

ICMCTF 2019

46th International Conference on
Metallurgical Coatings and Thin Films

Program

Technical Sessions

Abstracts

Exhibition

May 19-24, 2019

Town & Country Hotel and Convention Center
San Diego, California, USA

Presented and Sponsored by:

Advanced Surface Engineering Division of AVS



2019 ICMCTF Platinum Sponsors:

OERLIKON BALZERS and PLATIT



Start using the ICMCTF 2019 App

To login, enter your Registration Confirmation Number and Last Name to access messaging, enable the synchronization of notes, favorites, and scheduled items between devices and the online planner.

The new benchmark



INNOVENTA kila HIGH-PERFORMANCE PVD EQUIPMENT

INNOVENTA kila has the preferred coating system size for most production requirements and perfectly masters smaller to larger quantities. The successor of the best-selling INNOVA meets all your expectations with compelling elegance. It's the perfect coating system for tools, and also R&D.

www.oerlikon.com/balzers

oerlikon
balzers

Welcome to the 46th ICMCTF

ICMCTF 2019 will have eight technical symposia A through H and four topical symposia, addressing experimental, theoretical, and manufacturing issues associated with the development of new coating materials and processes, novel methods of analysis and characterization, and approaches for scale up of commercial applications. A special emphasis on flexible electronic materials for this year is evident with an opening plenary talk on Monday morning by Professor John Rogers from Northwestern University, USA, on 'Soft Electronics for the Human Body.' Another special highlight of the meeting is our Exhibitors Keynote Lecture, presented by Dr. Farwah Nahif, voestalpine eifeler Vacotec GmbH, Germany. She will present on the topic of "Advanced Performance of Tools in Sheet-metal Forming – The Synergy of Surface Technology and Tooling Material Selection." Two Special Interest Lectures will be featured throughout the conference week, as well. Professor Ivan Petrov from the University of Illinois, USA, and Linköping University, Sweden, will speak on his vast experience with "Linking Intrinsic Plasma Characteristics to the Microstructure and Properties of Diverse Thin Film Materials." Professor Gregory Abadias from the Université de Poitiers, France, will share his recent work on "Advanced Monitoring of Thin Film Growth from Real-time Diagnostics."

In addition to the technical program, the Conference features a two-day industrial exhibition, Tuesday and Wednesday, May 21–22, showcasing the latest in equipment, materials and services used for the deposition, monitoring, and characterization of coatings and thin films. The Exhibition is open to the public. An educational program of Short Courses and Focused Topic Sessions (FTS) will be offered throughout the week.

Each year, the R.F. Bunshah Award Laureate and three outstanding Graduate Student Award winners are celebrated during a special convocation late Wednesday afternoon, May 22, followed by a festive buffet reception in the evening.

ICMCTF will again publish excellent scientific and technical work in peer-reviewed issues of the two Elsevier journals *Surface and Coatings Technology* (SCT) and *Thin Solid Films* (TSF), so we hope you were able to submit your manuscript by May 8th. Stop in to see the Journal Editors in the Terrace Salon 3 with any questions.

The Town and Country Resort Hotel and Convention Center, located in sunny San Diego of Southern California, will be the official conference venue, providing a relaxed atmosphere for discussion and networking among attendees.



2019 General Chair
Michael Stüber
Karlsruhe Instit. of Technology, Germany



2019 Program Chair
Christopher Muratore
University of Dayton, USA



2020 Program Chair
Grzegorz (Greg) Greczynski
Linköping University, Sweden



The ICMCTF 2019 graphic is a composite of images provided courtesy of:

Dr. Adam Waite and Dr. Rachel Rai, University of Dayton, Department of Chemical and Materials Engineering/Air Force Research Laboratory, Materials and Manufacturing Directorate

Dr. Argelia Pérez Pacheco and Dr. Rosa Quispe, Investigadora en Ciencias Médicas, Unidad de Investigación y Desarrollo Tecnológico UIDT-HGM, Hospital General de México

Table of Contents

| | |
|--|---------|
| Welcome Message | 1 |
| ICMCTF Mobile App..... | 2 |
| 2019 ASED-EC, Editors & Chairs..... | 3 |
| 2019 ICMCTF Executive Organizing Committee | 4 |
| 2019 Symposium and Session Chairs | 5–7 |
| AVS Meetings Code of Conduct | 7 |
| Conference Overview & General Info | 8 |
| Schedule of Events..... | 9 |
| Plenary Session Lecture..... | 10 |
| Exhibition Keynote Lecture | 11 |
| Awards Night Invitation..... | 12 |
| ICMCTF Bunshah Award Laureates | 13 |
| R.F. Bunshah Award and Honorary Lecture | 14–15 |
| ICMCTF Graduate Student Award Finalists | 16 |
| 2020 Call for Award Nominations | 17 |
| Bunshah Awards Protocol | 18 |
| Student Awards Protocol | 19 |
| Short Courses..... | 20 |
| AVS Membership Promotion..... | 21 |
| Focused Topic Sessions | 22–24 |
| Sponsors..... | 26–27 |
| Town & Country Map | 28 |
| Program Key | 29 |
| Program at a Glance..... | 30 |
| Technical Program Schedule | 31–73 |
| Author Index | 74–82 |
| Abstracts (Arranged by Day)..... | 85–211 |
| Author Index | 212–220 |
| Exhibit Program..... | 221–248 |

ICMCTF MOBILE APP

DOWNLOAD THE AVS EVENTS & ACTIVITIES MOBILE APP!



The App Provides Year-round Access to AVS Publications, Technical Library, and Professional Development Activities and **contains the ICMCTF Conference Event App**. The AVS Events mobile app serves as your all-in-one event guide – giving you everything you need to know in the palm of your hand.

- Browse or search sessions, speakers, and posters
 - Locate exhibitors and tour the Exhibit Hall
 - Build your personal daily schedule
 - Receive reminders and updates
 - Engage and network with peers
 - Find what you are looking for
 - Take notes, bookmark, and filter
 - Synchronize across your devices
 - Access the conference program, schedule, or animated maps without WiFi
- Search for “AVSEvents” in the Apple Store or Google Play to locate and download the app. You can also scan the QR codes below to download the app directly.

| | |
|--|--|
| | |
| | |



THIS BOOK BELONGS TO:

Open access and 1 year retrieval of articles from the TSF and SCT Special Issues are compliments of ICMCTF 2019.



David Adams
2019 ASED Chair
Sandia National Lab.
USA



Jörg Patscheider
ASED Past Chair
Evatec AG
Switzerland



Paul Mayrhofer
ASED Chair-Elect
TU Wien
Austria

2019 ASED Executive Committee, Editors & Chairs



Secretary
Yip-Wah Chung
Northwestern Univ.
USA



Treasurer
Gregory J. Exarhos
Pacific Northwest
National Lab., USA



Awards Chair
Ivan Petrov
Univ. of Illinois, USA
Linköping Univ. Sweden



Short Course Chair
Jörg Patscheider
Evatec AG
Switzerland



Publications Chair
Samir Aouadi
Univ. of North Texas, USA



EC: Samir Aouadi
Univ. of North Texas
USA



EC: Andras Korenyi-Both
Tribologix Inc.
USA



EC: Aharon Inspektor
Carnegie Mellon Univ.
USA



EC: Christian Mitterer
Montanuniversität Leoben,
Austria



EC: Christopher Muratore
University of Dayton
USA



EC: Peter Polcik
Plansee AG
Austria



EC: Johanna Rosén
Linköpings Univ.
Sweden



EC: Roel Tietema
IHI Hauzer Techno Coatings
The Netherlands



Lead Editor
Esteban Broitman
SKF Res. & Tech. Dev.
The Netherlands



Editor
Carlos A. Figueroa
Univ. de Caxias do Sul
Brazil



Editor
Sandra E. Rodil
Univ. Nacional Autonoma de Mexico
Mexico



Editor
Juan Antonio Zapien
City Universit of Hong Kong
Hong Kong

2019 ICMCTF Executive Organizing Committee

2019 GENERAL CHAIR

Michael Stüber

Karlsruhe Institute of Technology (KIT), Germany
michael.stueber@kit.edu

IMMEDIATE PAST-CHAIR

Jörg Patscheider

Evatec AG, Switzerland
joerg.patscheider@evatecnet.com

AWARDS CHAIR

Ivan Petrov

University of Illinois, USA
Linköping University, Sweden
petrov@uiuc.edu

SHORT COURSE CHAIR

Jörg Patscheider

Evatec AG, Switzerland
joerg.patscheider@evatecnet.com

PUBLICATIONS CHAIR

Samir Aouadi

Department of Materials Science and Engineering
University of North Texas, USA
Samir.Aouadi@unt.edu

PROCEEDINGS EDITORS

Esteban Broitman (*Lead Editor*)

SKF Research & Technology Development Center
The Netherlands
esteban.daniel.broitman@skf.com

Carlos A. Figueroa

Center of Exact Sciences and Technology
University of Caxias do Sul, Brazil
cafiguer@ucs.br

Sandra E. Rodil

Instituto de Investigaciones en Materiales
Universidad Nacional Autonoma de Mexico
México
srodil@unam.mx

Juan Antonio Zapien

City University of Hong Kong
Hong Kong, SAR PRC
apjzas@cityu.edu.hk

2019 PROGRAM CHAIR

Christopher Muratore

University of Dayton, USA
cmuratore1@udayton.edu

2020 PROGRAM CHAIR

Grzegorz (Greg) Greczynski

Linköping University, Sweden
grzegorz.greczynski@liu.se

ASED CHAIR

David Adams

Sandia National Labs., USA
dadams205@comcast.net

ASED TREASURER

Greg Exarhos

Pacific Northwest National Laboratory, USA
greg.exarhos@pnnl.gov

CONFERENCE MANAGEMENT

Conference Administrator

Yvonne Towse
yvonne@avs.org

Conference Manager

Della Miller
della@avs.org

Registration Manager

Heather Korff
heather@avs.org

Exhibition Manager

Jeannette DeGennaro
jeannette@avs.org

Web Development

Keith Mitchell / Teddy Bhabikhan
keith@avs.org / teddy@avs.org

Conference Consultant

Mabel Zabinski
icmctf@icmctf.org

2019 Symposium and Session Chairs

SYMPOSIUM A

Coatings for Use at High Temperatures

Vladislav Kolarik
Fraunhofer ICT, Germany
vladislav.kolarik@ict.fraunhofer.de

Prabhakar Mohan
Solar Turbines, Inc., USA
Mohan_Prabhakar@solarturbines.com

Francisco Javier Pérez-Trujillo
Universidad Complutense de Madrid,
Spain
fjperez@ucm.es

A1. Coatings to Resist High-temperature Oxidation, Corrosion, and Fouling

Shigenari Hayashi
Hokkaido University, Japan
hayashi@eng.hokudai.ac.jp

Lars-Gunnar Johansson
Chalmers University of Technology,
Sweden
lg@chalmers.se

Justyna Kulczyk-Malecka
Manchester Metropolitan University, UK
J.Kulczyk-Malecka@mmu.ac.uk

A2. Thermal and Environmental Barrier Coatings

Sabine Faulhaber
University of California, San Diego, USA
sfaulhaber@eng.ucsd.edu

Kang Lee
NASA Glenn Research Center, USA
ken.k.lee@nasa.gov

Pantcho Stoyanov
Pratt & Whitney, USA
pantcho.stoyanov@pw.utc.com

A3. Materials and Coatings for Solar Power Concentration Plants

Pérez-Trujillo
Universidad Complutense de Madrid,
Spain
fjperez@ucm.es

Sebastien Dryepont
Oak Ridge National Laboratory, USA
dryepontsn@ornl.gov

Gustavo García-Martin
REP-Energy Solutions, Spain
gustavo.garcia@rep-energysolutions.com

SYMPOSIUM B

Hard Coatings and Vapor Deposition Technologies

Jyh-Wei Lee
Ming Chi University of Technology,
Taiwan
jefflee@mail.mcut.edu.tw

Farwah Nahif
Eifeler-Vacotec GmbH, Germany
farwah.nahif@eifeler-vacotec.com

Joerg Vetter
Oerlikon Balzers Coating Germany
GmbH, Germany
joerg.vetter@oerlikon.com

B1. PVD Coatings and Technologies

Frank Kaulfuss
Fraunhofer Institute for Material and
Beam Technology (IWS), Germany
frank.kaulfuss@iws.fraunhofer.de

Jyh-Ming Ting
National Cheng Kung University, Taiwan
jting@mail.ncku.edu.tw

Qi Yang
National Research Council of Canada,
Canada
qi.yang@nrc-cnrc.gc.ca

B2. CVD Coatings and Technologies

Raphaël Boichot
SIMaP, France
raphael.boichot@simap.grenoble-inp.fr

Kazunori Koga
Kyushu University, Japan
koga@ed.kyushu-u.ac.jp

B3. Deposition Technologies and Applications for Diamond-like Coatings

Laurent Espitalier
Wallwork Cambridge Ltd, UK
laurent.espitalier@wallworkht.com

Konrad Fadenberger
Robert Bosch GmbH, Germany
konrad.fadenberger@de.bosch.com

B4. Properties and Characterization of Hard Coatings and Surfaces

Naureen Ghafoor
Linköping Univ., IFM, Thin Film Physics
Div., Sweden
naureen.ghafoor@liu.se

Ulrich May
Robert Bosch GmbH, Germany
ulrich.may2@de.bosch.com

Fan-Bean Wu
National United University, Miaoli,
Taiwan
fbwu@nuu.edu.tw

B5. Hard and Multifunctional Nanostructured Coatings

Tomas Kozak
University of West Bohemia,
Czech Republic
kozakt@kfy.zcu.cz

Helmut Riedl
TU Wien, Institute of Materials Science
and Technology, Austria
helmut.riedl@tuwien.ac.at

B6. Coating Design and Architectures

Shou-Yi Chang
National Tsing Hua University, Taiwan
changsy@mx.nthu.edu.tw

Paul Heinz Mayrhofer
TU Wien, Institute of Materials Science
and Technology, Austria
paul.mayrhofer@tuwien.ac.at

B7. Plasma Diagnostics and Growth Processes

Arutun P. Ehasarian
Sheffield Hallam University, UK
a.ehasarian@shu.ac.uk

Yolanda Aranda Gonzalvo
University of Minnesota, USA
yarandag@umn.edu

SYMPOSIUM C

Fundamentals and Technology of Multifunctional Materials and Devices

Peter Kelly
Manchester Metropolitan University, UK
peter.kelly@mmu.ac.uk

Mathias Schubert
University of Nebraska-Lincoln, USA
schubert@engr.unl.edu

C1. Optical Metrology in Design, Optimization, and Production of Multifunctional Materials

Nikolas Podraza
University of Toledo, USA
nikolas.podraza@utoledo.edu

Juan Antonio Zapien
City University of Hong Kong,
Hong Kong
apjzajs@cityu.edu.hk

C2. Novel Oxide Films for Active Devices

Vanya Darakchieva
Linköping University, Sweden
vanya@ifm.liu.se

Marko Tadjer
Naval Research Laboratory, USA
marko.tadjer@nrl.navy.mil

C3. Thin Films for Energy-related Applications

Per Eklund
Linköping University, Sweden
per.eklund@liu.se

Tushar Shimpi
Colorado State University, USA
mechanical.tushar@gmail.com

C4. Fundamentals of Metallurgy in Thin Films and Coatings

I. Emre Gunduz

Naval Postgraduate School
igunduz@purdue.edu

Karsten Woll

Karlsruhe Institute of Technology (KIT),
Germany
karsten.woll@kit.edu

SYMPOSIUM D

Coatings for Biomedical and Healthcare Applications

Jean Gerlinger

Mines Saint-Etienne, France
geringer@emse.fr

Margaret Stack

University of Strathclyde, UK
margaret.stack@strath.ac.uk

D1. Surface Coating and Modification for Use in Biological Environments

Mathew T. Mathew

University of Illinois College of
Medicine, USA
mathewmathew@gmail.com

Kerstin Thorwarth

EMPA - Swiss Federal Laboratories for
Materials Science and Technology,
Switzerland
kerstin.thorwarth@empa.ch

D2. Bio-corrosion and Bio-tribology

Steve Bull

Newcastle University, UK
steve.bull@ncl.ac.uk

Jessica Jennings

University of Memphis, USA
jjennings@memphis.edu

D3. Surface and Coatings to Promote Tailored Biological Responses

Vincent Fridrici

Ecole centrale de Lyon, LTDS, France
vincent.fridrici@ec-lyon.fr

Sandra Rodil

Universidad Nacional Autonoma de
Mexico, Mexico
srodil@unam.mx

SYMPOSIUM E

Tribology and Mechanical Behavior of Coatings and Engineered Surfaces

Michael Chandross

Sandia National Laboratories, USA
mechand@sandia.gov

Giovanni Ramirez

Bruker Nano Surfaces, USA
giovanni.ramirez@bruker.com

E1. Friction, Wear, Lubrication Effects, and Modeling

Nazlim Bagcivan

Schaeffler AG, Germany
nazlim.bagcivan@schaeffler.com

Carsten Gachot

Vienna University of Technology, Austria
carsten.gachot@tuwien.ac.at

Tomas Polcar

University of Southampton, UK
t.polcar@soton.ac.uk

E2. Mechanical Properties and Adhesion

Megan Cordill

Erich Schmid Institute of Materials
Science, Austria
megan.cordill@oeaw.ac.at

Gerhard Dehm

MPI für Eisenforschung GmbH,
Germany
dehm@mpie.de

Ming-Tzer Lin

National Chung Hsing University,
Taiwan
mingtlin@dragon.nchu.edu.tw

E3. Tribology of Coatings for Automotive and Aerospace Applications

Nicolas Argiba

Sandia National Laboratories, USA
nargiba@sandia.gov

Christian Greiner

Karlsruhe Institute of Technology (KIT),
Institute for Applied Materials (IAM),
Germany
christian.greiner@kit.edu

Oliver Hunold

Oerlikon Balzers, Liechtenstein
oliver.hunold@oerlikon.com

SYMPOSIUM F

New Horizons in Coatings and Thin Films

Ramana Chintalapalle

University of Texas at El Paso, USA
rvchintalapalle@utep.edu

Daniel Lundin

Université Paris-Sud/CNRS, France
daniel.lundin@u-psud.fr

F1. Nanomaterials and Nanofabrication

Ulf Helmersson

Linköping University, Sweden
ulf.helmersson@liu.se

Vitezslav Stranak

University of South Bohemia,
Czech Republic
stranv00@centrum.cz

F2. HiPIMS, Pulsed Plasmas, and Energetic Deposition

Jon Tomas Gudmundsson

University of Iceland, Iceland
tumi@hi.is

Tiberiu Minea

Université Paris-Sud, France
tiberiu.minea@u-psud.fr

F3. 2D Materials: Synthesis, Characterization, and Applications

Suneel Kodambaka

UCLA, USA
kodambaka@ucla.edu

Eli Sutter

University of Nebraska-Lincoln, USA
esutter@unl.edu

F4. Functional Oxide and Oxynitride Coatings

Anders Eriksson

Oerlikon Balzers, Oerlikon Surface
Solutions AG, Liechtenstein
anders.o.eriksson@oerlikon.com

Marcus Hans

RWTH Aachen University, Germany
hans@mch.rwth-aachen.de

Jörg Patscheider

Evatec AG, Switzerland
joerg.patscheider@evatecnet.com

SYMPOSIUM G

Surface Engineering – Applied Research and Industrial Applications

Mats Ahlgren

Sandvik Coromant R&D, Sweden
mats.ahlgren@sandvik.com

Satish Dixit

Plasma Technology Inc., USA
dixsat@gmail.com

Chris Stoessel

Eastman Chemical Company, Inc., USA
stoessel@attglobal.net

Wan-Yu Wu

Da-Yeh University, Taiwan
wywu@cloud.dyu.edu.tw

G1. Advances in Industrial PVD, CVD and PCVD Processes and Equipment

Ladislav Bardos

Uppsala University, Sweden
ladislav.bardos@angstrom.uu.se

Emmanuelle Göthelid

Sandvik Coromant R&D, Sweden
emmanuelle.gothelid@sandvik.com

G2. Component Coatings for Automotive, Aerospace, Medical, and Manufacturing Applications

Etienne Bousser
Polytechnique Montreal, Canada
etienne.bousser@polymtl.ca

Satish Dixit
Plasma Technology Inc., USA
dixsat@gmail.com

Tetsuya Takahashi
Kobe Steel, Ltd., Japan
takahashi.tetsuya-1@kobelco.com

G3. Innovative Surface Engineering for Advanced Cutting and Forming Tool Applications

Ali Khatibi
Oerlikon Balzers, Oerlikon Surface
Solutions AG, Liechtenstein
ali.khatibi@oerlikon.com

Christoph Schiffers
CemeCon AG, Germany
christoph.schiffers@cemecon.de

G4. Pre-/Post-Treatment and Duplex Technology

Heidrun Klostermann
Fraunhofer FEP, Germany
heidrun.klostermann@fep.fraunhofer.de

Hiroyuki Kousaka
Gifu University, Japan
kousaka@gifu-u.ac.jp

Chris Stoessel
Eastman Chemical Company, Inc., USA
stoessel@attglobal.net

G5. Hybrid Systems, Processes and Coatings

Hana Barankova
Uppsala University, Sweden
hana.barankova@angstrom.uu.se

Sang-Yul Lee
Korea Aerospace University, Republic of
Korea
sylee@kau.ac.kr

G6. Application-Driven Cooperation between Industry and Research Institutions

Hamid Bolvardi
Oerlikon Balzers, Oerlikon Surface
Solutions AG, Liechtenstein
hamid.bolvardi@oerlikon.com

Tobias Brögelmann
Surface Engineering Institute - RWTH
Aachen University, Germany
broegelmann@iot.rwth-aachen.de

Joern Kohlscheen
Kennametal GmbH, Germany
joern.kohlscheen@kennametal.

SYMPOSIUM H

Advanced Characterization Techniques for Coatings, Thin Films and Small Volumes

Benoit Merle
Friedrich-Alexander-University Erlangen
Nürnberg (FAU), Germany
benoit.merle@fau.de

Marco Sebastiani
Roma TRE University, Italy
seba@uniroma3.it

H1. Spatially-resolved and In-Situ Characterization of Thin Films and Engineered Surfaces

Gregory Abadias
Université de Poitiers, France
gregory.abadias@univ-poitiers.fr

Xavier Maeder
Empa - Swiss Federal Laboratories for
Materials Science and Technology,
Switzerland
xavier.maeder@empa.ch

Michael Tkadletz
Montanuniversität Leoben, Austria
michael.tkadletz@unileoben.ac.at

H2. Advanced Mechanical Testing of Surfaces, Thin Films, Coatings and Small Volumes

Olivier Pierron
Georgia Institute of Technology, USA
olivier.pierron@me.gatech.edu

Timothy Rupert
University of California, Irvine, USA
trupert@uci.edu

H3. Characterization of Coatings and Small Volumes in Harsh Environments

James Gibson
RWTH Aachen University, Germany
gibson@imm.rwth-aachen.de

Jeffrey M. Wheeler
ETH Zürich, Switzerland
jeff.wheeler@mat.ethz.ch

TOPICAL SYMPOSIUM

TS1. High Entropy and Other Multi-principal-element Materials

Diederik Depla
Ghent University, Belgium
Diederik.Depla@ugent.be

Ulf Jansson
Uppsala University, Angstrom
Laboratory, Sweden
ulf.jansson@kemi.uu.se

TS2. Icephobic Surface Engineering

Alina Agüero Bruna
Instituto Nacional de Técnica
Aeroespacial (INTA), Spain
agueroa@inta.es

Jolanta Klemberg-Sapieha
Polytechnique Montréal, Canada
jolanta-ewa.sapieha@polymtl.ca

TS3. Surface Engineering for Lightweight Materials

Klaus Böbel
Robert Bosch GmbH, Germany
klaus.boebel@de.bosch.com

Fred Fietzke
Fraunhofer FEP, Germany
fred.fietzke@fep.fraunhofer.de

TS4. Thin Film Materials for Flexible Electronics

Nicholas Glavin
Air Force Research Laboratory, Materials
and Manufacturing Directorate, USA
Nicholas.Glavin.1@us.af.mil

Oleksandr Glushko
Austrian Academy of Sciences, Vienna



AVS Meetings Code of Conduct

It is the policy of the American Vacuum Society (AVS) that all participants, including attendees, vendors, AVS staff, volunteers, and all other stakeholders at AVS meetings will conduct themselves in a professional manner that is welcoming to all participants and free from any form of discrimination, harassment, or retaliation. Participants will treat each other with respect and consideration to create a collegial, inclusive, and professional environment at AVS Meetings. Creating a supportive environment to enable scientific disclosure at AVS meetings is the responsibility of all participants.

Participants will avoid any inappropriate actions or statements based on individual characteristics such as age, race, ethnicity, sexual orientation, gender identity, gender expression, marital status, nationality, political affiliation, ability status, educational background, or any other characteristic protected by law. Disruptive or harassing behavior of any kind will not be tolerated. Harassment includes but is not limited to inappropriate or intimidating behavior and language, unwelcome jokes or comments, unwanted touching or attention, offensive images, photography without permission, and stalking.

Violations of this code of conduct policy should be reported to the AVS Managing Director or Events Manager. Sanctions may range from verbal warning, to ejection from the meeting without refund, to notifying appropriate authorities. Retaliation for complaints of inappropriate conduct will not be tolerated. If a participant observes inappropriate comments or actions and personal intervention seems appropriate and safe, they should be considerate of all parties before intervening.

ICMCTF 2019 CONFERENCE OVERVIEW & GENERAL INFO

REGISTRATION HOURS

Atlas Foyer

| | |
|-------------------------------------|--------------------|
| Sunday, May 19: | 4:30 pm – 6:30 pm |
| Monday, May 20: | 7:00 am – 6:00 pm |
| Tuesday, May 21 – Thursday, May 23: | 7:30 am – 3:30 pm |
| Friday, May 24: | 7:30 am – 10:30 am |

EXHIBIT HOURS

Grand Hall

| | |
|--------------------|--------------------|
| Tuesday, May 21: | 12:00 pm – 7:00 pm |
| Wednesday, May 22: | 10:00 am – 2:00 pm |

TECHNICAL SESSIONS

All Technical Sessions are held at the Town & Country Convention Center. Consult the Program/Mobile App for the session and break times (AM/PM), locations, and maps. The Poster Session will be held in the Grand Hall on Thursday from 5:00–7:00 pm.

EDITORIAL OFFICE

Terrace Salon 3

| | |
|------------------------------------|--------------------|
| Monday, May 21 – Thursday, May 23: | 8:30 am – 5:00 pm |
| Friday, May 24: | 8:30 am – 12:00 pm |

Authors will be notified of the editorial decision concerning their manuscript(s) via email. Referees should return their reports, via the EES electronic system, to the Editorial Office as soon as possible.

PRESENTER PREVIEW ROOM

Terrace Salon 2

| | |
|------------------------------------|--------------------|
| Sunday, May 19: | 3:30 pm – 6:30 pm |
| Monday, May 20 – Thursday, May 23: | 7:30 am – 5:30 pm |
| Friday, May 24: | 7:30 am – 10:00 am |

ATTENDEE ROOM

The Royal Palm 1-3 Room has been designated as a “no-host” gathering room during ICMCTF 2019. The room will provide space for attendees to mingle with exhibitors, family members and companions. If you wish to reserve the room for a small meeting, please contact Della Miller (della@avs.org).

CYBER CAFÉ & WiFi

The ICMCTF Cyber Café sponsored by ELSEVIER is available to all ICMCTF attendees & Exhibitors at no charge Sunday through Friday, noon. Bring your laptop – the WiFi broadband signal can be found in the Atlas Foyer, most meeting rooms, the Exhibition Hall, and the adjacent Lion Fountain Courtyard. The complimentary WiFi service is LIMITED to 200 ICMCTF users at a time, Sunday–Friday.

CONFERENCE SPECIAL ISSUE

The ICMCTF 2019 Special Issues will be posted electronically on the Journals’ websites: *Surface and Coatings Technology* (Symposiums A, B, E, G, and TS1, and TS3) or *Thin Solid Films* (Symposiums C, D, F, H, TS2 and TS4). All attendees will receive an email notice when the Proceedings are posted as to when the *complimentary open access and retrieval is available* for one year compliments of ICMCTF 2019.

SHORT COURSES

Nine Short Courses: Sunday through Thursday, 8:30 am – 4:30 pm. Limited onsite registration is available at the Registration desk, Atlas Foyer. For more course details and descriptions, visit the website: <http://www2.avs.org/conferences/ICMCTF/2019/shortcourses.htm>

SPECIAL EXHIBIT HALL EVENTS

- **Exhibit Hall Raffles and Prizes during Exhibit Hours: Booth #320**
Visit the Hall during Tuesday and Wednesday session breaks!
- **AVS Membership: Get year-round access to benefits! Renew or Join at Booth #312** and receive a free gift and be entered in a drawing to receive an Amazon giftcard.

AVS MEETINGS CODE OF CONDUCT

It is the policy of the AVS that all participants, including attendees, vendors, staff, volunteers, and all other stakeholders at AVS meetings will conduct themselves in a professional manner that is welcoming to all participants and free from any form of discrimination, harassment, or retaliation. Participants will treat each other with respect and consideration to create a collegial, inclusive, and professional environment at AVS Meetings. Creating a supportive environment to enable scientific disclosure at AVS meetings is the responsibility of all participants. Participants will avoid any inappropriate actions or statements based on individual characteristics such as age, race, ethnicity, sexual orientation, gender identity, gender expression, marital status, nationality, political affiliation, ability status, educational background, or any other characteristic protected by law. Disruptive or harassing behavior of any kind will not be tolerated. Harassment includes but is not limited to inappropriate or intimidating behavior and language, unwelcome jokes or comments, unwanted touching or attention, offensive images, photography without permission, and stalking. Violations of this code of conduct policy should be reported to the AVS Managing Director or Events Manager. Sanctions may range from verbal warning, to ejection from the meeting without refund, to notifying appropriate authorities. Retaliation for complaints of inappropriate conduct will not be tolerated. If a participant observes inappropriate comments/actions personal intervention seems appropriate and safe, they should be considerate of all parties before intervening.

PHOTO & RECORDING POLICY

Attendees and exhibitors are encouraged to network and enjoy the meeting experience. As such, capturing memories of casual meeting activities and networking is permitted with the permission of those being prominently photographed. Photographing formal meeting presentations, posters or displays is forbidden without the permission of ICMCTF Conference Management and the presenter. Furthermore, the use of recording equipment, cameras, cell phone cameras, or audio equipment is prohibited at any AVS event without prior written approval of the Society. The Society reserves the right to reproduce, by any means selected, any or all of these presentations and materials.

2019 ICMCTF SCHEDULE OF EVENTS

| DAY | TIME | EVENT | LOCATION |
|-----------|----------------------------|---|--------------------------------|
| SUNDAY | 7:30 am – 8:30 am | Short Course Registration | Atlas Foyer |
| | 8:30 am – 4:30 pm | Short Course Program | Atlas Foyer |
| | 4:30 pm – 6:30 pm | Conference Registration | Atlas Foyer |
| MONDAY | 7:00 am – 6:00 pm | Conference Registration | Atlas Foyer |
| | 7:30 am – 8:30 am | Short Course Registration | Atlas Foyer |
| | 8:00 am – 9:45 am | Plenary Session Lecture: Professor John Rogers “Soft Electronics for the Human Body” | Town & Country Room |
| | 8:30 am – 4:30 pm | Short Course Program | Atlas Foyer |
| | 10:00 am – 5:40 pm | Technical Sessions | See Program/Mobile App |
| | 12:20 pm – 1:20 pm | Focused Topic Session: Anton Paar “Latest Developments in Advanced Mechanical Surface Characterization” | Town & Country Room |
| | 5:45 pm – 7:00 pm | ICMCTF 2019 Welcome Mixer | Lion Fountain Courtyard |
| TUESDAY | 7:00 am – 8:00 am | Focused Topic Session: Bruker “Advanced Technologies for the In-Depth Characterization of Surfaces” | Town & Country Room |
| | 7:30 am – 8:30 am | Short Course Registration | Atlas Foyer |
| | 7:30 am – 3:30 pm | Conference Registration | Atlas Foyer |
| | 8:00 am – 5:40 pm | Technical Sessions | See Program/Mobile App |
| | 8:30 am – 4:30 pm | Short Course Program | Atlas Foyer |
| | 11:00 am – 12:00 pm | Exhibition Keynote Lecture: Dr. Farwah Nahif “Advanced Performance of Tools in Sheet-metal Forming-The Synergy of Surface Technology and Tooling Material Selection” | Town & Country Room |
| | 12:00 pm – 7:00 pm | Exhibition Hall Opens Today | Grand Hall |
| | 12:00 pm – 1:40 pm | Light Lunch in Exhibit Hall (While Supplies Last) | Grand Hall |
| | 3:20 pm – 4:00 pm | Break – Complimentary Refreshments in Exhibit Hall | Grand Hall |
| | 5:30 pm – 7:00 pm | Exhibition Reception | Grand Hall |
| | 7:00 pm – 8:00 pm | Special Interest Talk: Grégory Abadias “Advanced Monitoring of Thin Film Growth from Real-time Diagnostics” | Town & Country Room |
| WEDNESDAY | 7:30 am – 3:30 pm | Conference Registration | Atlas Foyer |
| | 7:30 am – 8:30 am | Short Course Registration | Atlas Foyer |
| | 8:00 am – 5:40 pm | Technical Sessions | See Program/Mobile App |
| | 8:30 am – 4:30 pm | Short Course Program | Atlas Foyer |
| | 10:00 am – 2:00 pm | Visit the Exhibition! | Grand Hall |
| | 10:00 am – 11:00 am | Break – Complimentary Refreshments in Exhibit Hall | Grand Hall |
| | 12:20 pm – 2:00 pm | Light Lunch in Exhibit Hall (While Supplies Last) | Grand Hall |
| | 1:00 pm – 2:00 pm | Special Interest Talk: Ivan Petrov “Linking Intrinsic Plasma Characteristics to the Microstructure and Properties of Thin Films” | Town & Country Room |
| | 5:45 pm – 7:15 pm | Awards Convocation: Dr. Joe Greene “Some Highlights from over Four Decades of Thin-film Science” | Town & Country Room |
| | 7:30 pm – 10:00 pm | Awards Buffet Reception | Golden Ballroom |
| THURSDAY | 7:30 am – 3:30 pm | Conference Registration | Atlas Foyer |
| | 7:30 am – 8:30 am | Short Course Registration | Atlas Foyer |
| | 8:30 am – 4:30 pm | Short Course Program | Atlas Foyer |
| | 8:00 am – 5:00 pm | Technical Sessions | See Program/Mobile App |
| | 12:20 pm – 1:20 pm | ICMCTF 2020 Information Session | California |
| | 12:20 pm – 1:20 pm | Focused Topic Session: Elsevier “The Art of Publishing” | Golden West |
| | 5:00 pm – 7:00 pm | Poster Session (including 4 HDTV poster demonstrations) | Grand Hall |
| | 6:00 pm – 7:00 pm | Poster Reception | Grand Hall |
| FRIDAY | 7:30 am – 10:30 am | Conference Registration | Atlas Foyer |
| | 8:00 am – 12:00 pm | Technical Sessions | See Program/Mobile App |
| | 12:00 pm – 1:00 pm | Thank You, See You Next Year Party! | Lion Fountain Courtyard |

ICMCTF 2019 Plenary Session Lecture

Monday, May 20, 2019

8:00 am

Town & Country Room

Soft Electronics for the Human Body

Prof. John Rogers

Northwestern University, Evanston, IL, USA

Biological systems are mechanically soft, with complex, time-dependent 3D curvilinear shapes; modern electronic and microfluidic technologies are rigid, with simple, static 2D layouts. Eliminating this profound mismatch in physical properties will create vast opportunities in man-made systems that can intimately integrate with the human body, for diagnostic, therapeutic or surgical function with important, unique capabilities in biomedical research and clinical healthcare. Over the last decade, a convergence of new concepts in thin film materials science, mechanical engineering, electrical engineering and advanced manufacturing has led to the emergence of diverse, novel classes of ‘bio-compatible’ electronic and microfluidic systems with ultrathin, skin-like physical properties. This talk describes the key ideas and enabling materials, and it presents some of the most recent device examples, including wireless electronic ‘tattoos’, with applications in continuous monitoring of vital signs in neonatal intensive care; and microfluidic/electronic platforms that can capture, store and perform biomarker analysis on sweat, with applications in sports and fitness.



Prof. John Rogers has received an impossibly long list of awards including a MacArthur Foundation fellowship, reserved for inventive folks with the highest level of outstanding talent. He is also behind over 80 patents and patent applications, more than 50 of which are licensed or in active use by large companies and startups that he has co-founded.

In September of 2016, Professor John Rogers joined Northwestern University as the Louis Simpson and Kimberly Querrey Professor of Materials Science and Engineering, Biomedical Engineering, Mechanical Engineering, Electrical Engineering and Computer Science, Chemistry and Neurological Surgery, where he is also the founding Director of the newly endowed Center on Bio-Integrated Electronics.

At Northwestern, the Rogers Research Group, whose current research focuses on “soft materials for conformal electronics, nanophotonic structures, microfluidic devices, and microelectromechanical systems, all lately with an emphasis on bio-inspired and bio-integrated technologies.”

Rogers’ research includes fundamental and applied aspects of nano and molecular scale fabrication as well as materials and patterning techniques for unusual electronic and photonic devices, with an emphasis on bio-integrated and bio-inspired systems. He has published more than 550 papers and is an inventor on over 100 patents and patent applications, more than 70 of which are licensed or in active use by large companies and startups that he has co-founded.

John Rogers holds his BA and BS degrees in Chemistry and in Physics from the University of Texas, Austin. He obtained his Ph.D. in Physical Chemistry in 1995 from MIT and was a Junior Fellow in the Harvard University Society of Fellows from 1995–97.

2019 Exhibition Keynote Lecture

Tuesday, May 21, 2019

11:00 am

Town & Country Room

Advanced Performance of Tools in Sheet-metal Forming – The Synergy of Surface Technology and Tooling Material Selection

Farwah Nahif

voestalpine eifeler Vacotec GmbH, Germany

The requirement of the automotive industry for light weight construction parts has been followed by the introduction of new sheet metal materials for forming application, such as high-strength steels. Due to this development and progress in sheet-metal material properties, with high hardness and toughness, the requirements for forming tool design has evolved within the last years.

Thus, the talk will focus on the beneficial synergy of PVD-based surface technology and tooling material selection in order to meet the specific application demands and to obtain advanced functionality and performance of tools in sheet-metal forming in the automotive sector.



Dr. Farwah Nahif received her PhD in engineering from the RWTH Aachen University in 2013. Her dissertation was addressing the effect of Si and Y additives on the phase stability of arc-based Al_2O_3 thin films and has been performed at the Materials Chemistry Department under Prof. Jochen Schneider. In 2014 Dr. Nahif joined the Research & Development Department of voestalpine eifeler Vacotec GmbH as a research scientist specialized in PVD technology and PVD product development. Since July 2018 Dr. Nahif is Head of the Research & Development Department of voestalpine eifeler Vacotec GmbH.

-Join Us for-

Awards Night

ASED/ICMCTF 2019 Annual
Awards Convocation & Reception

WEDNESDAY

MAY
22

AT 5:45 PM



Town & Country Room



You are Invited to the ICMCTF Lecture by the
2019 R.F. Bunshah Award Recipient
Joe Greene

Univ. of Illinois, USA; Linköping Univ., Sweden; and
National Taiwan Univ. Science & Technology, Taiwan

"Some Highlights from Over Four Decades of
Thin-Film Science"

Graduate Student and Other Awards will be Announced

*The Awards Reception will be held
at 7:30 PM following the Convocation*

ICMCTF R.F. Bunshah Award Laureates



Joe Greene - 2019



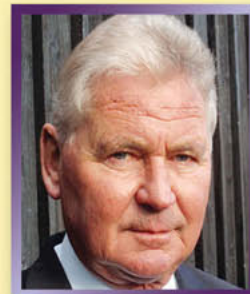
Wolf-Dieter Münz
2007



Stephen Rossnagel
2008



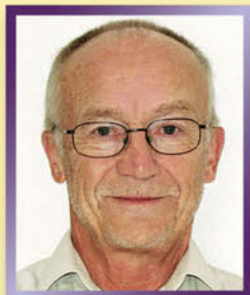
Ivan Petrov
2009



Helmut Holleck
2010



Stan Veprek
2011



Sture Hogmark
2012



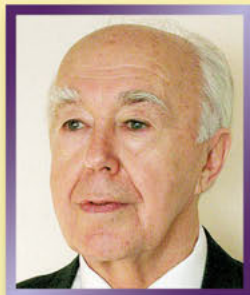
William D. Sproul
2013



Jindrich Musil
2014



Péter B. Barna
2015



Boris Movchan
2016



John Woollam
2017



Allan Matthews
2018

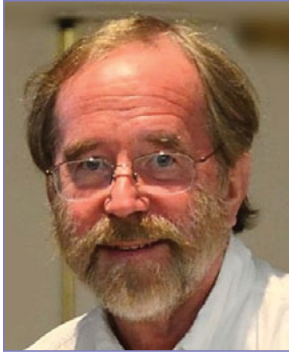
2020 Nominations are due October 1, 2019 - www.avs-ased.org

2019 R.F. Bunshah Annual Award & Honorary Lecture

Joe Greene

University of Illinois, USA, Linköping University, Sweden,
National Taiwan Univ. Science & Technology, Taiwan

Joe Greene, the 2019 ICMCTF laureate, is recognized for “*seminal contributions in areas of thin-film physics, surface science, and surface engineering.*”



Joe Greene is the D.B. Willett Professor of Materials Science and Physics at the University of Illinois, the Tage Erlander Professor of Materials Physics at Linköping University, Sweden, and a Chaired Professor at the National Taiwan University of Science and Technology. The focus of his research has been the development of an atomic-level understanding of adatom/surface interactions during the dynamic process of vapor-phase crystal growth in order to control-

ably manipulate nanochemistry, nanostructure, and, hence, physical properties. His work has involved nanoscience and film growth by all forms of sputter deposition, solid and gas-source MBE, UHV-CVD, MOCVD, and ALE. Joe has published more than 625 papers and review articles, 29 book chapters, and co-edited 4 books in the general areas of crystal growth, thin-film physics, and surface science. In particular, he has used hyperthermal condensing species and UV photochemistry for probing as well as stimulating surface reactions that do not proceed thermally. Joe has presented over 525 invited talks, 140 Plenary Lectures at international meetings, and has an h-factor of 78.

He is currently Editor-in-Chief of *Thin Solid Films* and past Editor of *CRC Critical Reviews in Solid State and Materials Sciences*. Joe is active in the AVS where he has served on the Trustees, twice as a member of the Board of Directors, as President of the society in 1989, and is currently Secretary. He has also Chaired the AVS Thin Film and Advanced Surface Engineering Divisions; the IUVSTA Education, Emerging Societies, and Thin Film Committees; and served on the Governing Board of the American Institute of Physics and the Executive Committee of the APS Division of Materials Physics. He is the US representative to the International Union of Vacuum Science and Techniques.

Joe is a Fellow of AVS, APS, and MRS.

A partial list of major awards:

- John Thornton Award (1991) from the AVS for “outstanding research in thin films”
- Tage Erlander Award (1991) from the Swedish Natural Science Research Council for “contributions to the physics and chemistry of thin films”
- Senior University of Illinois Scholar (1991) for “distinction as a member of the faculty”
- Honorary Doctor of Science in Materials Physics (1992) from Linköping Univ. (Sweden)
- Fellow of the American Vacuum Society (1993) for “outstanding research in thin film science with emphasis on the use of ion/surface interactions and photo-induced reactions to controllably alter film nucleation and growth kinetics”
- Technical Excellence Award from the Semiconductor Research Corporation (SRC) for “outstanding research contributions in the development of low-energy accelerated-ion doping during MBE Si and Si_{1-x}Ge_x film growth” (1994)
- 1996 DOE Award for Sustained Outstanding Research on “growth of new metastable nitride-based ceramic alloys, superlattices, and multilayers with enhanced properties”

- 1998 David Adler Award in Materials Physics from the American Physical Society for “outstanding research and lecturing on the physics and chemistry of thin films”
- 1998 Aristotle Award from SRC for “career achievement in outstanding graduate student teaching in its broadest sense; including innovation in student advising, instilling students with a love and respect for science, teaching students to carry out research at the highest level, contributing to student maturation and professional development, and continuing to impact student careers following graduation”
- Fellow of the American Physical Society (1998) for “original contributions to the experimental development, modeling, and understanding of Si, Ge, and Si_{1-x}Ge_x atomic-layer epitaxy and gas-source molecular-beam epitaxy”
- AVS Distinguished Lecturer (1998–present)
- Inaugural D.B. Willett Professor of Engineering Science (1999), University of Illinois
- David Turnbull Award, Materials Research Society (1999), for “contributions to the use of non-thermal methods in the growth of thin films and the engineering of their phase, composition, and microstructure; and for excellence in teaching and writing”
- Sustained research “Extending the Science of Transition-metal Nitrides” cited by the Department of Energy in 2001 as one of the most important scientific accomplishments in the last 25 years
- 2001 International Scientist of the Year for “contributions to thin-film science,” International Biographical Center, Cambridge, UK
- Elected to the European Academy of Science in 2002 for “outstanding contributions to materials science and education”
- Elected to the US National Academy of Engineering in 2003 for “pioneering studies in the synthesis and characterization of epitaxial and highly ordered polycrystalline materials”
- University Chaired Professor (2010), National Taiwan University of Science and Technology
- Fellow of the Materials Research Society (2013) for “foundational contributions to the understanding of thin film and nanostructure synthesis, particularly for pioneering work in thin film nitrides; distinguished leadership in the materials community”
- Lifetime Achievement Award (2013) from the Taiwan Association for Coatings and Thin Film Technology (TACT) for “seminal contributions to understanding the physics, chemistry, and materials science of thin films and nanoclusters”
- SVC Mentor Award (2015) for “seminal scientific and educational contributions to the evolving technologies of vacuum deposited coatings and thin-film materials”
- Named 2016 World Expert Lecturer, University of the Philippines
- 2016 George Sarton Annual International Award for “seminal contributions to the History of Science,” from the History of Science Society
- 2016 George Sarton Chair for the History of Science, Ghent University, Ghent, Belgium
- 2017: elected as a member of the EU Academy of Sciences
- 2017 Romanian Materials Science Crystal Growth Award for “outstanding international activity in promoting materials science”
- 2018 SVC Nathaniel H. Sugerman Memorial Award for “seminal scientific and educational contributions to the atomistic level understanding of the synthesis of nanostructured vacuum deposited coatings and thin film materials”
- 2019 AVS Advanced Surface Engineering Division R.F. Bunshah Award and ICMCTF Lecture “for his seminal contributions in areas of thin-film physics, surface science, and surface engineering”

Abstract: Some Highlights from over Four Decades of Thin-film Science

As a graduate student at USC, I was growing epitaxial GaAs(001) films by liquid-phase epitaxy. The layers were of very high purity as demonstrated by Hall and photoluminescence measurements, but we had no techniques sensitive enough to determine the remaining residual impurities. This led me to develop glow-discharge optical spectroscopy (GDOS), the optical analog of modern SIMS. As-deposited films were sputter etched and a spectrometer used to scan the emission peaks arising from the decay of sputtered atoms excited in the discharge. We found that the primary residual impurity was Sn and, via the use of calibration samples (based upon Hall measurements), we determined absolute Sn concentrations (initial detection limit = 3×10^{16} atoms/cm³, 680 ppb). Since then, we, and many others worldwide, have employed GDOS to quantitatively measure dopant diffusion and ion-implantation profiles in III-V, SiGe, and solar cell absorber layers. GDOS is also used to analyze bulk and thin-film alloys, for real-time process control (film growth rates and thicknesses) during sputter deposition, and for feedback control during high-rate reactive sputtering.

At UIUC, in addition to GDOS, I continued epitaxial semiconductor film growth, but switched to SiGe via UHV-CVD, metastable (III-V)_{1-x}(IV₂)_x (the “Greene” alloys) by UHV sputter deposition, and GaN by reactive-ion MBE. SiGe CVD was carried out in UHV in order to employ in-situ surface-science tools (RHEED, TPD, AES, XPS, UPS, HR-EELS, STM) to investigate atomic-scale growth kinetics. We developed models, with no fitting parameters, to accurately predict Si, Si_{1-x}Ge_x, Si_{1-x}C_x, and Ge_{1-x}Sn_x film growth rates, compositions, and doping profiles as a function of precursor partial pressures and deposition temperatures. The models are still used worldwide today. The Greene alloys (e.g.: (GaAs)_{1-x}(Ge₂)_x) were grown across pseudobinary phase diagrams and exhibited good thermal stability. They have interesting electronic transport, band structure, and phonon properties and are currently used in tunable photodetector and piezoelectric devices. The first high-resistivity single-crystal GaN films, both wurtzite and zincblende, were grown by MBE using evaporated Ga and 35 eV N₂₊ ions. The layers, which had the highest electron mobilities yet reported, were used to determine hexagonal and cubic GaN band structures.

Following an invitation to present a Swedish Academy of Science Lecture in the 1980s, colleagues from Linköping University ignited my interest in transition-metal (TM) nitrides (and, recently, TM diborides). The field of nitride hard-coatings was already developing rapidly, but reported properties varied by up to orders of magnitude. Thus, we hoped to make a contribution by growing and measuring fundamental properties of single-crystal compounds and alloys of groups IIIB, IVB, VB, and VIB TM nitrides using *tunable* magnetically-unbalanced magnetron sputtering which, together with Bill Sproul, Dieter Münz, and Ivan Petrov (all Bunshah Award winners), we developed in 1992. We also demonstrated vacancy hardening, enhanced hardness in superlattices with alternate layers chosen to have large differences in shear moduli, strong electron/phonon interactions, enhanced ductility using alloy design via electronic structure, and self-organized nanostructures. With polycrystalline TM nitrides, we developed a process for real-time control of preferred orientation using high-flux/low-energy ion irradiation and, recently, the growth of fully-dense/low-stress/high-hardness alloys, with no substrate heating, based upon a novel hybrid dc-magnetron/HiPIMS approach. Last year, we were the first to demonstrate controlled B/TM ratios in diboride layers using strong external magnetic fields during magnetron sputtering and controlling pulse lengths, at constant power and frequency, during HiPIMS.

ICMCTF 2019 Graduate Student Awards

These Awards were established by the Advanced Surface Engineering Division (ASED) of the AVS in 2006 to honor and encourage outstanding graduate students carrying out research in areas of interest to ASED, with emphasis on the fields of surface engineering, thin films, and related topics. The ASED seeks to recognize students of exceptional ability who show promise for significant future achievement.

The ASED is pleased to announce the two finalists for 2019, chosen based upon the quality of their written research summaries, resumes, and evaluation letters. The selection of the winners will take into consideration the application materials in addition to the quality and professionalism of their oral presentations/discussions and a brief interview with the Awards Committee at the 2019 ICMCTF.



Clarisse Furgeaud

Institut Prime – CNRS – ENSMA – Université de Poitiers, France
“Kinetics Dependence of Microstructure and Stress Evolutions in Polycrystalline Cu Films: Real-time Diagnostics and Atomistic Modelling”

H1-2-TuA4, Tuesday, 2:40 p.m., Pacific Salon 1



Rainer Hahn

Institute of Materials Science and Technology, TU Wien
“Fracture Toughness Enhancement in Superlattice Hard Coatings”

B4-2-TuA, 1:40 p.m., California

ASED 2020

AWARDS NOMINATIONS



Due
October 1
2019

*Call for
Nominations*

www.avs-ased.org

R.F. Bunshah Award and ICMCTF Lecture ICMCTF Graduate Student Awards

You are invited to submit nominations for the prestigious ASED Awards to be presented at ICMCTF 2020. The Awards were established to recognize outstanding research and/or technical innovation and to honor exceptional graduate students.

Protocol for the R. F. Bunshah Award and ICMCTF Lecture

Purpose

The R. F. Bunshah Award and Honorary ICMCTF lectureship, named after the founder of the ICMCTF, recognizes outstanding research or technological innovation in the areas of interest to the AVS Advanced Surface Engineering Division (ASED), with emphasis in the fields of surface engineering, thin films, and related topics.

Eligibility

The nominee shall have made pioneering contributions to the science or technology of surface engineering, thin films, or related fields of interest to ASED. The Award shall be granted without further restriction except that the current ICMCTF General and Program Chairs and current members of the ASED Executive and Awards Committees are not eligible.

Nomination Procedure

A nomination may be made by anyone qualified to evaluate, highlight, and validate the nominee's accomplishments. Any individual may submit one nominating or seconding letter for the award in any given year. Nominations remain active for three years and the nomination packages MUST include the following:

Nomination Letter: The letter nominating an individual for an award must describe the work for which the award is proposed and indicate the role the work has played in solving particular scientific or technological problems. The significance of these problems and the impact of the nominee's accomplishments in the field should be discussed. If the work was performed in collaboration with others, the contributions of the nominee should be clearly stated. A proposed citation, a one-sentence synopsis of the reason for selecting the nominee, and a list of individuals sending supporting letters, must also be included. The nominating letter should not exceed two pages in length, but should be as detailed as possible to allow the Award Committee to evaluate the nominee's contributions.

Supporting Letters: A minimum of two and a maximum of five supporting letters must be arranged by the nominator. Typically, the letters should not exceed one page. Their main purpose is to endorse the nomination and to provide additional evidence of the nominee's accomplishments. The supporting letters should be written by individuals at institutions other than that of the nominee.

Description of Research Highlights: A two-page summary of research accomplishments citing key papers and patents must be included. The purpose of the material is to document the scope of a nominee's technical career, placing in context the specific work being nominated for the award.

Biographical Materials: A Curriculum Vitae or biographical sketch of the nominee and a list of publications and patents must be submitted.

Nature of the Award

The award consists of a \$1500 cash award, an engraved statuette and an honorary lectureship at the ICMCTF conference at which the award is presented. This award is conferred annually, subject to availability of suitable candidates. The recipient shall receive complimentary meeting registration, travel expenses up to \$1500, and up to six nights lodging at the Town and Country Hotel.

Nomination Submission and Deadline: October 1, 2019

All nomination materials must be compiled by the nominator and submitted as one package. The **complete** nomination package is to be sent **electronically** to the current Chair of the ASED Awards Committee (asedawards@avs.org) such that it is received by **October 1, 2019**. Late or incomplete application packages will not be evaluated.

ASED Awards website: www.avs-ased.org
Protocol for the ICMCTF Graduate Student Awards

Purpose

The ICMCTF Graduate Student Awards are intended to honor and encourage outstanding graduate students in fields of interest to the AVS Advanced Surface Engineering Division (ASED). ASED seeks to recognize students of exceptional ability who show promise for significant future achievement in ASED-related fields.

Eligibility

The nominee must be a graduate student in science or engineering who is in good standing at a University with a recognized graduate degree program and the presenting author of an oral presentation at the annual ICMCTF conference. Nominees who receive their final research degree after the ICMCTF Abstract Submission deadline are still eligible for that year. However, previous Graduate Student Award winners are ineligible.

Nomination Procedure

The Student's Advisor must submit the following items to the current Chair of the ASED Awards Committee by the **Abstract Submission deadline, October 1, 2019** for the upcoming annual ICMCTF Conference (late or incomplete applications will not be evaluated):

- a completed application form can be downloaded from the ASED website: www.avs-ased.org
- one copy of the abstract that has been submitted separately to the ICMCTF Conference
- a two-page description of research associated with the abstract to be considered for the award, including a clear, concise description of the:
 - aim of the work and its relationship to the status of the field
 - a summary of the applicant's specific contributions and how they demonstrate exceptional ability and future promise
 - a summary of significant results of the work and how they relate to the specific research area
 - a list of any publications authored by the applicant that are relevant to this research.
- a resume which includes a list of publications with complete citations; a list of fellowships, scholarships, and/or other honors received; a list of past employment with dates; a list of technical/professional organizations, including AVS, in which you are a member; other activities or relevant information
- an Advisor's Student Evaluation Form completed by the student's advisor; please download the form from the ASED website: www.avs-ased.org
- a recommendation letter from the student's advisor(s).

Selection Process

Graduate Student Award Applications are accepted from graduate students who authored or co-authored a submitted abstract that is accepted for the current ICMCTF Conference. Applications are reviewed by the ASED Awards Committee; up to three finalists are selected. At the ICMCTF Conference, the finalists will present oral presentations which will be scheduled in an appropriate symposium on Monday, Tuesday, or Wednesday of the Conference week. The Awards Committee will meet and have discussions with the finalists. The committee will attend their presentations in order to evaluate for the Gold, Silver, and Bronze ASED Graduate Student Awards based upon: (1) the quality of their application materials and (2) the quality and professionalism of their presentation and discussion.

Selection Criteria

In the selection of finalists and award recipients, the judges look for evidence of:

- Excellence in scholarly research, including
 - thoroughness of the applicant's work
 - originality and independence of the applicant's contributions
 - depth of understanding of the research topic, the methodologies used, and the relationship of the results to the specific research area and the broader field
 - scholarship and ingenuity shown by the student in attacking the research project
- Promise for future substantial achievement in research fields of interest to ASED.

Nomination Submission and Deadline: October 1, 2019

All nomination materials must be compiled by the nominee's advisor and submitted as one package. The ***complete*** nomination package is to be sent ***electronically*** to the current Chair of the ASED Awards Committee (asedawards@avs.org) such that it is received by the **ICMCTF Abstract Submission deadline, October 1, 2019**.

ASED Awards website: www.avs-ased.org



ICMCTF 2019 Short Courses

Sunday, May 19 – Thursday, May 23, 2019

Nine Short Courses are being presented by leading experts in their respective fields:

- Sunday, May 19:** **NANOMECHANICS AND TRIBOLOGY OF THIN FILMS AND COATINGS**
Steve Bull, Newcastle University, Newcastle upon Tyne, UK, and
Adrian Leyland, University of Sheffield, UK
- Monday, May 20:** **PRACTICAL THIN FILM CHARACTERIZATION**
Jörg Patscheider, Evatec, Trübbach, Switzerland
- Monday, May 20:** **REACTIVE MAGNETRON SPUTTER DEPOSITION**
Diederik Depla, University Ghent, Belgium
- Tuesday, May 21:** **THIN FILM NUCLEATION, GROWTH, AND MICROSTRUCTURE EVOLUTION**
Joe Greene, University of Illinois, Urbana-Champaign, USA, Linköping University, Linköping, Sweden, and National Taiwan University of Science and Technology, Taipei, Taiwan
- Tuesday, May 21:** **INDUSTRIAL SURFACE ENGINEERING: FUNDAMENTALS, PRACTICE AND APPLICATIONS**
Aharon Inspektor, Carnegie Mellon University, Pittsburgh, USA, and
Satish Dixit, Plasma Technology Inc., USA
- Wednesday, May 22:** **IN-SITU AND EX-SITU ELLIPSOmetry CHARACTERIZATIONS OF THIN FILMS**
Thomas Tiwald, J.A.Woollam Co., Inc., USA and
Nikolas Podraza, University of Toledo, USA
- Wednesday, May 22:** **FUNDAMENTALS OF HiPIMS PLASMAS FOR THIN FILM DEPOSITION**
Arutjun Ehiasarian, Sheffield Hallam University, UK
- Thursday, May 23:** **PLASMAS IN PHYSICAL VAPOR DEPOSITION, INCLUDING ARCS AND HiPIMS**
André Anders, Lawrence Berkeley National Lab., USA
- Thursday, May 23:** **UNDERSTANDING AND CONTROL OF STRESSES IN PVD THIN FILMS**
Gregory Abadías, University of Poitiers, Poitiers, France

View the detailed Short Course descriptions on the web:

<https://www2.avs.org/conferences/ICMCTF/2019/shortcoursesform.htm>

Courses will run from 8:30 am–4:30 pm. Each of the nine courses cost \$500 per participant and \$130 per graduate student. Discounts are available, but do not apply to student rates. For all courses, extensive course notes will be provided.

Limited On-site Registration is available at the conference registration desk.

Please contact Heather Korff, heather@avs.org, 530-896-0477

**REMINDER: Please turn off CELL PHONES when you are attending
Technical Sessions & Short Courses.
See Photo & Recording Policy in General Info (page 8).**



AVS Membership

Get Year Round Access to Benefits

***Don't Miss Out!! Renew or Join at Booth 312
and Receive a **FREE Gift**
...AND be Entered into a Drawing to
Receive an **Amazon Gift Card*****

AVS Member Benefits:

Access to the **Publications Library**

Access to **Technical Library**
*(Presentations on Demand, Videos, Books,
Recommended Practices, and More)*

Discount on Individual
Subscription to AIP Journals



AVS

125 Maiden Lane, 15th Floor • New York, NY 10038
212-248-0200 • Fax 212-248-0245 • avsnyc@avs.org
For more details visit us online at www.avs.org

FOCUSED TOPIC SESSION



Latest Development in Advanced Mechanical Surface Characterization

Presented by Hasan Faisal, Ph.D. and Philippe Kempe

Monday, May 21, 2019

12:20–1:20 pm

Town & Country Room

Since 1922 Anton Paar (AP) has become the world leader in developing advanced testing instrumentation. Our state-of-the-art instruments support research and innovation in areas such as indentation, scratch testing, tribology and more recently, atomic force microscopy (AFM). Anton Paar instrumentation has long been recognized for extreme stability and accuracy.

As we continuously strive to provide the best instruments aligned with the needs of the research and industrial communities, we would like to share a couple of our advanced features to characterize nanoscale mechanical surface properties. The advanced features related to nanoscratch, nanoindentation and tribology testing and analysis will be introduced during this focus topic session.

Until today, AP scratch testers are well renowned in the industry as well as the academic research environment due to their well-known stability and optical analysis technique which are widely rated as an industry reference. The new “Generation 3” scratch testers provide the first automatic detection of critical loads on the market, with new algorithms for detection of slope changes on all the sensor signals (penetration depth, acoustic emission, or friction force). The patented “Panorama” mode (US 8261600,237, and EP 2065695) directly focuses on the scratch image to enable automation of scratch series measurements after the first focus.

Pin-on-disk tribology has been also used for many years under various environmental conditions (temperature, relative humidity, vacuum) but the continuous surface evolution in topography or chemical composition as a function of time is not easy to measure. A ball-on-disk high vacuum high temperature tribometer is combined at first with a digital holographic microscope (DHM) for in situ real-time measurement of the wear track. Advantages and limitations of these methods are explained.

Anton Paar presenters are also going to briefly present the recent introduction of three new laboratories, Los Angeles, Houston, and Chicago in addition to our Ashland, VA headquarters bringing new levels of local support and services to the USA coatings and materials community.

Complimentary food and beverages will be served at the Anton Paar FTS.

**Please visit the Anton Paar Booth #205
in the Exhibition Hall on Tuesday and Wednesday!**

FOCUSED TOPIC SESSION



Advanced Technologies for the In-Depth Characterization of Surfaces

Shraddha Vachhani, Ph.D. and Giovanni Ramirez, Ph.D.

Tuesday, May 21, 2019

7:00–8:00 am

Town & Country Room

Continuous advancement of technologies based on micro and nano surfaces requires uninterrupted efforts to develop innovative characterization techniques to perform measurements in a precise and realistic manner. For that reason, instrumentation has to be able to operate at these nano and micro scales. Specifically, Bruker is the leader in instrumentation that can measure surfaces in a very precise manner, and simulating environments that can correlate with real-world applications; those technologies are covering atomic, nano, micro and macro scales, with techniques like AFM, White Light Interferometry, Nanoindentation and Tribology.

The Atomic Force Microscope has evolved from a laboratory sensation to a widely used tool in materials and life science research today. Bruker's AFM technology includes both novel modes and probes that together provide new information enabling new research today. The evolution of modes from Contact to Tapping to PeakForce Tapping has enabled routine high resolution topography on various samples. In quantitative nanomechanics, we will cover our latest advances such as Contact Resonance, Fast Force Volume, and PeakForce QNM for high spatial resolution quantitative surface maps.

Bruker Nanoindentation technologies bring powerful hybrid testing techniques to enable understanding of the materials. In-situ nanomechanical and nanotribological testing performed inside the SEM or TEM provides direct observation of material deformation processes. Environmental stage designs offer a controlled micro-environment providing temperatures from -100°C to $+800^{\circ}\text{C}$, atmospheric control for incorporating specialized gases, and humidity control capabilities. Advancements in control and acquisition technologies have greatly increased the testing throughput of nanomechanical test instruments by performing up to 6 indentations per second for fast mapping of mechanical properties.

Bruker Tribometers evaluate the mechanical and tribological performance of surfaces and bulk materials, using multiple geometries and applying forces that can go from fractions of a Newton up to 2,000N. Easy setup of modules and sensors permits measuring important variables like forces, displacement, temperature, electrical contact resistant, acoustic emission and more.

Join us to learn about recent advancements and the future of morphological, mechanical and tribological characterization of nano- and micro-surfaces.

Complimentary food and beverages will be served at the Bruker FTS.

**Please visit the Bruker Booth #226
in the Exhibition Hall on Tuesday and Wednesday!**

FOCUSED TOPIC SESSION



The Art of Publishing

Presented by Samir Aouadi

Thursday, May 23, 2019

12:20–1:20 pm

Golden West Room

Good research deserves to be published, to be widely read, and to be recognized by your fellow researchers and community. The current research (and funding) climate makes it even absolutely necessary that you are successful in being able to be published: “Publish or Perish”. This then raises the question, how can you achieve that goal?

“Success” essentially depends on three components: 1) the ability to determine the best possible publication strategy for your research findings, 2) the best possible way to write your article, and 3) the most effective interaction with editors. Key to success in this context is your ability to put yourself in the position of **readers, reviewers and editors**.

Key considerations in journal selection are a realistic assessment of the quality of the research and the audience you intend to reach. The art of manuscript writing is not just applying one “golden tip”. It is essentially “telling your story” to your readers in an engaging way, and avoiding common mistakes and deficiencies including poor language. Avoidable mistakes can lead to unnecessary rejection of your manuscript. Finally, it is your open, non-defensive attitude towards the editors and the reviewer comments, that will not only increase the likelihood of getting your manuscript accepted for publication, it is also likely that your published paper has improved thanks to their comments.

By consistently applying these principles you are likely to become a more successful author.

Prof Aouadi, Editor of the Journal *Surface and Coatings Technology*, will give a presentation about “The Art of Publishing” from an Editor’s perspective. He will discuss the publication process, will outline the organization of a scientific journal, and will provide the important ingredients to get published.

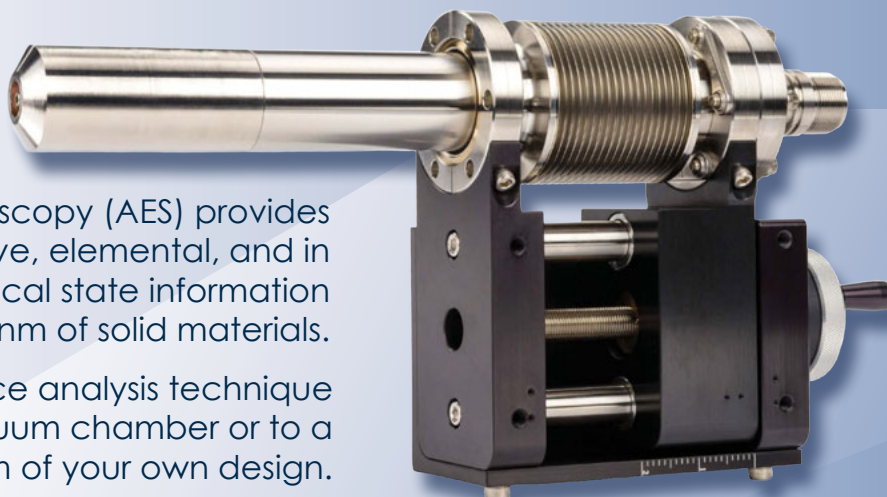
Elsevier is the world’s leading publisher of science and health information and publishes a number of journals that are highly relevant for ICMCTF attendees, such as *Thin Solid Films*, *Surface and Coatings Technology*, *Vacuum* and *Applied Surface Science*.

This FTS is aimed at new authors, but also at more experienced authors who want to hear how to bypass common publishing hurdles or have a discussion with the publisher and Editors who may be present during the session.

**Don’t forget to visit the Elsevier Literature Table at
Booth #108 in the Exhibition Hall.**

ADD ELEMENTAL ANALYSIS
TO ANY VACUUM CHAMBER

the **microCMA** Compact Auger Analyzer



Auger Electron Spectroscopy (AES) provides valuable quantitative, elemental, and in some cases chemical state information about the top 5 nm of solid materials.

Add this powerful surface analysis technique to your existing vacuum chamber or to a system of your own design.

It is ideal for in-situ analysis of thin films that are deposited onto metals and semiconductors.

The **microCMA** comprises a 2.75" CF flange-mount Cylindrical Mirror Analyzer with a 3 kV coaxial electron gun, Z-axis translator, USB analyzer controller, 9103 USB Picoammeter, and PC acquisition / data massage software.

INCLUDED WITH THE PURCHASE OF A **microCMA**: the **9103 USB Picoammeter**

With a built-in 90 V bias, the **9103** integrates with your **microCMA** to provide accurate target current measurement.



www.rbdinstruments.com

2437 NE Twin Knolls Drive • Suite 2 • Bend, OR 97701
541 • 330 • 0723

ICMCTF 2019 SPONSORS

PLATINUM & GOLD SPONSORS

oerlikon
balzers



Advanced Coating Systems
SWISS  QUALITY



ICMCTF sincerely thanks the 2019 Sponsors for their support of the ICMCTF Conference and Exhibit Hall Events.

ICMCTF 2019 SPONSORS

SILVER, BRONZE AND RAFFLE SPONSORS



ELSEVIER



Anton Paar

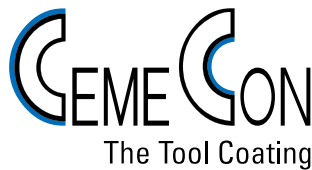


HAUZER

INDUSTRIAL PLASMA SOLUTIONS

BERNEX

SWISS CVD SOLUTIONS



The Tool Coating



PLASMATERIALS



ICMCTF sincerely thanks the 2019 Sponsors for their support of the ICMCTF Conference and Exhibit Hall Events.

Town and Country

SAN DIEGO

Legend

- Guest Rooms
- Restaurants
- Meeting Rooms
- Walking Path
- Accessible Guest
- Accessible Spaces
- Accessible Restrooms
- Accessible Lift
- Elevator
- Ice
- Restrooms
- Soft Drinks



Program Key

- A** Coatings for Use at High Temperatures
- B** Hard Coatings and Vapor Deposition Technologies
- C** Fundamentals and Technology of Multifunctional Materials and Devices
- D** Coatings for Biomedical and Healthcare Applications
- E** Tribology and Mechanical Behavior of Coatings and Engineered Surfaces
- EX** Exhibition Keynote Lecture
- F** New Horizons in Coatings and Thin Films
- G** Surface Engineering - Applied Research and Industrial Applications
- H** Advanced Characterization Techniques for Coatings, Thin Films, and Small Volumes
- HL** Awards Convocation and Honorary Lecture
- PL** Plenary Lecture
- SIT** Special Interest Talks
- TS** Topical Symposia
 - TS1** High Entropy and Other Multi-principal-element Materials
 - TS2** Icephobic Surface Engineering
 - TS3** Surface Engineering for Lightweight Materials
 - TS4** Thin Film Materials for Flexible Electronics

PROGRAM NUMBERS: They are listed with the Symposium letter first, the session number second, the Day of the Week, Morning (M) or Afternoon (A) and the presentation slot (e.g., **B1-1-MoM6**).

HELPFUL HINTS:

- Verify all technical session start times (morning and afternoon).
- Please note that on Monday, the technical sessions begin at 10:00 am following the 8:00 am Plenary Session. Morning sessions begin at 8:00 am but on some days the starting times may vary. Afternoon sessions start times vary between 1:20 – 2:00 p.m.
- Break times have been inserted into Tuesday and Wednesday programming and you are encouraged to use your extended lunches and breaks to visit the Exhibit Hall.
- Invited speakers are allotted 40 minutes and contributed speakers are allotted 20 minutes. Please verify your presentation time, as printed in the program book.
- Oral Presenters: All technical session rooms are equipped with computers, LCD projectors, screens, laser pointers and microphones. Please test your presentation materials to be certain that they are compatible with the equipment being provided in the technical session rooms. There will be a Presenter Preview Room for you to test your presentation on the conference equipment the day prior to your presentation.
- Poster Presenters: Please post a small photo of the presenter on the poster sign affixed to your assigned board. Boards will be available for posting materials from 11:00 am until 4:00 pm on Thursday, May 23. Prior to hanging your poster, poster presenters must check in at the Registration desk to show photo identification, as well as your registration badge. These forms of identification must match the name of the poster presenter listed in the ICMCTF program. The sign listing the paper's number, title, and presenting author will aid each presenter in locating your board. The board space provided is approximately four feet by four feet and all posters **MUST** be posted by 4:00 pm. Any posters not displayed by 4:00 pm will be removed from the Program and be listed as a No Show. All presenters are required to be at their poster during the entire session (5:00 - 7:00 pm), in order to promote discussion and for the author to answer attendee questions. Be forewarned, all poster materials will be discarded if not removed from the boards by 9:00 pm Thursday evening.

Reminder: Please turn off CELL PHONES when you are attending the Technical Sessions

ICMCTF 2019 Program at a Glance

| Room /Time | Atlas Foyer | Town & Country | Grand Hall | California | Golden West | Pacific Salon 1 | Pacific Salon 2 | Pacific Salon 3 | Pacific Salon 6-7 | San Diego |
|--------------------------------|---|--|--|--|---|--|---|---|--|---|
| Sun: am & pm | SC Reg: 7:30 - 8:30 am Conf. Registration: 4:30-6:30pm | | | | | | | | | |
| Mon: 8:00 am | SC Reg: 7:30-8:30 am Conf. Registration: 7:00 am – 6:00 pm | PLENARY: John Rogers 8:00–9:45 am | | | | | | | | |
| Mon am: 10:00 am Start | Registration Continues | FTS: Anton Paar 12:20-1:20 pm | | B3-1-MoM: Deposition Tech. & Applic. for Diamond-like Coatings I | B1-1-MoM: PVD Coatings and Technologies I | H2-1-MoM: Fatigue and Wear | D1-1-MoM: Surface Coating and Modification for Use in Biological Environments I | TS4-1-MoM: Thin Film Materials for Flexible Electronics | | |
| Mon pm: 1:40 pm Start | Welcome Mixer 5:45-7:00 pm Lion Fountain Courtyard | | Exhibit Staff Setup 3:00 pm | B3-2-MoA: Deposition Tech. & Applic. for Diamond-like Coatings II | B1-2-MoA: PVD Coatings and Technologies II | H2-2-MoA: Nanoscale Plasticity | D1-2-MoA: Surface Coating and Modification for Use in Biological Environments II | TS3+4-2-MoA: Surface Eng. for Lightweight Materials & TF Matls for Flexible Electronics | | |
| Tues am: 8:00 am Start | SC Reg: 7:30-8:30 am Conf. Registration: 7:30 am – 3:30 pm | FTS: Bruker 7:00-8:00 am Exhibition Keynote Farwah Nahif 11:00 am – 12:00 pm | Exhibit Staff Set up 8:00-10:00 am | B4-1-TuM: Properties and Characterization of Hard Coatings and Surfaces I | B1-3-TuM: PVD Coatings and Technologies III | H1-1-TuM: Spatially-resolved and In-Situ Charact. of TF & Engineered Surfaces I | A1-1-TuM: Coatings to Resist High-temperature Oxidation, Corrosion, and Fouling I | D3-TuM: Surfaces and Coatings to Promote Tailored Biological Responses | F1-TuM: Nanomaterials and Nanofabrication | E2-1-TuM: Mechanical Properties and Adhesion I |
| Tues pm: 1:40 pm Start | Registration Continues | SIT Gregory Abadías 7:00-8:00 pm | Exhibits 12:00-7:00 pm OPENS TODAY! Exhibits Reception 5:30-7:00 pm | B4-2-TuA: Properties and Characterization of Hard Coatings and Surfaces II | B7-TuA: Plasma Diagnostics and Growth Processes | H1-2-TuA: Spatially-resolved and In-Situ Charact. of TF & Engineered Surfaces II | A1-2-TuA: Coatings to Resist High-temperature Oxidation, Corrosion, and Fouling II | D2-TuA: Bio-corrosion and Bio-tribology | F3-TuA: 2D Materials: Synthesis, Characterization and Applications | E2-2-TuA: Mechanical Properties and Adhesion II |
| Wed am: 8:00 am Start | SC Reg: 7:30-8:30 am Conf. Registration: 7:30 am – 3:30 pm | SIT Ivan Petrov 1:00-2:00 pm | Exhibits 10:00 am – 2:00 pm CLOSES TODAY | B4-3-WeM: Properties and Characterization of Hard Coatings and Surfaces III | C3+C1-WeM: TF for Energy-rel App. I/Opt Metrology in Des., Opt, & Prod. of Multifunc Mtls | H3-1-WeM: Variable Temperature Nanomechanics | A1-3-WeM: Coatings to Resist High-temperature Oxidation, Corrosion, and Fouling III | TS1-1-WeM: High Entropy and Other Multi-principal-element Materials I | F4-1-WeM: Functional Oxide and Oxynitride Coatings I | E3-WeM: Tribology of Coatings for Automotive and Aerospace Applications |
| Wed pm: 2:00 pm Start | Registration Continues | Awards and Honorary Lecture: Joe Greene 5:45-7:00 pm | Exhibition Teardown: 2:00-6:00 pm | B4-4-WeA: Properties and Characterization of Hard Coatings and Surfaces IV | C2-WeA: Novel Oxide Films for Active Devices | H3-2-WeA: Degradation under Extreme Conditions | A3-WeA: Materials and Coatings for Solar Power Concentration Plants | TS1-2-WeA: High Entropy and Other Multi-principal-element Materials II | F4-2-WeA: Functional Oxide and Oxynitride Coatings II | E1-4-WeA: Friction, Wear, Lubrication Effects, and Modeling I |
| Thurs am: 8:00 am Start | SC Reg: 7:30-8:30 am Conf. Registration: 7:30 am – 3:30 pm | | Poster Set-up 11:00 am – 4:00 pm: Only Poster authors allowed to post materials | B6-ThM: Coating Design and Architectures ICMCTF 2020 Info Session 12:20-1:20 pm | TS2-ThM: Icephobic Surface Engineering FTS: Elsevier 12:20-1:20 pm | G1+G3-ThM: Adv. in Ind. PVD, CVD, PECVD & Equip/Inn. SE for Adv Cut & Form Tool Applications | A2-1-ThM: Thermal and Environmental Barrier Coatings I | C3+C2+C1-ThM: TF for Energy-rel Apps II/ Novel Oxide Films for Active Dev/ Opt Met in Design, Opt,& Prod of Multifunct. Matls | F2-1-ThM: HiPIMS, Pulsed Plasmas and Energetic Deposition I | E1-1-ThM: Friction, Wear, Lubrication Effects, and Modeling II |
| Thurs pm: 1:20 pm Start | Registration Continues | | Poster Session 5:00 – 7:00 pm Poster Reception 6:00-7:00 pm | B5-1-ThA: Hard and Multifunctional Nanostructured Coatings I | B2-1-ThA: CVD Coatings and Technologies I | G4+G5+G6-ThA: Pre/ Post Treat & Dup Tech/ Hyb Sys, Proc & Coat App-Driven Collaborations | A2-2-ThA: Thermal and Environmental Barrier Coatings II | C4-ThA: Fundamentals of Metallurgy in Thin Films and Coatings | F2-2-ThA: HiPIMS, Pulsed Plasmas and Energetic Deposition II | E1-2-ThA: Friction, Wear, Lubrication Effects, and Modeling III |
| Fri am: 8:00 am Start | Conference Registration: 7:30–10:30 am | See You Next Year Party! 12:00-1:00 pm Lion Fountain Courtyard | | B5-2-FrM: Hard and Multifunctional Nanostructured Coatings II | B2-2-FrM: CVD Coatings and Technologies II | G2-FrM: Comp. Coatings for Auto, Aerospace, Med., & Mfg Applications | | | | E1-3-FrM: Friction, Wear, Lubrication Effects, and Modeling IV |

Plenary Lecture

Town & Country Room - Session PL-MoPL

8:00 – 9:45 am

Moderators:

Christopher Muratore, University of Dayton, USA,

Michael Stüber, Karlsruhe Institute of Technology (KIT), Institute for Applied Materials (IAM), Germany

ICMCTF 2019 Plenary Session Lecture “Soft Electronics for the Human Body” Prof. John Rogers Northwestern University, Evanston, IL, USA

Biological systems are mechanically soft, with complex, time-dependent 3D curvilinear shapes; modern electronic and microfluidic technologies are rigid, with simple, static 2D layouts. Eliminating this profound mismatch in physical properties will create vast opportunities in man-made systems that can intimately integrate with the human body, for diagnostic, therapeutic or surgical function with important, unique capabilities in biomedical research and clinical healthcare. Over the last decade, a convergence of new concepts in thin film materials science, mechanical engineering, electrical engineering and advanced manufacturing has led to the emergence of diverse, novel classes of ‘biocompatible’ electronic and microfluidic systems with ultrathin, skin-like physical properties. This talk describes the key ideas and enabling materials, and it presents some of the most recent device examples, including wireless electronic ‘tattoos’, with applications in continuous monitoring of vital signs in neonatal intensive care; and microfluidic/electronic platforms that can capture, store and perform biomarker analysis on sweat, with applications in sports and fitness.

Prof. John Rogers has received an impossibly long list of awards including a MacArthur Foundation fellowship, reserved for inventive folks with the highest level of outstanding talent. He is also behind over 80 patents and patent applications, more than 50 of which are licensed or in active use by large companies and startups that he has co-founded.

In September of 2016, Professor John Rogers joined Northwestern University as the Louis Simpson and Kimberly Querrey Professor of Materials Science and Engineering, Biomedical Engineering, Mechanical Engineering, Electrical Engineering and Computer Science, Chemistry and Neurological Surgery, where he is also the founding Director of the newly endowed Center on Bio-Integrated Electronics.

At Northwestern, the Rogers Research Group, whose current research focuses on “soft materials for conformal electronics, nanophotonic structures, microfluidic devices, and microelectromechanical systems, all lately with an emphasis on bio-inspired and bio-integrated technologies.”

Rogers’ research includes fundamental and applied aspects of nano and molecular scale fabrication as well as materials and patterning techniques for unusual electronic and photonic devices, with an emphasis on bio-integrated and bio-inspired systems. He has published more than 550 papers and is an inventor on over 100 patents and patent applications, more than 70 of which are licensed or in active use by large companies and startups that he has co-founded.

John Rogers holds his BA and BS degrees in Chemistry and in Physics from the University of Texas, Austin. He obtained his Ph.D. in Physical Chemistry in 1995 from MIT and was a Junior Fellow in the Harvard University Society of Fellows from 1995–97.

Monday Morning, May 20, 2019

| | | |
|---------|---|---|
| | <p>Hard Coatings and Vapor Deposition Technologies Room Golden West - Session B1-1-MoM PVD Coatings and Technologies I Moderators: Frank Kaulfuss, Fraunhofer Institute for Material and Beam Technology (IWS), Germany, Jyh-Ming Ting, National Cheng Kung University, Taiwan, Qi Yang, National Research Council of Canada, Canada</p> | <p>Hard Coatings and Vapor Deposition Technologies Room California - Session B3-1-MoM Deposition Technologies and Applications for Diamond-like Coatings I Moderators: Laurent Espitalier, Wallwork Cambridge Ltd, UK, Konrad Fadenberger, Robert Bosch GmbH, Germany</p> |
| 10:00am | | |
| 10:20am | | <p>B3-1-MoM2 On the Deposition and Properties of Carbon-based Multilayer Systems Prepared by PLD, S. Weißmantel, University of Applied Sciences Mittweida, Germany; M. Hess, Fritz Stepper GmbH & Co. KG, Deutschland, Germany; R. Bertram, D. Haldan, T. Warnk, J. Maus, S. Rupp, University of Applied Sciences Mittweida, Germany</p> |
| 10:40am | <p>B1-1-MoM3 Structural, Optical and Wettability Properties of Thermally Evaporated CaF₂, MgF₂ and CaF₂/MgF₂ Films, R.K. Jain, J. Kaur, A. Khanna, Guru Nanak Dev University Amritsar India, India</p> | <p>B3-1-MoM3 Improved Adhesion of a-C and a-C:H Films with a CrC Interlayer on 16MnCr5 by HIPIMS-Pretreatment, W. Tillmann, N.F. Lopes Dias, D. Stangier, TU Dortmund University, Germany; W. Maus-Friedrichs, R. Gustus, Technical University Clausthal, Germany</p> |
| 11:00am | <p>B1-1-MoM4 Metal / ScAlN / Interdigital Transducer (IDT)/ LiNbO₃ Multilayer Structure for High K² Surface Acoustic Wave Device, Y.H. Huang, National Cheng Kung University, Taiwan; S. Wu, Tung-Fang Design University, Taiwan; J.L. Huang, National Cheng Kung University, Taiwan</p> | <p>B3-1-MoM4 Properties Of Diamond-Like Carbon Films With Incorporated CVD-Diamond Nanoparticles, R. Falcão, Institute of Science and Technology, Federal University of São Paulo (UNIFESP), Brasil; C. Wachesk, Federal University of São Paulo, Brazil, Brasil; T. Taiariol, National Institute for Space Research, Brazil; G. Vasconcelos, Instituto de Estudos Avançados, Brazil; E.J. Corat, V.J. Trava-Airoldi, National Institute for Space Research, Brazil</p> |
| 11:20am | <p>B1-1-MoM5 Sputter Deposited TiN_xO_y for Color Coatings and Solar Absorbers, L.Y. Chiu, J.-M. Ting, National Cheng Kung University, Taiwan</p> | <p>B3-1-MoM5 Influence of the Argon as an Ignitor and an Agent on DLC Properties Growth at Pressure as Low as 3 x 10⁻⁴ mbar by Modified Pulsed-DC PECVD Method, V.J. Trava-Airoldi, K. Nass, E.J. Corat, National Institute for Space Research, Brazil; N. Fukumasu, Sao Paulo University, Brazil; M. Ramirez, University of Vale do Paraiba, Brazil; G. Capote, National University of Bogota, Colombia</p> |
| 11:40am | <p>INVITED: B1-1-MoM6 High Power Impulse Magnetron Sputtering using Deep Oscillatory Micro Pulses for Surface Engineering, J.L. Lin, Southwest Research Institute, USA</p> | |
| 12:00pm | Invited talk continues. | <p style="text-align: center;">ANTON PAAR FOCUSED TOPIC SESSION “Latest Developments in Advanced Mechanical Surface Characterization” Hasan Faisal and Philippe Kempe MONDAY, 12:20 – 1:20 pm Town & Country Room REFRESHMENTS WILL BE SERVED</p> |

Monday Morning, May 20, 2019

| Coatings for Biomedical and Healthcare Applications Room Pacific Salon 2 - Session D1-1-MoM Surface Coating and Modification for Use in Biological Environments I Moderator: Mathew T. Mathew, University of Illinois College of Medicine, USA | | Advanced Characterization Techniques for Coatings, Thin Films, and Small Volumes Room Pacific Salon 1 - Session H2-1-MoM Fatigue and Wear Moderators: Olivier Pierron, Georgia Institute of Technology, USA, Timothy Rupert, University of California, Irvine, USA | |
|---|---|---|---|
| 10:00am | | | INVITED: H2-1-MoM1 Acoustic Emission Measurements to Quantifying Damage Accumulation and Crack Initiation in Nickel Single Crystals during High Frequency <i>In Situ</i> Cyclic Loading Experiments, <i>S. Lavenstein, J.A. El-Awady</i> , Johns Hopkins University, USA |
| 10:20am | D1-1-MoM2 Very Thin Gold Films Deposited on Collagen Fabric for Skin Cell Recover, <i>S.-Y. Huang</i> , Taichung Veterans General Hospital, Feng Chia University, Taiwan; <i>Y.-C. Chang</i> , Feng Chia University, Taiwan; <i>P.-Y. Hsieh</i> , Institute of Plasma, Feng Chia University, Taiwan; <i>C.M. Chou</i> , Taichung Veterans General Hospital, National Yang-Ming University, Taiwan; <i>C.J. Chung</i> , Central Taiwan University of Science and Technology, Taiwan; <i>J.L. He</i> , Feng Chia University, Taiwan | | Invited talk continues. |
| 10:40am | D1-1-MoM3 Effect of Calf Serum on Tribological Behavior of DLC Coating in Ti-6Al-4V / Ti-6Al-4V Contact for Application to STEM / NECK Contact of Modular Hip Implant, <i>H.H. Ding, V. Fridrici, G. Bouvard</i> , Ecole Centrale de Lyon, LTDS - Université de Lyon, France; <i>J. Géringier</i> , Ecole des Mines de St-Etienne - Université de Lyon, France; <i>P. Kapsa</i> , Ecole Centrale de Lyon, LTDS - Université de Lyon, France | | H2-1-MoM3 A Data-driven Approach to Describe Fatigue Damage Evolution and Crack Initiation in a BCC Steel Microstructure, <i>A.R.D. Durmaz, T.S. Straub, C. Eberl</i> , Fraunhofer IWM, Germany |
| 11:00am | INVITED: D1-1-MoM4 Accelerated Tests for Lifetime Prediction of Interlayers and Interfaces of Coated Implants in Body Fluid, <i>R. Hauert, E. Ilic, A. Pardo-Perez, K. Thorwarth, P. Schmutz</i> , Empa - Swiss Federal Laboratories for Materials Science and Technology, Switzerland; <i>S. Mischler</i> , Institut des Matériaux IMX, EPFL, Lausanne, Switzerland | | H2-1-MoM4 Low and High Cycle Fatigue Testing of Ni Microbeams, <i>A. Barrios</i> , Georgia Institute of Technology, USA; <i>E. Kakandar</i> , Cranfield University, UK; <i>X. Maeder</i> , Empa - Swiss Federal Laboratories for Materials Science and Technology, Switzerland; <i>G. Castelluccio</i> , Cranfield University, UK; <i>O.N. Pierron</i> , Georgia Institute of Technology, USA |
| 11:20am | Invited talk continues. | | H2-1-MoM5 Nanocrystalline Alloys with Disordered Complexions Probed by In Situ Mechanical Testing, <i>T. Rupert, J. Wardini, J.D. Schuler</i> , University of California, Irvine, USA |
| 11:40am | D1-1-MoM6 Thin Film Metallic Glass Coating as an Effective Antiadhesion Coating for Platelet and Cancer Cells, <i>J.P. Chu</i> , National Taiwan University of Science and Technology (NTUST), Taiwan; <i>C.L. Li, Y.L. Chen, S. Chyntara</i> , National Taiwan University of Science and Technology, Taiwan; <i>M.J. Chen</i> , Mackay Medical College, Taiwan; <i>S.H. Chang</i> , Mackay Memorial Hospital Tamsui Campus, Taiwan | | H2-1-MoM6 Structural Evolution and Wear-rate Transitions in Nanocrystalline Alloys, <i>O. Donaldson, J. Panzarino, T. Rupert</i> , University of California, Irvine, USA |
| 12:00pm | D1-1-MoM7 Improvement of Surface Properties of Nitinol Alloy through Deposition of Graphene by Electrophoretic Deposition Technique for Biomedical Applications, <i>M. Mallick, N. Arunachalam</i> , Indian Institute of Technology Madras, India | | H2-1-MoM7 Effects of Thermal Cycling on Nano-mechanical Properties of Thermal Barrier Coatings, <i>M. Sebastiani</i> , Roma TRE University, Italy |

Monday Morning, May 20, 2019

| | | |
|---|--|--|
| <p>Topical Symposia Room Pacific Salon 3 - Session TS4-1-MoM Thin Film Materials for Flexible Electronics Moderators: Oleksandr Glushko, Erich Schmid Institute of Materials Science, Austria, Nicholas Glavin, Air Force Research Laboratory, Materials and Manufacturing Directorate, USA</p> | | |
| 10:00am | <p>INVITED: TS4-1-MoM1 2D Materials Based Epidermal and Implantable Conformable Bioelectronics, N. Lu, University of Texas at Austin, USA</p> | |
| 10:20am | Invited talk continues. | |
| 10:40am | <p>TS4-1-MoM3 Performance Deterioration Characteristics of Silver-Nanoparticle-Printed Flexible Electric Wirings under Severe Bending Deformation, S. Kamiya, H. Izumi, Nagoya Institute of Technology, Japan; T. Sekine, Yamagata University, Japan; Y. Haga, H. Sugiyama, Nagoya Institute of Technology, Japan; N. Shishido, Green Electronics Research Institute, Kitakyushu, Japan; M. Koganemaru, Kagoshima University, Japan</p> | |
| 11:00am | <p>TS4-1-MoM4 Characterizing the Mechanical Reliability of Flexible and Stretchable Conductive Inks on Polymeric Substrates, G. Cahn, Georgia Institute of Technology, USA; M. Wolfe, DuPont Photovoltaic and Advanced Materials, USA; J. Meth, DuPont Electronics and Imaging, USA; S. Graham, O.N. Pierron, Georgia Institute of Technology, USA</p> | |
| 11:20am | <p>INVITED: TS4-1-MoM5 Printed Hybrid Materials for Flexible Electronic and Optoelectronic Devices, E. List-Kratochvil, F. Hermerschmidt, Humboldt-Universität zu Berlin, Germany</p> | |
| 11:40am | Invited talk continues. | |
| 12:00pm | | <p>ANTON PAAR FOCUSED TOPIC SESSION “Latest Developments in Advanced Mechanical Surface Characterization” Hasan Faisal and Philippe Kempe MONDAY, 12:20 – 1:20 pm Town & Country Room REFRESHMENTS WILL BE SERVED</p> |

Monday Afternoon, May 20, 2019

| Hard Coatings and Vapor Deposition Technologies Room Golden West - Session B1-2-MoA PVD Coatings and Technologies II Moderators: Frank Kaufuss, Fraunhofer Institute for Material and Beam Technology (IWS), Germany, Jyh-Ming Ting, National Cheng Kung University, Taiwan, Qi Yang, National Research Council of Canada, Canada | | Hard Coatings and Vapor Deposition Technologies Room California - Session B3-2-MoA Deposition Technologies and Applications for Diamond-like Coatings II Moderators: Laurent Espitalier, Wallwork Cambridge Ltd, UK, Konrad Fadenberger, Robert Bosch GmbH, Germany | |
|--|--|--|--|
| 1:40pm | B1-2-MoA1 Harlan™: High Rate-High Density Pulsed Magnetron Sputtering Source for Depositing Metal & Ceramic Coatings for Industrial Applications., <i>B. Abraham, R. Chistyakov</i> , Ionex Corp, USA | B3-2-MoA1 Transfer of DLC Coating Processes between Different Coating Machines Assisted by Plasma Simulation, <i>M. Günther, O. Schmidt, W. Dobrygin, G. Schütze</i> , Robert Bosch GmbH, Germany | |
| 2:00pm | B1-2-MoA2 Arc Sources for Low Defect Coatings and High Target Utilization, <i>V. Bellido-Gonzalez, D. Monaghan, B. Daniel, R. Brown, J. Price, A. Azzopardi</i> , Gencoa Ltd, UK | B3-2-MoA2 Stress-Free ta-C Industrially Deposited by PLD for High Performance Stamping Applications: Results and Challenges of 1st Production Year, <i>M. Hess, Fritz Stepper GmbH & Co. KG, Deutschland, Germany; S. Weißmantel, R. Bertram</i> , Hochschule Mittweida University of Applied Sciences, Germany | |
| 2:20pm | B1-2-MoA3 Cutting Tools in the Era of Industrial Internet of Things and Additive Manufacturing, <i>A. Inspektor, A.D. Rollett, P.A. Salvador</i> , Carnegie Mellon University, USA | INVITED: B3-2-MoA3 Hollow Cathode Discharges for Rapid DLC, <i>T. Casserly, S. Gennaro, F. Papa, A. Tudhope</i> , Duralar Technologies, USA | |
| 2:40pm | B1-2-MoA4 Overstoichiometric Transition Metal Nitride Films, <i>Z. Čiperová, J. Musil, Š. Kos, M. Jaroš</i> , European Centre of Excellence, University of West Bohemia, Czech Republic | Invited talk continues. | |
| 3:00pm | B1-2-MoA5 Introducing of New Hybrid LACS® Technology (Lateral ARC and Central Sputtering by Rotating Cathodes), <i>R. Zemlicka, M. Jilek (Sr.), M. Jilek (Jr.), A. Lümkmann, T. Cselle, D. Bloesch, V. Krsek</i> , Platit AG, Switzerland | B3-2-MoA5 Hard Cr-doped DLC Coatings Deposited by Low-frequency HiPIMS with Enhanced Tribomechanical Behavior at High Temperature, <i>J.A. Santiago Varela</i> , PVT Plasma und Vakuum Technik GmbH, Germany; <i>I. Fernandez</i> , Nano4Energy SL, Spain; <i>A. Wennberg</i> , Nano4Energy, Spain; <i>M.A. Monclus, J.M. Molina Aldareguia</i> , IMDEA Materials; <i>V. Bellido-Gonzalez</i> , Gencoa Ltd, UK; <i>T.C. Rojas, J.C. Sanchez Lopez</i> , ICMSe CSIC, Spain; <i>R. Gonzalez Arrabal</i> , Universidad Politécnica de Madrid, Spain; <i>N. Dams, H. Gabriel</i> , PVT Plasma und Vakuum Technik GmbH, Germany | |
| 3:20pm | B1-2-MoA6 Edge-related Effects During Arc-PVD Deposition Processes, <i>T. Krülle, F. Kaufuss, O. Zimmer, A. Leson, C. Leyens</i> , Fraunhofer Institute for Material and Beam Technology (IWS), Germany | B3-2-MoA6 Characterization of Diamond-like Carbon Coated Powders, <i>P.J. Heaney, A. Zeng, M. Efremov</i> , NCD Technologies, USA | |
| 3:40pm | B1-2-MoA7 Reactive Sputtering for Highly Oriented HfN Film Growth on Si(100) Substrate, <i>Y.S. Fang, K.A. Chiu, H. Do, L. Chang</i> , National Chiao Tung University, Taiwan | B3-2-MoA7 Effect of Pulse Shape and Plasma Composition (Ar + Ne) on the Properties of Hard DLC Films Deposited by HiPIMS: Correlation with Substrate Ion Fluxes, <i>J.C. Oliveira, F. Ferreira, R. Serra</i> , University of Coimbra, Portugal; <i>T. Kubart</i> , Uppsala University, Angstrom Laboratory, Sweden; <i>C. Vitelaru</i> , National Institute for Optoelectronics, Romania; <i>A. Cavaleiro</i> , University of Coimbra, Portugal | |
| 4:00pm | INVITED: B1-2-MoA8 Study of Orthorhombic ZnSnN ₂ Fabricated using Zn-Sn ₃ N ₄ Composition Spreads through Combinatorial Reactive Sputtering, <i>K.-S. Chang</i> , National Cheng Kung University, Taiwan | B3-2-MoA8 The Comparison of Deposition Processes, Composition and Properties of Hydrogenated W-C:H Coatings Prepared by Different Sputtering Techniques, <i>F. Lofaj, M. Kabatova, L. Kvetkova</i> , Institute of Materials Research of SAS, Slovakia; <i>J. Dobrovodsky</i> , ATRI, Slovakia | |
| 4:20pm | Invited talk continues. | B3-2-MoA9 The Mechanism of Graphite Nucleation in Amorphous Carbon Films Deposited with the Condition of Energetic Bombardment and High Temperature, <i>D. Zhang, P.Y. Yi, L.F. Peng, X.M. Lai</i> , Shanghai Jiaotong University, China | |
| 4:40pm | B1-2-MoA10 Angular Resolved Mass-energy Analyses of Species Emitted from a d.c. Magnetron Sputtered NiW-target, <i>M. Rausch</i> , Montanuniversität Leoben, Austria; <i>S. Mráz, J.M. Schneider</i> , RWTH Aachen University, Germany; <i>J. Winkler</i> , Plansee SE, Austria; <i>C. Mitterer</i> , Montanuniversität Leoben, Austria | | |
| 5:00pm | B1-2-MoA11 Effect Produced by Architecture of Nanolayer Composite Coatings Deposited with Filtered Cathodic Vacuum Arc Deposition (FCVAD) Technology on their Mechanical and Performance Properties, <i>A. Vereschaka, S. Grigoriev</i> , Mstu Stankin, Russian Federation; <i>N. Sitnikov</i> , National Research Nuclear University MEPhI, Russian Federation; <i>N. Andreev</i> , National University of Science and Technology "MISIS", Russian Federation | | |
| 5:20pm | B1-2-MoA12 Effects of Nitrogen Flow Rate and Substrate Bias on Structure and Properties of Molybdenum Nitride Thin Film, <i>C.C. Chou, J.-H. Huang</i> , National Tsing Hua University, Taiwan | WELCOME MIXER 5:45 – 7:00 pm Lion Fountain Courtyard | |

Monday Afternoon, May 20, 2019

| Coatings for Biomedical and Healthcare Applications Room Pacific Salon 2 - Session D1-2-MoA Surface Coating and Modification for Use in Biological Environments II Moderator: Mathew T. Mathew , University of Illinois College of Medicine, USA | | Advanced Characterization Techniques for Coatings, Thin Films, and Small Volumes Room Pacific Salon 1 - Session H2-2-MoA Nanoscale Plasticity Moderators: Timothy Rupert , University of California, Irvine, USA, Olivier Pierron , Georgia Institute of Technology, USA | |
|---|---|--|--|
| 1:40pm | INVITED: D1-2-MoA1 Recent Development of Biocompatible Thin Film Metallic Glass Materials, J.-W. Lee , Ming Chi University of Technology, Taiwan; B.-S. Lou , Chang Gung University, Taiwan; Y.-C. Yang , National Taipei University of Technology, Taiwan; C.-P. Lin , National Taiwan University, Taiwan | H2-2-MoA1 | Assessing the Mechanical Properties of Thin Organic Semiconductor Coatings, S.J. Bull , Newcastle University, UK |
| 2:00pm | Invited talk continues. | H2-2-MoA2 | <i>In Situ</i> TEM Activation Volume Measurements, S. Gupta , S. Stangebye , J. Kacher , O.N. Pierron , Georgia Institute of Technology, USA |
| 2:20pm | D1-2-MoA3 Synthesis and Characterization of Reactively Sputtered Platinum Group Metal Oxides for Stimulating and Recording Applications, G. Taylor , A. Marti , R. Paladines , N. Page , Rowan University, USA; A. Fones , S. Tint , Johnson Matthey Inc., USA; H. Hamilton , Johnson Matthey, Inc., USA; S. Amini , Johnson Matthey Inc., USA; J. Hettinger , Rowan University, USA | H2-2-MoA3 | In-situ Microscale Mechanical Testing of Metal/Ceramic Interfacial Regions, X. Zhang , Y. Mu , S. Shao , W.J. Meng , Louisiana State University, USA |
| 2:40pm | D1-2-MoA4 Antibacterial and Biocompatible Properties of Ga-doped TaON Thin Films, J.H. Hsieh , Q.W. Liu , Ming Chi University of Technology, Taiwan; C. Li , National Yang Ming University, Taiwan | H2-2-MoA4 | Nano-wedging: A Novel Test Method to Combine Nanoscale Strain Mapping with Multiaxial Stress States, T.E.J. Edwards , Empa - Swiss Federal Laboratories for Materials Science and Technology, Switzerland; F. Di Gioacchino , J.T. Pürstl , University of Cambridge, UK; X. Maeder , Empa - Swiss Federal Laboratories for Materials Science and Technology, Switzerland; W.J. Clegg , University of Cambridge, UK; J. Michler , Empa - Swiss Federal Laboratories for Materials Science and Technology, Switzerland |
| 3:00pm | D1-2-MoA5 TiO ₂ Nanotubes Produced in Aqueous Electrolytes with CMC for Biomaterials Application, R. Aguirre Ocampo , M. Echeverry-Rendón , S. Robledo , F. Echeverría , Universidad de Antioquia, Colombia | H2-2-MoA5 | Micromechanical Characterisation of Ag/Au Multilayers by Means of Bulge and Nanoindentation Testing, S. Krauß , M. Göken , B. Merle , Friedrich Alexander-University Erlangen-Nürnberg (FAU), Germany |
| 3:20pm | D1-2-MoA6 Electrochemical Evaluation of Titanium Oxide Coatings Deposited on Magnesium Alloys, B. Millan-Ramos , Universidad Nacional Autonoma de Mexico, México; J. Victoria-Hernandez , S. Yi , Magnesium Innovation Centre, Helmholtz-Zentrum, Germany; D. Letzig , Magnesium Innovation Centre, Helmholtz-Zentrum, Germany, Germany; P. Silva-Bermudez , Instituto Nacional de Rehabilitación, Mexico; S.E. Rodil , Universidad Nacional Autonoma de Mexico, México | H2-2-MoA6 | Size Effect on Superplastic Flow – In situ Micromechanical Characterization of Superplastic Zn-22% Al, P. Feldner , M. Göken , University Erlangen-Nürnberg, Germany; B. Merle , Friedrich Alexander-University Erlangen-Nürnberg (FAU), Germany |
| 3:40pm | D1-2-MoA7 Developments of Calcium Sulfate Coating on Ti6Al4V Substrate by Flame Spray, W.C. Wu , Y.-C. Yang , National Taipei University of Technology, Taiwan | INVITED: H2-2-MoA7 | Studies on the Mechanisms in Hexagonal Close Packed Metal Nanolaminates, I.J. Beyerlein , University of California, Santa Barbara, USA |
| 4:00pm | D1-2-MoA8 Metallization of Polymers for Medical Applications, A.R. Chacko , H.J. Hug , Empa - Swiss Federal Laboratories for Materials Science and Technology, Switzerland; S. Gauter , Christian-Albrechts-University Kiel, Germany; K. Thorwarth , Empa - Swiss Federal Laboratories for Materials Science and Technology, Switzerland | Invited talk continues. | |
| 4:20pm | D1-2-MoA9 Characteristics of a Composite Ceramic Coating Fabricated on Mg-1.2Zn-0.5Ca-0.5Mn Alloy Towards Biodegradable Bone Implants, H. Ibrahim , University of Tennessee at Chattanooga, USA; D. Dean , Ohio State University, USA; M. Elahinia , University of Toledo, USA | H2-2-MoA9 | Critical Assessment of the Criteria for Minimum Indentation Spacing, S.P. Pardhasaradhi , ARCI, India; W.C. Oliver , KLA-Tencor, USA |
| 4:40pm | WELCOME MIXER 5:45 – 7:00 pm Lion Fountain Courtyard | | H2-2-MoA10 Surface Laboratory Assistant – The New Combination of Measurement Device and Analysis Software, N. Bierwisch , N. Schwarzer , SIO, Germany |

Monday Afternoon, May 20, 2019

| | | |
|---|--|--|
| <p>Topical Symposia Room Pacific Salon 3 - Session TS3+4-2-MoA Surface Engineering for Lightweight Materials & Thin Film Materials for Flexible Electronics Moderators: Klaus Böbel, Robert Bosch GmbH, Germany, Oleksandr Glushko, Erich Schmid Institute of Materials Science, Austria, Nicholas Glavin, Air Force Research Laboratory, Materials and Manufacturing Directorate, USA</p> | | |
| 1:40pm | | |
| 2:00pm | | |
| 2:20pm | <p>TS3+4-2-MoA3 Electro-mechanical Reliability of Flexible Electronics: An Overview of Testing and Characterization Techniques, O. Glushko, <i>M.J. Cordill</i>, Erich Schmid Institute of Materials Science, Austria</p> | |
| 2:40pm | <p>TS3+4-2-MoA4 Bending Fatigue of Al/Mo Bilayers on Polymer Substrates with Varied Al Layer Thickness, P. Kreiml, <i>M. Rausch</i>, <i>V.L. Terziyska</i>, Montanuniversität Leoben, Austria; <i>J. Winkler</i>, Plansee SE, Austria; <i>C. Mitterer</i>, Montanuniversität Leoben, Austria; <i>M.J. Cordill</i>, Austrian Academy of Sciences, Austria</p> | |
| 3:00pm | <p>TS3+4-2-MoA5 Enabling High-Power Flexible Devices through Tailored Nanocomposite Interface Materials, K. Burzynski, University of Dayton, USA; <i>N. Glavin</i>, Air Force Research Laboratory, Materials and Manufacturing Directorate, USA; <i>E. Heller</i>, <i>M. Snure</i>, <i>E. Heckman</i>, Air Force Research Laboratory, Sensors Directorate, USA; <i>C. Muratore</i>, University of Dayton, USA</p> | |
| 3:20pm | <p>INVITED: TS3+4-2-MoA6 Plasma Polymers...A Family of Materials that is Full of Surprises, R. Snyders, University of Mons, Belgium</p> | |
| 3:40pm | Invited talk continues. | |
| 4:00pm | <p>TS3+4-2-MoA8 Environmental Challenges of Thin Film Systems on Polymer Substrates for Space Applications, B. Putz, Erich Schmid Institute of Materials Science, Austrian Academy of Sciences, Leoben, Austria; <i>G. Milassin</i>, <i>C. Semprinoschnig</i>, European Space Research and Technology Centre; <i>M.J. Cordill</i>, Erich Schmid Institute of Materials Science, Austrian Academy of Sciences, Leoben, Austria</p> | |
| 4:20pm | <p>TS3+4-2-MoA9 Sputtered Thin Film Sensors for Self-sensing Composite Materials, F.G. Cougnon, <i>A. Lamberti</i>, <i>W. Van Paepegem</i>, <i>D. Depla</i>, Ghent University, Belgium</p> | <p>WELCOME MIXER 5:45 – 7:00 pm Lion Fountain Courtyard</p> |
| 4:40pm | <p>TS3+4-2-MoA10 A New Method for Influencing Coating Properties on Polymer Substrates at Low Temperature: High Power Impulse Magnetron Sputtering (HIPIMS) with Positive Voltage Reversal, A. Wennberg, Nano4Energy SL, Spain; <i>M. Simmons</i>, Intellivation, USA; <i>F. Papa</i>, GP Plasma, Spain; <i>I. Fernandez</i>, Nano4Energy SL, Spain</p> | <p>TUESDAY 7:00 – 8:00 am BRUKER FOCUSED TOPIC SESSION “Advanced Technologies for the In-Depth Characterization of Surfaces” Shraddha Vachhani and Giovanni Ramirez Town & Country Room REFRESHMENTS WILL BE SERVED</p> |
| 5:00pm | <p>INVITED: TS3+4-2-MoA11 Tribological Challenges and Surface Engineering Solutions for Extreme Environments and Lightweight Materials, A.L. Korenyi-Both, Tribologix, Inc., USA</p> | |
| 5:20pm | Invited talk continues. | <p>EXHIBIT HALL OPENS TUESDAY 12:00 – 7:00 pm, Grand Hall Enjoy the Light Lunch at 12:00 pm (while supplies last)</p> |

Tuesday Morning, May 21, 2019

| | | |
|---------|---|---|
| | <p>Coatings for Use at High Temperatures Room Pacific Salon 2 - Session A1-1-TuM Coatings to Resist High-temperature Oxidation, Corrosion, and Fouling I Moderators: Justyna Kulczyk-Malecka, Manchester Metropolitan University, UK, Lars-Gunnar Johansson, Chalmers University of Technology, Sweden, Shigenari Hayashi, Hokkaido University, Japan</p> | <p>Hard Coatings and Vapor Deposition Technologies Room Golden West - Session B1-3-TuM PVD Coatings and Technologies III Moderators: Frank Kaulfuss, Fraunhofer Institute for Material and Beam Technology (IWS), Germany, Jyh-Ming Ting, National Cheng Kung University, Taiwan, Qi Yang, National Research Council of Canada, Canada</p> |
| 8:00am | <p>A1-1-TuM1 Modeling the Influence of Heat Treatment and Base Alloy Composition on the Performance of Aluminide Coatings for High Performance Engine Valve Alloys, <i>R.P. Pillai, S.N. Dreypondt, B.L. Armstrong, Q. Guo, K. Unocic, G.M. Muralidharan</i>, Oak Ridge National Laboratory, USA</p> | <p>B1-3-TuM1 PVD-AlTiN with High Al Content – How to Overcome the “Magic” 67%-Limit, <i>F. Fietzke, T. Modes, O. Zywitzki</i>, Fraunhofer Institute for Organic Electronics, Electron Beam and Plasma Technology FEP, Germany</p> |
| 8:20am | <p>A1-1-TuM2 Fabrication, Characterisation and Testing of Cr Coated Zr Alloy Nuclear Fuel Cladding for Enhanced Accident Tolerance, <i>A. Evans</i>, Manchester Metropolitan University, UK; <i>D. Goddard</i>, National Nuclear Laboratory, UK; <i>A. Cole-Baker</i>, Wood plc, UK; <i>G. Obasi, M. Preuss</i>, Manchester University, UK; <i>E. Vernon</i>, National Nuclear Laboratory, UK; <i>P. Kelly</i>, Manchester Metropolitan University, UK</p> | <p>INVITED: B1-3-TuM2 PVD Methods and Coatings for Protection of Aero Engine Components, <i>U. Schulz, R. Naraparaju, R. Braun, N. Laska</i>, German Aerospace Center (DLR), Germany</p> |
| 8:40am | <p>A1-1-TuM3 High-temperature Oxidation Resistance and Self-healing Capability of HiPIMS Cr-Al-C Coating on Zr-based Alloy, <i>M. Ougier, A. Michau, F. Lomello</i>, CEA, Université Paris-Saclay, France; <i>F. Schuster</i>, CEA Cross-Cutting Program on Materials and Processes Skills, France; <i>H. Maskrot, M.L. Schlegel</i>, CEA, Université Paris-Saclay, France</p> | <p>Invited talk continues.</p> |
| 9:00am | <p>INVITED: A1-1-TuM4 Ceramic Coatings for Protection of Ti and Zr Alloys at High Temperature, <i>P. Xiao, Z.H. Gao, X. Zhang, H. Liu</i>, University of Manchester, UK; <i>J. Kulczyk-Malecka, P. Kelly</i>, Manchester Metropolitan University, UK; <i>Z. Zhang</i>, University of Manchester, UK</p> | <p>B1-3-TuM4 High-temperature Nanoindentation and Microcantilever Deflection Tests of CrAlN and CrAlSiN Hard Coatings, <i>A. Drnovšek</i>, Montanuniversität Leoben, Austria; <i>H. Vo</i>, University of California Berkeley, USA; <i>A. Xia, M. Rebelo de Figueiredo</i>, Montanuniversität Leoben, Austria; <i>S. Kolosvári</i>, Plansee Composite Materials GmbH, Germany; <i>S. Vachhani</i>, Bruker Nano Surfaces, Germany; <i>P. Hosemann</i>, University of California at Berkeley, USA; <i>R. Franz</i>, Montanuniversität Leoben, Austria</p> |
| 9:20am | <p>Invited talk continues.</p> | <p>B1-3-TuM5 On Crystallization and Oxidation Behavior of Zr₅₄Cu₄₆ and Zr₂₇Hf₂₇Cu₄₆ Thin-film Metallic Glasses Compared to a Crystalline Zr₅₄Cu₄₆ Thin-film Alloy, <i>M. Kotrlová, M. Zitek, P. Zeman</i>, University of West Bohemia, Czech Republic</p> |
| 9:40am | <p>A1-1-TuM6 Multi-functional AlZr-TiO₂ Bilayer Coatings Combining Anticorrosion and Antifouling Properties, <i>C. Villardi de Oliveira</i>, ICD-LASMIS, Université de Technologie de Troyes, France, France; <i>A.A. Alhoussein</i>, University of Technology of Troyes (UTT), France; <i>C.J. Jiménez</i>, Univ. Grenoble Alpes, CNRS, France; <i>Z. Dong</i>, School of Materials Science and Engineering, Nanyang Technological University, Singapore; <i>F. Schuster</i>, CEA, PTCMP, France; <i>S. Narasimalu</i>, School of Materials Science and Engineering, Nanyang Technological University, Singapore; <i>M.L. Schlegel</i>, CEA, Université Paris-Saclay, France; <i>F. Sanchette</i>, Nogent International Center for CVD Innovation, LRC CEA-ICD LASMIS UMR6281, UTT, Antenne de Nogent, France</p> | <p>B1-3-TuM6 On the Origin of Multilayered Structure of W-B-C Coating Prepared by Non-Reactive Magnetron Sputtering from a Single Segmented Target, <i>M. Kroker, P. Soucek, M. Fekete, L. Zabransky, V. Bursikova</i>, Masaryk University, Brno, Czech Republic; <i>P. Zikan, A. Obrusnik</i>, Plasma Solve, Brno, Czech Republic; <i>Z. Czigany, K. Balazsi</i>, Hungarian Academy of Sciences, Hungary; <i>P. Vasina</i>, Masaryk University, Brno, Czech Republic</p> |
| 10:00am | <p>A1-1-TuM7 The Oxidation Behavior of ZrO₂-Coated Zircaloy-4 with ZrN Interlayer, <i>I.S. Ting, J.-H. Huang</i>, National Tsing Hua University, Taiwan</p> | |
| 10:20am | <p>A1-1-TuM8 Novel HIPIMS Deposited Nanostructured CrN/NbN Coatings for Environmental Protection of Steam Turbine Components., <i>P. Hovsepian, A.P. Ehasarian, Y. Purandare</i>, Sheffield Hallam University, UK; <i>P. Mayr, K.G. Abstoss</i>, Technische Universität Chemnitz, Germany; <i>M. Mosquera, W. Schulz, A. Kranzmann</i>, Federal Institute for Materials Research and Testing, Germany; <i>M.I. Lasanta Carrasco, J.P. Trujillo</i>, Universidad Complutense de Madrid, Spain</p> | <p>TUESDAY BRUKER FOCUSED TOPIC SESSION 7:00 – 8:00 am, Town & Country Room “Advanced Technologies for the In-Depth Characterization of Surfaces” Shraddha Vachhani and Giovanni Ramirez REFRESHMENTS WILL BE SERVED</p> |
| 10:40am | <p>A1-1-TuM9 NiAl Coatings Deposited on Inconel 600 by Using an Arc Ion Plating Process, <i>Y. Li</i>, University of Manchester, UK; <i>Y.L. Hung</i>, Feng Chia University, Taiwan; <i>M. Lin, A. Matthews</i>, University of Manchester, UK; <i>J.L. He</i>, Feng Chia University, Taiwan</p> | <p>EXHIBIT HALL OPENS TODAY! 12:00 – 7:00 pm, Grand Hall Enjoy the Light Lunch at 12:00 pm (while supplies last)</p> |

Tuesday Morning, May 21, 2019

| | | |
|---------|--|---|
| | <p>Hard Coatings and Vapor Deposition Technologies Room California - Session B4-1-TuM Properties and Characterization of Hard Coatings and Surfaces I Moderators: Naureen Ghafoor, Linköping Univ., IFM, Thin Film Physics Div., Sweden, Ulrich May, Robert Bosch GmbH, Germany, Fan-Bean Wu, National United University, Taiwan</p> | <p>Coatings for Biomedical and Healthcare Applications Room Pacific Salon 3 - Session D3-TuM Surfaces and Coatings to Promote Tailored Biological Responses Moderators: Sandra Rodil, Universidad Nacional Autonoma de Mexico, México, Vincent Fridrici, Ecole Centrale de Lyon, LTDS - Université de Lyon, France</p> |
| 8:00am | | |
| 8:20am | <p>INVITED: B4-1-TuM2 Preparation and Characterization of Hard and Tough Coatings of Ion-assisted Co-sputtered Transition Metal Borides, M.S. Wong, National Dong Hwa University, Taiwan</p> | <p>D3-TuM2 Tailoring the Microstructure of ZnO Thin Films for Antimicrobial Applications, P. Pereira-Silva, J. Borges, A. Costa-Barbosa, D. Costa, MS. Rodrigues, F. Vaz, P. Sampaio, University of Minho, Portugal</p> |
| 8:40am | Invited talk continues. | <p>D3-TuM3 <i>In Vitro</i> Evaluation of Macrophage Response to Ionic Liquid-Coated Titanium; S. Wheelis, L. Guida, D. C. Rodrigues, University of Texas at Dallas, USA</p> |
| 9:00am | <p>B4-1-TuM4 Strategy for Increasing Both Hardness and Toughness in Transition-metal Diboride Thin Films, B. Bakhit, Linköping Univ., IFM, Thin Film Physics Div., Sweden; I. Petrov, University of Illinois, USA, Linköping University, Sweden, USA; J.E. Greene, University of Illinois, USA, Linköping University, Sweden, National Taiwan Univ. Science & Technology, Taiwan; L. Hultman, J. Lu, J. Rosén, G. Greczynski, N. Ghafoor, Linköping Univ., IFM, Thin Film Physics Div., Sweden</p> | <p>INVITED: D3-TuM4 Materials To Control Biological Function, K. Anselme, CNRS, France</p> |
| 9:20am | <p>B4-1-TuM5 Tribocorrosion Resistance of Borided ASTM F1537 Alloy, I.E. Campos-Silva, A.M. Delgado-Brito, Instituto Politecnico Nacional Grupo Ingeniería de Superficies, México; J. Oseguera-Peña, Tecnológico de Monterrey-CEM, México; J. Martinez-Trinidad, Instituto Politecnico Nacional, Grupo Ingeniería de Superficies, México; R. Perez Pasten-Borja, Instituto Politecnico Nacional, SEPI ENCB, Mexico; D. Lopez-Suero, Instituto Politecnico Nacional, Grupo Ingeniería de Superficies, México; A. Mojica-Villegas, Instituto Politecnico Nacional, ENCB, México</p> | Invited talk continues. |
| 9:40am | <p>B4-1-TuM6 Corrosion Behavior of TiAlSiN Doped with Ag Coating Deposited by Co-sputtering in Physiological Fluids, A.D. Caïta Tapia, S.D. Rodriguez Arevalo, E.N. Borja Goyeneche, J.J. Olaya Florez, B.J. Gamboa Mendoza, Universidad Nacional de Colombia, Colombia</p> | <p>D3-TuM6 Comparison of Elution of Antibiotic and Biofilm Inhibitor from Manually Applied and Spray Deposited Phosphatidylcholine Coatings, Z. Harrison, R. Awais, R. Gopalakrishnan, J.A. Jennings, University of Memphis, USA</p> |
| 10:00am | <p>B4-1-TuM7 Adhesion Strength of Titanium Carbide Thin Film Coatings on Surface Microstructure Controlled WC-Co, T. Saito, C. Tanaka, N. Okamoto, Osaka Prefecture University, Japan; A. Kitajima, K. Higuchi, Osaka University, Japan</p> | <p>D3-TuM7 <i>In vitro</i> Osseointegration Analysis of Bio-functionalized Titanium Samples in a Protein-rich Medium, S. Rao, S. Hashemiastaneh, J. Villanueva, University of Illinois at Chicago, USA; F. Silva, University of Minho, Portugal; C. Takoudis, University of Illinois at Chicago, USA; D. Bijukumar, University of Illinois College of Medicine, USA; J. Souza, University of Illinois at Chicago, USA; M.T. Mathew, University of Illinois College of Medicine, USA</p> |
| 10:20am | <p style="text-align: center;">EXHIBITION KEYNOTE LECTURE Town & Country Room, 11:00 am – 12:00 pm “Advanced Performance of Tools in Sheet-metal Forming - The Synergy of Surface Technology and Tooling Material Selection” Dr. Farwah Nahif, voestalpine eifeler Vacotec GmbH, Germany</p> | <p>D3-TuM8 Microstructural and Electrochemical Properties of TiAlN- (Ag,Cu) Nanocomposite Coatings Deposited by DC Magnetron Sputtering for Medical Applications, H.D. Mejía, A.M. Echavarría, G. Bejarano, Universidad de Antioquia, Colombia</p> |

Tuesday Morning, May 21, 2019

| | | |
|--------|--|---|
| | <p>Tribology and Mechanical Behavior of Coatings and Engineered Surfaces Room San Diego - Session E2-1-TuM Mechanical Properties and Adhesion I Moderators: Megan J. Cordill, Erich Schmid Institute of Materials Science, Austrian Academy of Sciences, Leoben, Austria, Ming-Tzer Lin, National Chung Hsing University, Taiwan, Gerhard Dehm, Max-Planck Institut für Eisenforschung, Germany</p> | <p>New Horizons in Coatings and Thin Films Room Pacific Salon 6-7 - Session F1-TuM Nanomaterials and Nanofabrication Moderators: Ulf Helmersson, Linköping University, Sweden, Vitezslav Stranak, University of South Bohemia, Czech Republic</p> |
| 8:00am | <p>INVITED: E2-1-TuM1 Indentation Behavior of Metal-Ceramic Multilayer Coatings: Modeling vs. Experiment, Y.-L. Shen, University of New Mexico, USA</p> | <p>INVITED: F1-TuM1 Single and Multi-component Nanomaterials Prepared by Means of Cluster Beam Deposition, O. Kylian, Charles University, Czech Republic; A. Shelemin, D. Nikitin, Charles University, Czech Republic, Czechia; P. Pleskunov, J. Hanus, P. Solar, A. Choukourov, A. Kuzminova, M. Cieslar, H. Biederman, Charles University, Czech Republic</p> |
| 8:20am | <p>Invited talk continues.</p> | <p>Invited talk continues.</p> |
| 8:40am | <p>E2-1-TuM3 Indentation Induced Delamination for Adhesion Measurements, M.J. Cordill, A. Kleinbichler, Erich Schmid Institute of Materials Science, Austria</p> | <p>F1-TuM3 Preparation of High Activity and Stability of Cobalt Carbide Nanoparticles for Hydrogen Evolution Reaction, Y.H. Lin, National Cheng Kung University, Taiwan; S.C. Wang, Southern Taiwan University of Science and Technology, Taiwan; J.L. Huang, National Cheng Kung University, Taiwan</p> |
| 9:00am | <p>E2-1-TuM4 Intrinsic Stress in Polycrystalline Film: An Atomistic View, E. Vasco, Instituto de Ciencia de Materiales de Madrid, Spanish National Research Council (CSIC), Spain; D. Franco, Departamento de Física de la Materia Condensada, Universidad Autónoma de Madrid, Spain; E.G. Michel, C. Polop, Departamento de Física de la Materia Condensada and Condensed Matter Physics Center (IFIMAC), Universidad Autónoma de Madrid, Spain</p> | <p>F1-TuM4 Nanocluster-Based Metal Oxide Films for Hydrogen Gas Sensing, S. Haviar, J. Čapek, Š. Batková, N. Kumar, University of West Bohemia, Czech Republic</p> |
| 9:20am | <p>E2-1-TuM5 Development of a Methodology for Measuring the Elastic Constants of Anisotropic Coatings Using Impulse Excitation Technique, E. Zgheib, University of Technology of Troyes (UTT) and Lebanese University (UL), France; M.F. Slim, A.A. Alhussein, University of Technology of Troyes (UTT), France; K. Khalil, Lebanese University (UL), Lebanon; M. Francois, University of Technology of Troyes (UTT), France</p> | <p>F1-TuM5 Deposition of Magnetic Thin Films by High Power Impulse Magnetron Sputtering, J.T. Gudmundsson, H. Hajihoseini, M. Kateb, S. Ingvarsson, University of Iceland, Iceland</p> |
| 9:40am | <p>E2-1-TuM6 Oxidation Resistance of Ti6Al4V-Si₃N₄ Composites Fabricated through Spark Plasma Sintering Method, F. Kgoete, P.A. Popoola, Tshwane University of Technology, Pretoria, South Africa</p> | <p>F1-TuM6 Fluorination of the Magnesium Particle Surface: Enhancing the Reactivity of Magnesium, M. Pantoya, S. Islam, Texas Tech University, USA</p> |

Tuesday Morning, May 21, 2019

| | | |
|---|--|---|
| <p>Advanced Characterization Techniques for Coatings, Thin Films, and Small Volumes Room Pacific Salon 1 - Session H1-1-TuM Spatially-resolved and In-Situ Characterization of Thin Films and Engineered Surfaces I Moderators: Grégory Abadias, Institut Pprime - CNRS - ENSMA - Université de Poitiers, France, Xavier Maeder, Empa - Swiss Federal Laboratories for Materials Science and Technology, Switzerland, Michael Tkadletz, Montanuniversität Leoben, Austria</p> | | |
| 8:00am | | |
| 8:20am | <p>H1-1-TuM2 Evolution of the Nanoporous Structure of Sintered Ag Joints at High Temperature using In-Situ X-ray Nanotomography, X. Milhet, A. Nait-Ali, D. Tandiang, L. Signor, Institut Pprime - CNRS - ENSMA - Université de Poitiers, France; M. Legros, Cemes - Cnrs, France; Y. Liu, D. Van Campen, Stanford Synchrotron Radiation Lightsource - SLAC National Accelerator Laboratory, USA</p> | |
| 8:40am | <p>INVITED: H1-1-TuM3 Atom Probe Tomography to Help Understand Deformation Mechanisms in Metallic Alloys, B. Gault, Max-Planck Institute for Iron Research, Düsseldorf, Germany; P. Kontis, S.K. Makeneni, J. He, Z. Peng, Max-Planck Institut für Eisenforschung, Germany; S. Neumeier, Friedrich Alexander-University Erlangen-Nürnberg (FAU), Germany; J. Cormier, Institut Pprime - CNRS - ENSMA - Université de Poitiers, France; D. Raabe, Max-Planck Institut für Eisenforschung, Germany</p> | |
| 9:00am | Invited talk continues. | |
| 9:20am | <p>H1-1-TuM5 On the Chemical Composition of TiAlN Thin Films - Comparison of Ion Beam Analysis and Laser-assisted Atom Probe Tomography with Varying Laser Pulse Energy, M. Hans, J.M. Schneider, RWTH Aachen University, Germany</p> | <p>EXHIBITION KEYNOTE LECTURE Town & Country Room, 11:00 am – 12:00 pm “Advanced Performance of Tools in Sheet-metal Forming - The Synergy of Surface Technology and Tooling Material Selection” Dr. Farwah Nahif, voestalpine eifeler Vacotec GmbH, Germany</p> |
| 9:40am | <p>H1-1-TuM6 Microstructure and Oxidation States of Ni in Sub-Nanometric Layer Depending on its Seed-Layer (Zinc Oxide, Silver Layers): A Multi-Techniques Approach to Trespass Limits of Resolution, J. Voronkoff, H. Montigaud, Saint-Gobain Recherche/CNRS, France; L. Largeau, CNRS/C2N, France; S. Grachev, Saint-Gobain Recherche/CNRS, France</p> | <p>TUESDAY BRUKER FOCUSED TOPIC SESSION 7:00 – 8:00 am, Town & Country Room “Advanced Technologies for the In-Depth Characterization of Surfaces” Shraddha Vachhani and Giovanni Ramirez REFRESHMENTS WILL BE SERVED</p> |
| 10:00am | <p>H1-1-TuM7 Nanomechanical Investigation on Lateral fcc-w Phase Fields of a Partially Decomposed and Transformed Nano-lamellar CVD fcc-Ti_{0.2}Al_{0.8}N Coating, M. Tkadletz, A. Lechner, N. Schalk, Montanuniversität Leoben, Austria; B. Sartory, Materials Center Leoben Forschung GmbH (MCL), Austria; C. Mitterer, Montanuniversität Leoben, Austria; C. Czettl, CERATIZIT Austria GmbH, Austria</p> | <p>EXHIBIT HALL OPENS TODAY! 12:00 – 7:00 pm, Grand Hall Enjoy the Light Lunch at 12:00 pm (while supplies last)</p> |

Tuesday Morning, May 21, 2019

Exhibition Keynote Lecture

Town & Country Room - Session EX-TuEx

Exhibition Keynote Lecture, 11:00 am – 12:00 pm

Moderators:

Christopher Muratore, University of Dayton, USA,

Michael Stüber, Karlsruhe Institute of Technology (KIT), Institute for Applied Materials (IAM), Germany

ICMCTF 2019 EXHIBITION KEYNOTE LECTURE

“Advanced Performance of Tools in Sheet-metal Forming - The Synergy of Surface Technology and Tooling Material Selection”

Dr. Farwah Nahif

voestalpine eifeler Vacotec GmbH, Germany

The requirement of the automotive industry for light weight construction parts has been followed by the introduction of new sheet metal materials for forming application, such as high-strength steels. Due to this development and progress in sheet-metal material properties, with high hardness and toughness, the requirements for forming tool design has evolved within the last years. Thus, the talk will focus on the beneficial synergy of PVD-based surface technology and tooling material selection in order to meet the specific application demands and to obtain advanced functionality and performance of tools in sheet-metal forming in the automotive sector.

Dr. Farwah Nahif received her PhD in engineering from the RWTH Aachen University in 2013. Her dissertation was addressing the effect of Si and Y additives on the phase stability of arc-based Al₂O₃ thin films and has been performed at the Materials Chemistry Department under Prof. Jochen Schneider. In 2014 Dr. Nahif joined the Research & Development Department of voestalpine eifeler Vacotec GmbH as a research scientist specialized in PVD technology and PVD product development. Since July 2018 Dr. Nahif is Head of the Research & Development Department of voestalpine eifeler Vacotec GmbH.

EXHIBIT HALL OPENS TODAY!

12:00 – 7:00 pm, Grand Hall

Enjoy the Light Lunch at 12:00 pm

(while supplies last)

Tuesday Afternoon, May 21, 2019

| | | |
|--------|---|---|
| | <p>Coatings for Use at High Temperatures Room Pacific Salon 2 - Session A1-2-TuA Coatings to Resist High-temperature Oxidation, Corrosion, and Fouling II Moderators: Lars-Gunnar Johansson, Chalmers University of Technology, Sweden, Shigenari Hayashi, Hokkaido University, Japan, Justyna Kulczyk-Malecka, Manchester Metropolitan University, UK</p> | <p>Hard Coatings and Vapor Deposition Technologies Room California - Session B4-2-TuA Properties and Characterization of Hard Coatings and Surfaces II Moderators: Naureen Ghafoor, Linköping Univ., IFM, Thin Film Physics Div., Sweden, Ulrich May, Robert Bosch GmbH, Germany, Fan-Bean Wu, National United University, Taiwan</p> |
| 1:40pm | <p>INVITED: A1-2-TuA1 Nano Coatings To Achieve Cost Effective And Long Lifetime SOFC Interconnects, <i>J.-E. Svensson</i>, Chalmers University of Technology, Sweden</p> | <p>B4-2-TuA1 Fracture Toughness Enhancement in Superlattice Hard Coatings, <i>R. Hahn¹, M. Bartosik, H. Riedl</i>, TU Wien, Institute of Materials Science, Austria; <i>H. Bolvardi</i>, Oerlikon Balzers, Oerlikon Surface Solutions AG, Liechtenstein; <i>S. Koloszári</i>, Plansee Composite Materials GmbH, Germany; <i>P.H. Mayrhofer</i>, TU Wien, Institute of Materials Science, Austria</p> |
| 2:00pm | Invited talk continues. | <p>B4-2-TuA2 Simultaneous Topographical and Electrochemical Mapping using Scanning Ion Conductance Microscopy - Scanning Electrochemical Microscopy (SICM-SECM), <i>W. Shi, G.M. Mendoza, B.K. Kim, K. Lee</i>, Park Systems Corporation, USA</p> |
| 2:20pm | <p>A1-2-TuA3 Influence of Ta Content on Properties of TiAlTaN Films, <i>H.F. Shang, T.M. Shao</i>, State Key Laboratory of Tribology, Tsinghua University, China</p> | <p>B4-2-TuA3 Evaluation of the Cavitation Resistance of a Nitrided Stainless Steel, <i>J.L. Arciniaga-Martínez</i>, Instituto Politécnico Nacional, Escuela Superior de Ingeniería Mecánica y Eléctrica, Unidad Azcapotzalco., México; <i>G.A. Rodríguez-Castro</i>, Instituto Politecnico Nacional, Grupo Ingeniería de Superficies, Mexico, México; <i>A. Meneses-Amador</i>, Instituto Politecnico Nacional Grupo Ingeniería de Superficies, México; <i>J.E. Rivera-López, C.A. Juárez-Navarro</i>, Instituto Politécnico Nacional, Escuela Superior de Ingeniería Mecánica y Eléctrica, Unidad Azcapotzalco, México; <i>J.E. Campos-Silva</i>, Instituto Politecnico Nacional Grupo Ingeniería de Superficies, México</p> |
| 2:40pm | <p>A1-2-TuA4 Cr-Al-Si-N Quaternary Coating Applied on Zirconium Alloy: Combining Superior Resistance of High-temperature Steam Oxidation and Improved Mechanical Properties, <i>F.F. Ge, H. Zhu, F. Huang</i>, Ningbo Institute of Material Technology and Engineering, Chinese Academy of Sciences, China</p> | <p>B4-2-TuA4 Modeling Of Coating Thickness In Electrostatic Spray Deposition Using Response Surface Methodology And Artificial Neural Network, <i>U.M.R. Paturi</i>, Department of Mechanical Engineering, CVR College of Engineering, Hyderabad, India; <i>N. Subba Reddy</i>, Engineering Research Institute, GNU, Republic of Korea; <i>S.K.R. Narala</i>, BITS Pilani Hyderabad, India</p> |
| 3:00pm | | |
| 3:20pm | <p>SESSION BREAK: COMPLIMENTARY REFRESHMENTS IN EXHIBIT HALL</p> | <p>SESSION BREAK: COMPLIMENTARY REFRESHMENTS IN EXHIBIT HALL</p> |
| 3:40pm | | |
| 4:00pm | <p>A1-2-TuA8 Polyurethane Protective Coating with Self Polishing Property, <i>M.M. Rahman</i>, King Fahd University of Petroleum and Minerals, Saudi Arabia</p> | <p>B4-2-TuA8 Performance Comparison of Two Diffusion Models for Describing the Growth Kinetics of Iron Boride Layers, <i>M. Ortiz-Domínguez</i>, Universidad Autónoma del Estado de Hidalgo, México; <i>O. Gómez-Vargas, J. Solís-Romero</i>, Instituto Tecnológico de Tlalnepantla, México; <i>G. Ares de Parga</i>, Instituto Politécnico Nacional, México; <i>J. Oseguera-Peña</i>, Tecnológico de Monterrey, México</p> |
| 4:20pm | <p>A1-2-TuA9 Production of a Zinc Impregnated Stainless Steel Surface Utilizing Cathodic Plasma Electrolytic Deposition (CPED) for Retardation of Cobalt Ion Deposition in High Temperature Aqueous Conditions, <i>C. Fox, F. Scenini, A. Yerokhin, N. Laugel</i>, University of Manchester, UK; <i>R. Wain</i>, Rolls-Royce, UK</p> | <p>B4-2-TuA9 Microstructure and Surface Strength of Chemically Modified WC-Co for Adhesive Strength Improvement, <i>D. Kiyokawa, C. Tanaka, T. Saito, N. Okamoto</i>, Osaka Prefecture University, Japan; <i>A. Kitajima, K. Higuchi</i>, Osaka University, Japan</p> |
| 4:40pm | <p>EXHIBIT HALL OPENS TODAY! 12:00 – 7:00 pm, Grand Hall Exhibition Reception: 5:30 – 7:00 pm</p> | <p>B4-2-TuA10 Compositional and Processing Effects on Phase Transformations and Mechanical Properties of Additive Manufactured Ti-6Al-4V Alloy, <i>O.S. Fatoba, E.T. Akinlabi, S.A. Akinlabi</i>, University of Johannesburg, South Africa</p> |

Tuesday Afternoon, May 21, 2019

| Hard Coatings and Vapor Deposition Technologies Room Golden West - Session B7-TuA Plasma Diagnostics and Growth Processes Moderators: Arutiun P. Ehiastian, Sheffield Hallam University, UK, Yolanda Aranda Gonzalvo, University of Minnesota, USA | | Coatings for Biomedical and Healthcare Applications Room Pacific Salon 3 - Session D2-TuA Bio-corrosion and Bio-tribology Moderators: Jessica Jennings, University of Memphis, USA, Steve Bull, Newcastle University, UK | |
|---|--|---|---|
| 1:40pm | B7-TuA1 On the Growth of TiO _x Coatings by Reactive Magnetron Sputtering from Metallic and Ceramic (TiO _{1.8}) Targets: A Joint Modelling and Experimental Study, <i>R. Tonneau, P. Moskovkin</i> , University of Namur, Belgium; <i>W. De Bosscher</i> , Soleras Advanced Energy, Belgium; <i>A. Pflug</i> , Fraunhofer Institute for Surface Engineering and Thin Films, Germany; <i>S. Lucas</i> , University of Namur, Belgium | D2-TuA1 | Bio-Tribocorrosive Behavior of the Contact M30NW Stainless Steel against HDPE Reinforced with MoS ₂ Particles. New Polymer Implant: Promising Material?, <i>A. Salem, M. Guezmil, W. Bensalah, S. Mezzini</i> , Université de Monastir, Tunisia; <i>J. Géringier</i> , Mines Saint-Etienne, France |
| 2:00pm | B7-TuA2 Titanium Atom and Ion Number Density Evolution in Reactive HiPIMS with Oxygen, Nitrogen and Acetylene Gas, <i>M. Fekete</i> , Masaryk University, Brno, Czech Republic; <i>D. Lundin</i> , Université Paris-Sud/CNRS, France; <i>K. Bernatova, P. Klein, J. Hnilica, P. Vasina</i> , Masaryk University, Brno, Czech Republic | INVITED: D2-TuA2 Evaluation of the Adhesion of Electrospayed and Solution-Cast Chitosan Coatings on Titanium Surfaces, <i>V. Suresh, E.J. Chng, J. Bumgardner, R. Gopalakrishnan</i> , University of Memphis, USA | |
| 2:20pm | B7-TuA3 Phase Formation during Sputtering of Copper in Argon/Oxygen Mixtures, <i>D. Altangerel, D. Depla</i> , Ghent University, Belgium | Invited talk continues. | |
| 2:40pm | INVITED: B7-TuA4 Plasma Diagnostics During Growth of Transparent Conductive Oxide Thin Films by Magnetron Sputtering, <i>E. Stamate</i> , Technical University of Denmark, Denmark | D2-TuA4 Study of the Mechanical and Tribological Properties of the TaN with Ti Inclusion Multilayer Films on Si Substrate, <i>E. Garcia</i> , Cátedras-CONACYT, Universidad de Guadalajara, México; <i>J.O. Berumen</i> , ITESO, Universidad Jesuita de Guadalajara, Tlaquepaque, Jalisco, México; <i>M. Flores-Martinez</i> , Universidad de Guadalajara, México; <i>E. Camps</i> , Instituto Nacional de Investigaciones Nucleares, México; <i>S. Muhl</i> , Instituto de Investigaciones en Materiales-UNAM, México | |
| 3:00pm | Invited talk continues. | D2-TuA5 Enhancement of Tribocorrosion Properties of Ti6Al4V by Formation of a Carbide-Derived Carbon (CDC) Surface Layer, <i>K.Y. Cheng</i> , University of Illinois at Chicago, USA; <i>R. Nagaraj, D. Bijukumar, M.T. Mathew</i> , University of Illinois College of Medicine, USA; <i>M. McNallan</i> , University of Illinois at Chicago, USA | |
| 3:20pm | SESSION BREAK: COMPLIMENTARY REFRESHMENTS IN EXHIBIT HALL | SESSION BREAK: COMPLIMENTARY REFRESHMENTS IN EXHIBIT HALL | |
| 3:40pm | | | |
| 4:00pm | | INVITED: D2-TuA8 Considerations when using Additive Manufacturing to make Medical Devices, <i>A. Espinoza Orías</i> , Rush University Medical Center, USA | |
| 4:20pm | B7-TuA9 On Three Different Ways to Quantify the Degree of Ionization in Sputtering Magnetrons, <i>A. Butler</i> , Université Paris-Sud, Université Paris-Saclay, France; <i>N. Brenning</i> , Université Paris-Sud, Université Paris-Saclay, Sweden; <i>M.A. Raadu</i> , KTH Royal Institute of Technology, Sweden; <i>J.T. Gudmundsson</i> , University of Iceland, Iceland; <i>T. Minea, D. Lundin</i> , Université Paris-Sud, Université Paris-Saclay, France | Invited talk continues. | |
| 4:40pm | | D2-TuA10 Nanostructured Surfaces for (Bio)sensors, <i>V.S. Stranak</i> , University of South Bohemia, Czech Republic; <i>R. Bogdanowicz</i> , Gdansk University of Technology, Poland; <i>P. Sezemsky, V. Prysiaznyy, J. Kratochvil</i> , University of South Bohemia, Czech Republic; <i>M. Smietana</i> , Warsaw University of Technology, Poland; <i>O. Kylian</i> , Charles University, Czech Republic; <i>Z. Hubicka, M. Cada</i> , Institute of Physics CAS, v. i., Czech Republic | |
| 5:00pm | B7-TuA11 Characterization of Microwave Surfatron Plasma-enhanced-ALD System for Low-temperature Deposition of Thin Oxide Films, <i>M. Cada, D. Tvarog</i> , Institute of Physics CAS, v. i., Czech Republic; <i>J. Kim</i> , ISAC Research Inc., Republic of Korea; <i>A. Poruba, SVCS Process Innovation s.r.o.</i> , Czech Republic; <i>Z. Hubicka</i> , Institute of Physics CAS, v. i., Czech Republic | D2-TuA11 Electrochemical Performance of Agro-Industrial Waste as Green Corrosion Inhibitor for Stainless Steel Type 316 in Acid Environment, <i>O. Sanni, P.A. Popoola, S. Fayomi</i> , Tshwane University of Technology, Pretoria, South Africa | |
| 5:20pm | EXHIBIT HALL OPENS TODAY! 12:00 – 7:00 pm, Grand Hall Exhibition Reception: 5:30 – 7:00 pm | D2-TuA12 Electrochemical AC Impedance Analysis for Parylene AF4 Continuous Film, <i>W.-C. Kuo, C.-F. Wu</i> , National Kaohsiung University of Science and Technology, Taiwan | |

Tuesday Afternoon, May 21, 2019

| | | | | |
|---|--|---|---|--|
| <p>Tribology and Mechanical Behavior of Coatings and Engineered Surfaces Room San Diego - Session E2-2-TuA Mechanical Properties and Adhesion II Moderators: Megan J. Cordill, Erich Schmid Institute of Materials Science, Austrian Academy of Sciences, Leoben, Austria, Ming-Tzer Lin, National Chung Hsing University, Taiwan, Gerhard Dehm, Max-Planck Institut für Eisenforschung, Germany</p> | | <p>New Horizons in Coatings and Thin Films Room Pacific Salon 6-7 - Session F3-TuA 2D Materials: Synthesis, Characterization, and Applications Moderator: Eli Sutter, University of Nebraska-Lincoln, USA</p> | | |
| 1:40pm | | <p>INVITED: F3-TuA1 Roll-to-roll Plasma Chemical Vapor Deposition for Scalable Graphene Production, T.S. Fisher, UCLA, USA; M. Alrefae, Purdue University, USA</p> | | |
| 2:00pm | <p>E2-2-TuA2 Mechanical Behavior Study of 50 nm-thick Thin Film of Gold Single Crystal with In situ X-ray Pole Figures Measurements, P.O. Renault, Université de Poitiers, France; J. Drieu La Rochelle, P. Godard, M. Drauet, J. Nicolai, M.F. Beaufort, University of Poitiers, France; D. Thiaudière, C. Mocuta, SOLEIL Synchrotron, France</p> | <p>Invited talk continues.</p> | | |
| 2:20pm | <p>E2-2-TuA3 Evaluation of the Mechanical Properties in Antibacterial Multi-layer HA-Ag Coatings Deposited by RF Magnetron Sputtering, J.A. Lenis, M.A. Gómez, F.J. Bolivar, University of Antioquia, Colombia</p> | <p>F3-TuA3 Magnetron Sputtered MoS₂/C Nanocomposites as Highly Efficient Electrocatalyst in Hydrogen Evolution Reaction, S.J. Rowley-Neale, M. Ratova, Manchester Metropolitan University, UK; L.T.N. Fugita, University of Sao Paulo, Brazil; G.C. Smith, University of Chester, UK; A. Gaffar, J. Kulczyk-Malecka, P. Kelly, C.E. Banks, Manchester Metropolitan University, UK</p> | | |
| 2:40pm | <p>INVITED: E2-2-TuA4 Mechanical Deformation in Metal and Ceramic Nano Multilayers, A.M. Hodge, University of Southern California, USA</p> | <p>F3-TuA4 HIPIMS Graphene on Copper for Heat Spreading, C.M. Chen, E.Y. Liao, P.-Y. Hsieh, Y.H. Chen, J.L. He, Feng Chia University, Taiwan</p> | | |
| 3:00pm | <p>Invited talk continues.</p> | <p>F3-TuA5 Tailoring Optical Properties of Two-Dimensional Transition Metal Dichalcogenides Via Photonic Annealing, R. Rai, K. Gleibe, University of Dayton, Air Force Research Laboratory, USA; N. Glavin, Air Force Research Laboratory, Wright-Patterson AFB, USA; R. Wheeler, UES, Inc., Air Force Research Laboratory, USA; R. Kim, Air Force Research Laboratory, Wright-Patterson AFB, USA; A. Jawaid, UES, Inc., Air Force Research Laboratory, USA; L. Bissell, Air Force Research Laboratory, Wright-Patterson AFB, USA; C. Muratore, University of Dayton, USA</p> | | |
| 3:20pm | <p>SESSION BREAK: COMPLIMENTARY REFRESHMENTS IN EXHIBIT HALL</p> | | <p>SESSION BREAK: COMPLIMENTARY REFRESHMENTS IN EXHIBIT HALL</p> | |
| 3:40pm | | | | |
| 4:00pm | <p>E2-2-TuA8 Deposition of Highly Adhesive Ta Based Thin Films on a Biomedical Grade CoCrMo Alloy, J. Corona-Gomez, Q. Yang, Y. Li, University of Saskatchewan, Canada</p> | <p>F3-TuA8 Mechanism of Formation of Nitrogenated Doped Graphene Films, Investigated by In situ XPS During Thermal Annealing in Vacuum, Y. Bleu, Univ. Lyon, Université Jean Monnet, France; V. Barnier, F.C. Christien, Laboratoire Georges Friedel, Ecole Nationale Supérieure des Mines, France; F. Bourquard, Univ. Lyon, Laboratoire Hubert Curien, Université Jean Monnet, France; J. Avila, Synchrotron SOLEIL & Université Paris-Saclay, France; F. Garrelie, Univ. Lyon, Université Jean Monnet, France; M-C. Asensio, Synchrotron SOLEIL & Université Paris-Saclay, France; C.D. Donnet, Université de Lyon, Université Jean Monnet, France</p> | | |
| 4:20pm | <p>E2-2-TuA9 DIC on FIB Ring-Core of Thin Films for Depth Sensing Residual Stress Measurement, M.T. Lin, W.-C. Pan, National Chung Hsing University, Taiwan; Y-F. Chen, F-Y. Cheng, National Cheng Kung University, Taiwan; J.-H. Huang, National Tsing Hua University, Taiwan</p> | <p>INVITED: F3-TuA9 Engineering Point and Extended Defects in Transition Metal Dichalcogenides, H.-P. Komsa, Aalto University, Finland</p> | | |
| 4:40pm | <p>E2-2-TuA10 Metallic Glass/Crystalline Nanolayered Coatings with High Nanoscratch Resistance and Damage Tolerance, M. Abbaud, Middle East Technical University, Turkey; A. Motallebzadeh, Koç University, Turkey; S. Özerinç, Middle East Technical University, Turkey</p> | <p>Invited talk continues.</p> | | |
| 5:00pm | <p>E2-2-TuA11 Coatings Effect On Crack Initiation Behavior Of Ti Alloys, X.L. Pang, University of Science and Technology Beijing, China</p> | <p>F3-TuA11 Physicochemical and Mechanical Performance of Nylon 6.6 Coated Thin Free-standing Boron-doped Diamond Nanosheets, R. Bogdanowicz, M. Ficek, Gdansk University of Technology, Poland; V.S. Stranak, J. Kratochvil, University of South Bohemia, Czech Republic; M. Szkodo, J. Ryl, M. Sobaszek, Gdansk University of Technology, Poland</p> | | |

Tuesday Afternoon, May 21, 2019

| | |
|---|--|
| <p>Advanced Characterization Techniques for Coatings, Thin Films, and Small Volumes Room Pacific Salon 1 - Session H1-2-TuA Spatially-resolved and In-Situ Characterization of Thin Films and Engineered Surfaces II Moderators: Grégory Abadias, Institut Pprime - CNRS - ENSMA - Université de Poitiers, France, Xavier Maeder, Empa - Swiss Federal Laboratories for Materials Science and Technology, Switzerland, Michael Tkadletz, Montanuniversität Leoben, Austria</p> | |
| 1:40pm | <p>H1-2-TuA1 Complex Study of Thermally Induced Order Reactions in Cu-Au Thin Films, A.S. Sologubenko, <i>M. Volpi</i>, <i>P. Okle</i>, <i>R. Spolenak</i>, ETH Zürich, Switzerland</p> |
| 2:00pm | <p>H1-2-TuA2 Kinetics Dependence of Microstructure and Stress Evolutions in Polycrystalline Cu Films: Real-time Diagnostics and Atomistic Modelling, C. Furgeaud¹, <i>C. Mastail</i>, <i>A. Michel</i>, <i>L. Simonot</i>, Institut Pprime - CNRS - ENSMA - Université de Poitiers, France; <i>E. Chason</i>, Brown University, USA; <i>G. Abadias</i>, Institut Pprime - CNRS - ENSMA - Université de Poitiers, France</p> |
| 2:20pm | <p>H1-2-TuA3 Understanding the Crystallization of Amorphous Films with Embedded Seed Crystals using High-resolution STEM Composition and Structural Mapping, P. Rasmussen, <i>J. Rajagopalan</i>, <i>R. Berlia</i>, Arizona State University, USA</p> |
| 2:40pm | <p>H1-2-TuA4 <i>In-situ</i> Investigation of the Oxidation Behavior of Metastable CVD Ti_{1-x}Al_xN Using Combined Synchrotron XRD and DSC, C. Saringer, <i>M. Tkadletz</i>, Montanuniversität Leoben, Austria; <i>A. Stark</i>, Helmholtz Zentrum Geesthacht, Germany; <i>C. Czettl</i>, Ceratizit Austria GmbH, Austria; <i>N. Schalk</i>, Montanuniversität Leoben, Austria</p> |
| 3:00pm | <p>H1-2-TuA5 In-situ X-ray Characterization of Liquid-solid Transition Phase in Small Volume, M. Kbibou, <i>L. Barrallier</i>, Mechanics, Surfaces and Materials Processing Laboratory, France; <i>M. El Mansori</i>, Arts et Métiers ParisTech d'Aix en Provence, Laboratory of Mechanics, Surface and Materials Processing (MSMP-EA7350), France; <i>L. Heraud</i>, Mechanics, Surfaces and Materials Processing Laboratory, France</p> |
| 3:20pm | <p>SESSION BREAK: COMPLIMENTARY REFRESHMENTS IN EXHIBIT HALL</p> |
| 3:40pm | |
| 4:00pm | <p>H1-2-TuA8 Novel Quantitative Thin Film Thickness and Chemical State Analysis X-ray Techniques, W. Yun, <i>B. Stripe</i>, <i>S. Shesadri</i>, <i>S. Lewis</i>, <i>X. Yang</i>, <i>R. Qiao</i>, <i>S.H. Lau</i>, Sigray, Inc., USA</p> |
| 4:20pm | <p>H1-2-TuA9 Effect of Heat Treatment on Microstructure of Erbium Film on Steel Substrate with Yttria Buffer Layer Fabricated by MOCVD, K. Matsuda, <i>M. Tanaka</i>, <i>S.W. Lee</i>, University of Toyama, Japan; <i>Y. Hishinuma</i>, NIFS, Japan; <i>K. Nishimura</i>, <i>T. Tsuchiya</i>, University of Toyama, Japan</p> |
| 4:40pm | <p>H1-2-TuA10 Detailed Characterization of Interface Structure of Thin Aluminum Films Deposited on a Highly Reactive Metallic Surface, J.W. Yan, Institute of Materials, China Academy of Engineering Physics, China</p> |
| 5:00pm | <p>H1-2-TuA11 Study of Volmer-Weber Thin Film Growth Mechanisms by Coupling <i>in situ</i> Resistivity, Optical and Mechanical Measurements, Q. Heralut, <i>S. Grachev</i>, <i>I. Gozhyk</i>, <i>H. Montigaud</i>, Saint-Gobain Recherche/CNRS, France; <i>R. Lazzari</i>, Institut des Nano Sciences de Paris - Sorbonne Université, France</p> |
| <p>EXHIBIT HALL OPENS TODAY! 12:00 – 7:00 pm, Grand Hall Exhibition Reception: 5:30 – 7:00 pm</p> | |

Tuesday Evening, May 21, 2019

Special Interest Talk

Town & Country Room - Session SIT1-TuSIT

Special Interest Session I: 7:00 – 7:40 pm

Moderators:

Christopher Muratore, University of Dayton, USA,

Michael Stüber, Karlsruhe Institute of Technology (KIT), Institute for Applied Materials (IAM), Germany

Advanced Monitoring of Thin Film Growth from Real-time Diagnostics

G. Abadias, Institut Pprime - CNRS - ENSMA - Université de Poitiers, France

Thin metallic films deposited on Si are largely used in many technological areas, such as microelectronics, catalysis, architectural glazing or plasmonics. In the case of high-mobility metals on weakly interacting substrates (e.g. Ag on SiO₂), the growth proceeds in a 3D fashion, known as Volmer-Weber. The control of islands size and shape at the beginning of growth is vital for many applications as the characteristic length scales and physical attributes of ultrathin films are mostly set-in during the coalescence stage.

By employing a panel of *in situ* and real-time diagnostics, we could obtain valuable insights on the thin film growth dynamics as well as stress evolution in a variety of sputter-deposited metallic systems (Ag, Cu, Au, Ta and Mo). More particularly, the characteristic thickness of film percolation and film continuity can be determined from a combination of real-time electrical resistivity and wafer curvature measurements. This will be highlighted for the case of Ag and Cu deposited on amorphous carbon as a function of deposition flux F and substrate temperatures T_s .

We will also provide examples on how chemical alloying or interface reactivity can affect the growth morphology and stress evolution of Ag and Cu films. Growth monitoring was performed *in situ* by employing either surface differential reflectance spectroscopy or spectroscopic ellipsometry. We will show that strategies based on interfacial or alloying design can be efficiently employed to manipulate growth and obtain ultra-thin, ultra-smooth, continuous layers.

Finally, we will discuss the issue of phase transformation during growth of ultrathin layers, with special focus on silicide formation. By coupling simultaneously X-ray diffraction, X-ray reflectivity and wafer curvature during sputter-deposition of metal layers on amorphous Si, information about thickness-dependent crystalline phases, texture, grain growth and microstrain can be gained. This will be demonstrated for Mo/Si and Pd/Si systems. A complex nanostructure formation is uncovered from these synchrotron studies, pointing out to different silicide formation mechanisms and subsequent structural development.

Wednesday Morning, May 22, 2019

| Coatings for Use at High Temperatures Room Pacific Salon 2 - Session A1-3-WeM Coatings to Resist High-temperature Oxidation, Corrosion, and Fouling III Moderators: Justyna Kulczyk-Malecka, Manchester Metropolitan University, UK, Lars-Gunnar Johansson, Chalmers University of Technology, Sweden, Shigenari Hayashi, Hokkaido University, Japan | | Hard Coatings and Vapor Deposition Technologies Room California - Session B4-3-WeM Properties and Characterization of Hard Coatings and Surfaces III Moderators: Naureen Ghafoor, Linköping Univ., IFM, Thin Film Physics Div., Sweden, Ulrich May, Robert Bosch GmbH, Germany, Fan-Bean Wu, National United University, Taiwan | |
|---|---|---|--|
| 8:00am | | | |
| 8:20am | A1-3-WeM2 Corrosion Monitoring Of High-Temperature Protective Coatings Under Molten Salts Environments For CSP Applications, <i>F.J. Pérez Trujillo, V. Encinas Sánchez, T. de Miguel Gamo</i> , Universidad Complutense de Madrid, Spain; <i>M.I. Lasanta Carrasco</i> , Universidad Complutense de Madrid, Spain; <i>G. García-Martín</i> , Universidad Complutense de Madrid, Spain | B4-3-WeM2 Physical Properties of Nano-structured Chromium Nitride Hard Coatings obtained by RF Physical Vapor Dynamic Glancing Angle Deposition, <i>M.J.M. Jimenez, V. Antunes, S.C. Cucatti, A.R. Riul, L.F. Zaganel</i> , UNICAMP, Brazil; <i>C.A. Figueroa</i> , Universidade de Caxias do Sul, Brazil; <i>D. Wisnivesky</i> , UNICAMP, Brazil; <i>F. Alvarez</i> , Instituto de Física, UNICAMP, Brazil | |
| 8:40am | A1-3-WeM3 Development of a Ti _x Si _y Protective Layer on TiAl48-2Cr-2Nb for Increased Oxidation Resistance, <i>J. Crespo Villegas, S.L. Loquai, É. Bousser</i> , École Polytechnique de Montréal, Canada; <i>M. Cavarroc</i> , SAFRAN Tech, France; <i>S. Knittel</i> , SAFRAN Aircraft Engines, France; <i>L. Martinu, J.E. Klemberg-Sapieha</i> , École Polytechnique de Montréal, Canada | B4-3-WeM3 Synthesis and Characterization of Sputter Deposited Hard Coatings within the Quasibinary System TiB ₂ -VB ₂ , <i>C. Mitterer, V.L. Terziyska, M. Tkadletz, L. Hatzenbichler, D. Holec</i> , Montanuniversität Leoben, Austria; <i>V. Moraes</i> , Institute of Materials Science and Technology, TU Wien, Austria; <i>A. Lümkmann</i> , PLATIT AG Advanced Coating Systems, Switzerland; <i>M. Morstein</i> , Hightech Zentrum Aargau AG, Switzerland; <i>P. Polcik</i> , Plansee Composite Materials GmbH, Germany | |
| 9:00am | A1-3-WeM4 The Impact of Aluminide and MCrAlY Coatings on the Fatigue Properties of Ni-based Valve Alloys, <i>S.N. Dryepondt, B.L. Armstrong, G.M. Muralidharan</i> , Oak Ridge National Laboratory, USA | B4-3-WeM4 Deposition-controlled Stabilization of Metastable fcc-(Al,Ti)N in CVD and PVD Coatings, <i>U. Ratayski</i> , Technische Universität Bergakademie Freiberg, Germany; <i>M. Höhn</i> , Fraunhofer IKTS, Germany; <i>B. Scheffel</i> , Fraunhofer FEP, Germany; <i>F. Fietzke</i> , Fraunhofer Institute for Organic Electronics, Electron Beam and Plasma Technology FEP, Germany; <i>M. Motylenko, D. Rafaja</i> , Technische Universität Bergakademie Freiberg, Germany | |
| 9:20am | A1-3-WeM5 High Temperature Oxidation of γ-TiAl Produced by Additive Manufacturing, <i>R. Swadzba</i> , Institute for Ferrous Metallurgy, Poland; <i>B. Mendala, L. Swadzba, B. Witala, J. Tracz</i> , Silesian University of Technology, Poland; <i>L. Pyclik, K. Marugi, S. Sabbadini</i> , Avio Aero A GE Aviation Business, Poland | B4-3-WeM5 Oxidation Resistance of AIP Deposited AlCrN and AlTiN Coatings with High Al Compositions, <i>K. Yamamoto, H. Nii</i> , Kobe Steel, Ltd., Japan | |
| 9:40am | | B4-3-WeM6 Standing Contact Fatigue Behavior of Nitrided AISI 316L Steels, <i>D. Fernández-Valdés, A. Meneses-Amador, G.A. Rodríguez-Castro, I.E. Campos-Silva</i> , Instituto Politecnico Nacional Grupo Ingeniería de Superficies, México; <i>A. Mouftiez</i> , ICAM Lille, Matériaux, France; <i>J.L. Nava-Sánchez</i> , Tecnológico de Estudios Superiores de Chalco, México | |
| 10:00am | | | |
| 10:20am | SESSION BREAK: COMPLIMENTARY REFRESHMENTS IN EXHIBIT HALL | SESSION BREAK: COMPLIMENTARY REFRESHMENTS IN EXHIBIT HALL | |
| 10:40am | | | |
| 11:00am | A1-3-WeM10 High Temperature Oxidation Protection of Gamma-based TiAl by Sputtered Al-O-F Films, <i>F. Bergeron, S.L. Loquai, É. Bousser</i> , École Polytechnique de Montréal, Canada; <i>M. Cavarroc</i> , SAFRAN Tech, France; <i>S. Knittel</i> , SAFRAN Aircraft Engines, France; <i>L. Martinu, J.E. Klemberg-Sapieha</i> , École Polytechnique de Montréal, Canada | B4-3-WeM10 Effect of Composition on Toughening Mechanism of V _{1-x} Mo _x N Nanocrystalline Thin Film, <i>Y.Q. Feng, J.-H. Huang</i> , National Tsing Hua University, Taiwan | |
| 11:20am | A1-3-WeM11 Corrosion Behavior and Durability of Microstructure of Stainless Steel Rebars in Simulated Concrete Pore Solution Containing Chloride with Different Ph, <i>D.B. Subedi</i> , Chinese Academy of Sciences, China | B4-3-WeM11 Influence of Mo Contents on Elevated Temperature Tribological Characteristics of CrAlMoSiN Nanocomposite Coating, <i>Y.C. Lin, H. Tao, J.G. Duh</i> , National Tsing Hua University, Taiwan; <i>J.-W. Lee</i> , Ming Chi University of Technology, Taiwan | |
| 11:40am | | B4-3-WeM12 Characterization of Cosputtered W-Si-N Coatings, <i>Y.H. Liu</i> , National Taiwan Ocean University, Taiwan; <i>L.C. Chang</i> , Ming Chi University of Technology, Taiwan; <i>B.W. Liu, Y.I. Chen</i> , National Taiwan Ocean University, Taiwan | |
| 12:00pm | EXHIBIT HALL CLOSSES TODAY 10:00 am – 2:00 pm, Grand Hall Enjoy the Light Lunch at 12:20 pm (while supplies last) | B4-3-WeM13 RF Input Power Effect on Microstructure and Mechanical Properties of TaSiN Coatings, <i>Z.X. Lin, Y.C. Liu, S.T. Wang</i> , National United University, Taiwan; <i>M.G. Guillon</i> , Polytech Lyon, France; <i>F.B. Wu</i> , National United University, Taiwan | |

Wednesday Morning, May 22, 2019

| | | |
|---------|---|---|
| | <p>Fundamentals and Technology of Multifunctional Materials and Devices Room Golden West - Session C3+C1-WeM Thin Films for Energy-related Applications I/Optical Metrology in Design, Optimization, and Production of Multifunctional Materials Moderators: Per Eklund, Linköping Univ., IFM, Thin Film Physics Div., Sweden, Tushar Shimpi, Colorado State University, USA</p> | <p>Tribology and Mechanical Behavior of Coatings and Engineered Surfaces Room San Diego - Session E3-WeM Tribology of Coatings for Automotive and Aerospace Applications Moderators: John Curry, Sandia National Laboratories, USA, Christian Greiner, Karlsruhe Institute of Technology (KIT), Institute for Applied Materials (IAM), Germany, Oliver Hunold, Oerlikon Balzers, Oerlikon Surface Solutions AG, Liechtenstein</p> |
| 8:00am | | <p>INVITED: E3-WeM1 Self-assembly of Ultra-high Strength Nanoporous Metals for Multifunctional Coatings and Free-standing Films, J.H. Pikul, University of Pennsylvania, USA; N. Argibay, J. Curry, Sandia National Laboratories, USA; Z. Hsain, University of Pennsylvania, USA</p> |
| 8:20am | <p>C3+C1-WeM2 Avoiding Blistering of Magnetron Sputtered Thin Film CdTe Photovoltaic Devices, J.M. Walls, F. Bittau, R.C. Greenhalgh, A. Abbas, P. Hatton, R. Smith, Loughborough University, UK</p> | <p>Invited talk continues.</p> |
| 8:40am | <p>C3+C1-WeM3 Electrochromic Device Based on WO₃/NiO Complementary Electrodes Prepared by Using Vacuum Cathodic Arc Plasma, P.-W. Chen, Institute of Nuclear Energy Research, Taiwan</p> | <p>E3-WeM3 Elevated Temperature Sliding Wear of PEO-Chameleon Duplex Coating, A.A. Voevodin, A. Shirani, University of North Texas, USA; A. Yerokhin, The University of Manchester, UK; A.L. Korenyi-Both, Tribologix Inc., USA; D. Berman, University of North Texas, USA; J. Zabinski, Army Research Laboratory, USA</p> |
| 9:00am | <p>C3+C1-WeM4 Influence of Film Thickness on Growth, Structure and Properties of Magnetron Sputtered ITO Films, A. Subacius, Manchester University, UK; É. Bousser, École Polytechnique de Montréal, Canada; B. Baloukas, Polytechnique Montreal, Canada; S. Hinder, M. Baker, Surrey University, UK; D. Ngo, Manchester University, UK; C.G. Reholz, Cyprus University, Cyprus; A. Matthews, Manchester University, UK</p> | <p>E3-WeM4 Formation Mechanisms of Zn, Mo, S and P Containing Reaction Layers on a DLC Coating, K. Bobzin, T. Brögelmann, C. Kalscheuer, M. Thiex, Surface Engineering Institute - RWTH Aachen University, Germany</p> |
| 9:20am | <p>INVITED: C3+C1-WeM5 Metal/Semiconductor Superlattice Metamaterials: A New Paradigm in Solid-State Energy Conversion, B. Saha, Jawaharlal Nehru Centre for Advanced Scientific Research, India</p> | <p>E3-WeM5 ta-C Coatings for Tribological Applications, J. Becker, Oerlikon Balzers Coating Germany GmbH, Germany; N. Beganovic, A. Gies, J. Karner, Oerlikon Balzers, Oerlikon Surface Solutions AG, Liechtenstein; J. Vetter, Oerlikon Balzers Coating Germany GmbH, Germany</p> |
| 9:40am | <p>Invited talk continues.</p> | <p>E3-WeM6 Investigation on Effect of MgO-ZrO₂ and Al₂O₃-13%TiO₂ Coated Piston Crown on Performance and Emission Characteristics of a Variable Compression Ratio Engine, T. Raja, Sri Ramakrishna Institute of Technology, India; S. Periyasamy, Government College of Technology, Coimbatore, India</p> |
| 10:00am | <p>SESSION BREAK: COMPLIMENTARY REFRESHMENTS IN EXHIBIT HALL</p> | <p>SESSION BREAK: COMPLIMENTARY REFRESHMENTS IN EXHIBIT HALL</p> |
| 10:20am | | |
| 10:40am | | |
| 11:00am | | <p>E3-WeM10 Titanium Nitrides Coatings for Hard Chromium Replacement, M. Cavarroc, Safran Tech, France; B. Giroire, L. Teulé-Gay, D. Michau, A. Poulon-Quintin, ICMCB, France</p> |
| 11:20am | | <p>E3-WeM11 Tribological Coating Solutions and Lubrication Strategies for Gas Turbine Engines, P. Stoyanov, Pratt & Whitney, USA</p> |
| 11:40am | <p>EXHIBIT HALL CLOSES TODAY 10:00 am – 2:00 pm, Grand Hall Enjoy the Light Lunch at 12:20 pm (while supplies last)</p> | |
| 12:00pm | | |

Wednesday Morning, May 22, 2019

| New Horizons in Coatings and Thin Films Room Pacific Salon 6-7 - Session F4-1-WeM Functional Oxide and Oxynitride Coatings I Moderators: Anders Eriksson, Oerlikon Balzers, Oerlikon Surface Solutions AG, Liechtenstein, Marcus Hans, RWTH Aachen University, Germany, Jörg Patscheider, Evatec AG, Switzerland | | Advanced Characterization Techniques for Coatings, Thin Films, and Small Volumes Room Pacific Salon 1 - Session H3-1-WeM Variable Temperature Nanomechanics Moderators: Jeffrey M. Wheeler, ETH Zürich, Switzerland, James Gibson, RWTH Aachen University, Germany | |
|--|---|---|---|
| 8:00am | F4-1-WeM1 Microstructure and Piezoelectric Properties of Hexagonal Mg _x Zn _{1-x} O and Mg _x Zn _{1-x} O/ZnO Films at Lower Mg Compositions, H.-H. Chen, C.P. Liu, J.L. Huang , National Cheng Kung University, Taiwan | H3-1-WeM1 | On the Activation of Slip in the Mg-Al-Ca Laves Systems: A Combined Study Using High Temperature Indentation, Micropillar Compression and TEM, J. Gibson, C. Zehnder, S. Sandlöbes, S. Korte-Kerzel , RWTH Aachen University, Germany |
| 8:20am | F4-1-WeM2 Structure Optimization of Ta-O-N Films Prepared by Reactive HiPIMS for More Effective Water Splitting, Š. Batková , Department of Physics and NTIS - European Centre of Excellence, University of West Bohemia, Czech Republic; J. Čapek, S. Haviar, J. Houška, R. Čerstvý , University of West Bohemia, Czech Republic; M. Krbal , University of Pardubice, Czech Republic; T. Duchoň , Charles University, Czech Republic | H3-1-WeM2 | Recent Evolution of Instrumentation for Nanoindentation Measurements at Elevated Temperatures, P. Kempe, V. Haiblíková , Anton Paar, Switzerland |
| 8:40am | INVITED: F4-1-WeM3 A Sustainable and Viable Alternative to Low Cost Electronics based on Metal Oxides, E. Fortunato, R. Martins , New University of Lisbon, Portugal | H3-1-WeM3 | High Temperature Mechanical Characterization of Binary Cu-X Alloys Produced by Combinatorial Synthesis, V.G. Arigela , Max-Planck Institut für Eisenforschung, Germany; T. Oellers, A. Ludwig , Ruhr Universität Bochum, Germany; C.K. Kirchlechner, G. Dehm , Max-Planck Institut für Eisenforschung, Germany |
| 9:00am | Invited talk continues. | H3-1-WeM4 | Temperature and Strain-rate Dependence of the Mechanical Behavior of Freestanding Gold Thin Films, B. Merle , Friedrich Alexander-University Erlangen-Nürnberg (FAU), Germany |
| 9:20am | F4-1-WeM5 Photocatalytic Study for Indium Tantalum Oxide Thin Film in Visible Light, C. Li , National Yang Ming University, Taiwan; J.H. Hsieh , Ming Chi University of Technology, Taiwan; P. Hsueh , National Central University, Taiwan | INVITED: H3-1-WeM5 In-situ Investigation on Mechanical Properties at the Micrometer Scale in Cryogenic Environment, S.-W. Lee , University of Connecticut, USA | |
| 9:40am | | Invited talk continues. | |
| 10:00am | | | |
| 10:20am | SESSION BREAK: COMPLIMENTARY REFRESHMENTS IN EXHIBIT HALL | SESSION BREAK: COMPLIMENTARY REFRESHMENTS IN EXHIBIT HALL | |
| 10:40am | | | |
| 11:00am | F4-1-WeM10 Exploring Thin Film Zn-Sn-O (ZTO) Composition Spreads Using Combinatorial Sputtering, S.Y. Li, Y.H. Shen, K.-S. Chang, J.-M. Ting , National Cheng Kung University, Taiwan | EXHIBIT HALL CLOSING TODAY 10:00 am – 2:00 pm, Grand Hall Enjoy the Light Lunch at 12:20 pm (while supplies last) | |
| 11:20am | F4-1-WeM11 Can Thin-Film Technology Help to Realize The Einstein Gravity Quantum Computer?, N. Schwarzer , SIO, Germany | | |

Wednesday Morning, May 22, 2019

| | | |
|--|---|---|
| <p>Topical Symposia Room Pacific Salon 3 - Session TS1-1-WeM High Entropy and Other Multi-principal-element Materials I Moderators: Diederik Depla, Ghent University, Belgium, Ulf Jansson, Uppsala University, Angstrom Laboratory, Sweden</p> | | |
| 8:00am | <p>TS1-1-WeM1 Effect of Nitrogen Content on the Microstructure and Mechanical and Tribological Properties of Magnetron Sputtered FeMnNiCoCr Nitride Coatings, <i>C. Sha</i>, <i>P. Munroe</i>, University of New South Wales, Australia; <i>Z. Zhou</i>, City University of Hong Kong, Hong Kong; <i>Z. Xie</i>, University of Adelaide, Australia</p> | |
| 8:20am | <p>TS1-1-WeM2 Reactive Sputtering of High Entropy Alloys with Nitrogen – The Effect of Enthalpy and Entropy, <i>R. Dedoncker</i>, <i>D. Depla</i>, Ghent University, Belgium</p> | |
| 8:40am | <p>TS1-1-WeM3 Compositional Variations and Resulting Structure-property Correlations in Multicomponent Al-Cr-Nb-Y-Zr-N Thin Films, <i>K. Johansson</i>, <i>A. Srinath</i>, Uppsala University, Sweden; <i>L. Nyholm</i>, Uppsala University, Angstrom Laboratory, Sweden; <i>E. Lewin</i>, Uppsala University, Sweden</p> | |
| 9:00am | <p>TS1-1-WeM4 Exploring High Entropy Alloy Core Effects in Multi-principal Transition Metal-Al-Si-N, and Multi-principal Boride PVD Thin Films, <i>K. Yalamanchili</i>, <i>F. Doris</i>, <i>M. Arndt</i>, Oerlikon Balzers, Oerlikon Surface Solutions AG, Liechtenstein; <i>H. Rudigier</i>, Oerlikon Balzers, Oerlikon Surface Solutions AG, Switzerland</p> | |
| 9:20am | <p>TS1-1-WeM5 Mechanical Properties and Corrosion Resistance of Magnetron Sputtered Co-Cr-Fe-Mn-Ni-C Thin Films, <i>L. Zendejas Medina</i>, <i>P. Berastegui</i>, Uppsala University, Sweden; <i>L. Nyholm</i>, <i>U. Jansson</i>, Uppsala University, Angstrom Laboratory, Sweden</p> | |
| 9:40am | <p>TS1-1-WeM6 Thermal Property Evaluation of V-Nb-Mo-Ta-W and V-Nb-Mo-Ta-W-Cr-B High-entropy Alloy Thin Films, <i>S.B. Hung</i>, <i>C.J. Wang</i>, National Taiwan University of Science and Technology, Taiwan; <i>J.-W. Lee</i>, Ming Chi University of Technology, Taiwan</p> | |
| 10:00am | <p>SESSION BREAK: COMPLIMENTARY REFRESHMENTS IN EXHIBIT HALL</p> | |
| 10:20am | | |
| 10:40am | | |
| 11:00am | <p>INVITED: TS1-1-WeM10 Using Modeling and Machine Learning to Accelerate High-Throughput Experimental Materials Discovery, <i>J. Hattrick-Simpers</i>, <i>H. Joress</i>, National Institute of Standards and Technology, USA</p> | |
| 11:20am | <p>Invited talk continues.</p> | |
| 11:40am | <p>TS1-1-WeM12 Structure, Mechanical Properties and Thermal Stability of Magnetron Sputtered HfTaVWZr High-entropy Boride Coatings, <i>A. Kirnbauer</i>, <i>C.M. Koller</i>, TU Wien, Institute of Materials Science and Technology, Austria; <i>P. Polcik</i>, Plansee Composite Materials GmbH, Germany; <i>P.H. Mayrhofer</i>, TU Wien, Institute of Materials Science and Technology, Austria</p> | |
| | | <p>EXHIBIT HALL CLOSING TODAY 10:00 am – 2:00 pm, Grand Hall Enjoy the Light Lunch at 12:20 pm (while supplies last)</p> |

Special Interest Talk

Town & Country Room - Session SIT2-WeSIT

Special Interest Talk II: 1:00 – 1:40 pm

Moderators:

Christopher Muratore, University of Dayton, USA,

Michael Stüber, Karlsruhe Institute of Technology (KIT), Institute for Applied Materials (IAM), Germany

Linking Intrinsic Plasma Characteristics to the Microstructure and Properties of Thin Films

I. Petrov, University of Illinois, USA, Linköping University, Sweden, USA; *G. Greczynski*, *L. Hultman*, Linköping Univ., IFM, Thin Film Physics Div., Sweden; *J.E. Greene*, University of Illinois, USA, Linköping University, Sweden, National Taiwan Univ. Science & Technology, Taiwan

From its inception, the benefits of sputter deposition have stemmed from the presence of plasma in the vicinity of the growing film. Bombardment with charged particles and energetic photons affect the substrate initial condition and all stages of film growth: nucleation, coalescence, texture evolution, and recrystallization. Measuring and controlling the fluxes and energies of the charged particles incident at the substrate is essential to achieving low-temperature growth of high-quality thin films. Under typical direct current magnetron sputtering (DCMS) conditions, the dominant ion species incident at the growth surface while sputtering with N₂/Ar gas mixtures optimized to obtain stoichiometric nitride films is Ar⁺, while the ratio of the gas-ion flux to deposited metal flux J_i/J_{Me} is ≤ 1 . Densification is achieved by increasing the ion energy E_i commonly above 100 eV. However, at higher ion energies, a steep price is extracted in the form of residual ion-induced compressive stress resulting from both recoil implantation of surface atoms and trapping of rare-gas ions in the lattice. An alternative approach is offered by strongly magnetically-unbalanced magnetron sputter deposition systems, which allow ion-to-neutral flux ratios J_i/J_{Me} incident at the growing film to be varied over extremely wide ranges (up to > 20) at very low ion energies ($E_i \sim 10\text{-}20$ eV) (below the lattice displacement threshold). Using high-flux, low-energy ion irradiation during deposition opens new kinetic pathways to independently control the texture (from completely 111 to completely 200) and microstructure (from underdense to fully dense) in transition metal (TM) nitride films grown on amorphous substrates as well as to achieve low-temperature epitaxy of refractory materials and metastable alloys.

The invention of high power impulse magnetron sputtering (HiPIMS) opened the way to exploit metal-ion irradiation, which is particularly attractive for low-temperature growth of refractory ceramic thin films. HiPIMS discharges can ionize up to 90% of the sputtered metal flux; equally important is the time separation between metal- and gas-ion fluxes incident at the substrate. In recent years, it has been demonstrated that the use of synchronized bias to select the metal-rich portion of the ion flux provides a new dimension for ion-assisted growth in which momentum can be tuned by selection of the metal ion in the hybrid/cosputtering configuration and stresses can be eliminated/reduced since the metal ion is a component of the film. Thus, the control of intrinsic plasma conditions continues to drive research and caters to tooling-component, and microelectronics industry, as will be exemplified in the presentation.

Wednesday Afternoon, May 22, 2019

| Coatings for Use at High Temperatures Room Pacific Salon 2 - Session A3-WeA Materials and Coatings for Solar Power Concentration Plants Moderators: Vladislav Kolarik, Fraunhofer Institute for Chemical Technology ICT, Germany, Gustavo García-Martín, Universidad Complutense de Madrid, Spain | | Hard Coatings and Vapor Deposition Technologies Room California - Session B4-4-WeA Properties and Characterization of Hard Coatings and Surfaces IV Moderators: Naureen Ghafoor, Linköping Univ., IFM, Thin Film Physics Div., Sweden, Ulrich May, Robert Bosch GmbH, Germany, Fan-Bean Wu, National United University, Taiwan | |
|--|---|---|--|
| 2:00pm | INVITED: A3-WeA1 Materials and Coatings for Solar Power Concentration Plants, <i>C. Prieto Ríos</i> , Abengoa Research, Spain | B4-4-WeA1 Effect of Ti Interlayer on Stress Relief of ZrN/Ti Bilayer Thin Films on Si Substrate, <i>J.-H. Huang, T.-W. Zheng</i> , National Tsing Hua University, Taiwan | |
| 2:20pm | Invited talk continues. | B4-4-WeA2 In-situ Observation of Stress Fields during Crack Tip Shielding in Loaded Soft-hard Micro-Cantilevers using Cross-sectional X-ray Nanodiffraction, <i>M. Meindlhuber</i> , Montanuniversität Leoben, Department of Physical Metallurgy and Materials Testing, Austria; <i>J. Todt, J. Zálešák</i> , Erich Schmid Institute of Materials Science, Austrian Academy of Sciences, Leoben, Austria; <i>S. Klima, N. Jäger</i> , Montanuniversität Leoben, Department of Physical Metallurgy and Materials Testing, Austria; <i>M. Rosenthal, M. Burghammer</i> , ESRF Grenoble, France; <i>H. Hruby</i> , voestalpine eifeler Vacotec GmbH, Germany; <i>C. Mitterer, R. Daniel</i> , Montanuniversität Leoben, Department of Physical Metallurgy and Materials Testing, Austria; <i>J. Keckes</i> , Montanuniversität Leoben, Austria | |
| 2:40pm | A3-WeA3 Ductility and Creep Rupture Behavior of Diffusion Coatings Deposited on Grade 91 Steel for Concentrated Solar Power Applications, <i>C. Oskay, T. Meissner, C. Dobler, M.C. Galetz</i> , DECHEMA-Forschungsinstitut, Germany | B4-4-WeA3 Experimentally Parameterized Simulation of an Instrumented Dry Milling Arrangement – Parameter Study Identifying Damage-relevant Coating Properties for End Mills, <i>A.W. Nemetz, W. Daves, T. Klünsner, W. Ecker</i> , Materials Center Leoben Forschung GmbH, Austria; <i>C. Praetzas</i> , Institute of Production Management, Technology and Machine Tools (PTW), Germany; <i>C. Czettl, J. Schäfer</i> , CERATIZIT Austria GmbH, Austria | |
| 3:00pm | A3-WeA4 Long-term Molten Salt Corrosion of Aluminide Coatings for Heat Storage in Concentrated Solar Power Plants, <i>P. Audigié, S. Rodríguez, A. Agüero</i> , Instituto Nacional de Técnica Aeroespacial (INTA), Spain | B4-4-WeA4 Mechanical Properties and Cutting Performance of AlCrSiN and AlTiCrSiN Hard Coatings, <i>L.C. Chao, Y.-Y. Chang</i> , National Formosa University, Taiwan | |
| 3:20pm | A3-WeA5 Burn-in Heat Treatment to Form Aluminide Diffusion Coatings for Industrial Large Scale Application, <i>V. Kolarik, M. Juez Lorenzo, J. Bermejo Sanz, S. Weick</i> , Fraunhofer Institute for Chemical Technology ICT, Germany | B4-4-WeA5 Erosion, Corrosion Resistance and Hydrophobicity of Nano-layered and Multi-layered Nitride Coatings, <i>Q. Yang, L. Zhao, P. Patnaik</i> , National Research Council of Canada, Canada | |
| 3:40pm | A3-WeA6 High-Temperature Coatings For Protection of Steels in Contact with Molten Salt for CSP Technology, <i>G. García-Martín</i> , REP-Energy Solutions, Spain; <i>V. Encinas Sánchez</i> , Universidad Complutense de Madrid, Spain; <i>M.I. Lasanta Carrasco</i> , Universidad Complutense de Madrid, Spain; <i>T. de Miguel Gama, F.J. Pérez Trujillo</i> , Universidad Complutense de Madrid, Spain | B4-4-WeA6 Study of Erosion on Metals and Ceramic Coated Metals Using Magnetron Sputtering Process, <i>S. Hill, D.M. Mihut, A. Afshar, Z. Grantham, S. Sanchez-Lara, C.D. Raffield, N. Cordista, S. Sanchez Lara</i> , Mercer University, USA | |
| 4:00pm | AWARDS CONVOCATION: 5:45 pm, Town & Country Honorary R.F. Bunshah Award Lecture: Joe Greene “Some Highlights from over Four Decades of Thin-film Science” Awards Reception to follow at 7:30 pm, Golden Ballroom | B4-4-WeA7 Microstructure and Thermal Stability of Al-rich Ti-Al-Mo-N Protective Coatings, <i>C. Wüstefeld</i> , Institute of Materials Science, TU Bergakademie Freiberg, Germany; <i>M. Motylenko</i> , Technische Universität Bergakademie Freiberg, Germany; <i>S. Berndorf</i> , Institute of Materials Science, TU Bergakademie Freiberg, Germany; <i>M. Pohler, C. Czettl</i> , CERATIZIT Austria GmbH, Austria; <i>D. Rafaja</i> , Technische Universität Bergakademie Freiberg, Germany | |

Wednesday Afternoon, May 22, 2019

| Fundamentals and Technology of Multifunctional Materials and Devices Room Golden West - Session C2-WeA Novel Oxide Films for Active Devices Moderators: Marko Tadjer , Naval Research Laboratory, USA, Vanya Darakchieva , IFM, Linköping University, Sweden | | Tribology and Mechanical Behavior of Coatings and Engineered Surfaces Room San Diego - Session E1-4-WeA Friction, Wear, Lubrication Effects, and Modeling I Moderators: Nazlim Bagcivan , Schaeffler AG, Germany, Carsten Gachot , TU Wien, Institute for Engineering Design and Logistics Engineering, Austria | |
|--|--|---|---|
| 2:00pm | INVITED: C2-WeA1 The Physics of Low Symmetry Metal Oxides with Special Attention to Phonons, Plasmons and Excitons, A. Mock , Linköping University, Sweden | | |
| 2:20pm | Invited talk continues. | | E1-4-WeA2 Surface Characteristics of the Chameleon/PEO Coating after Fretting Wear Tests, M. Lin , A. Matthews , A. Yerokhin , University of Manchester, UK |
| 2:40pm | INVITED: C2-WeA3 Materials Interfaces for β -Ga ₂ O ₃ Power Devices, R.L. Peterson , University of Michigan, USA | | E1-4-WeA3 Characterization of W Alloyed DLC Coatings Deposited by a Hybrid DC / HIPIMS Magnetron Sputtering Process, M. Evaristo , A. Cavaleiro , SEG-CEMPRE - University of Coimbra, Portugal |
| 3:00pm | Invited talk continues. | | E1-4-WeA4 Tribological Improvement of Al with CNTs and Nb Nanopowder for Industrial Application, C.O. Ujah , P.A. Popoola , O.M. Popoola , Tshwane University of Technology, Pretoria, South Africa |
| 3:20pm | INVITED: C2-WeA5 Phase Selectivity in Heteroepitaxial Ga ₂ O ₃ Thin Films, V.D. Wheeler , N. Nepal , U.S. Naval Research Laboratory, USA; L.O. Nyakiti , Texas A&M University at Galveston, USA; D.R. Boris , S. Walton , D.J. Meyer , B.P. Downey , C.R. Eddy Jr. , U.S. Naval Research Laboratory, USA | | E1-4-WeA5 Influence of Interface Density on Tribological Performance of VN/TiN Multilayers, M.J. Rivera Chaverra , Universidad Nacional de Colombia Sede Manizales, Colombia; D. Escobar , Universidad Nacional de Colombia, Colombia; R. Ospina , Universidad Industrial de Santander, Bucaramanga, Santander, Colombia; M. Arroyave Franco , Universidad EAFIT A.A, Colombia; J.J. Olaya Florez , Universidad Nacional de Colombia, Colombia; E. Restrepo-Parra , Universidad Nacional de Colombia Sede Manizales, Colombia |
| 3:40pm | Invited talk continues. | | E1-4-WeA6 Analysis of Tribomechanical Behavior of Low-Temperature Plasma Blued Tool Steels, F. Santiago , ITESM Estado de México, Mexico; .R. Meza , Terminoynova, S.A. de C.V., Mexico; J. Oseguera-Peña , Tecnológico de Monterrey, México |
| 4:00pm | INVITED: C2-WeA7 Exfoliated β -Ga ₂ O ₃ Nano-layer based (Opto)electronic Devices, J. Kim , S. Oh , Korea University, Republic of Korea | | E1-4-WeA7 Improved Wear Resistance and Mechanical Properties of Multifunctional Polymer Nanocomposites for Advance Engineering Applications, U.O. Uyor , P.A. Popoola , O.M. Popoola , Tshwane University of Technology, Pretoria, South Africa |
| 4:20pm | Invited talk continues. | | |
| 4:40pm | C2-WeA9 Towards Controlled Exfoliation of β -Ga ₂ O ₃ through Ion Implantation, M.E. Liao , T. Bai , Y. Wang , M.S. Goorsky , UCLA, USA | | |
| 5:00pm | C2-WeA10 A Comparison of In-doped SnO ₂ (ITO) Films and Doped ZnO in Magnetron Sputtering: Both Thermodynamic and Kinetic Advantages of ITO Films, Y. Chen , F. Huang , F. Meng , Ningbo Institute of Materials Technology and Engineering, Chinese Academy of Sciences, China | AWARDS CONVOCATION: 5:45 pm, Town & Country Room Honorary R.F. Bunshah Award Lecture: Joe Greene “Some Highlights from over Four Decades of Thin-film Science” Awards Reception to follow at 7:30 pm, Golden Ballroom | |
| 5:20pm | C2-WeA11 Investigation on Microstructure and Piezoelectric Property of High Orientation Y-doped ZnO Thin Films via RF Magnetron Sputtering, L.C. Cheng , C.P. Liu , J.L. Huang , National Cheng Kung University, Taiwan | | |

Wednesday Afternoon, May 22, 2019

| | | |
|--------|--|---|
| | <p>New Horizons in Coatings and Thin Films Room Pacific Salon 6-7 - Session F4-2-WeA Functional Oxide and Oxynitride Coatings II Moderators: Anders Eriksson, Oerlikon Balzers, Oerlikon Surface Solutions AG, Liechtenstein, Marcus Hans, RWTH Aachen University, Germany, Jörg Patscheider, Evatec AG, Switzerland</p> | <p>Advanced Characterization Techniques for Coatings, Thin Films, and Small Volumes Room Pacific Salon 1 - Session H3-2-WeA Degradation under Extreme Conditions Moderators: James Gibson, RWTH Aachen University, Germany, Jeffrey M. Wheeler, ETH Zürich, Switzerland</p> |
| 2:00pm | | <p>H3-2-WeA1 Application of Micro-cantilever Bending to Probe the Fracture Behavior of Thin Film Interfaces, <i>J. Kabel, P. Hosemann</i>, University of California at Berkeley, USA; <i>T. Koyanagi, Y. Katah</i>, Oak Ridge National Laboratory, USA</p> |
| 2:20pm | | <p>H3-2-WeA2 Probing Fatigue Resistance in Multilayer DLC Coatings by Micro-impact: Correlation to Erosion Tests, <i>B.D. Beake</i>, Micro Materials Ltd, UK; <i>T. Liskiewicz, S. McMaster, A. Neville</i>, University of Leeds, UK</p> |
| 2:40pm | <p>F4-2-WeA3 Study on Silicon Carbide Based Metal Oxide Semiconductor Capacitor with Magnetron Sputtered ZrO₂ high-k Gate Dielectric, <i>R. Chandra, S. Mourya, G. Malik, J. Jaiswal</i>, IIC, IIT Roorkee, India</p> | <p>H3-2-WeA3 Development of an In-Situ Ion Irradiation and Nanomechanics Scanning Electron Microscope, <i>K. Hattar, N. Heckman, S.A. Briggs, C.M. Barr, A.M. Monterrosa, C. Chisholm, L. Treadwell, B.L. Boyce</i>, Sandia National Laboratories, USA</p> |
| 3:00pm | <p>F4-2-WeA4 Structural, Optical and Electrochromic Properties of Nanocrystalline WO₃ Thin Films, <i>M.V. Kalapala</i>, VFSTR University, India</p> | <p>H3-2-WeA4 Proton Radiation and He Implantation Effect on Radiation-resistant Zr/Nb Sputtered Multilayer Coatings, <i>T. Polcar</i>, Czech Technical University in Prague, Czech Republic; <i>M. Callisti</i>, University of Cambridge, UK; <i>S. Sen, H.Y. Yavas</i>, Czech Technical University in Prague, Czech Republic; <i>A. Lider</i>, Tomsk State University, Czech Republic</p> |
| 3:20pm | <p>F4-2-WeA5 Structure, Mechanical Characteristics and Thermal Stability of HS-PVD (Al,Cr)₂O₃ Coatings, <i>K. Bobzin, T. Brögelmann, C. Kalscheuer, M. Welters</i>, Surface Engineering Institute - RWTH Aachen University, Germany</p> | <p>H3-2-WeA5 Tracking the Temporal Oxidation Behavior in TiN Thin Films by In-situ Resistivity Measurements, <i>B. Stelzer, X. Chen, J.A. Sälker, J.M. Schneider</i>, RWTH Aachen University, Germany</p> |
| 3:40pm | <p>F4-2-WeA6 Reactive HiPIMS Deposition of γ-Al₂O₃ Thin Films using Transition Metal Doped Al Targets, <i>S. Kagerer, L. Zauner</i>, TU Wien, Institute of Materials Science, Austria; <i>S. Koloszári</i>, Plansee Composite Materials GmbH, Germany; <i>J. Čapek, T. Kozák, P. Zeman</i>, University of West Bohemia, Czech Republic; <i>H. Riedl</i>, TU Wien, Institute of Materials Science, Austria; <i>P.H. Mayrhofer</i>, Institute of Materials Science and Technology, TU Wien, Austria</p> | <p>H3-2-WeA6 Industrial XRF Coating Thickness Analyzer for Real Time Measurement of Aluminum Deposited on Rolled Steel, <i>J.I. Hasikova, A.D. Sokolov, A. Pecerskis, A. Pone, V. Gostilo</i>, Baltic Scientific Instruments, Latvia</p> |
| 4:00pm | <p>F4-2-WeA7 Influence of V Content on Phase Evolution and Thermal Stability of Reactive Pulsed DC Magnetron Sputtered (Al,V)₂O₃, <i>L.L. Landölv</i>, Linköping Univ., IFM, Thin Film Physics Div. and Sandvik Coromant R&D, Sweden; <i>C-F. Carlström</i>, Sandvik Coromant R&D, Sweden; <i>J. Lu</i>, Linköping Univ., IFM, Thin Film Physics Div., Sweden; <i>M.P. Johansson-Jöesaar</i>, SECO tools AB, Sweden; <i>M. Ahlgren, E. Göthelid</i>, Sandvik Coromant R&D, Sweden; <i>B. Alling, L. Hultman, P. Eklund</i>, Linköping Univ., IFM, Thin Film Physics Div., Sweden</p> | <p>H3-2-WeA7 In situ Characterization of Dual Phase Diamond-like Carbon (DLC) at Elevated Temperatures, <i>M. Chen</i>, ETH Zürich, Switzerland; <i>C. Liu, K.Y. Li</i>, City University of Hong Kong, China; <i>R. Spolenak, J.M. Wheeler</i>, ETH Zürich, Switzerland</p> |
| 4:20pm | <p>F4-2-WeA8 Al Vacancies in Wurtzite Al-(Si)-(O)-N: Theory and Experimental Assessment, <i>M. Fischer, M. Trant, K. Thorwarth, D. Scopece, C.A. Pignedoli, D. Passerone, H.J. Hug</i>, Empa - Swiss Federal Laboratories for Materials Science and Technology, Switzerland</p> | <p>H3-2-WeA8 In situ micro-Tensile Testing of TiN Coating: Deformation and Fracture in Relation to Residual Stress, <i>E.J. Herrera Jimenez</i>, École Polytechnique de Montréal, Canada; <i>N. Vanderesse</i>, École de Technologie Supérieure, Canada; <i>T. Schmitt, É. Bousser</i>, École Polytechnique de Montréal, Canada; <i>P. Bocher</i>, École de Technologie Supérieure, Canada; <i>L. Martinu, J.E. Klemberg-Sapieha</i>, École Polytechnique de Montréal, Canada</p> |
| 4:40pm | <p>INVITED: F4-2-WeA9 Thermal Atomic Layer Etching of Oxide and Nitride Thin Films, <i>S.M. George</i>, University of Colorado at Boulder, USA</p> | <p>H3-2-WeA9 Small Scale Fracture of Mo₂BC Coatings, <i>H.G. Gopalan, R.S. Soler, S.G. Gleich, C.K. Kirchlechner, C.S. Scheu</i>, Max-Planck Institut für Eisenforschung, Germany; <i>J.M. Schneider</i>, RWTH Aachen University, Germany; <i>G. Dehm, V.G. Arigela</i>, Max-Planck Institut für Eisenforschung, Germany</p> |
| 5:00pm | Invited talk continues. | <p>H3-2-WeA10 The Effect of Selected Laser Beam Micromilling Parameters on the Surface Layer Structure of HVOF Sprayed WC-CoCr Coating, <i>A. Iwaniak</i>, Silesian University of Technology, Poland; <i>L. Norymberczyk</i>, ANGA Uszczelnienia Mechaniczne Sp. z o.o., Poland</p> |
| 5:20pm | <p>F4-2-WeA11 Growth and Characterization ALD Films with a new Continuous Flow Process, <i>B. Kuyel, A. Alphonse, K.P. Hong</i>, Nano-Master, Inc., USA</p> | |

Wednesday Afternoon, May 22, 2019

| Topical Symposia Room Pacific Salon 3 - Session TS1-2-WeA High Entropy and Other Multi-principal-element Materials II Moderators: Diederik Depla, Ghent University, Belgium, Ulf Jansson, Uppsala University, Angstrom Laboratory, Sweden | |
|--|--|
| 2:00pm | TS1-2-WeA1 Structure and Mechanical Properties of Refractory Type High-entropy Alloy Thin Films Deposited by Vacuum-arc, M. Kuczyk, U. Nimsch, O. Zimmer, J. Kaspar, F. Kaufjuss, A. Leson, M. Zimmermann, C. Leyens , Fraunhofer Institute for Material and Beam Technology (IWS), Germany |
| 2:20pm | TS1-2-WeA2 Templated Stacking of Organic/Inorganic Semiconductors Crystals Upon Coalescence, Assembly and Split Behaviors of High-entropy Ferroelectric Lamellar Crystals, J.-J. Ruan, C.-H. Pan, J.-M. Ting, K.-S. Chang, Y.-H. Su , National Cheng Kung University, Taiwan |
| 2:40pm | TS1-2-WeA3 Angular-dependent Deposition of High Entropy Alloy Thin Films by DCMS, HiPIMS and Cathodic Arc, A. Xia , Montanuniversität Leoben, Austria; A. Togni , University of Modena and Reggio Emilia, Italy; S. Hirn , Montanuniversität Leoben, Austria; L. Lusvarghib , University of Modena and Reggio Emilia, Italy; R. Franz , Montanuniversität Leoben, Austria |
| 3:00pm | TS1-2-WeA4 Combustion Synthesis of High Entropy Alloys Thin Films: AlCrFeNi, AlCrCuFeNi, and AlCoCrFeNi, A.N. Wang, M. Hopfeld, T. Kups, D. Flock, H. Romanus, L.-B. Kellmann, H. Rupapara, P. Schaaf , Technische Universität Ilmenau, Germany |
| 3:20pm | TS1-2-WeA5 Nanostructured Highly Concentrated Solid Solution Alloy Coatings on a Zirconium Based Alloy, M.A. Tunes, S.E. Donnelly , Institute for Materials Science, University of Huddersfield, UK; P.D. Edmondson , Oak Ridge National Laboratory, USA; V. Vishnyakov , University of Huddersfield, UK |
| 3:40pm | TS1-2-WeA6 High Temperature Electrical Conductivity and Oxidation Resistance of V-Nb-Mo-Ta-W High Entropy Alloy Thin Films, Y.Y. Chen , Ming Chi University of Technology, Taiwan; S.B. Hung, C.J. Wang, W.-C.J. Wei , National Taiwan University of Science and Technology, Taiwan; J.-W. Lee , Ming Chi University of Technology, Taiwan |
| 4:00pm | INVITED: TS1-2-WeA7 Micro-mechanics of High Entropy Alloys: Size Effects and Rate Sensitivity, Y. Xiao, R. Spolenak, J.M. Wheeler , ETH Zürich, Switzerland |
| 4:20pm | Invited talk continues. |
| 4:40pm | TS1-2-WeA9 Is the Entropy of High Entropy Ceramics High?, J.M. Schneider, S. Evertz, D. Neuß, M.K. Steinhoff, D.M. Holzapfel , RWTH Aachen University, Germany; S. Koloszári , Plansee Composite Materials GmbH, Germany; P. Polcik , PLANSEE Composite Materials GmbH, Germany; H. Rueß , RWTH Aachen University, Germany |
| 5:00pm | TS1-2-WeA10 Next Generation Entropy Stabilized Material, J.-M. Ting, J.J. Ting, K.-S. Chang, Y.-H. Su , National Cheng Kung University, Taiwan |
| AWARDS CONVOCATION: 5:45 pm, Town & Country Room Honorary R.F. Bunshah Award Lecture: Joe Greene “Some Highlights from over Four Decades of Thin-film Science” Awards Reception to follow at 7:30 pm, Golden Ballroom | |

Awards Convocation and R.F. Bunshah Award Honorary Lecture

Town & Country Room - Session HL-WeHL

5:45 – 7:00 pm

“Some Highlights from over Four Decades of Thin-Film Science”

Joe Greene, Materials Science and Physics Departments, University of Illinois, Physics Department, Linköping University, Linköping, Sweden, Materials Science Dept., National Taiwan Univ. of Science & Technology

As a graduate student at USC, I was growing epitaxial GaAs(001) films by liquid-phase epitaxy. The layers were of very high purity as demonstrated by Hall and photoluminescence measurements, but we had no techniques sensitive enough to determine the remaining residual impurities. This led me to develop glow-discharge optical spectroscopy (GDOS), the optical analog of modern SIMS. As-deposited films were sputter etched and a spectrometer used to scan the emission peaks arising from the decay of sputtered atoms excited in the discharge. We found that the primary residual impurity was Sn and, via the use of calibration samples (based upon Hall measurements), we determined absolute Sn concentrations (initial detection limit = 3×10^{16} atoms/cm³, 680 ppb). Since then, we, and many others worldwide, have employed GDOS to quantitatively measure dopant diffusion and ion-implantation profiles in III-V, SiGe, and solar cell absorber layers. GDOS is also used to analyze bulk and thin-film alloys, for real-time process control (film growth rates and thicknesses) during sputter deposition, and for feedback control during high-rate reactive sputtering.

At UIUC, in addition to GDOS, I continued epitaxial semiconductor film growth, but switched to SiGe via UHV-CVD, metastable (III-V)_{1-x}(IV₂)_x (the “Greene” alloys) by UHV sputter deposition, and GaN by reactive-ion MBE. SiGe CVD was carried out in UHV in order to employ in-situ surface-science tools (RHEED, TPD, AES, XPS, UPS, HR-EELS, STM) to investigate atomic-scale growth kinetics. We developed models, with no fitting parameters, to accurately predict Si, Si_{1-x}Ge_x, Si_{1-x}C_x, and Ge_{1-x}Sn_x film growth rates, compositions, and doping profiles as a function of precursor partial pressures and deposition temperatures. The models are still used worldwide today. The Greene alloys (e.g.: (GaAs)_{1-x}(Ge₂)_x) were grown across pseudobinary phase diagrams and exhibited good thermal stability. They have interesting electronic transport, band structure, and phonon properties and are currently used in tunable photodetector and piezoelectric devices. The first high-resistivity single-crystal GaN films, both wurtzite and zincblende, were grown by MBE using evaporated Ga and 35 eV N₂₊ ions. The layers, which had the highest electron mobilities yet reported, were used to determine hexagonal and cubic GaN band structures.

Following an invitation to present a Swedish Academy of Science Lecture in the 1980s, colleagues from Linköping University ignited my interest in transition-metal (TM) nitrides (and, recently, TM diborides). The field of nitride hard-coatings was already developing rapidly, but reported properties varied by up to orders of magnitude. Thus, we hoped to make a contribution by growing and measuring fundamental properties of single-crystal compounds and alloys of groups IIIB, IVB, VB, and VIB TM nitrides using *tunable* magnetically-unbalanced magnetron sputtering which, together with Bill Sproul, Dieter Münz, and Ivan Petrov (all Bunshah Award winners), we developed in 1992. We also demonstrated vacancy hardening, enhanced hardness in superlattices with alternate layers chosen to have large differences in shear moduli, strong electron/phonon interactions, enhanced ductility using alloy design via electronic structure, and self-organized nanostructures. With polycrystalline TM nitrides, we developed a process for real-time control of preferred orientation using high-flux/low-energy ion irradiation and, recently, the growth of fully-dense/low-stress/high-hardness alloys, with no substrate heating, based upon a novel hybrid dc-magnetron/HiPIMS approach. Last year, we were the first to demonstrate controlled B/TM ratios in diboride layers using strong external magnetic fields during magnetron sputtering and controlling pulse lengths, at constant power and frequency, during HiPIMS.

Joe Greene is the D.B. Willett Professor of Materials Science and Physics at the University of Illinois, the Tage Erlander Professor of Materials Physics at Linköping University, Sweden, and a Chaired Professor at the National Taiwan University of Science and Technology. The focus of his research has been the development of an atomic-level understanding of adatom/surface interactions during the dynamic process of vapor-phase crystal growth in order to controllably manipulate nanochemistry, nanostructure, and, hence, physical properties. His work has involved nanoscience and film growth by all forms of sputter deposition, solid and gas-source MBE, UHV-CVD, MOCVD, and ALE. Joe has published more than 625 papers and review articles, 29 book chapters, and co-edited 4 books in the general areas of crystal growth, thin-film physics, and surface science. In particular, he has used hyperthermal condensing species and UV photochemistry for probing as well as stimulating surface reactions that do not proceed thermally. Joe has presented over 525 invited talks, 140 Plenary Lectures at international meetings, and has an h-factor of 78.

He is currently Editor-in-Chief of *Thin Solid Films* and past Editor of *CRC Critical Reviews in Solid State and Materials Sciences*. Joe is active in the AVS where he has served on the Trustees, twice as a member of the Board of Directors, as President of the society in 1989, and is currently Secretary. He has also Chaired the AVS Thin Film and Advanced Surface Engineering Divisions; the IUVESTA Education, Emerging Societies, and Thin Film Committees; and served on the Governing Board of the American Institute of Physics and the Executive Committee of the APS Division of Materials Physics. He is the US representative to the International Union of Vacuum Science and Techniques. Joe is a Fellow of AVS, APS, and MRS. For a list of his awards see page 14.

Thursday Morning, May 23, 2019

| Coatings for Use at High Temperatures Room Pacific Salon 2 - Session A2-1-ThM Thermal and Environmental Barrier Coatings I Moderators: Sabine Faulhaber, University of California, San Diego, USA, Kang N. Lee, NASA Glenn Research Center, USA, Pantcho Stoyanov, Pratt & Whitney, USA | | Hard Coatings and Vapor Deposition Technologies Room California - Session B6-ThM Coating Design and Architectures Moderators: Shou-Yi Chang, National Tsing Hua University, Taiwan, Paul Heinz Mayrhofer, Institute of Materials Science and Technology, TU Wien, Austria | |
|--|--|--|---|
| 8:00am | INVITED: A2-1-ThM1 Mechanical Characterization and Modelling Issues for Thermal Barrier Coating Lifetime Assessment, <i>V. Maurel, V. Guipont</i> , Mines-ParisTech, France | B6-ThM1 | The Mechanical and Tribological Properties of Boron Based Films Grown by HiPIMS Under Different N ₂ Contents, <i>A. Keles, I. Efeoğlu, Y. Totik</i> , Ataturk University, Turkey |
| 8:20am | Invited talk continues. | B6-ThM2 | Peculiar Oscillations in Nano-scale AlN/TiN and Other Nitride-based Superlattices, <i>N. Koutna</i> , Institute of Materials Science and Technology, TU Wien, Austria; <i>P.R. Řehák</i> , Institute of Physics of Materials, Academy of Sciences of the Czech Republic, Czech Republic; <i>Z. Zhang</i> , Erich Schmid Institute of Materials Science, Austrian Academy of Sciences, Leoben, Austria; <i>M. Černý</i> , Central European Institute of Technology, CEITEC VUT, Brno University of Technology, Czech Republic; <i>M. Bartosik</i> , Institute of Materials Science and Technology, TU Wien, Austria; <i>M.F. Friák, M.S. Šob</i> , Institute of Physics of Materials, Academy of Sciences of the Czech Republic, Czech Republic; <i>P.H. Mayrhofer</i> , Institute of Materials Science and Technology, TU Wien, Austria; <i>D. Holec</i> , Department of Physical Metallurgy and Materials Testing, Montanuniversität Leoben, Austria |
| 8:40am | A2-1-ThM3 The Effect of Bond Coat Asperity Removal on the Lifetime of Atmospheric Plasma Sprayed Thermal Barrier Coatings, <i>K.A. Kane</i> , Oak Ridge National Laboratory, USA; <i>M.L. Sweet</i> , Praxair, USA; <i>M.J. Lance, B.A. Pint</i> , Oak Ridge National Laboratory, USA | B6-ThM3 | Impact Fatigue and Mechanical Properties of AlTiCrN and AlTiCrSiN Hard Coatings with Optimal Design of Interlayers, <i>Y.J. Yang, Y.-Y. Chang, S.Y. Weng</i> , National Formosa University, Taiwan |
| 9:00am | A2-1-ThM4 Effect of Superalloy Substrate on the Lifetime of Electron Beam Physical Vapour Deposited Thermal Barrier Coatings, <i>C.L. Liu, Y.C. Chen, P. Xiao</i> , University of Manchester, UK | B6-ThM4 | Improvement of CrMoN/ SiN _x Multilayered Coatings on Mechanical and High Temperature Tribological Properties, <i>W.L. Lo, L.K. Yeh-Liu, J.W. Lee, J.G. Duh</i> , National Tsing Hua University, Taiwan |
| 9:20am | A2-1-ThM5 Self-Healing Thermal Barrier Coatings Produced by Laser Processing, <i>W. Wei, J. Gu, S.S. Joshi, T. Huang, N.B. Dahotre, S.M. Aouadi</i> , University of North Texas, USA | B6-ThM5 | Tuning the Hardness–toughness Relationship by Combining MoN with TaN, <i>F.F. Klimashin, N. Koutna, L. Lobmaier</i> , TU Wien, Institute of Materials Science and Technology, Austria; <i>D. Holec</i> , Montanuniversität Leoben, Austria; <i>P.H. Mayrhofer</i> , TU Wien, Institute of Materials Science and Technology, Austria |
| 9:40am | A2-1-ThM6 Influence of Heat Treatment on Thermal Cyclic Fatigue Lifetime of TBC System, <i>J.H. He, T. Sharobem</i> , Oerlikon Metco, USA | B6-ThM6 | Microstructure, Mechanical and Tribological Performance of Complex TiAlTaN-[TiAlN/TaN _n] Coatings: Understanding the Effect of Volume Fraction, <i>E. Contreras, J. Cortínez</i> , Universidad de Antioquia, Colombia; <i>A. Hurtado</i> , Centro de Investigación en Materiales Avanzados CIMA, Mexico; <i>M.A. Gómez</i> , Universidad de Antioquia, Colombia |
| 10:00am | A2-1-ThM7 Environmental Barrier Coating Development for High Temperature SiC Ceramic Matrix Composite Components, <i>M.M. Gentleman, M.L. Sweet, B. Richards</i> , Praxair Surface Technologies Inc., USA | INVITED: B6-ThM7 | Plastic Deformation in Transition-Metal Nitrides and Carbides via Density-Functional Molecular Dynamics, <i>D.G. Sangiovanni</i> , Linköping University, Sweden, Ruhr-Universität Bochum, Germany |
| 10:20am | A2-1-ThM8 Effects of Chemical Modification on Bond Coat Oxidation and Internal Stresses in Yb ₂ Si ₂ O ₇ Environmental Barrier Coatings, <i>B. Herren</i> , California Institute of Technology, USA; <i>J. Almer</i> , Argonne National Laboratory, USA; <i>K. Lee</i> , NASA Glenn Research Center, USA; <i>K.T. Faber</i> , California Institute of Tech., USA | | Invited talk continues. |
| 10:40am | A2-1-ThM9 Thermal Shock and CMAS Resistant Tunable Self-Healing Thermal Barrier Coatings, <i>J. Gu, W. Wei, T. Huang, S. Bakkar, D. Berman, R.F. Reidy, S.M. Aouadi</i> , University of North Texas, USA | B6-ThM9 | Phase Evolution and Mechanical Properties of Isostructural Decomposing W _{1-x} M _x B ₂ Thin Films, <i>V. Moraes, L. Zauner</i> , TU Wien, Institute of Materials Science, Austria; <i>H. Bolvardi</i> , Oerlikon Balzers, Oerlikon Surface Solutions AG, Liechtenstein; <i>P. Polcik</i> , Plansee Composite Materials GmbH, Germany; <i>H. Riedl, P.H. Mayrhofer</i> , TU Wien, Institute of Materials Science, Austria |
| 11:00am | A2-1-ThM10 Variables Affecting Steam Oxidation Kinetics of Environmental Barrier Coatings, <i>K. Lee</i> , NASA Glenn Research Center, USA | B6-ThM10 | Van der Waals Layer Promoted Heteroepitaxy in Sputter-deposited Thin Films, <i>K. Tanaka, P. Arias, M.E. Liao, Y. Wang, H. Zaid, A. Aleman, M.S. Goorsky, S. Kodambaka</i> , University of California, Los Angeles, USA |
| 11:20am | A2-1-ThM11 High Temperature Investigations of Thermochemistry and Phase Stability in the ZrO ₂ -Y ₂ O ₃ -Ta ₂ O ₅ System, <i>M. Lepple</i> , DECHEMA Forschungsinstitut, Technische Universität Darmstadt, Germany; <i>S.V. Ushakov, K. Lilova</i> , University of California, Davis, USA; <i>C.A. Macauley, C.G. Levi</i> , University of California, Santa Barbara, USA; <i>A. Navrotsky</i> , University of California, Davis, USA | B6-ThM11 | Improvement of Tribological Properties for Hard Coatings by Stress Control, <i>T.M. Shao</i> , State Key Laboratory of Tribology, Tsinghua University, China |
| 11:40am | ELSEVIER FOCUSED TOPIC SESSION THURSDAY, 12:20 – 1:20 pm, Golden West “The Art of Publishing” Samir Aouadi | | B6-ThM12 Is WB _{2-z} a Proper Base System for Designing Ternary Diboride based Thin Films?, <i>H. Riedl, V. Moraes, C. Fuger, H. Euchner, R. Hahn, T. Wojcik</i> , TU Wien, CDL AOS at the Institute of Materials Science, Austria; <i>M. Arndt</i> , Oerlikon Balzers, Oerlikon Surface Solutions AG, Liechtenstein; <i>P. Polcik</i> , Plansee Composite Materials GmbH, Germany; <i>P.H. Mayrhofer</i> , TU Wien, Institute of Materials Science, Austria |

Thursday Morning, May 23, 2019

| | | |
|---------|---|--|
| | <p>Fundamentals and Technology of Multifunctional Materials and Devices Room Pacific Salon 3 - Session C3+C2+C1-ThM Thin Films for Energy-related Applications II/Novel Oxide Films for Active Devices/Optical Metrology in Design, Optimization, and Production of Multifunctional Materials Moderators: Per Eklund, Linköping Univ., IFM, Thin Film Physics Div., Sweden, Tushar Shimpi, Colorado State University, USA</p> | <p>Tribology and Mechanical Behavior of Coatings and Engineered Surfaces Room San Diego - Session E1-1-ThM Friction, Wear, Lubrication Effects, and Modeling II Moderators: Nazlim Bagcivan, Schaeffler AG, Germany, Carsten Gachot, TU Wien, Institute for Engineering Design and Logistics Engineering, Austria, Tomas Polcar, Czech Technical University in Prague, Czech Republic</p> |
| 8:00am | | |
| 8:20am | | |
| 8:40am | <p>C3+C2+C1-ThM3 Nanoflaky Titanium Dioxide Grown on Titanium Foil for Capacitive Deionization Purpose, J.T. Huang, P.-Y. Hsieh, J.L. He, Feng Chia University, Taiwan</p> | <p>E1-1-ThM3 Sliding Wear Resistance of Nickel Boride Layers on Inconel 718 Superalloy, I.E. Campos-Silva, Instituto Politecnico Nacional Grupo Ingeniería de Superficies, México; A.D. Contla-Pacheco, Instituto Politecnico Nacional, Grupo</p> |
| 9:00am | <p>C3+C2+C1-ThM4 Mixed-oxide Coated Ni Foam for High Performance Supercapacitor, K.C. Lin, National Cheng Kung University, Taiwan</p> | <p>E1-1-ThM4 A Study of the Wear Mechanism of PTFE: The Effects of Temperature and Environment on its Mechanical and Tribological Properties, V. Saisnith, V. Fridrici, Ecole Centrale de Lyon, LTDS - Université de Lyon, France</p> |
| 9:20am | <p>INVITED: C3+C2+C1-ThM5 Wavefront Shaping: A New Tool in Optics, M. N'Gom, University of Michigan, USA</p> | <p>E1-1-ThM5 Harness Intrinsic Friction in Transition Metal Dichalcogenides, A. Cammarata, Czech Technical University in Prague, Czech Republic; T.P. Polcar, University of Southampton, UK</p> |
| 9:40am | Invited talk continues. | <p>E1-1-ThM6 Static Friction at High Temperature: from Methodology to Severe-Service Valve Application, T. Schmitt, J.A. Schmitt, Polytechnique Montréal, Canada; É. Bousser, École Polytechnique de Montréal, Canada; M. Azzi, Tricomat, Canada; F. Khelfaoui, V. Najarian, L. Vernhes, Velan; J.E. Klemberg-Sapieha, Polytechnique Montréal, Canada</p> |
| 10:00am | <p>C3+C2+C1-ThM7 Optical Optimisation of Semi-transparent a-Si:H Solar Cells for Photobioreactor Application, A. Brodu, C. Ducros, Univ. Grenoble Alpes, CEA, France; C. Dublanche-Tixier, Univ. Limoges, France; C. Seydoux, G. Finazzi, Univ. Grenoble Alpes, CNRS, CEA, France</p> | <p>INVITED: E1-1-ThM7 Coating Development, Characterization and Application-oriented Tests, L.P. Nielsen, K.P. Almqvist, B.H. Christensen, S. Louring, Danish Technological Institute, Denmark; H. Ronkainen, T.J. Hakala, VTT Technical Research Centre of Finland, Finland; D. Drees, FALEX Tribology, Belgium</p> |
| 10:20am | <p>C3+C2+C1-ThM8 Properties of Highly Transparent AlN/SiO_x Multilayer Systems, C. Appleget, A. Sáenz-Trevizo, A.M. Hodge, University of Southern California, USA</p> | Invited talk continues. |
| 10:40am | <p>C3+C2+C1-ThM9 Tailoring the Optical Properties of Highly Porous Superlattice-type Si-Au Slanted Columnar Heterostructure Thin Films, U. Kilic, University of Nebraska-Lincoln, USA; A. Mock, Linköping University, Sweden; R. Feder, The Fraunhofer Institute for Microstructure of Materials and Systems (IMWS), Germany; D. Sekora, M. Hilfiker, R. Korlacki, E. Schubert, C. Argyropoulos, M. Schubert, University of Nebraska Lincoln, USA</p> | |
| 11:00am | <p>C3+C2+C1-ThM10 Microstructures and Optoelectronic Properties of Cu₃N Thin Films and its Diode Rectification Characteristics, Y.H. Chen, S.C. Chen, S. Sakalley, S.Y. Huang, A. Paliwal, Ming Chi University of Technology, Taiwan; M.H. Liao, National Taiwan University, Taiwan; H. Sun, Shandong University at Weihai, China; S. Biring, Ming Chi University of Technology, Taiwan</p> | |
| 11:20am | <p>C3+C2+C1-ThM11 Effects of the Frequency of Pulsed DC Sputtering Power on Amorphous Carbon Film used for Metallic Bipolar Plates in Proton Exchange Membrane Fuel Cells, X.B. Li, P.Y. Yi, L.F. Peng, X.M. Lai, Shanghai Jiaotong University, China</p> | <p>2020 ICMCTF INFORMATION SESSION THURSDAY, 12:20 – 1:20 pm California Room</p> |
| 11:40am | <p>C3+C2+C1-ThM12 On the Mechanisms of Halloysite Nanotubes Incorporation in the Surface Layer of Forsterite Grown by Plasma Electrolytic Oxidation, B. Mingo, Y. Guo, A. Němcová, A. Gholinia, A. Matthews, A. Yerokhin, The University of Manchester, UK</p> | <p>ELSEVIER FOCUSED TOPIC SESSION THURSDAY, 12:20 – 1:20 pm, Golden West</p> |
| 12:00pm | <p>C3+C2+C1-ThM13 Inorganic-Organic Perovskites: Handle with Care, Properties May Depend on It, N.J. Podraza, B. Subedi, M.M. Junda, K. Ghimire, University of Toledo, USA</p> | <p>“The Art of Publishing” Samir Auadi</p> |

Thursday Morning, May 23, 2019

| | | |
|---------|---|---|
| | <p>New Horizons in Coatings and Thin Films Room Pacific Salon 6-7 - Session F2-1-ThM HiPIMS, Pulsed Plasmas and Energetic Deposition I Moderators: Jon Tomas Gudmundsson, University of Iceland, Iceland, Tiberiu Minea, LPGP, Université Paris-Sud, Orsay, France</p> | <p>Surface Engineering - Applied Research and Industrial Applications Room Pacific Salon 1 - Session G1+G3-ThM Advances in Industrial PVD, CVD, and PECVD Processes and Equipment/Innovative Surface Engineering for Advanced Cutting and Forming Tool Applications Moderators: Ladislav Bardos, Uppsala University, Sweden, Emmanuelle Göthelid, Sandvik Machining Solutions, Sweden, Ali Khatibi, Oerlikon Balzers, Oerlikon Surface Solutions AG, Liechtenstein, Christoph Schiffers, CemeCon AG, Germany</p> |
| 8:00am | | <p>G1+G3-ThM1 Predicting Coating Uniformity and Cathode Utilization in Magnetron Sputtering Applications using Numerical Simulation, A. Obrusnik, P. Zikan, Plasma Solve, Brno, Czech Republic</p> |
| 8:20am | | <p>G1+G3-ThM2 Multinary HiPIMS, T. Leyendecker, W. Koelker, S. Bolz, C. Schiffers, CemeCon AG, Germany</p> |
| 8:40am | <p>INVITED: F2-1-ThM3 Recent Insights into HiPIMS Physics via Coherent and Incoherent Thomson Scattering, S. Tsikata, CNRS, ICARE, France; T. Minea, Université Paris-Sud/CNRS, France; B. Vincent, CNRS, France; A. Revel, Université Paris-Sud/CNRS, France</p> | <p>G1+G3-ThM3 From Small Parts to Particles – Experiences in Bulk Coating, H. Klostermann, F. Fietzke, B.G. Kraetzschmar, Fraunhofer FEP, Germany</p> |
| 9:00am | Invited talk continues. | <p>G1+G3-ThM4 A Novel Industrial Coating System for the Deposition of Smooth Hard Coatings Combining HiPIMS V+ and Rotatable Magnetrons, H. Gabriel, J.A. Santiago Varela, PVT Plasma und Vakuum Technik GmbH, Germany; I. Fernandez, N4E Nano4Energy S.L.N.E, Spain; N. Dams, PVT Plasma und Vakuum Technik GmbH, Germany; A. Wennberg, N4E Nano4Energy S.L.N.E, Spain; J. Lu, PVT Harbin Coating Ltd, China</p> |
| 9:20am | <p>F2-1-ThM5 Process Gas Rarefaction and Other Transport Phenomena in High Power Impulse Magnetron Sputtering Discharges Studied by Particle Simulations, T. Kozák, University of West Bohemia, Czech Republic</p> | <p>INVITED: G1+G3-ThM5 From DCMS to HiPIMS: A Giant Leap for Cutting Tools?, B. Gaedike, Hartmetall-Werkzeugfabrik Paul Horn GmbH, Germany</p> |
| 9:40am | <p>F2-1-ThM6 Insight on the Sputtered Material in HiPIMS by 2D PIC-MCC Modeling, A. Revel, Université Paris-Sud/CNRS, France; T. Minea, Université Paris-Sud, Université Paris-Saclay, France</p> | Invited talk continues. |
| 10:00am | <p>F2-1-ThM7 Spoke Formation in Large Scale Rectangular Magnetrons, A.P. Ehasarian, Sheffield Hallam University, UK</p> | <p>G1+G3-ThM7 Application of Twin-Roll PECVD for Surface Functionalization on Flexible Substrate, Y. Isomura, Y. Ikari, T. Okimoto, Kobe Steel, Ltd., Japan</p> |
| 10:20am | <p>F2-1-ThM8 The Use of Bipolar-HiPIMS for the Design of Ion Energies in Thin Film Growth, U. Helmersson, J. Keraudy, R.P.B. Viloan, Linköping University, Sweden; N. Brenning, M.A. Raadu, KTH Royal Institute of Technology, Sweden; D. Lundin, Université Paris-Sud, Université Paris-Saclay, France; I. Petrov, University of Illinois, USA, Linköping University, Sweden, USA; J.E. Greene, University of Illinois, USA, Linköping University, Sweden, National Taiwan Univ. Science & Technology, Taiwan; J.T. Gudmundsson, University of Iceland, Iceland</p> | <p>G1+G3-ThM8 A New System Platform for Ultrafast Nitriding and Diamond Like Carbon (DLC) Deposition Based on a Hollow Cathode Discharge, F. Papa, T. Casserly, A. Tudhope, S. Gennaro, Duralar Technologies, USA</p> |
| 10:40am | <p>F2-1-ThM9 Latest Developments in HiPIMS with Positive Pulsing, I. Fernandez, Nano4Energy, Spain; A. Wennberg, Nano4Energy SL, Spain; F. Papa, GP Plasma, Spain</p> | <p>INVITED: G1+G3-ThM9 Combinatorial Development of Nitride and Oxide Thin Films on an Industrial Scale, R. Cremer, KCS Europe GmbH, Germany</p> |
| 11:00am | <p>F2-1-ThM10 HiPIMS- Advantages of a Positive Kick Pulse, J. Hrebik, Kurt J. Lesker Company, USA</p> | Invited talk continues. |
| 11:20am | <p>F2-1-ThM11 Plasma Parameter Determination in a HiPIMS Discharge Using Laser Thomson Scattering, P.J. Ryan, J.W. Bradley, M.D. Bowden, University of Liverpool, UK</p> | <p>G1+G3-ThM11 Protective, Tribological and Decorative PECVD Coatings Deposited with a New Microwave Source: Plasma and Layer Characterization for Appropriate Applications, R. Schäfer, T. Radny, K.-D. Nauenburg, robeko GmbH & Co.KG, Germany; S. Ulrich, Karlsruhe Institute of Technology (KIT), IAM, Germany</p> |
| 11:40am | <p>2020 ICMCTF INFORMATION SESSION THURSDAY, 12:20 – 1:20 pm California Room</p> | <p>G1+G3-ThM12 Complex Coating Technique for Smallest Part of Advanced Powertrain Fuel System, S.C. Cha, H.J. Park, J.H. Lee, Hyundai Motor Group-Hyundai Kefico, Republic of Korea; K.Y. Ko, C.H. Shin, Dongwoo HST Co. Ltd., Republic of Korea</p> |

Thursday Morning, May 23, 2019

| | | |
|--|---|---|
| <p>Topical Symposia Room Golden West - Session TS2-ThM Icephobic Surface Engineering Moderators: Alina Agüero Bruna, Instituto Nacional de Técnica Aeroespacial (INTA), Spain, Jolanta-Ewa Klemberg-Sapieha, École Polytechnique de Montréal, Canada</p> | | |
| 8:00am | | |
| 8:20am | <p>TS2-ThM2 Synthesis And Characterization Of Amphiphobic Hybrid Coatings For Industrial Applications, G. Boveri, M. Raimondo, F. Veronesi, Institute of Science and Technology for Ceramics, Italy</p> | |
| 8:40am | <p>TS2-ThM3 <i>In situ</i> Ice Growth Kinetics on Water-repellent Coatings in Atmospheric Icing Conditions, J. Lengaigne, P. Xing, É. Bousser, École Polytechnique de Montréal, Canada; A. Dolatabadi, Concordia University, Canada; L. Martinu, J.E. Klemberg-Sapieha, École Polytechnique de Montréal, Canada</p> | |
| 9:00am | <p>TS2-ThM4 Icephobic Elastomeric Surfaces?, P.F. Ibáñez, F.J. Montes Ruiz-Cabello, M.A. Rodríguez Valverde, M. Cabrerizo Vélchez, Universidad de Granada, Spain</p> | |
| 9:20am | <p>INVITED: TS2-ThM5 Design and Fabrication of Superhydrophobic, Ice-phobic Coatings for High Voltage (HV) Power Lines Application, M. Raimondo, G. Boveri, F. Veronesi, ISTECCNR - Institute of Science and Technology for Ceramics, Italy</p> | |
| 9:40am | Invited talk continues. | |
| 10:00am | <p>TS2-ThM7 Energy Saving Strategy for the Development of Icephobic Coating and Surface, Y. Zheng, J. Wang, J.L. Liu, K. Choi, X.H. Hou, The University of Nottingham, UK</p> | |
| 10:20am | <p>TS2-ThM8 Anti-Icing Hard Steel Coating Modified With Polymer Particles, P. Garcia, J. Mora, A. Agüero, Instituto Nacional de Técnica Aeroespacial (INTA), Spain</p> | |
| 10:40am | <p>INVITED: TS2-ThM9 Development of Superhydrophobic and Icephobic Coatings by Suspension Plasma Spraying, A. Dolatabadi, N. Sharifi, R. Attarzadeh, C. Moreau, M. Pugh, Concordia University, Canada</p> | <p>2020 ICMCTF INFORMATION SESSION THURSDAY, 12:20 – 1:20 pm California Room</p> |
| 11:00am | Invited talk continues. | <p>ELSEVIER FOCUSED TOPIC SESSION THURSDAY, 12:20 – 1:20 pm, Golden West</p> |
| 11:20am | <p>TS2-ThM11 Minimum Required Thickness of a Hydrophobic Topcoat to withstand Cycling in an Icing Wind Tunnel, S. Brown, École Polytechnique de Montreal, Canada; J. Lengaigne, Polytechnique Montréal, Canada; N. Sharifi, Concordia University, Canada; L. Martinu, J.E. Klemberg-Sapieha, École Polytechnique de Montreal, Canada</p> | <p>“The Art of Publishing” Samir Aouadi</p> |

Thursday Afternoon, May 23, 2019

| Coatings for Use at High Temperatures Room Pacific Salon 2 - Session A2-2-ThA Thermal and Environmental Barrier Coatings II Moderators: Sabine Faulhaber, University of California, San Diego, USA, Kang N. Lee, NASA Glenn Research Center, USA, Pantcho Stoyanov, Pratt & Whitney, USA | | Hard Coatings and Vapor Deposition Technologies Room Golden West - Session B2-1-ThA CVD Coatings and Technologies I Moderators: Kazunori Koga, Kyushu University, Japan, Raphaël Boichot, Université Grenoble Alpes, CNRS, France | |
|---|---|--|---|
| 1:20pm | INVITED: A2-2-ThA1 Design of Multiphase Environmental Barrier Coatings: Toward Multifunctional Molten Deposit Resistance, <i>D. Poerschke</i> , University of Minnesota, USA | B2-1-ThA1 | Impact of HfO ₂ as a Buffer Layer on the Electrical and Ferroelectric Memory Characteristics of Metal/Ferroelectric/High-K/Semiconductor Gate Stack for Nonvolatile Memory Applications, <i>R. Jha, P. Singh, M. Goswami</i> , Indian Institute of Information Technology Allahabad, India; <i>B.R. Singh</i> , Park Systems, India |
| 1:40pm | Invited talk continues. | B2-1-ThA2 | Studies on Properties and Cutting Performance of Al-rich AlTiN Coating with Controlled Orientation via LP-CVD, <i>Y. Kido, A. Paseuth, S. Okuno, S. Imamura</i> , Sumitomo Electric Hardmetal Corp., Japan |
| 2:00pm | A2-2-ThA3 Comparison of Oxidation Procedures of MCrAlY Coatings Deposited by PVD Cathodic Arc Evaporation, <i>X. Maeder, J. Ast</i> , Empa - Swiss Federal Laboratories for Materials Science and Technology, Switzerland; <i>M. Polyakov</i> , EMPA - Swiss Federal Laboratories for Materials Science and Technology, Switzerland; <i>M. Döbeli</i> , ETH Zürich, Switzerland; <i>A. Neels, A. Dommann</i> , Empa - Swiss Federal Laboratories for Materials Science and Technology, Switzerland; <i>B. Widrig, O. Hunold, J. Ramm</i> , Oerlikon Balzers, Oerlikon Surface Solutions AG, Liechtenstein | B2-1-ThA3 | Effects of Al Content and Growth Orientation on Mechanical Properties of AlTiN Coatings Prepared by CVD Method, <i>K. Yanagisawa, T. Ishigaki, H. Nakamura, H. Homma</i> , Mitsubishi Materials Corporation, Japan |
| 2:20pm | A2-2-ThA4 Effect of APS Flash Bond Coatings and Curvature on Furnace Cycle Lifetime of Rods, <i>M.J. Lance, J.A. Haynes, B.A. Pint</i> , Oak Ridge National Laboratory, USA; <i>E. Gildersleeve, S. Sampath</i> , Stony Brook University, USA | B2-1-ThA4 | Thermal Crack Network Formation in CVD TiCN/ α -Al ₂ O ₃ Coatings, <i>N. Schalk, R. Stylianou, M. Gassner</i> , Montanuniversität Leoben, Austria; <i>D. Velic, W. Daves, W. Ecker</i> , Materials Center Leoben Forschung GmbH, Austria; <i>M. Tkadletz</i> , Montanuniversität Leoben, Austria; <i>C. Czettl</i> , CERATIZIT Austria GmbH, Austria; <i>C. Mitterer</i> , Montanuniversität Leoben, Austria |
| 2:40pm | A2-2-ThA5 Investigation of Thermally Grown Oxide Stress in Plasma-spray Physical Vapor Deposition and Electron-beam Physical Vapor Deposition Thermal Barrier Coatings via Photoluminescence Spectroscopy, <i>L. Rossmann, M. Northam</i> , University of Central Florida, USA; <i>V. Viswanathan</i> , Praxair Surface Technologies, USA; <i>B. Harder</i> , NASA Glenn Research Center, USA; <i>S. Raghavan</i> , University of Central Florida, USA | B2-1-ThA5 | Nanostructure of Textured CVD TiAlN, <i>O. Bäcke</i> , Chalmers University of Technology, Sweden; <i>W. Janssen, T. Manns, J. Kümme, D. Stiens</i> , Walter AG, Germany; <i>M. Halvarsson</i> , Chalmers University of Technology, Sweden |
| 3:00pm | A2-2-ThA6 Thermally Conductive and Electrically Insulating Epoxy Nanocomposites with Intercalation of Aluminum Nitride Nanoparticles into Exfoliated Graphite, <i>C.J. Wu</i> , National Cheng Kung University, Taiwan | B2-1-ThA6 | Structural and Piezoelectric Properties of Chemical Vapor Deposited AlN Films on Metallic Substrates, <i>J. Su, M. Pons, F. Mercier, D.Y. Chen, R. Boichot</i> , Université Grenoble Alpes, CNRS, France |
| 3:20pm | A2-2-ThA7 Effect of Feedstock Species on Thermal Durability of Thermal Barrier Coatings, <i>S.W. Myoung, B.I. Yang, I.S. Kim</i> , Doosan Heavy Industries and Construction, Republic of Korea; <i>Y.G. Jung</i> , Changwon National University, Republic of Korea | B2-1-ThA7 | Aluminum Nitride Based Coatings for High Temperature Solar Receiver Systems, <i>D.Y. Chen</i> , Université Grenoble Alpes, CNRS, France; <i>J. Colas</i> , PROMES-CNRS, France; <i>J. Su</i> , Université Grenoble Alpes, CNRS, France; <i>L. Charpentier, M. Balat-Pichelin</i> , PROMES-CNRS, France; <i>F. Mercier, M. Pons</i> , Université Grenoble Alpes, CNRS, France |
| 3:40pm | A2-2-ThA8 Development of Environmental Barrier Coatings for SiC/SiC Ceramic Matrix Composites via CVD, <i>T. König, M.C. Galetz</i> , DEHEMA-Forschungsinstitut, Germany | B2-1-ThA8 | Residual Stress and Quantitative Texture of CVD Al ₂ O ₃ Coatings, <i>Z. Liu</i> , Kennametal Inc., USA; <i>S. Tan</i> , University of Pittsburgh, USA; <i>D. Banerjee</i> , Kennametal Inc., USA |
| 4:00pm | | INVITED: B2-1-ThA9 | Gas Source Chemical Vapor Deposition of Wafer-scale Mono- and few-layer MX ₂ (M=W or Mo and X=S or Se) and Their Alloys, <i>M. Chubarov, T. Choudhury, D. Reifsnnyder Hickey, S. Bachu, N. Alem, J. Redwing</i> , The Pennsylvania State University, USA |
| 4:20pm | | | Invited talk continues. |
| 4:40pm | <p style="text-align: center;">POSTER SESSION 5:00 – 7:00 PM, GRAND HALL Reception Begins at 6:00 pm</p> | B2-1-ThA11 | The Effect of Dopants and Bilayer Period on Microstructure and Mechanical Properties of CVD Ti(B,C)N Hard Coatings, <i>C. Kainz, N. Schalk, M. Tkadletz, C. Mitterer</i> , Montanuniversität Leoben, Austria; <i>C. Czettl</i> , CERATIZIT Austria GmbH, Austria |

Thursday Afternoon, May 23, 2019

| | | |
|--------|--|---|
| | <p>Hard Coatings and Vapor Deposition Technologies Room California - Session B5-1-ThA Hard and Multifunctional Nanostructured Coatings I Moderators: Tomas Kozak, University of West Bohemia, Czech Republic, Helmut Riedl, TU Wien, Institute of Materials Science and Technology, Austria</p> | <p>Fundamentals and Technology of Multifunctional Materials and Devices Room Pacific Salon 3 - Session C4-ThA Fundamentals of Metallurgy in Thin Films and Coatings Moderators: Karsten Woll, Karlsruhe Institute of Technology (KIT), Germany, Ibrahim Gunduz, Naval Postgraduate School, USA</p> |
| 1:20pm | | |
| 1:40pm | | <p>C4-ThA2 Analytical Modelling of Propagation Velocity in Electron Transparent Nanolaminates, M.J. Abere, Sandia National Laboratories, USA; G.C. Egan, Lawrence Livermore National Laboratory, USA; D.P. Adams, Sandia National Laboratories, USA</p> |
| 2:00pm | <p>B5-1-ThA3 Interfaces and Mechanisms: A Molecular Dynamics Approach to Fine Tuning Manipulation of Mechanical Properties, A.F. Fraile, H.Y. Yavas, E.F. Frutos, Department of Control Engineering, Faculty of Electrical Engineering, Czech Technical University in Prague, Czech Republic; T.H. Huminiuc, Engineering Science, Faculty of Engineering and the Environment, University of Southampton, Southampton, UK; T. Polcar, Czech Technical University in Prague, Czech Republic</p> | <p>INVITED: C4-ThA3 Bimetallic Solid State Diffusion During Extreme Mechano-Chemical Processing of Nanoheater Multilayers, C. Doumanidis, Nazarbayev University, Astana, Kazakhstan; M. Aureli, University of Nevada Reno, USA; C. Doumanidis, Aristotelian University of Thessaloniki, Greece; I.E. Gunduz, Purdue University, USA; A. Hussien, Khalifa University, Abu Dhabi, UAE; Y. Liao, University of Nevada Reno, USA; C.G. Rebholz, University of Cyprus, Cyprus</p> |
| 2:20pm | <p>B5-1-ThA4 Preparation of Hard Yet Fracture Resistant W-B-C Coatings Using High Power Impulse Magnetron Sputtering, P. Soucek, M. Polacek, P. Klein, L. Zabransky, V. Bursikova, M. Stupavska, Masaryk University, Brno, Czech Republic; Z. Czigany, K. Balazsi, Hungarian Academy of Sciences, Hungary; P. Vasina, Masaryk University, Brno, Czech Republic</p> | <p>Invited talk continues.</p> |
| 2:40pm | <p>B5-1-ThA5 Analytical Modelling of Misfit Dislocation Formation in Superlattice Coatings and its Effect on the Fracture Toughness, A. Wagner, TU Wien, Institute of Materials Science and Technology, Austria; D. Holec, Montanuniversität Leoben, Austria; M. Todt, TU Wien, Institute of Lightweight Design and Structural Biomechanics, Austria; P.H. Mayrhofer, M. Bartosik, TU Wien, Institute of Materials Science and Technology, Austria</p> | <p>C4-ThA5 Twin-Wire Arc Coatings for Repair of Structural Components, C. Jasien, N.J. Wagner, Cal Poly Pomona, USA</p> |
| 3:00pm | <p>B5-1-ThA6 The Electrical Response of PVD Deposited Nanocrystallized Carbon Film in Magnetic Field, C. Wang, J. Guo, X. Dai, Institute of Nanosurface Science and Engineering, College of Mechatronics and Control Engineering, Shenzhen University, China</p> | <p>C4-ThA6 Unstable Propagating Reactions in Sputter-Deposited Nanolaminates, D.P. Adams, M.J. Abere, Sandia National Laboratories, USA</p> |
| 3:20pm | <p>INVITED: B5-1-ThA7 Aluminium Nitride Based Piezoelectric MEMS: From Material Aspects to Low Power Devices, U. Schmid, M. Schneider, TU Wien - Institute of Sensor and Actuator Systems, Austria</p> | <p>C4-ThA7 Synthesis of Reactive Ni-Al Composites Using High Pressure Torsion, O. Renk, Austrian Academy of Sciences, Austria; M. Tkadletz, N.K. Kostoglou, Montanuniversität Leoben, Austria; I.E. Gunduz, Naval Postgraduate School, USA; C. Doumanidis, Nazarbayev University, Astana, Kazakhstan; R. Pippa, Austrian Academy of Sciences, Austria; C. Mitterer, Montanuniversität Leoben, Austria; C.G. Rebholz, University of Cyprus, Cyprus</p> |
| 3:40pm | <p>Invited talk continues.</p> | <p>C4-ThA8 Magnetic Field Induced Strain Transfer in FSMA/AlN Multilayered Structure, S. Pawar, A. Kumar, Indian Institute of Technology Roorkee, India; D. Kaur, Indian Institute Of Technology Roorkee, India</p> |
| 4:00pm | <p>B5-1-ThA9 Superamphiphobic Surface Produced by Femtosecond Laser Patterning and Pulsed Plasma Polymerization, C.W. Lin, Feng Chia University; Central Taiwan University of Science and Technology, Taiwan; G.H. Lu, X.X. Chang, P.-Y. Hsieh, Feng Chia University, Taiwan; C.M. Chou, Department of Surgery, Taichung Veterans General Hospital, National Yang-Ming University, Taiwan; C.J. Chung, Central Taiwan University of Science and Technology, Taiwan; J.L. He, Feng Chia University, Taiwan</p> | <p>C4-ThA9 Structure-Property Correlation of Spray Pyrolyzed Binary Chalcogenide Thermoelectric Thin Films, G.P. Badhirappan, PSG College of Technology, India; V. Shaleni, PSG Institute of Advanced Studies, India; G. Balaji, R. Balasundrappabu, A. Ashok, PSG College of Technology, India; D. Sathishkumar, CVRDE, India</p> |
| 4:20pm | | <p style="text-align: center;">POSTER SESSION 5:00 – 7:00 PM, GRAND HALL Reception Begins at 6:00 pm</p> |

Thursday Afternoon, May 23, 2019

| | | |
|--------|---|--|
| | <p>Tribology and Mechanical Behavior of Coatings and Engineered Surfaces Room San Diego - Session E1-2-ThA Friction, Wear, Lubrication Effects, and Modeling III Moderators: Nazlim Bagcivan, Schaeffler AG, Germany, Carsten Gachot, TU Wien, Institute for Engineering Design and Logistics Engineering, Austria, Tomas Polcar, Czech Technical University in Prague, Czech Republic</p> | <p>New Horizons in Coatings and Thin Films Room Pacific Salon 6-7 - Session F2-2-ThA HiPIMS, Pulsed Plasmas and Energetic Deposition II Moderators: Jon Tomas Gudmundsson, University of Iceland, Iceland, Tiberiu Minea, LPGP, Université Paris-Sud, Orsay, France</p> |
| 1:20pm | | |
| 1:40pm | <p>E1-2-ThA2 Exploring the Nanomechanical Properties of Transition Metal Dichalcogenides using Density Functional Theory, B.J. Irving, P. Nicolini, Czech Technical University in Prague, Czech Republic; T.P. Polcar, University of Southampton, UK</p> | <p>F2-2-ThA2 Pulsed Cathodic Arc for Deposition of ta-C and TiSiCN Films, X.B. Tian, Y.H. Ma, State Key Laboratory of Advanced Welding & Joining, Harbin Institute of Technology, China; C.Z. Gong, State Key Laboratory of Advanced Welding and Joining, Harbin Institute of Technology, China; Y. Kong, Q.X. Tian, State Key Laboratory of Advanced Welding & Joining, Harbin Institute of Technology, China</p> |
| 2:00pm | <p>INVITED: E1-2-ThA3 Mechanics, Materials, and Design Problems in Medical Device Technology and Information Storage, F.E. Talke, University of California, San Diego, USA</p> | <p>F2-2-ThA3 HiPIMS Deposition of W Thin Films, A. Engwall, S.J. Shin, Y.M. Wang, Lawrence Livermore National Laboratory, USA</p> |
| 2:20pm | Invited talk continues. | <p>F2-2-ThA4 Study and Development of Thermochromic VO₂ Thin Films Deposited by HiPIMS, J.L. Victor, C. Marcel, CEA Le Ripault, France; A. Rougier, CNRS, France; L. Sauques, DGA, France</p> |
| 2:40pm | <p>E1-2-ThA5 Frictional Anisotropy of MoS₂ During Sliding: A Molecular Dynamics Study on the Atomistic Understanding of Frictional Mechanisms, V.E.P. Claerbout, P. Nicolini, Czech Technical University in Prague, Czech Republic</p> | <p>INVITED: F2-2-ThA5 A Paradigm Shift in Thin Film Growth by Magnetron Sputtering: from Gas-ion to Metal-ion-controlled Irradiation, G. Greczynski, Department of Physics, Linköping Univ., Sweden; I. Petrov, University of Illinois, USA, Linköping University, Sweden, USA; J.E. Greene, University of Illinois, USA, Linköping University, Sweden, National Taiwan Univ. Science & Technology, Taiwan; L. Hultman, Department of Physics, Linköping Univ., Sweden</p> |
| 3:00pm | <p>E1-2-ThA6 Effect of the Presence of Small Molecules on the Entangled Electronic and Dynamic Features in Layered MX₂ Transition Metal Dichalcogenides: Systematic Quantum Mechanic Ab Initio Simulations, J. Missaoui, A. Cammarata, Czech Technical University in Prague, Czech Republic</p> | Invited talk continues. |
| 3:20pm | <p>E1-2-ThA7 Nanoscale Frictional Properties of Ordered and Disordered MoS₂, E. Serpini, A. Rota, Università di Modena e Reggio Emilia, Italy; S. Valeri, Istituto CNR-NANO S3, Italy; E. Ukraintsev, Academy of Science of the Czech Republic, Czech Republic; B. Rezek, Czech Technical University in Prague, Czech Republic; T.P. Polcar, University of Southampton, UK; P. Nicolini, Czech Technical University in Prague, Czech Republic</p> | <p>F2-2-ThA7 In Vitro and In Vivo Biocompatibility Evaluation of Zr-Ti-Si and Fe-Zr-Nb Thin Film Metallic Glasses, A.J. Chen, J.-B. Wang, Y.-C. Yang, National Taipei University of Technology, Taiwan; B.-S. Lou, Chang Gung University, Taiwan; J.-W. Lee, Ming Chi University of Technology, Taiwan</p> |
| 3:40pm | <p>E1-2-ThA8 Electrical Tuning of Vibrational Modes in Transition Metal Dichalcogenides, F. Belviso, Advanced Material Group, Czech Technical University in Prague, Czech Republic</p> | <p>F2-2-ThA8 Microstructural and Tribological Properties of Sputtered AlCrSiWN Films Deposited with Segmented Powder Metallurgical Target Materials, W. Tillmann, A. Fehr, D. Stangier, TU Dortmund University, Germany</p> |
| 4:00pm | <p>E1-2-ThA9 On the In-situ Formation of Transition Metal Disulphides in Lubricated WN or WC Coating Contacts, B. Kohlhauser, TU Wien, Institute of Materials Science and Technology, Austria; M. Rodríguez Ripoll, AC2T research GmbH, Austria; H. Riedl, C.M. Koller, N. Koutna, TU Wien, Institute of Materials Science and Technology, Austria; G. Ramirez, A. Erdemir, Argonne National Laboratory, USA; C. Gachot, TU Wien, Institute for Engineering Design and Logistics Engineering, Austria; P.H. Mayrhofer, TU Wien, Institute of Materials Science and Technology, Austria</p> | <p>F2-2-ThA9 Linking an Atmospheric-pressured Arc Reactor to a Magnetron Sputter Device to Synthesize Novel Nanostructured Thin Films, W. Tillmann, D. Kokalj, D. Stangier, TU Dortmund University, Germany; Q. Fu, E. Kruis, University of Duisburg-Essen, Germany</p> |
| 4:20pm | <p>E1-2-ThA10 Tribological Investigations of Coated Roller Finger Followers using Application Oriented Valve Train Test, R.H. Brugnara, E. Schulz, L. Dobrenizki, N. Bagcivan, C. Geers, Schaeffler AG, Germany</p> | |
| 4:40pm | <p>E1-2-ThA11 Physical Understanding to Nano-friction of C:H/D Thin Films: Coupling Mechanism by Atomic-scale Vibration Damping, F.G. Echeverrigaray, S.R.S. de Mello, Universidade de Caxias do Sul, Brazil; F. Alvarez, Universidade Estadual de Campinas, Brazil; A.F. Michels, C.A. Figueroa, Universidade de Caxias do Sul, Brazil</p> | <p style="text-align: center;">POSTER SESSION 5:00 – 7:00 PM, GRAND HALL Reception Begins at 6:00 pm</p> |

Thursday Afternoon, May 23, 2019

| | |
|---|---|
| <p>Surface Engineering - Applied Research and Industrial Applications Room Pacific Salon 1 - Session G4+G5+G6-ThA Pre-/Post-Treatment and Duplex Technology/Hybrid Systems, Processes and Coatings/Application-Driven Collaborations between Industry and Research Institutions Moderators: Heidrun Klostermann, Fraunhofer FEP, Germany, Kumar Yalamanchili, Oerlikon Balzers, Oerlikon Surface Solutions AG, Liechtenstein, Tobias Brögelmann, RWTH Aachen University, Germany, Hana Barankova, Uppsala University, Sweden</p> | |
| 1:20pm | <p>INVITED: G4+G5+G6-ThA1 From Detailed Understanding to In Operando Studies of Coated Cutting Tools: A Successful and Long Term Collaboration between Industry and Universities, <i>J. Anderson</i>, Seco Tools AB, Sweden</p> |
| 1:40pm | Invited talk continues. |
| 2:00pm | <p>G4+G5+G6-ThA3 Electrolytic Plasma Polishing of Titanium Alloys, <i>N. Laugel</i>, <i>A. Yerokhin</i>, <i>A. Matthews</i>, University of Manchester, UK</p> |
| 2:20pm | <p>G4+G5+G6-ThA4 Characterization of Surface Modification Mechanisms for Boron Nitride Films under Plasma Exposure, <i>T. Higuchi</i>, Kyoto University, Japan; <i>M. Noma</i>, Shinko Seiki Co., Ltd, Japan; <i>M. Yamashita</i>, Hyogo Prefectural Institute of Technology, Japan; <i>K. Urabe</i>, Kyoto University, Japan; <i>S. Hasegawa</i>, Osaka University, Japan; <i>K. Eriguchi</i>, Kyoto University, Japan</p> |
| 2:40pm | <p>G4+G5+G6-ThA5 Ultra-fast Decoating Method for PVD Coatings, <i>B. Wittel</i>, <i>C. Buechel</i>, <i>T. Cselle</i>, Platit AG, Switzerland; <i>B. Torp</i>, Platit Scandinavia, Denmark; <i>A. Lümkmann</i>, <i>D. Bloesch</i>, Platit AG, Switzerland</p> |
| 3:00pm | <p>G4+G5+G6-ThA6 Development of an Omni-phobic Spray Coating for the Oil and Gas Industry, <i>C. Ellis-Terrell</i>, <i>R. Wei</i>, <i>R. McKnight</i>, Southwest Research Institute, USA; <i>X. Huang</i>, <i>K. Lin</i>, Beijing Sanju Environmental Protection & New Materials Co., Ltd., China</p> |
| 3:20pm | <p>INVITED: G4+G5+G6-ThA7 Hybrid Reactive High Power Impulse Magnetron Sputtering System Combined with Electron Cyclotron Wave Resonance ECWR Plasma used for the Deposition of Semiconducting Thin Films., <i>Z. Hubicka</i>, <i>M. Cada</i>, Institute of Physics CAS, v. v. i., Czech Republic; <i>S. Kment</i>, Institute of Physics, Academy of Sciences of the Czech Republic, Czech Republic; <i>V. Stranak</i>, <i>R.H. Hippler</i>, Institute of Physics, Academy of Sciences of the Czech Republic; <i>J. Olejnicek</i>, Institute of Physics CAS, v. v. i., Czech Republic</p> |
| 3:40pm | Invited talk continues. |
| 4:00pm | <p>INVITED: G4+G5+G6-ThA9 Pre- and Post-Surface Treatments using Electron Beam Technology for Load-Related Application of Thermochemical and PVD Hard Coatings on Soft Substrate Materials, <i>A. Buchwalder</i>, <i>R. Zenker</i>, TU Bergakademie Freiberg, Germany</p> |
| 4:20pm | Invited talk continues. |
| 4:40pm | <p>G4+G5+G6-ThA11 Black Oxide and Carbon-Based Coatings for Roller Bearing Applications, <i>E. Broitman</i>, <i>X. Zhou</i>, SKF Research & Technology Development Center, Netherlands</p> |
| <p>POSTER SESSION 5:00 – 7:00 PM, GRAND HALL Reception Begins at 6:00 pm</p> | |

Coatings for Use at High Temperatures

Room Grand Hall - Session AP-ThP

Coatings for Use at High Temperatures (Symposium A)

Poster Session

5:00pm

AP-ThP1

Investigation of Microstructure and Properties of Thick Mo Coating obtained via Molten Salt Electrolysis, **R. Tripathi**, Homi Bhabha National Institute, India; **S.K. Ghosh**, Bhabha Atomic Research Centre, India

AP-ThP2

High Temperature Performance of CrAlN Coating on Stainless Steel Substrates in Simulated Diesel Exhaust Environment, **S. Yang**, Miba Coating Group, Teer Coatings Ltd., UK; **V. Vishnyakov**, Institute for Materials Science, University of Huddersfield, UK; **P. Navabpour**, Miba Coating Group, Teer Coatings Ltd., UK; **J. Allport**, Institute for Materials Science, University of Huddersfield, UK; **H. Sun**, Miba Coating Group, Teer Coatings Ltd., UK

AP-ThP3

e-Poster Presentation: Improvement of the Robustness of Time to Failure Assessment in Tbc System, **M. Theveneau**, **B. Marchand**, **V. Guipont**, Mines ParisTech, PSL Research University, MAT - Centre des Matériaux, France; **F. Coudon**, SAFRAN Tech, France; **V. Maurel**, Mines ParisTech, PSL Research University, MAT - Centre des Matériaux, France

AP-ThP4

Computational Modelling, Synthesis and Characterization of Direct Laser Metal Deposition of Nickel Based Coatings on Ti-6Al-4V Alloy, **O.S. Fatoba**, **S.A. Akinlabi**, **E.T. Akinlabi**, **M.J. Oboegbu**, University of Johannesburg, South Africa

AP-ThP5

Wear Resistance Performance of AlCrN and TiAlN Coated H13 Tools during Friction Stir Welding of A2124/SiC Composite, **Y. Adesina**, **A. Al-Badour**, **Z. Gasem**, King Fahd University of Petroleum and Minerals, Saudi Arabia

AP-ThP6

Diffusion Model for Estimating the Iron Boride Layer Thicknesses, **O. Gómez-Vargas**, Instituto Tecnológico de Tlalnepantla, México; **M. Ortiz-Domínguez**, Universidad Autónoma del Estado de Hidalgo, México; **J. Solís-Romero**, Instituto Tecnológico de Tlalnepantla, México; **M. Flores-Rentería**, **I. Morgado-Gonzalez**, **E. Cardoso-Legorreta**, Universidad Autónoma del Estado de Hidalgo, México; **M. Elias-Espinosa**, Tecnológico de Monterrey, México; **A. Cruz Avilés**, Universidad Autónoma del Estado de Hidalgo, México

AP-ThP7

STEM Investigations of Oxide Scales formed during Pre-oxidation of γ -TiAl, **R. Swadzba**, Institute for Ferrous Metallurgy, Poland

AP-ThP8

Enhancement of Corrosion Resistance in Electrodeposited Ni-B-SnCoatings., **U. Waware**, **A.M.S. Hamouda**, Qatar University, Qatar

AP-ThP9

Microstructure of MCrAlY Coatings Deposited Using HVOF after Heat Treatment and Aluminizing, **L. Swadzba**, **A. Iwaniak**, **R. Swadzba**, **B. Witala**, **B. Mendala**, Silesian University of Technology, Poland; **G. Wieclaw**, **P. Lubaszka**, Certech Sp. z o.o., Poland

AP-ThP10

Effect of Vanadium Content on the High-temperature Tribo-mechanical Properties of Cr-Al-V-N Coatings Deposited by DC UBMS, **H. Kim**, **I.-W. Park**, Korea Institute of Industrial Technology (KITECH), Republic of Korea

AP-ThP11

Tensile Behavior of Air Plasma Spray MCrAlY Coatings: Role of High Temperature Aging and Process Defects, **C. Cadet**, Mines ParisTech, PSL Research University, France; **T.S. Straub**, Fraunhofer Institute for Mechanics of Materials IWM, Germany; **D. Texier**, Mines Albi, ISAE-SUPAERO, France; **C. Eberl**, Fraunhofer Institute for Mechanics of Materials IWM, Germany; **V. Maurel**, Mines ParisTech, PSL Research University, France

AP-ThP13

Influence of Si-Al Coating on Mechanical Properties of EBMed TiAl Alloy, **L. Pyclik**, Avio Aero A GE Aviation Business, Poland; **L. Swadzba**, **B. Mendala**, **B. Witala**, **J. Tracz**, **R. Swadzba**, Silesian University of Technology, Poland; **K. Marugi**, Avio Aero A GE Aviation Business, Poland

Hard Coatings and Vapor Deposition Technologies

Room Grand Hall - Session BP-ThP

Hard Coatings and Vapor Deposition Technologies

(Symposium B) Poster Session

5:00pm

BP-ThP1

Low Stress AlTiN-Based Coating Systems, **C.J. Charlton**, Kennametal Inc., USA; **J. Kohlscheen**, Kennametal GmbH, Germany; **D. Banerjee**, Kennametal Inc., USA

BP-ThP2

Multi-Target Co-Sputtering Deposition and Mechanical Properties of Ti-Zr-Based High-Entropy Alloy and Nitride Coatings, **S.Y. Chang**, **Y.T. Hsiao**, National Tsing Hua University, Taiwan; **S.Y. Lin**, National Formosa University, Taiwan

BP-ThP3

(Ti_{1-x}Y_x)B_{2+ Δ} Thin Films - Structural Evolution and Mechanical Properties, **M. Truchlý**, **B. Grancic**, Comenius University in Bratislava, Slovakia; **P. Švec Jr.**, Slovak Academy of Sciences, Bratislava, Slovakia; **T. Roch**, **L. Satrapinsky**, **V. Izaii**, Comenius University in Bratislava, Slovakia; **M. Harsani**, Staton s.r.o., Slovakia; **O. Kohulak**, **P. Kus**, **M. Mikula**, Comenius University in Bratislava, Slovakia

BP-ThP4

Post-annealing of (Ti,Al,Si)N Coatings deposited by High-Speed Physical Vapor Deposition (HS-PVD), **K. Bobzin**, **T. Brögelmann**, **C. Kalscheuer**, **T. Liang**, **M. Welters**, Surface Engineering Institute - RWTH Aachen University, Germany

BP-ThP6

Discrete Thin-film Multilayer Structures of TiB₂ and ZrB₂ Ceramics for Super-hard and Tough Coating, **A. Ghimire**, National Tsing Hua University, National Dong Hwa University, Taiwan; **M.S. Wong**, National Dong Hwa University, Taiwan; **S.Y. Chang**, National Tsing Hua University, Taiwan

BP-ThP7

Effect of Bias Voltage on Mechanical Properties of Zr-Si-N Films Fabricated through HiPIMS/RFMS Cosputtering, **Y.I. Chen**, **Y.Z. Zheng**, National Taiwan Ocean University, Taiwan; **L.C. Chang**, Ming Chi University of Technology, Taiwan

BP-ThP9

Influence of the C/N Ratio on the Mechanical and Tribological Properties of the AlCrCN Coatings by Cathodic Arc Deposition, **D.Y. Wang**, **W.Y. Ho**, **W.C. Chen**, MingDao University, Taiwan; **L.C. Hsu**, **J. Hung**, Aurora Scientific Corp., Canada

BP-ThP11

The Effects of Pulse Frequency on the Growth of Diamond Using Pulse Microwave Plasma CVD, **Y. Zeng**, **Y. Sakamoto**, **T. Maruko**, Chiba Institute of Technology, Japan

BP-ThP12

Analysis of Reaction Gas States on Synthesis of Boron Doped Diamond by HF-CVD, **T. Maruko**, **Y. Sakamoto**, Chiba Institute of Technology, Japan

BP-ThP13

Effects of Boronizing Pretreatment on the Adhesion of B-doped Diamond on Ti Substrates, **Y. Izu**, Chiba Institute of Technology, Japan; **T. Sakuma**, Ogura Jewel Industry, Japan; **A. Suzuki**, **T. Maruko**, Chiba Institute of Technology Graduate School, Japan; **M. Imamiya**, **Y. Sakamoto**, Chiba Institute of Technology, Japan

BP-ThP14

High Entropy Nitride Thin Film (Cr_{0.35}Al_{0.25}Nb_{0.12}Si_{0.08}V_{0.20})N_x for Tribological Characteristics at High Temperature, **Y.C. Lin**, **J.G. Duh**, National Tsing Hua University, Taiwan

BP-ThP15

Search of New (Al_{0.25}Cr_{0.3}Nb_{0.1}Si_{0.08}Ti_{0.1}Mo_{0.17})N_x Coatings for Feasible Application at High Temperature, **W.L. Lo**, **J.G. Duh**, National Tsing Hua University, Taiwan

BP-ThP17

Mechanical Properties and Thermal Stability of Cr-X-N (X=Al, Zr, Si) Multilayered Coatings Synthesized by UBMS, **H.K. Kim**, **S.H. Lee**, **S.Y. Lee**, Korea Aerospace University, Republic of Korea

BP-ThP18

e-Poster Presentation: The Role of Vacancies in the W-N System, **F.F. Klimashin**, **P.H. Mayrhofer**, TU Wien, Institute of Materials Science and Technology, Austria

BP-ThP19

Probing Defected Layers of MoN/TaN and TiN/WN Superlattices, *N. Koutna, J. Buchinger, R. Hahn*, Institute of Materials Science and Technology, TU Wien, Austria; *J. Zálešák*, Erich Schmid Institute of Materials Science, Austrian Academy of Sciences, Leoben, Austria; *M. Bartosik*, Institute of Materials Science and Technology, TU Wien, Austria; *M.F. Friák, M.S. Šob*, Institute of Physics of Materials, Academy of Sciences of the Czech Republic, Czech Republic; *D. Holec*, Montanuniversität Leoben, Austria; *P.H. Mayrhofer*, Institute of Materials Science and Technology, TU Wien, Austria

BP-ThP20

Investigation of CVD Stability Windows for Tungsten Carbide Phases, *K. Bäär, J. Gerdin*, Uppsala University, Sweden; *R. Qiu*, Chalmers University of Technology, Sweden; *M. Boman*, Uppsala University, Sweden; *E. Lindahl*, Sandvik Coromant R&D, Sweden

BP-ThP22

Photocatalytic Activity of Metal Oxide Thin Films Deposited by MS-PVD and Layer-by-Layer for Hydrogen Production by Water Splitting, *P.J. Rivera*, Public University of Navarra, Spain; *J.A. Garcia*, Universidad Publica de Navarra, Spain; *R. Rodriguez*, Public University of Navarra, Spain; *J. Esparza*, AIN, Ingeniería Avanzada de Superficies, Spain; *G. Garcia Fuentes*, Public University of Navarra, Spain

BP-ThP23

Nanocomposite (Ti,Al,Cr,Si)N HPPMS Coatings for High Performance Cutting Tools, *K. Bobzin, T. Brögelmann, N.C. Kruppe, M. Carlet, M. Thiex*, RWTH Aachen University, Germany

BP-ThP24

Surface Hardening of AISI 1018 Steel: Microstructural Characterization of Boride and Nitride Layers, *M. Ortiz-Domínguez, I. Morgado-Gonzalez*, Universidad Autónoma del Estado de Hidalgo, México; *M. Elias-Espinosa*, Tecnológico de Monterrey, México; *O. Gómez-Vargas, J. Solís-Romero*, Instituto Tecnológico de Tlalneptantla, México

BP-ThP25

Microstructural Characterization of a New Powder-pack Carbo-boro-nitriding Process, *M. Elias-Espinosa*, Tecnológico de Monterrey, México; *M. Ortiz-Domínguez*, Universidad Autónoma del Estado de Hidalgo, México; *J. Solís-Romero, O. Gómez-Vargas*, Instituto Tecnológico de Tlalneptantla, México; *I. Morgado-Gonzalez, M. Flores-Rentería*, Universidad Autónoma del Estado de Hidalgo, México

BP-ThP26

Low Temperature Titanium Boron-Carbide Based Thin Film Coatings by Plasma Enhanced Chemical Vapor Deposition on Surface Microstructure Controlled WC-Co, *T. Saito, D. Kiyokawa, K. Fujii, N. Okamoto*, Osaka Prefecture University, Japan; *A. Kitajima, K. Higuchi*, Osaka University, Japan

BP-ThP27

Performance of the CrAlSiN and Hydrogen free DLC Combined Hard Coatings Deposited on Micro Tools Cutting Printed Circuit Board, *D.Y. Wang*, MingDao University, Taiwan; *L.C. Hsu, J. Hung*, Aurora Scientific Corp., Canada; *W.C. Chen, W.Y. Ho*, MingDao University, Taiwan

BP-ThP28

Study and Characterization of the Vanadium Carbide Interlayer Deposited by Laser Cladding over Carbon Steel for CVD Diamond Growth, *D. Damm, R.A. Pinheiro, J.S. Gomez*, National Institute for Space Research (INPE), Brazil; *A. Contín*, Federal University of Goiás (UFG), Brazil; *R.F.B. Correia*, Federal University of São Paulo (UNIFESP), Brazil; *R.M. Volu*, Institute for Advanced Studies (IEAV), Brazil; *V.J. Trava-Airoldi*, National Institute for Space Research (INPE), Brazil; *G. de Vasconcelos*, Institute for Advanced Studies (IEAV), Brazil; *D.M. Barquete*, Santa Cruz State University (UESC), Brazil; *E.J. Corat*, National Institute for Space Research (INPE), Brazil

BP-ThP29

Wafer Scale Growth of Ultra-smooth Nano-crystalline Diamond Thick Film for Nanostructure Fabrication, *J.J. Li, S. Yan, Y. Sun, G. Gu*, Institute of Physics CAS, China

BP-ThP30

Optimization for Adhesion Properties of c-BN Films Coated with HiPIMS, *I. Efeöglü, Y. Totik, A. Keleş*, Ataturk University, Turkey

BP-ThP31

Si-DLC Films Prepared by Magnetron Sputtering under Different Working Pressure, *C.Q. Guo, S.S. Lin, Q. Shi, C.B. Wei, L. Li, W. Wang, M.J. Dai*, Guangdong Institute of New Materials, China

BP-ThP32

Multielement Rutile-structured AlCrNbTaTi-oxide Coatings Synthesised by Reactive Magnetron Sputtering, *A. Kirnbauer, C.M. Koller*, TU Wien, Institute of Materials Science and Technology, Austria; *S. Kolosvári*, Plansee Composite Materials GmbH, Germany; *P.H. Mayrhofer*, TU Wien, Institute of Materials Science and Technology, Austria

BP-ThP33

Magnetron Sputtering of Tungsten-containing /TiN_xO_y Multilayered Solar Selective Coatings, *S.Y. Li, Y.H. Shen, K.-S. Chang, J.-M. Ting*, National Cheng Kung University, Taiwan

BP-ThP34

Electron-configuration Stabilized (W,Al)₂ Solid Solutions, *R. Hahn, V. Moraes, P.H. Mayrhofer*, Institute of Materials Science and Technology, TU Wien, Austria; *A. Limbeck*, Institute of Chemical Technologies and Analytics, TU Wien, Austria; *P. Polcik*, Plansee Composite Materials GmbH, Germany; *H. Euchner*, Helmholtz Institute for Electrochemical Energy Storage, Germany

BP-ThP35

Apparent Fracture Toughness of TiN Coatings with Alternating Stress Fields, *A. Wagner, J. Buchinger*, TU Wien, Institute of Materials Science and Technology, Austria; *M. Todt*, TU Wien, Institute of Lightweight Design and Structural Biomechanics, Austria; *D. Holec*, Montanuniversität Leoben, Austria; *P.H. Mayrhofer, M. Bartosik*, TU Wien, Institute of Materials Science and Technology, Austria

BP-ThP36

Synthesis and Structural Characterization of Nanostructured CN_{0.1} Films Deposited by RF Magnetron Sputtering at Different Bias Voltages, *A. Lousa, D. Cano, C. Villabos, J. Esteve*, University of Barcelona, Spain

BP-ThP37

An X-ray Diffraction Study on CrAlN and CrAlSiN PVD Coatings, *J. Latarius, D. Stangier, C. Albers, K. Berger, M. Elbers, A. Sparenberg, G. Surmeier, M. Paulus, C. Sternemann, W. Tillmann, M. Tolan*, TU Dortmund University, Germany

BP-ThP39

Wear Resistance of TiAlSiN with Nanoparticles of Ag Coating Deposited via Co-sputtering Method, *A.D. Caíta Tapia, S.D. Rodriguez Arevalo, E.N. Borja Goyeneche, J.J. Olaya Florez, B.J. Gamboa Mendoza*, Universidad Nacional de Colombia, Colombia

BP-ThP41

Influence of Oxygen Addition on Microstructure and Properties of TiAlN, *D.M. Holzapfel, M. Hans*, RWTH Aachen University, Germany; *A.O. Eriksson, M. Arndt*, Oerlikon Balzers, Oerlikon Surface Solutions AG, Liechtenstein; *D. Primetzhofer*, Uppsala University, Sweden; *J.M. Schneider*, RWTH Aachen University, Germany

BP-ThP42

An Investigation on Synthesis of Novel Oxide-Based Superhard Cr-Zr-O Coatings, *M. Mohammadtaheri, Q. Yang, Y. Li, J. Corona-Gomez*, University of Saskatchewan, Canada

Fundamentals and Technology of Multifunctional Materials and Devices

Room Grand Hall - Session CP-ThP

Fundamentals and Technology of Multifunctional Materials and Devices (Symposium C) Poster Session

5:00pm

CP-ThP1

Comparison of SiC_xN_y Barriers using Different Precursors Deposited on Porous Low-Dielectric-constant SiCOH Dielectric Films, *Y.L. Cheng, Y.L. Lin, C.Y. Lee*, National Chi-Nan University, Taiwan

CP-ThP2

Stretchable Ultrasonic Transducer Arrays for Three-Dimensional Imaging on Complex Surfaces, *H. Hu, X. Zhu, C. Wang, L. Zhang, S. Xu*, University of California, San Diego, USA

CP-ThP4

Electrospun TiO₂ Nanofiber Electrodes for High Performance Supercapacitor, *C.K. Kunche, S.P. Reddy*, Sri Venkateswara University, India

CP-ThP6

Fabrication and Characterization of Ni-coated Ag Nanowire Electrodes with Bubble-like Random Meshes, *J.S. Park, R. Yoo, T.G. Park, J.S. Park*, Hanyang University, Republic of Korea

CP-ThP7

Characteristics of Silver Nanowire Transparent Electrodes Optimized for High Stretchability, *R. Yoo, J.S. Park, T.G. Park, J.S. Park*, Hanyang University, Republic of Korea

CP-ThP9

Microstructure and Electrochemical Properties of rf Sputtered V₂O₅ Thin Films, *M. Dhananjaya*, Sri Venkateswara University, India

Thursday Afternoon Poster Sessions, May 23, 2019

CP-ThP12

Thin Film Deposition of Lithium and its Alloys for High Energy Density Battery, **S. Sardar**, *J. Koh, N. Hart, J. Xu*, NICE America Research Inc; *D. Kang, J. Lemmon*, National Institute of Clean-and-Low-Carbon Energy

CP-ThP13

Study of Stress-electrical Properties of ITO Film Deposited on Stretchable Substrate, **P.O. Renault**, Université de Poitiers, France; *C. Grossias, P. Goudeau, P. Godard, F. Paumier, S. Hurand*, University of Poitiers, France; *D. Thiaudière*, SOLEIL Synchrotron, France; *P. Guerin*, University of Poitiers, France

CP-ThP17

Effect of Magnetron Sputtering Metal/PET Process on Performance of Flexible Capacitors, **J Wang, J. Lin**, Harbin University of Commerce, China

CP-ThP18

Dual Box Model based *In situ* Ellipsometry Growth Characterization: Oxygen Plasma Enhanced Atomic Layer Deposition of Metal Oxide Ultra-thin Films, *U. Kilic*, University of Nebraska-Lincoln, USA; *A. Mock*, Linköping University, Sweden; *D. Sekora, N. Ianno, E. Schubert, M. Schubert*, University of Nebraska Lincoln, USA

CP-ThP19

Controlled Release of Encapsulated Agents Deposited on Plasma Electrolytic Oxidation (PEO) Coatings for Corrosion Resistance and Biomedical Applications, *Y. Guo, B. Mingo, A. Matthews, A. Yerokhin*, The University of Manchester, UK

CP-ThP20

Ag@Co₃O₄ Core-shell Nanocrystals for Oxygen Reduction Reaction via Solution Plasma Process, **H.K. Kim**, Korea Aerospace University, Republic of Korea; *S.M. Kim*, Korea Institute of Industrial Technology, Republic of Korea; *J.W. Kim*, University of Incheon, Republic of Korea; *S.Y. Lee*, Korea Aerospace University, Republic of Korea

CP-ThP21

Influence of Substrate Temperature on the Growth of Molybdenum Trioxide Thin Films, **M.V. Kalapala**, VFSTR University, India

CP-ThP22

Evaluation of the Influence of Pre-carburisation on the In-situ Performance of Chromized 304 Stainless Steel Bipolar Plate, **A. Oladoye**, University of Lagos, Nigeria; *J. Carton, J. Stokes*, Dublin City University, Ireland; *A. Olabi*, University of the West of Scotland, UK

CP-ThP23

Piezo- and Thermo-resistive Thin Films Integrated into a Polymer Injection Mold to Control Dynamically the Pressure and Temperature of the Injection Process, **F. Vaz, J. Ferreira, M. Barbosa**, University of Minho, Portugal; *J. Laranjeira*, Moldit, Portugal

CP-ThP24

Assembled Monolayer of 1D and 2D Nanomaterials for Flexible Resistive Switching Device, **G.D. Moon, H.J. Seo, Y.K. Park, E. Jeong**, Korea Institute of Industrial Technology, Republic of Korea

CP-ThP25

Investigation of Sb₂Se₃ Ultra-thin Hole-transporting Material for Perovskite/Sb₂Se₃ Heterojunction Solar Cells, **G.M. Wu**, Chang Gung University, Chang Gung Memorial Hospital, Taiwan

CP-ThP26

Enhanced Storage Modulus and Shear Strength of Poly (vinylidene fluoride) Nanocomposites for Aerospace Components, **U.O. Uyor, P.A. Popoola, O.M. Popoola**, Tshwane University of Technology, Pretoria, South Africa

CP-ThP27

Fabrication of a Thermoelectric Generator Device by Suspension Plasma Spray Technique, **F. Ambriz-Vargas, C. Moreau**, Concordia University, Canada

CP-ThP30

Bipolar Resistive Switching Characteristics of MoS₂ Based Memory Devices, **A. Kumar, S. Pawar, D. Kaur**, Indian Institute of Technology Roorkee, India

CP-ThP31

Morphology Controlled of Silver/Silver Oxide Nanoparticles-MnO₂ Nanocomposites for Supercapacitor Application, *F.N. Sari, K.C. Lin, J.-W. Ruan, J.L. Huang, J.-M. Ting*, National Cheng Kung University, Taiwan

Coatings for Biomedical and Healthcare Applications

Room Grand Hall - Session DP-ThP

Coatings for Biomedical and Healthcare Applications

(Symposium D) Poster Session

5:00pm

DP-ThP2

Parylene Based Blood Oxygen Sensing Array For Flexible Wearable Devices, **W.-C. Kuo, T.-C. Wu**, National Kaohsiung University of Science and Technology, Taiwan

DP-ThP4

Development of Multilayer HA-Ag and TiN-HA-Ag Coatings Deposited by RF Magnetron Sputtering with Potential Application in the Biomedical Field, **J.A. Lenis, G.B. Gaitán, F.J. Bolívar**, University of Antioquia, Colombia

DP-ThP5

Electrochemical Activated Iridium Oxide Film as a Bio-interface Electrode for Neurostimulation Applications, *Y.-C. Chiu, P.-C. Chen*, National Taipei University of Technology, Taiwan; *C.-M. Lei*, Chinese Culture University, Taiwan; *P.-W. Wu*, National Chiao Tung University, Taiwan

DP-ThP6

HIPIMS Titanium Dioxide on Laser Roughened PEEK Surface for Biomedical Application, *P.-Y. Hsieh*, Institute of Plasma, Department of Materials Science and Engineering, Feng Chia University, Taiwan; **C.J. Chung**, Central Taiwan University of Science and Technology, Taiwan; *H.K. Tsou*, Taichung Veterans General Hospital, Taiwan; *H.T. Chen*, China Medical University Hospital, Taiwan; *J.L. He*, Institute of Plasma, Department of Materials Science and Engineering, Feng Chia University, Taiwan

DP-ThP7

Corrosion Property and Biocompatibility Evaluation of Fe-Zr-Nb Thin Film Metallic Glasses, *B.-S. Lou*, Chang Gung University, Taiwan; *T.Y. Lin, J.-W. Lee*, Ming Chi University of Technology, Taiwan; *J.-B. Wang, Y.-C. Yang*, National Taipei University of Technology, Taiwan

DP-ThP9

Bone-like Nano-hydroxyapatite Coating on Low-modulus Ti-5Nb-5Mo Alloy Using Hydrothermal and Post-heat Treatments, *H.C. Hsu, S.C. Wu, S.K. Hsu*, Central Taiwan University of Science and Technology, Taiwan; **W.F. Ho**, National University of Kaohsiung, Taiwan

DP-ThP10

Surface Characteristics and Structure of Porous TiNi Alloy for Biomedical Applications, *W.F. Ho*, National University of Kaohsiung, Taiwan; *S.C. Wu, S.K. Hsu, W.Y. Hsiao, H.C. Hsu*, Central Taiwan University of Science and Technology, Taiwan

DP-ThP11

In vitro Wear Tests of the Dual-layer Grid Blasting-plasma Polymerized Superhydrophobic Coatings on Substrates Made into Dental Stainless Archwires, **C.W. Lin**, Feng Chia University, Central Taiwan University of Science and Technology, Taiwan; *C.M. Chou*, Taichung Veterans General Hospital, National Yang-Ming University, Taiwan; *C.J. Chung*, Central Taiwan University of Science and Technology, Taiwan; *J.L. He*, Feng Chia University, Taiwan

DP-ThP16

MgO-TiO₂ Coating on Magnesium, A Biomaterial, **C. Iñiguez**, Universidad de Guanajuato, México; *E.N. Hernandez-Rodriguez*, University of Guanajuato, Mexico; *A. Marquez*, Universidad de Guanajuato, México; *M. Zapata*, Centro de Investigación en Ciencia Aplicada y Tecnología Avanzada, Unidad Legaria IPN, México

DP-ThP19

Obtaining of CVD Nanodiamonds and Evaluation of the Cytotoxicity in B16f10 Cells for Treatment of Melanoma, *C. Wachesk*, Federal University of São Paulo (UNIFESP), Brasil; *C. Hurtado*, Institute of Science and Technology, Federal University of São Paulo (UNIFESP), Brazil; **R. Falcão**, Institute of Science and Technology, Federal University of São Paulo (UNIFESP), Brasil; *D.C. Arruda*, University of Mogi das Cruzes, Brasil; *D. Tada*, Institute of Science and Technology, Federal University of São Paulo (UNIFESP), Brasil; *V.T. Airoldi*, National Institute for Space Research (INPE), Brasil

DP-ThP22

Tantalum Oxynitride PVD Coatings a Potential Candidate for Dental Implants Application, *O. Banakh*, University of Applied Sciences (HES-SO), Switzerland; **P.-A. Steinmann**, Positive Coating SA, Switzerland

DP-ThP23

SIMS and AFM Analysis of Silver-doped DLC Films on Titanium Alloy (Ti6Al4V) Aiming Biomedical Application, *A. Oliveira*, Federal University of São Paulo, UNIFESP, São Jose dos Campos, São Paulo, Brazil; *A.S. da Silva Sobrinho*, *D.M.G. Leite*, Technological Institute of Aeronautics, ITA/DCTA, São Jose dos Campos, Brazil; *W.T. Miyakawa*, *J.J. Jakutis Neto*, Institute for Advanced Studies- IEAv/DCTA, São Jose dos Campos, São Paulo, Brazil; *I.H.J. Koh*, Federal University of São Paulo, UNIFESP, Brazil; *A.M.A. Liberatore*, *M.A. Santos*, Biotecnovale Research and Development Ltd - EPP, São Jose dos Campos, Brazil; *M. Massi*, Mackenzie Presbyterian University, School of Engineering-PPGEMN, Brazil

DP-ThP24

A Multi-scale Modeling and Simulation Study on PVAc-g-PDMS Based Transparent Self-clean Coating, *S.K. Sethi*, *M. Singh*, *G. Manik*, Indian Institute of Technology Roorkee, India

DP-ThP25

Influence of Ag-Cu Nanoparticles on the Microstructural and Bactericidal Properties of TiAlN- (Ag,Cu) Coatings Deposited by DC Magnetron Sputtering for Medical Applications, *H.D. Mejia*, *G. Bejarano*, *A.M. Echavarría*, Universidad de Antioquia, Colombia

DP-ThP26

Antibacterial Activity of Conductive Thin Films Deposited on Water Filter Paper, *D.M. Mihut*, *A. Afshar*, *S. Hill*, *L. Khang*, *N. Cordista*, Mercer University, USA

Tribology and Mechanical Behavior of Coatings and Engineered Surfaces

Room Grand Hall - Session EP-ThP

Tribology and Mechanical Behavior of Coatings and Engineered Surfaces (Symposium E) Poster Session 5:00pm

EP-ThP2

Deposition of DLC/Si-N Composite Films Synthesized by Sputtering-PBII Hybrid System and Their Thermal Stability, *A. Melih*, *K. Yamada*, *S. Watanabe*, Nippon Institute of Technology, Japan

EP-ThP3

Mechanical and Tribological Performance of TiAlN, TaN and Nanolayered TiAlN/TaN Coatings Deposited by DC Magnetron Sputtering, *E. Contreras*, *J. Cortínez*, *M.A. Gómez*, Universidad de Antioquia, Colombia; *A. Hurtado*, Centro de Investigación en Materiales Avanzados CIMAV, Mexico

EP-ThP4

Development of Catalytically Active Nano-Composite Coating for Severe Boundary Lubricated Conditions of Hydraulic Fluids, *V. DaSilva*, *O.L. Eryilmaz*, *A. Erdemir*, Argonne National Laboratory, USA

EP-ThP5

Size-Independent High Strength of CuTi/Ti Metallic Glass/Crystalline Nanolayers, *M. Abboud*, Middle East Technical University, Turkey; *A. Motallebzadeh*, Koç University, Turkey; *S. Özeriç*, Middle East Technical University, Turkey

EP-ThP6

Extended Crack-free Tensile Deformation of Ultrathin Metallic Glass Films Due to an Intrinsic Size Effect, *O. Glushko*, Erich Schmid Institute of Materials Science, Austria; *M. Mühlbacher*, Montanuniversität Leoben, Austria; *C. Gammer*, *M.J. Cordill*, Erich Schmid Institute of Materials Science, Austria; *C. Mitterer*, Montanuniversität Leoben, Austria; *J. Eckert*, Erich Schmid Institute of Materials Science, Austria

EP-ThP11

Effect of Surface Treatments on AISI H13 Steels, *M.A. Doñu Ruiz*, Universidad Politécnica del Valle de México, Mexico, México; *M.G. Buenrostro Arvizu*, Universidad Autónoma Metropolitana Azcapotzalco, Mexico; *N. Lopez Perrusquia*, Universidad Politécnica del Valle de México, Mexico, México; *V.J. Cortés Suárez*, Universidad Autónoma Metropolitana Azcapotzalco, Mexico; *C.R. Torres San Miguel*, Instituto Politécnico Nacional, Mexico; *G.J. Pérez Mendoza*, Universidad Politécnica del Valle de México

EP-ThP12

Mechanical Properties and Fretting Corrosion of Zr/ZrN/CNx Hierarchical Multilayers Deposited by HIPIMS on Ti Biomedical Alloy, *M. Flores*, *J. Perez*, *O. Jiménez*, *L.M. Flores*, Universidad de Guadalajara, Mexico

EP-ThP13

Quantum Tools for Life-Time Prediction of Coatings and Thin Films, *N. Schwarzer*, SIO, Germany

EP-ThP14

Study on the Tribological Properties of MoS₂ Coatings Deposited on Laster Textured Titanium Alloy Surface, *D.Z. Segu*, LB-E-P, Republic of Korea

EP-ThP16

Structure and Fretting Wear Behavior of CuNiIn/MoS₂-Ti Multilayers Fabricated by Magnetron Sputtering Method, *C.B. Wei*, *Q. Li*, *S.S. Lin*, *H.J. Hou*, *M.J. Dai*, Guangdong Institute of New Materials, China

EP-ThP17

Contact-focusing Electron Flow (CFEF) Induced Near-zero Running-in for Low Friction of Carbon-steel contact Interface, *D.F. Diao*, Institute of Nanosurface Science and Engineering, Shenzhen University, China

EP-ThP18

Misinterpreting Size-effects during Coating Nanoindentation, *E. Broitman*, SKF Research & Technology Development Center, Netherlands

EP-ThP19

e-Poster Presentation: Think You Have Produced DLC? Think Again!, *A.M. Khan*, *H. Wu*, *Y.W. Chung*, *Q.J. Wang*, Northwestern University, USA

EP-ThP20

Mechanical and Tribological Properties of Cr-Al-Si-N-O Coatings Prepared by Arc Ion Plating for Cutting Tools, *J.-H. Kim*, *W.R. Kim*, Korea Institute of Industrial Technology (KITECH), Republic of Korea

EP-ThP21

Wear of TiN in Reciprocating Soft Contacts, *S.H. van der Poel*, *D.T.A. Matthews*, University of Twente, Netherlands

EP-ThP22

Friction Property of Si-DLC with Scratch Damage Before and After Local Repairing Deposition to the Scratch Scar, *H. Takamatsu*, *K. Tanaka*, *A. Ito*, *H. Kousaka*, *T. Furuki*, Gifu University, Japan

EP-ThP23

Raman Scattering Characterizes Thermally Annealed HiPIMS Sputtered MoS₂ Coatings, *H. Moldenhauer*, *W. Tillmann*, *A. Wittig*, *D. Kokalj*, *D. Stangier*, *A. Brümmer*, *J. Debus*, TU Dortmund University, Germany

EP-ThP24

Friction Reduction in Sliding Between Si-DLC vs. Steel Ball by Ar Plasma Irradiation Using Microwave-excited Atmospheric Pressure Plasma Jet, *T. Hibino*, *H. Kousaka*, *T. Furuki*, Gifu University, Japan; *J. Kim*, *H. Sakakita*, National Institute of Advanced Industrial Science and Technology (AIST), Japan

EP-ThP26

Tribological Performance Dependence on Microstructure, Composition and Morphology of WTiN Coatings Obtaining by d.c. Magnetron Sputtering Varying the Working Pressure, *R.F. Londoño*, Universidad Nacional de Colombia Sede Manizales Colombia; *R. Ospina*, Universidad Industrial de Santander, Bucaramanga, Santander, Colombia; *D. Escobar*, *J.J. Olaya Florez*, Universidad Nacional de Colombia, Colombia; *J.H. Quintero*, Universidad Industrial de Santander, Colombia; *E. Restrepo-Parra*, Universidad Nacional de Colombia Sede Manizales, Colombia

EP-ThP27

Taguchi Method to Study Effects of Plasma Surface Texturing on Friction Reduction of Cast Iron at High Speed Sliding Lubricated Conditions, *W. Zha*, *C. Zhao*, *R. Cai*, *X. Nie*, University of Windsor, Canada

EP-ThP28

Discharge Behaviors of Plasma Electrolytic Oxidation in Porosol and Coating Characterization of Aluminum Alloy, *W.X. Bo*, *W. Xiaobo*, China Academy of Engineering Physics, China

EP-ThP30

Test Rig Development For Static Friction Assessment At High Temperature, *M. Azzi*, Lebanese University (UL), Lebanon; *E.B-N. Bitar-Nehme*, Tricomat, Canada; *J.A. Schmitt*, *T.S. Schmitt*, *L. Martinu*, *J.E. Klemberg-Sapieha*, École Polytechnique de Montréal, Canada

EP-ThP31

Improving the Tribological Performance of PVD-TiCN-Al₂O₃ Coating with Solid Lubricants for Maximum Wear Resistance, *R.K. Gunda*, Mahatma Gandhi Institute of Technology, India; *U.M.R. Paturi*, CVR College of Engineering, Hyderabad, India; *S.K.R. Narala*, BITS Pilani, India; *S. Palaparty*, Methodist College of Engineering and Technology, India

New Horizons in Coatings and Thin Films

Room Grand Hall - Session FP-ThP

New Horizons in Coatings and Thin Films (Symposium F)

Poster Session

5:00pm

FP-ThP3

Influencing the Cubic to Wurtzite Phase Transition in Ti-Al-N by Reactive HiPIMS Deposition, *L. Zauner*, TU Wien, CDLAOS at the Institute of Materials Science, Austria; *H. Riedl*, TU Wien, Institute of Materials Science, Austria; *T. Kozák, J. Čapek*, University of West Bohemia, Czech Republic; *T. Wojcik*, TU Wien, Institute of Materials Science, Austria; *H. Bolvardi*, Oerlikon Balzers, Oerlikon Surface Solutions AG, Liechtenstein; *S. Kolosvári*, Plansee Composite Materials GmbH, Germany; *P.H. Mayrhofer*, TU Wien, Institute of Materials Science, Austria

FP-ThP5

e-Poster Presentation: Vacancies to Compensate for Electronic Imbalances in Crystals, *M. Fischer, D. Scopece, M. Trant, C.A. Pignedoli, K. Thorwarth, D. Passerone, H.J. Hug*, Empa - Swiss Federal Laboratories for Materials Science and Technology, Switzerland

FP-ThP6

Role of the Thermalized Ions in the Reduction of the Atomic Shadowing Effect in HiPIMS, *J.C. Oliveira, F. Ferreira*, University of Coimbra, Portugal; *A. Anders*, Leibniz Institute of Surface Engineering, Germany; *A. Cavaleiro*, University of Coimbra, Portugal

FP-ThP7

Study of the Self-organizing Structures in Magnetron Plasma by a Pseudo 3D Model, *A. Revel*, Université Paris-Sud/CNRS, France; *T. Minea*, Université Paris-Sud, Université Paris-Saclay, France; *M. George, B. Vincent*, CNRS, France; *S. Tsikata*, CNRS, ICARE, France

FP-ThP9

Point Ion Beam Sputtering for Novel Applications, *V. Bellido-Gonzalez, D. Monaghan, R. Brown*, Gencoa Ltd, UK; *D. Perry*, Quorum Technologies, UK; *J. Brindley, A. Azzopardi*, Gencoa Ltd, UK

FP-ThP10

Reducing the Intrinsic Stress of TiN Films in HiPIMS, *F. Cemin*, LPGP, Université Paris-Sud, Orsay, France; *G. Abadias*, Institut Pprime - CNRS - ENSMA - Université de Poitiers, France; *T. Minea, D. Lundin*, LPGP, Université Paris-Sud, Orsay, France

FP-ThP11

Study on Tribological Behavior of ZrB₂-Zr Coatings Deposited on Ti6Al4V and CoCrMo Alloys by HiPIMS, *L. Flores-Cova, O. Jiménez, M. Flores, J. Pérez-Alvarez*, Universidad de Guadalajara, Mexico

FP-ThP12

SPS of Al-CNTs-Nb Nano-Composite for Power Transmission Conductor Core, *C.O. Ujah, P.A. Popoola, O.M. Popoola*, Tshwane University of Technology, Pretoria, South Africa

FP-ThP15

Temperature Dependent Photoluminescence Emission and Resonance Raman Spectra from WS₂ Nanostructures, *nil. Sharma*, Guru Nanak Dev University Amritsar India, India

FP-ThP16

Detecting the Direction of a Magnetic Field with a Nanocrystallized Carbon Film by Using its Anisotropic Magnetoresistance and Hall Effect, *C. Wang, T. Huang, W. Zhang, J. Guo, X. Dai*, Institute of Nanosurface Science and Engineering, College of Mechatronics and Control Engineering, Shenzhen University, China

FP-ThP17

Effect of Synchronized Bias on the Oxygen Content in r-HiPIMS Deposited γ -Al₂O₃ Thin Films, *S. Kagerer*, TU Wien, Institute of Materials Science, Austria; *S. Kolosvári*, Plansee Composite Materials GmbH, Germany; *T. Kozák, J. Čapek, P. Zeman*, University of West Bohemia, Czech Republic; *H. Riedl*, TU Wien, Institute of Materials Science and Technology, Austria; *P.H. Mayrhofer*, TU Wien, Institute of Materials Science and Technology, Österreich, Austria

FP-ThP18

Effect of Secondary Phases on the Thermoelectric Properties of Zn₂GeO₄ Thin Films Grown by Thermal Evaporation on Au Coated Si Substrate, *K. Mahmood*, Government College University Faisalabad, Pakistan

Surface Engineering - Applied Research and Industrial Applications

Room Grand Hall - Session GP-ThP

Surface Engineering - Applied Research and Industrial Applications (Symposium G) Poster Session

5:00pm

GP-ThP1

Effect of Plasma Nitriding and Modulation Structure on the Adhesion and Corrosion Resistance of CrN/Cr₂O₃ Coating, *C.H. Huang, C.H. Yang, Y.J. Tsai, C.L. Chang*, Ming Chi University of Technology, Taiwan

GP-ThP2

Study on SiN and SiCN Film Production using PE-ALD Process with High-density Multi-ICP Source at Low Temperature, *H. Song, H.Y. Chang*, Korea Advanced Institute of Science and Technology, Republic of Korea

GP-ThP3

PEO Coatings for Adhesive Bonded Aluminium Structures, *D. Shore, A. Rogov, A. Matthews, A. Yerokhin*, The University of Manchester, UK

GP-ThP5

Hydrogen Barrier Coatings Deposited by Magnetron Sputtering: A Study of Different Oxide Materials and Their Microstructure on the Hydrogen Permeability Properties, *S. Gimeno*, Fersa Bearings, Spain; *J.A. Garcia*, Universidad Publica de Navarra, Spain; *I. Quintana, L. Mendizabal, C. Zubizarreta*, Physic of Surfaces and Materials Unit, IK4 - TEKNIKER, Spain

GP-ThP6

Process for Obtaining TiO₂/SiO₂ Systems using Magnetron Sputtering RF from Ceramic Targets: Studies on their Anti-Reflective Response, *D. Zambrano, R. Villarroel, R. Espinoza*, Universidad de Chile, Chile

GP-ThP7

Microstructure Evolution of Overlay Welded Duplex Stainless Steel Joints, *P.A. Luchtenberg, R. Torres, P. Soares, P. Campos*, Pontificia Universidade Católica do Paraná, Brazil

GP-ThP8

Deposition of Diamond-like Carbon Films on Interior Surface of a Metallic Tube with High Aspect Ratio, *E.J.D. Mitma Pillaca*, National Institute for Space Research - INPE, Brazil; *V.J. Trava-Airoldi*, National Institute for Space Research, Brazil; *M. Ramirez*, University of Vale do Paraiba, Brazil

GP-ThP11

Ion Beam Assisted Deposition of DLC for Sheet Metal Forming Tools, *L.P. Nielsen, K.P. Almtoft, C.S. Jeppesen, C. Mathiasen, P.M. Pedersen*, Danish Technological Institute, Denmark

GP-ThP13

Effect of Interaction between Microbial Fluid and Electrode on Performance, *Y.C. Liu, Y.-C. Yang*, National Taipei University of Technology, Taiwan

GP-ThP15

Design of Low-Pressure Chemical Vapor Deposition Reactors Using Vertical Cavity Surface Emitting Lasers, *S. Park, Y. Noh, Y. Kim*, Hongik University, Seoul, Republic of Korea; *B.K. Kim, H.J. Kim*, Viatron Technologies, Republic of Korea

GP-ThP16

Optical, Mechanical and Anti-corrosive Property Investigation of Tantalum Oxynitride Thin Films for Hard Coating Applications, *J.G. Hirpara, R. Chandra*, Indian Institute of Technology Roorkee, India

GP-ThP17

Synthesis and Properties of Two-dimensional Zirconium Phosphate/Polyimide Nanocomposites as Anticorrosion Coatings, *G.-H. Lai*, National Chin-Yi University of Technology, Taiwan; *I-H. Tseng*, Feng Chia University, Taiwan; *T.-C. Huang, P.-S. Tsai, M.-H. Tsai*, National Chin-Yi University of Technology, Taiwan

GP-ThP18

Improvement of the Corrosion Resistance in the ASTM F75 Alloy by Ball Burnishing, *E.N. Hernandez-Rodriguez, D.F. Silvia Alvarez, A. Marquez Herrera, A. Saldana Rovles, J. Moreno Palmerin*, University of Guanajuato, Mexico

GP-ThP19

Surface Modification of Sputter Deposited γ -WO₃ Thin Film for Scaled Electrochromic Behaviour, *R. Chandra, G. Malik, S. Mourya, J. Jaiswal*, IIC, IIT Roorkee, India

Thursday Afternoon Poster Sessions, May 23, 2019

GP-ThP20

Studies of Corrosion Properties of Plasma Nitrided Steels, *P. Ghai*, Brock University, St. Catharines, Canada

GP-ThP21

Nanotexturization and Passivation of Single Crystalline Silicon Surface for Passivated Emitter and Rear Contact Solar Cells, *C.H. Hsu*, Xiamen University of Technology, China; *S.-M. Liu*, Da-Yeh University, Taiwan, Taiwan; *W.-Y. Wu*, Da-Yeh University, Taiwan; *S.-Y. Lien*, Xiamen University of Technology, China

GP-ThP22

Understanding the Electrochemical Mechanism of Cold Galvanizing and Zinc Electroplating on Steel Structure in Saline Conditions, *A. Farooq*, University of the Punjab, Pakistan; *A. Saleem*, University of the Punjab, Lahore, Pakistan; *K. Mairaj Deen*, University of British Columbia, Canada

GP-ThP23

FEM Analysis on the Cold Rolled Gd-B-Duplex Stainless Steels, *Y. Baik*, Dankook University, Republic of Korea

GP-ThP24

Optical Performances of Antireflective Moth-Eye Structures under Thermal and Humid Stress – Application to Outdoor Lighting LEDs., *C. Ducros*, *A. Brodus*, *G. Lorin*, *F. Emieux*, *A. Pereira*, Univ. Grenoble Alpes, CEA, France

Advanced Characterization Techniques for Coatings, Thin Films, and Small Volumes

Room Grand Hall - Session HP-ThP

Advanced Characterization Techniques for Coatings, Thin Films, and Small Volumes (Symposium H) Poster Session 5:00pm

HP-ThP1

Cyclic Tensile Deformation of Freestanding, Nanocrystalline NiTi Films using MEMS Stages, *P. Rasmussen*, *R. Sarkar*, *J. Rajagopalan*, Arizona State University, USA

HP-ThP3

Ion Irradiation Behavior of a Nanocrystalline BCC High-Entropy Alloy, *Y. Xiao*, *H. Ma*, *A.S. Sologubenko*, *R. Spolenak*, *J.M. Wheeler*, ETH Zürich, Switzerland

HP-ThP4

Evaluation of Properties in Steel with Hard Coating under Hydrogen, *N. Lopez Ferrusquia*, Universidad Politecnica Del Valle De México, México; *M.A. Doñu Ruiz*, Universidad Politecnica del Valle de México, México; *C.R. Torres San Miguel*, Sección de Estudios de Posgrado e Investigación de la Escuela Superior de Ingeniería Mecánica y Eléctrica Unidad Zacatenco, México; *V.J. Cortés Suárez*, *J.A. Garcia Sanchez*, Universidad Autonoma Metropolitana Azcapotzalco, Mexico; *L. Sánchez Fuentes*, Universidad Politecnica del Valle de México, Mexico

HP-ThP5

Effect of Zn Interlayer Microstructure on Corrosion Resistance and Adhesion Strength of Zn-Mg/Zn Coating on TRIP Steel, *M.G. Song*, *H.K. Kim*, *S.H. Lee*, *S.Y. Lee*, Korea Aerospace University, Republic of Korea

HP-ThP6

Coatings and Interfaces Characterization: Depth Profiling from the First Nanometer down to the Substrate using RF GD-OES, *P. Hunault*, HORIBA Instruments, USA; *M.F. Chausseau*, *K. Savadkouei*, HORIBA Scientific, USA; *P. Chapon*, *S. Gaiaschi*, HORIBA Scientific, France

HP-ThP7

In situ Measurement Setup for DC Magnetron Sputtering Thin Film Deposition, *Q. Herault*, *S. Grachev*, *I. Gozhyk*, *H. Montigaud*, Saint-Gobain Recherche/CNRS, France; *R. Lazzari*, Institut des Nano Sciences de Paris - Sorbonne Université, France

HP-ThP8

Preparation and Physical Properties of Multiferroic CaMn₇O₁₂ Thin Films, *Y.C. Tseng*, National Chiao Tung University, Taiwan; *S.R. Jian*, I-Shou University, Taiwan; *C.-M. Lin*, National Tsing Hua University, Taiwan; *J.Y. Juang*, National Chiao Tung University, Taiwan

HP-ThP9

SIO X-Ray: View Inside your Material with Contact Experiments, *N. Bierwisch*, *N. Schwarzer*, SIO, Germany

HP-ThP10

Classification of Aluminum Alloys by an Inexpensive Laser-Induced Breakdown Spectroscopy System, *K. Maldonado Dominguez*, *R.S. Sanginés de Castro*, Universidad Nacional Autonoma de México, México

HP-ThP11

Glow Discharge Optical Emission Spectroscopy: Advances toward Quantitative Coating Compositional Depth Profiling, *A.H. Tavakoli*, *F. Li*, Air Liquide - Balazs NanoAnalysis Laboratory, USA

HP-ThP12

Effect of the Cobalt Content on the Magnetic and Corrosion Properties of Electro-formed Fe-Ni-Co Thin Foils, *B.K. Kang*, *Y. Baik*, *M.Y. Jung*, *Y. Choi*, Dankook University, Republic of Korea

Topical Symposia

Room Grand Hall - Session TSP-ThP

Topical Symposia (TS) Poster Session 5:00pm

TSP-ThP1

Surface Modification of Multiwalled Carbon Nanotubes for Electro-Thermal Heating in Ice Protection, *F. Zangrossi*, *F. Xu*, *N. Warrior*, *X.H. Hou*, University of Nottingham, UK

TSP-ThP2

Nanostructured a-C:H:SiO_x Coatings with Superhydrophobic Properties, *D. Batory*, Lodz University of Technology, Poland; *J. Lengaigne*, Ecole Polytechnique de Montreal, Canada; *A. Jedrzejczak*, Lodz University of Technology, Poland; *S. Brown*, *J.E. Klemberg-Sapieha*, Ecole Polytechnique de Montreal, Canada

TSP-ThP4

Structural Investigation of the Stability in Temperature of Some High Entropy Alloys, *M. Calvo-Dahlborg*, University of Rouen Normandie-CNRS, France, Swansea University, UK; *U. Dahlborg*, *J. Cornide*, University of Rouen Normandie-CNRS, France; *S. Mehraban*, College of Engineering, Swansea University, UK; *R. Wunderlich*, University of Ulm, Germany; *N. Lavery*, College of Engineering, Swansea University, UK; *S.G.R. Brown*, Swansea University, UK

TSP-ThP6

Cu-nanoparticles /Polyfluoroacrylate Emulsion Nanocomposite Coating for Icephobic Applications, *T.B. Barman*, *H.C. Chen*, *J.L. Liu*, *X.H. Hou*, The University of Nottingham, UK

TSP-ThP7

Surface Characteristics and Diffusion Phenomenon of Ni₂FeCoCrAl_x Alloys Treated by Atmospheric Pressure Plasma, *C.R. Huang*, National United University, Taiwan; *J.G. Duh*, National Tsing Hua University, Taiwan; *F.B. Wu*, National United University, Taiwan

TSP-ThP8

Development of Microwave Remote Plasma Source for New Surface Functionalization, *Y. Isomura*, *Y. Ikari*, *T. Okimoto*, *Y. Tauchi*, *K. Nishiyama*, Kobe Steel, Ltd., Japan; *H. Toyoda*, *H. Suzuki*, Nagoya University, Japan

TSP-ThP9

Combinatorial Study of Dielectric and Piezoelectric High Entropy Oxides, *Z.-W. Huang*, *C.-M. Chou*, *J.-M. Ting*, *J.-J. Ruan*, *K.-S. Chang*, *Y.-H. Su*, National Cheng Kung University, Taiwan

Friday Morning, May 24, 2019

| Hard Coatings and Vapor Deposition Technologies Room Golden West - Session B2-2-FrM CVD Coatings and Technologies II Moderators: Kazunori Koga , Kyushu University, Japan, Raphaël Boichot , Université Grenoble Alpes, CNRS, France | | Hard Coatings and Vapor Deposition Technologies Room California - Session B5-2-FrM Hard and Multifunctional Nanostructured Coatings II Moderators: Tomas Kozak , University of West Bohemia, Czech Republic, Helmut Riedl , TU Wien, Institute of Materials Science and Technology, Austria | |
|---|---|---|--|
| 8:00am | | | |
| 8:20am | | | |
| 8:40am | | | |
| 9:00am | | B5-2-FrM4 Microstructural and Mechanical Stability of TaCu Composite Coatings, <i>A. Bahrami, C.F. Onofre, A. Delgado</i> , Universidad Nacional Autonoma de México, México; <i>T.H. Huminiuc, T.P. Polcar</i> , University of Southampton, UK; <i>S.E. Rodil</i> , Universidad Nacional Autonoma de México, México | |
| 9:20am | B2-2-FrM5 Scale up of the DLI-MOCVD Process to Treat 16 Nuclear Fuel Cladding Segments in Parallel with a Protective CrC _x Coating, <i>A. Michau, F. Addou</i> , CEA, Université Paris-Saclay, France; <i>Y. Gazal, F. Maury, T. Duguet</i> , CIRIMAT, France; <i>R. Boichot, M. Pons</i> , Université Grenoble Alpes, CNRS, France; <i>E. Monsifrot</i> , Dephis, France; <i>F. Schuster</i> , CEA, PTCMP, France | B5-2-FrM5 Hydrogen Permeation Behavior of Multi-Layered-Coatings, <i>M. Tamura</i> , University of Electro-Communications, Japan | |
| 9:40am | B2-2-FrM6 Assessment of Low Temperature CVD Routes to MAX Phases in the Cr-Si-C System, <i>A. Michau</i> , CEA, Université Paris-Saclay, France; <i>F. Maury</i> , CIRIMAT, France; <i>F. Schuster</i> , CEA Cross-Cutting Program on Materials and Processes Skills, France; <i>T. Duguet</i> , CIRIMAT, France; <i>E. Monsifrot</i> , Dephis, France | INVITED: B5-2-FrM6 Tantalum Alloying - Improvement of Thermal Stability and Mechanical Properties of Ternary and Quaternary Transition Metal Nitrides, <i>B. Grancic</i> , Comenius University in Bratislava, Slovakia; <i>D.G. Sangiovanni</i> , Linköping University, Sweden, Ruhr-Universität Bochum, Germany; <i>T. Roch, M. Truchlý, M. Mikula</i> , Comenius University in Bratislava, Slovakia | |
| 10:00am | B2-2-FrM7 Towards CVD of Hard Coatings Using Hetero-Metallic Precursors, <i>s.Ö. Öhman, M.E. Ek</i> , Uppsala University, Angstrom Laboratory, Sweden; <i>R.M. Brenning</i> , Sandvik Coromant R&D, Sweden; <i>M. Boman</i> , Uppsala University, Angstrom Laboratory, Sweden | Invited talk continues. | |
| 10:20am | B2-2-FrM8 CVD of Tungsten, Tungsten Nitride and Tungsten Carbide Multilayers, <i>J. Hulkko, K. Bööer</i> , Uppsala University, Angstrom Laboratory, Sweden; <i>R. Qiu</i> , Chalmers University of Technology, Sweden; <i>E. Lindahl</i> , Sandvik Coromant R&D, Sweden; <i>M. Boman</i> , Uppsala University, Angstrom Laboratory, Sweden | B5-2-FrM8 Interface Characteristics Between PVD- AlTiN and Electroplated Hard Chrome by Duplex Process, <i>D.Y. Wang</i> , MingDao University, Taiwan; <i>L.C. Hsu, J. Hung</i> , Aurora Scientific Corp., Canada; <i>C.H. Chen, H.C. Liu</i> , Surftech Corp., Taiwan; <i>W.Y. Ho</i> , MingDao University, Taiwan | |
| 10:40am | B2-2-FrM9 Deposition of Carbon Nanoparticles Using Multi-Hollow Discharge Plasma CVD for Synthesis of Carbon Nanoparticle Composite Films, <i>K. Koga, S.H. Hwang</i> , Kyushu University, Japan; <i>T. Nakatani</i> , Okayama University of Science, Japan; <i>J.S. Oh</i> , Osaka City University, Japan; <i>K. Kamataki, N. Itagaki, M. Shiratani</i> , Kyushu University, Japan | B5-2-FrM9 Manipulation of Bimodal Matrix in Plasma Sprayed Nanostructured YSZ Coating and Its Effect on the Microstructure, <i>P. Bijalwan</i> , Tata Steel Limited, India; <i>A. Islam, K.K. Pandey</i> , Indian Institute of Technology, India; <i>A. Pathak, M. Dutta</i> , Tata Steel Limited, India; <i>A.K. Keshri</i> , Indian Institute of Technology, India | |
| 11:00am | B2-2-FrM10 Hot Filament CVD Diamond Coating Technology for Cutting Tool Applications, <i>M. Woda, W. Puetz, M. Frank, C. Schiffers, W. Koelker, O. Lemmer, T. Leyendecker</i> , CemeCon AG, Germany | SEE YOU NEXT YEAR PARTY!! 12:00 – 1:00 pm, Lion Fountain Courtyard ICMCTF 2020: APRIL 26 – MAY 1, 2020 Abstract & Awards Submission Deadline: October 1, 2019 | |

Friday Morning, May 24, 2019

| Tribology and Mechanical Behavior of Coatings and Engineered Surfaces Room San Diego - Session E1-3-FrM Friction, Wear, Lubrication Effects, and Modeling IV Moderators: Nazlim Bagcivan, Schaeffler AG, Germany, Carsten Gachot, TU Wien, Institute for Engineering Design and Logistics Engineering, Austria, Tomas Polcar, Czech Technical University in Prague, Czech Republic | | Surface Engineering - Applied Research and Industrial Applications Room Pacific Salon 1 - Session G2-FrM Component Coatings for Automotive, Aerospace, Medical, and Manufacturing Applications Moderators: Tetsuya Takahashi, Kobe Steel, Ltd., Japan, Etienne Bousser, École Polytechnique de Montréal, Canada, Satish Dixit, Plasma Technology Inc., USA | |
|---|--|---|--|
| 8:00am | E1-3-FrM1 Numerical and Experimental Analyses on the Influence of Irregular Columnar Boundaries on Mechanical and Tribological Behavior of a WC/C Coating, <i>C. Bernardes, N. Fukumasu, R.M. Souza, I.F. Machado</i> , University of São Paulo, Brazil | | |
| 8:20am | E1-3-FrM2 Structure, Mechanical and Tribological Properties of Mo-S-N Solid Lubricant Coatings, <i>T. Hudec</i> , University of Southampton, UK; <i>M. Mikula, L. Satrapinsky, T. Roch, M. Truchlý</i> , Comenius University in Bratislava, Slovakia; <i>P. Švec Jr.</i> , Slovak Academy of Sciences, Bratislava, Slovakia; <i>T.H. Huminiuc, T.P. Polcar</i> , University of Southampton, UK | | |
| 8:40am | INVITED: E1-3-FrM3 Superlubricity with Carbon Coatings Lubricated by Organic Friction Modifiers, <i>M. Moseler</i> , Fraunhofer IWM, Germany | INVITED: G2-FrM3 YKK's Sustainable Development: Reduction of Mold Cleaning Load by Diecast Mold Coating and Release Agent, <i>M. Mizubayashi, T. Sakuragi, N. Watanabe, M. Ishida</i> , YKK Corporation, Japan; <i>K. Matsuda</i> , University of Toyama, Japan; <i>M. Nose</i> , Hokuriku Polytechnic College, Japan | |
| 9:00am | Invited talk continues. | Invited talk continues. | |
| 9:20am | E1-3-FrM5 Multipass and Reciprocating Microwear Study of TiN Based Films, <i>R.C. Vega-Marón</i> , Instituto Politecnico Nacional Grupo Ingeniería de Superficies, Mexico, México; <i>D.V. Melo-Máximo</i> , Tecnológico de Monterrey-CEM, México; <i>G.A. Rodríguez-Castro</i> , Instituto Politecnico Nacional, Grupo Ingeniería de Superficies, Mexico, México; <i>J. Oseguera-Peña</i> , Tecnológico de Monterrey-CEM, Mexico, México; <i>A. Bahrami</i> , Institute for Metallic Materials, Leibniz-Institute for Solid State and Materials Research Dresden, Germany; <i>S. Muhl</i> , Instituto de Investigaciones en Materiales-UNAM, México | G2-FrM5 Effect of Plasma Electrolytic Oxidation Process on Surface Characteristics and Tribological Behavior, <i>R. Cai, C. Zhao, X. Nie</i> , University of Windsor, Canada | |
| 9:40am | E1-3-FrM6 Correlation Between Wear Resistance of Ti/TiN Based Films and Deposition Temperature, <i>F. Toledo-Romo, R.C. Vega-Marón</i> , Instituto Politecnico Nacional, Grupo Ingeniería de Superficies, México; <i>G.A. Rodríguez-Castro</i> , Instituto Politecnico Nacional, Grupo Ingeniería de Superficies, Mexico, México; <i>D.V. Melo-Máximo, J. Oseguera-Peña, L. Melo-Máximo</i> , Tecnológico de Monterrey-CEM, México; <i>V.M. Araujo-Monsalvo</i> , Laboratorio de Biomecánica, Instituto Nacional de Rehabilitación "Luis Guillermo Ibarra Ibarra", México | G2-FrM6 Effectiveness of Electromagnetic Interference Shielding of Sputtered Nitrogen-Doped Carbon Thin Films, <i>D.H. Liu, Y.S. Lai</i> , National United University Miaoli, Taiwan | |
| 10:00am | E1-3-FrM7 Microstructure Evolution and Deposition Parameter Control on Sputtering MoSiN Coating, <i>Y.C. Liu, Z.X. Lin, S.T. Wang, F.B. Wu</i> , National United University, Taiwan | G2-FrM7 Challenges for Surface Solutions for Automotive Applications, <i>J. Vetter, J. Becker</i> , Oerlikon Balzers Coating Germany GmbH, Germany; <i>P. Ernst</i> , Oerlikon Metco AG, Switzerland; <i>J. Crummenauer</i> , Oerlikon Balzers Coating Germany GmbH, Germany; <i>A. Müller</i> , Oerlikon Surface Solutions AG, BTS, Balzers, Liechtenstein | |
| 10:20am | E1-3-FrM8 Influence of Ag Content on the Tribological and Oxidation Behaviour of TiSiN(AG) Thin Films Deposited by HIPIMS, <i>D. Cavaleiro, F. Fernandes, S. Carvalho</i> , University of Minho, Portugal; <i>A. Cavaleiro</i> , University of Coimbra, Portugal | G2-FrM8 Hard Turning with PVD Coated p-cBN, <i>C.J. Charlton</i> , Kennametal Inc., USA; <i>J. Kahlscheen</i> , Kennametal GmbH, Germany; <i>D. Banerjee</i> , Kennametal Inc., USA; <i>C. Bareiss</i> , Kennametal GmbH, Germany | |
| 10:40am | E1-3-FrM9 Wear Resistance of Titanium Oxynitride Coatings as a Function of the Relative Humidity, <i>C. Rojo-Blanco</i> , IIM-UNAM, Mexico; <i>S. Muhl</i> , Instituto de Investigaciones en Materiales-UNAM, México | G2-FrM9 Arc PVD (Cr,Al,Mo)N and (Cr,Al,Cu)N Coatings for Mobility Applications, <i>K. Bobzin, T. Brögelmann, C. Kalscheuer</i> , RWTH Aachen University, Germany | |
| 11:00am | E1-3-FrM10 Thermo-mechanical/chemical Contact Behavior of DLC Film under Molecularly Thin Lubricants, <i>S.M. Rahman</i> , Texas Tech University, USA; <i>J. Song</i> , Molex, USA, USA; <i>C.D. Yeo</i> , Texas Tech University, USA | G2-FrM10 Thermal Analysis on the Application of Plasma Electrolytic Oxidation (PEO) Coatings On Automobile Engines, <i>X. Shen, X. Nie</i> , University of Windsor, Canada; <i>J. Tjong</i> , Ford Motor Company, USA | |
| 11:20am | E1-3-FrM11 Investigation of the Wear Resistance of TiN/TiAlN, CrN/TiAlN and CrAlN/TiAlN Double Layer Coated Stainless Steel at Elevated Temperatures, <i>Y. Adesina, A. Sorour</i> , King Fahd University of Petroleum and Minerals, Saudi Arabia | G2-FrM11 Ion Beam Stripping Process for Cutting Tools Reconditioning, <i>A.G. Remnev</i> , ITAC Ltd., Group of ShinMaywa Industries, Japan | |
| 11:40am | E1-3-FrM12 Effect of Electrostatic Solid Lubrication on Tribological Behavior of Ti-6Al-4V Alloy, <i>R.K. Gunda, S.K.R. Narala</i> , BITS Pilani Hyderabad Campus, India; <i>P. Shailesh</i> , Methodist College of Engineering and Technology, India; <i>S.P. Regalla</i> , BITS Pilani Hyderabad Campus, India | SEE YOU NEXT YEAR PARTY!! 12:00 – 1:00 pm, Lion Fountain Courtyard ICMCTF 2020: APRIL 26 – MAY 1, 2020 Abstract & Awards Submission Deadline: October 1, 2019 | |

Bold page numbers indicate presenter

— A —

Abadias, G.: FP-ThP10, **70**; H1-2-TuA2, 46; SIT1-TuSIT1, **47**
 Abbas, A.: C3+C1-WeM2, 49
 Abboud, M.: E2-2-TuA10, 45; EP-ThP5, 69
 Abern, M.J.: C4-ThA2, **63**; C4-ThA6, 63
 Abraham, B.: B1-2-MoA1, 35
 Abstoss, K.G.: A1-1-TuM8, 38
 Adams, D.P.: C4-ThA2, 63; C4-ThA6, **63**
 Addou, F.: B2-2-FrM5, 72
 Adesina, Y.: AP-ThP5, **66**; E1-3-FrM11, **73**
 Afshar, A.: B4-4-WeA6, 53; DP-ThP26, 69
 Agüero, A.: A3-WeA4, **53**; TS2-ThM8, 61
 Aguirre Ocampo, R.: D1-2-MoA5, **36**
 Ahlgren, M.: F4-2-WeA7, 55
 Airoidi, V.T.: DP-ThP19, 68
 Akinlabi, E.T.: AP-ThP4, 66; B4-2-TuA10, 43
 Akinlabi, S.A.: AP-ThP4, 66; B4-2-TuA10, 43
 Al-Badour, A.: AP-ThP5, 66
 Albers, C.: BP-ThP37, 67
 Alem, N.: B2-1-ThA9, 62
 Aleman, A.: B6-ThM10, 58
 Alhussein, A.A.: A1-1-TuM6, 38; E2-1-TuM5, 40
 Alling, B.: F4-2-WeA7, 55
 Allport, J.: AP-ThP2, 66
 Almer, J.: A2-1-ThM8, 58
 Almqvist, K.P.: E1-1-ThM7, 59; GP-ThP11, 70
 Alphonse, A.: F4-2-WeA11, 55
 Alrefae, M.: F3-TuA1, 45
 Altangerel, D.: B7-TuA3, 44
 Alvarez, F.: B4-3-WeM2, **48**; E1-2-ThA11, 64
 Ambriz-Vargas, F.: CP-ThP27, **68**
 Amini, S.: D1-2-MoA3, 36
 Anders, A.: FP-ThP6, 70
 Anderson, J.: G4+G5+G6-ThA1, **65**
 Andreev, N.: B1-2-MoA11, 35
 Anselme, K.: D3-TuM4, **39**
 Antunes, V.: B4-3-WeM2, 48
 Aouadi, S.M.: A2-1-ThM5, 58; A2-1-ThM9, 58
 Appleget, C.: C3+C2+C1-ThM8, **59**
 Araujo-Monsalvo, V.M.: E1-3-FrM6, 73
 Arciniega-Martínez, J.L.: B4-2-TuA3, **43**
 Ares de Parga, G.: B4-2-TuA8, 43
 Argibay, N.: E3-WeM1, 49
 Argyropoulos, C.: C3+C2+C1-ThM9, 59
 Arias, P.: B6-ThM10, 58
 Arigela, V.G.: H3-1-WeM3, **50**; H3-2-WeA9, 55
 Armstrong, B.L.: A1-1-TuM1, 38; A1-3-WeM4, 48
 Arndt, M.: B6-ThM12, 58; BP-ThP41, 67; TS1-1-WeM4, 51
 Arroyave Franco, M.: E1-4-WeA5, 54
 Arruda, D.C.: DP-ThP19, 68
 Arunachalam, N.: D1-1-MoM7, 33
 Asensio, M.-C.: F3-TuA8, 45
 Ashok, A.: C4-ThA9, 63
 Ast, J.: A2-2-ThA3, 62
 Attarzadeh, R.: TS2-ThM9, 61
 Audigié, P.: A3-WeA4, 53
 Aureli, M.: C4-ThA3, 63
 Avila, J.: F3-TuA8, 45
 Awais, R.: D3-TuM6, 39
 Azzi, M.: E1-1-ThM6, 59; EP-ThP30, 69
 Azzopardi, A.: B1-2-MoA2, 35; FP-ThP9, 70

— B —

Bachu, S.: B2-1-ThA9, 62
 Bäcke, O.: B2-1-ThA5, **62**
 Badhirappan, G.P.: C4-ThA9, **63**
 Bagcivan, N.: E1-2-ThA10, 64
 Bahrami, A.: B5-2-FrM4, 72; E1-3-FrM5, 73
 Bai, T.: C2-WeA9, 54

Baik, Y.: GP-ThP23, **71**; HP-ThP12, 71
 Baker, M.: C3+C1-WeM4, 49
 Bakhit, B.: B4-1-TuM4, 39
 Bakkar, S.: A2-1-ThM9, 58
 Balaji, G.: C4-ThA9, 63
 Balasundraprabhu, R.: C4-ThA9, 63
 Balat-Pichelin, M.: B2-1-ThA7, 62
 Balazsi, K.: B1-3-TuM6, 38; B5-1-ThA4, 63
 Baloukas, B.: C3+C1-WeM4, 49
 Banakh, O.: DP-ThP22, 68
 Banerjee, D.: B2-1-ThA8, 62; BP-ThP1, 66; G2-FrM8, 73
 Banks, C.E.: F3-TuA3, 45
 Barbosa, M.: CP-ThP23, 68
 Bareiss, C.: G2-FrM8, 73
 Barman, T.B.: TSP-ThP6, 71
 Barnier, V.: F3-TuA8, 45
 Barquete, D.M.: BP-ThP28, 67
 Barr, C.M.: H3-2-WeA3, 55
 Barrallier, L.: H1-2-TuA5, 46
 Barrios, A.: H2-1-MoM4, **33**
 Bartosik, M.: B4-2-TuA1, 43; B5-1-ThA5, 63; B6-ThM2, 58; BP-ThP19, 67; BP-ThP35, 67
 Batková, Š.: F1-TuM4, 40; F4-1-WeM2, **50**
 Batory, D.: TSP-ThP2, **71**
 Beake, B.D.: H3-2-WeA2, **55**
 Beaufort, M.F.: E2-2-TuA2, 45
 Becker, J.: E3-WeM5, 49; G2-FrM7, 73
 Beganovic, N.: E3-WeM5, 49
 Bejarano, G.: D3-TuM8, 39; DP-ThP25, 69
 Bellido-Gonzalez, V.: B1-2-MoA2, **35**; B3-2-MoA5, 35; FP-ThP9, **70**
 Belviso, F.: E1-2-ThA8, **64**
 Bensalah, W.: D2-TuA1, 44
 Berastegui, P.: TS1-1-WeM5, 51
 Berger, K.: BP-ThP37, 67
 Bergeron, F.: A1-3-WeM10, **48**
 Berlia, R.: H1-2-TuA3, 46
 Berman, D.: A2-1-ThM9, 58; E3-WeM3, 49
 Bermejo Sanz, J.: A3-WeA5, 53
 Bernardes, C.: E1-3-FrM1, **73**
 Bernatova, K.: B7-TuA2, 44
 Berndorf, S.: B4-4-WeA7, 53
 Bertram, R.: B3-1-MoM2, 32; B3-2-MoA2, 35
 Berumen, J.O.: D2-TuA4, 44
 Beyerlein, I.J.: H2-2-MoA7, **36**
 Biederman, H.: F1-TuM1, 40
 Bierwisch, N.: H2-2-MoA10, **36**; HP-ThP9, **71**
 Bijalwan, P.: B5-2-FrM9, **72**
 Bijukumar, D.: D2-TuA5, 44; D3-TuM7, 39
 Bilek, M.M.: B5-1-ThA6, 63
 Biring, S.: C3+C2+C1-ThM10, 59
 Bissell, L.: F3-TuA5, 45
 Bitar-Nehme, E.B.-N.: EP-ThP30, 69
 Bittau, F.: C3+C1-WeM2, 49
 Bleu, Y.: F3-TuA8, **45**
 Bloesch, D.: B1-2-MoA5, 35; G4+G5+G6-ThA5, 65
 Bo, W.X.: EP-ThP28, 69
 Bobzin, K.: BP-ThP23, 67; BP-ThP4, 66; E3-WeM4, 49; F4-2-WeA5, 55; G2-FrM9, 73
 Bocher, P.: H3-2-WeA8, 55
 Bogdanowicz, R.: D2-TuA10, 44; F3-TuA11, **45**
 Boichot, R.: B2-1-ThA6, 62; B2-2-FrM5, 72
 Bolívar, F.J.: DP-ThP4, 68; E2-2-TuA3, 45
 Bolvardi, H.: B4-2-TuA1, 43; B6-ThM9, 58; FP-ThP3, 70
 Bolz, S.: G1+G3-ThM2, 60
 Boman, M.: B2-2-FrM7, 72; B2-2-FrM8, **72**; BP-ThP20, 67
 Böör, K.: B2-2-FrM8, 72; BP-ThP20, **67**
 Borges, J.: D3-TuM2, 39
 Boris, D.R.: C2-WeA5, 54

Borja Goyeneche, E.N.: B4-1-TuM6, 39; BP-ThP39, 67
 Bourquard, F.: F3-TuA8, 45
 Bousser, É.: A1-3-WeM10, 48; A1-3-WeM3, 48; C3+C1-WeM4, 49; E1-1-ThM6, 59; H3-2-WeA8, 55; TS2-ThM3, 61
 Bouvard, G.: D1-1-MoM3, 33
 Boveri, G.: TS2-ThM2, **61**; TS2-ThM5, 61
 Bowden, M.D.: F2-1-ThM11, 60
 Boyce, B.L.: H3-2-WeA3, 55
 Bradley, J.W.: F2-1-ThM11, **60**
 Braun, R.: B1-3-TuM2, 38
 Brenning, N.: B7-TuA9, 44; F2-1-ThM8, 60
 Brenning, R.M.: B2-2-FrM7, 72
 Briggs, S.A.: H3-2-WeA3, 55
 Brindley, J.: FP-ThP9, 70
 Brodu, A.: C3+C2+C1-ThM7, **59**; GP-ThP24, **71**
 Brögelmann, T.: BP-ThP23, 67; BP-ThP4, 66; E3-WeM4, 49; F4-2-WeA5, 55; G2-FrM9, 73
 Broitman, E.: EP-ThP18, **69**; G4+G5+G6-ThA11, **65**
 Brown, R.: B1-2-MoA2, 35; FP-ThP9, 70
 Brown, S.: TS2-ThM11, **61**; TSP-ThP2, 71
 Brown, S.G.R.: TSP-ThP4, 71
 Brugnara, R.H.: E1-2-ThA10, **64**
 Brümmer, A.: EP-ThP23, 69
 Buchinger, J.: BP-ThP19, 67; BP-ThP35, 67
 Buchwalder, A.: G4+G5+G6-ThA9, **65**
 Buechel, C.: G4+G5+G6-ThA5, **65**
 Buenrostro Arvizu, M.G.: EP-ThP11, 69
 Bull, S.J.: H2-2-MoA1, **36**
 Bumgardner, J.: D2-TuA2, 44
 Burghammer, M.: B4-4-WeA2, 38
 Bursikova, V.: B1-3-TuM6, 38; B5-1-ThA4, 63
 Bursynski, K.: TS3+4-2-MoA5, **37**
 Butler, A.: B7-TuA9, 44

— C —

C. Rodrigues, D.: D3-TuM3, 39
 Cabrero Vélchez, M.: TS2-ThM4, 61
 Cada, M.: B7-TuA11, **44**; D2-TuA10, 44; G4+G5+G6-ThA7, 65
 Cadet, C.: AP-ThP11, 66
 Cahn, G.: TS4-1-MoM4, **34**
 Cai, R.: EP-ThP27, 69; G2-FrM5, **73**
 Caita Tapia, A.D.: B4-1-TuM6, **39**; BP-ThP39, **67**
 Callisti, M.: H3-2-WeA4, 55
 Calvo-Dahlborg, M.: TSP-ThP4, **71**
 Cammarata, A.: E1-1-ThM5, **59**; E1-2-ThA6, 64
 Campos, P.: GP-ThP7, 70
 Campos-Silva, I.E.: B4-1-TuM5, 39; B4-2-TuA3, 43; B4-3-WeM6, 48; E1-1-ThM3, 59
 Camps, E.: D2-TuA4, 44
 Cano, D.: BP-ThP36, 67
 Čapek, J.: F1-TuM4, 40; F4-1-WeM2, 50; F4-2-WeA6, 55; FP-ThP17, 70; FP-ThP3, 70
 Capote, G.: B3-1-MoM5, 32
 Cardoso-Legorreta, E.: AP-ThP6, 66
 Carlet, M.: BP-ThP23, 67
 Carlström, C.-F.: F4-2-WeA7, 55
 Carton, J.: CP-ThP22, 68
 Carvalho, S.: E1-3-FrM8, 73
 Casserly, T.: B3-2-MoA3, **35**; G1+G3-ThM8, 60
 Castelluccio, G.: H2-1-MoM4, 33
 Cavaleiro, A.: B3-2-MoA7, 35; E1-3-FrM8, 73; E1-4-WeA3, 54; FP-ThP6, 70
 Cavaleiro, D.: E1-3-FrM8, **73**
 Cavarroc, M.: A1-3-WeM10, 48; A1-3-WeM3, 48; E3-WeM10, **49**
 Cemin, F.: FP-ThP10, 70
 Černý, M.: B6-ThM2, 58
 Čerstvý, R.: F4-1-WeM2, 50

Author Index

- Cha, S.C.: G1+G3-ThM12, **60**
 Chacko, A.R.: D1-2-MoA8, **36**
 Chandra, R.: F4-2-WeA3, 55; GP-ThP16, 70; GP-ThP19, 71
 Chang, C.L.: GP-ThP1, **70**
 Chang, H.Y.: GP-ThP2, 70
 Chang, K.-S.: B1-2-MoA8, **35**; BP-ThP33, 67; F4-1-WeM10, 50; TS1-2-WeA10, 56; TS1-2-WeA2, 56; TSP-ThP9, 71
 Chang, L.: B1-2-MoA7, 35
 Chang, L.C.: B4-3-WeM12, 48; BP-ThP7, 66
 Chang, S.H.: D1-1-MoM6, 33
 Chang, S.Y.: BP-ThP2, **66**; BP-ThP6, 66
 Chang, X.X.: B5-1-ThA9, 63
 Chang, Y.-C.: D1-1-MoM2, 33
 Chang, Y.-Y.: B4-4-WeA4, 53; B6-ThM3, 58
 Chao, L.C.: B4-4-WeA4, **53**
 Chapon, P.: HP-ThP6, 71
 Charlton, C.J.: BP-ThP1, 66; G2-FrM8, 73
 Charpentier, L.: B2-1-ThA7, 62
 Chason, E.: H1-2-TuA2, 46
 Chausseau, M.F.: HP-ThP6, 71
 Chen, A.J.: F2-2-ThA7, **64**
 Chen, C.H.: B5-2-FrM8, 72
 Chen, C.M.: F3-TuA4, 45
 Chen, D.Y.: B2-1-ThA6, 62; B2-1-ThA7, **62**
 Chen, H.C.: TSP-ThP6, 71
 Chen, H.-H.: F4-1-WeM1, **50**
 Chen, H.T.: DP-ThP6, 68
 Chen, M.: H3-2-WeA7, **55**
 Chen, M.J.: D1-1-MoM6, 33
 Chen, P.-C.: DP-ThP5, 68
 Chen, P.-W.: C3+C1-WeM3, **49**
 Chen, S.C.: C3+C2+C1-ThM10, 59
 Chen, W.C.: BP-ThP27, 67; BP-ThP9, 66
 Chen, X.: H3-2-WeA5, 55
 Chen, Y.: C2-WeA10, **54**
 Chen, Y.C.: A2-1-ThM4, 58
 Chen, Y.H.: C3+C2+C1-ThM10, **59**; F3-TuA4, 45
 Chen, Y.L.: B4-3-WeM12, 48; BP-ThP7, **66**
 Chen, Y.L.: D1-1-MoM6, 33
 Chen, Y.Y.: TS1-2-WeA6, **56**
 Chen, Y.-F.: E2-2-TuA9, 45
 Cheng, F.-Y.: E2-2-TuA9, 45
 Cheng, K.Y.: D2-TuA5, **44**
 Cheng, L.C.: C2-WeA11, **54**
 Cheng, Y.L.: CP-ThP1, 67
 Chisholm, C.: H3-2-WeA3, 55
 Chistyakov, R.: B1-2-MoA1, **35**
 Chiu, K.A.: B1-2-MoA7, 35
 Chiu, L.Y.: B1-1-MoM5, **32**
 Chiu, Y.-C.: DP-ThP5, 68
 Chng, E.J.: D2-TuA2, 44
 Choi, K.: TS2-ThM7, 61
 Choi, Y.: HP-ThP12, 71
 Chou, C.C.: B1-2-MoA12, **35**
 Chou, C.M.: B5-1-ThA9, 63; D1-1-MoM2, 33; DP-ThP11, 68
 Chou, C.-M.: TSP-ThP9, 71
 Choudhury, T.: B2-1-ThA9, 62
 Choukourou, A.: F1-TuM1, 40
 Christensen, B.H.: E1-1-ThM7, 59
 Christien, F.C.: F3-TuA8, 45
 Chu, J.P.: D1-1-MoM6, **33**
 Chubarov, M.: B2-1-ThA9, **62**
 Chung, C.J.: B5-1-ThA9, 63; D1-1-MoM2, 33; DP-ThP11, 68; DP-ThP6, **68**
 Chung, Y.W.: EP-ThP19, 69
 Chyntara, S.: D1-1-MoM6, 33
 Cieslar, M.: F1-TuM1, 40
 Číperová, Z.: B1-2-MoA4, **35**
 Claerbout, V.E.P.: E1-2-ThA5, **64**
 Clegg, W.J.: H2-2-MoA4, 36
 Colas, J.: B2-1-ThA7, 62
 Cole-Baker, A.: A1-1-TuM2, 38
 Contin, A.: BP-ThP28, 67
 Contla-Pacheco, A.D.: E1-1-ThM3, **59**
 Contreras, E.: B6-ThM6, **58**; EP-ThP3, **69**
 Corat, E.J.: B3-1-MoM4, 32; B3-1-MoM5, 32; BP-ThP28, 67
 Cordill, M.J.: E2-1-TuM3, **40**; EP-ThP6, 69; TS3+4-2-WeMoA3, 37; TS3+4-2-MoA4, 37; TS3+4-2-MoA8, 37
 Cordista, N.: B4-4-WeA6, 53; DP-ThP26, **69**
 Cormier, J.: H1-1-TuM3, 41
 Cornide, J.: TSP-ThP4, 71
 Corona-Gomez, J.: BP-ThP42, **67**; E2-2-TuA8, **45**
 Correia, R.F.B.: BP-ThP28, 67
 Cortés Suárez, V.J.: EP-ThP11, 69; HP-ThP4, 71
 Cortínez, J.: B6-ThM6, 58; EP-ThP3, 69
 Costa, D.: D3-TuM2, 39
 Costa-Barbosa, A.: D3-TuM2, 39
 Coudon, F.: AP-ThP3, 66
 Cougnon, F.G.: TS3+4-2-MoA9, **37**
 Cremer, R.: G1+G3-ThM9, **60**
 Crespo Villegas, J.: A1-3-WeM3, **48**
 Crummenauer, J.: G2-FrM7, 73
 Cruz Avilés, A.: AP-ThP6, 66
 Cselle, T.: B1-2-MoA5, 35; G4+G5+G6-ThA5, 65
 Cucatti, S.C.: B4-3-WeM2, 48
 Curry, J.: E3-WeM1, 49
 Czettl, C.: B2-1-ThA11, 62; B2-1-ThA4, 62; B4-4-WeA3, 53; B4-4-WeA7, 53; H1-1-TuM7, 41; H1-2-TuA4, 46
 Czigany, Z.: B1-3-TuM6, 38; B5-1-ThA4, 63
 — D —
 da Silva Sobrinho, A.S.: DP-ThP23, 69
 Dahlborg, U.: TSP-ThP4, 71
 Dahotre, N.B.: A2-1-ThM5, 58
 Dai, M.J.: BP-ThP31, 67; EP-ThP16, 69
 Dai, X.: B5-1-ThA6, 63; FP-ThP16, 70
 Damm, D.: BP-ThP28, 67
 Dams, N.: B3-2-MoA5, 35; G1+G3-ThM4, 60
 Daniel, B.: B1-2-MoA2, 35
 Daniel, R.: B4-4-WeA2, 53
 DaSilva, V.: EP-ThP4, 69
 Daves, W.: B2-1-ThA4, 62; B4-4-WeA3, 53
 De Bosscher, W.: B7-TuA1, 44
 de Mello, S.R.S.: E1-2-ThA11, 64
 de Miguel Gamó, T.: A1-3-WeM2, 48; A3-WeA6, 53
 de Vasconcelos, G.: BP-ThP28, 67
 Dean, D.: D1-2-MoA9, 36
 Debus, J.: EP-ThP23, 69
 Dedoncker, R.: TS1-1-WeM2, **51**
 Dehm, G.: H3-1-WeM3, 50; H3-2-WeA9, 55
 Delgado, A.: B5-2-FrM4, 72
 Delgado-Brito, A.M.: B4-1-TuM5, **39**
 Depla, D.: B7-TuA3, **44**; TS1-1-WeM2, 51; TS3+4-2-MoA9, 37
 Dhananjaya, M.: CP-ThP9, **68**
 Di Gioacchino, F.: H2-2-MoA4, 36
 Diao, D.F.: EP-ThP17, **69**
 Ding, H.H.: D1-1-MoM3, 33
 Do, H.: B1-2-MoA7, 35
 Döbeli, M.: A2-2-ThA3, 62
 Dobler, C.: A3-WeA3, 53
 Dobrenizki, L.: E1-2-ThA10, 64
 Dobrovodsky, J.: B3-2-MoA8, 35
 Dobrygin, W.: B3-2-MoA1, 35
 Dolatabadi, A.: TS2-ThM3, 61; TS2-ThM9, **61**
 Dommann, A.: A2-2-ThA3, 62
 Donaldson, O.: H2-1-MoM6, **33**
 Dong, Z.: A1-1-TuM6, 38
 Donnelly, S.E.: TS1-2-WeA5, 56
 Donnet, C.D.: F3-TuA8, 45
 Doñu Ruiz, M.A.: EP-ThP11, **69**; HP-ThP4, 71
 Doris, F.: TS1-1-WeM4, 51
 Doumanidis, C.: C4-ThA3, **63**; C4-ThA7, 63
 Downey, B.P.: C2-WeA5, 54
 Drees, D.: E1-1-ThM7, 59
 Drieu La Rochelle, J.: E2-2-TuA2, 45
 Drnovšek, A.: B1-3-TuM4, **38**
 Drouet, M.: E2-2-TuA2, 45
 Dryepondt, S.N.: A1-1-TuM1, 38; A1-3-WeM4, **48**
 Dublanche-Tixier, C.: C3+C2+C1-ThM7, 59
 Duchoň, T.: F4-1-WeM2, 50
 Ducros, C.: C3+C2+C1-ThM7, 59; GP-ThP24, 71
 Duguet, T.: B2-2-FrM5, **72**; B2-2-FrM6, 72
 Duh, J.G.: B4-3-WeM11, 48; B6-ThM4, 58; BP-ThP14, 66; BP-ThP15, 66; TSP-ThP7, 71
 Durmaz, A.R.D.: H2-1-MoM3, 33
 Dutta, M.: B5-2-FrM9, 72
 — E —
 Eberl, C.: AP-ThP11, 66; H2-1-MoM3, 33
 Echavarría, A.M.: D3-TuM8, **39**; DP-ThP25, **69**
 Echeverría, F.: D1-2-MoA5, 36
 Echeverrigaray, F.G.: E1-2-ThA11, 64
 Echeverry-Rendón, M.: D1-2-MoA5, 36
 Ecker, W.: B2-1-ThA4, 62; B4-4-WeA3, 53
 Eckert, J.: EP-ThP6, 69
 Eddy Jr., C.R.: C2-WeA5, 54
 Edmondson, P.D.: TS1-2-WeA5, 56
 Edwards, T.E.J.: H2-2-MoA4, **36**
 Efeoğlu, I.: B6-ThM1, **58**; BP-ThP30, **67**
 Efremov, M.: B3-2-MoA6, 35
 Egan, G.C.: C4-ThA2, 63
 Ehiassarian, A.P.: A1-1-TuM8, 38; F2-1-ThM7, **60**
 Ek, M.E.: B2-2-FrM7, 72
 Eklund, P.: F4-2-WeA7, 55
 El Mansori, M.: H1-2-TuA5, 46
 Elahinia, M.: D1-2-MoA9, 36
 El-Awady, J.A.: H2-1-MoM1, **33**
 Elbers, M.: BP-ThP37, 67
 Elias-Espinosa, M.: AP-ThP6, 66; BP-ThP24, 67; BP-ThP25, 67
 Ellis-Terrell, C.: G4+G5+G6-ThA6, **65**
 Emieux, F.: GP-ThP24, 71
 Encinas Sánchez, V.: A1-3-WeM2, 48; A3-WeA6, 53
 Engwall, A.: F2-2-ThA3, **64**
 Erdemir, A.: E1-2-ThA9, 64; EP-ThP4, 69
 Eriguchi, K.: G4+G5+G6-ThA4, **65**
 Eriksson, A.O.: BP-ThP41, 67
 Ernst, P.: G2-FrM7, 73
 Eryilmaz, O.L.: EP-ThP4, **69**
 Escobar, D.: E1-4-WeA5, 54
 EP-ThP26, 69
 Esparza, J.: BP-ThP22, 67
 Espinoza Orías, A.: D2-TuA8, **44**
 Espinoza, R.: GP-ThP6, 70
 Esteve, J.: BP-ThP36, 67
 Euchner, H.: B6-ThM12, 58; BP-ThP34, 67
 Evans, A.: A1-1-TuM2, 38
 Evaristo, M.: E1-4-WeA3, **54**
 Evertz, S.: TS1-2-WeA9, 56
 — F —
 Faber, K.T.: A2-1-ThM8, 58
 Falcão, R.: B3-1-MoM4, **32**; DP-ThP19, **68**
 Fang, Y.S.: B1-2-MoA7, **35**
 Farooq, A.: GP-ThP22, **71**
 Fatoba, O.S.: AP-ThP4, **66**; B4-2-TuA10, **43**
 Fayomi, S.: D2-TuA11, 44
 Feder, R.: C3+C2+C1-ThM9, 59
 Fehr, A.: F2-2-ThA8, **64**
 Fekete, M.: B1-3-TuM6, 38; B7-TuA2, 44
 Feldner, P.: H2-2-MoA6, **36**
 Feng, Y.Q.: B4-3-WeM10, **48**

Author Index

- Fernandes, F.: E1-3-FrM8, 73
 Fernandez, I.: B3-2-MoA5, 35; F2-1-ThM9, **60**;
 G1+G3-ThM4, 60; TS3+4-2-MoA10, 37
 Fernández-Valdés, D.: B4-3-WeM6, **48**
 Ferreira, F.: B3-2-MoA7, 35; FP-ThP6, 70
 Ferreira, J.: CP-ThP23, 68
 Ficek, M.: F3-TuA11, 45
 Fietzke, F.: B1-3-TuM1, **38**; B4-3-WeM4, 48;
 G1+G3-ThM3, 60
 Figueroa, C.A.: B4-3-WeM2, 48; E1-2-ThA11,
 64
 Figueroa-Lopez, U.: E1-1-ThM3, 59
 Finazzi, G.: C3+C2+C1-ThM7, 59
 Fischer, M.: F4-2-WeA8, **55**; FP-ThP5, **70**
 Fisher, T.S.: F3-TuA1, **45**
 Flock, D.: TS1-2-WeA4, 56
 Flores, L.M.: EP-ThP12, 69
 Flores, M.: EP-ThP12, **69**; FP-ThP11, 70
 Flores-Cova, L.: FP-ThP11, **70**
 Flores-Martinez, M.: D2-TuA4, 44
 Flores-Rentería, M.: AP-ThP6, 66; BP-ThP25,
 67
 Fones, A.: D1-2-MoA3, 36
 Fortunato, E.: F4-1-WeM3, **50**
 Fox, C.: A1-2-TuA9, **43**
 Fraile, A.F.: B5-1-ThA3, **63**
 Franco, D.: E2-1-TuM4, 40
 Francois, M.: E2-1-TuM5, 40
 Frank, M.: B2-2-FrM10, 72
 Franz, R.: B1-3-TuM4, 38; TS1-2-WeA3, 56
 Friák, M.F.: B6-ThM2, 58; BP-ThP19, 67
 Fridrici, V.: D1-1-MoM3, **33**; E1-1-ThM4, 59
 Frutos, E.F.: B5-1-ThA3, 63
 Fu, Q.: F2-2-ThA9, 64
 Fuger, C.: B6-ThM12, 58
 Fugita, L.T.N.: F3-TuA3, 45
 Fujii, K.: BP-ThP26, 67
 Fukumasu, N.: B3-1-MoM5, 32; E1-3-FrM1,
 73
 Furgeaud, C.: H1-2-TuA2, **46**
 Furuki, T.: EP-ThP22, 69; EP-ThP24, 69
 — G —
 Gabriel, H.: B3-2-MoA5, 35; G1+G3-ThM4, **60**
 Gachot, C.: E1-2-ThA9, 64
 Gaedike, B.: G1+G3-ThM5, **60**
 Gaffar, A.: F3-TuA3, 45
 Gaiaschi, S.: HP-ThP6, 71
 Gaitán, G.B.: DP-ThP4, 68
 Galetz, M.C.: A2-2-ThA8, 62; A3-WeA3, 53
 Gamboa Mendoza, B.J.: B4-1-TuM6, 39; BP-
 ThP39, 67
 Gammer, C.: EP-ThP6, 69
 Ganesan, G.V.R.: B5-1-ThA6, **63**
 Gao, Z.H.: A1-1-TuM4, 38
 Garcia Fuentes, G.: BP-ThP22, 67
 García Sanchez, J.A.: HP-ThP4, 71
 García, E.: D2-TuA4, **44**
 Garcia, J.A.: BP-ThP22, **67**; GP-ThP5, 70
 García, P.: TS2-ThM8, 61
 García-Martín, G.: A1-3-WeM2, 48; A3-WeA6,
 53
 Garrelie, F.: F3-TuA8, 45
 Gasem, Z.: AP-ThP5, 66
 Gassner, M.: B2-1-ThA4, 62
 Gault, B.: H1-1-TuM3, **41**
 Gauter, S.: D1-2-MoA8, 36
 Gazal, Y.: B2-2-FrM5, 72
 Ge, F.F.: A1-2-TuA4, **43**
 Geers, C.: E1-2-ThA10, 64
 Gennaro, S.: B3-2-MoA3, 35; G1+G3-ThM8,
 60
 Gentleman, M.M.: A2-1-ThM7, **58**
 George, M.: FP-ThP7, 70
 George, S.M.: F4-2-WeA9, **55**
 Gerdin, J.: BP-ThP20, 67
 Géringuer, J.: D1-1-MoM3, 33; D2-TuA1, **44**
 Ghafoor, N.: B4-1-TuM4, **39**
 Ghai, P.: GP-ThP20, **71**
 Ghimire, A.: BP-ThP6, 66
 Ghimire, K.: C3+C2+C1-ThM13, 59
 Gholinia, A.: C3+C2+C1-ThM12, 59
 Gibson, S.K.: AP-ThP1, 66
 Gibson, J.: H3-1-WeM1, **50**
 Gies, A.: E3-WeM5, **49**
 Gildersleeve, E.: A2-2-ThA4, 62
 Gimeno, S.: GP-ThP5, **70**
 Giroire, B.: E3-WeM10, 49
 Glavin, N.: F3-TuA5, 45; TS3+4-2-MoA5, 37
 Gleibe, K.: F3-TuA5, 45
 Gleich, S.G.: H3-2-WeA9, 55
 Glushko, O.: EP-ThP6, **69**; TS3+4-2-MoA3, **37**
 Godard, P.: CP-ThP13, 68; E2-2-TuA2, 45
 Goddard, D.: A1-1-TuM2, 38
 Göken, M.: H2-2-MoA5, 36; H2-2-MoA6, 36
 Gomez, J.S.: BP-ThP28, 67
 Gómez, M.A.: B6-ThM6, 58; E2-2-TuA3, 45;
 EP-ThP3, 69
 Gómez-Vargas, O.: AP-ThP6, **66**; B4-2-TuA8,
 43; BP-ThP24, 67; BP-ThP25, 67
 Gong, C.Z.: F2-2-ThA2, 64
 Gonzalez Arrabal, R.: B3-2-MoA5, 35
 Goorsky, M.S.: B6-ThM10, 58; C2-WeA9, 54
 Gopalakrishnan, R.: D2-TuA2, **44**; D3-TuM6,
 39
 Gopalan, H.G.: H3-2-WeA9, **55**
 Gostilo, V.: H3-2-WeA6, 55
 Goswami, M.: B2-1-ThA1, **62**
 Göthelid, E.: F4-2-WeA7, 55
 Goudeau, P.: CP-ThP13, 68
 Gozhyk, I.: H1-2-TuA11, 46; HP-ThP7, 71
 Grachev, S.: H1-1-TuM6, 41; H1-2-TuA11, 46;
 HP-ThP7, 71
 Graham, S.: TS4-1-MoM4, 34
 Grancic, B.: B5-2-FrM6, **72**; BP-ThP3, 66
 Grantham, Z.: B4-4-WeA6, 53
 Greczynski, G.: B4-1-TuM4, 39; F2-2-ThA5,
 64; SIT2-WeSIT1, 52
 Greene, J.E.: B4-1-TuM4, 39; F2-1-ThM8, 60;
 F2-2-ThA5, 64; HL-WeHL3, **57**; SIT2-WeSIT1,
 52
 Greenhalgh, R.C.: C3+C1-WeM2, 49
 Grigoriev, S.: B1-2-MoA11, 35
 Grossias, C.: CP-ThP13, 68
 Gu, G.: BP-ThP29, 67
 Gu, J.: A2-1-ThM5, 58; A2-1-ThM9, **58**
 Gudmundsson, J.T.: B7-TuA9, 44; F1-TuM5,
 40; F2-1-ThM8, 60
 Guerin, P.: CP-ThP13, 68
 Guezmil, M.: D2-TuA1, 44
 Guida, L.: D3-TuM3, 39
 Guillon, M.G.: B4-3-WeM13, 48
 Guipont, V.: A2-1-ThM1, 58; AP-ThP3, 66
 Gunda, R.K.: E1-3-FrM12, 73; EP-ThP31, 71
 Gunduz, I.E.: C4-ThA3, 63; C4-ThA7, 63
 Günther, M.: B3-2-MoA1, **35**
 Guo, C.Q.: BP-ThP31, **67**
 Guo, J.: B5-1-ThA6, 63; FP-ThP16, 70
 Guo, Q.: A1-1-TuM1, 38
 Guo, Y.: C3+C2+C1-ThM12, 59; CP-ThP19, 68
 Gupta, S.: H2-2-MoA2, 36
 Gustus, R.: B3-1-MoM3, 32
 — H —
 Haga, Y.: TS4-1-MoM3, 34
 Hahn, R.: B4-2-TuA1, **43**; B6-ThM12, 58; BP-
 ThP19, 67; BP-ThP34, 67
 Haiblíková, V.: H3-1-WeM2, 50
 Hajjoseini, H.: F1-TuM5, 40
 Hakala, T.J.: E1-1-ThM7, 59
 Haldan, D.: B3-1-MoM2, 32
 Halvarsson, M.: B2-1-ThA5, 62
 Hamilton, H.: D1-2-MoA3, 36
 Hamouda, A.M.S.: AP-ThP8, 66
 Hans, M.: BP-ThP41, 67; H1-1-TuM5, **41**
 Hanus, J.: F1-TuM1, 40
 Harder, B.: A2-2-ThA5, 62
 Harrison, Z.: D3-TuM6, **39**
 Harsani, M.: BP-ThP3, 66
 Hart, N.: CP-ThP12, 68
 Hasegawa, S.: G4+G5+G6-ThA4, 65
 Hashemiastaneh, S.: D3-TuM7, 39
 Hasikova, J.I.: H3-2-WeA6, **55**
 Hattar, K.: H3-2-WeA3, **55**
 Hatton, P.: C3+C1-WeM2, **49**
 Hattrick-Simpers, J.: TS1-1-WeM10, 51
 Hatzenbichler, L.: B4-3-WeM3, 48
 Hauert, R.: D1-1-MoM4, **33**
 Haviar, S.: F1-TuM4, **40**; F4-1-WeM2, 50
 Haynes, J.A.: A2-2-ThA4, 62
 He, J.: H1-1-TuM3, 41
 He, J.H.: A2-1-ThM6, **58**
 He, J.L.: A1-1-TuM9, 38; B5-1-ThA9, 63;
 C3+C2+C1-ThM3, 59; D1-1-MoM2, 33; DP-
 ThP11, 68; DP-ThP6, 68; F3-TuA4, 45
 Heaney, P.J.: B3-2-MoA6, **35**
 Heckman, E.: TS3+4-2-MoA5, 37
 Heckman, N.: H3-2-WeA3, 55
 Heller, E.: TS3+4-2-MoA5, 37
 Helmersson, U.: F2-1-ThM8, **60**
 Heraud, L.: H1-2-TuA5, 46
 Herault, Q.: H1-2-TuA11, **46**; HP-ThP7, **71**
 Hermerschmidt, F.: TS4-1-MoM5, **34**
 Hernandez-Rodrigues, E.N.: DP-ThP16, 68;
 GP-ThP18, **70**
 Herren, B.: A2-1-ThM8, **58**
 Herrera Jimenez, E.J.: H3-2-WeA8, **55**
 Hess, M.: B3-1-MoM2, 32; B3-2-MoA2, **35**
 Hettinger, J.: D1-2-MoA3, 36
 Hibino, T.: EP-ThP24, 69
 Higuchi, K.: B4-1-TuM7, 39; B4-2-TuA9, 43;
 BP-ThP26, 67
 Higuchi, T.: G4+G5+G6-ThA4, 65
 Hilfiker, M.: C3+C2+C1-ThM9, 59
 Hill, S.: B4-4-WeA6, 53; DP-ThP26, 69
 Hinder, S.: C3+C1-WeM4, 49
 Hippler, R.H.: G4+G5+G6-ThA7, 65
 Hirn, S.: TS1-2-WeA3, 56
 Hirpara, J.G.: GP-ThP16, **70**
 Hishinuma, Y.: H1-2-TuA9, 46
 Hnilica, J.: B7-TuA2, 44
 Ho, W.F.: DP-ThP10, 68; DP-ThP9, **68**
 Ho, W.Y.: B5-2-FrM8, 72; BP-ThP27, 67; BP-
 ThP9, 66
 Hodge, A.M.: C3+C2+C1-ThM8, 59; E2-2-
 TuA4, **45**
 Höhn, M.: B4-3-WeM4, 48
 Holec, D.: B4-3-WeM3, 48; B5-1-ThA5, 63;
 B6-ThM2, 58; B6-ThM5, 58; BP-ThP19, 67;
 BP-ThP35, 67
 Holzapfel, D.M.: BP-ThP41, **67**; TS1-2-WeA9,
 56
 Homma, H.: B2-1-ThA3, 62
 Hong, K.P.: F4-2-WeA11, 55
 Hopfeld, M.: TS1-2-WeA4, 56
 Hosemann, P.: B1-3-TuM4, 38; H3-2-WeA1,
 55
 Hou, H.J.: EP-ThP16, 69
 Hou, X.H.: TS2-ThM7, **61**; TSP-ThP1, 71; TSP-
 ThP6, **71**
 Houška, J.: F4-1-WeM2, 50
 Hovsepian, P.: A1-1-TuM8, **38**
 Hrebik, J.: F2-1-ThM10, **60**
 Hruby, H.: B4-4-WeA2, 53
 Hsain, Z.: E3-WeM1, 49
 Hsiao, W.Y.: DP-ThP10, 68
 Hsiao, Y.T.: BP-ThP2, 66

Author Index

- Hsieh, J.H.: D1-2-MoA4, **36**; F4-1-WeM5, 50
Hsieh, P.-Y.: B5-1-ThA9, 63; C3+C2+C1-ThM3, 59; D1-1-MoM2, 33; DP-ThP6, 68; F3-TuA4, **45**
Hsu, C.H.: GP-ThP21, 71
Hsu, H.C.: DP-ThP10, **68**; DP-ThP9, 68
Hsu, L.C.: B5-2-FrM8, **72**; BP-ThP27, **67**; BP-ThP9, 66
Hsu, S.K.: DP-ThP10, 68; DP-ThP9, 68
Hsueh, P.: F4-1-WeM5, 50
Hu, H.: CP-ThP2, **67**
Huang, C.H.: GP-ThP1, 70
Huang, C.R.: TSP-ThP7, **71**
Huang, F.: A1-2-TuA4, 43; C2-WeA10, 54
Huang, J.-H.: A1-1-TuM7, 38; B1-2-MoA12, 35; B4-3-WeM10, 48; B4-4-WeA1, **53**; E2-2-TuA9, 45
Huang, J.L.: B1-1-MoM4, 32; C2-WeA11, 54; CP-ThP31, 68; F1-TuM3, 40; F4-1-WeM1, 50
Huang, J.T.: C3+C2+C1-ThM3, **59**
Huang, S.Y.: C3+C2+C1-ThM10, 59
Huang, S.-Y.: D1-1-MoM2, **33**
Huang, T.: A2-1-ThM5, 58; A2-1-ThM9, 58; FP-ThP16, 70
Huang, T.-C.: GP-ThP17, 70
Huang, X.: G4+G5+G6-ThA6, 65
Huang, Y.H.: B1-1-MoM4, **32**
Huang, Z.-W.: TSP-ThP9, **71**
Hubicka, Z.: B7-TuA11, 44; D2-TuA10, 44; G4+G5+G6-ThA7, **65**
Hudec, T.: E1-3-FrM2, **73**
Hug, H.J.: D1-2-MoA8, 36; F4-2-WeA8, 55; FP-ThP5, 70
Hulkko, J.: B2-2-FrM8, 72
Hultman, L.: B4-1-TuM4, 39; F2-2-ThA5, 64; F4-2-WeA7, 55; SIT2-WeSIT1, 52
Huminiuc, T.H.: B5-1-ThA3, 63; B5-2-FrM4, 72; E1-3-FrM2, 73
Hunault, P.: HP-ThP6, **71**
Hung, J.: B5-2-FrM8, 72; BP-ThP27, 67; BP-ThP9, 66
Hung, S.B.: TS1-1-WeM6, **51**; TS1-2-WeA6, 56
Hung, Y.L.: A1-1-TuM9, 38
Hunold, O.: A2-2-ThA3, **62**
Hurand, S.: CP-ThP13, 68
Hurtado, A.: B6-ThM6, 58; EP-ThP3, 69
Hurtado, C.: DP-ThP19, 68
Hussien, A.: C4-ThA3, 63
Hwang, S.H.: B2-2-FrM9, 72
— | —
Ianno, N.: CP-ThP18, 68
Ibáñez, P.F.: TS2-ThM4, **61**
Ibrahim, H.: D1-2-MoA9, **36**
Ikari, Y.: G1+G3-ThM7, 60; TSP-ThP8, 71
Ilic, E.: D1-1-MoM4, 33
Imamiya, M.: BP-ThP13, 66
Imamura, S.: B2-1-ThA2, 62
Ingvarsson, S.: F1-TuM5, 40
Iñiguez, C.: DP-ThP16, **68**
Inspektor, A.: B1-2-MoA3, **35**
Irving, B.J.: E1-2-ThA2, **64**
Ishida, M.: G2-FrM3, 73
Ishigaki, T.: B2-1-ThA3, 62
Islam, A.: B5-2-FrM9, 72
Islam, S.: F1-TuM6, **40**
Isomura, Y.: G1+G3-ThM7, 60; TSP-ThP8, 71
Itagaki, N.: B2-2-FrM9, 72
Ito, A.: EP-ThP22, **69**
Iwaniak, A.: AP-ThP9, **66**; H3-2-WeA10, **55**
Izaii, V.: BP-ThP3, 66
Izu, Y.: BP-ThP13, **66**
Izumi, H.: TS4-1-MoM3, 34
— J —
Jäger, N.: B4-4-WeA2, 53
Jain, R.K.: B1-1-MoM3, **32**
Jaiswal, J.: F4-2-WeA3, 55; GP-ThP19, 71
Jakutis Neto, J.J.: DP-ThP23, 69
Jansson, W.: B2-1-ThA5, 62
Jansson, U.: TS1-1-WeM5, 51
Jaroš, M.: B1-2-MoA4, 35
Jasien, C.: C4-ThA5, 63
Jawaid, A.: F3-TuA5, 45
Jedrzczak, A.: TSP-ThP2, 71
Jennings, J.A.: D3-TuM6, 39
Jeong, E.: CP-ThP24, 68
Jeppesen, C.S.: GP-ThP11, 70
Jha, R.: B2-1-ThA1, 62
Jian, S.R.: HP-ThP8, 71
Jílek (Jr.), M.: B1-2-MoA5, 35
Jílek (Sr.), M.: B1-2-MoA5, 35
Jiménez, C.J.: A1-1-TuM6, 38
Jimenez, M.J.M.: B4-3-WeM2, 48
Jiménez, O.: EP-ThP12, 69; FP-ThP11, 70
Johansson, K.: TS1-1-WeM3, 51
Johansson-Jöesaar, M.P.: F4-2-WeA7, 55
Joress, H.: TS1-1-WeM10, **51**
Joshi, S.S.: A2-1-ThM5, 58
Juang, J.Y.: HP-ThP8, 71
Juárez-Navarro, C.A.: B4-2-TuA3, 43
Juez Lorenzo, M.: A3-WeA5, 53
Junda, M.M.: C3+C2+C1-ThM13, 59
Jung, M.Y.: HP-ThP12, 71
Jung, Y.G.: A2-2-ThA7, 62
— K —
Kabatova, M.: B3-2-MoA8, 35
Kabel, J.: H3-2-WeA1, 55
Kacher, J.: H2-2-MoA2, 36
Kagerer, S.: F4-2-WeA6, **55**; FP-ThP17, **70**
Kainz, C.: B2-1-ThA11, **62**
Kakandar, E.: H2-1-MoM4, 33
Kalapala, M.V.: CP-ThP21, **68**; F4-2-WeA4, **55**
Kalscheuer, C.: BP-ThP4, 66; E3-WeM4, 49; F4-2-WeA5, 55; G2-FrM9, **73**
Kamatagi, K.: B2-2-FrM9, 72
Kamiya, S.: TS4-1-MoM3, **34**
Kane, K.A.: A2-1-ThM3, **58**
Kang, B.K.: HP-ThP12, **71**
Kang, D.: CP-ThP12, 68
Kapsa, P.: D1-1-MoM3, 33
Karner, J.: E3-WeM5, 49
Kaspar, J.: TS1-2-WeA1, 56
Kateb, M.: F1-TuM5, 40
Katoh, Y.: H3-2-WeA1, 55
Kaulfuss, F.: B1-2-MoA6, 35; TS1-2-WeA1, 56
Kaur, D.: C4-ThA8, 63; CP-ThP30, 68
Kaur, J.: B1-1-MoM3, 32
Kbibou, M.: H1-2-TuA5, **46**
Keckes, J.: B4-4-WeA2, 53
Keleş, A.: B6-ThM1, 58; BP-ThP30, 67
Kellmann, L.-B.: TS1-2-WeA4, 56
Kelly, P.: A1-1-TuM2, **38**; A1-1-TuM4, 38; F3-TuA3, 45
Kempe, P.: H3-1-WeM2, **50**
Keraudy, J.: F2-1-ThM8, 60
Keshri, A.K.: B5-2-FrM9, 72
Kgoete, F.: E2-1-TuM6, **40**
Khalil, K.: E2-1-TuM5, 40
Khan, A.M.: EP-ThP19, **69**
Khang, L.: DP-ThP26, 69
Khanna, A.: B1-1-MoM3, 32
Khelfaoui, F.: E1-1-ThM6, 59
Kido, Y.: B2-1-ThA2, **62**
Kiilic, U.: C3+C2+C1-ThM9, 59; CP-ThP18, 68
Kim, B.K.: B4-2-TuA2, **43**; GP-ThP15, 70
Kim, H.: AP-ThP10, 66
Kim, H.J.: GP-ThP15, 70
Kim, H.K.: BP-ThP17, 66; CP-ThP20, **68**; HP-ThP5, 71
Kim, I.S.: A2-2-ThA7, 62
Kim, J.: B7-TuA11, 44; C2-WeA7, 54; EP-ThP24, 69
Kim, J.-H.: EP-ThP20, **69**
Kim, J.W.: CP-ThP20, 68
Kim, R.: F3-TuA5, 45
Kim, S.M.: CP-ThP20, 68
Kim, W.R.: EP-ThP20, 69
Kim, Y.: GP-ThP15, 70
Kirchlechner, C.K.: H3-1-WeM3, 50; H3-2-WeA9, 55
Kirnbauer, A.: BP-ThP32, **67**; TS1-1-WeM12, **51**
Kitajima, A.: B4-1-TuM7, 39; B4-2-TuA9, 43; BP-ThP26, 67
Kiyokawa, D.: B4-2-TuA9, **43**; BP-ThP26, 67
Klein, P.: B5-1-ThA4, 63; B7-TuA2, 44
Kleinbichler, A.: E2-1-TuM3, 40
Klemborg-Sapieha, J.E.: A1-3-WeM10, 48; A1-3-WeM3, 48; E1-1-ThM6, 59; EP-ThP30, **69**; H3-2-WeA8, 55; TS2-ThM11, 61; TS2-ThM3, 61; TSP-ThP2, 71
Klima, S.: B4-4-WeA2, 53
Klimashin, F.F.: B6-ThM5, 58; BP-ThP18, 67
Klostermann, H.: G1+G3-ThM3, **60**
Klünsner, T.: B4-4-WeA3, 53
Kment, S.: G4+G5+G6-ThA7, 65
Knittel, S.: A1-3-WeM10, 48; A1-3-WeM3, 48
Ko, K.Y.: G1+G3-ThM12, 60
Kodambaka, S.: B6-ThM10, 58
Koelker, W.: B2-2-FrM10, 72; G1+G3-ThM2, 60
Koga, K.: B2-2-FrM9, **72**
Koganemaru, M.: TS4-1-MoM3, 34
Koh, I.H.J.: DP-ThP23, 69
Koh, J.: CP-ThP12, 68
Kohlhauser, B.: E1-2-ThA9, **64**
Kohlscheen, J.: BP-ThP1, **66**; G2-FrM8, **73**
Kohulak, O.: BP-ThP3, 66
Kokalj, D.: EP-ThP23, 69; F2-2-ThA9, **64**
Kolarik, V.: A3-WeA5, **53**
Koller, C.M.: BP-ThP32, 67; E1-2-ThA9, 64; TS1-1-WeM12, 51
Kolosvári, S.: B1-3-TuM4, 38; B4-2-TuA1, 43; BP-ThP32, 67; F4-2-WeA6, 55; FP-ThP17, 70; FP-ThP3, 70; TS1-2-WeA9, 56
Komsa, H.-P.: F3-TuA9, **45**
Kong, Y.: F2-2-ThA2, 64
König, T.: A2-2-ThA8, **62**
Kontis, P.: H1-1-TuM3, 41
Korenyi-Both, A.L.: E3-WeM3, 49; TS3+4-2-MoA11, **37**
Korlacki, R.: C3+C2+C1-ThM9, 59
Korte-Kerzel, S.: H3-1-WeM1, 50
Kos, Š.: B1-2-MoA4, 35
Kostoglou, N.K.: C4-ThA7, 63
Kotrlóvá, M.: B1-3-TuM5, **38**
Kousaka, H.: EP-ThP22, 69; EP-ThP24, **69**
Koutna, N.: B6-ThM2, **58**; B6-ThM5, 58; BP-ThP19, **67**; E1-2-ThA9, 64
Koyanagi, T.: H3-2-WeA1, 55
Kozák, T.: F2-1-ThM5, **60**; F4-2-WeA6, 55; FP-ThP17, 70; FP-ThP3, 70
Kraetzschmar, B.G.: G1+G3-ThM3, 60
Kranzmann, A.: A1-1-TuM8, 38
Kratochvil, J.: D2-TuA10, 44; F3-TuA11, 45
Krauβ, S.: H2-2-MoA5, **36**
Krbal, M.: F4-1-WeM2, 50
Kreiml, P.: TS3+4-2-MoA4, **37**
Kroker, M.: B1-3-TuM6, **38**
Krssek, V.: B1-2-MoA5, 35
Kruis, E.: F2-2-ThA9, 64
Krülle, T.: B1-2-MoA6, **35**
Kruppe, N.C.: BP-ThP23, 67
Kubart, T.: B3-2-MoA7, 35
Kuczyk, M.: TS1-2-WeA1, **56**

Author Index

- Kulczyk-Malecka, J.: A1-1-TuM4, 38; F3-TuA3, **45**
- Kumar, A.: C4-ThA8, 63; CP-ThP30, **68**
- Kumar, N.: F1-TuM4, 40
- Kümmel, J.: B2-1-ThA5, 62
- Kunche, C.K.: CP-ThP4, 67
- Kuo, W.-C.: D2-TuA12, **44**; DP-ThP2, **68**
- Kups, T.: TS1-2-WeA4, 56
- Kus, P.: BP-ThP3, 66
- Kuyel, B.: F4-2-WeA11, **55**
- Kuzminova, A.: F1-TuM1, 40
- Kvetkova, L.: B3-2-MoA8, 35
- Kylian, O.: D2-TuA10, 44; F1-TuM1, **40**
- L —
- Lai, G.-H.: GP-ThP17, 70
- Lai, X.M.: B3-2-MoA9, 35; C3+C2+C1-ThM11, 59
- Lai, Y.S.: G2-FrM6, 73
- Lamberti, A.: TS3+4-2-MoA9, 37
- Lance, M.J.: A2-1-ThM3, 58; A2-2-ThA4, **62**
- Landälv, L.L.: F4-2-WeA7, **55**
- Larangeira, J.: CP-ThP23, 68
- Largeau, L.: H1-1-TuM6, 41
- Lasanta Carrasco, M.I.: A1-1-TuM8, 38; A1-3-WeM2, 48; A3-WeA6, 53
- Laska, N.: B1-3-TuM2, 38
- Latarius, J.: BP-ThP37, **67**
- Lau, S.H.: H1-2-TuA8, 46
- Laugel, N.: A1-2-TuA9, 43; G4+G5+G6-ThA3, **65**
- Lavenstein, S.: H2-1-MoM1, 33
- Lavery, N.: TSP-ThP4, 71
- Lazzari, R.: H1-2-TuA11, 46; HP-ThP7, 71
- Lechner, A.: H1-1-TuM7, 41
- Lee, C.Y.: CP-ThP1, **67**
- Lee, J.H.: G1+G3-ThM12, 60
- Lee, J.W.: B6-ThM4, 58
- Lee, J.-W.: B4-3-WeM11, 48; D1-2-MoA1, **36**; TS1-1-WeM6, 51; TS1-2-WeA6, 56
- Lee, J.-W.: F2-2-ThA7, 64
- Lee, J.-W.: DP-ThP7, **68**
- Lee, K.: A2-1-ThM10, **58**; A2-1-ThM8, 58; B4-2-TuA2, 43
- Lee, S.H.: BP-ThP17, **66**; HP-ThP5, 71
- Lee, S.W.: H1-2-TuA9, 46
- Lee, S.-W.: H3-1-WeM5, **50**
- Lee, S.Y.: BP-ThP17, 66; CP-ThP20, 68; HP-ThP5, 71
- Legros, M.: H1-1-TuM2, 41
- Lei, C.-M.: DP-ThP5, **68**
- Leite, D.M.G.: DP-ThP23, 69
- Lemma, O.: B2-2-FrM10, 72
- Lemmon, J.: CP-ThP12, 68
- Lengaigne, J.: TS2-ThM11, 61; TS2-ThM3, **61**; TSP-ThP2, 71
- Lenis, J.A.: DP-ThP4, **68**; E2-2-TuA3, **45**
- Lepple, M.: A2-1-ThM11, **58**
- Leson, A.: B1-2-MoA6, 35; TS1-2-WeA1, 56
- Letzig, D.: D1-2-MoA6, 36
- Levi, C.G.: A2-1-ThM11, 58
- Lewin, E.: TS1-1-WeM3, **51**
- Lewis, S.: H1-2-TuA8, 46
- Leyendecker, T.: B2-2-FrM10, 72; G1+G3-ThM2, 60
- Leyens, C.: B1-2-MoA6, 35; TS1-2-WeA1, 56
- Li, C.: D1-2-MoA4, 36; F4-1-WeM5, **50**
- Li, C.L.: D1-1-MoM6, 33
- Li, F.: HP-ThP11, 71
- Li, J.J.: BP-ThP29, **67**
- Li, K.Y.: H3-2-WeA7, 55
- Li, L.: BP-ThP31, 67
- Li, Q.: EP-ThP16, 69
- Li, S.Y.: BP-ThP33, **67**; F4-1-WeM10, **50**
- Li, X.B.: C3+C2+C1-ThM11, **59**
- Li, Y.: A1-1-TuM9, **38**; BP-ThP42, 67; E2-2-TuA8, 45
- Liang, T.: BP-ThP4, 66
- Liao, E.Y.: F3-TuA4, 45
- Liao, M.E.: B6-ThM10, 58; C2-WeA9, **54**
- Liao, M.H.: C3+C2+C1-ThM10, 59
- Liao, Y.: C4-ThA3, 63
- Liberatore, A.M.A.: DP-ThP23, 69
- Lider, A.: H3-2-WeA4, 55
- Lien, S.-Y.: GP-ThP21, 71
- Lilova, K.: A2-1-ThM11, 58
- Limbeck, A.: BP-ThP34, 67
- Lin, C.-M.: HP-ThP8, 71
- Lin, C.-P.: D1-2-MoA1, 36
- Lin, C.W.: B5-1-ThA9, **63**; DP-ThP11, **68**
- Lin, J.: CP-ThP17, **68**
- Lin, J.L.: B1-1-MoM6, **32**
- Lin, K.: G4+G5+G6-ThA6, 65
- Lin, K.C.: C3+C2+C1-ThM4, **59**; CP-ThP31, **68**
- Lin, M.: A1-1-TuM9, 38; E1-4-WeA2, **54**
- Lin, M.T.: E2-2-TuA9, **45**
- Lin, S.S.: BP-ThP31, 67; EP-ThP16, 69
- Lin, S.Y.: BP-ThP2, 66
- Lin, T.Y.: DP-ThP7, 68
- Lin, Y.C.: B4-3-WeM11, **48**; BP-ThP14, **66**
- Lin, Y.H.: F1-TuM3, **40**
- Lin, Y.L.: CP-ThP1, 67
- Lin, Z.X.: B4-3-WeM13, **48**; E1-3-FrM7, 73
- Lindahl, E.: B2-2-FrM8, 72; BP-ThP20, 67
- Liskiewicz, T.: H3-2-WeA2, 55
- List-Kratochvil, E.: TS4-1-MoM5, 34
- Liu, B.W.: B4-3-WeM12, 48
- Liu, C.: H3-2-WeA7, 55
- Liu, C.L.: A2-1-ThM4, **58**
- Liu, C.P.: C2-WeA11, 54; F4-1-WeM1, 50
- Liu, D.H.: G2-FrM6, **73**
- Liu, H.: A1-1-TuM4, 38
- Liu, H.C.: B5-2-FrM8, 72
- Liu, J.L.: TS2-ThM7, 61; TSP-ThP6, 71
- Liu, Q.W.: D1-2-MoA4, 36
- Liu, S.-M.: GP-ThP21, 71
- Liu, Y.: H1-1-TuM2, 41
- Liu, Y.C.: B4-3-WeM13, 48; E1-3-FrM7, **73**; GP-ThP13, **70**
- Liu, Y.H.: B4-3-WeM12, **48**
- Liu, Z.: B2-1-ThA8, **62**
- Lo, W.L.: B6-ThM4, **58**; BP-ThP15, **66**
- Lobmaier, L.: B6-ThM5, 58
- Lofaj, F.: B3-2-MoA8, **35**
- Lomello, F.: A1-1-TuM3, 38
- Londoño, R.F.: EP-ThP26, 69
- Lopes Dias, N.F.: B3-1-MoM3, **32**
- Lopez Perrusquia, N.: EP-ThP11, 69; HP-ThP4, **71**
- Lopez-Suero, D.: B4-1-TuM5, 39
- Loqui, S.L.: A1-3-WeM10, 48; A1-3-WeM3, 48
- Lorin, G.: GP-ThP24, 71
- Lou, B.-S.: D1-2-MoA1, 36; DP-ThP7, 68; F2-2-ThA7, 64
- Louring, S.: E1-1-ThM7, 59
- Lousa, A.: BP-ThP36, **67**
- Lu, G.H.: B5-1-ThA9, 63
- Lu, J.: B4-1-TuM4, 39; F4-2-WeA7, 55; G1+G3-ThM4, 60
- Lu, N.: TS4-1-MoM1, **34**
- Lubaszka, P.: AP-ThP9, 66
- Lucas, S.: B7-TuA1, 44
- Luchtenberg, P.A.: GP-ThP7, **70**
- Ludwig, A.: H3-1-WeM3, 50
- Lümkemann, A.: B1-2-MoA5, 35; B4-3-WeM3, 48; G4+G5+G6-ThA5, 65
- Lundin, D.: B7-TuA2, 44; B7-TuA9, 44; F2-1-ThM8, 60; FP-ThP10, 70
- Lusvarghib, L.: TS1-2-WeA3, 56
- M —
- Ma, H.: HP-ThP3, 71
- Ma, Y.H.: F2-2-ThA2, 64
- Macauley, C.A.: A2-1-ThM11, 58
- Machado, I.F.: E1-3-FrM1, 73
- Maeder, X.: A2-2-ThA3, 62; H2-1-MoM4, 33; H2-2-MoA4, 36
- Mahmood, K.: FP-ThP18, **70**
- Mairaj Deen, K.: GP-ThP22, 71
- Makineni, S.K.: H1-1-TuM3, 41
- Maldonado Dominguez, K.: HP-ThP10, **71**
- Malik, G.: F4-2-WeA3, **55**; GP-ThP19, **71**
- Mallick, M.: D1-1-MoM7, **33**
- Manik, G.: DP-ThP24, 69
- Manns, T.: B2-1-ThA5, 62
- Marcel, C.: F2-2-ThA4, 64
- Marchand, B.: AP-ThP3, 66
- Marquez Herrera, A.: GP-ThP18, 70
- Marquez, A.: DP-ThP16, 68
- Marti, A.: D1-2-MoA3, 36
- Martinez-Trinidad, J.: B4-1-TuM5, 39; E1-1-ThM3, 59
- Martins, R.: F4-1-WeM3, 50
- Martino, L.: A1-3-WeM10, 48; A1-3-WeM3, 48; EP-ThP30, 69; H3-2-WeA8, 55; TS2-ThM11, 61; TS2-ThM3, 61
- Marugi, K.: A1-3-WeM5, 48; AP-ThP13, 66
- Maruko, T.: BP-ThP11, 66; BP-ThP12, **66**; BP-ThP13, 66
- Maskrot, H.: A1-1-TuM3, 38
- Massi, M.: DP-ThP23, **69**
- Mastail, C.: H1-2-TuA2, 46
- Mathew, M.T.: D2-TuA5, 44; D3-TuM7, **39**
- Mathiasen, C.: GP-ThP11, 70
- Matsuda, K.: G2-FrM3, 73; H1-2-TuA9, **46**
- Matthews, A.: A1-1-TuM9, 38; C3+C1-WeM4, 49; C3+C2+C1-ThM12, 59; CP-ThP19, 68; E1-4-WeA2, 54; G4+G5+G6-ThA3, 65; GP-ThP3, 70
- Matthews, D.T.A.: EP-ThP21, **69**
- Maurel, V.: A2-1-ThM1, **58**; AP-ThP11, 66; AP-ThP3, **66**
- Maury, F.: B2-2-FrM5, 72; B2-2-FrM6, **72**
- Maus, J.: B3-1-MoM2, 32
- Maus-Friedrichs, W.: B3-1-MoM3, 32
- Mayr, P.: A1-1-TuM8, 38
- Mayrhofer, P.H.: B4-2-TuA1, 43; B5-1-ThA5, 63; B6-ThM12, 58; B6-ThM2, 58; B6-ThM5, **58**; B6-ThM9, 58; BP-ThP18, **67**; BP-ThP19, 67; BP-ThP32, 67; BP-ThP34, 67; BP-ThP35, 67; E1-2-ThA9, 64; F4-2-WeA6, 55; FP-ThP17, 70; FP-ThP3, 70; TS1-1-WeM12, 51
- McKenzie, D.R.: B5-1-ThA6, 63
- McKnight, R.: G4+G5+G6-ThA6, 65
- McMaster, S.: H3-2-WeA2, 55
- McNallan, M.: D2-TuA5, 44
- Mehraban, S.: TSP-ThP4, 71
- Meindlhummer, M.: B4-4-WeA2, **53**
- Meissner, T.: A3-WeA3, 53
- Mejía, H.D.: D3-TuM8, 39; DP-ThP25, 69
- Melih, A.: EP-ThP2, **69**
- Melo-Máximo, D.V.: E1-3-FrM5, 73; E1-3-FrM6, 73
- Melo-Máximo, L.: E1-3-FrM6, 73
- Mendala, B.: A1-3-WeM5, 48; AP-ThP13, 66; AP-ThP9, 66
- Mendizabal, L.: GP-ThP5, 70
- Mendoza, G.M.: B4-2-TuA2, 43
- Meneses-Amador, A.: B4-2-TuA3, 43; B4-3-WeM6, 48
- Meng, F.: C2-WeA10, 54
- Meng, W.J.: H2-2-MoA3, **36**
- Mercier, F.: B2-1-ThA6, 62; B2-1-ThA7, 62
- Merle, B.: H2-2-MoA5, 36; H2-2-MoA6, 36; H3-1-WeM4, **50**

Author Index

- Meth, J.: TS4-1-MoM4, 34
Meyer, D.J.: C2-WeA5, 54
Meza, J.R.: E1-4-WeA6, 54
Mezlini, S.: D2-TuA1, 44
Michau, A.: A1-1-TuM3, 38; B2-2-FrM5, 72; B2-2-FrM6, 72
Michau, D.: E3-WeM10, 49
Michel, A.: H1-2-TuA2, 46
Michel, E.G.: E2-1-TuM4, 40
Michels, A.F.: E1-2-ThA11, 64
Michler, J.: H2-2-MoA4, 36
Mihut, D.M.: B4-4-WeA6, 53; DP-ThP26, 69
Mikula, M.: B5-2-FrM6, 72; BP-ThP3, 66; E1-3-FrM2, 73
Milassin, G.: TS3+4-2-MoA8, 37
Milhet, X.: H1-1-TuM2, 41
Millan-Ramos, B.: D1-2-MoA6, 36
Minea, T.: B7-TuA9, 44; F2-1-ThM3, 60; F2-1-ThM6, 60; FP-ThP10, 70; FP-ThP7, 70
Mingo, B.: C3+C2+C1-ThM12, 59; CP-ThP19, 68
Mischler, S.: D1-1-MoM4, 33
Missouli, J.: E1-2-ThA6, 64
Mitma Pillaca, E.J.D.: GP-ThP8, 70
Mitterer, C.: B1-2-MoA10, 35; B2-1-ThA11, 62; B2-1-ThA4, 62; B4-3-WeM3, 48; B4-4-WeA2, 53; C4-ThA7, 63; EP-ThP6, 69; H1-1-TuM7, 41; TS3+4-2-MoA4, 37
Miyakawa, W.T.: DP-ThP23, 69
Mizubayashi, M.: G2-FrM3, 73
Mock, A.: C2-WeA1, 54; C3+C2+C1-ThM9, 59; CP-ThP18, 68
Mocuta, C.: E2-2-TuA2, 45
Modes, T.: B1-3-TuM1, 38
Mohammadtaheri, M.: BP-ThP42, 67
Mojica-Villegas, A.: B4-1-TuM5, 39
Moldenhauer, H.: EP-ThP23, 69
Molina Aldareguia, J.M.: B3-2-MoA5, 35
Monaghan, D.: B1-2-MoA2, 35; FP-ThP9, 70
Monclus, M.A.: B3-2-MoA5, 35
Monsifrot, E.: B2-2-FrM5, 72; B2-2-FrM6, 72
Monterrosa, A.M.: H3-2-WeA3, 55
Montes Ruiz-Cabello, F.J.: TS2-ThM4, 61
Montigaud, H.: H1-1-TuM6, 41; H1-2-TuA11, 46; HP-ThP7, 71
Moon, G.D.: CP-ThP24, 68
Mora, J.: TS2-ThM8, 61
Moraes, V.: B4-3-WeM3, 48; B6-ThM12, 58; B6-ThM9, 58; BP-ThP34, 67
Moreau, C.: CP-ThP27, 68; TS2-ThM9, 61
Moreno Palmerin, J.: GP-ThP18, 70
Morgado-Gonzalez, I.: AP-ThP6, 66; BP-ThP24, 67; BP-ThP25, 67
Morstein, M.: B4-3-WeM3, 48
Moseler, M.: E1-3-FrM3, 73
Moskovkin, P.: B7-TuA1, 44
Mosquera, M.: A1-1-TuM8, 38
Motallebzadeh, A.: E2-2-TuA10, 45; EP-ThP5, 69
Motylenko, M.: B4-3-WeM4, 48; B4-4-WeA7, 53
Mouftiez, A.: B4-3-WeM6, 48
Mourya, S.: F4-2-WeA3, 55; GP-ThP19, 71
Mraz, S.: B1-2-MoA10, 35
Mu, Y.: H2-2-MoA3, 36
Muhl, S.: D2-TuA4, 44; E1-3-FrM5, 73; E1-3-FrM9, 73
Mühlbacher, M.: EP-ThP6, 69
Müller, A.: G2-FrM7, 73
Munroe, P.: TS1-1-WeM1, 51
Muralidharan, G.M.: A1-1-TuM1, 38; A1-3-WeM4, 48
Muratore, C.: F3-TuA5, 45; TS3+4-2-MoA5, 37
Musil, J.: B1-2-MoA4, 35
Myoung, S.W.: A2-2-ThA7, 62
- N —
- N'Gom, M.: C3+C2+C1-ThM5, 59
Nagaraj, R.: D2-TuA5, 44
Nahif, F.: EX-TuEx1, 42
Nait-Ali, A.: H1-1-TuM2, 41
Najarian, V.: E1-1-ThM6, 59
Nakamura, H.: B2-1-ThA3, 62
Nakatani, T.: B2-2-FrM9, 72
Narala, S.K.R.: B4-2-TuA4, 43; E1-3-FrM12, 73; EP-ThP31, 71
Naraparaju, R.: B1-3-TuM2, 38
Narasimalu, S.: A1-1-TuM6, 38
Nass, K.: B3-1-MoM5, 32
Nauenburg, K.-D.: G1+G3-ThM11, 60
Navabpour, P.: AP-ThP2, 66
Nava-Sánchez, J.L.: B4-3-WeM6, 48
Navrotsky, A.: A2-1-ThM11, 58
Neels, A.: A2-2-ThA3, 62
Němcova, A.: C3+C2+C1-ThM12, 59
Nemetz, A.W.: B4-4-WeA3, 53
Nepal, N.: C2-WeA5, 54
Neumeier, S.: H1-1-TuM3, 41
Neuß, D.: TS1-2-WeA9, 56
Neville, A.: H3-2-WeA2, 55
Ngo, D.: C3+C1-WeM4, 49
Nicolai, J.: E2-2-TuA2, 45
Nicolini, P.: E1-2-ThA2, 64; E1-2-ThA5, 64; E1-2-ThA7, 64
Nie, X.: EP-ThP27, 69; G2-FrM10, 73; G2-FrM5, 73
Nielsen, L.P.: E1-1-ThM7, 59; GP-ThP11, 70
Nii, H.: B4-3-WeM5, 48
Nikitin, D.: F1-TuM1, 40
Nimsch, U.: TS1-2-WeA1, 56
Nishimura, K.: H1-2-TuA9, 46
Nishiyama, K.: TSP-ThP8, 71
Noh, Y.: GP-ThP15, 70
Noma, M.: G4+G5+G6-ThA4, 65
Northam, M.: A2-2-ThA5, 62
Norymberczyk, L.: H3-2-WeA10, 55
Nose, M.: G2-FrM3, 73
Nyakiti, L.O.: C2-WeA5, 54
Nyholm, L.: TS1-1-WeM3, 51; TS1-1-WeM5, 51
- O —
- Obasi, G.: A1-1-TuM2, 38
Oboegbu, M.J.: AP-ThP4, 66
Obrusnik, A.: B1-3-TuM6, 38; G1+G3-ThM1, 60
Oellers, T.: H3-1-WeM3, 50
Oh, J.S.: B2-2-FrM9, 72
Oh, S.: C2-WeA7, 54
Öhman, S.Ö.: B2-2-FrM7, 72
Okamoto, N.: B4-1-TuM7, 39; B4-2-TuA9, 43; BP-ThP26, 67
Okimoto, T.: G1+G3-ThM7, 60; TSP-ThP8, 71
Okle, P.: H1-2-TuA1, 46
Okuno, S.: B2-1-ThA2, 62
Olabi, A.: CP-ThP22, 68
Oladoye, A.: CP-ThP22, 68
Olaya Florez, J.J.: B4-1-TuM6, 39; BP-ThP39, 67; E1-4-WeA5, 54; EP-ThP26, 69
Olejnicki, J.: G4+G5+G6-ThA7, 65
Oliveira, A.: DP-ThP23, 69
Oliveira, J.C.: B3-2-MoA7, 35; FP-ThP6, 70
Oliver, W.C.: H2-2-MoA9, 36
Onofre, C.F.: B5-2-FrM4, 72
Ortega-Aviles, M.: E1-1-ThM3, 59
Ortiz-Domínguez, M.: AP-ThP6, 66; B4-2-TuA8, 43; BP-ThP24, 67; BP-ThP25, 67
Oseguera-Peña, J.: B4-1-TuM5, 39; B4-2-TuA8, 43; E1-3-FrM5, 73; E1-3-FrM6, 73; E1-4-WeA6, 54
Oskay, C.: A3-WeA3, 53
Ospina, R.: E1-4-WeA5, 54; EP-ThP26, 69
- Ougier, M.: A1-1-TuM3, 38
Özerinç, S.: E2-2-TuA10, 45; EP-ThP5, 69
- P —
- Page, N.: D1-2-MoA3, 36
Paladines, R.: D1-2-MoA3, 36
Palaparty, S.: EP-ThP31, 71
Paliwal, A.: C3+C2+C1-ThM10, 59
Pan, C.-H.: TS1-2-WeA2, 56
Pan, W.-C.: E2-2-TuA9, 45
Pandey, K.K.: B5-2-FrM9, 72
Pang, X.L.: E2-2-TuA11, 45
Pantoya, M.: F1-TuM6, 40
Panzarino, J.: H2-1-MoM6, 33
Papa, F.: B3-2-MoA3, 35; F2-1-ThM9, 60; G1+G3-ThM8, 60; TS3+4-2-MoA10, 37
Pardhasaradhi, S.P.: H2-2-MoA9, 36
Pardo-Perez, A.: D1-1-MoM4, 33
Park, H.J.: G1+G3-ThM12, 60
Park, I.-W.: AP-ThP10, 66
Park, J.S.: CP-ThP6, 67; CP-ThP7, 68
Park, S.: GP-ThP15, 70
Park, T.G.: CP-ThP6, 67; CP-ThP7, 68
Park, Y.K.: CP-ThP24, 68
Paseuth, A.: B2-1-ThA2, 62
Passerone, D.: F4-2-WeA8, 55; FP-ThP5, 70
Pathak, A.: B5-2-FrM9, 72
Patnaik, P.: B4-4-WeA5, 53
Paturi, U.M.R.: B4-2-TuA4, 43; EP-ThP31, 71
Paulus, M.: BP-ThP37, 67
Paumier, F.: CP-ThP13, 68
Pawar, S.: C4-ThA8, 63; CP-ThP30, 68
Pecerskis, A.: H3-2-WeA6, 55
Pedersen, P.M.: GP-ThP11, 70
Peng, L.F.: B3-2-MoA9, 35; C3+C2+C1-ThM11, 59
Peng, Z.: H1-1-TuM3, 41
Pereira, A.: GP-ThP24, 71
Pereira-Silva, P.: D3-TuM2, 39
Pérez Mendoza, G.J.: EP-ThP11, 69
Perez Pasten-Borja, R.: B4-1-TuM5, 39
Pérez Trujillo, F.J.: A1-3-WeM2, 48; A3-WeA6, 53
Perez, J.: EP-ThP12, 69
Pérez-Alvarez, J.: FP-ThP11, 70
Periyasamy, S.: E3-WeM6, 49
Perry, D.: FP-ThP9, 70
Peterson, R.L.: C2-WeA3, 54
Petrov, I.: B4-1-TuM4, 39; F2-1-ThM8, 60; F2-2-ThA5, 64; SIT2-WeSIT1, 52
Pflug, A.: B7-TuA1, 44
Pierron, O.N.: H2-1-MoM4, 33; H2-2-MoA2, 36; TS4-1-MoM4, 34
Pignedoli, C.A.: F4-2-WeA8, 55; FP-ThP5, 70
Pikul, J.H.: E3-WeM1, 49
Pillai, R.P.: A1-1-TuM1, 38
Pinheiro, R.A.: BP-ThP28, 67
Pint, B.A.: A2-1-ThM3, 58; A2-2-ThA4, 62
Pippan, R.: C4-ThA7, 63
Pleskunov, P.: F1-TuM1, 40
Podraza, N.J.: C3+C2+C1-ThM13, 59
Poerschke, D.: A2-2-ThA1, 62
Pohler, M.: B4-4-WeA7, 53
Polacek, M.: B5-1-ThA4, 63
Polcar, T.: B5-1-ThA3, 63; H3-2-WeA4, 55
Polcar, T.P.: B5-2-FrM4, 72; E1-1-ThM5, 59; E1-2-ThA2, 64; E1-2-ThA7, 64; E1-3-FrM2, 73
Polcik, P.: B4-3-WeM3, 48; B6-ThM12, 58; B6-ThM9, 58; BP-ThP34, 67; TS1-1-WeM12, 51; TS1-2-WeA9, 56
Polop, C.: E2-1-TuM4, 40
Polyakov, M.: A2-2-ThA3, 62
Pone, A.: H3-2-WeA6, 55
Pons, M.: B2-1-ThA6, 62; B2-1-ThA7, 62; B2-2-FrM5, 72

Author Index

- Popoola, O.M.: CP-ThP26, 68; E1-4-WeA4, 54; E1-4-WeA7, 54; FP-ThP12, 70
- Popoola, P.A.: CP-ThP26, 68; D2-TuA11, 44; E1-4-WeA4, 54; E1-4-WeA7, 54; E2-1-TuM6, 40; FP-ThP12, 70
- Poruba, A.: B7-TuA11, 44
- Poulon-Quintin, A.: E3-WeM10, 49
- Praetzas, C.: B4-4-WeA3, 53
- Preuss, M.: A1-1-TuM2, 38
- Price, J.: B1-2-MoA2, 35
- Prieto Ríos, C.: A3-WeA1, **53**
- Primetzhofer, D.: BP-ThP41, 67
- Prysiazyni, V.: D2-TuA10, 44
- Puetz, W.: B2-2-FrM10, 72
- Pugh, M.: TS2-ThM9, 61
- Purandare, Y.: A1-1-TuM8, 38
- Pürstl, J.T.: H2-2-MoA4, 36
- Putz, B.: TS3+4-2-MoA8, **37**
- Pyclik, L.: A1-3-WeM5, 48; AP-ThP13, **66**
- **Q** —
- Qiao, R.: H1-2-TuA8, 46
- Qiu, R.: B2-2-FrM8, 72; BP-ThP20, 67
- Quintana, I.: GP-ThP5, 70
- Quintero, J.H.: EP-ThP26, 69
- **R** —
- Raabe, D.: H1-1-TuM3, 41
- Raadu, M.A.: B7-TuA9, 44; F2-1-ThM8, 60
- Radny, T.: G1+G3-ThM11, 60
- Rafaja, D.: B4-3-WeM4, 48; B4-4-WeA7, 53
- Raffield, C.D.: B4-4-WeA6, 53
- Raghavan, S.: A2-2-ThA5, 62
- Rahman, M.M.: A1-2-TuA8, **43**
- Rahman, S.M.: E1-3-FrM10, **73**
- Rai, R.: F3-TuA5, **45**
- Raimondo, M.: TS2-ThM2, 61; TS2-ThM5, **61**
- Raja, T.: E3-WeM6, **49**
- Rajagopalan, J.: H1-2-TuA3, 46; HP-ThP1, 71
- Ramirez, G.: E1-2-ThA9, 64
- Ramirez, M.: B3-1-MoM5, 32; GP-ThP8, 70
- Ramm, J.: A2-2-ThA3, 62
- Rao, S.: D3-TuM7, 39
- Rasmussen, P.: H1-2-TuA3, **46**; HP-ThP1, **71**
- Ratayski, U.: B4-3-WeM4, **48**
- Ratova, M.: F3-TuA3, 45
- Rausch, M.: B1-2-MoA10, **35**; TS3+4-2-MoA4, 37
- Rebelo de Figueiredo, M.: B1-3-TuM4, 38
- Rebholz, C.G.: C3+C1-WeM4, 49; C4-ThA3, 63; C4-ThA7, **63**
- Reddy, S.P.: CP-ThP4, **67**
- Redwing, J.: B2-1-ThA9, 62
- Regalla, S.P.: E1-3-FrM12, 73
- Řehák, P.R.: B6-ThM2, 58
- Reidy, R.F.: A2-1-ThM9, 58
- Reifsnnyder Hickey, D.: B2-1-ThA9, 62
- Remnev, A.G.: G2-FrM11, **73**
- Renault, P.O.: CP-ThP13, **68**; E2-2-TuA2, **45**
- Renk, O.: C4-ThA7, 63
- Restrepo-Parra, E.: E1-4-WeA5, **54**; EP-ThP25, 69; EP-ThP26, **69**
- Revel, A.: F2-1-ThM3, 60; F2-1-ThM6, **60**; FP-ThP7, **70**
- Rezek, B.: E1-2-ThA7, 64
- Richards, B.: A2-1-ThM7, 58
- Riedl, H.: B4-2-TuA1, 43; B6-ThM12, **58**; B6-ThM9, 58; E1-2-ThA9, 64; F4-2-WeA6, 55; FP-ThP17, 70; FP-ThP3, **70**
- Riul, A.R.: B4-3-WeM2, 48
- Rivera Chaverra, M.J.: E1-4-WeA5, 54
- Rivera-López, J.E.: B4-2-TuA3, 43
- Rivero, P.J.: BP-ThP22, 67
- Robledo, S.: D1-2-MoA5, 36
- Roch, T.: B5-2-FrM6, 72; BP-ThP3, 66; E1-3-FrM2, 73
- Rodil, S.E.: B5-2-FrM4, **72**; D1-2-MoA6, 36
- Rodrigues, M.S.: D3-TuM2, 39
- Rodríguez Arevalo, S.D.: B4-1-TuM6, 39; BP-ThP39, 67
- Rodríguez Ripoll, M.: E1-2-ThA9, 64
- Rodríguez Valverde, M.A.: TS2-ThM4, 61
- Rodríguez, R.: BP-ThP22, 67
- Rodríguez, S.: A3-WeA4, 53
- Rodríguez-Castro, G.A.: B4-2-TuA3, 43; B4-3-WeM6, 48; E1-3-FrM5, 73; E1-3-FrM6, 73
- Rogers, J.: PL-MoPL3, **31**
- Rogov, A.: GP-ThP3, 70
- Rojas, T.C.: B3-2-MoA5, 35
- Rojo-Blanco, C.: E1-3-FrM9, 73
- Rollett, A.D.: B1-2-MoA3, 35
- Romanus, H.: TS1-2-WeA4, 56
- Ronkainen, H.: E1-1-ThM7, 59
- Rosén, J.: B4-1-TuM4, 39
- Rosenthal, M.: B4-4-WeA2, 53
- Rossmann, L.: A2-2-ThA5, **62**
- Rota, A.: E1-2-ThA7, 64
- Rougier, A.: F2-2-ThA4, 64
- Rowley-Neale, S.J.: F3-TuA3, 45
- Ruan, J.-J.: TS1-2-WeA2, **56**; TSP-ThP9, 71
- Ruan, J.-W.: CP-ThP31, 68
- Rudigier, H.: TS1-1-WeM4, 51
- Rueß, H.: TS1-2-WeA9, 56
- Ruiz-Rios, A.: E1-1-ThM3, 59
- Rupapara, H.: TS1-2-WeA4, 56
- Rupert, T.: H2-1-MoM5, **33**; H2-1-MoM6, 33
- Rupp, S.: B3-1-MoM2, 32
- Ryan, P.J.: F2-1-ThM11, 60
- Ryl, J.: F3-TuA11, 45
- **S** —
- Sabbadini, S.: A1-3-WeM5, 48
- Sáenz-Trevizo, A.: C3+C2+C1-ThM8, 59
- Saha, B.: C3+C1-WeM5, **49**
- Saisnith, V.: E1-1-ThM4, **59**
- Saito, T.: B4-1-TuM7, **39**; B4-2-TuA9, 43; BP-ThP26, **67**
- Sakakita, H.: EP-ThP24, 69
- Sakalley, S.: C3+C2+C1-ThM10, 59
- Sakamoto, Y.: BP-ThP11, 66; BP-ThP12, 66; BP-ThP13, 66
- Sakuma, T.: BP-ThP13, 66
- Sakuragi, T.: G2-FrM3, 73
- Saldana Rovles, A.: GP-ThP18, 70
- Saleem, A.: GP-ThP22, 71
- Salem, A.: D2-TuA1, 44
- Sälker, J.A.: H3-2-WeA5, 55
- Salvador, P.A.: B1-2-MoA3, 35
- Sampaio, P.: D3-TuM2, 39
- Sampath, S.: A2-2-ThA4, 62
- Sanchette, F.: A1-1-TuM6, 38
- Sánchez Fuentes, L.: HP-ThP4, 71
- Sanchez Lara, S.: B4-4-WeA6, 53
- Sanchez Lopez, J.C.: B3-2-MoA5, 35
- Sanchez-Lara, S.: B4-4-WeA6, **53**
- Sandlöbes, S.: H3-1-WeM1, 50
- Sanginés de Castro, R.S.: BP-ThP8, 66; HP-ThP10, 71
- Sangiovanni, D.G.: B5-2-FrM6, 72; B6-ThM7, **58**
- Sanni, O.: D2-TuA11, **44**
- Santiago Varela, J.A.: B3-2-MoA5, **35**; G1+G3-ThM4, 60
- Santiago, F.: E1-4-WeA6, **54**
- Santos, M.A.: DP-ThP23, 69
- Sardar, S.: CP-ThP12, **68**
- Sari, F.N.: CP-ThP31, 68
- Saringer, C.: H1-2-TuA4, **46**
- Sarkar, R.: HP-ThP1, 71
- Sartory, B.: H1-1-TuM7, 41
- Sathishkumar, D.: C4-ThA9, 63
- Satrapinsky, L.: BP-ThP3, 66; E1-3-FrM2, 73
- Sauques, L.: F2-2-ThA4, 64
- Savadkouei, K.: HP-ThP6, 71
- Scenini, F.: A1-2-TuA9, 43
- Schaaf, P.: TS1-2-WeA4, 56
- Schäfer, J.: B4-4-WeA3, 53
- Schäfer, R.: G1+G3-ThM11, **60**
- Schalk, N.: B2-1-ThA11, 62; B2-1-ThA4, **62**; H1-1-TuM7, 41; H1-2-TuA4, 46
- Scheffel, B.: B4-3-WeM4, 48
- Scheu, C.S.: H3-2-WeA9, 55
- Schiffers, C.: B2-2-FrM10, 72; G1+G3-ThM2, **60**
- Schlegel, M.L.: A1-1-TuM3, 38; A1-1-TuM6, 38
- Schmid, U.: B5-1-ThA7, **63**
- Schmidt, O.: B3-2-MoA1, 35
- Schmitt, J.A.: E1-1-ThM6, 59; EP-ThP30, 69
- Schmitt, T.: E1-1-ThM6, **59**; H3-2-WeA8, 55
- Schmitt, T.S.: EP-ThP30, 69
- Schmutz, P.: D1-1-MoM4, 33
- Schneider, J.M.: B1-2-MoA10, 35; BP-ThP41, 67; H1-1-TuM5, 41; H3-2-WeA5, 55; H3-2-WeA9, 55; TS1-2-WeA9, **56**
- Schneider, M.: B5-1-ThA7, 63
- Schubert, E.: C3+C2+C1-ThM9, **59**; CP-ThP18, **68**
- Schubert, M.: C3+C2+C1-ThM9, 59; CP-ThP18, 68
- Schuler, J.D.: H2-1-MoM5, 33
- Schulz, E.: E1-2-ThA10, 64
- Schulz, U.: B1-3-TuM2, **38**
- Schulz, W.: A1-1-TuM8, 38
- Schuster, F.: A1-1-TuM3, 38; A1-1-TuM6, 38; B2-2-FrM5, 72; B2-2-FrM6, 72
- Schütze, G.: B3-2-MoA1, 35
- Schwarzer, N.: EP-ThP13, **69**; F4-1-WeM11, **50**; H2-2-MoA10, 36; HP-ThP9, 71
- Scopece, D.: F4-2-WeA8, 55; FP-ThP5, 70
- Sebastiani, M.: H2-1-MoM7, **33**
- Segu, D.Z.: EP-ThP14, **69**
- Sekine, T.: TS4-1-MoM3, 34
- Sekora, D.: C3+C2+C1-ThM9, 59; CP-ThP18, 68
- Semprimoschnig, C.: TS3+4-2-MoA8, 37
- Sen, S.: H3-2-WeA4, 55
- Seo, H.J.: CP-ThP24, 68
- Serpini, E.: E1-2-ThA7, 64
- Serra, R.: B3-2-MoA7, 35
- Sethi, S.K.: DP-ThP24, **69**
- Seydoux, C.: C3+C2+C1-ThM7, 59
- Sezemsky, P.: D2-TuA10, 44
- Sha, C.: TS1-1-WeM1, **51**
- Shailesh, P.: E1-3-FrM12, **73**
- Shaleni, V.: C4-ThA9, 63
- Shang, H.F.: A1-2-TuA3, **43**
- Shao, S.: H2-2-MoA3, 36
- Shao, T.M.: A1-2-TuA3, 43; B6-ThM11, **58**
- Sharifi, N.: TS2-ThM11, 61; TS2-ThM9, 61
- Sharma, nil.: FP-ThP15, **70**
- Sharobem, T.: A2-1-ThM6, 58
- Shelemin, A.: F1-TuM1, 40
- Shen, X.: G2-FrM10, 73
- Shen, Y.H.: BP-ThP33, 67; F4-1-WeM10, 50
- Shen, Y.-L.: E2-1-TuM1, **40**
- Shesadri, S.: H1-2-TuA8, 46
- Shi, Q.: BP-ThP31, 67
- Shi, W.: B4-2-TuA2, 43
- Shin, C.H.: G1+G3-ThM12, 60
- Shin, S.J.: F2-2-ThA3, 64
- Shirani, A.: E3-WeM3, 49
- Shiratani, M.: B2-2-FrM9, 72
- Shishido, N.: TS4-1-MoM3, 34
- Shore, D.: GP-ThP3, **70**
- Signor, L.: H1-1-TuM2, 41
- Silva, F.: D3-TuM7, 39
- Silva-Bermudez, P.: D1-2-MoA6, **36**

Author Index

- SilviaAlvarez, D.F.: GP-ThP18, 70
 Simmons, M.: TS3+4-2-MoA10, 37
 Simonot, L.: H1-2-TuA2, 46
 Singh, B.R.: B2-1-ThA1, 62
 Singh, M.: DP-ThP24, 69
 Singh, P.: B2-1-ThA1, 62
 Sitnikov, N.: B1-2-MoA11, 35
 Slim, M.F.: E2-1-TuM5, 40
 Smietana, M.: D2-TuA10, 44
 Smith, G.C.: F3-TuA3, 45
 Smith, R.: C3+C1-WeM2, 49
 Snure, M.: TS3+4-2-MoA5, 37
 Snyders, R.: TS3+4-2-MoA6, 37
 Soares, P.: GP-ThP7, 70
 Šob, M.S.: B6-ThM2, 58; BP-ThP19, 67
 Sobaszek, M.: F3-TuA11, 45
 Sokolov, A.D.: H3-2-WeA6, 55
 Solar, P.: F1-TuM1, 40
 Soler, R.S.: H3-2-WeA9, 55
 Solis-Romero, J.: AP-ThP6, 66; B4-2-TuA8, 43;
 BP-ThP24, 67; BP-ThP25, 67
 Sologubenko, A.S.: H1-2-TuA1, 46; HP-ThP3,
 71
 Song, H.: GP-ThP2, 70
 Song, J.: E1-3-FrM10, 73
 Song, M.G.: HP-ThP5, 71
 Sorour, A.: E1-3-FrM11, 73
 Soucek, P.: B1-3-TuM6, 38; B5-1-ThA4, 63
 Souza, J.: D3-TuM7, 39
 Souza, R.M.: E1-3-FrM1, 73
 Sparenberg, A.: BP-ThP37, 67
 Spolenak, R.: H1-2-TuA1, 46; H3-2-WeA7, 55;
 HP-ThP3, 71; TS1-2-WeA7, 56
 Srinath, A.: TS1-1-WeM3, 51
 Stamate, E.: B7-TuA4, 44
 Stangebye, S.: H2-2-MoA2, 36
 Stangier, D.: B3-1-MoM3, 32; BP-ThP37, 67;
 EP-ThP23, 69; F2-2-ThA8, 64; F2-2-ThA9, 64
 Stark, A.: H1-2-TuA4, 46
 Steinhoff, M.K.: TS1-2-WeA9, 56
 Steinmann, P.-A.: DP-ThP22, 68
 Stelzer, B.: H3-2-WeA5, 55
 Sternemann, C.: BP-ThP37, 67
 Stiens, D.: B2-1-ThA5, 62
 Stokes, J.: CP-ThP22, 68
 Stoyanov, P.: E3-WeM11, 49
 Stranak, V.: G4+G5+G6-ThA7, 65
 Stranak, V.S.: D2-TuA10, 44; F3-TuA11, 45
 Straub, T.S.: AP-ThP11, 66; H2-1-MoM3, 33
 Stripe, B.: H1-2-TuA8, 46
 Stupavaska, M.: B5-1-ThA4, 63
 Stylianou, R.: B2-1-ThA4, 62
 Su, J.: B2-1-ThA6, 62; B2-1-ThA7, 62
 Su, Y.-H.: TS1-2-WeA10, 56; TS1-2-WeA2, 56;
 TSP-ThP9, 71
 Subacius, A.: C3+C1-WeM4, 49
 Subba Reddy, N.: B4-2-TuA4, 43
 Subedi, B.: C3+C2+C1-ThM13, 59
 Subedi, D.B.: A1-3-WeM11, 48
 Sugiyama, H.: TS4-1-MoM3, 34
 Sun, H.: AP-ThP2, 66; C3+C2+C1-ThM10, 59
 Sun, Y.: BP-ThP29, 67
 Suresh, V.: D2-TuA2, 44
 Surmeier, G.: BP-ThP37, 67
 Suzuki, A.: BP-ThP13, 66
 Suzuki, H.: TSP-ThP8, 71
 Švec Jr., P.: BP-ThP3, 66; E1-3-FrM2, 73
 Svensson, J.-E.: A1-2-TuA1, 43
 Swadzba, L.: A1-3-WeM5, 48; AP-ThP13, 66;
 AP-ThP9, 66
 Swadzba, R.: A1-3-WeM5, 48; AP-ThP13, 66;
 AP-ThP7, 66; AP-ThP9, 66
 Sweet, M.L.: A2-1-ThM3, 58; A2-1-ThM7, 58
 Szkodo, M.: F3-TuA11, 45
- T —
- Tada, D.: DP-ThP19, 68
 Taiariol, T.: B3-1-MoM4, 32
 Takamatsu, H.: EP-ThP22, 69
 Takoudis, C.: D3-TuM7, 39
 Talke, F.E.: E1-2-ThA3, 64
 Tamura, M.: B5-2-FrM5, 72
 Tan, S.: B2-1-ThA8, 62
 Tanaka, C.: B4-1-TuM7, 39; B4-2-TuA9, 43
 Tanaka, K.: B6-ThM10, 58; EP-ThP22, 69
 Tanaka, M.: H1-2-TuA9, 46
 Tandiand, D.: H1-1-TuM2, 41
 Tao, H.: B4-3-WeM11, 48
 Tauchi, Y.: TSP-ThP8, 71
 Tavakoli, A.H.: HP-ThP11, 71
 Taylor, G.: D1-2-MoA3, 36
 Terziyska, V.L.: B4-3-WeM3, 48; TS3+4-2-
 MoA4, 37
 Teulé-Gay, L.: E3-WeM10, 49
 Texier, D.: AP-ThP11, 66
 Theveneau, M.: AP-ThP3, 66
 Thiaudière, D.: CP-ThP13, 68; E2-2-TuA2, 45
 Thiex, M.: BP-ThP23, 67; E3-WeM4, 49
 Thorwarth, K.: D1-1-MoM4, 33; D1-2-MoA8,
 36; F4-2-WeA8, 55; FP-ThP5, 70
 Tian, Q.X.: F2-2-ThA2, 64
 Tian, X.B.: F2-2-ThA2, 64
 Tillmann, W.: B3-1-MoM3, 32; BP-ThP37, 67;
 EP-ThP23, 69; F2-2-ThA8, 64; F2-2-ThA9, 64
 Ting, I.S.: A1-1-TuM7, 38
 Ting, J.J.: TS1-2-WeA10, 56
 Ting, J.-M.: B1-1-MoM5, 32; BP-ThP33, 67;
 CP-ThP31, 68; F4-1-WeM10, 50; TS1-2-
 WeA10, 56; TS1-2-WeA2, 56; TSP-ThP9, 71
 Tint, S.: D1-2-MoA3, 36
 Tjong, J.: G2-FrM10, 73
 Tkadletz, M.: B2-1-ThA11, 62; B2-1-ThA4, 62;
 B4-3-WeM3, 48; C4-ThA7, 63; H1-1-TuM7,
 41; H1-2-TuA4, 46
 Todt, J.: B4-4-WeA2, 53
 Todt, M.: B5-1-ThA5, 63; BP-ThP35, 67
 Togni, A.: TS1-2-WeA3, 56
 Tolan, M.: BP-ThP37, 67
 Toledo-Romo, F.: E1-3-FrM6, 73
 Tonneau, R.: B7-TuA1, 44
 Torp, B.: G4+G5+G6-ThA5, 65
 Torres San Miguel, C.R.: EP-ThP11, 69; HP-
 ThP4, 71
 Torres, R.: GP-ThP7, 70
 Totik, Y.: B6-ThM11, 58; BP-ThP30, 67
 Toyoda, H.: TSP-ThP8, 71
 Tracz, J.: A1-3-WeM5, 48; AP-ThP13, 66
 Trant, M.: F4-2-WeA8, 55; FP-ThP5, 70
 Trava-Airoldi, V.J.: B3-1-MoM4, 32; B3-1-
 MoM5, 32; BP-ThP28, 67; GP-ThP8, 70
 Treadwell, L.: H3-2-WeA3, 55
 Tripathi, R.: AP-ThP1, 66
 Truchlý, M.: B5-2-FrM6, 72; BP-ThP3, 66; E1-
 3-FrM2, 73
 Trujillo, J.P.: A1-1-TuM8, 38
 Tsai, M.-H.: GP-ThP17, 70
 Tsai, P.-S.: GP-ThP17, 70
 Tsai, Y.J.: GP-ThP1, 70
 Tseng, I.-H.: GP-ThP17, 70
 Tseng, Y.C.: HP-ThP8, 71
 Tsikata, S.: F2-1-ThM3, 60; FP-ThP7, 70
 Tsou, H.K.: DP-ThP6, 68
 Tsuchiya, T.: H1-2-TuA9, 46
 Tudhope, A.: B3-2-MoA3, 35; G1+G3-ThM8,
 60
 Tunes, M.A.: TS1-2-WeA5, 56
 Tvarog, D.: B7-TuA11, 44
- U —
- Ujah, C.O.: E1-4-WeA4, 54; FP-ThP12, 70
 Ukraintsev, E.: E1-2-ThA7, 64
- Ulrich, S.: G1+G3-ThM11, 60
 Unocic, K.: A1-1-TuM1, 38
 Urabe, K.: G4+G5+G6-ThA4, 65
 Ushakov, S.V.: A2-1-ThM11, 58
 Uyor, U.O.: CP-ThP26, 68; E1-4-WeA7, 54
- V —
- Vachhani, S.: B1-3-TuM4, 38
 Valeri, S.: E1-2-ThA7, 64
 Van Campen, D.: H1-1-TuM2, 41
 van der Poel, S.H.: EP-ThP21, 69
 Van Paeppegem, W.: TS3+4-2-MoA9, 37
 Vanderesse, N.: H3-2-WeA8, 55
 Vasco, E.: E2-1-TuM4, 40
 Vasconcelos, G.: B3-1-MoM4, 32
 Vasina, P.: B1-3-TuM6, 38; B5-1-ThA4, 63; B7-
 TuA2, 44
 Vaz, F.: CP-ThP23, 68; D3-TuM2, 39
 Vega-Morón, R.C.: E1-3-FrM5, 73; E1-3-FrM6,
 73
 Velic, D.: B2-1-ThA4, 62
 Vereschaka, A.: B1-2-MoA11, 35
 Vernhes, L.: E1-1-ThM6, 59
 Vernon, E.: A1-1-TuM2, 38
 Veronesi, F.: TS2-ThM2, 61; TS2-ThM5, 61
 Vetter, J.: E3-WeM5, 49; G2-FrM7, 73
 Victor, J.L.: F2-2-ThA4, 64
 Victoria-Hernandez, J.: D1-2-MoA6, 36
 Villabos, C.: BP-ThP36, 67
 Villanueva, J.: D3-TuM7, 39
 Villardi de Oliveira, C.: A1-1-TuM6, 38
 Villarroel, R.: GP-ThP6, 70
 Viloloan, R.P.B.: F2-1-ThM8, 60
 Vincent, B.: F2-1-ThM3, 60; FP-ThP7, 70
 Vishnyakov, V.: AP-ThP2, 66; TS1-2-WeA5, 56
 Viswanathan, V.: A2-2-ThA5, 62
 Vitelaru, C.: B3-2-MoA7, 35
 Vo, H.: B1-3-TuM4, 38
 Voevodin, A.A.: E3-WeM3, 49
 Volpi, M.: H1-2-TuA1, 46
 Volu, R.M.: BP-ThP28, 67
 Voronkoff, J.: H1-1-TuM6, 41
- W —
- Wachesk, C.: B3-1-MoM4, 32; DP-ThP19, 68
 Wagner, A.: B5-1-ThA5, 63; BP-ThP35, 67
 Wagner, N.J.: C4-ThA5, 63
 Wain, R.: A1-2-TuA9, 43
 Walls, J.M.: C3+C1-WeM25, 49
 Walton, S.: C2-WeA5, 54
 Wang, A.N.: TS1-2-WeA4, 56
 Wang, C.: B5-1-ThA6, 63; CP-ThP2, 67; FP-
 ThP16, 70
 Wang, C.J.: TS1-1-WeM6, 51; TS1-2-WeA6, 56
 Wang, D.Y.: B5-2-FrM8, 72; BP-ThP27, 67; BP-
 ThP9, 66
 Wang, J.: CP-ThP17, 68
 Wang, J.: TS2-ThM7, 61
 Wang, J.-B.: DP-ThP7, 68; F2-2-ThA7, 64
 Wang, Q.J.: EP-ThP19, 69
 Wang, S.C.: F1-TuM3, 40
 Wang, S.T.: B4-3-WeM13, 48; E1-3-FrM7, 73
 Wang, W.: BP-ThP31, 67
 Wang, Y.: B6-ThM10, 58; C2-WeA9, 54
 Wang, Y.M.: F2-2-ThA3, 64
 Wardini, J.: H2-1-MoM5, 33
 Warnk, T.: B3-1-MoM2, 32
 Warrior, N.: TSP-ThP1, 71
 Watanabe, N.: G2-FrM3, 73
 Watanabe, S.: EP-ThP2, 69
 Waware, U.: AP-ThP8, 66
 Wei, C.B.: BP-ThP31, 67; EP-ThP16, 69
 Wei, R.: G4+G5+G6-ThA6, 65
 Wei, W.: A2-1-ThM5, 58; A2-1-ThM9, 58
 Wei, W.-C.J.: TS1-2-WeA6, 56
 Weick, S.: A3-WeA5, 53

Author Index

- Weißmantel, S.: B3-1-MoM2, **32**; B3-2-MoA2, 35
 Welters, M.: BP-ThP4, **66**; F4-2-WeA5, **55**
 Weng, S.Y.: B6-ThM3, 58
 Wennberg, A.: B3-2-MoA5, 35; F2-1-ThM9, 60; G1+G3-ThM4, 60; TS3+4-2-MoA10, **37**
 Wheeler, J.M.: H3-2-WeA7, 55; HP-ThP3, **71**; TS1-2-WeA7, **56**
 Wheeler, R.: F3-TuA5, 45
 Wheeler, V.D.: C2-WeA5, **54**
 Wheelis, S.: D3-TuM3, **39**
 Widrig, B.: A2-2-ThA3, 62
 Wieclaw, G.: AP-ThP9, 66
 Winkler, J.: B1-2-MoA10, 35; TS3+4-2-MoA4, 37
 Wisnivesky, D.: B4-3-WeM2, 48
 Witala, B.: A1-3-WeM5, 48; AP-ThP13, 66; AP-ThP9, 66
 Wittel, B.: G4+G5+G6-ThA5, 65
 Wittig, A.: EP-ThP23, 69
 Woda, M.: B2-2-FrM10, **72**
 Wojcik, T.: B6-ThM12, 58; FP-ThP3, 70
 Wolfe, M.: TS4-1-MoM4, 34
 Wong, M.S.: B4-1-TuM2, **39**; BP-ThP6, **66**
 Wu, C.-F.: D2-TuA12, 44
 Wu, C.J.: A2-2-ThA6, **62**
 Wu, F.B.: B4-3-WeM13, 48; E1-3-FrM7, 73; TSP-ThP7, 71
 Wu, G.M.: CP-ThP25, **68**
 Wu, H.: EP-ThP19, 69
 Wu, P.-W.: DP-ThP5, 68
 Wu, S.: B1-1-MoM4, 32
 Wu, S.C.: DP-ThP10, 68; DP-ThP9, 68
 Wu, T.-C.: DP-ThP2, 68
 Wu, W.C.: D1-2-MoA7, 36
 Wu, W.-Y.: GP-ThP21, **71**
 Wunderlich, R.: TSP-ThP4, 71
 Wüstefeld, C.: B4-4-WeA7, **53**
 — **X** —
 Xia, A.: B1-3-TuM4, 38; TS1-2-WeA3, **56**
 Xiao, P.: A1-1-TuM4, **38**; A2-1-ThM4, 58
 Xiaobo, Y.: HP-ThP3, 71; TS1-2-WeA7, 56
 Xiaobo, W.: EP-ThP28, **69**
 Xie, Z.: TS1-1-WeM1, 51
 Xing, P.: TS2-ThM3, 61
 Xu, F.: TSP-ThP1, 71
 Xu, J.: CP-ThP12, 68
 Xu, S.: CP-ThP2, 67
 — **Y** —
 Yalamanchili, K.: TS1-1-WeM4, **51**
 Yamada, K.: EP-ThP2, 69
 Yamamoto, K.: B4-3-WeM5, **48**
 Yamashita, M.: G4+G5+G6-ThA4, 65
 Yan, J.W.: H1-2-TuA10, **46**
 Yan, S.: BP-ThP29, 67
 Yanagisawa, K.: B2-1-ThA3, **62**
 Yang, B.L.: A2-2-ThA7, 62
 Yang, C.H.: GP-ThP1, 70
 Yang, Q.: B4-4-WeA5, **53**; BP-ThP42, 67; E2-2-TuA8, 45
 Yang, S.: AP-ThP2, 66
 Yang, X.: H1-2-TuA8, 46
 Yang, Y.-C.: D1-2-MoA1, 36; D1-2-MoA7, **36**; DP-ThP7, 68; F2-2-ThA7, 64; GP-ThP13, 70
 Yang, Y.J.: B6-ThM3, **58**
 Yavas, H.Y.: B5-1-ThA3, 63; H3-2-WeA4, 55
 Yeh-Liu, L.K.: B6-ThM4, 58
 Yeo, C.D.: E1-3-FrM10, 73
 Yerokhin, A.: A1-2-TuA9, 43; C3+C2+C1-ThM12, **59**; CP-ThP19, **68**; E1-4-WeA2, 54; E3-WeM3, 49; G4+G5+G6-ThA3, 65; GP-ThP3, 70
 Yi, P.Y.: B3-2-MoA9, 35; C3+C2+C1-ThM11, 59
 Yi, S.: D1-2-MoA6, 36
 Yoo, R.: CP-ThP6, 67; CP-ThP7, 68
 Yun, W.: H1-2-TuA8, **46**
 — **Z** —
 Zabinski, J.: E3-WeM3, 49
 Zabransky, L.: B1-3-TuM6, 38; B5-1-ThA4, 63
 Zagonel, L.F.: B4-3-WeM2, 48
 Zaid, H.: B6-ThM10, 58
 Zálešák, J.: B4-4-WeA2, 53; BP-ThP19, 67
 Zambrano, D.: GP-ThP6, **70**
 Zangrossi, F.: TSP-ThP1, **71**
 Zapata, M.: DP-ThP16, 68
 Zauner, L.: B6-ThM9, 58; F4-2-WeA6, 55; FP-ThP3, 70
 Zehnder, C.: H3-1-WeM1, 50
 Zeman, P.: B1-3-TuM5, 38; F4-2-WeA6, 55; FP-ThP17, 70
 Zemlicka, R.: B1-2-MoA5, **35**
 Zendejas Medina, L.: TS1-1-WeM5, **51**
 Zeng, A.: B3-2-MoA6, 35
 Zeng, Y.: BP-ThP11, **66**
 Zenker, R.: G4+G5+G6-ThA9, 65
 Zgheib, E.: E2-1-TuM5, **40**
 Zha, W.: EP-ThP27, 69
 Zhang, D.: B3-2-MoA9, **35**
 Zhang, L.: CP-ThP2, 67
 Zhang, W.: FP-ThP16, 70
 Zhang, X.: A1-1-TuM4, 38; H2-2-MoA3, 36
 Zhang, Z.: A1-1-TuM4, 38; B6-ThM2, 58
 Zhao, C.: EP-ThP27, 69; G2-FrM5, 73
 Zhao, L.: B4-4-WeA5, 53
 Zheng, T.-W.: B4-4-WeA1, 53
 Zheng, Y.: TS2-ThM7, 61
 Zheng, Y.Z.: BP-ThP7, 66
 Zhou, X.: G4+G5+G6-ThA11, 65
 Zhou, Z.: TS1-1-WeM1, 51
 Zhu, H.: A1-2-TuA4, 43
 Zhu, X.: CP-ThP2, 67
 Zikan, P.: B1-3-TuM6, 38; G1+G3-ThM1, 60
 Zimmer, O.: B1-2-MoA6, 35; TS1-2-WeA1, 56
 Zimmermann, M.: TS1-2-WeA1, 56
 Zitek, M.: B1-3-TuM5, 38
 Zubizarreta, C.: GP-ThP5, 70
 Zywitzki, O.: B1-3-TuM1, 38

NOTES

NOTES

Monday Morning, May 20, 2019

Plenary Lecture

Room Town & Country - Session PL-MoPL

Plenary Lecture

Moderators: Christopher Muratore, University of Dayton, USA, Michael Stüber, Karlsruhe Institute of Technology (KIT), Institute for Applied Materials (IAM), Germany

8:40am **PL-MoPL3 Soft Electronics for the Human Body, J. Rogers (jrogers@northwestern.edu), Northwestern University, USA** **INVITED**

Biological systems are mechanically soft, with complex, time-dependent 3D curvilinear shapes; modern electronic and microfluidic technologies are rigid, with simple, static 2D layouts. Eliminating this profound mismatch in physical properties will create vast opportunities in man-made systems that can intimately integrate with the human body, for diagnostic, therapeutic or surgical function with important, unique capabilities in biomedical research and clinical healthcare. Over the last decade, a convergence of new concepts in thin film materials science, mechanical engineering, electrical engineering and advanced manufacturing has led to the emergence of diverse, novel classes of 'biocompatible' electronic and microfluidic systems with ultrathin, skin-like physical properties. This talk describes the key ideas and enabling materials, and it presents some of the most recent device examples, including wireless electronic 'tattoos', with applications in continuous monitoring of vital signs in neonatal intensive care; and microfluidic/electronic platforms that can capture, store and perform biomarker analysis on sweat, with applications in sports and fitness.

Hard Coatings and Vapor Deposition Technologies

Room Golden West - Session B1-1-MoM

PVD Coatings and Technologies I

Moderators: Frank Kaulfuss, Fraunhofer Institute for Material and Beam Technology (IWS), Germany, Jyh-Ming Ting, National Cheng Kung University, Taiwan, Qi Yang, National Research Council of Canada, Canada

10:40am **B1-1-MoM3 Structural, Optical and Wettability Properties of Thermally Evaporated CaF₂, MgF₂ and CaF₂/MgF₂ Films, R.K. Jain (ravishphy.rsh@gndu.ac.in), J. Kaur, A. Khanna, Guru Nanak Dev University Amritsar India, India**

In this work, thin films of CaF₂, MgF₂ and their multilayered stacks have been deposited on microscopy glass substrates by thermal evaporation and their structural, optical and wettability properties have been studied. Four different sets of samples i.e. glass/CaF₂, glass/MgF₂, glass/CaF₂/MgF₂ and glass/CaF₂/MgF₂/CaF₂/MgF₂ were prepared. X-ray diffraction studies revealed that crystalline CaF₂ film grows in glass/CaF₂ and in the 2-layer stacked glass/CaF₂/MgF₂ samples whereas, it grows in the amorphous phase in 4-layered stacked glass/CaF₂/MgF₂/CaF₂/MgF₂ sample. On the other hand, MgF₂ layer in all the samples grows in the amorphous phase. Field emission scanning electron microscopy (FESEM) was used to study the surface morphology and thicknesses of the samples. The surface FESEM image of CaF₂ film shows very small flake-like morphology whereas the MgF₂ film has a smooth morphology due to its amorphous nature. The cross-sectional FESEM images found that the thickness of the pure CaF₂ film (102 nm) is lesser than that of pure MgF₂ film (127 nm). The optical transmittance and reflectance properties were studied by UV-Vis spectroscopy which confirmed that all the films possess good anti-reflecting properties. The average specular reflectance values in the wavelength range: 350-1100 nm are 10.8%, 7.9%, 8.6%, 6.4% and 8.4% for bare glass slide, MgF₂, CaF₂, 2-layer and 4-layer stacked films respectively which confirms that the reflectance decreases with the top coating of the fluoride films. The water contact angle studies were carried out to study the wettability properties of the samples and it is found that the pure CaF₂ and MgF₂ films are hydrophobic with an average water contact angle 131±1° and 98±1°, respectively. The wettability properties of the 2-layer and 4-layer stacked structures were found to be completely different compared to single layer thin films and showed hydrophilic nature with water contact angles of 20±1° and 47±1° respectively with reflectance values that were comparable to those of MgF₂ and CaF₂ films. It is concluded that CaF₂ films have a very good potential to be used as hydrophobic anti-reflecting coatings and stacking with other well known optical material such as MgF₂, can tailor its wettability and anti-reflecting properties.

11:00am **B1-1-MoM4 Metal / ScAlN / Interdigital Transducer (IDT) / LiNbO₃ Multilayer Structure for High K² Surface Acoustic Wave Device, Y.H. Huang (igs200388@gmail.com), National Cheng Kung University, Taiwan; S. Wu, Tung-Fang Design University, Taiwan; J.L. Huang, National Cheng Kung University, Taiwan**

We reported a high electromechanical coupling coefficient (K²) Surface acoustic wave (SAW) devices on metal / ScAlN/interdigital transducer (IDT) / LiNbO₃ structure and we used Al/ Ti / Mo as metal layer. The Sc_{0.31}Al_{0.69}N films in different thickness (0.5, 1, 1.5, 2 μm) were deposited on Y-128° lithium niobate (LiNbO₃) substrate which possesses high K² by reactive magnetron co-sputtering using Sc and Al as targets. In the previous research, the replacement of Al by Sc increases piezoelectricity because of the phase transition. The Sc_xAl_{1-x}N films 2D-XRD result showed that high c-axis (002) orientation and 2D-XRD χ angle showed that there is a critical thickness. The (002) plane tilting from a normal direction of LiNbO₃ substrate before 1μm and it growth normal direction after critical thickness. The SEM cross-section result showed that ScAlN films have tilting from substrate and have columnar structures. The SEM top view indicated that spindle-like morphology and grain cover the whole surface when thickness over 1μm. The piezoelectric coefficient (d₃₃) measured the highest value 42.8 pm/V of Sc_{0.31}Al_{0.69}N film. The K² values are increasing with the metal layer deposited on. The highest K² value is three time larger than IDT/ LiNbO₃ (4.9%) structure. The metal / ScAlN/ IDT/ LiNbO₃ structure have a great potential in high frequency and high K² SAW devices.

11:20am **B1-1-MoM5 Sputter Deposited TiN_xO_y for Color Coatings and Solar Absorbers, L.Y. Chiu (andy22453464@gmail.com), J.-M. Ting, National Cheng Kung University, Taiwan**

Titanium oxynitride (TiN_xO_y) coatings were deposited using RF and DC pulse reactive magnetron sputtering techniques. Aluminum (2.5 x 2.5 cm) and stainless steel (2.5 x 2.5 cm) were used as substrates for decorative TiN_xO_y

coating and solar absorber TiN_xO_y coatings, respectively. In this works, various deposition parameters including sputtering power, N₂ flow rate, working pressure, and deposited time were investigated. The resulting coatings therefore exhibit various compositions, crystal structures, grain sizes, and thicknesses. The obtained coatings were examined using field emission scanning electron microscopes, X-Ray diffraction, X-Ray photoelectron spectroscopy, Colorimeter technique (CIELab 1976 color space), UV/vis/NIR spectrometer, and Fourier-transform infrared spectroscopy. Effects of the material characteristics on the coating performance is discussed.

11:40am **B1-1-MoM6 High Power Impulse Magnetron Sputtering using Deep Oscillatory Micro Pulses for Surface Engineering, J.L. Lin (jlin@swri.org), Southwest Research Institute, USA INVITED**

As one version of high power impulse magnetron sputtering (HiPIMS) technique, deep oscillation magnetron sputtering (DOMS) is developed from the early modulated pulsed power magnetron sputtering (MPPMS) technique. In DOMS, large oscillatory high power micro-pulses (e.g. tens of μs) are generated within long modulation pulses (up to 3~5 ms). The magnitude of the peak power can be adjusted by controlling the on and off times of the oscillatory micro-pulses. By using optimal combinations of on and off times of these oscillatory micro-pulses, virtually arc free reactive HiPIMS process can be achieved for many insulating coating materials (e.g. Al₂O₃, AlN, SiO₂, etc.). The paper presents an introduction of the DOMS technique with key processing features and parameters. The observation and mechanisms of generating arc-free discharge for reactive sputtering insulating coatings using deep oscillatory micro-pulses will be discussed. Recent technological development in DOMS for surface engineering will be presented. Specific examples will be focused on high rate deposition of transparent metal oxide coatings for optical and wear resistant applications, super hard hydrogen free diamond like carbon (DLC) coatings for low friction and wear applications, strongly (0002) textured AlN films for piezoelectric applications, and thick superlattice nitride coatings for solid particle erosion and high temperature wear protection. It is shown that the enhanced target ionization in combination with excellent process stability in DOMS enables the deposition of a variety of high quality coating materials with improved properties.

Hard Coatings and Vapor Deposition Technologies

Room California - Session B3-1-MoM

Deposition Technologies and Applications for Diamond-like Coatings I

Moderators: Laurent Espitalier, Wallwork Cambridge Ltd, UK, Konrad Fadenberger, Robert Bosch GmbH, Germany

10:20am **B3-1-MoM2 On the Deposition and Properties of Carbon-based Multilayer Systems Prepared by PLD, S. Weißmantel (steffen.weissmantel@hs-mittweida.de), University of Applied Sciences Mittweida, Germany; M. Hess, Fritz Stepper GmbH & Co. KG, Deutschland, Germany; R. Bertram, D. Haldan, T. Warnk, J. Maus, S. Rupp, University of Applied Sciences Mittweida, Germany**

The layer deposition technique Pulsed Laser Deposition (PLD) provides a feasible way to produce pure carbon films in a wide range of mechanical properties. These properties cover, depending on the deposition parameters, indentation hardness H_{IT} from 20 GPa up to 70 GPa and indentation modulus E_{IT} from 300 GPa up to 700 GPa. As we are going to show, the variation of these mechanical properties over wide ranges can be correlated with the Raman spectra of the films. In particular, the intensity ratio of the disordered and graphitic peak provides an efficient way to determine the mechanical properties of the hydrogen free amorphous carbon films.

Based on the fact that the variation of hardness can be done simply by varying the laser fluence, layered structures consisting of sublayers of alternating or continuously changing sp³ content and hardness were deposited. The periodicity of the bilayer stacks were varied from 500 nm down to 2.5 nm resulting in an immense increase of interfaces up to 800 since the total film thickness was kept constant at 2 micron. Keeping the ta-C film component constant at some 65 GPa, the hardness of the soft a-C layer component has been changed in the range of 20 up to 50 GPa. The toughness and resistivity against wear and cracking of these multilayered films were evaluated and compared to super-hard single ta-C films. We could show that properly designed multilayered structures have in this respect much improved properties compared to the single layer. In scratch tests,

these multilayers show besides an excellent adhesion to various substrate materials a significantly improved, very high cohesive breaking strength. In addition, by testing the abrasive wear of such coating systems against polycrystalline diamond suspension using calotte grinding and against various ceramics and metals using a pin-on-disk tribotester, superior durability was identified, surpassing conventional wear protection layers by up to 3 orders of magnitude.

A computational analysis of the stress distribution in the film substrate systems was used to get an idea of the positions and values of stress under different load scenarios. Based on that film architectures were designed and deposited that show optimized stress distributions to relieve the strain at the substrate layer-system interface. It will be shown that a proper film design enables the deposition and application of extremely hard, durable and yet tough diamond like carbon coating systems. These outstanding layer properties such as high hardness, elasticity, toughness and wear resistance show the great potential of such carbon-based films, i.e. for application as wear protection coatings.

10:40am B3-1-MoM3 Improved Adhesion of a-C and a-C:H Films with a CrC Interlayer on 16MnCr5 by HiPIMS-Pretreatment, *W. Tillmann, N.F. Lopes Dias (filipe.dias@tu-dortmund.de), D. Stangier*, TU Dortmund University, Germany; *W. Maus-Friedrichs, R. Gustus*, Technical University Clausthal, Germany

A high adhesion of amorphous carbon films to steel substrates remains a challenging task, sustaining continuous research efforts to improve the adhesion strength. Besides the interlayer system and the substrate material, surface pretreatments have a crucial role on the adhesion behavior. Within this context, the influence of the High Power Impulse Magnetron Sputtering (HiPIMS) pretreatment on the adhesion of hydrogenfree (a-C) and hydrogenated (a-C:H) amorphous carbon films with a chromium carbide (CrC) interlayer on 16MnCr5 steel is investigated. The plasma treatment consisted of 30 min Ar ion etching as well as a sequential 5 min of HiPIMS-pretreatment with a Cr cathode, subsequently comparing this procedure to a procedure without the HiPIMS technique. The impact of the HiPIMS-pretreatment on the structure of the film was systematically analyzed by taking the CrC interlayer as well as the entire film structure into consideration.

The adhesion strength of the a-C and a-C:H films is significantly improved by HiPIMS-pretreating the 16MnCr5 steel. In scratch tests, the critical load L_{c3} for a total film delamination increases from 43 ± 4 to 59 ± 3 N and from 48 ± 2 to 64 ± 3 N for the a-C and a-C:H film. The improved adhesion behavior of the carbon films is ascribed to the increased adhesion of the CrC interlayer, which did not delaminate when scratched with a load up to 159 ± 18 N. Complementary Rockwell indentation tests reveal that the HiPIMS-pretreatment improves the adhesion class from HF6 to HF4 and from HF5 to HF3 for a-C and a-C:H. The enhanced adhesion is essential to exploit the properties of a-C and a-C:H films in applications with high loads. In conclusion, the HiPIMS-pretreatment has proven to be a promising technique to increase the adhesion strength of carbon films.

11:00am B3-1-MoM4 Properties Of Diamond-Like Carbon Films With Incorporated CVD-Diamond Nanoparticles, *R. Falcão (rebecafalcaoborjacorreia@yahoo.com.br)*, Institute of Science and Technology, Federal University of São Paulo (UNIFESP), Brasil; *C. Wachesk*, Federal University of São Paulo, Brazil, Brasil; *T. Taiariol*, National Institute for Space Research, Brazil; *G. Vasconcelos*, Instituto de Estudos Avançados, Brazil; *E.J. Corat, V.J. Trava-Airoldi*, National Institute for Space Research, Brazil

Diamond-like carbon (DLC) films have been extensively applied as a surface coating due their attractive mechanical, chemical and tribological properties. The properties of the a-C:H films can be significantly enhanced by the presence of diamond nanoparticles in their structure with some apparent advantages by combining hardness, low roughness, coefficient of friction, biocompatibility, etc., of both materials. However, functionalization of diamond nanoparticles and their severe big clusters formations represent some challenges to be overcome. Therefore, the innovative aspect of this work is the growth of DLC films with incorporated CVD nanodiamonds (NDs), obtained by high energy ball milling technique with controlled sizes and functionalization avoiding a lot of clusters formation. In this work, CVD NDs, obtained at the first time, were chemically processed due to the high levels of contamination by using fluoric and nitric acid chemical attack. The DLC films were deposited on a metallic substrate by using a modified Pulsed DC Plasma-Enhanced Chemical Vapor Deposition (PECVD) technique, and the incorporation of the NDs into the DLC films structure was carried using a colloidal solution of NDs and DLC films precursor. The influence of the CVD

NDs size on physical and chemical properties of the hybrid film, such as hardness, coefficient of friction, morphology, and chemical inertia were investigated. Nanoparticles size and the level of purity was analyzed by dynamic light scattering and X-Ray diffractometry (XRD) technique, respectively. The hybrid DLC films were characterized by scanning electronic microscopy-field emission gun, XRD and Raman scattering spectroscopy. Also, the qualitative adhesion of the film was analyzed by RHC 1500 N indentations in accordance with the VDI3198 standard. An apparent application with preliminary results is also a part of this work.

Acknowledgments:

The authors want to thanks to the Fundação de Amparo à Pesquisa do Estado de São Paulo – FAPESP (grants n. 2017/08899-3 and 2012/15857-1), CNPq and Capes.

11:20am B3-1-MoM5 Influence of the Argon as an Ignitor and an Agent on DLC Properties Growth at Pressure as Low as 3×10^{-4} mbar by Modified Pulsed-DC PECVD Method, *V.J. Trava-Airoldi (vladimir.airoldi@inpe.br), K. Nass, E.J. Corat*, National Institute for Space Research, Brazil; *N. Fukumasu*, Sao Paulo University, Brazil; *M. Ramirez*, University of Vale do Paraiba, Brazil; *G. Capote*, National University of Bogota, Colombia

As reported for many years, hydrogenated DLC films (a-C:H) have been a choice of a protective coatings for many applications due to their set of superior mechanical, chemical, tribological and biological properties such as: high hardness, high wear resistance, low coefficient of friction, high chemical inertness, good biocompatibility, bactericide, etc.. However, in order to improve the adhesion between the DLC and the different metals substrates a huge modification of a Pulsed DC PECVD technique has been obtained introducing an additional cathode working as electron and ion confinement. With these modifications pressure as low as 10^{-3} mbar allow operating in collisionless regime improving not only the adhesion but also a set of DLC properties cited above. So, in this work we present studies concerning more improvement properties of the DLC films as a function of confinement of electrons and ions parameters in a plasma discharge by using argon as an ignitor gas for the interlayer precursor and keeping it during all the process of DLC deposition. In this case the best conditions of collisionless operation was reached at pressure as low as 3.10^{-4} mbar. Basically, due to the condition of operating in very low pressure, this technique allows to grow the DLC film with very good uniformity and higher hardness, higher adhesion, lower coefficient of friction, less porosity and, also, provide to be able to get a DLC deposition in the form of multilayer, like thicker films, promoting less residual stress. So, studies at the first time, of DLC with superior properties has been carried out from PECVD technique. More specifically, studies of the DLC film properties as a function of the argon buffer gas density and as a function of bias voltage has been done. Raman scattering spectroscopy, Rockwell indentation, nano indentation, FEG, and tribological analyses are discussed. Also, the operating parameters of this modified PECVD system are well controlled, so that a scaling up studies will also be presented as an important part of this work.

Keywords: DLC films; DC pulsed PECVD; additional cathode; argon ignitor, mechanical and tribological properties.

Coatings for Biomedical and Healthcare Applications

Room Pacific Salon 2 - Session D1-1-MoM

Surface Coating and Modification for Use in Biological Environments I

Moderator: Mathew T. Mathew, University of Illinois College of Medicine, USA

10:20am D1-1-MoM2 Very Thin Gold Films Deposited on Collagen Fabric for Skin Cell Recover, *S.-Y. Huang (drugholic@vghtc.gov.tw)*, Taichung Veterans General Hospital, Feng Chia University, Taiwan; *Y.-C. Chang*, Feng Chia University, Taiwan; *P.-Y. Hsieh*, Institute of Plasma, Feng Chia University, Taiwan; *C.M. Chou*, Taichung Veterans General Hospital, National Yang-Ming University, Taiwan; *C.J. Chung*, Central Taiwan University of Science and Technology, Taiwan; *J.L. He*, Feng Chia University, Taiwan

The goal of this study is to develop a novel biomedical material, where gold thin film is deposited on collagen fabrics for skin tissue engineering. Type I Collagen had been used in many products for its biocompatibility and critical role in skin recovery. Gold, in the form of nanoparticles (AuNPs), had been proven to improve biomaterial properties, such as mechanical strength, elasticity, degradation resistance, cell attachment, cell proliferation and wound healing. Unlike chemically prepared AuNPs in most of present literature, very thin gold films deposited by high-power

Monday Morning, May 20, 2019

impulse magnetron sputtering (HIPIMS) on collagen fibers reveal the advantage of green synthesis process and free from chemical ligand of gold particles.

Scanning electron microscopy (SEM) and X-ray diffraction (XRD) are used to observe the surface morphology and microscopic characteristics of the composites. Fourier transform infrared spectroscopy (FTIR) and circular dichroism spectroscopy (CD) are used to evaluate functional groups and secondary structure of collagen, respectively. Process of biomedical fabrics with collagen and gold thin film in different thickness is established.

Keywords: gold thin films, HIPIMS, collagen fabric, skin cell recovery

10:40am D1-1-MoM3 Effect of Calf Serum on Tribological Behavior of DLC Coating in Ti-6Al-4V / Ti-6Al-4V Contact for Application to STEM / NECK Contact of Modular Hip Implant, H.H. Ding, V. Fridrici (vincent.fridrici@ec-lyon.fr), G. Bouvard, Ecole Centrale de Lyon, LTDS - Université de Lyon, France; J. Géringier, Ecole des Mines de St-Etienne - Université de Lyon, France; P. Kapsa, Ecole Centrale de Lyon, LTDS - Université de Lyon, France
Influences of new-born calf serum on the fretting behaviors of Ti-6Al-4V and diamond-like carbon coating were investigated using a fretting-wear test rig with a cylinder-on-flat contact. The results indicated that, for the Ti-6Al-4V / Ti-6Al-4V contact, the friction coefficients were high (0.8-1.2) and the wear volumes presented an increase with the increase in the displacement amplitude under dry laboratory-air conditions. Under serum-liquid conditions, the Ti-6Al-4V / Ti-6Al-4V contact presented significantly larger wear volumes under the displacement of $\pm 40 \mu\text{m}$; however, it presented significantly lower friction coefficients (0.25-0.35) and significantly smaller wear volumes under the displacement of $\pm 70 \mu\text{m}$. The opposite effects of lubrication and corrosion are studied and analyzed. For the DLC coating / Ti-6Al-4V contact, the coating response wear maps could be divided into two areas: the coating working area (low normal force conditions) and the coating failure area (high normal force conditions). In the coating working area, the DLC coating could protect the substrate with low friction, low wear volume, and mild damage in the coating. The presence of serum had a positive influence on the tribological performance of the DLC coating. Furthermore, the positive influence was more significant under larger displacement amplitudes condition.

11:00am D1-1-MoM4 Accelerated Tests for Lifetime Prediction of Interlayers and Interfaces of Coated Implants in Body Fluid, R. Hauert (roland.hauert@empa.ch), E. Ilic, A. Pardo-Perez, K. Thorwarth, P. Schmutz, Empa - Swiss Federal Laboratories for Materials Science and Technology, Switzerland; S. Mischler, Institut des Matériaux IMX, EPFL, Lausanne, Switzerland
INVITED

Hard coatings such as diamond like carbon (DLC) on articulating joints can result in desired surface properties showing extremely low wear. However, an interlayer material or a single row of contamination atoms at the coating/substrate interface can result in altered corrosion behavior and possible adhesion instability. A method to determine the chemical composition of the few atomic rows of altered material at an interface, buried under several microns of coatings, will be shown by low angle polishing down to less than 0.06 degrees (less than 1/1000 steepness). Corrosion effects such as crevice corrosion, which can cause coating delamination after some years in vivo, cannot be accelerated in simulator testing since it evolves only as a function of time in media. A new setup for accelerated crevice corrosion testing in body fluid, as well as preliminary results, will be presented. Furthermore, stress corrosion cracking and corrosion-fatigue can damage the few rows of reacted atoms present at an interface. By simulating in vivo conditions, we are developing an accelerated test to assess these deteriorating effects at the interface. First results of coating adhesion lifetime expectations, including the influence of small detrimental contaminations, will be shown.

11:40am D1-1-MoM6 Thin Film Metallic Glass Coating as an Effective Antiadhesion Coating for Platelet and Cancer Cells, J.P. Chu (jpchu@mail.ntust.edu.tw), National Taiwan University of Science and Technology (NTUST), Taiwan; C.L. Li, Y.L. Chen, S. Chyntara, National Taiwan University of Science and Technology, Taiwan; M.J. Chen, Mackay Medical College, Taiwan; S.H. Chang, Mackay Memorial Hospital Tamsui Campus, Taiwan

The adhesion of platelet cells is viewed as a first step in thrombus formation, and cancer cell attachment can lead to cancer seeding. The amorphous structure of metallic glasses (MGs) is a new group of coating materials exhibiting excellent hydrophobicity and resistance to bacterial colonization, as well as relatively low coefficient of friction. In this presentation, we will report a study which has been published in *Surface and Coatings Technology*,

Vol. 344, p. 312-321 (2018), describing the feasibility of utilizing $\text{Zr}_{53}\text{Cu}_{33}\text{Al}_9\text{Ta}_5$ thin film metallic glass (TFMG) to minimize the adhesion of various human cancer cells (breast cancer cell, colon cancer cell, and esophageal cancer cell), human and animal platelets. TFMG was respectively grown on glass substrates to a thickness of 200 nm using magnetron sputtering. TFMG was shown to reduce surface roughness of glass. The concentrations of all major ions released from the TFMG were well below toxic levels. TFMG surfaces were effective in increasing the contact angle of water, phosphate buffer saline and blood from different animal species. The application of TFMG to bare surfaces was shown to reduce the attachment area of human platelets by 77 % and that of pig platelets by 63%. TFMG also reduced the attachment of cancer cells by up to ~87%. These characteristics can be attributed to a low surface free energy of TFMG-coated surfaces (31.89 mN/m), which is far below that of bare glass (47.80 mN/m). These findings demonstrate the considerable potential of TFMG coatings in the fabrication of medical instruments aimed at preventing the adhesion of platelet and cancer cells.

12:00pm D1-1-MoM7 Improvement of Surface Properties of Nitinol Alloy through Deposition of Graphene by Electrophoretic Deposition Technique for Biomedical Applications, M. Mallick (madhusmita1509@gmail.com), N. Arunachalam, Indian Institute of Technology Madras, India

The superelastic nature of biocompatible material nitinol & its alloys is utilized for the application of orthodontic archwires due to its ability to prevent strain localization & plastic deformation. However, they tend to wear over time due to continual contact with body fluids and release toxic metal ions (Ni^{2+}) into the body. In order to overcome this limitation smooth layers of graphene was deposited on Nitinol wires by Electrophoretic Deposition technique to improve its wear resistance and other mechanical properties.

The electrodeposited coatings were characterized by Scanning electron microscopy (SEM), Transmission electron microscopy (TEM), X-Ray diffraction, Raman spectroscopy and Potentiodynamic polarization technique. Raman spectroscopy showed the presence of graphene & 2-D graphitic phase. Finally, a post deposition treatment was done to evaluate in-vitro bioactivity by Simulated Body Fluid (SBF) immersion test. The results showed that graphene coating onto Nitinol substrate improved anti-corrosion rate and anti-bacterial properties while reducing friction as compared to bare Nitinol wires.

Hence, this bioactive coating exhibited better mechanical strength, enhanced wear and corrosion resistance indicating high potential for biomedical applications.

Advanced Characterization Techniques for Coatings, Thin Films, and Small Volumes

Room Pacific Salon 1 - Session H2-1-MoM

Fatigue and Wear

Moderators: Olivier Pierron, Georgia Institute of Technology, USA, Timothy Rupert, University of California, Irvine, USA

10:00am H2-1-MoM1 Acoustic Emission Measurements to Quantifying Damage Accumulation and Crack Initiation in Nickel Single Crystals during High Frequency In Situ Cyclic Loading Experiments, S. Lavenstein, J.A. El-Awady (jelawady@jhu.edu), Johns Hopkins University, USA
INVITED

We present a new methodology, coupling between acoustic emission measurements and high frequency *in situ* scanning electron microscopy experiments to quantify the evolution of damage and crack initiation in single crystal nickel microcrystals. The mechanical properties are continuously monitored during the cyclic loading using dynamic measurements and signal analysis. The experimental results show that persistent slip bands (PSBs) form in these microcrystals in the absence of any apparent dislocation dense regions as commonly observed in bulk crystals. In addition, the speed of propagation of these PSBs is measured. Quantification of crack initiation and propagation is also analyzed from acoustic emission measurements, and the statistics of these measurements at different stages of crack propagation (i.e. short crack and long crack regimes) are quantified.

Monday Morning, May 20, 2019

10:40am **H2-1-MoM3 A Data-driven Approach to Describe Fatigue Damage Evolution and Crack Initiation in a BCC Steel Microstructure**, *A.R.D. Durmaz, T.S. Straub (Thomas.Straub@iwf.fraunhofer.de)*, C. Eberl, Fraunhofer IWM, Germany

A material's fatigue lifetime is determined by the crack formation process: damage accumulation in individual grains, micro crack initiation, and finally short crack formation. In the past years, a testing methodology for fatigue damage evolution investigation was developed. This methodology reduced sample sizes and cycled them at their resonant frequency, using sensitive measurements of the resonant frequency for correlation with damage initiation.

Building on this work, a multi modal approach has been developed employing in-situ optical images of the sample surface to better understand damage evolution kinetics and improve crack initiation analysis. The processed image data allows the creation of labels for machine learning (ML) methods, such as random forests, which are based on decision trees. As ML attributes various microstructure characteristics are extracted for each grain using complementing ex-situ EBSD measurements and MTEX. In order to generate a sufficient and balanced dataset the SEM and EBSD methods were automated.

11:00am **H2-1-MoM4 Low and High Cycle Fatigue Testing of Ni Microbeams**, *A. Barrios (alejandro.barrios@gatech.edu)*, Georgia Institute of Technology, USA; *E. Kakandar*, Cranfield University, UK; *X. Maeder*, Empa - Swiss Federal Laboratories for Materials Science and Technology, Switzerland; *G. Castelluccio*, Cranfield University, UK; *O.N. Pierron*, Georgia Institute of Technology, USA

Small-scale fatigue is an active area of research due to the widespread use of metallic films and micrometer-scale structures in applications such as flexible electronics, and micro electromechanical systems (MEMS). New techniques are required to characterize the fatigue damage and its size effects in metallic microcomponents under loading conditions relevant to their applications. This work presents two small-scale fatigue testing techniques to characterize the fatigue behavior of electroplated Ni microbeams subjected to in-situ high cycle and low cycle fatigue loading conditions. The in-situ high cycle fatigue technique consists of MEMS microresonators that are driven at resonance inside a Scanning Electron Microscope (SEM), leading to fully-reversed loading of microbeams at a frequency of ~8 kHz. The fatigue damage leads to a decrease of the microresonator's resonance frequency and is measured to quantify crack growth rates. The low cycle fatigue technique consists of the external mechanical actuation of the microresonator using a micromanipulator, which exerts a close to fully reversed bending fatigue loading on the microbeam. The micromanipulator is attached to a load cell and the decrease in load needed to actuate the device as cycling increases is used to characterize fatigue damage. Both techniques were complemented with Focused Ion Beam (FIB) cross sectioning that allow for a better understanding of the mechanisms of crack nucleation and propagation.

The crack propagation rates on the surface of the microbeam in the high cycle regime are extremely low (average values down to $\sim 10^{-14}$ m/cycle) indicating that the fatigue mechanism in high cycle fatigue does not follow the common crack tip stress intensification. Instead, crack nucleation and propagation are caused by the formation of voids that nucleate from the condensation of vacancies. However, in the low cycle fatigue regime, the microbeam does follow the conventional fatigue mechanisms observed in literature. Results will highlight the comparison in fatigue life and mechanisms of the low cycle and high cycle fatigue regimes. In addition, further testing will evaluate the frequency effects by comparing low cycle and high cycle tests at similar stress amplitudes. Electron backscatter diffraction (EBSD) scans will also allow for a better understanding of the microstructural variation along the crack path in the microbeam.

Furthermore, modeling efforts with 3D crystal plasticity will complement experimental results by giving a more complete understanding of the stress/strain states at crack initiation sites and a prediction of the low cycle fatigue life of the microbeam at various loadings.

11:20am **H2-1-MoM5 Nanocrystalline Alloys with Disordered Complexions Probed by In Situ Mechanical Testing**, *T. Rupert (trupert@uci.edu)*, J. Wardini, J.D. Schuler, University of California, Irvine, USA

Recent innovations in materials processing have enabled the creation of nanostructured materials with unique grain boundary structures. Here, we focus on nanocrystalline metals with amorphous intergranular films, which have been predicted to add a toughening effect. Due to the limited volumes of materials that can be made on lab scales or the geometry of typical parts, it is difficult to accurately probe the mechanical properties of these

materials. In this talk, we first describe the use of in situ mechanical testing in the scanning electron microscope, with the goal of measuring important properties only from the regions of interest. We focus on properties of fundamental importance, such as yield strength, strain hardening rate, ductility, and rate sensitivity, with measurements made by microtension and microcompression of very small samples. In addition, in situ fatigue testing inside of the transmission electron microscope provides an atomic scale view of plasticity near a developing crack in materials with and without the amorphous films. Using these results, we revisit the design of these materials, to suggest paths for improvement in the future.

11:40am **H2-1-MoM6 Structural Evolution and Wear-rate Transitions in Nanocrystalline Alloys**, *O. Donaldson (odonalds@uci.edu)*, J. Panzarino, T. Rupert, University of California, Irvine, USA

Nanocrystalline alloys have shown great potential as wear resistant coatings due to their high strength and hardness, but cyclic plastic deformation associated with sliding contact can lead to grain coarsening. In this study, we explore near-surface microstructural changes resulting from scratch wear tests in a nanoindenter, with a focus on understanding how such evolution affects subsequent wear properties. Electrodeposited Ni-W films, with an initial grain size of 3 nm, underwent transmission electron microscopy characterization of the grain structure and texture following scratch wear under normal loads of 10 to 50 mN. Additional Ni-W films with a grain size of 45 nm, achieved through annealing, underwent wear testing as well to provide a contrasting example where damage appears as grain refinement. A clear connection between instantaneous wear rate and subsurface microstructure was found. In addition, the final grain size for the damage layer near the surface was observed to be strongly dependent on the applied normal force, suggesting that local stresses near the surface affect the metastable, near-surface grain size that forms during wear. Finally, a wear map which captures microstructural changes due to different experimental testing variables was constructed and preliminary experiments on Cu-rich alloys were performed to provide a comparison.

12:00pm **H2-1-MoM7 Effects of Thermal Cycling on Nano-mechanical Properties of Thermal Barrier Coatings**, *M. Sebastiani (seba@uniroma3.it)*, Roma TRE University, Italy

In the present work, we analysed the nano-mechanical properties of high- and low-porosity Yttria-partially stabilized zirconia – YSZ top coats and of the thermally grown oxide (TGO) layer in a thermal barrier coating (TBC), produced by thermal spray.

High-speed nanoindentation and micro-pillar splitting were used for spatially-resolved analysis of elastic modulus, hardness and fracture toughness of the materials as a function of the number of thermal cycles.

In this way, the degradation of both elastic modulus and hardness of the YSZ top-coat is quantified, and a correlation with observed microstructures is proposed.

In addition, the micro-scale fracture toughness of the TGO layer is measured, for the very first time, as a function of the number of thermal cycles.

The existence of a critical TGO thickness of $\approx 5 \mu\text{m}$, postulated by previous research, is confirmed.

Until this threshold, the TGO is solely based on aluminium oxide, it grows slowly and generally remains dense and compact, except for some prominent asperities where the TGO becomes thicker. As a result, its micro-scale fracture toughness of the TGO also tends to increase up to maxima of 2.5 – 3 MPa $\cdot\sqrt{\text{m}}$.

These findings have implications on the failure mechanisms. Indeed, in addition to large stress concentrations along the interface, it is inferred that a reduction in the properties of both the TGO and the top coat contribute to failure of the TBC.

Topical Symposia

Room Pacific Salon 3 - Session TS4-1-MoM

Thin Film Materials for Flexible Electronics

Moderators: **Oleksandr Glushko**, Erich Schmid Institute of Materials Science, Austria, **Nicholas Glavin**, Air Force Research Laboratory, Materials and Manufacturing Directorate, USA

10:00am **TS4-1-MoM1 2D Materials Based Epidermal and Implantable Conformable Bioelectronics**, **N. Lu (nanshulu@utexas.edu)**, University of Texas at Austin, USA

INVITED

Bio-tissues are soft, curvilinear and dynamic whereas wafer-based electronics are hard, planar, and fragile. Such mismatch fundamentally impedes their integration with each other. As atomically thin, optically transparent, mechanically robust, and highly functional electronic materials, 2D materials are ideal for conformable bioelectronics. We have invented a cost- and time-effective "wet transfer, dry patterning" process for the freeform manufacture of graphene e-tattoos (GETs) [1-2]. Our GET has a total thickness of less than 500 nm, an optical transparency of ~85%, and a stretchability of more than 40%. Tensile fracture of PMMA-supported graphene has been experimentally investigated and different stages of fracture have been identified [3]. GET can be directly laminated on human skin exactly like a temporary transfer tattoo and can fully conform to the microscopic morphology of the skin surface via just van der Waals forces. Analytical models are developed to guide the GET design for full skin conformability even under skin deformation [4]. As a dry electrode, GET-skin interface impedance is found to be as low as medically used Ag/AgCl gel electrodes. GET has been successfully applied to measure electrocardiogram (ECG), electromyogram (EMG), electroencephalogram (EEG), skin temperature, and skin hydration. When applied around human eyes, imperceptible GET electrooculogram (EOG) sensors can capture eye movement with an angular resolution of 4 degrees, which can be used to wirelessly control a quadcopter in real-time [2]. In addition to noninvasive e-tattoos, we have engineered human eye-inspired soft implantable optoelectronic device using atomically thin MoS₂-graphene heterostructure and strain-releasing, retina conformable designs [5]. The hemispherically curved image sensor array exhibits infrared blindness and successfully acquires pixelated optical signals. We propose the ultrathin hemispherically curved image sensor array as a promising imaging element in the soft retinal implant with minimum mechanical loading to the retina. Optical signals obtained by this curved image array can be converted to electrical stimulations applied to optic nerves to restore visualization.

[1] Ameri et al, *Acs Nano* 2017, 11 (8), 7634-7641.

[2] Ameri et al, *npj 2D Materials and Applications* 2018, in revision.

[3] Jang, et al. To be submitted 2017.

[4] Wang, et al. *Journal of Applied Mechanics* 2017, 84 (11), 111003.

[5] Choi, et al. *Nat Commun* 2017, 8, 1664.

10:40am **TS4-1-MoM3 Performance Deterioration Characteristics of Silver-Nanoparticle-Printed Flexible Electric Wirings under Severe Bending Deformation**, **S. Kamiya (kamiya.shoji@nitech.ac.jp)**, **H. Izumi**, Nagoya Institute of Technology, Japan; **T. Sekine**, Yamagata University, Japan; **Y. Haga**, **H. Sugiyama**, Nagoya Institute of Technology, Japan; **N. Shishido**, Green Electronics Research Institute, Kitakyushu, Japan; **M. Koganemaru**, Kagoshima University, Japan

One of the important issues in flexible electronic devices is certainly their mechanical robustness. For further development of devices and wider applications in markets, how to characterize performance deterioration behavior under large scale bending deformation and how such information should be shared among suppliers and users of devices must be established for the sake of quantitative risk management in the actual operation toward the society of so-called IoT or ubiquitous sensor networks.

Mechanical robustness of flexible devices is most commonly demonstrated by bending them to a certain curvature while they are working. However, such a demonstration is mere consolation because no one knows what happens with even a bit of severer curvature. Therefore, in order to appropriately understand their robustness, bending test must be once carried out to the end of possibility, i.e., to folding them in half, while their performance is being evaluated. This is indeed a similar concept to common strength tests of materials, where materials are loaded until breakage to know safety margins of operation conditions.

To examine such a concept on flexible devices, a new type of bending test method was proposed in this study. Silver nano-particle wirings printed on flexible films were selected for the actual experiment, since wirings are utilized as the component most commonly found in any kinds of flexible devices, and tested not only under monotonic but also repeated bending loadings. Depending on the levels of loading, their resistance increased not always gradually but occasionally also suddenly. Such sudden behavior could hardly be deduced with the data obtained under less severe loading conditions and in shorter time of testing.

On the basis of deterioration behavior of performance observed above as an example, a number of new possibilities will be discussed in the presentation to share knowledge for the evaluation of operation risks associated with flexible devices to be distributed as a new type of infrastructures in the next step of society.

11:00am **TS4-1-MoM4 Characterizing the Mechanical Reliability of Flexible and Stretchable Conductive Inks on Polymeric Substrates**, **G. Cahn (gcahn3@gatech.edu)**, Georgia Institute of Technology, USA; **M. Wolfe**, DuPont Photovoltaic and Advanced Materials, USA; **J. Meth**, DuPont Electronics and Imaging, USA; **S. Graham**, **O.N. Pierron**, Georgia Institute of Technology, USA

Flexible hybrid electronic (FHE) devices are produced through precision printing of electrically conductive inks onto flexible substrates. A fundamental understanding of the inks' conductivity evolution under mechanical strain is required to properly address mechanical reliability of these devices and develop better conductors for mechanically-demanding applications such as wearable devices. This work investigates the behavior of DuPont's 5025 ("flexible") and PE874 ("stretchable") silver conductors under strain and on different polymer substrates (Kapton Polyimide (PI), Polyethylene Terephthalate (PET), and Thermoplastic Polyurethane (TPU)). Both inks are composite materials made of silver flakes embedded at high volume density within an insulating polymer matrix. While contacts between the flakes form electrically conductive pathways within the ink, their evolution under strain due to inhomogeneous deformation and local cracking, and the effect on conductivity has not been explored yet. This work specifically investigates this aspect using an *in situ* optical microscopy technique to measure the resistance evolution during monotonic, stress relaxation and creep loadings. As the applied strain is increased, the resistance of both inks increases as well, but at a much lower rate for PE874. Under stress relaxation, both inks see similar recovery in resistance, the amount of which is a function of the polymer substrate. The local deformation is investigated using digital image correlation to interpret these results and understand the role of polymer matrix and ink/substrate elastic modulus mismatch on ink conductivity.

11:20am **TS4-1-MoM5 Surface-engineered Nanostructured GaN Thin Film Based Ultraviolet Photodetectors**, **M. Mishra (monumishra.phy@gmail.com)¹**, **G. Gupta**, National Physical Laboratory, India

We report the formation of wet chemical etching induced nanostructures on polar and nonpolar epitaxial GaN films. Morphological transformations from planar to faceted pyramidal, flat/trigonal rod like nanostructures along with development of porous structures on the film were observed. The oxidation states of chemically modified (etched) surface were probed via photoemission spectroscopic measurements which revealed the elimination of hydroxyl species and adsorbed water molecules in polar GaN. Further, dissociation of Ga-N bonds and traces of metallic gallium were observed on the surface of porous GaN film after repeated etching. Fermi level pinning, band bending & alteration in the surface polarity with significant change in the electron affinities were also perceived. The wettability of the samples was reduced drastically and surfaces became highly hydrophilic. A great extent of stress relaxation with negligible in-plane compressive stress was pragmatic in the developed nanostructures. The temperature dependent I-V analysis displayed significant enhancement in current conduction with reduced sample resistance. Finally, the fabricated ultraviolet (UV) photodetectors (PDs) revealed an enhancement in photocurrent (5.5 folds) as well as device responsivity (6 folds) along with a significant increment in detectivity (7 folds) and very low noise equivalent power ($\sim 10^{-10}$ WHz^{-1/2}). The fast photoswitching of the PDs were ensured via a response and decay time of 151 ms and 453 ms which were >5 times faster with respect to pristine film based UV Photodetector. The improvement in device performance was attributed to increased light absorption, efficient transport of photogenerated carriers and enhancement in conduction cross section via

¹ Student Award Nominee

Monday Morning, May 20, 2019

elimination of recombination/trap centres related defects states which could be a promising approach to enhance the performance of GaN based photodetector technology.

11:40am **TS4-1-MoM6 Printed Hybrid Materials for Flexible Electronic and Optoelectronic Devices**, *E. List-Kratochvil* (emil.list-kratochvil@hu-berlin.de), **F. Hermerschmidt**, Humboldt-Universität zu Berlin, Germany

INVITED

Beyond the use in home and office-based printers, inkjet printing (IJP) has become a popular structuring and selective deposition technique across many industrial sectors. More recently great interest also exists in new industrial areas like in the manufacturing of printed circuit boards (PCBs), solar cells, flexible organic electronic and medical products. In all these cases IJP allows for a flexible (digital), additive, selective and cost-efficient material deposition, which can be used in an in-line production process. Due to these advantages, there is the prospect that up to now used standard processes can be replaced through this low cost innovative material deposition technique. However, using IJP as a production process in manufacturing, beyond the use in research laboratories, still requires rigorous development of cost and performance optimised functional electronic inks and processes, in particular those allowing for the fabrication on low cost flexible substrates polyethylene terephthalate. By this means this important aspect also addresses the trend in industry for high-throughput, roll-to-roll device processing, where the use of common plastic substrates instead of glass poses problems concerning the thermal stability of the substrate and the mechanical stability of the deposited device layers, including the transparent conductive electrode (TCEs) against damages caused by substrate bending during the production and operation lifetime of the flexible devices. In this contribution we report on the design, realisation and characterization of novel low temperature processes for printed metals, active and passive IJP electronic devices on flexible low cost substrates. We will present examples of resistive memories, printed TCEs and related electrode structures for organic light emitting diodes and organic solar cells based on IJP. [1]

[1] F. Hermerschmidt, S. A. Choulis, E. J. W. List-Kratochvil, "Implementing Inkjet-Printed Transparent Conductive Electrodes in Solution-Processed Organic Electronics", *Adv. Mater. Technol.* (2019) 1800474.

Monday Afternoon, May 20, 2019

Hard Coatings and Vapor Deposition Technologies

Room Golden West - Session B1-2-MoA

PVD Coatings and Technologies II

Moderators: Frank Kaulfuss, Fraunhofer Institute for Material and Beam Technology (IWS), Germany, Jyh-Ming Ting, National Cheng Kung University, Taiwan, Qi Yang, National Research Council of Canada, Canada

1:40pm **B1-2-MoA1 Harlan™: High Rate-High Density Pulsed Magnetron Sputtering Source for Depositing Metal & Ceramic Coatings for Industrial Applications.**, B. Abraham, R. Chistyakov (rchistyakov@ionexcorp.com), Ionex Corp, USA

A patented & proprietary high density/high rate magnetron deposition source developed in-house from the ground up. The development includes a newly designed high-density plasma generator and an improved magnetron deposition source far more superior to any conventional magnetron technology in the market today. The data presented will include deposition rates and X-SEM images of different thin films such as DLC, High Rate Metal Nitrides (MeN) and High Rate Metal Oxide (MeO), Highly Ionized Metal (Me).

2:00pm **B1-2-MoA2 Arc Sources for Low Defect Coatings and High Target Utilization**, V. Bellido-Gonzalez (victor@gencoa.com), D. Monaghan, B. Daniel, R. Brown, J. Price, A. Azzopardi, Gencoa Ltd, UK

Cathodic arc deposition, also known as arc ion plating or arc evaporation, is a PVD technique utilizing arc sources to deposit non-reactive and reactive coatings, such as carbide, nitride, carbonitrides, diamond like carbon, etc. Compared to traditional magnetron sputtering, denser coatings can be obtained by arc sources due to a higher degree of ionization and thus higher potential energy of the vapour flux towards the substrate. Also the ability of generating metal ions enables adhesion enhancement in some particular processes, like hard coating on cutting tools. Usually, target evaporation by arcs rather than momentum transfer in sputtering leads to a higher deposition rate in arc deposition, and provides a higher degree of heat on the substrate, which is beneficial for some processes. Unlike in Reactive Magnetron Sputtering, reactive arc has a very wide window of process conditions for a successful reactive process. However the deposition conditions all affect the arc parameters and the levels of macroparticle defect on the coating. Different solutions for filtering of the macroparticles have been devised, such as venetian blinds and Magnetic Guidance Filters. It is desired however that the basic level of macroparticles is reduced at its origin.

This work aims to obtain low defect coatings without using macroparticle filters and to obtain high target utilization by controlling the arc travelling. A 125mm circular arc source with optimized design will be employed for nitride deposition. Reliable arc triggering has been realized without mechanical trigger. The arc source will be powered by an arc generator with the capability to vary the arc current during deposition. A small but effective and easily adjustable controller will be used for varying the magnetic field. The effects of varying the arc current and the magnetic field on the defect generation and the target erosion will be investigated. SEM/EDX will be used to characterize the coating defects.

2:20pm **B1-2-MoA3 Cutting Tools in the Era of Industrial Internet of Things and Additive Manufacturing**, A. Inspektor (ainspekt@andrew.cmu.edu), A.D. Rollett, P.A. Salvador, Carnegie Mellon University, USA

The Industrial Internet of Things (IIoT), which involves multi-level internet-connectivity of machines and systems, and additive manufacturing (AM) of complex 3D printed items hold great promise to revolutionize the manufacturing industry. In this paper we will discuss the impact of IIoT and AM on the machining sector and anticipated challenges and opportunities for cutting tools and hard coatings. We will examine how sensors that provide real-time internet-connected feedback on the conditions of the cutting edge will allow confident increase in cutting speeds and other machining parameters. This will lead to expansion of the safe zone in wear maps and call for improvements in tool materials and coatings. We will then review the structure and surface properties of AM 3D printed metal parts. Economic, large scale finish machining of rough 3D printed metals will challenge current finish cutting routines and accelerate suitable changes in design and structure of cutting tools. The IIoT sensors will affect, primarily, machining of bulk materials. AM and 3D printed metals will speed up progress in finish cutting. We will discuss both cases with appropriate examples of tools and coatings for machining high temperature alloys, gray cast iron, and carbon composites.

2:40pm **B1-2-MoA4 Overstoichiometric Transition Metal Nitride Films**, Z. Čiprová (ciprovz@kfy.zcu.cz), J. Musil, Š. Kos, M. Jaroš, European Centre of Excellence, University of West Bohemia, Czech Republic

Transition metal nitride films TMN_x with a high stoichiometry $x = N/TM > 1$ are advanced films with new unique properties; here TM are the transition metals such as Ti, Zr, Mo, Ta, Nb, W, etc. We report on their properties and formation by the reactive magnetron sputtering using dual hybrid magnetron. The principle of formation of overstoichiometric $TMN_{x>1}$ films is explained. Three $TMN_{x>1}$ coatings were investigated in detail: $ZrN_{x>1}$, $Ti(Al,V)N_{x>1}$ and TiN_2 dinitride films [1]. It was found that (1) the overstoichiometric $ZrN_{x>1}$ films are two-phase films with c-ZrN and o- Zr_3N_4 structure, (2) the overstoichiometric $Ti(Al,V)N_{x>1}$ and $TiN_{x>1}$ films are one-phase films with c-TiN structure, (3) the one-phase overstoichiometric $TMN_{x>1}$ nitride films can form the TMN_2 dinitride films such as TiN_2 dinitride, (4) the film stoichiometry x is a strong parameter which enables to control its mechanical properties and electric conductivity; for example, the electrical resistivity of the ZrN_x film varies with increasing x from well electrically conducting films with $x \leq 1$ through the semi-conducting films with x ranging from 1 to ≤ 1.26 to non-conductive with $x \geq 1.3$, and (5) the high base pressure $p_0 \geq 0.001$ Pa in the deposition chamber after its evacuation strongly influences the structure and phase composition of sputtered nitride films.

Reference

[1] J. Musil, M. Jaroš, Š. Kos, R. Čerstvý, S. Haviar: Hard TiN_2 dinitride films prepared by magnetron sputtering, J. Vac. Sci. Technol. A 36(4) 2018, 040602-1 to -3.

3:00pm **B1-2-MoA5 Introducing of New Hybrid LACS® Technology (Lateral ARC and Central Sputtering by Rotating Cathodes)**, R. Zemlicka (r.zemlicka@platit.com), M. Jilek (Sr.), M. Jilek (Jr.), A. Lümkmann, T. Cselle, D. Bloesch, V. Krsek, Platit AG, Switzerland

The flexible coating units which are able to work with ARC, sputtering and PACVD technologies are very suitable for the small and medium size enterprise. While the ARC brings the highest performance for cutting tools in cca 85% of the applications, the sputtering achieves very smooth surfaces for better chip evacuation and DLC coatings, made by PACVD, avoids build up edges at cutting sticky materials. The combination of these 3 technologies in one coating unit enables the use of advantages of all of them.

We would like to introduce the new LACS® technology (Lateral ARC and Central Sputtering by rotating cathodes). The new feature of this hybrid technology is the combination of arc evaporated non-alloyed metallic (Ti, Al, Cr, W, etc) and magnetron sputtered ceramic (TiB₂, B₄C) targets, resp. cathodes.

It allows to deposit different high-performance coatings, like AlCrN/BN, AlTiN/BN, TiWN, TiCNWCC or TiB₂. On the other hand, the supplementary electron injection provided by ARC discharge can improve the microstructure and performance of the plasma-enhanced magnetron sputtered coatings.

On the example of BN-containing coatings we would like to illustrate how it is possible to optimize mechanical parameters of the coating by tuning of the process parameters. We will also present industrial applications of the optimized coating.

3:20pm **B1-2-MoA6 Edge-related Effects During Arc-PVD Deposition Processes**, T. Krülle (tim.kruelle@iws.fraunhofer.de), F. Kaulfuss, O. Zimmer, A. Leson, C. Leyens, Fraunhofer Institute for Material and Beam Technology (IWS), Germany

The deposition of different coatings on shaped surfaces, such as on cutting tools (drills) faces problems especially on edges [1-2]. Normally the radii of such cutting edges are dramatically increased, if the coating thickness is increased. Also defects, damaging or resputtering of material on edges may occur. A multilayered coating based on AlCrSiN instead showed an interesting effect of edge sharpening during the deposition process. With this approach it would be possible to overcome the problem of edge rounding in PVD coating technology. The pictures below show different edge radii varying with the negative bias voltage and leading to a smaller edge radius as compared to the uncoated tools or tools without additional bias voltage [3].

Therefore the deposition process and important deposition parameters were investigated and the geometry of such edges was measured. Accompanying nano indentation hardness measurements give an overview of mechanical properties around the surface also in dependence of position and chemical composition of the coating.

REFERENCES:

- [1] H. A. Jehn, "PVD coating of 3D parts studied with model samples", Surface and Coating Technologies, Vol. 94-95, pp 232-236, 1997.
- [2] J. Bohlmark, "Evaluation of arc-evaporated coatings on rounded surfaces and sharp edges", Materials Science Forum, Vol. 681, pp 145-150, 2011.
- [3] T. Krülle, FHI-IWS Dresden, Annual Report 2016, "Sharp edges thanks to coatings", pp 106-107.

3:40pm **B1-2-MoA7 Reactive Sputtering for Highly Oriented HfN Film Growth on Si(100) Substrate**, *Y.S. Fang (lacus830618@gmail.com)*, *K.A. Chiu, H. Do, L. Chang*, National Chiao Tung University, Taiwan

Hafnium nitride have excellent properties such as high melting point, high hardness, low resistivity, which makes them potential in many technological fields. HfN have been investigated for diffusion barriers in semiconductor devices. HfSi₂ has been used for high temperature oxidation resistant coatings. However, there are no detailed studies for growth of epitaxial HfN/HfSi₂ films on Si substrate.

HfN films were grown on Si(100) substrates by reactive DC magnetron sputtering with Ar/N₂ gas mixture using a Hf target. The deposition was carried out by varying N₂ flow ratio and the power at 5 mTorr and 850°C

XRD results with cross-sectional TEM/STEM show that low N₂ flow ratio favors the formation of the HfSi₂ interlayer between HfN and Si, while no HfSi₂ diffraction peaks can be seen for high N₂ flow ratio of 12.5%. Also, increasing the applied power for sputtering results in the increase of the HfN peak intensity ratio of (200)/(111). Furthermore, it is shown that the orthorhombic HfSi₂ interlayer is in epitaxy with Si (100) and those (100) oriented HfN grains are found in epitaxy with both HfSi₂ and Si as well. The epitaxial relationship is HfN (100) [011] // HfSi₂ (020) [100] // Si (100) [011].

4:00pm **B1-2-MoA8 Study of Orthorhombic ZnSnN₂ Fabricated using Zn-Sn₃N₄ Composition Spreads through Combinatorial Reactive Sputtering**, *K.-S. Chang (kschang@mail.ncku.edu.tw)*, National Cheng Kung University, Taiwan

INVITED

The piezo-related properties of ZnSnN₂ (ZTN) will be presented. Natural Sn₃N₄ and Zn thickness gradients were fabricated using combinatorial magnetron sputtering to form Zn-Sn₃N₄ composition spreads to enhance the relative variation of the cation ratios and to promote the formation of orthorhombic ZTN. Sn₃N₄ and the single crystallinity of orthorhombic (Pna2₁) ZTN nanocolumn arrays growing along the [001] direction were confirmed by locked-coupled XRD and TEM. The diffusion and variation of the atomic binding state of constituent elements were studied using SIMS depth profiling and XPS. The band gap of ZTN was estimated to be approximately 2.0 eV from a UV-vis measurement. The piezotronic and piezophototronic effects of ZTN were ascertained and illustrated by the Schottky barrier height variations. Excellent piezophotocatalysis was also observed, which was attributed to the reduced recombination of the photogenerated e⁻-h⁺ pairs. In addition, *O₂ radicals were predominate in the photodecomposition process.

4:40pm **B1-2-MoA10 Angular Resolved Mass-energy Analyses of Species Emitted from a d.c. Magnetron Sputtered NiW-target**, *M. Rausch (martin.rausch@unileoben.ac.at)*, Montanuniversität Leoben, Austria; *S. Mraz, J.M. Schneider*, RWTH Aachen University, Germany; *J. Winkler*, Plansee SE, Austria; *C. Mitterer*, Montanuniversität Leoben, Austria

Advanced thin film applications e.g. in thin film transistors, electrochromic glasses or hard coatings frequently require sputtering targets consisting of multiple chemical elements with large differences in atomic weight. An understanding of sputtering, gas-phase transport and deposition characteristics of thin film systems deposited from such multi-element targets becomes increasingly important. For the previously investigated system Mo_{0.70}Al_{0.20}Ti_{0.10} (m_{Mo}=95.95 u, m_{Al}=26.98 u, m_{Ti}=47.87 u) it was shown that not only (i) element-specific differences in sputter yield and initial emission angle, but also the (ii) transport of sputtered particles through the gas, accompanying (iii) collisions with background gas atoms with concomitant energy loss of sputtered particles, and (iv) the interaction of transmitted energetic particles with the surface of the growing thin film, such as preferential re-sputtering, will have an impact on the film morphology as well as the chemical composition of the films [1]. For the system NiW, which is used for the deposition of electrochromic thin films, the difference in atomic weight of the target constituents is significant (m_{Ni}=58.69 u, m_W=183.84 u), making it an ideal model system to study the mechanisms mentioned above. Since it was concluded in [1] that the initial emission angle and the corresponding energy of sputtered atoms have a substantial impact on differences in morphology and chemical composition of the films, a 180 ° turnable magnetron with a mass-energy analyzer

Monday Afternoon, May 20, 2019

mounted opposite the target at a distance of 80 mm was used to d.c. sputter a Ni_{0.80}W_{0.20} target at Ar pressures ranging from 0.01 to 1 Pa. This setup allowed measuring both, flux and energy of sputtered Ni and W, but also of Ar reflected from the target and ionized in the plasma, at any given angle between 0 and 90° with respect to the target normal. Subsequent thin film deposition with a spherical-shell substrate holder covering the examined angles at deposition positions from 0 to 80 ° in 10 ° steps allowed correlating the mass-energy measurements with thin film growth experiments. Film thickness measurements, structure and composition analysis yielded insights into the relation between emission angle and energy of transmitted particles and angular dependent structure and composition evolution of the deposited films.

[1] M. Rausch, M. Pavlovič, P. Kreiml, M.J. Cordill, J. Winkler, C. Mitterer, Applied Surface Science 455 (2018) 1029–1036.

5:00pm **B1-2-MoA11 Effect Produced by Architecture of Nanolayer Composite Coatings Deposited with Filtered Cathodic Vacuum Arc Deposition (FCVAD) Technology on their Mechanical and Performance Properties**, *A. Vereschaka (dr.a.veres@yandex.ru)*, *S. Grigoriev*, Mstu Stankin, Russian Federation; *N. Sitnikov*, National Research Nuclear University MEPhI, Russian Federation; *N. Andreev*, National University of Science and Technology "MISIS", Russian Federation

The paper deals with the technique of forming coatings with nanolayer structure, including nanolayers (formed due to rotation of a turntable in a chamber) and subnanolayers (formed due to planetary rotation of rigging elements). The SEM and TEM methods were used to study the coating structure. In particular, the Ti-TiN-(Ti,Al,Si)N, Zr-ZrN-(Zr,Cr,Al,Si)N and ZrNb-ZrNbN-(Zr,Nb,Cr,Al,Si)N coatings were considered. The thickness of binary nanolayers in the coatings under study was 20-70 nm, while the thickness of subnanolayers was 2-20 nm. The study also considered the mechanism of coating failure in scratch testing, depending on thickness of nanolayers and subnanolayers. The investigation found significant differences in the value of the critical failure force L_{c2} and the pattern of failure, depending on the thickness of coating nanolayers. The change in the value of adhesion component of the friction coefficient for samples with the coatings under study within the temperature range of 20-1000°C was studied. Cutting tests were conducted for carbide tools with the coatings under study in turning steel C45 at f = 0.25 mm/rev, a_p = 1.0 mm, v_c = 200-350 m/min. The patterns of wear and failure for coated tools were studied, as well as oxidation and diffusion processes. As a result of the conducted studies, a range of values for optimal thickness of nanolayers was determined to make it possible to increase the cutting speed by 25-30% while maintaining the tool life period and the high quality of the machined surface.

5:20pm **B1-2-MoA12 Effects of Nitrogen Flow Rate and Substrate Bias on Structure and Properties of Molybdenum Nitride Thin Film**, *C.C. Chou (alanchou2003@msn.com)*, *J.-H. Huang*, National Tsing Hua University, Taiwan

Molybdenum nitride is well known as a wear resistant material with high hardness, which has three different thermodynamic stable crystal structures, tetragonal β-Mo₂N, cubic γ-Mo₂N, and hexagonal δ-MoN, among which γ-Mo₂N possesses the best mechanical performance. However, there is little research on the relationship of β- and γ-Mo₂N transformation. The purposes of this study are to investigate the order-disorder phase transformation of Mo_{2-x}N thin film by controlling the deposition parameters, including nitrogen flow rate and substrate bias, and to explore the relationship between mechanical properties of different phases. The Mo_{2-x}N thin films were prepared on Si substrate using unbalanced magnetron sputtering with different nitrogen flow rate and substrate bias. After deposition, the film hardness and crystal orientation were characterized by nanoindentation and X-ray diffraction, respectively. The residual stress of the thin film was measured using laser curvature and XRD cos²αsin²ψ methods, which may affect hardness and adhesion of the thin film. The microstructure was observed by scanning electron microscopy and atomic force microscopy. The electrical resistivity and chemical compositions were measured by a 4-point probe and X-ray photoelectron spectroscopy. Based on the experimental results, the mechanical properties were correlated to structure of the thin films.

Monday Afternoon, May 20, 2019

Hard Coatings and Vapor Deposition Technologies

Room California - Session B3-2-MoA

Deposition Technologies and Applications for Diamond-like Coatings II

Moderators: Laurent Espitalier, Wallwork Cambridge Ltd, UK, Konrad Fadenberger, Robert Bosch GmbH, Germany

1:40pm B3-2-MoA1 Transfer of DLC Coating Processes between Different Coating Machines Assisted by Plasma Simulation, M. Günther (marcus.guenther2@de.bosch.com), O. Schmidt, W. Dobrygin, G. Schütze, Robert Bosch GmbH, Germany

Hydrogenated amorphous carbon films (a-C:H) as a kind of diamond-like carbon (DLC) coatings combine unique optical, electrical and mechanical properties, resulting in numerous industrialized applications. These plasma coatings are continuously of high interest for research and industry because of the possibility to adjust their layer properties in a wide range by varying the deposition conditions like pressure, temperature or bias voltage. DLC films are widely used in the automotive industry due to their unique tribological properties, e.g. as an enabler for modern fuel injection equipment.

Important goals of a modern flexible industrial production especially for automotive mass production are the realization of good adhesion, functionality of the layer system and the fundamental control of the deposition process regardless of the kind of coating machine and coated component geometry. The combination of plasma simulation, coating experiments and plasma diagnostics enables the monitored deposition of hydrogenated amorphous carbon films and the prediction of the resulting layer properties, e.g. hardness, intrinsic stress or hydrogen content.

The study will present a global model for acetylene and argon plasmas to support the process development for the functional a-C:H-layer and the process transfer between different coating machines for the industrialized deposition to guarantee consistent a-C:H-layer quality. With the presented simulation, it is possible to calculate all partial pressures of reaction products, relevant plasma parameters and particle fluxes. By transferring all relevant machine parameters (e.g. bias voltage, gas flow, ...) into only one main virtual parameter, the energy per deposited carbon atom, it is possible to compare and generically predict the coating quality of various coating machines with different chamber sizes and vacuum pumping systems.

2:00pm B3-2-MoA2 Stress-Free ta-C Industrially Deposited by PLD for High Performance Stamping Applications: Results and Challenges of 1st Production Year, M. Hess (martin.hess@stepper.de), Fritz Stepper GmbH & Co. KG, Deutschland, Germany; S. Weißmantel, R. Bertram, Hochschule Mittweida University of Applied Sciences, Germany

At the 45th ICMCTF conference, we presented PLD as a new system technology for the production of stress-free ta-C coatings which are summarizable by a very high hardness of over 60 GPa while retaining the common layer thicknesses of 3 to 4 μm (which are previously and still used for our PVD tool coatings coated by Sputter- and Arc-PVD). Among other things PLD allowed us to deposit ta-C without changing tool drawings (which are proven over many years) if we mix ta-C- with PVD coatings in our high performance progressive die tools. Moreover we can avoid egg shell effects, which may be a drawback if very hard but relatively thin (ca. 1 μm) coatings are used in highly stressed applications.

PLD ta-C achieves, compared to so far used PVD coatings, almost double hardness in combination with a significantly artifact less surface. As a result the abrasion resistance against some stamping strips and active component lifetime are boosted by a magnitude and more – which saves tool cost and press down time. As presented in 2018 our daily quantities and tool sizes are relatively small, even for compliance with compact PVD systems, we decided to design a PLD system dedicated to our requirements for our final products: Complex modular die tools (with more than 1000 coated active elements) which are able to produce multi-millions of electrical contacts in a 24/7 operation without any maintenance.

In the meantime our PLD coating system has been in operation for more than one year. Driven by demanding applications, such as Si-containing high-strength bronze, stainless steel, the ta-C coatings became smarter (e.g. integrated run-in layer, tailored hardness and Young's modulus, etc.) and more performing. Significant progress was e. g. also made regarding the coating of die cavities.

The purpose of the present contribution is to introduce latest developments of ta-C produced by PLD. For this purpose, relevant mechanical properties as well as new successful applications will be presented.

2:20pm B3-2-MoA3 Hollow Cathode Discharges for Rapid DLC, T. Casserly (tcasserly@duralar.com), S. Gennaro, F. Papa, A. Tudhope, Duralar Technologies, USA

INVITED

The application of Diamond Like Carbon coatings has been limited by the cost and time required to deploy the coating. Hollow cathode discharges are characterized by their high ion densities and hot oscillating electrons capable of multiple ionization events. Through harnessing the power of hollow cathode discharges internal surfaces of conductive hollow articles can be coated rapidly with DLC (and other materials). This internal deposition technology enables numerous applications of DLC for low wear and low friction in engine cylinders, actuators, hydraulic cylinders, and more as well as anti-wear, anti-fouling and anti-corrosion applications in upstream oil and gas and adjacent markets. Deposition rates in excess of 5 μm per minute have been achieved for specific geometries allowing for cost effective deployment of advanced coatings. This high rate hollow cathode deposition technology has been extended to coat external surfaces as well; initially, for shafts, plungers, and other cylindrical objects through the application of annular hollow cathode geometries. Using a similar approach designed for high throughput, the deposition technology has been developed to coat the external and internal surfaces of complex objects with applications in armaments, sporting, and automotive components, as well as functional decorative coatings for consumer products. The high deposition rates and throughput afforded by hollow cathode discharge technology greatly reduces the cost of deploying advanced DLC coatings and enables a diverse set of applications.

3:00pm B3-2-MoA5 Hard Cr-doped DLC Coatings Deposited by Low-frequency HiPIMS with Enhanced Tribomechanical Behavior at High Temperature, J.A. Santiago Varela (j.santiago@PVTvacuum.de), PVT Plasma und Vakuum Technik GmbH, Germany; I. Fernandez, Nano4Energy SL, Spain; A. Wennberg, Nano4Energy, Spain; M.A. Monclus, J.M. Molina Aldareguia, IMDEA Materials; V. Bellido-Gonzalez, Gencoa Ltd, UK; T.C. Rojas, J.C. Sanchez Lopez, ICMSe CSIC, Spain; R. Gonzalez Arrabal, Universidad Politécnica de Madrid, Spain; N. Dams, H. Gabriel, PVT Plasma und Vakuum Technik GmbH, Germany

Diamond-like Carbon (DLC) coatings have been recognized as one of the most valuable engineering materials for various industrial applications including manufacturing, transportation, biomedical and microelectronics. Among its many properties, DLC stands out for a good frictional behaviour combined with high surface hardness, offering an elevated protection against abrasive wear. Nevertheless, a factor limiting the widespread application of DLC coatings is their thermal stability. DLC is very temperature-sensitive since its sp^3 - sp^2 structure undergoes a graphitization process at high temperatures that deteriorates both hardness and coefficient of friction. In order to overcome this limitation, new ways to modify DLC coatings for acceptable high temperature performance have been explored. In this work, we investigated the deposition of hard DLC coatings doped with Cr using HiPIMS technique at industrial scale. Extraordinary highly ionized plasma discharges were obtained during chromium and carbon codeposition at low HiPIMS frequencies. The high ion energy bombardment at low HiPIMS frequencies allowed doping with Cr the DLC structure while reaching high sp^3 contents. EELS spectroscopy was used to evaluate sp^3 content and Raman was used for sp^2 structural characterization of the films. Enhanced mechanical properties (hardness up to 35 GPa) were observed with nanoindentation for Cr-doped DLC at low frequencies. High temperature nanoindentation tests were also performed from room temperature to 450°C in order to evaluate the evolution of hardness and Young Modulus with temperature. The results confirm that the mechanical properties at high temperature mainly depend on the sp^3 content. Tribological tests were carried out in air from room temperature to 250°C. Cr-doped DLC coatings showed lower friction and wear compared to pure DLC. The increased toughness that Cr provides to the carbon matrix together with a high sp^3 bonding structure obtained with low frequency HiPIMS deposition improves the stability of DLC coatings for high temperature applications.

3:20pm B3-2-MoA6 Characterization of Diamond-like Carbon Coated Powders, P.J. Heaney (patrick@ncdtechnologies.com), A. Zeng, M. Efmov, NCD Technologies, USA

General characterization is needed to show a coating is meeting applications' needs, optimizing coatings performance, and general quality control. Characterizing diamond-like carbon (DLC) coated powders is challenging with conventional techniques. These challenges significantly increase as the particle size decrease from the micro to the nanoscale. Many coating processes use flat coupons to provide samples that can be easily characterized with a variety of samples, however flat coupons are not

Monday Afternoon, May 20, 2019

representative of the same coating that is deposited on micro and nano scaled powders.

Determining coating thickness for many samples of coated powder can be difficult. TEM can work well to measure thickness; however sample throughput is slow. We have validated a few methods including using depth profiling and XPS to help determine thickness. Measuring the hydrophobicity of a material is difficult as contact angle measurements do not work on powders. We have developed a method of stirring powder in aquatic solutions to determine hydrophobicity. We have also developed solutions for testing corrosion resistance by exposure to various compounds and measuring with UV-VIS spectrometer. We have further developed an oxidation resistance test through measuring gas output while exposing our DLC coated powders to elevated temperatures in high humidity environments.

In developing technologies to coat nano and micro scaled powders with DLC, NCD Technologies has developed new techniques for standard quality control characterization. We will discuss the limitations of standard measurements on nanoscaled powders and new techniques that can measure the specific aspects of the coating performance. We will provide a variety of results based on DLC coated nano and micro scaled powders.

3:40pm B3-2-MoA7 Effect of Pulse Shape and Plasma Composition (Ar + Ne) on the Properties of Hard DLC Films Deposited by HiPIMS: Correlation with Substrate Ion Fluxes, J.C. Oliveira (joao.oliveira@dem.uc.pt), F. Ferreira, R. Serra, University of Coimbra, Portugal; T. Kubart, Uppsala University, Angstrom Laboratory, Sweden; C. Vitelaru, National Institute for Optoelectronics, Romania; A. Cavaleiro, University of Coimbra, Portugal
High Power Impulse Magnetron Sputtering (HiPIMS) has been under consideration for hard Diamond Like Carbon (DLC) thin films deposition in recent years. The major driver to use HiPIMS is the possibility of C ions formation in the plasma and their subsequent subplantation upon substrate biasing to promote the formation of sp³ bonds in a similar way to ARC deposition. However, the low electron impact ionization cross-section of C limits the C_s/C ratio in HiPIMS plasmas to some few percent (~ 5 %). Adding Ne to the discharge gas allows increasing the electron temperature of the plasma and, thus, increasing the C ionization fraction. On the other hand, the use of short pulse on-times (<10 μs) together with high target voltages (>1 kV) has been reported to result in large target current densities.

In this work the effect of adding Ne to a pure Ar discharge and the use of different HiPIMS pulse shapes are investigated. DLC films were deposited by HiPIMS using two different power supplies providing HiPIMS pulses with different temporal duration and peak voltages. The structural and mechanical properties of the DLC films were evaluated by micro-Raman Spectroscopy and Nanoindentation, respectively. The tribological behavior of the DLC films was evaluated by pin-on-disk tests in ambient atmosphere (room temperature and ~ 40% relative humidity). The friction coefficients of the DLC films were obtained by averaging over last 1000 m of the sliding tests. The specific wear rate (k) of the DLC films was calculated from the cross-section profiles of the wear tracks. Additionally, the time-resolved substrate current densities (SCDs) were measured using a flat probe mounted at the substrate position. The measured Ion Saturation Currents (ISCs) were correlated to the structural, mechanical and tribological properties of DLC films.

Adding Ne to the HiPIMS plasma results in a significant increase of both the sp³ content and the hardness (> 20 GPa) of the DLC films while their friction coefficient remains within the range typical of DLC films tested under relatively humid conditions (< 0.2). The specific wear rate of the DLC films decreases with Ne addition down to a minimum value of 4 x10⁻¹⁷ m³/Nm.

4:00pm B3-2-MoA8 The Comparison of Deposition Processes, Composition and Properties of Hydrogenated W-C:H Coatings Prepared by Different Sputtering Techniques, F. Lofaj (lofaj@saske.sk), M. Kabatova, L. Kvetkova, Institute of Materials Research of SAS, Slovakia; J. Dobrovodsky, ATRI, Slovakia

The work reviews the processes and subsequent mechanical and tribological properties of hybrid PVD/PECVD sputtering during deposition of hydrogenated W-C:H coatings prepared by High Power Impulse Magnetron Sputtering (HiPIMS) and High Target Utilization Sputtering (HiTUS) as a function of acetylene and hydrogen additions in the Ar atmosphere. The results are compared with those from analogous coatings deposited by conventional direct current magnetron sputtering. TEM observations revealed that a transition from nanocrystalline WC_{1-x} to nanocomposite and amorphous structure occurred with the increase of acetylene addition in all coatings but at different acetylene contents. The concentrations of carbon and hydrogen in the studied coatings measured by Rutherford

Backscattering (RBS) and Elastic Recoil Detection Analysis (ERDA) methods depended on the amount of acetylene and hydrogen addition but also on the applied technique. The obtained results were analyzed and the main differences in the possible growth mechanisms between DCMS and HiPIMS were discussed within the von Keudell model for a-C:H growth. The increase of free carbon content in HiTUS W-C:H coatings when C₂H₂ was added resulted to a degradation of indentation hardness and indentation modulus similarly as in DCMS coating. However, almost no degradation was observed in HiPIMS coatings. Low coefficients of friction in HiTUS and DCMS coatings were attributed to the formation of lubricious tribolayer whereas uniform structure was considered to be a property controlling parameter in HiPIMS coatings. The main advantage of HiPIMS compared to HiTUS and DCMS coatings includes lower coefficients of friction at higher hardness values.

4:20pm B3-2-MoA9 The Mechanism of Graphite Nucleation in Amorphous Carbon Films Deposited with the Condition of Energetic Bombardment and High Temperature, D. Zhang (zhangdi2015@sjtu.edu.cn), P.Y. Yi, L.F. Peng, X.M. Lai, Shanghai Jiaotong University, China

Amorphous carbon (a-C) films exhibit many properties that make them attractive for applications in coating technology. The property of a-C films closely depends on their microscopic structures and a-C films with a graphite-like structure may exhibit high electrical conductivity and excellent corrosion resistance, mainly due to the nucleation of graphite nanocrystals observed in a-C matrix. However, the mechanism of graphite nucleation remains unclear. This work aims to develop a fundamental understanding of the graphite nucleation in a-C films deposited with energetic bombardment and high temperatures. Our experiments revealed that different sizes of graphite nanocrystals were observed in a-C films produced by applying varying deposition bias voltages and temperatures, thus leading to a different durability under the a typical corrosive environment of proton exchange membrane fuel cells. Moreover, we developed an atomistic model to simulate the nucleation of graphite nanocrystals in a-C films using Molecular Dynamics and Monte Carlo methods. Investigations on the structural properties of the atomistic model provide fresh insights into the microscopic structure of graphite-like a-C films.

Coatings for Biomedical and Healthcare Applications Room Pacific Salon 2 - Session D1-2-MoA

Surface Coating and Modification for Use in Biological Environments II

Moderator: Mathew T. Mathew, University of Illinois College of Medicine, USA

1:40pm D1-2-MoA1 Recent Development of Biocompatible Thin Film Metallic Glass Materials, J.-W. Lee (jefflee@mail.mcut.edu.tw), Ming Chi University of Technology, Taiwan; B.-S. Lou, Chang Gung University, Taiwan; Y.-C. Yang, National Taipei University of Technology, Taiwan; C.-P. Lin, National Taiwan University, Taiwan

INVITED

The thin film metallic glass (TFMG) materials have been intensively studied due to their promising physical and mechanical properties, such as high strength, flexibility, and excellent corrosion resistance. Recently, the biomedical applications of TFMGs also attracted lots of attentions from researchers. Improved sharpness and non-stick effects of the dermatome and syringe needles have been reported, respectively, by the coating of thin film metallic glass. In this work, several Zr-, Ti- and Fe-based TFMGs were fabricated using magnetron sputtering method. The corrosion resistance and in-vitro biocompatibility tests of TFMGs were studied. The antimicrobial test of some Cu or Ag containing TFMGs was also evaluated. The in-vivo animal test on Zr-Ti-Si and Fe-Zr-Nb TFMGs was further investigated. In addition, fracture resistance evaluation of dental Ni-Ti rotary instruments with TFMG coating was conducted. It is found that excellent anti-corrosion properties were observed for these TFMGs. Remarkable antimicrobial performance was obtained for the Cu or Ag containing TFMGs. In-vitro test showed that the TFMGs had good proliferation and differentiation of cultured cell. The in-vivo animal test also indicated that no allergy, toxicity or carcinogenic reaction was caused by the TFMGs to the rats. The Ti-based TFMG coating can effectively improve the fatigue fracture resistance of dental Ni-Ti rotary files. We can conclude that the biocompatible Zr-, Ti- and Fe-based TFMGs show very promising application on the dental and orthodontic surgical tools.

Monday Afternoon, May 20, 2019

2:20pm D1-2-MoA3 Synthesis and Characterization of Reactively Sputtered Platinum Group Metal Oxides for Stimulating and Recording Applications, *G. Taylor (taylor6q@students.rowan.edu), A. Marti, R. Paladines, N. Page, Rowan University, USA; A. Fones, S. Tint, Johnson Matthey Inc., USA; H. Hamilton, Johnson Matthey, Inc., USA; S. Amini, Johnson Matthey Inc., USA; J. Hettinger, Rowan University, USA*

A range of materials have been examined as coatings over the past several decades to improve the performance of implantable devices used in neurostimulation and recording applications. Iridium oxide (IrO₂) has been widely investigated due to its biocompatibility and high charge storage capacity. Modification of the synthesis conditions, as one means of improving the coating performance, led to reports of surface platelets forming at high deposition pressures. This study complements earlier research by extending the range of deposition parameters for the IrO₂ system and investigates the ruthenium oxide (RuO₂) system under the same experimental conditions. The results show that the platelet microstructure in tetragonal IrO₂ is due to the formation of a specific orientation of crystallite. In contrast to previous reports that platelet formation coincided with a decrease in coating performance, it will be shown that the presence of platelets can improve the electrochemical performance of the coatings as measured by cyclic voltammetry in a phosphate buffered saline electrolyte. Furthermore, the platelet microstructure, and thereby the effective surface area, can be systematically controlled by adjusting deposition parameters, including temperature and oxygen partial pressure, used during the reactive sputtering. No such platelet formation has yet been observed in the RuO₂ system.

2:40pm D1-2-MoA4 Antibacterial and Biocompatible Properties of Ga-doped TaON Thin Films, *J.H. Hsieh (jhhsieh@mail.mcut.edu.tw), Q.W. Liu, Ming Chi University of Technology, Taiwan; C. Li, National Yang Ming University, Taiwan*

Recently, gallium ions have been studied for its multi-functional bio-activity. While gallium has no known function in human physiology, the chemical properties that it shares with iron allow it to bind to iron-containing proteins (Trojan Horse effect), including the iron transport protein transferrin. Thus, malignant cells and microorganisms may be tricked into incorporating gallium in place of iron for iron-dependent processes essential for bacterial viability and growth. Hence, rather than facilitate iron-dependent cellular function, gallium disrupts it. As a result, the interaction between gallium and iron-proteins can be exploited for therapeutic purposes in cancers and bactericidal treatments. Accordingly, it is of great interest to know how Ga can be doped into surface coatings.

In this study, the deposition processes of tunable TaOxNy-Ga thin film coatings were studied systematically. Following this, the resultant mechanical, structural, and, bio-related properties were examined, in terms of O/N ratio, surface roughness and Ga contents. However, due to low melting point of Ga (~29 °C), it is relatively difficult to sputter Ga into those oxynitride coatings. Therefore, Ga₂O₃ target was used in this study to provide oxygen and Ga. According to the results, it was learned that small amount of oxygen (2~5%) and gallium (1~3%) in the coatings could be beneficial to the improvement of mechanical and antibacterial properties. The enhanced dissolution of Ga ions was observed with the addition of oxygen. The highest hardness could reach 30 GPa, while an antibacterial efficiency of >90% could be found after 48 hrs of immersion. The films showed good biocompatibility with MG63 cells.

3:00pm D1-2-MoA5 TiO₂ Nanotubes Produced in Aqueous Electrolytes with CMC for Biomaterials Application, *R. Aguirre Ocampo (robinson.aguirre@udea.edu.co), M. Echeverry-Rendón, S. Robledo, F. Echeverría, Universidad de Antioquia, Colombia*

Nanotubular structures were produced on the c.p. Titanium surface by anodization in an aqueous electrolyte that contains carboxymethylcellulose (CMC) and NaF. The internal diameter obtained at voltages of 20, 10 and 2 V was about 100, 48 and 9.5 nm, respectively. Those diameters were measured using Scanning Electron Microscopy (SEM), Transmission Electron Microscopy (TEM) and Atomic Force Microscopy (AFM). Scientific reports about nanotube produced by anodization with internal diameters upper than 30 nm are very common, however, reports about lower nanotube diameters (<20 nm) are scarce. Several heat treatments at 200, 350 and 600 °C were made to produce nanotubes with different TiO₂ polymorphs (Anatase, Rutile), at 200 °C no phase change was observed, at 350 °C the nanotubes change from amorphous phase to Anatase, and at 600 °C the rutile phase was predominant. These phases were corroborated by XRD and Micro-Raman microscopy. All the tested surfaces were superhydrophilic (high surface free energy), and the superhydrophilic behavior is maintained

after at least 25 days, regardless of the heat treatment. The aim of produce nanotubes with different diameters and various heat treatments was to correlate the nanotube characteristics (morphology, internal diameter, composition) and the biologic behavior (cell adhesion and proliferation and antibacterial properties). The heat treated samples showed higher antibacterial properties in contrast to the as anodized samples. All nanotube coatings of TiO₂ were non-cytotoxic, nevertheless the anodization parameter or electrolyte composition used. However, some differences in terms of cell adhesion were found. Based on those results, these coatings can be applied as drug carriers, surface modification of biomaterial devices and catalyst, among others.

3:20pm D1-2-MoA6 Electrochemical Evaluation of Titanium Oxide Coatings Deposited on Magnesium Alloys, *B. Millan-Ramos, Universidad Nacional Autonoma de Mexico, México; J. Victoria-Hernandez, S. Yi, Magnesium Innovation Centre, Helmholtz-Zentrum, Germany; D. Letzig, Magnesium Innovation Centre, Helmholtz-Zentrum, Germany, Germany; P. Silva-Bermudez, Instituto Nacional de Rehabilitación, Mexico; S.E. Rodil (srodil@unam.mx), Universidad Nacional Autonoma de Mexico, México*

Titanium oxide (TiO₂) has been recognized as the active layer responsible for the good biocompatibility and osteogenic properties of the Ti-based medical alloys used for dental and orthopedic applications. Meanwhile, magnesium (Mg) and its alloys are currently widely researched for orthopedic applications, since their mechanical properties are more adequate to balance load transfer between bone and implant, but also due to its biodegradability. Extensive mechanical, in-vitro and in-vivo studies have been done to improve the biomedical performance of Mg alloys through alloying, processing conditions and surface modifications, including coating deposition. The main purpose of such modifications is to extend the degradation rate of the alloy in order to match it with bone self-healing time. In this work, we are investigating the use of titanium oxide coatings deposited by reactive magnetron sputtering on high purity Mg alloys.

Here, we present the electrochemical response of TiO₂-coated Mg-alloys in simulated physiological fluids. The results indicate that independently of the TiO₂ film thickness (60 - 250 nm) and the use of a Ti-buffer layer, the corrosion rate of the Mg alloy is not significantly reduced. Such response is probably associated to specific chemical reactions occurring between Mg and Ti that were not expected.

3:40pm D1-2-MoA7 Developments of Calcium Sulfate Coating on Ti6Al4V Substrate by Flame Spray, *W.C. Wu, Y.-C. Yang (ycyang@ntut.edu.tw), National Taipei University of Technology, Taiwan*

Due to the aging of global population, the demand of artificial joints is gradually rising. And in dental and orthopedic prosthesis, the outcome of the procedure depends greatly on the fixation of the implant. Covering the artificial joints with proper bio-ceramic can help the bone tissue grow into the porous structure. Thus, the purpose of this study is to create a ceramic-metal composites to accelerate the recovery after implanting. Calcium sulfate is a degradable bio-ceramics used widely as bone filler in current. It has good biocompatibility, no toxicity, osteoconductivity and abundant as well. In this study, calcium sulfate coating was successfully prepared on the Ti-6Al-4V substrate by flame spraying technique, and each property of the coating was analyzed. The experiment results showed that the bonding strength between substrate and calcium sulfate coating prepared by flame spraying could reach 37.02 MPa. The average porosity of the coating was 18.9% and the porous structure led the coating to rapid degradation and collapse. In the degradation test, the accumulated weight loss of the coating soaked in Hank's solution reached 100% on the fifth day. Besides, the high temperature of flame spray caused the calcium sulfate to decompose into calcium oxide and led the pH value of the SBF (simulated body fluid) to rise to 12 after 1 day of immersion. The power of flame spray was then lower to avoid the calcium oxide to appear. The pH value of the SBF after 1 day of immersion dropped to 11.3.

4:00pm D1-2-MoA8 Metallization of Polymers for Medical Applications, *A.R. Chacko (aarati.chacko@empa.ch), H.J. Hug, Empa - Swiss Federal Laboratories for Materials Science and Technology, Switzerland; S. Gauter, Christian-Albrechts-University Kiel, Germany; K. Thorwarth, Empa - Swiss Federal Laboratories for Materials Science and Technology, Switzerland*

Metallization of polymers has been of interest for years, as a means to achieve barrier coatings in packaging, biocompatible interfaces for medical implants, or to produce light-weight alternatives to metal parts in the automotive and aerospace industries, to cite a few examples. As the performance requirements of metalized plastics increase, so too must our understanding of plasma-polymer and metal-polymer interactions that occur in coating processes. High Power Impulse Magnetron Sputtering

Monday Afternoon, May 20, 2019

(HiPIMS) is a physical vapor coating method that allows one to span a whole range of energetic regimes; close to direct current sputtering, with low metallic ion discharge, up to almost fully ionized discharges. This versatile technique is our method of choice to study and tailor the substrate-film interphase region responsible for 'good' and long-lived coating adhesion.

In our study we vary the pulse-on/off time, thus controlling the time allowed for surface processes to occur between metal-species fluxes. We evaluate the chemical state of our interface using XPS and gauge the practical adhesion of the resulting films using a modified ASTM D4541 pull-off test. In addition, we study the effect of sample pre-treatment on adhesion, also using the above methods. The test metal-polymer system for this study is titanium on PEEK, which has shown exemplary adhesion in the case of orthopedic implants for use in spinal fusion surgery.

4:20pm D1-2-MoA9 Characteristics of a Composite Ceramic Coating Fabricated on Mg-1.2Zn-0.5Ca-0.5Mn Alloy Towards Biodegradable Bone Implants, H. Ibrahim (HAMDY-IBRAHIM@UTC.EDU), University of Tennessee at Chattanooga, USA; **D. Dean,** Ohio State University, USA; **M. Elahinia,** University of Toledo, USA

INTRODUCTION: Mg and its alloys possess a biodegradable nature that has recently made them attractive for developing biomedical devices that are expected to degrade and bioresorb completely *in-vivo* after the healing of the body tissue. In addition to their biodegradable nature, Mg alloys are biocompatible, and they have low density and modulus of elasticity, close to the bone. We have developed a patent-pending alloy, Mg-1.2Zn-0.5Ca-0.5Mn produced using biocompatible alloying elements, and a heat treatment process that is likely to provide the needed mechanical stability during bone healing and reliably resorb following the healing of a reconstructed skeletal segment. Our goal is to investigate the use of a composite ceramic-based coating to delay device corrosion (weakening) for 4-6 months.

METHODS: We heat-treated Mg-1.2Zn-0.5Ca-0.5Mn alloy samples to achieve significant mechanical strength and then coated them using plasma electrolyte oxidation (PEO) and layer-by-layer coating techniques to achieve corrosion resistance. The coated samples were characterized for their morphological and chemical properties using SEM, EDS and XRD methods. Finally, the corrosion characteristics before and after coating were determined using Potentiodynamic polarization test conducted in a simulated body fluid (SBF).

RESULTS: PEO-coated samples show pitting and pores, a common observation following PEO coating, and a tight junction with the subsequent layer-by-layer coatings. The composite coated samples showed a major enhancement in the corrosion resistance compared to the only PEO-coated and uncoated samples. The XRD patterns showed the presence of the incorporated compounds on the coating surface in addition to the presence of biocompatible corrosion products on the surface after corrosion such as hydroxyapatite (HA) and magnesium hydroxide (Mg(OH)₂). The use of heat treatment followed by composite ceramic coating may be beneficial for the fabrication of Mg-1.2Zn-0.5Ca-0.5Mn skeletal fixation devices with predictable resorption rates.

Advanced Characterization Techniques for Coatings, Thin Films, and Small Volumes Room Pacific Salon 1 - Session H2-2-MoA

Nanoscale Plasticity

Moderators: Timothy Rupert, University of California, Irvine, USA, **Olivier Pierron,** Georgia Institute of Technology, USA

1:40pm H2-2-MoA1 Assessing the Mechanical Properties of Thin Organic Semiconductor Coatings, S.J. Bull (steve.bull@ncl.ac.uk), Newcastle University, UK

A wide range of organic semiconductor coatings have been developed for optical and electronic applications and have been extensively characterised for their electronic and optical properties. What mechanical measurements have been made are focused on assessing the average properties of a film (e.g. using buckling to assess elastic moduli) but are not suitable to assess point-to-point variation in mechanical response which may be related to changes in coating microstructure due to crystallisation and/or phase separation. The assessment of time-dependent mechanical response is also lacking. This presentation will address the challenges of testing 100-300nm thin films of a range of organic semiconductors on a glass substrate to extract mechanical properties using nanoindentation at very low loads (peak loads less than 50µN). The importance of surface contamination and adhesion of
Monday Afternoon, May 20, 2019

the tip to the film, the effect this has on setting the conditions of first contact and the effect this has on measured properties will be discussed. The use of extrapolation methods to determine coating only properties will be assessed for both quasi-static and dynamic measurement techniques. Finally the effect of coating microstructure and surface roughness on the measured results will be discussed.

2:00pm H2-2-MoA2 In Situ TEM Activation Volume Measurements, S. Gupta, S. Stangebye, J. Kacher, O.N. Pierron (olivier.pierron@me.gatech.edu), Georgia Institute of Technology, USA

Signature parameters such as true activation volume are often characterized to identify the governing plastic deformation mechanisms. The current state-of-the-art for characterizing thermally-activated dislocation mechanisms consist of measuring activation volume (using transient tests), along with separate *in situ* TEM observations to provide hints about the actual mechanisms. In this work, we take advantage of recent advances in quantitative *in situ* TEM nanomechanics to simultaneously measure activation volume and perform *in situ* TEM observations of the governing mechanisms. This talk will demonstrate the use of a MEMS device to measure true activation volume based on repeated stress relaxation experiments performed inside the TEM. The technique is demonstrated on 100-nm-thick Au and 200-nm-thick Al micro-specimens, providing true activation volume values of 5 and 10 b³, respectively. These values will be interpreted in light of the TEM observations performed during these experiments, highlighting mechanisms dominated by grain boundary – dislocation interactions.

2:20pm H2-2-MoA3 In-situ Microscale Mechanical Testing of Metal/Ceramic Interfacial Regions, X. Zhang, Y. Mu, S. Shao, W.J. Meng (wmeng1@lsu.edu), Louisiana State University, USA

Application of ceramic coatings onto substrates is an important means of tuning the near-surface mechanical, chemical, and tribological properties of machining tools and mechanical components for improved performance and durability. Successful application of coatings demands adequate interfacial mechanical integrity [1]. Effective engineering of the coating/substrate interfacial region is predicated on establishing experimental protocols for quantitative measurement of interfacial mechanical response and understanding key mechanisms governing interfacial mechanical failure.

We will summarize our results on using in-situ microscale mechanical testing for quantitatively assessing mechanical integrity of metal/ceramic interfacial regions under shear, compression, and tension loading. Quantitative mechanical testing of interfacial regions was accomplished through in-situ SEM instrumented compression and tension loading of focused ion beam fabricated micro-pillars, in which metal/ceramic interfacial regions are placed at various inclinations with respect to the pillar axis [2,3,4]. Such testing, in combination with in-situ SEM observations and detailed post-mortem characterizations, provides new data and new insights on interfacial mechanical failures under different loading conditions. Accompanying simulations, combining density functional theory, molecular dynamics, and crystal plasticity finite element, provide additional mechanistic interpretations for observed interfacial failures [5,6]. Results of testing on metal/ceramic epitaxial interfaces will also be discussed.

References:

- [1] J.C. Jiang, W.J. Meng, A.G. Evans, C.V. Cooper, Structure and mechanics of W-DLC coated spur gears, Surf. Coat. Technol. 176, 50-56 (2003).
- [2] K. Chen, Y. Mu, W.J. Meng, A new experimental approach for evaluating the mechanical integrity of interfaces between hard coatings and substrates, MRS Comm. 4, 19-23 (2014).
- [3] Y. Mu, J.W. Hutchinson, W.J. Meng, Micro-pillar measurements of plasticity in confined Cu thin films, Extreme Mech. Lett. 1, 62-69 (2014).
- [4] Y. Mu, X. Zhang, J.W. Hutchinson, W.J. Meng, Measuring critical stress for shear failure of interfacial regions in coating/interlayer/substrate systems through a micro-pillar testing protocol, J. Mater. Res. 32, 1421-1431 (2017).
- [5] X. Zhang, B. Zhang, Y. Mu, S. Shao, C. D. Wick, B.R. Ramachandran, W.J. Meng, Mechanical failure of metal/ceramic interfacial regions under shear loading, Acta Mater. 138, 224-236 (2017).
- [6] X. Zhang, Y. Mu, M. Dodaran, S. Shao, D. Moldovan, W.J. Meng, Mechanical failure of CrN/Cu/CrN interfacial regions under tensile loading, Acta Mater., doi.org/10.1016/j.actamat.2018.08.046 (2018).

Monday Afternoon, May 20, 2019

2:40pm **H2-2-MoA4 Nano-wedging: A Novel Test Method to Combine Nanoscale Strain Mapping with Multiaxial Stress States, T.E.J. Edwards (thomas.edwards@empa.ch)**, Empa - Swiss Federal Laboratories for Materials Science and Technology, Switzerland; *F. Di Gioacchino, J.T. Pürstl*, University of Cambridge, UK; *X. Maeder*, Empa - Swiss Federal Laboratories for Materials Science and Technology, Switzerland; *W.J. Clegg*, University of Cambridge, UK; *J. Michler*, Empa - Swiss Federal Laboratories for Materials Science and Technology, Switzerland

A novel small-scale mechanical test geometry is presented, which enables a multi-axial stress state to be generated and the deformation characterised in-situ by two non-destructive strain mapping techniques – digital image correlation (nDIC) of a nanoscale Pt speckle pattern e-beam deposited on the side surface of testpieces, and high resolution electron backscatter diffraction (HR-EBSD). To date, such strain mapping methods have only been applied to small-scale mechanical test geometries where the stress state is nominally uniaxial – micropillars, microcantilevers – or at crack tips. By indenting a vertical wall, supported at both ends, with a wedge-shaped indenter, a stress state can be generated which is similar to that produced by standard surface indentation techniques. This method hence gives insight into the evolution of plastic and elastic strains throughout the depth of the material as indentation progresses, in the loaded or unloaded state. Finite element modelling of the test geometry has enabled the nominal stress distribution to be assessed.

This experimental method has been applied to several pure metals – f.c.c., b.c.c and h.c.p – to investigate the evolution of slip band spacing as a function of indentation depth and local plastic strain. It has also been used on MAX phases investigated as novel coating materials for zirconium-based nuclear reactor fuel rod cladding alloys, where certain deformation mechanisms in the MAX phases are not activated in simple uniaxial straining test geometries.

3:00pm **H2-2-MoA5 Micromechanical Characterisation of Ag/Au Multilayers by Means of Bulge and Nanoindentation Testing, S. Krauß (sebastian.s.krauss@fau.de)**, *M. Göken, B. Merle*, Friedrich Alexander-University Erlangen-Nürnberg (FAU), Germany

The mechanical properties of metallic thin films are of paramount importance for the performance and reliability of MEMS devices. An approach to further improve the mechanical properties is to introduce a multilayered structure of alternating materials. Therefore metallic Ag/Au multilayered thin film systems were fabricated by thermal evaporation. The overall thickness of the thin film stacks was kept constant to 800 nm, whereas the number of layers in the film and therefore the individual layer thickness were modified. Multilayered systems containing two to sixteen layers were created, resulting in individual layer thicknesses ranging from 400 nm to 50 nm. The microstructure and morphology of the thin films were investigated by atomic force microscopy (AFM) and by cross-sectioning with a focused ion beam system (FIB). The mechanical properties of the thin films were investigated by nanoindentation on glass substrates and by bulge testing of released membranes. The investigations include hardness, yield stress and fracture toughness analysis and are correlated to the microstructure produced by the evaporation process.

3:20pm **H2-2-MoA6 Size Effect on Superplastic Flow – In situ Micromechanical Characterization of Superplastic Zn-22% Al, P. Feldner (Patrick.Feldner@fau.de)**, *M. Göken*, University Erlangen-Nürnberg, Germany; *B. Merle*, Friedrich Alexander-University Erlangen-Nürnberg (FAU), Germany

Superplastic micro & nanoforming has a great potential for a high throughput production of small-scale structural devices with complex geometries. However, it has not yet been established if the macroscopically observed superplastic behavior also persists at microscopic length scales and which fundamental processes govern structural superplasticity in metallic alloys.

For this reason, the micro & nanomechanical properties of the superplastic alloy Zn-22% Al were characterized as a function of the specimen size, using different, complementary in situ micromechanical testing techniques, including micropillar compression in a scanning electron microscope as well as in a X-ray microscope and tensile testing in a transmission electron microscope.

The resulting deformation kinetics clearly reveal a superplastic trend even at the micro scale. However, below a critical specimen volume a breakdown of the superplastic flow behavior is revealed, which is associated with a loss of ductility. Based on the intra as well as intercrystalline deformation morphology observed during in situ testing, this change of the rate-

controlling deformation process is discussed in terms of a transition from boundary mediated ductility to boundary mediated brittleness.

3:40pm **H2-2-MoA7 Studies on the Mechanisms in Hexagonal Close Packed Metal Nanolaminates, I.J. Beyerlein (beyerlein@ucsb.edu)**, University of California, Santa Barbara, USA

INVITED

The goal of this study is to better understand the mechanisms underlying the mechanical response of nanolayered composites containing either pseudo-morphic body center cubic (BCC) Mg or hexagonal close packed (HCP) Mg phases. Nanolayered composites comprised of 50% volume fraction of Mg and Nb were synthesized using physical vapor deposition with individual layer thicknesses h ranging from 2.5 nm to 50 nm. At the lower layer thicknesses of $h < 5$ nm the Mg phase was found to have undergone a phase transition from HCP to BCC, such that it formed a coherent interface with the adjoining Nb phase. Hardness testing and micropillar compression testing normal, 45 degrees, and parallel to the interface plane showed that the BCC Mg composite is much stronger and can sustain higher strains to failure. A multiscale, crystal plasticity model incorporating a confined layer slip model for h -dependent critical resolved shear stresses was developed and applied to understand the linkage between the observed deformation response and underlying mechanisms. Calculations from the model predict that the more homogeneous deformation and reduced plastic anisotropy of the bcc Mg/Nb material compared to the hcpMg/Nb results from dislocation-mediated plasticity on the {110} and {112} slip systems in the Mg phase. The hcp Mg/Nb phase exhibits significant plastic anisotropy due to large differences among the slip strengths of the three HCP slip systems.

4:20pm **H2-2-MoA9 Critical Assessment of the Criteria for Minimum Indentation Spacing, S.P. Pardhasaradhi (spphani@yahoo.com)**, ARCI, India; **W.C. Oliver**, KLA-Tencor, USA

With the advances in nanoindentation measurement instrumentation and the associated testing methodologies, high speed indentation mapping with indents that take less than a second to perform, is now possible. This enables mapping large areas with thousands of indents within a few hours which is extremely useful to measure the local mechanical properties of multi-phase alloys, coatings and small volumes of materials. The combination of high-speed mapping techniques and the continuous push towards understanding the mechanical properties of small volumes of materials, has now put greater emphasis on the minimum spacing of indents. In this work, a critical assessment of the minimum spacing of indents is performed, by a combination of extensive indentation experiments (~ 50000) and finite element simulations at different spacings for a wide range of materials including bulk materials and coatings. It was found that a minimum indent spacing of 10 times the indentation depth is sufficient to obtain accurate results for a Berkovich indenter. This is less than half of the commonly followed criteria of spacing the indents three times the size of the indent, which for a Berkovich indent, is approximately 20 times the indent depth. Similar results were also found for other indenter geometries. Finite element simulations are carried out to visualize the plastic zone beneath the indents and to rationalize the experimental findings. It was found that non-overlapping plastic zones is not a requirement for determining the minimum indent spacing and the observed minimum spacing criteria can be rationalized by simple indentation energy arguments. These results were also found to be applicable for a gold film on a glass substrate, which is an extreme case of soft film on hard substrate that shows significant pile-up. These results have significant ramifications for indentation mapping wherein the indents can now be placed much closer than what was traditionally accepted which enables high resolution mechanical property mapping.

4:40pm **H2-2-MoA10 Surface Laboratory Assistant – The New Combination of Measurement Device and Analysis Software, N. Bierwisch (n.bierwisch@siomec.de)**, *N. Schwarzer*, SIO, Germany

Nowadays the used materials or material combinations in all application fields (e.g. optical, avionic or automotive industry) are getting more and more complex. These complex structures are needed in order to increase the performance and lifetime of the components. Such improvements of each part of your complex device, tool or structural element are necessary to reach the performance goals demanded by the desired application. This increased complexity demands extended analysis and optimization methods. Classical engineering methods and rules of thumb aren't enough anymore.

Proper characterization and optimization of such structures requires invertable mathematical tools of sufficient holistic character. Unfortunately, as such tools are often unavailable trial and error or half empirical sensitivity analysis methods in combination with FEM or BEM are applied. Thereby faster tools could help significantly to save development time and costs [1].

Monday Afternoon, May 20, 2019

All models (FEM or analytical based) will need exact and generic material parameters for each part of the material system.

SIO [2] has developed several software modules to determine these parameters from different measurement types and created a variety of easy to use software packages which combine these modules.

There are many different measurement devices, where the results could – in principle – be wonderfully combined and successively be applied to obtain a very holistic picture of the strength and weaknesses of a piece of material one is interested in. Only problem there: So far there was no proper joint sewing all these tests and the results they produce seamlessly together.

This unsatisfying situation has changed now.

The talk will demonstrate how the so-called “Surface-Laboratory-Assistant” automatically not only combines various tests, but also improves them, makes suggestions for the next – higher level – test and even automatically starts and subsequently analyses it.

This way and just by the press of a button and in one go, you could get a most comprehensive and sophisticated holistic material analysis from a simple indentation test, via physical scratch up to complex and application orientated tribo-tests.

Topical Symposia

Room Pacific Salon 3 - Session TS3+4-2-MoA

Surface Engineering for Lightweight Materials & Thin Film Materials for Flexible Electronics

Moderators: Klaus Böbel, Robert Bosch GmbH, Germany, **Oleksandr Glushko**, Erich Schmid Institute of Materials Science, Austria, **Nicholas Glavin**, Air Force Research Laboratory, Materials and Manufacturing Directorate, USA

2:20pm **TS3+4-2-MoA3 Electro-mechanical Reliability of Flexible Electronics: An Overview of Testing and Characterization Techniques, O. Glushko (oleksandr.glushko@oeaw.ac.at), M.J. Cordill**, Erich Schmid Institute of Materials Science, Austria

In this presentation an overview of three main mechanical test concepts will be given along with numerous examples of the reliability parameters which can be gained from these tests. Monotonic tensile test is a standardized technique which is used for characterization of general mechanical reliability parameters of a flexible system under tension. It will be shown how to describe general material behavior (from brittle to ductile), determine the crack onset strain or estimate the density and lengths of cracks with the help of tensile test combined with in-situ measurements of electrical resistance. Cyclic tensile (fatigue) testing is a well-established method to examine the stability of flexible components when small amounts of mechanical strain are repeatedly applied. Examples of different types of damage development with the cycle number will be given for materials with different microstructures. Finally, bending tests are required to prove the mechanical performance under conditions which closely simulate the real usage conditions of a flexible electronic device. Because there is no unified approach or standard for flexible electronics, different available bending test methods will be reviewed along with the typical cases of mechanical response. A special emphasis on the correlation between mechanical damage and the degradation of electrical conductivity will be made. It will be shown that, under given conditions, significant topological changes in metallization layers might occur without pronounced growth of measured electrical resistance.

2:40pm **TS3+4-2-MoA4 Bending Fatigue of Al/Mo Bilayers on Polymer Substrates with Varied Al Layer Thickness, P. Kreiml (patrice.kreiml@unileoben.ac.at), M. Rausch, V.L. Terziyska**, Montanuniversität Leoben, Austria; **J. Winkler**, Plansee SE, Austria; **C. Mitterer**, Montanuniversität Leoben, Austria; **M.J. Cordill**, Austrian Academy of Sciences, Austria

In traditional display technologies for rigid flat panel displays, magnetron sputter deposited Mo thin films, acting both as diffusion barrier and adhesion layer, are often used in combination with Al thin films, acting as charge carrying layer. With the increasing demand for flexible displays, for instance for the application in foldable smartphones, the mechanical limitations of these systems have to be systematically investigated and fully understood. *In situ* straining experiments, combining optical and electrical failure analyses, demonstrated the dominance of the brittle Mo layer on the bilayer fracture and increasing the Al-layer thickness has proved to lighten its impact. Although general trends can be made visible from that approach,

no quantified lifetime predictions under conditions close to reality can be drawn. Due to that a series of Al/Mo bilayers was magnetron sputter deposited on polymer substrates, keeping the thickness of the Mo layer at constant 30 nm and varying the thickness of the Al layer on top from 30 over 75 to 150 nm. These thin films were then tested on a custom-built bending device at different modi: (i) 20,000 cycles of compressive bending strains, (ii) 20,000 cycles of tensile bending strains and (iii) alternating 10 cycles compressive and 10 cycles tensile bending strains, leading to overall 20,000 cycles of mixed applied bending strains at strains of 0.5, 1.3 and 3.1 %. In combination with intermittent optical and resistance measurements, a quantification of the electro-mechanical behavior could be conducted. The data gained from these experiments reveal the physical limits of the Al/Mo system. It will be shown that an optimized thickness ratio, an adequate choice of bending load and bending strain lead to acceptable lifetimes for flexible back-plane electrodes.

3:00pm **TS3+4-2-MoA5 Enabling High-Power Flexible Devices through Tailored Nanocomposite Interface Materials, K. Burzynski (burzynskik1@udayton.edu)**, University of Dayton, USA; **N. Glavin**, Air Force Research Laboratory, Materials and Manufacturing Directorate, USA; **E. Heller, M. Snure, E. Heckman**, Air Force Research Laboratory, Sensors Directorate, USA; **C. Muratore**, University of Dayton, USA

Consumers and military personnel are demanding faster data speeds only available through fifth generation (5G) wireless communication technology. Furthermore, as wearable sensors and other devices become more ubiquitous, devices demonstrating enhanced flexibility and conformality are necessary. A fundamental challenge for flexible electronics is thermal management. Even on rigid substrates with significantly higher thermal conductivity than polymeric and other flexible substrates, the full potential of semiconducting materials is often thermally limited. The flexible gallium nitride (GaN) high electron mobility transistors (HEMTs) employed in this work are grown on a two-dimensional boron nitride (BN) release layer that allows the conventionally processed devices on sapphire wafers to be transferred using a polymeric stamp and placed onto a variety of rigid and flexible substrates. Characterization of the GaN device behavior on the as-grown sapphire wafers (prior to transfer) provide a baseline for evaluation of the thermal performance of engineered interfaces and substrates. With conventional substrates, device performance (specifically, the saturation current) is reduced when the device is transferred to polymeric substrates. The thermal dissipation is further restricted due to the addition of an adhesive layer to the substrate. Thermal imaging of devices in operation reveals that the current passing through an as-grown GaN transistor on a sapphire wafer reaches the target operating temperature at approximately five times the power of the same device transferred to a flexible substrate. Printable, thermally conductive nanocomposites integrating 1D, 2D, and 3D forms of carbon in a flexible polymer matrix, as well as metal nanoparticles, were developed to maximize heat transfer from GaN devices. The thermal conductivity of the candidate substrate materials was measured experimentally to have more than a 300 percent increase in thermal conductivity, and the performance of devices transferred to these novel flexible composite substrates was characterized. The measured thermal data was used in computational simulations to predict flexible substrate architectures effectively promoting point-to-volume heat transfer to further improve device performance. Additive manufacturing for engineered architectures of the flexible, thermally conductive substrate materials was demonstrated to substantially reduce the thermal limitation of high-power flexible electronics.

3:20pm **TS3+4-2-MoA6 Plasma Polymers...A Family of Materials that is Full of Surprises, R. Snyders (rony.snyders@umons.ac.be)**, University of Mons, Belgium

INVITED

Through the years, plasma polymerization has become a well-established technique for the synthesis of almost atomically flat functionalized organic thin films which are nowadays mostly used in the biomedical field. Nevertheless, in order to further extend the application fields of these materials (supports for nanoparticles, active surface for the detection of biomolecules...), a large surface area is often necessary. In this work, we develop plasma-polymer based platforms for the stabilization of gold nanoparticles that are active in the degradation of VOC molecules. In addition to the approach consisting to grow this material onto powders or paper substrates in order to increase the surface to volume ratio, we also develop strategies allowing for a structuration, at the micro/nano-scale, of these surfaces. The present presentation will focus on this part of the work. It will be described how we have established a method that allow the self nano-structuration of plasma polymers coatings by adapting their mechanical properties. Specifically, it is demonstrated that a fine control of

Monday Afternoon, May 20, 2019

the latter by tuning of their crosslinking degree is a promising strategy to generated wrinkling phenomenon in these materials. In this context, our results unambiguously reveal the key role of the growth temperature on the mechanical properties of the deposited layer. Particularly, it has been reported that soft viscoelastic plasma polymer layer can be synthesized by depositing the coating at temperature below 273 K. Taking advantage of this discovery, it was possible to design nano/micro patterned surfaces by combining such a viscoelastic plasma polymer surfaces with a more elastic (plasma polymer) layer. The obtained patterns are generated by complex wrinkling and degassing mechanisms that will be discussed in the presentation.

4:00pm **TS3+4-2-MoA8 Environmental Challenges of Thin Film Systems on Polymer Substrates for Space Applications, B. Putz (barbara.putz@oeaw.ac.at)**, Erich Schmid Institute of Materials Science, Austrian Academy of Sciences, Leoben, Austria; *G. Milassin, C. Semprinoschnig*, European Space Research and Technology Centre; *M.J. Cordill*, Erich Schmid Institute of Materials Science, Austrian Academy of Sciences, Leoben, Austria

Multilayer thin film systems on flexible polymer substrates build up optical solar reflectors (OSR) for thermal insulation of satellites and spacecraft. During one year of operation a satellite in low earth orbit (LEO) typically encounters 6000 thermal cycles of $\pm 100^\circ\text{C}$. Due to the different coefficients of thermal expansion between the individual layers and the substrate it is important to investigate the thermo-mechanical stability of the composites as a function of the cyclic heat load. Scanning electron microscopy and focused ion beam cross-sectioning revealed, that the Inconel-Ag-Teflon system, currently used as OSR material in orbit, forms through thickness cracks and cavities in the Ag layer during thermal cycling of $\pm 150^\circ\text{C}$ in a gaseous N_2 atmosphere. Crack and cavity formation start at very low cycle numbers, which is detrimental to the reflectivity (Ag) corrosion protection (Inconel) and considerably diminish the insulation capacity of the OSR. Combined in-situ surface imaging, film resistance (4 Point Probe setup) and film stress measurements (X-ray diffraction $+\sin^2\psi$) during straining revealed that also electro-mechanical properties of the bi-layer system are dramatically influenced, emphasizing the need to improve multilayer design and resistance of versatile metal-polymer compounds against thermal cycling. In this work, sputter deposited thin film metallic glasses (TFMG), combining metallic bonding and an amorphous microstructure, are introduced as novel coatings to overcome the problems of current multilayer OSR systems. Results indicate that this new and innovative type of thin films are ideal candidates to withstand the extreme thermal cycling as well as the harsh space environment.

4:20pm **TS3+4-2-MoA9 Sputtered Thin Film Sensors for Self-sensing Composite Materials, F.G. Cougnon (Florian.Cougnon@ugent.be), A. Lamberti, W. Van Paepegem, D. Depla**, Ghent University, Belgium

The wide-spread use of fibre-reinforced composite materials in big structures such as planes, windmills or pedestrian bridges, combined with the unacceptably high cost of material-failure, has vastly pushed the demand for structural health monitoring of composite materials. Structural health monitoring nowadays evolved from periodic quality inspections and surface-bounded sensing networks towards continuous monitoring of the entire in-service life time by sensing networks embedded in the material. In order not to degrade the structural integrity of the host material, the spatial dimensions of the embedded sensors should be as small as possible. Therefore we focus on the development of embedded thin film sensors – deposited by magnetron sputtering – such as thermocouples for measuring temperature and antennas for wireless measurements of strain and temperature through shift in resonance frequency. It is a challenging task to deposit well-performant thin film sensors onto temperature sensitive polymeric substrates. On the one hand, the electrical properties of the thin films mainly scale with the energy flux delivered towards the growing film. The temperature sensitivity of the substrate however demands tuning of the energy flux in order not to degrade the quality of the polymer. On the other hand, tuning the energy flux is often unambiguously correlated with an increased impurity flux towards the substrate. These impurities originate from residual gasses in the vacuum chamber and outgassing from the polymeric substrate and can have a large impact on the overall film properties as well. In this work, the link between energy flux, impurity flux and electrical properties of thin films grown by magnetron sputtering is unraveled from a fundamental point-of-view and exploited to fine-tune embedded thin film sensors towards applications for smart composite materials.

4:40pm **TS3+4-2-MoA10 A New Method for Influencing Coating Properties on Polymer Substrates at Low Temperature: High Power Impulse Magnetron Sputtering (HIPIMS) with Positive Voltage Reversal, A. Wennberg (ambiorn.wennberg@nano4energy.eu)**, Nano4Energy SL, Spain; *M. Simmons*, Intellivation, USA; *F. Papa*, GP Plasma, Spain; *I. Fernandez*, Nano4Energy SL, Spain

Current engineering and material advances are shifting manufacturing in many areas from solid bulk materials to flexible lightweight materials. Although these materials, such as polymers, are lightweight, flexible and tough, there are challenges to engineering coatings on such substrates as they insulating and not able to withstand high temperatures. This gives rise to the challenge of how to deposit high quality thin film coatings on such substrates. High Power Impulse Magnetron Sputtering (HIPIMS) has shown many advantages over conventional sputtering which is commonly used to deposit metals, metal nitrides and metal oxides on polymer web. With HIPIMS, a fraction of the target material will be ionized while the ion energy distribution function will shift to energies about 10 times greater than those for DC discharges. However, this increase in ionization and energy will give only modest changes on an unbiased substrate. With the addition of a positive voltage reversal pulse adjacent to the negative HIPIMS sputtering pulse, these ions can be accelerated towards the substrate providing energy for film nucleation and densification.

In this study, an industrial scale (330 mm wide web) web coater was used to deposit TiO_2 and Cu coatings as well as other metal nitride and metal oxide coatings on PET at room temperature. Improvements in film density and grain size can be clearly seen compared to DC or pulsed DC sputtering. The effect on the index of refraction, extinction coefficient and barrier properties are also investigated.

5:00pm **TS3+4-2-MoA11 Tribological Challenges and Surface Engineering Solutions for Extreme Environments and Lightweight Materials, A.L. Korenyi-Both (Andy@tribologix.com)**, Tribologix, Inc., USA **INVITED**

Moving mechanical assemblies that are used in extreme environments are often coupled with unique challenges for maintaining intended operational requirements. Conventional material selection becomes narrow and often native surfaces are not robust enough to handle extreme requirements. Surface modification techniques that are uniquely suited for special materials and their relevant operating environments must be carefully chosen from trusted knowledge bases or heritage based know-how. To further assure mission success modeling through simulation and specialized mechanical testing becomes critical. Surface analytical techniques, including in-situ data monitoring become an integral part of testing and simulation. To help offset the high costs often associated with placing moving mechanical assemblies in to extreme or high distance environments the choice of materials is further narrowed by intentional light-weighting for gains in economy. Lightweight material performance also needs to have careful attention placed on surface interactions and coating techniques to improve these surfaces are typically novel in nature. With a clear understanding of interacting surfaces, environmental factors, available options for treatments/coatings, risks associated with wear can usually be successfully mitigated. Several interesting and challenging extreme environment tribological cases are highlighted to provide further in-sight in to this area of science and engineering.

Coatings for Use at High Temperatures

Room Pacific Salon 2 - Session A1-1-TuM

Coatings to Resist High-temperature Oxidation, Corrosion, and Fouling I

Moderators: Justyna Kulczyk-Malecka, Manchester Metropolitan University, UK; Lars-Gunnar Johansson, Chalmers University of Technology, Sweden; Shigenari Hayashi, Hokkaido University, Japan

8:00am **A1-1-TuM1 Modeling the Influence of Heat Treatment and Base Alloy Composition on the Performance of Aluminide Coatings for High Performance Engine Valve Alloys**, R.P. Pillai (pillairr@ornl.gov), S.N. Dreypondt, B.L. Armstrong, Q. Guo, K. Unocic, G.M. Muralidharan, Oak Ridge National Laboratory, USA

Ni-based alloys are currently being used for engine valves in internal combustion engines. The currently employed valve alloys have reached their operational limit and the need to increase engine efficiency and hence operating temperatures combined with the added challenge of low component cost tolerance makes high temperature materials selection for durability and cost a primary concern since there are fewer lower-cost materials which possess sufficient oxidation, creep and fatigue resistance.

Protective metallic nickel aluminide (NiAl) diffusion coatings enhance the oxidation and corrosion resistance of the underlying high temperature materials. However, the substrate composition and specimen geometry influence the final coating microstructure during the aluminising process and govern the high temperature behavior of the coating system during subsequent exposure. Potentially detrimental phases may form in the interdiffusion zone (IDZ) during the aluminizing process. The formation of a protective alumina scale and the diffusion from the coating into the substrate during subsequent service result in the loss of Al and thereby the dissolution of the β -NiAl phase in the coating. The compatibility of a given type of a coating with its base material substantially influences the performance of a coated material during service. Evaluation of the coating's high temperature behavior requires extensive experimental testing, but computational methods can substantially reduce these efforts required for coating evaluation and qualification.

In the current work, a coupled thermodynamic and kinetic computational model was employed to predict the microstructural evolution in nickel aluminide (NiAl) diffusion coatings on the Ni-base 31V alloy (UNS N07032) and new recently developed high strength alloys during the coating (aluminising) process. Various heat treatment procedures were assessed to optimize the coating microstructure. The model was also used to predict the microstructural evolution of coated 31V coupons exposed at 800°C for up to 5,000h.

Element concentrations and phase distribution were obtained by scanning electron microscopy (SEM). Phases were identified by energy/wavelength dispersive X-ray spectroscopy (EDX/WDX) and electron backscatter diffraction (EBSD). The model predicted the formation of sigma phase and carbides of the MC-type in the IDZ of the coating on 31V which was in agreement with experimental observations. The computational approach provides a general approach in predicting the IDZ microstructure during manufacturing and estimating the extent of microstructural changes in the coating as a function of alloy/coating composition, time and temperature.

8:20am **A1-1-TuM2 Fabrication, Characterisation and Testing of Cr Coated Zr Alloy Nuclear Fuel Cladding for Enhanced Accident Tolerance**, A. Evans, Manchester Metropolitan University, UK; D. Goddard, National Nuclear Laboratory, UK; A. Cole-Baker, Wood plc, UK; G. Obasi, M. Preuss, Manchester University, UK; E. Vernon, National Nuclear Laboratory, UK; P. Kelly (peter.kelly@mmu.ac.uk), Manchester Metropolitan University, UK

The deposition of an oxidation resistant Cr coating on Zr alloy nuclear fuel cladding is an advanced concept for deployment of an accident tolerant fuel, which is attracting considerable interest in the market. Improvements have been shown relative to uncoated Zr alloys in both operational conditions and when subjected to high temperature steam. Initial irradiation testing of this concept is also in progress. In the UK, a collaborative programme of research is investigating Cr deposition using magnetron sputtering. This research is examining how the integrity and microstructure of the coating is affected by deposition conditions and coating thickness for both flat coupons and short lengths of Zr alloy tube. Test coatings have been subjected to static autoclave tests under standard PWR operating conditions, as well as accelerated tests in air at 900°C and in 400°C steam. The as-deposited and post-testing coatings have been characterised using SEM/EDX and XRD to determine structure, texture and residual stress and, in the latter case, damage arising from testing. Initial results have shown significant

Tuesday Morning, May 21, 2019

differences in the stress condition in the coatings as a function of deposition parameters. Furthermore, selected coatings have successfully undergone accelerated oxidation tests with little or no discernible detrimental effects.

8:40am **A1-1-TuM3 High-temperature Oxidation Resistance and Self-healing Capability of HiPIMS Cr-Al-C Coating on Zr-based Alloy**, M. Ougier (michael.ougier@cea.fr), A. Michau, F. Lomello, CEA, Université Paris-Saclay, France; F. Schuster, CEA Cross-Cutting Program on Materials and Processes Skills, France; H. Maskrot, M.L. Schlegel, CEA, Université Paris-Saclay, France

The development of nuclear accident-tolerant fuels (ATF) claddings has gained new momentum since Fukushima Daiichi accident. The primary goal of this study is to develop alternative fuel claddings which are more resilient to high-temperature steam oxidation to reduce hydrogen generation during loss-of-coolant-accident (LOCA). A promising solution is to protect the claddings by metallic or ceramic coatings, such as MAX phases. In order to resist such accidental conditions, the oxide coatings need to be physically and chemically stable in normal operating conditions and accidental (steam) situations; also, they should act as protective barrier against oxygen diffusion. Al-containing MAX phases, as Cr₂AlC, possess excellent high-temperature oxidation resistance both in air and in humid atmosphere due to the formation of a dense and adherent alumina scale. In this work, Cr-Al-C thin films were synthesized as coatings on Zr-based alloy from a Cr₂AlC compound target by high-power magnetron sputtering (HiPIMS) and subsequent thermal annealing. The crystal structure, microstructure and oxidation behavior of these films were investigated in air. As-deposited coatings are dense and amorphous regardless the deposition temperature (between 25 to 450°C). The effect of the annealing post-treatment was studied by *in situ* X-ray diffraction from 550 to 650°C in helium for up to 12 h. In such conditions, HRTEM analysis demonstrated that the amorphous coating partially crystallized into Cr₂AlC nanocrystals above 600°C. Microcracks also appear on the surface for very thick films, due to the release of residual stresses originating from both the mismatch in thermal expansion coefficients of the coating and the substrate, and from internal stresses. Oxidation at temperatures up to 1200°C in air reveals no significant oxidation of the substrate thanks to the growth of a dense and protective Al₂O₃ layer fully covering residual Cr carbides. Voids also formed at the interface between oxide and Cr carbides. The relative weight gain of coated samples typically decreases by 80% compared with uncoated Zr-based alloy. Furthermore, coatings also possess a self-healing capability due to the formation of alumina within microcracks. In addition, water quenching tests prove that coatings demonstrate high adherence and thermal-shock resistance. As a comparison, the oxidation behavior of the crystalline film is also conducted. Results indicate that Cr-Al-C thin films grown by HiPIMS process are promising candidates for ATF cladding coatings.

Keywords : Accident-Tolerant Fuels, MAX phase coating, physical vapor deposition, oxidation resistance, self-healing

9:00am **A1-1-TuM4 Ceramic Coatings for Protection of Ti and Zr Alloys at High Temperature**, P. Xiao (p.xiao@manchester.ac.uk), Z.H. Gao, X. Zhang, H. Liu, University of Manchester, UK; J. Kulczyk-Malecka, P. Kelly, Manchester Metropolitan University, UK; Z. Zhang, University of Manchester, UK

INVITED

SiAlN coating have been produced with use of magnetron sputtering on both Ti and Zr alloy substrates for protection from oxidation in both air and steam environments. The coatings have demonstrated excellent oxidation resistance tested in both air and steam and the strong coating/substrate bonding, measured with use of scratch testing. Electron microscopy has been used to understand the oxidation mechanisms and the mechanisms controlling the coating/substrate adhesion. The study has presented that the coatings are very promising for protection of Ti and Zr alloys from oxidation in air and steam at high temperature.

9:40am **A1-1-TuM6 Multi-functional AlZr-TiO₂ Bilayer Coatings Combining Anticorrosion and Antifouling Properties**, C. Villardi de Oliveira (caroline.villardi_de_oliveira@utt.fr), ICD-LASMIS, Université de Technologie de Troyes, France; A.A. Alhussein, University of Technology of Troyes (UTT), France; C.J. Jiménez, Univ. Grenoble Alpes, CNRS, France; Z. Dong, School of Materials Science and Engineering, Nanyang Technological University, Singapore; F. Schuster, CEA, PTCMP, France; S. Narasimalu, School of Materials Science and Engineering, Nanyang Technological University, Singapore; M.L. Schlegel, CEA, Université Paris-Saclay, France; F. Sanchette, Nogent International Center for CVD Innovation, LRC CEA-ICD LASMIS UMR6281, UTT, Antenne de Nogent, France

Fouling in marine environment is a costly problem and can be described by the development of biofilms containing various types of micro and macro-

organisms, which can enhance the processes and rates of steel corrosion in saline seawater. TiO₂ coating shows photocatalytic activity and hydrophilic behavior which can promote antifouling properties in order to minimize the biofouling process in the marine structures. Photocatalytic oxidation is a non-toxicity low cost promising technology to control fouling in submerged surfaces by generation of reactive oxygen species [1]. In this work we present a multi-functional coating made by an anticorrosion Al-Zr interlayer covered by an antibiofouling TiO₂ top layer. Al-Zr film is proposed as a potential candidate for affording sacrificial corrosion resistance of steels since it presents a good compromise between the mechanical reinforcement and the electrochemical properties[2].

Steel substrates were initially coated by magnetron sputtering with Al-Zr alloy (3 μm thick films) containing 5 at.% Zr. TiO₂ films were deposited on the top of the Al-Zr layer by atmospheric pressure Aerosol-Chemical Vapor Deposition (AACVD). The structure and morphology of the multi-functional coatings were analyzed by XRD and SEM. Photocatalytic activity using Orange G under UV light and electrochemical tests in saline solution were performed. The biofouling behavior and performance in natural seawater were also tested by in situ immersion tests.

Keywords: Al-Zr alloys, magnetron sputtering, steel protection, biofouling, TiO₂, AACVD, Photocatalysis.

References

[1] Liu, H., Raza, A., Aili, A., Lu, J., AlGhaferi, A., & Zhang, T. (2016). Sunlight-sensitive anti-fouling nanostructured TiO₂ coated Cu meshes for ultrafast oily water treatment. *Scientific reports*, 6, 25414.

[2] Sanchette, F. & Billard, A. Main features of magnetron sputtered aluminium transition metal alloy coatings. *Surf. Coatings Technol.* 218–224 (2001).

10:00am **A1-1-TuM7 The Oxidation Behavior of ZrO₂-Coated Zircaloy-4 with ZrN Interlayer**, I.S. Ting (gary820902@yahoo.com.tw), J.-H. Huang, National Tsing Hua University, Taiwan

The purposes of this study were to investigate the oxidation behavior of ZrO₂-coated Zircaloy-4 (Zry-4) with different crystal structure and evaluate the effect of ZrN interlayer. Oxidation is a crucial problem for the Zry-4 fuel cladding in light water nuclear reactor. In general, when reacting with water, Zry-4 will naturally form a surface oxide layer that is composed of both tetragonal and monoclinic ZrO₂. Although ZrO₂ is a well-known protective material, the naturally formed oxide layer is only several nanometers, which is insufficient to protect the Zry-4 substrate from the severe water-corrosion environment in nuclear reactor. Several transition metal nitride coatings (TMeN), such as CrN, TiN, and TiAlN have been proposed to improve the oxidation resistance of Zry-4. Owing to the excellent thermal and chemical stability, TMeN can act as a diffusion barrier and prevent the substrate from further oxidation. In addition, TMeN possess superior mechanical properties that may enhance the service time of the Zry-4 claddings. Therefore, this study aimed to investigate the oxidation behavior of ZrO₂-coated Zry-4 with tetragonal, monoclinic, and yttria-stabilized cubic crystal structure, and evaluate whether the ZrN interlayer can act as an efficient diffusion barrier. ZrO₂ thin films with three different crystal structure and ZrN interlayer were deposited on both sides of the Zry-4 plate by unbalanced magnetron sputtering (UBMS). After the deposition of ZrO₂ thin films, the crystal structure was characterized by X-ray diffraction (XRD), and the chemical composition was measured using X-ray photoelectron spectroscopy (XPS). Thermogravimetric analysis (TGA) was carried out at 700, 800 and 900°C in argon atmosphere for 1 h. After the TGA oxidation, the uniformity of the multi-phases ZrO₂ oxide layer was examined using azimuthal cos²asin²ψ technique, which combines cos²asin²ψ XRD method [1] with average X-ray strain (AXS) method [2]. The surface morphology of the ZrO₂ thin films and the precipitation of nonuniform surface oxides after TGA oxidation were observed by SEM equipped with EDX.

[1] C. H. Ma, J. H. Huang, H. Chen, *Thin Solid Films* 418 (2002) 73-78.

[2] A.N. Wang, C.P. Chuang, G.P. Yu, J.H. Huang, *Surf. Coat. Technol.* 262 (2015) 40-47.

10:20am **A1-1-TuM8 Novel HIPIMS Deposited Nanostructured CrN/NbN Coatings for Environmental Protection of Steam Turbine Components.**, P. Hovsepian (p.hovsepian@shu.ac.uk), A.P. Ehiasarian, Y. Purandare, Sheffield Hallam University, UK; P. Mayr, K.G. Abstoss, Technische Universität Chemnitz, Germany; M. Mosquera, W. Schulz, A. Kranzmann, Federal Institute for Materials Research and Testing, Germany; M.I. Lasanta Carrasco, J.P. Trujillo, Universidad Complutense de Madrid, Spain

A significant reduction of CO₂ emissions is expected by increasing the efficiencies of the steam turbines to η > 50% which can be achieved by

moving from subcritical low pressure/ low temperatures, to high pressure/high temperature, ultra-supercritical regime of operation. The main challenges faced by different steel components of the power plant with this approach however, consist of material failure due to high temperature oxidation, and phenomenon such as creep, erosion and descaling after a stipulated period of time.

In the current work, 4 μm thick CrN/NbN coating utilising nanoscale multilayer structure with bi-layer thickness of Δ = 3.4 nm has been used to protect low Cr content P92 steel widely used in steam power plants. The novel High Power Impulse Magnetron Sputtering (HIPIMS) deposition technology has been used to deposit CrN/NbN with enhanced adhesion (critical scratch adhesion value of Lc = 80N) and very dense microstructure as demonstrated by XTEM imaging.

P92 coated samples were oxidised at 600°C in 100% high pressure, 50 bar steam atmosphere up to 1500 h. The gas-flow velocity through the reaction zone of the test rig was 0.0133 m/s. In these conditions CrN/NbN provided reliable protection of the P92 steel.

This research also revealed that unlike other state-of-the-art PVD technologies, HIPIMS does not have an adverse effect on the mechanical properties of the substrate material, which is of paramount importance in case of turbine blade applications. In high temperature (650°C) tensile strength test uncoated P92 steel showed Ultimate Tensile Strength (UTS) values of 229 MPa and Yield Strength, (YS) values of 222 MPa compared to UTS = 307 MPa and YS = 291 MPa measured for CrN/NbN coated P92 steel. Similarly in strain controlled, (0.4% strain) Low Cycle Fatigue tests at 650°C both uncoated and coated specimens failed after similar number of cycles, N_f = 1700 and N_f = 1712 respectively and showed similar half-life stress drop of -37% and -43% respectively. Finally high temperature creep tests at 650°C, tensile stress of 120 MPa revealed that the HIPIMS coating improved the creep lifetime by almost factor of two from 564 hours to 908 hours whereas the creep rate was decreased from 17.6 10⁻⁶ s⁻¹ to 13.5 10⁻⁶ s⁻¹.

The protection properties of the coating against water droplet erosion attack were tested using specialized test rig. The coating shows high resistance against water droplet erosion. After 2.4E⁶ impacts no measurable weight loss was detected.

10:40am **A1-1-TuM9 NiAl Coatings Deposited on Inconel 600 by Using an Arc Ion Plating Process**, Y. Li (yli070320@gmail.com), University of Manchester, UK; Y.L. Hung, Feng Chia University, Taiwan; M. Lin, A. Matthews, University of Manchester, UK; J.L. He, Feng Chia University, Taiwan

To protect against the most demanding environments in gas turbines, thermal barrier coatings (TBCs) made of a ceramic top coat and an intermetallic bond coat are applied throughout the hot sections. In a TBC system, a top coat of partially yttria stabilized zirconia (PYSZ) presently offers the main thermal insulation, whilst a bond coat of Ni(Pt),Al or MCrAlY provides the vital oxidation resistance. Currently, these coatings are typically deposited by electron beam physical vapour deposition (EB-PVD). A potential alternative processing route is to deposit both top coat and bond coat by an arc PVD method in a single coating cycle. Little work has been carried out on arc PVD NiAl and PYSZ coatings, which may offer benefits (e.g. in the degree of ionisation achieved, and therefore coating structure and uniformity improvements) compared to other methods.

In this study, the arc ion plating (AIP) method is used to deposit NiAl films on nickel-based alloy (Inconel 600) and AISI 304 stainless steel substrates. The composition of the cathode target is Ni₅₀Al₅₀. In order to study the influence of processing conditions on microstructure and phase composition, the parameters of substrate bias voltage and current, target pulse current and working pressure are controlled during the deposition. Thermal cyclic oxidation testing is carried out to evaluate the cyclic oxidation resistance. The results demonstrate the benefits of the process in terms of improved morphology and performance.

Hard Coatings and Vapor Deposition Technologies

Room Golden West - Session B1-3-TuM

PVD Coatings and Technologies III

Moderators: Frank Kaulfuss, Fraunhofer Institute for Material and Beam Technology (IWS), Germany, Jyh-Ming Ting, National Cheng Kung University, Taiwan, Qi Yang, National Research Council of Canada, Canada

8:00am **B1-3-TuM1 PVD-AITiN with High Al Content – How to Overcome the “Magic” 67%-Limit, F. Fietzke (fred.fietzke@fep.fraunhofer.de), T. Modes, O. Zywitzki, Fraunhofer Institute for Organic Electronics, Electron Beam and Plasma Technology FEP, Germany**

Since first investigations in the 1980's, TiAlN has become the most widespread coating material for wear protection in cutting applications. For the use at high temperatures, its corrosion resistance can be further improved by increasing the aluminum content in the cubic rock salt (Ti,Al)N phase. However, the solubility of Al in this phase is limited, and above a certain threshold AlN with hexagonal wurtzite structure is formed in addition. This leads to a sharp drop of hardness and a general deterioration of wear resistance.

Whereas the application of CVD techniques allows the deposition of single phase cubic $Al_xTi_{1-x}N$ layers with $x > 0.8$, the accepted state of the art for PVD is a maximum x-value of 0.67.

To find out how the effective maximum-x-value depends on the deposition conditions, a co-sputtering approach was used and compositionally graded layers with increasing Al content in growth direction were deposited. By FE-SEM investigation of cross sections in crystal orientation contrast it could be shown that the microstructure is changed at a certain depth, from large columnar crystallites with lateral dimensions of about 60 nm to a nanocrystalline structure with globulitic crystallites in the range of 10 nm.

XRD measurements showed that the initially deposited columnar structure is single-phase cubic, whereas the nanocrystalline layer arising on top is hexagonal with wurtzite structure. Hardness measurements by nanoindentation gave results up to 40 GPa for the lower and around 20 GPa for the upper layer. The depth profiles of chemical composition were determined by GD-OES. The results show that the layers are stoichiometric and exhibit aluminum gradients of different slope.

The location of the phase change from cubic to hexagonal could be affected by deposition conditions like pressure, temperature, and bias voltage. By optimization of the process parameters, it was possible to shift the phase transformation from x-values of 0.67 to 0.75.

8:20am **B1-3-TuM2 PVD Methods and Coatings for Protection of Aero Engine Components, U. Schulz (uwe.schulz@dlr.de), R. Naraparaju, R. Braun, N. Laska, German Aerospace Center (DLR), Germany** **INVITED**

Advanced aero engines aim at reduced specific fuel consumption and increased thrust-to-weight ratio. This ultimately calls for materials with increased high temperature capability and lightweight components that are pushed to its limits. Usage of coatings offers the potential to prolong lifetime, to increase operating temperatures, and to protect turbine components. Several PVD coating techniques that are used to protect turbine parts will be presented.

Thermal barrier coatings (TBCs) are applied to increase lifetime and efficiency of turbine blades and vanes in aero-engines and land-based gas turbines by reducing the average metal temperature and mitigating the detrimental effects of hot spots. The presentation highlights the interplay between processing, microstructure, and lifetime of the coatings that are produced by electron beam-physical vapor deposition (EB-PVD). Those coatings possess a superior strain and thermo-shock tolerance due to their columnar microstructure. The influence of substrate material, bond coat composition, and top coat composition is discussed. New topcoat chemistries have been developed that offer low thermal conductivity, improved sinter resistance, higher phase stability, and especially enhanced resistance against degradation by volcanic ash and calcium-magnesium aluminosilicate (CMAS) deposits that are ingested in aero-engines during the flight. The presentation provides results on several new TBCs, especially their behavior under the influence of deposits and under thermo-cyclic loading.

Gamma-TiAl based alloys are attractive light-weight materials for high temperature applications in automotive and aero engines. However, their oxidation resistance is poor at temperatures above 800°C. To improve the oxidation behavior of TiAl components, the use of protective coatings is a suitable method. Furthermore, the application of TBCs on TiAl would allow a further increase in operating temperature of internally cooled

components. In the presentation several alumina forming coatings such as PtAl, Ti-Al-Cr based coatings and TBCs of yttria partially stabilized zirconia (YSZ) are discussed. They were deposited on gamma-TiAl alloys using magnetron sputtering and electron-beam physical vapour deposition, respectively. The oxidation behavior of the protective layers and the lifetime of the TBC systems are presented in the temperature range between 900 and 1000°C performing thermal cyclic tests.

PVD methods are also capable to protect CFRPs against erosion which is another damaging effect in aero-engines. Here multilayers of metallic and hard coatings are favored to effectively protect the underlying material.

9:00am **B1-3-TuM4 High-temperature Nanoindentation and Microcantilever Deflection Tests of CrAlN and CrAlSiN Hard Coatings, A. Drnovšek (aljaz.drnovsek@ijs.si), Montanuniversität Leoben, Austria; H. Vo, University of California Berkeley, USA; A. Xia, M. Rebelo de Figueiredo, Montanuniversität Leoben, Austria; S. Koloszári, Plansee Composite Materials GmbH, Germany; S. Vachhani, Bruker Nano Surfaces, Germany; P. Hosemann, University of California at Berkeley, USA; R. Franz, Montanuniversität Leoben, Austria**

Mechanical properties of protective coatings are commonly determined by nanoindentation methods. The development of nanoindentation in recent years led to new ex-situ and in-situ systems that are capable of measuring mechanical properties such as hardness, elastic modulus and fracture toughness at high temperatures (HT). For hard protective coatings it is of paramount value to gain knowledge of their mechanical properties close to the real operation temperature.

In the current work, we tested two magnetron sputter deposited coatings that are widely used in industrial cutting applications, namely CrAlN and CrAlSiN. Although the coatings consist of similar elements, the addition of Si interrupts the columnar growth of CrAlN coatings resulting in a nanocomposite composed of CrAl(Si)N grains surrounded by an amorphous SiN_x grain boundary phase. We measured their HT hardness and elastic modulus up to 700°C in steps of 100°C. The hardness value reduced from 30 GPa and 36 GPa for CrAlN and CrAlSiN, respectively, by approximately 2 GPa per temperature step. In contrast to a gradual decrease of hardness over the whole temperature range for CrAlN, the hardness of CrAlSiN revealed only minor changes at temperatures exceeding 500 °C. The HT fracture toughness was measured by microcantilever deflection using in-situ nanoindentation. These measurements were conducted in a similar way as the hardness measurements, up to 700°C in 100°C steps. We found that the trend is similar to the HT hardness results with CrAlSiN exhibiting a slightly better performance.

This data set is intended to serve as a first step towards a more comprehensive understanding of the HT mechanical properties of hard coatings which is vital for their further development and improvement for use in HT applications.

9:20am **B1-3-TuM5 On Crystallization and Oxidation Behavior of $Zr_{54}Cu_{46}$ and $Zr_{27}Hf_{27}Cu_{46}$ Thin-film Metallic Glasses Compared to a Crystalline $Zr_{54}Cu_{46}$ Thin-film Alloy, M. Kotrlová (kotrlova@kfy.zcu.cz), M. Zitek, P. Zeman, University of West Bohemia, Czech Republic**

Zr- and Cu-based metallic glasses are one of the most studied systems because of their high crystallization temperature and a wide supercooled liquid region. Their unique properties make them attractive for miscellaneous applications. An important prerequisite to use them in industry is their ability to resist an oxidizing environment at elevated temperatures.

Therefore, this work is focused on the investigation of the crystallization and oxidation behavior of $Zr_{54}Cu_{46}$ and $Zr_{27}Hf_{27}Cu_{46}$ thin-film metallic glasses and on the comparison of their oxidation behavior with that of a crystalline $Zr_{54}Cu_{46}$ thin-film alloy. The amorphous $Zr_{54}Cu_{46}$ and $Zr_{27}Hf_{27}Cu_{46}$ thin-film metallic glasses were prepared by non-reactive magnetron co-sputtering of Zr, Hf and Cu in pure argon. The magnetrons with the Zr and Hf targets were operated in dc regimes while the magnetron with the Cu target in high-power impulse regime. Several as-deposited $Zr_{54}Cu_{46}$ films were post-annealed in high vacuum to create a crystalline thin-film alloy of the identical composition. The non-isothermal crystallization behavior of the amorphous $Zr_{54}Cu_{46}$ and $Zr_{27}Hf_{27}Cu_{46}$ films and the effect of a substitution of Hf for Zr on the crystallization process were studied by differential scanning calorimetry. The oxidation behavior of the amorphous and crystalline $Zr_{54}Cu_{46}$, and amorphous $Zr_{27}Hf_{27}Cu_{46}$ films was investigated by thermogravimetric analysis.

The results showed that the $Zr_{54}Cu_{46}$ film crystallized at a lower temperature ($\approx 422^\circ\text{C}$) and in two successive steps in contrast to the $Zr_{27}Hf_{27}Cu_{46}$ film (\approx

477°C). The activation energy of the $Zr_{27}Hf_{27}Cu_{46}$ film was higher for all conversion fractions, which indicates that the substitution of Hf for Zr enhanced the thermal stability of the glassy state. Dynamical thermogravimetric curves revealed that the onset of the oxidation of the amorphous $Zr_{54}Cu_{46}$ film ($\approx 475^\circ\text{C}$) was shifted by about 120°C to a higher temperature than for the crystalline $Zr_{54}Cu_{46}$ film. Moreover, the substitution of Hf for Zr shifted the onset of the oxidation to an even higher temperature ($\approx 550^\circ\text{C}$). As for oxidation kinetics, all isothermal thermogravimetric curves in the temperature range from 400 to 575°C obeyed the parabolic law. The activation energy of the oxidation process was 112, 143 and 208 kJ/mol for the crystalline $Zr_{54}Cu_{46}$ film, and the amorphous $Zr_{54}Cu_{46}$ and $Zr_{27}Hf_{27}Cu_{46}$ films, respectively. The highest activation energy for the $Zr_{27}Hf_{27}Cu_{46}$ film indicates that the most protective oxide layer was formed on the surface of this film.

9:40am **B1-3-TuM6 On the Origin of Multilayered Structure of W-B-C Coating Prepared by Non-Reactive Magnetron Sputtering from a Single Segmented Target**, *M. Kroker (kroker@physics.muni.cz)*, *P. Soucek, M. Fekete, L. Zabransky, V. Bursikova*, Masaryk University, Brno, Czech Republic; *P. Zikan, A. Obrusnik*, Plasma Solve, Brno, Czech Republic; *Z. Czigany, K. Balazi*, Hungarian Academy of Sciences, Hungary; *P. Vasina*, Masaryk University, Brno, Czech Republic

Machining tools are routinely coated with thin films to enhance their performance and durability. Nowadays used hard protective coatings exhibit high hardness and high stiffness; however, these positive features are often accompanied by negative brittle deformation behaviour, which facilitates formation and spreading of cracks. This leads to a premature degradation of the coated tool. A solution would be to prepare coatings simultaneously exhibiting high hardness together with enhanced ductility. Recently, there has been an increased interest in crystalline metal-boron-carbon based coatings [1] with X2BC stoichiometry which is inherently nanolaminated within the unit cell. According to the ab-initio models [1], these materials should exhibit an unusual combination of high stiffness and moderate ductility. A systematic theoretical study revealed that the nanolaminates with $X = W$ should exhibit the best mechanical properties [1] making them the best candidates for experimental synthesis. Thus W-B-C coatings were sputter deposited in non-reactive atmosphere onto substrates performing a planetary motion around a central rotating cylindrical target composed from boron-carbide, tungsten and graphite segments in an industrial scaled deposition system of company SHM, Sumperk, Czech Republic. The coatings were deposited at the temperature of 450°C and bias of -100 V by direct current magnetron sputtering. The SEM and TEM cross-section view revealed the presence of multilayered structure. The pattern of the multilayered structure was dependent on the type of planetary rotation around the central target. According to EDX and GDOES, the multilayered structure consisted of tungsten-rich layers alternating with boron- and carbon-rich layers. The whole structure consisted of thin layers with the thickness not exceeding 15 nm. The number of the multilayers was correlated with the number of the revolutions the sample performed during the deposition process. The multilayered structure was attributed to different transport pathways of heavy (W) and light (C and B) atoms sputtered from the target and scattered by working gas. 3D DSMC model was developed to explain the transport of sputtered atoms. The model is using the experiment geometry and initial velocities of sputtered particles calculated by TRIM. Results obtained with this model are in good agreement with experiment.

[1]H. Bolvardi, J. Emmerlich, M. to Baben, J, von Appen, R. Dronskowski, J.M. Schneider, Systematic study on the electronic structure and mechanical properties of X BC ($X = \text{Mo, Ti, V, Zr, Nb, Hf, Ta}$ and W), J. Phys.-Condens. Mat. 25 (2013) 045501.

Hard Coatings and Vapor Deposition Technologies

Room California - Session B4-1-TuM

Properties and Characterization of Hard Coatings and Surfaces I

Moderators: Naureen Ghafoor, Linköping Univ., IFM, Thin Film Physics Div., Sweden, Ulrich May, Robert Bosch GmbH, Germany, Fan-Bean Wu, National United University, Taiwan

8:20am **B4-1-TuM2 Preparation and Characterization of Hard and Tough Coatings of Ion-assisted Co-sputtered Transition Metal Borides**, *M.S. Wong (mswong@gms.ndhu.edu.tw)*, National Dong Hwa University, Taiwan

INVITED

Transition metal borides (TMeB) are frequently explored around the globe due to their superior mechanical, tribological, electrical properties and chemical stability. Titanium diboride (TiB_2) is the most promising and explored material, while the other TMeBs like zirconium and tantalum diboride (ZrB_2 and TaB_2) sharing the same crystal structure and common properties receive relatively low attention. TMeBs are usually hard but brittle, which limit their wide spread applications. To prepare both hard and tough coatings of TMeBs, various approaches have been taken including doping, solid solution, ion bombardment, and multilayer. In the Ti-Zr-Ta-B system, ceramic-meal composites like TiB_2 -Zr, ZrB_2 -Ta composites, $TiZrB_2$ and $TiTaB_2$ solid solution and TiB_2/ZrB_2 multilayer films were explored by co-sputtering the corresponding TMeB ceramic target and/or metal target under various substrate bias voltages. Appropriate doping, solid solution, multilayer and ion bombardment could result in textured films with preferred structure with enhanced properties. Ion bombardment on the growing film greatly affects the crystal preferred orientation, crystallinity, composition, grain size, surface roughness, stress, toughness and hardness of the TMeB films. The change in target power ratio for solid solution films and in bilayer thickness for multilayer all affected the structure of the obtained films influencing intensity of texture, distortion of crystal lattice and residual stress. Superhard and tough films with hardness over 50 GPa and fracture toughness over $3\text{ MPa}\cdot\text{m}^{1/2}$ have been achieved consistently

9:00am **B4-1-TuM4 Strategy for Increasing Both Hardness and Toughness in Transition-metal Diboride Thin Films**, *B. Bakhit (babak.bakhit@liu.se)*, Linköping Univ., IFM, Thin Film Physics Div., Sweden; *I. Petrov*, University of Illinois, USA, Linköping University, Sweden, USA; *J.E. Greene*, University of Illinois, USA, Linköping University, Sweden, National Taiwan Univ. Science & Technology, Taiwan; *L. Hultman, J. Lu, J. Rosén, G. Greczynski, N. Ghafoor*, Linköping Univ., IFM, Thin Film Physics Div., Sweden

Refractory transition-metal (TM) diborides exhibit inherent hardness. However, this is not always sufficient to prevent failure in applications involving high mechanical and thermal stresses, since hardness is typically accompanied by brittleness leading to crack formation and propagation. Toughness, the combination of hardness and ductility, is required to avoid brittle fracture. Here, we propose a strategy for enhancing both the hardness and ductility of ZrB_2 thin films, selected as a model TM diboride, grown by hybrid high-power pulsed and dc magnetron co-sputtering (HiPIMS/DCMS) in pure Ar. A Ta target operated in HiPIMS mode, with a substrate bias synchronized to metal-rich portions of HiPIMS pulses, supplies energetic Ta ions to the growing film, while a compound ZrB_2 target operated in DCMS mode provides a continuous flux of Zr and B atoms. The average power P_{Ta} applied to the HiPIMS Ta target, and the HiPIMS pulse frequency, are varied from 0 to 1800 W (300 Hz) in increments of 600 W. All other deposition parameters are maintained constant. The resulting boron-to-metal ratio, $\gamma = B/(Zr + Ta)$, in as-deposited $Zr_{1-x}Ta_xB_\gamma$ films continuously decreases from 2.4 to 1.5 as P_{Ta} is increased from 0 to 1800 W, while x increases from 0 to 0.3. A combination of XTEM, analytical Z-contrast STEM, EELS, EDX, and XRD analyses, reveal that all films have the AlB_2 hexagonal crystal structure with a columnar microstructure. Layers with $x < 0.2$ have B-rich column boundaries, whereas those with $x \geq 0.2$ have Ta-rich column boundaries. This microstructural transition results in an increase of $\sim 20\%$ in hardness, from 35 to 42 GPa, with a simultaneous increase of $\sim 50\%$ in the nanoindentation toughness, from 3.5 to 5.2 $\text{MPa}\cdot\text{m}$.

Tuesday Morning, May 21, 2019

9:20am **B4-1-TuM5 Tribocorrosion Resistance of Borided ASTM F1537 Alloy**, *I.E. Campos-Silva, A.M. Delgado-Brito (angel_manuel05@hotmail.com)*, Instituto Politecnico Nacional Grupo Ingenieria de Superficies, México; *J. Oseguera-Peña*, Tecnologico de Monterrey-CEM, México; *J. Martinez-Trinidad*, Instituto Politecnico Nacional, Grupo Ingenieria de Superficies, México; *R. Perez Pasten-Borja*, Instituto Politecnico Nacional, SEPI ENCB, Mexico; *D. Lopez-Suero*, Instituto Politecnico Nacional, Grupo Ingenieria de Superficies, México; *A. Mojica-Villegas*, Instituto Politecnico Nacional, ENCB, México

New results about the tribocorrosion resistance of borided ASTM F1537 alloy, immersed in Hanks' solution were estimated in this study. A CoB-Co₂B layer, with around 30 microns of thickness, was obtained at the surface of the alloy using the powder-pack boriding process at 1273 K with 6 h of exposure. Before the tribocorrosion tests, indentation properties such as hardness, fracture toughness, the residual stresses were obtained at the surface of the borided cobalt alloy. Otherwise, the tribocorrosion tests were carried out in a linear reciprocating tribometer coupled with a standard three-electrode electrochemical cell, in which a 5 mm diameter alumina ball worn the specimen surface immersed in Hanks' solution. A constant load of 20 N was applied over the surface of the material considering a stroke length of 2.5 m, and a total sliding distance of 100 m.

To estimate the material loss due to wear only, corrosion only, and the component due to the wear-corrosion synergism, four tests were conducted according to the ASTM G119 procedure: two wear tests, a) one in which the total material loss due to wear and corrosion (T) was estimated, b) another performed at 1 V cathodic of the open circuit to eliminate the corrosion component, defined as W_0 . In the case of the corrosion tests, c) the polarization resistance was evaluated (C_p), without the influence of the wear component, and finally, d) the influence of the wear component in the corrosion behavior (C_w) was estimated. In all the cases, and to evaluate the influence of the boride layer developed at the surface of the ASTM F175 alloy, the experimental procedure was also established on the untreated material.

The results established that the presence of CoB-Co₂B layer decreases the total material loss due to wear and corrosion synergy compared to the untreated material. For the untreated material, the 62 % of the material loss was attributed to the wear-corrosion synergism in comparison with the 38 % estimated for the borided cobalt alloy. Finally, the influence of wear affected in greater extent than corrosion in the untreated material, while for the borided alloy the interaction between corrosion and wear was equal.

9:40am **B4-1-TuM6 Corrosion Behavior of TiAlSiN Doped with Ag Coating Deposited by Co-sputtering in Physiological Fluids**, *A.D. Caita Tapia (adcaitat@unal.edu.co)*, *S.D. Rodriguez Arevalo, E.N. Borja Goyeneche, J.J. Olaya Florez, B.J. Gamboa Mendoza*, Universidad Nacional de Colombia, Colombia

In this work it was studied the influence of the variation on weight percentage of Ag in TiAlSiN coating deposited on TiAlV substrate with co-sputtering technique. The structural analysis was performed by X-ray diffraction (XRD) and chemical composition was performed using Energy-dispersive X-ray spectroscopy (EDS). It was evaluated the corrosion response at one hour of Electrochemical Impedance Spectroscopy (EIS) performed on samples in different solutions that simulate physiological fluids such as 3.5%NaCl at human body temperature (aprox. 38°C), physiological serum and ringer lactate. Those results were compared with an EIS corrosion test in 3.5%NaCl solution at an ambient temperature. It is shown that there is a peak in silver content for which is reached the best corrosion resistance performance, wich in addition to the antibacterial capacities of Ag, makes this coating an optimal candidate for biomedical applications.

10:00am **B4-1-TuM7 Adhesion Strength of Titanium Carbide Thin Film Coatings on Surface Microstructure Controlled WC-Co**, *T. Saito (tsaito@chemeng.osakafu-u.ac.jp)*, *C. Tanaka, N. Okamoto*, Osaka Prefecture University, Japan; *A. Kitajima, K. Higuchi*, Osaka University, Japan
Chemical vapor deposited (CVD) or physical vapor deposited (PVD) hard material coating technique on the cemented-tungsten carbide (WC-Co) is widely used for molds and cutting tools, which plays an important role in a lot of manufacturing industry. Plasma enhanced chemical vapor deposition (PECVD) and PVD have some merits like lower deposition temperature (< 500°C) than thermal CVD and high through-put, however, the films usually have low adhesion strength. Then, life of molds and cutting tools obtained PVD are usually shorter than that with CVD.

In this study, several surface pretreatment methods were investigated to increase surface roughness to enhance adhesion strength. The procedure include, dry etching by CF₄ plasma discharge for 15 to 120 min in the

temperature change from R.T. to 500°C. Chemical treatment with aqua regia (3HCl:HNO₃) for 3 min at 25 to 60°C. After pretreatment, TiC coatings were formed by sputtering with TiC target or PECVD with TiCl₄ and CH₄. Surface roughness, deposition rate, composition ratio and chemical bond, hardness and adhesion strength of WC-Co and TiC coating film ewre evaluated AFM, surface profiler, XPS, dynamic ultra-micro hardness tester, and scratch tester, respectively.

Figure 1 shows the relationship between the surface roughness (Ra) and critical load of sputtered TiC hard coating layer on surface treated WC-CO. With the CF₄ plasma treatment, the maximum load of 12.1 N with Ra = 46 nm. However, with the aqua regia treatment, the maximum load of ca. 70 N more than Ra = 80 nm. There are still scatters less than Ra = 80 nm. The cause of delamination was thought to be the detailed substrate morphology or chemical states after etching and poor step coverage of sputtered TiC coating layer. Figure 2 shows the relationship between the surface roughness (Ra) and critical load of PECVD TiC hard coating layer on surface treated WC-CO with aqua regia. Compared with fig. 2(right), the critical load is worse. We are still investigating the reason but are considering that the quality PECVD TiC film is poor at this moment

Coatings for Biomedical and Healthcare Applications Room Pacific Salon 3 - Session D3-TuM

Surfaces and Coatings to Promote Tailored Biological Responses

Moderators: *Sandra Rodil*, Universidad Nacional Autonoma de Mexico, México, *Vincent Fridrici*, Ecole Centrale de Lyon, LTDS - Université de Lyon, France

8:20am **D3-TuM2 Tailoring the Microstructure of ZnO Thin Films for Antimicrobial Applications**, *P. Pereira-Silva, J. Borges, A. Costa-Barbosa, D. Costa, MS. Rodrigues, F. Vaz (fvaz@fisica.uminho.pt), P. Sampaio*, University of Minho, Portugal

Nosocomial infections are microbial infectious diseases that are acquired in healthcare settings, and are a worldwide health problem. The surfaces are involved in the spread of these infections, thus there is an urgent need to eliminate this route of transmission. Nanotechnology allows the production of materials with improved properties and effective action against pathogens. Zinc oxide (ZnO) is frequently used due to its excellent antimicrobial properties.

This work focused on the evaluation of the antimicrobial activity of ZnO thin films. All the samples were produced by reactive DC magnetron sputtering and tested against the fungus *Candida albicans*. A first set of thin films were produced with different O₂ flows, which affected the thin films' chemical composition and morphology. Additionally, some of the thin films were subjected to an annealing treatment, which promoted the crystallization of the ZnO matrix. A second set of thin films was produced modifying the deposition angle, using the Glancing Angle Deposition technique, GLAD, with a fixed O₂ flow. These changes were performed to increase the porosity and roughness of the thin films, which may allow the tailoring of the film's biological response. To evaluate the ZnO thin films surface antimicrobial properties, a direct contact assay was performed, and the results revealed no significant cell growth after five hours of incubation. Analysing possible molecular mechanisms responsible for the antimicrobial activity, it was observed that the loss of membrane integrity and the increase of Reactive Oxygen Species (ROS) within *C.albicans* cells was correlated with the incapacity of the cells to grow.

As a general conclusion, one may claim that all the thin films showed a significant antifungal activity, and the observed differences among them can be correlated with the evolution of the (micro)structural features.

8:40am **D3-TuM3 In Vitro Evaluation of Macrophage Response to Ionic Liquid-Coated Titanium:**, *S. Wheelis (sxw110230@utdallas.edu), L. Guida, D. C. Rodrigues*, University of Texas at Dallas, USA

Introduction: Dicationic Imidazolium-based ionic liquids with amino acid anions (IonL) have been proposed as a multifunctional coating approach for dental implants. IonL are able to form a temporary, stable coating on the surface of titanium (cpTi), providing lubrication and antimicrobial properties to address the multiple causes of early dental implant failures while maintaining bone and soft tissue cell compatibility *in vitro*. However, there is limited information regarding the response of immune cells to this coating, which is significant as they are often determining factors in implant healing. The aim of this study is to evaluate the proliferation and cytokine gene expression of human macrophages in response IonL-coated cpTi *in vitro* to

Tuesday Morning, May 21, 2019

infer the possible effect of the coating on the onset of the acute immune response *in vivo*.

Methods: IonLs with the best combination of antimicrobial and host cell compatibility properties (IonL-Phe, IonL-Met) were chosen as the coatings for investigation. CpTi disks (5 X 2 mm) were drop coated in 1 μ mol of each IonL on the disk surface. Uncoated cpTi disks and 1 μ mol of pure IonL were used as controls. Samples and controls were plated individually in 6 well plates in experimental duplicates (n = 36), seeded with primary human macrophages (M0, Cellprogen), then incubated for 1 or 3 days with a 135,000 or 50,000 cells per well. One set of experiments underwent a 3-[4,5-dimethylthiazol-2-yl]-2,5-diphenyltetrazolium bromide (MTT) assay to determine cell proliferation in each well. The other experimental replicate were evaluated with a quantitative polymerase chain reaction (qPCR) to determine changes in IL6, TNF α , TGF β 1, iNOS, ARG1 and FIZZ1 gene expression to determine M0 polarization. Statistical analysis was performed using ANOVA (α = 0.05)

Results: Results from 1 day MTT assays showed a significant difference in viability in IonL-Met coated samples and uncoated cpTi control. Results from 3 days showed a significant difference in viability of the control versus both IonL coatings, as well as between IonL-Met and IonL-Phe coated samples. However, in both 1 and 3 day experiments, viability in all samples did not drop below 70% when scaled to the uncoated cpTi.

Conclusions: MTT assays show that although there is a significant drop in viability after 3 days of IonL exposure, the coating is still not considered cytotoxic. Similar viability results were seen when the same assay was performed on bone and soft tissue cells. Therefore, the IonLs retain their cell compatibility and qPCR results will likely corroborate viability results, showing a lack of significant stimulation towards pro- or anti-inflammatory phenotypes.

9:00am **D3-TuM4 Materials To Control Biological Function**, **K. Anselme** (karine.anselme@uha.fr), CNRS, France **INVITED**

Surface modifications of materials are used to monitor and evaluate cellular function for several decades. An example of this is the ability to control tissue integration of medical prostheses by changing their composition, surface topography, chemistry, energy, or their mechanical properties. Similarly, control of the surface of materials is also a key element in the effectiveness of diagnostic tools, devices for cell culture, bio-sensors or drug delivery systems (1).

The cells have the ability to discriminate and specifically react to surface characteristics of the materials considered at the micrometer scale as well as the nanometer scale. In this talk, I will present our experience on the response of cells to functionalization of implants with mixed coatings associating inorganic and organic compounds such as hydroxyapatite and biologically active proteins (fibronectin, bone morphogenetic proteins) (2). Also, our last experience on response of living cells to topography at their own scale will be detailed and in particular our recent discovery of a new cellular ability which we term "curvotaxis" (3).

References:

1. **K. Anselme***, A. Ponche, L. Ploux, Materials to control and measure cell function in Comprehensive Biomaterials, ed. P. Ducheyne, D. Huttmacher, K. Healy, J. Kirkpatrick, Elsevier (2011), Volume 3, Chapter 3-314, 235-256.
2. I. Brigaud, R. Agniel, J. Leroy Dudal, S. Kellouche, A. Ponche, T. Bouceba, N. Mihailescu, M. Sopronyi, E. Viguier, C. Ristoscu, F. Sima, I.N. Mihailescu, A.C.O. Carreira, M. Cleide Sogayar, O. Gallet, **K. Anselme***, Synergistic effects of BMP-2, BMP-6 or BMP-7 with human plasma fibronectin onto hydroxyapatite coatings: a comparative study, Acta Biomaterialia (2017) 55, 481-492.
3. L. Pieuchot*, M. Vassaux, J. Marteau, T. Cloatre, T. Petithory, I. Brigaud, P-F. Chauvy, A.Ponche, J-L. Milan, P. Rougerie, M. Bigerelle, **K. Anselme**, Curvotaxis directs cell migration through cell-scale curvature landscapes (2018) Nature Communications, 9:3995

9:40am **D3-TuM6 Comparison of Elution of Antibiotic and Biofilm Inhibitor from Manually Applied and Spray Deposited Phosphatidylcholine Coatings**, **Z. Harrison** (zlhrrson@memphis.edu), **R. Awais**, **R. Gopalakrishnan**, **J.A. Jennings**, University of Memphis, USA

When implanting medical devices, the resultant wounds are often at high risk of infection. This infection is often caused by the formation of a biofilm, which occurs when microorganisms attach to the surface of the implanted device. Previous work in our lab has shown the effectiveness of cis-2-decenoic acid (C2DA) to disperse and inhibit biofilm, especially when combined with antibiotics. Previous studies have shown that

phosphatidylcholine (PtC) can be loaded with C2DA and antibiotics to create a crayon-like solid, which can be used to "draw" a thick layer of coating onto an implant and thus prevent infection. While this application method showed promising results for drug elution and prevention of bacterial growth, this method of application has drawbacks of slow application process and uneven coating, especially for devices with complex shapes. To overcome these clinical issues, a system has been developed to spray phosphatidylcholine directly onto the device via an aerosol sprayer. This study seeks to determine if this aerosol spraying method provides similar drug elution capabilities as the previously manual coating method. PtC crayons loaded with 15% ciprofloxacin and 15% C2DA were dispersed in water and sprayed onto stainless steel coupons. Manually applied coatings were used as controls. Elution over 7 days in PBS was analyzed using high performance liquid chromatography. Results indicate that though mass of coating applied was lower using the spray setup, coating uniformity is improved with this method. Elution study results indicate that while the thicker manual coating showed higher elution of ciprofloxacin per day, the spray coating only eluted concentrations above inhibitory levels of ciprofloxacin through day 3. Current studies are being conducted to test the efficacy of sprays dispersed in polyethylene glycol 400 (PEG 400) and phosal 53 MCT (a 50/50 blend of PtC and medium chain triglycerides), which may increase elution and spray deposition. Furthermore, modifications are being made to the aerosol sprayer to improve the portability of the system, the speed of coating, and the thickness of the sprayed coating.

10:00am **D3-TuM7 In vitro Osseointegration Analysis of Bio-functionalized Titanium Samples in a Protein-rich Medium**, **S. Rao**, **S. Hashemiastaneh**, **J. Villanueva**, University of Illinois at Chicago, USA; **F. Silva**, University of Minho, Portugal; **C. Takoudis**, University of Illinois at Chicago, USA; **D. Bijukumar**, University of Illinois College of Medicine, USA; **J. Souza**, University of Illinois at Chicago, USA; **M.T. Mathew** (mtmathew@uic.edu), University of Illinois College of Medicine, USA

Titanium (Ti) or Ti-based alloys are commonly used for the biomedical implant applications. The long-term survivability of the implants is strongly influenced by the osteointegration aspects of the metal-bone interface. Several techniques on Ti surface modification have been reported in the literature to improve osteointegration of implants to bone. Here, biological materials such as protein are used to functionalize titanium surfaces to enhance the ability of implants to interact with human tissues for accelerated osseointegration. The main aim of this study is to functionalize titanium surfaces in a medium enriched with fibrinogen.

Commercially pure titanium grade IV discs (8 mm Dia x 3 mm thick) are etched using two different acidic substances (HF/HNO₃ and H₂SO₄/HCl). Fibrinogen is processed and precipitated by a standard procedure to obtain high molecular weight fibrinogen under repeated centrifugation. Fibrin gel is prepared by adding thrombin to fibrinogen. Surfaces coated with and without fibrin are analyzed by white light microscope, SEM, and WCA to check for the surface properties. Osteoblasts are cultured on the surfaces to assess cell proliferation, adhesion as well as the mineralization process. Osteoblastic proliferation on these surfaces is quantified by Alamar blue assay and visualized under confocal microscope and SEM; qPCR is performed to investigate the expression of genes specific to osteogenic cells and mineralization assay is done to check calcium and phosphate deposits.

This study demonstrates a method of increasing roughness and hydrophilicity of the implant surface by etching followed by protein functionalization. Such a method can reduce the time for osseointegration that can decrease risks in early failures of implants. Also, the adsorption of fibrinogen on titanium surfaces is influenced by the method of acid etching.

10:20am **D3-TuM8 Microstructural and Electrochemical Properties of TiAlN- (Ag,Cu) Nanocomposite Coatings Deposited by DC Magnetron Sputtering for Medical Applications**, **H.D. Mejia** (hdario.mejia@udea.edu.co), **A.M. Echavarría**, **G. Bejarano**, Universidad de Antioquia, Colombia

AlSi 420 stainless steel is currently used in the manufacture of surgical and dental instrumentation due to its hardenability, acceptable biocompatibility and resistance to corrosion. However its resistance to wear is relatively low, and therefore multiple strategies of surface modification are offered such as plasma nitriding, hard coatings and self-lubricating ceramic coatings deposited by the physical vapor deposition techniques PVD, among others, to reduce the wear rate and to confer this steel other variety of specific properties. In the case of coatings that include metallic solid lubricants, the anticorrosive properties can be affected by the formation of galvanic pairs and the high chemical reactivity of the metallic phase. Therefore, it is absolutely necessary to evaluate the electrochemical behavior and the

corrosion resistance of these composite coatings. In this work TiAlN coatings doped with four different contents of Ag and Cu nanoparticles (11 at.% to 20 at.%) were deposited onto 420 steel by means of DC magnetron sputtering equipment using two composited targets of Ti/Al and Ag/Cu (both 50/50 at.% and 99,95 purity), which were facing each other at 180 degrees. The microstructure, chemical and phase composition were analyzed by scanning and transmission electron microscopy (SEM/TEM), energy dispersive X-ray spectroscopy (EDX) and X-ray diffraction, while the roughness were determined using atomic force microscopy (AFM), respectively. The corrosion rates were obtained from the polarization curves and the electrochemical behavior was evaluated by electrochemical impedance spectroscopy (EIS) in artificial saliva. The reduction in the corrosion rates of the steel was evident once it was superficially modified with the TiAlN (Ag,Cu) nanocompound, forming a substrate protection barrier when exposed to the selected body fluids. The TiAlN (Ag-Cu) coatings presented an electrochemical activity superior to the TiAlN matrix, and consequently exhibited higher corrosion current densities. This behavior becomes greater with the increase of the Ag-Cu content in the compound and is correlated mainly with the continuous and increasing dissolution of silver and copper in the surrounding medium and to the greater chemical activity of the Ag-particles as compared to the ceramic matrix. However, all coated samples showed an enhanced corrosion resistance compared to the steel substrate, obtaining the best electrochemical behavior by the sample coated with TiAlN (Ag-Cu) with 17at.% Ag-Cu. The development of this nanostructured coating system might be considered for potential application in surgical and dental instrumentation.

Tribology and Mechanical Behavior of Coatings and Engineered Surfaces

Room San Diego - Session E2-1-TuM

Mechanical Properties and Adhesion I

Moderators: **Megan J. Cordill**, Erich Schmid Institute of Materials Science, Austrian Academy of Sciences, Leoben, Austria, **Ming-Tzer Lin**, National Chung Hsing University, Taiwan, **Gerhard Dehm**, Max-Planck Institut für Eisenforschung, Germany

8:00am **E2-1-TuM1 Indentation Behavior of Metal-Ceramic Multilayer Coatings: Modeling vs. Experiment**, **Y.-L. Shen** (shenyl@unm.edu), University of New Mexico, USA **INVITED**

Thin films consisting of alternating metal and ceramic layers are an exciting subset of materials with many promising attributes. This presentation highlights our recent studies on mechanical characterization of such coatings using nanoindentation. We focus on aluminum (Al)/silicon carbide (SiC) nanolayers, which serves as a model system for investigating the constraining effect due to the highly mismatched mechanical properties of the constituents. How this structural heterogeneity responds to nanoindentation is a current a subject of active research. The development of complex deformation patterns underneath the indentation, dictated by the structural heterogeneity, can lead to various forms of local damage. Our studies focus on the employment of numerical finite element modeling to corroborate with experimental observations as well as to extract meaningful constitutive properties. Special attention is given to the analyses of (i) plastic deformation in the metal layers, (ii) cyclic indentation response and composite modulus measurement, (iii) indentation-induced delamination, and (iv) indentation-induced shear band formation.

8:40am **E2-1-TuM3 Indentation Induced Delamination for Adhesion Measurements**, **M.J. Cordill** (megan.cordill@oeaw.ac.at), **A. Kleinbichler**, Erich Schmid Institute of Materials Science, Austria

Silicon nitride (Si₃N₄) is a frequently used passivation layer as well as an ion barrier in microelectronic devices. Its most outstanding properties are high fracture toughness and thermal stability, but in order to have a reliable device the adhesion to other thin films is of great importance. Qualitative tests like tape tests have shown that the adhesion of the brittle interface of Si₃N₄ and silicon glass (BPSG) is rather poor. In order to determine a quantitative measure of the adhesion of Si₃N₄ to BPSG other techniques such as nanoindentation are necessary. Indentation induces well-defined areas of delamination at the Si₃N₄-BPSG interface only when used in conjunction with a stressed overlayer of WTi. In this film system, the stressed overlayer helps the underlying Si₃N₄ film to buckle and supports the delaminated, brittle Si₃N₄ film from spalling from the substrate. Utilizing the delaminated areas and well established methods the adhesion of brittle thin films can be determined, which could not be measured before.

9:00am **E2-1-TuM4 Intrinsic Stress in Polycrystalline Film: An Atomistic View**, **E. Vasco** (enrique.vasco@csic.es), Instituto de Ciencia de Materiales de Madrid, Spanish National Research Council (CSIC), Spain; **D. Franco**, Departamento de Física de la Materia Condensada, Universidad Autónoma de Madrid, Spain; **E.G. Michel**, **C. Polop**, Departamento de Física de la Materia Condensada and Condensed Matter Physics Center (IFIMAC), Universidad Autónoma de Madrid, Spain

Most of the current applications based on films and coatings use continuous and compact polycrystalline films. They are easy to produce and integrate in many devices, cost-effective and suitable for common applications. However, their reliability suffers as the applications demand more resources, intensive use of medium properties or nonstandard working conditions. These limitations are due to the heterogeneous structure of the polycrystalline films, which are made up of misorientated grains separated by boundaries and other defects. Where the crystal lattice of the films has defects, a local field of intrinsic stress is generated. This stress field, which is reversible and cumulative with the working conditions, determines the short-range properties of the films and shortens the lifespan of devices.

The evolution of the intrinsic stress during the preparation of polycrystalline films has been investigated over decades. Nowadays, it is well known that the continuous compact films grow under compression, whose strength is closely linked with the density of grain boundaries (GB). However, the origin of the compression has not been clarified yet despite many models have been proposed. Recently, we measured the local distribution of residual intrinsic stress in polycrystalline films using a pioneering method¹ of nanoscale stress mapping based on AFM. Our results² demonstrated that, at odds with expectations, compression is not generated inside GBs, but at the edges of gaps where the boundaries intercept the surface. We report now a "definitive" model^{2,3}, wherein the compression is caused by Mullins-type surface diffusion towards the GBs, which generates a kinetic surface profile different from the equilibrium profile predicted by Laplace-Young. Where the curvatures of both profiles differ (mainly, at the edges of gaps where diffusing atoms accumulate), the intrinsic compression rises in the form of Laplace pressure. Our model³ addresses successfully all the major evidences reported so far regarding the behavior of stress with experimental conditions. However, owing to the mesoscopic nature of our model, it is difficult to correlate it with atomistic processes that provide a physical vision (rather than mathematical one) of the phenomenon. In this work, we update our model in atomistic terms, namely, we address the origin and behavior of the intrinsic compression from the density of surface species (i.e., monomers and steps) and random walk diffusion with aggregation/nucleation leading to step-flow/second-nucleation growths.

1) C. Polop et al., *Nanoscale* **9**, 13938 (2017)

2) E. Vasco et al., *PRL* **119**, 256102 (2017)

3) E. Vasco et al., *PRB* **98**, 195428 (2018)

9:20am **E2-1-TuM5 Development of a Methodology for Measuring the Elastic Constants of Anisotropic Coatings Using Impulse Excitation Technique**, **E. Zgheib** (elia.zgheib@utt.fr), University of Technology of Troyes (UTT) and Lebanese University (UL), France; **M.F. Slim**, **A.A. Alhussein**, University of Technology of Troyes (UTT), France; **K. Khalil**, Lebanese University (UL), Lebanon; **M. Francois**, University of Technology of Troyes (UTT), France

New processes for obtaining advanced materials, in the form of coatings, are developing more and more to meet the socio-economic and the environmental needs. Coatings, as protective layers, improve the surface properties of a material. For example, in biomedical, elastic properties are must to be considered for the good insertion of the prostheses into the bone tissues. Thus, the deposit of Micro metric and/or Nano metric layers to obtain gradient functional materials is a promising approach for achieving impedance matching or reduction of stress concentrations on structures, such as prostheses or implants.

The project is part of the developments of Impulse Excitation Technique (IET) measuring constants of elasticity of thin layers [1, 2]. The IET is based on the analysis of vibrational frequencies created by an impact on a specimen. In this project, deposition will be developed using low-pressure process: PVD (Physical Vapor Deposition); and the parameters influencing the elasticity of the coatings will be identified. In the literature and for a designed anisotropic coating, no technique is available to go back to the values of the elastic constants of each layer and stack. This difficulty motivates the researcher to innovate methods and characterizations. What the project proposes is developing an inverse method using a multilayer model and the global analysis of vibration modes obtained by IET.

The methodology being used is a multi-scale approach to correlate the microstructural state of the coating and its resulting properties. The objectives that will be achieved rely on the development of IET measurement technique for mono and multi anisotropic coatings, by understanding the link between the parameters of elaboration, the physical-chemical properties, the microstructures and the elastic constants of the materials.

Keywords: Coatings, Elastic constants, Anisotropy, Multilayers, Impulse Excitation Technique, PVD.

Acknowledgements: The authors would like to thank the co-founders of CERA project: The European Union (Fond Européen de Développement Régional)

References:

[1] M.F. Slim, A. Alhoussein, F. Sanchette, B. Guelorget, M. François, A new enhanced formulation to determine Young's and shear moduli of thin films by means of Impulse Excitation Technique, Thin solid films, 2017.

[2] M.F. Slim, A. Alhoussein, A. Billard, F. Sanchette, M. François, On the determination of Young's modulus of thin films with Impulse Excitation Technique, Journal of Materials Research, 2016.

9:40am **E2-1-TuM6 Oxidation Resistance of Ti6Al4V-Si₃N₄ Composites Fabricated through Spark Plasma Sintering Method**, *F. Kgoete (f.kgoete@gmail.com)*, P.A. Popoola, Tshwane University of Technology, Pretoria, South Africa

In this work, elevated temperature oxidation of Ti6Al4V and Ti6Al4V-xSi₃N₄ composites using thermal gravimetric analyser (TGA) in air at 45-800°C are reported. Specimens prepared for the study were established through spark plasma sintering method at a temperature of 1000°C with a holding time of 6 mins under a pressure of 50MPa. The alloy was consolidated with varying Si₃N₄ proportions of 5wt. %, 10wt. % and 15wt%. The effects of the ceramic reinforcements on the thermally gravimetric analyzed samples were explored. Scanning electron microscope attached with energy dispersive spectroscopy (SEM-EDS) was employed to explore the oxide layer formed on the surface of the samples. The phases present in the oxidized samples were observed by energy dispersive X-ray diffraction spectrometer (XRD). Microhardness property was considered by means of high impact diamond Dura scan micro hardness tester. The results showed that the addition of Si₃N₄ to Ti6Al4V alloy considerably enhanced the oxidation resistance, and hardness of Ti6Al4V alloy which is compactable and useful for aerospace application.

New Horizons in Coatings and Thin Films

Room Pacific Salon 6-7 - Session F1-TuM

Nanomaterials and Nanofabrication

Moderators: Ulf Helmersson, Linköping University, Sweden, Vitezslav Stranak, University of South Bohemia, Czech Republic

8:00am **F1-TuM1 Single and Multi-component Nanomaterials Prepared by Means of Cluster Beam Deposition**, *O. Kylian (ondrej.kylian@gmail.com)*, Charles University, Czech Republic; *A. Shelemin, D. Nikitin*, Charles University, Czech Republic, Czechia; *P. Pleskunov, J. Hanus, P. Solar, A. Choukourov, A. Kuzminova, M. Cieslar, H. Biederman*, Charles University, Czech Republic

INVITED

Cluster beam deposition by means of gas aggregation sources (GAS) based either on magnetron sputtering or plasma polymerization become very attractive tool for the production of metal, metal-oxide or plasma polymer nanoparticles (NPs). The increasing popularity of GAS systems is caused by many advantageous features that these sources offer such as their relative simplicity, high efficiency, no or only limited use of potentially harmful solvents and precursors, cleanness of produced NPs as well as the possibility to combine gas aggregation sources with another vacuum-based deposition methods that in turn enables production of functional nanocomposite or nanostructured materials. Furthermore, recent studies showed that not only single material NPs, but also more complex multi-component NPs may be produced by GAS systems including dumbbell-like, janus-like or core@shell nanoparticles.

In this study we introduce and compare three different strategies that allow producing multi-component heterogeneous metal/plasma polymer NPs. The first one is based on the use of a composite metal/polymer target. An example of this approach is the use of Cu/nylon target mounted onto a planar magnetron introduced into the aggregation chamber of GAS. As it was found this system makes it possible to produce metal/plasma polymer

nanoparticles with multiple small metallic cores embedded in a plasma polymer shell. Similar multi-core@shell structure of created NPs was observed also when the second approach was used, in which a high amount of precursor (HMDSO) was introduced into the aggregation chamber of the GAS equipped with planar magnetron used for metal sputtering (Ag in our case). The formation of multi-core@shell NPs in both of these arrangements may be explained by the competitive growth of metal NPs and plasma polymerization process and phase segregation of metals and polymers caused by the differences between the cohesive forces of metal atoms and interaction energies of metals and organics. In order to achieve single-core@shell NPs, the third strategy was developed. This is based on the in-flight coating of metallic NPs by a thin plasma polymer shell. This is realized by an auxiliary plasma deposition source positioned in between the output orifice of the GAS and substrate. It is shown that this approach enables to fully decouple the core production from the shell deposition and it is suitable for effective production of metal/plasma polymer single-core@shell NPs.

Acknowledgments: This work was supported by the grant GACR 17-22016S from the Czech Science Foundation

8:40am **F1-TuM3 Preparation of High Activity and Stability of Cobalt Carbide Nanoparticles for Hydrogen Evolution Reaction**, *Y.H. Lin (x01n01n01n@gmail.com)*, National Cheng Kung University, Taiwan; *S.C. Wang*, Southern Taiwan University of Science and Technology, Taiwan; *J.L. Huang*, National Cheng Kung University, Taiwan

Hydrogen is one of the promising renewable energy in substitution for petroleum energy. The hydrogen produced by splitting water using renewable energy is the key to becoming a sustainable and environmentally friendly green energy. The catalyst plays an important role in hydrogen evolution reaction (HER) to enhance the efficiency. Among the transition metal carbides (TMCs), cobalt carbide is considered to be a potentially active catalyst from theoretical calculations and literature reports. However, the common syntheses are solid phase or chemical vapor deposition processed at high temperature. Here we report two wet-chemistry synthesis methods to prepare nano-sized transition metal carbide. For the first process, Co(CHOCOO)₂ and triethylene glycol (TEG) are used as cobalt and carbon source precursor, respectively. With increasing temperature and time of the reaction, TEG decomposes and Co²⁺ becomes carbonized. By controlling the amount of NaOH addition, we can adjust the ratio of Co₂C and Co₃C in the product. In the other process we use TEG and oleylamine (OLA) as precursor and without participation of NaOH, and the product will be only Co₂C. The X-ray diffraction pattern peaks show that there is the presence of Co₃C in the former process, and Co₂C dominate in the latter process. The detailed analysis of the product such as TEM, SEM, FT-IR and electrochemical properties on HER will be reported in future.

9:00am **F1-TuM4 Nanocluster-Based Metal Oxide Films for Hydrogen Gas Sensing**, *S. Haviar (haviar@ntis.zcu.cz)*, *J. Čapek, Š. Batková, N. Kumar*, University of West Bohemia, Czech Republic

Advances in the field of hydrogen-based technologies bring new challenges for material researchers working in the field of gas sensors.

Metal oxide semiconductors (MOSs) are well established as active materials in gas sensor assemblies. Especially nanostructured MOSs attract the attention because of the unique electronic properties of nanomaterials and a high reactive area. Here, we present the study of nanostructured MOS films prepared by use of a gas aggregation cluster source (GAS).

To assemble a functional hydrogen gas sensor we combined sputter-deposited thin film of tungsten oxide with cupric oxide nanoclusters prepared by GAS. Sputtering conditions were tuned to vary the chemical composition and structure of the prepared films. Various architectures were examined for their sensorial response when assembled into a hydrogen gas sensor. The specimens were tested for the response to a time-varied hydrogen concentration in synthetic air at various temperatures. The sensitivity and the response time were evaluated. It is shown that optimization of the structure, architecture and/or composition results in enhanced sensorial properties.

The prepared materials were characterized by means of X-ray diffraction (XRD), scanning electron microscopy (SEM), atomic force microscopy (AFM) and Raman spectroscopy. The chemical composition was studied using X-Ray Photoemission Spectrometry (XPS) and Near Ambient Pressure XPS (NAP).

With further expansion of mobile and portable hydrogen-based technologies the demand on miniaturization of gas sensor rises. That is why it is of a key importance that both the magnetron sputtering and deposition of clusters are techniques compatible with industrial microcircuit technologies. Moreover, in contrary to commonly used wet-techniques the

Tuesday Morning, May 21, 2019

GAS process provides nanoparticles which are clean and ready to use for catalytic purposes in the "as-deposited" condition.

Therefore the technique is very attractive for the research of new catalytic materials.

9:20am F1-TuM5 Deposition of Magnetic Thin Films by High Power Impulse Magnetron Sputtering, J.T. Gudmundsson (tumi@hi.is), H. Hajihoseini, M. Kateb, S. Ingvarsson, University of Iceland, Iceland

We study the microstructure and magnetic properties of Ni and Ni₈₀Fe₂₀ thin films grown by high power impulse magnetron sputtering (HiPIMS), and compare with films grown by dc magnetron sputtering (dcMS). The nickel films were grown under tilt angles ranging from 0 (substrate faces to the target) to 70 degrees. The magnetic hysteresis was characterized using a home-made high sensitivity magneto-optical Kerr effect (MOKE) loop. It is shown that both deposition methods exhibit in-plane biaxial anisotropy when deposited at small tilt angles while larger tilt angles result in uniaxial anisotropy. However, the angle of transition for anisotropy type is different when depositing with dcMS (35 degrees) compared to HiPIMS deposition (60 degrees). The Ni₈₀Fe₂₀ films were grown under a tilt angle of 35 degrees to identical thickness of 37 nm using both dcMS and HiPIMS [1]. All the films exhibit effective in-plane uniaxial anisotropy with square easy axis and linear hard axis magnetization traces. X-ray diffraction reveals that there is very little change in grain size within the pressure and temperature ranges explored. However, variations in film density, obtained by x-ray reflectivity measurements, with pressure have a significant effect on magnetic properties such as anisotropy field (H_k) and coercivity (H_c). We find that HiPIMS deposition results in dense films with low H_k and H_c. For epitaxial growth of Ni₈₀Fe₂₀ film on MgO (001) we find the film deposited with HiPIMS has very well defined in-plane uniaxial anisotropy along the <100> direction while the dcMS deposited film presents biaxial anisotropy in-plane, the easy directions are along the [110], indicating that crystalline anisotropy is dominant in that case.

[1] Kateb et al., J. Phys. D: Appl. Phys. 51 (2018) 285005

9:40am F1-TuM6 Fluorination of the Magnesium Particle Surface: Enhancing the Reactivity of Magnesium, M. Pantoya, S. Islam (shancita.islam@ttu.edu), Texas Tech University, USA

Most metal fuel particles are inherently passivated with their native metal oxide to prevent the pyrophoric metal core from spontaneous reaction with the surrounding environment. The metal oxide is typically a heat sink and barrier to diffusion limited oxidation reactions. One strategy for increasing the energy release rate of nanoparticle fuels is to activate surface reactions that promote faster and more complete main oxidation reactions. Recent work with aluminum (Al) nanoparticles has shown that the native oxide shell can be used to exothermically contribute to the overall energy generated. The goal of this study was to assess reactivity spurred from surface exothermic reactions to other fuels, namely magnesium, Mg. The objective was to examine surface reactions of Mg particles including nano and micron scale particles coated with a liquid fluorinated perfluoro-polyether (PFPE) polymer. To closely observe the properties of the exothermic surface reaction, magnesium-oxide (MgO) nanoparticles were also examined. Many experimental techniques including differential scanning calorimetry (DSC), thermogravimetric analysis (TGA), powder X-ray diffraction (PXRD) and transmission electron microscopy (TEM) are used to characterize the Mg-PFPE and MgO-PFPE reactions. The results showed that all samples generate a pre-ignition reaction (PIR) including micron Mg particles, and the PIR enthalpy increases with decreasing particle size. The XRD results confirm MgF₂ in all product samples. Further, activation of surface exothermic reactions was shown to affect the overall reactivity of Mg particles by combining the Mg-PFPE coated particles with another solid oxidizer, polytetrafluoroethylene (PTFE) and measuring the flame speed compared with uncoated Mg particles. Results from this study extend previous work promoting surface reactions on Al to other fuels that also benefit from this strategy.

Advanced Characterization Techniques for Coatings, Thin Films, and Small Volumes

Room Pacific Salon 1 - Session H1-1-TuM

Spatially-resolved and In-Situ Characterization of Thin Films and Engineered Surfaces I

Moderators: Grégory Abadias, Institut Pprime - CNRS - ENSMA - Université de Poitiers, France, Xavier Maeder, Empa - Swiss Federal Laboratories for Materials Science and Technology, Switzerland, Michael Tkadletz, Montanuniversität Leoben, Austria

8:20am H1-1-TuM2 Evolution of the Nanoporous Structure of Sintered Ag Joints at High Temperature using In-Situ X-ray Nanotomography, X. Milhet (xavier.milhet@ensma.fr), A. Nait-Ali, D. Tondiang, L. Signor, Institut Pprime - CNRS - ENSMA - Université de Poitiers, France; M. Legros, Cemes - Cnrs, France; Y. Liu, D. Van Campen, Stanford Synchrotron Radiation Lightsource - SLAC National Accelerator Laboratory, USA

Silver pastes sintering is a potential candidate for die bonding in power electronic modules. The thin Ag joints, obtained by sintering, exhibit a significant pore fraction thus reducing the density of the material compared to bulk silver. This was shown to alter drastically the mechanical properties (Young's modulus, yield strength and ultimate tensile stress) at room temperature. However, while careful analysis of the nanoporous structure has been reported in 2D, little is known about its quantitative spatial evolution during thermal aging and more specifically during temperature jumps. In this context, high temperature evolutions of the 3D nanoporous structure were observed in-situ using a heater fitted into the beamline 6-2C of SSRL. Segmentation of the porosity and subsequent statistical analysis of the tomographic dataset reveal pore shape, size and spatial distributions evolution during continuous heating. Such an analysis provides insight into the microstructural evolution of sintered nanoporous Ag joints in-service.

8:40am H1-1-TuM3 Atom Probe Tomography to Help Understand

Deformation Mechanisms in Metallic Alloys, B. Gault (b.gault@mpie.de), Max-Planck Institute for Iron Research, Düsseldorf, Germany; P. Kontis, S.K. Mäkinen, J. He, Z. Peng, Max-Planck Institut für Eisenforschung, Germany; S. Neumeier, Friedrich Alexander-University Erlangen-Nürnberg (FAU), Germany; J. Cormier, Institut Pprime - CNRS - ENSMA - Université de Poitiers, France; D. Raabe, Max-Planck Institut für Eisenforschung, Germany
INVITED
Atom probe tomography (APT) is a burgeoning materials characterization technique that enables elemental mapping in three-dimensions at the nanoscale and with high elemental sensitivity. APT exploits the effect of an intense electrostatic field to cause the departure of individual atoms, in the form of ions, from the end of a very sharp needle-specimen. The very particular geometry of the specimen gives rise to a highly magnified image formed by the projected ions that are accelerated away from the specimen's surface by the electric field itself. This projection microscope is then coupled with a time-of-flight mass spectrometer to reveal the elemental identity of each of the detected ions. In this presentation, I will cover some of the basics of the technique, I will be showcasing some applications to investigate segregation phenomena induced by the plastic deformation of high-temperature alloys.

9:20am H1-1-TuM5 On the Chemical Composition of TiAlN Thin Films - Comparison of Ion Beam Analysis and Laser-assisted Atom Probe Tomography with Varying Laser Pulse Energy, M. Hans (hans@mch.rwth-aachen.de), J.M. Schneider, RWTH Aachen University, Germany

We compare the chemical composition of TiAlN thin films determined by ion beam analysis and laser-assisted atom probe tomography (APT). The laser pulse energy during APT was increased subsequently from 10 to 20, 30, 40, 50, 100 and 200 pJ within a single measurement, covering the range that is typically employed for the analysis of transition metal nitrides. The laser pulse energy-dependent Ti, Al and N concentrations were compared to ion beam analysis data, combining Rutherford backscattering spectrometry and elastic recoil detection analysis with the total measurement uncertainty of 2.5% relative deviation. It can be learned that the absolute N concentration from APT is underestimated by at least 9% and the absolute Al concentration from APT is overestimated by at least 16%, while absolute Ti concentration values are for both techniques in good agreement. The here presented comparative analysis clearly shows that absolute Al and N concentration values obtained by ion beam analysis deviate significantly to the APT data for the laser pulse energy range from 10 to 200 pJ.

9:40am **H1-1-TuM6 Microstructure and Oxidation States of Ni in Sub-Nanometric Layer Depending on its Seed-Layer (Zinc Oxide, Silver Layers): A Multi-Techniques Approach to Trespass Limits of Resolution, J. Voronkoff** (justine.voronkoff@saint-gobain.com), H. Montigaud, Saint-Gobain Recherche/CNRS, France; L. Largeau, CNRS/C2N, France; S. Grachev, Saint-Gobain Recherche/CNRS, France

Functional glazing for thermal isolation consist of stack of layers deposited by PVD magnetron sputtering on flat glass substrates at room temperature. They combine metallic and dielectric thin layers in order to optimize reflectance in the IRs and transmission in the visible. The determination of layers microstructures and chemical states is of great interest for industrials to understand the macroscopic (optical, mechanical) properties of such stacks. Literature is restricted and suffers a lack of adapted techniques. Hence, this is of major interest to develop tools to understand those stacks microstructures.

For this study, we have focused our works on the behavior of ultra-thin layers of nickel or nichrome (< 1 nm) deposited on silver (10-20nm) and zinc oxide layers (5-20nm), which could be found in such functional stacks. First part is dedicated to investigations on the seed layer (ZnO and Ag) which are polycrystalline. AFM images and GIXRD in coplanar and non-coplanar modest to reach key parameters such as crystal size, density of grain boundaries and surface morphology which drastically influences the NiCr layer characteristics. In addition to the heterogeneous environment and the small thicknesses, the oxidation state of Ni and Cr itself impact the layer morphology, which make it challenging to characterize. In order to characterize the NiCr layer depending on the sputtering deposition conditions and its under-layers as best as possible, we use a multi-approach using combined high resolution techniques: AFM, GIXRD, XPS in situ, TEM and STEM-HAADF, Atom Probe Tomography. We use a XPS directly connected to the deposition chamber that enables following the growth at the first stages of the NiCr layer along the deposition process. Using a tilted XPS mode could give us information regarding the growth of NiCr (island or homogeneous layer) without any contact to the atmosphere. Moreover, XPS analysis gives access to the oxidation states of the different species in presence (Ni, Cr and the topmost part of the seed-layer). Coupled with ex situ STEM-HAADF it permits a 2D characterization of crystallites size and distributions, Ni coverage and microstructure depending on the different substrates (Ag, ZnO) and to have chemical information. ATP first results complete those revealed by STEM with the 3D distribution of the species with a sensibility much higher than EDS. All those techniques give complementary information with more or less advantages at different resolutions, which would be discuss and justify their combined use. Deposition conditions for the sputtered layers will be compared as they directly determine the properties discussed above.

10:00am **H1-1-TuM7 Nanomechanical Investigation on Lateral fcc-w Phase Fields of a Partially Decomposed and Transformed Nano-lamellar CVD fcc-Ti_{0.2}Al_{0.8}N Coating, M. Tkadletz** (michael.tkadletz@uniloben.ac.at), A. Lechner, N. Schalk, Montanuniversität Leoben, Austria; B. Sartory, Materials Center Leoben Forschung GmbH (MCL), Austria; C. Mitterer, Montanuniversität Leoben, Austria; C. Czettl, CERATIZIT Austria GmbH, Austria

In metastable, nano-lamellar chemical vapor deposited (CVD) fcc-Ti_{1-x}Al_xN coatings, at elevated temperatures, intact fcc-TiAlN areas co-existing with non-lamellar fully decomposed and transformed fcc-Ti(Al)N and w-Al(Ti)N areas could be observed. It is assumed that the observed phase fields and their microstructure strongly correlate with their mechanical properties. To study this correlation, this work focuses on the investigation of a nano-lamellar CVD fcc-Ti_{0.2}Al_{0.8}N coating in an intermediate sample state annealed at 1050 °C for 5 min, exhibiting fcc- and w-phase fractions side by side. A cross-section of the coating was characterized by means of scanning electron microscopy (SEM) and electron backscatter diffraction (EBSD) measurements and subsequently used for nanomechanical testing. Modulus mappings were performed by evaluating the elastic response after superimposing a dynamically oscillating load to the contact force applied during scanning probe microscopy imaging. Arrays of low load quasistatic indentations on the respective positions provided the basis to create maps of the lateral hardness distribution with a resolution of ~100-200 nm. A cross-correlation of the results with SEM images and EBSD inverse pole figure maps allowed to clearly identify the lateral phase fields and their effects on the mechanical properties. Obtained moduli and hardness values were in good agreement with values measured on the as-deposited and fully decomposed/transformed state. The results of this study clearly demonstrate the power of correlative characterization techniques for the investigation of advanced hard coating materials at the nanoscale.

Tuesday Morning, May 21, 2019

Exhibition Keynote Lecture

Room Town & Country - Session EX-TuEx

Exhibition Keynote Lecture

Moderators: Christopher Muratore, University of Dayton, USA, Michael Stüber, Karlsruhe Institute of Technology (KIT), Institute for Applied Materials (IAM), Germany

11:00am EX-TuEx1 **Advanced Performance of Tools in Sheet-metal Forming - The Synergy of Surface Technology and Tooling Material Selection, F. Nahif (farwah.nahif@eifeler-vacotec.com)**, voestalpine eifeler Vacotec GmbH, Germany **INVITED**

Within the last years the global trend towards reduction of CO₂ emission and resource efficiency have significantly influenced the product design within the automotive industry and enhanced the relevance of light weight construction parts. This trend has been followed by the development and introduction of new sheet materials for forming application, such as high-strength steels with optimized properties to compete with the performance and functionality of alternative lightweight materials.

Due to this development and progress in sheet-metal material properties for automotive applications, the requirements for forming tool design are evolving permanently.

Although the application of PVD coatings in forming and cutting tool application has become common practice, the improvement of forming tool design is strongly dependent on the optimal matched value chain.

To obtain advanced functionality and performance the focus of the forming tool design has to be set on the synergy of high quality tool steels, pre-treatment and PVD surface technology.

A profound knowledge of the tool conditions during forming of high strength steel grades is prerequisite to understand the wear mechanisms and the most possible tool failure types. The transfer of this information into requirements for the forming tool and an in-depth analysis of the most suitable combination of physical and mechanical properties of tool steel and PVD coating as well as the appropriate choice of pre-treatment are the key factors of a superior forming tool design.

The talk will cover the beneficial synergy of PVD-based surface technology and tooling material selection, by discussing industrial application examples and highlighting the importance of an optimal matched value chain to obtain advanced functionality and performance of PVD-coated tools in sheet-metal forming.

Coatings for Use at High Temperatures

Room Pacific Salon 2 - Session A1-2-TuA

Coatings to Resist High-temperature Oxidation, Corrosion, and Fouling II

Moderators: Lars-Gunnar Johansson, Chalmers University of Technology, Sweden, Shigenari Hayashi, Hokkaido University, Japan, Justyna Kulczyk-Malecka, Manchester Metropolitan University, UK

1:40pm **A1-2-TuA1 Nano Coatings To Achieve Cost Effective And Long Lifetime SOFC Interconnects**, J.-E. Svensson (jes@chalmers.se), Chalmers University of Technology, Sweden

INVITED
Ferritic stainless steel interconnects are widely used in solid oxide fuel cells (SOFC) due to a combination of low cost, compatible thermal expansion properties and ease of manufacturing. Nonetheless, their viability is hindered by several key technical hurdles. Most stainless steels suggested for SOFC applications rely on the formation of a fairly protective chromium oxide scale. However, in air side environments Cr species evaporation leads to material failure and insufficient lifetimes. Additionally even a protective oxide scale grows with time and since chromium oxide is only a moderate electronic conductor, this results in an increase of Area Specific Resistance (ASR). This work investigates nano coatings to mitigate both degradation mechanisms. FeCr steels have been coated with Co and/or Ce using Physical Vapor Deposition (PVD). The materials were exposed in air at 600-850 °C for up to 3000 h and oxide scale growth, chromium evaporation and electrical resistance were studied using mass gain data, the Cr-evaporation denuder technique and ASR measurements respectively. The effect of dual atmosphere exposure are also investigated. Exposed samples were additionally examined by Scanning Electron Microscopy/Energy Dispersive X-Ray (SEM/EDX) analysis. The results show that thin Co coatings effectively mitigate Cr volatilization. By adding Ce to the coating the performance was further improved as the oxidation rate was significantly reduced, thus resulting in substantially reduced ASR values. These results imply that the duplex, Co + Ce thin film coating is suitable for ferritic stainless steel interconnects in SOFCs.

2:20pm **A1-2-TuA3 Influence of Ta Content on Properties of TiAlTaN Films**, H.F. Shang (shanghongfei@tsinghua.edu.cn), T.M. Shao, State Key Laboratory of Tribology, Tsinghua University, China

Binary and ternary nitrides of transition metal elements, such as Ti, Cr, Zr, V, Nb, or Ta, exhibit outstanding mechanical, chemical, and thermal properties, and are utilized as protective coatings in machining, automobile and other industrial areas. Recently, alloying titanium aluminium nitride (TiAlN) with tantalum can improve cutting performance. Titanium aluminium tantalum nitride (TiAlTaN) films have been reported on improved mechanical and tribological properties.

In this work, a series of TiAlTaN films with different Ta contents were deposited using an ion beam assisted deposition. Microstructure of the as-deposited films was characterized by using X-ray diffraction (XRD), X-ray photoelectron spectroscopy (XPS) and scanning electron microscope (SEM). Mechanical properties of the TiAlTaN films were also tested. Tribological behavior and corrosion performance of the TiAlTaN films were analyzed and compared to that of the TiAlN film. Results show that the TiAlTaN films demonstrated better mechanical properties, tribological behavior and corrosion resistance than the TiAlN film. Ta content has a great influence on the properties of the TiAlTaN films.

2:40pm **A1-2-TuA4 Cr-Al-Si-N Quaternary Coating Applied on Zirconium Alloy: Combining Superior Resistance of High-temperature Steam Oxidation and Improved Mechanical Properties**, F.F. Ge (gefangan@nimte.ac.cn), H. Zhu, F. Huang, Ningbo Institute of Material Technology and Engineering, Chinese Academy of Sciences, China

Accident tolerant fuel claddings are extremely urgent to increase the safety margin of light water reactors. Cr-Al-Si-N quaternary coatings were proposed to increase mechanical properties and high-temperature steam oxidation resistance of Zr-based alloy. $(Cr_{60}Al_{30}Si_{10})_xN_{1-x}$ coatings with three kinds of microstructure, were prepared on Zr coupons, followed by evaluation of their mechanical properties and oxidation resistance under high-temperature steams. Moreover, to reveal the anti-oxidation mechanism, much examination was performed on the microstructure the oxidized samples. Compared to the "dense & columnar" coating, the "dense & featureless" coating exhibits a combination of the best mechanical properties and the highest oxidation resistance. It increases the H and the E* of the uncoated Zr coupon by ~4 times has a and ~twice, respectively. After coated on the "dense & featureless" coating with the thickness of ~5 μm,

the oxidation of the Zr coupon was completely suppressed in the 1000 °C steam for 15 min, and the thickness of the α-Zr(O) layer decreased by 40% - 92% in the 1200 °C steam for 30 min. Furthermore, a ~10 μm thick "dense & featureless" coating can prevent the Zr coupon from oxidizing in the 1200 °C steam for >1 h. By contrast, the "porous & columnar" coating can hardly provide any protection for the uncoated Zr substrate in the high-temperature steam. It demonstrates that the densely fine-grained or amorphous microstructure could effectively suppress the inner-diffusion of O and favor the formation of a dense and coherent scale on surface, which would be highly desirable for the protection coatings of Zr claddings.

4:00pm **A1-2-TuA8 Polyurethane Protective Coating with Self Polishing Property**, M.M. Rahman (mohammadmizanur@gmail.com), King Fahd University of Petroleum and Minerals, Saudi Arabia

Waterborne Polyurethane (WBPU) coatings are widely used to protect metals from corrosion and fouling. Owing to restrictions on using toxic materials scientists are attempting to develop new, more environmentally-friendly coatings that maintain their performance over extended periods. Unfortunately, these coatings are inadequate to prevent metal corrosion and fouling under adverse conditions especially marine condition. Self-polishing coatings (SPC) are considered to be among the most effective technologies. Self-polishing coatings facilitate the continuous renewal of the surface and the release of active compound via a hydrolysis reaction or an ion exchange reaction with seawater. In this study, WBPU coatings were synthesized by in-situ polymerization. Synthesis and properties of coatings were investigated by Fourier transform-infrared spectrometer, proton-nuclear magnetic resonance and dynamic light scattering. The polishing rate of coating was determined from the reduction in dry film thickness after artificial seawater immersion under a dynamic condition. The corrosion and fouling resistance of coatings were also considered after certain interval.

4:20pm **A1-2-TuA9 Production of a Zinc Impregnated Stainless Steel Surface Utilizing Cathodic Plasma Electrolytic Deposition (CPED) for Retardation of Cobalt Ion Deposition in High Temperature Aqueous Conditions**, C. Fox (ciara.fox@manchester.ac.uk), F. Scenini, A. Yerokhin, N. Laugel, University of Manchester, UK; R. Wain, Rolls-Royce, UK

The majority of the radiation field present in light water nuclear reactors is the result of the build-up of radioactive cobalt species on structural components and this can lead to occupational radiation exposure to personnel during maintenance and inspections. However, it has been shown that zinc added to the high temperature coolant water hinders the deposition of aqueous cobalt cations onto the surface of stainless steel because it is preferentially incorporated into the inner spinel corrosion layer on stainless steel surfaces over cobalt. This work looks at the feasibility of preconditioning the stainless steel surface with zinc to remove the need for zinc additions into the coolant water.

In this work the surface modification of a 316 stainless steel to promote superficial zinc enrichment is explored. The modified alloy is created utilised Cathodic Plasma Electrolytic Deposition (CPED). The stainless steel work piece is used as the cathode in an aqueous electrolyte bath containing zinc cations and a voltage between 110V – 150V is applied to generate plasma discharges at the surface of the cathode. The superficial layer was characterised by scanning electron microscopy (SEM), energy-dispersive X-ray spectroscopy (EDS), grazing angle X-ray diffraction (G-XRD) and glow discharge optical emission spectroscopy (GDOES) to identify the phases present on the treated samples.

The high surface temperatures generated during plasma discharges were shown to promote the diffusion of zinc which has been detected up to 3 micrometres in depth into the stainless steel substrate. In addition to zinc penetration into the stainless steel matrix, zinc is also deposited on the surface as a rough and porous zinc oxide coating which can be mechanically removed from the stainless steel surface. The effect of process parameters on zinc diffusion into the substrate as well as the treatment time and composition of the electrolyte, are discussed.

Hard Coatings and Vapor Deposition Technologies

Room California - Session B4-2-TuA

Properties and Characterization of Hard Coatings and Surfaces II

Moderators: Naureen Ghafoor, Linköping Univ., IFM, Thin Film Physics Div., Sweden, Ulrich May, Robert Bosch GmbH, Germany, Fan-Bean Wu, National United University, Taiwan

1:40pm **B4-2-TuA1 Fracture Toughness Enhancement in Superlattice Hard Coatings**, R. Hahn (rainer.hahn@tuwien.ac.at), M. Bartosik, H. Riedl, TU Wien, Institute of Materials Science, Austria; H. Bolvardi, Oerlikon Balzers, Oerlikon Surface Solutions AG, Liechtenstein; S. Koloszári, Plansee Composite Materials GmbH, Germany; P.H. Mayrhofer, TU Wien, Institute of Materials Science, Austria

Physical vapour deposited (PVD) ceramic hard coatings are widely used in industrial applications as protective, wear reducing coatings. Their combination of good mechanical properties such as high hardness, a low friction coefficient, and their chemical resistance enable the application in harsh environments. However, a strong limitation is the relatively low fracture tolerance (brittle behaviour), depicting especially in cutting applications a major challenge.

In this contribution, we show experimental results of *in-situ* microcantilever bending tests on nanolayered TiN-CrN coatings, referred to as superlattices, overcoming this unfavourable behaviour. We found a maximum in fracture toughness (K_{IC}) at bilayer periods of ~6 nm [1], similar to the well-known peak for the indentation hardness reported by Helmersson et al. [2]. For both, K_{IC} and the hardness, we observe an increase by ~50 % compared to the rule of mixture of the constituents. The beneficial effect of a careful structural design on the fracture toughness will be shown for reactive magnetron sputtered as well as arc evaporated superlattice coatings. Importantly, the coatings synthesized in the industrial scale arc evaporation plant (Oerlikon Balzers Innova) show an even more pronounced superlattice effect and thus unite high hardness with reasonable toughness.

While mechanisms based on dislocation activity explain the increase in hardness, the linear elastic behaviour during our micromechanical tests suggests a different mechanism responsible. To describe this, we conducted density functional theory (DFT) calculations as well as finite element studies.

Complementary, we studied the microstructure of our coatings by X-ray diffraction experiments, scanning electron microscopy and high-resolution transmission electron microscopy. The thermal stability of our films was investigated by annealing in vacuum and ensuing experiments (XRD, hardness and fracture toughness) [3] along with differential scanning calorimetry (DSC) investigations.

[1] R. Hahn, M. Bartosik, R. Soler, C. Kirchlechner, G. Dehm, P.H. Mayrhofer, Superlattice effect for enhanced fracture toughness of hard coatings, *Scripta Mat.* 124 (2016) 67.

[2] U. Helmersson, S. Todorova, S.A. Barnett, J.-E. Sundgren, L.C. Markert, J.E. Greene, Growth of single-crystal TiN/VN strained-layer superlattices with extremely high mechanical hardness, *J. Appl. Phys.* 62 (1987) 481.

[3] R. Hahn, M. Bartosik, M. Arndt, P. Polcik, P.H. Mayrhofer, Annealing effect on the fracture toughness of CrN/TiN superlattices, *Int. J. Refract. Met. H.* 71 (2018) 352-356.

2:00pm **B4-2-TuA2 Simultaneous Topographical and Electrochemical Mapping using Scanning Ion Conductance Microscopy - Scanning Electrochemical Microscopy (SICM-SECM)**, W. Shi, G.M. Mendoza (gabriela@parksystems.com), B.K. Kim, K. Lee, Park Systems Corporation, USA

Lately, scanning ion conductance microscopy (SICM), has emerged as a versatile non-contact imaging tool. To obtain spatially-resolved electrochemical information, scanning electrochemical microscopy (SECM), also known as the chemical microscope, has been developed. Hybrid SICM-SECM techniques have been developed, in which the SICM compartment provides the accurate probe-sample distance control, while the SECM compartment measures the faradaic current for electrochemical information collection.

In this work, we demonstrate the use of an Atomic Force Microscopy (Park NX10) in combination with an ammeter for concurrent topography imaging and electrochemical mapping. The SICM-SECM probe consisted of a Au crescent electrode (AuE) on the peripheral of a nanopipette. High resolution

probe-substrate distance control was obtained by the ion current feedback from SICM, while simultaneous electrochemical signal collection was achieved via the AuE from SECM. As a proof-of-concept experiment, a Au/Pyrex pattern standard sample was imaged with the SICM-SECM technique. The Au bar and the Pyrex substrate were clearly resolved from the SICM topography image, with the bar height and pitch width closely matching the actual values. In terms of the electrochemical property mapping, higher Faradaic current was seen when the probe was scanned over Au bar as a result of redox cycling, while lower Faradaic current was observed when the probe was over Pyrex substrate due to hindered diffusion. The capability of the SICM-SECM technique described here holds promise of many exciting applications in the field of electrochemistry, battery research and metallurgical coatings.

2:20pm **B4-2-TuA3 Evaluation of the Cavitation Resistance of a Nitrided Stainless Steel**, J.L. Arciniega-Martinez (jarciniega@ipn.mx), Instituto Politécnico Nacional, Escuela Superior de Ingeniería Mecánica y Eléctrica, Unidad Azcapotzalco., México; G.A. Rodríguez-Castro, Instituto Politécnico Nacional, Grupo Ingeniería de Superficies, Mexico, México; A. Meneses-Amador, Instituto Politécnico Nacional Grupo Ingeniería de Superficies, México; J.E. Rivera-López, C.A. Juárez-Navarro, Instituto Politécnico Nacional, Escuela Superior de Ingeniería Mecánica y Eléctrica, Unidad Azcapotzalco, México; I.E. Campos-Silva, Instituto Politécnico Nacional Grupo Ingeniería de Superficies, México

The cavitation erosion resistance of nitrided AISI 304L Steel was evaluated. The stainless steel was subjected to the Tenifer nitride process at a temperature of 580 °C for 2 and 8 h; subsequently the cooling was carried out at room temperature and in oxidizing salts to evaluate its effect. To evaluate the morphology of the layer, chemical composition and phases, scanning electron microscopy (SEM), energy dispersion spectroscopy (EDS) and X-ray diffraction (XRD) were used. Once the coatings were formed, they were exposed to the cavitation cloud, venture type, causing dynamic impact degradation; the tests were carried out with a throat/inlet ratio (B) = 0.24 and cavitation coefficients (s) = 0.86, 1.2 and 2.9 at room temperature. Curves of mass loss, erosion rate and roughness parameters were plotted as a function of exposure time. The relationship between microstructure, time-variation curves and wear mechanisms are discussed.

2:40pm **B4-2-TuA4 Modeling Of Coating Thickness In Electrostatic Spray Deposition Using Response Surface Methodology And Artificial Neural Network**, U.M.R. Paturi (maheshpaturi@cvr.ac.in), Department of Mechanical Engineering, CVR College of Engineering, Hyderabad, India; N. Subba Reddy, Engineering Research Institute, GNU, Republic of Korea; S.K.R. Narala, BITS Pilani Hyderabad, India

To extend the quality and efficiency of any process before resorting to expensive and time consuming experimental investigations, it is essential to model and estimate the process performance with regard to its operational factors. Predictive modeling through artificial neural network (ANN) is one of the most used soft computing methods, alternative to traditional statistical response surface methodology (RSM) technique. Present study attempts to model the coating thickness in complex electrostatic spray deposition (ESD) coating process using RSM technique and match its prediction capability with ANN model. For this objective, RSM and ANN models were established for the real time ESD experiments conducted according to Taguchi's L27 (3¹³) orthogonal array based design of experiments (DOE). Statistical approach by analysis of variance (ANOVA) and Anderson-Darling p-value is engaged to examine the rationality of RSM model. In ANN modeling, a multilayer feed-forward neural network built back-propagation training algorithm is used with input parameters of electric potential, feed pressure and substrate distance. The optimum ANN model with 3-6-6-1 architecture consists of 0.6 momentum term and 0.3 learning rate with attained mean squared error (MSE), absolute error in prediction (AEP) of trained and test data are 0.000334, 0.197 and 0.54365 respectively. The coating thickness values obtained from RSM and ANN models and the experimental results obtained in this study are related and error in prediction was computed. From the results presented, the Pearson's correlation coefficient (R) value with ANN model for the training and testing data were determined as 0.993, 0.921 respectively; whereas, with RSM model, Rvalue for corresponding data was estimated to be 0.949 and 0.882 respectively. Although, the degree of linear dependency of fit between model predicted and experimental results confirmed to be fairly convincing, the degree of precision in coating thickness prediction with ANN model was realized to be quite high than that of traditional RSM model. The outcome of this study conclude that the use of ANN modeling approach can endow a

possible substitute to ESD process optimization as well as curtailing time consuming and expensive experimental investigations.

Keywords: Electrostatic spray deposition, Coating thickness, Response surface methodology, Artificial neural network

4:00pm **B4-2-TuA8 Performance Comparison of Two Diffusion Models for Describing the Growth Kinetics of Iron Boride Layers**, *M. Ortiz-Domínguez*, Universidad Autónoma del Estado de Hidalgo, México; *O. Gómez-Vargas, J. Solís-Romero (jsolis@ittla.edu.mx)*, Instituto Tecnológico de Tlalnepantla, México; *G. Ares de Parga*, Instituto Politécnico Nacional, México; *J. Oseguera-Peña*, Tecnológico de Monterrey, México

In selecting and designing materials for certain engineering applications is an important factor. Likewise, one of the most important reasons for the machinery parts to suffer damage and fail is wear. The boriding process is adequate to increase the surface hardness and a very significant resistance against some acids, bases, metal solutions and high temperature oxidizing are among the advantages of boriding over other surface hardening methods to extend its lifetime. An indispensable tool to choose the suitable process parameters for obtaining boride layer of an adequate thickness is the modeling of the boriding kinetics. Moreover, the simulation of the growth kinetics of boride layers has gained great interest in the recent years. In this study, the AISI O1 steel was pack-borided in the temperature range of 1123-1273 K for different treatment times ranging from 2 to 8 h. Two kinetic models were proposed for estimating the boron diffusion coefficients through the Fe₂B layers. Displacements of the interface (Fe₂B/substrate) resulted from a difference of the arrival flux of the interstitial boron atoms to one phase. The mass balance equations were formulated. The measurements of the thickness (Fe₂B), for different temperature of boriding, were used for calculations. As a result, the boron activation energy for the AISI O1 steel was estimated as 197.20 kJ mol⁻¹. This value of energy was compared between both models and with other literature data. In addition, to extend the validity of the present models, two additional boriding conditions were done. The Fe₂B layers grown on AISI O1 steel were characterized by use of the following experimental techniques: X-Ray Diffraction (XRD), Scanning Electron Microscopy (SEM) and Energy Dispersive X-Ray Spectroscopy (EDS).

4:20pm **B4-2-TuA9 Microstructure and Surface Strength of Chemically Modified WC-Co for Adhesive Strength Improvement**, *D. Kiyokawa (dkiyokawa@chemeng.osakafu-u.ac.jp)*, *C. Tanaka, T. Saito, N. Okamoto*, Osaka Prefecture University, Japan; *A. Kitajima, K. Higuchi*, Osaka University, Japan

Chemical vapor deposited (CVD) or physical vapor deposited (PVD) hard material coating technique is widely used the cemented-tungsten carbide (WC-Co) for molds and cutting tools, which plays an important role in a lot of manufacturing industry. However, the adhesive strength is one of the issues for reliable mold preparation.

In this study, substrate is pretreated by chemical treatment with aqua regia (3HCl:HNO₃) for 1 to 5 min at 25 to 60°C to remove Co from the WC-Co surface and to increase surface roughness to enhance adhesion strength. The hardness of films was measured by dynamic ultra-micro hardness tester (Shimadzu Co. DUH-211). Pretreated WC-Co substrates are measured for bulk strength with 200 gf of test load as well as for surface strength with 25 gf of test load.

Figure 1 shows Martens hardness (HM) of WC-Co bulk after pretreatment. Hardness of pretreated substrate became gradually lower. Figure 2 shows HM of WC-Co surface after pretreatment. Hardness of pretreated substrate became lower, even after 1min/25°C treatment. In addition, the difference in HM increased with higher temperature and longer treatment period. The brittleness of WC-Co surface after surface treatment should be eliminated. The TiC-based hard coating deposition of surface treated WC-Co will be discussed.

4:40pm **B4-2-TuA10 Compositional and Processing Effects on Phase Transformations and Mechanical Properties of Additive Manufactured Ti-6Al-4V Alloy**, *O.S. Fatoba (drfatobasameni@gmail.com)*, *E.T. Akinlabi, S.A. Akinlabi*, University of Johannesburg, South Africa

Titanium Alloy (Ti-6Al-4V) unlocks a wide range of useful applications in aerospace industries; these industries make use of different additive manufacturing (AM) techniques to obtain parts of different properties for different uses by this titanium alloy. titanium alloy mainly stands out due to the properties such as high specific strength to weight ratio, and excellent corrosion resistance. Despite these benefits, the formation of defects such as pores and cracks play a vital role in the quality of the deposited coatings. The presence of these unwanted artefacts on laser deposited coatings

depends on the melting, cooling and solidification of the melt pool, dilution rate and process parameters. This research paper focuses on the effect of hybrid coating of Ti-Cu-Al on a grade five titanium alloy (Ti-6Al-4V) using laser metal deposition (LMD) process at different laser process parameters.

A 3kW continuous wave ytterbium laser system (YLS) attached to a KUKA robot which controls the movement of the cladding process was utilized for the fabrication of Ti-Cu-Al coatings on Ti-6Al-4V alloy.

The titanium clad surfaces were investigated for its microstructure, mechanical properties and corrosion resistance characteristics at different laser processing conditions. The samples were cut to corrosion coupons and immersed into 4M NaCl solution at 28°C using Potentiodynamic Polarization (LP) and Electrochemical Impedance Spectroscopy (EMS) techniques. Hardness measurements were done using a Vickers micro-hardness tester. Ti-6Al-4V/Ti-Cu-Al composites were analysed using optical microscopy, scanning electron microscopy (SEM) with energy dispersive microscopy (EDS), and x-ray diffraction (XRD). The enhanced tensile strength, yield strength and micro-hardness were attributed to the formation of hard intermetallic compounds (TiCu, Ti₂Cu, CuTi₃, TiCu₃, Al₃Ti) produced through the in-situ metallurgical reactions during the LMD process. In addition, the rapidly solidified homogeneous fine microstructure imparts the coatings good combination of strength and toughness, which also contributes to the excellent resistance of the coating to spallation and delamination during dry sliding wear process. The addition of Cu impacts positively on the Young's modulus of the coatings. The enhanced Young's modulus was because of copper interlayer which is attributed to the presence of Ti-Cu intermetallics (like CuTi₃ and Cu₃Ti). The intermetallic also provides an enveloping effect giving rise to a protective barrier against corrosion.

Keywords: Ti-6Al-4V alloy; Corrosion; Mechanical Properties; Microstructure; Ti-Cu-Al coating; Process Parameters.

Hard Coatings and Vapor Deposition Technologies Room Golden West - Session B7-TuA

Plasma Diagnostics and Growth Processes

Moderators: Arutiun P. Eghasarian, Sheffield Hallam University, UK, Yolanda Aranda Gonzalvo, University of Minnesota, USA

1:40pm **B7-TuA1 On the Growth of TiO_x Coatings by Reactive Magnetron Sputtering from Metallic and Ceramic (TiO_{1.8}) Targets: A Joint Modelling and Experimental Story**, *R. Tonneau (romain.tonneau@unamur.be)*, *P. Moskovkin*, University of Namur, Belgium; *W. De Bosscher*, Soleras Advanced Energy, Belgium; *A. Pflug*, Fraunhofer Institute for Surface Engineering and Thin Films, Germany; *S. Lucas*, University of Namur, Belgium

This work reports the study of the growth mechanisms involved in TiO_x thin film deposition by magnetron sputtering. An Ar-O₂ plasma chemistry obtained by dual magnetron setup operating in DC mode is used. Growth from both metallic and TiO_{1.8} targets are compared. Isotopic ¹⁸O₂ is used as reactive gas for all different configurations. The aim is to differentiate oxygen coming from ceramic targets and oxygen coming from the gas phase. Indeed, using ion beam analysis techniques such as Rutherford Backscattering Spectroscopy it is possible to precisely analyze Ti, ¹⁶O and ¹⁸O content of the samples. Other investigation techniques such as AFM, SEM ... are also used to fully characterize deposited coatings. In order to study the effect of energetic ions bombardment of samples during deposition, 70° and normal incidence samples are compared. In addition to sample's characterization, Langmuir probe and energy flux probe are used to obtain plasma phase properties.

In a second part, simulations tools are used to predict both discharge and coating's properties. In order to simulate the complete plasma process, three different software are used. Each one is handling a defined step of the process (i) neutral particle motion, (ii) charged particle motion and (iii) film growth. We will discuss the comparison between simulation predictions and experimental investigations. Those two approaches allow us to achieve a better understanding on the growth of oxide layers by reactive magnetron sputtering and how plasma parameters influence coating properties.

2:00pm B7-TuA2 Titanium Atom and Ion Number Density Evolution in Reactive HiPIMS with Oxygen, Nitrogen and Acetylene Gas, *M. Fekete*, Masaryk University, Brno, Czech Republic; *D. Lundin*, Université Paris-Sud/CNRS, France; *K. Bernatova*, *P. Klein*, *J. Hnilica*, *P. Vasina* (vasina@physics.muni.cz), Masaryk University, Brno, Czech Republic

Reactive high power impulse magnetron sputtering (R-HiPIMS) offers a great opportunity for high quality coating production thus understanding the processes accompanying deposition is of great importance. The hysteresis curve in R-HiPIMS generally exhibits a narrower shape compared to dCMS, or it can even be entirely suppressed, which is beneficial for high-rate deposition of stoichiometric compound films. The main reason of the hysteresis suppression is not yet completely understood. A recently developed effective branching fraction method is utilized to determine absolute ground state number densities of sputtered titanium species from the optical-emission signal. We report on evolutions of titanium atom and ion ground state densities in R-HiPIMS discharges in oxygen, nitrogen and acetylene gases for constant mean power and pulse duration, when varying the repetition frequency. A fast feedback system is employed to allow working in the transition region of the hysteresis curve in a well-controlled manner. The ionization fraction of sputtered species increases with the partial pressure of the reactive gas. The increased ionization of titanium is attributed to the combination of the following effects: a longer residual time of sputtered species in the target vicinity; a higher maximal discharge current attained at the end of the pulse; lower amount of sputtered species due to the target poisoning which may positively affect electron distribution function. It is furthermore found that the hysteresis curve shape changes when varying the repetition frequency at the same mean power. The difference is more pronounced for R-HiPIMS with higher sputtered species ionization fraction. The experimental results are compared to the results obtained by a reactive ionization region model (R-IRM). The absolute ground state number densities of Ti atoms and Ti ions measured at the target vicinity are also substituted into the Berg model modified to include ion back attraction, and a rather good match between the measurements and simulation results for different experimental conditions is found.

2:20pm B7-TuA3 Phase Formation during Sputtering of Copper in Argon/Oxygen Mixtures, *D. Altangerel*, *D. Depla* (Diederik.Depla@ugent.be), Ghent University, Belgium

Structure zone models give an overview of the microstructure as a function of the deposition conditions. It has been shown by our research team that these overviews can be interpreted in a quantitative way by studying the ratio between the diffusivity (D) and the deposition flux (F)[1-3]. The deposition flux can easily be derived from the deposition rate. To calculate the diffusivity the available energy per deposited atom (EPA) needs to be quantified which becomes possible by measuring the total energy flux with a passive calorimetric probe. In this paper, this approach is applied to understand the phase formation during reactive sputtering of copper in an argon/mixture. The influence of the total pressure, and the discharge current was investigated. Within the experimental range hardly any changes in the EPA could be noticed, illustrating that the phase formation in the case of copper oxide thin films is solely defined by the oxygen partial pressure in the system. In the case of pure tenorite (CuO) thin films deposited at relative high oxygen partial pressures, the EPA could be increased, and it is shown that this leads to less crystalline films. The origin of this behavior is further investigated by energy-resolved mass spectrometry.

[1] Review paper : S. Mahieu, D. Depla, Journal of Physics D: Applied Physics 42 (2009) 053002

[2] Critical review paper : D. Depla, B. Braeckman, Thin Solid Films, (2016) 90-93

[3] J. Xia, W. Liang, Q. Miao, D. Depla, Applied Surface Science 439 (2018) 545–551

2:40pm B7-TuA4 Plasma Diagnostics During Growth of Transparent Conductive Oxide Thin Films by Magnetron Sputtering, *E. Stamate* (eust@dtu.dk), Technical University of Denmark, Denmark

Transparent and conductive materials are important for a large number of applications including: touch screens, solar cells, smart windows and light emitting diodes. Oxides doped with metals, generically known as transparent conductive oxides (TCO) are successfully used nowadays, with indium tin oxide (ITO) as the best material. However, the high demand for large area applications, conflicts with the reduced abundance of indium. This motivation sustains an intensive research on alternative materials with aluminum doped zinc oxide (AZO) as one of the most promising choices. There are several methods used to deposit AZO. Among them, magnetron plasma sputtering is successfully used for ITO on large area substrates and it

is also investigated as a viable cost effective method for AZO. However, the resistivity of AZO thin films is about 5 to 10 time higher than ITO, with promising values only for limited areas on the substrate. One of the main reasons is the electronegativity of oxygen that forms negative ions, resulting in a growth mechanism assisted by energetic ions with a spatial distribution correlated with the erosions tracks. In this context, a proper deposition process requires spatially-resolved plasma diagnostics in direct correlation with spatially-resolved thin film properties. This work reviews the status in plasma diagnostics during TCO growth with special emphasis on AZO. New results by mass spectrometry, optical emission and probes are also presented, both for disk and rotatable cathodes operated in DC, RF and MF using oxide (ZnO/Al₂O₃, 2, 2.5 and 3% Al) and metallic targets (Zn, 2 and 3% Al). Pressure, target to substrate distance and discharge power have been investigated as discharge parameters with the aim of obtaining a resistivity below 10⁻³ W cm over the whole length of the sample (50 mm for disk cathode and 200 mm for rotatable cathode). The resistivity, transmittance and film thickness were measured with a spatial resolution of 2 mm. XPS, XRD, TOF-SIMS and SEM were used for surface characterization. It is shown that the AZO resistivity can change with two orders of magnitude over 10 mm span on the substrate, a behavior that can be correlated with plasma parameters and the growth mechanism.

4:20pm B7-TuA9 On Three Different Ways to Quantify the Degree of Ionization in Sputtering Magnetrons, *A. Butler*, Université Paris-Sud, Université Paris-Saclay, France; *N. Brenning*, Université Paris-Sud, Université Paris-Saclay, Sweden; *M.A. Raadu*, KTH Royal Institute of Technology, Sweden; *J.T. Gudmundsson*, University of Iceland, Iceland; *T. Minea* (tiberiu.minea@u-psud.fr), *D. Lundin*, Université Paris-Sud, Université Paris-Saclay, France

Quantification and control of the fraction of ionization of the sputtered species are crucial in magnetron sputtering, and in particular in high-power impulse magnetron sputtering (HiPIMS), yet proper definitions of the various concepts of ionization are still lacking. In this contribution, we distinguish between three approaches to describe the degree (or fraction) of ionization: the ionized flux fraction F_{flux} , the ionized density fraction $F_{density}$, and the fraction α of the sputtered metal atoms that become ionized in the plasma (sometimes referred to as probability of ionization). By studying a reference HiPIMS discharge with a Ti target, we show how to extract absolute values of these three parameters and how they vary with peak discharge current. Using a simple model, we also identify the physical mechanisms that determine F_{flux} , $F_{density}$, and α , as well as how these three concepts of ionization are related. This analysis finally explains why a high ionization probability does not necessarily lead to an equally high ionized flux fraction or ionized density fraction.

5:00pm B7-TuA11 Characterization of Microwave Surfatron Plasma-enhanced-ALD System for Low-temperature Deposition of Thin Oxide Films, *M. Cada* (cada@fzu.cz), *D. Tvarog*, Institute of Physics CAS, v. v. i., Czech Republic; *J. Kim*, ISAC Research Inc., Republic of Korea; *A. Poruba*, SVCS Process Innovation s.r.o., Czech Republic; *Z. Hubicka*, Institute of Physics CAS, v. v. i., Czech Republic

The preparation of ultra-thin film is crucial for the development of cutting-edge technologies in the field of microelectronics, optoelectronics, nanotechnology or catalysts. Furthermore, covering 3-D objects in a nanometer scale requires a high degree of uniformity of deposited thin films preserving high aspect ratio of complex shape objects. Atomic layer deposition (ALD) has proven to be almost an indispensable deposition technique for conformal deposition of mostly metal or oxide thin films. Plasma-enhanced ALD (PE-ALD) process brings energy for surface reactions between precursors and reactants through electrons, ions, radicals or excited particles. Many studies have shown that the PE-ALD process is able to operate at significantly lower substrate temperatures. In this work, a microwave surfatron plasma source as alternative to CCP, ICP or other remote plasma sources was used for activation of reactants during the PE-ALD process. We carried out measurements with the Langmuir probe to obtain spatial map of electron temperature, plasma density and potentials in the ALD chamber designed for deposition on wafers with diameter 100 mm during typical deposition conditions of TiO₂, Al₂O₃ and TiN thin films. The plasma parameters were investigated for different working gas pressures and mixtures. Obtained results proved that radial homogeneity of the plasma density could be improved if mass flow rate of working gas is reduced. On the other hand, for higher pressure of the working gas the plasma density rapidly decreased in axial distance from the surfatron nozzle outlet. Results clearly demonstrated that spatial inhomogeneity of the plasma parameters correlates with thin film properties. The possibilities of deployment of the multi-nozzle surfatron system for achieving a sufficient

level of homogenization of the plasma parameters was suggested. Effect of substrate temperature and microwave power delivered into the surfatron on deposited thin film properties was studied too. The Raman spectroscopy proved that substrate temperature above 200°C led to anatase phase formation of TiO₂ thin films whilst lower temperatures produced amorphous thin films. Further, gradually increased microwave power resulted in the rise of thin film thickness measured by the spectroscopic ellipsometry for constant number of ALD cycles. Impact of the microwave power on the Growth per Cycle (GPC) parameter was studied by the optical emission spectroscopy detecting evolution of oxygen or nitrogen atoms and radicals.

The authors would like to thank for the financial support from Technology Agency of the Czech Republic under project no. TF03000025.

Coatings for Biomedical and Healthcare Applications

Room Pacific Salon 3 - Session D2-TuA

Bio-corrosion and Bio-tribology

Moderators: *Jessica Jennings*, University of Memphis, USA, *Steve Bull*, Newcastle University, UK

1:40pm D2-TuA1 Bio-Tribocorrosive Behavior of the Contact M30NW Stainless Steel against HDPE Reinforced with MoS₂ Particles. New Polymer Implant: Promising Material?, *A. Saleh, M. Guezmil, W. Bensalah, S. Mezlini*, Université de Monastir, Tunisia; *J. Géringier (geringer@emse.fr)*, Mines Saint-Etienne, France

Some new polymer composites are under investigation in order to enhance the biocompatible usage of new biomaterials. This paper deals with the tribological behavior of High Density PolyEthylene/molybdenum disulphide (MoS₂-HDPE) composites against M30NW stainless steel. As received HDPE pellets were milled and blended with MoS₂ particles using a ball milling machine. The reinforced HDPE specimens with different contents of MoS₂ were elaborated using a compression molding machine. Tribological characterization including wear rate and friction coefficient was investigated using a linear reciprocating pin-on-disc tribometer under dry conditions. Tribocorrosion tests were carried out in the presence of bovine serum solution. It is highlighted that the use of MoS₂ enhances the tribological performances of HDPE composites compared to the unfilled polymer under dry and lubricated conditions. In both cases, an optimal content of MoS₂ was around 4 wt.%. Morphological and chemical investigations using SEM and EDS analyses were carried out on the composite discs after wear tests. Thus the wear scenario was discussed in relation to the MoS₂ content.

2:00pm D2-TuA2 Evaluation of the Adhesion of Electrospayed and Solution-Cast Chitosan Coatings on Titanium Surfaces, *V. Suresh, E.J. Chng, J. Bumgardner, R. Gopalakrishnan (rgplkrsh@memphis.edu)*, University of Memphis, USA

INVITED

Biomedical implant devices for dental/craniofacial and orthopedic applications are a reliable and effective means for repairing/re-storing function of damaged, diseased or missing tissues. Despite the success of these devices, there are still challenges in their use with respect to improving their integration into boney tissues, promoting healing and resisting/preventing infection. Electrospay coating technologies provide an additive manufacturing route to endow implant surfaces with new properties to improve their performance by controlled deposition of desired materials, compounds and/or agents in the form of nano- or micro-particles on the surface of implant devices under relatively mild conditions. This ensures that the biomaterials do not get denatured under high temperature or harsh chemical environments commonly employed in many coating methods. They also provide a means to control the structure of coatings with high precision that allows the functionalization of complex 3D geometries of the implants with a range of physical and bioactive properties. Devices such as dental implants, total joint replacement devices, bone plates and screws that cannot be easily coated by other manufacturing methodologies such as solution casting, sputter coatings, or electrochemical treatments can be robustly handled by the electrospay technique. This project focuses on assessing the adhesion of electrospayed chitosan coatings on model titanium surfaces and screws to explore their potential as an implant treatment technology. Currently, the most widely used technique for implant coating with biomaterials is solution casting. This method limits the coverage of chitosan on complex surfaces of implants, and provides little control on the thickness of the coating and leads to excessive wastage. This research also evaluates the effectiveness of the electrospay as a delivery method of aerosolized chitosan to coat complex implants with precise thickness control, multilayer coatings for controlled drug delivery and to

reduce wastage. Adhesion strength values are reported and compared between electrospayed and solution cast chitosan coatings.

2:40pm D2-TuA4 Study of the Mechanical and Tribological Properties of the TaN with Ti Inclusion Multilayer Films on Si Substrate, *E. García (edgb007@hotmail.com)*, Cátedras-CONACyT, Universidad de Guadalajara, México; *J.O. Berumen*, ITESO, Universidad Jesuita de Guadalajara, Tlaquepaque, Jalisco, México; *M. Flores-Martinez*, Universidad de Guadalajara, México; *E. Camps*, Instituto Nacional de Investigaciones Nucleares, México; *S. Muhl*, Instituto de Investigaciones en Materiales-UNAM, México

The hip prosthesis surfaces are exposed to high mechanical, chemical and tribological stress conditions. For that binary and ternary transition metallic nitride films have been studied in order to improve the wear and corrosion resistance of the metallic surfaces of the prosthesis. This work shows the first studies of the TaN with Ti inclusion multilayers films. These were produced using DC magnetron cosputtering with a Ta and Ti targets in an N₂/Ar atmosphere in a multilayer arrangement with similar thickness, incremental layer and decremented layer thickness on a silicon substrate. The films were structural, chemical and topologically characterized, using X-Ray diffraction (in theta-2 theta and in-plane configuration), Raman spectroscopy and Electronic microscopy, respectively. The mechanical properties were studied using nanoindentation (at 10 mN) and scratch test (from 0 to 8N) with a Rockwell C indenter. The tribological characterization was carried out with a linear reciprocating with a Rockwell C indenter, with at 0.5, 1 and 2 N of load and 5 cycles of 5 mm of length. The wear track produced for the scratch and the tribological test were studied with optical and electronic microscopy. The layers had a combined structure of a cubic of TaN and hexagonal and cubic of Ta. The coating presented a lower Hardness than the reported for the TaN films. The coating with the incremental arrangement presented a better tribological performance but with lower hardness.

3:00pm D2-TuA5 Enhancement of Tribocorrosion Properties of Ti6Al4V by Formation of a Carbide-Derived Carbon (CDC) Surface Layer, *K.Y. Cheng (kcheng24@uic.edu)*, University of Illinois at Chicago, USA; *R. Nagaraj, D. Bijukumar, M.T. Mathew*, University of Illinois College of Medicine, USA; *M. McNellan*, University of Illinois at Chicago, USA

Metal implant materials not only face corrosion or friction individually but the synergism of tribology and corrosion, which has been called "tribocorrosion". Especially, on the bearing of hip implant in the synovial fluid, the usual CoCrMo alloy endures severe tribocorrosion reaction, sometimes resulting in the formation of wear and corrosion products which cause the adverse local tissue reaction. In 2011, a graphitic tribolayer was discovered on retrieved hip implants at Rush Medical Center, which suggested that the tribolayer might offer lubrication and corrosion protection. Therefore, a coating of graphitic material might be beneficial to the performance of orthopedic implants.

Carbide-derived carbon (CDC) is a primarily graphitic material formed on silicon carbide, which improved tribological performance in non-biomedical applications. If CDC can be applied on the metal substrate, its high lubrication and chemical inertness should provide the same improvement as the graphitic tribolayer found on the retrieved hip implant. To produce a CDC layer on a metal, the metal is first carburized to form a surface layer of metal carbide, and subsequently the carbide is decomposed to form CDC. In this study, Ti6Al4V alloy was chosen as our substrate due to its high affinity to form carbides on its surface and its poor tribocorrosion property, by which CDC's protection can be demonstrated. As long as CDC can properly protect Ti6Al4V alloy, it is possible to reproduce the same effect on other metal surfaces.

In this presentation, recent tribocorrosion results obtained in the hip simulator at Rockford Medical Center, CDC treated metal shows a smaller voltage drop during ($\Delta E_{\text{CDC}} = -0.2 \pm 0.047(\text{V}) < \Delta E_{\text{Ti6Al4V}} = -0.89 \pm 0.13(\text{V})$) testing in an open-circuit potential condition, a smaller induced current ($\Delta I_{\text{CDC}} = -4.8\text{E-}6 \pm 4.4\text{E-}6(\text{A}) < \Delta I_{\text{Ti6Al4V}} = -3.94\text{E-}4 \pm 8.02\text{E-}5(\text{A})$) when tested under potentiostatic conditions, a smaller wear loss ($\Delta V_{\text{CDC}} = -0.001 \pm 5.85\text{E-}4(\text{mm}^3) < \Delta V_{\text{Ti6Al4V}} = -0.43 \pm 0.025(\text{mm}^3)$) and smaller values of friction coefficient ($\mu_{\text{CDC}} = 0.0045 \pm 0.0025 < \mu_{\text{Ti6Al4V}} = 0.47 \pm 0.135$). The biocompatibility tests have shown CDC is as biocompatible as the Ti6Al4V substrate. In general, the CDC protected Ti6Al4V performs better in tribocorrosion without sacrificing biocompatibility.

4:00pm **D2-TuA8 Considerations when using Additive Manufacturing to make Medical Devices, A. Espinoza Orias (Alejandro_Espinoza@rush.edu)**, Rush University Medical Center, USA **INVITED**

Additive Manufacturing has demonstrated to be and gone beyond being a disruptive technology as many industries have adopted it to mass-produce parts on demand. In the medical arena, however, there are some concepts that part manufacturers need to be familiar with before going to mass production. A big part of the orthopedic market is that of hip and knee implants that have seen steady growth in the last decade. Corrosion is a natural process and changes the properties of metallic structures. In the case of orthopedic implants, such as total hip replacements, titanium alloys are the most frequently used metal due to their elevated resistance to corrosion, compared to other alloys suitable for implantation in the body. Some of these considerations are as diverse as the patient population meant to benefit from AM: patient privacy, metallurgy, mechanical properties and cleanliness. The aspects of bio-corrosion and bio-tribology have received little attention when new additively manufactured implants hit the market. A big reason for this is the 510(k) process that allows manufacturers to 'grandfather-in' the designs. However, we know little about the differences in metallurgy that are related to the additive manufacturing process that has key contrasts to that of traditional subtractive manufacturing. The most relevant aspect of utility from the additive manufacturing point of view is the direct ability to print highly rough and porous surfaces that are meant for bone ingrowth. While this manufacturing method is capable of producing high-resolution surface finishes with or without built-in designed porosity, not much is known about the surface interaction properties of said finished surfaces. The need for better and more accurate methods to describe bio corrosion and bio tribological aspects of additively manufactured implants makes this type of characterization crucial since the durability of the implant is in play. Current traditionally manufactured designs, last about 15 years not without their own survivability issues. It remains to be seen if the materials and the processes involved in additive manufactured can match the same type of performance benchmarks of the standard manufactured implants.

4:40pm **D2-TuA10 Nanostructured Surfaces for (Bio)sensors, V.S. Stranak (stranv00@centrum.cz)**, University of South Bohemia, Czech Republic; R. Bogdanowicz, Gdansk University of Technology, Poland; P. Sezemsky, V. Prysiashnyi, J. Kratochvil, University of South Bohemia, Czech Republic; M. Smietana, Warsaw University of Technology, Poland; O. Kylian, Charles University, Czech Republic; Z. Hubicka, M. Cada, Institute of Physics CAS, v. i., Czech Republic

The contribution reports our study of nanostructured surfaces preferentially used for bio-sensing applications. Nanostructured surfaces were prepared by low-temperature plasma assisted deposition employing magnetron sputtering of bulk target. The advantages of nanostructures for sensor applications have been demonstrated several times. Here we focus on two approaches: (i) the first one utilizes homogeneous transparent conductive oxide (TCO) films for Lossy Mode Resonance (LMR) sensors while (ii) the second employs Ag nanoparticles for detection and signal calibration of matrix assisted laser desorption/ionization mass spectrometry.

Bio-sensors working on LMR principle represent rather new concept which appeared a few years ago. The LMR sensors, equipped by precisely tailored TCO film (in our case indium doped tin oxide - ITO) are based on the optical fibre and allow optical as well as electrochemical sensing. The optical sensitivity is achieved by spectral shift of transmission spectra of the light passing through the optical fibre, while the electrochemical effects can occur on the sensor surface. Our main aim represents tailoring of the ITO film deposition to achieve relevant optical and electrochemical properties of ITO with adequate LMR and electrochemical response [1]. The detection of substances as, e.g. ketoprofen [2], will be reported, too.

The second part will be devoted to nanostructures for independent mass-charge calibration of laser desorption/ionization mass spectrometry (LDI MS). Properly tailored Ag nanostructured surface - formed as homogeneous thin film, isolated nanoislands, and spherical nanoparticles - can effectively substitute protonation agent for low-mass molecules instead of conventionally used matrices. Beside the surface characterization, the impact of LDI MS laser, irradiating the nanostructured surfaces responsible for Ag cluster production, will be discussed [3]. It is the nanoparticle size and the surface coverage that play a key role and have to be optimized.

[1] V. Stranak, R. Bogdanowicz, P. Sezemsky, H. Wulff, A. Kruth et al, Surf. Coat. Technol. 335, (2018), 126.

[2] R. Bogdanowicz, P. Niedziałkowski, M. Sobaszek, D. Burnat, W. Białobrzaska et al, Sensors 18, (2018), 1361.

[3] V. Prysiashnyi, F. Dycka, J. Kratochvil, V. Stranak, P. Ksirova et al. J. Vac. Sci. Technol. B 37, (2019), 012906.

Acknowledgement: This work was supported by project NATO SPS G5147. Furthermore, support by project GACR 19-20168S is acknowledged, too.

5:00pm **D2-TuA11 Electrochemical Performance of Agro-Industrial Waste as Green Corrosion Inhibitor for Stainless Steel Type 316 in Acid Environment, O. Sanni (tayo.sanni@yahoo.com)**, P.A. Popoola, S. Fayomi, Tshwane University of Technology, Pretoria, South Africa

The objective of this study is to investigate the inhibition of industrial waste, as a green source of corrosion inhibitor against stainless steel Type 316 corrosion in 0.5 M H₂SO₄ solution. The corrosion inhibition effects of methanol extract of coconut shell powder (CSP) on stainless steel in 0.5 molar sulphuric acid solution was studied by weight loss and electrochemical techniques. The results showed that the tested CSP is a promising inhibitor because of its high inhibition efficiency at low concentrations. The results of polarization test revealed that CSP acted as mixed type inhibitor and retarded both anodic and cathodic reactions. It was found that corrosion potential (E_{corr}) increases with increasing CSP concentrations, while, corrosion current (i_{corr}) decreases. Results revealed that the adsorption behavior of the CSP onto the stainless steel surface follow Langmuir model isotherm. Scanning electron microscopy (SEM) and energy x-ray dispersive spectroscopy (EDX) supported the adsorption conclusions indicating the formation of passive film on the surface of stainless steel samples in the presence of CSP. Activation energy (E_a) and ΔG_{ads} for adsorption of CSP is calculated.

5:20pm **D2-TuA12 Electrochemical AC Impedance Analysis for Parylene AF4 Continuous Film, W.-C. Kuo (rkuo@nkust.edu.tw)**, C.-F. Wu, National Kaohsiung University of Science and Technology, Taiwan

The purpose of the study was to research the corrosion resistance of Parylene AF4 with minimal continuous film thickness. Parylene AF4 has good anti-ultraviolet ability and low hygroscopicity. It can be used in implantable sensors, medical components and outdoor electronic components. Through minimum continuous film, we can strike the best balance between the film thickness corrosion resistance and sensor sensitivity.

In this study, Parylene AF4 coating was performed by interdigital electrodes. The film thickness was controlled to 10nm, 15nm, 20nm, 30nm, 40nm, 80nm, 100nm respectively. The film thickness was measured by surface profilometer and controlled within a reasonable error range. After that, we soaked the device in the phosphate buffered saline under 50°C, 80°C accelerated aging test, through the electrochemical impedance measurement, We can then realize the different stages of solution penetration film from the Bode diagram and Nyquist diagram. The corresponding electrode parameters can be simulated according to the equivalent circuit model to see whether the film impedance value is a definite value after a period of time. Therefore, we can judge whether the present film thickness is a continuous film.

Experimental results show that according to the equivalent circuit simulation parameters, the film thickness of 10 nm, 15 nm and 20 nm immersed in phosphate buffered saline at 50 °C. is immersed in the solution immediately, the film impedance is a fixed value, the solution has infiltrated the film and the 30 nm film Thickness was infiltrated by the solution in 72 hours, whereas the 40 nm film thickness was 96 hours permeated by the solution; 50 nm, the 60 nm film thickness was infiltrated by the solution for 120 hours; the 80 nm film thickness was 192 hours infiltrated by the solution; the 100 nm film thickness was 216 hours permeated by the solution. 10nm, 15nm, 20nm film thickness Immediately immersed in the solution, the film resistance value is a fixed value, so 10nm, 15nm, 20nm film thickness of the discontinuous film; and 30nm, 40nm, 50nm, 60nm, 80nm, 100nm film thickness and so on The effective circuit simulation parameters show that the film resistance value will continue to decrease with increasing time, so as a continuous film. Experimental results show that immersed in phosphate-buffered saline at 80 °C 30nm, 40nm film thickness, the solution has begun to penetrate the film in 24 hours phenomenon, 50nm, 60nm film thickness at 48 hours, 80nm and 100nm film thickness at 72 hour.

Tribology and Mechanical Behavior of Coatings and Engineered Surfaces

Room San Diego - Session E2-2-TuA

Mechanical Properties and Adhesion II

Moderators: Megan J. Cordill, Erich Schmid Institute of Materials Science, Austrian Academy of Sciences, Leoben, Austria, **Ming-Tzer Lin**, National Chung Hsing University, Taiwan, **Gerhard Dehm**, Max-Planck Institut für Eisenforschung, Germany

2:00pm E2-2-TuA2 Mechanical Behavior Study of 50 nm-thick Thin Film of Gold Single Crystal with In situ X-ray Pole Figures Measurements, P.O. Renault (pierre.olivier.renault@univ-poitiers.fr), Université de Poitiers, France; **J. Drieu La Rochelle**, **P. Godard**, **M. Drouet**, **J. Nicolai**, **M.F. Beaufort**, University of Poitiers, France; **D. Thiaudière**, **C. Mocuta**, SOLEIL Synchrotron, France

For a few years, thanks to the development of mechanical tests on nanometer-size objects, the question of how the mechanical plastic behavior of metallic materials change as their characteristic sizes are reduced down to nanometer range has attracted significant interest. In addition to slip by dislocation glide, deformation twinning is one of the plastic deformation mechanisms in metallic crystalline materials. In this way, size-dependent twin propagation behaviors in nanowires such as face-centered cubic metals has been reported in literature.

In this work, the mechanical behavior of gold single crystal is studied thanks to in situ pole figures measurements during controlled biaxial loadings. The gold thin film 50 nm thick is deposited on NaCl single crystal by physical vapor deposition technique at 400°C. The film is then transferred on a polyimide cruciform substrate to be deformed on a biaxial tensile tester in situ during synchrotron x-ray measurements. The as-deposited gold single crystal contains a given amount of small twins. The twins are rather narrow and small, i.e. they have a thickness of about 10 nm and a size of about 50-100 nm.

In the presentation, the first results obtained on in situ uniaxial applied deformation in the [110] direction of Au monocrystalline film are reported. The in situ x-ray pole figure measurements show a huge evolution of the intensity of the diffracting pole related to the twins. Hence, the amount of twins is increasing during deformation, either by thickening or growing of the pre-existing twins, either by creating new twins. The twins' volume is quantified as a function of applied deformation.

2:20pm E2-2-TuA3 Evaluation of the Mechanical Properties in Antibacterial Multi-layer HA-Ag Coatings Deposited by RF Magnetron Sputtering, J.A. Lenis (julian.lenis@udea.edu.co), M.A. Gómez, F.J. Bolívar, University of Antioquia, Colombia

The use of osteoconductive coatings such as Hydroxyapatite (HA) in surgical implants is a great alternative in order to improve the acceptance of these devices in the human body. On the other hand, in order to avoid possible problems associated with bacterial infections, which can be generated during the surgical or postoperative procedure, researchers have been developing antibacterial coatings that act locally inhibiting the bio-film formation. One of the strategies that has been adopted to induce these properties is the incorporation of silver (Ag) nano-particles in HA coatings. In the literature it has been found that these coatings exhibit a good antibacterial behavior, however, there are few studies about the mechanical behavior of these systems deposited like multi-layer coatings. Therefore, in the present report the effect of the process parameters such as deposit temperature and substrate-target distance, on the chemical composition, structure, morphology and mechanical properties of multilayer coatings HA-Ag deposited by magnetron sputtering on Ti6Al4V is shown. The characterization of the obtained films was carried out by means of energy dispersive spectroscopy, micro-Raman spectroscopy, scanning electron microscopy, atomic force microscopy and nano indentation tests. A relationship between the target-substrate distance and the chemical composition of the coatings was found, obtaining a decrease in the Ca/P ratio, as function of the decrease between the target and substrates. Additionally, the critical load of the deposited coatings shown an increasing tendency as function of the decrease in the target-substrate distance, whereas for the first level of cohesive failure an inverse behavior was obtained. Furthermore, both mechanical characteristics were improved with the increase of the deposit temperature.

Key words: magnetron sputtering, hydroxyapatite, multi-layer coating, critical load, first level of cohesive failure.

2:40pm E2-2-TuA4 Mechanical Deformation in Metal and Ceramic Nano Multilayers, A.M. Hodge (ahodge@usc.edu), University of Southern California, USA

INVITED

Nano multilayers (NMs) consist of alternating layers of materials with thicknesses on the order of nanometers and typically display many attractive properties which are attributed to the fact that, as the layer thicknesses decrease, the individual layer behavior changes and the interface volume increases. In general, studies on the mechanical behavior of NMs have been focused mostly on metal systems, followed by metal/ceramic systems and even fewer studies on ceramic multilayers. Thus, the behavior of metallic NMs is well characterized and general trends such as a Hall-Petch type strengthening behavior has been observed for variety of material systems as result of the layered structure. In contrast, for ceramic NMs, the research is limited and overall trends and mechanisms have not been well determined. Furthermore, for NM ceramics, the role of dislocations is limited and therefore the role of the interfaces increase and hold the key to understanding their mechanical behavior.

In this study, we present a comprehensive microstructural evaluation of metal and ceramic multilayers with various layer thicknesses and compositions in order to elucidate on the role of their interfaces during mechanical deformation. Several NM configurations including SiO₂/TiO₂, AlN/SiO₂, AlN/Ag, Cu/Nb, Mo/Au and Hf/Ti will be presented. The role of bilayer thickness and composition is evaluated in both compression and tension using nanoindentation and micro-tensile tests.

4:00pm E2-2-TuA8 Deposition of Highly Adhesive Ta Based Thin Films on a Biomedical Grade CoCrMo Alloy, J. Corona-Gomez, Q. Yang (qiy866@mail.usask.ca), Y. Li, University of Saskatchewan, Canada

Tantalum (Ta) based thin films including alpha and beta tantalum, TaN, and Ta doped diamond-like carbon (Ta-DLC) thin films deposited by radio frequency (RF) magnetron sputtering were investigated as potential interlayers to enhance DLC coating adhesion on a biomedical grade CoCrMo alloy. The deposited interlayers and DLC thin films were characterized by X-ray diffraction, Raman spectroscopy, and Rockwell C indentation. The correlation between the adhesion and the structure of interlayers was investigated. The results show that the deposition temperature and bias voltage play an important role in determining the structure and adhesion of the interlayers and thus the adhesion of DLC coatings.

4:20pm E2-2-TuA9 DIC on FIB Ring-Core of Thin Films for Depth Sensing Residual Stress Measurement, M.T. Lin (mingtlin@nchu.edu.tw), W.-C. Pan, National Chung Hsing University, Taiwan; Y.-F. Chen, F.-Y. Cheng, National Cheng Kung University, Taiwan; J.-H. Huang, National Tsing Hua University, Taiwan

Reliable measurement and modeling of residual stresses at the micrometer scale is a great challenging task for small-scale structures and nanostructured thin films. Moreover, the specific location on microscale evaluation of residual stress gradients is a very critical issue in the hard coating of thin films. The analysis of the residual strain depth profiles requires detailed knowledge of the in-depth lattice strain function, so the residual stress profile calculation can be carried out in a manner that takes into account the mechanical anisotropy and texture of the materials. The development of a microstructure independent procedure for depth-resolved measurement of residual stress is an issue of strategic interest. Here, we perform a digital correlation (DIC) of the specimen images acquired by incremental focused ion beam (FIB) ring-core drilling with various depth steps. A translation test was performed first to study the applicability of DIC to FIB images, and a proper procedure was established to obtain more accurate results. Next, 2 μm thick sputtered Ag and ZrN thin films were used for this measurement. To observe the depth-resolved residual stress profiles of each step on thin film samples, two FIB images of the specimen, one before and one after being drilled, were processed to extract the surface deformation from tiny changes in the FIB images using DIC. This combined with high-resolution in situ SEM imaging of the relaxing surface and a full field strain analysis by digital image correlation (DIC). A parallel residual stress measurement was also performed using a four-circle diffractometer with grazing incidence X-ray diffraction (XRD) $\cos^2\alpha\sin^2\psi$ method at several azimuthal angles to obtain the average X-ray strain (AXS) and thus the residual stress can be accurately determined and compared.

4:40pm E2-2-TuA10 Metallic Glass/Crystalline Nanolayered Coatings with High Nanoscratch Resistance and Damage Tolerance, M. Abboud, Middle East Technical University, Turkey; A. Motallebzadeh, Koç University, Turkey; S. Özerinç (ozeric@metu.edu.tr), Middle East Technical University, Turkey
Metallic glass/crystalline metal nanolayers provide a balanced combination of high hardness and ductility, making them promising materials for wear

resistant coating applications. However, there has been no study to date investigating the wear behavior of these materials. In this study, we investigated the nanoscratch behavior of nanolayered CuZr/Zr composed of alternating CuZr metallic glass and nanocrystalline Zr layers.

A magnetron sputterer deposited the 1 μm thick coatings on polished 316 stainless steel substrates. Layer thickness varied in the range 10-100 nm. X-ray diffraction and transmission electron microscopy characterized the microstructure of the coatings and nanoindentation measurements probed the hardness and elastic modulus. A nanoindenter equipped with a spherical diamond tip of 5 μm radius performed nanoscratch measurements on the coatings.

Hardness and elastic modulus of nanolayered coatings do not vary with layer thickness and are close to that of the monolithic metallic glass, about 5.5 GPa, and 105 GPa, respectively. A comparison of nanoscratch residual depths, on the other hand, indicate that monolithic CuZr has higher scratch resistance than the layered samples. Among the nanolayers, CuZr/Zr with 100 nm layer thickness shows the highest scratch resistance, and the resistance diminishes with decreasing layer thickness. All coatings showed considerably smaller penetration depth when compared to uncoated stainless steel demonstrating the superior wear resistance and damage tolerance of the coatings.

A close observation of scratch tracks showed outstanding adhesion and conformity of the coatings to the substrates. The most damage tolerant coating was the CuZr/Zr with 10 nm layers, showing no sign of delamination or fracture at compressive strain levels exceeding 80%. Monolithic CuZr showed local delamination and microfracture at relatively lower strain levels, but without any gross failure.

Although the hardness and elastic modulus of the coatings are virtually the same, the nanoscratch results indicated distinct patterns. We attribute the layer-thickness dependent behavior to the low interfacial shear strength in these layers previously reported in literature. While low interfacial strength does not play a major role in nanoindentation response where plastic strain is mostly perpendicular to the interface, it affects the scratch resistance where shear strain is dominant. Our findings give insight to the behavior of metallic glass/crystalline composites under sliding loading conditions for the first time in the literature, and present a model system for the development of protective coatings suitable for compliant substrates.

5:00pm E2-2-TuA11 Coatings Effect On Crack Initiation Behavior Of Ti Alloys, X.L. Pang (pangxl@mater.ustb.edu.cn), University of Science and Technology Beijing, China

Titanium has high strength/weight ratio, stiffness and corrosion properties, but at the same time different kinds of surface treatments are employed due to the poor wear resistance, and surface coating is one of the most popular ones. Since fatigue is one of the most important properties of titanium alloys and fatigue crack initiation period occupy an important position in the fatigue failure process, so the study on coating effect on fatigue crack initiation should play an important role. However, the effect of coatings on fatigue crack initiation of Ti-alloys has not been taken seriously, and the mechanism is not clear. This paper deposited CrAlN and TiN hard coatings by PVD on the surface of TC4 titanium alloy to study the coating effects on fatigue crack initiation and propagation. Hard coatings significantly decreased fatigue properties of TC4, since the 510-530 MPa TC4 fatigue limit was reduced to 315-330 MPa for the CrAlN coated samples. The existence of coatings prevented deformation of the TC4 samples at the beginning of fatigue tests, and had a positive effect on sample deformation in the middle of the fatigue process. For the coated samples, the fatigue crack initiated in the coatings and propagated to the interface, and induced a micro crack at the substrate surface. Then the micro crack propagated into the bulk material and formed the distinct propagation path in the fracture surface. The mechanism of non-propagation fatigue cracks and influence of coating thickness were also studied. A corresponding model is proposed.

New Horizons in Coatings and Thin Films

Room Pacific Salon 6-7 - Session F3-TuA

2D Materials: Synthesis, Characterization, and Applications

Moderator: Eli Sutter, University of Nebraska-Lincoln, USA

1:40pm F3-TuA1 Roll-to-roll Plasma Chemical Vapor Deposition for Scalable Graphene Production, T.S. Fisher (tsfisher@ucla.edu), UCLA, USA; **M. Alrefae,** Purdue University, USA

INVITED

Recently, roll-to-roll (R2R) chemical vapor deposition (CVD) processes have been implemented to produce graphene with substrate feed rates ranging from 5-100 mm/min. However, this production rate must increase much further to make graphene a feasible product in semiconductor and materials manufacturing industries. Plasma sources can be applied to increase the graphene deposition rate, and additionally, to decrease energy input. This work will describe the implementation of a radio frequency plasma R2R CVD process to deposit graphene on copper and nickel foils, and carbon fibers. The growth process takes advantage of the high-temperature plasma gas that produces active carbon species to accelerate growth kinetics. Thus, supplemental heating of the substrate is unnecessary when using plasma, in contrast to thermal CVD systems that consume energy to heat the substrate and to decompose the carbon gas source. *In situ* temperature measurements of the substrate in the plasma region confirm the plasma's ability to heat the substrate to the 1200-1500 K range depending on the plasma power. From these real-time temperature measurements, a heat transfer model is developed and validated to determine the substrate temperature profile during R2R graphene growth. The effects of plasma power and web speed on substrate temperature are explored and correlated to graphene quality. The results indicate that graphene growth on Cu foil is most significantly influenced by the in-plasma substrate temperature, whereas growth on Ni foil is controlled by the substrate cooling rate, which is evaluated from the heat transfer model. Furthermore, the plasma environment is characterized by optical emission spectroscopy (OES) to optimize graphene growth and assess the impact of ion bombardment. The OES results suggest that the quality of graphene deposited on Cu foil is enhanced with increased CH emission and decreased emission from O, H, Ar⁺, C₂, and CN. The process characterization techniques aid in controlling and optimizing graphene growth in a large-scale setup, including graphene quality as a function of reactor pressure and nitrogen mole fraction with associated uncertainties obtained from statistical analysis. The talk will include a discussion of applications of the resulting materials in energy and biosensing technologies, as well as plans for a new MHz plasma R2R system supplemented by solar heating.

2:20pm F3-TuA3 Magnetron Sputtered MoS₂/C Nanocomposites as Highly Efficient Electrocatalyst in Hydrogen Evolution Reaction, S.J. Rowley-Neale, M. Ratova, Manchester Metropolitan University, UK; **L.T.N. Fugita,** University of Sao Paulo, Brazil; **G.C. Smith,** University of Chester, UK; **A. Gaffar, J. Kulczyk-Malecka (J.Kulczyk-Malecka@mmu.ac.uk), P. Kelly, C.E. Banks,** Manchester Metropolitan University, UK

The design and fabrication of an inexpensive and highly efficient electrocatalyst for the hydrogen evolution reaction (HER), were performed by the route of magnetron sputtering. Molybdenum disulfide (MoS₂) was coated directly onto the nanocarbon (C) powder support. Sputtering time was explored as a function of physicochemical composition of MoS₂/C nanocomposites, and its performance in HER. Increased sputtering time gave rise to materials with different compositions and oxidation states of Mo ions, Mo⁴⁺ and Mo⁶⁺, associated with sulfur anions (sulfide, elemental and sulfate) and improved HER outputs. The physicochemical characterisation of the MoS₂/C nanocomposites as a function of sputtering time was evaluated using scanning electron microscope (SEM) equipped with an energy-dispersive X-ray spectroscopy (EDS), transmission electron microscopy (TEM), X-ray photoelectron spectroscopy (XPS), X-ray diffraction (XRD) and Raman Spectroscopy. An optimised sputtering time of 45 minutes was used to fabricate MoS₂/C nanocomposites. This gave rise to an optimal HER performance in regards to its onset potential (-0.44 mV vs saturated calomel electrode (SCE)), achievable current (-1.45 mVs⁻¹) and Tafel value (43 mVdec⁻¹) for the compositions rich in Mo⁴⁺ and sulfide (MoS₂). This bespoke fabricated MoS₂/C nanocomposites were incorporated into the bulk ink utilised in the fabrication of screen-printed electrodes (SPEs) to allow improved electrical wiring to the MoS₂/C and to produce scalable and reproducible electrocatalytic platforms. The MoS₂/C-SPEs displayed far greater HER catalysis with a 450 mV reduction in the HER onset potential and a 1.70 mA cm⁻² increase in the achievable current density (recorded at -0.75 V vs SCE), compared to a bare/unmodified graphitic SPE. The approach of using magnetron sputtering to modify carbon with MoS₂ facilitates the mass

Tuesday Afternoon, May 21, 2019

production of stable and effective electrode materials for possible use in electrolyzers, which are cost competitive to platinum (Pt) and mitigate the need to use time consuming and low-yield exfoliation techniques, typically used to fabricate pristine MoS₂.

2:40pm **F3-TuA4 HIPIMS Graphene on Copper for Heat Spreading**, *C.M. Chen, E.Y. Liao, P.-Y. Hsieh (pingyehsieh@mx.nthu.edu.tw), Y.H. Chen, J.L. He*, Feng Chia University, Taiwan

The heat generated from electronic devices such as light emitting diodes, batteries, and highly integrated transistors is one of the major causes limiting their performance and reliability. The extraordinarily high thermal conductivity of graphene has let intensive studies for use as a heat spreader. A strategy of further enhancing the thermal conductivity by growing graphene layer on copper will thus proposed in this study. Based on our previous study, it is able to grow graphene layer on copper foil at relative low temperature by using high power impulse magnetron sputtering (HIPIMS) equipped with synchronized substrate bias. The thermal conductivity of the graphene-on-copper (GOC) layer structure was measured, here in this study, based on Angstrom's method. The thermal conductivity of GOC was significantly enhanced as compared to bare copper foil alone. This is due to epitaxial graphene on copper generated low interfacial thermal resistance, and intrinsic high thermal conductivity of graphene. Finally, a strong correlation between graphene layer thickness and thermal conductivity was reported.

3:00pm **F3-TuA5 Tailoring Optical Properties of Two-Dimensional Transition Metal Dichalcogenides Via Photonic Annealing**, *R. Rai (rair01@udayton.edu), K. Gleibe*, University of Dayton, Air Force Research Laboratory, USA; *N. Glavin*, Air Force Research Laboratory, Wright-Patterson AFB, USA; *R. Wheeler*, UES, Inc., Air Force Research Laboratory, USA; *R. Kim*, Air Force Research Laboratory, Wright-Patterson AFB, USA; *A. Jawaid*, UES, Inc., Air Force Research Laboratory, USA; *L. Bissell*, Air Force Research Laboratory, Wright-Patterson AFB, USA; *C. Muratore*, University of Dayton, USA

Semiconducting transition metal dichalcogenides (TMDs) exhibit unique combinations of physical properties at thicknesses of less than 5 molecular layers. For example, mechanical flexibility and photoluminescence (PL) in the visible to near infrared (NIR) frequencies are not properties that are commonly observed in a single material, but are routinely measured for materials such as 2D MoS₂ and WSe₂. Such properties make TMDs attractive candidates for the next generation of flexible and wearable opto-electronic technologies. Incorporation of TMDs into commercial applications is currently limited, however, by challenges associated with synthesis of large area, device-quality films with tunable properties. Our work encompasses diverse innovative techniques to tailor optical properties of TMD thin films by controlling their area, thickness, crystalline domain size, defect density and uniformity during and after processing. We begin by application of thin amorphous films of WSe₂ and other TMDs on both flexible and rigid substrates via vapor phase and liquid phase application over large areas. We then illuminate the amorphous film with diverse light sources, including lasers (visible-IR), broad-band xenon lamps, and nanoscale electron beams. WSe₂ was selected as a model material due to high quantum yield at room temperature. Tailoring the 'structure' of the amorphous material via modulation of the energy flux during magnetron sputtering provides an opportunity to model homogeneous or heterogeneous crystallization during illumination by controlling the density of pre-existing nuclei. Crystallization kinetics were examined by *in situ* analysis of real-time images and electron diffraction patterns. The amorphous-crystalline conversion is correlated to 2D growth theory and contrasting elements of 2D versus 3D growth are highlighted. A significant increase in photoluminescence intensity is accompanied by a change in crystal edge density, consistent with observations that PL originates preferentially from defective regions of 2D WSe₂. Furthermore, we examine quantum confinement effects on photoluminescence yield in nanoscale crystalline areas (~10 nm) via electron beam irradiation.

4:00pm **F3-TuA8 Mechanism of Formation of Nitrogenated Doped Graphene Films, Investigated by In situ XPS During Thermal Annealing in Vacuum**, *Y. Bleu (yannick.bleu@univ-st-etienne.fr)*, Univ. Lyon, Université Jean Monnet, France; *V. Barnier, F.C. Christien*, Laboratoire Georges Friedel, Ecole Nationale Supérieure des Mines, France; *F. Bourquard*, Univ. Lyon, Laboratoire Hubert Curien, Université Jean Monnet, France; *J. Avila*, Synchrotron SOLEIL & Université Paris-Saclay, France; *F. Garrelie*, Univ. Lyon, Université Jean Monnet, France; *M.-C. Asensio*, Synchrotron SOLEIL & Université Paris-Saclay, France; *C.D. Donnet*, Université de Lyon, Université Jean Monnet, France

The introduction of dopants, such as nitrogen, into the graphene network, is paramount for many applications such as nanoelectronics, nanophotonics, sensor devices and green energy technology. One way consists in thermal heating of a doped solid carbon source, such as an amorphous a-C:N film, in the presence of a metal catalyst, to obtain nitrogenated graphene (NG) layers. The control of such a process requires to investigate diffusion and segregation mechanisms of the graphene precursor through the metal catalyst.

In the present study, the mechanism of atomic diffusion and NG film growth through a nickel catalyst thin film was investigated using *in situ* X-ray photoelectron spectroscopy (XPS) performed during thermal heating responsible for NG synthesis. Amorphous a-C:N films, containing 16%at. nitrogen, 10 nm thick, were synthesized by femtosecond pulsed laser ablation on fused silica substrates. A 150 nm thick nickel film was subsequently deposited by thermal evaporation on the a-C:N films. Thermal annealing at various temperatures (200, 300, 500 and 650°C), with different time durations, were performed in ultra-high vacuum during *in situ* XPS analysis, to carry out the top surface genesis of the NG film onto the nickel catalyst. FEG-SEM, Raman and X-ray absorption (XAS) spectroscopies were also performed to elucidate the nature and chemical composition of NG films. The diffusion of carbon and nitrogen through the nickel film towards the surface from 300°C was observed, without any graphene signature. Graphene films are formed at the highest temperatures, with a final 3%at. nitrogen content, in both pyrrolic and pyridinic configurations. In addition, the kinetics of carbon surface enrichment observed using *in-situ* XPS is discussed in the frame of the interface segregation theory and modelled using the Du Plessis approach. The solid-state transformation mechanism responsible for the formation of few-layer NG films is thus investigated.

4:20pm **F3-TuA9 Engineering Point and Extended Defects in Transition Metal Dichalcogenides**, *H.-P. Komsa (Hannu-pekka.komsa@aalto.fi)*, Aalto University, Finland

INVITED

Two-dimensional (2D) materials such as graphene, hexagonal boron nitride, and transition metal dichalcogenides have recently received lots of attention due to their unique material properties and numerous potential applications. The 2D atomic structure can also facilitate distinct defect formation mechanisms and offer new possibilities for defect engineering.

In my talk, I will present the results from layered molybdenum dichalcogenides (MoS₂, MoSe₂, and MoTe₂), where vacancy, substitutional, interstitial, and grain boundary defects are introduced by electron irradiation or by various chemical treatments. Due to the 2D nature, transmission electron microscopy and scanning tunneling microscopy imaging allows direct monitoring of formation and agglomeration of defects as well as of larger structural changes. First-principles calculations are used to provide microscopic insight into the energetics and kinetics of these processes. The gained understanding together with the computationally predicted defect properties can be used to guide future efforts in tailoring the 2D material properties via defect engineering.

5:00pm **F3-TuA11 Physicochemical and Mechanical Performance of Nylon 6.6 Coated Thin Free-standing Boron-doped Diamond Nanosheets**, *R. Bogdanowicz (rbogdan@eti.pg.edu.pl), M. Ficek*, Gdansk University of Technology, Poland; *V.S. Stranak, J. Kratochvil*, University of South Bohemia, Czech Republic; *M. Szkodo, J. Ryl, M. Sobaszek*, Gdansk University of Technology, Poland

In the following work, we describe studies on the fabrication and the physicochemical performance of thin and free-standing heavy boron-doped diamond (BDD) nanosheets coated by thin nylon 6.6. First, the diamond nanosheets with less than 400 nm of thickness were grown and doped by boron on Ta substrate by using microwave plasma-enhanced chemical vapor deposition technique (MPECVD) [1]. Then, the BDD/Ta samples were covered by 6.6 nylon to improve their stability in harsh environments.

The plasma polymer films, the thickness in the range 500-1000 nm, with different surface energies were obtained by magnetron sputtering of a bulk target. The hydrophilic nitrogen-rich C:H:N :O were prepared by sputtering

of nylon 6.6. C:H:N :O as films with high surface energy improves adhesion at ambient condition. However, their disadvantage lays in a natural swelling increasing its volume about of 15% after immersion into an aqueous liquid. This behavior influences diamond-C:H:N :O structure in a wet environment.

The C:H:N :O coated diamond nanosheets were delaminated from Ta substrate creating free-standing nanostructures (Diamond-on-Nylon). The C:H:N :O film fixtures the thin polycrystalline diamond sheets enhancing its mechanical stability and enabling transfer and integration with microelectronic systems.

We have manifested that investigated Diamond-on-Nylon nanostructures possess altered morphology and physicochemical properties, revealed by electron microscopy and Raman spectroscopy. Moreover, the electrical response of investigated nanostructures as conductive electrodes is time-stable and indicates the high activity of the sheets with higher dopant concentrations.

Moreover, the Diamond-on-Nylon is characterized with altered mechanical properties like Young modulus or internal stress. These properties varied strongly with the thickness and density of nylon coverage.

In summary, the Diamond-on-Nylon nanostructures show excellent electrical and thermal conductivity along with high mechanical strength. Composite diamond-on-polymer structures could be further developed for flexible and robust electronic devices or thermal heat spreaders.

Acknowledgments

The authors gratefully acknowledge the financial support of the National Centre for Science and Development Grant Techmatstrateg No. 347324. This work was partially supported by the Science for Peace Programme of NATO (Grant no. G5147). The DS funds of the Faculty of Electronics, Telecommunications, and Informatics are also acknowledged.

References

[1]. Bogdanowicz, Robert, et al. *Advanced Functional Materials* (2018): 1805242.

[2]. Ryl, Jacek, et al. *Carbon* 96 (2016): 1093-1105.

Advanced Characterization Techniques for Coatings, Thin Films, and Small Volumes

Room Pacific Salon 1 - Session H1-2-TuA

Spatially-resolved and In-Situ Characterization of Thin Films and Engineered Surfaces II

Moderators: Grégory Abadias, Institut Pprime - CNRS - ENSMA - Université de Poitiers, France, Xavier Maeder, Empa - Swiss Federal Laboratories for Materials Science and Technology, Switzerland, Michael Tkadletz, Montanuniversität Leoben, Austria

1:40pm H1-2-TuA1 Complex Study of Thermally Induced Order Reactions in Cu-Au Thin Films, A.S. Sologubenko (alla.sologubenko@mat.ethz.ch), M. Volpi, P. Okle, R. Spolenak, ETH Zürich, Switzerland

The development of thermally and structurally stable Cu- and Au- based thin films or nano-modulated materials for modern electronic and catalytic applications is the main goal of our work. In our study we follow an effect of thermal treatment on microstructure evolution in Cu-X at.% Au thin films sputter-deposited on rigid and viscoelastic substrates. Complex characterization of thermally induced changes of the material microstructure was carried out by a combination of techniques, transmission electron microscopy (TEM), including time-resolved in-situ heating TEM, and reflectance anisotropy spectroscopy (RAS). While TEM is a well-established technique for phase analyses of nano-dimensional objects, RAS is hardly known as a tool for the microstructure and phase analyses [1]. The validation of RAS as a technique for phase finger-printing is an alternative goal of our work. Most simple specimen preparation requirements, a non-destructive nature of the optical set-up, high sensitivity to the microstructure state of the material are very attractive features of RAS. The comparison of the TEM and RAS data sets acquired from the same material confirms the unprecedented phase sensitivity of the optical technique and justifies its employment as a prompt, high quality and throughout, routine material characterization method.

Thermally induced phase reactions in Cu-Au bulk alloys are well studied. However, there is little information reported on phase evolution and microstructure stability against thermal annealing in continuous Cu-Au thin

films or dewetted nano-modulated structures. A balance between kinetic rates of phase reactions, grain growth and dewetting is affected by an increase of the interface and strain energy contributions to the Gibbs free energy of the thin film system, which in turn can have an effect on the temperature-composition phase fields and the grain morphology.

Our studies confirmed that phase configurations in Cu-Au thin films of 80 and 200 nm thicknesses, accord with the 350°C section of the Cu-Au binary phase diagram [2]. Both, TEM and RAS revealed the stable solid-solution state of Cu-15 at.% Au films in annealed films. The formation of intermetallic phases in Cu-25 at.% Au and Cu-50 at.% Au films upon 350°C annealing was also detected by both, TEM and RAS, but only RAS could reveal the two-phase state of the annealed Cu-25 at.% Au and Cu-50 at.% Au films. The in-situ heating TEM studies show that the 350°C annealing results in nearly concurrent ordering and grain growth in the films with Au content higher than 15 at.%. The time-resolved in-situ heating TEM studies are performed to estimate kinetic rates of both processes.

2:00pm H1-2-TuA2 Kinetics Dependence of Microstructure and Stress Evolutions in Polycrystalline Cu Films: Real-time Diagnostics and Atomistic Modelling, C. Furgeaud (clarisse.furgeaud@univ-poitiers.fr), C. Mastail, A. Michel, L. Simonot, Institut Pprime - CNRS - ENSMA - Université de Poitiers, France; E. Chason, Brown University, USA; G. Abadias, Institut Pprime - CNRS - ENSMA - Université de Poitiers, France

Thin films are currently used in order to decrease the size and improve performances of integrated components in electronic devices. Sputter-deposition is commonly used for growth of metallization layers. It's well established that microstructure, morphology and residual intrinsic stress are strongly correlated to deposition parameters. By combining *in situ* and real-time diagnostics tools a better understanding of the development of film microstructure and intrinsic stress could be achieved for high-mobility metals [1] highlighting the key role of the early stages of growth in the design of thin films morphology.

However, the interplay between deposition parameters and growth kinetics is unexplored, such as the interdependence between growth rate, pressure, flux interruption/resumption on stress build-up and post-growth-relaxation kinetics. In this study, we propose a methodology based on three different *in situ* and real-time diagnostics tools: Multiple-beam optical stress sensor (MOSS), electrical resistance and surface differential reflectance spectroscopy (SDRS) implemented during sputter-deposition of a model system Cu thin film. Such methodology allows us to obtain relevant and quantitative information on growth and relaxation kinetics. This study was complemented by a systematic *ex situ* characterization by AFM, XRD, and TEM to relate film morphology and microstructure to deposition parameters used.

Besides this experimental approach, we have addressed the atomistic mechanisms responsible for these kinetic effects by computational modelling. We have developed a versatile kinetic Monte Carlo (kMC) code based on a 3D rigid lattice to mimic as much closely as possible the real sputter-deposition conditions. The originality of this code lies on its ability to capture the energetic deposition conditions intrinsic to the sputtering deposition process. Indeed, energetic species constituting the incoming flux are able to drastically alter (sub-)surface processes, such as adatom diffusion and defect creation, and subsequent morphology, microstructure and stress. Finally, the capability of the code to predict stress caused by the diffusion of adatoms in and out of the grain boundaries will be further examined with the final objective to provide a multiscale, predictive computational tool to study the growth and stress kinetics.

[1] G. Abadias *et al.*, Volmer-Weber growth stages of polycrystalline metal films probed by in situ and real time optical diagnostics, *APL*, 107, 183105 (2015)

2:20pm H1-2-TuA3 Understanding the Crystallization of Amorphous Films with Embedded Seed Crystals using High-resolution STEM Composition and Structural Mapping, P. Rasmussen (pjrasmu1@asu.edu), J. Rajagopalan, R. Berlia, Arizona State University, USA

It has been shown recently [1] that by systematically embedding nanometer sized seed crystals into amorphous thin films, their thermally induced crystallization process and final microstructure (mean grain size, grain aspect ratio, and spatial distribution) can be explicitly controlled. Here, we describe the characterization of the seed crystals and their relation to the final grain size, size dispersion and texture of the crystallized films through a combination of spatially resolved, composition and structural mapping in a scanning transmission electron microscope (STEM). We examined two

Tuesday Afternoon, May 21, 2019

different films (NiTi and TiAl) with a variety of seed crystals (Ti, Cu, Cr) in this work. First, we used energy dispersive X-ray spectroscopy (STEM-EDXS) to obtain the chemical composition with nanometer scale spatial resolution and identified seed crystals (regions with sharply elevated seed element content) in the films. To complement this information, we used automated crystal orientation mapping (ACOM) via precession electron diffraction to identify amorphous (film matrix) and crystalline regions (seed crystals) as well as the orientation of the seed crystals. The combination of STEM-EDXS and ACOM analysis allowed us to map the size dispersion, areal density and spatial distribution of seed crystals and correlate them with the final microstructure of the crystallized film.

1. R. Sarkar and J. Rajagopalan, "Synthesis of thin films with highly tailored microstructures," *Materials Research Letters* 6, 398-405, 2018

2:40pm **H1-2-TuA4 *In-situ* Investigation of the Oxidation Behavior of Metastable CVD Ti_{1-x}Al_xN Using Combined Synchrotron XRD and DSC.** C. Saringer (christian.saringer@unileoben.ac.at), M. Tkadletz, Montanuniversität Leoben, Austria; A. Stark, Helmholtz Zentrum Geesthacht, Germany; C. Czetti, Ceratizit Austria GmbH, Austria; N. Schalk, Montanuniversität Leoben, Austria

Although hard protective Ti_{1-x}Al_xN coatings deposited by physical vapor deposition methods are well investigated today, their microstructure and properties when synthesized by chemical vapor deposition (CVD) still offer new and scientifically challenging questions. This is mainly owing to the extraordinary structure of CVD Ti_{1-x}Al_xN coatings, typically consisting of Al-enriched Al(Ti)N and Al-depleted Ti(Al)N epitaxial nanolamellae. Within this work, the oxidation behavior of such a nanolamellar coating has been examined using a combination of *in-situ* analytical methods. The coating investigated was composed of approximately 66 wt.-% Al(Ti)N and 32 wt.-% Ti(Al)N face centered cubic phase fractions as well as small amounts of wurtzitic AlN (< 2 wt.-%) deposited on a TiN baselayer. Differential scanning calorimetry (DSC) and X-ray diffraction (XRD) on a powdered sample were simultaneously performed at the P07 beamline at the synchrotron PETRA III in Hamburg during a continuous annealing cycle from 100 to 1400 °C in ambient atmosphere. Together with the DSC signal a sequential Rietveld refinement of the XRD data allowed to precisely determine the onset temperatures of phase transformations and oxidation reactions along with the quantitative phase composition at any given temperature. The results showed that while the TiN baselayer already started to oxidize to rutile at temperatures below 550 °C, the Al-containing phases still retained their chemical stability. For the Ti(Al)N and Al(Ti)N phases the onset of oxidation could be observed at approximately 700 and 850 °C, respectively, evidencing the positive influence of Al on the oxidation resistance of Ti_{1-x}Al_xN based coatings. At 1000 °C, oxidation of the coating to rutile and alumina was completed, however, upon further annealing above 1250 °C rutile and alumina were found to form the ternary oxide Al₂TiO₅. The sophisticated combination of *in-situ* DSC and XRD at a synchrotron with subsequent Rietveld analysis is a novel approach for the investigation of the thermal stability of metastable coating systems and the results presented demonstrate the potential power of this method. Additionally, annealing in ambient air of the same CVD Ti_{1-x}Al_xN coating on single crystalline alumina substrates with subsequent microstructural analysis allowed to validate the results provided by the *in-situ* investigation of the powdered sample with the behavior of the solid coating.

3:00pm **H1-2-TuA5 In-situ X-ray Characterization of Liquid-solid Transition Phase in Small Volume.** M. Kbibou (Mohamed.kbibou@ensam.eu), L. Barrallier, Mechanics, Surfaces and Materials Processing Laboratory, France; M. El Mansori, Arts et Métiers ParisTech d'Aix en Provence, Laboratory of Mechanics, Surface and Materials Processing (MSMP-EA7350), France; L. Heraud, Mechanics, Surfaces and Materials Processing Laboratory, France
This research paper presents a novel *in-situ* X-ray characterization of microstructure and evolution of residual stress during solidification process in small volume, which involves the occurrence of various mechanisms operating concurrently. This is illustrated by the solidification of binary eutectic alloy Bi58%wt-Sn42%wt using *in-situ* X-ray diffraction cell of laboratory instrument to understand the fundamental physical mechanisms that control the liquid-solid transition phase. The diffraction cell is outfitted with a heater under inert atmosphere, temperature control system, thermal isolation and transparent window making X-ray scattering analysis possible at higher temperature. The experimentally obtained temperature dependence of crystal mesh parameters, phase's percent and residual stress is discussed. A Radial Distribution Function Analysis (RDFA) is given at the melting phase of the alloy to describe the short-range order (SRO) and atomic distribution. Also discussed is the evolution of phase transformations

and residual stresses on the surface of alloys from room temperature to melting point. The possibilities of this *in-situ* X-ray characterization method to master interplay between microstructure, solidification process variables and functional properties of compounds are highlighted.

4:00pm **H1-2-TuA8 Novel Quantitative Thin Film Thickness and Chemical State Analysis X-ray Techniques.** W. Yun (wuyun@sigray.com), B. Stripe, S. Shesadri, S. Lewis, X. Yang, R. Qiao, S.H. Lau, Sigray, Inc., USA

X-ray based techniques have long been used for thin film characterization, and commonly known approaches include total fluorescence x-ray spectrometry (TXRF) and grazing incidence x-ray scattering systems. However, these laboratory-based approaches have poor spatial resolution due to the limited brightness of the x-ray sources used. On the other hand, techniques based on synchrotron facilities (large particle accelerators that provide intense beams of x-rays) such as micro x-ray fluorescence and micro x-ray absorption spectroscopy (microXRF and microXAS) can provide powerful, spatially resolved information, including: thickness variation, chemistry (e.g. oxidation state and bond lengths), and compositional variation. Such information can be achieved by rastering a focused, high brilliance x-ray beam at microns-scale resolution across the thin film.

Until now, such capabilities at high, microns-scale resolution have been exclusively available at synchrotron facilities, which have limited accessibility and a competitive application process. Sigray, through patented breakthroughs in x-ray source and x-ray optic technologies, has developed two major systems for spatially resolved thin film studies: the AttoMap microXRF system and the QuantumLeap x-ray absorption spectroscopy system.

Here we present the two breakthrough systems and their recent applications, which both provide non-destructive capabilities and the ability to spatially resolve thin films *in situ*, for instance under high temperature and mechanical strain. The microXRF system has spatial resolution down to microns and sub-Angstrom sensitivities, which has enabled it to map thickness variations of coatings and on the order of angstroms with high repeatability and accuracy. The x-ray absorption spectroscopy (XAS) system provides important chemical information for a given element of interest, such as oxidation state and reactivity, bond lengths, atomic geometry, and nearest neighbor information (such as atomic type).

We will present recent trace-level results of thin films with ~1% repeatability, such as Ar, Hf, Ni and Ti measurements and standard-less ratios for fast and non-destructive characterization. Moreover, we will also present some recent findings on chemical state analysis using the XAS system for applications including battery electrodes and catalyst layers.

4:20pm **H1-2-TuA9 Effect of Heat Treatment on Microstructure of Erbium Film on Steel Substrate with Yttria Buffer Layer Fabricated by MOCVD.** K. Matsuda (matsuda@sus.u-toyama.ac.jp), M. Tanaka, S.W. Lee, University of Toyama, Japan; Y. Hishinuma, NIFS, Japan; K. Nishimura, T. Tsuchiya, University of Toyama, Japan

Erbium and yttria are the promising materials to realize an advanced breeding blanket system because of good electrical resistivity and effective hydrogen permeation suppression. Erbium thin film fabricated via MOCVD process with the yttria buffer layer was formed on steel (SUS316) substrate before and after thermal cycles to investigate the effect of thermal cycling, and their microstructure was confirmed by electron microscopes (SEM, TEM and STEM) and atomic force microscope (AFM) in the present work.

The surface morphology of samples after thermal cycling has small granular structure than samples before thermal cycling and without yttria buffer layer. According to cross sectional observation by TEM and STEM, erbium and yttria have different columnar structure, while yttria buffer layer did not avoid diffusion of elements from SUS316 substrate to erbium layer. The thermal cycling test had not been affected to the growth direction of erbium and yttria layers, which is mostly cube-cube relationship

4:40pm **H1-2-TuA10 Detailed Characterization of Interface Structure of Thin Aluminum Films Deposited on a Highly Reactive Metallic Surface.** J.W. Yan (jwyan@alum.imr.ac.cn), Institute of Materials, China Academy of Engineering Physics, China

Thin Aluminum films were deposited on depleted uranium surface using magnetron sputtering techniques under different working pressure ranging from 1⁻³Pa to 1⁻⁴Pa. Interface structure were analyzed using AES, XPS and TEM techniques. Present of oxygen at film substrate interfaces were confirmed by both AES and XPS depth profile scanning. TEM examinations revealed a laminated structure at interface, composed by a mixed layer and an oxide layer about 100 nm thick, from film to substrate, respectively. Results obtained from EDAX line scanning profile and diffraction ring

Tuesday Afternoon, May 21, 2019

patterns suggest that, mixed layer is composed by UAl₂ and oxide layer by UO_{2+x}, respectively. A laminated interface model is proposed to assess the interface adhesion properties of uranium aluminum interface.

5:00pm **H1-2-TuA11 Study of Volmer-Weber Thin Film Growth Mechanisms by Coupling *in situ* Resistivity, Optical and Mechanical Measurements, Q. Hérault (quentin.herault@saint-gobain.com), S. Grachev, I. Gozhyk, H. Montigaud, Saint-Gobain Recherche/CNRS, France; R. Lazzari, Institut des Nano Sciences de Paris - Sorbonne Université, France**

Völmer-Weber growth mode is characteristic of some materials, such as Ag and Au. Before obtaining a uniform film, this growth mode involves complex steps of growth: island nucleation, island growth, percolation and coalescence. It is still a challenge to study these steps with *ex situ* techniques, especially when thin films are not stable after deposition and oxidation. Indeed, low melting points materials -Ag for example- are very mobile due to their low diffusion energy. *In situ* measurements become important to obtain representative information about growth phenomenon happening during deposition process.

To do so, we decided to develop a homemade *in situ* resistivity measurement setup into our DC magnetron sputtering chamber. Coupled to an existing *in situ* mechanical stress measurement setup, this system provided information about coalescence start (mechanical compressive pick), percolation threshold (resistivity fall) and uniform film (mechanical tensile pick). In parallel, our measurements were compared to optical measurement, providing complementary information about coalescence start.

With this setup and playing on deposition technique (continuous and sequentially interrupted), we measured a more or less delayed percolation threshold. We also measured a change in grain size distribution. In addition, using different deposition conditions (power and pressure) and sublayers, we tuned growth in order to finally propose growth mechanisms during Ag thin film deposition, function of deposition rate and diffusion.

Tuesday Evening, May 21, 2019

Special Interest Talks

Room Town & Country - Session SIT1-TuSIT

Special Interest Session I

Moderators: Christopher Muratore, University of Dayton, USA, Michael Stüber, Karlsruhe Institute of Technology (KIT), Institute for Applied Materials (IAM), Germany

7:00pm **SIT1-TuSIT1 Advanced Monitoring of Thin Film Growth from Real-time Diagnostics**, G. Abadias (gregory.abadias@univ-poitiers.fr), Institut Pprime - CNRS - ENSMA - Université de Poitiers, France **INVITED**

Thin metallic films deposited on Si are largely used in many technological areas, such as microelectronics, catalysis, architectural glazing or plasmonics. In the case of high-mobility metals on weakly interacting substrates (e.g. Ag on SiO₂), the growth proceeds in a 3D fashion, known as Volmer-Weber. The control of islands size and shape at the beginning of growth is vital for many applications as the characteristic length scales and physical attributes of ultrathin films are mostly set-in during the coalescence stage.

By employing a panel of *in situ* and real-time diagnostics, we could obtain valuable insights on the thin film growth dynamics as well as stress evolution in a variety of sputter-deposited metallic systems (Ag, Cu, Au, Ta and Mo). More particularly, the characteristic thickness of film percolation and film continuity can be determined from a combination of real-time electrical resistivity and wafer curvature measurements. This will be highlighted for the case of Ag and Cu deposited on amorphous carbon as a function of deposition flux F and substrate temperatures T_s.

We will also provide examples on how chemical alloying or interface reactivity can affect the growth morphology and stress evolution of Ag and Cu films. Growth monitoring was performed *in situ* by employing either surface differential reflectance spectroscopy or spectroscopic ellipsometry. We will show that strategies based on interfacial or alloying design can be efficiently employed to manipulate growth and obtain ultra-thin, ultra-smooth, continuous layers.

Finally, we will discuss the issue of phase transformation during growth of ultrathin layers, with special focus on silicide formation. By coupling simultaneously X-ray diffraction, X-ray reflectivity and wafer curvature during sputter-deposition of metal layers on amorphous Si, information about thickness-dependent crystalline phases, texture, grain growth and microstrain can be gained. This will be demonstrated for Mo/Si and Pd/Si systems. A complex nanostructure formation is uncovered from these synchrotron studies, pointing out to different silicide formation mechanisms and subsequent structural development.

Wednesday Morning, May 22, 2019

Coatings for Use at High Temperatures

Room Pacific Salon 2 - Session A1-3-WeM

Coatings to Resist High-temperature Oxidation, Corrosion, and Fouling III

Moderators: Justyna Kulczyk-Malecka, Manchester Metropolitan University, UK; Lars-Gunnar Johansson, Chalmers University of Technology, Sweden; Shigenari Hayashi, Hokkaido University, Japan

8:20am **A1-3-WeM2 Corrosion Monitoring Of High-Temperature Protective Coatings Under Molten Salts Environments For CSP Applications, F.J. Pérez Trujillo (fjperez@ucm.es), V. Encinas Sánchez, T. de Miguel Gamo, Universidad Complutense de Madrid, Spain; M.I. Lasanta Carrasco, Universidad Complutense de Madrid, Spain; G. García-Martín, Universidad Complutense de Madrid, Spain**

In recent years there has been a substantial increase in interest in renewable energy, this being particularly high in the field of concentrated solar power (CSP). Commercial CSP plants usually use molten salt mixtures as thermal energy storage medium. The currently used industrial compound is an alkali-nitrate mixture composed of 60 wt.% NaNO₃/40 wt.% KNO₃. One of the main drawbacks of this medium consists in the severe corrosion problems to which its composition and high temperature lead. Thus, the development of protective coatings for steels could be an economical alternative for increasing the lifetime of pipes and tanks in CSP plants against molten salt corrosion. This solution would allow CSP plants to reduce the levelized cost of electricity (LCOE), which is one of the major objectives currently set.

The conventional methods used for assessing the corrosion in molten salt environments are not the optimal methods when monitoring the real-time corrosion process. A better understanding of the process requires a monitoring system that allows recording corrosion rates in real-time. In this respect, electrochemical impedance spectroscopy (EIS) is a powerful technique for monitoring corrosion processes that take place in steels under molten salt environments.

Thus, this work aimed at developing sol-gel protective coatings on low alloyed steels and monitoring the protective behavior in contact with molten salts by employing EIS technique. To this end, electrochemical sensors, patented under the reference code WO2017046427, were employed. Corrosion tests were performed at 500°C up to 2000 h and EIS results were supported by gravimetric and microstructural characterizations. All results were compared to the uncoated steels.

Results showed the good behavior of the coated substrates. Corrosion monitoring system showed the protective behavior of the coatings, these being compared with the uncoated samples, where widespread corrosion was determined. Results were supported by gravimetric analyses, with very little weight variations after 2000 h of test in comparison to uncoated samples.

8:40am **A1-3-WeM3 Development of a Ti_xSi_y Protective Layer on TiAl48-2Cr-2Nb for Increased Oxidation Resistance, J. Crespo Villegas (joseffina.crespo@polymtl.ca), S.L. Loquai, É. Bousser, École Polytechnique de Montréal, Canada; M. Cavarroc, SAFRAN Tech, France; S. Knittel, SAFRAN Aircraft Engines, France; L. Martinu, J.E. Klemberg-Sapieha, École Polytechnique de Montréal, Canada**

Given the extreme and wide range of operational conditions of jet engines, the aircraft industry has been a driving force in the development of high performance materials. There is a well-known need for lowered fuel consumption and greenhouse gas emission. Weight reduction of the aircraft engine is essential to meet these needs. In this context, γ -TiAl alloys have been extensively studied to be used as a replacement for Nickel-based alloys, due to their well-balanced ratio of density and mechanical properties. In fact, these alloys have recently been introduced as a material candidate for low-pressure turbine blades by several engine manufacturers. However, their application is limited by a maximum operating temperature around 750°C due to their limited oxidation resistance. Indeed, the formation of an outer mixed oxide scale (Al₂O₃-TiO₂) and oxygen inward diffusion, due to the high affinity for oxygen, lead to material degradation and embrittlement of the component.

To increase the thermal stability of γ -TiAl alloys over 750°C, the development of coatings that promote stable and slow growing protective oxide scales is one of the preferred methods. Consequently, this work presents a study on the growth of Ti_xSi_y layers on a γ -TiAl alloy by Si deposition using RF magnetron sputtering and subsequent vacuum thermal annealing at 900°C. The composition and microstructural evolution of the coating are investigated by X-Ray Diffraction (XRD), Scanning Electron Microscopy and

Energy-Dispersive X-Ray Spectroscopy (SEM-EDS). To evaluate the efficiency of the Ti_xSi_y coatings, the oxidation resistance of the coating is investigated by isothermal measurements at 900°C.

The deposition of Si and the subsequent thermal annealing step resulted in the formation of a continuous coating of mixed Ti_xSi_y compounds. A significant dependence of the coating microstructure on the diffusion process conditions at the Ti_xSi_y coating/ γ -TiAl interface was demonstrated. The oxidation behavior of Ti_xSi_y coated γ -TiAl and uncoated γ -TiAl were compared and the protective behavior of the Ti_xSi_y coating was confirmed. The chemical composition remained stable, no delamination was observed, and only a thin external layer of mainly protective SiO₂ was formed. Finally, the effect of the diffusion process of Ti_xSi_y promoted by the thermal annealing conditions is discussed.

9:00am **A1-3-WeM4 The Impact of Aluminide and MCrAlY Coatings on the Fatigue Properties of Ni-based Valve Alloys, S.N. Dryepondt (dryepondtsn@ornl.gov), B.L. Armstrong, G.M. Muralidharan, Oak Ridge National Laboratory, USA**

Increasing temperature in light and heavy-duty internal combustion engines offers a straightforward solution for increasing engine efficiency. Development of new Ni-based high temperature alloys is, however, burdensome due to the need for both high strength and high oxidation resistance. One solution is to apply corrosion-resistant coatings to high strength materials, but the coating must not affect the alloy mechanical properties. The impact of diffusion aluminides and MCrAlY overlay coatings on the high cycle fatigue (HCF) properties of alloy 31V ((57Ni-23Cr-13Fe-2Mo-2.3Ti-1.3Al-0.9Nb) was evaluated at 20, 500 and 800° C. At all temperatures, the numbers of cycles to failure for the bare and coated specimens were similar, as long as the specimen heat treatments were identical. A 3h at 1100° C heat treatment was initially used to fabricate a ~50um thick slurry aluminide coating but it was shown that a similar coating thickness can be achieved at temperature as low as 850° C. For the slurry and pack aluminide coatings, cracks initiated in the interdiffusion zone, whereas cracks initiated at the substrate/coating interface for the NiCoCrAlY-coated specimens. Initial characterization of aluminide and MCrAlY coatings deposited on advanced high strength Ni-based alloys will also be presented. This research was sponsored by the U.S. Department of Energy's (DOE), Vehicle Technologies Office, Propulsion Materials Program

9:20am **A1-3-WeM5 High Temperature Oxidation of γ -TiAl Produced by Additive Manufacturing, R. Swadzba (rswadzba@gmail.com), Institute for Ferrous Metallurgy, Poland; B. Mendala, L. Swadzba, B. Witala, J. Tracz, Silesian University of Technology, Poland; L. Pyclik, K. Marugi, S. Sabbadini, Avio Aero A GE Aviation Business, Poland**

Recently γ -TiAl intermetallics have been successfully applied on low pressure turbine blades mostly due to their low density, high specific strength and creep resistance, all of which make them excellent alternatives for Ni-based superalloys. The paper presents the results of analytical TEM and STEM investigations on the microstructure and scale growth on γ -TiAl 48-2 alloy produced by EBM (Electron Beam Melting) in the range of 750 – 900 °C during short term experiments in air and pure oxygen. Moreover, the results of research works performed on Si-modified aluminide coatings for γ -TiAl are presented. The coatings were produced using pack cementation method with varying content of Si and Al in the pack. Total of five different pack chemistries were utilized to obtain coatings of different microstructure and high temperature oxidation performance. Moreover, a comparison of the high temperature oxidation behavior of 48-2-2 alloy produced by Additive Manufacturing and cast TNB-V5 alloy is presented. The samples were thermally cycled at 850 °C in 23 h cycles to a total of over 3000 hours in order to obtain mass change curves. The results of cyclic oxidation tests were related to the microstructure of the as-deposited coatings. Special effort has been done in order to perform a detailed investigation of the growth of protective oxide scales using high resolution Scanning Transmission Electron Microscopy (STEM), energy filtered TEM (EFTM) and EELS (Electron Energy Loss Spectroscopy).

11:00am **A1-3-WeM10 High Temperature Oxidation Protection of Gamma-based TiAl by Sputtered Al-O-F Films, F. Bergeron (florence.bergeron@polymtl.ca), S.L. Loquai, É. Bousser, École Polytechnique de Montréal, Canada; M. Cavarroc, SAFRAN Tech, France; S. Knittel, SAFRAN Aircraft Engines, France; L. Martinu, J.E. Klemberg-Sapieha, École Polytechnique de Montréal, Canada**

γ -based TiAl alloys are considered for major components of aircraft engines. Indeed, their excellent mechanical properties and relative light weight make them good candidates to replace nickel-based alloys for blades and vanes in the low-pressure stages of the turbine. However, the use of TiAl for other

Wednesday Morning, May 22, 2019

engine parts is limited by its high sensitivity to oxidation phenomena at temperatures above 750°C. The presence of TiO₂ in the generated oxide scale is an issue, as it grows faster than Al₂O₃ and hinders the formation of a continuous protective Al₂O₃ oxide scale. Indeed, alumina is a slow growing oxide, and offers good protection against oxygen diffusion.

Therefore, a solution to protect gamma-based TiAl is to form an α -Al₂O₃ layer at its surface, for which the halogen effect can be very effective approach. The addition of a halogen on the surface or the subsurface of TiAl promotes the growth of alumina by preferentially forming gaseous aluminum halides instead of titanium halides. Specifically, fluorine has been shown to offer excellent performance during high-temperature oxidation, as aluminum fluorides react with oxygen to form Al₂O₃. Fluorination of TiAl can be performed using either F ion implantation or fluorocarbon overlay coatings applied by spraying, painting, dipping, etc.

In the present work, we propose a new approach to deposit Al-O-F coatings based on low-pressure RF reactive magnetron sputtering of Al in an atmosphere composed of an O₂ and fluorocarbon mixture. The resulting coating microstructure was characterized by Scanning Electron Microscopy (SEM) coupled to Energy Dispersive X-Ray Spectroscopy (EDS) and Rutherford Backscattering Spectrometry (RBS) chemical analysis. Their oxidation performance was then tested using isothermal oxidation at 850°C in laboratory air. The fluorine content of the coatings varied between 50 and 70 at.% and it was found that the Al-O-F coatings protect TiAl against damaging oxidation. The resulting outer oxide scale at the surface was thin and was composed of a continuous Al₂O₃ layer at the interface, covered by a mixed TiO₂ and Al₂O₃ oxide layer.

In parallel, the discharge was studied using mass spectrometry and the relationships between gaseous precursor concentrations, power, pressure and the plasma's chemistry and coating composition are discussed.

11:20am **A1-3-WeM11 Corrosion Behavior and Durability of Microstructure of Stainless Steel Rebars in Simulated Concrete Pore Solution Containing Chloride with Different Ph**, *D.B. Subedi (dhrubacsubedi@gmail.com)*, Chinese Academy of Sciences, China

Corrosion is a problem of science and technology. It cannot eliminate completely although the corrosion control is becoming more practical and achievable to decrease its rate. Nowadays, the corrosion control method of metals and alloys using various types of eco-friendly coating to save passive film on metal surface is becoming a fundamental academic and research concerns corrosion scientists.

All the experiments were conducted under static or dynamic flow conditions at room temperature. The corrosion rate evaluations were implemented by electrochemical measurements (open circuit potential, linear polarization, potentiodynamic polarization, and electrochemical impedance spectroscopy), while surface analytical techniques (SEM/EDS, XRD and XPS) were employed to examine and characterize the compositions, microstructure of alloys and the corrosion product films.

Fig1; Nyquist plot, 1-28day Austenitic Stainless Steel Fig1; Nyquist plot of three Stainless Steel

The corrosion resistance performance of the different stainless steel, 304ss, 410ss and 2304ss

Were evaluated in different chloride condition at 9.3 pH comparing with microstructure and mechanism of passivation film formation. EIS results of both accelerated corrosion tests showed the corrosion resistance performance of different alloys

Fig; Phase and Bode plot of Austenitic stainless steel for 1- 28day

The results of a study examining the Cl₋ induced corrosion resistance of austenitic, duplex, and ferritic high-strength stainless steels in simulated alkaline and carbonated concrete solutions during exposed to carbonated solutions, corrosion resistance was reduced and only duplex grades 2304SS exhibited high corrosion resistance.

Fig; surface structure of duplex stainless steel after 14 days

A strong correlation between microstructural defects and corrosion damage was observed by the help of morphology of SEM picture and optical observations. The pitting corrosion behavior of 304ss, 2304ss and 410ss in 3.5% NaCl solution has been investigated by electrochemical noise M-S Curve and the experimental data was analyzed based on stochastic theory. The change in the pit initiation site and the outstanding repassivation ability of 2304ss thin film determined that metastable pit events occurred more frequently and the probability of stable pits developing from metastable pits was lower than that of 304ss and 410ss, which improved the pit corrosion resistance of duplex thin film. The difference between growth mechanisms of

stable pits on two materials led to different corrosion resistance, thus enhancing the pit corrosion resistance of duplex thin film compare to other two alloys.

11:40am **A1-3-WeM12 High-temperature Sulfidation of Hot-dip Aluminized 9Cr-1Mo Steel**, *M.A. Abro (abromdali@gmail.com)*, Mehran University of Engineering and Technology, Pakistan; *D.B. Lee*, Sungkyunkwan University, Republic of Korea

The 9Cr-1Mo ferritic steel is used frequently in petroleum refining, petrochemical units, and coal power plants due to its good combination of weldability, ductility and high-temperature creep resistance. However, it could suffer serious corrosion in the H₂S gas that is produced as the byproduct during processing in plants. The H₂S gas could accelerate the corrosion and structural deterioration through forming the nonprotective FeS scale and causing the hydrogen dissolution. Hence, the Al hot-dipping was performed in order to protect this steel from the serious H₂S gas corrosion. Aluminum hot-dipped coatings behavior applied on 9Cr-1Mo steels have been studied under N₂/0.1%H₂S gas corrosion for up to 50 h at 800 and 900 °C, which suffered little general corrosion on the exterior, due to the frequent incorporation and dissolution of foreign ions such as S to a certain extent. The results have shown that initially, the coating forms by outward growth possibly due to the dissolution of the Fe and matrix elements in molten aluminum. At a later stage, during exposure to N₂/0.1%H₂S at 800-900 °C, aluminum diffuses inward and Fe diffuses outward resulting in the progressive development of Kirkendall voids. A protective aluminum oxide scale (α -Al₂O₃) forms on the surface which remains homogenous, continuous and non-adherent to the alloy layer, but constitutes a protective behavior against sulfurized corrosion attack to a certain extent. The corrosion resistance of hot-dipped steels was much better than that without hot-dipping was largely attributed to its Cr, Mo and Si content in the matrix and Al-rich alloy layer formed at the oxide scale/substrate interface.

The samples without were also sulfidized at similar conditions for comparison purposes and in order to find the diffusion mechanism using Pd marker testing. The samples were inspected using SEM equipped with an EDS, an EPMA and a high-power X-ray diffractometer with Cu-K α radiation at 40 kV and 300 mA. The microstructures of the aluminized layer and the steel substrate were etched using Keller's reagent and Vilella's reagent, respectively. Vickers microhardness was measured using a microhardness tester.

Acknowledgment. This research was supported by Basic Science Research Program through the National Research Foundation of Korea (NRF) funded by the Ministry of Education (2017R1D1A1B03028792). Authors are also thankful to HEC Pakistan to provide the travel grant.

Hard Coatings and Vapor Deposition Technologies Room California - Session B4-3-WeM

Properties and Characterization of Hard Coatings and Surfaces III

Moderators: **Naureen Ghafoor**, Linköping Univ., IFM, Thin Film Physics Div., Sweden, **Ulrich May**, Robert Bosch GmbH, Germany, **Fan-Bean Wu**, National United University, Taiwan

8:20am **B4-3-WeM2 Physical Properties of Nano-structured Chromium Nitride Hard Coatings obtained by RF Physical Vapor Dynamic Glancing Angle Deposition**, *M.J.M. Jimenez*, *V. Antunes*, *S.C. Cucatti*, *A.R. Riul*, *L.F. Zagonel*, UNICAMP, Brazil; *C.A. Figueroa*, Universidade de Caxias do Sul, Brazil; *D. Wisnivesky*, UNICAMP, Brazil; **F. Alvarez (alvarez@ifi.unicamp.br)**, Instituto de Física, UNICAMP, Brazil

Nanostructures CrN films are obtained by combining RF Physical Vapor Dynamic Glancing Angle Deposition (PV-DGAD) and Logic Programmable Computer (PLC) controlled substrate motion. By appropriated substrate oscillation frequency, the physical properties such as the micro-nanostructure, morphology, hardness, texture, crystallite size are feasible to be tailored. Samples are deposited by moving the substrate forward ($-\phi \Rightarrow +\phi$) a back ($+\phi \Rightarrow -\phi$) by controlling the angular velocity $\omega = d\phi/dt$. The angle ϕ is measured perpendicular to the substrate ($\phi=0$, Cr target parallel to the substrate). We report the physical properties of samples obtained by moving the substrate with $\omega(t)$ constant and square shape functions. The time dependence angle of the precursors atoms impinging the substrate prompts the formation of wavy-like and zigzag periodic nano-crystalline columnar nano-structures with interesting physical properties. The physical characteristics of the CrN coating such as morphology, residual stress, nano-

Wednesday Morning, May 22, 2019

hardness, crystallite size and texture of the columnar multi-structured films are customized by the PLC motion of the substrate. Also, X-ray spectra show that the oscillation of the substrate allows the appearance of a periodic crystalline orientations that strongly depends on $\omega(t)$. Finally, these properties of the deposition technique open the possibility to control the (un)isotropy of the hard coatings for specific applications.

Keywords: Hard Coating, Chromium nitride, Dynamic Glancing angle deposition

8:40am **B4-3-WeM3 Synthesis and Characterization of Sputter Deposited Hard Coatings within the Quasibinary System TiB₂-VB₂**, *C. Mitterer (christian.mitterer@unileoben.ac.at)*, V.L. Terziyska, M. Tkadletz, L. Hatzenbichler, D. Holec, Montanuniversität Leoben, Austria; V. Moraes, Institute of Materials Science and Technology, TU Wien, Austria; A. Lümkmann, PLATIT AG Advanced Coating Systems, Switzerland; M. Marstein, Hightech Zentrum Aargau AG, Switzerland; P. Polcik, Plansee Composite Materials GmbH, Germany

TiB₂ coatings on cutting tools have become state-of-the-art in high-performance machining of nonferrous alloys, due to their superior hardness, thermal stability and low adhesion tendency to workpiece material. These properties stem from strong covalent B-B bonds within the hexagonal TiB₂ lattice, which consequently results in high brittleness limiting their application. Thus, in this work, coatings within the quasibinary system TiB₂-VB₂ have been investigated, with the goal to tune their chemical bonds to overcome these limitations. Coatings with thicknesses of $2 \pm 0.5 \mu\text{m}$ have been synthesized by d.c. magnetron sputter deposition from powder metallurgically produced (Ti,V)B₂ composite targets with 2-inch-diameter and VB₂ fractions of 0, 7, 13, 25, and 100 mol%. All coatings are characterized by a strongly (001) oriented hexagonal AlB₂-type (Ti,V)B₂ solid solution phase with a Vegards-like gradual shift of X-ray diffraction peaks from TiB₂ to VB₂. While the compressive stress within the TiB₂ coatings reaches a maximum of -1.4 GPa, VB₂ addition results in stress relaxation to about -0.3 GPa, independent of the VB₂ content. Despite this low stress of (Ti,V)B₂ coatings, their hardness and elastic modulus is largely unaffected by the VB₂ addition, reaching values of about 45 GPa and 420 GPa, respectively. In addition, (Ti,V)B₂ coatings sputter deposited from targets with 25 mol% VB₂ show superior friction and wear properties during ball-on-disk testing against Al₂O₃ at room temperature and at 400°C, outperforming pure TiB₂ coatings. Finally, the results obtained are corroborated by ab-initio calculations of elastic properties within the TiB₂-VB₂ quasibinary system.

9:00am **B4-3-WeM4 Deposition-controlled Stabilization of Metastable fcc-(Al,Ti)N in CVD and PVD Coatings**, *U. Ratayski (ulrike.ratayski@iwu.tu-freiberg.de)*, Technische Universität Bergakademie Freiberg, Germany; M. Höhn, Fraunhofer IKTS, Germany; B. Scheffel, Fraunhofer FEP, Germany; F. Fietzke, Fraunhofer Institute for Organic Electronics, Electron Beam and Plasma Technology FEP, Germany; M. Motylenko, D. Rafaja, Technische Universität Bergakademie Freiberg, Germany

The addition of aluminum nitride to titanium nitride is known to improve the high-temperature oxidation resistance of TiN-based coatings. Furthermore, low or medium concentrations of Al increase also the hardness of the (Ti,Al)N coatings [1]. High Al contents lead typically to an enhanced decomposition of titanium aluminum nitride into Ti-rich (Ti,Al)N with the face centered cubic (fcc) structure and wurtzitic AlN, and to the degradation of the mechanical properties of the Al-rich (Al,Ti)N coatings. In order to be able to achieve good high-temperature oxidation resistance and high hardness concurrently, metastable Al-rich fcc-(Al,Ti)N must be stabilized.

In this comparative study, the mechanisms stabilizing metastable Al-rich fcc-(Al,Ti)N are discussed and tested on the Al-rich (Al,Ti)N coatings containing more than 50 mol % AlN, which were deposited using chemical vapor deposition (CVD), spotless arc evaporation (SAD) and pulsed magnetron sputtering (PMS). The mechanisms stabilizing the thermodynamically metastable phases were concluded from the microstructure analyses that were performed using X-ray diffraction, transmission electron microscopy with high resolution, X-ray spectroscopy (EDX) and electron-energy loss spectroscopy (EELS).

In the (Al,Ti)N coatings prepared by CVD, three-phase composites consisting of fcc-(Ti,Al)N, fcc-(Al,Ti)N and w-AlN have formed. Although w-AlN is known to deteriorate the mechanical properties of the (Al,Ti)N coatings, the interaction of these phases retarded the decline of the hardness up to $x_{\text{AlN}} \sim 0.9$. In the (Al,Ti)N coatings deposited by PMS, the formation of w-AlN was avoided up to $x_{\text{AlN}} \sim 0.65$. The Al-rich fcc-(Al,Ti)N phase was apparently stabilized by fluctuations of the Al (and Ti) concentration. The concentration of Al (and Ti) showed almost bimodal distribution in these coatings. In the (Al,Ti)N coatings deposited using SAD, the Al-rich fcc-(Al,Ti)N was stabilized

mainly by a low ad-atom mobility, which promoted the formation of supersaturated fcc-(Al,Ti)N.

[1]D. Rafaja, C. Wüstefeld, M. Dopita, V. Klemm, D. Heger, G. Schreiber, M. Šíma, Surf. Coat. Technol. 203 (2008) 572-578]

Keywords: metastable fcc-(Al,Ti)N, microstructure, chemical vapor deposition, spotless arc evaporation, pulsed magnetron sputtering, XRD, TEM

9:20am **B4-3-WeM5 Oxidation Resistance of AlP Deposited AlCrN and AlTiN Coatings with High Al Compositions**, *K. Yamamoto (Yamamoto.kenji1@kobelco.com)*, H. Nii, Kobe Steel, Ltd., Japan

Al containing transition metal nitrides undergo a characteristic phase transition from cubic B1 to hexagonal B4 structure as the Al content is increased. This change in crystal structure is known to affect not only mechanical property, but also chemical property such as oxidation resistance [1]. AlCrN and AlTiN are one of compounds among such system and applied tribological components such as cutting tool, die and molds for superior mechanical and oxidation resistance at elevated temperatures. A series of AlCrN and AlTiN coating with different Al contents were deposited by cathodic arc ion plating with different substrate bias voltage. Crystal structure of the coatings were examined by XRD and oxidation behavior was investigated by annealing samples in air at 800, 900 and 1000 °C for 30min and surface O composition was measured by EDX and AES for O depth profiling.

Both AlCrN and AlTiN coating showed change in crystal structure depending on the substrate bias, especially Al content is more than 70 at% for AlCrN and 50 at% for AlTiN. These coatings contain hexagonal phase in the coating at low substrate biases and became cubic single phase as the substrate bias is increased. In case of AlCrN, the oxidation behavior seems influenced by the crystal structure and much better oxidation resistance was observed for cubic single phase coating independent of Al content. In case of AlTiN, however, such crystal structure dependent oxidation behavior was not observed. X-ray diffraction analysis of these AlCrN and AlTiN coatings suggests systematic change in grain size corresponding to the change in substrate bias as indicated by width of the diffraction peak. From this observation, it can be concluded that change in oxidation resistance is more likely correlating to the change in grain size of the coating rather than crystal structure.

References:

[1] Reiter et al. Surf. Coat. Technol., Vol. 200, (2005) 2114

9:40am **B4-3-WeM6 Standing Contact Fatigue Behavior of Nitrided AISI 316L Steels**, *D. Fernández-Valdés (amenesa@ipn.mx)*, A. Meneses-Amador, G.A. Rodríguez-Castro, I.E. Campos-Silva, Instituto Politécnico Nacional Grupo Ingeniería de Superficies, México; A. Mouftiez, ICAM Lille, Matériaux, France; J.L. Nava-Sánchez, Tecnológico de Estudios Superiores de Chalco, México

In this work an experimental-numerical evaluation of the standing contact fatigue testing of a nitrided AISI 316L steel is developed. The nitride layers were formed at the surface of a AISI 316L steel by salt bath nitriding process at a temperature of 580 °C for 1, 3 and 5 hours of exposure time, obtaining three different layer thicknesses. In order to know the mechanical response and the different mechanisms of damage associated with the standing contact fatigue test, Hertzian tests were performed on a MTS machine by cyclic loading of a sphere on a flat surface formed by the layer / substrate system. The standing contact fatigue test was developed through two main stages. Firstly, the critical loads for each treatment condition were determined by monotonic tests, where the appearance of circular cracks were considered as a failure criterion. Subsequently, cyclic subcritical loads were applied at a frequency of 5 Hz. A numerical model based on the finite element method was developed to evaluate the stress field generated in the mechanical contact. The results indicate that the thinner coating exhibits better resistance to standing contact fatigue.

11:00am **B4-3-WeM10 Effect of Composition on Toughening Mechanism of V_{1-x}Mo_xN Nanocrystalline Thin Film**, *Y.Q. Feng (fengyiqun0124@gmail.com)*, J.-H. Huang, National Tsing Hua University, Taiwan

The purpose of this study were to investigate the toughening mechanism of V_{1-x}Mo_xN nanocrystalline thin film with different composition of Mo, and compare the texture, residual stress and fracture toughness with each specimen. It is commonly acknowledged that nanocrystalline ceramics with high strength and hardness, while always show low ductility, which limits their applications. Recently, Sangiovanni et al. [1] predicted the V_{0.5}Mo_{0.5}N coating with high hardness and ductility by ab initio density functional theory

Wednesday Morning, May 22, 2019

(DFT), and it has been verified by experiments that $V_{0.5}Mo_{0.5}N$ is more ductile than VN. However, there is lack of studies on the accurate stress and fracture toughness measurements of $V_{1-x}Mo_xN$ and the associated fracture mechanisms. Also it is important to understand the toughness enhancing mechanisms compared with different compositions of $V_{1-x}Mo_xN$. Therefore, this study aimed to investigate the relationship of texture, residual stress and toughness of the different compositions of $V_{1-x}Mo_xN$. $V_{1-x}Mo_xN$ thin films about 1000 nm were deposited on Si substrate by unbalanced magnetron sputtering (UBMS), the compositions of Mo were set to 0.1, 0.2, 0.3, 0.4 and 0.5 by adjusting Mo target currents. After deposition, the ratio of V/Mo and (V+Mo)/N were determined by X-ray photoelectron spectroscopy (XPS), the thickness of all specimens were confirmed by auger electron spectroscopy (AES) and scanning electron microscope (SEM). X-ray diffraction (XRD) was used to characterize the structure and the texture. Besides, the residual stress of the specimens was measured by laser curvature method (LCM) and average X-ray strain (AXS) combined with elastic constant from nanoindentation [2], the hardness was assessed by nanoindentation, and the internal energy induced cracking (IEIC) method was used to evaluate the fracture toughness.

[1] D. G. Sangiovanni, V. Chirita, L. Hultman, Phys. Rev. B, 81 (2010) 104107.

[2] A.-N. Wang, C.-P. Chuang, G.-P. Yu, J.-H. Huang, Surf. Coat. Technol., 262 (2015) 40.

11:20am **B4-3-WeM11 Influence of Mo Contents on Elevated Temperature Tribological Characteristics of CrAlMoSiN Nanocomposite Coating**, **Y.C. Lin (jay85621@kimo.com)**, H. Tao, J.G. Duh, National Tsing Hua University, Taiwan; J.-W. Lee, Ming Chi University of Technology, Taiwan

CrAlMoSiN nanocomposite coatings were produced by doping Mo into the CrAlSiN nanocomposite matrix via radio frequency magnetron sputtering. CrAlMoSiN thin films with different Mo contents were deposited on both Si-wafer and Inconel-718 substrate by controlling the Mo target working power. Since CrAlSiN nanocomposite coatings exhibit superior high temperature wear resistance, the addition of Mo into CrAlSiN nitride coatings will offer extra self-lubricating characteristic, which leads to lower friction coefficient. By doping Mo in to CrAlSiN coating via composition control, CrAlMoSiN coatings with high temperature wear resistance and reduced friction coefficient could be developed.

The chemical compositions of as-deposited coatings were identified by a FE-EPMA. The tribological property was evaluated by a tribometer with temperature control unit. The wear tracks were analyzed by an Alpha-step to calculate the wear rate. The nano-hardness (HIT) and reduced elastic modulus (EIT*) were examined by a nano-indenter. Further, microstructure of wear tracks was analyzed by FE-SEM and HR-TEM. The phase transformations were observed by a Gazing Incidence XRD and XPS.

11:40am **B4-3-WeM12 Characterization of Cosputtered W-Si-N Coatings**, **Y.H. Liu (10655003@email.ntou.edu.tw)**, National Taiwan Ocean University, Taiwan; L.C. Chang, Ming Chi University of Technology, Taiwan; B.W. Liu, Y.I. Chen, National Taiwan Ocean University, Taiwan

Monolithic and multilayered W-N and W-Si-N coatings were fabricated through direct current magnetron cosputtering with a nitrogen flow ratio ($N_2/(N_2 + Ar)$) of 0.4 at substrate holder rotation speeds of 0 and 5 rpm, respectively. The characteristics and oxidation behaviors of the W-N and W-Si-N coatings were investigated by nanoindentation technique, X-ray diffraction, X-ray photoelectron spectroscopy, and transmission electron microscopy. The mechanical properties of crystalline W-N coatings correlated to their texture and residual stress. The monolithic $W_{77}N_{23}$ samples located nearest to the W target exhibited a high deposition rate of 18.0 nm/min, a strong (200) texture coefficient, a high nanoindentation hardness of 32.7 GPa, a high Young's modulus of 392 GPa and a residual stress of -3.2 GPa. The addition of Si into the W-N matrix transformed the coatings to be an X-ray amorphous phase dominated structure comprising constitutions of Si_3N_4 , W_2N , and W. The preferential formation of Si_3N_4 declined the residual stress and mechanical properties of the W-Si-N coatings with increasing the Si contents. By contrast, the oxidation resistance was improved by adding a Si content > 24 at.% after annealing at 600 °C in a 1% O_2 -99% Ar atmosphere.

12:00pm **B4-3-WeM13 RF Input Power Effect on Microstructure and Mechanical Properties of TaSiN Coatings**, **Z.X. Lin (x52088520@gmail.com)**, Y.C. Liu, S.T. Wang, National United University, Taiwan; M.G. Guillon, Polytech Lyon, France; F.B. Wu, National United University, Taiwan

The TaSiN nanocomposite thin films were fabricated by a reactive radio frequency r.f., magnetron sputtering system with pure Ta and Si sources. The Ar/ N_2 flow ratio was fixed at 18/2 sccm/sccm, while r.f. input powers for

Ta and Si were from 50 to 200W and from 50 to 150W, respectively. The Si contents doped in the coating ranged from 0 to approximately 25 at.%. The plasma of various process conditions were investigated by Optical Emission Spectroscopy. Characterizations by XRD, TEM, SEM revealed the dependence of Si doping and SiN_x phases on the preferred orientation, crystalline behavior, microstructure. Mechanical properties through wear tester, Rockwell.C and nano-indentation were evaluated to check the durability, adhesion and hardness, respectively. When the content of silicon reaches 17 at.%, the TaSiN structure evolved from crystallization to amorphous, leading to a significant degradation of mechanical properties. The TaSiN with lower Si contents exhibited TaN with SiN_x phase and processed superior mechanical strength.

Fundamentals and Technology of Multifunctional Materials and Devices

Room Golden West - Session C3+C1-WeM

Thin Films for Energy-related Applications I/Optical Metrology in Design, Optimization, and Production of Multifunctional Materials

Moderators: Per Eklund, Linköping Univ., IFM, Thin Film Physics Div., Sweden, Tushar Shimpi, Colorado State University, USA

8:20am **C3+C1-WeM2 Avoiding Blistering of Magnetron Sputtered Thin Film CdTe Photovoltaic Devices**, **J.M. Walls (j.m.walls@lboro.ac.uk)**, F. Bittau, R.C. Greenhalgh, A. Abbas, P. Hatton, R. Smith, Loughborough University, UK

Magnetron sputtering is an industrially scalable technique for thin film deposition. It provides excellent coating uniformity and the deposition can be conducted at relatively low substrate temperatures. It is widely used in the manufacture of solar modules. However, its use for the deposition of thin film CdTe photovoltaics results in unusual problems. Blisters appear on the surface of the device and voids occur in the CdTe absorber. These problems appear after the cadmium chloride activation treatment at 400°C. The voids often occur at the p-n junction interface causing catastrophic delamination. This problem has been known for more than 25 years, but the mechanisms leading to blistering have not been understood. Using High Resolution Transmission Electron Microscopy we have discovered that during the activation process, argon trapped during the sputtering process diffuses in the lattice to form gas bubbles. The gas bubbles grow by agglomeration particularly at grain boundaries and at interfaces. The growth of the bubbles eventually leads to void formation and blistering. Switching the working gas to xenon overcomes these problems.

8:40am **C3+C1-WeM3 Electrochromic Device Based on WO_3/NiO Complementary Electrodes Prepared by Using Vacuum Cathodic Arc Plasma**, **P.-W. Chen (powen@iner.gov.tw)**, Institute of Nuclear Energy Research, Taiwan

Smart windows based on electrochromic (EC) materials, which are controlled to change their optical properties of reflectance, transmittance, and absorption can be effectively reduced the heating or cooling loads of building interiors. Electrochromism can produce interesting phenomenon based on redox reaction that gives a reversible, persistent changing in color, thus with an optical modulation by a small applied DC voltage pulse difference. In this study, we prepared a complementary electrochromic device (ECD) with ITO/ $WO_3/LiClO_4-PC/NiO/ITO$ structure was assembled. This work focuses on the influence of thickness of NiO layers on the ECD electrochemical and optical properties. For the fabrication of ECD, WO_3 and NiO electrode films were used as the cathodic and anodic coloring materials, which are fabricated by vacuum cathodic arc plasma (CAP). We achieve a high performance electrochromic electrode, producing porous deposited by the CAP technique is promising smart window for potential electrochromic application. Our results are observed the highest oxidation/reduction ion diffusion coefficient (9.38×10^{-9} / 8.12×10^{-8} cm^2/s , respectively) with NiO(60 nm)/ITO films, meaning that enhanced electrochromic properties compared to the other samples. The performance of the 5×5 cm^2 ECD demonstrated optical contrast of 52 % and switching times 4.6 sec and 8.1 sec for coloring and bleaching state at the wavelength of 633 nm. During the durability test, the transmittance change (ΔT) of ECD remained 45% after 2500 cycles, which was about 85% of original state.

Wednesday Morning, May 22, 2019

9:00am **C3+C1-WeM4 Influence of Film Thickness on Growth, Structure and Properties of Magnetron Sputtered ITO Films, A. Subacius (andrius.subacius@manchester.ac.uk), Manchester University, UK; É. Bousser, École Polytechnique de Montréal, Canada; B. Baloukas, Polytechnique Montreal, Canada; S. Hinder, M. Baker, Surrey University, UK; D. Ngo, Manchester University, UK; C.G. Rebholz, Cyprus University, Cyprus; A. Matthews, Manchester University, UK**

Indium tin oxide (ITO) is one of the most widely used transparent conducting oxides due to its electrical conductivity and optical transparency, and it can be used for many applications, such as LEDs, flat-panel displays, smart windows and architectural windows. As typical for transparent conducting films, there is a trade-off between conductivity and transparency.

In this work, the effect of film thickness on the evolution of growth, microstructure and electrical and optical properties was studied. ITO coatings with different thickness values (200, 800 and 3000 nm) were deposited onto unheated soda lime glass substrates by r.f. sputtering from a ceramic ($\text{In}_2\text{O}_3:\text{SnO}_2$, 90:10 wt.%) target. X-ray diffraction (XRD), transmission Kikuchi diffraction (TKD) and transmission electron microscopy (TEM) analysis revealed an increase in crystallinity with growing ITO film thickness. While the 200 nm thin film appeared amorphous in XRD measurements, the 800 and 3000 nm coatings were found to be crystalline. The 3000 nm thick film displayed preferred orientations in the (440) and (400) directions. In the case of the 200 nm film, TKD results showed local crystallinity with 50-200 nm grains imbedded in an amorphous or possibly nanocrystalline matrix. The luminous transmittance in the visible range was found to decrease with increasing film thickness from 81.7 % for the 200 nm film down to 70 % for the 800 nm one and 44.6 % for the 3000 nm film. On the other hand, electrical resistivity values only slightly decreased with increasing film thickness from $6.15 \times 10^{-4} \Omega \cdot \text{cm}$ to $5.36 \times 10^{-4} \Omega \cdot \text{cm}$ and $5.23 \times 10^{-4} \Omega \cdot \text{cm}$ for 200 nm, 800 nm and 3000 nm films, respectively.

9:20am **C3+C1-WeM5 Metal/Semiconductor Superlattice Metamaterials: A New Paradigm in Solid-State Energy Conversion, B. Saha (bsaha@jncasr.ac.in), Jawaharlal Nehru Centre for Advanced Scientific Research, India**

INVITED

Since the 1960s, researchers exploring the potential of artificially-structured materials for applications in quantum electronic devices have sought combinations of metals and semiconductors that could be combined on the nano-scale with atomically-sharp interfaces. Early work with multilayers of polycrystalline elemental metals and amorphous semiconductors showed promise in tunneling devices. More recently, similar metal/semiconductor multilayers have been utilized to demonstrate novel optical metamaterials. These metal/semiconductor multilayers, however, are not amenable to atomic-scale control of interfaces. We developed the first epitaxial metal/semiconductor multilayer and superlattice heterostructures that are free of extended defects. These rocksalt nitride superlattices have atomically sharp interfaces and properties that are tunable by alloying, doping and quantum size effects. Furthermore, these nitride superlattices exhibit exceptional mechanical hardness, chemical stability and thermal stability up to $\sim 1000^\circ\text{C}$.

In this presentation, I will describe the growth, structural characterization and transport properties of nitride metal/semiconductor superlattices including (Ti,W)N/(Al,Sc)N and (Hf, Zr)N/ScN. ScN and $\text{Al}_x\text{Sc}_{1-x}\text{N}$ ($x < 0.82$) are rocksalt semiconductors in thin film and bulk form that can be doped preferentially with *n*-type or *p*-type carriers. $\text{Al}_x\text{Sc}_{1-x}\text{N}$ can also be stabilized in rocksalt phase for high AlN mole fractions by lattice-matched epitaxy. TiN, ZrN, HfN and similar transition metal nitride films can be good metals with carrier concentrations approaching 10^{22} cm^{-3} . Potential applications of these single crystalline superlattice and thin films in thermoelectric devices and plasmonic metamaterials will be discussed. Furthermore, recent experimental efforts to employ these superlattices as model materials for investigating the fundamentals of heat transport in nanostructured materials will be addressed.

Reference:

1. B. Saha, A. Shakouri and T. D. Sands, "Rocksalt Nitride Metal/Semiconductor Superlattices: A New Class of Artificially-Structured Materials". *Appl. Phys. Rev. 5*, 021101 (2018).

Tribology and Mechanical Behavior of Coatings and Engineered Surfaces

Room San Diego - Session E3-WeM

Tribology of Coatings for Automotive and Aerospace Applications

Moderators: John Curry, Sandia National Laboratories, USA, **Christian Greiner**, Karlsruhe Institute of Technology (KIT), Institute for Applied Materials (IAM), Germany, **Oliver Hunold**, Oerlikon Balzers, Oerlikon Surface Solutions AG, Liechtenstein

8:00am **E3-WeM1 Self-assembly of Ultra-high Strength Nanoporous Metals for Multifunctional Coatings and Free-standing Films, J.H. Pikul (pikul@seas.upenn.edu), University of Pennsylvania, USA; N. Argibay, J. Curry, Sandia National Laboratories, USA; Z. Hsain, University of Pennsylvania, USA**

INVITED

This talk will describe the fabrication and characterization of nickel-based cellular materials which have the strength of titanium and the density of water. These materials can be made free-standing or as thin film coatings by electroplating metal through self-assembled particles. The gap between self-assembled particles confines the dimension of the metal struts to diameters as small as 17 nm. The nanoscale confinement increases the local yield strengths of the nickel struts to 8 GPa, which exceeds that of bulk nickel by up to 4X. The mechanical properties of this material can be controlled by varying the nanometer-scale geometry, with strength varying over the range 90-880 MPa, modulus varying over the range 5-40 GPa, and density varying over the range 880 – 14500 kg/m³. In addition to characterizing the mechanical strength of these nickel-based cellular materials, I will discuss their wear performance when the pores are infiltrated with solid lubricants. These materials present a new class of films that can achieve high wear resistance while also maintaining high thermal conductivity, electrical conductivity, or other tailored properties.

8:40am **E3-WeM3 Elevated Temperature Sliding Wear of PEO-Chameleon Duplex Coating, A.A. Voevodin (andrey.voevodin@unt.edu), A. Shirani, University of North Texas, USA; A. Yerokhin, The University of Manchester, UK; A.L. Korenyi-Both, Tribologix Inc., USA; D. Berman, University of North Texas, USA; J. Zabinski, Army Research Laboratory, USA**

Plasma electrolytic oxidation (PEO) is an attractive technology for improving wear and corrosion resistance of aluminum and titanium alloys exposed to different temperature and environment. PEO results in formation of 50-150 micrometer thick hard ceramic (AlSiO and TiSiO) coatings with good adhesion to the substrate and with morphology gradient from a dense region near the substrate interface to a porous outside region [1]. Such properties potentially make a PEO coating an ideal underlying layer for the application of solid lubricants which can be entrapped in outside porous and provide reservoirs for the tribological contact lubrication. In this study we investigate the wear behavior of the PEO-based coatings during sliding in air at elevated temperatures. The PEO produced 11-12 GPa hardness AlSiO and TiSiO coatings are covered with a top layer of an MoS₂-Sb₂O₃-graphite chameleon solid lubricant, the composition of which was previously reported to self-adapt in variable humidity environments resulting in friction and wear reduction [2]. Coupons of aluminum and titanium alloys were coated by the PEO process and then were over-coated by a burnishing process with a MoS₂-Sb₂O₃-graphite chameleon coating to prepare such duplex coating combination. The coated surfaces were then subjected to sliding wear tests against silicon nitride counterparts with variable normal loads (2- 10 N) and temperatures (room to 400 °C). At room temperature, the humid air friction coefficients were of the order of 0.10-0.15, which is typical for graphite lubricant in humid air. However, when the temperature was increased first to 100°C and then up to 400 °C, the coefficient of friction was reduced to about 0.03-0.05 level which was linked with removing the water and promoting lubrication with the MoS₂ chameleon coating component. Raman, SEM and cross-sectional FIB/SEM/EDX analyses of the wear tracks were used to investigate the mechanisms of the temperature adaptation and sliding wear performance. The study demonstrate the effectiveness of the PEO-chameleon coating system performance for the sliding wear mitigation and friction reduction.

[1] A.L. Yerokhin et al., *Surface and Coatings Technology*, 122 (1999) 73.

[2] J.S. Zabinski et al., *Tribology Letters*, 23 (2006) 155.

Wednesday Morning, May 22, 2019

9:00am **E3-WeM4 Formation Mechanisms of Zn, Mo, S and P Containing Reaction Layers on a DLC Coating**, *K. Bobzin, T. Brögelmann, C. Kalscheuer, M. Thiex (thiex@iot.rwth-aachen.de)*, Surface Engineering Institute - RWTH Aachen University, Germany

Environmental restrictions on the climate-damaging CO₂ emissions in the field of mobility are increasingly tightened due to political requirements. Thus, there are requirements on saving fossil resources in tribological contacts, e.g., by reducing friction and wear as well as the amounts of additives and lubricants. A successful approach is the application of diamond-like carbon (DLC) coatings on components such as pistons, piston rings and bearings in lubricated tribological contacts due to their significant effects in friction and wear reduction. Lubricants and additives nowadays are designed for tribological steel/steel contacts, whereby the knowledge on tribochemical layer formation on steel surfaces is comprehensive in contrast to the physical-chemical interactions between DLC coatings, lubricants and additives. That is in contradiction to the increasing usage of DLC coated components in tribological applications. Within this study, the formation mechanisms of Zn, Mo, S and P containing reaction layers on a Zr modified DLC coating a-C:H:Zr (ZrC_z) in lubricated tribological DLC/DLC contacts were studied by means of pin-on-disc (PoD) tribometer. Motivated by the loading conditions in applications, the tests were conducted by varying the distances in a range 200 m ≤ s ≤ 5,000 m under boundary and mixed friction conditions at a temperature T = 90 °C and a Hertzian contact pressure p = 1,300 MPa. The synthetic base lubricant poly-alpha-olefin (PAO) was formulated using the anti-wear (AW) and extreme pressure (EP) additive zinc dialkyldithiophosphate (ZnDTP), PAO/ZnDTP, the friction modifier (FM) additive molybdenum dialkyldithiophosphate (MoDTP), PAO/MoDTP, as well as a combined additivation of MoDTP and ZnDTP at a ratio of 1:3, PAO/MoDTP/ZnDTP/1:3. Based on the results of confocal laser scanning microscopy (CLSM), tribochemical layers form inside and at the edge region of the wear track. The chemical and structural formation process can also be influenced by increasing the sliding distance s in PoD tests. Hereby, the thickness of the tribochemical layers increases too. The chemical composition of the tribochemical reaction layers (Zn,Mo,S,P) and molybdenum disulphide (MoS₂) determined by energy-dispersive X-ray spectroscopy (EDX) and Raman spectroscopy differs by changing the additivation and sliding distance s. Similar conclusion can be made considering the structure and texture of the tribochemical reaction layers, which differ significantly in size and appearance for all analyzed tribological contacts. Hereby, the results show the importance of a differentiated consideration of the interaction between DLC coating, lubricant and additive.

9:20am **E3-WeM5 ta-C Coatings for Tribological Applications**, *J. Becker, Oerlikon Balzers Coating Germany GmbH, Germany; N. Beganovic, A. Gies (astrid.gies@oerlikon.com), J. Karner, Oerlikon Balzers, Oerlikon Surface Solutions AG, Liechtenstein; J. Vetter, Oerlikon Balzers Coating Germany GmbH, Germany*

Diamond Like Carbon (DLC) coatings and in particular the hydrogenated a-C:H coatings are widely used where friction and wear reduction is required. However, a-C:H coatings have a limited thermal stability and start to graphitize at temperatures higher than about 300°C. Depending on the contact pressure, graphitization might even occur at much lower temperatures. In addition, the tribological performance of a-C:H coatings can be negatively influenced by different lubricants and additives.

To overcome the drawbacks of a-C:H coatings hydrogen-free DLC coatings like ta-C and a-C are currently investigated as a possible solution. ta-C shows a significant higher coating hardness than a-C:H coatings and due to the lack of hydrogen a different surface chemistry which results in a different behaviour under lubricants. ta-C is usually deposited by high-energy deposition processes like arc evaporation; the arc evaporation is possible with or without filtering. Inherent to these processes is the generation of coating defects like droplets. A suitable post-treatment is mandatory to reduce the roughness to an acceptable level. High roughness in combination with a high coating hardness would lead to significant counter body wear.

In this work, ta-C coatings were submitted to tribological testing in a wide temperature range (room temperature to 480°C) in dry running conditions under air. Surprisingly the maximum operation temperature in dry running systems was not as high as expected. The results were compared to those obtained in the past for a-C:H coatings [1]. The investigations were completed by Raman measurements for a better understanding of the tribological behavior of the coatings. In addition, we investigated the compatibility of ta-C with different lubricants and additives and compared it to a-C:H.

[1] J. Becker et al., Thermal effects influencing stability and performance of coatings in automotive applications, *Surface & Coatings Technology* 284 (2015), pp. 166-172

9:40am **E3-WeM6 Investigation on Effect of MgO-ZrO₂ and Al₂O₃-13%TiO₂ Coated Piston Crown on Performance and Emission Characteristics of a Variable Compression Ratio Engine**, *T. Raja (thirunaarasu821@gmail.com)*, Sri Ramakrishna Institute of Technology, India; *S. Periyasamy*, Government College of Technology, Coimbatore, India
Piston crown of a single cylinder Diesel engine is coated with MgO-ZrO₂ and Al₂O₃-13%TiO₂ and tested under different loading conditions. The impact of thermal barrier coating performance and emissions compared with standard CI diesel engine characteristics are investigated. MgO-ZrO₂ and Al₂O₃-13%TiO₂ are selected as an additional material to coat the piston crown because these materials have physical and stable properties like low heat conductivity, high melting point, high thermal expansion and stable at high temperature. This experimental work has shown an increase in brake thermal efficiency (BTE) of 32.11 % for TBC engine and 23.4 % for UC engine. Therefore, there is a decrease in brake specific fuel consumption (BSFC) for TBC engine 0.27 kg/kWh and uncoated engine 0.37 kg/kWh at 9 kg of load. which ultimately decreases the effect of gases CO and HC due to increasing complete combustion by the thermal barrier coating.

11:00am **E3-WeM10 Titanium Nitrides Coatings for Hard Chromium Replacement**, *M. Cavarroc (marjorie.cavarroc@safrangroup.com)*, Safran Tech, France; *B. Giroire, L. Teulé-Gay, D. Michau, A. Poulon-Quintin*, ICMCB, France

High-power impulse magnetron sputtering (HIPIMS or HiPIMS, also known as high-power pulsed magnetron sputtering, HPPMS) is a method for physical vapor deposition of thin films which is based on magnetron sputtering deposition. Very high power densities (of the order of a few kW·cm⁻²) are applied in very short pulses (few tens of microseconds) at low duty cycle (< 10%).

HiPIMS allows reaching a high ionization degree of the sputtered material around several tens of percent versus a few percent for conventional magnetron sputtering. The ionization and dissociation degree increase as a function of the peak cathode power. The limit is determined by the transition of the discharge from glow to arc phase. In the system we used, a continuous voltage is applied to the discharge in order to maintain continuously the plasma and increase its stability.

Work was focused on Titanium Nitride (TiN) deposition on steel coupons. After optimizing parameters for Titanium sputtering, the following parameters were chosen: 1 Pa total pressure, gas mixture 5% N₂ diluted in 95% Ar. High power pulses of 20 μs @ 200 Hz were delivered with a voltage comprised between 800V and 900V and a continuous voltage comprised between 90V and 150V. In those conditions, maximum intensities around a few tens of amperes are observed. TiN coatings we obtained exhibit a cubic crystalline structure, with a low film texturation and nanometric crystallites.

Coatings are continuous and fully covering the substrate. TiN morphology and roughness are directly linked to the substrate's ones. Coatings are homogeneous in all the thickness: micro-stress, crystallite size and chemical composition are the same from the surface to the interface with the substrate.

We will present the influence of deposition parameters on the coating microstructure (crystallinity, stoichiometry, grain size and interface). Tribological properties will also be discussed.

11:20am **E3-WeM11 Tribological Coating Solutions and Lubrication Strategies for Gas Turbine Engines**, *P. Stoyanov (pantcho.stoyanov@pw.utc.com)*, Pratt & Whitney, USA

The advancement of durable gas turbine engine components depends heavily on the development of high-performance materials that can withstand extreme environmental and contact conditions (e.g. large temperature ranges, high contact pressures, and continuous bombardment of abrasive particles, all of which degrade the physical properties). In particular, due to the large number of complex contacting and moving mechanical assemblies in the engine, the lifetime of certain structures is limited by the tribological performance of the employed materials and coatings. This talk will provide an overview of tribological solutions and lubrication strategies employed in several sections of gas turbine engines. After a general review of aircraft engine tribology, the talk will focus on tribological coatings and materials used to minimize fretting type of wear. A series of studies on the friction and wear behavior of Ni-based and Co-based superalloys at elevated temperatures will be presented. Emphasis will be placed on the correlation between the third body formation process (e.g.

oxide layer formation, transferfilms) and the tribological behavior of the superalloys. This talk will conclude with the future strategies of tribological coating solutions in gas turbine engines.

New Horizons in Coatings and Thin Films Room Pacific Salon 6-7 - Session F4-1-WeM

Functional Oxide and Oxynitride Coatings I

Moderators: Anders Eriksson, Oerlikon Balzers, Oerlikon Surface Solutions AG, Liechtenstein, Marcus Hans, RWTH Aachen University, Germany, Jörg Patscheider, Evatec AG, Switzerland

8:00am **F4-1-WeM1 Microstructure and Piezoelectric Properties of Hexagonal Mg_{1-x}Zn_xO and Mg_{1-x}Zn_xO/ZnO Films at Lower Mg Compositions, H.-H. Chen (n56064012@mail.ncku.edu.tw), C.P. Liu, J.L. Huang, National Cheng Kung University, Taiwan**

We investigate the piezoelectric coefficient(d_{33}) of Mg_{1-x}Zn_xO and Mg_{1-x}Zn_xO/ZnO with various Mg content. The films were grown on Si (111) substrate using MgO and ZnO targets by radio frequency magnetron sputtering. Thickness of all films are fixed at around 600nm for Mg_{1-x}Zn_xO and 300/300nm for Mg_{1-x}Zn_xO/ZnO. There shows high crystallinity with preferred orientation along c-axis in XRD pattern, and columnar structures are clearly observed in SEM images, indicating that the films still remain wurtzite structures. Besides, XRD pattern, PL and XPS spectra proved that substitution of smaller magnesium ions at zinc sites causes lattice distortion and therefore enhance the d_{33} at maximum 48.7pm/V of Mg_{1-x}Zn_xO and 39.1pm/V of Mg_{1-x}Zn_xO/ZnO ($x=0.17$ for both) by PFM measurement. These values are nearly four and three times larger than pure ZnO films. We consider these films as a promising candidate for nanogenerators(NGs) and ultraviolet photodetectors(UV-PDs).

8:20am **F4-1-WeM2 Structure Optimization of Ta-O-N Films Prepared by Reactive HiPIMS for More Effective Water Splitting, Š. Batková (sbatkova@kfy.zcu.cz), Department of Physics and NTIS - European Centre of Excellence, University of West Bohemia, Czech Republic; J. Čapek, S. Haviar, J. Houška, R. Čerstvý, University of West Bohemia, Czech Republic; M. Krbal, University of Pardubice, Czech Republic; T. Duchoň, Charles University, Czech Republic**

The TaON material is a promising candidate for application as a visible-light-driven photocatalyst splitting water into H₂ and O₂ and thus converting solar energy into chemical energy. The photo-generated electron-hole pairs act here as the active water splitting species. In order to work as a water splitting photocatalyst, the material must satisfy certain conditions: (i) band gap of proper width (preferably corresponding to visible light absorption) and (ii) suitable alignment of the band gap with respect to the water splitting redox potentials. The subsequent transport of the charge carriers through the material (particularly across the films thickness) plays an important role in the effectivity of the process.

In this work we first demonstrate that using reactive high-power impulse magnetron sputtering (HiPIMS) as the deposition technique followed by post-annealing of the amorphous as-deposited film at 900°C in a vacuum furnace allows us to prepare a polycrystalline film exhibiting a pure TaON phase. Such film satisfies the above mentioned conditions for a water splitting photocatalyst (band gap of ~2.6 eV). However, as it is desirable to prepare the TaON phase in situ, we investigate the possibilities of substrate heating and biasing during deposition while focusing on fine-tuning of the elemental composition. Additionally, as the monoclinic TaON phase exhibits anisotropic charge carrier conductivity, tailoring of the texture of the film can further improve the charge carrier transport in a desired direction. In this work, we therefore also investigate the possibilities of deposition at high power densities in a pulse (up to 4 kW/cm²) and/or deposition onto suitable substrates providing proper seeding layers (e.g., Pt, ZrO₂) to prepare textured TaON film allowing enhanced charge carrier mobility across the film thickness.

8:40am **F4-1-WeM3 A Sustainable and Viable Alternative to Low Cost Electronics based on Metal Oxides, E. Fortunato (emf@fct.unl.pt), R. Martins, New University of Lisbon, Portugal**

INVITED

In the last 50 years we observed a drastic change in our daily life since society was never before so efficient and interconnected. This provides a collaborative environment that is essential for economic growth and progress like: Silicon Valley for microelectronic technology and Boston for biotechnology. This breakneck development has been in part dictated by an empirical technologically and economically driven rule known as "Moore's law". Indeed today a microprocessor has more than 7 billion integrated

transistors in an area of 350 mm². This unbelievable integration capability with higher processing speeds, memory capacity and functionality gives rise to what we call today: ubiquitous electronics. Despite the importance of silicon technology there are applications where it is impossible, either technically or economically use it. Displays are the most notorious example, more if we want them to be flexible and conformable. On the other hand, 10 years ago it was pure science fiction the notion of fully transparent, flexible and conformable displays, like those used by T. Cruise in the Minority Report movie fully based on materials away from silicon! Thanks to the Hollywood vision and the hard work of scientists this is now a reality. After the huge success and revolution of transparent electronics where we must highlight the low process temperatures that turn possible the use of low cost eco-friendly materials and substrates such biopolymer or paper, where CENIMAT is pioneer and with the worldwide interest in displays/smart interfaces where metal oxide thin films have proved to be truly semiconductors, display backplanes have already gone commercial due to the huge investment of several high profile companies such: SAMSUNG, SHARP, LG, BOE, in a very short period of time. Recently IDTechEx estimated that 8 km sq of metal oxide-based backplanes will be used in the OLED and LCD industry by 2024, enabling a 16 billion USD market at the display module level alone. We can anticipate that the metal oxide based industry will be in the near future a so-called multi billion euro market similar to what is observed with the pharmaceutical industry, due to the number of different applications that can serve, ranging from information technology, biotechnology/life sciences and energy to food/consumer products. In this talk we will present results on recent new technologies developed at CENIMAT|i3N where it is possible to have the use of sustainable materials used in disruptive applications.

9:20am **F4-1-WeM5 Photocatalytic Study for Indium Tantalum Oxide Thin Film in Visible Light, C. Li (cli10@yahoo.com), National Yang Ming University, Taiwan; J.H. Hsieh, Ming Chi University of Technology, Taiwan; P. Hsueh, National Central University, Taiwan**

Indium tantalum oxide thin film was deposited by sputtering using three different designs: 5-7 and 10-14 nm alternative layers of Ta₂O₅ and In₂O₃, and co-sputtering of In₂O₃ and Ta₂O₅. Then as-deposited films were rapidly annealed at different temperatures to assess the thermal effects on microstructures and photocatalytic functions. Results from XRD and EDS indicate that crystalline InTaO₄ emerges in 5-7 and 10-14 nm stacks of films but absent in the co-sputtered films. Since crystalline InTaO₄ is capable of photocatalysis under both ultraviolet and visible light, we particularly tested the annealed films in water to degrade methylene blue under visible light. The photo-induced degradation on methylene blue by 5-7 and 10-14 nm stacks can reach 45% after 6-hour continuous exposure. Using UV-Visible-NIR spectroscopy, we can estimate the optical band gaps in these annealed films and from these estimations, a mechanism for the photocatalysis is discussed following. This mechanism is similar to other electron-hole separation and transfer across the heterogeneous junctions in semiconductors.

11:00am **F4-1-WeM10 Exploring Thin Film Zn-Sn-O (ZTO) Composition Spreads Using Combinatorial Sputtering, S.Y. Li (m9810217@gmail.com), Y.H. Shen, K.-S. Chang, J.-M. Ting, National Cheng Kung University, Taiwan**

Transparent conducting oxide (TCO) films are extensively applied as electrodes in the fields of solar cells and displays, due to their high transparency and excellent electrical conductivity. Multicomponent oxides such as Zn-Sn-O (ZTO) have attracted much attention due to the low cost elements of indium (In). In addition, thermal stability and mechanical strength of ZTO can be tailored by varying its stoichiometry. However, making compounds having different ratios of Zn/Sn systematically is not trivial.

Combinatorial methodology has been proven its validity in such an application. This approach allows the Zn/Sn ratio continuously to change across a single sample area and a feasible intimate mix of Zn and Sn. Therefore, a single ZTO composition spread sample essentially includes a full spectrum of properties to be investigated. A Zn-Sn-O (ZTO) composition spread, consisting of thickness wedges of SnO and ZnO, was prepared using a state-of-the-art combinatorial sputtering system, equipped with a moving shutter and two RF guns for the targets of Zn and Sn, respectively. The thickness gradient was determined using SEM, α -step and SIMS. It was found a smooth thickness variation across the sample area for both ZnO and SnO with the coefficient of determination (R^2) \cong 0.99, indicating a good control of the ZTO composition spread. Structure evolution was characterized using XRD. We found in-situ 500 °C annealing resulted in crystallization of the samples, where ZnO, Zn₂SnO₄, ZnSnO₃, and SnO₂ phases were observed,

Wednesday Morning, May 22, 2019

depending upon the ZnO/SnO ratios on the ZTO composition spread. The resistivity was characterized using a four-point probe on different substrates, which revealed lower resistivity near ZnO-rich. Morphology and optical characteristics were studied as well using AFM, SEM and UV-Vis spectrometry. A clear variation trend of both properties was observed. A systematic study of physical properties of ZTO has been successfully demonstrated.

11:20am **F4-1-WeM11 Can Thin-Film Technology Help to Realize The Einstein Gravity Quantum Computer?**, **N. Schwarzer** (n.schwarzer@esae.de), SIO, Germany

After it became clear that quantum computers are more powerful than originally thought [1], we were asked by the industry to find the most fundamental form of a Turing machine based on Quantum Theory. Do this job in a very comprehensive manner, we found that the deepest layer for the Quantum Computer was not to be found inside the theoretical apparatus of Quantum Theory. Surprising as this may be, it is the General Theory of Relativity which "contained it all". We found that an extremely simple solution of the Einstein-Field-Equations, using pairwise dimensional entanglement, sports the principle structural elements of computers [2]. We will derive these structural elements and show that the classical computer technology of today and even the quantum computers are just degenerated derivatives of this general solution. In the talk we will discuss thin-film technology- and smart material-options potentially helping us to one day realize the general computer concept.

[1] J. Aron, "Quantum computers are weirder and more powerful than we thought", www.newscientist.com/article/2170746

[2] N. Schwarzer, "Einstein had it, but he did not see it – Part XXXIX: EQ or The Einstein Quantum Computer", www.amazon.com, ASIN: B07D9MBRS3

Keywords— Quantum Computer, Smart Materials, Quantum Dots, Quantum Gravity

Advanced Characterization Techniques for Coatings, Thin Films, and Small Volumes

Room Pacific Salon 1 - Session H3-1-WeM

Variable Temperature Nanomechanics

Moderators: **Jeffrey M. Wheeler**, ETH Zürich, Switzerland, **James Gibson**, RWTH Aachen University, Germany

8:00am **H3-1-WeM1 On the Activation of Slip in the Mg-Al-Ca Laves Systems: A Combined Study Using High Temperature Indentation, Micropillar Compression and TEM**, **J. Gibson** (gibson@imm.rwth-aachen.de), **C. Zehnder**, **S. Sandlöbes**, **S. Korte-Kerzel**, RWTH Aachen University, Germany

The mechanical properties of modern, creep-resistant Mg-Al-Ca alloys are significantly influenced by the properties of the intermetallic skeleton at their grain boundaries. During application, these alloys will be thermally cycled from room- to application-temperatures, therefore it is essential to understand how the properties of these intermetallic components vary over this range.

A combination of nanoindentation, AFM, micropillar compression and TEM have been employed to study the behaviour of the Mg₂Ca Laves phase between room temperature and 250°C. Statistical analysis of the slip lines around inclusions - confirmed by TEM cross-sections - allow rapid analysis of relative CRSS values, supported by direct measurement in micropillar compression.

We show a constant hardness of ~3.5 GPa from room-temperature to 250°C, revealing that Mg₂Ca is likely the high-temperature strengthening phase of the parent alloy. The trends in slip-plane activation frequency and CRSS with temperature are analysed to explain the overall measurements of hardness.

8:20am **H3-1-WeM2 Recent Evolution of Instrumentation for Nanoindentation Measurements at Elevated Temperatures**, **P. Kempe** (philippe.kempe@anton-paar.com), **V. Haibliková**, Anton Paar, Switzerland

Characterization of thin film mechanical properties at elevated temperatures has been of scientific and industrial interests for many years, and Instrumented Indentation Testing (IIT) on PVD coatings is bringing useful information. The major limitations in high temperature measurements have been seen as the thermal drift, signal stability (noise) of instrumentation and oxidation of the surface. A defined setup of instrumentation allows to reduce these factors.

The vacuum nanoindentation system is designed to perform reliable load-displacement measurements over a wide temperature range (up to 800 °C). Vacuum has become an essential part of the instrument in order to prevent sample/tip oxidation at elevated temperatures. Independent tip and sample heating as well as an active thermal management of the system answer to the concern of temperature stability. Nevertheless, different experimental aspects of instrumentation are still investigated. It includes frame compliance, indenter tip calibration and verification, and reference samples. The manufacturing of indenter tips and their stability with temperatures is also discussed.

Recent measurements at high temperatures with system characterization and experimental protocol will be presented.

8:40am **H3-1-WeM3 High Temperature Mechanical Characterization of Binary Cu-X Alloys Produced by Combinatorial Synthesis**, **V.G. Arigela** (v.arigela@mpie.de), Max-Planck Institut für Eisenforschung, Germany; **T. Oellers**, **A. Ludwig**, Ruhr Universität Bochum, Germany; **C.K. Kirchlechner**, **G. Dehm**, Max-Planck Institut für Eisenforschung, Germany

Due of their excellent electrical properties copper-based material systems form the metallization components of most of the thin-film circuits today. The current trend of ever harsher environments and power densities brings the need of enhanced electrical and mechanical properties. It is of particular interest to develop copper alloys with improved strength, which requires the mechanical characterization of these systems at their service conditions on a micrometer length scale. We have used combinatorial material synthesis approaches to synthesize binary Cu-Ag and Cu-Zr alloys with the aim of enhancing the mechanical properties while preserving the electrical properties. The mechanical properties of the alloys were investigated by fabricating free-standing tensile specimens with photolithography techniques from the thin-film material libraries, which were produced by sputtering. Our approach enables high throughput mechanical characterization of a composition range of Cu-(1-8%) X. The alloys were tested both in the as deposited and in the annealed state. In addition, mechanical properties were also investigated at elevated temperatures (400°C) by tensile testing with a micro deformation stage with a novel method of temperature measurement. The investigations show a substantial improvement of the thin film strength both at elevated and at room temperature along the compositional gradient and a mild influence on the thin film conductivity. Beside the testing protocol and results we will also discuss the mechanism based origin of this behavior with respect to the thin film microstructure.

9:00am **H3-1-WeM4 Temperature and Strain-rate Dependence of the Mechanical Behavior of Freestanding Gold Thin Films**, **B. Merle** (benoit.merle@fau.de), Friedrich Alexander-University Erlangen-Nürnberg (FAU), Germany

The plastic deformation of freestanding gold films is shown to strongly depend on the testing temperature and strain-rate. These findings were achieved by both creep and constant strain-rate tensile tests, which were performed on evaporated gold films with columnar microstructure. The creep tests were carried out with an upgraded bulge tester operated between 23°C and 100°C. The measurements evidenced a critical temperature of about 75°C, corresponding to a transition in deformation mechanisms from a dislocation based to grain boundary and diffusion mediated plasticity. The influence of the stress was found to be rather low within the investigated range. Constant strain-rate tests were performed in-situ in a TEM, using a novel method for preparing tensile specimens from evaporated thin films. With decreasing strain-rate, the films exhibited a clear transition from shear-coupled grain boundary migration and grain growth to grain boundary sliding, which resulted in strong changes in strength and ductility.

9:20am **H3-1-WeM5 In-situ Investigation on Mechanical Properties at the Micrometer Scale in Cryogenic Environment**, **S.-W. Lee** (seok-woo.lee@uconn.edu), University of Connecticut, USA **INVITED**

Due to the significant advances in nanotechnology, a structural material at small length scales is becoming more important to develop mechanically robust small devices such as micro-/nano-electro-mechanical systems (MEMS/NEMS). MEMS and NEMS sensor systems that operate in the presence of high/low temperature, corrosive media and/or high radiation can reduce weight, improve machine reliability, and reduce cost in strategic market sectors such as automotive, avionics, oil well logging, nuclear power, and space exploration. Performance of all these small mechanical devices is directly related to mechanical properties of structural materials at small length scales, which are usually "different" from mechanical properties at bulk scale. In order to design a mechanically reliable small device working

under various environments, therefore, it is critical to understand “how sample dimension influence mechanical properties of materials” as well as “how environmental conditions influence small-scale mechanical properties.” For the last two decades, small-scale plasticity has been extensively investigated by using micro-mechanical tests, and “Smaller is Stronger” and “Smaller is More Ductile” phenomena were observed in various material systems. As briefly mentioned before, the development of sensors and actuators that operates in harsh environment brings a strong attention in small-scale plasticity community. Therefore, materials research, which combines both “size effects” and “environmental effects”, is now regarded as next generation research in the field of materials science.

In this presentation, we are going to introduce our ongoing efforts to develop an in-situ nanomechanical testing system operating in cryogenic environments and describe its potential use for materials science research. Then, we will present several examples showing how temperature influences mechanical behaviors of materials at the micrometer scale. The size effects in body-centered-cubic single crystalline metals in cryogenic environments will be discussed, and the strong temperature dependence of power-law exponent will be explained. The size effects in metallic glassy nanolattices will also be presented. Here, we will discuss how thickness of metallic glass and temperature controls ductile-to-brittle transition in nanolattice structures. Finally, we will introduce our recent discovery of superelasticity in ThCr_2Si_2 -structured intermetallic compounds, and their strong temperature dependence on their superelastic performance and structural transition will be discussed. Their potential use in cryogenic actuators or superconductivity switches for space exploration will be explained, too.

Topical Symposia

Room Pacific Salon 3 - Session TS1-1-WeM

High Entropy and Other Multi-principal-element Materials I

Moderators: Diederik Depla, Ghent University, Belgium, Ulf Jansson, Uppsala University, Angstrom Laboratory, Sweden

8:00am **TS1-1-WeM1 Effect of Nitrogen Content on the Microstructure and Mechanical and Tribological Properties of Magnetron Sputtered FeMnNiCoCr Nitride Coatings**, C. Sha (c.sha@student.unsw.edu.au), P. Munroe, University of New South Wales, Australia; Z. Zhou, City University of Hong Kong, Hong Kong; Z. Xie, University of Adelaide, Australia

Extensive research has been carried out on high entropy alloys (HEAs) in bulk form. These alloys exhibit many attractive physical and mechanical properties, and more recently are being investigated in the form of thin film coatings. In pursuit of improved mechanical performance of HEA coatings, nitrides based on these compositions have been investigated in this study. We have examined a series of FeMnNiCoCr nitride coatings deposited onto M2 steels using a DC closed field unbalanced magnetron sputtering system. The target was composed of a FeMnNiCoCr alloy in equal atomic ratio. The nitrogen content in the nitride coatings was controlled by nitrogen gas flow rate. The phase compositions, microstructure, mechanical, and tribological properties of the as-prepared coatings were examined by XRD, TEM/EDS, nanoindentation, scratch and wear tests. A phase transformation from FCC to BCC, with higher nitrogen contents was observed in these coatings. A relatively high hardness value of ~ 17 GPa was measured in the coating with the highest nitrogen content. A reduction in the adhesion strength with increasing nitrogen content was also found by the scratch test. In contrast, an improved wear resistance was achieved at higher nitrogen concentrations. It is believed the evolution of mechanical and tribological properties is related with the compositional changes and phase transformations as a function of gas flow rate. That is, the low-nitrogen content coatings exhibit FCC structures with higher ductility and toughness, whilst the high-nitrogen content coatings exhibit BCC structures but greater brittleness.

8:20am **TS1-1-WeM2 Reactive Sputtering of High Entropy Alloys with Nitrogen – The Effect of Enthalpy and Entropy**, R. Dedoncker (robin.dedoncker@ugent.be), D. Depla, Ghent University, Belgium

High entropy alloys are a new class of materials with at least 5 different metals in near-equimolar concentrations with promising properties such as a high degree of corrosion resistance and mechanical strength. Despite the multi-elemental composition, these alloys can form simple solid solutions when they are deposited by magnetron sputtering. The formation of a solid solution was initially believed to originate from the large contribution of the entropy of mixing, but this has recently become subject of discussion. Upon

sputtering in a mixed argon/nitrogen atmosphere, a nitride is formed. This nitride shows a rock salt (B1) structure, with the metals in solid solution on the cation sites. Studies on different alloys where the incorporation of nitrogen was investigated, reveal a Langmuir adsorption mechanism. The latter could be quantified with the calculation of the sticking coefficient of nitrogen on each alloy. This made it possible to examine the influence of enthalpy and entropy, and to reveal what the role of both thermodynamic quantities are in the phase formation of these alloys.

8:40am **TS1-1-WeM3 Compositional Variations and Resulting Structure-property Correlations in Multicomponent Al-Cr-Nb-Y-Zr-N Thin Films**, K. Johansson, A. Srinath, Uppsala University, Sweden; L. Nyholm, Uppsala University, Angstrom Laboratory, Sweden; E. Lewin (erik.lewin@kemi.uu.se), Uppsala University, Sweden

Initial studies on multicomponent Al-Cr-Nb-Y-Zr-based nitride coatings exhibited a single NaCl-type (B1) solid solution phase, and promising corrosion performance in electrochemical testing.[1] Further studies have now been conducted. Samples have once more been synthesised using reactive magnetron deposition from elemental and segmented targets. Coating composition has been varied, both with regards to nitrogen (from pure alloy to nitride) and metals (several different multicomponent compositions, as well as ternary references). Samples have been analysed using X-ray diffraction (XRD), X-ray photoelectron spectroscopy (XPS), and electron microscopy (SEM and TEM). The present results are combined with the previously attained results where coating have been deposited under different process conditions,[1] to attain an overview of structure and properties of multicomponent coating materials within the Al-Cr-Nb-Zr-Y-N system. Pure alloy samples, as well as samples with lower amounts of nitrogen show both diffuse scattering connected with amorphous alloys, as well as broad diffraction peaks pointing to the presence of a nanocrystalline alloy phase. Thus low nitrogen content coatings are nanocomposites with nanocrystallites in a metallic amorphous matrix. For nitrogen contents above about 37 at.% (corresponding to a N_2/Ar ratio of 1), only a single NaCl-type crystalline phase is observed, without any indications of secondary phases. Coating performance has been evaluated using polarisation tests, as well as more in-depth electrochemical testing. The formed passive layer has been investigated with hard X-ray photoelectron spectroscopy (HAXPES) for non-destructive depth profiling. Also mechanical testing, using nanoindentation, has been performed.

[1] K. Johansson et al. *Multicomponent Al-Cr-Nb-Y-Zr-N Thin Films*, poster presentation (TSP-6) at 45th ICMTF, San Diego 2018.

9:00am **TS1-1-WeM4 Exploring High Entropy Alloy Core Effects in Multi-principal Transition Metal-Al-Si-N, and Multi-principal Boride PVD Thin Films**, K. Yalamançhili (kumar.yalamançhili@oerlikon.com), F. Doris, M. Arndt, Oerlikon Balzers, Oerlikon Surface Solutions AG, Liechtenstein; H. Rudigier, Oerlikon Balzers, Oerlikon Surface Solutions AG, Switzerland

Several metallic high entropy alloys (HEA), also known as multi-principal element alloys were reported with fascinating structural and functional properties. These properties are mainly attributed to (1) unpredicted favourable cocktail mixture of alloying elements, (2) a severe distortion of their lattice, (3) sluggish diffusion kinetics, and most importantly (4) formation of entropy stabilized solid solutions enabled by a high configurational entropy ($S_{\text{config}} > 1.61 R$), where R is the gas constant.

Recent studies also indicate that HEA core effects are operative in ceramic alloys. It was experimentally shown that the entropy predominates the thermodynamic landscape, resulting in a reversible entropy stabilized solid solution in an equimolar mixture of MgO, CoO, NiO, CuO and ZnO [1]. In contrast, entropy stabilization could not be achieved in (AlTiVNbCr)N alloy [2]. This leads to a question of what should be the pre-qualifying criterion to form entropy stabilization in ceramic alloys.

In this contribution, we have explored the above mentioned HEA core effects in two different alloy system with an estimated S_{config} 1.4 R in their cation sub-lattice, (a) multi-principal transition metal (Ti,Nb,V,Cr,W)-Al-Si-N, and (b) multi-principal (Ti-Zr-Ta-Hf-Cr) B₂ alloys. Nitride alloys are synthesized in a reactive arc and boride alloys are synthesized in S3p™ process in thin film form.

As deposited nitride alloys crystallized in a metastable cubic B1 (NaCl) and boride alloys crystallized in hexagonal AlB₂ structure, with a hardness of 40 GPa. Subsequently, these films are subjected to post vacuum annealing up to a temp of 1100 °C. Key properties like structural and hardness evolution as a function of annealing temperature, indentation-induced fracture resistance, and high temp. Oxidation resistance of the multi-principal high entropy alloys are measured and compared with their selective low entropy

Wednesday Morning, May 22, 2019

binary and ternary alloys. These observations are cross-compared with above mentioned HEA core effects.

Ref:

[1] C.M. Rost, et al., Nat. Commun. 6 (2015) 8485

[2] K.Yalamanchili et al., Thin Solid Films, Vol.636, 346-352, 2017

9:20am **TS1-1-WeM5 Mechanical Properties and Corrosion Resistance of Magnetron Sputtered Co-Cr-Fe-Mn-Ni-C Thin Films**, **L. Zendejas Medina** (leon.zendejas.medina@kemi.uu.se), **P. Berastegui**, Uppsala University, Sweden; **L. Nyholm**, **U. Jansson**, Uppsala University, Angstrom Laboratory, Sweden

In this project we aim to deposit thin films which combine high hardness and wear resistance with a high ductility and oxidation resistance. This combination of properties is uncommon as there is often a trade-off between hardness and ductility. Multicomponent or high entropy alloys (HEAs) are a new generation of materials, which is corrosion resistant and has characteristically high strength compared to traditional alloys. There are many HEAs with promising qualities, but the correlation between the mechanical properties and corrosion behavior is less well studied.

The HEA CoCrFeMnNi system with small amounts of C was chosen as a starting point. Carbon is known to increase the corrosion resistance and strength of metal films [1]. However, in the CrCoFeNi system, the ductility starts decreasing above 4 at-% C due to carbide formation [2]. By using magnetron sputtering, which can form metastable phases, the formation of carbides can be suppressed, and the amount of carbon increased beyond the maximum equilibrium solubility. In this project we have used combinatorial sputtering to study the influence of C on the two alloy systems CrFeNi and CrCoFeMnNi.

In the first system, targets of Fe, Cr, Ni and graphite were used to deposit compositional gradient films with up to 10 at-% C at 300 °C. The structure was a mixture of fcc, bcc and σ -phases. All films were highly ductile, and the addition of carbon gave an increase in both hardness and ductility. Films as hard as 11 GPa were obtained for near-equimolar metal contents and 10 at% C. No indication of carbide formation was observed, suggesting that the carbon was dissolved on interstitial sites in the structure. The corrosion of the films was investigated with impedance and potentiodynamic polarization measurements in 0.6 M NaCl. The carbon containing films exhibited higher pitting corrosion resistance than a 316L steel reference.

In a second set of experiments, a compound CoCrFeMnNi HEA and a graphite target were used to deposit gradients with up to 20 at-% C. The structure was a mixture of fcc and bcc, and the crystallinity decreased with increasing carbon content. The hardness at 10 at-% C was 15 GPa, an increase compared to the carbon free films at 7 GPa. The corrosion behavior of the films, and the influence of carbon, have been studied and will be described in more detail.

[1] Fritze, S. et al. Hard and crack resistant carbon supersaturated refractory multicomponent nanostructured coatings. *Sci. Rep.*, 8:14508, 2018.

[2] Huang, T. D. et al. Effect of carbon addition on the microstructure and mechanical properties of CoCrFeNi high entropy alloy. *Sci China Tech Sci*, 61(1):117-123, 2018.

9:40am **TS1-1-WeM6 Thermal Property Evaluation of V-Nb-Mo-Ta-W and V-Nb-Mo-Ta-W-Cr-B High-entropy Alloy Thin Films**, **S.B. Hung** (a0973353952@gmail.com), **C.J. Wang**, National Taiwan University of Science and Technology, Taiwan; **J.-W. Lee**, Ming Chi University of Technology, Taiwan

Refractory high entropy alloys (HEAs) have drawn lots of attentions from researchers and industries because of their outstanding properties, such as high hardness, good wear resistance, and good corrosion resistance and stable thermal properties. In this work, the V-Nb-Mo-Ta-W and carbon contained V-Nb-Mo-Ta-W-B-C refractory HEA thin films were fabricated by a sputtering system on the Al₂O₃, AISI304 stainless steel, AISI420 stainless steel and P-type (100) Si wafers substrates. The structures of thin films were determined by an X-ray diffractometer. The cross-sectional morphologies of thin films were examined by a field emission scanning electron microscopy (FE-SEM). A nanoindenter and scratch test were used to evaluate the hardness and adhesion properties of thin films, respectively. The thermal properties of the V-Nb-Mo-Ta-W and V-Nb-Mo-Ta-W-B-C coatings were evaluated at the temperature ranging from 500 to 1000 °C. The influence of carbon contents on the thermal stability of the V-Nb-Mo-Ta-W and V-Nb-Mo-Ta-W-B-C coatings were discussed in this study.

11:00am **TS1-1-WeM10 Using Modeling and Machine Learning to Accelerate High-Throughput Experimental Materials Discovery**, **J. Hattrick-Simpers** (jason.hatrick-simpers@nist.gov), **H. Jorress**, National Institute of Standards and Technology, USA

INVITED

Over the past 10 years there has been a resurgent interest in the development of novel metallic alloys, both as multiple principle component solid solution alloys, so-called high entropy alloys (HEA) as well as amorphous metallic glasses. Although a number of empirical rules have been proposed for the prediction of potential alloy compositions, calculating their stability and quantifying their properties of interest at operating temperatures from first principles represents a significant challenge. In fact, even high-throughput experimental studies struggle to effectively explore such large composition-processing-property parameter spaces efficiently. Here, I will discuss an approach that seeks to address the rational experimental exploration of such alloys by combining theory, experiment and data science. Our approach is to use insights from the literature, theory, and/or data mining to identify the regions of parameter space most likely to yield interesting materials. We then employ computationally guided high-throughput synthesis techniques to strategically probe composition and processing space. In situ synchrotron diffraction studies yield tens of thousands of data sets describing the evolution of the alloy phase and corrosion products. The data are evaluated using automated knowledge extraction techniques, enabling us to assess our experiments, update the models used to generate the initial lead materials, and plan the next material system to study. In this talk, I will emphasize our recent work using these techniques to investigate phase stability in metallic glasses.

11:40am **TS1-1-WeM12 Structure, Mechanical Properties and Thermal Stability of Magnetron Sputtered HfTaVWZr High-entropy Boride Coatings**, **A. Kirnbauer** (alexander.kirnbauer@tuwien.ac.at), **C.M. Koller**, TU Wien, Institute of Materials Science and Technology, Austria; **P. Polcik**, Plansee Composite Materials GmbH, Germany; **P.H. Mayrhofer**, TU Wien, Institute of Materials Science and Technology, Austria

In the field of materials research, a novel alloying concept of so-called high-entropy alloys (HEAs), has gained particular attention within the last decade. These alloys contain 5 or more elements in equiatomic or near-equiatomic composition. Properties, like hardness, strength, and toughness can be attributed to the specific elemental distribution and are often superior to those of conventional alloys. In parallel to HEAs also high-entropy ceramics (HECs) moved into in the focus of research. These consist of a solid solution of 5 or more binary borides, carbides, nitrides, or oxides. Within this work, we investigate the structure and mechanical properties of thin films based on the high-entropy materials concept with emphasis on their behaviour at elevated temperatures, as their structural integrity should be improved with increasing temperature according to the Gibbs free energy.

Therefore, HfTaVWZr boride coatings were synthesised in a lab-scale sputter deposition facility using a single powder-metallurgically produced composite target (nominal target composition 20 mole % of HfB₂, TaB₂, VB₂, W₂B₅, and ZrB₂, respectively). The coatings crystallise in a single-phased hexagonal α -structure (AlB₂ prototype) with a fine columnar morphology. The hardness in as-deposited state is 45.6 ± 1.5 GPa and these films can thus be considered super hard. The structural evolution of free-standing powdered coating material upon annealing was investigated by DSC and X-ray diffraction, showing only marginal structural changes between 900 and 1200 °C, which can be interpreted by a stabilisation due to the high-entropy effect. Upon annealing up to 1400 °C slight indication for the initiation of decomposition processes is given by emergence of low intensity XRD peaks. Yet, the hardness after annealing at 1400 °C remains at least ~42 GPa.

Compared to their binary boride constituents a significant structural stability and mechanical enhancement at elevated temperatures could be achieved by applying the high-entropy concept to HfTaVWZr boride thin films.

Special Interest Talks

Room Town & Country - Session SIT2-WeSIT

Special Interest Talk II

Moderators: Christopher Muratore, University of Dayton, USA, Michael Stüber, Karlsruhe Institute of Technology (KIT), Institute for Applied Materials (IAM), Germany

1:00pm SIT2-WeSIT1 Linking Intrinsic Plasma Characteristics to the Microstructure and Properties of Thin Films, *I. Petrov (petrov@illinois.edu)*, University of Illinois, USA, Linköping University, Sweden, USA; *G. Greczynski, L. Hultman*, Linköping Univ., IFM, Thin Film Physics Div., Sweden; *J.E. Greene*, University of Illinois, USA, Linköping University, Sweden, National Taiwan Univ. Science & Technology, Taiwan
INVITED

From its inception, the benefits of sputter deposition have stemmed from the presence of plasma in the vicinity of the growing film. Bombardment with charged particles and energetic photons affect the substrate initial condition and all stages of film growth: nucleation, coalescence, texture evolution, and recrystallization. Measuring and controlling the fluxes and energies of the charged particles incident at the substrate is essential to achieving low-temperature growth of high-quality thin films. Under typical direct current magnetron sputtering (DCMS) conditions, the dominant ion species incident at the growth surface while sputtering with N₂/Ar gas mixtures optimized to obtain stoichiometric nitride films is Ar⁺, while the ratio of the gas-ion flux to deposited metal flux J_i/J_{Me} is ≤ 1 . Densification is achieved by increasing the ion energy E_i commonly above 100 eV. However, at higher ion energies, a steep price is extracted in the form of residual ion-induced compressive stress resulting from both recoil implantation of surface atoms and trapping of rare-gas ions in the lattice. An alternative approach is offered by strongly magnetically-unbalanced magnetron sputter deposition systems, which allow ion-to-neutral flux ratios J_i/J_{Me} incident at the growing film to be varied over extremely wide ranges (up to > 20) at very low ion energies ($E_i \sim 10$ -20 eV) (below the lattice displacement threshold). Using high-flux, low-energy ion irradiation during deposition opens new kinetic pathways to independently control the texture (from completely 111 to completely 200) and microstructure (from underdense to fully dense) in transition metal (TM) nitride films grown on amorphous substrates as well as to achieve low-temperature epitaxy of refractory materials and metastable alloys.

The invention of high power impulse magnetron sputtering (HiPIMS) opened the way to exploit metal-ion irradiation, which is particularly attractive for low-temperature growth of refractory ceramic thin films. HiPIMS discharges can ionize up to 90% of the sputtered metal flux; equally important is the time separation between metal- and gas-ion fluxes incident at the substrate. In recent years, it has been demonstrated that the use of synchronized bias to select the metal-rich portion of the ion flux provides a new dimension for ion-assisted growth in which momentum can be tuned by selection of the metal ion in the hybrid/cosputtering configuration and stresses can be eliminated/reduced since the metal ion is a component of the film. Thus, the control of intrinsic plasma conditions continues to drive research and caters to tooling-component, and microelectronics industry, as will be exemplified in the presentation.

Coatings for Use at High Temperatures

Room Pacific Salon 2 - Session A3-WeA

Materials and Coatings for Solar Power Concentration Plants

Moderators: Vladislav Kolarik, Fraunhofer Institute for Chemical Technology ICT, Germany, Gustavo García-Martín, Universidad Complutense de Madrid, Spain

2:00pm **A3-WeA1 Materials and Coatings for Solar Power Concentration Plants, C. Prieto Ríos (Cristina.Prieto@abengoa.com)**, Abengoa Research, Spain

INVITED

CSP (concentrated solar power) is the technology that concentrated the solar radiation to produce electrical energy. The CSP power plant are increasing worldwide in the recent years as the electrical generation is impacting in the climate change. Its development until they compete with traditional power plants, demands decrease the cost of electricity. There are initiatives as Sun Shot by NREL promoting new developments to obtain a lower target cost per kWh. Focusing decrease the costs, the researches point to use higher temperatures, to increase the power plant performance and maximizing the solar radiation uses. The Energy storage let the CSP be dispatchable, and the developments look up higher temperature used too and decreased its costs.

The coatings are using in CSP from the beginning of the technology as they let functionalize the raw materials. Optical and protective layers are the most used coatings in this area. The optical properties are modified with solar selective and with absorptance coatings to enhance the radiation using. The next generation of reflectors is being developed with anti-soiling, protective and antireflection transparent coatings. The molten salts employed as storage media is a high corrosive fluid increasing it with the temperature. These fluids are requiring high inert materials a characteristic easy give from hard coatings. The disruptive developments are proposing and testing new heat transfer fluids, as liquid metals and new mixtures of molten salts, this type of fluids requires high resistance corrosion materials as well, the use of specific protective coatings will be a solution to use this fluid in commercial power plants.

Which are the keys, the methods and the boundary conditions to implement coatings in the CSP technology are the first step to produce solutions based in coated materials properly. The coated material will offer new solutions to temperature increment and resist the corrosion in the power plant functionalizing base materials, always considering cost effectiveness to obtain a feasible optimal designs.

The article gives an overview of the optical and protective coatings employed in CSP and how they must performance their functions. Analyzing and systematization working condition and requirements to design coatings for CSP or to link new developments, to improve the CSP competitiveness.

2:40pm **A3-WeA3 Ductility and Creep Rupture Behavior of Diffusion Coatings Deposited on Grade 91 Steel for Concentrated Solar Power Applications, C. Oskay (oskay@dechema.de), T. Meissner, C. Dobler, M.C. Galetz**, DECHEMA-Forschungsinstitut, Germany

Energy transition aims at the abandoning of fossil-fuel based power generation and shifting to renewable energy technologies. In the course of energy transition concentrated solar power (CSP) technology is qualified as one of the most promising energy generation methods. In CSP systems, solar radiation is concentrated to a receiver via heliostats and molten nitrate salts are employed in the absorber tubes to store and transfer the thermal energy for the consequential generation of electricity via a steam turbine. While offering beneficial thermal and physical properties such as a high heat capacity, thermal conductivity and stability, the utilization of molten nitrate salts, particularly the eutectic mixture of 60 wt.% NaNO₃ – 40 wt. KNO₃ (known as the solar salt) is accompanied with an increased corrosion rate and thus limits the selection of structural materials to high-alloyed steels as well as Ni-based alloys due to their high corrosion resistance. As an alternative, cheaper structural materials such as ferritic-martensitic steels can be used by enhancing their molten salt corrosion resistance via the application of diffusion coatings. This can result in a substantial increase in the cost efficiency of the CSP technology and thus improve its competitiveness with respect to other energy generation methods such as photovoltaics.

In this study, three different types of diffusion coatings were deposited on P91 steel substrates by the industrially well-established method of pack cementation. The first two coatings were aimed at Cr and Al enrichment at the surface respectively; whereas the third coating was manufactured by a

two-step process involving chromizing followed by aluminizing. Subsequently coated and uncoated specimens were exposed to isothermal oxidation in laboratory air at 650°C for 100, 300 and 1000 h in order to characterize the scaling behavior of coatings by thermogravimetric analysis. Four-point bending tests with in-situ acoustic emission (AE) measurement were conducted to determine the fracture strain at RT, while creep rupture tests at 650°C in laboratory air were undertaken to compare the creep strength of coated specimens with respect to their uncoated counterparts. X-ray diffraction (XRD), scanning electron microscopy (SEM) and electron probe microanalysis (EPMA) were utilized for the phase identification and microstructural characterization. Detailed microstructural analysis enabled the correlation of mechanical behavior with the microstructural degradation of coated and uncoated specimens during exposure.

3:00pm **A3-WeA4 Long-term Molten Salt Corrosion of Aluminide Coatings for Heat Storage in Concentrated Solar Power Plants, P. Audigé, S. Rodríguez, A. Agüero (agueroba@inta.es)**, Instituto Nacional de Técnica Aeroespacial (INTA), Spain

Concentrating solar power (CSP) plants represent a valuable technology in terms of baseload and dispatchable renewable energy. However, due to its complicated nature and its difficulty to become an economically viable technology CSP struggle to gain the upper hand over solar photovoltaic and wind power. To overcome the main drawback of intermittency, improving the heat storage system by targeting 15h to 24h storage in the mid- or long-term will bring added-value to CSP. In that sense, advanced molten salts used as heat transfer fluids are investigated but corrosion issues for tubes and tanks materials in contact with them are of concern. To protect base materials with coatings can resolve or moderate corrosion degradation and therefore improve the plant efficiency. This alternative also allows to reduce the capital expenditure when designing a new plant because coatings can be applied on lower cost ferritic-martensitic steels instead of current expensive Ni-base alloys. Slurry aluminide coatings have already demonstrated high corrosion resistance to molten salt after short term exposure (1000h). But the protection mechanism still remains under investigation and long-term exposure is required to confirm the lifetime gain brought by the coatings. This study focuses on the corrosion resistance of slurry aluminide coatings after long-term exposure in contact with the currently employed heat storage system, the so-called Solar Salt (60% NaNO₃-40% KNO₃). To do that, slurry applied aluminides to 9 wt.% Cr P91 and 11.5 wt.% Cr VM12-SHC alloys have been deposited, heat treated at high temperature and both systems have been tested at 580°C in contact with the Solar Salt under static isothermal and cyclic conditions. All the coated systems in all conditions performed much better than the uncoated materials as they exhibited very slight weight variations and formed very thin oxides rich in Na, Al and Fe. Moreover, the coating's morphology and composition were maintained after 5000h with the presence of the same FeAl and Fe₃Al phases than in the initial state suggesting that the Al reservoir is still large enough to protect the underlying metals. On the contrary, both uncoated P91 and VM12-SHC developed a complex, fast growing multilayered oxides rich in Fe, Cr and Na which easily spalled in particular after testing in the more aggressive cyclic conditions. Moreover, as corrosion in molten salt results from the competition between dissolution reactions and corrosion product formation, removing the corrosion products by chemical etching was performed to determine the corrosion kinetics and both substrates experienced parabolic kinetics with significant metal loss.

3:20pm **A3-WeA5 Burn-in Heat Treatment to Form Aluminide Diffusion Coatings for Industrial Large Scale Application, V. Kolarik (vladislav.kolarik@ict.fraunhofer.de), M. Juez Lorenzo, J. Bermejo Sanz, S. Weick**, Fraunhofer Institute for Chemical Technology ICT, Germany

Aluminide diffusion coatings, deposited as Al slurries, are an efficient and economic technique to protect steels against oxidation and corrosion at high temperatures. Moreover, the coating suppresses the evaporation of volatile chromium VI species, which form especially in the presence of water vapor. The typical applications of such coatings are boilers and heat exchangers in all kind of power plants and recently, the application to tubes and storage tanks for molten salt in the up-coming technique of concentrated solar power (CSP) is being investigated.

The diffusion heat treatment, however, is a crucial process step when applied to large scale components, such as a CSP storage tank and even more when aiming at application on-site. Furthermore, the temperature of the heat treatment has to stay below the annealing temperature of the steel for not affecting the microstructure, e.g. 700°C for the ferritic steel P92.

A superficial BURN-IN process was applied to form the aluminide diffusion coating using a heating source with a defined temperature moving with a

defined velocity over the slurry coated surface at a defined distance to it. Pre-oxidation forming an alumina scale on top of the coating can be achieved with a proper adjustment of the burn-in process.

A viscosity and rheology adapted slurry formulation was prepared using spherical high purity aluminum particles with an average diameter of 15 μm and was deposited by brushing or spraying on the surface of the ferritic steel P92. A commercially available radiation heating element was used to heat the sample surface. During the burn-in process the temperatures of the heating source, the slurry coating surface as well as the back-side of the sample were recorded as a function of time. Temperatures in the range of 800°C were applied to the slurry coated surface for times up to 5 hours. With these parameters, the back-side temperature of a 3 mm thick sample was around 500°C.

The resulting aluminide diffusion coatings exhibit very low porosity and a very smooth surface forming a two layers-structure, an outer Fe_2Al_5 layer and an inner FeAl layer. Transversal micro-cracks across the aluminide coating are observed locally as it is typical for such coatings. Underneath the diffusion coating the P92 substrate shows an unaffected microstructure as it is found in the case of the conventional heat treatment at 650°C. The superficial burn-in process is a suitable heat treatment for slurry coatings allowing higher temperatures on the surface and applicable to large components.

3:40pm A3-WeA6 High-Temperature Coatings For Protection of Steels in Contact with Molten Salt for CSP Technology, G. García-Martín (gusgarci@ucm.es), REP-Energy Solutions, Spain; V. Encinas Sánchez, Universidad Complutense de Madrid, Spain; M.I. Lasanta Carrasco, Universidad Complutense de Madrid, Spain; T. de Miguel Gamo, F.J. Pérez Trujillo, Universidad Complutense de Madrid, Spain

The dramatic increase in demand for energy independence has led research groups all over the world to concentrate their investigation on renewable energies. As renewable energy penetration grows, the need for utility-scale renewable generation with storage technology is increasingly important to mitigate intermittency problems, deliver power to peak demand periods and support transmission system reliability. Therefore, concentrated solar power has gained momentum as an attractive technology. Molten nitrate salts are currently considered ideal candidates for heat transfer and storage applications because of their properties. However, this technology is still expensive compared to other renewable sources, which lead to propose solutions for reducing costs. One of these solutions is the development of high-temperature corrosion-resistant coatings, which would avoid the use of expensive alloys. The use of high-temperature corrosion-resistant coatings would be a very suitable option, even more if they were deposited on cheap steels, such as ferritic-martensitic ones. This solution not only would help to overcome the corrosion problems, but also would allow the CSP industry to improve the Levelized Cost of Energy. In this respect, zirconia-based sol-gel coatings seem to be a suitable option, both from an operational and economical point of view.

Thus, in this work, sol-gel zirconia-based coatings were deposited on ferritic-martensitic steels and tested in contact with Solar Salt at 500°C, results being compared with the uncoated substrate. Results were also compared to other steels of interest in CSP industry, such as austenitic stainless steels. The study was developed up to 1000 h under static conditions. Samples were characterized via gravimetric, SEM-EDX, and XRD.

Results showed the good behavior of the coated substrates, with very little weight variations after 1000 h of test in comparison with the uncoated ones, which exhibited significant weight gain and spallation. The good behavior of the proposed coatings was also observed by SEM-EDX and XRD. Furthermore, results also showed the promising behavior when comparing with steels currently used in CSP industry.

Hard Coatings and Vapor Deposition Technologies

Room California - Session B4-4-WeA

Properties and Characterization of Hard Coatings and Surfaces IV

Moderators: Naureen Ghafoor, Linköping Univ., IFM, Thin Film Physics Div., Sweden, **Ulrich May,** Robert Bosch GmbH, Germany, **Fan-Bean Wu,** National United University, Taiwan

2:00pm B4-4-WeA1 Effect of Ti Interlayer on Stress Relief of ZrN/Ti Bilayer Thin Films on Si Substrate, J.-H. Huang (jhhuang@ess.nthu.edu.tw), T.-W. Zheng, National Tsing Hua University, Taiwan

Pure metal interlayers have been widely used to enhance adhesion and relieve residual stress in hard coatings. However, the design of interlayer thickness for stress relief was mostly empirical without quantitative basis. The objectives of this study were to investigate the effect of metal interlayer on stress relief of hard coatings, and to establish a physical model correlating plastic deformation of the interlayer with stress relief. ZrN/Ti bilayer thin films on Si substrate was chosen as the model system. ZrN/Ti specimens with different interlayer thicknesses and with ZrN coatings deposited at different bias voltages were prepared using unbalanced magnetron sputtering. Wafer curvature method and average X-ray strain combined with nanoindentation technique [1,2] were employed to accurately measure the residual stresses in the entire specimen and individual layer, respectively. Experimental results showed that the extent of stress relief, ranging from 59.7 to 80.4%, increased with interlayer thickness, while decreased with increasing stress transferring from top ZrN layer. The efficiency of stress relief decreased with increasing interlayer thickness, but varied irregularly with the stress transferring from ZrN layer. A physical model was developed to account for the stress relief due to plastic deformation of the interlayer, based on the energy balance between elastic stored energy in ZrN and plastic work of metal interlayer. The upper limit of stress relief by the interlayer was assumed to be the necking strain of the interlayer under equibiaxial stress state. The model was verified by the experimental results. Furthermore, a critical experiment was conducted and confirmed that the model could provide a conservative estimation on stress relief for practical applications. The proposed model also indicated that the stress relief was mainly due to plastic deformation of Ti interlayer. Using the model, we could quantitatively estimate the allowable stress relief with a specific interlayer thickness or the required interlayer thickness to relieve certain amount of stress.

[1] A.-N. Wang, C.-P. Chuang, G.-P. Yu, J.-H. Huang, *Surf. Coat. Technol.*, 262 (2015) 40.

[2] A.-N. Wang, J.-H. Huang, H.-W. Hsiao, G.-P. Yu, Haydn Chen, *Surf. Coat. Technol.*, 280(2015) 43.

2:20pm B4-4-WeA2 In-situ Observation of Stress Fields during Crack Tip Shielding in Loaded Soft-hard Micro-Cantilevers using Cross-sectional X-ray Nanodiffraction, M. Meindlhuber

(michael.meindlhuber@unileoben.ac.at), Montanuniversität Leoben, Department of Physical Metallurgy and Materials Testing, Austria; J. Todt, J. Zálešák, Erich Schmid Institute of Materials Science, Austrian Academy of Sciences, Leoben, Austria; S. Klima, N. Jäger, Montanuniversität Leoben, Department of Physical Metallurgy and Materials Testing, Austria; M. Rosenthal, M. Burghammer, ESRF Grenoble, France; H. Hruby, voestalpine eifeler Vacotec GmbH, Germany; C. Mitterer, R. Daniel, Montanuniversität Leoben, Department of Physical Metallurgy and Materials Testing, Austria; J. Keckes, Montanuniversität Leoben, Austria

In recent years, cross-sectional X-ray nanodiffraction (CSnanoXRD) with a resolution down to ~ 30 nm has been proven to resolve depth gradients and residual stresses within individual sublayers of multi-layered thin films. In this work, the in-situ CSnanoXRD setup was used to perform micromechanical testing on a 20 μm thick film composed of four alternating hard CrN and soft Cr sublayers, each 5 μm thick, on a high-strength steel substrate. Notched freestanding and clamped cantilevers of the film thickness and a length and width of 150 and 35 μm and 200 and 40 μm , respectively, machined using focused ion beam (FIB), were tested. Multiaxial stress distributions were evaluated in stationary, stepwise loaded and unloaded cantilevers with a spatial resolution of 200 x 200 nm^2 in a cross-sectional area of ± 20 μm around the FIB-fabricated notches.

While the freestanding cantilever was nearly relaxed before loading, the clamped cantilever exhibited residual stresses up to -4 GPa within the CrN sublayers and up to -500 MPa in the Cr sublayers. During the loading, high in-plane, out-plane and shear compressive stresses up to ~ 10 GPa were observed in CrN under the indenter and at the crack tip. In the Cr sublayers, the loading resulted in a formation of cross-sectional stress gradients and

Wednesday Afternoon, May 22, 2019

compressive-tensile-compressive stress switching at different stages of the experiments. Interestingly, it was observed in both cantilevers that the multi-axial stress concentrations at the crack tips in CrN and in Cr sublayers were blunted when approaching CrN-Cr interfaces. After the unloading, only minor changes in residual stresses in CrN were observed, compared to the stress state before loading.

In summary, the pioneering in-situ micromechanical approach coupled with X-ray nanodiffraction screening was used for the first time to determine multi-axial X-ray elastic strain/stress fields in the vicinity of notches/cracks with sub μm -resolution. The experimental data provide an understanding of the nanoscale deformation processes in nanolaminates and will be integrated into finite element simulations dealing with the evolution of crystallite size- and interface-dependent stress concentrations during elasto-plastic deformation.

2:40pm B4-4-WeA3 Experimentally Parameterized Simulation of an Instrumented Dry Milling Arrangement – Parameter Study Identifying Damage-relevant Coating Properties for End Mills, A.W. Nemetz (andreas.nemetz@mcl.at), W. Daves, T. Klünsner, W. Ecker, Materials Center Leoben Forschung GmbH, Austria; C. Praetzas, Institute of Production Management, Technology and Machine Tools (PTW), Germany; C. Czettl, J. Schäfer, CERATIZIT Austria GmbH, Austria

Solid hard metal end mills, both coated and uncoated, are used to machine difficult-to-cut materials, such as titanium alloys. Experience shows that the tool life varies greatly depending on the applied coating and the chosen process parameters. At the end of the tool life, the cutting situation is not the same as at the beginning of the process and the product quality suffers. Therefore it is of high relevance to recognize and interpret the signals, given within the process to assess its quality and estimate the remaining tool life. Especially in the field of process monitoring, temperature monitoring is a valuable addition to the prevailing force measurement. Within an instrumented milling arrangement, the measured temperature inside the coated end mill is documented. The process is numerically simulated to relate the measured core temperature in the end mill to the temperature at the cutting edge. This information is essential for the model based tool health monitoring. The synergetic use of 2D thermo-mechanical milling models and 3D thermal and mechanical models enables the prediction of the transient temperature field in milling tools. The material models describing the hard coatings and the WC-Co hard metal substrate are parameterized experimentally. The influence of hard coatings on the evolution of the evolving temperature field in end mills is investigated during dry milling. A parameter study identifies improved thermal coating material properties.

3:00pm B4-4-WeA4 Mechanical Properties and Cutting Performance of AlCrSiN and AlTiCrSiN Hard Coatings, L.C. Chao (514two503@gmail.com), Y.-Y. Chang, National Formosa University, Taiwan

Transition metal nitride coatings based on Cr, Ti and Al, such as AlTiN, AlCrN and AlCrSiN, have been used as protective coating materials of cutting and forming tools due to their high hardness and thermal stability. In this study, AlCrSiN and AlTiCrSiN coatings were deposited onto high-speed steels and tungsten carbide tools using AlTi, TiSi, Cr and ternary AlCrSi alloy targets in a Cathodic-arc evaporation (CAE) system. Optimal design of interlayers of the AlCrSiN and AlTiCrSiN can offer an efficient way of controlling residual stress, improving adhesion strength and enhancing toughness. During the coating process of AlCrSiN and AlTiCrSiN, AlCrN and AlTiN were deposited, respectively, as interlayers with different structures to control residual stress, toughness and adhesion strength between the coatings and substrates. By controlling the different interlayers and negative bias voltages, the AlCrSiN and AlTiCrSiN possessed different microstructures and mechanical properties. The microstructure of the deposited coatings was investigated by field emission scanning electron microscope (FE-SEM) and field emission gun high resolution transmission electron microscope (FEG-HRTEM), equipped with an energy-dispersive x-ray analysis spectrometer (EDS). Glancing angle X-ray diffraction was used to characterize the microstructure and phase identification of the coatings. Mechanical properties, such as the hardness and young's modulus, were measured by means of nanoindentation. The adhesion strength of the coatings was evaluated by a standard Rockwell indentation test. In order to evaluate the impact fatigue behavior of the coated samples, an impact test was performed using a cyclic loading device with a tungsten carbide indenter as an impact probe. For the cutting experiment, 316L stainless steel was machined by the coated end mills under oil mist condition using a CNC milling machine. The design of AlCrTiSiN coatings were anticipated to increase the hardness, toughness, thermal stability and impact resistance by optimizing the interlayers and bias condition of the deposition.

Keywords : Mechanical property; Cutting; Hard coating; Interlayer

3:20pm B4-4-WeA5 Erosion, Corrosion Resistance and Hydrophobicity of Nano-layered and Multi-layered Nitride Coatings, Q. Yang (qi.yang@nrc-cnrc.gc.ca), L. Zhao, P. Patnaik, National Research Council of Canada, Canada
Nano-layered CrTiN, CrTiAlN, CrAlTiN, multi-layered CrAlTiN-CrN and CrAlTiN-AlTiN coatings were deposited on 17-4 PH stainless steel substrate by the cathodic arc evaporation technique. Solid particle erosion tests were performed to investigate their erosion resistance. All of these coatings, CrAlTiN and CrAlTiN-AlTiN coatings in particular, demonstrated higher resistance to solid particle erosion at both low and high impingement angles when compared to the single layered CrN coating. For example, the mass erosion rates of the nano-layered CrAlTiN coating were less than 1/3 and 1/7 of the corresponding erosion rates of the CrN coating at 30° and 90° respectively. The excellent erosion performance of the coatings was attributed to the improved hardness. Potentiodynamic polarization tests of the coatings in 3.5% NaCl aqueous solution indicated that these coatings had higher corrosion potentials and much wider passive ranges with comparable or lower current densities, when compared to 17-4 PH. Water contact angle measurements illustrated that the nitride coatings also had good hydrophobic characteristics.

3:40pm B4-4-WeA6 Study of Erosion on Metals and Ceramic Coated Metals Using Magnetron Sputtering Process, S. Hill, D.M. Mihut (dorinamm@yahoo.com), A. Afshar, Z. Grantham, S. Sanchez-Lara, C.D. Raffield, N. Cordista, S. Sanchez Lara, Mercer University, USA

Solid particle impact erosion is a progressive loss of the materials' mass that results from repeated impact of the erodent particles on the material surface. Materials selection for equipment components working in this type of aggressive environmental condition is a great challenge. These materials must possess high strength, hardness, toughness, corrosion resistance but also high erosion resistance. This study uses an impact erosion tester to observe the effects of accelerated erosion on aluminum 6061 alloy and 4140 heat treated steel and assess their erosion behavior improvement after coating with titanium nitride and chromium nitride ceramics. A two phase mixture of water/sand is circulated in a custom test fixture and allowed to impact test coupons at specified angles. The set of experiments uses multiple sand concentrations, a fixed liquid flow rate, and a constant impact angle during the testing procedure to determine the improvement of erosion with the thin film coating. The ceramic thin film coatings on the samples are deposited using magnetron sputtering equipment, the thickness of the coatings is measured using a profilometer and the compositional structures of the coatings are characterized using X-Ray diffraction. The coating morphology and thin films adherence was investigated using Scanning Electron Microscopy (SEM).

4:00pm B4-4-WeA7 Microstructure and Thermal Stability of Al-rich Ti-Al-Mo-N Protective Coatings, C. Wüstefeld (wuestefeld@ww.tu-freiberg.de), Institute of Materials Science, TU Bergakademie Freiberg, Germany; M. Motylenko, Technische Universität Bergakademie Freiberg, Germany; S. Berndorf, Institute of Materials Science, TU Bergakademie Freiberg, Germany; M. Pohler, C. Czettl, CERATIZIT Austria GmbH, Austria; D. Rafaja, Technische Universität Bergakademie Freiberg, Germany

Ti-Al-N coatings are known as protective coatings in metal cutting applications. Further improvements of the mechanical properties and thermal stability of Ti-Al-N coatings are aspired by the addition of alloying elements like tantalum, niobium or molybdenum and by the adjustment of the microstructure via the deposition parameters. In this study, the Mo content and the bias voltage were varied in order to investigate the impact on the microstructure and thermal stability of Al-rich Ti-Al-Mo-N coatings. The coatings were deposited using cathodic arc evaporation (CAE) in nitrogen atmosphere from $\text{Ti}_{32}\text{Al}_{65.5}\text{Mo}_{2.5}$ and $\text{Ti}_{28}\text{Al}_{62}\text{Mo}_{10}$ targets at different bias voltages that ranged between -40 V and -120 V. In order to study the influence of the Mo addition on the thermal stability, selected samples were annealed in argon atmosphere up to 1000 °C. The as deposited and annealed Ti-Al-Mo-N coatings were characterized by using a combination of X-ray diffraction and transmission electron microscopy (TEM) with high resolution and in scanning mode. TEM in scanning mode was supplemented by electron energy loss spectroscopy and energy dispersive spectroscopy.

The microstructure of the coatings was described in terms of the chemical and phase composition, stress-free lattice parameters of the fcc-phase, macroscopic residual stresses as well as the sizes and preferred orientations of fcc crystallites. It could be shown that the bias voltage can be used to control the fractions of fcc-(Ti,Al,Mo)N and wurtzitic AlN in Al-rich Ti-Al-Mo-N coatings. The correlation between the microstructure characteristics, the parameters of the deposition process and the hardness is discussed.

Fundamentals and Technology of Multifunctional Materials and Devices

Room Golden West - Session C2-WeA

Novel Oxide Films for Active Devices

Moderators: Marko Tadjer, Naval Research Laboratory, USA, Vanya Darakchieva, IFM, Linköping University, Sweden

2:00pm C2-WeA1 The Physics of Low Symmetry Metal Oxides with Special Attention to Phonons, Plasmons and Excitons, A. Mock (alyssalynnmock@gmail.com), Linköping University, Sweden **INVITED**

We discuss the analysis of the dielectric function tensor for monoclinic metal oxides. We investigate the potential high-power device material gallium oxide and derive dispersions of transverse, longitudinal and plasmon coupled modes [M. Schubert *et al.*, Phys. Rev. B 93, 125209 (1-18) (2016); Editors' Suggestion], the band-to-band transitions and excitons and their eigenvectors [A. Mock *et al.*, Phys. Rev. B 96, 245205 (1-12) (2017)], the effective electron mass tensor using optical Hall effect measurements [S. Knight, A. Mock *et al.*, Appl. Phys. Lett. 112, 012103 (2018); Editors' Pick], and the temperature dependence of band-to-band transitions energies [A. Mock *et al.*, Appl. Phys. Lett. 112, 041905 (2018)]. We present the Lyddane-Sachs-Teller relation for monoclinic and triclinic semiconductors [M. Schubert, Phys. Rev. Lett. 117, 215502 (2016)]. We also discuss the identification of transverse and longitudinal phonons in scintillator material cadmium tungstate [A. Mock *et al.*, Phys. Rev. B 95, 165202 (1-15) (2017)], and the dielectric and inverse dielectric tensor analysis method for transverse and longitudinal phonon mode dispersion characterization in high-power laser material yttrium orthosilicate [A. Mock *et al.*, Phys. Rev. B, 97 165203 (1-17) (2018)]. Additionally, we discuss the application of these analysis techniques to triclinic single crystalline oligoclase. Further, we apply our methods to epilayers of beta-phase gallium oxide and discuss strain induced effects.

2:40pm C2-WeA3 Materials Interfaces for β -Ga₂O₃ Power Devices, R.L. Peterson (blpeters@umich.edu), University of Michigan, USA **INVITED**

Beta-phase gallium oxide (β -Ga₂O₃) is an ultra-wide bandgap semiconductor that holds great promise for future power electronics due to its ease of bulk crystal growth and facile ability to extrinsically dope *n*-type over a wide range of dopant concentrations. Power devices often operate at elevated temperature with large surge currents and high blocking voltages. Reliable operation under these aggressive conditions requires that the metal and dielectric interfaces, as well as the doping profiles within the device, be highly stable under thermal and electrical stress, including thermal cycling. Obtaining stable materials interfaces is a particular challenge for oxide semiconductors, due to the ready supply of oxygen within the bulk, and to thermodynamic competition amongst adjacent metal atoms to oxidize or reduce. This property has been exploited in other oxide devices, for instance in oxygen-vacancy based resistive memory (ReRAM). However such behavior must be strictly avoided in power devices to ensure reliable and stable operation.

In this talk, I will present our experimental investigations on the stability of dielectric and contact electrode interfaces to beta-phase gallium oxide, using comprehensive materials characterization and electrical measurements. We study novel dielectrics that can be used as gate insulators in field-effect transistors, and for field plates and passivation layers. We also investigate metal contacts to bulk Ga₂O₃ with a variety of dopants and doping levels, to determine pathways to form low-resistance and stable ohmic contacts. The experimental results will be compared to thermodynamic predictions based on Gibbs' free energies of reactions. Using these results, we will identify and discuss strategies for designing stable dielectric and contact interfaces in order to enable high-performance Ga₂O₃ power electronics.

3:20pm C2-WeA5 Phase Selectivity in Heteroepitaxial Ga₂O₃ Thin Films, V.D. Wheeler (virginia.wheeler@nrl.navy.mil), N. Nepal, U.S. Naval Research Laboratory, USA; L.O. Nyakiti, Texas A&M University at Galveston, USA; D.R. Boris, S. Walton, D.J. Meyer, B.P. Downey, C.R. Eddy Jr., U.S. Naval Research Laboratory, USA **INVITED**

Ga₂O₃ has emerged as a promising material for next generation power electronics and UV photodetectors applications due to its large bandgap (4.9 eV) and the availability of affordable native substrates from melt-grown bulk crystals. While β -Ga₂O₃ (monoclinic) is the most stable and studied of five Ga₂O₃ polymorphs, the slightly less energetically favorable α - and ϵ -Ga₂O₃ phases have unique characteristics that can be exploited. The α -Ga₂O₃ (rhombohedral corundum) has the largest bandgap of 5.3 eV and can be alloyed with α -Al₂O₃ and α -In₂O₃ for bandgap engineering. The ϵ -Ga₂O₃

(hexagonal wurtzite) is a polar phase, with a calculated polarization strength that is 10 and 3 times larger than that of GaN and AlN, respectively. Like the III-N system, polarization induced charges can lead to higher charge densities and mobilities in two-dimensional electron gases formed at heterojunctions, which would improve the viability of Ga₂O₃ electronic devices. In this work, we use atomic layer epitaxy (ALEp) to produce high-quality heteroepitaxial Ga₂O₃ films and investigate phase selectivity as a function of substrate type and orientation, growth temperature (*T_g*), plasma gas phase chemistry and gas pressure.

All ALE Ga₂O₃ films were deposited in a Veeco Fiji G2 reactor equipped with a load lock and turbo pump using trimethylgallium and O₂ plasma precursors. Initial studies on *c*-plane sapphire substrates showed that decreasing chamber pressure an order of magnitude during the plasma step resulted in a shift from mostly ϵ -Ga₂O₃ to pure α -Ga₂O₃. Additionally, at 350°C and 8 mTorr, the phase could be altered by a varying the O₂ plasma flow from 5-100 sccm. Optical emission spectroscopy indicate that the ratio of O*/O₂ is critical for phase selectivity while the high ion flux to the surface can contribute to the crystallinity at low *T_g*. By varying *T_g* from 300 to 500°C at 8 mTorr, films went from mixed β/ϵ phase at <350°C, to pure α -Ga₂O₃ at 350°C, to pure β -Ga₂O₃ at 500°C. Using the optimum growth conditions for α -Ga₂O₃ on *c*-sapphire, the influence of substrate was explored using a variety of substrates including AlN, GaN (bulk and epilayers), SiC, diamond, and Si. Deposition on III-N and β -Ga₂O₃ substrates all resulted in crystalline β -Ga₂O₃ films, while amorphous films were deposited on both SiC and Si. This suggests that a clean crystalline substrate interface is critical to obtaining high quality films and promoting metastable phases is more dependent on growth parameters than underlying crystal symmetry. Finally, we will discuss simple electrical properties of optimum films of each phase to validate feasibility of the process in device applications.

4:00pm C2-WeA7 Exfoliated β -Ga₂O₃ Nano-layer based (Opto)electronic Devices, J. Kim (hyunhyun7@korea.ac.kr), S. Oh, Korea University, Republic of Korea **INVITED**

β -Ga₂O₃, which is an ultra-wide band-gap semiconductor (>4.8 eV at room temperature), is an attractive material for next-generation power electronics devices and solar-blind photodetectors. Owing to its ultra-high (theoretical) critical field strength of ~8 MV/cm, Baliga's figure of merit of β -Ga₂O₃ (at 3214) outperforms other wide bandgap semiconductors including SiC (at 317) and GaN (at 846), indicating that β -Ga₂O₃ offers a superior power switching capability. In β -Ga₂O₃ electronic devices, high breakdown voltage by using field plate structures has been demonstrated. In addition, a hetero-junction field-effect transistor by the integration with *p*-type semiconductor was reported. In β -Ga₂O₃ optoelectronic devices, various types of solar-blind (deep-UV) photodetectors have been demonstrated, including photoconductive-type, MSM-type, and Schottky barrier-type photodetectors. The details of the results will be presented at the ICMCTF2019.

4:40pm C2-WeA9 Towards Controlled Exfoliation of β -Ga₂O₃ through Ion Implantation, M.E. Liao (meliao@g.ucla.edu), T. Bai, Y. Wang, M.S. Goorsky, UCLA, USA

β -Ga₂O₃ is a wide bandgap semiconductor that has the potential for high-power device applications. While heterostructures of thin film β -Ga₂O₃ grown on various materials such as GaN^{1,2} and sapphire^{3,4} have been reported, the understanding of direct wafer bonding β -Ga₂O₃ to form heterostructures is still limited. The benefits of wafer bonding β -Ga₂O₃ would be two-fold: (1) enables even more novel materials combinations to be realized and (2) other unprecedented orientations of β -Ga₂O₃ could be integrated with various materials. This last point is important for β -Ga₂O₃ due to its anisotropic properties especially since β -Ga₂O₃ exhibits the low-symmetry monoclinic crystal structure.

Currently there are reports of mechanically exfoliating β -Ga₂O₃ along cleavage planes parallel to the (100) and (001) planes.^{5,6} However, this approach will be challenging to integrate in large-scale processing. Demonstrated with Si_i^{7,8} III-V's⁹⁻¹² and CdZnTe,¹³ the "SMART-Cut" method¹⁴ is more compatible with large-scale processing. In this approach, ions are implanted in a handle substrate and subsequently annealed. Under the appropriate processing conditions, the implanted ions diffuse and agglomerate into bubbles during annealing and surface blistering, accompanied by exfoliation, can occur. In this work, (010) β -Ga₂O₃ substrates are implanted with hydrogen ions and subsequently annealed. Both high-resolution X-ray diffraction (XRD) measurements and transmission electron microscopy (TEM) images were employed to monitor the structural evolution with annealing. Symmetric ω :2 θ XRD scans showed that annealing at 150 °C and 300 °C did not change the implantation-induced strain

appreciably; while annealing at 500 °C for 1 hour was sufficient in removing this strain. Additionally, TEM images showed subsurface hydrogen bubble formation. Despite implanting along a non-cleavage plane, ion implantation for exfoliation provides a promising pathway for obtaining thin layers of β -Ga₂O₃ with orientations other than (100) and (001).

References

- 1.A. Kalra, et al., Appl. Phys. Ex. 11, 2018
- 2.P. Li, et al., J. Mat. Chem. C. 5, 2017
- 3.S. Ghose, et al., J. Appl. Phys. 122, 2017
- 4.V.I. Nikolaev, et al., Mat. Sci. Semi. Proc. 47, 2016
- 5.Y. Kwon, et al., Appl. Phys. Lett. 110, 2017
- 6.M.J. Tadjer, et al., ECS 1233 2017
- 7.C.M. Varma, Appl. Phys. Lett. 71, 1997
- 8.C. Miclaus, et al., J. Phys. D: Appl. Phys. 36, 2003
- 9.S. Hayashi, et al., Appl. Phys. Lett. 85, 2004
- 10.S. Hayashi, et al., J. Electro. Soc. 153, 2006
- 11.S. Hayashi, et al., J. Electro. Soc. 154, 2007
- 12.E. Padilla, et al., ECS Trans. 33, 2010
- 13.C. Miclaus, et al., J. Elec. Mat. 34, 2005
- 14.M. Bruel, et al., Jpn. J. Appl. Phys. 36, 1997

5:00pm C2-WeA10 A Comparison of In-doped SnO₂ (ITO) Films and Doped ZnO in Magnetron Sputtering: Both Thermodynamic and Kinetic Advantages of ITO Films, Y. Chen (chenyuyun@nimte.ac.cn), F. Huang, F. Meng, Ningbo Institute of Materials Technology and Engineering, Chinese Academy of Sciences, China

Replacement of In-doped SnO₂ (ITO) films by doped ZnO [i.e., Al-doped ZnO (AZO) and Ga-doped ZnO (GZO), etc.] has been widely investigated in many studies about large-area magnetron sputtered transparent conductive oxides. However, whether the magnetron sputtered ITO films can be replaced has not been well understood yet. To answer this question, we compared the resistivity of magnetron sputtered ITO, AZO, and GZO films prepared at various discharge voltages ($|V_d|$) and substrate temperatures (T_s), both of which are the key process parameters in energetic vapor deposition. We found that (i) low $|V_d|$ and sufficient T_s are necessary for AZO and GZO films to achieve high conductivity, but the latter needs lower $|V_d|$ and higher T_s than the former; (ii) adequate T_s (>100 °C) enables ITO films to show high conductivity, irrespective of $|V_d|$; and (iii) compared with AZO and GZO films under same conditions, ITO films show higher conductivity. Such differences are discussed in terms of the thermodynamic stability and kinetic diffusion of their dopants during the formation of substitutional solid solution. Our results show that ITO films exhibit both thermodynamic and kinetic advantages over AZO or GZO films. Therefore, ITO replacement by AZO or GZO is difficult in large-area magnetron sputtering.

5:20pm C2-WeA11 Investigation on Microstructure and Piezoelectric Property of High Orientation Y-doped ZnO Thin Films via RF Magnetron Sputtering, L.C. Cheng (n56064428@mail.ncku.edu.tw), C.P. Liu, J.L. Huang, National Cheng Kung University, Taiwan

In this study, we focused on the piezoelectric coefficients (d_{33}) depended on doping rare earth element, yttrium (Y), into ZnO thin films. Pure ZnO and Y doped ZnO (Y:ZnO) thin films with different yttrium contents were synthesized on p-type Si (111) substrates via RF magnetron sputtering, and the thickness of these thin films were fixed at 650 nm. In X-ray diffraction (XRD) patterns, Y:ZnO films with low yttrium contents (<3 at%) showed preferential orientation of (002) plane and still maintained columnar wurtzite structures. The positions of diffraction peaks shifted to lower angle as the concentration of yttrium increased due to the substitution of smaller host ions (Zn²⁺: 0.74Å) by larger dopant ions (Y³⁺: 1.04Å). When the concentration of yttrium is over 3 at%, the drastic transformation of morphology was observed in scanning electron microscopy (SEM) images, which consisted with the results of XRD analysis. This phenomenon caused by the lattice distortion, owing to the larger radii of Y³⁺ ions. The piezoelectric coefficients of pure ZnO and Y:ZnO thin films were measured by piezoresponse force microscopy (PFM) as well. The piezoelectric coefficients had achieved higher values ($d_{33} \sim 86.8$ pm/V) when the contents of yttrium was 3 at%, which compared to the theoretical values of pure ZnO thin films ($d_{33} = 12.4$ pm/V). Therefore, Y doped ZnO thin film was regarded as the promising candidate for piezoelectric nanogenerators (NGs).

Tribology and Mechanical Behavior of Coatings and Engineered Surfaces

Room San Diego - Session E1-4-WeA

Friction, Wear, Lubrication Effects, and Modeling I

Moderators: Nazlim Bagcivan, Schaeffler AG, Germany, Carsten Gachot, TU Wien, Institute for Engineering Design and Logistics Engineering, Austria

2:20pm E1-4-WeA2 Surface Characteristics of the Chameleon/PEO Coating after Fretting Wear Tests, M. Lin (linmy19911001@gmail.com), A. Matthews, A. Yerokhin, University of Manchester, UK

A duplex MoS₂/Sb₂O₃/graphite chameleon and PEO coating deposited on 6082 series Al alloy substrate have been established using burnishing process and plasma electrolytic oxidation (PEO) technique, respectively. A series of fretting wear tests were then applied on the surface of the chameleon/PEO coating sample under various amplitudes and environment (ambient humid air or nitrogen atmosphere) with two different counterpart materials. The X-ray diffraction (XRD), nano indentation, scanning electron microscopy (SEM), energy dispersive spectrometer (EDS), laser confocal microscope and Raman spectroscopy were employed to examine the phase composition, nanohardness, surface microstructure, element distribution and 3D surface topographies of the wear scars. It was found that the wear scars on the chameleon coating were mainly composed of MoS₂, Sb₂O₃ and Al₂O₃ phases while the underneath PEO coating was consisted of crystalline α/γ -Al₂O₃ mixtures. This study demonstrated the efficient wear properties enhancement of the chameleon/PEO coating against alumina counterpart by reducing friction coefficient from 0.88-0.92 to 0.07-0.09 in N₂ and 0.58-0.62 to 0.10-0.12 in air. The specific stick sliding (~3 μ m amplitude), partial slip (5-10 μ m amplitude) and gross slip (>10 μ m amplitude) regimes were observed at the fretting wear with the amplitudes increase from 3 μ m to 100 μ m. The steel counterpart and oxidized atmosphere were proved could seriously affect the performance of the duplex coating, resulted in the mass generation of the metal oxides/hydroxides in the contact region, long penetration micro-cracks in the PEO coating and gradually severely oxidation in the aluminium substrate.

2:40pm E1-4-WeA3 Characterization of W Alloyed DLC Coatings Deposited by a Hybrid DC / HIPIMS Magnetron Sputtering Process, M. Evaristo (manuel.evaristo@dem.uc.pt), A. Cavaleiro, SEG-CEMMPRE - University of Coimbra, Portugal

Tribology is a key feature to sustainable and environmental friendly engineering as it is directly related to energy consumption, wear and component failures across all industries. Energy losses worldwide due to friction and wear have a significant impact on the economy, reduction of friction and wear can reduce economic losses by energy saving and increase time between maintenance stops. One of the most efficient way to reach those objectives is modifying the surfaces in contact by means of thin films in dry and lubricated conditions. DLC coatings provide low friction and good wear resistance in dry sliding; however in lubricated conditions the efficiency is not so good due to inertness of the surface. Therefore, to maintain a good performance in both situations, improving the reactivity of the surface, by doping the coating with a metal, is necessary.

W-DLC coatings were deposited in a four magnetron semi-industrial PVD TEER Coatings deposition chamber with HIPIMS and DC power supplies connected to the W target and C/Cr (used for the deposition of the interlayer) targets, respectively. The depositions were set to have a W content close to 10 at. % for all coatings. The coatings were deposited with two peak power levels, high 140 kW and low 55 kW. For both powers the substrate bias voltage was varied from 0 to -110V. The mechanical properties are influenced by both peak power and bias voltage with the lowest value of 9.7 GPa achieved for the lower peak power and 0 substrate bias and the highest of 14.1 GPa for the higher peak power and 110 V of substrate bias. A coating deposited in a reactive atmosphere (Ar + CH₄) with the latter conditions, with same W content, also showed a similar hardness value 14.9 GPa. The adhesion of the coatings was similar for all coatings tested. The XRD analysis showed typical diffraction patterns of an amorphous structure without visible differences among the coatings. However, both bias and peak power influenced the coatings morphology, with a more compactness columnar aspect with their increase. In the case of the coatings deposited in a reactive atmosphere, a dense and featureless morphology was produced.

Two coatings were selected for the tribological characterization, the ones deposited high peak power and -110V substrate bias, with and without CH₄ as reactive gas. The coatings were tested in different conditions with wear

rates and coefficient of friction values lower than $0.15 \times 10^{-6} \text{ mm}^3/\text{Nm}$ and 0.25 respectively.

3:00pm E1-4-WeA4 Tribological Improvement of Al with CNTs and Nb Nanopowder for Industrial Application, C.O. Ujah (omega.ujah@gmail.com), P.A. Popoola, O.M. Popoola, Tshwane University of Technology, Pretoria, South Africa

Unreinforced Al alloy lacks adequate Tribological property required in service. To improve on this property, it must be reinforced with materials having good wear properties. Hence, Al was reinforced with CNTs and Nb and consolidated with spark plasma sintering (SPS). The wear experiment was conducted on a ball-on-disc Tribometer where loads of 10 N, 20 N and 30 N were systematically applied on the sintered samples and their corresponding coefficients of friction generated. The samples were weighed before and after each run to determine their weight losses which were used to compute their wear volumes. The experiment was designed and analyzed with Taguchi and ANOVA. Results obtained showed that Al-8CNTs-8Nb composite gave the best wear characteristics, recording 79 % improvement in Tribology which is suitable for most of the industrial applications.

3:20pm E1-4-WeA5 Influence of Interface Density on Tribological Performance of VN/TiN Multilayers, M.J. Rivera Chaverra, Universidad Nacional de Colombia Sede Manizales, Colombia; D. Escobar, Universidad Nacional de Colombia, Colombia; R. Ospina, Universidad Industrial de Santander, Bucaramanga, Santander, Colombia; M. Arroyave Franco, Universidad EAFIT A.A, Colombia; J.J. Olaya Florez, Universidad Nacional de Colombia, Colombia; E. Restrepo-Parra (erestrepopa@unal.edu.co), Universidad Nacional de Colombia Sede Manizales, Colombia

VN/TiN multilayers were produced by means of the reactive sputtering technique provided with two independent magnetrons, each with a titanium and vanadium target. Coatings were deposited on AISI 304 substrates varying the number of bilayers from 3 to 5 and maintaining the total thickness at a value of 500 nm and hence varying the amount of interfaces in a constant thickness. Structural characterization was carried out through X-ray diffraction (XRD) showing the presence of both TiN and VN cubic phases. Surface morphology obtained by atomic force microscopy (AFM) revealed a granular topography and variations in surface grain size as the number of interfaces is modified. X-ray photoelectron spectroscopy (XPS) showed the composition and the formation of each nitride. Finally, tribological performance were evaluated carrying out pin on disc tests and measuring the displaced material. Also these tests revealed the existence of both abrasive and adhesive wear mechanisms. Finally, sample with 5 VN/TiN bilayers was the most wear resistant sample, even with no changes in coefficient of friction, which attribute low wear to its higher amount of interfaces.

3:40pm E1-4-WeA6 Analysis of Tribomechanical Behavior of Low-Temperature Plasma Blued Tool Steels, F. Santiago (A01101427@itesm.mx), ITESM Estado de México, Mexico; .R. Meza, Termoinnova, S.A. de C.V., Mexico; J. Oseguera-Peña, Tecnológico de Monterrey, México

The tribomechanical behavior of tool steels AISI 4140T and AISI 8620 steel treated by the novel low-temperature plasma blued (LTPB) process. An amorphous solid carbon film (Diamond-like Carbon, DLC) layer is obtained using an atmosphere of methane (CH_4) and molecular hydrogen (H_2) at low-temperature and a short period of time. The microstructure of treated samples was characterized using XPS spectroscopy, Raman spectroscopy, and X-ray diffraction, and the compound layer thickness was measured by optical microscopy. Raman spectroscopy finds D and G bands, and XPS spectroscopy shows a mixture of sp^2 and sp^3 hybridized bonds of a typical DLC coating. Vickers microhardness profiles were correlated with a reduction of friction coefficient in the treated samples. Wear test was performed on a pin-on-disc tribometer in dry-sliding conditions using a counter-face of WC-Co ball. Wear tracks on the ball and surface of the treated sample were analyzed by optical micrograph and SEM.

4:00pm E1-4-WeA7 Improved Wear Resistance and Mechanical Properties of Multifunctional Polymer Nanocomposites for Advance Engineering Applications, U.O. Uyor (UyorUO@tut.ac.za), P.A. Popoola, O.M. Popoola, Tshwane University of Technology, Pretoria, South Africa

Polymeric materials have shown great properties required for various engineering applications such as surface coating, solid or self-lubricant, electronic, electrical, mechanical and structural applications. Their wide applications are due to their desired properties such as light weight, chemical resistance, flexibility, toughness and low cost. However, polymers generally suffer from low wear resistance and poor mechanical strength.

These challenges have limited some applications of polymers, especially where high mechanical strength and wear resistance are required. Therefore, research interests have focused on advancement of various polymers' properties. This was achieved in this study by incorporation of surface modified graphene and titanium dioxide nano-powder in poly(vinylidene fluoride) matrix through solution blending and melt compounding. The morphology of the nanocomposites was studied using scanning electron microscope (SEM). The nanocomposites showed significant reduction in wear volume and enhanced mechanical properties due to the present of surface modified fillers. About 76.5% reduction in wear volume, 52% and 186.5% increase in tensile strength and Young modulus respectively were achieved in this study. The surface modification of the fillers was essential in homogeneous dispersion of the fillers in the polymer matrix and the improved properties recorded. Such nanocomposites can find applications as solid lubricant, automobile and aerospace components.

Keywords: Polymer, graphene, titanium dioxide, wear and mechanical properties.

New Horizons in Coatings and Thin Films Room Pacific Salon 6-7 - Session F4-2-WeA

Functional Oxide and Oxynitride Coatings II

Moderators: Anders Eriksson, Oerlikon Balzers, Oerlikon Surface Solutions AG, Liechtenstein, Marcus Hans, RWTH Aachen University, Germany, Jörg Patscheider, Evatec AG, Switzerland

2:40pm F4-2-WeA3 Study on Silicon Carbide Based Metal Oxide Semiconductor Capacitor with Magnetron Sputtered ZrO₂ high-k Gate Dielectric, R. Chandra (ramesfic@gmail.com), S. Mourya, G. Malik, J. Jaiswal, IIC, IIT Roorkee, India

A silicon carbide (SiC) based two terminal metal oxide semiconductor (MOS) capacitors with magnetron sputtered zirconium oxide (ZrO_2) as a high-k dielectric material using titanium (Ti) gate has been synthesized at room temperature. The structural, morphological and compositional analysis of the dielectric layer has been carried out using X-ray diffraction (XRD), scanning electron microscopy (SEM), Atomic force microscopy (AFM), energy dispersive spectroscopy (EDS) and X-ray photoelectron spectroscopy (XPS). The current-voltage (I-V) and capacitance-voltage (C-V) characteristics of MOS capacitor were studied at room temperature by applying the dc bias gate voltage swept from -3V to 3V for both, high and low-frequency operation using semiconductor parameter analyzer. The thermal stability of the MOS capacitor is of critical importance for use in the fabrication of electronics for deployment in extreme environments. Hence, the effects of post-deposition annealing (PDA) temperatures (200-1000 °C) on the electrical properties of the MOS capacitor have been investigated. MOS characteristics of Ti/ZrO₂/SiC/Ni capacitor were correlated with structural and morphological properties of an insulating dielectric layer at different PDA temperatures. It has been observed that a synergetic contribution of lowest effective oxide charge, semiconductor-oxide interface-trap density and total interface-trap density improve the electric breakdown field of MOS capacitor for PDA samples.

3:00pm F4-2-WeA4 Structural, Optical and Electrochromic Properties of Nanocrystalline WO₃ Thin Films, M.V. Kalapala (kvmsvu@gmail.com), VFSTR University, India

In the present work, WO_3 thin films were coated onto well cleaned corning 7059 glass, Silicon and ITO coated glass substrates by electron beam evaporation (EBE) technique under an oxygen partial pressure of 2×10^{-4} mbar by maintaining the substrate temperature at 6-8 °C and room temperature (RT). The deposited films were subsequently annealed at 400 °C in air at about 2 hours and the films were systematically characterised to analyse the electrochromic properties which are useful in emerging chromogenic technology. The structural, morphological, vibrational, optical and electrochromic properties of WO_3 films were studied by XRD, AFM, Raman, UV-VIS spectroscopy and Cyclic voltammetry respectively. XRD studies reveal that the prepared WO_3 films are completely monoclinic structure with different orientations. The AFM images and the grain sizes are comparable with the XRD data. The optical transmission and energy bandgap of the films increases with the lowering of temperatures to 6-8 °C. Finally it is found that, the coloration efficiency at the wavelength of 550 nm for the annealed films deposited at 6-8 °C is maximum $72.60 \text{ cm}^2\text{C}^{-1}$.

3:20pm **F4-2-WeA5 Structure, Mechanical Characteristics and Thermal Stability of HS-PVD (Al,Cr)₂O₃ Coatings**, *K. Bobzin, T. Brögelmann, C. Kalscheuer, M. Welters (welters@iot.rwth-aachen.de)*, Surface Engineering Institute - RWTH Aachen University, Germany

Alumina coatings with corundum structure, α -Al₂O₃, bear great potential concerning the application under harsh conditions even at temperatures above $T \geq 900$ °C and in corrosive or oxidative environments. Typically, α -Al₂O₃ is used on cutting and molding tools. However, the industrial deposition of α -alumina coatings is typically performed by chemical vapor deposition (CVD) at temperatures between 800 °C $\leq T \leq 1,100$ °C, which limits the choice of base materials. In the last decades (Al,Cr)₂O₃ coatings deposited by physical vapor deposition (PVD) attract great interest as an alternative to CVD α -Al₂O₃, due to their potential to form corundum-type structure at lower process temperatures. (Al,Cr)₂O₃ coatings with high Al content promise similar characteristics to α -alumina. However, the deposition of crystalline α -(Al,Cr)₂O₃ by PVD technology with high alumina content, $x_{Al} > 70$ at.%, is still one of the greatest challenges. So far, various PVD technologies, such as cathodic arc deposition and magnetron sputtering, were investigated concerning the deposition of α -(Al,Cr)₂O₃. The investigations showed that low deposition temperatures, $T \leq 650$ °C, and high aluminum contents, $x_{Al} > 70$ at.%, frequently led to the formation of metastable amorphous or crystalline alumina phases. Further drawbacks are low coating thicknesses and deposition rates for the deposition of oxide coatings as well as challenges regarding the coating of complex geometries. A promising technology to overcome these challenges is the high speed (HS)-PVD technology, basing on a hollow cathode discharge. Owing to the promising technology characteristics, the potential of HS-PVD concerning the deposition of α -(Al,Cr)₂O₃ was fundamentally investigated. After successful process adjustment, the deposition of crystalline tetragonal (Al,Cr)₂O₃ coatings and semi-crystalline α -(Al,Cr)₂O₃ coatings with high Al content, $x_{Al} \geq 70$ at.%, was possible by HS-PVD at a substrate temperature of $T_s = 570$ °C. The analyses regarding structural characteristics confirm that the deposition of thick, $s \geq 20$ μ m, oxide coatings with high deposition rates above 35 μ m/h is possible by HS-PVD. Furthermore, nanoindentation shows that an indentation hardness of $H_{IT} = 24$ GPa can be achieved for the crystalline (Al,Cr)₂O₃ coatings. Moreover, the oxidation and diffusion behavior of the thick (Al,Cr)₂O₃ coatings was investigated by thermal annealing up to $T = 1,300$ °C in ambient air. Thereby, the annealing tests were evaluated by scanning electron microscopy, X-ray diffraction and nanoindentation. Analog annealing tests in vacuum confirmed the stability of the α -(Al,Cr)₂O₃ phase up to $T = 1,300$ °C.

3:40pm **F4-2-WeA6 Reactive HiPIMS Deposition of γ -Al₂O₃ Thin Films using Transition Metal Doped Al Targets**, *S. Kagerer (stefan.kagerer@tuwien.ac.at)*, *L. Zauner*, TU Wien, Institute of Materials Science, Austria; *S. Kolosvári*, Plansee Composite Materials GmbH, Germany; *J. Čapek, T. Kozák, P. Zeman*, University of West Bohemia, Czech Republic; *H. Riedl*, TU Wien, Institute of Materials Science, Austria; *P.H. Mayrhofer*, Institute of Materials Science and Technology, TU Wien, Austria
The outstanding oxidation resistance, thermo-mechanical stability, and chemical inertness of alumina attracts particular attention in academia and industry. Especially, in the field of hard protective coatings there are many research activities focusing on the synthesis of the different polymorphs α - and γ -Al₂O₃ (corundum and cubic), respectively. To overcome the thermodynamic barrier stabilizing these structure types, extremely high deposition temperatures are crucial during film growth (either in CVD or PVD). Apart from this fact, the formation of isolating Al₂O₃ layers on the target surface may lead to massive arc events, and hence destabilizes PVD based deposition process.

Therefore, alternative concepts involving PVD based synthesis at low temperatures are extremely interesting. Within this study, we investigated in detail the influence of small amounts of transition metals such as M = Cr or W on the process stability and phase formation of DC as well as high power impulse magnetron sputtered (Al_{1-x}M_x)₂O₃ thin films in reactive gas atmospheres (Ar/O₂ mixtures). Through the introduction of high amplitude impulses at relatively low duty cycles, the amount of ionized species, either for the target-near gas or sputtered target-atoms, can be increased drastically. To gain an in-depth understanding on the influence of small amounts of tungsten compared to pure Al targets but also on different HiPIMS parameters (e.g. frequency, pulse length, power density, or synchronized bias signals), the ionization of e.g. Al⁺, Al⁺⁺ or O₂⁺ was investigated by ion mass spectroscopy methodically. In addition, the obtained coating structures were analyzed with respect to phase formation and morphology applying X-ray diffraction combined with electron imaging techniques (SEM and HR-TEM).

4:00pm **F4-2-WeA7 Influence of V Content on Phase Evolution and Thermal Stability of Reactive Pulsed DC Magnetron Sputtered (Al,V)₂O₃**, *L.L. Landälv (ludvig.landalv@liu.se)*, Linköping Univ., IFM, Thin Film Physics Div. and Sandvik Coromant R&D, Sweden; *C-F. Carlström*, Sandvik Coromant R&D, Sweden; *J. Lu*, Linköping Univ., IFM, Thin Film Physics Div., Sweden; *M.P. Johansson-Jöesaar*, SECO tools AB, Sweden; *M. Ahlgren, E. Göthelid*, Sandvik Coromant R&D, Sweden; *B. Alling, L. Hultman, P. Eklund*, Linköping Univ., IFM, Thin Film Physics Div., Sweden

Physical vapor deposited corundum structured α -Al₂O₃ coatings have been a long sought goal for the cutting tool industry. Various PVD synthesis routes have been evaluated comprising, e.g., Cr alloying in (Al,Cr)₂O₃ to stabilize the corundum phase [1, 2]. Correspondingly, based on V₂O₃ crystallization in the corundum structure, similar possibilities are indicated for phase stabilization in (Al,V)₂O₃ alloys, although this material system has not yet been studied as much.

This work aims to investigate the influence of V concentration in reactive co-sputtered (Al,V)₂O₃ coatings on phase stabilization and phase evolution, correlated to its mechanical properties by nanoindentation. XRD and SEM characterization of the as-deposited coatings reveal three different phase-regions as a function of V content in the coating with a solid solution γ -(Al,V)₂O₃ for low V content, a defect spinel at around 50 at % metal fraction V and a corundum phase at large V content.

The phase stability and mechanical properties of (Al,V)₂O₃ coatings were studied after annealing in air at different temperatures up to a maximum of 1100 °C. SEM, XRD and nanoindentation was performed after each temperature step. The annealing resulted in formation of vanadiumoxide phases, predominantly V₂O₅, at the coating surface with an onset temperature correlated to the amount of V in the coating. A higher V-content resulting in a lower onset temperature. The effect of the oxidation behavior of the coatings with respect to mechanical properties will be discussed.

[1] Ramm, J., et al., Surf. Coat. Technol., 2007, **202**(4–7): p. 876-883.

[2] Khatibi, A., et al., Acta Mater., 2013, **61**(13): p. 4811-4822.

4:20pm **F4-2-WeA8 Al Vacancies in Wurtzite Al-(Si)-(O)-N: Theory and Experimental Assessment**, *M. Fischer (maria.fischer@empa.ch)*, *M. Trant, K. Thorwarth, D. Scopece, C.A. Pignedoli, D. Passerone, H.J. Hug*, Empa - Swiss Federal Laboratories for Materials Science and Technology, Switzerland

Transparent hard films can be fabricated from Al, Si, O and N by reactive direct current magnetron sputter (R-DCMS) deposition. Al-Si-N and Al-O-N are two possible ternary combinations. Up to 6% Si / 8% O, the coatings can maintain the crystalline structure of wurtzite AlN and incorporate Si / O in the form of a solid solution. As Si is an electron donor like Al, it will substitute the latter on a cationic lattice site. O, in contrast, is an electron acceptor like N, and thus replaces the latter on an anionic lattice site.

These two contrary substitutions induce the same microstructural evolution in wurtzite. The reason for this was found in the formation of cationic Al vacancies (V(Al)) in both cases, because both Si and O impose an electron excess onto the crystal system. The presence of V(Al) in Al-Si-N and Al-O-N has previously been supported by X-ray diffraction measurements, *ab initio* calculations and entropic considerations. With the present study, further experimental evidence for V(Al)s has been provided through Positron Annihilation Spectroscopy (PAS) and Lifetime (PALS) measurements of the latter. To corroborate the hypothesis on vacancy formation, PA(L)S has also been performed on a complementary material system containing anionic vacancies.

4:40pm **F4-2-WeA9 Thermal Atomic Layer Etching of Oxide and Nitride Thin Films**, *S.M. George (Steven.george@colorado.edu)*, University of Colorado at Boulder, USA

Nanofabrication requires atomic layer control over both material deposition and removal. Thermal atomic layer etching (ALE) is based on sequential, self-limiting surface reactions. Thermal ALE is the reverse of atomic layer deposition (ALD). Thermal ALE yields isotropic etching. Thermal Si ALE complements plasma ALE processes that utilize directional ions and produce anisotropic etching. This talk will focus on the thermal ALE of oxide and nitride thin films.

Thermal Al₂O₃ will be described using sequential fluorination and ligand-exchange reactions [1]. During these reactions, HF is utilized to fluorinate the Al₂O₃ surface and produce an AlF₃ surface layer. Trimethylaluminum (TMA) is then used to remove the AlF₃ surface layer through a ligand-exchange reaction. During this ligand-exchange, fluorine transfers from AlF₃ to TMA and, concurrently, methyl groups transfer from TMA to AlF₃. This

Wednesday Afternoon, May 22, 2019

ligand-exchange process yields volatile $\text{AlF}(\text{CH}_3)_2$ products. Al_2O_3 etch rates of $0.51 \text{ \AA}/\text{cycle}$ are observed at 300°C [1].

Thermal SiO_2 ALE will also be demonstrated using a "conversion-etch" mechanism with TMA and HF as the reactants [2]. During SiO_2 ALE, the TMA is able to convert the SiO_2 surface to an Al_2O_3 surface layer. The Al_2O_3 surface layer is then removed by thermal Al_2O_3 ALE as described above. The conversion of SiO_2 to Al_2O_3 requires higher TMA pressures. Larger SiO_2 etch rates are observed at higher TMA pressures [2]. In addition, thermal TiN ALE will be presented using oxidation of TiN to TiO_2 and then the removal of the TiO_2 surface layer by fluorination to a volatile fluoride [3]. TiN ALE at 250°C using O_3 and HF as the reactants yields a TiN etch rate of $0.2 \text{ \AA}/\text{cycle}$.

[1] Y. Lee, J.W. DuMont and S.M. George, *Chem. Mater.***28**, 2994 (2016).

[2] J.W. DuMont et al., *ACS Appl. Mater. & Interfaces***9**, 10296 (2017).

[3] Y. Lee and S.M. George, *Chem. Mater.***29**, 8202 (2017).

5:20pm F4-2-WeA11 Growth and Characterization ALD Films with a new Continuous Flow Process, B. Kuyel (b.kuyel@nanomaster.com), A. Alphonse, K.P. Hong, Nano-Master, Inc., USA

Growth and film deposition characteristic in a downstream ICP PEALD reactor are studied using a unique new process called Continuous Flow Process* that cuts the cycle time in half. This process is implemented in an PEALD reactor where uniform variable density O_2 and N_2 or H_2 plasmas is produced but any contact of the plasma with the substrate is prevented. Precursors are not allowed to enter the plasma production region making it possible to obtain repeatable operation free of deposits or instabilities. Design features will be discussed and application of this Continuous Flow Process in depositing PEALD GaN, Al_2O_3 , AlN, SiO_2 and Si_3N_4 films on Si substrates will be shown. Examples of Continuous Flow process is presented showing ultra-smooth and uniform films with thickness linearly proportional to the number of cycles are deposited. Future applications will also be discussed.

*US Patent # 9,972,501 B1 May 15, 2018

Advanced Characterization Techniques for Coatings, Thin Films, and Small Volumes Room Pacific Salon 1 - Session H3-2-WeA

Degradation under Extreme Conditions

Moderators: James Gibson, RWTH Aachen University, Germany, **Jeffrey M. Wheeler**, ETH Zürich, Switzerland

2:00pm H3-2-WeA1 Application of Micro-cantilever Bending to Probe the Fracture Behavior of Thin Film Interfaces, J. Kabel, P. Hosemann (peterh@berkeley.edu), University of California at Berkeley, USA; T. Koyanagi, Y. Katoh, Oak Ridge National Laboratory, USA

Thin film coatings are proposed as a dual-purpose corrosion barrier and hermetic seal for accident tolerant fuel cladding in light water nuclear reactors (LWR). The bulk cladding structure is a SiC/SiC composite as it exhibits high temperature mechanical properties and superior oxidation kinetics in accident scenarios. However, operational LWR coolant conditions and inherent SiC micro-cracking cause matrix dissolution and fission product release respectively. It has been shown that coating technology can mitigate both challenges. A critical aspect of qualifying these coatings for application is to understand the mechanical stability of the interface. Two coating materials, Cr and CrN, have shown promising corrosion behavior and are the subject of this research. Approximately 45 micro-cantilevers, $\sim 2 \mu\text{m}^2$ cross-section and $6 \mu\text{m}$ length, were fabricated using focused ion beam milling techniques and tested *in situ* SEM to evaluate the interfacial fracture stress. Ductility was observed in the Cr coating, leading a lower-bound fracture stress $3.25 \pm 0.23 \text{ GPa}$. Neutron irradiated SiC/Cr interfaces ($\sim 0.5 \text{ dpa-SiC}$ at 330°C) also showed ductility and a lower-bound fracture stress $2.9 \pm 0.21 \text{ GPa}$. SiC/CrN cantilevers showed brittle failure at $5.55 \pm 0.46 \text{ GPa}$. Fracture stress was evaluated via the flexural formula following linear elastic beam mechanics assumptions. FEA modelling was pursued to further quantify the complex stress state at the interface, allowing for improved interpretation of the results. Additionally, micro-beam 3pt-bending is being investigated to extract interfacial fracture toughness.

2:20pm H3-2-WeA2 Probing Fatigue Resistance in Multilayer DLC Coatings by Micro-impact: Correlation to Erosion Tests, B.D. Beake (ben@micromaterials.co.uk), Micro Materials Ltd, UK; T. Liskiewicz, S. McMaster, A. Neville, University of Leeds, UK

Improving the fatigue resistance of multilayered DLC coatings on hardened steel under the harsh environment of highly loaded repetitive contact is key to increasing their performance in demanding applications, such as in automotive engines.

This has been studied directly by (1) micro-scale rapid impact tests at significantly higher strain rate and energy than in the nano-impact test, enabling the study of coating fatigue with spherical indenters (2) dry erosion testing. Good correlation between micro-impact results and erosion results was found.

Hard multilayered a-C:H and Si:a-C:H coatings were found to be significantly less durable under fatigue loading than a multi-layered WC/C coating. The influence of the coating mechanical properties on these differences is discussed. The results of this study provide further strong evidence that in highly loaded mechanical contact applications requiring a combination of load support and resistance to impact fatigue, the optimum lifetime of coated components may be achieved by designing the coating system to combine these properties rather than by solely aiming to maximise coating hardness as this may be accompanied by brittle fracture and higher wear.

2:40pm H3-2-WeA3 Development of an In-Situ Ion Irradiation and Nanomechanics Scanning Electron Microscope, K. Hattar (khattar@sandia.gov), N. Heckman, S.A. Briggs, C.M. Barr, A.M. Monterrosa, C. Chisholm, L. Treadwell, B.L. Boyce, Sandia National Laboratories, USA

Understanding the response of coatings and thin films to harsh and often superimposed extreme environments is important for materials selection and prediction of device performance lifetimes. In order to explore the response of materials in these extreme environments, Sandia National Labs is developing, as part of the Center for Integrated Nanotechnologies (CINT) user facility, an in-situ ion irradiation and nanomechanics scanning electron microscope (SEM). The facility being developed couples a JEOL IT300-HRLV SEM with a HVE 6 MV Tandem accelerator and a 1.2 kV KRI KDC10 gridded ion source. This large-chamber field emission SEM can obtain 1.5 nm resolution, while supporting large samples and high tilt capabilities. The SEM can be operated at a range of pressures (up to 650 Pa) and temperatures (up to 800 C). In-situ SEM ion irradiation is achieved with a 6 MV tandem with available beam species ranging from 800 keV protons to 100 MeV Au ions. Low energy ions can be introduced directly from the tandem ion sources at 46 keV or from the directly connected 1.2 kV ion source that can implant gaseous species at high flux and at energies ranging from 100 eV to 1.2 keV. There are three options for in-situ SEM nanomechanical testing (MTI Fullham heating-straining stage, Hysitron PI-85 nanoindenter, and the custom-built piezo fatigue tester) that significantly expand the range of mechanical properties that can be explored in the SEM. To aid rapid structure and composition analysis during in-situ experiments, the SEM is being outfitted with high speed CMOS based EBSD and large area SSD EDS system. Finally, to provide automated in-situ SEM experiments, a LabVIEW code is being refined that permits direct communication between the SEM, the accelerators, and the nanomechanical stages. To demonstrate these new capabilities, a range of initial experiments will be highlighted including, but not limited to: in-situ compression of additively manufactured (AM) miniature bear figurines, in-situ SEM fatigue in Pt and Pt-Au tensile bars, and in-situ irradiation degradation of an AM composite resulting from 20 MeV Au.

This work was performed, in part, at the Center for Integrated Nanotechnologies, an Office of Science User Facility operated for the U.S. Department of Energy (DOE) Office of Science. Sandia National Laboratories is a multi-mission laboratory managed and operated by National Technology and Engineering Solutions of Sandia, LLC, a wholly owned subsidiary of Honeywell International, Inc., for the U.S. DOE's National Nuclear Security Administration under contract DE-NA-0003525.

3:00pm H3-2-WeA4 Proton Radiation and He Implantation Effect on Radiation-resistant Zr/Nb Sputtered Multilayer Coatings, T. Polcar (polcar@fel.cvut.cz), Czech Technical University in Prague, Czech Republic; M. Callisti, University of Cambridge, UK; S. Sen, H.Y. Yavas, Czech Technical University in Prague, Czech Republic; A. Lider, Tomsk State University, Czech Republic

Nanoscale metallic multilayers (NMMs) represent prospective material resistant to intensive radiation damage. Zr/Nb multilayered coatings with a periodicity (L) in the range $6 - 167 \text{ nm}$ were prepared by magnetron

sputtering and studied by a combination of transmission electron microscopy analyses and nanomechanical measurements to reveal deformation and strengthening mechanisms. We can control the mechanical properties by selected deposition conditions leading to various crystallographic orientation or even amorphous Zr layer, whereas Nb layer was kept identical (crystalline) for all depositions. For $L > 60$ nm, the strengthening mechanism is well described by the Hall-Petch model, while for $27 < L < 60$ nm the refined CLS model comes into picture. For $L < 27$ nm; plastic strain measured across compressed NMMs revealed a strong dependence of actual interface between layers. For selected crystallographic orientation Zr layer experiences a hard-to-soft transition. This transition can be avoided by change of crystallographic orientation of Zr layer. In such case, deformation causes structural transformation of Zr from hcp to bcc. The interfaces obtained by experiments are used as an input for DFT simulations to identify helium diffusion and agglomeration in pristine and radiation-damaged Zr/Nb interfaces. Finally, irradiation experiments will be discussed in detail.

3:20pm H3-2-WeA5 Tracking the Temporal Oxidation Behavior in TiN Thin Films by In-situ Resistivity Measurements, B. Stelzer (stelzer@mch.rwth-aachen.de), X. Chen, J.A. Sälker, J.M. Schneider, RWTH Aachen University, Germany

In order to estimate the expected remaining lifetime and safety of thin film components employed in high temperature applications, knowledge of the progress of oxidation is indispensable. A method to estimate the remaining film thickness by in-situ resistivity measurements during oxidation is introduced. To this end, Van-der-Pauw resistivity measurements were performed during oxidation at temperatures up to 720 °C on high power pulsed magnetron sputtered TiN thin films with dc magnetron sputtered Pt electrodes. Based on correlative ex-situ film morphology, structure and local composition data it is evident that the resistivity changes are caused by oxidation of TiN. Thickness measurements of the remaining TiN film thickness under the oxide layer are in very good agreement with calculated TiN thickness data deduced from in-situ resistivity measurements. Hence, we have demonstrated that the temporal oxidation behavior of TiN thin films can be tracked by time resolved in-situ resistivity measurements.

3:40pm H3-2-WeA6 Industrial XRF Coating Thickness Analyzer for Real Time Measurement of Aluminum Deposited on Rolled Steel, J.I. Hasikova (office@bsi.lv), A.D. Sokolov, A. Pecerskis, A. Pone, V. Gostilo, Baltic Scientific Instruments, Latvia

Aluminium coatings, deposited by Physical Vapour deposition on the rolled steel products, are more resistant to corrosion in the atmosphere than Zinc coatings. Real time monitoring of coating thickness is very important for the automatic quality control of coating deposition [1].

The industrial coating thickness analyser consists of XRF measuring head, integrated in the vacuum chamber, and remote electrical control unit, containing embedded microprocessor, spectrometric device, electronic circuits, power supply, etc. The measuring head of the analyzer is designed to generate and detect a secondary XRF line, radiated by the Aluminium coating on steel in vacuum. The measuring head is specially designed in order to protect vacuum in process chamber. It is also protected against overheating.

The industrial coating thickness analyser is integrated in the PVD Pilot Line. Measurement of coating thickness is performed directly in the process vacuum chamber. Cold rolled steel strips of different steel grades are used as substrates for PVD process. The amount of aluminium deposited on the surface of the steel strip is in the range from 1 to 20 g/m² on studied samples. Accuracy of thin film thickness measurement shown during pre-acceptance test was less than 10 % relative and precision was less than 5 % relative.

Thickness Analyser is included in the factory automatic control system for the technology processes. All data on current measurements in operating and calibration modes, of the status of all spectrometric equipment, including the state of X-ray tube and detector etc. can be transmitted to the computer of upper (factory) level. Based on real-time information about the thickness of the coating, the process engineer and operator can make the right decision to correct the deposition process.

1. A.Sokolov
[https://www.mdpi.com/search?authors=Aleksandr%20Sokolov&orcid=], J. Hasikova
[https://www.mdpi.com/search?authors=Jelena%20Hasikova&orcid=], A. Pecerskis
[https://www.mdpi.com/search?authors=Aleksej%20Pecerskis&orcid=], V.Gostilo
[https://www.mdpi.com/search?authors=Vladimir%20Gostilo&orcid=],
Wednesday Afternoon, May 22, 2019

K.Y.Lee
[https://www.mdpi.com/search?authors=Ki%20Yong%20Lee&orcid=], H.Jung
[https://www.mdpi.com/search?authors=Hoobok%20Jung&orcid=], J.H.Lim
[https://www.mdpi.com/search?authors=Jung%20Hyun%20Lim&orcid=]. Application of Industrial XRF Coating Thickness Analyzer for Phosphate Coating Thickness on Steel. *Coatings*2018, 8(4), 126.

4:00pm H3-2-WeA7 In situ Characterization of Dual Phase Diamond-like Carbon (DLC) at Elevated Temperatures, M. Chen (ming.chen@mat.ethz.ch), ETH Zürich, Switzerland; C. Liu, K.Y. Li, City University of Hong Kong, China; R. Spolenak, J.M. Wheeler, ETH Zürich, Switzerland

Diamond-like carbon (DLC) is routinely used as protective coatings due to their superior wear and friction resistance. However, DLC film is extremely brittle at ambient temperature because of covalent bonds and also notably degraded at elevated temperatures due to graphitization [1]. In this study, dual phases DLC films, i.e. sp² and sp³ phases, were deposited via closed-field unbalanced magnetron sputtering (CFUBMS) with various bias voltages. The microcompression testing at room temperature has revealed a high yield strength of $\sim E/11$ (E: elastic modulus) and a large plasticity of $\sim 70\%$ (engineering strain) [2]. This is attributed to the phase transformation of the bonding from sp² to sp³ under stress, which accommodates plastic strain and densifies the materials. The *in situ* micromechanical tests, e.g. microcompression and cantilever bending, were conducted at the elevated temperature range of 100–300 °C to further study the mechanical properties of DLC films at the detrimental temperature conditions. Raman spectroscopy and electron energy loss spectroscopy (EELS) were both applied to quantitatively determine the effect from the content of sp² and sp³ bonds on the mechanical performance. The microstructures after deformation were inspected using high resolution transmission electron microscopy (HRTEM) to elucidate the relationship of processing-structure-property.

[1] Y. Liu, E. Meletis, Evidence of graphitization of diamond-like carbon films during sliding wear, *Journal of Materials Science* 32(13) (1997) 3491-3495.

[2] C. Liu, Y. Lin, Z. Zhou, K.-Y. Li, Dual phase amorphous carbon ceramic achieves theoretical strength limit and large plasticity, *Carbon* 122 (2017) 276-280.

4:20pm H3-2-WeA8 In situ micro-Tensile Testing of TiN Coating: Deformation and Fracture in Relation to Residual Stress, E.J. Herrera Jimenez (erika.hj.06@gmail.com), École Polytechnique de Montréal, Canada; N. Vanderesse, École de Technologie Supérieure, Canada; T. Schmitt, É. Bousser, École Polytechnique de Montréal, Canada; P. Bocher, École de Technologie Supérieure, Canada; L. Martinu, J.E. Klemberg-Sapieha, École Polytechnique de Montréal, Canada

Interface engineering is essential to maintain the performance of protective coatings on metallic substrates during the entire product life. In particular, mechanical and microstructural properties of the coating/substrate system are of great importance in order to minimize material failure and improve durability. Deposition of hard coatings and plasma treatment processes can be used to induce compressive residual stress (RS) on the surface of the substrate and to delay the appearance of cracks and thus the material failure. This work presents a study of the effect of substrate plasma pre-treatment by different methods (ion bombardment, ion implantation, nitriding) on the RS of titanium nitride (TiN) coatings, which subsequently affects fracture behaviour of the coating-substrate system. TiN hard coatings with a hardness of $\sim 23 \pm 2$ GPa, Young's modulus = $\sim 250 \pm 20$ GPa were deposited by reactive magnetron sputtering onto Ti-6Al-4V aerospace alloy. Glancing angle X-ray diffraction (GAXRD) was used to assess RS profiles of the different coating/substrate interfaces, aiming to elucidate the effect of coating and plasma treatments processes on the Ti-alloy's RS. Each substrate treatment process affected the TiN coating compressive RS from 1 to 4 GPa. Failure mechanism of the coating/substrate interfaces was investigated through *in situ* micro tensile testing employing two configurations: 1) under a laser scanning confocal microscope for non-continuous test and 2) under a monochrome camera for continuous test using digital image correlation (DIC). The Stress-strain curves were obtained from both configuration tests, and for each coating/substrate interface were investigated the formation and propagation of multiple cracks in the thin hard coating, the crack onset strain (COS), energy release rate, stress intensity factor among others. Ti implantation, Ar bombardment and nitriding plasma treatments induced compressive RS into the substrate surface of the Ti-alloy of ~ 900 , ~ 1250 and ~ 1600 MPa respectively, with higher RS value the crack onset strain (COS) was delayed, while fracture toughness and energy release rate increased.

4:40pm **H3-2-WeA9 Small Scale Fracture of Mo₂BC Coatings**, **H.G. Gopalan** (h.gopalan@mpie.de), R.S. Soler, S.G. Gleich, C.K. Kirchlechner, C.S. Scheu, Max-Planck Institut für Eisenforschung, Germany; J.M. Schneider, RWTH Aachen University, Germany; G. Dehm, V.G. Arigela, Max-Planck Institut für Eisenforschung, Germany

A density functional theory based approach was used to identify Mo₂BC as a promising candidate for hard coatings with improved fracture properties. A bipolar pulsed direct current magnetron sputtering system was used to deposit a 3 mm thick film on silicon from room temperature to 630°C. An additional thin film was synthesized on sapphire substrate at 900°C. The microstructure of the coatings characterized by transmission electron microscopy reveals that the degree of crystallinity increased with increasing deposition temperatures. The crystalline films possess a columnar morphology with nanocrystalline dimensions. The micro fracture behavior of the free standing coating was characterized by focused ion beam milled pre-notched microcantilever bending tests performed *in situ* in a scanning electron microscope. All cantilevers fractured after purely elastic loading. The fracture toughness of the coatings showed a weak dependence on the substrate deposition temperatures with a maximum of 5 MPa m^{0.5}. Fractography revealed the fracture path was either intergranular or through amorphous regions. Additional nanoindentation based fracture toughness estimates were obtained on the coating substrate system showing substantially higher toughness values. The disagreement between the nanoindentation and microcantilever bending experiments was rationalized in terms of a difference in the residual stress in the films which were characterized by wafer curvature measurements. Microfracture experiments in conjunction with nanoindentation revealed Mo₂BC coatings are excellent candidates as coating materials with high hardness and respectable fracture toughness confirming density functional theory studies.

5:00pm **H3-2-WeA10 The Effect of Selected Laser Beam Micromilling Parameters on the Surface Layer Structure of HVOF Sprayed WC-CoCr Coating**, **A. Iwaniak** (aleksanderi@interia.eu), Silesian University of Technology, Poland; L. Norymberczyk, ANGA Uszczelnienia Mechaniczne Sp. z o.o., Poland

This study investigated the effect of laser beam micromilling on the surface layer structure of HVOF sprayed WC-CoCr coating. The carbide layer was HVOF sprayed onto flat test samples made of austenitic stainless steel 1.4571 using the Thermico system and CJS K5.2-N gun. Ultra fine-grained WC-CoCr (84/12/4) powder, particle size 10 µm, was used for coat spraying application. The surfaces of test pieces were ground and polished after spraying. Then surface ablation was carried out by micromilling pre-set rectangular-shaped recesses with a nanosecond MOPA pulsed fiber laser. The experiment was planned using the Taguchi method (L9 3³ orthogonal array). The process parameters examined were: laser power, pulse duration and laser beam scanning speed. Scanning Electron Microscopy / Energy Dispersive X-Ray Spectroscopy (SEM/EDS), X-ray Diffraction (XRD) phase analysis and 3D profilometry were used to evaluate structural changes. The effect of ablation process parameters (laser work parameters) on the treated coating surface condition, removed layer depth, surface roughness after the ablation process and treated coat phase composition was analysed. It was demonstrated that scanning speed reduction and laser pulse duration increase caused the increase of removed material layer thickness at a single beam pass. It was noted that laser treatment resulted in W₂C carbide formation on the treated WC-CoCr coating surface and molten material accumulated at the edges of the openings bored affecting their shapes and topography.

Acknowledgement:

The work was performed under the project co-financed under the European Regional Development Fund of the Silesian Center of Entrepreneurship (Agreement No.: UDA-RPSL01.02.00-24-0698/16-00).

Topical Symposia

Room Pacific Salon 3 - Session TS1-2-WeA

High Entropy and Other Multi-principal-element Materials II

Moderators: **Diederik Depla**, Ghent University, Belgium, **Ulf Jansson**, Uppsala University, Angstrom Laboratory, Sweden

2:00pm **TS1-2-WeA1 Structure and Mechanical Properties of Refractory Type High-entropy Alloy Thin Films Deposited by Vacuum-arc**, **M. Kuczyk** (martin.kuczyk@iws.fraunhofer.de), U. Nimsch, O. Zimmer, J. Kaspar, F. Kaulfuss, A. Leson, M. Zimmermann, C. Leyens, Fraunhofer Institute for Material and Beam Technology (IWS), Germany

High-entropy alloys (HEA), comprised of five or more principal elements in near equimolar ratios, have attained increasing attention, since they have demonstrated many exciting properties such as high hardness and wear resistance, high strength at elevated temperatures and high thermal stability or a desirable balance of structural and functional properties. Hence, it is supposed that coatings from HEAs will also exhibit such promising properties.

In the current work a series of refractory type HEA metal and nitride thin films were synthesized by means of vacuum-arc deposition technique. For this pre-alloyed targets of TiVbZrMo, TiVbZrHf and TiNbZrHfTa were vaporized in argon and nitrogen atmosphere. The film microstructure was analyzed applying high resolution electron microscopy (SEM and TEM) as well as X-ray diffraction. Moreover nanoindentation was used to determine the hardness and elastic modulus of the different coatings.

The results of the structural analysis reveal, that all metallic coatings exhibit a single phase bcc and all nitride layers a single phase fcc structure with more or less strong columnar grain growth. The hardness of the metallic HEA coatings is typically about 10 GPa, whereas the hardness of the nitride coatings is above 25 Gpa, clearly depending on the chosen material system.

Due to their high hardness the obtained multi-element nitride coatings are regarded as promising candidates for cutting tool application. It is furthermore concluded, that further improvement of mechanical properties of the metallic and nitride HEA coatings should be feasible by additionally applying a nanostructured design.

2:20pm **TS1-2-WeA2 Templated Stacking of Organic/Inorganic Semiconductors Crystals Upon Coalescence, Assembly and Split Behaviors of High-entropy Ferroelectric Lamellar Crystals**, **J.-J. Ruan** (jjrjeng@mail.ncku.edu.tw), C.-H. Pan, J.-M. Ting, K.-S. Chang, Y.-H. Su, National Cheng Kung University, Taiwan

The cocrystallization of multiple principle elements with near-equimolar ratio has been widely pursued as an approach to create high-entropy alloys, which likely involves plentiful spatial distribution patterns of constituent elements within crystal lattices and therefore fruitful physical properties. In the field of organic materials, the cocrystallization of two disparate organic compounds is also feasible, but, nevertheless is rarely found. Upon the random incorporation of trifluoroethylene (TrFE) and vinylidene fluoride (VDF) motif within random copolymer poly(vinylidene fluoride trifluoroethylene) (PVDF-TrFE), possible routes of cocrystallization of VDF and TrFE motifs are studied, and several ferroelectric crystalline phases were found able to grow concurrently. For the development of each crystalline form, there is an appropriate composition range of TrFE motif, instead of a specific composition. Above the Curie temperature, all the crystals transform into the high-temperature phase, and unique secondary crystallization behaviours are involved, which initiates lamellar coalescence and assembly. As a result, previous crystals lattices composed of various compositions and helical conformers are integrated together into one crystals, rendering the high-temperature lattice packing as a kind of high-entropy crystalline form.

For the transportation of charge carrier within organic/inorganic semiconducting thin films, continuous pathways are realized to critically rely on stacking and growth pattern of semiconductive crystals. Hence, based on initiated coalescence and assembly behavior of crystalline lamellar of PVDF-TrFE, adjustable stacking pattern of PVDF-TrFE lamellar crystals upon the mixing with poly(methyl methacrylate) (PMMA) have been further studied and adopted as the guiding template for the crystallization of organic/inorganic semiconductors. With the presence of regular stacking arrays of ferroelectric PVDF-TrFE lamellar crystals, oriented crystals growth of convention organic semiconductor like 6,13-bis(triisopropylsilyl)ethynyl pentacene (TIPS pentacene) and fullerene derivative of [6,6]-phenyl C61 butyric acid methyl ester (PCBM) has been identified. In addition, oriented

Wednesday Afternoon, May 22, 2019

crystallization of 2D lead-free perovskite (PEA)₂SnI₄ crystals were explored in this research as well, which is classified as a kind of 2D materials and less subject to environmental moisture. Based on unveiled guiding effects of stacking arrays of PVDF-TrFE lamellar crystals, the physics and also possible routes to harvest the merits of coexistent constituent phases have been acknowledged.

2:40pm TS1-2-WeA3 Angular-dependent Deposition of High Entropy Alloy Thin Films by DCMS, HIPIMS and Cathodic Arc, A. Xia (ao.xia@unileoben.ac.at), Montanuniversität Leoben, Austria; A. Togni, University of Modena and Reggio Emilia, Italy; S. Hirn, Montanuniversität Leoben, Austria; L. Lusvarghib, University of Modena and Reggio Emilia, Italy; R. Franz, Montanuniversität Leoben, Austria

In recent years, high entropy alloys (HEAs) have emerged as a new class of materials. These typically metallic alloys consist of 5 to 13 metallic elements in an approximately equimolar ratio. Studies conducted on HEA bulk materials revealed promising combinations of properties, such as high strength, corrosion resistance, high wear resistance, high hardness and sluggish diffusion. While research on bulk HEAs has seen quite a boost over the past years, HEAs as thin films are still a relatively unexplored area.

The current work examines the influence of different physical vapor deposition methods on structure, chemical composition and properties of HEA thin films at different deposition angles. MoNbTaVW and AlCuCrTaTi HEA thin films were deposited by cathodic arc deposition (CAD), direct current magnetron sputtering (DCMS) and high-power impulse magnetron sputtering (HIPIMS). The HEA thin films were deposited on Si substrates which were positioned at angles from 0° up to 90° in steps of 15° with respect to the cathode surface normal. The achieved coating thickness varied from 0.3 to 3.2 μm depending on deposition technique and angle. According to scanning electron microscopy and X-ray diffraction, the HEA thin films revealed a smooth surface with columnar growth characteristics and a bcc crystal structure regardless of the deposition method. The chemical composition of the coatings was analyzed by energy dispersive X-ray spectroscopy which revealed, e.g., that W and Ta, the heaviest elements in the composition, are the most abundant elements at a deposition angle of 0° in the MoNbTaVW films deposited by CAD. However, their atomic percentage decreases with increasing deposition angle and at 90° the HEA thin films were enriched in V, the lightest element. Finally, mechanical properties of the synthesized HEA thin films were determined by nanoindentation to compare the impact of the deposition technique on the hardness and elastic modulus of the synthesized HEA films.

3:00pm TS1-2-WeA4 Combustion Synthesis of High Entropy Alloys Thin Films: AlCrFeNi, AlCrCuFeNi, and AlCoCrFeNi, A.N. Wang (anni.wang@tu-ilmenau.de), M. Hopfeld, T. Kups, D. Flock, H. Romanus, L.-B. Kellmann, H. Rupapara, P. Schaaf, Technische Universität Ilmenau, Germany

This study presents combustion synthesized High Entropy Alloy (HEA) thin films through physical vapor deposition (PVD). By that, metallic multilayer coatings were produced with different multilayer scales in a total thickness of around 900 nm. AlCrFeNi, AlCrCuFeNi, and AlCoCrFeNi were selected due to their large negative enthalpy of formation and superior physical and chemical properties. Several stacking sequences of CrNi, AlFe, CoFe, Cu were deposited onto an as-prepared Ni-Al reactive layer on a Cu substrate; afterward, the coatings were removed from the Cu substrate to form a free-standing HEA thin film. Two fabrication methods were conducted in comparison: combustion synthesis via spark ignition and thermal treatment via rapid thermal annealing. The propagation velocity and temperature during combustion synthesis were monitored by using a high-speed camera and a pyrometer. The reaction products were then analyzed by means of a scanning electron microscope (SEM), X-ray diffraction (XRD) and transmission electron microscopy (TEM) to identify the phase transformation and stability related to the layer stacking as well as annealing temperature. The compositional profile and uniformity were measured via EDX analysis with SEM, and Auger electron spectroscopy. A spark voltage of 12 V for stacking layers of 30 nm was shown to be sufficient despite the unstable and partial reaction. In the reacted region, grain sizes of 200 to 300 nm were observed from TEM images. In contrary to the annealed samples with random texture, the combustion synthesized ones showed highly textured HEA thin films as seen from XRD patterns. In this research, a new synthesis path for developing HEA thin films is first introduced, and the attempt to optimize a stable reaction through individual metal layers and thickness is demonstrated.

Acknowledgment

This study is supported by the postdoctoral fellowship program to promote the academic career of women at TU Ilmenau for habilitation. The author,

Wednesday Afternoon, May 22, 2019

Anni Wang, would like to especially thank the financial add of internal research funding from TU Ilmenau for her traveling expense to ICMCTF.

3:20pm TS1-2-WeA5 Nanostructured Highly Concentrated Solid Solution Alloy Coatings on a Zirconium Based Alloy, M.A. Tunes, S.E. Donnelly, Institute for Materials Science, University of Huddersfield, UK; P.D. Edmondson, Oak Ridge National Laboratory, USA; V. Vishnyakov (v.vishnyakov@hud.ac.uk), University of Huddersfield, UK

Highly Concentrated Alloys (HCAs) are a class of multicomponent alloys formed with two or more elements in close to equiatomic composition. The materials are lately also known as High Entropy Alloys (HEA). The alloys have enhanced phase stability in extreme environments. Aiming at to establish a protective coating on Zr-based alloys (or Zircalloys), equiatomic and non-equiatomic thin films from the FeCrMnNi system were deposited on both Si and Zircaloy-4 substrates at room temperature by ion sputtering. The microstructural features of the films has been performed by means of Transmission Electron Microscopy (TEM). The non-equiatomic thin film exhibited polycrystalline structure with nanometre-sized grains while in the equiatomic thin film, grains are bigger with sizes around of 100-200 nm. Planar defects, surface roughening and Ar bubbles were also observed in the microstructure of the films. Current theories of concentrated solid solution alloys and crystal nucleation have been applied to reflect on the results. Metallic alloys are well suited to form protective coatings on Zircalloys for the future Accident Tolerant Fuel (ATF) reactor assemblies. The experimental results obtained demonstrate the possibility of depositing highly concentrated solid solution alloy thin films as protective coatings for future ATF systems using Zircalloys as the nuclear-fuel cladding material at low homologous temperature. A study on their radiation resistance conducted using *in situ* TEM heavy ion irradiation will also be presented.

3:40pm TS1-2-WeA6 High Temperature Electrical Conductivity and Oxidation Resistance of V-Nb-Mo-Ta-W High Entropy Alloy Thin Films, Y.Y. Chen (yenyu0619@gmail.com), Ming Chi University of Technology, Taiwan; S.B. Hung, C.J. Wang, W.-C.J. Wei, National Taiwan University of Science and Technology, Taiwan; J.-W. Lee, Ming Chi University of Technology, Taiwan

Multi-principal element alloys, such as high entropy alloys (HEA), show outstanding thermodynamic, mechanical or thermal properties as compared with pure metals or binary alloys. Among several kinds of HEAs, the refractory element containing HEAs exhibit relatively high thermal stability and better mechanical properties at elevated temperature. In this study, the V-Nb-Mo-Ta-W high entropy alloy thin films with and without nitrogen doping were deposited on the substrate of AISI 316 stainless steel by a magnetron sputtering process. The oxidation resistance and electric conductivities of HEA thin films at elevated temperatures were evaluated for high temperature application. Crystal phases, chemical compositions, microstructures and mechanical property of these thin films were characterized by the x-ray diffraction, energy dispersive spectra, scanning and transmission electron microscopes, and nanoindenter, respectively. The electrical conductivity of V-Nb-Mo-Ta-W thin films are around 10⁷ S·cm⁻¹. The electrical conductivities of V-Nb-Mo-Ta-W and V-Nb-Mo-Ta-W-N thin films gradually decreased when the oxidation temperature increased. The decreasing tendency of electrical conductivity is due to the surface oxidation of thin films and formation of amorphous phase. The influence of nitrogen content, microstructure and phase evolution on the oxidation resistance and electrical conductivity of thin films under high temperature conditions will be discussed in this work.

4:00pm TS1-2-WeA7 Micro-mechanics of High Entropy Alloys: Size Effects and Rate Sensitivity, Y. Xiao, R. Spolenak, J.M. Wheeler (jeff.wheeler@mat.ethz.ch), ETH Zürich, Switzerland

INVITED
High-entropy alloys (HEAs) are comprised of four or more major alloying elements, where the individual elements typically exhibit concentrations between 5 and 35 at%. These alloys demonstrate exceptional properties (e.g. high strength, high toughness, good corrosion performance, et cetera) and represent a fascinating new field of metallurgy and materials science. Over the last few years, great advances have been made to understand the mechanical behavior of these alloys in the micron and submicron regimes. However, a systematic, experimental investigation of the influence of increasing the number of major components on the fundamental plasticity mechanisms is still missing. In this study, the deformation behavior of the medium-entropy alloy CrCoNi and high-entropy alloy FeCrCoNi is compared with more traditional unary and binary alloys (pure Ni and NiCo) by using *in situ* strain rate jump micropillar compression. This allows us to simultaneously determine both size effects and rate effects, which give a fingerprint of the fundamental plasticity behaviour, from a single sample set. From these results, we discuss the relationship between solid solution

Wednesday Afternoon, May 22, 2019

strengthening mechanisms and the number of major alloying elements and how this quantitatively relates to the observed deformation mechanisms.

4:40pm **TS1-2-WeA9 Is the Entropy of High Entropy Ceramics High?**, *J.M. Schneider (schneider@mch.rwth-aachen.de)*, *S. Evertz*, *D. Neuß*, *M.K. Steinhoff*, *D.M. Holzapfel*, RWTH Aachen University, Germany; *S. Koloszári*, Plansee Composite Materials GmbH, Germany; *P. Polcik*, PLANSEE Composite Materials GmbH, Germany; *H. Rueß*, RWTH Aachen University, Germany

Several reports have extended the high entropy alloy notion to ceramics and ultrahigh temperature ceramics. Here the configurational entropy of several so called ceramic high entropy alloys is estimated. Furthermore, (TiCrMoW)N, (TiVNbTa)N, (VNbTaCrMoW)N and (TiVZrNbHfTa)N thin films were grown and their thermal stability was evaluated. Based on the obtained thermal stability data of compounds with similar configurational entropy the conceptual significance of the high entropy ceramics notion is critically appraised.

5:00pm **TS1-2-WeA10 Next Generation Entropy Stabilized Material**, *J.-M. Ting (jting@mail.ncku.edu.tw)*, *J.J. Ting*, *K.-S. Chang*, *Y.-H. Su*, National Cheng Kung University, Taiwan

High entropy alloy (HEA) has been one of the most focused materials in the last decade and continues to be one that is still drawing a tremendous amount of attentions from academia and industry. While the research and development of HEA is being conducted world-wide, recent attention has also been paid to high entropy oxides (HEOs) and nitrides (HENS). Limited studies have shown the synthesis of various HEOs that exhibits unique structures and improved, unexpected properties. The studies in HEOs and HENS are still in its infant stage such that unlimited explorations are there. Also, in these studies, the vast majority of the materials are made in bulk, including powders. As a result, we have recently launched a study to investigated HEOs and HENS thin films as well as powders. Combinatorial deposition techniques are applied to make the films and non-conventional, facile methods are used to made the powders. The resulting materials, including a number of new HEOs, are subjected to microstructural analysis and a number of different physical/chemical characterizations. In particular, the thin film samples are investigated with tools that are capable of mapping the characteristics of the entire films. The materials are also examined for use in energy generation/storage and photocatalysis.

Awards Convocation and Honorary Lecture

Room Town & Country - Session HL-WeHL

Bunshah Award Honorary Lecture

6:25pm HL-WeHL3 R.F. Bunshah Award and ICMCTF Lecture: **Some Highlights from over Four Decades of Thin-film Science, J.E. Greene (jgreene@illinois.edu)¹**, University of Illinois, USA, Linköping University, Sweden, National Taiwan Univ. Science & Technology, Taiwan **INVITED**

As a graduate student at USC, I was growing epitaxial GaAs(001) films by liquid-phase epitaxy. The layers were of very high purity as demonstrated by Hall and photoluminescence measurements, but we had no techniques sensitive enough to determine the remaining residual impurities. This led me to develop glow-discharge optical spectroscopy (GDOS), the optical analog of modern SIMS. As-deposited films were sputter etched and a spectrometer used to scan the emission peaks arising from the decay of sputtered atoms excited in the discharge. We found that the primary residual impurity was Sn and, via the use of calibration samples (based upon Hall measurements), we determined absolute Sn concentrations (initial detection limit = 3×10^{16} atoms/cm³, 680 ppb). Since then, we, and many others worldwide, have employed GDOS to quantitatively measure dopant diffusion and ion-implantation profiles in III-V, SiGe, and solar-cell absorber layers. GDOS is also used to analyze bulk and thin-film alloys, for real-time process control (film growth rates and thicknesses) during sputter deposition, and for feedback control during high-rate reactive sputtering.

At UIUC, in addition to GDOS, I continued epitaxial semiconductor film growth, but switched to SiGe via UHV-CVD, metastable (III-V)_{1-x}(IV₂)_x (the "Greene" alloys) by UHV sputter deposition, and GaN by reactive-ion MBE. SiGe CVD was carried out in UHV in order to employ *in-situ* surface-science tools (RHEED, TPD, AES, XPS, UPS, HR-EELS, STM) to investigate atomic-scale growth kinetics. We developed models, with no fitting parameters, to accurately predict Si, Si_{1-x}Ge_x, Si_{1-x}C_x, and Ge_{1-x}Sn_x film growth rates, compositions, and doping profiles as a function of precursor partial pressures and deposition temperatures. The models are still used worldwide today. The Greene alloys (e.g.: (GaAs)_{1-x}(Ge₂)_x) were grown across pseudobinary phase diagrams and exhibited good thermal stability. They have interesting electronic transport, band structure, and phonon properties and are currently used in tunable photodetector and piezoelectric devices. The first high-resistivity single-crystal GaN films, both wurtzite and zincblende, were grown by MBE using evaporated Ga and 35 eV N₂⁺ ions. The layers, which had the highest electron mobilities yet reported, were used to determine hexagonal and cubic GaN band structures.

Following an invitation to present a Swedish Academy of Science Lecture in the 1980s, colleagues from Linköping University ignited my interest in transition-metal (TM) nitrides (and, recently, TM diborides). The field of nitride hard-coatings was already developing rapidly, but reported properties varied by up to orders of magnitude. Thus, we hoped to make a contribution by growing and measuring fundamental properties of single-crystal compounds and alloys of groups IIIB, IVB, VB, and VIB TM nitrides using tunable magnetically-unbalanced magnetron sputtering which, together with Bill Sproul, Dieter Münz, and Ivan Petrov (all Bunshah Award winners), we developed in 1992. We also demonstrated vacancy hardening, enhanced hardness in superlattices with alternate layers chosen to have large differences in shear moduli, strong electron/phonon interactions, enhanced ductility using alloy design via electronic structure, and self-organized nanostructures. With polycrystalline TM nitrides, we developed a process for real-time control of preferred orientation using high-flux/low-energy ion irradiation and, recently, the growth of fully-dense/low-stress/high-hardness alloys, with no substrate heating, based upon a novel hybrid dc-magnetron/HiPIMS approach. Last year, we were the first to demonstrate controlled B/TM ratios in diboride layers using strong external magnetic fields during magnetron sputtering and controlling pulse lengths, at constant power and frequency, during HiPIMS.

¹ R.F. Bunshah Awardee

Thursday Morning, May 23, 2019

Coatings for Use at High Temperatures

Room Pacific Salon 2 - Session A2-1-ThM

Thermal and Environmental Barrier Coatings I

Moderators: Sabine Faulhaber, University of California, San Diego, USA, Kang N. Lee, NASA Glenn Research Center, USA, Pantcho Stoyanov, Pratt & Whitney, USA

8:00am A2-1-ThM1 Mechanical Characterization and Modelling Issues for Thermal Barrier Coating Lifetime Assessment, V. Maurel (vincent.maurel@mines-paristech.fr), V. Guipont, Mines-ParisTech, France INVITED

One of the major challenges for protective coatings is to determine the time to failure of ceramic layer during ageing for both TBC and EBC. For TBC, scenarios of damage have been well established from decades, based on microstructure to damage analysis with an increase use of 3D measurement tools (synchrotron tomography, FIB). The aim of this paper is to review some experiments to modeling issues.

Firstly, the characterization of adhesion is a key factor in the evaluation of time to failure. The measurement of adhesion should be addressed including the analysis of scatter induced by both the methodology of measurement and the "natural" scatter associated to TBC process. Recently, the use of LASER Shock Adhesion Test (LASAT) has shown its capability for both ranking different coating solutions and evaluating the evolution of a given coating as a function of aging [1-2], limiting the scatter associated to measurement. Besides, the laser shock could be used to introduce a defect, an interfacial delaminated area, known in size and location. Thus, local adhesion properties could be determined [2].

Secondly, dealing with modeling of lifetime, different strategies have been discussed in the literature taking into consideration a typical multi-scaled problem. Local analysis of failure has shown its efficiency to model the link to microstructure and aging to local failure. However, for the time being, only macroscopic analysis enables to derive lifetime at the scale-length of a typical component (eg turbine blade). We develop macroscopic lifetime model based on adhesion testing [3,5]. Finally, the robustness of this kind of models has been analyzed through sensitivity analysis based on large numerical sampling. As a conclusion, the propagation of scatter from measurement to life modeling is evaluated and guidelines for experimental focus points have been derived.

References

- [1] Guipont, et al (2010). Journal of Biomedical Materials Research Part A, 95(4), 1096-1104.
- [2] Guipont, et al. "Interfacial toughness evolution under thermal cycling by laser shock and mechanical testing of an EB-PVD coating system." (2018). <http://dc.engconfintl.org/cgi/viewcontent.cgi?article=1033&context=tbvc>
- [3] Thourcier, C et al (2011). Interfacial damage based life model for EB-PVD thermal barrier coating. Surface and Coatings Technology, 205(13-14), 3763-3773.
- [4] Dennstedt, et al (2018). Crack Morphology in a Columnar Thermal Barrier Coating System. https://opus4.kobv.de/opus4-zib/files/6938/3DMS2018_AnneDennstedt.pdf
- [5] Theveneau, M. (2018). Internal report, Mines-ParisTech.

8:40am A2-1-ThM3 The Effect of Bond Coat Asperity Removal on the Lifetime of Atmospheric Plasma Sprayed Thermal Barrier Coatings, K.A. Kane (kenalankane@gmail.com), Oak Ridge National Laboratory, USA; M.L. Sweet, Praxair, USA; M.J. Lance, B.A. Pint, Oak Ridge National Laboratory, USA

Atmospheric plasma sprayed (APS) MCrAlY (M = Co, Ni) bond coats are inherently rough, typically being comprised of a mixture of convex and concave regions. Initially the roughness provides a high surface area platform for mechanical interlocking of a yttria stabilized zirconia (YSZ) top coat however after high temperature oxidation the convex asperities of the bond coat are prone to form multiphasic, nonhomogeneous thermally grown oxide (TGO). Non-uniform TGO growth is generally thought to have a deleterious effect on top coat adhesion and the removal of these regions should impact coating performance. In the presented work, CoNiCrAlY APS bond coats deposited onto Hastelloy-X substrates were modified to varying degrees (unmodified, lightly modified, and heavily modified) prior to YSZ deposition. The modifications resulted in large asperities being replaced with flat regions, leaving intact concavities and smaller asperities. Samples were isothermally exposed at 1100°C for 100 h to evaluate the effect modification has on TGO formation. Furnace cycle testing (FCT) at 1100°C/1-

h was used to gauge the effect modification has on coating lifetime. BS-SEM and EDS analysis of TGO formation and cracking behavior was used to elucidate the changes in FCT lifetime due to modification.

9:00am A2-1-ThM4 Effect of Superalloy Substrate on the Lifetime of Electron Beam Physical Vapour Deposited Thermal Barrier Coatings, C.L. Liu (liuchen126123@outlook.com), Y.C. Chen, P. Xiao, University of Manchester, UK

Previous studies have reported that the cyclic oxidation lifetime of thermal barrier coatings (TBCs) is affected by the composition of superalloy substrates [1-3]. The presence of titanium (Ti) in CMSX-4 has been reported to be detrimental to TBC lifetime because the Ti-rich oxides can degrade the thermally grown oxide (TGO)/bond coat interface adherence [4]. However, the mechanism of how the chemical composition of the substrate affect the lifetime of TBCs is still not fully understood. To further elucidate the effect of substrates on TBCs, the CMSX-4 and René N5 single crystal superalloys have been used as substrates for TBCs with Pt-diffused γ/γ' bond coats and electron beam-physical vapour deposited (EBPVD) yttria-stabilized zirconia (YSZ) top coats. The cyclic oxidation (1 h holding time at 1200°C) test has been carried out on TBCs with different substrates. It was found that TBC deposited on the CMSX-4 substrate exhibited an average lifetime 20% higher than that deposited on the René N5 substrate. Specifically, spallation of TBC occurred mainly along the bond coat/TGO interface for TBC with the René N5 substrate whereas, for TBC with the CMSX-4 substrate, failure occurred mostly along the TGO/YSZ interface and sometimes within the TGO. This suggests that the bond coat/TGO interface for TBC with the René N5 substrate might be degrade by the chemical composition diffused from the substrate into the coating. To confirm this, transmission electron microscope (TEM) with STEM (scanning transmission electron microscope)/EDX (energy-dispersive X-ray) detector was used to examine the TGO/coating interface of TBCs. Segregation of sulfur has been found at the bond coat/TGO interface of TBC with the René N5 substrate, while no impurity segregation was observed at the bond coat/TGO interface of TBC with CMSX-4 substrate. In addition, no Ti-rich oxides was found in the TGO on the CMSX-4 substrate, indicating that the lifetime of this TBC system is not affected by the presence of Ti in the substrate.

Reference

- [1] Pint BA, Haynes JA, Zhang Y. Surf Coat Tech 2010;205:1236-40.
- [2] Bouhanek K, Adesanya OA, Stott FH, Skeldon P, Lees DG, Wood GC. High Temperature Corrosion and Protection of Materials 5, Pts 1 and 2 2001;369-3:615-22.
- [3] Tawancy HM, Al-Hadhrami LM. J Eng Gas Turb Power 2011;133.
- [4] Tawancy HM, Mohamed AI, Abbas NM, Jones RE, Rickerby DS. J Mater Sci 2003;38:3797-807.

9:20am A2-1-ThM5 Self-Healing Thermal Barrier Coatings Produced by Laser Processing, W. Wei (BowenWei@my.unt.edu), J. Gu, S.S. Joshi, T. Huang, N.B. Dahotre, S.M. Aouadi, University of North Texas, USA

Thermal barrier coatings (TBCs) are widely applied to protect superalloy blades in gas turbines and jet engines that are subjected to high temperatures and corrosive environments. However, the dissimilarities between the coefficients of thermal expansion of the ceramic coatings and metallic substrates will cause thermal stresses and lead to the generation and growth of cracks. This will facilitate oxygen diffusion through the TBC, and a thermally grown oxide (TGO) will be generated between the TBC and the bond coat, which will ultimately lead to failure. A potential effective solution to overcoming this challenge is to grow a self-healing layer on the TBC. In this work, YSZ/Al₂O₃/SiC and YSZ/Al₂O₃/TiC self-healing model systems were produced by laser processing with the premise that the healing process occurs as a result of the oxidation of the carbide phase. The formation of the healing oxide phase was observed using X-Ray diffraction and its formation in the crack site was confirmed using cross-sectional scanning electron microscopy. The optimum process parameters to create a self-healing composite were determined. Finally, the impact of the self-healing overlayer on deformation and failure resistance as well as corrosion resistance at elevated temperatures was investigated.

9:40am A2-1-ThM6 Influence of Heat Treatment on Thermal Cyclic Fatigue Lifetime of TBC System, J.H. He (Jianhong.He@Oerlikon.com), T. Sharobem, Oerlikon Metco, USA

Heat treatment of a component with TBC coating in vacuum is a common industrial practice. However, there is no systematic investigation on its cause. This paper tested thermal cyclic fatigue lifetime of TBC systems heat treated in different levels of vacuum (as sprayed, heat treated in atmosphere, 0.5 mbar and 6.67 x 10⁻⁴ mbar) and found there are significant

Thursday Morning, May 23, 2019

difference in thermal cyclic fatigue lifetime. Detailed TGO examinations on cross section and EDS analysis indicate that TGO configurations in samples heat treated in different levels of vacuum is rationale of the differences in thermal cyclic fatigue lifetime.

10:00am **A2-1-ThM7 Environmental Barrier Coating Development for High Temperature SiC Ceramic Matrix Composite Components, M.M. Gentleman (Molly_Gentleman@praxair.com), M.L. Sweet, B. Richards, Praxair Surface Technologies Inc., USA**

The use of environmental barrier coatings (EBC) for the protection of ceramic matrix composites (CMC) has gained significant momentum among engine manufacturers to address increased operating temperatures in turbine engines. The development and success of these coatings is highly dependent on both the materials performance capabilities as well as the ability to develop dense and steam impermeable layers. For materials including the commonly used rare earth silicates, this requires tightly controlled powder feedstock, with high levels of composition and phase uniformity, and thermal spray deposition parameters, that result in uniform processing of all particles in the plume. In this talk, the advances made in the deposition capabilities of EBCs at Praxair Surface Technologies, Inc. will be presented. A focus will be placed on the deposition of rare earth silicate using advanced deposition technologies and feedstock production that meet the requirements of these complex materials coatings systems.

10:20am **A2-1-ThM8 Effects of Chemical Modification on Bond Coat Oxidation and Internal Stresses in Yb₂Si₂O₇ Environmental Barrier Coatings, B. Herren (bherren@caltech.edu), California Institute of Technology, USA; J. Almer, Argonne National Laboratory, USA; K. Lee, NASA Glenn Research Center, USA; K.T. Faber, California Institute of Technology, USA**

A key failure mode of environmental barrier coatings in steam environments is spallation, often caused by a thermally grown oxide (TGO) resulting from oxidation of the bond coat. Safeguarding against this failure mode can increase the usable lifespan of EBCs, with one approach focused on limiting oxide growth rate. This study examines the effects of topcoat compositional modification on oxide growth rate and internal stresses, by addition of Al₂O₃ or Al₂O₃-containing compounds, e.g., mullite and yttrium-aluminum-garnet, of a current state-of-the-art EBC (Si/Yb₂Si₂O₇). Cyclic steam oxidation tests of these EBC systems and post-exposure analyses were used to study the effects of oxide additions on TGO growth rate and microstructure; after 1000-hour exposures to high-temperature steam conditions, some modified EBC compositions showed significant reductions to TGO growth – in certain cases, larger than 80 percent. (K. N. Lee, J. Am. Ceram. Soc., doi: 10.1111/jace.15978). X-ray scattering of these same EBC systems at the Advanced Photon Source at Argonne National Laboratory was used to evaluate strain in the multilayer systems as steam oxidation progressed. Strain and the associated internal stresses for modified EBCs were evaluated with respect to TGO thickness and chemistry and compared to the baseline EBC composition for the same exposure conditions.

10:40am **A2-1-ThM9 Thermal Shock and CMAS Resistant Tunable Self-Healing Thermal Barrier Coatings, J. Gu (Jingjingu@my.unt.edu), W. Wei, T. Huang, S. Bakkar, D. Berman, R.F. Reidy, S.M. Aouadi, University of North Texas, USA**

Thermal barrier coatings (TBCs) are used to protect gas turbine blades from oxidation and corrosion. Commercial TBCs often exposed to sand, dust, ash, and other particulates in addition to elevated temperatures. Found in desert sands and volcanic ash, calcia-magnesia-alumina-silicate (CMAS) particles can degrade TBCs through chemical attack, and coating delamination and spallation, thus, limiting the durability of gas turbines in these environments. In this work, laser cladding was used to create a self-healing protective overlayer on TBC coatings to improve chemical and thermal resistance. Self-healing coatings were applied onto traditional yttria-stabilized zirconia (YSZ) layers. YSZ/Al₂O₃/SiC and YSZ/Al₂O₃/TiC overlayer coatings were deposited using a Nd:YAG laser. Within the overlayer, the carbide phase oxidizes and seals the porosity in the TBCs. After thermal cycling and CMAS tests, resulting phases were identified X-Ray diffraction. In addition, cross-sectional scanning electron microscopy was used to investigate the subsurface and interlayer damage and CMAS penetration occurring resulting from thermal cycling. The performance of these overlayers TBC was compared to the traditional TBCs.

11:00am **A2-1-ThM10 Variables Affecting Steam Oxidation Kinetics of Environmental Barrier Coatings, K. Lee (ken.k.lee@nasa.gov), NASA Glenn Research Center, USA**

Increased fuel efficiency is obtained through increased thermal efficiency of turbine engines by increasing the overall pressure ratio (OPR). Increased OPR

requires increased turbine inlet temperature, which is paced by advances in turbine hot section materials. SiC/SiC Ceramic Matrix Composites (CMCs) are the most promising materials to enable a quantum leap in temperature capability. Environmental Barrier Coatings (EBCs) are an enabling technology for CMCs by protecting them from water vapor-induced recession. Spallation of EBC induced by thermally grown oxide (TGO) resulting from steam oxidation is a key EBC failure mode. A logical approach to improve EBC life, therefore, is to reduce TGO growth rates. A study was undertaken to investigate the effect of two variables, EBC chemistry and CMC substrate, on TGO growth rates. Using Si/Yb₂Si₂O₇ as the baseline, various oxides were added in Yb₂Si₂O₇ to investigate the former, while various CMC substrates were used to investigate the latter. EBC was processed using air plasma spraying. Oxidation kinetics was determined using steam cycling test in 90% H₂O + 10% O₂. Correlations between oxidation kinetics, chemistry, phase, and microstructure are used to explain the effect of EBC chemistry and CMC substrate on TGO growth rates.

11:20am **A2-1-ThM11 High Temperature Investigations of Thermochemistry and Phase Stability in the ZrO₂-Y₂O₃-Ta₂O₅ System, M. Lepple (mlepple@web.de), DECHEMA Forschungsinstitut, Technische Universität Darmstadt, Germany; S.V. Ushakov, K. Lilova, University of California, Davis, USA; C.A. Macauley, C.G. Levi, University of California, Santa Barbara, USA; A. Navrotsky, University of California, Davis, USA**

Compositions in the ZrO₂-Y₂O₃-Ta₂O₅ system are of interest for new high performance thermal barrier coating applications due to their promising high-temperature properties. Alongside an extended tetragonal phase field stable to temperatures at least up to 1500 °C obtained by equimolar co-doping of Y³⁺ and Ta⁵⁺, the YTaO₄ phase field recently attracted attention. Both phase fields of interest lie on the ZrO₂-YTaO₄ quasibinary investigated in this work.

For high temperature applications, it is essential to understand phase stabilities and relations as well as energies and driving forces of the stable and metastable phases. Experimental and computational thermodynamics using the method CALPHAD (Computer Coupling of Phase Diagrams and Thermochemistry) gives a self-consistent description of the materials system, facilitating materials development. In this work, the energetics and phase stabilities of several compounds in the ZrO₂-Y₂O₃-Ta₂O₅ system were investigated experimentally. The enthalpies of formation of different phases as a function of composition were determined using high-temperature oxide melt solution calorimetry. Transition temperatures and enthalpies and phase stabilities were explored by differential thermal analysis (DTA) up to 2400 °C and in-situ high temperature synchrotron X-ray diffraction. The very high melting temperatures of the refractory oxides were investigated by measurement of cooling traces using laser melting. The enthalpy of fusion of YTaO₄ was determined using drop calorimetry on a laser heated aerodynamically levitated samples. The results will be used for CALPHAD modeling to obtain a comprehensive understanding of the thermochemistry of the quasibinary.

Hard Coatings and Vapor Deposition Technologies Room California - Session B6-ThM

Coating Design and Architectures

Moderators: Shou-Yi Chang, National Tsing Hua University, Taiwan, Paul Heinz Mayrhofer, Institute of Materials Science and Technology, TU Wien, Austria

8:00am **B6-ThM1 The Mechanical and Tribological Properties of Boron Based Films Grown by HiPIMS Under Different N₂ Contents, A. Keleş, I. Efeoğlu (iefeoğlu@atauni.edu.tr), Y. Totik, Ataturk University, Turkey**

The cubic phase of boron nitride (c-BN) has significant technological potential for thin film applications. It is generally compared with diamonds due to c-BN properties. c-BN is a semi-stable, high temperature and high pressure (HPHT) stable phase with high strength covalent bond and the second highest hardness. However, c-BN film has low adhesion at the interface due to high compressive internal stress. To overcome this problem, c-BN films were coated with HiPIMS-CFUBMS under three different N₂ contents (2.5 sccm, 3 sccm, 3.5 sccm). Before deposition of c-BN film, Ti-TiN-TiB₂-TiBN-TiBCN graded composite layers were coated for improving the adhesion. The structural properties were identified using SEM. The chemical properties were determined using XPS. The c-BN content and internal compressive stress were calculated using FT-IR. The mechanical properties were carried out by microhardness tester and scratch tester. The tribological properties were experimented with pin-on-disc tribometer. The maximum

Thursday Morning, May 23, 2019

hardness (45GPa) and minimum critical load ($L_c \gg 69N$) values were obtained from the lowest N_2 content (2.5sccm). Also, the minimum friction coefficient value was 0.622. The results showed that c-BN films coated with HiPIMS is very up-and-coming.

8:20am B6-ThM2 Peculiar Oscillations in Nano-scale AlN/TiN and Other Nitride-based Superlattices, N. Koutna (nikola.koutna@tuwien.ac.at), Institute of Materials Science and Technology, TU Wien, Austria; P.R. Řehák, Institute of Physics of Materials, Academy of Sciences of the Czech Republic, Czech Republic; Z. Zhang, Erich Schmid Institute of Materials Science, Austrian Academy of Sciences, Leoben, Austria; M. Černý, Central European Institute of Technology, CEITEC VUT, Brno University of Technology, Czech Republic; M. Bartosik, Institute of Materials Science and Technology, TU Wien, Austria; M.F. Friák, M.S. Šob, Institute of Physics of Materials, Academy of Sciences of the Czech Republic, Czech Republic; P.H. Mayrhofer, Institute of Materials Science and Technology, TU Wien, Austria; D. Holec, Department of Physical Metallurgy and Materials Testing, Montanuniversität Leoben, Austria

Superlattices with layer thicknesses of only a few nm cannot be simply understood based on the knowledge of their monolithic building components. Different phases and/or their mutual orientation together with the presence of interfaces may lead to peculiar physical phenomena, such as partial structural transformations, superhardening or supertoughening effects.

This talk centers around an AlN/TiN multilayered system, combining materials that are very popular in industrial applications. Though considerable experimental as well as modelling efforts have been devoted to AlN/TiN system, the atomic-scale effects of the interface are not fully understood. Our ab initio calculations reveal interplanar spacing oscillations stemming from the presence of the interface and the corresponding changes in the electronic structure. The character of these oscillations differs significantly in each material–AlN and TiN–based on the superlattice-forming phases (metallic TiN vs. semiconducting AlN, or cubic vs. hexagonal AlN) and their orientation (e.g., (001) vs. (111)), influencing the critical distance from the interface above which the oscillations disappear. The oscillatory behaviour of atomic displacements have also important consequences for elastic constants as well as the cleavage properties in terms of theoretical critical stress and energy for brittle cleavage. Our Density Functional Theory calculations are corroborated with observations from high resolution transmission electron microscopy. Consequently, atomistic reasons for superior mechanical properties of AlN/TiN multilayered systems are proposed. Our findings are compared with the relevant predictions for other superlattice architectures containing (meta)stable phases of transition metal nitrides.

8:40am B6-ThM3 Impact Fatigue and Mechanical Properties of AlTiCrN and AlTiCrSiN Hard Coatings with Optimal Design of Interlayers, Y.J. Yang (40371203@gm.nfu.edu.tw), Y.-Y. Chang, S.Y. Weng, National Formosa University, Taiwan

Optimal design of interlayers of a hard coating can offer an efficient way of controlling residual stress, improving adhesion strength and enhancing toughness. Transition metal nitrides, such as AlTiCrN, have been used as protective hard coatings due to their high hardness and high resistance to high temperature oxidation. In this study, AlTiCrN and AlTiCrSiN coating was deposited by cathodic-arc evaporation (CAE). During the coating process of AlTiCrN and AlTiCrSiN, TiN and CrN were deposited, respectively, as interlayers with different graded structures to control residual stress, toughness and adhesion strength between the coatings and substrates. The microstructure of the coatings was characterized by using a field emission scanning electron microscope (FE-SEM), equipped with an energy-dispersive x-ray analysis spectrometer (EDS). Glancing angle X-ray diffraction (XRD) was used to characterize the microstructure, phase identification and residual stress. The chemical composition was also evaluated. The thickness and alloy content of the deposited coating were correlated with the evaporation rate of cathode materials. Mechanical properties, such as the hardness and elastic modulus, were measured by means of nanoindentation and Vickers hardness measurement. To study the correlation between impact fracture resistance and hardness/elastic modulus ratio of the deposited coatings, an impact test was performed at 500 °C using a cyclic loading device with a tungsten carbide indenter as an impact probe. The results indicated that all the AlTiCrN and AlTiCrSiN coatings exhibited (Al,Ti,Cr)N solid solution phases with NaCl-type structure. The design of AlTiCrN hard coatings with optimal designed interlayers of CrN and AlTiCrN/CrN can decrease residual stress, enhance hardness and toughness, which were effective to elimination of cracking of hard coatings. The AlTiCrN and AlTiCrSiN hard coatings with

multilayered interlayers of CrN and AlTiCrN/CrN possessed the best resistance to plastic deformation and the highest impact fatigue resistance. The AlTiCrN and AlTiCrSiN hard coatings with optimal design of interlayers can be good candidates for piercing, punching and molding applications.

9:00am B6-ThM4 Improvement of CrMoN/ SiN_x Multilayered Coatings on Mechanical and High Temperature Tribological Properties, W.L. Lo (lowelly85@gmail.com), L.K. Yeh-Liu, J.W. Lee, J.G. Duh, National Tsing Hua University, Taiwan

In this study, CrMoN/SiN_x multilayered coatings were deposited by controlling the shutter-open time of two sputtering guns in a radio frequency magnetron sputtering system. CrMoN/SiN_x thin films with different bi-layer periods were fabricated on both Si-wafer and Inconel-718 substrates. The chemical composition of as-deposited CrMoN/ SiN_x coatings were obtained by a field emission electron probe micro-analyzer (FE-EPMA). The confirmation of multilayered structure and crystallization characterization were carried out using a transmission electron microscope (TEM). The phases of the coatings were analyzed by a grazing incidence X-ray diffraction (XRD). Mechanical and high-temperature tribological properties were estimated using a nano-indenter and a high-temperature tribometer (ball-on-disc), respectively.

The grain refinement phenomenon was verified using XRD peak broadening at high angles, indicating inhibition in the column structure and the formation of an amorphous phase. The CrMoN/SiN_x multilayered coatings exhibited high-temperature tribological properties for a specific bi-layer period, which was attributed to the multilayer strengthening mechanism. Multilayered structure provided enormous benefit to COF improvement, which was reduced by 50% of the value of CrMoN. In the meanwhile, the toughening effect of the multilayered structure design also improved the wear resistance ability of the coatings. Moreover, the best bi-layer period was identified, resulting in favorable mechanical and high-temperature tribological properties. Eventually, a CrMoN/SiN_x multilayer coating with enhanced high-temperature characteristics was demonstrated and discussed in this study.

9:20am B6-ThM5 Tuning the Hardness–toughness Relationship by Combining MoN with TaN, F.F. Klimashin, N. Koutna, L. Lobmaier, T. Wien, Institute of Materials Science and Technology, Austria; D. Holec, Montanuniversität Leoben, Austria; P.H. Mayrhofer (paul.mayrhofer@tuwien.ac.at), TU Wien, Institute of Materials Science and Technology, Austria

Recently we showed that cubic-structured Mo–N and Ta–N exhibit an inherent driving force for vacancies at the nitrogen and metal sublattice, respectively. To shed light on their interaction and effects on structural evolution and mechanical properties within the ternary system Mo–Ta–N, we have synthesised coatings by means of reactive magnetron sputtering with varying nitrogen partial pressure. Low nitrogen partial pressures, resulting in high concentration of vacancies on the N sublattice, allow one to stabilise single-phase cubic-structured solid solutions up to a high metal fraction of Ta of $x = Ta/(Mo+Ta)$ of at least 0.76. These solid solutions form with vacancies predominantly at the nitrogen sublattice, with increasing vacancy concentration upon increasing x . Furthermore, with increasing x to 0.56, also the compressive residual stresses increase to -2 GPa, the hardness increases to 36 GPa, and the fracture toughness increases to 7 MPaVm. Schottky defects, energetically favoured at higher tantalum concentration (at least up to $x = 0.76$), cause in turn the relaxation of compressive residual stresses to -1.3 GPa and reduction in hardness to 29 GPa and fracture toughness to 5 MPaVm. On the contrary, high nitrogen partial pressures favour vacant sites on the metal sublattice of cubic-structured solid solutions, which are the major constituent in these dual-phased coating. The hardness of these dual-phase coatings is mainly determined by the fraction of the coexisting hexagonal phase, which appears to be the harder constituent. However, neither hexagonal phases nor vacancies at the metal sublattice are desirable when aiming to combine high hardness with high fracture toughness in this Mo–Ta–N system. The fracture toughness would be reduced to 2.5 MPaVm. The binary γ -MoN_{0.89} with partially ordered vacancies on metal and non-metal sublattices possesses the highest toughness among all coatings studied with 8 MPaVm, while showing a moderate compressive residual stress of -2 GPa and hardness of 28 GPa. Our findings show that by combining materials with a driving force for metal or nitrogen vacancies, both routes of structural evolution can be designed, allowing to tune their mechanical and elastic properties.

Thursday Morning, May 23, 2019

9:40am **B6-ThM6 Microstructure, Mechanical and Tribological Performance of Complex TiAlTaN-[TiAlN/TaN_n] Coatings: Understanding the Effect of Volume Fraction, E. Contreras (elbert.contreras@udea.edu.co), J. Cortínez, Universidad de Antioquia, Colombia; A. Hurtado, Centro de Investigación en Materiales Avanzados CIMAV, Mexico; M.A. Gómez, Universidad de Antioquia, Colombia**

Recent studies have shown that by modifying the coatings architecture it is possible to obtain significant improvements in their mechanical and tribological properties. In the present work four complex TiAlTaN-[TiAlN/TaN_n] coatings were deposited, varying the volume fraction of the top quaternary coating (TiAlTaN) and the base multilayer coating (TiAlN/TaN) with percentages of: 20/80, 40/60, 60/40 and 80/20, and evaluating their effect on mechanical and tribological performance of the complex coatings. The cross-sectional images obtained by FIB-SEM showed the interface between each of the constituent monolayers, a well-defined columnar structure was also observed for the TiAlN/TaN multilayer coating, while in the quaternary TiAlTaN coating a refinement was observed in the columns with denser and compact structures. High-resolution TEM analysis revealed well-formed multilayer composites with very smooth layers. The complex TiAlTaN-[TiAlN/TaN_n] coatings did not exhibit a significant difference in their crystalline structure, however, once calculating the residual stresses by XRD, it was found that by increasing the volume fraction of the multilayer in the coatings there is a decrease in the compressive residual stresses. Regarding the mechanical properties, it was possible to observe an increase between 20-25% when increasing the volume fraction of the multilayer, as well as an increase in resistance to plastic deformation (H^3/E^2), fracture toughness and in the adhesion of complex architecture coatings. With respect to tribological properties, TiAlTaN-[TiAlN/TaN_n] coatings exhibited lower friction coefficients and wear rates compared to constituent monolayers. Using cross-section FIB it was possible to observe initial deformation in the constituent layers followed by the propagation of cracks along the interfaces between TiAlTaN, TiAlN and TaN layers, in nanoindentation tests, scratch tests and tribological tracks.

10:00am **B6-ThM7 Plastic Deformation in Transition-Metal Nitrides and Carbides via Density-Functional Molecular Dynamics, D.G. Sangiovanni (davide.sangiovanni@liu.se), Linköping University, Sweden, Ruhr-Universität Bochum, Germany**

INVITED

Hard refractory transition-metal nitrides and carbides (TMN and TMC) possess unique combinations of outstanding physical and mechanical properties. As most ceramics, however, TMN and TMC are typically inherently brittle. Recent theoretical and experimental results have demonstrated that TMN can be made *both hard* (~20 – 25 GPa) *and ductile* via manipulation of electronic structures and control of phase stability. This surprising finding addressed a long-standing question in materials science on whether hardness and ductility are necessarily mutually exclusive properties in a single-crystal ceramic phase. Nevertheless, it is still puzzling how high hardness and excellent ductility may coexist given that the two properties are affected in opposite manner by plastic deformation.

This seminar will be divided in three parts. (i) I will first describe density-functional theory results to explain the effects induced by valence electron concentrations and phase stabilities on toughness of TMN and TMC; (ii) Then, I will show the results of finite-temperature *ab initio* molecular dynamics (AIMD) simulations of tensile, shear deformation, and nanopillar compression to clarify the atomistic pathways with associated changes in electronic structures responsible for brittleness (TiN and VN) vs. supertoughness (VMoN, VN_x); (iii) Finally, I will give an overview of AIMD simulations for slip system activation/quenching as a function of temperature and pressure to demonstrate unusual non-Schmid behavior in TMC. All first-principles results will be discussed in comparison with, and supported by, experimental findings.

10:40am **B6-ThM9 Phase Evolution and Mechanical Properties of Isostructural Decomposing W_{1-x}M_xB₂ Thin Films, V. Moraes (vincent.moraes@tuwien.ac.at), L. Zauner, TU Wien, Institute of Materials Science, Austria; H. Bolvardi, Oerlikon Balzers, Oerlikon Surface Solutions AG, Liechtenstein; P. Polcik, Plansee Composite Materials GmbH, Germany; H. Riedl, P.H. Mayrhofer, TU Wien, Institute of Materials Science, Austria**

The increasing demand in various industrial applications calls for a target-driven development of protective coatings with exceptional properties. Therefore, transition metal nitrides have been studied and developed extensively. However, the exploration of new protective coating systems is required to meet upcoming challenges not only in machining applications. A rather new promising class of materials – to be used as protective thin films – are borides. Especially, multinary borides are rather unexplored compared

to their nitride-based counterparts. Coherent phase separation effects of supersaturated single-phased structures such as age hardening in Ti_{1-x}Al_xN based thin films was a key-factor for the success being nowadays one of the most important material combination in thin film industries. The formation of coherent domains through spinodal decomposition (Ti_{1-x}Al_xN into TiN- and AlN-rich cubic domains) allows for significant strengthening effects at elevated temperatures (for example, as obtained during application). Transferring the concept of two competing phases from nitrides to borides is a promising approach to find new materials with outstanding properties already in the as deposited state. Different *ab initio* and experimental studies [1-3] already showed that WB_{2-x} thin films preferable crystallize in their metastable α -AlB₂ modification (space group 191), being an excellent origin for ternary alloying concepts considering the decomposition to its stable ω -W₂B_{5-x} configuration (space group 194).

In this study, we experimentally investigated the structural and mechanical evolution for selected ternary W_{1-x}M_xB₂ based thin films concerning spinodal decomposition. Especially, not only the effect of coherent phase separation on the hardness but also fracture toughness has been correlated with temperature. This aspect is highly important, as most of the α -AlB₂ structured diborides (e.g. TiB₂, ZrB₂, or CrB₂) suffer extremely low damage tolerance. In addition, the phase evolution with respect to structural defects (e.g. metal or boride vacancies) was also investigated by *ab initio* based calculations.

Keywords: W₂B_{5-x} based diborides; multinary borides; mechanical properties; coherent phase separation;

[1] B. Alling, H. Högborg, R. Armiento, J. Rosen, L. Hultman, *Sci. Rep.* 5 (2015) 9888.

[2] V. Moraes, H. Riedl, C. Fuger, P. Polcik, H. Bolvardi, D. Holec, P.H. Mayrhofer, *Sci. Rep.* 8 (2018) 9288.

[3] V. Moraes, C. Fuger, V. Paneta, D. Primetzhofer, P. Polcik, H. Bolvardi, M. Arndt, H. Riedl, P.H. Mayrhofer, *Scr. Mater.* 155 (2018) 5–10.

11:00am **B6-ThM10 Van der Waals Layer Promoted Heteroepitaxy in Sputter-deposited Thin Films, K. Tanaka (koichitanaka@ucla.edu), P. Arias, M.E. Liao, Y. Wang, H. Zaid, A. Aleman, M.S. Goorsky, S. Kadambaka, University of California, Los Angeles, USA**

We demonstrate that the crystallinity of sputter-deposited thin films can be significantly improved using two-dimensional (2D) van der Waals (vdW) layered materials as the buffer layers on substrates. Using hexagonal boron nitride (hBN) ($a = 0.250$ nm and $c = 0.667$ nm) as the 2D vdW buffer layer, we grow trigonal-structured Ta₂C ($a = 0.310$ nm and $c = 0.494$ nm) thin films of desired thickness ($t = 17 \sim 75$ nm) on Al₂O₃(0001) substrates via ultra-high vacuum direct current magnetron sputtering of TaC compound target in 20 mTorr pure Ar gas atmospheres at 1373 K. hBN layers are deposited via pyrolytic cracking of borazine (~600 L) onto Al₂O₃(0001) substrates at 1373 K. The as-deposited Ta₂C films are characterized *in situ* using Auger electron spectroscopy and low-energy electron diffraction and *ex situ* using X-ray diffraction (XRD) and transmission electron microscopy (TEM) based techniques. For the same Ta₂C film thickness, the notable differences in the layers deposited on hBN-covered Al₂O₃(0001) compared to those grown on bare substrates are: observation of 6-fold symmetric LEED pattern, significantly stronger (20x) 0002 reflection intensity in ω -2 θ XRD scans, and observation of Laue oscillations around the 0002 peak. Furthermore, we show that inserting hBN layers at regular intervals results in highly-0002-oriented growth and suppression of polycrystallinity in thicker Ta₂C films.

11:20am **B6-ThM11 Improvement of Tribological Properties for Hard Coatings by Stress Control, T.M. Shao (shaotm@tsinghua.edu.cn), State Key Laboratory of Tribology, Tsinghua University, China**

For the application of hardcoatings, stress level in coating/substrate systems is one of the main factors influencing their tribological properties. In many applications, effective control of stresses is of great importance for the performance and working life of hard coatings. Generally, the stress inside coatings subjected during service is a combination of external stress and intrinsic stress. The external stress is mainly determined by the applied working load, and the intrinsic stress depends on the coating material, the structure of coating, property mismatch between coating and substrate, coating production process, etc. In this presentation, control of intrinsic stress by properly design of coating/substrate system is studied. As examples, studies on stress control by textured coating technique and design of layered structures are introduced. Tribological properties of several hard coatings are experimentally studied and the results are discussed based on stress analysis. Results show that both textured coating and layered

structure can be used for stress control of coating/substrate systems, and eventually improving their tribological properties.

Keywords: stress control; tribological property; hard coating; textured coating; layered structure

11:40am B6-ThM12 Is WB_{2-x} a Proper Base System for Designing Ternary Diboride based Thin Films?, H. Riedl (helmut.riedl@tuwien.ac.at), V. Moraes, C. Fugger, H. Euchner, R. Hahn, T. Wojcik, TU Wien, CDL AOS at the Institute of Materials Science, Austria; M. Arndt, Oerlikon Balzers, Oerlikon Surface Solutions AG, Liechtenstein; P. Polcik, Plansee Composite Materials GmbH, Germany; P.H. Mayrhofer, TU Wien, Institute of Materials Science, Austria

Future tasks in many different fields of academia and industry are directed towards environmental sustainability, and hence the application of ultra-stable materials featuring novel properties. A rather new and highly promising class of thin film materials are borides. Especially, transition metal borides (TMBs) exhibit a tremendous potential to be applied in various applications ranging from wear and corrosion resistant coatings, to superconductive thin films, or as superhard and extremely stable protective layers in diverse fields of engineering. In contrast to classic diborides – such TiB₂, ZrB₂, WB₂, or ReB₂, which has been theoretically predicted to be the most incompressible material exceeding the properties of diamond – are ternary or even multinary diborides (e.g. W_{1-x}M_xB₂) relatively unexplored. Based on atomistic modelling studies [1,2] (Density Functional Theory calculations) is the stabilization of ternary diborides dominated by two hexagonal competing structure types – α -AlB₂-prototype (SG-191) vs. ω -W₂B_{5-x}-prototype (SG-194) – as well as structural defects (especially vacancies). These facts emphasize distinct difficulties for PVD based synthesis of ternary diboride thin films.

Within this study, we want to address the challenges in depositing ternary diborides in a prototype based on α -W_{1-x}M_xB₂ solid solutions, applying non-reactive sputtering processes, whereas M represents different transition metals such as Ta or Ti [2]. Due to the strong tendency of WB₂ to be stabilized through structural defects in the AlB₂ structure type – exhibiting distinct advantages concerning the relatively low ductility of TMBs in general – it can be an excellent base system for studying various alloying concepts utilizing physical vapour deposition (PVD) techniques. To gain an in-depth insight on the specific effects of selected transition metals on α structured W_{1-x}M_xB₂ coatings, we correlated the synthesis parameter with structure property relationships applying a set of high-resolution characterization techniques as well as micro-mechanical testing methods – also after exposing to diverse aggressive- environments in terms of oxidation and thermal treatments.

References

- [1] B. Alling, et al., A theoretical investigation of mixing thermodynamics, age-hardening potential, and electronic structure of ternary M(1)_{1-x}M(2)_xB₂ alloys with AlB₂ type structure, *Sci. Rep.* 5 (2015) 9888.
- [2] H. Euchner, et al., Solid solution hardening of vacancy stabilized Ti_xW_{1-x}B₂, *Acta Mater.* 101 (2015) 55–61.

Fundamentals and Technology of Multifunctional Materials and Devices

Room Pacific Salon 3 - Session C3+C2+C1-ThM

Thin Films for Energy-related Applications II/Novel Oxide Films for Active Devices/Optical Metrology in Design, Optimization, and Production of Multifunctional Materials

Moderators: Per Eklund, Linköping Univ., IFM, Thin Film Physics Div., Sweden, Tushar Shimpi, Colorado State University, USA

8:40am C3+C2+C1-ThM3 Nanoflaky Titanium Dioxide Grown on Titanium Foil for Capacitive Deionization Purpose, J.T. Huang (jacky841008@gmail.com), P.-Y. Hsieh, J.L. He, Feng Chia University, Taiwan
Capacitive deionization (CDI) is considered to be one of the most promising technologies for many water treatment and purification applications. To meet the demand for pursuing high efficiency of desalination, the key component, CDI electrode, requires high chemical stability, high specific surface area, high water wetting ability, and suitable porous structure for ion electrosorption. In this study, a facile approach involving alkali treatment followed by post-annealing was utilized to develop nanoflaky titanium dioxide (TiO₂) structure on titanium (Ti) foil. Furthermore, the feasibility of using nanoflaky TiO₂ grown Ti as electrode for CDI application was evaluated.

The results showed that the grown TiO₂ possessed a porous nanoflaky structure with a mixed-phase of anatase and rutile; in addition, the porous size is in the range of 30 ~ 100 nm. Such microstructure characteristics implies a high specific surface area. Superhydrophilic surface property was also obtained for this nanoflaky TiO₂ structure. According to the cyclic voltammetry results, the nanoflaky TiO₂ grown Ti electrode exhibited electrosorption/electrodesorption ability in 1 M sodium chloride solution, indicating the stability and regeneration. Finally, the deionization performance of flow-through CDI device using nanoflaky TiO₂ grown Ti electrode was demonstrated.

9:00am C3+C2+C1-ThM4 Mixed-oxide Coated Ni Foam for High Performance Supercapacitor, K.C. Lin (joelin820516@gmail.com), National Cheng Kung University, Taiwan

Supercapacitors have become a popular energy storage device in the past ten years, owing to its excellent properties in many aspects, like electrical conductivity, cycle stability, and higher power density than lithium battery. However, the biggest challenge for supercapacitors to compete with the Li battery is energy density, i.e., its discharging time is still insufficient to satisfy for many desired applications. Therefore, we have studied a novel supercapacitor electrode made out of a mixed transition metal oxide grown on Ni foam to combat this problem. The mixed transition metal oxide is MnCo₂O₄ was synthesized using a one-pot synthesis involving hydrothermal treatment. We show that simply varying the precursor concentration would lead to the formation of MnCo₂O₄ nanostructures having different morphologies. The resulting MnCo₂O₄ provides more oxidation states that can participate in the electron transfer than monoxide. Several material characterizations and electrochemical tests were performed. Moreover, we demonstrate that the novel electrode gives very excellent specific capacitance of 1,740 F/g and stability after 5,000 cycles. Effect of the material characteristics on the electrochemical performance is discussed.

9:20am C3+C2+C1-ThM5 Wavefront Shaping: A New Tool in Optics, M. N'Gom (mngom@umich.edu), University of Michigan, USA INVITED

The newly emerging field of optical wavefront shaping involves the ability to manipulate light fields both spatially and temporally. It has largely been enabled by the availability of spatial light modulators (SLM). SLMs are used to create arbitrarily complex light fields that are now powerful elements of the optics toolbox. An SLM provides means to manipulate the fundamental constituents of classical light or single photons, which obey the laws of quantum physics. These new tools open up novel ways to address topics where conventional optical techniques are hard to apply, such as the control of light propagation in biological tissues, complex photonic structures, plasmonic systems, and multimode fibers. In this talk, I outline how I exploit the versatility of wavefront shaping to focus through and beyond highly scattering media. I will show its potential to manipulate entangled structured light fields to address coherence degradation in optical communication transmission channels and to address challenges in biomedical imaging.

10:00am C3+C2+C1-ThM7 Optical Optimisation of Semi-transparent a-Si:H Solar Cells for Photobioreactor Application, A. Brodu (agathe.brodu@cea.fr), C. Ducros, Univ. Grenoble Alpes, CEA, France; C. Dublanche-Tixier, Univ. Limoges, France; C. Seydoux, G. Finazzi, Univ. Grenoble Alpes, CNRS, CEA, France

One of the main limitations of microalgae culture in a photobioreactor is the low efficiency of sunlight conversion. To improve the overall photoconversion efficiency and provide energy support, a photobioreactor (PBR) and photovoltaic technology (PV) coupled system can be developed.

Semi-transparent thin film solar cells based on hydrogenated amorphous silicon technology could be directly placed on the PBR's surface. PV cells absorb a part of the incident light to produce electricity while being transparent in the specific photosynthesis wavelength range. To reach this objective, very thin solar cells must be produced. Decreasing the active layer thickness (intrinsic a-Si:H layer) of solar cells induces a better transparency but also a lower efficiency. As a consequence, we worked on the compensation of efficiency losses of thin solar cells by improving optical properties of substrate surfaces. Texturing process using reactive ion etching was applied on glass substrate to obtain a light scattering property on its back side and an antireflective property on the upper side. We studied the influence of those both textured surfaces on a-Si:H solar cells properties.

First, by texturing the back side of the substrate, the influence of light scattering was investigated. That should improve the light absorption in PV solar cells. The best result shows a raise of the short circuit current (J_{sc}) of the thin solar cells from 8.5 to 10 mA/cm², while the other parameters (the

Thursday Morning, May 23, 2019

open circuit voltage (Voc) and the fill factor (FF) remained the same. Thus the efficiency increased from 3.7 to 4.5 %.

In a second step, the influence of an antireflective texture of the substrate upper side was studied. The antireflection texture with light scattering effect gives the best results on PV cells. Short circuit current of this thin solar cell goes to 11.2 mA/cm² and its efficiency increased to 5.2 %.

The influence of these solar cells, used as optical filter, on the microalgae production rate was investigated. The photosynthesis peaks of microalgae correspond to wavelengths [400 - 500 nm] and [550 - 700 nm]. The first peak of photosynthesis is absorbed by the solar cell. Furthermore, an important diffusion of light in the solar cells also induces losses of transmitted light to microalgae for the second peak of photosynthesis. Finally growing test of *Phaeodactylum Tricornutum* shows that PV optical filtering does not have influence on growth rate. Optical modifications of substrate applied to very thin solar cells allowed to keep a high PV efficiency while maintaining the growing rate of microalgae.

10:20am C3+C2+C1-ThM8 Properties of Highly Transparent AlN/SiO_x Multilayer Systems, C. Appleget, A. Sáenz-Trevizo, A.M. Hodge (ahodge@usc.edu), University of Southern California, USA

The new generation of engineered materials is required to perform under extreme conditions of stress, temperature and irradiation, among others. Nano multilayer (NM) materials have been shown to be promising candidates to overcome current structural and functional limitations. To date, most of the studied NM systems are comprised of metal/metal layers, where the optical properties do not represent an area of interest. Therefore, in this work we extended the structural potential of metal/metal NM configurations to ceramic/ceramic NMs which display a broad range of properties but in particular, they offer the possibility to modulate the optical properties depending on their morphology, grain size, layer thickness, and composition. Three different systems composed of alternated layers of AlN and SiO_x were studied. For each sample, the number of layers and the individual thicknesses were varied until a total thickness of 1 μm was reached. The optical properties of the multilayers were determined using UV-Vis-NIR spectroscopy, revealing the formation of uniform and smooth interfaces with an average optical transparency above 80% that extends through the entire region. Furthermore, the microstructure and plastic behavior were also studied and correlated with the multilayer configuration of the synthesized systems.

10:40am C3+C2+C1-ThM9 Tailoring the Optical Properties of Highly Porous Superlattice-type Si-Au Slanted Columnar Heterostructure Thin Films, U. Kilic (ufuk.kilic@huskers.unl.edu), University of Nebraska-Lincoln, USA; A. Mock, Linköping University, Sweden; R. Feder, The Fraunhofer Institute for Microstructure of Materials and Systems (IMWS), Germany; D. Sekora, M. Hilfiker, R. Korlacki, E. Schubert, C. Argypoulos, M. Schubert, University of Nebraska Lincoln, USA

The subwavelength scale periodic arrangement of nanostructures, so-called artificially engineered nano-structures exhibit distinct optical, mechanical, and magnetic properties when they are compared with their bulk counterparts which has recently gained a growing interest due to its potential applications in various optical and optoelectronic systems such as lenses, solar cells, photodetectors, and sensors [1-3]. Tailoring aforementioned inherent properties cannot merely possible with the material choices (ie. elemental composition), but also the size and shape of these artificial structures play a significant role. Unraveling the mechanisms that influence and control the optical properties of highly-porous, periodic, and three dimensional arrangements of nanoplasmonic structures can offer new approaches for the development of next generation sensors. Particularly, both glancing angle deposition and atomic layer deposition can be used to create periodic nanostructures with multiple constituent materials, so-called heterostructured metamaterials.[4]

In this study, we employ a two-source (ie. Au and Si) electron-beam-evaporated, ultra-high-vacuum glancing angle deposition which allows for the fabrication of highly-ordered and spatially-coherent super-lattice type Au-Si slanted columnar heterostructured thin films. We perform a combinatorial spectroscopic generalized ellipsometry and finite-element method calculation analysis to determine anisotropic optical properties. We observe the occurrence of a strong locally enhanced dark quadrupole plasmonic resonance mode (bow-tie mode) in the vicinity of the gold junctions, with a tunable and geometry dependent frequency in the near-infrared spectral range. In addition, inter-band transition-like modes are observed in the visible to ultra-violet spectral regions. Using finite element method, we demonstrate that changes in the index of refraction due to the concentration variation of a chemical substance environment (gaseous or

liquid) within a porous nanoplasmonic structure can be detected by transmitted intensity alterations down to 1 ppm sensitivity.

References

- [1] Kabashin, A. V., et al. Nature materials 8.11 (2009): 867.
- [2] Schmidt, Daniel, and Mathias Schubert. Journal of Applied Physics 114.8 (2013): 083510.
- [3] Frölich, Andreas, and Martin Wegener. Optical Materials Express 1.5 (2011): 883-889.
- [4] Sekora, Derek, et al. Applied Surface Science 421 (2017): 783-787.

11:00am C3+C2+C1-ThM10 Microstructures and Optoelectronic Properties of Cu₃N Thin Films and its Diode Rectification Characteristics, Y.H. Chen (m07188016@mail2.mcut.edu.tw), S.C. Chen, S. Sakalley, S.Y. Huang, A. Paliwal, Ming Chi University of Technology, Taiwan; M.H. Liao, National Taiwan University, Taiwan; H. Sun, Shandong University at Weihai, China; S. Biring, Ming Chi University of Technology, Taiwan

Rapidly growing applications of p-type Copper nitride (Cu₃N) films in optical storage media, photovoltaics etc. has motivated us to study Cu₃N thin films which were deposited on glass and silicon substrates by reactive magnetron sputtering at 150°C from a metallic copper target. Until now, few researchers have studied the p-type conductivity of Cu₃N films which is low compared to the result obtained in our experiment. In this work, we discuss the effects of working pressure on the microstructures, electrical, and optical properties of the Cu₃N films. The working pressures were varied from 5 mtorr to 23 mtorr while gas flow rate was kept constant at N₂/(Ar+N₂)%=40%. When the working pressure increases, the Cu₃N (111) peak intensity decreases as evident from XRD studies. Meanwhile, conduction type changes from n-type to p-type. When working pressure is increased to 15 mtorr, the resistivity is 1.575 Ω•cm and the sample shows p-type conduction. This is possibly due to the formation of many copper vacancies (i.e. vacancies at Cu cation sites) in the films. When the working pressure is 5 mtorr, a Cu (111) pattern was observed from selected area electron diffraction (SAED) by TEM analysis. It disappears upon increasing the working pressure to 15 mtorr. It was also found that the ratio of Cu²⁺/Cu⁺ increases from 0.39 to 0.93 when the working pressure is raised from 5 mtorr to 20 mtorr. More substitution of Cu²⁺ for Cu⁺ results in the formation of more Cu vacancies, which leads to the transition in conduction from n-type to p-type. Finally, n-type Cu₃N/p-type Cu₃N homojunctions and n-type ZnO/p-type Cu₃N heterojunctions diodes were fabricated. It was found that homojunction devices Al/n-type Cu₃N/p-type Cu₃N do not show significant rectification effects. As we observed, at ±3Volts, the I_{on}/I_{off} was only 0.24. Whereas, in heterojunction devices Al/n-type ZnO/p-type Cu₃N, a higher I_{on}/I_{off} of 3118 can be achieved. Heterojunction devices outperform the homojunction devices instead of interfacial issues indicating the superior electrical properties which are explained considering the mismatch in the built-in potentials of the p-n junctions.

11:20am C3+C2+C1-ThM11 Effects of the Frequency of Pulsed DC Sputtering Power on Amorphous Carbon Film used for Metallic Bipolar Plates in Proton Exchange Membrane Fuel Cells, X.B. Li (lxbsj@sytu.edu.cn), P.Y. Yi, L.F. Peng, X.M. Lai, Shanghai Jiaotong University, China

Amorphous carbon (a-C) film is a promising material serving as a protective film for metallic bipolar plates in proton exchange member fuel cells (PEMFCs) due to its high electrical conductivity and corrosion resistance. However, the performance of a-C needs to be further improved to meet the commercial requirements of PEMFCs. During the process of preparing a-C film by magnetron sputtering, the sputtering power supply has significant influences on the structure and performance of the film. In this paper, the influence of the frequency of pulsed DC sputtering power supply are investigated to further improve the performance of a-C. The corrosion and interfacial contact resistance (ICR) test results show that the film prepared at 200 kHz exhibits excellent performance. The compactness of the films can be enhanced by the bombardment of high-energy sputtering particles produced by pulsed DC sputtering power. In addition, the proper frequency is beneficial to the formation of graphite nanocrystalline, which is embedded into a-C and improve the sp² fraction of the film and decrease the ICR synchronously. Furthermore, the a-C containing graphite nanocrystalline exhibits better stability in simulated acid environment of PEMFCs. This study provides a new direction for further improving the performance of a-C films on bipolar plates in PEMFCs.

11:40am **C3+C2+C1-ThM12 On the Mechanisms of Halloysite Nanotubes Incorporation in the Surface Layer of Forsterite Grown by Plasma Electrolytic Oxidation**, *B. Mingo, Y. Guo, A. Němcová, A. Gholinia, A. Matthews, A. Yerokhin (aleksey.yerokhin@manchester.ac.uk)*, The University of Manchester, UK

Increasing demand for high-performance lightweight metallic materials underlies the interest to Plasma Electrolytic Oxidation (PEO) as one of the most promising techniques for surface engineering of Mg alloys. In order to enable smart and multifunctional performance, it can be beneficial to incorporate into ceramic PEO coatings nanocontainers to carry appropriate active and functionalising agents. In situ incorporation of nanocontainers is challenging since their integrity may be compromised by plasma discharge assisting coating formation. We studied incorporation of halloysite nanotubes (HNTs) as potential nanocontainers into forsterite, Mg_2SiO_4 , formed during PEO processing of AM50 Mg alloy. Detailed analysis of the coating microstructure, chemical and phase composition carried out by Scanning Electron Microscopy/Energy Dispersive X-ray Spectroscopy, Transmission Kikuchi Diffraction and X-ray Diffraction enabled evaluation of a pattern of surface temperature evolution during current pulses underpinning the PEO process. Consequent thermal transient analysis revealed that at pulses longer than 10^{-4} s, the surface heating becomes affected by the metal substrate acting as a heat sink. As the pulse duration approaches 10^{-3} s, raising surface temperature and increasing thermal gradients across the coating cause crystallisation of forsterite and grain growth towards the surface; this triggers thermally induced degradation and decomposition of HNTs adsorbed on the surface. In contrast, at short pulse durations (2×10^{-5} s), the energy released is insufficient to induce forsterite crystallisation and incorporated HNTs are retained in their original tubular structure. Due to the fine porosity and good structural integrity, such coatings show the highest corrosion resistance in saline solution. Strong correlations between surface thermodynamic conditions and evolution of coating microstructure disambiguate the fundamental mechanisms underlying incorporation of nanoparticles into growing PEO coatings, thus creating the basis for efficient design of PEO processes and development of novel smart and multifunctional coatings with potential applications in many industrial sectors.

12:00pm **C3+C2+C1-ThM13 Inorganic-Organic Perovskites: Handle with Care, Properties May Depend on It**, *N.J. Podraza (nikolas.podraza@utoledo.edu)*, *B. Subedi, M.M. Junda, K. Ghimire*, University of Toledo, USA

Inorganic-organic lead halide based perovskites (ABX_3) have been applied as the absorbing, current-generating layer in thin film photovoltaics over the last decade. In that time, device efficiency has increased from virtually nothing to 22.7% at the time of writing this abstract (that number is likely now higher at the time you are reading it). In spite of the ability to manipulate band gap to absorb different parts of the solar irradiance spectrum, the low deficit between the open circuit voltage and band gap, and the overall high electronic quality of the material based on fill factor and device efficiency, these perovskites still pose challenges—namely related to instability in atmosphere and under external heat, moisture, and electric field driven stimuli. Some instability is mitigated when layers are within solar cell devices, as the perovskites are over-coated with other layers and do not share an interface with the ambient. The susceptibility of thin films to atmosphere leads to a disconnect between measured properties for films and what those properties of similarly prepared materials are in the final device structure. Spectroscopic ellipsometry over the near infrared to ultraviolet is applied for perovskite (A: MA, FA, Cs; B: Pb, Sn; X: I, Br, Cl) thin films and layers in solar cells to deduce structure in the form of thickness and surface roughness as well as complex optical response in the form of the complex index of refraction and complex dielectric function spectra. Photothermal deflection spectroscopy probes the optical response in the vicinity of the band gap for improved sensitivity to low values of the absorption coefficient resulting from Urbach tails and other sub-band gap absorption. For both techniques, measurements are performed for films with no exposure to atmospheric ambient and those exposed for controlled amounts of time. From these comparisons, changes appear in the complex optical response both above and below the band gap, including higher energy electronic transitions, Urbach energies, and other sub-gap absorption features. Understanding the origin of differences due to sample handling allows for more realistic comparison of samples and results in literature. Expectedly, upon continued atmospheric exposure Urbach energies increase and very prominent sub-gap absorption features develop. Samples characterized without atmospheric exposure have comparable properties to layers of the same composition in device structures, and

correlations between Urbach energies and photovoltaic device performance parameters are identified.

Tribology and Mechanical Behavior of Coatings and Engineered Surfaces

Room San Diego - Session E1-1-ThM

Friction, Wear, Lubrication Effects, and Modeling II

Moderators: *Nazlim Bagcivan*, Schaeffler AG, Germany, **Carsten Gachot**, TU Wien, Institute for Engineering Design and Logistics Engineering, Austria, **Tomas Polcar**, Czech Technical University in Prague, Czech Republic

8:40am **E1-1-ThM3 Sliding Wear Resistance of Nickel Boride Layers on Inconel 718 Superalloy**, *I.E. Campos-Silva*, Instituto Politecnico Nacional Grupo Ingeniería de Superficies, México; **A.D. Contla-Pacheco (aldani.90@hotmail.com)**, Instituto Politecnico Nacional, Grupo Ingeniería de Superficies, México; *U. Figueroa-Lopez*, Tecnológico de Monterrey-CEM, Mexico; *J. Martinez-Trinidad, A. Ruiz-Rios, M. Ortega-Aviles*, Instituto Politecnico Nacional Grupo Ingeniería de Superficies, México

New results about the wear resistance of nickel boride layers under dry sliding conditions were estimated in this work. For this purpose, an Inconel 718 superalloy was borided using the powder-pack process at two different conditions to estimate the influence of the nickel boride layer thicknesses on the sliding wear resistance. The first condition was at 1173 K with 2 h of exposure (B1), while 1223 K with 6 h of exposure was used for the second condition (B2). A flat-uniform nickel boride layer was developed at the surface of the borided Inconel 718 superalloy with a layer thicknesses ranged between 19 to 50 microns according to the boriding conditions. The microstructure of the nickel boride layer consisted of a mixture of Ni_4B_3 , Ni_2B and Ni_3B phases with a presence of a diffusion zone beneath the layers. Otherwise, the indentation properties such as hardness, Young's modulus and the distribution of residual stresses across the boride layer-substrate system were estimated for both boriding conditions.

The sliding wear tests were performed on both boriding conditions and over the untreated material (Inconel 718 superalloy), using a ball-on-flat configuration comprised with an alumina ball of 6 mm diameter as a counterpart, in which a constant load of 20 N was employed with different sliding distances between 50 to 200 m. In addition, during the wear tests, the friction coefficient was monitored for the overall set of experimental conditions.

As it expected, the presence of the nickel boride layers at the surface of the Inconel 718 superalloy enhanced the wear resistance than that of the untreated material. However, for the B2 condition, an increase of the nickel boride layer thickness produced a more wear-resistant layer, in which the values of the wear rate remained constant for the entire set of sliding distances, in contrast with the results estimated for the B1 condition. Finally, the failure mechanisms developed over the surface of the wear tracks for the borided Inconel 718 superalloys (B1 and B2 conditions), and untreated material were discussed and correlated as a function of the friction coefficients and the mechanical properties estimated by indentation tests.

9:00am **E1-1-ThM4 A Study of the Wear Mechanism of PTFE: The Effects of Temperature and Environment on its Mechanical and Tribological Properties**, *V. Saisnith (vilayvone.saisnith@gmail.com)*, *V. Fridrici*, Ecole Centrale de Lyon, LTDS - Université de Lyon, France

Polytetrafluoroethylene (PTFE) coatings are widely employed in various industrial applications due to their low coefficient of friction, low surface energy, good chemical and high temperature resistances. However, PTFE exhibits relatively weak mechanical strength and its wear resistance (particularly in abrasion conditions) has been a critical issue which needs to be understood and to be overcome. In the present work, we set up a methodology to obtain a measure of the durability of PTFE coatings. Experiments to study the effect of both temperature (from room temperature to 180°C) and environment (dry, in water and in an oil) on the mechanical and tribological properties of PTFE have been carried out. The interactions between temperature and environment are also investigated. Scanning Electron Microscopy (SEM) was used to investigate the worn surfaces and debris and thus understand the wear mechanisms under various conditions. As expected, experimental results showed that the tribological resistance of PTFE significantly decreases with increase in temperature. In addition, the coefficient of friction exhibits no significant difference as a function of the environment. The morphological study of wear debris observed after tests at different temperatures and the measurements of mechanical properties of the coating by nano-indentation

Thursday Morning, May 23, 2019

at different temperatures helped us understand the various wear mechanisms occurring during these tests. In particular, the higher wear observed in an oil environment could be attributed to a different tribological behavior of the transfer film on the abrasive counterbody, with its ease of formation and regeneration.

9:20am **E1-1-ThM5 Harness Intrinsic Friction in Transition Metal Dichalcogenides**, **A. Cammarata** (cammaant@fel.cvut.cz), Czech Technical University in Prague, Czech Republic; **T.P. Polcar**, University of Southampton, UK

One of the main difficulties in understanding and predicting frictional response is the intrinsic complexity of highly non-equilibrium processes in any tribological contact, which include breaking and formation of multiple interatomic bonds between surfaces in relative motion. Moreover, under tribological conditions, local charge accumulation may take place and produce a tribological response different than that of the corresponding neutral structure.

To understand the physical nature of the microscopic mechanism of friction and design new tribological materials, we conducted a systematic quantum mechanic investigation at the atomic scale on prototypical Transition Metal Dichalcogenides at different charge content and applied external load. We combined group theoretical analysis and phonon band structure calculations with the characterisation of the electronic features using non-standard methods such as orbital polarization and the recently formulated bond covalency and cophononity analyses. We proposed a phonon-mode based method, named Normal-Modes Transition Approximation, to identify possible sliding paths from only the analysis of the phonon modes of the stable geometry and to tune the corresponding sliding energy barriers. We formulated guidelines on how to engineer intrinsic friction at nanoscale, and finally applied them to design a new Ti-doped MoS₂ phase with expected improved tribological properties.

Finally, thanks to the general formulation of our approaches, the present outcomes can be promptly used to finely tune physical properties for the design of new materials with diverse applications beyond tribology such as tuning of Metal-Insulator transitions, dielectric response, Second Harmonic Generation, phase matchability, and ionic conduction among others.

9:40am **E1-1-ThM6 Static Friction at High Temperature: from Methodology to Severe-Service Valve Application**, **T. Schmitt** (thomas.schmitt@polymtl.ca), **J.A. Schmitt**, Polytechnique Montréal, Canada; **É. Bousser**, École Polytechnique de Montréal, Canada; **M. Azz**, Tricomat, Canada; **F. Khelifaoui**, **V. Najarian**, **L. Vernhes**, Velan; **J.E. Klemberg-Sapieha**, Polytechnique Montréal, Canada

An international effort is being made to increase the thermodynamic efficiency of thermal power plants up to 50%. To achieve this goal, the temperature and pressure of the steam powering the turbines must be increased up to 760°C and 35 MPa. For such grueling application, Metal-Seated Ball Valves are usually the preferred solution for safety valves. Their sealing surfaces being inherently protected in both open and closed positions, they can be exposed to long periods of immobility in harsh environments. Consequently, new materials are being developed to withstand this new application, driving the development of new equipment and methodologies to characterize these materials under severe conditions.

To investigate this specific static contact, a new tribometer has been developed to measure the coefficient of static friction (μ_s) between a pin and a plane up to a 800°C and after several hours of immobility. In parallel, a methodology was established to simulate the contact condition in a valve consisting of Stellite 6 and hard chrome plating. The evolution of the static coefficient of friction was measured according to three parameters: the contact pressure (P_c), the temperature (T_c) and the holding time (t_c). The microstructure, chemical composition, and topography of the contact was then analyzed.

The study revealed that μ_s was not affected by the contact condition at RT. However, at higher temperatures, the coefficient of static friction depended on both contact pressure and holding time. Particularly, at 800°C, the friction behavior was characterized by an increase in μ_s as a function of holding time up to values greater than 1. In addition, much more pronounced adhesive damage was observed compared to other testing temperatures. The above observations were attributed to the evolution of the contact as a function of the testing conditions. In particular, the formation of a mixed oxide inside the contact seemed to have a major influence on the tribological response of the system. Finally, an adhesion mechanism was proposed to explain the origin of the evolution of the static coefficient of friction.

10:00am **E1-1-ThM7 Coating Development, Characterization and Application-oriented Tests**, **L.P. Nielsen** (lpn@dti.dk), **K.P. Almqvist**, **B.H. Christensen**, **S. Lourcing**, Danish Technological Institute, Denmark; **H. Ronkainen**, **T.J. Hakala**, VTT Technical Research Centre of Finland, Finland; **D. Drees**, FALEX Tribology, Belgium **INVITED**

Developing new coatings and bringing them out of the R&D phase into actual applications is not an easy task. The presentation illustrates how we have developed new coatings based on reactive sputtering processes utilizing different plasma techniques, HiPIMS, pulsed DC and DC magnetron sputtering. The HiPIMS platform was used to develop a very hard TiB₂ coating characterized by having a low residual stress level. Pulsed DC magnetron sputtering was used to deposit a stable 50 μm thick amorphous Al₂O₃ coating for CERN's next generation superconducting magnets. Finally, DC magnetron sputtering was used to deposit different types of low friction carbon-based coatings tailored for different applications such as a low-friction coating for dental application and a Si-containing a-C:H:Si coating revealing increased hardness and improved temperature stability as compared to a-C:H.

The developed coatings were characterized by SEM, nanoindentation, RBS, XPS, GDOES, XRD, etc. The presentation will provide examples of model tests including different types of wear tests as e.g. pin-on-disk, reciprocal sliding tests, scratch testing as well as more application-oriented tests that might be more useful when bringing new coatings into industrial applications.

New Horizons in Coatings and Thin Films Room Pacific Salon 6-7 - Session F2-1-ThM

HiPIMS, Pulsed Plasmas and Energetic Deposition I

Moderators: **Jon Tomas Gudmundsson**, University of Iceland, Iceland, **Tiberiu Minea**, LPGP, Université Paris-Sud, Orsay, France

8:40am **F2-1-ThM3 Recent Insights into HiPIMS Physics via Coherent and Incoherent Thomson Scattering**, **S. Tsikata** (Sedina.tsikata@cnrs-orleans.fr), CNRS, ICARE, France; **T. Minea**, Université Paris-Sud/CNRS, France; **B. Vincent**, CNRS, France; **A. Revel**, Université Paris-Sud/CNRS, France **INVITED**

The emergence of the HiPIMS operating regime for planar magnetrons offers new possibilities for the generation of thin films. HiPIMS operation, characterized by high-current, short-duration plasma pulsing, produces high plasma densities which can favor improved mechanical properties of thin films. For HiPIMS plasmas to be fully exploited and for their adoption to become commonplace in industry, it is necessary to understand the basic physical processes associated with this operation.

HiPIMS operation involves complex, transient plasma states and processes which are much more challenging to model than conventional DC operation. Although a consensus has emerged that fully kinetic, three-dimensional models offer the best chance at capturing the physics of this state, such codes are in their infancy and cannot be feasibly applied to large-scale industrial development. A key missing ingredient for such codes remains the knowledge of the particle dynamics and properties.

In this talk, we report on recent new approaches to understanding the HiPIMS plasma using a combination of advanced laser diagnostics. With coherent Thomson scattering, we have recently obtained for the first time information on the nature of microturbulence affecting the confinement of electrons in the planar magnetron magnetic trap [1]. Studies with this experimental technique show that large-scale and small-scale behavior are inextricably linked. With incoherent Thomson scattering [2], we have also obtained time-resolved measurements of electron density and temperature during the evolution of a HiPIMS pulse, establishing the link between these properties and the current characteristics. The implementation of these diagnostics gives access to information on electron dynamics and properties which was previously inaccessible. We discuss the import of these experimental findings in the context of recent numerical models [3], and explain our current understanding of the physics of the HiPIMS state.

[1] S. Tsikata and T. Minea. Phys. Rev. Lett. 114, 185001 (2015)

[2] B. Vincent, S. Tsikata, S. Mazouffre, T. Minea and J. Fils. Plasma Sources Sci. Technol. 27, 055002 (2018)

[3] A. Revel, T. Minea and S. Tsikata. Phys. Plasmas 23, 100701 (2016)

Thursday Morning, May 23, 2019

9:20am **F2-1-ThM5 Process Gas Rarefaction and Other Transport Phenomena in High Power Impulse Magnetron Sputtering Discharges Studied by Particle Simulations**, *T. Kozák*, University of West Bohemia, Czech Republic

The high power impulse magnetron sputtering (HiPIMS) technique has recently been increasingly used in the coating industry. For tailoring film properties, it is necessary to know and control the energy delivered to the film by process gas and film-forming particles. Computer simulations can help understand the relations between discharge process parameters and fluxes of particles onto the substrate. Due to the complexity of the HiPIMS discharge, it is not feasible to simulate the deposition process self-consistently. Various modelling approaches have been used to give simplified predictions of the HiPIMS plasma parameters.

A fully three-dimensional simulation using the Direct Simulation Monte Carlo (DSMC) method was developed to model the transport of neutral and ion species in a vacuum chamber of realistic size, to improve upon the existing volume-average [1,2] or Monte Carlo [3] models. The time-dependent evolution of gas and target material species densities in the discharge chamber during sputtering pulses as well as the fluxes of particles onto the substrate and their energy distributions were studied under various conditions.

First, the effect of process gas rarefaction by momentum transfer from sputtered target material atoms (Zr, Al and C) was systematically investigated. The effect of target material mass and the target current amplitude is reported. The argon density decreases during the pulse-on time to 50% of its initial value for the current density of sputtered Al atoms of around 0.5 Acm^{-2} . For Zr and C, the minimum argon density is 43% and 57%, respectively. Thus, the dependence on the mass of the target material was found to be rather weak. During the pulse-off time, argon density returns back to equilibrium within 1 ms after the pulse end.

Second, ionization of sputtered target material atoms and the transport of ions in a given electrostatic potential is further investigated. This will help us understand the complex dynamics of HiPIMS discharges and the energies of ions incident onto the substrate observed in diagnostic experiments.

References

- [1] M.A. Raadu et al., *Plasma Sources Sci. Technol.* **20** (2011) 65007
- [2] J.T. Gudmundsson et al., *Plasma Sources Sci. Technol.* **25** (2016) 65004
- [3] S. Kadlec, *Plasma Process. Polym.* **4** (2007) S419–23

9:40am **F2-1-ThM6 Insight on the Sputtered Material in HiPIMS by 2D PIC-MCC Modeling**, *A. Revel (adrien.revel@u-psud.fr)*, Université Paris-Sud/CNRS, France; *T. Minea*, Université Paris-Sud, Université Paris-Saclay, France

The development of High Power Impulse Magnetron Sputtering (HiPIMS) since the early 2000 has boosted the research much beyond the Conventional Magnetron Sputtering (CMS), worldwide used in industries. In HiPIMS regime, the quantity of sputtered material from the target is greatly improved during the on time compared to the DC regime. Combined with the higher plasma density, the fraction of the sputtered material being ionized is considerably increased reaching a value between 10% and 80% depending on the discharge parameters and target characteristics. An important part of these ionized particles come back to target leading to the self-sputtering effect.

Beyond this, the plasma behavior in magnetron discharge involves complex phenomena such as ExB gradient, curvature and drift coupled with kinetic reactions and plasma-surface interactions. Hence, the motion of individual particles and the whole plasma is subject to intricate phenomena difficult to apprehend and not completely understood yet. The presence of important quantities of sputtered particles complicate even more the study of magnetron plasma, especially when focusing on their spatial distribution and evolution and not only on the global balance of plasma species.

Over the past few years, the OHiPIC model (Orsay High density Particle-in-Cell) has been developed at the LPGP (Laboratoire de Physique des Gaz et des Plasmas) for the modeling of magnetron plasma. OHiPIC code has been used in DC and in HiPIMS regime. It now takes into account the sputtered particles and their ionization. The results provided by OHiPIC are insightful and give a better understanding of the process involved in magnetron discharges. The OHiPIC and its latest improvements will be presented. The 2D density map of the different species and their evolution will be presented and discussed.

10:00am **F2-1-ThM7 Spoke Formation in Large Scale Rectangular Magnetrons**, *A.P. Ehasarian (a.ehasarian@shu.ac.uk)*, Sheffield Hallam University, UK

Rectangular magnetron cathodes are widely used in the sputter deposition industry, however spokes have been studied mainly in the circular target geometry. The variation in magnetic field strength between the corners and straight sections of the cathode as well as the smaller spoke-to-cathode size ratio influence the motion and formation of the spokes. Fast camera imaging was used to study High Power Impulse Magnetron Sputtering (HiPIMS) discharges on $200 \times 600 \text{ mm}$ cathodes in a Hauzer HTC 1000/4 system. Spokes were observed at peak current densities as low as 0.6 Acm^{-2} . Spoke number (mode) was found to decrease and the velocity increase with magnetic field. Spokes were triangular for strong fields and diffusive for weaker fields for the same peak current of 1 Acm^{-2} . The splitting of spokes due to acceleration of a portion was observed. At low pressure the spoke shape was a diffuse triangle which widened and advanced in the $\mathbf{E} \times \mathbf{B}$ direction. The spokes turned diffusive at the corners and narrow sections of the magnetron and reformed upon re-entry into the straight sections. The shape of the spokes is generally triangular due to the sequential processes of build-up of ionisation to a critical value, rupture of the field and restoration of confinement. In strong confinement fields these processes are faster and produce triangular spokes. In weaker fields the triangle is stretched out resulting in larger volumes of escaping plasma. The behaviour of spokes in the corners is discussed in terms of electron dynamics and the weaker magnetic fields. At low pressures the spokes may be dominated by metal sputtering and ionisation which are initiated in the centre of the racetrack and spread across.

It is argued that spoke formation could be linked to the ratio of plasma density and magnetic field (β , θ). Spokes are associated with localised rupture in confinement and ejection of intense particle beams. Thus spokes are a route for the escape of plasma from the confinement field which leads to a greater degree of freedom, greater number of accessible states and greater entropy. It is suggested that the increase in entropy is the driving force for the creation of zones of intense ionisation which leads to high plasma pressure and localised rupture of the confinement field.

10:20am **F2-1-ThM8 The Use of Bipolar-HiPIMS for the Design of Ion Energies in Thin Film Growth**, *U. Helmersson (ulf.helmersson@liu.se)*, J. Keraudy, R.P.B. Viloan, Linköping University, Sweden; N. Brenning, M.A. Raadu, KTH Royal Institute of Technology, Sweden; D. Lundin, Université Paris-Sud, Université Paris-Saclay, France; I. Petrov, University of Illinois, USA, Linköping University, Sweden, USA; J.E. Greene, University of Illinois, USA, Linköping University, Sweden, National Taiwan Univ. Science & Technology, Taiwan; J.T. Gudmundsson, University of Iceland, Iceland

The effect of a positive pulse following a high-power impulse magnetron sputtering (HiPIMS) pulse are studied using energy- and time-resolved mass spectrometry. This includes exploring the influence of a $200 \mu\text{s}$ long positive voltage pulse ($U_{\text{rev}} = 10\text{-}150 \text{ V}$) following a typical HiPIMS pulse on the ion-energy distribution function (IEDF) of the various ions. We find that, a portion of the Ti^+ flux is affected by gaining energy which corresponds to the acceleration over the full potential U_{rev} . The Ar^+ IEDF on the other hand illustrates that a large fraction of the Ar^+ accelerated, gain energy only to a portion of U_{rev} . The Ti^+ IEDFs are consistent with the assumption that practically all the Ti^+ that become accelerated during the reverse pulse come from a region adjacent to the target, in which the potential is uniformly increased with the applied potential U_{rev} , while much of the Ar^+ come from a region further away from the target that contains a boundary with a drop in potential from U_{rev} to a lower potential consistent with the plasma potential achieved without the application of U_{rev} . The deposition rate is only slightly affected and decreases with U_{rev} to $\sim 90\%$ at $U_{\text{rev}} = 150 \text{ V}$. Both the Ti^+ IEDF and the small deposition rate change indicate that the potential increase in the region close to the target is uniform and essentially free of electric fields, with the consequence that the motion of the ions inside it are not much influenced by the application of U_{rev} . In this situation, Ti^+ will flow towards the outer boundary of the target-adjacent region, due to their momentum achieved during the HiPIMS discharge pulse, independent whether the positive pulse is applied or not. The metal ions that cross the boundary in the direction towards the substrate, and do this during the positive pulse, all gain an energy corresponding to the full positive applied potential U_{rev} .

10:40am **F2-1-ThM9 Latest Developments in HiPIMS with Positive Pulsing**, *I. Fernandez (ivan.fernandez@nano4energy.eu)*, Nano4Energy, Spain; A. Wennberg, Nano4Energy SL, Spain; F. Papa, GP Plasma, Spain
Recently, it has been demonstrated for highly ionized discharges that the application of a positive voltage reversal pulse adjacent to the negative

Thursday Morning, May 23, 2019

sputtering pulse gives rise to the generation of high fluxes of energetic ions. This effect allowed unprecedented benefits for the coating industry, where the key factor is the ability to tailor both the energy and flux of the high fraction of ionized material present in a HiPIMS discharge. Now, this can also be achieved by controlling the amplitude of the positive voltage reversal. A description of this technology as well as the experimental results obtained in different coating systems from a wide variety of industrial sectors (hard metal nitrides, optical coatings, semiconductor trench filling, roll-to-roll applications...) will be presented in this paper.

11:00am F2-1-ThM10 HIPIMS- Advantages of a Positive Kick Pulse, J. Hrebik (jasonh@lesker.com), Kurt J. Lesker Company, USA

HiPIMS is an ionized PVD technique that produces a high density, high performance films. The extreme power densities in HiPIMS create a higher ionized plasma that creates a very high energy of material being deposited onto the substrate.

A key feature to the maturing HiPIMS technology is the ability to apply a positive kick pulse. Having a full range of control over this kick pulse is key in the ability to dial out stress, build thicker deposition layers, increase rate, and tune for specific film morphology and or crystallinity and microstructures. This presentation will share examples of applications and performance data to support the many advantages of the IMPULSE power supply. The available configurations and examples of ideal operating parameters will be shared.

11:20am F2-1-ThM11 Plasma Parameter Determination in a HiPIMS Discharge Using Laser Thomson Scattering, P.J. Ryan, J.W. Bradley (j.w.bradley@liv.ac.uk), M.D. Bowden, University of Liverpool, UK

The temporal evolution of the electron density and temperature in a HiPIMS discharge has been measured using laser Thomson scattering and Langmuir probing as comparative techniques. Measurements were performed (non-simultaneously) at two positions within the plasma; in the low magnetic field region on the discharge centreline and in the high magnetic field region of the magnetic trap above the racetrack, for peak power densities of 450 Wcm⁻² and 900 Wcm⁻² respectively. The maximum plasma densities and temperatures were found to be 6.9 × 10¹⁹ m⁻³ and 3.7 eV in the pulse-on time, decaying to values of 4.5 × 10¹⁷ m⁻³ and 0.1 eV some 300 μs into the afterglow. The results indicate that although intrusive, the Langmuir probe can provide a good indication of electron properties in regions of different electron magnetization in the HiPIMS discharge.

Surface Engineering - Applied Research and Industrial Applications

Room Pacific Salon 1 - Session G1+G3-ThM

Advances in Industrial PVD, CVD, and PECVD Processes and Equipment/Innovative Surface Engineering for Advanced Cutting and Forming Tool Applications

Moderators: Ladislav Bardos, Uppsala University, Sweden, **Emmanuelle Göthelid**, Sandvik Machining Solutions, Sweden, **Ali Khatibi**, Oerlikon Balzers, Oerlikon Surface Solutions AG, Liechtenstein, **Christoph Schiffers**, CemeCon AG, Germany

8:00am G1+G3-ThM1 Predicting Coating Uniformity and Cathode Utilization in Magnetron Sputtering Applications using Numerical Simulation, A. Obrusnik (obrusnik@plasmasolve.com), P. Zikan, Plasma Solve, Brno, Czech Republic

In many disciplines of applied science, numerical simulation and computer-aided engineering (CAE) are well established and are being commonly used in process design and utilization. This is not the case in plasma processing science, where numerical simulation is still largely considered an academic endeavour. This is partly due to the complexity of the problem and partly due to the lack of tools available.

In this contribution, we aim to illustrate that numerical models of PVD processes and the codes necessary for implementation of these models have matured enough and are ready to be used on the industrial scale. We provide real-life examples as to how a numerical simulation can be instrumental in optimization of magnetron sputtering processes and low-pressure cathodic arc PVD. To that end, we utilize solvers relying both on continuum plasma models and particle-based models (DSMC, direct-simulation Monte Carlo). These solvers are largely based on open-source computational libraries OpenFOAM and Elmer, which allows for excellent computational scalability and computation in realistic 2D and 3D geometries. The codes presented are capable of predicting application-

relevant observables, e.g. magnetron cathode consumption, multilayer structure and coating uniformity on 3D rotating samples.

The contribution illustrates the potential of open-source computational solutions as well as cloud computing, which might be necessary for addressing industrial-scale plasma simulations.

8:20am G1+G3-ThM2 Multinary HiPIMS, T. Leyendecker, W. Koelker, S. Bolz, C. Schiffers (christoph.schiffers@cemecon.de), CemeCon AG, Germany

The almost unlimited choice of materials is one of the biggest strength of HiPIMS. It offers a variety of opportunities for tailoring coatings by alloying of the chemical composition or by using species from certain elements to densify the film by heavy ion bombardment.

Carbon based coatings are mainly used for tribological applications. However, coatings such as TiCN and WC/C are of high relevance for tap tool applications – a market of about 100 Mio tools per year. Commercial coating products for the threading industry are most frequently multilayer designs of an AlTiN with a carbon containing top layer. This gives HiPIMS a new challenge: multinary coatings of materials with rather different properties.

This paper will introduce a new HiPIMS control concept offering for every source an individual set of HiPIMS pulse parameters. Now the coating designer can take the very different ionization potential of different materials into account or select a source for heavy ion bombardment while the other ones are optimized for highest sputtering rate.

All this with full synchronization of the HiPIMS cathodes to the HiPIMS table bias. Hence, the film's designer can actively go for the ionized target species while suppressing the incorporation of sputtering gas into the film.

Data from plasma analysis as well as hardness and stress measurement reveal a huge effect of the pulse parameters such as frequency and pulse length on the film properties.

Multinary HiPIMS gives freedom to coating engineers and broadens the application range of HiPIMS.

Case stories from the thread tool industry underline the industrial relevance of the concept.

8:40am G1+G3-ThM3 From Small Parts to Particles – Experiences in Bulk Coating, H. Klostermann (heidrun.klostermann@fep.fraunhofer.de), F. Fietzke, B.G. Kraetzschmar, Fraunhofer FEP, Germany

Bulk coating seems to be an intriguing variant of vacuum coating for small mass parts. Compared to individual part coating, the handling effort is considerably reduced. This applies to indirect and direct labor such as the production and maintenance of adapted fixtures and the charging and de-charging of individual parts. Furthermore, the utilization of processing volume can be maximized, avoiding void space between the parts. This benefit grows with decreasing part size. However, when it comes to particles, new challenges arise in bulk coating that thwart the fast success.

The surface to be coated per volume increases with decreasing size of the parts/particles. Therefore, high deposition rates are required in order to keep the processing time reasonably low. The economic assessment of bulk vacuum coating has to be made for every individual coating task including a specific substrate, the intended function of the coating, the production volume and the costs. Certainly, for many high volume bulk goods vacuum coating is not an option. However, novel high tech materials are often composites in which bulk materials are included and combined with metals or polymers to result in improved properties and/or reduced weight. Correspondingly, surface functionalization of bulk material becomes more important and more requested.

Fraunhofer FEP has pursued the objective of vacuum bulk coating for several years. We have developed a technology for corrosion resistance coating of rivets. Based on the barrel coating device ALMA 1000, which includes the high rate plasma activated evaporation technique as well as the magnetron sputtering technique, other bulk materials are envisaged for surface functionalization. The challenge starts with the handling of particulate material, its behavior in the rotating substrate drum and its implication for the vacuum process.

First experiences with different particulate materials will be presented that illustrate options and limitations. The contribution is thought to stimulate new ideas for surface functionalized bulk materials that can eventually be solved by vacuum plasma treatment and coating processes.

Thursday Morning, May 23, 2019

9:00am **G1+G3-ThM4 A Novel Industrial Coating System for the Deposition of Smooth Hard Coatings Combining HiPIMS V+ and Rotatable Magnetrons**, **H. Gabriel** (h.gabriel@PVTvacuum.de), *J.A. Santiago Varela*, PVT Plasma und Vakuum Technik GmbH, Germany; *I. Fernandez*, N4E Nano4Energy S.L.N.E, Spain; *N. Dams*, PVT Plasma und Vakuum Technik GmbH, Germany; *A. Wennberg*, N4E Nano4Energy S.L.N.E, Spain; *J. Lu*, PVT Harbin Coating Ltd, China

Multi-layered, nano-structured metal-nitride and carbo-nitride coatings are very well established in the cutting tool industry as well as in other industries. For years most of such coatings have been deposited by arc evaporation despite the badmouthed "droplets", since arc evaporation is an extremely economic process with significant advantages such as high intrinsic ionization which is particularly beneficial during metal etching.

Magnetron sputtering with its low ionization and its deficiencies in adhesion and productivity significantly improved with the development of HiPIMS. An even more significant improvement is the HiPIMS V+ process where adding positive reverse pulses creates enhanced ion assistance and incorporation to the growing film, thus also increasing the deposition rate.

On the other hand, rotatable magnetrons are well known to provide better material usage, longer operation and higher operation power levels.

The novel industrial system introduced in this paper shows the unique combination of HiPIMS V+ with rotatable magnetrons in a batch coater system, thus enhancing system productivity. This process is applied in a multi-cathode magnetron sputtering system using 4 pieces of 1 m long rotatable cathodes equipped with a strong unbalanced magnetic design allowing high ion-to-neutral ratios to the substrate. The system can be configured to operate in unipolar HiPIMS, Dual Bipolar HiPIMS or DC-Pulsed.

Besides a description of the newly designed coating system, nitride and carbo-nitride nano-structured multilayered coating structures based on Ti, AlTi, AlCr and TiSi deposited in such system are shown and characterized, concerning their micro-structure, adhesion, microhardness and composition.

Wear and performance data are presented.

9:20am **G1+G3-ThM5 From DCMS to HiPIMS: A Giant Leap for Cutting Tools?**, **B. Gaedike** (Bastian.Gaedike@phorn.de), Hartmetall-Werkzeugfabrik Paul Horn GmbH, Germany **INVITED**

Carbide cutting tools for machining (e.g. milling or turning) are coated with physical (PVD) or chemical vapor deposition (CVD) to meet the high requirements. Arc and DCMS (Direct Current Magnetron Sputtering) have dominated the PVD sector for decades.

In recent years the PVD process HiPIMS (High Power Impulse Magnetron Sputtering) has moved more and more into the focus of the cutting tools industry. Research in this area has already progressed considerably. Since the observation of high peak currents by high-frequency pulsing by Kouznetsov in 1999, researchers have published several hundred publications on HiPIMS. While the technical details of the HiPIMS process are highly interesting for researchers and developers, the focus for users and manufacturers of cutting tools is more on the use of coatings.

The machining of new materials for aerospace and medical technology has greatly increased the demands on cutting materials and cutting edge geometries. In general steel and stainless steel processing, there is also an increase in downtimes and cycle times. For the manufacturers themselves, not only the performance of the layers is decisive, but also the economic efficiency in production. The low deposition rates of HiPIMS, which are often reported in publications, are a major topic here.

The main topic of the presentation is the requirements of users and manufacturers of cutting tools and the resulting challenges for research and development. In addition to various applications and problems in machining, the coating of sharp cutting edges and the problem of the deposition rates of HiPIMS are under discussion.

10:00am **G1+G3-ThM7 Application of Twin-Roll PECVD for Surface Functionalization on Flexible Substrate**, *Y. Isomura* (isomura.yoshiyuki@kobelco.com), *Y. Ikari*, *T. Okimoto*, Kobe Steel, Ltd., Japan

Technological development of surface functionalization is of great significance today in the wide field of application. This ranges, for instance, from hard nitride coating for cutting tools to functional transparent electrode on a flexible polymer film. For this purpose, plasma deposition and treatment techniques of cathodic arc, sputtering, Plasma Enhanced CVD (PECVD) are largely used in an industrial production scale. A batch type system is commonly employed in hard coating application where a variety

of individual components is deposited by tailor-made coatings while a continuous production with Roll to Roll process, hereafter referred to as R2R, provides a high productivity for surface functionalization on a flexible substrate. Application of R2R has been expanding due to a recent increase in demand for smart devices such as functional display, wearable devices and sensors, energy conversion and storage, contributing towards realization of sustainable smart society in the near future.

We have developed the so-called Twin-Roll PECVD technique integrated into R2R process in an industrial scale. A unique feature of Twin-Roll PECVD is that the winding rolls themselves for flexible substrate serve as the electrode for discharge of PECVD process. This provides a stable discharge for a long time compared to a conventional pulse PECVD since no deposition occurs on the surface of electrode, which often limits productivity of deposition of non-conductive coating such as oxide and nitride. Optimization of magnetic field on the electrode enables to sustain the discharge at a relatively low pressure of 1~10 Pa. The low pressure PECVD process suppresses the formation of dust particles, and hence the film deposition with a low defect density is realized.

In this work we report the basic principle of Twin-Roll PECVD as for a new type of plasma processing as well as some applications of surface functionalization on flexible substrate using this technology. We have deposited and characterized SiOx films exhibiting a high water vapor barrier property, SiOx/SiNx films with a high refractive index, and DLC (Diamond-Like Carbon) films showing a high infrared transmissivity. Spectrophotometry, XPS, TOF-SIMS, water vapor transmissivity measurement were mainly used for film characterization. In addition an application of Twin-Roll PECV for deposition of heat-ray reflecting film is demonstrated.

10:20am **G1+G3-ThM8 A New System Platform for Ultrafast Nitriding and Diamond Like Carbon (DLC) Deposition Based on a Hollow Cathode Discharge**, **F. Papa** (fpapa@duralar.com), *T. Casserly*, *A. Tudhope*, *S. Gennaro*, Duralar Technologies, USA

Diamond Like Carbon (DLC) has become one of the most important coatings in the Physical Vapor Deposition (PVD) industry due to its chemical inertness, hardness and low coefficient of friction. For mass production, these coatings are usually produced in large batch coaters with PVD interlayers for adhesion and load absorption with a Plasma Enhanced Chemical Vapor Deposition (PECVD) DLC layer on top. Typical cycle times for such a batch system are on the order of 6-9 hours. A new PECVD system platform based on hollow cathode technology has been developed for the deposition of DLC (a-C:H) with a complete door to door cycle time of less than 30 minutes for a 2-3 µm DLC coating. In addition to high rate DLC coating (0.5 to 1 µm/minute), ultrafast plasma nitriding can also be done before the DLC process in order to harden and chemically modify the surface before DLC coating. Titanium alloys, stainless, carbon and alloy steels are suitable materials for such processes. In addition to the short cycle times, three dimensional parts with aspect ratios of 15:1 (length:diameter) can also be coated with coating on both external and internal surfaces. DLC coating thicknesses greater than 50 µm can be achieved.

10:40am **G1+G3-ThM9 Combinatorial Development of Nitride and Oxide Thin Films on an Industrial Scale**, **R. Cremer** (CREMER@KCS-EUROPE.COM), KCS Europe GmbH, Germany **INVITED**

The ever increasing complexity of modern coatings triggers the need of sophisticated technologies for rapid and commercially advantageous development methods. One possibility to significantly increase the speed of materials development is the use of combinatorial approaches.

In this paper, the applicability of such combinatorial methods in industrial development of advanced materials is illustrated presenting various examples for the deposition and characterization of one- and two-dimensionally laterally graded coatings. These coatings were deposited by means of magnetron sputtering, arc ion plating and plasma-enhanced chemical vapor deposition.

To illustrate the advantages of this approach for the industrial development of advanced materials, the multi-component metastable hard coatings (Ti,Al)N, (Ti,Al,Cr)N and (Ti,Al,Si)N as well as various non conductive oxides and nitrides were investigated with respect to the relations between structure and composition on one hand and physical properties like hardness, erosion resistance, cutting performance and oxidation behavior of these coatings on the other.

Thursday Morning, May 23, 2019

11:20am **G1+G3-ThM11 Protective, Tribological and Decorative PECVD Coatings Deposited with a New Microwave Source: Plasma and Layer Characterization for Appropriate Applications**, *R. Schäfer, T. Radny, K.-D. Nauenburg* (*nauenburg.klaus@robeko.de*), robeko GmbH & Co.KG, Germany; *S. Ulrich*, Karlsruhe Institute of Technology (KIT), IAM, Germany

The KIT designed a novel MW source with a parabolic reflector to focus the high microwave plasma density directly onto the substrates during the deposition of scratch, corrosion and wear protective, tribological, biocompatible and decorative coatings by a PECVD processes using e.g. siloxane and hydrocarbons as precursor compounds. A number of MW sources can be arranged in line or even lateral to form a larger coating area to be used in inline coaters or larger batch coating systems, also being easily combined with other PVD sources e.g. planar and rotatable sputter magnetrons, both with the option to be driven with a HiPIMS generator to create new and promising combination of diverse plasma effects. At the very first it is necessary to characterize the plasma by different diagnostic methods, e.g. Langmuir probe measurements, OES, RFA and others, but also work out the influence of the plasma parameter settings for the properties of the deposited layers, e.g. diamond - or quartz-like-coatings. At least the design has to be optimized in details to ensure a long-lasting reliable stability of process conditions and product properties in industrial production. First results for all issues will be presented.

11:40am **G1+G3-ThM12 Complex Coating Technique for Smallest Part of Advanced Powertrain Fuel System**, *S.C. Cha* (*SungChul.Cha@kefco.co.kr*), *H.J. Park, J.H. Lee*, Hyundai Motor Group-Hyundai Kefico, Republic of Korea; *K.Y. Ko, C.H. Shin*, Dongwoo HST Co. Ltd., Republic of Korea

The objective of this paper is to achieve the high quality SiO-DLC (Diamond Like Carbon) coating on small spherical part with diameter of 2-4 mm applied to the advanced powertrain fuel system. Silicon and oxygen incorporated DLC reduces internal residual stress and improves high temperature stability compared to DLC. The spherical part moves continuously up and down and hits their counterpart. Therefore this part is required to have high hardness and wear resistance. Conventional process, this part firstly welded with bar shaped part and then assembled with further parts, finally coated as assembled state. However in this manner, the maximum amount of charging in one coating batch of coating machine is limited due to big size of whole component, causing cost increasing. Furthermore the assembled component can be contaminated by alkali cleaning agent during cleaning process before and after coating and discolored by the process gas during coating process. Therefore the spherical part is to be coated before welding on the bar shaped part.

One of the challenges of this work was mounting the spherical parts in the coating jig. To maximize the production amount, parts shall be mounted in vertical direction in the coating machine. Therefore the appropriate jig is designed and installed with a magnet substrate backside of the jig to magnetically hold parts. The other challenge was designing for masking in the jig. At least 0.7 mm height of non-coating region must be secured concerning heat damage on coating by laser welding process. Thus the parts should be mounted on the masking jig with high precision. The tolerance of the jig had to be as small as possible to block the inflow of coating material into the gap between spherical part and jig. Moreover the jig should be as thin and narrow as possible to maximize the production amount.

The coating is composed of three layers, Cr as bonding layer, WC or CrN as buffer layer and SiO-DLC as functional top layer. Bonding and buffer layers are coated with reactive or non-reactive sputtering method and top SiO-DLC layer is coated by reactive sputtering with HMDSO (Hexamethyldisiloxane). The minimum properties of hardness was 20 GPa, of coating thickness 1.5-2.5 μm and of roughness lower than R_a 0.05 μm . With only PACVD, coating hardness of part's equator zone could not be satisfied due to the limitation of complex shape. In conclusion, SiO-DLC coating technique by reactive sputtering with high precise jiggling and masking technique resulted best properties for modern powertrain fuel system, detailed described in this paper.

Topical Symposia

Room Golden West - Session TS2-ThM

Icephobic Surface Engineering

Moderators: *Alina Agüero Bruna*, Instituto Nacional de Técnica Aeroespacial (INTA), Spain, *Jolanta-Ewa Klemberg-Sapieha*, École Polytechnique de Montréal, Canada

8:20am **TS2-ThM2 Synthesis And Characterization Of Amphiphobic Hybrid Coatings For Industrial Applications**, *G. Boveri* (*giulio.boveri@istec.cnr.it*), *M. Raimondo, F. Veronesi*, Institute of Science and Technology for Ceramics, Italy

In the coming few years, the control of materials repellence against liquids is one of the biggest challenge to make innovation in many industrial fields. Gathering on the same material the ability of repelling liquids with physical properties (typically surface tension γ) in a wide range of values represents the topic of many scientific efforts. Materials wetting strictly depends on surface chemistry and reactivity and on structural features at nanoscale as well.

This work is based on the surface modification of aluminum substrates by deposition of thin layers of ceramic oxide nanoparticles, in particular Al_2O_3 and SiO_2 synthesized by sol-gel routes, in order to introduce nano features which, coupled with the organic modification of the surface chemistry, lead to an almost complete repellence against water (*superhydrophobicity*, contact angles approaching 180° and contact angle hysteresis $<5^\circ$) and liquids with γ as low as 25 mN/m (*superhydrophobicity* plus *oleophobicity* = *amphiphobicity*). *Amphiphobic* materials are drawing much interest in different industrial sectors, such as naval, aerospace, energy and automotive, so that great efforts have been making to improve their durability and wearing resistance simulating their application in real environments.

Two different approaches were typically used to produce non-wetting surfaces: the so-called *Lotus Leaf (LF)* and the *Slippery Liquid Infused Porous Surfaces (SLIPS)* ones, both introducing textural and chemical modifications at surface level that, in turn, is working in a solid-liquid-air (LF) or liquid-liquid-air three phasic environment. Self-cleaning, anti-icing and anti-soiling behavior was assessed on these surfaces and the detected performances correlated to the nature of the coatings, other than to the physical state of the working interfaces.

Keywords: Amphiphobicity, hybrid coatings, ceramic nanoparticles, surface modifications.

8:40am **TS2-ThM3 In situ Ice Growth Kinetics on Water-repellent Coatings in Atmospheric Icing Conditions**, *J. Lengaigne* (*jacques.lengaigne@polymtl.ca*), *P. Xing, É. Bousser*, École Polytechnique de Montréal, Canada; *A. Dolatabadi*, Concordia University, Canada; *L. Martinu, J.E. Klemberg-Sapieha*, École Polytechnique de Montréal, Canada

Ice accretion on the surface of airplanes during flight and in other similar situations presents significant safety concerns and economic loss. Icing occurs when micrometric Supercooled Water Droplets (SWD) impact at high speed and freeze on exposed components. Current de-icing systems (chemical agents, heaters or inflatable boots) are energy intensive and prone to failure. To address these shortcomings, research has focused on the development of so-called icephobic surfaces or coatings. These surfaces could provide an efficient passive protection: inhibiting ice nucleation, reducing ice growth or improving the efficiency of current de-icing technology. At the forefront of these new coatings, superhydrophobic surfaces, combining materials with low surface energy and high multiscale roughness, are regarded as one of the most promising avenues. In this work, we investigated the performance of water-repellent coatings against SWD ice accretion.

To replicate realistic SWD icing conditions, we used a small-scale icing wind-tunnel to generate microdroplets with diameters ranging from 10 to 90 μm , and an air speed of 10 m/s impinging at a temperature of -17°C . The test section was equipped with a sample holder incorporating a thermoelectric module for heating/cooling the sample, a side camera to visually record the ice formation, and an *in situ* ice growth monitoring system. This latter module was developed to measure ice thickness during the testing cycle. It functions by following the displacement of a laser beam using a dedicated digital camera. Moreover, the laser spot spreading offers insights into the evolution of the roughness of the ice layer.

Three types of surfaces with different wettability and roughness R_q values were studied in this experiment: hydrophilic mirror-polished Ti-6Al-4V alloy ($\theta_c=74\pm 1^\circ$, $R_q=51\pm 4\text{nm}$), hydrophobic spray coating ($\theta_c=107\pm 1^\circ$, $R_q=$

Thursday Morning, May 23, 2019

0.35±0.04 μm) and superhydrophobic hierarchical spray coating ($\theta_c=173\pm3^\circ$, $R_a=12\pm2\ \mu\text{m}$).

The ice growth cycle follows a similar behavior on all samples: first the ice nucleation occurs followed by an incubation period before the continuous ice growth. Once the ice has formed a continuous layer, the growth rate is linear. It was found that the incubation period is longer when the surface is more hydrophobic. In fact, the superhydrophobic coating showed twice longer incubation time compared to the substrate. However, ice growth rate increased on the water-repellent coatings (up 34% faster on the superhydrophobic surface) compared to the pristine titanium alloy. Finally, de-icing of each sample showed that the conductive substrate is de-iced faster compared to both water-repellent coatings.

9:00am **TS2-ThM4 Icephobic Elastomeric Surfaces?**, *P.F. Ibáñez (pabloi@ugr.es)*, *F.J. Montes Ruiz-Cabello*, *M.A. Rodríguez Valverde*, *M. Cabrerizo Vilchez*, Universidad de Granada, Spain

It is well-accepted that superhydrophobic surfaces may lead to interesting properties such as anti-fogging, self-cleaning, or anti-icing. However, some studies have reported that superhydrophobicity does not assure anti-icing/de-icing performance. Icephobic surfaces should hold three requirements: subcooled-water repellency, freezing delay and low ice-adhesion energy. Superhydrophobic surfaces are rough and ice adhesion is mostly increased by interlocking. Lubricant-Impregnated Surfaces (LIS) are also proposed to repel water. Moreover, there are evidences of that these surfaces also mitigate icing and reduce ice-adhesion. For this reason, we are investigating others approaches to prepare low ice-adhesion surfaces.

In this work, to absorb the surface shear stresses of freezing water, we focus on elastic hydrophobic surfaces such as fluorosilicones. We study the ice-adhesion strength on PDMS surfaces with different elastic modulus and thickness. Further, we study oil-infused elastomeric surfaces. Finally, we evaluate the durability of the prepared surfaces (wear, abrasion).

9:20am **TS2-ThM5 Design and Fabrication of Superhydrophobic, Ice-phobic Coatings for High Voltage (HV) Power Lines Application**, *M. Raimondo (mariarosa.raimondo@istec.cnr.it)*, *G. Boveri*, *F. Veronesi*, ISTEC CNR - Institute of Science and Technology for Ceramics, Italy

INVITED

The interaction between water under many different forms – dry or wet snow, ice, frost, rime or their combination – and materials is a complex matter to investigate, depending on many parameters, among which composition and surface texturing, outside temperature, wind velocity, etc. The deposition of water, ice, etc. on structural installations, facilities and infrastructures represents a huge problem in many cold regions. To overcome heavy risks on HV lines, such as the overloading and electricity blackout, new effective strategies - other than the mostly used based on the Joule effect, mechanical removal, electro-impulse methods and application of chemical de-icing fluids - need to be adopted.

New frontiers for superhydrophobic (SH) materials lie in their potential ability to hinder the interaction with water under many different forms so that they might be able to reduce snow, ice or even frost formation and accretion on structural installations, facilities and infrastructures under critical conditions (e.g. at temperatures below 0°C). Here, SH surfaces were obtained by deposition of hybrid nanostructured coatings on aluminum alloy cables commonly used for HV power lines. Two different design approaches to water repellence were pursued: the typical Lotus leaf (*LF*) and the one referring to Slippery Liquid-Infused Porous Surfaces (*SLIPS*), both obtained by the initial deposition of Al₂O₃ nanoparticles, followed by chemical hybridization with a fluoropolymer, plus additional infusion with an ultrasmooth, water-immiscible lubricant overlayer for *SLIPS*. Given the well-known role of surface texture on superhydrophobicity, sandblasted substrates with different roughness were used to assess its influence on the wetting-related performances. Indoor experimental test at lab scale revealed that superhydrophobicity involves the decreasing of shear stress on coated cables even if the ice adhesion strength varies in a more complex way depending on the surface roughness. Materials were also exposed outdoor at test facilities located in the west of Italian Alps, at an altitude of 959 m asl. At T of about -2°C under the conditions of dry snow with a low liquid water content (LWC) and spherical snowflakes morphology, *LF*-like designed sandblasted cables showed a significant delay (some hours) in snow deposition if compared to both the untreated and the *SLIPS* ones. This behavior stood out as the most relevant with respect to the other coated cables, whether smooth or sandblasted. However, under different conditions (-2°C < T < 0°C and wet snow with higher LWC), sandblasted *LF* materials seem to partially lose their ability of delaying snow and ice accretion.

10:00am **TS2-ThM7 Energy Saving Strategy for the Development of Icephobic Coating and Surface**, *Y. Zheng*, *J. Wang*, *J.L. Liu*, *K. Choi*, *X.H. Hou (xianghui.hou@nottingham.ac.uk)*, The University of Nottingham, UK

Aircrafts are frequently exposed to cold environments and ice accumulation on aircraft surface may lead to catastrophic failures. An appropriate solution of ice protection is a critical issue in the aerospace industry. In the R&D of icephobic coating, the current coating design target mainly aims on lowering the ice adhesion strength between the ice and the coating surface. However, as a passive ice protection approach, the use of icephobic coating is often combined with an active ice protection solution (e.g. electro-thermal heating and hot air bleeding), especially for the in-flight application where the reliability of ice protection must be ensured. Therefore, ice adhesion strength is no longer the sole criterion to evaluate the icephobic performance of a coating and a surface. It is a need to establish a better strategy for the design of icephobic coating and surface. In this work, an energy saving strategy has been proposed to assess the de-icing performance of the icephobic coating and surface when heating is involved. The energy consumed for the de-icing operation is used as the key criterion for the overall performance of icephobic coating and surface. Successful validation has been clearly obtained in the evaluation of the de-icing performance of selected coatings and surfaces, which demonstrates a new criterion on the R&D of icephobic coating and surface for ice protection.

10:20am **TS2-ThM8 Anti-Icing Hard Steel Coating Modified With Polymer Particles**, *P. García (garciagp@inta.es)*, *J. Mora*, *A. Agüero*, Instituto Nacional de Técnica Aeroespacial (INTA), Spain

Icing is a severe problem, in particular on aircrafts, with important consequences in safety, energy consumption, ecologic impact, and economy. To fight it, ice protection systems have been developed and have evolved over the last decades, from the highly energy consumption active de-icing systems based on heating, and non-eco-friendly use of de-icing fluids on-ground, to the recent boom that have experimented the technology of passive, anti-icing materials, as well as alternative more efficient new active technologies.

Indeed, very attractive passive surface modification systems have been proposed, decreasing ice accretion and adhesion, but until now, these solutions are not durable and capable of withstanding the harsh conditions to which aircraft surfaces are exposed. A practical approximation would be the development of durable passive solutions that contribute to reduce the power required by the active deicing systems saving energy.

Durable anti-icing coatings with high thermal conductivity deposited over metallic aerodynamic surfaces have been developed and applied by HVOF (High velocity oxyfuel) thermal spray. Mixtures of powders of a high hardness steel and polymer particles were sprayed on stainless steel alloy 304L, and dense 50-100 microns coatings were obtained, with improved anti-icing properties in comparison with the untreated substrate. Extensive preliminary testing of the newly developed coatings has been carried out, including ice accretion in an icing wind tunnel (IWT), employing representative in-cloud icing conditions, allowing to obtain different types of ice: glaze, mixed-glaze, mixed-rime and rime ice. The developed systems showed a significant reduction in ice accretion in comparison with the untreated substrates, with some variations depending on the type of ice and the concentration of added polymer.

Moreover, the durability of the coatings was also examined by repeating icing cycles and by testing for sand and rain erosion resistance. The so tested samples maintained the hydrophobicity with a good water droplet mobility, and in general very promising results in terms of durability after repeated icing/deicing cycles in an IWT.

10:40am **TS2-ThM9 Development of Superhydrophobic and Icephobic Coatings by Suspension Plasma Spraying**, *A. Dolatabadi (ali.dolatabadi@concordia.ca)*, *N. Sharifi*, *R. Attarzadeh*, *C. Moreau*, *M. Pugh*, Concordia University, Canada

INVITED

Suspension plasma spraying (SPS) technique has been used to develop microtextured TiO₂ coatings with a hierarchical surface roughness to develop superhydrophobic surfaces. Superhydrophobic coatings demonstrate extremely water repellent properties and can be potentially used for applications such as anti-icing, reduced drag and friction, self-cleaning and corrosion resistance purposes. The focus of this presentation is on engineering the hierarchical morphology or so-called "cauliflower" features using a parametric study approach to optimize the wetting properties of the coatings. It is demonstrated that by carefully designing and controlling the process parameters, rather fine and uniform dual-scale (hierarchical) surface textured coatings can be generated. Finally, icephobic performance of superhydrophobic surfaces are assessed both experimentally and also

Thursday Morning, May 23, 2019

through a detailed numerical modeling of cloud-sized droplet impact and solidification.

11:20am **TS2-ThM11 Minimum Required Thickness of a Hydrophobic Topcoat to withstand Cycling in an Icing Wind Tunnel**, **S. Brown** (stephen.brown@polymtl.ca), Ecole Polytechnique de Montreal, Canada; *J. Lengaigne*, Polytechnique Montréal, Canada; *N. Sharifi*, Concordia University, Canada; *L. Martinu*, *J.E. Klemberg-Sapieha*, Ecole Polytechnique de Montreal, Canada

Atmospheric icing occurs on aircraft when supercooled water droplets impact exposed surfaces, and quickly freeze in place. This leads to numerous issues such as increased fuel consumption, flight delays, and even crashes. Superhydrophobic surfaces have been shown to reduce icing by allowing droplets to bounce off the surface upon contact, as well as reducing ice adhesion compared to bare metals. A common technique for the creation of a superhydrophobic surface is to develop a surface with hierarchical roughness, and then to coat this surface with a hydrophobic material. If the hydrophobicity comes purely from the topcoat, however, then the durability of the entire system is limited to the durability of this topcoat.

In the present study, we explore the effect of topcoat thickness on sample durability, with the goal of defining a minimum required thickness to withstand repeated icing/deicing cycles. To achieve the desired hierarchical morphology, a $\sim 100 \mu\text{m}$ TiO₂ coating is first deposited on stainless steel by suspension-plasma-spray. Samples are then coated with a fluoropolymer by thermal evaporation, with thicknesses ranging from 7 to 75 nm. These surfaces show contact angles up to $164 \pm 5^\circ$, with hysteresis values as low as $5.8 \pm 0.9^\circ$ prior to cycling. The durability of the developed surfaces is tested by performing icing/deicing cycles in an icing wind tunnel, exposing the samples to supercooled microdroplets at a temperature of -10°C and a velocity of 43 m/s. Contact angle and contact angle hysteresis measurements are performed every 10 cycles. It is shown that samples with topcoats thinner than 20 nm completely lose their superhydrophobic properties after only 10 cycles, while samples with 75 nm topcoats retain at least some droplet mobility after as many as 100 cycles.

Coatings for Use at High Temperatures

Room Pacific Salon 2 - Session A2-2-ThA

Thermal and Environmental Barrier Coatings II

Moderators: Sabine Faulhaber, University of California, San Diego, USA, Kang N. Lee, NASA Glenn Research Center, USA, Pantcho Stoyanov, Pratt & Whitney, USA

1:20pm **A2-2-ThA1 Design of Multiphase Environmental Barrier Coatings: Toward Multifunctional Molten Deposit Resistance**, *D. Poerschke (poerschke@umn.edu)*, University of Minnesota, USA **INVITED**

The ceramic thermal and environmental barrier coatings (T/EBC) employed to protect SiC-based composited in gas turbine engines must satisfy multiple interrelated performance requirements including phase stability, tolerance to thermal strains, and resistance to environmental degradation (e.g., via molten deposits or foreign object impact). It is increasingly evident that rare earth disilicate coatings, which offer good phase stability and minimize the coefficient of thermal expansion (CTE) mismatch with SiC, are not sufficiently resistant to degradation caused by silicate deposits. Reactions between the coatings and deposits progressively consume the coating and produce phases with increased CTE mismatch. Upon thermal cycling, the penetration of channel cracks originating in the reaction layer through the remaining coating and into the composite accelerates the failure of both the coating and the underlying component. Due to the limited number of materials satisfying all of the design requirements, achieving improved performance likely requires multiphase coating systems. This presentation presents a multi-pronged approach to new develop new coating materials. The effort combines new understanding of the thermochemistry of the coating-deposit interactions in order to identify material combinations that minimize the coating recession depth upon exposure to various deposits while developing composite materials with precisely tunes CTEs to manage thermal strains over a wide range of operating conditions.

2:00pm **A2-2-ThA3 Comparison of Oxidation Procedures of MCrAlY Coatings Deposited by PVD Cathodic Arc Evaporation**, *X. Maeder (xavier.maeder@empa.ch)*, *J. Ast*, Empa - Swiss Federal Laboratories for Materials Science and Technology, Switzerland; *M. Polyakov*, EMPA - Swiss Federal Laboratories for Materials Science and Technology, Switzerland; *M. Döbeli*, ETH Zürich, Switzerland; *A. Neels*, *A. Dommann*, Empa - Swiss Federal Laboratories for Materials Science and Technology, Switzerland; *B. Widrig*, *O. Hunold*, *J. Ramm*, Oerlikon Balzers, Oerlikon Surface Solutions AG, Liechtenstein

Development of superalloys which can sustain higher operating temperatures is necessary to increase efficiency of land-based and aero turbines. This requires enhanced surface stability of the components with respect to oxidation and corrosion. The coatings applied to superalloys substrates need therefore to form a well adherent and stable interface towards the substrate by diffusion process and create a protective oxide at their surface. We will show here the capability of depositing MCrAlY coatings by cathodic arc evaporation on Ni-based superalloy substrates. MCrAlY targets were produced by spark plasma sintering and processed in non-reactive mode and in mix non-reactive and reactive modes on directional solidified CM247 and single crystalline PWA1483 substrates. The phases, microstructure and composition of the targets and synthesized coatings are characterized by TEM, transmission EBSD, X-ray diffraction and RBS analyses and discussed. The interface between the MCrAlY coatings and the different Ni-based superalloy substrates before and after annealing is investigated and different approaches to form an oxide scale on top of the MCrAlY coating are discussed.

2:20pm **A2-2-ThA4 Effect of APS Flash Bond Coatings and Curvature on Furnace Cycle Lifetime of Rods**, *M.J. Lance (lancem@ornl.gov)*, *J.A. Haynes*, *B.A. Pint*, Oak Ridge National Laboratory, USA; *E. Gildersleeve*, *S. Sampath*, Stony Brook University, USA

The addition of an air plasma sprayed (APS) "flash" bond coating layer on top of a high velocity oxy-fuel (HVOF) bond coating significantly extended the lifetime of APS yttria stabilized zirconia (YSZ) top coatings on rod specimens of superalloy 247 tested using 100-h cycles in air+10% H_2O at 1100°C. The flash coatings of both NiCoCrAlY and NiCoCrAlYHfSi powder were compared to an HVOF-only and a vacuum plasma sprayed (VPS) NiCoCrAlYHfSi bond coating. The flash coatings appear to form a mixed oxide-metal zone that appeared to inhibit crack formation and extend lifetime compared to conventional bond coatings. The underlying HVOF layer acted as a source of Al for this intermixed zone and prevented the oxide from penetrating deeper. Residual stress in the thermally grown Al_2O_3 scale was measured using photo-luminescence piezospectroscopy (PLPS) as a function of time for

each coating variation, including a comparison of concave and convex surfaces.

Research sponsored by the U. S. Department of Energy, Office of Fossil Energy's Turbine Program.

2:40pm **A2-2-ThA5 Investigation of Thermally Grown Oxide Stress in Plasma-spray Physical Vapor Deposition and Electron-beam Physical Vapor Deposition Thermal Barrier Coatings via Photoluminescence Spectroscopy**, *L. Rossmann (lin.rossmann@knights.ucf.edu)*, *M. Northam*, University of Central Florida, USA; *V. Viswanathan*, Praxair Surface Technologies, USA; *B. Harder*, NASA Glenn Research Center, USA; *S. Raghavan*, University of Central Florida, USA

Gas turbine engines for aircraft propulsion require thermal barrier coatings (TBCs) to protect metallic components in the hot section from the extreme temperatures of operation, which may exceed 1200 °C. These coatings are typically 6-8% yttria-stabilized zirconia (YSZ), and the standard methods of coating deposition are air plasma spray (APS) and electron-beam physical vapor deposition (EB-PVD). EB-PVD produces a higher-quality coating than APS due to its resulting columnar microstructure that increases the strain tolerance of the coating. Plasma-spray physical vapor deposition (PS-PVD) is a promising technique that offers several advantages over EB-PVD, including lower cost, shorter coating time, customizability of microstructure by varying processing parameters, and possibility of non-line-of-sight coating. However, the effect of this process on the resulting microstructure, properties, and performance is not fully understood. In this work, TBCs manufactured by both EB-PVD and PS-PVD were investigated via photoluminescence spectroscopy after varying amounts of thermal cycling, to investigate the effect of deposition process on the stress state of the thermally grown oxide (TGO) layer.

This work investigates the residual stress in the TGO of samples made by EB-PVD and PS-PVD, thermally cycled in the same way at multiple lifetimes (as-deposited, 300 cycles, and 600 cycles), to evaluate the effects of deposition method. As-deposited PS-PVD samples were given a 1-hour heat treatment, during which they developed a TGO. This was found to be in compression on the order of 2-3 GPa, consistent with published data on EB-PVD TBCs. Other PS-PVD samples were cycled for 300 and 600 hours, and these exhibited stress relaxation compared to the 1-h heat treated, suggesting some stress relief from damage. The findings from these investigations will be presented in the paper.

In this study, we compare the TGO residual stress evolution in PS-PVD and EB-PVD TBCs to shed light on their respective responses to thermal cycling. These results contribute to understanding how the PS-PVD process compares to the EB-PVD process with respect to coating life and durability.

3:00pm **A2-2-ThA6 Thermally Conductive and Electrically Insulating Epoxy Nanocomposites with Intercalation of Aluminum Nitride Nanoparticles into Exfoliated Graphite**, *C.J. Wu (terry205502013@gmail.com)*, National Cheng Kung University, Taiwan

In this study, the enhancement of thermal conductive of epoxy-based nanocomposites without scarifying electrical insulating were demonstrated. This was done by introducing intercalated aluminum nitride (AlN) into expanded graphite in the nanocomposite. Intercalation of AlN nanoparticles into adjacent exfoliated graphite were firstly prepared via solution mixing with supercritical fluid CO_2 (SCCO₂). SCCO₂'s low surface tension and viscosity lead to greater penetration into porous solid. Epoxy composites with an intercalated of AlN nanoparticles into exfoliated graphite were fabricated using a three roll mills machine. Scanning electron microscopy images reveal that intercalation of AlN into exfoliated graphite structures were formed and were uniformly dispersed in the epoxy matrix. The in-plane and through-plane electrical and thermal conductivities of thin thermal interface layers of epoxy composites were discussed. Compare to epoxy composites with only exfoliated graphite, epoxy composites with intercalation of AlN nanoparticles into exfoliated graphite not only maintain epoxy's electrically insulation but also enhance through-plane thermal conductivity, which make this material an attractive candidate for electronic field applications especially thermal interface materials (TIMs).

3:20pm **A2-2-ThA7 Effect of Feedstock Species on Thermal Durability of Thermal Barrier Coatings**, *S.W. Myoung (sangwon.myoung@doosan.com)*, *B.I. Yang*, *I.S. Kim*, Doosan Heavy Industries and Construction, Republic of Korea; *Y.G. Jung*, Changwon National University, Republic of Korea
Thermal durability and stability of thermal barrier coatings (TBCs) are closely related with its microstructure and feedstock species. Numerous factors, besides the thermal and mechanical properties, have to be considered in practical applications of TBCs. There is therefore a need to the reliability and

lifetime performance of the plasma sprayed TBC system. In this study, the microstructures in the top and bond coats of TBCs have been deposited different plasma spray process. The TBC system with the thicknesses of 500 and 200 nm in the top and bond coats, respectively, were prepared with the air plasma sprayed (APS) coating system using $ZrO_2-8wt\% Y_2O_3$ powders for the top coats and vacuum-plasma sprayed coating system using Ni-based metallic powders for the bond coats. In order to investigate the improvement of thermal durability, the furnace cyclic test (FCT) was performed for the TBC samples at a temperature of 1100°C with a dwell time of 1 h for 1000 cycles. Porosity and pore size distribution were measured with the FCT, and the effects of feedstock species in the TBC on mechanical properties such as hardness and toughness were observed, including the adhesive strength before and after the FCT. The nominal pore size of as-prepared TBC system is dramatically reduced with increasing thermal exposed cycle. The hardness and toughness values are increased to 1000 cycles. The influence of feedstock species on the microstructural evolution and thermal durability of TBC is discussed.

3:40pm A2-2-ThA8 Development of Environmental Barrier Coatings for SiC/SiC Ceramic Matrix Composites via CVD, T. König (till.koenig@dechema.de), M.C. Galetz, DECHEMA-Forschungsinstitut, Germany

With increasing combustion temperature of turbine engines the commonly used nickel-based superalloys are getting closer to their melting point and excessive cooling along with thermal barrier coatings are used to maintain the properties at the desired level. The substitution of these alloys by Ceramic Matrix Composites (CMC) for applications in the high temperature region of turbines is widely discussed and first parts are in service. Due to their mechanical properties at high temperatures especially SiC/SiC-CMC are investigated. Their advantages include a low density, high specific strength and a low creep rate even at very high temperatures. Therefore the efficiency of the turbines can be increased by using higher combustion temperatures, the abandonment of cooling and reducing the mass. In oxidizing atmospheres these materials form silica scales, which are generally considered protective. But the presence of water vapor, which forms during the combustion process, results in the volatilization of the silica scale by the formation of hydroxides. The simultaneous process of oxidation and evaporation follows parabolic kinetics and makes it necessary to apply coatings that reduce the evaporation and result at best in parabolic kinetics. Under investigation are multi layered environmental barrier coatings (EBC) that reduce the silica activity by mixed oxides (e.g. rare earth silicates) or by forming oxides not prone to evaporation (e.g. Al_2O_3).

In this study the chemical vapor deposition process (CVD) was used instead of or in addition to the commonly used thermal spraying with the aim to apply coatings that show a better adherence and cover the whole surface (line of sight). A layered chromium aluminide, chromium silicide coating was applied by chromizing and subsequent aluminizing in a second step, both via pack cementation. Aluminum nitride was applied by a two-step process consisting of aluminizing via pack cementation and subsequent nitriding as well as by direct deposition via high temperature CVD. The evaporation of these coatings was tested in comparison to the uncoated CMC in water vapor containing atmospheres. The adherence was investigated in synthetic air under thermal cycling conditions to test the influence of possible thermal expansion mismatches. To identify the phases and the microstructure X-ray diffraction (XRD), scanning electron microscope (SEM) and electron probe microanalysis (EPMA) were used.

Hard Coatings and Vapor Deposition Technologies Room Golden West - Session B2-1-ThA

CVD Coatings and Technologies I

Moderators: Kazunori Koga, Kyushu University, Japan, Raphaël Boichot, Université Grenoble Alpes, CNRS, France

1:20pm B2-1-ThA1 Impact of HfO_2 as a Buffer Layer on the Electrical and Ferroelectric Memory Characteristics of Metal/Ferroelectric/High-K/Semiconductor Gate Stack for Nonvolatile Memory Applications, R. Jha (rajajha25@gmail.com), P. Singh, M. Goswami, Indian Institute of Information Technology Allahabad, India; B.R. Singh, Park Systems, India
For the proposed work, the electrical properties of metal-ferroelectric-insulator-silicon (MFeIS) capacitors with $Sr_{0.8}Bi_{0.2}Ta_{0.9}O_9$ (SBT) ferroelectric film deposited on HfO_2/Si substrate has been investigated. The SBT film was deposited by RF sputtering and HfO_2 film by plasma enhanced atomic layer deposition (PEALD). The structural characteristic of the deposited

ferroelectric and dielectric films was obtained using X-ray diffraction and multiple angle ellipsometric analysis. Metal/Ferroelectric/Silicon (MFeS), Metal/Ferroelectric/Metal (MFeM), Metal/Insulator/Silicon (MIS) and Metal/Ferroelectric/Insulator/Silicon (MFeIS) structures were fabricated to obtain the electrical and ferroelectric properties. MFeIS structure with 10 nm buffer layer shows the improved memory window of 5 V as compared to the 3.07 V in the MFeS structures. MFeIS structure even show endurance higher than 10^{12} read/write cycles and data retention for more than 8 hours. The effect of thickness and annealing temperature of buffer layer has also been investigated. The improvement in remnant polarization and coercive field due to the introduction of high-K layer has also been studied and compared with previous results.

1:40pm B2-1-ThA2 Studies on Properties and Cutting Performance of Al-rich AlTiN Coating with Controlled Orientation via LP-CVD, Y. Kido (kido-yasuki@sei.co.jp), A. Paseuth, S. Okuno, S. Imamura, Sumitomo Electric Hardmetal Corp., Japan

Al-rich AlTiN is one of the important hard coatings for cutting tool. Among them, cubic phase AlTiN (c-AlTiN) comprising c-Al(Ti)N/c-Ti(Al)N nanolamellae structure with high Al content and controlled orientation via LP-CVD has been modern coating due to high hardness and strength, compared to conventional CVD coating also AlTiN by PVD. The aim of this study is to investigate the effect of c-AlTiN coated carbide tools, as a function of component (Al/Ti ratio) and orientation, on mechanical and thermal properties also cutting performance. Deposition of c-AlTiN with controlled component and orientation was conducted by LP-CVD using $AlCl_3-TiCl_4-NH_3$ precursor system. High-resolution transmission electron microscopy revealed formation of c-AlN and c-TiN-rich domains in nanometer scale. The c-AlTiN coating showed high hardness and compressive stress with adhesion by indentation technique, X-ray diffraction and scratch test. Also thermal property was measured. Furthermore, a cutting test for cast iron milling was performed with different kinds of component and orientation c-AlTiN coating on carbide tools.

2:00pm B2-1-ThA3 Effects of Al Content and Growth Orientation on Mechanical Properties of AlTiN Coatings Prepared by CVD Method, K. Yanagisawa (kyanagis@mmc.co.jp), T. Ishigaki, H. Nakamura, H. Homma, Mitsubishi Materials Corporation, Japan

AlTiN coatings with high aluminum content have attracted attention due to its beneficial properties such as high oxidation resistance and age hardening effect on metal cutting. It is well-known that conventional AlTiN coatings are deposited by PVD method and the maximum aluminum content Al/(Al+Ti) is limited to lower than 0.67 to maintain a single phase cubic. Otherwise, in the range of aluminum content Al/(Al+Ti) higher than 0.67, they contain hexagonal phase which has lower hardness.

In this work, (111)- and (100)- oriented cubic AlTiN coatings with aluminum content higher than 0.67 were prepared on cemented carbide substrates by CVD method. Microstructure of the deposited coatings was observed by scanning electron microscopy, and the crystallographic orientation of these coatings was examined by X-ray diffraction analysis. Additionally, the hardness of these coatings was measured using nanoindentation and crack resistance property was evaluated by crack length induced by Vickers indentation, respectively.

From SEM observation, all of these coatings had columnar microstructures which contained self organized nano-lamellae structures in grains. Nanolamellae structure in (100)-oriented coatings had a tendency to be smaller periods of the compositional fluctuation compared with those of (111)-oriented coatings, despite the almost same composition. As for the mechanical properties, the coatings with higher aluminum content or preferred (111) orientation showed higher hardness and higher crack resistance property. Thus, it was suggested that the hardness or crack resistance property of coatings was correlated to not only aluminum content but also the morphology of nano-lamellae structure.

One of possible explanation for the higher hardness, the deforming energy caused by indentation was dissipated by nano-lamellae structure. This effect is similar to a pinning effect for the propagation of the dislocations at interfaces of a multilayered coating. Regarding the superior crack resistance, it was attributed to crack deflection at the nano-lamellae structure.

Besides, these coatings were tested for the dry milling operation of 42CrMo4 steel blocks. It was indicated that CVD – AlTiN coatings with higher aluminum content showed superior wear and thermal crack resistance. On the other hand, the difference of coating orientation did not affect to the cutting results in this work.

Thursday Afternoon, May 23, 2019

2:20pm **B2-1-ThA4 Thermal Crack Network Formation in CVD TiCN/ α -Al₂O₃ Coatings**, *N. Schalk (nina.schalk@unileoben.ac.at)*, R. Stylianou, M. Gassner, Montanuniversität Leoben, Austria; D. Velic, W. Daves, W. Ecker, Materials Center Leoben Forschung GmbH, Austria; M. Tkadletz, Montanuniversität Leoben, Austria; C. Czettl, CERATIZIT Austria GmbH, Austria; C. Mitterer, Montanuniversität Leoben, Austria

TiCN/ α -Al₂O₃ coatings grown by thermally activated chemical vapor deposition on cemented carbide substrates typically exhibit a crack network as a result of the different thermal expansion coefficients (TEC) of coating and substrate material. Thus, the present work focuses on the investigation of these thermal cracks and on strategies to avoid them. The thermal cracks in industrially applied TiCN/ α -Al₂O₃ coatings were studied in different conditions, i.e. in as-deposited state, after post-treatment by wet-blasting and annealing as well as after face turning, by scanning electron microscopy techniques. While wet-blasting results in closure of the thermal cracks near the coating surface due to the introduction of compressive stresses, annealing and turning lead to a relaxation of these stresses and thus in the reappearance of the cracks. In an attempt to avoid the formation or to reduce the density of cracks, TiCN/ α -Al₂O₃ coatings were deposited on a series of cemented carbide substrates with cobalt contents of 6, 7.5, 10, 12.5 and 15 wt.%. The determination of the TEC of both, substrates and coating yielded a decreasing mismatch of the TECs with increasing cobalt content. At the highest cobalt content, no cracks and only low tensile stresses are observed in the coating. Decreasing the cobalt content yields first a tensile stresses maximum, followed by decreasing tensile stresses at even lower cobalt contents as a result of stress relaxation due to promoted crack formation. Finally, finite element simulations of the residual stresses in the coating after deposition, considering different crack distances, corroborate the experimental results.

2:40pm **B2-1-ThA5 Nanostructure of Textured CVD TiAlN**, *O. Bäcke (obacke@chalmers.se)*, Chalmers University of Technology, Sweden; W. Janssen, T. Manns, J. Kümmel, D. Stiens, Walter AG, Germany; M. Halvarsson, Chalmers University of Technology, Sweden

TiAlN is today a common choice for wear-resistant coatings on cutting tools used for metal machining due to its high hardness and excellent oxidation resistance. For long, physical vapour deposition (PVD) has been the standard method for producing commercial available TiAlN coatings. Using PVD it has been impossible to reach Ti_(1-x)Al_xN coatings with a higher Al content than x = 0.65. A few years ago however a new low pressure CVD technique was developed that makes it possible to deposit Ti_(1-x)Al_xN coatings with a very high Al content, x = 0.9. These high Al content TiAlN coatings show improved hardness compared to other TiAlN coatings and commercially available CVD grown TiAlN coatings are just reaching the market. However, how TiAlN start to nucleate and grow during CVD is not very well understood. Film growth is very sensitive to deposition parameters and h-AlN can easily form alongside TiAlN. TiAlN layers show large variations in nanostructure, stemming from local variations in Ti, Al and N ratio. The variations can be either periodic, non-periodic, or not exist at all depending on deposition parameters. The large variations in nanostructure can affect properties such coating hardness and thermal stability. TiAlN is metastable and will with time decompose to c-TiN and h-AlN when exposed to elevated temperatures. It is thus of interest to investigate how the nanostructure of TiAlN layers can differ with deposition and have been the focus of the work performed. TiAlN coatings with 111 texture were produced on standard WC/Co cemented carbide substrates. The coatings were characterized by X-ray diffraction, high resolution scanning and transmission electron microscopy (STEM and TEM), and energy dispersive X-ray analysis with a focus on when and when not a nanostructure consisting of nanosized lamellas is obtained.

3:00pm **B2-1-ThA6 Structural and Piezoelectric Properties of Chemical Vapor Deposited AlN Films on Metallic Substrates**, *J. Su (juan.su@grenoble-inp.fr)*, M. Pons, F. Mercier, D.Y. Chen, R. Boichot, Université Grenoble Alpes, CNRS, France

To monitor the state of stress and damage in cutting tools or critical equipment working under extreme conditions such as high temperature, high pressure or aggressive chemical environment, the strongly textured AlN as a piezoelectric layer was successfully deposited on metals by Chemical Vapor Deposition (CVD) method. Low temperature textured TiN by CVD from TiCl₃-H₂-NH₃ system or AlN by Atomic Layer Deposition (ALD) is applied as a buffer layer to avoid the instability of metal substrates in CVD reactor during growth and decrease the huge mismatch between substrates and AlN layer. A design of experiment (DOE) is used to analyze the influence of 7 main process parameters and find a suitable experimental condition for depositing dense, covering and textured AlN. The morphology, XRD results and piezoelectric coefficient d₃₃ are compared and analyzed. Unexpectedly,

the results show that (200) textured TiN is a good buffer layer to obtain (002) textured AlN on WC-Co. On the contrary, the AlN with the thickness of 90 nm deposited by ALD is the best buffer layer for TZM. At last, the relationship between texture coefficient and d₃₃ is studied considering 10 different orientations of AlN. It proves that when (002) texture coefficient is less than 2, d₃₃ almost keeps constant at 0.14 pC/N, then it increases linearly to more than 2 pC/N while the theoretical bulk piezoelectric coefficient for AlN is around 6 pC/N.

3:20pm **B2-1-ThA7 Aluminum Nitride Based Coatings for High Temperature Solar Receiver Systems**, *D.Y. Chen (danying.chen@grenoble-inp.fr)*, Université Grenoble Alpes, CNRS, France; J. Colas, PROMES-CNRS, France; J. Su, Université Grenoble Alpes, CNRS, France; L. Charpentier, M. Balat-Pichelin, PROMES-CNRS, France; F. Mercier, M. Pons, Université Grenoble Alpes, CNRS, France

There is a growing interest in concentrating solar power plants as electricity generation systems, whereby the sunlight is redirected and focused onto a receiver heated to high temperature. One of the challenges is to build the solar receiver which can work at temperatures near or higher than 1000 °C for optimizing the yield. Current candidate materials are metallic alloys such as Inconel, or bulk ceramics like silicon carbide, but their operating temperatures may be limited due to oxidation or mechanical problems. Aluminum nitride (AlN) coating, deposited by chemical vapor deposition at 1100 °C, was selected for its high thermal conductivity, low thermal expansion coefficient, high temperature stability and its oxidation resistance. It forms stable and protective alumina scales at temperatures higher than 1000°C. Oxide dispersion strengthened (ODS) FeCrAl alloy (Kanthal APMT), also alumina-forming, was chosen as a model substrate to study the potential of AlN coatings. Accelerated cyclic oxidation and high temperature emissivity measurements were performed in Odeillo solar furnace facilities (France), confirming the potential of aluminum nitride coatings as materials for high temperature central receivers. The AlN based multilayered system exhibits low degradation after 1500 h of oxidation at 1100 °C in air. The modelling and simulation of stresses during thermal cycles taking into account the creep and growth of the oxide layer are used to show the limits of use of these materials.

3:40pm **B2-1-ThA8 Residual Stress and Quantitative Texture of CVD Al₂O₃ Coatings**, *Z. Liu (Zhenyu.Liu@kennametal.com)*, Kennametal Inc., USA; S. Tan, University of Pittsburgh, USA; D. Banerjee, Kennametal Inc., USA

Conventional CVD coatings on cemented carbide are characterized by tensile stress, due to high temperature of deposition and thermal expansion mismatch between substrate and coating materials. The stress results in a mesh like cracking pattern in the coating, and may reduce toughness of coating leading to premature failure. It has been demonstrated that the tensile stress can be reduced, or reversed into compression by different postcoat blasting treatment. It is clear that postcoat blasting can reduce the extent of tensile stress in functional layer or even modified the stress state into compressive. At the same time, the residual stress of deposited coating and stress relieve during the high temperature caused by *in situ* heating during the metal-cutting practice, in another word, the stress situation in the coating, will affect the ultimate metal-cutting performance as well.

Anisotropic properties of crystal material make the texture of coated thin films a very important factor to affect the metal-cutting performance. Most of investigations on coating texture are determined by texture coefficient. There is still lack of the quantitative textural analysis of the tool coatings. With the aid of XRD/EBSD, the quantitative analysis of texture components can be determined then provide better evaluation on the highly textured coatings, such as Al₂O₃.

4:00pm **B2-1-ThA9 Gas Source Chemical Vapor Deposition of Wafer-scale Mono- and few-layer MX₂ (M=W or Mo and X=S or Se) and Their Alloys**, *M. Chubarov (mikhail.chubarov@gmail.com)*, T. Choudhury, D. Reifsnnyder Hickey, S. Bachu, N. Alem, J. Redwing, The Pennsylvania State University, USA

INVITED

Transition metal dichalcogenides (TMD) like WS₂, WSe₂, MoS₂ and MoSe₂, when thinned to a monolayer (ML) thickness show direct bandgap, valley spin polarization, reasonable charge carrier mobilities and relatively high optical absorption; properties relevant to many applications. In addition to binary materials, alloys of TMD materials are also promising. It was reported that electronic transport properties are not dramatically deteriorated for the TMD alloys, and alloying allows for bandgap engineering over a wide range between 1.56 eV (794.8 nm) for MoSe₂ and 2.01 eV (590.4 nm) for WS₂. To push these materials towards practical applications, wafer-scale epitaxial growth of ML and few-layer (FL) films is necessary which can be achieved using CVD. In this study, to achieve ML and FL epitaxial layers of TMD

materials and their alloys, we use gas source CVD and sapphire ((0001) α - Al_2O_3) as substrates.

For the growth we employ metal hexacarbonyls ($\text{W}(\text{CO})_6$ and $\text{Mo}(\text{CO})_6$) and hydrides (H_2S , H_2Se) as precursors diluted in hydrogen (H_2) carrier gas. Deposition temperature for this class of materials is in the range between 800 and 1000 °C at a pressure of 50 Torr for sulfides and 200 Torr for selenides. For the growth of binary compounds, a previously developed multistep growth process was employed while for the alloys, a single step was implemented to minimize routes for the formation of compositional gradients in the resulting layers.

As a result, we obtained ML and FL films of TMD materials. Acquired samples showed epitaxial relation with the substrate, high intensity photoluminescence and, for the alloys, composition control was achieved over a wide range as determined using X-ray photoelectron spectroscopy. Growth of WS_2 films resulted in growth of epitaxial ML films ((10-10) WS_2 //((10-10) α - Al_2O_3) with in plane twist of 0.1°, room temperature photoluminescence (PL) showed emission maximum at 2 eV and width of 0.04 eV with pronounced exciton and trion components as well as defect-bound exciton emission. Domain size and distribution of antiphases were studied using transmission electron microscopy (TEM). This showed a relatively low fraction of isolated antiphase regions.

WMoS_2 alloys showed variation in the PL peak position as well as a change in the Raman scattering spectra which can be correlated with the composition of the film. Microstructure of the films was studied using TEM that showed no distinct segregation of the metal atoms when continuous flows of metal precursors were used.

Further details on the growth and characterization of MoS_2 , WSe_2 and MoSe_2 will be presented along with the results obtained from ternary alloy growth and characterization.

4:40pm B2-1-ThA11 The Effect of Dopants and Bilayer Period on Microstructure and Mechanical Properties of CVD Ti(B,C)N Hard Coatings, C. Kainz (christina.kainz@unileoben.ac.at), N. Schalk, M. Tkadletz, C. Mitterer, Montanuniversität Leoben, Austria; C. Czettel, CERATIZIT Austria GmbH, Austria

The cutting performance of CVD TiN hard coatings can be improved by both, the alloying with additional elements, or through the application of a multilayered coating design. However, limited literature is available on the mutual influence of chemical composition and architecture on the properties of CVD Ti(B,C)N coatings. Thus within this work, a comparison of mono- and multilayered CVD hard coatings within the system Ti(B,C)N with a particular focus on their microstructure, mechanical properties and microscopic fracture behavior is presented. The coatings were grown onto cemented carbide substrates in an industrial-scale thermal CVD plant using BCl_3 , CH_4 , TiCl_4 , N_2 and H_2 precursors. Transmission electron microscopy investigations showed a higher defect density and grain refinement in the ternary and quaternary coatings compared to binary TiN. X-ray diffraction confirmed the presence of the hexagonal TiB_2 phase embedded in the B-containing coatings within the face-centered cubic TiN or TiCN matrix. Nanoindentation revealed an increase of hardness with decreasing bilayer period for the multilayer coatings and the highest hardness (32.2 ± 1.0 GPa) and Young's modulus (587 ± 29 GPa) for the TiBCN monolayer coating. Finally, bending tests, performed with free-standing coating micro-cantilevers prepared by focused ion beam milling, provided insights into the effect of alloying and bilayer period on coating strength and toughness. This juxtaposition of different chemical compositions and architectures enables to identify the most promising coating for application in metal cutting.

Keywords: CVD, Ti(B,C)N, hard coatings, TEM, micromechanical testing

Hard Coatings and Vapor Deposition Technologies

Room California - Session B5-1-ThA

Hard and Multifunctional Nanostructured Coatings I

Moderators: Tomas Kozak, University of West Bohemia, Czech Republic, Helmut Riedl, TU Wien, Institute of Materials Science and Technology, Austria

2:00pm B5-1-ThA3 Interfaces and Mechanisms: A Molecular Dynamics Approach to Fine Tuning Manipulation of Mechanical Properties, A.F. Fraile (frazilb@fel.cvut.cz), H.Y. Yavas, E.F. Frutos, Department of Control Engineering, Faculty of Electrical Engineering, Czech Technical University in Prague, Czech Republic; T.H. Huminiuc, Engineering Science, Faculty of Engineering and the Environment, University of Southampton, Southampton, UK; T. Polcar, Czech Technical University in Prague, Czech Republic

With the advent of more and more powerful supercomputers, Molecular Dynamics (MD) is playing today a capital role in the understanding of the deformation mechanisms at the atomic scale of all kind of materials under different scenarios. Many investigations have demonstrated that the peculiar features of nanoplasticity generated during indentation can be analyzed in detail by this technique.

Using MD we are constructing deformation-mechanism maps based on fundamental physical processes in the deformation of nanostructured materials. The knowledge for these processes comes from modelling the nanostructures at the atomic level by using atomistic simulations. The power of our approach is that it integrates the most important physics associated with deformation phenomena, in a self-consistent description of the effects of stress, interfaces and grain size on the mechanical properties in nanocrystalline structures, thereby avoiding the empiricism of other methods.

We have prepared different Zr/Nb layered systems (with different Nb/Zr geometries and/or structures) and indentation hardness close to the theoretical limits was measured for special cases. Then, our theoretical calculations were compared to the experimental results. Special attention was devoted to the effect of interlayers, grain boundaries, dislocation reactions as well as the effect of phase transitions in Zr.

The dominant deformation mechanism of metallic multilayered systems is the confined volume dislocation reactions, however, we also showed that there is a high possibility to control the deformation by tuning phase transformations at the nanoscale. This knowledge will open new doors to shed light into hidden features of the deformation and strengthening mechanisms guiding the design the next generation of metallic coatings and alloys.

2:20pm B5-1-ThA4 Preparation of Hard Yet Fracture Resistant W-B-C Coatings Using High Power Impulse Magnetron Sputtering, P. Soucek (soucek@physics.muni.cz), M. Polacek, P. Klein, L. Zabransky, V. Bursikova, M. Stupavska, Masaryk University, Brno, Czech Republic; Z. Czigany, K. Balazsi, Hungarian Academy of Sciences, Hungary; P. Vasina, Masaryk University, Brno, Czech Republic

As the demands for the quality and speed of machining increase, the application of protective coatings on the used cutting tools becomes ever more important. Nowadays used ceramic protective coatings exhibit high hardness and toughness, however, they suffer from inherent brittleness. This can lead to a premature failure of the coating and of therefore of the cutting tool as a whole due to rapid crack propagation. Thus, a new generation of coatings combining hardness and moderate ductility is sought for.

Such a combination of seemingly mutually exclusive properties was recently predicted by ab-initio calculations in inherently nanolaminated X_2BC crystalline coatings, where X is a metallic element [1]. W_2BC system was found the most promising regarding its mechanical properties with predicted Young's modulus of ~ 470 GPa, B/G ratio of 1.91 and Cauchy pressure of 71 GPa. However, only a near zero negative value of its formation enthalpy of -0.16 eV/atom predicts problems with crystallization of this phase [1]. Indeed, previous works using mid-frequency pulsed DC sputtering did not report the formation of the crystalline W_2BC phase [2].

This contribution reports on the synthesis and comparison of W-B-C coatings sputtered from a compound W_2BC target using DCMS and HiPIMS, respectively. Different substrate temperatures up to 700°C were used in each case. The differences in the DCMS and HiPIMS deposition processes will be discussed. The microstructure of the coatings is investigated and is correlated to their mechanical properties. The fracture resistance and the

deformation behaviour of the coatings will be discussed. Simultaneous achievement of high hardness and fracture resistance will be shown as well as the means of its achievement will be discussed.

This research has been supported by project LO1411 (NPU I) funded by the Ministry of Education, Youth and Sports of the Czech Republic.

[1] H. Bolvardi, J. Emmerlich, M. to Baben, D. Music, J. von Appen, R. Dronskowski, J.M. Schneider, *J. Phys.: Condens. Matter* 25 (2013) 045501

[2] M. Alishahi, S. Mirzaei, P. Soucek, L. Zabransky, V. Bursikova, M. Stupavska, V. Perina, K. Balazsi, Zs. Czigany, P. Vasina, *Surf. Coat. Technol.* 340 (2018) 103-111

2:40pm B5-1-ThA5 Analytical Modelling of Misfit Dislocation Formation in Superlattice Coatings and its Effect on the Fracture Toughness, A. Wagner (antonia.wagner@tuwien.ac.at), TU Wien, Institute of Materials Science and Technology, Austria; D. Holec, Montanuniversität Leoben, Austria; M. Todt, TU Wien, Institute of Lightweight Design and Structural Biomechanics, Austria; P.H. Mayrhofer, M. Bartosik, TU Wien, Institute of Materials Science and Technology, Austria

Coherently grown multilayer coatings with a bilayer period in the nanometer range exhibit a superlattice (SL) effect in mechanical properties like hardness and fracture toughness [1, 2]. While the superlattice effect in hardness is well described by the model after Chu and Barnett [3] based on dislocation plasticity, the fracture toughness enhancement in 'all-ceramic' SL coatings is not primarily governed by plasticity and the underlying mechanisms are less well understood.

The aim of the present work is to study the effect of the residual stress state in SL coatings on the fracture toughness. In general, extrinsic residual stresses (due to a mismatch of the coefficients of thermal expansion) and intrinsic stresses (stemming from the film growth process) contribute to the overall stress state. A major part of the intrinsic stresses, in turn, are coherency stresses, which originate from the epitaxial growth and the lattice mismatch of the film forming phases and the substrate material. While the thermal mismatch stresses are almost independent of the individual layer thicknesses, coherency stresses show a strong dependency when considering the formation of misfit dislocations. Up to a critical thickness of the layers, the misfit in the lattice parameters is accommodated by elastic strain, thereafter misfit dislocations form, preferably at the interface to the substrate or the previously deposited layer [4, 5].

We have calculated the dislocation density as a function of the layer thickness by an energy balance considering the strain energy of the system and the dislocation energy. An analytical model - with layerwise deposition of the individual layers including misfit dislocations - was developed to predict the stress state of superlattice systems as a function of the bilayer period. Finally, the fracture toughness and its dependence on the bilayer period was calculated taking into account the stress state, the intrinsic fracture toughness of the phases and the spatial variation of elastic properties of respective SL architectures.

[1] U. Helmersson, S. Todorova, S.A. Barnett, J.-E. Sundgren, L.C. Markert, J.E. Greene, *J. Appl. Phys.* 62 (1987) 481.

[2] R. Hahn, M. Bartosik, R. Soler, C. Kirchlechner, G. Dehm, P.H. Mayrhofer, *Scr. Mater.* 124 (2016) 67.

[3] X. Chu, S.A. Barnett, *J. Appl. Phys.* 77 (1995) 4403.

[4] L.B. Freund, S. Suresh, *Thin Film Materials: Stress, Defect Formation, and Surface Evolution*, Cambridge University Press, Cambridge, 2003.

[5] D. Holec, P.M.F.J. Costa, M.J. Kappers, C.J. Humphreys, *J. Crystal Growth* 303 (2007) 314.

4:20pm B5-1-ThA6 The Electrical Response of PVD Deposited Nanocrystallized Carbon Film in Magnetic Field, C. Wang (cwang367@szu.edu.cn), J. Guo, X. Dai, Institute of Nanosurface Science and Engineering, College of Mechatronics and Control Engineering, Shenzhen University, China

Nano-crystallized carbon film has gained much attentions due to its excellent electrical and mechanical properties, especially its magnetoresistance (MR) at room temperature. The novel electrical response of this film under external magnetic field shed light on a new-type carbon based magnetic sensing device. Recently, it is found that the MR performances of the film can be strongly improved by introducing Si as substrate instead of SiO₂. Transport study implied that the film has high carrier density and ultra low mobility, which may be originated from the modulation effect of n-type doping substrate.

In this study, nanocrystallized carbon films were deposited on silica and N-type silicon substrates with plasma assisted PVD method. The nanocrystallized structure were observed through high resolution TEM and Raman spectra. The change of electrical resistances along with temperature and magnetic field strength were measured by using Quantum Design physical property measurement system (PPMS). The results showed that the nanocrystallized films showed large magnetoresistance at 300K, which is favorable for room temperature applications. The magnetic response behavior of the carbon films on different substrates were compared, which suggested that the n-silicon substrate can remarkably improved the magnetoresistance coefficient. The influences of gas flow, bias voltage, and deposition time on the structure, carrier density and magnetoresistance of the carbon films were investigated, and the transport mechanism of carriers in the films were discussed. We also found the large magnetoresistance of the film when using alternating current as stimulating source, when the largest rate of magnetoresistance can reach to 1000% per tesla at room temperature. This is ascribed to the inductive as well as spin-enhanced magnetoresistance effect due to the oriented graphene nanocrystallites inside the semiconductive film matrix.

3:20pm B5-1-ThA7 Aluminium Nitride Based Piezoelectric MEMS: From Material Aspects to Low Power Devices, U. Schmid (schmid@isas.tuwien.ac.at), M. Schneider, TU Wien - Institute of Sensor and Actuator Systems, Austria

INVITED

In a compact introduction, I will motivate the benefits of piezoelectric thin films for MEMS and will give a short overview to state of art application scenarios on device level. Next, I will highlight latest results on the electrical, mechanical and piezoelectrical characterization of sputter-deposited aluminium nitride (AlN) including the impact of sputter parameters, film thickness and substrate pre-conditioning [1,2]. I will present the impact of doping of AlN with scandium, which leads to an increase of the moderate piezoelectric coefficient of AlN up to a factor of four. In a next step, these films are implemented into fabrication processes of cantilever-type MEMS devices. In combination with a tailored electrode design, resonators are realized featuring Q factors up to about 300 in liquids covering the frequency range of 1-2 MHz. This enables the precise determination of the viscosity and density of fluids up to dynamic viscosity values of almost 300 mPas [3]. Besides this application, such high Q factors are useful when targeting mass-sensitive sensors, thus paving the way to e.g. particle detection even in highly viscous media. Given the low increase in permittivity of ScAlN compared to AlN, another field of application for this material are vibrational energy harvesters, where the benefit of ScAlN compared to pure AlN is demonstrated [4]. Finally, I will present some selected results of ScAlN thin films within SAW devices ranging from high temperature applications to droplet manipulation in microfluidics [5].

References:

[1] M. Schneider, A. Bittner, F. Patocka, M. Stöger-Pollach, E. Halwax and U. Schmid, Impact of the surface-near silicon substrate properties on the microstructure of sputter-deposited AlN thin films, *Applied Physics Letters* 101 (2012) 221602.

[2] M. Schneider, A. Bittner and U. Schmid, Improved piezoelectric constants of sputtered aluminium nitride thin films by pre-conditioning of the silicon surface, *Journal of Physics D: Applied Physics* 48 (2015) 405301.

[3] G. Pfusterschmied, M. Kucera, E. Wistrela, T. Manzaneeque, V. Ruiz-Díez, J. L. Sánchez-Rojas, A. Bittner and U. Schmid, Temperature dependent performance of piezoelectric MEMS resonators for viscosity and density determination of liquids, *Journal of Micromechanics and Microengineering* 25 (2015).

[4] P. M. Mayrhofer, C. Rehlendt, M. Fischeneder, M. Kucera, E. Wistrela, A. Bittner and U. Schmid, ScAlN MEMS Cantilevers for Vibrational Energy Harvesting Purposes, *Journal of Microelectromechanical Systems* 26 (2017) 102-112.

[5] W. Wang, P. M. Mayrhofer, X. He, M. Gillingner, Z. Ye, X. Wang, A. Bittner, U. Schmid and J. K. Luo, High performance AlScN thin film based surface acoustic wave devices with large electromechanical coupling coefficient, *Applied Physics Letters* 105 (2014).

Thursday Afternoon, May 23, 2019

4:00pm **B5-1-ThA9 Superamphiphobic Surface Produced by Femtosecond Laser Patterning and Pulsed Plasma Polymerization**, *C.W. Lin (cwlino126@gmail.com)*, Feng Chia University; Central Taiwan University of Science and Technology, Taiwan; *G.H. Lu, X.X. Chang, P.-Y. Hsieh*, Feng Chia University, Taiwan; *C.M. Chou*, Department of Surgery, Taichung Veterans General Hospital, National Yang-Ming University, Taiwan; *C.J. Chung*, Central Taiwan University of Science and Technology, Taiwan; *J.L. He*, Feng Chia University, Taiwan

The superamphiphobic surface may be widely applied, including medical devices, kitchen wares, architectures, and automobiles, but is a challenging technique, with the unique characteristics of water and low surface tension liquids repelling, self-cleaning, anti-freezing and anti-bacterial activity. In this study, a dual-technique of surface modification by employing femtosecond laser patterning and pulsed plasma polymerization of octafluorocyclobutane was used to develop a superamphiphobic surface on the AISI 304 stainless steel substrate. Experimental results showed that the treated surfaces exhibited high water and oil contact angle, which may be attributed to nano/micro surface structure and low-surface-energy of fluorocarbon coating, as identified by SEM and FTIR analysis. In the steel wool scratch test, the superamphiphobic surface showed high mechanical durability even under harsh conditions. This indicates that such technique may have the potential in regulating surface properties of medical devices for different purposes.

Fundamentals and Technology of Multifunctional Materials and Devices

Room Pacific Salon 3 - Session C4-ThA

Fundamentals of Metallurgy in Thin Films and Coatings

Moderators: *Karsten Woll*, Karlsruhe Institute of Technology (KIT), Germany, *Ibrahim Gunduz*, Naval Postgraduate School, USA

1:40pm **C4-ThA2 Analytical Modelling of Propagation Velocity in Electron Transparent Nanolaminates**, *M.J. Abere (mjabere@sandia.gov)*, Sandia National Laboratories, USA; *G.C. Egan*, Lawrence Livermore National Laboratory, USA; *D.P. Adams*, Sandia National Laboratories, USA

The ignition of sputter deposited bimetallic nanolaminate films results in rapid, self-propagating reactions. Analytical models of the measured propagation velocities have been typically performed using a framework developed by Mann et al. (J. Appl. Phys. 1997). This work seeks to expand upon this model to handle electron transparent Co/Al samples for experiments in dynamic TEM. This work utilizes a three resistor thermal circuit model to account for thermal conductivity in the intermixed zone that is an order of magnitude less than that predicted by rule of mixtures. Also, this work utilizes cross-sectional scanning transmission electron microscope energy-dispersive X-ray spectroscopy data to calculate the Fourier coefficients in the Mann et al. model from the physical composition profile in the intermixed region. The effect of radiation loss for 150 nm thick foils is calculated as a perturbation to the difference in the heat of reaction measured in calorimetry and the adiabatic heat of product formation. Finally, the model considers two independent activation energies for when the reaction proceeds via co-melted reactants versus solid Co dissolution into molten Al.

This work was supported by the Sandia National Laboratory Directed Research and Development

(LDRD) program. Sandia National Laboratories is a multimission laboratory managed and operated by National Technology and Engineering Solutions of Sandia, LLC., a wholly owned subsidiary of Honeywell International, Inc., for the U.S. Department of Energy's National Nuclear Security Administration under Contract No. DE-NA0003525. This work describes objective technical results and analysis. Any subjective views or opinions that might be expressed in the paper do not necessarily represent the views of the U.S.

Department of Energy or the U.S. Government.

2:00pm **C4-ThA3 Bimetallic Solid State Diffusion During Extreme Mechano-Chemical Processing of Nanoheater Multilayers**, *C. Doumanidis (haris.doumanidis@nu.edu.kz)*, Nazarbayev University, Astana, Kazakhstan; *M. Aureli*, University of Nevada Reno, USA; *C. Doumanidis*, Aristotelian University of Thessaloniki, Greece; *I.E. Gunduz*, Purdue University, USA; *A. Hussien*, Khalifa University, Abu Dhabi, UAE; *Y. Liao*, University of Nevada Reno, USA; *C.G. Rebholz*, University of Cyprus, Cyprus

INVITED

Based on a real-time simulation of thermal and diffusion distributions in ball milled bimetallic Ni-Al particulates, this research investigates

mechanochemical synthesis of ignitable nanoheater pellets. The impact and contact conditions between Ni and Al domains and the temperature distribution generated via friction and plastic deformation determine diffusive flux through their interfaces and concentration field via Green's functions, with mirror images reflecting the boundary conditions. Predictions of this model are validated against laboratory open-loop SEM micrographs and XRD spectra at steady state, defining the threshold of diffusion penetration to avoid early exothermic reaction in the ball milling vial. Then, dynamic descriptions of diffusion saturation and internal temperature are developed and employed for the design of a closed-loop regulator by computer simulation. Finally this feedback controller is implemented on an experimental device with infrared measurement of external vial temperature, adjusting the efficiency of the previous model implemented in parallel to the laboratory process as a real-time observer of internal temperature and diffusion saturation. By modulating the process duration, this control system is shown to successfully replicate the material composition in the open-loop reference tests.

2:40pm **C4-ThA5 Twin-Wire Arc Coatings for Repair of Structural Components**, *C. Jasien, N.J. Wagner (njwagner@cpp.edu)*, Cal Poly Pomona, USA

There has been a growing interest in additive manufacturing technologies for the repair of metallic structural components. Among the proposed techniques, twin-wire arc plasma spraying offers the advantage of providing high deposition and growth rate capabilities, coupled with process robustness and versatility, which are always desirable in real-life applications. In addition to these considerations, the fundamental materials science of these plasma-sprayed coatings is surprisingly still under-explored. Nanostructured depositions and coatings should be achievable with this additive technique given its high temperature and fast quenching rate. Motivated by these considerations, we have performed a study on the deposition of metallic coatings on steel substrates using an Oerlikon Metco FlexiArc 300 twin-wire arc plasma spraying system. We used 1.6mm diameter stainless steel wires and compressed air as a carrier gas. The process conditions that were varied include power, standoff distance and coating thickness. Dense coatings, approximately 150 micrometers thick, were achievable at the highest electrical input power of 10 kW within a few seconds of deposition time. Structural and morphological characterization has been performed using scanning electron microscopy (SEM) and energy dispersive x-ray spectroscopy (EDS). We have found that substrate temperature has a significant influence on the adhesion layer between the substrate and the coating.

3:00pm **C4-ThA6 Unstable Propagating Reactions in Sputter-Deposited Nanolaminates**, *D.P. Adams (dpadams@sandia.gov)*, *M.J. Abere*, Sandia National Laboratories, USA

Reactive metal multilayers are a form of energetic material that continue to attract attention for various applications. Generally composed of two layered reactants, these heterogeneous solids can be stimulated at a point or in bulk to initiate internal, self-sustained chemical reactions that give off heat and light. Their reactions are characterized by propagating high temperature wavefronts, little or no gas emission, and rapid local heating rates of ~106 K/s. Reactions often propagate in a stable manner characterized by a uniform propagation speed and smooth wavefront morphology. Other less reactive forms exhibit unstable reactions characterized by stalled wavefronts, spatially non-uniform temperatures, and variable propagation speeds. Unfortunately, unstable reaction modes are poorly understood, thus limiting the use of reactive multilayers in emerging applications. In order to better understand the various behaviors of reactive multilayers, we have investigated how surrounding gaseous environment affects wavefront stability. Rare-earth / transition metal multilayers (e.g., Sc/Ag) of different periodicity were deposited by DC magnetron sputtering and tested as freestanding foils in different environments. Their reaction in 1e-3 Torr vacuum demonstrates inherent unstable intermetallic reaction fronts. Reactions in air are complicated by oxidation of the rare earth metal species which produces metal oxide and residual elemental metal. A separate oxidation wavefront trails the intermetallic reaction wavefront when reacted in air. In some cases, oxidation occurs long after the passage of the intermetallic reaction and there is little effect on the intermetallic reaction dynamics. However, large-period (low speed) multilayers show evidence for interference between intermetallic and trailing oxidation reaction waves. Prompt oxidation after the passage of the slow intermetallic reaction wave leads to a complex oscillatory behavior. The high exothermicity oxidation reaction repeatedly transitions the intermetallic front from an unstable mode to a stable form, while boosting its net velocity.

Thursday Afternoon, May 23, 2019

This work was supported by a Sandia Laboratory Directed Research and Development (LDRD) program. Sandia National Laboratories is a multi-mission laboratory managed and operated by National Technology and Engineering Solutions of Sandia, LLC., a wholly owned subsidiary of Honeywell International, Inc., for the U.S. Department of Energy's National Nuclear Security Administration under contract DE-NA-0003525.

3:20pm **C4-ThA7 Synthesis of Reactive Ni-Al Composites Using High Pressure Torsion**, *O. Renk*, Austrian Academy of Sciences, Austria; *M. Tkadletz*, *N.K. Kostoglou*, Montanuniversität Leoben, Austria; *I.E. Gunduz*, Naval Postgraduate School, USA; *C. Doumanidis*, Nazarbayev University, Astana, Kazakhstan; *R. Pippan*, Austrian Academy of Sciences, Austria; *C. Mitterer*, Montanuniversität Leoben, Austria; *C.G. Rebholz (claus@ucy.ac.cy)*, University of Cyprus, Cyprus

Mechanical mixing methods provide a bottom-up scalable route for fabricating nanostructured bulk materials. These include high energy ball milling (HEBM) used in metal-based reactive systems such as Nickel-Aluminum that can yield high performance NiAl and Ni₃Al intermetallic alloys upon combustion synthesis or used for in-situ welding with the heat generated from the exothermic reactions. The drawback of HEBM is the final product form, which consists of fine hardened powders that need to be processed further to form a dense part. This study investigates an alternative route, high pressure torsion (HPT), which applies a combination of large normal and shear stresses to a powder mixture in a die to yield nanostructured materials. HPT was used for fabricating consolidated reactive pellets of Ni-Al with microstructures comparable to HEBM and magnetron sputtering. The results show that materials undergoing HPT beyond 5 full rotations at processing temperatures of up to 473 K are highly reactive and can be ignited below the Al melting point, yielding a product phase of NiAl with residual Ni₂Al₃ and Ni₃Al, while reaching very high reaction temperatures near 1900 K.

3:40pm **C4-ThA8 Magnetic Field Induced Strain Transfer in FSMA/AlN Multilayered Structure**, *S. Pawar*, *A. Kumar*, Indian Institute of Technology Roorkee, India; *D. Kaur (dkaurfph@iitr.ac.in)*, Indian Institute Of Technology Roorkee, India

In the present work, thin film multilayered structure of Aluminium Nitride (AlN) and ferromagnetic Shape Memory alloy were fabricated on silicon substrates using reactive magnetron sputtering technique. The AlN thin films were deposited at 550 °C with 30% nitrogen concentration on FSMA layer. The AlN film shows high (002) orientation suggesting an enhancement in the magnetoelectric coupling. To confirm the presence of magnetoelectric coupling between NiMnIn and AlN layer, the dielectric measurements of the multiferroic heterostructure were measured with temperature and magnetic field. The dielectric result exhibits a hump like structure overlapping with the martensite phase transformation region of Ni-Mn-In layer with variation in temperature whereas an increase of dielectric constant was observed with increment in the magnetic field. Such novel NiMnIn/AlN multilayered structures with strong ME coupling are promising candidates for electrical and micro-electro-mechanical system (MEMS) and sensors applications.

4:00pm **C4-ThA9 Structure-Property Correlation of Spray Pyrolyzed Binary Chalcogenide Thermoelectric Thin Films**, *G.P. Badhirappan (bgp@psgias.ac.in)*, PSG College of Technology, India; *V. Shaleni*, PSG Institute of Advanced Studies, India; *G. Balaji*, *R. Balasundrprabhu*, *A. Ashok*, PSG College of Technology, India; *D. Sathishkumar*, CVRDE, India

Thermoelectric (TE) materials are very promising in the area of waste heat energy recovery and can be an efficient energy harvesting devices. Particularly, certain groups of chalcogenides based materials are most attractive owing to its interesting crystal structure leading to intrinsically low thermal conductivities. However, in most of the cases, heat sources have arbitrary shapes rather than flat surfaces. It is therefore difficult to capture the waste heat efficiently with the conventional flat and inflexible thermoelectric devices. Nowadays, various fabrication methods are employed to develop a thin film Thermoelectric Generators (TEGs) with high of figure-of-merit ($ZT > 1$) by introducing low dimensional quantum confinement and lowering the lattice thermal conductivity. Therefore, a thin film flexible TE device offers an economical viability to produce TEGs with faster response speed enabling new device configurations and perhaps higher power output with the use of efficient heat exchangers.

In this work binary chalcogenide thermoelectric thin films were grown on soda lime glass substrates by spray pyrolysis in the temperature range from 270-300°C. TE thin films were subsequently annealed at three different annealing temperatures (250 °C, 350 °C, and 400 °C) under vacuum conditions and associated structural modification was systematically

examined. Elemental compositions of the TE films were analyzed using Energy dispersive spectroscopy respectively. The annealing induced morphological evolution was studied using Scanning electron microscopy. Surface topography and surface roughness of the films were analyzed by atomic force microscopy. Further, X-Ray diffraction patterns depicts that for temperatures 270 °C and 300 °C, the films are largely composed of hexagonal and orthorhombic phases associated with change in the preferential crystallographic orientation from (001) to (101) plane.

Tribology and Mechanical Behavior of Coatings and Engineered Surfaces

Room San Diego - Session E1-2-ThA

Friction, Wear, Lubrication Effects, and Modeling III

Moderators: *Nazlim Bagcivan*, Schaeffler AG, Germany, *Carsten Gachot*, TU Wien, Institute for Engineering Design and Logistics Engineering, Austria, *Tomas Polcar*, Czech Technical University in Prague, Czech Republic

1:40pm **E1-2-ThA2 Exploring the Nanomechanical Properties of Transition Metal Dichalcogenides using Density Functional Theory**, *B.J. Irving (irvinben@fel.cvut.cz)*, *P. Nicolini*, Czech Technical University in Prague, Czech Republic; *T.P. Polcar*, University of Southampton, UK

Low-dimensional materials have recently attracted immense interest due to their fascinating physical properties and potential for application in diverse fields such as (opto)electronics, energy harvesting and dry lubrication. Transition metal dichalcogenides (TMDs), of general form MX₂ (M = Mo, W; X = S, Se, Te), are posited as being some of the best solid-state lubricants currently available. They exhibit a lamellar structure in which covalently-bonded MX₂ layers are held together by weak van der Waals forces, which, together with very low ideal shear strengths (i.e., the maximum load applied parallel to the face of the material that can be resisted prior to the onset of sliding) render them suitable for use in the mitigation of friction. Our extensive density functional calculations highlight the dependence of important nanomechanical properties of TMDs on their chemical composition and bilayer orientation (sliding direction); in particular, our calculations underscore the intrinsic relationship between incommensurate layers and superlubricity.[1] Our latest calculations have focused on TMD-based van der Waals heterostructures (e.g. WS₂ sliding on MoS₂), with the aim of formalizing the relationship between fundamental quantum chemical parameters of the constituent elements and the nanomechanical properties of the material. Ultimately, we wish to improve the predictive capabilities of *in silico* methods during the material design process.

[1] B. Irving, P. Nicolini and T. Polcar, *Nanoscale*, 2017, 9, 5597-5607

2:00pm **E1-2-ThA3 Mechanics, Materials, and Design Problems in Medical Device Technology and Information Storage**, *F.E. Talke (ftalke@ucsd.edu)*, University of California, San Diego, USA

INVITED

Current research in medical device technology and information storage at the Center for Memory and Recording Research will be discussed with emphasis on mechanics and materials issues.

In the area of medical device technology, the design of a miniaturized pressure sensor for implantation in the eye will be discussed to help in the understanding and treatment of glaucoma. The sensor is a passive device, based on interferometry, and does not require a power source to be implanted in the eye. Another materials related topic is concerned with the design and development of a 3-d printed disposable endoscope to avoid spread of antibiotic resistant superbugs, a serious medical infection and contamination problem. Materials and manufacturing issues will be discussed. In the area of information storage on hard disks, mechanics and materials problems will be discussed that are encountered during flying of a magnetic recording head at a head disk separation on the order of 1 nano meter. In order to increase the storage density further, the flying height of the read/write element must be reduced to less than 1 nm, and the track width to less than 20 nm (500,000 tracks per inch). To achieve sub-nano meter head disk spacing, the flying height of the head disk interface is controlled using the so-called thermal flying height control technology. In this approach, a controlled thermal deformation of the slider is achieved in the read write area of the slider by energizing a miniaturized resistance heater, causing a reduction in the flying height of the read write element to the order of 1 nm. Voltage biasing will be discussed to minimize materials transfer at the head disk interface. Another approach to achieve higher storage densities is the use of heat assisted magnetic recording where the magnetic medium is heated up to the Curie temperature just prior to

Thursday Afternoon, May 23, 2019

recording using a laser beam. Current and future problems in the mechanics and materials area of information storage on hard disks will be presented.

2:40pm E1-2-ThA5 Frictional Anisotropy of MoS₂ During Sliding: A Molecular Dynamics Study on the Atomistic Understanding of Frictional Mechanisms, V.E.P. Claerbout (claervic@fel.cvut.cz), P. Nicolini, Czech Technical University in Prague, Czech Republic

The tribological characteristics of molybdenum disulfide (MoS₂) as solid lubricants are well-described starting from the discovery of the super low friction behavior of MoS₂ by Martin et al. in 1993 [1]. However, despite numerous experimental and theoretical efforts, a fundamental understanding of the frictional mechanisms at the nanoscale is lacking.

In this contribution, we aim to elucidate the phenomena taking place at the nanoscale when several layers of MoS₂ slide atop another. In particular, by means of molecular dynamics simulations, we studied the effect of rotational sliding anisotropy [2] (i.e., the changing frictional behavior upon introducing a misfit angle between the layers or by varying the relative sliding angle) on the energy dissipation due to friction. We simulated different sliding conditions (varying e.g. normal load) in order to highlight their effect on the lubricating properties. These results will help on the one hand to identify the fundamental mechanisms that govern friction at an atomistic level, as well as providing guidelines for the design of novel layered materials with improved tribological properties.

[1] J.M. Martin et al., Phys. Rev. B, 48, 10583(R) (1993). [2] Onodera et al., J. Phys. Chem. B, 114, 15832 (2010).

3:00pm E1-2-ThA6 Effect of the Presence of Small Molecules on the Entangled Electronic and Dynamic Features in Layered MX₂ Transition Metal Dichalcogenides: Systematic Quantum Mechanic Ab Initio Simulations, J. Missaoui (missajam@fel.cvut.cz), A. Cammarata, Czech Technical University in Prague, Czech Republic

Great attention has been paid to the problem of friction in materials because of its enormous practical and technological importance in a vast range of scales including nanomaterials. In particular, control of intrinsic friction is mandatory in nano-electro mechanical devices (NEMS), mainly based on multi-layered Transition Metal Dichalcogenides (TMD). In this perspective, the present work is aimed to study the entangled electronic and dynamic features of selected TMD in the presence of small molecules of contaminants from the atmosphere.

We conducted systematic quantum mechanic ab initio simulations on prototypical layered MX₂ (M = transition metal, X = chalcogen anion) TMDs with hexagonal structure in the presence of small molecules in the inter-layer region. We combined group theoretical analysis and phonon band structure calculations with the characterization of the electronic features using non-standard methods such as orbital polarization and the recently formulated bond covalency and cophonicity analyses. We will then study how the vibrational frequencies of the pristine material are shifted in the presence of the contaminant, by relating such shift to the nanoscale friction between adjacent MX₂ layers. Finally, we will present guidelines on how to engineer intrinsic friction in TMDs at the atomic level.

Thanks to the generality of the used simulation protocol, the outcomes of the present study can be exploited to harness the macroscopic response of electro-dynamic entangled systems; the latter find application in fields beyond tribology based on physical phenomena like metal-insulator transition, second harmonic generation, and exciton effects (optoelectronics), among others.

3:20pm E1-2-ThA7 Nanoscale Frictional Properties of Ordered and Disordered MoS₂, E. Serpini, A. Rota, Università di Modena e Reggio Emilia, Italy; S. Valeri, Istituto CNR-NANO S3, Italy; E. Ukraintsev, Academy of Science of the Czech Republic, Czech Republic; B. Rezek, Czech Technical University in Prague, Czech Republic; T.P. Polcar, University of Southampton, UK; P. Nicolini (nicolpao@fel.cvut.cz), Czech Technical University in Prague, Czech Republic

One third of energy produced by industrial countries is lost as friction. High wear caused by friction means approx. 35% of industrial production is used to replace degraded products, whilst causing the breakdown of machinery, resulting in safety risks and environmental pollution. Controlling and reducing friction is a fundamental step in attaining the sustainable development of our society, as detailed in the Brundtland report. In this contribution I will present the results of a study on the nanometric sliding of molybdenum disulfide against itself both from the experimental and from the computational point of view. The differences between ordered material (single crystal) and disordered material (sputtered coating) were investigated. Tribological experiments were performed using Lateral Force

Microscopy. Atomic Force Microscopy tips modified by sputter deposition of molybdenum disulfide were used for the first time. This feature opened up the possibility for close comparison with classical molecular dynamics simulations. In both cases, the coefficient of friction for the ordered system in inert conditions was found to be smaller than for disordered system. This result demonstrates the impact of morphology at the nanoscale and highlights the importance of molecular dynamics as a diagnostic and predictive tool in nano-friction. Furthermore, experiments show that the effects of the environment on nanoscale friction are reduced with respect to the macroscale case. These findings can expedite the process of fabricating molybdenum disulfide-based coatings with superior tribological properties, with the ultimate aim of reducing the energy dissipation due to friction.

3:40pm E1-2-ThA8 Electrical Tuning of Vibrational Modes in Transition Metal Dichalcogenides, F. Belviso (belviflo@fel.cvut.cz), Advanced Material Group, Czech Technical University in Prague, Czech Republic

Transition metal dichalcogenides (TMDs) have been shown to be a promising source of applications in multiple fields, such as nanoelectronics, photonics, sensing, energy storage, and opto-electronics.

We investigated the atomic scale tribological properties of TMDs, using ab-initio techniques. Such compounds are formed by triatomic layers with MX₂ stoichiometry (M: transition metal cation, X: chalcogen anion) held together by van der Waals forces.

We considered 6 prototypical MX₂ TMDs (M=Mo, W; X=S, Se, Te) with hexagonal P6₃/mmc symmetry, focusing on how specific phonon modes contribute to their intrinsic friction. Within the DFT framework, we described the exchange-correlation interaction energy by means of the PBE functional, including long range dispersion interactions in the Grimme formulation (DFT-D3 van der Waals).

We identified and disentangled the electro-structural features that determine the intra- and inter-layer motions affecting the intrinsic friction by means of electro-structural descriptors such as orbital polarization, bond covalency and cophonicity.¹

We show how the phonon modes affecting the intrinsic friction can be adjusted by means of an external electrostatic field. In this way, the electric field turns out to be a knob to control the intrinsic friction.

We also show the structural distortion induced by some various cation substitution.

The presented outcomes are a step forward in the development of layer exfoliation and manipulation methods, which are fundamental for the production of TMD-based optoelectronic devices and nanoelectromechanical systems.

[1] Cammarata, Antonio and Polcar, Tomas (2015) DOI 10.1039/C5RA24837J

4:00pm E1-2-ThA9 On the In-situ Formation of Transition Metal Disulfides in Lubricated WN or WC Coating Contacts, B. Kohlhauser (bernhard.kohlhauser@tuwien.ac.at), TU Wien, Institute of Materials Science and Technology, Austria; M. Rodríguez Ripoll, AC2T research GmbH, Austria; H. Riedl, C.M. Koller, N. Koutna, TU Wien, Institute of Materials Science and Technology, Austria; G. Ramirez, A. Erdemir, Argonne National Laboratory, USA; C. Gachot, TU Wien, Institute for Engineering Design and Logistics Engineering, Austria; P.H. Mayrhofer, TU Wien, Institute of Materials Science and Technology, Austria

In recent years, solid lubricants such as transition metal dichalcogenides have attracted attention in form of nanoparticle additives for conventional oil-based lubricants. Those nanoparticle additives entail several disadvantages, including the need to compose a stable dispersion. An in-situ formation of lubricating solid compounds via a tribochemical reaction path between a coating and conventional S containing extreme pressure additives could prove to be much more advantageous.

While MoS₂ can easily be formed on metallic Mo surfaces, the conditions in lubricated tungsten contacts are not severe enough to produce WS₂. A new generation of functional coatings is helping to overcome this energetic barrier, which is linked to the formation of intermediate tungsten oxide phases. WN and WC based coatings are able to facilitate this in-situ formation of WS₂ and combine excellent mechanical properties with an optimization of friction and wear via the formation of a low friction tribofilms.

The coatings were prepared by magnetron sputtering and their mechanical, structural and chemical properties were investigated with nanoindentation, energy dispersive x-ray spectroscopy, X-ray diffraction, and transmission electron microscopy.

Thursday Afternoon, May 23, 2019

The tribofilms, resulting from lubricated pin on disk tests, were studied in detail and consist of a fraction of amorphous WS₂ and C based oil derived debris, but also of nanocrystalline WS₂ domains along the surface. These lubricating WS₂ sheets lead to a low coefficient of friction around 0.05 and the tribofilm protects coating and counter body from any wear, even after 100 h of testing.

4:20pm **E1-2-ThA10 Tribological Investigations of Coated Roller Finger Followers using Application Oriented Valve Train Test**, *R.H. Brugnara (ricardo.brugnara@schaeffler.com)*, *E. Schulz, L. Dobrenizki, N. Bagcivan, C. Geers*, Schaeffler AG, Germany

Due to the increasing demand to reduce emissions, friction reduction is an important topic in the automotive industry. Among the various possibilities to reduce mechanical friction, the usage of a low-viscosity lubricant in the engine is one option. Thus, continuously lower viscosity lubricants are being developed and offered on the market. Other approach is to adjust the properties of the components using surface technology in order to minimize friction losses and meet the more stringent environmental requirements. Coated components using thin film vacuum technology offers the possibility to reduce CO₂-emissions and fuel consumption of the vehicle by mandatory lightweight design, reducing friction losses in tribological contacts. In present study, uncoated and DLC (Diamond-like Carbon) coated roller finger followers were investigated for the first time using application oriented driven cylinder head tests with 0W20 low viscosity oil under relevant conditions. The results show a significant friction reduction in rolling contact with coated cam rollers compared to the uncoated reference.

4:40pm **E1-2-ThA11 Physical Understanding to Nano-friction of C:H/D Thin Films: Coupling Mechanism by Atomic-scale Vibration Damping**, *F.G. Echeverrigaray, S.R.S. de Mello*, Universidade de Caxias do Sul, Brazil; *F. Alvarez*, Universidade Estadual de Campinas, Brazil; *A.F. Michels, C.A. Figueroa (carlos.cafiguer@gmail.com)*, Universidade de Caxias do Sul, Brazil

Friction phenomenon is a complex manifestation of the nature originated in energy dissipation events owing to the lost work of non-conservative forces. In spite of phenomenological laws describe the friction force at different scales, the fundamental physical understanding of such a phenomenon still did not achieve consensus. Phononic, electronic, magnetic and electrostatic effects were considered and theoretical models were developed in order to explain the nano-friction behavior of materials. The surface structure of deuterated and/or hydrogenated amorphous carbon (a-C:D/H) thin films in air, which plays an important role in nanoscale friction research, is constituted by deuterium and/or hydrogen terminated bonds and physisorbed oxygen, nitrogen and water molecules. There are well established models to explain the tribological behavior of carbon-based thin films in different atmospheres, however, the fundamental physical mechanism at the interfacial atomic-scale remains open. In this study, we report the friction forces at the nanoscale on amorphous carbon thin films with different [D]/[C] and [H]/[C] contents by nanoindentation followed of unidirectional sliding (NUS) and friction force microscopy (FFM). Two different experimental setups are reported. Firstly, for samples where hydrogen was replaced by deuterium in the thin film the friction force decreases with the increasing of deuterium content, this behavior is associated to a fononic phenomenon owing to isotope effect. Secondly, for samples where hydrogen content is increased at the surface, the friction force decreases with the increasing of the ratio H/C at the surface, which is explored by an electronic interaction analysis. We discuss these two different frictional damping mechanisms by dissipation effects associated with phonon/van der Waals (vdW) coupling by sliding interface polarizability.

New Horizons in Coatings and Thin Films

Room Pacific Salon 6-7 - Session F2-2-ThA

HiPIMS, Pulsed Plasmas and Energetic Deposition II

Moderators: *Jon Tomas Gudmundsson*, University of Iceland, Iceland, *Tiberiu Minea*, LPGA, Université Paris-Sud, Orsay, France

1:40pm **F2-2-ThA2 Pulsed Cathodic Arc for Deposition of ta-C and TiSiCN Films**, *X.B. Tian (Xiubotian@163.com)*, *Y.H. Ma*, State Key Laboratory of Advanced Welding & Joining, Harbin Institute of Technology, China; *C.Z. Gong*, State Key Laboratory of Advanced Welding and Joining, Harbin Institute of Technology, China; *Y. Kong, Q.X. Tian*, State Key Laboratory of Advanced Welding & Joining, Harbin Institute of Technology, China

Cathodic arc evaporation has been widely utilized due to the advantages of high ionization rate and ion energy, high deposition rate and good adhesion between film and substrate. However, with the development of industrial technology, high-quality films are increasingly required. Novel techniques or processes are proposed and investigated. Many studies have confirmed that higher plasma density is very critical for optimal microstructure and surface properties. In the conventional cathodic arc processes, the plasma density may be increased by larger target current, however it may lead to more macroparticles and larger heat load to the target as well. So power supply for pulsed arc has been developed, and pulsed arc discharge has been investigated. Afterwards the films including ta-C, TiN and TiSiCN were deposited. The OES results demonstrate that spectral intensity of all species is greatly enhanced with pulsed arc mode. With the same average target current, substrate current has been substantially increased by pulsed arc mode. It means much higher plasma density near the substrate, which produces the denser microstructure. A thicker film is also achieved by pulsed arc, which may be attributed to the magnetic field of high current and higher pulsed power. The pulsed arc has proven to be a versatile tool to fabricate the films with denser structure, good adhesion and higher resistance of high temperature oxidation and a larger processing window as well.

Keywords: pulsed cathodic arc, OES, microstructure, Ta-C, TiSiCN

2:00pm **F2-2-ThA3 HiPIMS Deposition of W Thin Films**, *A. Engwall (engwall1@llnl.gov)*, *S.J. Shin, Y.M. Wang*, Lawrence Livermore National Laboratory, USA

High power impulse magnetron sputtering (HiPIMS) has been shown to deposit W films with desirable physical characteristics including higher strength and uniformity than films deposited with traditional direct current magnetron sputtering (DCMS) under similar processing conditions. In-situ stress measurements paired with ex-situ film characterization and Langmuir probe plasma measurements were used to investigate the fundamental differences between DCMS and HiPIMS film deposition over a range of chamber pressures with and without applied substrate biasing.

LLNL-ABS-758580

This work was performed under the auspices of the U.S. Department of Energy by Lawrence Livermore National Laboratory under Contract DE-AC52-07NA27344. Support was provided by LDRD program 17-ERD-048 at LLNL.

2:20pm **F2-2-ThA4 Study and Development of Thermochromic VO₂ Thin Films Deposited by HiPIMS**, *J.L. Victor (jean-louis.victor@cea.fr)*, *C. Marcel*, CEA Le Ripault, France; *A. Rougier*, CNRS, France; *L. Sauques*, DGA, France
Vanadium dioxide (VO₂) has attracted a great interest for smart coating applications because of its promising thermochromic properties. Its main characteristic is to transit from a semiconductive state to a metallic state at a phase transition temperature (T_c) of 341 K which is closer to room temperature (300 K) than any other thermochromic material. Nevertheless, the fabrication of high-quality VO₂ films by conventional direct current or radio-frequency Magnetron sputtering (DCMS or RFMS) requires an annealing step over 450°C which limits its compatibility with temperature-sensitive substrates. High power impulse magnetron sputtering (HiPIMS) is a novel sputtering method, developed recently for the deposition of VO₂ films. It is characterized by its high ionization degree of the sputtered species, which allows the control of film microstructure through ion bombardment. Due to this additional energy, the annealing temperature can be reduced for the development of functional VO₂. In this work, we show that HiPIMS supply permits to deposit dense stoichiometric crystalline VO₂ thin films at lower temperature.

Thursday Afternoon, May 23, 2019

2:40pm **F2-2-ThA5 A Paradigm Shift in Thin Film Growth by Magnetron Sputtering: from Gas-ion to Metal-ion-controlled Irradiation**, *G. Greczynski (grzegorz.greczynski@liu.se)*, Department of Physics, Linköping Univ., Sweden; *I. Petrov*, University of Illinois, USA, Linköping University, Sweden, USA; *J.E. Greene*, University of Illinois, USA, Linköping University, Sweden, National Taiwan Univ. Science & Technology, Taiwan; *L. Hultman*, Department of Physics, Linköping Univ., Sweden

INVITED

Traditionally, growth of dense refractory thin films by means of dc magnetron sputtering employs gas-ion bombardment to ensure sufficient adatom mobility during deposition at lower temperatures $T_s/T_m < 0.3$ (T_s and T_m : growth and melting temperature in K). This approach often results in significant concentrations of trapped inert gas atoms with accompanying high film stresses leading to cohesive failure and film/substrate delamination. A possible remedy is offered by metal-ion-synchronized bias during high-power pulsed magnetron sputtering (HIPIMS). The inherent separation of metal- and gas-ion fluxes that stems from gas rarefaction, provides the ability to separate, in both time and energy domains, metal ions and gas ions incident at the substrate. In this approach, a substrate bias potential is synchronized with the metal-ion-rich portion of the HIPIMS pulse. Metal-ions, as opposed to noble-gas ions, are primarily incorporated at lattice sites. This, together with dramatically-reduced concentrations of trapped gas ions, results in lower compressive stresses. Moreover, the metal-ion mass, incident flux, and impact energy can be independently controlled to optimize momentum transfer and provide the recoil density and energy necessary to eliminate film porosity at low deposition temperatures. This novel approach expands the PVD process envelope to allow the use of temperature-sensitive substrates as well as synthesis of supersaturated alloys.

In the first part of the talk, results of time-resolved ion mass spectrometry analyses performed at the substrate plane during HIPIMS sputtering of TM targets in Ar and Ar/N₂ atmospheres are reviewed. Detailed knowledge of the time evolution of metal- and gas-ion fluxes incident at the growing film surface is essential for precise choice of synchronous bias pulse, and, hence, control over the incident metal-ion energy, while minimizing the role of gas-ion irradiation. In the second part of the talk, several examples of metal-ion-synchronized HIPIMS will be discussed including the growth of (i) nanostructured N-doped bcc-CrN_{0.05} films possessing atomically-smooth surfaces with unique properties which are characteristic of both metals (bcc-Cr crystal structure, electrical resistivity, and toughness) and ceramics (high hardness); (ii) fully-dense, hard, and stress-free Ti_{0.39}Al_{0.61}N; (iii) single-phase cubic Ti_{1-x}Si_xN with record-high SiN concentrations; (iv) single-phase NaCl-structure V_{1-x}Al_xN layers with unprecedented AlN supersaturation; and (v) dense and hard dilute Ti_{0.92}Ta_{0.08}N alloys deposited with no external heating ($T_s/T_m < 0.15$).

3:20pm **F2-2-ThA7 In Vitro and In Vivo Biocompatibility Evaluation of Zr-Ti-Si and Fe-Zr-Nb Thin Film Metallic Glasses**, *A.J. Chen (sophia40101@gmail.com)*, *J.-B. Wang*, *Y.-C. Yang*, National Taipei University of Technology, Taiwan; *B.-S. Lou*, Chang Gung University, Taiwan; *J.-W. Lee*, Ming Chi University of Technology, Taiwan

Thin film metallic glass (TFMG) has been considered in the biomedical applications due to its better corrosion resistance, which attracts lots of attention from academic and industry. In this study, a co-deposition system consisting of a high power impulse magnetron sputtering (HiPIMS) and a radio frequency (RF) power supply was used to prepare Zr-Ti-Si and Fe-Zr-Nb TFMGs on the surface of 316 L stainless steel specimen.

The chemical composition, microstructure and surface roughness of Zr-Ti-Si, Fe-Zr-Nb TFMGs were analyzed by a FE-EPMA, FE-SEM and AFM respectively. The nanoindentation, scratch test and HRC-DB adhesion test were employed to evaluate the mechanical and adhesion properties of TFMGs. The corrosion resistance of TFMGs in 3.5 wt. % NaCl aqueous solution was conducted by a potentiodynamic polarization test. The MG-63 cell line (human osteosarcoma) was used to investigate the biocompatibility of coatings. Finally, the animal tests were executed to examine any allergy, poisoning or carcinogenic reaction was brought by the TFMGs to the rats.

Through the in-vitro cell test and in-vivo animal tests, both Zr-Ti-Si and Fe-Zr-Nb TFMGs exhibited better biocompatibility because of their good corrosion resistance, good hydrophilic properties and improved adhesion on the 316L surface. We can conclude that Zr-Ti-Si and Fe-Zr-Nb TFMGs have very excellent potential application in the biomedical field.

3:40pm **F2-2-ThA8 Microstructural and Tribological Properties of Sputtered AlCrSiWN Films Deposited with Segmented Powder Metallurgic Target Materials**, *W. Tillmann*, *A. Fehr (alexander.fehr@tu-dortmund.de)*, *D. Stangier*, TU Dortmund University, Germany

When synthesizing magnetron sputtered films with a complex stoichiometry, integrating the desired coating constituents in one target material is favorable to avoid a nanolaminar film depositions and to enable a homogenous film growth. In contrast to alloyed targets, segmented plug targets allow to merge elements with different physical properties in one target material. Two targets, amalgamating 20 and 48 hot-pressed 80Cr5Si15W (wt. %) plugs, respectively, into a monolithic aluminum target were fabricated and employed in a direct current magnetron sputtering process to deposit AlCrSiWN films on high-speed steel (AISI M3:2, 1.3344). Furthermore, an AlCrSiN film, which served as a reference, was deposited using Cr, Si, and AlCr24 targets. The cathode powers for the Al(CrSiW)20 and Al(CrSiW)48 targets were varied between 3 and 7 kW to analyze how differently composed targets and various cathode powers affect the microstructure and tribological properties of the sputtered films.

The results revealed that the chemical composition as well as the thickness of the films are strongly dependent on the target setup. For all AlCrSiWN films, the Cr and Al contents predominated (19–29 at%), while the Si and W contents varied between 2–3 at. %. This indicates that chromium is preferentially sputtered from the alloyed CrSiW plugs. The film, which was deposited by applying 7 kW to the Al(CrSiW)20 and 3 kW to the Al(CrSiW)48 targets had the highest hardness (27.66 ± 1.87 GPa) due to a dense coating growth and a finer crystalline structure. All AlCrSiWN films had a preferred (111)–(CrN/WN) orientation, which exhibited a finer crystalline growth with an increasing cathode power. Analyses of the tribological behavior of the AlCrSiWN films further revealed a significantly lower friction coefficient ($\leq 0.4 \pm 0.04 \cdot 10^{-5}$ mm³/Nm) when sliding against Al₂O₃ balls when compared to the AlCrSiN reference system.

4:00pm **F2-2-ThA9 Linking an Atmospheric-pressured Arc Reactor to a Magnetron Sputter Device to Synthesize Novel Nanostructured Thin Films**, *W. Tillmann*, *D. Kokalj (david.kokalj@tu-dortmund.de)*, *D. Stangier*, TU Dortmund University, Germany; *Q. Fu*, *E. Kruis*, University of Duisburg-Essen, Germany

Due to their properties, nanocomposite coatings offer outstanding advantages compared to single-phase coatings. However, the choice of materials to produce such nanocomposite coatings is severely limited. Basically, there are only three mechanisms that lead to the formation of nanocomposite structures. One possibility is the use of two metals which, in certain compositions, reveal a miscibility gap and form mixed crystals with different structures. Alternatively, metals with strongly different nitrogen affinities also form the desired nanocomposite structure. The third mechanism is based on the use of a nitride-forming transition metal, which is nanocrystalline embedded in an amorphous matrix.

To allow an unrestricted combination of materials, the approach in this project is a decentralized production of nanoparticles and the thin film, whereby the films growth of both phases is combined on the substrate material. For this attempt, an atmospheric pressured arc reactor is used to generate the TiN nanoparticles with mean primary particle sizes of 7 nm to 20 nm agglomerated to clusters of about 120 nm. To inject these nanoparticles in-situ into the vacuum PVD process, an aerodynamic lens is utilized. The purpose of the aerodynamic lens is to separate the process gas from the nanoparticles to only introduce the nanoparticles into the PVD process. Thus, depending on the coating materials used, nanostructured thin films of type nc-MeN / nc-MeN or nc-MeN / nc-Me can be produced in addition to already existing systems, such as nc-MeN/a-nitride and nc-MeC/a-C, synthesized by conventional PVD processes. Within this context, the metal (Me) can also be nitrogen-affine in the new approach.

In this project, TiN nanoparticles are employed and embedded into magnetron sputtered CrN thin films. Initially, the influence of selected PVD deposition parameters, such as the temperature, chamber pressure, and bias voltage, is examined on the morphology and crystallite size of the TiN nanoparticles. Additionally, the influence on the particle distribution on the substrate is discussed. The nanoparticles were successfully deposited on silicon wafer and it was found out that the particle distribution is affected more by the deposition parameters than the particle properties mentioned. This enables the production of nanostructured PVD thin films by means of external nanoparticle injection without the particle properties being subsequently influenced by the deposition parameters during the coating process.

Thursday Afternoon, May 23, 2019

Surface Engineering - Applied Research and Industrial Applications

Room Pacific Salon 1 - Session G4+G5+G6-ThA

Pre-/Post-Treatment and Duplex Technology/Hybrid Systems, Processes and Coatings/Application-Driven Collaborations between Industry and Research Institutions

Moderators: Heidrun Klostermann, Fraunhofer FEP, Germany, Kumar Yalamanchili, Oerlikon Balzers, Oerlikon Surface Solutions AG, Liechtenstein, Tobias Brügelmann, RWTH Aachen University, Germany, Hana Barankova, Uppsala University, Sweden

1:20pm G4+G5+G6-ThA1 From Detailed Understanding to In Operando Studies of Coated Cutting Tools: A Successful and Long Term Collaboration between Industry and Universities, J. Anderson (jon.andersson@secotools.com), Seco Tools AB, Sweden **INVITED**

The truth is in the details when it comes to development of materials, so also for cutting tool coatings. For example, two coating materials CVD Al₂O₃ and PVD TiAlN have been the dominating commercial wear resistant coatings for the last 20-30 years. Over the same period, both the coating properties and their performance during machining have improved dramatically. This has been made possible by paying attention to the details of the coating synthesis coupled to its structure, properties and performance during service. The key to finding these details as well as deciding which to focus on to achieve the desired results is advanced characterization and an in-depth analysis combined with the feedback from focused material, process or functional modeling studies. At Seco Tools we have a long and fruitful experience of collaborating with universities around these issues with an open and creative mindset. Here we will present the outcome of a few case studies, ranging from fundamental arc plasma studies vs. coating synthesis including particle-in-cell (PIC) simulation of the same, correlated to coating structure and properties, to atomic-level materials characterization and in operando synchrotron investigations of the tool/chip contact during metal cutting.

2:00pm G4+G5+G6-ThA3 Electrolytic Plasma Polishing of Titanium Alloys, N. Laugel (nicolas.laugel@manchester.ac.uk), A. Yerokhin, A. Matthews, University of Manchester, UK

Electrolytic plasma polishing (EPPo) is a method for metals surface finishing. Its applications see a fast growing interest in line with its advantages over more established competing methods, in particular in the field of additive manufacturing. The promises of additive manufacturing include a disruptive impact on metals manufacturing in virtually all high value applications, from aerospace to automotive and medical industries. However it suffers to this day from entirely unsatisfactory surface states, both for direct use or for subsequent surface treatment or coatings. The most promising approach to the issue is arguably contactless post-treatment and EPPo as one of the best fitting contenders.

EPPo consists in setting a workpiece as the anode in an electrolytic cell, and apply voltages in the hundreds of volts. The energy liberated due to this strong polarization is transferred primarily through the production of large quantities of electrolysis gases and of water vapor, resulting in a relatively stable isolating sheath. This envelope hinders dramatically the passage of current, ultimately mediating the electrochemical dissolution of the metallic workpiece. Compared to traditional electropolishing, EPPo notably features slower material removal for more control over geometry conservation and electrolyte compositions much more benign to the workplace and to the environment. Yet it retains all the advantages of contactless, geometry-independent polishing.

Titanium and its alloys are of notorious interest to a wide range of industries and as such are a particularly valuable application for EPPo. The electro-dissolution of titanium, and of some of the elements commonly alloyed to it like aluminum, proves however significantly more difficult to control than that of other EPPo metals. These difficulties are rooted in a strong competition against the formation of insoluble oxides into a compact and process-blocking layer. A range of electrolytes and Ti-complexing agents were combined with different electrical and thermodynamical parameters to investigate this race between electro-dissolution and oxide formation. *In situ* measurements of the electric response from the system and of the glow light emitted by the process were collected and analyzed. Characterization of the treated surfaces was performed, in terms of elemental and chemical composition, morphology and topography, to help elucidate the interactions at play during EPPo. The range of surface states that can be produced by the method is explored, both in topological and chemical terms, with the

ultimate goal of enabling pathways to subsequent surface treatment and coating.

2:20pm G4+G5+G6-ThA4 Characterization of Surface Modification Mechanisms for Boron Nitride Films under Plasma Exposure, T. Higuchi, Kyoto University, Japan; M. Noma, Shinko Seiki Co., Ltd, Japan; M. Yamashita, Hyogo Prefectural Institute of Technology, Japan; K. Urabe, Kyoto University, Japan; S. Hasegawa, Osaka University, Japan; K. Eriguchi (eriguchi.koji.8e@kyoto-u.ac.jp), Kyoto University, Japan

Boron nitride (BN) film has attracted much attention recently because of the superior mechanical properties (hardness) and the unique electronic structure. [1][2] In addition, BN films have potential applications to the usage in harsh environment such as space, e.g. (1) solid lubricant material with a low friction coefficient in ultra-high vacuum [3] and (2) coating material on the inner wall of an electric propulsion system for a long-term mission. [4] Recently, we proposed a reactive plasma-assisted coating (RePAC) system [5] and fabricated high-hardness (cubic) BN stack structures on a Si substrate with anti-delamination feature. Regarding the application to solid lubricant, we showed friction coefficient lowering phenomena in BN films under ultra-high vacuum ($\sim 10^{-6}$ Pa), which is in sharp contrast to usually-observed "friction coefficient increase". [6] In this study, we focus on the other issue, the surface modification mechanisms under plasma exposure. A (cubic) BN film consisting of the surface (35 nm) and bulk regions was formed on a Si substrate using the RePAC system. The mechanical property degradation after low-pressure Ar plasma exposure was investigated in detail. The energy of incident ions was controlled to be 170 or 690 eV with a constant ion flux (4.5×10^{13} cm⁻²s⁻¹). A nano-indentation test identified a plasma-damaged layer in the vicinity of the surface region (a few nm thick), where the indentation hardness (H_{IT}) was modified. On the basis of a three-layer BN structure model, we revealed that the H_{IT} of the damaged layer increased in the case of 170 eV, while the H_{IT} decreased in the case of 690 eV. We performed a molecular dynamics (MD) simulation to predict the surface structure change by particle impacts, where the Tersoff- and Wilson-type potential models [7][8] were used for B-N and Ar-(N or B) systems, respectively. The MD simulation clearly assigned that a change of the cubic BN fraction in the rhombohedral-/hexagonal-BN background within the surface region leads to the H_{IT} change. The present findings should be implemented in designing BN films for harsh environment applications.

[1] C. B. Samantaray and R. N. Singh, *Int. Mater. Rev.* **50** (2005) 313.

[2] Y. Hattori et al., *ACS Appl. Mater. Interfaces* **8** (2016) 27877.

[3] G. Colas et al., *Wear* **305** (2013) 192.

[4] T. Burton et al., *J. Propul. Power.* **30** (2014) 690.

[5] M. Noma et al., *Jpn. J. Appl. Phys.* **53** (2014) 03DB02.

[6] M. Noma et al., *AVS 63rd Int. Symp. & Exhibition, TR+BI+SE+TF-ThA8* (2016).

[7] K. Albe and W. Moller, *Computational Mater. Sci.* **10** (1998) 111.

[8] K. Eriguchi, *J. Phys. D* **50** (2017) 333001.

2:40pm G4+G5+G6-ThA5 Ultra-fast Decoating Method for PVD Coatings, B. Wittel, C. Buechel (c.buechel@platit.com), T. Cselle, Platit AG, Switzerland; B. Torp, Platit Scandinavia, Denmark; A. Lümekmann, D. Bloesch, Platit AG, Switzerland

Production of cutting tools requires energy and materials which are getting scarce and thus, more expensive. To save these resources, repeated use of a refurbished cutting tool is an important issue. A PVD coated cutting tool can be decoated, reground and recoated. The conventional ways to remove a worn PVD coating from a cutting tool are slow and expensive. This paper introduces a fast electrochemical decoating system with computer control, using pulsed voltage and end-point detection. The decoating times are in the range of minutes. A thin TiN adhesion layer is used under the coating to be removed. Cobalt leaching is prevented. A PVD coating applied after decoating shows excellent adhesion.

3:00pm G4+G5+G6-ThA6 Development of an Omni-phobic Spray Coating for the Oil and Gas Industry, C. Ellis-Terrell (carol.ellis@swri.org), R. Wei, R. McKnight, Southwest Research Institute, USA; X. Huang, K. Lin, Beijing Sanju Environmental Protection & New Materials Co., Ltd., China

In the oil and gas (O&G) industry, low surface energy coatings are of great interest. In the upstream industry, specifically in crude oil exploration and production, where the accumulation of asphaltenes and paraffin wax can clog production tubing completely. Clogging of the tubing may result in the abandonment of the upstream exploration and a significant loss in a multi-million dollar investment. In the downstream petrochemical refinery, the accumulation of carbon deposits, known as coking, is regularly encountered

on the walls of reactors. The periodic cleaning of the reactor vessel is not only a very costly process due to the interruption in production; it is also an unsafe operation because manual operation is still heavily involved.

Low surface energy coatings are used to prevent foreign substances from sticking to the surface. Water contact angle (WCA), or oil contact angle (OCA) measurements are commonly used to characterize the surface energy. When both the WCA and OCA are $>90^\circ$, the surface is termed as omni-phobic, reducing/inhibiting the adhesion of oil or water to the surface. Even though, there are a number of techniques used to fabricate omni-phobic surfaces, many are very expensive, short-lived, and impractical for real-world applications. In this study, we will discuss the solution-based spray coating, which is generated by synthesizing and functionalizing nanoparticles. We will present the particle synthesizing process, the chemical composition, the structural and morphological properties, wetting properties, thermal resistance, and the durability. Finally, we will present a few application examples of the omni-phobic coating in the O&G industry.

3:20pm G4+G5+G6-ThA7 Hybrid Reactive High Power Impulse Magnetron Sputtering System Combined with Electron Cyclotron Wave Resonance ECWR Plasma used for the Deposition of Semiconducting Thin Films., Z. Hubicka (hubicka@fzu.cz), M. Cada, Institute of Physics CAS, v. v. i., Czech Republic; S. Kment, Institute of Physics, Academy of Sciences of the Czech Republic, Czech Republic; V. Stranak, R.H. Hippler, Institute of Physics, Academy of Sciences of the Czech Republic; J. Olejnicek, Institute of Physics CAS, v. v. i., Czech Republic

INVITED

A hybrid reactive high power impulse magnetron sputtering system (HiPIMS) combined with a RF electron cyclotron wave resonance ECWR plasma (HiPIMS+ECWR) was investigated as a source for the deposition of oxide semiconductor thin films for photoelectrochemical applications as solar water splitting cells and dye sensitized solar cells (DSSC). It includes various forms of TiO_2 thin films working as barrier layers with enhanced electron transport in DSSC perovskite solar cells. Furthermore thin films of Fe_2O_3 and WO_3 working like photoanodes in solar water splitting cells were deposited with this hybrid plasma source. The non-stoichiometric oxide thin films have recently gained a huge attention due to their practical applications. These semiconducting materials can have interesting optical, electrical and photoelectrochemical properties with possible applications in various types of optoelectronic devices or different types of solar electrochemical cells working here as the cocatalysts. The defect engineering (DE) has become an attractive research direction for improving the optical and electronic properties of these materials towards highly efficient PEC processes. The main limitation related to the current DE approaches is that they are predominantly realized via a high-pressure high-temperature gas reduction. In the presented work the non-stoichiometric oxide thin films such as WO_{3-x} , TiO_{2-x} were deposited by the HiPIMS+ECWR plasma system. By adjusting the deposition conditions, we can regulate the extent of induced defects and, moreover under significantly reduced temperature. Defined $\text{Ar}+\text{O}_2$ working gas mixture at different pressures in the range from 0.05- 5 Pa were used for the deposition process with eventual additional substrate annealing in the RF-ECWR reactive plasma after the deposition process. This annealing could further control the stoichiometry of deposited films and change the crystal structure with other semiconducting properties. The plasma was monitored during the deposition process by a time resolved ion mass spectroscopy with energetic resolution, Langmuir probes, RF impedance probe and calorimetric probe. Deposited films were analyzed by XRD, Raman scattering, electrical conductivity and optical absorption measurements. Photoelectrochemical properties of these films in connection with other materials were investigated by photoelectrochemical measurement in three electrode cell.

4:00pm G4+G5+G6-ThA9 Pre- and Post-Surface Treatments using Electron Beam Technology for Load-Related Application of Thermochemical and PVD Hard Coatings on Soft Substrate Materials, A. Buchwalder (anja.buchwalder@ww.tu-freiberg.de), R. Zenker, TU Bergakademie Freiberg, Germany

INVITED

With their specific layer features and properties, surface treatments such as thermochemical treatment (nitriding, boriding) and hard coating (PVD) cover a broad field of application, and in particular for the wear and corrosion protection of steels. Limitations exist, however, when applying these surface treatments to cast irons and aluminum alloys with respect to both their treatability and load-bearing capacity.

The current contribution deals with investigations into duplex surface treatments, where a pre- and post-electron beam (EB) surface treatment (e.g. hardening, remelting, alloying etc.) was combined with one of the above-mentioned treatments. Among other factors, the thermal EB surface

treatments were characterized by high heating and cooling rates that facilitated the generation of a variety of non-equilibrium microstructures, which exhibited increased hardness and had minimal thermal effects on the surrounding base material. Furthermore, the layer thicknesses were one or two orders of magnitude higher than those generated by thermochemical treatment or hard coating.

Based on the extensive results, the study should demonstrate (using cast irons as an example) the extent to which duplex treatments can overcome the aforementioned limitations, and how the tribological and/or corrosive load behavior is affected. The property profiles achieved after duplex surface treatment were strongly dependent on the inherent microstructural and chemical processes. These complex processes were influenced by a range of parameters, such as the respective temperature and time of the secondary process, the thermal stability of the EB surface layer generated firstly etc..

The matrix microstructures of cast irons are comparable with those of steels. As is known from steel processing, however, the additional presence of soft graphite and high silicon contents changes the structures and properties of the surface layers generated. This was demonstrated by means of three different treatments and temperature/time regimes: PVD hard coating (575 K/3 h), nitriding (815 K/8-16 h) and boriding (>975 K/3-10 h) performed as both single and duplex surface treatments.

Thus, the focus of the investigations was on comparable investigations of the graphite containing states (single treatment) and the graphite eliminated states after EB liquid surface treatments (duplex treatments).

Hardness measurements, scratch tests and unlubricated pin-on-disc wear tests using different normal loads were realized to facilitate characterization of the different load-bearing capacities of the single- and duplex-treated layers.

4:40pm G4+G5+G6-ThA11 Black Oxide and Carbon-Based Coatings for Roller Bearing Applications, E. Broitman (esteban.daniel.broitman@skf.com), X. Zhou, SKF Research & Technology Development Center, Netherlands

It is widely accepted the advantages of using coatings to improve bearings performance. In some applications, they can provide different properties like electrical insulation, low friction, and resistance to corrosion, contact fatigue, abrasive wear, and plastic deformation. Several bearing producers are putting a great effort on coated bearings development as an added value in their product. Among different kind of available industrial coatings, there are two standing out: "Black Oxide" and "Carbon-based" coatings.

In the first part of the presentation we will introduce two typical carbon-based coatings used by the bearing industry: "diamond-like coatings" (DLC) and WC/C nanostructured coatings. We will show how carbon-based coatings can be deposited at industrial scale on hardened steel bearings and gears which are temperature-sensitive using low deposition temperatures. We will explain how it is possible to deposit films with different amount of sp^2 - sp^3 bonding ratios by just changing fundamental deposition parameters, leading to six different microstructures: graphite, non-hydrogenated a-C (amorphous) and ta-C (tetrahedral) carbon coatings, hydrogenated a-C:H and ta-C:H films, and a soft polymeric coatings. We will show films containing nanometric-thick multilayers of different nanostructure that can be tailored according to the applications to obtain coatings with high toughness, high elasticity, and/or very low friction coefficient.

In the second part we will introduce Black Oxide, which is a coating formed by a chemical reaction on the surface of the bearing steel. We will describe the coating process consisting of about 15 steps where the parts to be coated are immersed in alkaline aqueous salt solutions at defined temperatures in the range 130-150 °C. The reaction produces a dark conversion layer of approximately 1 μm thick formed by mainly magnetite Fe_3O_4 . Compared to non-coated bearing steels, we will show experimental results demonstrating Black Oxide benefits: increasing moisture corrosion resistance, steel chemical attack preservation from some aggressive lubricant additives, steel embrittlement protection by hydrogen permeation reduction, enhancing micropitting protection, and improved smearing resistance from bearing sliding during high-load conditions.

In the last part we will present some applications of SKF Black-Oxide and NoWear® carbon-based bearings to extend maintenance and life expectancy of specialized bearings in different areas, like the automotive and wind-energy.

Thursday Afternoon Poster Sessions, May 23, 2019

Coatings for Use at High Temperatures

Room Grand Hall - Session AP-ThP

Coatings for Use at High Temperatures (Symposium A) Poster Session

AP-ThP1 Investigation of Microstructure and Properties of Thick Mo Coating obtained via Molten Salt Electrolysis, R. Tripathi (ramtripath@barc.gov.in), Homi Bhabha National Institute, India; S.K. Ghosh, Bhabha Atomic Research Centre, India

Refractory metals and their alloy coatings have got tremendous attention in recent years because of their inherent high temperature oxidation resistance properties, corrosion resistance to molten salt and hydrogen permeation barrier applications in ITER and hydrogen storage purposes. In this study, thick metallic Molybdenum (Mo) coating was electrodeposited on various metallic substrates by molten salt electrolysis from oxide-fluoride based electrolyte. The effect of current density and electrolyte temperature on coating thickness and quality of the coating were studied. Detail parameter optimization was done to obtain compact, defect free smooth thick Mo-coating. Grazing incidence X-ray diffraction (GIXRD) of the coatings confirmed about the deposition of bcc Mo metal with strong texture along <110> direction. Cross-section field emission scanning electron microscopy (FESEM) attached energy dispersive spectroscopy (EDS) of the coating revealed deposition of nonporous and uniform deposition of Mo coating with high chemical purity. The qualitative nature of the coating/substrate interface was also investigated under FESEM. For quantitative estimation of adhesion with substrate, adhesion tester was used and the results were analyzed in detail. The measured microhardness of the coatings was correlated with microstructure and composition. In addition to this, the results related to hydrogen permeation across the Mo-coating will also be discussed.

AP-ThP2 High Temperature Performance of CrAlN Coating on Stainless Steel Substrates in Simulated Diesel Exhaust Environment, S. Yang (shicai.yang@miba.com), Miba Coating Group. Teer Coatings Ltd., UK; V. Vishnyakov, Institute for Materials Science, University of Huddersfield, UK; P. Navabpour, Miba Coating Group. Teer Coatings Ltd., UK; J. Allport, Institute for Materials Science, University of Huddersfield, UK; H. Sun, Miba Coating Group. Teer Coatings Ltd., UK

CrAlN coatings on stainless steels were subjected to temperature cycling up to 750 °C in air, simulated diesel engine exhaust composition and actual diesel engine exhaust. Scanning electron microscopy (SEM), X-ray diffraction (XRD) and glow discharge optical emission spectrometry (GDOES) were used to study the surface morphology, phase microstructures and composition coating depth profiles. It was found that high temperature corrosion on the coating surface induced formation of passive oxides, which provided a barrier function to further corrosion. The microstructure of the coatings did not change significantly in ambient air at temperature of 750 °C. The results show that CrAlN coatings have high hardness, thermal stability, corrosion and erosion resistance. The coatings have potential for applications to protect surface of mechanical components in diesel exhaust systems.

Key words: Thermal stability, high temperature, oxidation, corrosion, erosion.

AP-ThP3 e-Poster Presentation: Improvement of the Robustness of Time to Failure Assessment in Tbc System, M. Theveneau, B. Marchand, V. Guipont, Mines ParisTech, PSL Research University, MAT - Centre des Matériaux, France; F. Coudon, SAFRAN Tech, France; V. Maurel (vincent.maurel@mines-paristech.fr), Mines ParisTech, PSL Research University, MAT - Centre des Matériaux, France

One of the major challenges for TBC system is to determine the time to failure of ceramic layer during ageing. The aim of this paper is to propose new methodologies for both experimental assessment of adhesion and for analyzing the robustness of model of lifetime to spallation.

Recently, the use of Laser Shock Adhesion Test (LASAT) has shown its capability for both ranking different coating solutions and evaluating the evolution of a given coating as a function of aging [1-2]. The methodology developed in this study is based on the evaluation of interfacial crack propagation from a defect introduced by laser shock, an interfacial delaminated area, known in size and location. The evolution of interfacial delamination during thermal cycling was shown to be consistent with measured interfacial delamination measured by cross-sectioning. Thus, the influence of dwell time at high temperature has been clearly established, confirming that short dwell time was very detrimental as compared to long

dwell at high temperature [3-4]. Moreover, this new method has shown a very small scatter as compared to other adhesion testing [2].

On the other hand, some lifetime to spallation models have been tested, focusing on two main aspects. Firstly, the ability of existing models to reproduce the influence of loading parameters has been tested (e.g. the influence of dwell time at high temperature or the influence of maximum temperature) [3-5]. Secondly, the robustness of this kind of models has been analyzed through sensitivity analysis based on large numerical sampling. As a conclusion, the propagation of scatter from measurement to life modeling has been evaluated and guidelines for experimental focus points have been derived.

References

- [1] Guipont, et al (2010). Journal of Biomedical Materials Research Part A, 95(4), 1096-1104.
- [2] Guipont, et al. "Interfacial toughness evolution under thermal cycling by laser shock and mechanical testing of an EB-PVD coating system." (2018). <http://dc.engconfintl.org/cgi/viewcontent.cgi?article=1033&context=tbcv>
- [3] Courcier, C et al (2011). Interfacial damage based life model for EB-PVD thermal barrier coating. Surface and Coatings Technology, 205(13-14), 3763-3773.
- [4] Soullignac, Romain, et al. "Cohesive zone modelling of thermal barrier coatings interfacial properties based on three-dimensional observations and mechanical testing." Surface and Coatings Technology 237 (2013): 95-104.
- [5] Chaboche, J. L., et al "Lifetime assessment tools for thermal barrier systems" in "Thermal Barrier Coatings IV", Eds, ECI Symposium Series, (2015). http://dc.engconfintl.org/thermal_barrier_iv/34

AP-ThP4 Computational Modelling, Synthesis and Characterization of Direct Laser Metal Deposition of Nickel Based Coatings on Ti-6Al-4V Alloy, O.S. Fatoba (drfatobasameni@gmail.com), S.A. Akinlabi, E.T. Akinlabi, M.J. Oboegbu, University of Johannesburg, South Africa

Super alloys have been developed for specific, specialized properties and applications. One of the main applications for titanium alloy and nickel based super alloys is gas turbine engine disc components for land based power generation and aircraft propulsion. Turbine engines create harsh environments for materials due to the high operating temperatures and stress levels. Hence, alloys used in the high temperature turbine sections such as the exhaust nozzle of aircraft engines have to be developed from specialized and sophisticated materials with advanced properties. Nickel based super alloy has been widely used for components manufacturing for aerospace engines and high temperature applications due to its ability to retain very high mechanical strength up to 650°C for prolonged periods, the alloy however can be susceptible to crack propagation. This research work seeks to develop an innovative super alloy via Direct Laser Metal Deposition (DLMD) technique for improved thermal, mechanical, and tribological properties, which can withstand adverse environmental conditions. A 3kW continuous wave ytterbium laser system (YLS) attached to a KUKA robot which controls the movement of the cladding process was utilized for the fabrication of Nickel-based coatings on Ti-6Al-4V alloy. The mechanical and thermal properties of the developed composite coatings were investigated. Hardness measurements were done using a Vickers micro-hardness tester. While the composite coatings were also analysed using optical microscopy, scanning electron microscopy (SEM) with energy dispersive microscopy (EDS), and X-ray diffraction (XRD). The results showed improved mechanical, thermal and tribological properties of the coatings due to the rapid solidification of the DLMD technique. The improved properties were as a result of combinations of optimized process parameters, coating composition, intermetallic phases formed, rapid cooling, and controlled thermal stresses in the coatings. The COMSOL multiphysics modelling developed corroborated the experimental results, determined predictive mechanisms and matched the proposed hypothesis.

Keywords: Ti-6Al-4V alloy; Ni-based coating; Computational modelling; Characterization; Microstructure; Process Parameters.

AP-ThP5 Wear Resistance Performance of AlCrN and TiAlN Coated H13 Tools during Friction Stir Welding of A2124/SiC Composite, Y. Adesina (akyadesina@gmail.com), A. Al-Badour, Z. Gasem, King Fahd University of Petroleum and Minerals, Saudi Arabia

Tool wear during friction stir welding (FSW) of hard particulate reinforced aluminum metal matrix composites

(Al MMCs) are more prominent due to the tool interaction with the particulates at high strain rate. Considering

Thursday Afternoon Poster Sessions, May 23, 2019

the excellent mechanical and wear resistance properties of cathodic arc PVD coatings, they are expected to abate

the wear of tools during FSW of Al MMCs. Hence, it is the aim of this study to investigate the contribution of

cathodic arc PVD deposited AlCrN and TiAlN coatings in alleviating tool wear during FSW of Al MMCs. AlCrN

and TiAlN coated H13 FSW tools were used to butt weld 8 mm thick aluminum alloy 2124 reinforced with 17 vol

% SiC of 3 μm particle size. Interestingly, the coated tools exhibited significant improvement in wear resistance

of about 92 and 80%, respectively, over the bare H13 tool. Over 97% reduction in the wear of the FSW tool was

recorded during the plunging stage with the use of the coated tools. Additionally, AlCrN and TiAlN coated tools

considerably improved the surface finish of the welded Al MMC. The coated tools demonstrated superior wear

resistance due to the improved scratch crack resistance, high mechanical and oxidation resistance properties of

the coatings. Dominant wear mechanisms on AlCrN and TiAlN coated tools were abrasive erosion and chipping

off by sharp and hard SiC particles while severe striation and oxidation characterized the wear mechanism of the

bare tool. The use of these coatings did not deteriorate the weld properties, rather somewhat improvement in the

hardness of the nugget zone was observed due to the characteristic dynamic stirring and refinement of the Al

matrix and SiC particles.

AP-ThP6 Diffusion Model for Estimating the Iron Boride Layer Thicknesses, O. Gómez-Vargas (ogomezv@ittla.edu.mx), Instituto Tecnológico de Tlalnepantla, México; *M. Ortiz-Domínguez*, Universidad Autónoma del Estado de Hidalgo, México; *J. Solís-Romero*, Instituto Tecnológico de Tlalnepantla, México; *M. Flores-Rentería, I. Morgado-Gonzalez, E. Cardoso-Legorreta*, Universidad Autónoma del Estado de Hidalgo, México; *M. Elías-Espinosa*, Tecnológico de Monterrey, México; *A. Cruz Avilés*, Universidad Autónoma del Estado de Hidalgo, México

Surface hardening, a process that includes a wide variety of techniques (Carburizing, Nitriding, Nitrocarburizing, Boriding, and Thermal diffusion process), is used to improve the wear resistance of parts without affecting the more soft, tough interior of the part. In particular, resistant layers of borides are produced in ferrous and non-ferrous materials through the well-developed process of boriding. In the present work, the AISI 9840 steel was pack-borided in the temperature range 1123-1273 K for 2- 8 h to form a compact layer of Fe₂B at the material surface. A recent kinetic approach, based on the integral method, was proposed to estimate the boron diffusion coefficients in the Fe₂B layers formed on AISI 9840 steel in the temperature range 1123-1273 K. In the present model, the boron profile concentration in the Fe₂B layer is described by a polynomial form based on the Goodman's method. As a main result, the value of activation energy for boron diffusion in AISI 9840 steel was estimated as 193.08 kJmol⁻¹ by the integral method and compared with the values available in the literature. Three extra boriding conditions were used to extend the validity of the kinetic model based on the integral method as well as other diffusion models. An experimental validation was made by comparing the values of Fe₂B layers' thicknesses with those predicted by different diffusion models. Finally, an iso-thickness diagram was proposed for describing the evolution of Fe₂B layer thickness as a function of boriding parameters.

AP-ThP7 STEM Investigations of Oxide Scales formed during Pre-oxidation of γ -TiAl, R. Swadzba (rswadzba@gmail.com), Institute for Ferrous Metallurgy, Poland

The paper presents results of pre-oxidation experiments of γ -TiAl alloy with Si-modified aluminide coatings intended for application as bondcoatings for Thermal Barrier Coatings. The goal of this work was to provide insight into the effect of different oxidation atmospheres and temperatures on the initial stages of oxide scale formation on bare and coated γ -TiAl. It is assumed that the formation of a thin (several hundreds of nanometers) and slow growing TGO consisting of α -alumina will enhance the adherence and lifetime of the TBCs on γ -TiAl.

The coatings were produced by pack cementation method applying a mixture consisting of Si and Al-containing powders and NH₄Cl activator. The

additional surface modification by pre-oxidation under various atmospheres was performed to foster the formation of oxide scales characterized by various thicknesses as well as phase and chemical compositions. The pre-oxidation experiments were performed in various gases including a mixture of Ar and O₂ (from 0.01 to 10 %) as well as pure O₂ at 900 °C for 0.5, 2 and 4 hours. After the pre-oxidation experiments systematic studies were performed using Scanning Transmission Electron Microscopy (STEM) method in order to characterize the phenomena at the metal-scale interface and study the phase and chemical compositions as well as the microstructures of the formed oxide scales.

AP-ThP8 Enhancement of Corrosion Resistance in Electrodeposited Ni-B-SnCoatings., U. Waware (uswaware@gmail.com), A.M.S. Hamouda, Qatar University, Qatar

In this work, Novel Ni-B-Sn coatings were developed through electrodeposition by reinforcing Sn particles in to Ni-B matrix. The effect of Sn particles on surface, structural, electrochemical properties were studied by comparing properties of Ni-B and Ni-B-Sn composites. The composite coatings were deposited on 22 x 2 mm mild steel substrates through electrodeposition process and dimethylamine borane (DMAB) is used as reducing agent. The incorporation of Sn particles into Ni-B matrix has been explained on the basis of Guglielmi's model. A substantial effect on surface roughness, thermal properties, crystal structure, and corrosion resistance was observed by addition of Sn particles to Ni-B coatings. Ni-B coatings in their as deposited state are amorphous in nature. Crystallinity of the composite coatings was significantly improved by addition of Sn particles. Surface analyses however shows increase in surface roughness confirms the formation of fine and dense structures in both Ni-B and Ni-B-Sn coatings. Corrosion resistance has improved greatly by incorporation of Sn into Ni-B matrix due to reduction in active area of Ni-B matrix. The enhancement in corrosion resistance has been explained in the light of the existing literature.

Keywords: Coating, electrodeposition, amorphous, morphology, crystalline, corrosion.

***Corresponding authors:** Tel.: +974-55019813

E-mails: uswaware@gmail.com [mailto:uswaware@gmail.com%20] (U. S. Waware), hamouda@qu.edu.qa [mailto:hamouda@qu.edu.qa] (A. M.S. Hamouda)

AP-ThP9 Microstructure of MCrAlY Coatings Deposited Using HVOF after Heat Treatment and Aluminizing, L. Swadzba, A. Iwaniak (aleksanderi@interia.eu), R. Swadzba, B. Witala, B. Mendala, Silesian University of Technology, Poland; *G. Wieclaw, P. Lubaszka*, Certech Sp. z o.o., Poland

Effective oxidation and corrosion protection of turbine blades in aircraft engines used at high temperature in the atmosphere of exhaust gases is still a major technological challenge and is the subject of intensive research. In this work, the microstructure of coatings deposited on Inconel 738 alloy used for turbine blades was investigated. In the first stage of the research work MCrAlYHfSi (M=Ni) coatings made of Amperit 405.001 material with granulation +22-45 μm were deposited using HVOF method. The coatings were applied with variable process parameters by HVOF method using the Thermico system and the CJS K5.2-N burner. Then thermal treatment of the sprayed coatings was performed at 1050°C for 4 hours in argon atmosphere. After the heat treatment vapor phase aluminizing using the "out-of-pack" method was carried out at 1050°C for 5 hours. After each treatment thickness of the coatings was measured, the microstructures were investigated using SEM and chemical composition analysis (EDS) and their surface topography and roughness were determined using 3D profilometry.

AP-ThP10 Effect of Vanadium Content on the High-temperature Tribo-mechanical Properties of Cr-Al-V-N Coatings Deposited by DC UBMS, H. Kim, I.-W. Park (ipark@kitech.re.kr), Korea Institute of Industrial Technology (KITECH), Republic of Korea

Quaternary Cr-Al-V-N coatings with vanadium content ranging from 0 to 13 at.% were deposited on WC-Co alloy substrates by an d.c. unbalanced magnetron sputtering using Cr-Al composite targets and pure vanadium target in an N₂/(Ar+N₂) gas mixture for applications of the high-strength steel and aluminum alloys entails increasing demands on the surfaces of tools used for forming processes. The microstructure, mechanical, wear, tribological properties of the coatings were investigated by XRD, XPS, FESEM, HRTEM, surface 3D profiler, nano-indentation, scratch tester, and ball-on-disc tribo-meter. As the vanadium content increased, the nanohardness of the Cr-Al-V-N coatings showed higher hardness values (~30GPa) than that of CrAlN coating (~25GPa). Ball-on-disc tri-tests were used to assess the friction at 700°C, the friction coefficient of the Cr-Al-V-N coatings drastically

Thursday Afternoon Poster Sessions, May 23, 2019

decreased from 0.6 to 0.35 with increasing vanadium content up to 7 at.% in the coatings due to the formation of a tribolayer containing the lubricious oxide V_2O_5 as evidenced by XPS. Moreover, it was found that the improved friction coefficient and nanohardness with incorporated small amount of the vanadium contents contributed to excellent wear resistance of the coatings.

AP-ThP11 Tensile Behavior of Air Plasma Spray MCrAlY Coatings: Role of High Temperature Aging and Process Defects, C. Cadet, Mines ParisTech, PSL Research University, France; T.S. Straub (Thomas.Straub@iwm.fraunhofer.de), Fraunhofer Institute for Mechanics of Materials IWM, Germany; D. Texier, Mines Albi, ISAE-SUPAERO, France; C. Eberl, Fraunhofer Institute for Mechanics of Materials IWM, Germany; V. Maurel, Mines ParisTech, PSL Research University, France

MCrAlY coatings are used as a protection layer against high temperature oxidation and corrosion for components working in an aggressive environment. In order to predict both coating and substrate lifetime, the characterization of thermomechanical properties of the coating is a challenging issue [1-3]. As these coatings are only a few hundreds of micrometers thick, their properties should be investigated with experimental tests adapted at this small scale [1-4].

In the present study, the mechanical properties of a free-standing MCrAlY coating and their evolution were scrutinized when it is aged in air for a large range of time and temperature. Free-standing micro-tensile specimens were prepared [1] and tested after different time/temperature ageing [4]. Based on digital image correlation to derive the strain evolution during loading, the stress-strain behavior has been identified. Thus a crucial effect of intrusive oxidation from deposition process defects and surface oxidation has been evidenced to drive both the ductility and the fracture mechanism of the tested material. For coarse intrusive oxidation, a loss of ductility has been identified, whereas metallic phase transformation (from b to g) increases the ductility of the material from 0.5 up to 3%. This composite effect will be analyzed through systematic microstructure and homogenization analyses. This methodology could be straightforward to determine the coupling between coating cracking and substrate failure under thermo-mechanical fatigue conditions [5].

References

- [1] D. Texier, D. Monceau, J. C. Salabura, R. Mainguy, E. Andrieu, *Materials at High Temperatures*, 33 (2016) 325–337.
- [2] D. Texier, D. Monceau, Z. Hervier, E. Andrieu, *Surface and Coatings Technology*, 307 (2017) 81–90
- [3] Alam, M.Z., Satyanarayana, D.V.V., Chatterjee, D., Sarkar, R., Das, D. K., *Materials Science and Engineering: A*, 641 (2015) 84-95.
- [4] Straub, T., Baumert, E.K., Eberl, C., Pierron, O.N., *Thin Solid Films*, 526 (2012) 176–182.
- [5] Esin, V.A., Maurel, V., Breton, P., Köster, A., Selezneff, S., *Acta Materialia*, 105 (2016) 505–518.

AP-ThP13 Influence of Si-Al Coating on Mechanical Properties of EBMed TiAl Alloy, L. Pyclik (Lukasz.Pyclik@avioaero.it), Avio Aero A GE Aviation Business, Poland; L. Swadzba, B. Mendala, B. Witala, J. Tracz, R. Swadzba, Silesian University of Technology, Poland; K. Marugi, Avio Aero A GE Aviation Business, Poland

The paper presents the results of investigations concerning the effect of silicon modified aluminide coatings on EBMed Ti-48Al-2Cr-2Nb (48-2-2) alloy. The study was performed on specimens machined from EBMed rods. The rods were printed by Avio Aero Cameri, Italy, and met heat treatment by hiping and solutioning. The specimens were manufactured by Silesian University of Technology, Poland, for coating or heat treatment. The anti-oxidation coating was applied on pre-machined specimens by a pack cementation process. The test results revealed difference between specimens in three conditions: bare, coated and heat treated corresponding to coating deposition process. The mechanical tests ensure environments as close as possible to current application in commercial novel engine, GE9X, where EBMed blades are applied on last stages of Low-Pressure Turbine designed by Avio Aero. All tests covered work at elevated temperatures at and above 1500F. All tests shown impact of coating on mechanical properties.

Avio Polska Proprietary Information The information contained in this document is Avio Polska Sp. z o.o proprietary information and is disclosed in confidence. It is the property of Avio Polska Sp. z o.o and shall not be used, disclosed to others or reproduced without the express written consent of Avio Polska Sp. z o.o, including, but without limitation, it is not to be used in the creation, manufacture, development, or derivation of any repairs,

modifications, spare parts, designs, or configuration changes or to obtain EASA, FAA or any other government or regulatory approval to do so. If consent is given for reproduction in whole or in part, this notice and the notice set forth on each page of this document shall appear in any such reproduction in whole or in part.

Hard Coatings and Vapor Deposition Technologies Room Grand Hall - Session BP-THP

Hard Coatings and Vapor Deposition Technologies (Symposium B) Poster Session

BP-ThP1 Low Stress AlTiN-Based Coating Systems, C.J. Charlton (corinne.charlton@kennametal.com), Kennametal Inc., USA; J. Kohlscheen, Kennametal GmbH, Germany; D. Banerjee, Kennametal Inc., USA

In this study, we deposited AlTiN coatings with reduced intrinsic stress for metal cutting applications. Stress management is important to maintain coating integrity during machining operations, especially at the cutting edge. Deposition was done in an industrial scale PVD unit using cathodic arc evaporation. Coating thickness was adjusted to about 3 μm . Al content in the metal fraction was varied between 60 and 70 atomic %. A reduction in compressive stress was achieved in four different ways: lowering bias voltage, layering of coating architecture, increasing pressure, and varying the cathode confinement ring system. Samples of cemented carbide and carbon steel strips were used for analyses. Chemical composition was measured by EDX. The microstructure of the obtained films was evaluated by x-ray diffraction (XRD). Stress was estimated using Stoney's equation considering the resulting curvature of the partially coated steel strip. The values were validated using XRD peak shift measurements of the dominant cubic phase. It will be shown that a combination of bias and layer variation leads to an optimized ratio of low stress and wear resistance. Metal cutting data obtained by turning are showing that such coatings are able to outperform mono-layer coatings with higher stress.

BP-ThP2 Multi-Target Co-Sputtering Deposition and Mechanical Properties of Ti-Zr-Based High-Entropy Alloy and Nitride Coatings, S.Y. Chang (changsy@mx.nthu.edu.tw), Y.T. Hsiao, National Tsing Hua University, Taiwan; S.Y. Lin, National Formosa University, Taiwan

Protective hard coatings with good mechanical properties and high thermal stability have been widely used in cutting tools and machinery components. Because of the strict conditions in practical applications, multi-component, nanocomposite and multilayered coatings have been developed to replace conventional single-phase, single-layered binary nitrides. Among them, multi-component high-entropy alloy and nitride coatings with a simple solid-solution structure have been intensively studied in recent years and been found to present excellent mechanical properties, thermal stability and wear resistance. In this study, several coatings of Ti-Zr-based quinary high-entropy alloys with the additions of Al, Cr, Mo, Hf, Nb, Ta, and/or V, and their nitrides with various nitrogen contents, were deposited using a multi-target co-sputtering system in an N_2/Ar mixed atmosphere. The microstructures, crystal structures and chemical compositions of these coatings were characterized, and the mechanical properties were measured. Because of the effect of high mixing entropies, all the coatings presented an amorphous or a simple face-centered cubic solid-solution structure. The nitrogen contents of the coatings increased with N_2/Ar flow ratio. The alloy coatings had a hardness of 6-8 GPa, while the nitride coatings with a low nitrogen content of about 20 at.% easily showed a hardness up to 16-20 GPa. With a high nitrogen content of 50 at.%, very large residual stresses caused the cracking of the coatings and needed to be reduced for preparing more robust and reliable coatings.

BP-ThP3 $(Ti_{1-x}Y_x)B_{2+\delta}$ Thin Films - Structural Evolution and Mechanical Properties, M. Truchlý (martin.truchly@fjmph.uniba.sk), B. Grancic, Comenius University in Bratislava, Slovakia; P. Švec Jr., Slovak Academy of Sciences, Bratislava, Slovakia; T. Roch, L. Satrapinskyy, V. Izaii, Comenius University in Bratislava, Slovakia; M. Harsani, Staton s.r.o., Slovakia; O. Kohulak, P. Kus, M. Mikula, Comenius University in Bratislava, Slovakia

The transition metals boride family offers a lot of stoichiometric modifications (TMB, TMB_2 , TMB_6 , TMB_{14} , etc.) with different crystalline structure and excellent physical properties. From the point of view of mechanical properties, TM diborides seem to be the most interesting. The best-known overstoichiometric TiB_{2+x} thin film prepared by magnetron sputtering exhibits extremely high hardness $H > 40$ GPa [1]. However, the application potential of TiB_{2+x} and other binary coatings (ZrB_2 , NbB_{2-x} and

Thursday Afternoon Poster Sessions, May 23, 2019

W_2B_{5-x}) and the use of their excellent mechanical properties are heavily limited. This is in particular a low fracture toughness expressed by the very high values of Young's modulus (500±600 GPa) and low oxidation resistance due to formation of volatile boron oxide at 450°C.

Recently, Alling et al. [2] performed extensive theoretical study of 45 ternary diborides with AlB_2 type structure, where the possibility to obtain beneficial age hardening through isostructural clustering, including spinodal decomposition in $M^{1-x}M^2_xB_2$ ($M^{1,2} = Mg, Al, Sc, Y, Ti, Zr, Hf, V, Nb, Ta$) were presented. It has been shown that a significant influence on the formation of a metastable alloy, in which thermally-induced processes led to isostructural clustering, accompanied by age hardening is combination of lattice mismatch between binary constituents and bulk modulus of resulting ternaries.

According to aforementioned results, $(Ti_{1-x}Y_x)B_{2+\Delta}$ seems to be potential candidate for films with clustering tendency what can bring interesting mechanical behavior and extend the possibilities of application potential of diborides.

Here, we present experimental methods and analyzes to investigate structure evolution and mechanical behavior of ternary systems $(Ti_{1-x}Y_x)B_{2+\Delta}$ prepared by magnetron co-sputtering. We discuss the relationship between chemical composition, structural evolution and mechanical properties of as-deposited and annealed thin films based on results obtained from scanning electron microscopy (SEM), X-ray diffraction analysis (XRD), transmission electron microscopy (TEM), and nanoindentation measurements.

[1] M. Mikula et al., The influence of low-energy ion bombardment on the microstructure development and mechanical properties of TiB_x coatings Vacuum 85 (2011) 866–870.

[2] B. Alling et al., A theoretical investigation of mixing thermodynamics, age hardening potential, and electronic structure of ternary $M^{1-x}M^2_xB_2$ alloys with AlB_2 type structure. Sci. Rep. 5, 9888; (2015)

This work was supported by the Slovak Research and Development Agency [grant number APVV-17-0320], and Operational Program Research and Development [project ITMS: 26210120010].

BP-ThP4 Post-annealing of (Ti,Al,Si)N Coatings deposited by High-Speed Physical Vapor Deposition (HS-PVD), K. Bobzin, T. Brägelmann, C. Kalscheuer, T. Liang, M. Welters (welters@iot.rwth-aachen.de), Surface Engineering Institute - RWTH Aachen University, Germany

Gas turbine engines operating in environments containing solid particles such as sand, dust and ice particles are challenged by the problem of solid particle erosion (SPE), which causes contour changes especially on compressor blades. Consequently, the performance and efficiency of the engines as well as the maintenance intervals will be reduced. In order to minimize the effects of SPE and to extend the lifetime of compressor blades, the application of erosion resistant coatings represents a promising way.

In the present work, (Ti,Al,Si)N coatings with different Si contents were deposited onto martensitic steel X3CrNiMo13-4 used for compressor blades by High-Speed Physical Vapor Deposition (HS-PVD) technology. Morphology of the coatings investigated by scanning electron microscopy (SEM) shows a dense microstructure with coating thicknesses up to $s \approx 20 \mu m$. Owing to hollow cathode discharge (HCD) and the transport function of the plasma-forming gas Ar, which are specific in HS-PVD deposition processes, high deposition rates $ds/dt > 20 \mu m$ were achieved. The coated samples were then post-annealed in N_2 atmosphere with bias voltage induced Ar plasma directly in the coating chamber. The annealing temperature, time and atmosphere were varied. The post-annealing effects on the microstructure, indentation hardness as well as chemical and phase compositions were investigated by energy dispersive spectroscopy (EDS), X-ray diffraction (XRD) and nanoindentation, respectively. The erosion resistance of annealed, as-deposited and uncoated samples was investigated using a fine sand blasting facility. Basing on measured erosion rates and inspection of the eroded surfaces, a much higher erosion resistance of the (Ti,Al,Si)N coated samples compared to uncoated substrates could be revealed. Moreover, the post-annealing process led to a further improvement of the erosion resistance. Therefore, the thick (Ti,Al,Si)N coatings deposited by HS-PVD in combination with a post-annealing in N_2 atmosphere provide a high potential for the protection of compressor blades against SPE.

BP-ThP6 Discrete Thin-film Multilayer Structures of TiB_2 and ZrB_2 Ceramics for Super-hard and Tough Coating, A. Ghimire, National Tsing Hua University, National Dong Hwa University, Taiwan; M.S. Wong (mswong@gms.ndhu.edu.tw), National Dong Hwa University, Taiwan; S.Y. Chang, National Tsing Hua University, Taiwan

Multilayer films consisting alternating ZrB_2 and TiB_2 layers with nanometer scale bilayer thickness λ ($7nm \sim 1nm$) were deposited on silicon substrate by using unbalance magnetron dc sputtering system. The effect of bilayer thickness design on the structure and mechanical properties of the resulting multilayer films has been investigated. The films of bilayer thickness 6 nm and 7 nm possess polycrystalline structure with low crystallinity, however, below 6 nm bilayer thickness, highly [001] textured films with high intensity XRD peaks were witnessed to be lying between ZrB_2 and TiB_2 [001] phase. For 6 nm \sim 2nm bilayer samples, there also exist a unique X-ray diffraction peak along with the alloy phase which is distinct than the conventionally observed superlattice peaks in most of the multilayer works. The hardness increment concurs with the phase transition to aforementioned unique structure. The maximum hardness reached up to 44 GPa for the 2nm bilayer sample with a compressive stress of 4.9 GPa. Over the explored range of λ , all the multilayer films generated shorter cracks than single layer TiB_2 and ZrB_2 films upon Vickers indentation fracture test. Furthermore, the microstructure and growth mechanism of ZrB_2/TiB_2 multilayer system by cross sectional TEM analysis is discussed.

BP-ThP7 Effect of Bias Voltage on Mechanical Properties of Zr-Si-N Films Fabricated through HIPIMS/RFMS Cosputtering, Y.I. Chen (yichen@mail.ntou.edu.tw), Y.Z. Zheng, National Taiwan Ocean University, Taiwan; L.C. Chang, Ming Chi University of Technology, Taiwan

A previous study has fabricated Zr-Si-N films with Si content of 2–10 at.% through the co-deposition of high-power impulse magnetron sputtering (HIPIMS) and radio-frequency magnetron sputtering (RFMS). The mechanical properties, hardness and Young's modulus, of the HIPIMS/RFMS co-sputtered Zr-Si-N films exhibited linear relationships to their compressive residual stresses. In this work, a negative bias voltage of 50–150 V was applied on the substrates to increase the compressive residual stress of the Zr-Si-N films and the effects on mechanical properties were investigated. The results indicated that the compressive residual stress was increased from -5.0 to -8.8 GPa as increasing the bias voltage from 0 to -150 V; however, the hardness and Young's modulus values exhibited decreasing trends varying from 34.4 to 28.3 GPa and 369 to 299 GPa, respectively, which were accompanied with the decrease in the Si content of the fabricated films from 3.2 to 0.4 at.%.

BP-ThP9 Influence of the C/N Ratio on the Mechanical and Tribological Properties of the AlCrCN Coatings by Cathodic Arc Deposition, D.Y. Wang (mdu.aurora@gmail.com), W.Y. Ho, W.C. Chen, MingDao University, Taiwan; L.C. Hsu, J. Hung, Aurora Scientific Corp., Canada

CrAlCN coatings with different C/N ratio were deposited using a cathodic arc deposition (CAD) technique from $Cr_{50}Al_{50}$ and Cr targets in a various mixture of N_2 and C_2H_2 gases. Scanning electron microscopy (SEM), nanoindentation, and pin-on-disc tribometer were used to characterize the cross-sectional microstructure, hardness, wear rate, and friction coefficient of the AlCrCN coatings. The increase in the C_2H_2 fraction leads to a continuous increase in the deposition rate of the AlCrCN coatings. Nano-indentation results indicate that with an increase of the C/N ratio in the coatings, the hardness and elastic modulus increase to a maximum value, then decreases rapidly, which results from the increase in the defect density in the coatings. Tribological test results show that when tested against WC-Co balls, there is no significant change in the friction coefficient (0.2–0.3) of the AlCrCN coatings with a C/N ratio of above 5, but the friction coefficient increases rapidly to 0.6 with the C/N ratio below 2. In addition, the wear rate decreases remarkably by observation on the worn track showing increasing C content in the coatings. The result shows the low friction coefficient and the formation of a transfer layer correspond to the low wear rate for the AlCrCN coatings with high C content.

Keywords: Cathodic arc deposition, AlCrCN, friction coefficient, wear

BP-ThP11 The Effects of Pulse Frequency on the Growth of Diamond Using Pulse Microwave Plasma CVD, Y. Zeng (s1871032NN@s.chibakoudai.jp), Y. Sakamoto, T. Maruko, Chiba Institute of Technology, Japan

Diamond has many excellent properties such as high hardness, and high thermal conductivity. Usually diamond is grown on 973-1273 K substrate. However high temperature may cause the film to break or peel off. Pulse oscillation plasma can reduce electron temperature and gas temperature while maintaining electron density. For this purpose, pulse oscillation is used to reduce the synthetic temperature. In this study research of diamond

Thursday Afternoon Poster Sessions, May 23, 2019

deposition at lower substrate temperature using pulse microwave CVD apparatus and the effect of the pulse frequency on growth rate and quality of the deposit.

Diamond synthesis use pulse microwave CVD. Use Si (100) as the substrate. The pretreatment method is scratched with diamond powder and then clean under ultrasonic environment with acetone. Microwave adopt two modes of continuous oscillation and pulse oscillation. The duty ratio is 50%. The pulse frequency is 250,500,750,1000Hz, respectively. Adjust the microwave output power to control the substrate temperature at 673 K under each condition. The substrate temperature during synthesis is measured by the thermocouple mounted on the bottom of the substrate holder. the flow rate of CH₄-CO-H₂ is 2-25-200 sccm, and synthesis time is 5 hours. For the synthetic pressure, 5.3kPa is used for pulse oscillation, and 1.3kPa is used for continuous oscillation. Analysis of the surface and section of diamond films are observed by SEM. Qualitative evaluation is carried out by Raman spectroscopy. The plasma state is evaluated by emission spectroscopic analysis by OES.

As a result of SEM observation, the crystal size of diamond by pulse oscillation is larger than continuous oscillation. Although the pressure staying at 5.3kPa, the orientation of the crystal changes from (100) to (111) as the pulse frequency increases. The growth rate of pulse oscillation is 1.5-3 times faster than continuous oscillation. The growth rate is 0.3-0.6 μ m/h when pulse oscillation is used. Under the condition of this experiment, the growth rate of 500Hz was maximum. In the OES, H α has the highest emission intensity at 500 Hz. Comparing the H α emission intensity and the film growth rate, it is recognized that the film growth rate tends to be faster with the condition of high emission intensity. In the Raman spectra, D band (1350 cm⁻¹) and G band (1580 cm⁻¹) are observed under any conditions. On the condition at 500 Hz and 1000 Hz, apparent peak 1000-1200cm⁻¹ can be observed. This peak is caused by the miniaturization of diamond crystal. It can be concluded that crystal size is miniaturized by pulse frequency 500Hz and 1000Hz.

BP-ThP12 Analysis of Reaction Gas States on Synthesis of Boron Doped Diamond by HF-CVD, T. Maruko (s1321321HE@s.chibakoudai.jp), Y. Sakamoto, Chiba Institute of Technology, Japan

Boron doped diamond (BDD) electrodes are expected to be applied to various applications. The performance of BDD electrodes varies depending on the amount of doped B in diamond. Therefore, it is necessary to synthesize BDD which controlled amount of B in diamond depended on the used applications. In synthesis of BDD, B₂H₆, B(CH₃), B(OCH₃)₃ are often used as B dopants, nevertheless there is a disadvantage that B₂H₆ and B(CH₃)₃ are toxic. Conversely, B(OCH₃)₃ has the advantage of lower toxic relatively. However, it is difficult to control B(OCH₃)₃ flow rate, because B(OCH₃)₃ is liquid and introduced into the chamber by evaporation or bubbling. Therefore, if it is possible to control the amount of doped B in diamond by in-situ measurement of the reaction gas states, it is considered that more efficient production of BDD electrodes are possible.

In this study, the BDD synthesis was performed by HF-CVD using B(OCH₃)₃ as a B source, and analysis of reaction gas states using QMS during synthesis was attempted.

BDD was synthesized by HF-CVD using H₂-CH₄-B(OCH₃)₃ as a reaction gas. The B(OCH₃)₃ flow rate was varied from 0.1 to 0.4 sccm and CH₄ / H₂ ratio was 2%. The synthesis pressure was 4 kPa, filament temperature was 2273 K. The reaction gas states were measured using QMS. The deposits were evaluated using SEM, XRD, and Raman spectroscopy.

As a result of observation of deposits, facets of diamond crystals were observed under all conditions from surface observation by SEM. The peaks of diamond were recognized in the XRD patterns of the deposits under all conditions. The peaks due to B-doped diamond were recognized in the Raman spectra of the deposits for all synthesis conditions. Therefore, the synthesis of BDD was confirmed under all conditions. Additionally, the position of the peak caused diamond at 1333cm⁻¹ in the Raman spectrum was changed lower wavenumber with increasing of the B(OCH₃)₃ flow rate. This result suggests that the amount of doped B in the diamond was increased with increasing of the B(OCH₃)₃ flow rate.

As a result of measurements of reaction gas states during synthesis by QMS, it was confirmed that peak of OCH₃ molecule was decomposed from B(OCH₃)₃. Additionally, the peak height of OCH₃ increased with increase of B(OCH₃)₃ flow rate.

In summary, the correlation was confirmed between the peak height of OCH₃ molecules measured from QMS and amount of B in diamond.

BP-ThP13 Effects of Boronizing Pretreatment on the Adhesion of B-doped Diamond on Ti Substrates, Y. Izu (s1521031JZ@s.chibakoudai.jp), Chiba Institute of Technology, Japan; T. Sakuma, Ogura Jewel Industry, Japan; A. Suzuki, T. Maruko, Chiba Institute of Technology Graduate School, Japan; M. Imamiya, Y. Sakamoto, Chiba Institute of Technology, Japan

BDD is an ideal electrode material because the potential window is wide, the background current is extremely low and it is insoluble in any solution. Ti / BDD electrodes are promising for application in wastewater treatment, because it has advantages of both materials. However, the delamination occurs at the intermediate layer between BDD coating and Ti substrate. Consequently, it is necessary to design intermediate layer having high bond dissociation energy.

Since the bonding dissociation energy is TiB > TiB₂ > TiC, the introducing Ti-B into the intermediate layer of the BDD on the Ti substrate can be expected to be improved the adhesion strength between the Ti substrate and the BDD film.

The boronizing of each Ti substrate with different reaction time and deposition of BDD on each Ti substrate with different reaction time were conducted using a mode-conversion type microwave plasma chemical vapor deposition apparatus, which is able to consistently process boronizing pretreatment and deposition of BDD, with solution of trimethyl borate as boron source.

From the results of chemical bonding analysis by X-ray photoelectron spectroscopy of the surface of each Ti substrate after the boronizing, it was observed that the amount of synthesizing Ti-B increased with the increase of the boronizing time. In adhesion strength of each BDD / Ti, increasing adhesion strength was accompanied the increase of boronizing time upto 20 minutes. However, adhesion strength at 30 minutes of boronizing time was decreased more than at 20 minutes.

It is considered that the adhesion strength was decreased by progressing hydrogen embrittlement was indicated.

BP-ThP14 High Entropy Nitride Thin Film (Cr_{0.35}Al_{0.25}Nb_{0.12}Si_{0.08}V_{0.20})N_x for Tribological Characteristics at High Temperature, Y.C. Lin (jay85621@kimo.com), J.G. Duh, National Tsing Hua University, Taiwan

High entropy nitride thin films have already been reported because of its outstanding mechanical properties. In this study, adding self-lubricating element Vanadium in high entropy nitride system improved the wear performance due to the formation of Magnéli phase. High entropy nitride thin films (Cr_{0.35}Al_{0.25}Nb_{0.12}Si_{0.08}V_{0.2})N_x with different nitrogen ratio were fabricated by controlling the nitrogen flow ratio in a radio frequency magnetron sputtering system. The variation of nitrogen ratio in thin film will affect the mechanical properties or even the crystal structure, thus investigating the difference of material characteristic induced from different nitrogen ratio become essential.

The chemical composition of as-deposited coatings was detected by a FE-EPMA. The crystal structure was evaluated from a Grazing Incidence XRD. The layer thickness of nitride thin films was measured from SEM. The mechanical properties at ambient temperature and high-temperatures were evaluated by a nano-indenter. The tribological properties were tested by ball-on-disc wear test in a high-temperature tribometer. The results of annealing test in air were also addressed in this study. Finally, a high entropy nitride thin film with the favorable wear performance in high temperature will be briefly discussed. It is expected to be a potential candidate applied in high temperature wearing industry.

BP-ThP15 Search of New (Al_{0.25}Cr_{0.3}Nb_{0.1}Si_{0.08}Ti_{0.1}Mo_{0.17})N_x Coatings for Feasible Application at High Temperature, W.L. Lo (lowelly85@gmail.com), J.G. Duh, National Tsing Hua University, Taiwan

Recently, mechanical and tribological properties of high entropy alloy(HEA) and HEA nitride coatings have been widely discussed, yet the high-temperature tribology of HEA nitride coatings have not been investigated. In this study, (Al_{0.25}Cr_{0.3}Nb_{0.1}Si_{0.08}Ti_{0.1}Mo_{0.17})N_x coatings with various nitrogen ratios were fabricated on Inconel 718 substrate by RF magnetron sputtering. The chemical composition analysis of (Al_{0.25}Cr_{0.3}Nb_{0.1}Si_{0.08}Ti_{0.1}Mo_{0.17})N_x coating was carried out using a FE-EPMA. The cross-sectional microstructure was observed by a FE-SEM. The phases of the HEA nitride coatings were verified by a Grazing Incidence XRD. The intrinsic mechanical properties of the coatings were measured by a high-temperature nano-indenter. The high-temperature tribological properties were estimated by a ball-on-disc tribometer equipped with a Al₂O₃ ball at high temperature.

(Al_{0.25}Cr_{0.3}Nb_{0.1}Si_{0.08}Ti_{0.1}Mo_{0.17})N_x coating with a specific nitrogen ratio exhibits favorable mechanical properties, which could be attributed to the

Thursday Afternoon Poster Sessions, May 23, 2019

formation of stable crystalline structure. In addition, the MoO₃ Magnéli phase could be observed at elevated temperature, which also improves the high-temperature tribological properties by providing a lubricating surface. Surface morphology and microstructure of the wear track were observed by FE-SEM and HR-TEM. The elemental redistribution and phase transformations in the wear track were analyzed by XPS and XRD. Finally, a HEA nitride coating with optimal high-temperature mechanical and tribological properties will be investigated and discussed.

BP-ThP17 Mechanical Properties and Thermal Stability of Cr-X-N (X=Al, Zr, Si) Multilayered Coatings Synthesized by UBMS, *H.K. Kim (ndkim2@naver.com), S.H. Lee, S.Y. Lee,* Korea Aerospace University, Republic of Korea

Among many kinds of transition metal nitride hard coatings, the (CrN)-based coatings have been paid much attention to cutting tool's film due to their excellent mechanical properties. Recently, industrial necessity of multilayered hard coatings with various interlayers are increasing due to their advanced mechanical properties and high temperature oxidation resistance. In this work the influence of coating structure on their various properties of multilayered Cr-X-N (X=Al, Zr, Si) coating was investigated. The microstructure, residual stress, hardness and elastic modulus, and friction coefficient were evaluated by field-emission scanning electron microscopy (FE-SEM), laser reflectance system, nano-indentation, and ball-on-disc type wear tester, respectively.

The hardness and compressive residual stress were measured to be in a range from 30.4 to 38.7 GPa, and from 4.3 to 6.2 GPa, respectively. After the scratch test to investigate adhesion property, the critical load gradually decreased from 48 to 41 N. Generally, the high residual stress causes the low adhesion, and the compressive residual stress could be considered as a factor on the adhesion decrement. During the wear test, the friction coefficient of the CrAlN coatings with the CrN and CrN/CrZrN interlayer exhibited improved values of 0.34 compared to that of the CrAlN coating with the CrZrN interlayer (COF 0.41). These improved friction coefficient could be attributed to the H/E ratio of the interlayer between the CrAlN coating and the WC substrate. In view of the coating structure, there exists a gradual increase in the H/E ratio from the WC substrate (H/E, 0.040), to the CrN interlayer (H/E, 0.076), and CrZrSiN interlayer (H/E, 0.083), and the CrAlN coating (H/E, 0.089). The CrN and CrZrSiN interlayers induced a smooth transition of the stress effectively under loading conditions, and wear properties could be improved significantly by structuring the coating with an optimal gradient of the H/E ratio of the coating/interlayer/substrate.

Acknowledgement

This research was supported by a grant from the Fundamental R&D Program for Core Technology of Materials funded by the Ministry of Commerce, Industry and Energy, Republic of Korea.

BP-ThP18 e-Poster Presentation: The Role of Vacancies in the W-N System, *F.F. Klimashin, P.H. Mayrhofer (paul.mayrhofer@tuwien.ac.at),* TU Wien, Institute of Materials Science and Technology, Austria

Our experimental and computational investigations afford an insight into the role of vacancies in the structure-properties relationship within the binary system tungsten-nitrogen. The vacancies on metal and nitrogen lattice sites favour the formation of the face-centred cubic structure. The lower the synthesis temperature, the lower the needed nitrogen partial pressure to stabilise the cubic structure. Among cubic γ -W_{0.50}N and γ -WN_{0.50}, also compositions with nearly 1:1 stoichiometry were prepared. Our results indicate clustering of vacancies on metal and nitrogen lattice sites rather than single-phased structures of NaCl (mechanically unstable) or NbO (nearly twice as high elastic modulus as experimentally observed) types. All cubic structures show hardness values of 30–33 GPa (up to 37 GPa on austenitic steel) with the tendency to slightly higher values for lower N/W ratios. In contrast, higher N/W ratios tend to increase fracture toughness, as for example 3.4 MPaVm is obtained for γ -W_{0.5}N but only 2.4 MPaVm is obtained for γ -WN_{0.5}. Coatings with a 1:1 stoichiometry, where clustered vacancies seem to be present, exhibit 2.8 MPaVm. The fracture toughness clearly scales with the compressive residual stresses, which clearly increase with the N/W ratio.

BP-ThP19 Probing Defected Layers of MoN/TaN and TiN/WN Superlattices, *N. Koutna (nikola.koutna@tuwien.ac.at), J. Buchinger, R. Hahn,* Institute of Materials Science and Technology, TU Wien, Austria; *J. Zálešák,* Erich Schmid Institute of Materials Science, Austrian Academy of Sciences, Leoben, Austria; *M. Bartosik,* Institute of Materials Science and Technology, TU Wien, Austria; *M.F. Friák, M.S. Šob,* Institute of Physics of Materials, Academy of Sciences of the Czech Republic, Czech Republic; *D. Holec,* Montanuniversität Leoben, Austria; *P.H. Mayrhofer,* Institute of Materials Science and Technology, TU Wien, Austria

Superlattices composed of coherently stacked materials with bi-layer periods in the nm range are an important concept to alter energetic, structural, mechanical, or electronic properties of coatings. Exceptional performance and hardness enhancement beyond the limits of the superlattice building components has been demonstrated for a series of nitride-based superlattices, e.g., TiN/AlN, TiN/CrN, TiN/NbN, TiN/VN, TiN/TaN or AlN/CrN. Yet the fundamental structure-stability-elasticity relationships and their origin remain mostly unknown for superlattices combining even simple binary transition metal nitrides. The complexity of these multilayered systems mainly stems from a strong driving force of transition metal nitrides for vacancies.

Our combined first-principles and experimental study focuses on two cubic-based multilayered systems: MoN/TaN and TiN/WN. MoN, TaN, and WN are often used to improve ductility, but they are metastable (MoN, TaN), or even unstable (WN) in a perfect stoichiometric configuration. Vacancies play an important role for these binaries, since they can largely improve their thermodynamic stability, ensure mechanical stability, or even eliminate (some) soft phonon modes (i.e., contribute to a vibrational stabilisation). By employing Density Functional Theory calculations, we reveal the impact of vacancies on the structural stability as well as on the electronic structure and elastic constants. Theoretical findings are corroborated with X-ray diffraction patterns, energy-dispersive X-ray spectroscopy as well as nanoindentation data. Furthermore, we formulate design rules for MoN/TaN and TiN/WN multilayered coatings with superior elastic properties and/or exceptional tensile strength.

BP-ThP20 Investigation of CVD Stability Windows for Tungsten Carbide Phases, *K. Bőör (katalin.boor@kemi.uu.se), J. Gerdin,* Uppsala University, Sweden; *R. Qiu,* Chalmers University of Technology, Sweden; *M. Boman,* Uppsala University, Sweden; *E. Lindahl,* Sandvik Coromant R&D, Sweden
Tungsten carbides are widely used in bulk materials such as cemented carbides, primarily due to their high hardness and chemical resistance. Although there has been extensive research on tungsten carbides, their potential as materials for wear and corrosion resistant coatings has not been widely utilized yet. A few attempts have been made to deposit tungsten carbides with chemical vapor deposition. Typically WF₆, H₂ and a hydrocarbon such as propane were used as precursors. Usually, multiple metallic or carbide phases were obtained such as W, W₃C, W₂C, WC_{1-x} or WC. In addition to the metallic or carbide phases amorphous carbon was also observed to be formed in some cases during the CVD process. Single-phase coatings, however, have only been obtained in a few cases and it has been difficult to control the microstructure and/or morphology of those.

In order to achieve a better control on the characteristics of the coating, a deeper understanding on the influence of the CVD process parameters on the resulted coatings is needed. A systematic study carried out to find the stability window of the single phases in a CVD process will be presented. The study will include the phase content, the microstructure, the morphology of the deposited single-phase tungsten carbide coatings and the growth kinetics behind.

The tungsten carbide thin films were deposited using WF₆, C₂H₄, H₂ as precursors with Ar as the carrier gas on different metallic and ceramic substrates in a newly constructed hot-wall CVD reactor. XRD, GI-XRD, SEM, XPS and TEM- analysis were used to characterize the coatings.

BP-ThP22 Photocatalytic Activity of Metal Oxide Thin Films Deposited by MS-PVD and Layer-by-Layer for Hydrogen Production by Water Splitting, *P.J. Rivero,* Public University of Navarra, Spain; *J.A. Garcia (joseantonio.garcia@unavarra.es),* Universidad Publica de Navarra, Spain; *R. Rodriguez,* Public University of Navarra, Spain; *J. Esparza,* AIN, Ingenieria Avanzada de Superficies, Spain; *G. Garcia Fuentes,* Public University of Navarra, Spain

Two different deposition techniques, Magnetron Sputtering Physical Vapour Deposition (MS-PVD) and Layer-by-Layer (LbL) technique, have been utilized to compare the photocatalytic activity of various metal oxides, including single metal oxides: Fe₂O₃, WO₃, binary metal oxides: SrTiO₃, and a combination of these compounds. The coatings were deposited on stainless

Thursday Afternoon Poster Sessions, May 23, 2019

steel (AISI 304) substrates, glass slides and silicon wafers. Photocatalytic activity has been tested by visible spectrophotometry, through monitoring the degradation of Methylene Blue under direct exposure to simulated solar light. Additionally, UV-Vis-NIR spectrophotometry tests have been carried out to measure the changes in the resultant light absorbance of the oxide films. Further characterization has been performed, including Field Emission Scanning Electron Microscopy (FE-SEM), X-Ray Diffraction (XRD), chemical composition profiles by Glow Discharge Optical Emission Spectrometry (GDOES), corrosion performance by potentiodynamic polarization tests, light interferometry, contact angle measurements and wetting properties. Finally, an exhaustive study of the mechanical properties of the thin films has been carried out.

BP-ThP23 Nanocomposite (Ti,Al,Cr,Si)N HPPMS Coatings for High Performance Cutting Tools, K. Bobzin, T. Brögelmann, N.C. Kruppe, M. Carlet, M. Thiex (thiex@iot.rwth-aachen.de), RWTH Aachen University, Germany

During the machining of high-speed steels, thermal and mechanical loads occur, which can influence the performance and cause damaging of the cutting tools. Due to their high hardness, wear resistance and toughness, hard coatings are used to improve productivity. The development of a complex coating (Ti,Al,Cr,Si)N for cutting tools and comprehensive analyses of them are the main objectives of the current research. The coating deposition was conducted in an industrial scale coating unit using a hybrid technology, consisting of direct current and high power pulse magnetron sputtering (dcMS/HPPMS). Cemented carbide was used as substrate material. To enhance the cutting performance, a nanocomposite architecture was developed, which consists of crystalline (Ti,Al,Cr)N phases in an amorphous Si₃N₄ matrix. The amorphous matrix aims to reduce the oxygen diffusion into grains and thus, to increase the oxidation resistance. Reduced grain sizes can further improve the mechanical properties such as the resistance of the coating against plastic deformation. The oxide reaction layer formed on the coating's surface upon exposure to the atmosphere has a significant influence on the tool performance. Thus, the design of a diffusion resistant coating system was proceeded by the synthesis of a thin oxynitride toplayer (Ti,Al,Cr,Si)ON, which is not sufficiently studied in the literature. The oxidation behavior of the coated samples under atmospheric conditions and the phase stability under inert gas atmosphere were comprehensively analyzed at high temperatures up to T = 1,300°C. Under both conditions, detailed analysis on diffusion between the workpiece material AISI M2 and the bilayer coatings were additionally performed. By reducing the pulse duration of the HPPMS cathodes, the non-metal to metal ratio was taken into account to study its influence on the reaction layer. Furthermore, the influence of cathode power and bias voltage on the coating properties was investigated. The microstructure was investigated by transmission electron microscopy (TEM). Sputter depth profiles determined using X-ray photoelectron spectroscopy (XPS) and X-ray diffraction (XRD) were applied after the heat treatments. Based on the results, the incorporation of oxygen tends to modify the nanocrystalline morphology of the nitride interlayer having grain sizes of d ≈ 10 nm to an amorphous microstructure, which is characteristic for the oxynitride top layer. The coated samples possess high oxidation resistance and diffusion resistivity. Moreover, the coating systems exhibit a significant phase stability.

BP-ThP24 Surface Hardening of AISI 1018 Steel: Microstructural Characterization of Boride and Nitride Layers, M. Ortiz-Domínguez, I. Morgado-Gonzalez (imorgadog@hotmail.com), Universidad Autónoma del Estado de Hidalgo, México; M. Elias-Espinosa, Tecnológico de Monterrey, México; O. Gómez-Vargas, J. Solís-Romero, Instituto Tecnológico de Tlalnepantla, México

There are several thermochemical treatments which alter the surface of a material changing its chemical composition and the microstructure thereof. Using thermochemical treatments, wear resistance can be improved, having a greater effect when the predominant phenomenon is the abrasive. In this study, the microstructure of the ε - Fe₃N and Fe₂B layers formed on an AISI 1018 steel surface have been investigated at different temperatures by the powder-pack process. Cubic commercial samples were cut from an AISI 1018 steel with composition: Mn, 0.60-0.90 wt.%; Carbon, 0.15-0.20 wt.% and P, 0.04 wt.%; and S, 0.05 wt.%. This grade of steel is used for forged motor shafts, hydraulic shafts and pump shafts, as well as machinery parts. The boro-nitriding treatment was carried out in two stages: boriding and then nitriding. Powder-pack boriding and powder-pack nitriding procedures were preferred in this study for its cost-effectiveness, and simplicity of the required equipment. The samples were embedded in a closed in a closed cylindrical case (AISI 316L stainless steel) having a boron powder mixture inside with an average particle size of 30 μm. The boriding agent contained

an active source of boron (B₄C), an inert filler (SiC), and an activator (KBF₄). The powder-pack boriding process was carried out in a conventional furnace under a pure argon atmosphere at 1123, 1173, 1223 and 1273 K for 2, 4, 6, and 8 h of exposure for each temperature. Once the boriding treatment was finished the container was removed from the furnace and slowly cooled to room temperature. In the second step, the pre-boriding iron samples were nitrided by the pack method in the powder mixture consisting of calcium cyanamide (CaCN₂, ~24% of N) and calcium silicate (CaSi, ~35 wt.% of the mixture) as an activator. The samples were directly immersed in the powder mixture in another stainless steel cylindrical case. The nitriding temperatures were 773, 795, 823, and 848 K for 2, 4, 6, and 8 h respectively, using the same furnace and conditions. The depth of the surface coatings and morphology were analysed by SEM and EDS (JEOL JSM-6360 LV at 20 kV). The distribution of alloying elements across the multicomponent coating was measured using the GDOES technique utilising a Horiba Jobin Yvon RF GD. X-Ray Diffraction (XRD) analyses of the layers were carried out with 2θ varying 20° to 90°, using CuK_α radiation and λ = 1.54 Å. Finally, the Daimler-Benz Rockwell-C indentation technique was employed to assess the cohesion of multicomponent layers on AISI 1018 steel. In addition, the pin-on-disc and wear scratch tests were carried out for investigating the wear behaviour of hardened AISI 1018 steel.

BP-ThP25 Microstructural Characterization of a New Powder-pack Carbo-boro-nitriding Process, M. Elias-Espinosa, Tecnológico de Monterrey, México; M. Ortiz-Domínguez, Universidad Autónoma del Estado de Hidalgo, México; J. Solís-Romero (jsolis@ittla.edu.mx), O. Gómez-Vargas, Instituto Tecnológico de Tlalnepantla, México; I. Morgado-Gonzalez, M. Flores-Rentería, Universidad Autónoma del Estado de Hidalgo, México

Corrosion, wear and fatigue involve chemical and/or mechanical interaction of the material component considered with loads imposed by the environment. Hence, materials performance and service life rely in many cases to a high degree on the properties of a material component in its surface region. In this study, the microstructure of a mixture of γ' - Fe₃N_{1-x}, ε-Fe₂N, Fe₂B and CaC₂ layers formed on an AISI 1018 steel surface have been investigated at different temperatures by the combination of two chemical agents. Cubic commercial samples were cut from an AISI 1018 steel with composition: Mn, 0.60-0.90 wt.%; Carbon, 0.15-0.20 wt.% and P, 0.04 wt.%; and S, 0.05 wt.%. This grade of steel is used for forged motor shafts, hydraulic shafts and pump shafts, as well as machinery parts. It would be used for such applications in a surface-hardened condition. Likewise, the substrate used in this work was selected to curb the effect of alloying elements in order to solely analyse the characteristic of a mixture layers and some of their mechanical effects. The carbo-boro-nitriding treatment was carried out in one stage process. The samples were embedded in a closed cylindrical case (AISI 316L stainless steel) the powder mixture having the composition of: CaCN₂ (calcium cyanamide) + CaSi (calcium silicate) + B₄C (boron carbide) + SiC (silicon carbide) + KBF₄ (potassium fluoroborate). The powder-pack carbo-boro-nitriding process was carried out in a conventional furnace under a pure argon atmosphere at 1123, 1173, 1223 and 1273 K for 2, 4, 6 and 8 h of exposure for each temperature using the same furnace and conditions. The depth of the surface coatings and morphology were analysed by SEM and EDS (JEOL JSM-6360 LV at 20 kV). X-Ray Diffraction (XRD) analyses of the layers were carried out with 2θ varying 20° to 90°, using CuK_α radiation and λ = 1.54 Å. Finally, the Daimler-Benz Rockwell-C indentation technique was employed to assess the cohesion of multicomponent layers on AISI AISI 1018 steel. In addition, the pin-on-disc and wear scratch tests were carried out for investigating the wear behaviour of borided AISI AISI 1018 steel.

BP-ThP26 Low Temperature Titanium Boron-Carbide Based Thin Film Coatings by Plasma Enhanced Chemical Vapor Deposition on Surface Microstructure Controlled WC-Co, T. Saito (tsaito@chemeng.osakafu-u.ac.jp), D. Kiyokawa, K. Fuji, N. Okamoto, Osaka Prefecture University, Japan; A. Kitajima, K. Higuchi, Osaka University, Japan

Chemical vapor deposited (CVD) or physical vapor deposited (PVD) hard material carting technique is widely used for molds and cutting tools, which plays an important role in a lot of manufacturing industry. For example, titanium carbide (TiC), titanium nitride (TiN) and titanium carbonitride (TiCN) is used in order to increase lifetime or to decrease friction coefficient of molds, tools etc. Recently, titanium boronitride-based hard coating films (TiBCN) have been attracted much attention.

The film prepared by thermal CVD typically carried out around 1000°C has good uniformity and mechanical properties, which restricts substrates having low melting points, and also causes deformation of substrates. Plasma enhanced chemical vapor deposition (PECVD) has some merits like

Thursday Afternoon Poster Sessions, May 23, 2019

lower deposition temperature (< 500°C) than thermal CVD, however, the films usually have low adhesion strength.

In this study, TiBCN coatings were formed by PECVD with $\text{TiCl}_4/\text{CH}_4/\text{BBr}_3/\text{N}_2$ reaction system. Growth rate, surface morphologies, crystallographic properties, and composition ratio/chemical states were evaluated by surface profiler, FE-SEM, XRD, and XPS. Several surface pretreatment methods were investigated to increase surface roughness to enhance adhesion strength, which include, CF_4 plasma etching and aqua regia ($3\text{HCl}:\text{HNO}_3$) etching.

Figure 1 shows XRD results of TiBC thin films from $\text{TiCl}_4/\text{BBr}_3/\text{CH}_4$ with different CH_4 concentration. Clear TiB_2 peaks were recognized and C(004) peak became recognized when the C/Ti ratio is over 3. Figure 2 shows XRD results of TiBN thin films from $\text{TiCl}_4/\text{BBr}_3/\text{N}_2$ with different N_2 concentration. $\text{TiN}(110)$ increased and $\text{TiB}_2(101)$ became weak with increasing N/Ti ratio. Both TiN and TiB_2 peaks exist, suggesting that deposited films contain Ti, B and N when N/Ti ratio = 3.5. Based on the results shown in figs. 1 and 2, the deposition properties of TiBCN thin films will be discussed.

BP-ThP27 Performance of the CrAlSiN and Hydrogen free DLC Combined Hard Coatings Deposited on Micro Tools Cutting Printed Circuit Board, D.Y. Wang, MingDao University, Taiwan; L.C. Hsu (lhsu@aurorasci.com), J. Hung, Aurora Scientific Corp., Canada; W.C. Chen, W.Y. Ho, MingDao University, Taiwan

Coating systems, including CrAlSiN coatings and various CrAlSiN +DLC combined coatings were deposited using a cathodic arc evaporation system. All the coatings were finished by using technology of modified pulsed current output to the arc evaporators. The DLC coatings were obtained with graphitic target and various mixture of $\text{N}_2 + \text{Ar}$ gases. All the coating systems with the effects of various conditions on the properties and performance in field of machining printed circuit boards were studied. The properties of the CrAlSiN coating was used as a reference coating. The various CrAlSiN+DLC coatings were evaluated using ball-on-disc wear tests. The wear behavior of the CrAlSiN+DLC combined coatings was affected by the various mixture of $\text{N}_2 + \text{Ar}$ gases. The hardness of the CrAlSiN+DLC combined coatings increase up to 40GPa as compared to CrAlSiN coating of 35GPa. Furthermore, the cutting performance of micro tools with the various coatings were evaluated by cutting the PCB board. Micro tool with CrAlSiN coatings increased the significant amount of cutting distance as compared to the blank tool. Meanwhile, the tools deposited with CrAlSiN+DLC combined coatings showed the maximum cutting distance of the PCB board which helped to improve tool wear and cutting performance.

Keywords: Pulsed current, cathodic arc evaporation, CrAlSiN, DLC

BP-ThP28 Study and Characterization of the Vanadium Carbide Interlayer Deposited by Laser Cladding over Carbon Steel for CVD Diamond Growth, D. Damm (djoilled.damm@hotmail.com), R.A. Pinheiro, J.S. Gomez, National Institute for Space Research (INPE), Brazil; A. Contin, Federal University of Goiás (UFG), Brazil; R.F.B. Correia, Federal University of São Paulo (UNIFESP), Brazil; R.M. Volu, Institute for Advanced Studies (IEAV), Brazil; V.J. Trava-Airoldi, National Institute for Space Research (INPE), Brazil; G. de Vasconcelos, Institute for Advanced Studies (IEAV), Brazil; D.M. Barquete, Santa Cruz State University (UESC), Brazil; E.J. Corat, National Institute for Space Research (INPE), Brazil

Vanadium carbide has been used in the industry to improve the steel properties. It was extensively studied and explored by Toyota a few decades ago. Vanadium has high hardness, as well as carbides forming ability, chemical compatibility with carbon steel and CVD diamond and an intermediate thermal expansion coefficient (TEC) between these materials. These characteristics make vanadium carbide attractive as an intermediate layer for CVD diamond applications. There are many techniques to obtain a vanadium carbide interface such as thermomdiffusion and sputtering. In this work, we will discuss the vanadium carbide deposition by laser cladding on carbon steel surface. The main problems in growing CVD diamond directly on steel surface are related crystallinity, purity and adhesion. The crystallinity issue is due to the fact that the gas phase carbon goes in to the steel substrate bulk causing its embrittlement and reducing diamond growth rate. The problem regarding purity is related to the transition metals present in the steel surface (such as iron and cobalt) that inhibit the sp^3 bond over the sp^2 bond, providing the appearance of graphite on CVD film that reduces the film quality. As for the Adhesion challenge, the TEC mismatch results in a high residual compressive tension in the diamond film, which causes delamination during cooling. Therefore, an intermediate layer is necessary to create a transition zone able to relieve the thermal residual stress and also to act as a diffusional barrier. The laser cladding was selected because of its rapid processing, excellent metals adhesion by melting, good

surface finish reducing roughness and capacity to preserve the original properties of the material substrate interacting only with the up layers of the material. In this study, we analyze vanadium carbide phase formation by varying systematically the following parameters: resolution (300 – 900 DPI); scanning speed (100 – 500 mm/s); and output power (40 – 125 W). For the substrate we used AISI D6, AISI O1 and AISI M2 steels. The HFCVD films were grown using the following parameters: 2 sscm of CH_4 ; 98scm of H_2 ; 2h deposition process time; 700°C and 5mm of work distance. The results of LCVC coating and HFCVD films characterizations were obtained by X-ray diffraction, scanning electron microscope field emission (SEM-FEG) and Raman spectroscopy.

BP-ThP29 Wafer Scale Growth of Ultra-smooth Nano-crystalline Diamond Thick Film for Nanostructure Fabrication, J.J. Li (jjli@iphy.ac.cn), S. Yan, Y. Sun, G. Gu, Institute of Physics CAS, China

Nano-crystalline Diamond (NCD) films exhibit excellent physical and chemical properties, such as low surface roughness, low friction factor, low resistivity, and high infrared transmittance. However, wafer scale NCD films either were too thin to fabricate deep nanostructure, or have very rough surface. This dilemma is caused by unmanageable nucleation density and fast growth rate of diamond grain. Both Nucleation density and grain size have complicated relations with temperature field, pressure, H_2/CH_4 ratio and the distance between filament and wafer. To obtain wafer scale thick high quality NCD film, a hot filament chemical vapor deposition (HFCVD) system was used in this work. Arrangement of filament and the variation of temperature field were studied. Finally,

20.54 μm thick NCD film was obtained on a 4 inch wafer. Grain size of this NCD film is below 30nm, and surface roughness (R_q) is about 25.0nm, which is almost the same with only 2~6 μm thickness NCD films^{1,2}. For NCD film, this R_q number can be considered as an ultra-smooth surface, and the film is very suitable for micro/nano-devices fabrication. Then, using e-beam lithography (EBL) and inductively coupled plasma (ICP) etching method, high-aspect-ratio nanopillar arrays were fabricated on this high quality NCD film. The as-fabricated diamond nanopillar arrays have a controllable aspect ratio and tunable period with good repeatability and uniformity, and the highest aspect ratio of above 10 with 200 nm in diameter can be obtained. Thus, wafer-scale thick film (>20 μm) with ultra-smooth surface and small grain size and smooth surface are important conditions for the fabrication of nanopillar arrays. Such development of CVD-diamond deposition and nanostructure fabrication process will likely impact the application of CVD-diamond film. Especially for nanostructure based nanoscale sensors, nanoelectronic devices, and NEMS/MEMS manufacturing.

Reference:

1. Subramanian, K., Kang, W. P., Davidson, J. L., Choi, B. K. & Howell, M. Single-mask multiple lateral nanodiamond field emission devices fabrication technique. *J. Vac. Sci. Technol. B* **24**, 953-957, doi:10.1116/1.2185653 (2006).
2. Zhang, W. J., Wu, Y. *et al.* Structuring nanodiamond cone arrays for improved field emission. *Appl. Phys. Lett.* **83**, 3365-3367, doi:10.1063/1.1619563 (2003).

BP-ThP30 Optimization for Adhesion Properties of c-BN Films Coated with HiPIMS, I. Efeoglu (iefeoglu@atauni.edu.tr), Y. Totik, A. Keleş, Ataturk University, Turkey

Friction and wear are one of the most important problems for machine components working in contact with each other. In order to reduce friction and wear, films with desired properties are usually coated on the surface of component. One of the most phenomena of these coatings is c-BN films. Although c-BN films have superior properties, their low adhesion property needs to be improved. Therefore, in this study, optimum adhesion properties were investigated for c-BN film coated with HiPIMS. Taguchi L9 orthogonal array test setup was used to determine the optimum adhesion. The scratch tester was conducted to define adhesion property. Three different parameters (N_2 content, duty cycle and B_4C target voltage) and three different levels for each parameter have been selected in Taguchi. The results obtained from the experiments were converted to signal/noise rate (S/N) and used to optimize the adhesion value of c-BN films. These values are in order of N_2 content, duty cycle and B_4C target voltage 3.5 sccm, 4.5% and 900V, respectively. Verification coating and test were performed for the optimum values obtained.

Thursday Afternoon Poster Sessions, May 23, 2019

BP-ThP31 Si-DLC Films Prepared by Magnetron Sputtering under Different Working Pressure, C.Q. Guo (guochaoqian@gdinnm.com), S.S. Lin, Q. Shi, C.B. Wei, L. Li, W. Wang, M.J. Dai, Guangdong Institute of New Materials, China

Si-DLC films were prepared on cemented carbides by high power impulse magnetron sputtering combined with middle-frequency magnetron sputtering. A graphite target providing carbon source was driven by high power impulse magnetron sputtering while silicon was originated from two SiC targets powered by middle-frequency magnetron sputtering. Mechanical and tribological properties of Si-DLC films deposited under different working pressure were studied. Scanning electron microscope, Raman spectroscopy and X-ray photoelectron spectroscopy were applied to investigate film microstructure and bonding states of elements. Nanoindentation, scratch tester and tribometer were used to test films' mechanical and tribological properties. The results showed that working pressure affects Si-DLC films' structure and properties greatly.

BP-ThP32 Multielement Rutile-structured AlCrNbTaTi-oxide Coatings Synthesised by Reactive Magnetron Sputtering, A. Kirnbauer (alexander.kirnbauer@tuwien.ac.at), C.M. Koller, TU Wien, Institute of Materials Science and Technology, Austria; *S. Kolozsvári,* Plansee Composite Materials GmbH, Germany; *P.H. Mayrhofer,* TU Wien, Institute of Materials Science and Technology, Austria

A new alloying concept gained tremendous attraction in the field of materials research within the last years—so-called high-entropy alloys. These are defined as alloys with a configurational entropy of at least 1.5 R (R being the universal gas constant). To reach this specific value, the alloy ought to consist of at least 5 elements in a compositional range between 10 and 30 at.%. This concept may also be transferred to ceramic-based materials, in which the respective constituents are binary ceramics borides, carbides, nitrides, or oxides—the latter of which are subject to the present study.

AlCrNbTaTi-oxide coatings were prepared by reactive magnetron sputtering in a lab-scaled deposition system using a single powder-metallurgically produced compound target (composition AlCrNbTaTi 20/20/20/20/20 at.%). Systematic variations of the O₂/Ar-ratio used for the deposition of these high-entropy films to determine basic structure-property-relationships.

The coatings crystallise partly in a single-phased rutile structure, are slightly enriched in Ta and exhibit nearly a MeO₂ stoichiometry with an oxygen content of ~64 at.%. The indentation hardness of ~20 GPa in the as-deposited state is for some of the coatings slightly higher than compared to binary or ternary oxides. The thermal stability was investigated by vacuum annealing treatments with subsequent XRD and indentation measurements to gain information about the evolution of the structure and the mechanical properties.

Our results clearly show that a high-entropy concept applied to oxide thin films using a single powder-metallurgically-produced compound target is a promising strategy in promoting single-phased and mechanically/thermally-stable AlCrNbTaTi oxide coatings.

BP-ThP33 Magnetron Sputtering of Tungsten-containing TiN_xO_y Multilayered Solar Selective Coatings, S.Y. Li (m9810217@gmail.com), Y.H. Shen, K.-S. Chang, J.-M. Ting, National Cheng Kung University, Taiwan

In this study, we prepared multilayer coatings of tungsten-containing TiN_xO_y having different compositions for use as solar selective absorbers. First, we sputtered a tungsten reflective layer on stainless steel substrate and W/TiN_xO_y layers having two different compositions as the solar absorption layers. Finally, we sputtered HfO₂ as the outermost reflective layer. We adjusted the N/O ratio and film thickness to optimize the performance of TiN_xO_y multilayered solar selective coatings. The coatings were characterized using before and after 600-800 C heat treatment. Effects of the materials characteristics on the optical properties were discussed.

BP-ThP34 Electron-configuration Stabilized (W,Al)B₂ Solid Solutions, R. Hahn, V. Moraes (vincent.moraes@tuwien.ac.at), P.H. Mayrhofer, Institute of Materials Science and Technology, TU Wien, Austria; *A. Limbeck,* Institute of Chemical Technologies and Analytics, TU Wien, Austria; *P. Polcik,* Plansee Composite Materials GmbH, Germany; *H. Euchner,* Helmholtz Institute for Electrochemical Energy Storage, Germany

Recent investigations on boride based materials, pointed out, that WB_{2,2} - in its metastable α -structure (AlB₂-prototype) - draws an interesting base system for the development of ternary material systems with exceptional performances in the field of hard and tough coatings.

In this study, we present a combined experimental and theoretical study of the ternary diboride system W_{1-x}Al_xB_{2-z}. Tungsten rich solid solutions of W_{1-x}Al_xB_{2-z} were prepared by physical vapor deposition and investigated for

structure, mechanical properties and thermal stability. All crystalline films show hardness values above 35 GPa, while the highest thermal stability was found for low Al contents. In this context, the impact of point defects on the stabilization of the AlB₂ structure type is discussed, using ab initio methods. Most notably, we are able to show that vacancies on the boron sublattice are detrimental for the formation of Al-rich W_{1-x}Al_xB_{2-z}, thus providing an explanation why only tungsten rich phases are crystalline.

Keywords: W_{1-x}Al_xB_{2-z}, sputtering, vacancies, density functional theory

BP-ThP35 Apparent Fracture Toughness of TiN Coatings with Alternating Stress Fields, A. Wagner (antonia.wagner@tuwien.ac.at), J. Buchinger, TU Wien, Institute of Materials Science and Technology, Austria; *M. Todt,* TU Wien, Institute of Lightweight Design and Structural Biomechanics, Austria; *D. Holec,* Montanuniversität Leoben, Austria; *P.H. Mayrhofer, M. Bartosik,* TU Wien, Institute of Materials Science and Technology, Austria

In general, ceramic thin films show a low fracture toughness and tend to catastrophic brittle failure. One of the most important approaches to increase the crack growth resistance of ceramic components is to introduce compressive residual stresses. When considering coatings manufactured by physical vapor deposition the intrinsic residual stresses can be modified by applying a negative bias voltage to the substrate and hence altering the degree of ion bombardment. Depositing a chemically homogeneous material with a sequential variation of the bias voltage leads to a multilayer coating in the sense of residual stresses, whereas the material properties are kept more or less constant over the film thickness. This approach allows studying the effect of residual stresses on the fracture behavior of multilayers decoupled from other mechanisms like elastic mismatch.

Herein, TiN coatings are deposited on Si (100) substrates by reactive magnetron sputtering and different multilayer architectures with respect to the residual stress state are realized by changing between a bias voltage of -30V and -60V. The curvature of the substrate is measured and an analytical model based on Euler-Bernoulli-beam theory is applied to investigate the stress distribution within the coating. Fracture experiments are performed on micro cantilevers fabricated by focused ion beam milling which eventually are compared with fracture toughness estimations based on the calculated stress distributions.

BP-ThP36 Synthesis and Structural Characterization of Nanostructured CN_{0.1} Films Deposited by RF Magnetron Sputtering at Different Bias Voltages, A. Lousa (alousa@ub.edu), D. Cano, C. Villabos, J. Esteve, University of Barcelona, Spain

Nitrogen content of about 10% can be considered as the border between nitrogen doped amorphous carbon (DLC:N) and fullerene-like carbon nitride (CN_x) thin films. In this sense, this material can be a good alternative to reduce the high values of stress usually found in pure DLC coatings while keeping most of its good mechanical, tribological and biocompatible properties.

The present investigation is centered on the deposition of relatively thick films (0.5 mm) of CN_{0.1} with N concentration of around 10% by RF magnetron sputtering. Samples were deposited at negative bias voltage between -20 and -150 V in order to study the effect of different intensities of ion bombardment during the film growth on the film structure. Monocrystalline Silicon wafers were used as substrates for all the deposited samples, and CoCrMo substrates were occasionally used in order to test the applicability on biomedical components. These films were characterized by X-ray photoelectron spectroscopy, (XPS) Raman spectroscopy, FTIR scanning and transmission electron microscopy (HRTEM). Hardness an elastic modulus were measured by the nanoindentation technique.

The deposition rate was 0,5 mm/h. Films showed a columnar structure with atomic composition of 10% N and 90 % C, with a relative composition of sp³ C-C bonds which decreased slightly as the negative bias voltage was increased. The Raman spectra were deconvoluted in four Gaussians showing more complex contributions than the two conventional G and D. The FTIR results corresponds to electrical conductive samples, with an absorption band corresponding to four different vibration modes of the C-N bonds. The HRTEM diffraction patterns of selected area reveal an essentially amorphous condition. However, as the bias is smaller, some ordering is observed oriented parallel to the substrate. The images of bright field show a homogeneous aspect with a coherent interface and a uniform thickness, with a presence of a distribution of nanometric clusters in an amorphous matrix, denser and with smaller cluster size as the negative bias voltage decreases. Hardness values are in the range of 21–24 GPa, and the modulus of elasticity are in the range of 140–180 GPa with a slight tendency to increase as the negative bias voltage is increased.

Thursday Afternoon Poster Sessions, May 23, 2019

BP-ThP37 An X-ray Diffraction Study on CrAlN and CrAlSiN PVD Coatings, J. Latarius (jan.latarius@tu-dortmund.de), D. Stangier, C. Albers, K. Berger, M. Elbers, A. Sparenberg, G. Surmeier, M. Paulus, C. Sternemann, W. Tillmann, M. Tolan, TU Dortmund University, Germany

As the demand for highly resistant tools for milling and drilling applications is rising, this translates to more sophisticated coatings, to cope with special requirements as high temperature or corrosion resistance. Very promising candidates are coatings produced by physical vapor deposition (PVD).

Here, CrAlN based PVD coatings have proven to be quite capable to match the claims and CrAlSiN as a possible successor might feature improvement in many critical aspects like hardness, wear resistance, thermal and mechanical stability. These macroscopic properties are reflected in microscopic structural properties and can therefore be studied through means of X-ray diffraction (XRD) by determination of phase composition, residual stresses, micro strains and crystallite size, etcetera.

We present an XRD study on different CrAlN and CrAlSiN PVD coatings. These coatings were produced with varied bias potentials and tempered under air at temperatures between room temperature and 1000° C. The coatings were investigated at beamline BL9 at the synchrotron light source DELTA (Dortmund, Germany). The phase composition, micro strain and crystallite size were determined. The CrAlSiN coatings show a much higher oxidation temperature indicating great benefits of doping with silicon.

BP-ThP39 Wear Resistance of TiAlSiN with Nanoparticles of Ag Coating Deposited via Co-sputtering Method, A.D. Caïta Tapia (adcaitat@unal.edu.co), S.D. Rodriguez Arevalo, E.N. Borja Goyeneche, J.J. Olaya Florez, B.J. Gamboa Mendoza, Universidad Nacional de Colombia, Colombia

It was evaluated the tribological response of TiAlSiN coating doped with nanoparticles of Ag varying the wt% of Ag on different samples. The chemical composition analysis was performed using Energy-dispersive X-ray spectroscopy (EDS) and structural analysis was performed by X-ray diffraction (XRD). The abrasive wear resistance was evaluated by a three-body system on the ASTM standard G65 and the friction coefficient was determined by the ball-on disk test. The morphology of the wear track was characterized by 3D optic microscopy. The silver content changes the wear mechanism inducing plastic deformations, so it is reported the optimal Ag content to take advantage of corrosion properties avoiding a tribological underperformance.

BP-ThP41 Influence of Oxygen Addition on Microstructure and Properties of TiAlN, D.M. Holzapfel (holzapfel@mch.rwth-aachen.de), M. Hans, RWTH Aachen University, Germany; A.O. Eriksson, M. Arndt, Oerlikon Balzers, Oerlikon Surface Solutions AG, Liechtenstein; D. Primetzhofer, Uppsala University, Sweden; J.M. Schneider, RWTH Aachen University, Germany
Industrial cutting and forming processes have high demands regarding chemical and mechanical properties of coatings, to serve as effective wear protection. Coatings in the TiAlN-system are widely used in industry. In this study TiAlN and (TiAl)_x(O,N_{1-x})_{1-x} thin films were deposited by cathodic arc evaporation onto cemented carbide substrates. Structure and composition were investigated by X-ray diffraction, scanning transmission electron microscopy, elastic recoil detection analysis and atom probe tomography. The effect on microstructure and properties as influenced by O were characterized.

BP-ThP42 An Investigation on Synthesis of Novel Oxide-Based Superhard Cr-Zr-O Coatings, M. Mohammadtaheri (msctaheri@gmail.com), Q. Yang, Y. Li, J. Corona-Gomez, University of Saskatchewan, Canada

Synthesis of ternary Cr-Zr-O coatings was performed on silicon wafers and glass substrates by Reactive dual radio-frequency (RF) magnetron sputtering technique. The zirconium concentration of coatings changed in a range of 0-10 at. % by tuning the RF power of Zr target. The correlation between the chemical composition, crystal structure, phase composition, and hardness of coatings was investigated by Energy Dispersive Spectroscopy (EDS), X-ray diffraction (XRD), Raman spectroscopy, and Nanoindentation, respectively. Annealing procedures were conducted for 3 hours at 300, 700, 800, and 1000 °C to evaluate the structural stability of the Cr-Zr-O coatings. The results indicated that incorporation of zirconium increases the crystallization temperature of coatings and the excess of zirconium transferred the coatings to a completely amorphous structure. The superhardness (Hardness ≥ 40 GPa) in Cr-Zr-O system was achieved in a specific chemical composition where the Zr content was about 2 at. %. According to the XRD results obtained after annealing treatments, it was confirmed that the zirconium was in a super-saturated solid solution state in the chromium oxide crystal structure where the superhardness was achieved. However,

the thermal stability of Cr-Zr-O coatings was higher than pure chromium oxide coatings, their structure was not stable at a temperature higher than 700 °C and their high hardness dropped to 30 GPa after 3 hours annealing at 800 °C. A heat treatment at 1000 °C is required to completely segregate Zr from the chromium oxide crystal structure to create a ZrO₂-Cr₂O₃ composite microstructure in the superhard coatings.

Fundamentals and Technology of Multifunctional Materials and Devices

Room Grand Hall - Session CP-ThP

Fundamentals and Technology of Multifunctional Materials and Devices (Symposium C) Poster Session

CP-ThP1 Comparison of SiC_xN_y Barriers using Different Precursors Deposited on Porous Low-Dielectric-constant SiCOH Dielectric Films, Y.L. Cheng, Y.L. Lin, C.Y. Lee (ck7766@gmail.com), National Chi-Nan University, Taiwan

In this study, two different SiC_xN_y films using different deposition precursors were deposited onto the porous SiOCH low-*k* films. Their impacts on the electrical characteristics and reliability of a SiCOH/SiC_xN_y dielectric stack were compared. A lower plasma damage on the SiOCH low-*k* film was made as SiC_xN_y film was deposited onto the SiOCH low-*k* film using single-source precursor compared to that using the conventional multi-source precursors. This results in a lower capacitance of SiCOH/SiC_xN_y dielectric stack. Moreover, better TDDB reliability and comparable Cu barrier performance were detected. As a result, the SiC_xN_y layer deposited using a single precursor is a promising method to serve as a capping barrier for porous low-*k* dielectrics.

CP-ThP2 Stretchable Ultrasonic Transducer Arrays for Three-Dimensional Imaging on Complex Surfaces, H. Hu (h4hu@eng.ucsd.edu), X. Zhu, C. Wang, L. Zhang, S. Xu, University of California, San Diego, USA

Ultrasonic imaging has been implemented as a powerful tool for noninvasive subsurface inspections of both structural and biological media. Current ultrasound probes are rigid and bulky and cannot readily image through nonplanar three-dimensional (3D) surfaces. However, imaging through these complicated surfaces is vital because stress concentrations at geometrical discontinuities render these surfaces highly prone to defects. This study reports a stretchable ultrasound probe that can conform to and detect nonplanar complex surfaces. The probe consists of a 10 × 10 array of piezoelectric transducers that exploit an "island-bridge" layout with multilayer electrodes, encapsulated by thin and compliant silicone elastomers. The stretchable probe shows excellent electromechanical coupling, minimal cross-talk, and more than 50% stretchability. Its performance is demonstrated by reconstructing defects in 3D space with high spatial resolution through flat, concave, and convex surfaces. The results hold great implications for applications of ultrasound that require imaging through complex surfaces.

CP-ThP4 Electrospun TiO₂ Nanofiber Electrodes for High Performance Supercapacitor, C.K. Kunchu, S.P. Reddy (psreddy4@gmail.com), Sri Venkateswara University, India

Nanofibers are one dimensional (1-D) nanostructured materials having high surface-to-volume ratio which provides improved ion diffusion and high mechanical strength to prevent volume expansion during electrochemical process and enhance the cycle stability. In the present study, TiO₂ nanofibers (TNF) were successfully synthesized on an aluminium collector with a polymer concentration of 9 wt % and a needle diameter of 500 μm followed by subsequent annealing at a temperature of 500 °C respectively by cost-effective electrospinning technique. The XRD spectrum of electrospun TNF exhibited predominant (101) orientation corresponding to anatase TiO₂ with I₄₁/amd symmetry. The estimated average crystallite size is 18 nm. The strongest Raman vibrational mode at 143 Cm⁻¹ confirms the phase purity of TNF. The surface morphological features depicts highly interconnected network fibers with a variation in the fiber diameter and the estimated average diameter is ~ 150±20 nm. Homogenously distributed very smooth surface ultra-long nanofibers are observed from TEM analysis. The newly fabricated TNF electrode delivered a specific capacitance of 533 F g⁻¹ and retained 91% capacity even after 4000 cycles. The large capacitance, high columbic efficiency and good structural stability demonstrates that TNF should open up new opportunities for next-generation high performance supercapacitors.

Thursday Afternoon Poster Sessions, May 23, 2019

CP-ThP6 Fabrication and Characterization of Ni-coated Ag Nanowire Electrodes with Bubble-like Random Meshes, J.S. Park (pdk927@naver.com), R. Yoo, T.G. Park, J.S. Park, Hanyang University, Republic of Korea

Recently, as the applications of flexible electronic devices have been expanded, transparent electrode materials are required to be flexible and stretchable in addition to having excellent electrical and optical properties. Examples of such materials include carbon nanotubes, metal meshes, metal nanowires, and graphene. Among them, metal nanowires along with metal meshes, are evaluated to be advantageous in terms of commercialization because they have a low electrical sheet resistance and a high visible light transmittance. In particular, compared to other materials, metal nanowires are the most advantageous in terms of flexibility and have the advantage of being able to fabricate electrodes using simple and relatively inexpensive solution-based methods. However, metal nanowires have a relatively high reflectance, high haze, and high contact resistance between their wires. They also have oxidation problems when exposed to the atmosphere. As an example of inhibiting the oxidation of metal nanowires, studies have been introduced to coat the nanowires with oxidation resistant materials. Also, in the case of the widely adopted grid-type electrode, there is another disadvantage in that it is difficult to secure high visibility due to the diffraction of light or the moiré phenomenon due to a regularly repeated lattice structure. To solve this problem, studies on the fabrication of random-type electrodes using the irregular patterns of crack, leaf, spider web, and bubble have been reported.

In this study, embedded-type nickel (Ni)-coated silver nanowire (AgNW) transparent electrodes with random-mesh patterns were fabricated via solution processes. The major manufacturing processes of the Ni-coated AgNW random mesh electrodes are summarized as follows. The AgNW bubble solution was prepared by mixing a surfactant with the AgNW solution and agitating it. The surface modification of polyethylene terephthalate (PET) substrate was performed using corona plasma. Using a spin-coating method, the AgNW bubble solution was deposited on the PET substrate with various surface energies. Then, the bubble solution was evaporated through the baking process to form a bubble-like random pattern. This was transferred to polydimethylsiloxane (PDMS) and coated with Ni by electroplating. The line width and line-to-line spacing of the fabricated electrodes were estimated according to the number of corona treatments and baking temperature on the PET substrate. For the electrodes fabricated, we have measured and characterized their morphology, transmittance and reflectance at visible light region, electrical sheet resistance, flexibility, stretchability, and oxidation-stability.

CP-ThP7 Characteristics of Silver Nanowire Transparent Electrodes Optimized for High Stretchability, R. Yoo (wnltor1777@naver.com), J.S. Park, T.G. Park, J.S. Park, Hanyang University, Republic of Korea

With the development of electronic communication devices, transparent electrodes are required not only to have high light transmittance and low electric sheet resistance, but also excellent flexibility and stretchable properties. However, indium tin oxide (ITO), which has been widely used, is fragile due to structural problems and requires a high process temperature in order to maintain crystallinity. So, there is a serious problem when ITO is applied to next generation electronic devices requiring stretchable characteristics. Therefore, researches on novel transparent electrode materials that replace ITO, such as carbon nanotubes (CNT), graphene, metal meshes, metal-nanowires, and conducting polymers, are actively being carried out. Among these materials, metal nanowires are expected to be commercialized first because they are evaluated to have advantages in terms of optical and electrical properties as well as stretchable characteristics. In order to fabricate a transparent electrode with excellent stretchability, a suitable substrate material may be selected and the electrode may be embedded in the substrate or the shape of the electrode may be varied to minimize deformation of the electrode during stretchable operations. However, systematic researches regarding the above issue have not been studied yet, and there have been few reports in the literature on the flexible and stretchable characteristics of the electrode structures especially in metal nanowires.

In this paper, we fabricated silver nanowire (AgNW) meshes with various geometric shapes using microcontact printing, which is one of the soft lithography methods, and systematically analyzed their flexible and stretchable characteristics. First, 3D simulation was performed on various types of mesh patterns, and a mesh structure with the best stretchability was selected. According to the selected mesh structure, photoresist (PR) coated on a glass substrate was patterned by using photo-lithography method. Polydimethylsiloxane (PDMS), which is one of the stretchable

substrate materials, was coated on the patterned PR, then hardened and peeled off to prepare a PDMS mold. Finally, the PDMS mold was coated with AgNW. The surface morphology, sheet resistance, and visible light transmittance of the electrodes fabricated were measured via a FESEM (field-emission scanning electron microscope), a non-contact sheet-resistance measurement system, and a spectrophotometer. In addition, bending, twist, rolling, and stretching tests were carried out on the electrodes fabricated.

CP-ThP9 Microstructure and Electrochemical Properties of rf Sputtered V₂O₅ Thin Films, M. Dhananjaya (msdhananjaya51@gmail.com), Sri Venkateswara University, India

Vanadium pentoxide with orthorhombic layered structure is a multifunctional electrode material for both Li-ion microbatteries as well as supercapacitors. V₂O₅ thin films have been prepared using rf magnetron sputtering by varying the substrate temperature from 200 to 450 °C and maintained partial pressure ratio of Oxygen to Argon at 1:8. The predominant (001) X-ray diffraction peak corresponds to the orthorhombic V₂O₅ structure. The scanning electron microscopy (SEM) images confirm nanorods like structure and the dimensions of nanorods increased with increasing the substrate temperature. The thin films prepared at substrate temperature of 300 °C exhibited pseudo capacitive behavior because of low crystallite size and demonstrated a specific capacitance of 960 mF cm⁻² at current density of 1 mA cm⁻². Whereas the films prepared at substrate temperature of 400 °C exhibited sharp oxidation and reduction peaks due to high crystallite size, which signifies the cathodic behavior with discharge capacity of 62.5 μAh cm⁻² μm⁻¹ at current rate of 50 μA.

Keywords: Substrate temperature, V₂O₅ thin films, microstructure, electrochemical properties.

CP-ThP12 Thin Film Deposition of Lithium and its Alloys for High Energy Density Battery, S. Sardar (saydulsardar@nicenergy.com), J. Koh, N. Hart, J. Xu, NICE America Research Inc; D. Kang, J. Lemmon, National Institute of Clean-and-Low-Carbon Energy

The biggest technical challenge of lithium ion battery (LIB) for electric vehicles (EVs) is the relatively low energy density compared to the internal combustion engine (ICE). The current state-of-the-art EVs can drive approximately 200 miles upon single charge which is still less than the mileage of ICE vehicles. The battery community has been working hard to increase the energy density of LIB from its current 150-200 Wh/g to over 400 Wh/g. The key enabling technology for high energy density LIB is to use pure lithium or its alloys as the anode material. To maximize the energy density and efficiency, the desired thickness of lithium or alloy electrode is 30 microns or less. Due to the extremely high reactivity of lithium and its physical properties (low melting point and soft nature), the processing of thin film lithium electrode has not been established in the LIB industry. Physical vapor deposition of lithium film can be a reliable tool. We built an in-house system that allows for deposition of lithium thin film and assembly of battery cells without exposing them to air. This presentation demonstrates high quality thin film lithium or alloy electrodes deposited by vapor-phase processing for high energy density battery applications.

CP-ThP13 Study of Stress-electrical Properties of ITO Film Deposited on Stretchable Substrate, P.O. Renault (pierre.olivier.renault@univ-poitiers.fr), Université de Poitiers, France; C. Grossias, P. Goudeau, P. Godard, F. Paumier, S. Hurand, University of Poitiers, France; D. Thiaudière, SOLEIL Synchrotron, France; P. Guerin, University of Poitiers, France

Indium Tin Oxide (ITO) is one of the most widely used material with the unusual property of being transparent and conductor. The fabrication and characterization of these materials, called transparent conductive oxides (TCO), is a very active field of research motivated by their potential applications in optical and optoelectronic devices. ITO is almost always used as a thin film in a more or less complex stacking deposited on substrates. The mechano-electro-optical properties of transparent conductive oxide thin films deposited onto substrates depend on many elaboration parameters as well as their piezoresistive response.

In the present work, 400 nm thick ITO films have been prepared by ion beam sputtering controlling the oxygen partial pressure. Each thin film has been deposited on a polyimide stretchable substrate. The deformations are applied thanks to a biaxial tensile tester in situ during x-ray diffraction measurements at the french synchrotron SOLEIL. Thus, x-ray stress or x-ray strain (measured by x-ray diffraction technique), true strain (measured by digital image correlation technique) and electrical resistivity (Van der Pauw method) measurements are performed during in situ biaxial straining. The first results obtained on x-ray stress- true strain – electrical conductivity

Thursday Afternoon Poster Sessions, May 23, 2019

relation are reported. A negative gauge factor is observed for all thin films. The influence of oxygen residual pressure does not seem to have a large effect on gauge factor contrary to the mechanical behavior.

CP-ThP17 Effect of Magnetron Sputtering Metal/PET Process on Performance of Flexible Capacitors, J Wang, J. Lin (linlin681020@126.com), Harbin University of Commerce, China

Herein, we report a rational synthesis of flower like CoMoO₄ nanostructures with remarkable supercapacitors performance on PET conductive film. PET as conductive substrates with magnetron sputtering metal in composite electrodes is fabricated highly flexible energy storage devices with high mechanical strength and excellent electrical stability. The influence of the uniaxial tensile strain on the electrical resistance of these films was evaluated in situ for the first time during tensile elongation. In addition, the role of the thickness on the mechanical behavior of the films was also evaluated. The preliminary results reveal that the increase in electrical resistance is related to the number of cracks, as well as the crack width, which also depends on the film thickness. The flexibility of the electrode influence on the electrochemical performance were explored by compared the GCD curves and cyclic performance of the flexible hybrid electrode under flat and bending for electrochemical test at the same current density of 3 A g⁻¹. The results indicated slight attenuation of charge-discharge interval of the bent electrode compared to its flat state. The corresponding GCD curves of the first tenth cycles for the three forms without obvious changing. And the specific capacitance is a slight decreased after bending. The Coulomb efficiency for the flat one is 99.3 % and the other two bent forms are still keeping 98.9 % and 98.5 %, respectively. The results confirmed the electrode is mechanically robust. And the PET film as conductive substrate will be a good candidate for applications in flexible devices.

Key words: magnetron sputtering; PET film; flexible electrodes; supercapacitors

CP-ThP18 Dual Box Model based *In situ* Ellipsometry Growth Characterization: Oxygen Plasma Enhanced Atomic Layer Deposition of Metal Oxide Ultra-thin Films, U. Kilic (ufuk.kilic@huskers.unl.edu), University of Nebraska-Lincoln, USA; A. Mock, Linköping University, Sweden; D. Sekora, N. Ianno, E. Schubert, M. Schubert, University of Nebraska Lincoln, USA

Atomic Layer Deposition (ALD) of conformal ultra-thin films has been shown to have potential for applications in microelectronics, photovoltaics, photoluminescence and fuel cells [1]. The integration of spectroscopic ellipsometry (SE), an optical, contactless, and non-invasive technique, into the ALD instrumentation has been a powerful and widely-used process monitoring method[2] which paves the way to unravel the surface roughness and thickness evolution during the ALD process.

In this study, we successfully optimized the oxygen plasma enhanced ALD recipes for two different metal-oxides: WO₃ and TiO₂, in which employs (tBuN)₂(Me₂N)₂W and Ti(OC₃H₇)₄ organometallic precursors, respectively. Multi-sample analysis method is employed in order to obtain both thickness and optical constants from SE data analysis[3]. Thus, three films are deposited by using 75, 100, and 150 ALD cycles under the same conditions and *ex-situ* SE data is collected in the spectral range from 0.7-6.5 eV.

The as-grown WO₃ and TiO₂ dielectric functions are determined along with the respective film thicknesses. With this information, the *in-situ* SE data is retroactively analyzed to attain inherent layer-by-layer deposition parameters. We employed the dual-box model in order to obtain sub-angstrom scale in-cycle resolution time evolution of thin film thickness and effective surface roughness layer thickness parameters during the growth process. Our model analysis permits determination of growth rate and identification of cyclic surface modifications during exposure to individual cycle steps. Further implementation of this method allows for precise control and real-time optimization of deposition parameters ultimately providing us with the ability to develop ALD recipes *in-situ*.

References:

- [1]: George, Steven M., Chemical reviews 110.1 (2009): 111-131.
- [2]: Leick, N., et al. Journal of Physics D: Applied Physics 49.11 (2016): 115504.
- [3]: Kilic, U., et al., Journal of Applied Physics:1805.04171 (2018).

CP-ThP19 Controlled Release of Encapsulated Agents Deposited on Plasma Electrolytic Oxidation (PEO) Coatings for Corrosion Resistance and Biomedical Applications, Y. Guo (yue.guo-4@postgrad.manchester.ac.uk), B. Mingo, A. Matthews, A. Yerokhin, The University of Manchester, UK

A number of surface treatment methods has been developed in order to increase the protective and functional properties of magnesium alloys. Plasma Electrolytic Oxidation (PEO) is an environmentally friendly treatment resulting in ceramic coatings with high hardness, excellent adhesion to the substrate and good wear and corrosion resistance. However, the passive corrosion protection provided by PEO coatings can be undermined if the coating is worn off or damaged.

Therefore, the aim of this work is to investigate a possibility functionalisation of PEO coating surfaces in order to achieve: i) sustained release of corrosion inhibitors encapsulated by halloysite nanotubes (HNT) for non – biological applications of magnesium alloys, in order to achieve self-healing effect; and ii) sustained release of encapsulated drugs for biological applications of degradable magnesium alloys, in order to develop the next generation of ‘smart’ biomedical implants materials.

Halloysite nanotubes (HNT) represent a type of bio-compatible naturally occurring clay with the walls consisting of two layered aluminosilicates. The hollow tubular structure of HNT allows different agents to be loaded by vacuum-induced capillarity. The release of the agents can be triggered by e.g. changes in the pH of environment, on mechanical impact or simply by osmotic pressure. The corrosion inhibitors in this study (vanadate, molybdate and 8-hydroxyquinoline) consist both negatively charged particles and electrically neutral molecules. For biological applications, the drugs are mostly electrically neutral molecules, and in this study is penicillin.

The main challenge of this work is ensure the adequateness of the deposited agents. The incorporation of encapsulated agents onto PEO coatings can be achieved by two approaches: hybrid and sequential. The hybrid approach is to incorporate the particles as the same time as the coating synthesis whereas the sequential approach is by post-treatment. In this work, post-treatment will be discussed. There are two post-treatment methods: electrophoretic deposition (EPD) and immersion. Both of the post-treatment methods require aqueous suspension of loaded HNT. So, the release kinetics of the loaded agents is of great importance since there are possibility of release during the deposition process. Ultraviolet-visible (UV-VIS) spectroscopy is employed for the release kinetics.

Successfully encapsulated and deposited corrosion inhibitors significantly improves the corrosion resistance of magnesium alloys. And for drugs, observation of zone of inhibition (ZOI) on Gram-positive bacteria *Staphylococcus Aureus* indicates the success of drug loading.

CP-ThP20 Ag@Co₃O₄ Core-shell Nanocrystals for Oxygen Reduction Reaction via Solution Plasma Process, H.K. Kim (ndkim2@naver.com), Korea Aerospace University, Republic of Korea; S.M. Kim, Korea Institute of Industrial Technology, Republic of Korea; J.W. Kim, University of Incheon, Republic of Korea; S.Y. Lee, Korea Aerospace University, Republic of Korea

Ag is considered to be among the most promising electrocatalysts for the oxygen reduction reaction (ORR) in alkaline media for fuel cell applications since the cost is roughly 100 times cheaper than Pt and more stable than Pt in base. However, their synthetic route has been still issued because the synthesis of Ag nanocrystals is mostly performed by a chemical method. Typically, such a synthesis uses precursors (usually a salt of the desired metals), reducing agents, and capping agents that may be hard to completely remove from the final products, which can affect some of the physical and chemical properties of the crystals. Therefore, the synthesis method to control size, shape and surface uniformity without capping agent is highly desirable and technologically important.

Recently, a method for the synthesis of the Ag nanocrystals by means of plasma discharge in liquid phase is introduced, in which plasma is generated at room temperature and under atmospheric pressure. Plasma discharge in liquid phase is an attractive method for the synthesis of nanoparticles because it is faster (microseconds), simpler (one-step method) and more cost-effective (only requiring an ion source) than traditional colloid methods. The novelty of this method consists in the fact that the size, shape, and crystalline structure can be controlled by discharge conditions.

In this work, we report on the preparation of the Ag@Co₃O₄ core-shell nanocrystals using bi-polar pulsed plasma discharge in water for catalytic oxygen reduction in alkaline solutions. Microstructural and compositional analysis using HRTEM equipped with high resolution EDX elemental mapping verified that the reactive oxygen species generated from plasma-assisted decomposition of water molecules played important role in controlling the phase structure of the nanoparticles. From cyclic voltammetry results, it was

Thursday Afternoon Poster Sessions, May 23, 2019

found that the electrochemically active surface area of Ag@Co₃O₄ core-shell nanocrystals was much higher than pure Ag. The electrochemical measurements for oxygen reduction reaction revealed that the electrocatalytic activity of the Ag@Co₃O₄ core-shell nanocrystals were higher than that of pure Ag and Co₃O₄ nanoparticles.

Acknowledgement

This study was supported by the National Research Foundation of Korea (NRF) funded by the Korean Government (No. 2016R1D1A1A09918072).

CP-ThP21 Influence of Substrate Temperature on the Growth of Molybdenum Trioxide Thin Films, *M.V. Kalapala (kvmvsu@gmail.com)*, VFSTR University, India

Molybdenum oxide is one of the most important inorganic materials which exhibit several phases such as MoO₃, MoO₂, Mo₄O₁₁, Mo₅O₁₄, etc.. Out of this molybdenum trioxide (MoO₃) can crystallize in various phases such as Orthorhombic, Monoclinic etc., which lead it to be useful for potential applications in chemical, electrical and electrochemical industry. In the present work MoO₃ thin films were prepared by pulsed laser deposition techniques at various substrate temperatures from room temperature to 400°C. The films were deposited on to glass and FTO coated substrates at a base pressure of 10⁻⁵mbar. The crystal structure morphology and elemental analysis were recorded by XRD, SEM, EDS and AFM. The substrate temperature strongly influences the structure and surface topography. The films prepared at base pressures are found to be oxygen deficient and after annealing the films were found to be transparent. The presence of oxygen atmosphere at the time of deposition makes the films to show better properties.

CP-ThP22 Evaluation of the Influence of Pre-carburisation on the In-situ Performance of Chromized 304 Stainless Steel Bipolar Plate, *A. Oladoye (atinuke.oladoye2@mail.dcu.ie)*, University of Lagos, Nigeria; *J. Carton, J. Stokes*, Dublin City University, Ireland; *A. Olabi*, University of the West of Scotland, UK

This paper reports preliminary attempts at improving the in-situ performance of chromized 304 stainless steel (304SS) bipolar plates via the introduction of a pre-carburisation step prior to chromising. 304 stainless steel bipolar plates with parallel flow field design were pre-carburised at 900°C for 3 hours and subsequently chromised at 1040°C for 3 hours. The surface modified plates were tested in a 5cm² active area single proton exchange membrane fuel cell at room temperature for performance and durability. Results obtained was compared to that of non-carburised chromised 304SS bipolar plate tested under identical conditions. It was found that the single fuel cell with pre-carburised chromised bipolar plates attained a peak power density of 18.20 mW/cm², which was a double-fold increase in that of the single fuel cell with non carburised chromised 304SS bipolar plates. The ten-hour durability test, however, indicated the need for further research efforts to enhance the stability of the pre-carburised-chromised stainless steel bipolar plates.

CP-ThP23 Piezo- and Thermo-resistive Thin Films Integrated into a Polymer Injection Mold to Control Dynamically the Pressure and Temperature of the Injection Process, *F. Vaz (fvaz@fisica.uminho.pt)*, *J. Ferreira, M. Barbosa*, University of Minho, Portugal; *J. Laranjeira*, Moldit, Portugal

The present work reports on the development of metallic piezoresistive thin films, aiming to investigate an innovative solution to control dynamically the temperature of the injection molding process of polymeric parts using technologies of thin films. The general idea was to analyse the signal response of the Ti_{1-x}Cu_x and ZnO/Ag based transducers exploring the possibility to use this thin film system in force, deformation and temperature sensor devices. Ti_{1-x}Cu_x and ZnO/Ag thin films were produced by the Glancing Angle Deposition technique (GLAD).

The results reveal that the zigzag microstructure has an evident influence on the overall response of the films as well as the influence of the Cu or Ag doping level. The values of temperature coefficient of resistance reach 8.73×10⁻³ °C⁻¹ for pure copper films and 4.38 ×10⁻³ °C⁻¹ for films with an intermedium composition. The values of the gauge factor show that a longer distance between Ag particles, which varies from 0.1 to 120 nm, leads to enhanced GF, which ranges from 8 ± 1 to 120 ± 3, respectively.

In order to demonstrated the sensing capabilities of the system, a proof-of-concept experiment was carried out by integrated the thin films of Ti_{1-x}Cu_x and ZnO/Ag with the best response in an injection steel mold and connected to a data acquisition system based on a homemade dedicated read circuit hardware and LabVIEW software, connected to a radio-frequency access point, plugged to a universal serial bus (USB) port. The most challenging part

in this work is to quantify the results obtained from this experiment which has not been done in literature yet.

CP-ThP24 Assembled Monolayer of 1D and 2D Nanomaterials for Flexible Resistive Switching Device, *G.D. Moon (gmoon@kitech.re.kr)*, *H.J. Seo, Y.K. Park, E. Jeong*, Korea Institute of Industrial Technology, Republic of Korea

Self-assembly is a general technique fabricating ordered arrangement of small building blocks. The assembly is driven by forces such as intermolecular force, electrostatic force, capillary force, or convective motion of solvents. Various types of self-assembly have been explored to produce hexagonally closely-packed 2D or 3D array for photonic crystals, inverse opals, and chemical sensors and biosensors. Some of the simplest techniques include sedimentation and centrifugation procedures, which are time-consuming and cause macroscopic defects in the crystalline order. Alternative methods have been tried to increase the speed of crystal formation and to enhance the colloidal ordering with a controlled thickness of the assembly. Capillary deposition, spin-coating, electrophoretic assembly, convective assembly, vertical deposition, and other initiative designs are included in the category. However, these methods often require complex configurations or long deposition time.

In this study, we demonstrated a flexible resistive switching device based on ultrathin Ag₂Te nanowire (NW) film and Au nanosheet (NS) electrode by exploiting a monolayer assembly on water surface for macroscale two-dimensional structures. Firstly, ultrathin TeNWs (diameter ≈ 10 nm) are, rapidly, assembled on water surface as a form of monolayer and transferred to fabricate TeNW film on various substrates with any available size. An assembled TeNW film was used as a template to produce Ag₂TeNW film through chemical transformation. A well-aligned Ag₂TeNW film device showed reversible resistive switching properties when the Ag composition of silver telluride NW becomes the stoichiometric Ag₂Te. Additionally, non-stoichiometric Ag_{2-x}TeNW film shows increased On/Off ratio. For a flexible memory device, ultrathin AuNS (thickness ≤20 nm) was adopted as working electrodes, since thermally-deposited gold electrodes tend to go through cracks under strain, which can fail to maintain the electrical properties. A paper-like flexibility of AuNS proved its capability as optimal electrodes of ultrathin Ag₂TeNW film-based resistive memory devices.

CP-ThP25 Investigation of Sb₂Se₃ Ultra-thin Hole-transporting Material for Perovskite/ Sb₂Se₃ Heterojunction Solar Cells, *G.M. Wu (wu@mail.cgu.edu.tw)*, Chang Gung University, Chang Gung Memorial Hospital, Taiwan

Sb₂Se₃ thin film photovoltaic has a low energy band gap for effective and wide solar-spectrum utilization. This report presents a new solar cell architecture with ultra-thin Sb₂Se₃ hole-transporting material (HTM) layer (<300 nm) in between bi-layer Mo metal-electrode layer and CH₃NH₃PbI₃ (MAPbI₃) perovskite active absorber layer. The solar cell nano-structures were prepared as Mo/ Sb₂Se₃/perovskite/ ZnS/Ag multi-layers on FTO (fluorine-doped tin oxide) glass substrates. The hole-transporting layer, active absorber layer, electron-transporting buffer layer, and top metal-electrode contact layer, were made of Sb₂Se₃, perovskite, zinc-sulfide, and silver, respectively. The ultra-thin Sb₂Se₃ HTM layers were annealed at temperature of 400, 500, and 600°C. The nano-crystal grain size, revealed by scanning electron microscopy, was enhanced with the increasing annealing temperature. The advantages of using Sb₂Se₃ HTM on perovskite photovoltaics included better device performance, reduced HTM film thickness, and diminished HTM film cost. The Sb₂Se₃ HTM has acted to maintain perovskite absorber layer's optical-current and stability. The device photo power-conversion efficiency can reached about 14.4%, and the related photo-electronic characteristics will be summarized and further discussed. This work was supported in part by the Ministry of Science and Technology under research grants MOST105-2221-E182-059-MY3/BMRP246 and CGMH CMRPD3G0062.

Keywords: Sb₂Se₃, Hole-transporting material, perovskite, MoSe₂, ZnS,

CP-ThP26 Enhanced Storage Modulus and Shear Strength of Poly (vinylidene fluoride) Nanocomposites for Aerospace Components, *U.O. Uyor (UyorUO@tut.ac.za)*, *P.A. Popoola, O.M. Popoola*, Tshwane University of Technology, Pretoria, South Africa

Some aerospace components require materials with good mechanical strength, stiffness and high noise or vibration absorption capability. Polymeric materials show good vibration absorption capacity due to their high damping coefficient or factor, which is the measure of vibration absorption capacity. Increase in damping factor often result to decrease in other mechanical properties. This is because damping property has to do with loss of heat generated from interfacial slippage of polymer chains as

Thursday Afternoon Poster Sessions, May 23, 2019

external load is applied. Therefore, to obtain appreciable damping factor materials with good mechanical properties has been of research interest. Hence, this study focused on improvement of storage modulus and shear strength of polymer, while maintaining appreciable damping coefficient. These were studied using modular compact rheometer at temperature of 200°C, frequency of 0.1rad/sec and strain rate of 0.05%. The nanocomposites used for this study were fabricated by solution blending and melt compounding. Surface modified graphene and titanium dioxide nano-powder were used as reinforcements in poly(vinylidene fluoride) matrix. Dispersion of the fillers was investigated using scanning electron microscope. The nanocomposites showed huge increase in storage modulus from about 67.5Pa for pure polymer to 3.2x10⁵Pa for the composite material. Shear strength was also significantly enhanced with appreciable damping factor. Such composites have great potentials in aerospace and automobile industries due to their improved properties.

Keywords: Storage modulus, Shear strength, Damping factor and Polymer

CP-ThP27 Fabrication of a Thermoelectric Generator Device by Suspension Plasma Spray Technique, F. Ambriz-Vargas (fabian.ambrizvargas@mail.concordia.ca), C. Moreau, Concordia University, Canada

About seventy percent of the world energy production is lost in the form of heat dissipation which is one of the most significant contributions in the global warming. Thermoelectric generators are one of the most viable devices to recover waste heat (generated by the vehicles, factories, houses etc.) and convert it into electricity. With the rising cost of fuel and increasing demand for clean energy, solid-state thermoelectric devices are good candidates to reduce fuel consumption and CO₂ emissions. Although, they are reliable energy converters, there are several issues that have limited their implementation into the market. These issues include toxicity of the thermoelectric materials (coatings-based lead and tellurium) and the limited ability to mass-manufacture thermoelectric materials. Recent theoretical predictions have demonstrated that titanium dioxide (TiO₂) can overcome the above issues, since they are non-toxic, relatively abundant and present excellent thermoelectric properties. However, formation of high quality TiO₂ phase is not feasible. Among the different emerging synthesis process, suspension plasma spray technique is a good candidate to synthesize TiO₂ coatings since it presents several advantages such as control over the chemical stoichiometry, industry-scalable and low-cost process. Then, this work presents the evaluation of the thermoelectric properties of TiO₂ coatings produced by suspension plasma spray technique. This research strategy involves the study of the effect of the synthesis technique parameters on the microstructural, structural and thermoelectric properties of TiO₂.

CP-ThP30 Bipolar Resistive Switching Characteristics of MoS₂ Based Memory Devices, A. Kumar, S. Pawar, D. Kaur (dkaurfph@iitr.ac.in), Indian Institute of Technology Roorkee, India

This report explore the resistive switching characteristics of MoS₂ thin film based memory devices with ferromagnetic shape memory alloys (FSMA, e.g. Ni-Mn-In) as bottom electrode. The Cu/MoS₂/NiMnIn, Ti/MoS₂/NiMnIn and Ag/MoS₂/NiMnIn memory devices has been fabricated by D.C. magnetron sputtering technique. The field emission scanning electron microscopy images reveals the nano-worm growth of the MoS₂ layer. The Cu/MoS₂/NiMnIn and Ag/MoS₂/NiMnIn devices exhibits bipolar resistive switching behavior while no resistive switching phenomenon is observed for Ti/MoS₂/NiMnIn nanostructure. Therefore, the top electrode has been observed to play a significant role in resistive switching memory characteristics. The conduction mechanism based on metallic filament formation across MoS₂ layer is proposed and well explained. Such MoS₂ based devices with excellent resistive switching characteristics have the potential to be used as next generation memory devices.

Keywords: MoS₂, ferromagnetic shape memory alloys, thin film, resistive switching.

CP-ThP31 Morphology Controlled of Silver/Silver Oxide Nanoparticles-MnO₂ Nanocomposites for Supercapacitor Application, F.N. Sari, K.C. Lin, J.-W. Ruan, J.L. Huang, J.-M. Ting (jting@mail.ncku.edu.tw), National Cheng Kung University, Taiwan

Ag nanoparticles (NPs)-MnO₂ having various morphology have been synthesized through a facile method. It was found that by controlling the amount of Ag NPs, temperature, and time of reaction lead to the formation of urchin-like structure with Ag₂O NPs on the tips of MnO₂ nanowires, while the addition of surfactant agent poly(vinylpyrrolidone) (PVP) leads to the formation of nanoflower-like structure with Ag NPs distribute well on the

δ-MnO₂ nanosheets surface. Moreover, the formation of the Ag sub-oxides such as Ag₂O and Ag₂O₂ were also investigated. Varied dimension and different morphology resulting the different of specific surface area. Supercapacitors having the obtained Ag/Ag sub-oxides-MnO₂ nanocomposite as the electrodes were evaluated. We demonstrated the synergistic effect of high specific surface area with the Ag/Ag₂O NPs, which provide more active sites and effectively reduce the resistance. As a result, the obtained nanocomposite with optimum specific surface area of 250.9 m²g⁻¹ and low Rct of 84 ohm showing high Csp of 226 F g⁻¹ at 5 mV s⁻¹ which is three times compare to pure MnO₂. The nanocomposites also show no degradation after 1000 cycles, indicating excellent electrochemical stability.

Keywords: MnO₂, Ag nanoparticles, Ag₂O, supercapacitor

Coatings for Biomedical and Healthcare Applications Room Grand Hall - Session DP-ThP

Coatings for Biomedical and Healthcare Applications (Symposium D) Poster Session

DP-ThP2 Parylene Based Blood Oxygen Sensing Array For Flexible Wearable Devices, W.-C. Kuo (rkuo@nku.edu.tw), T.-C. Wu, National Kaohsiung University of Science and Technology, Taiwan

The performance of flexible and wearable pulse oximetry is highly influenced by motion artifact. The signal originally comes from photolethysmographic (PPG) during walking and running at different conditions. The measurement of SpO₂ in pulse oximetry extracts the dc part (the absorption of human tissue and vessel) and the ac part (the absorption of fluctuating wave of pulsing blood) of the red and IR PPG signals. Improper site selection or fitting misalignment will receive the less light intensity to generate the error SpO₂. The intensity of light detection is the case of larger the better quality characteristic. The purpose of this research is to develop the reflective array type of flexible wrist pulse oximetry in order to get the correct SpO₂. The parylene based flexible device can fit the curvature of wrist and locate the array of photo diodes around the radial artery of wrist, and the maximum intensity of light can be extracted to get the optimum SpO₂ to reduce the wrong value coming from improper fitting or misalignment.

DP-ThP4 Development of Multilayer HA-Ag and TiN-HA-Ag Coatings Deposited by RF Magnetron Sputtering with Potential Application in the Biomedical Field, J.A. Lenis (julian.lenis@udea.edu.co), G.B. Gaitán, F.J. Bolívar, University of Antioquia, Colombia

The use of composite coatings emerges as a great alternative to induce superficially the combination of properties widely desired in surgical implants, such as: osteointegration and bactericidal character, which can not be conferred by a single material. In the present investigation, the effect of the incorporation of an intermediate layer of titanium nitride (TiN) on the chemical composition, structure, morphology, phases and adherence of a multi-layer Hydroxyapatite (HA) - silver (Ag) coating deposited on Ti-6Al-4V by magnetron RF sputtering was evaluated. The elemental composition analysis was performed by energy dispersive spectroscopy, while the techniques of micro-Raman spectroscopy, scanning electron microscopy and atomic force microscopy were used to determine the structure and morphology of the obtained coatings. A variation in the Ca/P ratio, the Ag content and the thickness in the HA-Ag coatings deposited on the TiN layer was found compared to the HA-Ag system deposited on the metallic alloy. In the same way, the roughness and structure of this coating was modified according to the surface where it was deposited.

Key words: Magnetron sputtering, Hydroxyapatite, Ca/P ratio, structure, multi-layer coating, intermediate layers, critical load.

DP-ThP5 Electrochemical Activated Iridium Oxide Film as a Bio-interface Electrode for Neurostimulation Applications, Y.-C. Chiu, P.-C. Chen, National Taipei University of Technology, Taiwan; C.-M. Lei (ljm9@faculty.pccu.edu.tw), Chinese Culture University, Taiwan; P.-W. Wu, National Chiao Tung University, Taiwan

Electrode materials for neural stimulation have been widely investigated for implantable devices. Among them, iridium and iridium oxide are attractive materials for bio-interface applications due to their desirable stability, electrochemical performance, and biocompatibility. In this study, metallic iridium thin film was deposited on a transparent conducting oxide substrate (ITO-coated glass) by radio-frequency (RF) magnetron sputtering, and we carried out an electrochemical activation to produce iridium oxide film through a repetitive biphasic pulsed current. The process parameters for sputtering of iridium film and electrochemical activation of iridium oxide film

Thursday Afternoon Poster Sessions, May 23, 2019

were optimized. The activated iridium oxide film exhibited superior electrochemical performance, including large charge storage capacity (CSC), high charge injection capability, low electrochemical impedance, and excellent stability. In addition, the biocompatibility of activated iridium oxide was evaluated by cytotoxicity, and the iridium oxide/iridium film showed high cell-viability. These findings suggest that the activated iridium oxide film is a promising candidate as an electrode material for the development of neurostimulating devices.

DP-ThP6 HIPIMS Titanium Dioxide on Laser Roughened PEEK Surface for Biomedical Application, P.-Y. Hsieh, Institute of Plasma, Department of Materials Science and Engineering, Feng Chia University, Taiwan; C.J. Chung (cjchung@ctust.edu.tw), Central Taiwan University of Science and Technology, Taiwan; H.K. Tsou, Taichung Veterans General Hospital, Taiwan; H.T. Chen, China Medical University Hospital, Taiwan; J.L. He, Institute of Plasma, Department of Materials Science and Engineering, Feng Chia University, Taiwan

Polyetheretherketone (PEEK), known for its comparable elastic modulus to human cancellous bone characteristics and X-ray radiolucency, is greatly considered for spinal implant material. However, the bio-inertness and hydrophobic surface properties of PEEK results in poor osseointegration when implanted into human bodies. The aim of this study is to develop a combination method, viz., laser roughening process and titanium dioxide (TiO₂) deposition, for modifying the biological properties of PEEK surface. A femtosecond pulse laser was utilized to avoid the thermal damage on PEEK, while high power impulse magnetron sputtering (HIPIMS) was employed to deposited high crystalline TiO₂ coating at low temperature. The results showed that the hierarchically patterned PEEK surfaces composed of nano- and microstructures can be obtained by adjusting laser parameters. Such structure resulted in varied surface roughness and water wetting ability. On the other hand, the highest rank (5B) in adhesion tape test proved the superior adhesion of the HIPIMS prepared TiO₂ coating even on roughened PEEK surface. The strong adhesion is believed to arise from the advantage of high ion energy and high-density plasma characteristics of the HIPIMS discharge. Under proper laser roughening condition followed by HIPIMS-TiO₂, the *in vitro* osteoblast compatibility test performed a much higher level than bare PEEK.

DP-ThP7 Corrosion Property and Biocompatibility Evaluation of Fe-Zr-Nb Thin Film Metallic Glasses, B.-S. Lou (blou@mail.cgu.edu.tw), Chang Gung University, Taiwan; T.Y. Lin, J.-W. Lee, Ming Chi University of Technology, Taiwan; J.-B. Wang, Y.-C. Yang, National Taipei University of Technology, Taiwan

The amorphous thin film metallic glasses (TFMGs) have drawn lots of attention by researchers due to their unique properties and ease of fabrication. Recently, the biocompatibility of Zr-based TFMG becomes an important issue because of its excellent corrosion resistance and bio safety. In this work, six Zr-Ti-Si TFMGs with different Si concentrations were fabricated on the bio-grade 316L stainless steel plates and Si wafer, respectively, by a hybrid bipolar high power impulse magnetron sputtering and radio frequency sputtering technique. The chemical composition of Si increased gradually from 3.3 to 34.7 at.%, respectively, as the Si target power increased from 25 to 250 W. The crystalline structure was observed for TFMG containing 3.3 at.% Si, whereas the amorphous phase was found for the TFMG containing higher than 9.6 at.% Si. The cross-sectional morphology changed from columnar to fine and featureless microstructure as more silicon contents were added into the thin film. Acceptable adhesion qualities, HF1 to HF 3, were obtained for all Zr-Ti-Si thin films. The maximum hardness, 15.7 GPa, and the highest H/E value around 0.088 were achieved for TFMG containing 34.7 at.% Si. The corrosion resistance of 316L stainless steel disk can be improved effectively by TFMGs. The lowest corrosion current density around 0.02 mA/cm², and the highest polarization resistance around 1042.1 kWcm², were achieved for TFMG containing 31.6 at.%. Six thin films had better biocompatibility than that of 316L stainless steel substrate. The hybrid HIPIMS-RF grown Zr-Ti-Si TFMGs with adequate hardness, good biocompatibility can be used as a promising candidate to improve the surface biocompatibility of biomaterials.

DP-ThP9 Bone-like Nano-hydroxyapatite Coating on Low-modulus Ti-5Nb-5Mo Alloy Using Hydrothermal and Post-heat Treatments, H.C. Hsu, S.C. Wu, S.K. Hsu, Central Taiwan University of Science and Technology, Taiwan; W.F. Ho (fuji@nuk.edu.tw), National University of Kaohsiung, Taiwan

Titanium and its alloys have been widely used as biomaterials for orthopedic and dental implants because of their excellent biocompatibility and mechanical properties. However, they are considered to be bioinert, such that when they are inserted into the human body these implants cannot

bond directly to the surrounding living bone. This study aimed to improve the bioactivity of a low-modulus Ti-5Nb-5Mo alloy with a hydroxyapatite (HA) surface coating using eggshells as a Ca source through hydrothermal reaction and heat treatment. The results showed that the whole alkali-treated alloy surface was covered with amorphous calcium phosphate nanoparticles after hydrothermal reaction at 200 °C for 48 h. When subsequently heat-treated at various temperatures (400, 500 or 600 °C) for 48 h, the surface coating of Ti-5Nb-5Mo alloy was transformed into crystalline rod-like HA nanoparticles. Also, heat treatment enhanced the adhesion between the HA coating and the Ti alloy substrate. Additionally, FTIR analysis confirmed the production of HA containing mixed AB-type carbonate substitutions. To evaluate bioactivity of the bone-like HA-coated Ti-5Nb-5Mo alloy, the capability of calcium phosphate apatite formation on the alloy surface was assessed by immersion in a simulated body fluid (SBF). Dune-like apatite layer was observed to densely deposit on the surface of HA-coated Ti alloy after 6 h of immersion in the SBF. Notably, the ability of Ti-5Nb-5Mo alloy subjected to sequential process with alkali, hydrothermal, and heat treatments to form bone-like HA nanoparticle coating was obviously greater than that of its counterpart without HA coating.

DP-ThP10 Surface Characteristics and Structure of Porous Ti-5Nb-5Mo Alloy for Biomedical Applications, W.F. Ho, National University of Kaohsiung, Taiwan; S.C. Wu, S.K. Hsu, W.Y. Hsiao, H.C. Hsu (hchsu@ctust.edu.tw), Central Taiwan University of Science and Technology, Taiwan

Titanium (Ti) and some of its alloys have been used widely as load-bearing implants because of their excellent mechanical properties, superior biocompatibility, and good corrosion resistance. Lately, there has been an increasing interest in studying porous alloy, which could imitate bone structures by altering the porosity of alloy. In this study, a biomedical porous Ti-5Nb-5Mo (wt.%) alloy was fabricated by mechanical alloying (MA) process for different ball-milling times. The metal powders of Ti (99.9% pure), Nb (99.9% pure), Mo (99.95% pure) were milled in a planetary ball milling machine for 3 h, 15 h and 30 h. The ball milled Ti-5Nb-5Mo powders were compacted of 7 mm in diameter and 11 mm in height. The sintering process was carried out in two steps. The compacts were initially sintered at 175 °C for 2 h and then increased to 1100 °C for 5, 10 and 15 h respectively. The results found in this study are summarized as follows: The Ti-5Nb-5Mo particle size increased with the ball-milling time increased from 3 h (35 μm) to 15 h (72 μm). The ball milling produced alloy particles gather together, and caused a larger particle size. The ball milled Ti-5Nb-5Mo particles were significantly refined, and the Nb and Mo was integrated and uniformly distributed in the matrix. XRD analysis shown that the porous Ti-5Nb-5Mo was a α phase and has no obvious diffraction peaks of elemental Nb and Mo remained which confirmed Nb and Mo was integrated and uniformly distributed in the matrix. While the sintering of powder by ball milling enhances the homogeneity. The compressive strength and modulus of all the porous Ti-5Nb-5Mo match the necessary mechanical property of cancellous bones. Especially for the B3S15 specimen (Balling 3 h and sintering 15 h) which shows the highest strength. After soaking in a SBF solution for 7 days, the porous Ti-5Nb-5Mo alloy formed a dense apatite layer on the surface. It exhibited a better apatite-forming ability. The study reveals that the use of porous Ti-5Nb-5Mo alloy satisfies the need of implants with an adequate mechanical strength and elastic modulus for the patients.

DP-ThP11 In vitro Wear Tests of the Dual-layer Grid Blasting-plasma Polymerized Superhydrophobic Coatings on Substrates Made into Dental Stainless Archwires, C.W. Lin (cwwlin0126@gmail.com), Feng Chia University, Central Taiwan University of Science and Technology, Taiwan; C.M. Chou, Taichung Veterans General Hospital, National Yang-Ming University, Taiwan; C.J. Chung, Central Taiwan University of Science and Technology, Taiwan; J.L. He, Feng Chia University, Taiwan

Dental stainless archwires, frequently used in orthodontics and dentofacial orthopedics, may accumulate food debris, promote bacterial overgrowth, and subsequently result in dental caries. A dual-layer grid-blasting plasma-polymerized (GB-PP) superhydrophobic coating was developed in a previous work by changing the micro- and nano-structured surface morphology on AISI 304 stainless substrates. In this study, *in vitro* wear tests were performed in artificial saliva that mimicked tooth brushing, peanut-chewing, and nougat-chewing modes to determine the durability of the superhydrophobic layer. Experimental results show that peanut-chewing causes more damage to the superhydrophobic surface than nougat-chewing because the carbohydrate, protein and oil ingredients in peanut and nougat might be transferred onto the surface, subsequently masking some of the fluorocarbon layer (also verified by SEM, EDS, and FTIR analyses). In conclusion, the GB-PP coatings deposited on medical-purposed stainless

Thursday Afternoon Poster Sessions, May 23, 2019

steel substrates exhibit good durability after tooth brushing and nougat-chewing wear tests.

DP-ThP16 MgO-TiO₂ Coating on Magnesium, A Biomaterial, C. Iñiguez (cm.iniguezcontreras@ugto.mx), Universidad de Guanajuato, México; E.N. Hernandez-Rodriguez, University of Guanajuato, Mexico; A. Marquez, Universidad de Guanajuato, México; M. Zapata, Centro de Investigación en Ciencia Aplicada y Tecnología Avanzada, Unidad Legaria IPN, México

The research of biomaterials has experienced a spectacular breakthrough in recent years. The idea of increasing life expectancy by improving surgical techniques brought with it the need to create materials that can be used in prostheses, implants, systems and medical devices. To make this possible the biomaterials should be biocompatible, non-toxic, no carcinogen, chemically stable, good mechanical resistance, proper density and weight, shape and size, cheap, reproducible and easy to manufacture. The low corrosion resistance of Mg makes Mg alloys appropriate candidates for degradable biomaterials due to their biocompatibility combined with outstanding physical and mechanical properties. The focus of this research concerns the development of biocompatible and biodegradable coatings for Magnesium, with the intent of reducing and controlling the corrosion rate and increasing their initial biocompatibility. To solve this problem, magnesium substrates of a square inch area each were made and a coating of MgO-TiO₂ was applied through reactive rf-sputtering by varying the concentrations of oxides for different samples. To evaluate the efficiency of the coating, the corrosion resistance in the Hanks solution, which simulates the physiological fluid, was measured through the Tafel curves and the hardness was measured by a Vickers hardness tester at each of the samples. These tests showed that corrosion resistance and the hardness were incremented with the application of the coating and that it is possible to control the characteristics by modifying the oxide ratios in the coating.

DP-ThP19 Obtaining of CVD Nanodiamonds and Evaluation of the Cytotoxicity in B16f10 Cells for Treatment of Melanoma, C. Wachesk (cris_cw@hotmail.com), Federal University of São Paulo (UNIFESP), Brazil; C. Hurtado, Institute of Science and Technology, Federal University of São Paulo (UNIFESP), Brazil; R. Falcão, Institute of Science and Technology, Federal University of São Paulo (UNIFESP), Brazil; D.C. Arruda, University of Mogi das Cruzes, Brazil; D. Tada, Institute of Science and Technology, Federal University of São Paulo (UNIFESP), Brazil; V.T. Airoldi, National Institute for Space Research (INPE), Brazil

Recent studies have shown the potential use of nanodiamonds (NDs) as drug carriers for the therapy of cancer due to their high stability and small size. With the aim of obtaining a new system to be applied as drug delivery platform for the therapy of metastatic melanoma, a new technique of obtaining NDs from CVD diamond thin film was developed. The synthetic CVD-diamond film has similar physical and chemical properties to natural diamond: extreme hardness, excellent thermal conductivity, biological compatibility and chemical stability at temperatures below 800°C. Herein, CVD NDs were prepared by using laser ablation. The NDs were characterized by X-ray (XRD), (MEV-FEG), (TEM), energy dispersion spectroscopy (EDS), (XPS), Raman spectroscopy and dynamic light scattering. Furthermore, since cytocompatibility is one of the main features required for a drug delivery platform, the cytotoxicity of NDs was evaluated in B16-F10-Nex2 cells by MTT assay. The results showed that the laser ablation process reduced CVD particle size. The mean hydrodynamic diameter in aqueous suspension after the centrifugation changed from 54 nm. The high stability of aqueous suspension of CVD NDs was indicated by the low polydispersity index (0,2) and a small increase in the mean value of hydrodynamic diameter during the observed period (D = 215 nm). The high stability was provided by the high charge density on NDs surface as suggested by the high value of Zeta-potential (-36.39 and -30.94 mV). EDS analysis showed that NDs were composed of carbon (77.2%) and oxygen (22.2%). By X-ray diffraction analysis, it could be observed the characteristic peak of NDs at 43°. Raman spectrum of CVD NDs showed three peaks at: 1332, 1500 and 1600 cm⁻¹, corresponding to D and G bands of diamond. Cytotoxicity assay showed 60% and 80% of cell viability after 24h 48h 72h and 96h of incubation with NDs. The high value of cell viability is an indicative of the cytocompatibility of NDs, indicating the potential use of NDs in biomedical applications such as drug delivery platforms.

DP-ThP22 Tantalum Oxynitride PVD Coatings a Potential Candidate for Dental Implants Application, O. Banakh (oksana.banakh@he-arc.ch), University of Applied Sciences (HES-SO), Switzerland; P.-A. Steinmann, Positive Coating SA, Switzerland

Coating technology offers innovative solutions to improve the quality and durability of medical devices. Among new materials, titanium oxynitride

coatings (TiOxNy) are considered promising for applications in implantology (cardiovascular stents) due to their high biocompatibility. The purpose of this study is to test tantalum oxynitride coatings (TaOxNy) as a potential candidate in dental implants application. Coatings with different nitrogen and oxygen contents were deposited by conventional reactive magnetron sputtering and by High Power Impulse Magnetron Sputtering (HIPIMS) in mixed Ar-O₂-N₂ atmosphere. The coatings were deposited onto titanium micro-rough substrates (Ti-SLA) and stainless steel substrates. In some experiments water vapor was used as a reactive gas, instead of oxygen. The Ti-SLA uncoated sample was chosen as control in cellular response biological tests. None of the specimens presented any signs of cytotoxicity. Their biological response was similar to that of Ti-SLA. The coatings produced with water vapor showed an improvement of the corrosion resistance as well as a slight enhancement of cell adhesion. Even though the tantalum oxynitride coatings didn't show a noticeable enhancement of biological response on Ti-SLA surfaces, their application looks promising on other substrates such as stainless steel.

DP-ThP23 SIMS and AFM Analysis of Silver-doped DLC Films on Titanium Alloy (Ti6Al4V) Aiming Biomedical Application, A. Oliveira, Federal University of São Paulo, UNIFESP, São Jose dos Campos, São Paulo, Brazil; A.S. da Silva Sobrinho, D.M.G. Leite, Technological Institute of Aeronautics, ITA/DCTA, São Jose dos Campos, Brazil; W.T. Miyakawa, J.J. Jakutis Neto, Institute for Advanced Studies- IEAv/DCTA, São Jose dos Campos, São Paulo, Brazil; I.H.J. Koh, Federal University of São Paulo, UNIFESP, Brazil; A.M.A. Liberatore, M.A. Santos, Biotecnovale Research and Development Ltd - EPP, São Jose dos Campos, Brazil; M. Massi (massi.marcos@gmail.com), Mackenzie Presbyterian University, School of Engineering-PPGEMN, Brazil

A PECVD and hollow cathode conjugate reactor was used to deposit silver-doped DLC films on Ti6Al4V alloy. SIMS depth profile showed the hollow cathode effectiveness to form a silver concentration gradient from the substrate up to the film surface, what is desired in biomedical applications. Atomic Force Microscopy - AFM detected that the ranging of the argon flow from 20 to 80 sccm became the relief most acicular and promoted an increasing in sp³ hybridization. These results indicate the possibility of tuning the film roughness according its biomedical application. The results of in vivo trials suggested that the silver doping of DLC films promoted a faster biointegration in comparison with non-doped DLC films and can be a nice alternative for elderly patients.

Keywords: Diamond-like carbon, PECVD, hollow cathode, silver, titanium.

Acknowledgments: This work was partially supported by FAPESP (Grant 2014/21690-8).

DP-ThP24 A Multi-scale Modeling and Simulation Study on PVAc-g-PDMS Based Transparent Self-clean Coating, S.K. Sethi, M. Singh, G. Manik (manikfpt@iitr.ac.in), Indian Institute of Technology Roorkee, India

Interest in the development of self-clean coatings has gained strong attention among the scientific community during the last few years. However, the commercially available coatings are majorly fluoro based polymers that generate toxic gases during their processing and are non-biodegradable. Keeping this in mind, bio-degradable poly(vinylacetate) (PVAc) and bio-compatible poly(dimethylsiloxane) (PDMS) have been used as graft-copolymer system in order to fabricate durable, weather resistant, transparent and eco-friendly self-clean coatings. While PDMS contributes suitable hydrophobicity, PVAc provides useful substrate adhesion to ensure durability.

Molecular simulations are increasingly being used as an advanced tool for modeling and simulating complex structures in polymer and biomedical sectors. They help investigate the structure-property relationships through an understanding of atomistic/molecular level interactions which is difficult to be achieved through experiments. Here, we employ a multi-scale molecular simulation approach to investigate the self-clean nature of the PVAc-g-PDMS. Properties such as hydrophobicity, oleophobicity, surface energy, interaction energy, glass transition (T_g) and transparency were estimated from molecular dynamics (MD) simulations for pristine PDMS, PVAc and their grafted copolymers. Several properties such as density, solubility parameter and T_g of pristine polymers were found to be in close agreement with available previously reported literature, thereby, validating the simulation protocols adopted. Properties like hydrophobicity and oleophobicity have been investigated from mesoscopic simulation with higher M_w of the polymers to ensure similarity with the real-time situation, and duly compared with the atomistic simulation estimates and experimental characterization results.

Additionally, ZnO filler was incorporated into the grafted polymer at different concentrations in order to improve the hydrophobicity and

Thursday Afternoon Poster Sessions, May 23, 2019

oleophobicity further without compromising with its transparency and binding energy with the substrate. These systems are completely non-hazardous, good water repellent, transparent and durable in nature. They are thus serious potential candidates for self-clean coatings for several automobiles, aircraft, structural, biomedical and healthcare applications.

DP-ThP25 Influence of Ag-Cu Nanoparticles on the Microstructural and Bactericidal Properties of TiAlN- (Ag,Cu) Coatings Deposited by DC Magnetron Sputtering for Medical Applications, *H.D. Mejía (hdario.mejia@udea.edu.co), G. Bejarano, A.M. Echavarría,* Universidad de Antioquia, Colombia

Most of the surgical and odontological instrumentation is manufactured using martensitic stainless steel AISI 420 and 440 due to their acceptable biocompatibility, good hardenability, proper hardness and resistance to corrosion. However, the resistance to wear of this type of steels is relatively low and may be susceptible to contamination with bacteria representing a potential risk to the health of patients. This research work focused on the development of a coating system of titanium-aluminum-nitride doped with silver and copper nanoparticles TiAlN (Ag, Cu) to provide it with an appropriate bactericidal effect for possible biomedical applications.

TiAlN coatings doped with four different contents of Ag and Cu nanoparticles (11 at.% to 20 at.%) were deposited onto 420 steel by means of self-manufactured DC unbalanced magnetron sputtering using two composited targets of Ti/Al and Ag-Cu (both 50/50 at.% and 99.9% purity), which were facing each other at 180 degrees. The diffusion of the Ag-Cu nanoparticles to the sample surface, as well as their quantity, size, shape and distribution was controlled by an appropriate adjustment of the power applied to the Ag/Cu- target, the temperature and time of the deposition process, since the mechanical, tribological and bactericidal properties of the compound depend, among others, on these characteristics of the nanoparticles. The microstructure, surface topography, chemical and phase composition were analyzed by scanning and transmission electron microscopy (SEM/TEM), energy dispersive X-ray spectroscopy (EDX) and X-ray diffraction. To evaluate the bactericidal effect of steel and coated samples in vitro inhibition and adhesion test were carried out selected *Staphylococcus aureus* and *Escherichia coli*, two of the major pathogen frequently found in surgery and dentistry rooms and associated with infections. The coating without doping presents a structure of columnar growth, which becomes densified with the increase of the Ag-Cu content and takes a glassy appearance accompanied by an increased size of the Ag-Cu particles and consequently also in the surface roughness. All the coated samples exhibited a higher bactericidal effect in comparison with the uncoated and with TiAlN coated steel, however the greater inhibition (100%) and less adherence to both bacteria was showed by the sample coated with 17% at Ag-Cu. Based on the results obtained, the developed nanostructured coating system might be considered for potential application in surgical and dental instrumentation.

DP-ThP26 Antibacterial Activity of Conductive Thin Films Deposited on Water Filter Paper, *D.M. Mihut (dorinamm@yahoo.com), A. Afshar, S. Hill, L. Khang, N. Cordista,* Mercer University, USA

There is a high interest to investigate nanomaterials that can work effectively against different types of bacteria and provide alternative substitution for chemical substances and antibiotics. In this research, conductive materials nanoparticles in the form of thin films were deposited on water filter papers by using direct current (DC) high vacuum magnetron sputtering technique. The effectiveness of the nanoparticles to remove bacteria from polluted water was tested during the experiment. The morphology of the coatings and their adherence to the water filter paper was examined using the Scanning Electron Microscopy and their chemical composition was investigated using the X-ray diffraction technique. All thin films showed good adhesion to water filter fibers and ensured a high area of exposure to contaminated water. The antibacterial effect of different conductive thin films was characterized by using the standardized membrane filtering technique for water and wastewater examination. The testing media (i.e. contaminated water) containing bacterial samples were collected from local wastewater basins. Water was tested for the bacterial content before and after the exposure to conductive thin films coated filters.

Tribology and Mechanical Behavior of Coatings and Engineered Surfaces

Room Grand Hall - Session EP-ThP

Tribology and Mechanical Behavior of Coatings and Engineered Surfaces (Symposium E) Poster Session

EP-ThP2 Deposition of DLC/Si-N Composite Films Synthesized by Sputtering-PBII Hybrid System and Their Thermal Stability, *A. Melih (anasmelih525@hotmail.com), K. Yamada, S. Watanabe,* Nippon Institute of Technology, Japan

Diamond-like carbon (DLC) is a metastable amorphous film that exhibits unique properties. However, many limitations exist regarding the use of DLC, for example, its tribological characteristics at high temperature, as well as its limited thermal stability. In this study, silicon/nitrogen incorporated diamond-like carbon (DLC/Si-N) composite films are studied, taking into account the thermal stability and tribological performance of these films compared with pure DLC. All the films were synthesized using RF magnetron sputtering combination with PBII techniques (so-called Sputtering-PBII Hybrid System). High purity of Silicon nitride (99.9%) disk was used as a target with RF power of 500-700 W. The substrates were also applied with negative-pulsed bias voltage of 5 kV. The mixtures of Ar-CH₄ were used as reactive gas by varying CH₄ partial pressure between 0 and 0.15 Pa, while total gas pressure and total gas flow were fixed at 0.30 Pa and 30 sccm, respectively. The structure of the films was characterized using Raman spectroscopy. The thermal stability of the films was measured using thermogravimetric and differential thermal analysis (TG-DTA). The friction coefficient of the films was assessed using ball-on-disk friction testing. The results indicate that DLC/Si-N composite films present better thermal stability due to the presence of Si-O networks in the films. The DLC/Si-N (about 11 at.%Si, 18.5 at.%N) film was showed good thermal stability in an air atmosphere with increasing temperature until 800°C. Further, the films exhibit excellent tribological performance at 500°C in an air atmosphere. It is concluded that the DLC/Si-N composite films improve upon the thermal stability and tribological performance of DLC at a high temperature.

EP-ThP3 Mechanical and Tribological Performance of TiAlN, TaN and Nanolayered TiAlN/TaN Coatings Deposited by DC Magnetron Sputtering, *E. Contreras (elbert.contreras@udea.edu.co), J. Cortínez, M.A. Gómez,* Universidad de Antioquia, Colombia; *A. Hurtado,* Centro de Investigación en Materiales Avanzados CIMAV, Mexico

Nanoscale multilayer systems have become the most important way to increase the mechanical and tribological performance of wear protective coatings. In the present research, nanoscale TiAlN/TaN multilayer coatings were deposited by DC magnetron sputtering, controlling the substrate rotation speed in order to obtain different periods and to evaluate their effect on mechanical and tribological properties; additionally, monolayer TiAlN and TaN coatings were deposited to compare the effect of multilayer architecture on the coatings performance. SEM images showed a well defined columnar and homogenous microstructure, it was possible to observe the multilayer architecture with higher bilayer periods. TEM images exhibited well defined interface and diffusion between both TiAlN and TaN layers. A high crystalline coatings, change in the growth direction of coatings and residual stresses was the most relevant results obtained by XRD. Regarding to the residual stresses, it was observed that monolayer coatings exhibit high compressive stresses reaching values up to 8 GPa. On the other hand, the residual stresses of nanoscale multilayer coatings exhibit considerable lower values and decrease progressively as the bilayer period of the coatings decreases, reaching values below 2 GPa. TiAlN and TaN coatings exhibited hardness of 16 GPa and 17 GPa, respectively, while TiAlN/TaN coatings showed a progressive increase as the coating period decreases, reaching values up to 22 GPa with bilayer periods lower than 10 nm. Scratch test results showed that all nanoscale multilayer coatings exhibit better adherence compared to TiAlN and TaN monolayer coatings. Additionally, it was also observed a slight tendency to increase the adherence once the bilayer period decreases reaching values up to $L_c = 42$ N. Fracture toughness was evaluated by nanoindentation, it was possible to calculate a significant improvement in the toughness of multilayer coatings and a significant increase in the H^3/E^2 ratio. With respect to the tribological performance, it was possible to observe a decrease in friction coefficient and wear rates of nanoscale multilayer coatings compare to TiAlN and TaN monolayer coatings. Using cross-section FIB it was possible to observe initial deformation in the constituent layers followed by the propagation of cracks along the interfaces between TiAlN and TaN layers, in nanoindentation tests, scratch tests and tribological tracks.

Thursday Afternoon Poster Sessions, May 23, 2019

EP-ThP4 Development of Catalytically Active Nano-Composite Coating for Severe Boundary Lubricated Conditions of Hydraulic Fluids, V. DaSilva, O.L. Eryilmaz (eryilmaz@anl.gov), A. Erdemir, Argonne National Laboratory, USA

Applying thin coatings onto bulk materials is a surface benefactor favorable in tribology because of its ability to lower friction and copiously improve wear performance. These phenomena result in more reliable mechanical systems and improve energy efficiency. In this work, Vanadium Nitride - Copper coatings were produced and optimized (power of each target was adjusted to achieve a range of Cu concentration within the hard nitride phase) using HIPIMS magnetron sputtering system. The thin coatings were deposited onto 52100 steel flat, cylinders, and ball samples for tribological testing. Characterization such as surface roughness, composition, coating thickness, and adhesion were analyzed using a wide range of characterization techniques prior to testing. The coatings were evaluated in hydraulic fluids under unidirectional sliding (ball on flat) using two different test configurations. The results showed that, use of coating on both static and moving surfaces significantly improved wear resistance and lowered the coefficient of friction when tested under severe conditions (1 GPa maximum Hertzian contact pressure). Post-test microscopy and profilometry analysis confirmed ultralow wear on sliding surfaces. Furthermore, the VN-Cu coated surfaces showed an astounding 30-40% reduction in coefficient of friction compared to baseline 52100 ball on 52100 flat in hydraulic fluid.

EP-ThP5 Size-Independent High Strength of CuTi/Ti Metallic Glass/Crystalline Nanolayers, M. Abboud, Middle East Technical University, Turkey; A. Motallebzadeh, Koç University, Turkey; S. Özerinc (ozercinc@metu.edu.tr), Middle East Technical University, Turkey

Thin film metallic glasses (MG) offer a wide design space for the development of hard, corrosion resistant and biocompatible coatings. However, one of the major disadvantages of MGs is their brittle nature. Utilizing a nanolayered MG – crystalline structure is a promising approach for improving the ductility of these materials. Hardness of these nanocomposites usually increases with decreasing layer thickness, and it is lower than that of the corresponding monolithic MG. In this work, we demonstrated a nanolayered model system composed of CuTi MG and nanocrystalline Ti layers (CuTi/Ti) that shows unusually high hardness, comparable to that of monolithic CuTi MG. Furthermore, we did not observe any significant dependence of strength on layer thickness.

We prepared thin films of nanocrystalline Ti, CuTi MG, and nanolayered CuTi/Ti. A magnetron sputterer deposited 1 μm -thick films on oxidized silicon substrates, and layer thickness was varied in the range 10–100 nm. X-ray diffraction and electron microscopy verified the microstructure with alternating layers, and nanoindentation experiments measured the mechanical properties.

Nanocrystalline Ti sample has an average grain size of ≈ 20 nm and the grain size of Ti layers in the CuTi/Ti samples varies in the range 5–16 nm; monotonically increasing with increasing layer thickness. Hardness of all CuTi/Ti nanolayers are in the range 7.1–7.3 ± 0.3 GPa with no observable layer thickness dependence; and are comparable to that of monolithic CuTi MG (7.0 ± 0.3 GPa). On the other hand, 1 μm -thick nanocrystalline Ti has a hardness of only 0.9 GPa. An order of magnitude higher hardness of the nanocomposite when compared to the crystalline Ti suggests that the confinement of hexagonal close-packed Ti in between amorphous layers results in unexpected levels of extrinsic strengthening. In order to have a comparison, we also prepared nanolayered CuTi MG/crystalline Cu samples. These layers are softer than CuTi for all layer thicknesses, and show the usual size dependence of increasing hardness with decreasing layer thickness, in the range 5.1–6.3 GPa. These differences between the samples containing HCP Ti layers and FCC Cu layers suggest that crystal structure plays an important role in the mechanical behavior of nanolayered MG-crystalline composites.

The results demonstrate that by the appropriate selection of the constituent layers, it is possible to design size-independent high strength nanolayered metals. This enables the opportunity of engineering the layer thicknesses for optimizing other properties of nanolayers such as ductility, corrosion resistance and biocompatibility for application requirements.

EP-ThP6 Extended Crack-free Tensile Deformation of Ultrathin Metallic Glass Films Due to an Intrinsic Size Effect, O. Glushko (oleksandr.glushko@oaeaw.ac.at), Erich Schmid Institute of Materials Science, Austria; M. Mühlbacher, Montanuniversität Leoben, Austria; C. Gammer, M.J. Cordill, Erich Schmid Institute of Materials Science, Austria; C. Mitterer, Montanuniversität Leoben, Austria; J. Eckert, Erich Schmid Institute of Materials Science, Austria

Although metallic glasses (MGs) exhibit a unique combination of mechanical and chemical properties (high strength, hardness, elastic strain, wear and corrosion resistance, biocompatibility), their application as structural or functional materials is hindered by the lack of ductility which leads to catastrophic brittle-like fracture. When the size of a MG sample is reduced below some critical value, typically of the order of a few hundred nanometers, then considerable ductility can be observed. However, this size effect was demonstrated so far mostly by nanomechanical testing inside a transmission electron microscope using samples prepared by focused ion beam (FIB) milling. Whether the ductile-like behavior of submicrometer-sized metallic glasses is a real “intrinsic” size effect or it is rather caused by extrinsic factors like sample shape, ion beam effect or parameters of the testing setup is currently a subject of extensive discussions in the community.

In this contribution the tensile properties of thin film PdSi MGs grown by sputter deposition on a polymer substrate are considered. The integrity of the MG films during stretching was monitored by in-situ measurements of the electrical resistance. Although the 250 nm thick films fail in a brittle manner at 2% strain, considerable local ductility originating from the substrate constraint is observed. A strong size effect on the deformation behavior appears when the film thickness drops below 16 nm. The 7 nm thick films with the same composition show a crack-free deformation up to a strain of 7%. Even at higher strains no brittle-like failure but rather short and isolated cracks are observed. Cyclic tensile loading revealed extreme fracture resistance of ultrathin amorphous films showing no cracks after 30000 stretching cycles with a strain amplitude of 2%. Since all tests are performed at ambient conditions on films deposited using an industrially scalable process, the demonstrated size effect can be directly utilized for applications, such as protective coatings, nanoelectromechanical devices or half-transparent conductive layers for flexible electronics.

EP-ThP11 Effect of Surface Treatments on AISI H13 Steels, M.A. Doñu Ruiz (marckdr_69@hotmail.com), Universidad Politecnica del Valle de México, Mexico, México; M.G. Buenostro Arvizu, Universidad Autónoma Metropolitana Azcapotzalco, Mexico; N. Lopez Perrusquia, Universidad Politecnica del Valle de México, Mexico, México; V.J. Cortés Suárez, Universidad Autónoma Metropolitana Azcapotzalco, Mexico; C.R. Torres San Miguel, Instituto Politecnico Nacional, Mexico; G.J. Pérez Mendoza, Universidad Politecnica del Valle de México

Mechanical properties can be improved by thermochemical treatments, the present work studied the effect of surface treatment on AISI H13. Nitriding was performed according to TENIFER® process under two conditions; i) samples of were employed in the salt bath component at temperature of 853 K with exposure time of 1h 3min ii) sample were austenized in a vacuum furnace at a temperature of 1283 K for 90 minutes and cooled with nitrogen to 333 K. After all the samples were tempered, the first was carried out at 813 K and the second at 878 K, with 2 h, respectively. After hardening and tempering (HT), the samples HT were nitride (HTN).

Boro nitride coating was applied on samples on AISI H13 in two stage: i) samples were boride by paste dehydrated pack at temperatures 1173 K for 3 hours and then nitriding on sample boride at temperature of 853 K with exposure time of 1h 30 min.

The microstructural and phases composition were characterized using scanning electron microscopy (SEM) and X-ray diffractometer (XRD). The samples were mechanical characterization by three-point bend test and microhardness test.

Nitrided coating thicknesses are over thicknesses of 4.97 μm with zone of diffusion of 52.8 μm of thickness, for the case of boronitride a depth of 26.42 μm is observed. For the condition AISI H13 hardening, tempering and nitriding a maximum bending stress of 10990 MPa was obtained in comparison with the AISI H13 as received with a value of 3677 MPa.

Thursday Afternoon Poster Sessions, May 23, 2019

EP-ThP12 Mechanical Properties and Fretting Corrosion of Zr/ZrN/CNx Hierarchical Multilayers Deposited by HIPIMS on Ti Biomedical Alloy, M. Flores (majflores66@gmail.com), J. Perez, O. Jiménez, L.M. Flores, Universidad de Guadalajara, Mexico

The hierarchical multilayers of hard ceramic coatings can improve the adhesion to substrates and the tribocorrosion resistance of biomedical alloy as Ti6Al4V. The coatings deposited by HIPIMS have a more compact growth respect to films deposited by DC magnetron sputtering; this diminishes the presence of pinholes and defects that permit to predict a reduction in permeability. The design of the multilayer was made with a top layer of CNx in order to reduce the friction coefficient. In this work we study the mechanical and fretting corrosion behaviour of Ti6Al4V biomedical alloys coated with multilayers of Zr/ZrN/CNx and Zr/ZrN deposited by HIPIMS (High Power Impulse Magnetron Sputtering). The fretting corrosion tests were made in fetal bovine serum (FBS) to simulate the proteins in synovial liquid. The tribocorrosion was studied using open circuit potential (OCP) and potentiostatic polarization in the passive region during the relative movement of samples. The friction coefficient was measured as a function of the applied potential. The worn surface at wear track was analysed by SEM, XRD and Raman spectroscopy. We report the results on composition and structure of tribolayer and removed material of the wear tracks, and the comparative study in mechanical properties fretting corrosion and friction behaviour of coatings of Zr/ZrN and Zr/ZrN with a top layer of CNx.

EP-ThP13 Quantum Tools for Life-Time Prediction of Coatings and Thin Films, N. Schwarzer (n.schwarzer@esae.de), SIO, Germany

Everybody who ever tried to do some life-time prediction on parts subjected to erosion or tribology or any other form of complex and potentially multi-body interaction full well understands and values Mark Twain's famous dictum about the simple fact that making predictions is very complicated... especially if they concern the future. The smaller the objects and the more complex their internal structure the even more complicated this task becomes. In thin-film physics the most principle uncertainties come on top of the already rather nonlinear and often chaotic behavior the objects of interest are subjected to.

Instead of seeing this increase of complexity due to the incorporation of roughness, defects, impurity and quantum effects as an additional problem in our efforts to come to better life-time predictions with respect to all sorts of coating-applications, this author actually saw an interesting potential in the apparently tedious "add-on-effects" coming into play with smaller and smaller scales.

By incorporating quantum theoretical concepts into highly sophisticated physical models [1] we obtained a very compact, rather general and powerful tool to handle practical applications in many different fields, leading to a much more holistic uncertainty budget calculation and – as a surprise – even a more comfortable and secure life-time prediction.

[1] N. Schwarzer, "The Theory of Everything - Quantum and Relativity is everywhere – A Fermat Universe", Pan Stanford Publishing, July 2018, ISBN-10: 9814774472

EP-ThP14 Study on the Tribological Properties of MoS₂ Coatings Deposited on Laser Textured Titanium Alloy Surface, D.Z. Segu (zenebedawit@yahoo.com), LB-E-P, Republic of Korea

Laser surface texturing (LST) is a surface engineering procedure used to improve tribological characteristics of materials by generating patterned micro-structures on the sliding contact surface. In LST technology, a pulsed laser beam is used to make arranged dimples on surface by a material ablation process. The present study concerns a detailed understanding of friction, wear, and solid lubrication behaviors of laser surface textured titanium alloy (Ti-6Al-4V) with combined geometry patterns developed by using Nd:YAG laser. A pulsed Nd:YAG laser was applied on titanium alloy to create arranged dimples. To optimize the surface texturing effect on friction and wear, combined texture dimples with some specific formula arrays were fabricated by laser ablation process by combining ellipses and circles. Surface topography, residual stress, and micro-hardness of the fabricated micro dimple arrays on polished titanium surfaces have been characterized. The tribological testing of textured surface was performed by a ball-on-flat unidirectional tribometer under dry and coated MoS₂, and the results compared with that of untextured surface. The effect of density and diameter were also determined by assessing factors that affect friction, including load and speed. Results show that the textured surface had excellent tribological characteristics than the untextured surface under dry and coated MoS₂ revealed the prospective of surface modification for better tribological properties. The ploughing and abrasion were the key wear mechanisms of the surface of textured titanium alloy.

EP-ThP16 Structure and Fretting Wear Behavior of CuNiIn/MoS₂-Ti Multilayers Fabricated by Magnetron Sputtering Method, C.B. Wei (weichunbei@gdinn.com), Q. Li, S.S. Lin, H.J. Hou, M.J. Dai, Guangdong Institute of New Materials, China

Fretting denotes a tribological phenomenon related to movements of small amplitudes between two surfaces in contact. This working condition occurs in many mechanical assemblies where the parts are occasionally subjected to a vibrating environment or are sustaining variable stresses directly. It often results in damage that may lead to premature component failure. A thick soft CuNiIn coating prepared by plasma sprayed is usually used to cover engine components from fretting due to its great capacity of accommodation by plastic deformation. However, CuNiIn coating has limited life because of its high friction coefficient. Some researches combine CuNiIn+polymer bonded lubricant MoS₂ to improve the tribological behavior due to the cohesion, ductility and adhesion of third bodies inside the contact.

In this paper, CuNiIn/MoS₂-Ti multilayer was fabricated by magnetron sputtering method. As a comparison, CuNiIn monolayer and MoS₂-Ti monolayer was also prepared. The linear fretting wear was used to study the fretting wear behavior of the coatings. The results show that the interface of multilayer prevented the growth of thick columnar crystal of CuNiIn interlayer and MoS₂-Ti interlayer, whereas the monolayer showed thick columnar structure. A compact, fine crystal structure has formed for CuNiIn/MoS₂-Ti multilayers. The microhardness of the multilayers was in the range of 350~500HV, which was higher compared with that of the CuNiIn and MoS₂-Ti monolayer. After 12000 cycles of fretting wear, the friction coefficient of CuNiIn monolayer was more than 1.0, and its wear trace depth reached to 108µm, indicated the failure of the coating. However, the friction coefficient of MoS₂-Ti monolayer was about 0.1, and the wear trace depth was 4.5µm. MoS₂-Ti monolayer exhibited good lubricant properties, leading to the improvement of the tribological performance. The friction coefficient of CuNiIn/MoS₂-Ti multilayer was lower to 0.07, and the wear trace depth was 0.5 µm, demonstrated that the better wear properties of the multilayer compared with that of the monolayer. These can attribute to the more compact structure and higher ductile of the multilayers, as well as its good lubricant characteristic.

EP-ThP17 Contact-focusing Electron Flow (CFEF) Induced Near-zero Running-in for Low Friction of Carbon-steel contact Interface, D.F. Diao (dfdiao@szu.edu.cn), Institute of Nanosurface Science and Engineering, Shenzhen University, China

Under air condition, a-C film sliding against steel surface often shows high friction coefficients ($\mu=0.1\sim0.3$), which largely impedes its potential in industrially. In this study, we report a new method of contact-focusing electron flow (CFEF) by applying direct current (DC) at the sliding interface between a-C film and steel ball to trigger the in-situ formation of nanosized graphene sheets, and induce a fast low-friction behavior. The developments of the friction behavior with different DC values and normal loads were examined. The typical friction coefficient dropped one order of magnitude from 0.2 to 0.02 and the run-in period was close to zero under CFEF-condition. The low friction interface, especially the carbon-transfer film was examined at nanoscale by using the newest detecting avenues. The nanostructure of the transfer films was observed by Cs-corrected TEM and EELS analysis. The elemental composition of the transfer film was investigated by using EDS, XPS and Raman spectra analysis. Based on these analyses, we found three key factors for the fast low friction (near-zero running-in). (1) CFEF excited the carbon structural transition from amorphous to graphene sheet at the contact area. (2) Friction transferred the nanosized graphene sheets to the steel ball surface. (3) CFEF-friction coupling effect supplied the nanosized graphene sheets into the sliding interface. This work shed light on the CFEF-method for the in-situ fabrication of nanosized graphene sheets at the carbon-steel contact interface for low friction with near-zero running-in period.

EP-ThP18 Misinterpreting Size-effects during Coating Nanoindentation, E. Broitman (esteban.daniel.broitman@skf.com), SKF Research & Technology Development Center, Netherlands

The hardness of a material is a multifunctional physical property depending on a large number of internal and external factors. The transition from macroscale to microscale, and from microscale to nanoscale indentation hardness measurement is accompanied by a decreasing influence of some of these factors and by an increasing contribution from others.

The Vickers indenter used in macro-indentation tests has been designed to give geometrically similar indentations (i.e. the strain generated within the material is independent of the load), so the hardness should be independent

Thursday Afternoon Poster Sessions, May 23, 2019

of the indentation size. This fact results to be true for macroscale indentations. However, for microscale indentations (loads of less than 1N), it is well established that the hardness decreases or, more frequently, increases with the decrease of the applied load. This effect is known as the "indentation size effect" (ISE). The same phenomena has also been observed during coating nanoindentations at very low loads (low indentation depths), using either Berkovich or cube-corner indenters.

The gradient plasticity theory attributes ISE to the evolution of the so-called geometrically necessary dislocations beneath the indenter, which gives rise to strain gradients that affect the measurements at low penetration depths. In this presentation we will show that most of the ISE reported in the literature are, in fact, related to artifacts originated from a wrong surface preparation that generates work hardening, or the lack of surface microstructural characterization, which leads to ignore the presence of surface roughness, grain precipitates, or very thin surface oxide layers. Furthermore, we will show also that ignoring pile-ups or the use of an incorrect indenter geometric calibration generate false ISE results. We conclude that most of reported ISE have been misinterpreted and can be suppressed when proper data interpretation and processing are used.

EP-ThP19 e-Poster Presentation: Think You Have Produced DLC? Think Again!, *A.M. Khan (armankhan2020@u.northwestern.edu)*, *H. Wu, Y.W. Chung, Q.J. Wang*, Northwestern University, USA

Carbon-containing tribofilms have been widely reported to form in lubricated tribological contacts. These films show the same Raman *D* and *G* signatures as those of graphite- or diamond-like carbon (DLC) films. As a result, these films are commonly assumed to be DLC. Our work has revealed that this interpretation may not be always correct. In our experiments, we formed such tribofilms in standard pin-on-disk tribotesting using steel counter-faces and polyalphaolefin (PAO) base oil with cyclopropanecarboxylic acid (CPCA) as an additive. Raman spectra obtained from these tribofilms have *D* and *G* features identical to those from DLC. Multiple analytical techniques (micro-FTIR, mass spectrometry, and proton NMR) coupled with reactive molecular dynamics simulations demonstrate that these tribofilms are not DLC, but are in fact high molecular weight hydrocarbons acting as a solid lubricant.

EP-ThP20 Mechanical and Tribological Properties of Cr-Al-Si-N-O Coatings Prepared by Arc Ion Plating for Cutting Tools, *J.-H. Kim (jhkim81@kitech.re.kr)*, *W.R. Kim*, Korea Institute of Industrial Technology (KITECH), Republic of Korea

Quinary Cr-Al-Si-N-O nanocomposite films were deposited onto WC-Co substrate by a filtered arc ion plating system using CrAl₂ and Cr₄Si composite targets under N₂/Ar atmosphere. XRD and XPS analyses revealed that the synthesized Cr-Al-Si-N-O films were nanocomposite consisting of nanosized (Cr,Al,Si)_n crystallites embedded in an amorphous Si₃N₄/SiO₂ matrix. The hardness of the Cr-Al-Si-N-O films exhibited the maximum hardness values of ~40 GPa at a Si content of ~2.78 at.% due to the microstructural change to a nanocomposite as well as the solid-solution hardening. Besides, Cr-Al-Si-N-O film with Si content of around 2.78 at.% also showed perfect adhesive strength value of 109 N. These excellent mechanical properties of Cr-Al-Si-N-O films could be help to improve the performance of machining tools and cutting tools with application of the film. Also X-ray diffractometer (XRD) analysis was conducted to investigate the crystallinity and phase transformation of the films. Moreover, it was found that the improved nanohardness and the H/E ratio contributed to excellent wear resistance of the coatings. The friction coefficient and wear rate of the Cr-Al-Si-N-O coatings first decreased and then increased with increasing silicon content. The friction coefficient and wear rate were also mainly related to the lubricant wear debris in this work.

EP-ThP21 Wear of TiN in Reciprocating Soft Contacts, *S.H. van der Poel, D.T.A. Matthews (d.t.a.matthews@utwente.nl)*, University of Twente, Netherlands

In this study, TiN coatings were prepared by PVD on CoCrMo substrate material. The coatings were subjected to reciprocating sliding wear tests in both demineralised water and dry lubrication conditions against polyethylene ball counter-surfaces. Low contact pressures (approximately 20MPa) and low speeds (11 and 21 mm/s) were used during the tribological tests. Friction coefficients of approximately 0.3 were found in both wet and dry cases. However, surprisingly, the TiN coating was found to abrade significantly in wet contact cases, and mild wear of the TiN coating was seen in dry lubrication conditions. This work explores reasons for these observations.

EP-ThP22 Friction Property of Si-DLC with Scratch Damage Before and After Local Repairing Deposition to the Scratch Scar, *H. Takamatsu, K. Tanaka, A. Ito (ito.a@rc-logo.jp)*, *H. Kousaka, T. Furuki*, Gifu University, Japan

Diamond-Like Carbon (DLC) has excellent mechanical properties such as high hardness (over 10GPa), high wear resistance, and low friction. However, DLC film has low impact resistance and toughness because of its high hardness and brittleness, and thus it is often damaged by cracking from film surface and peeling from base material.

DLC film with local damages is repaired through the following process: (1) Removal of all the DLC film, (2) Recoating of new DLC film. However, this process is not efficient. We have proposed a new way of repairing, or recoating only to local damaged points of DLC by using a micro coating device. In this paper, we discuss the friction property of Si-DLC on which a local damaged point is repaired by recoating.

A local damage was introduced to Si-DLC pre-coated steel disk (SUJ2, JIS) by scratching at an almost constant load. Recoating of Si-DLC was conducted to the Si-DLC disk with a slit mask so that only the area near the scratch is recoated.

In order to evaluate the friction behavior of pre-coated, damaged and repaired Si-DLC films, these films were slid against a steel ball (SUJ2, JIS) at a vertical load of 15N and a rotation speed of 10m/min by ball on disk friction tester.

During running-in process, damaged Si-DLC showed frequent fluctuation of friction coefficient, which appeared from the sliding distance of about 60m. After the process has done, large increase of friction coefficient was sometimes confirmed with passing through the scratch scar. On the other hand, such fluctuation and unstable transition of friction coefficient were not confirmed in the repaired Si-DLC.

Transfer film formed onto the mating steel ball surface is considered to easily re-adhere to the metal exposed part in the damaged Si-DLC. Such transfer film detached from the ball surface can easily stick back to the ball surface, because of initial oxide film on the ball which prevents the formation of transfer film is already removed during the initial stage of sliding. We assume the fluctuation of friction coefficient in the damaged Si-DLC was caused by such detachment and re-attachment of transfer film at the sliding interface. In addition, we consider that such detachment of transfer film was suppressed in the repaired Si-DLC because the metal exposed part is covered by recoating of Si-DLC. As result, it is possible that partially repairing local damaged DLC shows better friction properties.

EP-ThP23 Raman Scattering Characterizes Thermally Annealed HiPIMS Sputtered MoS₂ Coatings, *H. Moldenhauer (henning.moldenhauer@tu-dortmund.de)*, *W. Tillmann, A. Wittig, D. Kokalj, D. Stangier, A. Brümmer, J. Debus*, TU Dortmund University, Germany

Omnipresent friction forces and wear limit the service time of machine parts. The usage of lubricants increases the service time remarkably due to a reduction in the wear. In that context, solid lubricants, like MoS₂ coatings grown by physical vapor deposition (PVD), are highly promising. However, the friction coefficient and, consequently, the lifetime of the coating depend on its oxidation resistance which in turn depends on several microscopic parameters, like its structure. In order to produce highly oxidation resistant coatings, high-power impulse magnetron sputtering (HiPIMS) is used. Their structural properties at the nanoscale are characterized by laser-light scattering methods; in particular, Raman scattering studies on HiPIMS sputtered MoS₂ thin films are performed aiming at their structural and tribological properties under multiple annealing conditions.

Raman scattering spectroscopy is a non-destructive and contactless tool for identifying the structure, morphology and chemistry of material surfaces. The material's quantized lattice vibrations are laser-excited and optically measured, thus generating a physicochemical fingerprint of the surface at the atomic scale. Raman scattering spectroscopy provides a high spatial resolution of about one micrometer and can be used for practically any sample geometry.

Using this technique, a microscopic layering of MoS₂ is detected: Interlayer-phonon modes at low frequency (38 cm⁻¹) build up for increasing annealing temperatures of the coatings (until 600°C). Changes in the intensity ratio of the in-plane and out-of-plane Raman modes moreover hint at crystal symmetry changes. To assess the tribological performance, ball-on-disc experiments are performed in combination with Raman scattering. A dependence of the friction coefficient on the annealing temperature and the layering of the MoS₂ is found. Furthermore, the MoS₂ typical needle-like structure and a denser morphology of the MoS₂ thin films compared to a DC sputtered reference are revealed by scanning-electron microscopy. A

Thursday Afternoon Poster Sessions, May 23, 2019

hexagonal crystallization structure and the crystallite size are evaluated from X-ray diffraction.

EP-ThP24 Friction Reduction in Sliding Between Si-DLC vs. Steel Ball by Ar Plasma Irradiation Using Microwave-excited Atmospheric Pressure Plasma Jet, T. Hibino, H. Kousaka (kousaka@gifu-u.ac.jp), T. Furuki, Gifu University, Japan; J. Kim, H. Sakakita, National Institute of Advanced Industrial Science and Technology (AIST), Japan

Diamond-like carbon (DLC) has widespread applications in many fields due to its excellent mechanical properties such as high hardness, low friction, chemical inertness, and so on. Recently, DLC is applied to machine parts as surface coating to improve frictional property. The interface between DLC and mating surface shows low friction through running-in period, in which shear strength at the interface decreases gradually; in other words, the interface between as-deposit DLC and mating surface does not show low-friction from the very beginning of sliding. Since high-friction during running-in period may cause severe damage to sliding interface such as the fracture of DLC coating, shortening of running-in period is desired. In our previous work, Okumura et al. investigated the influence of atmospheric He plasma irradiation to the sliding interface between a polyacetal ball and Si-doped DLC disk, demonstrating that the running-in period is shortened by plasma irradiation [1]. In this work, we further tried to use plasma irradiation for shortening the running-in period in the sliding between a steel ball and Si-doped DLC disk. A Si-doped DLC (a-C:H:Si) with a Si content of 27 at % was coated by using DC plasma enhanced chemical vapor deposition (PECVD) onto a steel disk (SUS304, JIS) 25 mm in diameter. The Si-DLC disk was slid against a stainless-steel ball (SUS440C, JIS) 8mm in diameter under dry condition at a normal load of 1 N and rotation speed of 0.67 m/s for 1800 m. During the initial sliding distance of 100 m, atmospheric Ar plasma was irradiated to the sliding track on the Si-DLC disk by using microwave-excited atmospheric pressure plasma jet [2]. In the case of plasma irradiation, friction coefficient decreased to 0.1 rapidly just after stopping the plasma irradiation and it was kept from 100 to 1800 m, or the end of sliding test; on the other hand, friction coefficient without plasma irradiation was always higher than 0.1 and fluctuated more largely from 100 m to 1800 m. It was shown in the sliding between a steel ball and Si-doped DLC disk that the plasma irradiation shortened the running-in period and decreased friction coefficient. (The authors gratefully acknowledge the funding by JST CREST, Japan.)

[1]. S. Okumura, et. al, Effect of plasma irradiation on the interface between DLC and plastic, ISPlasma2017 (2017), Paper No.04P80.

[2]. J. Kim, et. al, Microwave-excited atmospheric pressure plasma jet with wide aperture for the synthesis of carbon nanomaterials, Japanese Journal of Applied Physics 54, 01AA02 (2015).

EP-ThP26 Tribological Performance Dependence on Microstructure, Composition and Morphology of WTiN Coatings Obtaining by d.c. Magnetron Sputtering Varying the Working Pressure, R.F. Londoño, Universidad Nacional de Colombia Sede Manizales Colombia; R. Ospina, Universidad Industrial de Santander, Bucaramanga, Santander, Colombia; D. Escobar, J.J. Olaya Florez, Universidad Nacional de Colombia, Colombia; J.H. Quintero, Universidad Industrial de Santander, Colombia; E. Restrepo-Parra (erestrepopa@unal.edu.co), Universidad Nacional de Colombia Sede Manizales, Colombia

In this work, WTiN thin films were produced on silicon substrates using the D.C. magnetron sputtering technique varying the working pressure and keeping constant the working temperature and power at 25°C and 90W, respectively. The structure of the coatings were analyzed using techniques as X ray diffraction (XRD), that allows to identify a showed a non-stoichiometry β -W_xTi_yN_z phase, with high lattice parameter values (~4.3 Å) for samples grown at pressure of 0.27 and 0.67 Pa. Lattice parameter reduction for remaining samples is due to decrease in titanium content. Also was found relative low microstrain reaching values between 1.6% and 6.4 % and measured crystallite sizes between 12.8 nm and 82.8 nm. Highest microstrain values were for samples P1 and P2 due to re-sputtering processes, which is consistent with high defect content due to non-stoichiometry state. Using XPS, the chemical composition of the WTiN thin films was determined for the different working pressure. N1s, Ti2p, W4f, O1s and C1s peaks were identified and the W/Ti ratio was obtained showing values lower than the expected Ti/W = 10/90. Surface grain size and roughness (on average approximately 34 nm and 8.7 nm respectively) of coatings were determined using atomic force microscopy (AFM) and furthermore, for determining the tribological behavior, scratch and pin on disc tests were conducted. According to the results, the film grown at 0.27 Pa exhibited the best performance. This sample also presented lower

roughness, lower coefficient of friction and wear rate such behavior was attributed to the formation of wear debris, accumulated in the wear-track and acting as third-body particles.

EP-ThP27 Taguchi Method to Study Effects of Plasma Surface Texturing on Friction Reduction of Cast Iron at High Speed Sliding Lubricated Conditions, W. Zha, C. Zhao, R. Cai, X. Nie (xnie@uwindsor.ca), University of Windsor, Canada

Cathodic plasma electrolysis (CPE) is used to create surface texture on cast iron for the purpose of friction reduction. Micro craters formed by the explosion of gas bubbles can generate hydrodynamic force that separate two sliding surface, increase the oil film thickness and thus, decrease the friction. The Taguchi method is used to find the optimal process parameters (voltage and roughness) for surface texturing. The orthogonal array and the signal-to-noise ratio are employed to study the effect of each process parameter on friction. The results show that with higher voltage and lower roughness, the friction coefficient can be reduced to a lower value.

EP-ThP28 Discharge Behaviors of Plasma Electrolytic Oxidation in Porosol and Coating Characterization of Aluminum Alloy, W.X. Bo, W. Xiaobo (yize24@163.com), China Academy of Engineering Physics, China

Al₂O₃ coatings were fabricated on aluminum alloy by plasma electrolytic oxidation in porosol. The Discharge Behaviors of PEO and microstructure and composition of the coating were studied by SEM and EDS. The corrosion resistance was evaluated by potentiodynamic polarization techniques. The results show that the temperature raising obviously decreases the working voltage and increases the thickness of the coatings. The temperature has no effect on the coating phase and composition. While the coating fabricated in porosol (>80 degree) has a smaller roughness and a better corrosion resistance. This can widen the application on PEO technique.

EP-ThP30 Test Rig Development For Static Friction Assessment At High Temperature, M. Azzi (marwanazzi@ul.edu.lb), Lebanese University (UL), Lebanon; E.B-N. Bitar-Nehme, Tricomat, Canada; J.A. Schmitt, T.S. Schmitt, L. Martin, J.E. Klemberg-Sapieha, École Polytechnique de Montréal, Canada

The oil and gas industry uses steam-turbine power generation valves are vital equipment components that are used to control the flow of steam. Sealing surfaces in the valve must withstand high contact and friction stresses at high temperature. The main cause of valve failure is the degradation of sealing surfaces that can result in valves not cycling on demand due to high static friction. Development of materials or coatings with high tribological performance (high wear resistance and low friction) at high temperatures is the key for manufacturing valves with long service life.

In the present work, a novel experimental test rig has been developed to rigorously investigate the evolution of static friction in a tribological contact at high temperature in terms of holding time and contact stress. Pin-on-Flat configuration has been adopted in the design with the flat sample being mounted in a furnace that heats up to 800°C. The furnace moves vertically on a well-guided structure to bring the sample into contact with its counterface that moves in a linear motion generating friction.

Here, we present an approach to assess static friction, and we illustrate it by the results for stainless steel 304 and for Alumina counterface. The measurements showed that static friction increases with the number of passes to reach a plateau at 0.7 after a certain number of passes that depends on the contact stress. In addition, friction was shown to strongly depend on temperature and more importantly on the holding time at high temperature which might be related to processes such as diffusion that take place at the interface.

EP-ThP31 Improving the Tribological Performance of PVD-TiCN-Al₂O₃ Coating with Solid Lubricants for Maximum Wear Resistance, R.K. Gunda, Mahatma Gandhi Institute of Technology, India; U.M.R. Paturi, CVR College of Engineering, Hyderabad, India; S.K.R. Narala, BITS Pilani, India; S. Palaparty (palapartyshailesh@gmail.com), Methodist College of Engineering and Technology, India

The growing demand for green manufacturing to enhance the tribological properties has gaining extensive attention in industrial engineering. Applying negligible amount of lubricant under sliding interference is an appealing research direction. Another important variable is wettability of lubricants under sliding surface to decrease the rate of wear and frictional force under sliding surfaces. TiCN coating layer offers balanced combination of deformation resistance which offers abrasion resistance and crater wear resistance for high-speed machining. In the present work, TiCN-Al₂O₃ double-layered coatings were prepared by PVD-coating deposition. Tribology experimental investigations were performed under pin-on-disc tribometer under coated TiCN-Al₂O₃ and uncoated WC carbide pin material. X-ray

Thursday Afternoon Poster Sessions, May 23, 2019

diffraction (XRD), Scanning Electronic Microscopy (SEM) were employed to characterize the wear surface. The tribological studies demonstrated that significant improvement can be achieved by tribological properties of a green composite coating by incorporating MoS₂ nanoparticle additives into PVD-TiCN-Al₂O₃ coatings.

New Horizons in Coatings and Thin Films

Room Grand Hall - Session FP-ThP

New Horizons in Coatings and Thin Films (Symposium F) Poster Session

FP-ThP3 Influencing the Cubic to Wurtzite Phase Transition in Ti-Al-N by Reactive HiPIMS Deposition, L. Zauner, TU Wien, CDL AOS at the Institute of Materials Science, Austria; H. Riedl (helmut.riedl@tuwien.ac.at), TU Wien, Institute of Materials Science, Austria; T. Kozák, J. Čapek, University of West Bohemia, Czech Republic; T. Wojcik, TU Wien, Institute of Materials Science, Austria; H. Bolvardi, Oerlikon Balzers, Oerlikon Surface Solutions AG, Liechtenstein; S. Kolosvári, Plansee Composite Materials GmbH, Germany; P.H. Mayrhofer, TU Wien, Institute of Materials Science, Austria

High power impulse magnetron sputtering (HiPIMS) is often seen as one key-technology in the deposition of future hard and multifunctional coating materials. Through the introduction of high amplitude impulses at relatively low duty cycles, the amount of ionized species, either target near gas atoms or sputtered target atoms, can be increased drastically. These highly dense plasmas have various consequences on the film growth and hence coating properties, as well as on the sputter behavior of the target material itself. Applying reactive gas mixtures such as N₂/Ar atmospheres, e.g. for the deposition of TiN coatings, lead to further complex effects within the plasmas. However, several studies clearly highlighted the outstanding coating properties as well as metastable phases accessible, using HiPIMS compared to conventional DC magnetron sputtering, whereas a majority of these investigations concentrate on the plasma physics itself. Therefore, we focused in this study on the reactive HiPIMS deposition of Ti-Al-N coatings using Ti_{1-x}Al_x compound targets (x = 0.40 between 0.70) in mixed Ar/N₂ atmospheres. The influence of the HiPIMS parameters such as frequency, pulse length, or synchronized bias potentials, but also of the deposition parameters like partial pressure, deposition temperature, or total pressure were investigated methodically. The so obtained coating structures were analyzed with respect to phase stability, thermomechanical properties, and morphology applying nanoindentation, X-ray diffraction combined with electron imaging techniques (SEM and HR-TEM). In addition, to correlate the observed phase stabilizing effects in relation to the deposition parameters various plasma analysis methods have been applied. Especially, the amount and type of ionized species was quantified for specific parameter settings utilizing mass spectroscopy.

FP-ThP5 e-Poster Presentation: Vacancies to Compensate for Electronic Imbalances in Crystals, M. Fischer (maria.fischer@empa.ch), D. Scopece, M. Trant, C.A. Pignedoli, K. Thorwarth, D. Passerone, H.J. Hug, Empa - Swiss Federal Laboratories for Materials Science and Technology, Switzerland

The elements Al, Si, O and N can be combined to yield hard and transparent thin coatings. The binary combination AlN readily adopts the hexagonal crystal structure of wurtzite in thin films deposited by reactive direct current magnetron sputtering (R-DCMS). Si and O can be added to form the ternary combinations Al-Si-N and Al-O-N. Si up to 6% and O up to 8% integrate into wurtzite crystallites in the form of a solid solution. For 6-30% Si and 8-35% O, a nanocomposite forms, and higher Si / O contents lead to a fully amorphous coating.

In the crystalline solid solution regime, Si replaces Al on cationic lattice sites, while O replaces N on anionic lattice sites. Despite the different nature of these two substitutions, they induce the same microstructural evolution in the thin films. The underlying mechanism is hypothesized to be the formation of Al vacancies (V(Al)) in both cases. A model explaining this mechanism has been developed and corroborated theoretically and experimentally with *ab initio* calculations, entropic considerations, X-ray diffraction and positron annihilation lifetime spectroscopy.

FP-ThP6 Role of the Thermalized Ions in the Reduction of the Atomic Shadowing Effect in HiPIMS, J.C. Oliveira (joao.oliveira@dem.uc.pt), F. Ferreira, University of Coimbra, Portugal; A. Anders, Leibniz Institute of Surface Engineering, Germany; A. Cavaleiro, University of Coimbra, Portugal Traditionally, the most influential deposition parameters regarding both bombardment and shadowing effect in magnetron sputtering-based

deposition processes are the deposition pressure and substrate biasing. In constant power mode, decreasing the process pressure results in an increased discharge voltage and less collisions with gas atoms and molecules and thus it increases the average energy of the sputtered species. On the other hand, the high-angle component of the angular distribution of the impinging species, as measured relatively to the substrate normal, also decreases thus weakening of the shadowing effect. Substrate biasing allows us to bombard the growing film with ions extracted from the plasma with an energy proportional to the applied voltage (and ion charge state). This triggers re-sputtering if a high enough voltage is used. However, the vast majority of the sputtered species in magnetron sputtering are neutrals, not ions, and thus mostly Ar ions are involved in re-sputtering.

Additional control of the bombarding flux can be obtained by ionizing the sputtered flux because ions can be controlled with respect to their energy and impinging direction. In the last decade, High-Power Impulse Magnetron Sputtering (HiPIMS) has been popularized for this purpose. In a previous paper it was shown that Deep Oscillation Magnetron Sputtering (DOMS), a variant of HiPIMS, allowed us to overcome the shadowing effect and, thus, to deposit Cr thin films with much smoother surfaces and densely packed columns even at relatively high pressure (up to 1 Pa). The main objective of the present work is to identify the mechanisms which effectively decreases the shadowing effect in DOMS. For this purpose, the deposition conditions and properties of two Cr films deposited by DOMS at higher pressure and DCMS at lower pressure were studied and compared. In both cases the energy distributions of the energetic particles bombarding the substrate during film growth were evaluated by energy-resolved mass analysis (ERMS) and the angular distribution of the Cr species impinging on the substrate was simulated using Monte Carlo-based programs. The microstructure, structure and mechanical properties of the deposited Cr films were characterized by SEM and AFM, X-Ray diffraction and nano-indentation.

FP-ThP7 Study of the Self-organizing Structures in Magnetron Plasma by a Pseudo 3D Model, A. Revel (adrien.revel@u-psud.fr), Université Paris-Sud/CNRS, France; T. Minea, Université Paris-Sud, Université Paris-Saclay, France; M. George, B. Vincent, CNRS, France; S. Tsikata, CNRS, ICARE, France Magnetron plasma and Hall thrusters are magnetized plasma which presents common feature such as the formation of self-organizing structures rotating over the central axis. The, so called, spokes appear both in direct current (DC) and high power impulse magnetron sputtering (HiPIMS) and they can be at the origin of the abnormal electron transport. The spokes are only visible using fast camera (100 ns), the plasma appearing homogeneous otherwise.

Because this phenomenon is intrinsically 3D, the numerical modeling of the spokes needs to take into account all the three space dimensions. However, a straight 3D Particle-in-Cell modeling of the magnetron discharge is not feasible due to the computation cost. Hence, we developed a *pseudo* 3D approach which allows to follow the spoke formation and behavior in the three dimensions with a reasonable computation time. The results undoubtedly show high frequency instabilities lying in the range of MHz, in addition to centimetric space structured plasma as previously observed by other groups.

In addition, Incoherent and Coherent Thomson Scattering (ITS and CTS) experimental techniques have been successfully used to measure the electron density, temperature and its fluctuations in the magnetized region without disturbing the plasma. The measurements found the same MHz fluctuations as the modeling for plasma electrons, which is compatible with the electron cyclotron drift instabilities.

Particle modeling results show the microscopic information missing from almost all experiments, particularly on the electron energy distribution function, the ionization region of the spoke, the trajectories of confined electrons, the space distribution of the electric field, etc. Also, macroscopic information can be obtained, such as spoke velocity that is in good agreement with the experiments reported in the literature. Moreover, the variation of this velocity during the pulse (current rise) is presented and commented.

FP-ThP9 Point Ion Beam Sputtering for Novel Applications, V. Bellido-Gonzalez (victor@gencoa.com), D. Monaghan, R. Brown, Gencoa Ltd, UK; D. Perry, Quorum Technologies, UK; J. Brindley, A. Azzopardi, Gencoa Ltd, UK Sputtering (magnetron sputtering and ion beam sputtering) is widely used to deposit coatings onto substrates. Ion beam sputtering utilizes an ion source to generate an ion beam which sputters the target. This work will show a grid/filament-less point ion source recently developed for ion beam sputtering of small targets. The point ion source being small in size together with the low target material cost makes it suitable for research and

Thursday Afternoon Poster Sessions, May 23, 2019

development. It also has a number of novel applications, including high quality biological specimen preparations for electron microscope examination, multilayer or multicomponent coating deposition using rotating targets, integrated into minimal fab systems for revolutionary microelectronics, etc. In this work, point beam sputtering for microscope specimen preparations will be addressed. Metal and compound coatings will be deposited onto silicon and latex nanoballs at varied conditions. Optimal coating conditions for fine coating structures will be obtained. The coatings will be assessed by atomic force microscopy and scanning electron microscope, and will be compared with those prepared by magnetron sputtering in terms of surface morphology.

FP-ThP10 Reducing the Intrinsic Stress of TiN Films in HiPIMS, F. Cemin, LPGP, Université Paris-Sud, Orsay, France; G. Abadias (gregory.abadias@univ-poitiers.fr), Institut Pprime - CNRS - ENSMA - Université de Poitiers, France; T. Minea, D. Lundin, LPGP, Université Paris-Sud, Orsay, France

TiN is one of the most common hard coatings with applications in high-speed steel cutting tools and drill bits due to its high hardness and high wear resistance. It is also used in semiconductor devices as a diffusion barrier as well as anti-reflective or adhesion-promoting layers. It is well known that the stress levels acquired during TiN growth by ionized physical vapor deposition (IPVD) often lead to premature failure and delamination of the coated tool or device. Hence, the stress can drastically limit the industrial appeal of deposition technologies such as high power impulse magnetron sputtering (HiPIMS). Moreover, reducing stress through structure modification is required to enhance the performance and lifetime of components coated with compound-based films. Therefore, the purpose of this work is to identify HiPIMS process conditions for reduced intrinsic stress of TiN films by controlling the quantity, energy, charge state, and chemical nature of the incident ions, *i.e.*, inert gas vs. metal, which are impinging on the substrate during film growth.

Different discharge conditions comprising high and low energy ion bombardment as well as different substrate bias configurations (DC or pulsed bias synchronized or delayed with respect to the HiPIMS discharge pulse) were investigated. The intrinsic stress evolution during TiN growth was monitored *in situ* by wafer curvature measurement using a multi-beam optical stress sensor (MOSS). The results show that for standard HiPIMS discharges and biased substrates, the energetic metal ion irradiation during film growth results in dense but highly stressed TiN films (~11 GPa), which is not unexpected for refractory films. On the other hand, when using less energetic HiPIMS discharges and pulsed-biased substrates synchronized to the HiPIMS pulse, the compressive stress was considerably reduced (between 0 and -1 GPa). Although slightly less dense structures are observed in this latter case, the films are still significantly denser than TiN films deposited by direct-current magnetron sputtering (DCMS) under similar conditions.

FP-ThP11 Study on Tribological Behavior of ZrB₂-Zr Coatings Deposited on Ti6Al4V and CoCrMo Alloys by HiPIMS, L. Flores-Cova (luis.fcova@alumnos.udg.mx), O. Jiménez, M. Flores, J. Pérez-Alvarez, Universidad de Guadalajara, Mexico

CoCrMo alloys are used due to their high wear and relatively high oxidation resistance, whereas Ti6Al4V is widely used in orthopedic and dental implants due to their excellent corrosion resistance and biocompatibility. Nevertheless, the main disadvantage of titanium alloys is their poor wear resistance. Consequently, many coating systems have been deposited on these alloys in order to improve their wear resistance. In this study ZrB₂-Zr coatings were deposited by High Power Impulse Magnetron Sputtering (HiPIMS) under a selection of parameters. The thickness and the growth morphology of the films were studied from cross-sectional SEM images. The structure of the coatings was analyzed by XRD technique. The mechanical properties (hardness and Elastic Modulus) were studied through nanoindentation techniques. The adhesion of coatings to the substrate was measured by means of scratch tests. Wear tests were performed using a tribometer with a reciprocating sliding motion, using a 10 mm diameter Al₂O₃ ball, frequency of 1 Hz, a stroke length of 10 mm, sliding time of 30 minutes and at different normal loads (0.5, 1 and 1.5 N). The wear tracks were analyzed by optical profilometry. In general, the thickness of the coatings resulted between 1 and 2 μm. Hardness on the other hand, was found to be above 20 GPa and wear results showed a better resistance of coatings in comparison to substrates.

FP-ThP12 SPS of Al-CNTs-Nb Nano-Composite for Power Transmission Conductor Core, C.O. Ujah (omega.ujah@gmail.com), P.A. Popoola, O.M. Popoola, Tshwane University of Technology, Pretoria, South Africa

In powder metallurgy, conventional sintering is challenged with grain growth and formation of voids which result in the depreciation of the characteristics of the developed material. Spark Plasma Sintering (SPS) has the potentials of addressing these challenges, according to researchers. The bulk nature of Aluminium can be partially modified by the addition of a small amount of reinforcement to alter the matrix thus producing an advanced material with superior properties. Hence, this work involves SPS of Aluminium-Carbon nanotubes-Niobium composite for application in power transmission conductor core. Taguchi Design of Experiment (DOE) was used in designing the experiment where two factors were randomized at three levels to generate nine experimental samples. As-received nanopowders were mixed with tubular mixer at dry mode and sintered with SPS machine at the sintering parameters of 600°, 50 MPa, 5 mins, 200°/mins. The sintered samples were sand-blasted to clean graphite contamination and cut into sizes for characterisation. The thermal test was conducted with Thermogravimetric Analyser; the Electrical conductivity was measured with a Four-Point Probe meter. Results were analysed with ANOVA and Regression equations generated include: Thermal stability (Deg. C) = 430.24 + 8.395 CNTs% + 6.305 Nb%; Electrical conductivity (MS/m) = 0.224 + 1.26e-4 CNTs% + 3.15e-4 Nb%. Al-8CNTs-8Nb was the best thermally stable composite at 562° while the electrical conductivity increased from 0.224MS/m to 0.230MS/m. This composite can serve as a robust material for power conductor core due to its good thermal and electrical properties and low density.

FP-ThP15 Temperature Dependent Photoluminescence Emission and Resonance Raman Spectra from WS₂ Nanostructures, nil. Sharma (shivanisha18@gmail.com), Guru Nanak Dev University Amritsar India, India

Recently, two-dimensional transition metal di-chalcogenides (TMDCs) of the type MX₂ (M= Mo or W and X = S, Se or Te) have attracted worldwide attention due to their exceptional physical properties [1]. These materials have layered structure with weak Van der Waals forces, enabling their easy exfoliation. These materials possess an indirect band gap in bulk form and a direct band gap in monolayer form. Due to the larger atomic size of transition metal atom, they possess large spin-orbit coupling enabling their use in spintronics devices. Their tunable band gap, larger spin-orbit coupling and high surface area to volume ratio make them favourable for photovoltaic, optoelectronic, sensing and spintronics devices [3]. Recently, photoluminescence emission from MoS₂ and WS₂ nanostructures has been reported [2-3]. But studies investigating the impact of various factors, such as temperature on the emission properties are rare.

In present work, we will report one step synthesis of the WS₂ nanostructure. The resonance Raman spectra from these nanostructure reveals various higher order modes. The photoluminescence emission from these nanostructures displayed linear temperature dependence in the range 293 K to 363 K. The negative temperature coefficients are very small and may arise from anharmonicity and thermal expansion. Weak red-shift displayed by emission spectra is attributed to anharmonic effects in the lattice.

References:

1. Andre. Geim and Kostya Novoselov "The rise of graphene" **6**, (2007): 183–191
2. Qing Hua Wang, Kourosh Kalantar-Zadeh, Andras Kis, Jonathan N. Coleman and Michael S. Strano " Electronics and optoelectronics of two-dimensional transition metal dichalcogenides" *Nature Nanotechnology* **7** (2012): 699-712
3. A. Kuc, N. Zibouche, and T. Heine *Phys. Rev. B* **83**(2011): 245213

FP-ThP16 Detecting the Direction of a Magnetic Field with a Nanocrystallited Carbon Film by Using its Anisotropic Magnetoresistance and Hall Effect, C. Wang (cwang367@szu.edu.cn), T. Huang, W. Zhang, J. Guo, X. Dai, Institute of Nanosurface Science and Engineering, College of Mechatronics and Control Engineering, Shenzhen University, China

The graphene nanocrystallited carbon film has been found not only with low friction performance and fast run-in behavior, but also with unique magnetic properties and room temperature magnetoresistance (RT-MR). Compared to magnetic alloys and rare earth semiconductors which are mostly used as magnetic sensitive materials, nanocrystallited carbon films are much lighter, cheaper, and possess better mechanical properties such as higher hardness, better flexibility and less friction coefficient, which make it an ideal candidate for next generating magnetic sensors in micro/nano-

Thursday Afternoon Poster Sessions, May 23, 2019

electromechanical systems and wearable devices. Therefore it is of great significance to explore carbon films with better RT-MR behaviors. In recent study, it has been found that the RT-MR performance of graphene nanocrystallized film is originated from its self-magnetism enhancement, and is highly related to the relative angles between the orientations of graphene layers inside the film and the external magnetic field. This gives us an inspiration that the graphene nanocrystallized carbon film can be utilized to detect the direction of magnetic field, which may lead to its further applications as an carbon based angle sensor or spin rate sensor.

In this study, graphene nanocrystallized carbon films were deposited with plasma assisted PVD method, and the orientation of nanocrystallites were demonstrated with high resolution TEM images. The TEM results showed that the graphene nanocrystallites aligned perpendicular to the growing direction of the film, which is vertical to the substrate plane. The hall effect and magnetoresistance were measured under different directions of magnetic field with respect to the film surface. The results showed that the hall voltage and film resistance varied periodically as the film rotated along its surface axial, exhibiting a sinusoidal trend for hall voltage, and absolute value of a sinusoidal trend for magnetoresistance. In room temperature, the angle resolution of the film was better than 2 degree, and the largest changing rate of the film resistance can reach 200%. The mechanism of this performance was investigated through electrical transport measurement and magnetic Raman spectra, as well as magnetic hysteresis loops, which revealed the spin-enhanced magnetism of the nanocrystallites were the main origin of this anisotropic magnetic response behaviors.

FP-ThP17 Effect of Synchronized Bias on the Oxygen Content in r-HiPIMS Deposited γ -Al₂O₃ Thin Films, S. Kagerer (stefan.kagerer@tuwien.ac.at), TU Wien, Institute of Materials Science, Austria; S. Kolosvári, Plansee Composite Materials GmbH, Germany; T. Kozák, J. Čapek, P. Zeman, University of West Bohemia, Czech Republic; H. Riedl, TU Wien, Institute of Materials Science and Technology, Austria; P.H. Mayrhofer, TU Wien, Institute of Materials Science and Technology, Österreich, Austria

Reactive high-power impulse magnetron sputtering (r-HiPIMS) is a highly complex but also versatile PVD based deposition technique establishing a broad field of parameters influencing thin film growth in general. Especially, for the synthesis of alumina-based polymorphs, such as cubic (γ) or corundum (α) type crystals, r-HiPIMS allows for novel approaches to overcome the thermodynamic barrier stabilizing α - or γ -Al₂O₃ crystals at feasible deposition temperatures. During conventional magnetron sputtering, the excellent properties of γ -Al₂O₃, such as thermomechanical resistance or chemical inertness, are usually unattainable due to the formation of nano crystalline or even amorphous structures. In addition, target poisoning and hence instable process accompanied by the formation of non-stoichiometric Al₂O₃ strongly limits the deposition of alumina-based coatings.

Therefore, within this study we combine two novel approaches depositing highly crystalline and stoichiometric γ -Al₂O₃ thin films by means of r-HiPIMS depositions. One of the key issues during HiPIMS is the ionization of ejected target species leading especially in reactive atmospheres to specific time resolved mass spectra. Here, the separation of metal and gas ions is most important, allowing for targeted species selection by specific synchronized bias impulses. Based on time resolved mass spectroscopy, a promising time window could be established, suggesting for a maximum amount of ionized oxygen compared to all other species – e.g. Ar⁺ and Al⁺. To validate the positive effect of synchronized bias impulses four different target to bias on-time variations have been deposited. Based on former studies, we additionally utilized transition metal alloyed Al_{1-x}TM_x targets (x = 2 at.% TM = Cr or W) – retarding the poisoning behaviour in oxygen rich atmospheres – for specific on-time variations. The so obtained coatings have been analyzed with respect to phase formation and chemistry applying X-ray diffraction combined with electron imaging techniques (SEM, EDS and HR-TEM).

FP-ThP18 Effect of Secondary Phases on the Thermoelectric Properties of Zn₂GeO₄ Thin Films Grown by Thermal Evaporation on Au Coated Si Substrate, K. Mahmood (khalid_mahmood856@yahoo.com), Government College University Faisalabad, Pakistan

This study reported the growth of Zn₂GeO₄ thin films on Au coated Si substrate by thermal evaporation technique using vacuum tube furnace. The thermoelectric properties of nano-crystals were improved by generating the secondary phases in the grown samples using the post-growth annealing at various temperatures (600-900 °C). The low energy carriers filtered out at the interface of secondary phases and caused an enhancement in Seebeck coefficient and power factor. The emergence of secondary phases with

annealing temperature was confirmed by various characterization techniques. XRD data suggested that samples annealed at 800 and 900 °C consisted of three extra secondary phases along with the phases related to Zn₂GeO₄, ZnO, Si and Au. Raman spectroscopy data demonstrated the presence of strong peak due to Si substrate for all samples but two weak peaks appeared at 375 and 800 cm⁻¹ for samples annealed at 800 and 900 °C. The SEM images shows the presence of randomly oriented nano structures as annealing temperature increase up to 900°C. The Hall measurements were also performed to strengthened our argument.

Surface Engineering - Applied Research and Industrial Applications

Room Grand Hall - Session GP-ThP

Surface Engineering - Applied Research and Industrial Applications (Symposium G) Poster Session

GP-ThP1 Effect of Plasma Nitriding and Modulation Structure on the Adhesion and Corrosion Resistance of CrN/Cr₂O₃ Coating, C.H. Huang, C.H. Yang, Y.J. Tsai, C.L. Chang (clchang@mail.mcut.edu.tw), Ming Chi University of Technology, Taiwan

The increasing demand for high performance coatings has led to the production of coatings which are becoming more sophisticated in terms of their engineered microstructure and properties. An extensive interest of high power impulse magnetron sputtering (HiPIMS) as a novel PVD technology in academia and industry owing to their dense and smooth coatings properties when compared to traditional PVD technologies. However, the adhesion strength still not insufficient, therefore a plasma nitriding process is introduced before the HiPIMS process. On the other hand, the carbon steel has a very poor corrosion resistance in an atmospheric environment, which one is needed to solve by various surface treatment technologies in environmentally friendly.

In this study, a continuous process combines both vacuum plasma nitriding and HiPIMS CrN/Cr₂O₃ multilayered coating technology is used. Before CrN/Cr₂O₃ multilayer coating, the vacuum plasma nitriding is carried out at different nitrogen flow rate for 1~5 h with a bias output of HiPIMS power between 0.5 and 2.5 kW, which is at a fixed temperature of 400°C. After that CrN/Cr₂O₃ multilayer films with different bi-layer thickness were deposited onto carbon steel and silicon p-type (100) wafer substrates at 400°C. Using Cr targets with a nitrogen (or oxygen)/argon flow ratio of 0.2, by high power impulse magnetron sputtering technique. The bi-layer thickness was varied by time-controlled with a switch in between the nitrogen and oxygen to obtain different nanoscale multilayered period thickness. The modulation structure characteristics of the CrN/Cr₂O₃ multilayer films between 100 nm to 5 nm were systematically investigated. The results have demonstrated that both the nitriding effect and the modulation period (Λ) was strongly to affect adhesion strength between carbon steel and the coating. In addition, the corrosion resistance of carbon steel is strongly improved by the CrN/Cr₂O₃ multilayer film.

GP-ThP2 Study on SiN and SiCN Film Production using PE-ALD Process with High-density Multi-ICP Source at Low Temperature, H. Song (shh817@kaist.ac.kr), H.Y. Chang, Korea Advanced Institute of Science and Technology, Republic of Korea

SiN and SiCN film production using plasma-enhanced atomic layer deposition (PE-ALD) is investigated in this study. A developed high-power and high-density multiple inductively coupled plasma (multi-ICP) source is used for a low temperature PE-ALD process. High plasma density and good uniformity are obtained by high power N₂ plasma discharge. Silicon nitride films are deposited on a 300-mm wafer using the PE-ALD method at low temperature. To analyze the quality of the SiN and SiCN films, the wet etch rate, refractive index, and growth rate of the thin films are measured. Experiments are performed by changing the applied power and the process temperature (300–500 °C).

GP-ThP3 PEO Coatings for Adhesive Bonded Aluminium Structures, D. Shore (dominic.shore@postgrad.manchester.ac.uk), A. Rogov, A. Matthews, A. Yerokhin, The University of Manchester, UK

Plasma Electrolytic Oxidation (PEO) has received much attention in research for the production of oxide coatings with excellent tribological performance and corrosion resistance. This study looks into a further application of PEO as an alternative to conventional anodizing techniques for the preparation of aluminium for adhesive bonding. Conventional anodizing processes have been applied to adhesive bonded aluminium components to promote

Thursday Afternoon Poster Sessions, May 23, 2019

increased bond durability tracing back to the first half of the 20th century. However, Conventional anodizing procedures generally use strongly acidic electrolytes which have a substantial environmental impact. Anodizing procedures are generally multi-stage processes which can be resource intensive and time consuming. PEO offers an alternative route for the production of well adhered oxide coatings where weak alkaline electrolytes can be utilised in place of the highly acidic electrolytes associated with conventional anodizing processes. PEO has the further potential to reduce the number of additional treatments prior to and after the anodizing stage offering scope for resource and time saving. To provide bond durability comparable to that offered by the conventional anodizing techniques currently used, PEO coatings must promote sufficient mechanical interlocking and physical/chemical affinity between the surface and adhesive in addition to good corrosion resistance.

Work has been carried out on the optimisation of PEO coatings on aluminium alloys with regards to the application of adhesion bonding. Through the use of varying processing parameters and different electrolyte compositions, coatings with properties designed to promote enhanced bond strength are being developed. Topological features of the developed PEO coatings, including surface porosity which is important for the promotion of mechanical interlocking in the adhesive bond have been analysed. Chemical analysis of the surface composition of the oxide and the adsorption groups formed at the oxide/adhesive interface has been carried out to deduce the chemical nature of the adhesive bonding occurring on PEO coatings formed under different conditions. As a result, a scientific description as to how the surface features of PEO coatings contribute to adhesive bond durability is being summated, which will lead to further optimisation of PEO coatings for this application.

GP-ThP5 Hydrogen Barrier Coatings Deposited by Magnetron Sputtering: A Study of Different Oxide Materials and Their Microstructure on the Hydrogen Permeability Properties, S. Gimeno (sofia.gimeno@fersa.com), Fersa Bearings, Spain; J.A. Garcia, Universidad Publica de Navarra, Spain; I. Quintana, L. Mendizabal, C. Zubizarreta, Physic of Surfaces and Materials Unit, IK4 – TEKNIKER, Spain

White Etching Cracks (WEC) is the main cause of premature failure on bearings used in wind turbine sector. This premature failure mode is still under debate due to the lack of a clear theory about how it is produced and which are the factors involved in the WEC damage. One of the most important theories is based on Hydrogen embrittlement, due to hydrogen diffusion in steel under rolling contact fatigue (RCF) [1].

The development of novel surfaces which are able to avoid or delay the diffusion of Hydrogen would be considered as a key point to solve the WEC problem. In this study, films based on WO₃, SiO₂ & Al₂O₃ oxides grown by pulsed dc magnetron sputtering have been designed to act as barrier to Hydrogen permeation, delaying or avoiding the diffusion of this in 100Cr6 steel. The objective of this study is to analyze the behaviour of the different oxide materials, as well as the influence of the morphology of coatings on the permeation of Hydrogen.

WO₃, SiO₂ & Al₂O₃ thin films were deposited on 100Cr6, Niquel and silicon substrates. The adhesion, microstructure and crystal structure of oxide films were investigated and correlated with barrier properties against hydrogen permeation.

Hydrogen permeability of different films was studied using differential pressure method described in ISO 15105-1:2007. Nickel was used as substrate due to the known and high permeability of this material to hydrogen.

GP-ThP6 Process for Obtaining TiO₂/SiO₂ Systems using Magnetron Sputtering RF from Ceramic Targets: Studies on their Anti-Reflective Response, D. Zambrano (dario.zambrano@ug.uchile.cl), R. Villarroel, R. Espinoza, Universidad de Chile, Chile

Nanostructured systems of SiO₂ and TiO₂ produced by magnetron sputtering technique have allowed the development of optical filters that maximize the conversion of light in different devices and applications [1–4]. The anti-reflective coatings (ARCs) of SiO₂ / TiO₂ systems allow obtaining a greater contrast and better image quality in applications such as TV screens, cell phones, projectors, among others. In addition, they improve the quantum efficiency in photovoltaic panels, increasing the power generation capacity [5].

In this research nanostructured films composed by multilayer stacking of SiO₂ and TiO₂ were studied, considering the working pressure and the partial pressure of O₂ as variables for the modification of the microstructure of each

monolayer and the influence on the anti-reflective response of the multilayer SiO₂/TiO₂ system.

The nanostructured layers of TiO₂ and SiO₂ were synthesized by magnetron sputtering RF, using ceramic targets of TiO₂ and SiO₂. The modulation of the optical performance of the ARCs were measured using spectrophotometry and ellipsometry. On the other hand, the microstructure of the ARC's was obtained using FE-SEM, AFM, XRD, and FTIR.

REFERENCES

- [1] M. Mazur, D. Wojcieszak, D. Kaczmarek, J. Domaradzki, S. Song, D. Gibson, F. Placido, P. Mazur, M. Kalisz, A. Poniedzialek, Functional photocatalytically active and scratch resistant antireflective coating based on TiO₂ and SiO₂, Appl. Surf. Sci. 380 (2016) 165–171. doi:10.1016/j.apsusc.2016.01.226.
- [2] M.A. Green, S.P. Bremner, Energy conversion approaches and materials for high-efficiency photovoltaics, Nat. Mater. 16 (2016) 23–34. doi:10.1038/nmat4676.
- [3] S. Chu, Y. Cui, N. Liu, The path towards sustainable energy, Nat Mater. 16 (2017) 16–22. doi:10.1038/nmat4834.
- [4] H.K. Raut, V.A. Ganesh, A.S. Nair, S. Ramakrishna, Anti-reflective coatings: A critical, in-depth review, Energy Environ. Sci. 4 (2011) 3779– 3804. doi:10.1039/c1ee01297e.
- [5] W.-J. Ho, J.-C. Lin, J.-J. Liu, W.-B. Bai, H.-P. Shiao, Electrical and Optical Characterization of Sputtered Silicon Dioxide, Indium Tin Oxide, and Silicon Dioxide/Indium Tin Oxide Antireflection Coating on Single-Junction GaAs Solar Cells, Materials (Basel). 10 (2017) 700-709. doi:10.3390/ma10070700.

GP-ThP7 Microstructure Evolution of Overlay Welded Duplex Stainless Steel Joints, P.A. Luchtenberg (paolaluchtenberg@gmail.com), R. Torres, P. Soares, P. Campos, Pontificia Universidade Católica do Paraná, Brazil

Duplex stainless steels have a good mechanical properties, wear and corrosion resistance and fatigue strength. This material have a higher price compared to austenitic steel, in some cases to lower the cost, companies use low carbon steel or low alloy coated with duplex stainless steel, than this material can be employed through overlay welded coatings on mild steel components and equipment. In this work, the aim was to evaluate the overlay properties obtained through deposition of ER 2209 duplex stainless steel alloy on a mild steel ASTM A 516 Gr 60. The deposition was performed through GMAW welding process. The coatings were deposited using four heat input levels, which showed influence in phase balance in weld metal austenite/ferrite morphology. Microstructural characterization by optical microscopy and quantification of ferrite by ferritscope, showed that heat input, cooling rate and grain size influences on the formation of secondary phases, because this type of phase precipitate from ferrite or primary austenite. The reheating change the microstructure influencing positively or negatively in corrosion behavior of DSSs. The secondary austenite that precipitates due to the welding process in DSSs are grain boundary austenite (GBA), Widmanstätten austenite (WA), partially transformed austenite (PTA) and intragranular austenite (IGA) and each of them has their characteristic precipitation, like temperature, grain size, cooling rate. However, the corrosion resistance can be avoided by means of appropriate welding procedures and the phase control such as ferrite/austenite balance.

GP-ThP8 Deposition of Diamond-like Carbon Films on Interior Surface of a Metallic Tube with High Aspect Ratio, E.J.D. Mitma Pillaca (mitma.elver@gmail.com), National Institute for Space Research - INPE, Brazil; V.J. Trava-Airoldi, National Institute for Space Research, Brazil; M. Ramirez, University of Vale do Paraiba, Brazil

Recently, we have studied the growth of DLC film on the inner surface of a stainless steel AISI 304 tube with high aspect ratio (length/diameter = 20) by using the Plasma Enhanced Chemical Vapor Deposition (PECVD) technique. In this configuration, a tube with 200 cm in length and 10 cm in diameter was used as a reactor. The inlet and the pumping of the gas is performed by both side of the tube-ends. Thus, in the present work are reports the results about the effect of the pulse width on the plasma discharge and on the adherence of DLC film. The coating was performed by using the pulsed-DC PECVD technique and the acetylene gas, as precursor. Five samples of AISI 304 were distributed longitudinally on the tube inner for the film growth and subsequent characterization. The system was pumped down to a base pressure of 10⁻⁴ Torr by a set of mechanical and diffusion pump. The working pressure was kept constant at approximately 3 mTorr in all the experiments. The voltage was kept at 1 kV (SiH₄ plasma) and at 0.7 kV (Ar and C₂H₂ plasma). The repetition rate was 21 kHz whereas the pulse width was varied from 5 to 20 μs. Various results were obtained: (a) high voltages can be applied by using lower pulse width; (b) the confinement of the plasma is affected; (c)

Thursday Afternoon Poster Sessions, May 23, 2019

the temperature on the tube surface was reduced significantly during the plasma discharge; (d) amorphous carbon hydrogenated (a-C:H) films with a remarkable improvement on the adherence of the DLC film were obtained. Results of Raman scattering spectroscopy have shown dependence of structure and quality of the DLC film with the longitudinal distribution.

GP-ThP11 Ion Beam Assisted Deposition of DLC for Sheet Metal Forming Tools, L.P. Nielsen (lpn@dti.dk), K.P. Almqvist, C.S. Jeppesen, C. Mathiasen, P.M. Pedersen, Danish Technological Institute, Denmark

A deposition process combining high-energy ion implantation of chromium ions into a condensing Fomblin-oil has been developed and characterized. The composition of the IBAD-DLC film was measured by RBS and contain a mixture of elements (C, H, O, F and Si) from the condensing oil (Penta Phenyl Trimethyl Trisiloxane) besides the impinging high-energy Cr ions. The friction properties have been evaluated by pin-on-disk to be below 0.05. The hardness of the IBAD-DLC was measured to 10.7 GPa. Hardness, scratch tests and friction properties will be compared with PVD-based DLCs. Examples of different industrial applications of the IBAD-DLC coating in connection with sheet metal forming in the food sector will be presented.

GP-ThP12 Laser-clad Induced Reaction Synthesis of TiC/WC Reinforced Co-based Composite Coatings on Copper Alloy, H. Yan (yanhua@foxmail.com), P.L. Zhang, Shanghai University of Engineering Science, China

Co-based composite coatings reinforced by nickel coated WC (Ni/WC) and in-situ synthesized TiC particles has been fabricated from precursor mixtures of HG-Co01(Co-based alloy), Ni/WC, graphite and pure titanium powders by laser cladding on Cr-Zr-Cu alloy substrate. The microstructure, phase and wear properties were investigated by means of optical microscopy (OM), X-ray diffraction (XRD) and scanning electron microscopy (SEM), as well as dry sliding wear test. Results show that reinforcements dispersed uniformly in the Co-based matrix. TiC showed the morphology of dendritic and particle. During laser-clad processing, the laser heating effect caused inter-diffusion action between the precursor mixtures and generated Ti_xC_y and some Ti element diffused into Ni/WC particles formation of $TiWC_2$ alloyed layer. The laser-clad TiC/WC reinforced Co-based composite coatings exhibited higher microhardness and better wear resistance than copper alloy. The highest microhardness was up to 1007 HV0.2 which was improved 8 times comparing to the Cr-Zr-Cu substrate. The friction coefficients of the laser-clad composite coatings were reduced significantly to about 0.15 and relatively smooth wear surface could be observed.

GP-ThP13 Effect of Interaction between Microbial Fluid and Electrode on Performance, Y.C. Liu (jack21324@gmail.com), Y.-C. Yang, National Taipei University of Technology, Taiwan

For the electrode reaction controlled by electron transfer, the electrode material has a great influence on the reaction rate. In terms of the material's conductivity, the reaction rate of the MFC will be improved by the high electron conductivity of the anode and the cathode. About the electrode area, as the electrode reaction is carried out at the electrode-solution interface, the reaction rate will be proportional to the electrode area, so a high surface area of the electrode development is extremely important. In addition, the metal surface modification, in order to develop a corrosion-resistant and highly collectible metal electrode modification is also an important research topic.

Electrodes of the Microbial fuel cell whether used in sewage treatment plants or marine rivers or lakes, the purpose of the production of electricity will be associated with the behavior of the fluid. Fluid behavior for the system efficiency and electrode usefulness would have a great impact. In this study, we focused on the interaction of microfluidic fluids with multi-morphological metal electrodes in the system. Through the observation of fluid mechanics and numerical simulation, we hope to understand the interaction between fluid and electrode, understand the interaction between bacteria and electrodes.

GP-ThP15 Design of Low-Pressure Chemical Vapor Deposition Reactors Using Vertical Cavity Surface Emitting Lasers, S. Park (spark@hongik.ac.kr), Y. Noh, Y. Kim, Hongik University, Seoul, Republic of Korea; B.K. Kim, H.J. Kim, Viatron Technologies, Republic of Korea

VCSEL modules were investigated to design a LPCVD reactor for promising industrial applications due to advantages of excellent irradiation uniformity, rapid power controllability, and especially extended spatial scalability. Each VCSEL cell radiates perpendicularly from the wafer surface, differently from the conventional EEL.

A laser beam emitted from the VCSEL diffuses slightly as its power load increases, which is critical to irradiation uniformity and spatial scalability.

The divergence angles best-fitting the radiative fluxes that were measured experimentally increased monotonically with a very small slope.

Through the experimental investigation on the temperature distribution on the silicon wafer irradiated by the high-power VCSEL beams, the optimal structure for the VCSEL heating system that ensured the uniform irradiation was obtained for wafers of 300 mm in diameter.

Based on the single-step chemical reaction mechanism for the deposition of polycrystalline silicon with silane gas species, the factors for the Arrhenius equation depicting the deposition process were obtained by the comparisons of numerical simulations and the available experimental results.

A simple reactor structure was used to investigate the variation in deposition rates on the wafer during the VCSEL LPCVD process. On the wafer surface the boundary condition of the energy conservation equation for the numerical simulation was given by the heat flux distribution calculated from the radiative irradiation from the VCSEL arrays, rather than the temperature distribution that has been widely used in simulations.

Comparisons of the deposition thicknesses calculated from the simulations under static and practical rotative conditions indicated that the wafer exclusion region increased considerably in the rotative condition due to the decrease in deposition rates in the edge region of the wafer. In order to minimize the wafer exclusion region, the VCSEL emitters which exerted influence on the wafer edge region were controlled to increase the emissive power slightly. As a result, the wafer exclusion zone was reduced considerably, without the help of additional structures to stabilize the gas flow and to reduce the energy loss in the wafer edge region commonly applied in practice.

GP-ThP16 Optical, Mechanical and Anti-corrosive Property Investigation of Tantalum Oxynitride Thin Films for Hard Coating Applications, J.G. Hirpara (jigneshghirpara@gmail.com), R. Chandra, Indian Institute of Technology Roorkee, India

Mechanically hard coating with anti-corrosive behaviour is high in demand for the coating of metal surface in the medicine and industries. Tantalum oxynitride film deposited through reactive magnetron sputtering was investigated for its mechanical and anti-corrosive behaviour. XRD study revealed monoclinic phase with average crystalline size 270Å. Surface topographic was studied through AFM. Micrographs showed high uniformity with low roughness (<100 nm). Highly magnified FE-SEM imaging cleared the formation of nanoscale granules. Optical spectroscopic results demonstrated good transparency of the film (around 85%). Potentiodynamic polarization test and electrochemical impedance spectroscopy were performed with 0.1 M NaCl electrolyte, which demonstrated the high anticorrosive behaviour of the film. The measurement of mechanical hardness of the film was done using the Nanoindentation technique, which has presented the high value of reduced modulus (E_r) 132.98 GPa and hardness (H) 7.30 GPa. Hence, this material with high mechanical strength, transparency and anti-corrosive behaviour is quite suitable for the protective coating of the metal surface.

GP-ThP17 Synthesis and Properties of Two-dimensional Zirconium Phosphate/Polyimide Nanocomposites as Anticorrosion Coatings, G.-H. Lai, National Chin-Yi University of Technology, Taiwan; I.-H. Tseng, Feng Chia University, Taiwan; T.-C. Huang, P.-S. Tsai, M.-H. Tsai (tsaimh@ncut.edu.tw), National Chin-Yi University of Technology, Taiwan

In this study, novel zirconium phosphate/polyimide (ZrP/PI) nanocomposite was developed as an anti-corrosion coating material. The two-dimensional ZrP was prepared by the thermal reflux method and modified by the surfactant Jeffamine M1000. Various contents (0.5 ~ 5 wt.%) of ZrP were then homogeneously blended within PI matrix to obtain ZrP/PI coatings with enhanced anticorrosion effect on cold-rolled steel electrodes. The characteristics of two-dimensional ZrP and nanocomposites were confirmed by Fourier-transform infrared spectroscopy (FTIR), X-ray diffraction (XRD), and scanning electron microscope (SEM) analyses. A series of electrochemical measurements such as corrosion potential (E_{corr}), polarization resistance (R_p), corrosion current (I_{corr}) and electrochemical impedance spectroscopy (EIS) were performed to evaluate the performance of the anticorrosion coatings.

GP-ThP18 Improvement of the Corrosion Resistance in the ASTM F75 Alloy by Ball Burnishing, E.N. Hernandez-Rodriguez (noe.hernandez@ugto.mx), D.F. Silvia Alvarez, A. Marquez Herrera, A. Saldana Rovles, J. Moreno Palmerin, University of Guanajuato, Mexico

The ball burnishing is a process in which the surface of a material is compressed causing plastic deformation, and therefore changing the

Thursday Afternoon Poster Sessions, May 23, 2019

mechanical and chemical surficial properties. ASTM F75 alloy is used in the field of health for fabrication of orthopedic implants. In this application, the alloy is exposed to physiological fluids which are corrosive media. Therefore, improving the corrosion resistance is desirable in order to extend the lifetime of the implants. In this work, we propose the ball burnishing for improving the corrosion resistance of the ASTM F75 alloy. We implemented a design of experiments (DoE) methodology to minimize the corrosion. Two factors were analyzed in the DoE: burnishing force (F_B) and number of tool passes (N_p). The response variable was the corrosion current (I_{corr}). Tests were conducted in cylindrical ASTM F75 alloy samples (ϕ 25.4 mm x L 12 mm). The ball burnishing process was carried out in a conventional lathe and was only applied to one flat face of the samples. Burnishing force was varied from 150 N to 450 N, while tool passes was varied from 2 to 6. After burnishing, corrosion tests were performed by means of electrochemical polarization. Hank's balanced salt solution was employed as the corrosive media. Tafel plots were used for determining I_{corr} . Under studied experimental conditions, F_B was the more significant factor in determining I_{corr} . It was found that as N_p is set constant (at 2, 4 or 6 passes) and F_B is varied from 150 to 450 N, I_{corr} decreases (and therefore corrosion) when ball burnishing is performed with lower F_B values. On the other hand, when F_B is set constant (at 150, 300 and 450 N) little influence was found when N_p changes. A minimum I_{corr} value was found for 150 N and 4 tool passes. Under this condition I_{corr} was 4.9 nA in contrast to I_{corr} in unburnished samples which was 65.2 nA. These values showed a reduction of I_{corr} up to 92.5% in burnished samples, and therefore, a great improving in corrosion resistance.

GP-ThP19 Surface Modification of Sputter Deposited γ -WO₃ Thin Film for Scaled Electrochromic Behaviour, R. Chandra (ramesfjc@gmail.com), G. Malik, S. Mourya, J. Jaiswal, IIC, IIT Roorkee, India

Here, we have reported the electrochromic properties of the highly ordered γ -WO₃ nanoporous thin film grown directly on the indium tin oxide glass (ITO) coated glass substrate using DC magnetron sputtering in a reactive environment (Ar:O₂) at room temperature. To achieve the nanoporous-nanocrystalline behaviour of the active material, a thermal treatment (250°) was given to the active material, which modified the compact film surface into nanospheres. This surface modification is responsible to alter the physical, optical and electrochromic properties of the active material. The physical properties of the active material were characterized in detail using X-ray diffraction, scanning electron microscopy, atomic force microscopy, and energy-dispersive X-ray analysis. The optical and electrochromic behaviour of the active electrode material was analyzed using UV-Vis spectroscopy and cyclic voltammetry. The proposed device revealed large optical modulation, high reversible redox behaviour and good cyclic stability at least up to 1000 cycles. This electrochemically active architecture allows one to fabricate the device for energy harvesting applications at an elevated temperature. Our work indorses human comfort with financial benefits and plays a crucial role in "green nanotechnology".

GP-ThP20 Studies of Corrosion Properties of Plasma Nitrided Steels, P. Ghai (priyanka16ghai@gmail.com), Brock University, St. Catharines, Canada

With the development of science and technology, surface engineering has immersed as a new branch dealing with modification and treatment of surfaces of sophisticated components, which are being used, in various shapes, sizes, etc in different environments. Steel is a material, which is almost universally utilized in various applications in corrosive atmospheres, non-corrosive atmospheres, wear and abrasion and other combinations. Surface nitriding, a thermo-chemical diffusion process provides a solution to most of the problems related to degradation of materials due to corrosion, wear, abrasion, fatigue and creep, etc. Plasma nitriding is a modern technique of nitriding which has drawn the attention of researchers all over the globe.

In the present investigation an attempt has been made to produce low temperature plasma which is employed for diffusion of nitrogen atoms into varying thicknesses of the steel (En-9, En-19, En-24, En-31 and S.S 304) components and then characterize the surface with regard to hardness and corrosion behavior using standard potentiodynamic tests.

It is known that corrosion resistance of low and medium alloy steels for example En-9, En-19, En-24, En-31 and S.S 304 improves with plasma nitriding. However for S.S the results depend on the process temperature. The results of the investigation show that the obtained results are similar, i.e. corrosion resistance has improved for En-9, En-19, En-24 and En-31. But for S.S 304 it was observed that corrosion resistance improvement is best at 450°C thereafter it deteriorates. In a nutshell the present investigation validates that plasma nitriding not only improves surface hardness (wear

resistance) but also improves corrosion resistance of various grades of steels with appropriate process variables.

GP-ThP21 Nanotexturization and Passivation of Single Crystalline Silicon Surface for Passivated Emitter and Rear Contact Solar Cells, C.H. Hsu, Xiamen University of Technology, China; S.-M. Liu, Da-Yeh University, Taiwan, Taiwan; W.-Y. Wu, Da-Yeh University, Taiwan; S.-Y. Lien (sylien@xmut.edu.cn), Xiamen University of Technology, China

Passivated emitter and rear contact (PERC) solar cells are currently the most promising product in solar cell market. One way to improve the cell efficiency is to reduce the reflectance at incident surface while maintaining high passivation quality. In this study, nanostructured black silicon has been prepared by using metal catalysed chemical etching with a solution mixture of silver nitrate (AgNO₃) and hydrogen fluoride. The AgNO₃ concentration is varied from 0.015 to 0.075 M. An aluminum oxide and silicon nitride stack is deposited for passivation and antireflection. The experimental results show that the AgNO₃ concentration of 0.06 M produces the most prominent nanostructures, but the silicon nitride cannot well-deposited on the surface. The silicon wafer etched at the AgNO₃ concentration of 0.03 M exhibits the lowest average reflectance of 1.6% while not compromising on passivation quality. Solar cell simulation reveals that PERC cells with the optimal black silicon nanostructure can have short-circuit current two percent higher than that of traditional PERC cells, and reach a conversion efficiency of 22.04%.

Keywords: Nanostructure, Black silicon, Single crystalline, PERC, Passivation

GP-ThP22 Understanding the Electrochemical Mechanism of Cold Galvanizing and Zinc Electroplating on Steel Structure in Saline Conditions, A. Farooq (ameeq.farooq@gmail.com), University of the Punjab, Pakistan; A. Saleem, University of the Punjab, Lahore, Pakistan; K. Mairaj Deen, University of British Columbia, Canada

The aim of this research is to understand the electrochemical mechanism of two zinc rich coatings on steel. Zinc rich coatings are mostly used as sacrificial coatings to protect steel structures. Commercial Zinc electroplating was performed on mild carbon steel with controlled thickness of (35 ± 1) μ m and with the same thickness of Roval[®] cold galvanizing compound paint. The cold galvanizing was applied on the substrate by brush and dipping method. The dry thickness was measured by electronic thickness meter. Open circuit potential (OCP), Cyclic Polarization (CP) and Electrochemical Impedance spectroscopy (EIS) techniques were used to assess the mechanism of corrosion of zinc electroplated and cold galvanized coatings in both 3.5% NaCl and soil containing 10% NaCl solution. The OCP and EIS were conducted in both aggressive environments with 0 hour and 24 hours immersion times. Salt spray technique was also conducted for 500 hrs on both coatings in the saline environments for the quality assessment. In 3.5% NaCl, the OCP of coatings shift towards more active potential of around -950mV_{vs} Ag/AgCl, as compare to un-coated mild steel substrate which is about -693mV_{vs} Ag/AgCl. The OCP is more negative for electroplated sample which is -1000mV_{vs} Ag/AgCl as compared to brush and dipped cold galvanized paint which is -961mV_{vs} Ag/AgCl and -989mV_{vs} Ag/AgCl respectively. There is no significant change in the value of OCP after 24 hours of immersion. In soil, the OCP of zinc electroplated again shift towards more active potential of around -1061mV_{vs} Cu/CuSO₄ as compare to un-coated mild steel substrate which is about -535mV_{vs} Cu/CuSO₄. All the CP scans was conducted after 24 hours of immersion, the mild steel and zinc electroplated samples shows positive reverse loop which indicate pitting formation in the coatings in both electrolyte. The kinetic parameter and corrosion rate was calculated from CP curves. In 3.5 % NaCl the electroplated zinc has the greater corrosion rate as compare cold galvanizing paint of 4.715 mm/year while in soil it has 0.030 mm/year. The results of EIS for all coatings and substrate was fitted in five different times of equivalent circuit models which generally shows the absorbed and charge transfer resistance phenomenon. The resistance of the coating decreases after 24 hours immersion time. The dipped coated cold galvanized paint shows good results in salt spray test after 500 hours.

GP-ThP23 FEM Analysis on the Cold Rolled Gd-B-Duplex Stainless Steels, Y. Baik (youlboy@gmail.com), Dankook University, Republic of Korea

Finite element method (FEM) analysis is required to find an optimum cold rolling condition of the Gd-B-duplex stainless steels for the storage and transportation of the spent nuclear fuel (SNF) because the process may introduce surface cracks of the alloy. The objective of this study is to find an optimum condition of cold-rolling process of the Gd-B-DSTS by FEM. FEM analysis to find an optimum cold rolling condition was carried out by modelling based on the cold roller size and materials values of the Gd-B-duplex stainless steels. The duplex stainless steels to confirm FEM analysis were prepared by inductive melting and casting followed by hot rolling. The hot rolled specimens with 5 mm thick were cold rolled to be 1 and 3 mm

Thursday Afternoon Poster Sessions, May 23, 2019

thick, separately. The mechanical properties of the stainless steels were determined by universal testing machine (RB302ML, R&B, Korea). The morphology of the deformed surface of the specimen was observed by optical microscopy. The ultimate tensile strength, yield strength and elongation of the cold rolled Gd-B-stainless steels were , respectively. The cold-rolling with 25% of reduction of area (RA) of the Gd-B- duplex stainless steels showed that the strain of the left side, right side and center area of the specimen were 35%, 36% and 54%, respectively. For 15% of RA, the strain decreased about 19%, 18% and 34%, respectively. In case of 10% of RA, the strain of the left side, right side and center area of the specimen were 11%, 12% and 17%, respectively. This means that less than 10% of RA is one of the cold rolling conditions not to form surface cracks because of the lower value than the elongation. Visual and optical inspections of the cold rolled specimen also supported the FEM analysis result.

GP-ThP24 Optical Performances of Antireflective Moth-Eye Structures under Thermal and Humid Stress – Application to Outdoor Lighting LEDs.
C. Ducros (cedric.ducros@cea.fr), A. Brodu, G. Lorin, F. Emieux, A. Pereira, Univ. Grenoble Alpes, CEA, France

Antireflective moth-eye structures were studied in order to increase optical properties of protection windows for outdoor LED lighting. This antireflective structure was compared to “standard” antireflective coatings elaborated by electron-beam evaporation: MgF₂ single layer and broadband SiO₂/ZrO₂ multilayers. Two types of substrates, glass and polycarbonate (PC) have been treated in order to determine the influence of substrates on failure mechanisms generated during ageing tests.

In a first time, effective refractive index and surface morphology were respectively determined by ellipsometry and scanning electron microscopy (SEM). Reactive ion etching process was then optimised on both substrates materials for maximising transmission in normal and angular incidence in the wavelength range of white LEDs (400-750nm). Best results with moth-eye structure were achieved on glass substrate treated on both sides: we measured an increase of 7% of white LED light transmission comparatively to untreated substrate.

In a second time, three standard ageing tests, normative for outdoor applications, were then enforced in climatic chamber on different antireflective treatments in order to estimate their optical properties degradation. First one is an extreme heat test at 130°C with 50% of relative humidity (RH) during 1 hours. Humid heat test consists in testing coated samples during 4 days at 70°C and 95% RH. Third test is a high humidity heat test at 40°C, 98% RH with condensation during 2 days. Surface energy measurement, ellipsometry and SEM were performed on aged surfaces in order to highlight the main degradation mechanisms. The influence of environmental stress on optical properties were then described for all antireflective surfaces. Three main observations can be pointed out from this study: First, degradation of MgF₂ coating under high humidity conditions was mainly due to its high hydrophilic property: a lowering of 3% of light transmission is measured on PC after high humidity heat test. The second main observation is surface cracking of SiO₂/ZrO₂ multilayer antireflective coating on PC leading to losses of 2% in light transmission under extreme heat test. Finally, only moth-eye structures gives high environmental stability as they maintain their white LED light transmission after ageing tests.

Advanced Characterization Techniques for Coatings, Thin Films, and Small Volumes

Room Grand Hall - Session HP-ThP

Advanced Characterization Techniques for Coatings, Thin Films, and Small Volumes (Symposium H) Poster Session

HP-ThP1 Cyclic Tensile Deformation of Freestanding, Nanocrystalline NiTi Films using MEMS Stages.
P. Rasmussen (pjrasmu1@asu.edu), R. Sarkar, J. Rajagopalan, Arizona State University, USA

Controlling the micro/nanostructure of thin films would enable us to explicitly tailor their mechanical behavior. Here, a new process is described in which thin films can be synthesized with precise microstructural control via systematic deposition of nanometer-sized seed crystals, and subsequent crystallization of amorphous precursor films. Using this process, austenitic NiTi (nitinol) films with submicron grain sizes are synthesized. We then co-fabricated freestanding samples of the films with MEMS testing stages and performed cyclic tensile load-unload experiments. Chromium seeded samples showed a high phase transformation stress (> 700 MPa) during the first cycle, with a further increase in transformation stress during

subsequent cycles. Unlike the pseudo-elastic behavior typically observed in microcrystalline nitinol, the film showed a continuous decrease in stress-strain slope during unloading. Preliminary in-situ TEM straining studies suggest that this unusual loading behavior is caused by a combination of reverse phase transformation and reverse plasticity.

HP-ThP3 Ion Irradiation Behavior of a Nanocrystalline BCC High-Entropy Alloy.
Y. Xiao, H. Ma, A.S. Sologubenko, R. Spolenak, J.M. Wheeler (jeff.wheeler@mat.ethz.ch), ETH Zürich, Switzerland

Refractory high-entropy alloys (HEAs) have attracted significant attention due to their superior mechanical properties at elevated temperature, making them potential candidates for structural nuclear materials. However, there is little known about their radiation resistance, particular at harsh environment relevant for fission and fusion applications. Here, strongly textured, columnar and nanometer-size-grain NbMoTaW HEA thin films with and without ion beam assisted deposition (IBAD) are produced. They are irradiated with 4.5 MeV Au ions at 77 K and room temperature with doses up to 1000 displacement per atom at ion-channeling direction. Electron backscatter diffraction (EBSD) and transmission electron microscopy (TEM) are used to characterize the microstructural changes. The examined HEA thin film with IBAD technique exhibits superior microstructural radiation resistance compared to normal deposited HEA and W ones. The radiation resistance can be correlated to mechanical properties via nanoindentation.

HP-ThP4 Evaluation of Properties in Steel with Hard Coating under Hydrogen.
N. Lopez Perrusquia (noeperrusquia@hotmail.com), Universidad Politecnica Del Valle De México, México; M.A. Doñu Ruiz, Universidad Politecnica del Valle de México, México; C.R. Torres San Miguel, Sección de Estudios de Posgrado e Investigación de la Escuela Superior de Ingeniería Mecánica y Eléctrica Unidad Zacatenco, Mexico; V.J. Cortés Suárez, J.A. García Sanchez, Universidad Autonoma Metropolitana Azcapotzalco, Mexico; L. Sánchez Fuentes, Universidad Politecnica del Valle de México, Mexico

In this study, on ASTM A36 steel surface with hardened, at 950 °C for 3, 5 and 7h; through dehydrated paste-pack boriding process. Then, They were investigated, the behavior of the specimen hardened superficially in the microstructure, the hardness, the present XRD phases and characteristics by three point bending. Simultaneously, was investigated the hydrogen permeation effect on the coating formed in the surface of the material and the mechanical characteristics, were evaluated by three point bending and hardness. Obtained a layer sawn with the time and temperatures study; likewise the growth of FeB/Fe₂B layers. There is a hardness change of the boron coating subjected to hydrogen permeation and without hydrogen permeation for each time and temperature. The three-point test showed changes in properties with the coating formed on the surface of the study material subjected to hydrogen permeation and without hydrogen permeation. Showing that the coating boron an efficient alternative to lessen the effect by hydrogen permeation.

HP-ThP5 Effect of Zn Interlayer Microstructure on Corrosion Resistance and Adhesion Strength of Zn-Mg/Zn Coating on TRIP Steel.
M.G. Song (mksongshr@naver.com), H.K. Kim, S.H. Lee, S.Y. Lee, Korea Aerospace University, Republic of Korea

The high-strength steels (HSS) such as dual phase (DP) steel, transformation-induced plasticity (TRIP) steel, and twinning-induced plasticity (TWIP) steel have been used extensively in automotive industries to reduce the weight and to improve the safety of automobiles. To ensure the corrosion resistance of HSS, advanced coating material and process to replace conventional galvanizing coating and process are necessary. Zn-Mg coating is a strong candidate for the corrosion protective coating of HSS, and physical vapor deposition (PVD) process is a promising process for deposition of Zn-Mg coating on HSS. As reported in previous works, however, the Zn-Mg coating showed the insufficient adhesion strength compared to Zn coating due to the high brittleness of the Zn-Mg coating. In this study, to improve the adhesion strength of the Zn-Mg coating, the Zn-Mg/Zn coatings were synthesized on TRIP steel substrate using evaporation deposition process, and the microstructure control of Zn interlayer was carried out. Microstructure, chemical composition depth profile, corrosion resistance and adhesion strength of Zn-Mg/Zn coatings were investigated by field emission scanning electron microscopy (FE-SEM), glow discharge optical emission spectroscopy (GDOES), potentiodynamic polarization test, lap shear test respectively. The Zn-Mg/Zn coatings were synthesized successfully with various deposition temperature and applied power. The Zn-Mg/Zn coating showed an improved corrosion resistance and adhesion strength, and this indicated that the corrosion resistance and adhesion strength of Zn-Mg coating could be improved by the microstructure change

Thursday Afternoon Poster Sessions, May 23, 2019

of Zn interlayer from porous to dense. Detailed experimental results will be presented.

Acknowledgement

This work was financially supported by the Smart Coating Steel Development Center operating for the execution of WPM (World Premier Materials) Program funded by the Ministry of Trade, Industry and Energy, Republic of Korea.

HP-ThP6 Coatings and Interfaces Characterization: Depth Profiling from the First Nanometer down to the Substrate using RF GD-OES, P. Hunault (philippe.hunault@horiba.com), HORIBA Instruments, USA; M.F. Chausseau, K. Savadkouei, HORIBA Scientific, USA; P. Chapon, S. Gaiaschi, HORIBA Scientific, France

With its capability to perform depth profiling on conductive and non-conductive materials with a nanometric resolution and to go up to 150 μm deep into the sample within few minutes, GD-OES is an ideal tool to evaluate depth profiles on materials and to study interfaces between layers, diffusion processes or to optimize coatings processes. Many elements can be analyzed simultaneously, including Oxygen, Hydrogen, Deuterium, Carbon, Fluorine, Sulfur, Lithium... GD-OES is a versatile tool to study materials that complements other techniques such as XPS and SIMS. Since recently, GD-OES can also be used for the measurement of layer thickness and odd shape samples can be characterized.

Results obtained on various nm thin and thick coatings will be shown during this presentation: The use of RF GD-OES for the optimization of electroplating processes will be described with depth profiles of coatings on both inorganic and organic substrates and the direct determination of thickness using Differential Interferometry. Some results obtained on non-conductive organic coatings used for Aluminum packaging will be shown as well as how GD-OES can be used for thickness measurement on Zinc coatings with a comparison with cross-sectional SEM data. Other examples will include the use of GD to manage quality issues such as unexpected elements at the coating/steel interface or for hot-rolled pipe production.

HP-ThP7 In situ Measurement Setup for DC Magnetron Sputtering Thin Film Deposition, Q. Heraut (quentin.heraut@saint-gobain.com), S. Grachev, I. Gozhyk, H. Montigaud, Saint-Gobain Recherche/CNRS, France; R. Lazzari, Institut des Nano Sciences de Paris - Sorbonne Université, France
DC magnetron sputtering is a common technique of deposition at the industrial scale. It involves complex phenomenon due to the variety of species involved, such as electron, ions, neutral, etc. Consequently, deposition parameters are the key to improve thin film quality. Among them, sample holder potential, deposition speed, deposition pressure, target-sample distance are generally identified as the most pertinent.

To understand the effect of these parameters, we developed different *in situ* measurements methods in the same chamber used during thin film deposition. Surface temperature, mechanical stress, optical reflectivity and resistivity measurement were chosen as complementary methods. Our *in situ* results, correlated to thin film morphology measured by *ex situ* measurements gave a good overview of the impact of deposition parameters on grain size and deposition steps for example.

We propose here to describe this setup and results obtained in the particular case of silver thin film deposition.

HP-ThP8 Preparation and Physical Properties of Multiferroic $\text{CaMn}_7\text{O}_{12}$ Thin Films, Y.C. Tseng, National Chiao Tung University, Taiwan; S.R. Jian, I-Shou University, Taiwan; C.-M. Lin, National Tsing Hua University, Taiwan; J.Y. Juang (jyjuang@nctu.edu.tw), National Chiao Tung University, Taiwan
This study is aiming at how to prepare epitaxial $\text{CaMn}_7\text{O}_{12}$ (CMO) films on various substrates by pulsed laser deposition (PLD). The growth temperature for preparing CMO thin films can be between 600 and 700°C. We have tried a wide range of deposition parameters, for example, varying the oxygen pressure from 0.1 to 8×10^{-5} torr and also tried to change the laser energy. When using the parameters of 8×10^{-2} torr at the 700°C can successfully grow the CMO on the STO(100) substrates. The XRD results reveal that all of the diffraction peaks can be indexed to belong the CMO phase with no obvious preferred orientation and we further used synchrotron radiation sources for XRD measurements to confirm that the obtained samples are indeed with correct phases. In addition, we used phi scan technique to check the symmetry of our thin films. It is could obtain both the CMO thin film and the STO(100) substrate are displaying very clean 4-fold symmetry and displaces 45° with respect to each other. It is also interesting to note that, although the laser energy appeared to have little effects on the formation of crystalline phase and orientation, the AFM examination does reveal significant differences in the film surface morphologies. It is evident that
Thursday Afternoon Poster Sessions, May 23, 2019

with smaller laser energy, the grain structure appears to be more square-like and when the laser energy was increased, the film grain morphology became more spherical. The typical magnetic properties of the obtained CMO thin films are shown that the present CMO thin films exhibit two magnetic transitions at $\sim 96\text{K}$ (T_{N1}) and $\sim 42\text{K}$ (T_{N2}), respectively that measured by SQUID, which in good agreement with the two antiferromagnetic transitions occurring at $T_{N1} \sim 90\text{K}$ and $T_{N2} \sim 48\text{K}$ reported previously. The fact that our CMO films shows higher T_{N1} and lower T_{N2} is also interesting. Nevertheless, the reason that is most likely to cause this phenomenon at present is that the epitaxial strain introduced during film growth.

* To whom correspondence should be addressed. Electronic mail: yctseng101@gmail.com

HP-ThP9 SIO X-Ray: View Inside your Material with Contact Experiments, N. Bierwisch (n.bierwisch@siomec.de), N. Schwarzer, SIO, Germany

Caused by the increasing complexity of materials, be it as coatings, multi-layers, fiber or particle reinforced structures or other forms of compounds, classical engineering methods, linear material models and rules of thumb aren't enough anymore.

Proper characterization and optimization of such structures requires invertible mathematical tools of sufficient holistic character. Therefore, SIO developed analytical models which can dramatically speed up the analysis and simulation of complex contact situations compared to FEM, BEM or other numerical systems.

Together with sophisticated measurement devices it's now possible to characterize even extremely complex material structures in a still completely generic (physical) manner.

The knowledge gained thereby, almost literary allows a view inside the material without cutting it open. In fact, our noninvasive (partially even non-destructive) X-ray technology, which is to say the combination of suitable material test with sophisticated physical analysis, allows a stunning presentation of the material interior with all field components, be it stresses, strains, energies etc.

This way a much easier and - what is more - almost entertaining method of finding initial failure mechanisms and detect weak material spots came into existence.

HP-ThP10 Classification of Aluminum Alloys by an Inexpensive Laser-Induced Breakdown Spectroscopy System, K. Maldonado Dominguez (madk96@comunidad.unam.mx), R.S. Sanginés de Castro, Universidad Nacional Autonoma de México, México

Laser-induced breakdown spectroscopy (LIBS) has been widely used for elemental analysis of solid, liquid and gaseous samples due to its portability and the practical null sample preparation. Due to the changing nature of the induced plasma the necessity of using a time-resolved spectroscopy system, consisting of an Echelle spectrograph and an ICCD camera, is usually mandatory; however, these systems are delicate and the portability could be difficult. Although field spectrometers with a CCD detector could have a relatively high spectral resolution, their main drawback is the trouble to synchronize the laser beam trigger to the beginning of the spectral acquisition. If the trigger issue is resolved with a relatively low jitter, these spectrometers could be an attractive alternative for characterization of material composition via LIBS.

In this work, a CCD spectrometer (Avantes, AvaSpec) is tested to determine the composition of several aluminum alloys and is compared to the results of an Echelle spectrometer by identifying spectral lines from the NIST database and applying statistical tools. Different experimental parameters were studied and results are discussed in terms of the correct identification of the Al alloy.

HP-ThP11 Glow Discharge Optical Emission Spectroscopy: Advances toward Quantitative Coating Compositional Depth Profiling, A.H. Tavakoli (amir.tavakoli@airliquide.com), F. Li, Air Liquide - Balazs NanoAnalysis Laboratory, USA

As of key analytical data for understanding of functional coatings behavior are (i) coating compositional depth profile, (ii) potential chemical interaction of the coating material with the substrate, and (iii) possible impact of processing environment on the coating composition. Glow discharge optical emission spectroscopy (GDOES) is known as a fast elemental analysis technique for qualitative compositional depth profiling and capable of detecting almost all elements at ppm level. Balazs NanoAnalysis Laboratory with many years of R&D efforts on the GDOES methodology development has proven records of semi-quantitative compositional depth profiling for a variety of metal and ceramic coatings in a range of thickness from 10 nm to

Thursday Afternoon Poster Sessions, May 23, 2019

50 μm . In this presentation, a systematic GDOES research work on a series of widely used coatings on aluminum alloys with emphasis on anodized coatings is reported. It is shown how major, minor, and trace element concentrations change from the top-coating surface to the substrate, how the surface elemental composition can be affected from the processing conditions, and how the coating composition is influenced by the diffusion of the substrate constituent elements (coating-substrate interdiffusion). In addition, the reliability of the elemental quantification by GDOES measurements are cross checked using the other elemental analysis techniques.

HP-ThP12 Effect of the Cobalt Content on the Magnetic and Corrosion Properties of Electro-formed Fe-Ni-Co Thin Foils, B.K. Kang (kangbk0906@naver.com), Y. Baik, M.Y. Jung, Y. Choi, Dankook University, Republic of Korea

Fe-Ni-Co thin foil for electromagnetic device has been attractive attention for their good electromagnetic properties, which significantly depends on cobalt content. The objectives of this study are to fabricate Fe-Ni-Co thin foil by electroforming in a modified Watt solution and determine their magnetic and corrosion properties with cobalt content to make a high performance electromagnetic device. The electroforming conditions were under 10 A/dm², 50°C, pH=2.2. The X-ray diffractometry for phase identification was performed with Cu-K α radiation ($\lambda=1.5406\text{\AA}$). Electrochemical corrosion test of the Fe-Ni-Co thin foil was carried out in aerated 10% sulfuric acid at 25°C with a potentiostat. Magnetic hysteresis curves of the Fe-Ni-Co thin foil were obtained under $-10\sim 10$ [kOe] magnetic field at 25°C with a vibrating sample magnetometer. The final chemical compositions of the electroformed thin foils were Fe-41%Ni and Fe-40%Ni-7%Co. The Fe-41%Ni thin foil included γ -[Fe, Ni] (Fm-3m) phase, which was mainly (111) and (200) planes. 7% Cobalt addition denoted the appearance of α -[Fe, Ni] (Im-3m) and Co₃Fe₇ (Pm3m) phases. The corrosion potential and corrosion rate of the Fe-41%Ni and Fe-40%Ni-7%Co thin foils were -831.7 , -813.7 [mV_{SHE}], 2.53, 2.70 [10^{-3}xA/cm^2], respectively. Maximum magnetization, coercivity and susceptibility of the Fe-41%Ni and Fe-40%Ni-7%Co thin foil were 74.6, 57.2 [emu/g], 135.8, 48.6 [G], 0.0282, 0.1069 [H/m], respectively.

Topical Symposia

Room Grand Hall - Session TSP-ThP

Topical Symposia (TS) Poster Session

TSP-ThP1 Surface Modification of Multiwalled Carbon Nanotubes for Electro-Thermal Heating in Ice Protection, F. Zangrossi (ezz fz1@nottingham.ac.uk), F. Xu, N. Warrior, X.H. Hou, University of Nottingham, UK

Icing inevitably occurring on the surfaces of aircraft causes a serious concern of flight safety. Various de-icing strategies have been developed to overcome the icing problems on aircraft. Electro-thermal technique is categorized as heat generated by internal electrical component and transferred to the outer surface for ice protection. Given the increased use of composites on aircrafts structure, self-heating fibre reinforced polymer composite have been studied as de-icing system for the new generation aircraft. In the present work, electrical resistance of multi-walled carbon nanotubes (MWCNTs) was modified by two approaches: functionalisation by acid treatment and silver decoration techniques. The aim was to reduce the electrical resistance of the carbon nanotube networks. To evaluate the electrical resistance of carbon nanotubes, MWCNTs coated glass fibres samples prepared by filtration method. The results showed that MWCNTs treated by silver decoration via Tollen reaction had increased the electrical resistance. On contrast, the functionalisation by acid treatment of the carbon nanotubes reduced the resistance by approximate 50%. Treated MWCNTs with improved electrical conductivity were used to produce multiwalled carbon nanotube paper (MWCNP) and a composite structure with glass fibres and epoxy matrix. De-icing tests will be carried out to verify the electro-thermal performance in a climate chamber.

TSP-ThP2 Nanostructured a-C:H:SiO_x Coatings with Superhydrophobic Properties, D. Batory (damian.batory@p.lodz.pl), Lodz University of Technology, Poland; **J. Lengaigne,** Ecole Polytechnique de Montreal, Canada; **A. Jedrzejczak,** Lodz University of Technology, Poland; **S. Brown, J.E. Klemberg-Sapieha,** Ecole Polytechnique de Montreal, Canada

The main aim of the work was to obtain carbon and silicon based amorphous layers with different surface morphology allowing to obtain superhydrophobic properties. SiO_x incorporated diamond-like carbon coatings with different thicknesses were synthesized onto reactive ion

etched silicon wafers with previously deposited thin layer of gold. An island shape of the thin golden layer made it possible to obtain selectively etched pillar-like structure of silicon surface with morphology depending on the time of etching. A combination of different structures of the silicon substrates with three thicknesses of subsequently deposited a-C:H:SiO_x layers enabled to obtain six sets of samples with respect to the thickness of the coatings and morphology of the substrate. The obtained coatings were characterized using scanning electron microscopy, Raman spectroscopy and atomic force microscopy. Finally the contact angle was measured using sessile drop technique. Additionally the contact angle hysteresis and roll-off angle were determined. As the result of the investigation it was noticed that the structure and morphology of the silicon substrates change with the time of etching. The deposition of a-C:H:SiO_x coatings onto the reactive ion etched silicon substrates decreases the roughness parameters and surface area, which progress with increasing thickness. However, an optimal surface morphology correlated with a proper thickness of the coating resulted in contact angle exceeding 150 deg.

TSP-ThP4 Structural Investigation of the Stability in Temperature of Some High Entropy Alloys, M. Calvo-Dahlborg (monique.calvo-dahlborg@univ-rouen.fr), University of Rouen Normandie-CNRS, France, Swansea University, UK; **U. Dahlborg, J. Cornide,** University of Rouen Normandie-CNRS, France; **S. Mehraban,** College of Engineering, Swansea University, UK; **R. Wunderlich,** University of Ulm, Germany; **N. Lavery,** College of Engineering, Swansea University, UK; **S.G.R. Brown,** Swansea University, UK

It has been shown in a previous study [1] that High Entropy Alloys (HEA) can be classified in three domains according to their e/a and r values, e/a being the number of itinerant valence electrons as calculated by Massalski [2] and r being the average radius for a 12 local neighborhood [3]. CoCr_zFeNi-XY (with X and Y = Al, Cu, Pd, Ru, Ti and z=0 or 1) HEAs from the three domains identified by e/a have been investigated in as cast conditions (T0), after 3 hours homogenization at 1100°C (T1) and after 3 hours annealing at 700°C (T3). The comparison is based mainly on diffraction and calorimetry results.

It is observed that for the alloys from domain I which contains fcc structures, the microstructure transforms from multi- to almost single-phase under homogenization. In Domain III which contains cubic (Bcc+B2) structures very small multi-structural changes are observed. The alloys in domain II have mixed structure which is changing under heat treatments. Moreover, an additional heat treatment at T3 after homogenization leads in all domains to the appearance of other phases. All results are confirmed by the calorimetric results. The effect of heat treatments on hardness is discussed for some compositions.

[1] M. Calvo-Dahlborg, S.G.R. Brown, *J. Alloys and Compds* **724** (2017) 353-364. <http://dx.doi.org/10.1016/j.jallcom.2017.07.074>

[2] T.B. Massalski, *Materials Transactions* **51** (2010) 583-596. <https://doi.org/10.2320/materia.49.192>

[3] E.T. Teatum, K.A. Gschneidner Jr., J.T. Waber, 1968. Report LA-4003. UC-25. Metals, Ceramics and Materials. TID-4500, Los Alamos Scientific Laboratory.

TSP-ThP6 Cu-nanoparticles /Polyfluoroacrylate Emulsion Nanocomposite Coating for Icephobic Applications, T.B. Barman, H.C. Chen, J.L. Liu, X.H. Hou (xianghui.hou@nottingham.ac.uk), The University of Nottingham, UK

Atmospheric ice accumulation and adhesion on component surfaces often causes great concerns in various industries, especially for aerospace in which catastrophic accidents may occur under inflight or ground icing conditions. Applying icephobic coatings on the components surface has been considered as a promising solution for minimising the accumulation of ice and prompting the removal of the ice from the surface. In the present work, a nanocomposite coating has been developed by mixing Cu- nanoparticles with synthesized polyfluoroacrylate (PFA) emulsion and depositing the mixture on the substrates by spin coating method. Surface hydrophobicity of 140 ° was achieved on the surface of the nanocomposite coating, which has the average surface roughness (R_a) in the range of 0.2 to 0.3 μm . Ice adhesion of the coating was measured by centrifugal approach and it was found that the ice adhesion strength has been effectively reduced as compared to reference surface. De-icing performance of the coating was also evaluated using electro-thermal heating method and 35 % decrease in energy consumption was observed as compared to uncoated aluminium surface.

Thursday Afternoon Poster Sessions, May 23, 2019

TSP-ThP7 Surface Characteristics and Diffusion Phenomenon of $\text{Ni}_2\text{FeCoCrAl}_x$ Alloys Treated by Atmospheric Pressure Plasma, C.R. Huang (zx8110256zx@gmail.com), National United University, Taiwan; J.G. Duh, National Tsing Hua University, Taiwan; F.B. Wu, National United University, Taiwan

High entropy alloys, HEAs, recently attracted intense attention due to its outstanding performance in mechanical properties, thermal stability, sluggishness in diffusion, anti-sticking, corrosion resistance, etc... However the knowledge of the evolution of microstructure and surface characteristic of HEAs under treatments through atmospheric pressure plasma jet, APPJ, was limited. In present study, Al incorporated Ni_2FeCoCr high entropy alloys were treated by APPJ to investigate the surface property evolution and diffusion characteristics on HEAs surface. The treatment parameters included gas source, input power, flow rate, and torch-surface distance, ranged from dry air to N_2 , 850 to 1100 W, 35 to 50 sccm, and 15 to 50 mm, respectively. The slow and stable Ni showed limited diffusion and reaction even against highest power input under air. The surface microstructure and property evolution were attributed to the elemental redistribution of the active Al in the designed HEAs. The detailed concentration profiles, phase, and surface characteristics were analysed and discussed in consideration of concentration gradient, microstructure evolution, and chemical potential.

TSP-ThP8 Development of Microwave Remote Plasma Source for New Surface Functionalization, Y. Isomura (isomura.yoshiyuki@kobelco.com), Y. Ikari, T. Okimoto, Y. Tauchi, K. Nishiyama, Kobe Steel, Ltd., Japan; H. Toyoda, H. Suzuki, Nagoya University, Japan

We developed the so-called Twin-Roll Plasma Enhanced CVD (PECVD) integrated into an industrial roll to roll process for surface functionalization of a flexible substrate. In Twin-Roll PECVD process the winding rolls themselves function as the electrode for plasma discharge and hence provide a stable deposition process for a long time even for deposition of non-conductive films as compared to typical pulse PECVD process. In this technique, however, the direct plasma discharge occurs between the electrode winding rolls and hence the substrate material needs to be electrically non-conductive. The application of the direct plasma method to a conductive substrate is therefore practically limited.

We have been developing a microwave remote plasma source and its integration into roll to roll process as for demonstration of a new surface functionalization technique. In direct plasma discharge process such as in the case of Twin-Roll PECVD, for instance, ion bombardment/irradiation is expected during the film growth by application of a negative bias potential to the electrode. The ion bombardment effect is known to be quite effective for microstructural control of the growing film and hence the film properties. Application of bias voltage to the electrode is however not feasible when a conductive substrate is employed. In the remote plasma source developed, a positive bias potential is applied at a point of plasma source, and the plasma potential is increased with respect to a grounding substrate, accordingly. This source is a linear type exhibiting a possible plasma treatment on a large area with high uniformity. In this work we present the basic principle and function of this remote plasma source. We also demonstrate some applications thereof for film deposition, contributing towards a new technique for surface functionalization.

TSP-ThP9 Combinatorial Study of Dielectric and Piezoelectric High Entropy Oxides, Z.-W. Huang (ylliwq@gmail.com), C.-M. Chou, J.-M. Ting, J.-J. Ruan, K.-S. Chang, Y.-H. Su, National Cheng Kung University, Taiwan

The related studies of high entropy alloys (HEAs) have been ongoing extensively. However, few studies are conducted to explore high entropy oxides (HEOs). HEOs may exhibit more diverse properties than those of HEAs. The goal of this study aims the following aspects: 1) fabrication of various HEO systems using combinatorial methodology, 2) enhancement of physical and functional properties of HEOs through coupling high entropy lamellar crystals of polymers, and 3) theoretical calculations to predict and support our experimental results.

Potential high-k and piezoelectric HEOs were explored in this study. Sputtering and hydrothermal processes were employed to systemically study the physical and functional properties of various HEOs. In the field of high-k HEOs, two systems of $(\text{Al,Ti,Zr,Ta,Hf})\text{O}_2$ and $(\text{Al,Ti,Zr,V,Hf})\text{O}_2$ were examined. A single element (Al) target and a 4-sliced metal (Ti,Zr,Ta,Hf) target were prepared for a sputtering deposition. Our preliminary results indicated the formation of amorphous $(\text{Ti,Zr,Ta,Hf})\text{O}$ films on Si (100), which is excellent for advanced gate stacks. Hydrothermal synthesis of $(\text{Al,Ti,Zr,V,Hf})\text{O}_2$ indicated that the equimolar ratio of constituent elements was achieved by tuning the relative amounts of precursors.

In the field of piezoelectric HEOs, two systems of $\text{Ba}(\text{Ti,Zr,Ta,Hf,Mo})\text{O}_3$ and $\text{Ba}(\text{Ti,Zr,Sn,Hf,Mo})\text{O}_3$ were explored. A BaTiO_3 (BTO) target and 4-sliced metal (Zr,Ta,Hf,Mo) target were used for a sputtering deposition. Both as-deposited films of BTO and (Zr,Ta,Hf,Mo) were amorphous. However, the crystalline BTO and (Zr,Ta,Hf,Mo) films were obtained after a postanneal although the oxide phases of each component in the (Zr,Ta,Hf,Mo) films were observed. Hydrothermal synthesis of $\text{Ba}(\text{Ti,Zr,Sn,Hf,Mo})\text{O}_3$ assisted by poly lactic-co-glycolic acid (PLGA) indicated the formation of a single phase of crystalline BaMoO_4 films before any heat treatment. A forming gas anneal above 900 °C will be applied to reduce BaMoO_4 to BaMoO . EDS will be also applied to analyze the ratio of each component in the film. Band structures of the two systems were also theoretically evaluated and will be reported.

Hard Coatings and Vapor Deposition Technologies

Room Golden West - Session B2-2-FrM

CVD Coatings and Technologies II

Moderators: Kazunori Koga, Kyushu University, Japan, Raphaël Boichot, Université Grenoble Alpes, CNRS, France

9:20am **B2-2-FrM5 Scale up of the DLI-MOCVD Process to Treat 16 Nuclear Fuel Cladding Segments in Parallel with a Protective Cr_x Coating**, A. Michau (alexandre.michau@cea.fr), F. Addou, CEA, Université Paris-Saclay, France; Y. Gazal, F. Maury, T. Duguet, CIRIMAT, France; R. Boichot, M. Pons, Université Grenoble Alpes, CNRS, France; E. Monsifrot, Dephis, France; F. Schuster, CEA, PTCMP, France

Direct liquid injection – metalorganic chemical vapor deposition (DLI-MOCVD) is the most advanced process dedicated to the internal protection of nuclear fuel cladding in accident conditions such as loss of coolant. A coating composed of amorphous chromium carbide Cr_x can be grown by DLI-MOCVD. It is resistant against high-temperature oxidation in air and steam. A joint development between experimental and numerical studies has led to a coating of uniform thickness inside the cladding. Optimized reactor parameters consist in a combination of low temperature (~ 600 K) and low pressure (~ 600 Pa) with a high vapor flow rate ensuring a short residence time of reactive species in the reactor.

Interestingly, Cr_x coatings deposited from the decomposition of a bis(arene)chromium(0) precursor at low temperatures, around 600 K, exhibit the same characteristics than the coatings grown at higher temperatures (623, 648, 673 and 723 K). A similar glassy-like and dense microstructure is achieved; specific to the amorphous nature of the material. No significant differences are detected in TEM, XRD, EPMA and Raman spectroscopy, regardless of the substrate (silicon wafers, 304L and zirconium alloy coupons). It indicates a strong flexibility of the DLI-MOCVD process when combined with an adequate selection of metalorganic precursor.

Since the above-mentioned materials characterizations demonstrate that low temperature coatings possess the appropriate protection properties, the low-temperature DLI-MOCVD process can be scaled-up. The final geometry to be coated is the internal surface of 4 m-long tubes with a diameter < 1 cm. Several runs are successfully achieved with a single segment, 3 segments in parallel, and finally a batch of 16 segments. 3D computational simulations of the deposition process validate the design of the gas-phase distributor flanges (for 3 and 16 segments) which are required to split homogeneously the reactive gas flow towards each segment. Experimental conditions have been extrapolated from 1 to 3 and to 16 cladding segments, resulting in the deposition of the Cr_x coating inside all segments with a uniform partition. Indeed, the total mass intakes over deposition time (g/min) are similar in all 3 or 16 segments.

Overall, this paper demonstrates the feasibility of the deposition of Cr_x coating in a bundle of several, up to 16, nuclear fuel cladding segments of 1 m in length, in order to protect them during accident conditions. This “batch demonstration” is a first step in the course of industrialization. Next step will be the deposition in a full-length cladding (4 m).

9:40am **B2-2-FrM6 Assessment of Low Temperature CVD Routes to MAX Phases in the Cr-Si-C System**, A. Michau, CEA, Université Paris-Saclay, France; F. Maury (francis.maury@ensiacet.fr), CIRIMAT, France; F. Schuster, CEA Cross-Cutting Program on Materials and Processes Skills, France; T. Duguet, CIRIMAT, France; E. Monsifrot, Dephis, France

Different CVD routes have explored for the growth of mixed carbide coatings in the system Cr-Si-C, especially the MAX phases of this ternary system. The goal was to find suitable precursors and typical growth conditions, which could be further optimized to develop an advanced process for industrial applications. For this objective, DLI-MOCVD is an emerging CVD process that combines the use of metalorganic precursors (MO) and direct liquid injection (DLI) of the reactive sources. The main advantages are a significant reduction of deposition temperatures (required for sensitive substrates and energy saving) and the production of high vapor flow rates to feed large-scale reactor.

The solid compound Cr[CH₂Si(CH₃)₃]₄, has been used as single-source precursor by DLI-MOCVD in a hot-wall reactor. A solution in toluene (2.9 × 10⁻² mol.l⁻¹) was injected in a flash vaporization chamber directly connected to the reactor containing the substrates. The coatings were obtained under low pressure (6.7 kPa) in the temperature range 613-733 K. They are XRD amorphous and exhibit a smooth surface morphology with a dense and homogenous microstructure. Growth rates in the range 0.5-1 μm/h were obtained but the films were partially oxidized due to the high sensitivity of

this single-source precursor to oxygen. The Si:Cr atomic ratio of coatings is about 1.1 which significantly lower than the amount bring by the precursor (4). This atomic ratio is relatively close to the value 0.6 of a previously reported ternary phase (Cr₅Si₃C₂) but far from the MAX phases Cr₂SiC (0.5) and Cr₃SiC₂ (0.33). Finally this route did not allow to control the Si:Cr atomic ratio in a sufficiently wide range, especially that of MAX phases.

To gain flexibility in the DLI-MOCVD process, a simple one-pot dual-source process has been investigated in a similar reactor. In this 2nd route, bis(ethylbenzene)chromium(0), Cr(C₆H₅C₂H₅)₂, and diphenylsilane, (C₆H₅)₂SiH₂, were used as liquid molecular precursor of Cr and Si, respectively. A solution containing both precursors in toluene with various mole ratios was used to produce the reactive gas phase via a single pulsed injector. Depositions were carried out under low pressure (6.7 kPa) in the temperature range 723-773 K on various substrates. Cr_xSi_yC_z coatings have been obtained with growth rates as high as 5 μm.h⁻¹ and compositions depending mainly on the composition of the injected solution. The coatings were characterized by many techniques (SEM, XRD, TEM, EPMA...) and preliminary properties including thermal stability and oxidation resistance have been investigated. It is demonstrated that DLI-MOCVD process is a promising route to deposit MAX phases.

10:00am **B2-2-FrM7 Towards CVD of Hard Coatings Using Hetero-Metallic Precursors**, S.Ö. Öhman (sebastian.ohman@kemi.uu.se), M.E. Ek, Uppsala University, Angstrom Laboratory, Sweden; R.M. Brenning, Sandvik Coromant R&D, Sweden; M. Boman, Uppsala University, Angstrom Laboratory, Sweden
CVD of hard coatings used for machining and cutting is a field in fast development. However, progress in this area is impeded by the lack of adequate control for nucleation and film growth, which governs the desired mechanical and physical properties of these films. In addition, today's wear resistant coatings are commonly based on single phased binary material systems, yet the increasing demands put on tomorrow's coatings will require the development of new, multicomponent and multifunctional coatings. Such coatings can be made by combining conventional CVD with the development of new hetero-metallic precursors. This opens for new chemical pathways, better stoichiometric control, higher yields, more versatility and simplified CVD processing.

In this session, a presentation will be made regarding the use of hetero-metallic precursors for CVD. Audience will also be introduced to a newly developed 3-zone hot-wall reactor that enables the flexible deposition from such precursors, in particular those based on titanium and aluminium alkoxides. With the current experimental set-up, it is possible to use several hetero-metallic precursors at once or sequentially (i.e. pulsed CVD).

The synthesised CVD films were characterised using several methods, including XRD, SEM/EDS, TEM, Raman and RBS.

10:20am **B2-2-FrM8 CVD of Tungsten, Tungsten Nitride and Tungsten Carbide Multilayers**, J. Hulkko (johan.gerdin@kemi.uu.se), K. Böör, Uppsala University, Angstrom Laboratory, Sweden; R. Qiu, Chalmers University of Technology, Sweden; E. Lindahl, Sandvik Coromant R&D, Sweden; M. Boman, Uppsala University, Angstrom Laboratory, Sweden

Tungsten-based CVD has been investigated since the early 1960. Today, tungsten-based coatings can be found in many technological areas, ranging from electrical contacts and diffusion barriers to wear- and corrosion resistant films as well as absorber coatings in solar cells.

The aim in this study was to create new multi-layered coatings of W/WN, W/WC and WN/WC by varying the thickness and phase composition of the layers.

W/WC/WN thin films were deposited from a reaction gas mixture containing WF₆ and H₂ using Ar as carrier gas. NH₃ and C₂H₄ were added during the nitride- and carbide formation steps. The films were deposited on n-type Si(111)- and Al₂O₃(0001)-substrates, in a newly constructed CVD-equipment built in-house. This equipment is characterised by excellent repeatability using a custom software controller and a wide parameter space to work within, for instance partial pressures and temperature.

The coatings were characterised using several XRD techniques. SEM images provide microstructural information and thickness. Additionally XPS and TEM were used to gain more in-depth chemical and structural information. Vickers nano-indentation was used for hardness investigation.

10:40am **B2-2-FrM9 Deposition of Carbon Nanoparticles Using Multi-Hollow Discharge Plasma CVD for Synthesis of Carbon Nanoparticle Composite Films**, *K. Koga (koga@ed.kyushu-u.ac.jp)*, *S.H. Hwang*, Kyushu University, Japan; *T. Nakatani*, Okayama University of Science, Japan; *J.S. Oh*, Osaka City University, Japan; *K. Kamataki*, *N. Itagaki*, *M. Shiratani*, Kyushu University, Japan

Carbon Coating films are receiving much attention as an alternative to improve the physical and chemical characteristics of material surfaces. Meanwhile, as the application field diversifies, there have been increasing requests for an improvement in optoelectronic, physical, and chemical properties of the films. Nanoparticle composite films are very promising, since they are expected to improve the film performance [1]. To further understand the films, nanoparticle synthesis and their deposition are important. In this study, gas flow and bias voltage effects on their deposition were studied, using a multi-hollow discharge plasma CVD (MHDPCVD) method. The experiment was carried out in room temperature with CH₄+Ar MHDPCVD, which can continuously produce nanoparticles [2]. Carbon nanoparticles were synthesized at 8 hollows of 5 mm in diameter where Ar and CH₄ pass through. They were transported to the substrate set 50 mm away from the multi-hollow electrode and then deposited. During the process, 60 MHz rf power of 40 W was applied and working pressure and gas ratio of Ar and CH₄ were kept at 2 Torr and 6:1 respectively. Also, carbon nanoparticles that were deposited under the control of total gas flow rate from 10 sccm to 200 sccm were analyzed through a transmission electron microscope (TEM). The average size gradually decreased from about 250 nm at 10 sccm to 31.7nm at 120 sccm and the area density increased, but nanoparticles were not detected at conditions over 125 sccm. When the substrate was biased at +50V DC, the nanoparticles of 24 nm in average size were deposited at 125 sccm, because negatively charged nanoparticles were attracted to the positively biased substrate. Hence, the gas flow rate and the bias voltage are the keys to control of nanoparticles for carbon nanoparticle composite films.

[1] Peter Greil, *Advanced engineering materials* / volume 17, issue 2, 2014.

[2] K. Koga, et al., *Thin Solid Films* 506 (2006) 656.

11:00am **B2-2-FrM10 Hot Filament CVD Diamond Coating Technology for Cutting Tool Applications**, *M. Woda (michael.woda@cemecon.de)*, *W. Puetz*, *M. Frank*, *C. Schiffers*, *W. Koelker*, *O. Lemmer*, *T. Leyendecker*, CemeCon AG, Germany

Besides a variety of DLC based coatings for tribological applications, pure diamond (100% sp³ bonded, crystalline carbon) is a very useful coating material system in the group of carbon based coatings for cutting of hard to machine materials. Nowadays Diamond coatings are typically applied to cutting tools with complex geometries by means of Hot Filament CVD thin film deposition. The technology is well established on an industrial scale. The basic principle of this Hot filament CVD diamond deposition technology and the details on the corresponding coating equipment are presented here. Results of case studies dealing with cutting applications on machining of various examples of highly abrasive materials with pure CVD Diamond thin films are discussed in this work. These case studies include applications with Carbon Fiber Reinforced Plastics (CFRP) systems for aerospace industry, ceramic materials as zirconium oxides for dental applications up to direct milling of sintered cemented carbide.

Hard Coatings and Vapor Deposition Technologies Room California - Session B5-2-FrM

Hard and Multifunctional Nanostructured Coatings II

Moderators: *Tomas Kozak*, University of West Bohemia, Czech Republic, *Helmut Riedl*, TU Wien, Institute of Materials Science and Technology, Austria

9:00am **B5-2-FrM4 Microstructural and Mechanical Stability of TaCu Composite Coatings**, *A. Bahrami*, *C.F. Onofre*, *A. Delgado*, Universidad Nacional Autonoma de México, México; *T.H. Huminiuc*, *T.P. Polcar*, University of Southampton, UK; *S.E. Rodil (srodil@unam.mx)*, Universidad Nacional Autonoma de México, México

In this study, binary Cu-Ta alloys with Ta content between 0 and 100 % were prepared by co-magnetron sputtering. The effect of elevated temperature vacuum annealing on the morphological stability and mechanical properties of Cu-Ta films was studied. Their structural and mechanical properties were characterized by X-ray photoelectron spectroscopy (XPS), X-ray diffraction (XRD), Scanning electron microscopy (SEM), Transmission electron microscopy (TEM) and nanoindentation methods. The XRD results show that

a Ta-rich CuTa amorphous phase is formed in the coatings with 15-67 at. % Ta along with nanocrystalline Cu. TEM analyses of two selected samples with 25 and 67 at. % Ta depict formation of crystalline Cu islands in an amorphous CuTa matrix in both as-deposited and annealed coatings. XPS profiles show that the coatings are mainly metallic, with a thin oxide layer. Moreover, analysis of the oxide layer, indicated that Cu nanocrystals are protected against oxidation by the Ta-rich CuTa amorphous layer. A significant increase in hardness values from 0.9 for pure annealed Cu to 11.89 GPa for the samples with 98 at. % Ta, is observed. Also, it was observed that the coatings preserve their microstructural and mechanical stability after vacuum annealing at 550 °C.

9:20am **B5-2-FrM5 Hydrogen Permeation Behavior of Multi-Layered Coatings**, *M. Tamura (tamura@uec.ac.jp)*, University of Electro-Communications, Japan

Hydrogen permeation tests of hard coatings such as TiN, TiC, TiAlN, and multilayer of TiAlN/TiMoN were performed based on the differential-pressure methods described in ISO15105. Coatings were deposited by ion plating on a stainless steel substrate (SUS316L). This study focused on the impact of differences in thin film microstructures on hydrogen permeation behavior. Ceramics coatings consisting of fine crystal grains, with diameters of about 100 nm or less, provided superior hydrogen-permeation barriers. On the other hand, the test specimens coated with columnar crystals grown vertically on the substrate, tended to exhibit higher hydrogen permeability. Applying TiN, TiC or TiAlN coatings reduced the hydrogen permeation by a factor of about 100 compared with uncoated substrates. In addition, multilayer of TiAlN-TiMoN coatings was effective to obtain lower hydrogen permeability. The grain boundaries and layer interface of the coatings could be trap sites for hydrogen.

9:40am **B5-2-FrM6 Tantalum Alloying - Improvement of Thermal Stability and Mechanical Properties of Ternary and Quaternary Transition Metal Nitrides**, *B. Grancic (branislav.grancic@fmph.uniba.sk)*, Comenius University in Bratislava, Slovakia; *D.G. Sangiovanni*, Linköping University, Sweden, Ruhr-Universität Bochum, Germany; *T. Roch*, *M. Truchly*, *M. Mikula*, Comenius University in Bratislava, Slovakia

INVITED

Combining the high hot-hardness to enhanced toughness and good oxidation resistance is one of the greatest challenges in material-design of transition metal nitride (TMN) ceramics, which are widely employed as protective coatings in machining industry.

In Ti-Al-N and Cr-Al-N, well-known Al-containing TMNs, the thermally-induced decomposition of the cubic solid solution via spinodal mechanism or precipitation leads to the formation of fine-grained nanostructures and the associated age hardening. However, continuous thermal load/unload cycling during industrial machining cause transformation into thermodynamically more stable coarse-grained structures containing hexagonal AlN and cubic TiN or hexagonal CrN_x phases resulting in degradation of mechanical properties. In addition, brittleness limits the use of TMN-AlN alloys in applications demanding a high fracture-resistance.

The concept of multicomponent alloying with elements from groups IIIB – VIB (Y, Zr, Hf, V, Nb, Ta, Mo, and W) represents a suitable way to improve the properties of Al-containing TMNs. From this group, pentavalent tantalum is a very attractive substitutional element which is used, for example, in Ti-Al superalloys to improve ductility, and to reduce oxidation at high temperatures. Moreover, the Ta-N phase diagram exhibits a large variety of Ta_xN_x structures, characterized by different electronic properties.

Here, the role of tantalum as a substitution atom improving thermal stability and mechanical properties is presented in several ternary and quaternary systems. In the first case, we combine experiments and *ab initio* calculations to investigate thermally induced age hardening in tough Ta-Al-N coatings via spinodal decomposition. The increase in hardness from 29 GPa to 35 GPa was observed during early stages of phases separations when temperature exceeded 1000°C. In the next case, a significant improvement in toughness of nitride coatings was observed in highly TaN-alloyed Ti-Al-N. While the hardness of Ti_{0.46}Al_{0.54}N (32.5 GPa) is not significantly affected by alloying with TaN, the elastic stiffness monotonically decreases from 442 to 354 GPa with increasing Ta contents indicating enhanced toughness in TiAlTaN. In the last presented Cr-Al-Ta-Y-N system, the presence of Ta in the solid solution shifts the decomposition process to higher temperatures (>1000°C) compared to Cr-Al-Y-N (~900°C), thus enhancing the alloy thermal stability. The improved thermal stability may be attributed to increased cohesive energy, as revealed from *ab initio* calculations.

This work was supported by the Slovak Research and Development Agency [Grant No. APVV-17-0320]

Friday Morning, May 24, 2019

10:20am **B5-2-FrM8 Interface Characteristics Between PVD- AlTiN and Electroplated Hard Chrome by Duplex Process**, D.Y. Wang, MingDao University, Taiwan; L.C. Hsu (lhsu@aurorascicorp.com), J. Hung, Aurora Scientific Corp., Canada; C.H. Chen, H.C. Liu, Surftech Corp., Taiwan; W.Y. Ho, MingDao University, Taiwan

Most of the hard coatings have good corrosion resistance on certain applications. The traditional way for corrosion resistance accepted by industries are electroplated hard chrome. However, in some severe environment, hard chrome can not pass corrosion tests, as a result, PVD hard coatings are applied on hard chrome to even further enhance corrosion resistance in some special applications. In this research, we are investigating the unique application of cathodic arc technology in depositing AlTiN hard coating film onto electroplated hard chrome PH17-4 stainless steel 1-inch OD shafts. The requirement for the AlTiN multi-layer coating is to take into consideration of residual stress between the hard chrome layer and AlTiN coating to ensure great adhesion between two materials. Also, the residual chemicals from hard chroming process will be analyzed and the removal of chromium oxide will be addressed in both pre-coating cleaning and in-chamber cleaning processes. This research will reveal the effect of coating process on the sensitive to temperature of the duplex coatings which related to the residual stress. Meanwhile, it is critical to monitor whether any released on the hard chrome surface, causing contamination of chrome surface in the coating process. Results of this research will enhance corrosion resistance by applying both hard chrome and hard coating by PVD cathodic arc process.

10:40am **B5-2-FrM9 Manipulation of Bimodal Matrix in Plasma Sprayed Nanostructured YSZ Coating and Its Effect on the Microstructure**, P. Bijalwan (shivi273@gmail.com), Tata Steel Limited, India; A. Islam, K.K. Pandey, Indian Institute of Technology, India; A. Pathak, M. Dutta, Tata Steel Limited, India; A.K. Keshri, Indian Institute of Technology, India
Nanostructured YSZ (n-YSZ) based ceramic TBCs have attracted widespread attention because of the exceptionally higher toughness, bond strength and thermal cycling life compared to the conventional YSZ. However, the primary concern is to control the melting of nanostructured powders in the plasma jet by adjusting the plasma spray parameters, resulting the formation of the bimodal structured coatings. Further, by controlling the size, shape, and morphology of the nanozones, it is possible to engineer coatings with enhanced properties. There is a complete scarcity in correlating the effect of the content of nanostructured zone on the performance of the coating. In this work, attempts have been made to control the melting states of nanoparticles by changing the plasma process parameters and to manipulate the different contents of nanozones in the coating. Temperature and velocity profile of the in-flight particle was captured at several plasma process parameters using Accuraspray in-flight particle diagnostic sensor. Free standing coating will be synthesized after analyzing the temperature and velocity profile of the in-flight particle. These free-standing coating will be evaluated in detail for the porosity and the bimodal matrix. At the optimized parameter, final coating will be fabricated and various abovementioned properties will be evaluated.

Tribology and Mechanical Behavior of Coatings and Engineered Surfaces

Room San Diego - Session E1-3-FrM

Friction, Wear, Lubrication Effects, and Modeling IV

Moderators: Nazim Bagcivan, Schaeffler AG, Germany, Carsten Gachot, TU Wien, Institute for Engineering Design and Logistics Engineering, Austria, Tomas Polcar, Czech Technical University in Prague, Czech Republic

8:00am **E1-3-FrM1 Numerical and Experimental Analyses on the Influence of Irregular Columnar Boundaries on Mechanical and Tribological Behavior of a WC/C Coating**, C. Bernardes (cassiano@usp.br), N. Fukumasu, R.M. Souza, I.F. Machado, University of São Paulo, Brazil

Many commercial coating deposition systems produce microstructures with defects that can affect the tribological performance of a given component. Instabilities during the deposition process or variations on local surface topography can lead to macroscale defects, such as irregular columnar boundaries. Those columnar defects can present interfacial discrepancies between two consecutive columns, leading to local lower mechanical and fracture properties. This work explores the influence of irregular columnar growth of a Tungsten Carbide / Carbon (WC/C) multilayer coating, on local and global tribological behavior. The samples consisted of a commercial version of a WC/C coating deposited onto polished AISI H13 discs and AISI

52100 balls. Mechanical, fracture and microscale tribological behaviors were analysed using a Bruker T1950 triboindenter. Macroscale tribological behavior was evaluated by reciprocating tests using the Optimol SRV v4 tribometer in the ball-on-disk configuration. X-ray diffraction (XRD), x-ray photoemission spectroscopy (XPS) and Raman spectroscopy techniques were used to characterize the coating microstructure. Numerical simulations of the microscale scratch test, using the digital tribology package TRIBOCODE, allowed the analyses of the local columnar irregularities on the tribological behavior of the coating. The macroscale reciprocating results showed variable tribological behavior of the coating induced by the defects, in which only part of the tests presented coating failure (cohesive cracks and spallation). XRD and XPS analyses indicated a presence of crystalline phases of type WC_{1-x}, while the presence of amorphous carbon matrix was identified during the Raman analyses. The numerical simulations indicated a correlation between the orientation of the mechanical and fracture properties of the irregular columnar structures and boundaries and the scratch direction, which could lead to selective failure modes of the coating.

8:20am **E1-3-FrM2 Structure, Mechanical and Tribological Properties of Mo-S-N Solid Lubricant Coatings**, T. Hudec (t.hudec@soton.ac.uk), University of Southampton, UK; M. Mikula, L. Satrapinskyy, T. Roch, M. Truchlý, Comenius University in Bratislava, Slovakia; P. Švec Jr., Slovak Academy of Sciences, Bratislava, Slovakia; T.H. Huminiuc, T.P. Polcar, University of Southampton, UK

Self-lubricant thin solid films produced by physical vapour deposition (PVD) techniques represent modern approach to reduce friction in highly demanding situations where traditional liquid lubricants cause problems (environmental, excessive costs, frequent maintenance) or cannot be used at all (vacuum, extremely high/low temperatures and contact pressures). Transition metal dichalcogenides (TMDs), especially molybdenum disulphide (MoS₂), are the most known and applied solid lubricant coatings; however, its use is limited by environmental sensitivity and low hardness. To improve mechanical and tribological properties, we doped MoS₂ coating with nitrogen.

Mo-S-N solid lubricant films were deposited by pulsed d. c. High Target Utilisation Sputtering (HiTUS) in Ar + N₂ atmosphere. The effect of deposition parameters on chemical composition, structure, mechanical and tribological properties of MoS_x and Mo-S-N coatings was studied; films with the most promising properties have been selected for tribological testing. MoS_x films with S/Mo ratio 1.6 exhibited the coefficient of frictions (COFs) in humid air 0.12 and 0.05 for loads 2 and 15 N, respectively. Mo-S-N films were prepared with nitrogen content in a range of 19 to 50 at., whereas S/Mo ratio varied from 1.2 to 0.4. Mo-S-N films were amorphous or nanostructured with nanograins of molybdenum disulphide. Hardness increased with N doping up to 14 GPa for film with the highest nitrogen content. Friction behaviour in humid air was evaluated using a ball-on-disk tribometer. Globally, the doping with N resulted in hardness in Mo-S-N films one order of magnitude higher than in an undoped one, keeping the friction coefficient at the same level or even lower. These coatings showed remarkable friction coefficients in humid air from 0.18 to 0.06 with loads from 2 to 15 N, respectively. The excellent friction properties were attributed to the formation of a thin molybdenum disulphide tribofilm on the top of the wear track of the film and on the counterpart surface. HiTUS represents a very promising way of depositing thin coatings on the thermally sensitive substrates (e.g. bearing steel) with desired properties.

8:40am **E1-3-FrM3 Superlubricity with Carbon Coatings Lubricated by Organic Friction Modifiers**, M. Moseler (mos@iwm.fhg.de), Fraunhofer IWM, Germany

INVITED

Superlubricity of tetrahedral amorphous carbon (ta-C) coatings lubricated with unsaturated organic friction modifiers or glycerol is a well-known phenomenon, but the underlying mechanisms remain elusive. Here, combined experiments and simulations unveil a universal tribochemical mechanism leading to superlubricity of ta-C/ta-C tribopairs. Pin-on-disc sliding experiments show that ultra- and superlow friction with negligible wear can be achieved by lubrication with unsaturated fatty acids or glycerol, but not with saturated fatty acids and hydrocarbons. Atomistic simulations reveal that, due to the simultaneous presence of two reactive centers (carboxylic group and C=C double bond), unsaturated fatty acids can concurrently chemisorb on both ta-C surfaces and bridge the triboagap. Sliding-induced mechanical strain triggers a cascade of molecular fragmentation reactions releasing passivating hydroxyl, keto, epoxy, hydrogen and olefinic groups. Similarly, glycerol's three hydroxyl groups react simultaneously with both ta-C surfaces, causing the molecule's

Friday Morning, May 24, 2019

complete mechano-chemical fragmentation and formation of aromatic passivation layers with superlow friction.

9:20am **E1-3-FrM5 Multipass and Reciprocating Microwear Study of TiN Based Films**, *R.C. Vega-Morón (vega.moron@gmail.com)*, Instituto Politecnico Nacional Grupo Ingeniería de Superficies, Mexico, México; *D.V. Melo-Máximo*, Tecnológico de Monterrey-CEM, México; *G.A. Rodríguez-Castro*, Instituto Politecnico Nacional, Grupo Ingeniería de Superficies, Mexico, México; *J. Oseguera-Peña*, Tecnológico de Monterrey-CEM, Mexico, México; *A. Bahrami*, Institute for Metallic Materials, Leibniz-Institute for Solid State and Materials Research Dresden, Germany; *S. Muhl*, Instituto de Investigaciones en Materiales-UNAM, México

Titanium nitride-based films were deposited on AISI 316L steel by D.C. unbalanced magnetron sputtering. Adhesion and wear resistance at the micrometric range of the films were studied by changing the gas mixture ratio and the temperature of the substrate during the deposition process. Scanning electronic microscope (SEM), elemental analysis (EDS) and X-Ray diffraction (XRD) were carried out to investigate films physico-chemical characteristics. Also, the examination of topography was conducted by atomic force microscopy (AFM). Mechanical properties were studied by nanoindentation test. Scratch tests were performed with a chrome steel ball (1 mm of diameter) on a 3 mm scratch track and the critical loads were estimated. Additionally, reciprocating microwear and multipass sliding tests were conducted at 0.5 and 1 N using an alumina ball (3 mm of diameter) as counterpart. The coefficient of friction behavior was analyzed and the identification of damage mechanisms were conducted by SEM and optical profilometry.

9:40am **E1-3-FrM6 Correlation Between Wear Resistance of Ti/TiN Based Films and Deposition Temperature**, *F. Toledo-Romo (fer.toledoromo@gmail.com)*, *R.C. Vega-Morón*, Instituto Politecnico Nacional, Grupo Ingeniería de Superficies, México; *G.A. Rodríguez-Castro*, Instituto Politecnico Nacional, Grupo Ingeniería de Superficies, Mexico, México; *D.V. Melo-Máximo*, *J. Oseguera-Peña*, *L. Melo-Máximo*, Tecnológico de Monterrey-CEM, México; *V.M. Araujo-Monsalvo*, Laboratorio de Biomecánica, Instituto Nacional de Rehabilitación "Luis Guillermo Ibarra Ibarra", México

Ti/TiN bilayer films deposited on AISI 316L by D.C. unbalanced magnetron sputtering were investigated. The mechanical properties, adhesion and wear resistance of Ti/TiN films were evaluated according to the temperature of the substrate during the deposition process. Four temperatures were used for the study, these were: at room temperature, 80, 120 and 200 ° C. The power and gas mixture ratio during the deposition process remained constant. The bilayer system optical inspection was carried out by scanning electronic microscopy (SEM) and the physico-chemical characterization was performed by energy dispersion spectroscopy (EDS) and X-ray diffraction (XRD). Hardness and Young's modulus were determined by instrumented indentation. Scratch tests were performed to evaluate adhesion using a Rockwell C indenter and loads of up to 100 N. Critical loads (Lc) were estimated based on optical microscope observations of the scratch tracks. The wear coefficients of TiN and Ti formed on 316L steel were evaluated by a micro-abrasion tester using SiC particles dissolved in deionized water as abrasive slurry. The wear coefficients were obtained by relating the Archard law and the wear area (obtained by optical profilometry).

10:00am **E1-3-FrM7 Microstructure Evolution and Deposition Parameter Control on Sputtering MoSiN Coating**, *Y.C. Liu (com35518617@gmail.com)*, *Z.X. Lin*, *S.T. Wang*, *F.B. Wu*, National United University, Taiwan
Transition metal nitride, TMN, coating due to its excellent surface and mechanical characteristics, was applied in surface finishing, decoration, and protective coating. In present study, the molybdenum silicon nitride, MoSiN, films were produced by RF magnetron sputtering technique for protective application. Microstructure evolution and composition variation were found for the MoSiN coating due to the change of the input power and gas flow ratio during the manufacturing process. The effect of input power control on microstructure evolution and indentation cracking behavior were analyzed. When input powers on Si and Mo were fixed at 105W and 135W, respectively, the Si/MoSi contents varied from 0.27 to 0.44 when Ar/N₂ flow changed from 18/2 to 10/10. The microstructure possessed a featureless structure as a high content Si was incorporated. Hardness, Young's modulus, abrasion characteristics of the MoSiN monolayer films were further investigated and discussed.

10:20am **E1-3-FrM8 Influence of Ag Content on the Tribological and Oxidation Behaviour of TiSiN(Ag) Thin Films Deposited by HIPIMS**, *D. Cavaleiro (diogoacavaleiro@gmail.com)*, *F. Fernandes*, *S. Carvalho*, University of Minho, Portugal; *A. Cavaleiro*, University of Coimbra, Portugal
Titanium alloys are one of the most common materials used in several important industries (aerospace, automotive, etc.) due to its multiple excellent properties. Nonetheless, they are also known as a "difficult-to-machine" material, leading to the premature wear and/or failure of the machining tools and consequently to the increase of the production costs. Self-lubricating coatings (highly oxidation resistant coatings alloyed with a lubricious element) are one of the most promising solutions to overcome this problem. The main challenge nowadays in these type of coatings is to control the diffusion of the lubricious element to the surface. Here, we propose to control the diffusion of silver, using the TiSiN system deposited as nanocomposite structure. Si-N matrix of this coating system is well known to have diffusion barrier properties which with proper tailoring of the structure, could avoid the lubricious agent diffusion. This work reports the influence of Ag additions on the properties of TiSiN(Ag) films deposited by high power impulse magnetron sputtering- HIPIMS. All of the coatings displayed a fcc NaCl-type crystalline structure. Silver addition to the TiSiN coating significantly lowers the TiN crystallites size however, grain size of Ag containing coatings was independent of the coatings chemical composition. Mechanical properties of the coatings deteriorated with the increasing silver content. Ag additions decreases the oxidation behavior of films, however it improves their tribological performance.

10:40am **E1-3-FrM9 Wear Resistance of Titanium Oxynitride Coatings as a Function of the Relative Humidity**, *C. Rojo-Blanco (rojo.blanco.c@gmail.com)*, IIM-UNAM, Mexico; *S. Muhl*, Instituto de Investigaciones en Materiales-UNAM, México

For this study we used titanium oxynitride thin films because of their many uses as coatings in biological, aeronautics, automotive applications. Each application has its own environment with different conditions that can influence the wear of the films. These conditions can involve physical (applied force and temperature, etc.) or chemical (acid, basic, relative humidity, etc.) factors.

The five groups of titanium oxynitride coated samples, with different oxygen to nitrogen ratios, were deposited by RF reactive sputtering on to stainless steel substrates. To analyze the wear we employed the reciprocating sliding test, one of the most common tests. With this technique we could observe the change of the coefficient of friction during the wear process, and subsequently measured the wear volume and study the wear track. In order to control the relative humidity surrounding the point of contact between the deposited film and the counter-body (alumina) we modified our standard reciprocating sliding test machine to include an enclosure connected to the gas flow from a humidity generator. In this way we measured the variation of the wear, using an optical profilometer, as a function of the relative humidity for each group of oxynitride coatings.

11:00am **E1-3-FrM10 Thermo-mechanical/chemical Contact Behavior of DLC Film under Molecularly Thin Lubricants**, *SM. Rahman (shahriar.rahman@ttu.edu)*, Texas Tech University, USA; *J. Song*, Molex. USA, USA; *C.D. Yeo*, Texas Tech University, USA

Diamond like carbon (DLC) has been widely used as a surface protective coating due to its outstanding tribological performance. When a DLC coating is required to sustain high speed surface contact at hot/wet condition, its surface is susceptible to critical damage by mechanical and chemical degradation of carbon atoms. In this study, the thermo-mechanical/chemical contact behavior of DLC film under molecularly thin lubricants is investigated through molecular dynamics (MD) simulations. Three different designs of PFPE lubricants (i.e., D4OH, Z-tetraol and ZTMD) are applied onto amorphous DLC film. Under the high-speed sliding contact with an asperity made of diamond, the friction and wear of DLC film is quantitatively measured and compared. From MD simulation results, it could be found that all three lubricants significantly improved the tribological performance of DLC film, and the lubricants with higher molecular weight made further improvements. It is expected that the research outcome can provide more physical insight into the tribological performance of DLC film and PFPE lubricants, which can deliver their key design rules to achieve the long-term reliability of a system.

Friday Morning, May 24, 2019

11:20am **E1-3-FrM11 Investigation of the Wear Resistance of TiN/TiAlN, CrN/TiAlN and CrAlN/TiAlN Double Layer Coated Stainless Steel at Elevated Temperatures**, *Y. Adesina (akyadesina@gmail.com)*, *A. Sorour*, King Fahd University of Petroleum and Minerals, Saudi Arabia

TiAlN coating is now widely being used as protective coatings against wear and abrasion in turbomachinery, cutting tools and aerospace applications. This is due to its superior mechanical and tribological properties at both low and high temperatures over commonly used TiN coating. However, increasing demands on hard coatings due to increased productivity, new tool applications such as high-speed cutting, dry cutting and/or extreme operating environment have necessitated the need for improved coating performance. Coating architecture, microstructural and compositional modification, as well as advanced deposition technologies, are among methods currently being researched to further improve properties of TiAlN and other hard coatings. The use of an interlayer coating is well known to improve adhesion, corrosion and wear resistance properties. Several efforts are being tailored in order to improve the performance efficiency of TiAlN at elevated temperatures through the use of layers and multi-layered deposits.

This study is aimed at investigating the wear resistance and the effect of TiN, CrN and CrAlN as interlayers for TiAlN at elevated temperatures. The wear behavior of these double layer coatings will be evaluated under reciprocating wear test configuration at room temperature, 250 and 500 °C and compared to the monolayer TiAlN coating (without interlayer) to reveal the role of the interlayer coatings. An attempt will be made to investigate both surface and subsurface damages during wear. 3D optical profilometer, scanning electron microscope (FE-SEM) and energy dispersion spectroscopy (EDS) will be utilized to understand the wear damages and underlying mechanisms. The structural and mechanical characterization of the coatings analyzed using X-ray diffraction (XRD) technique and microindentation, respectively, will also be examined and discussed in light of the wear behavior.

11:40am **E1-3-FrM12 Effect of Electrostatic Solid Lubrication on Tribological Behavior of Ti-6Al-4V Alloy**, *R.K. Gunda (kumarrakeshgunda@gmail.com)*, *S.K.R. Narala*, BITS Pilani Hyderabad Campus, India; *S. Palaparty*, Methodist College of Engineering and Technology, India; *S.P. Regalla*, BITS Pilani Hyderabad Campus, India

The advanced science of tribology offers challenges for the cooling/lubrication of hard-to-cut materials in sliding and machining processes. Modern tribology has facilitated the use of solid lubricants with low cost and eco-friendly, which can sustain and provide lubricity over a wide range of temperature in controlling heat and frictional effect on interface zone. The aim of the paper is to study the effect of innovative ECSL spray technique and the existing results are compare with MQSL and dry sliding conditions under various speed and load conditions. Sliding tests were performed under pin-on-disc tribometer against WC pin and Ti-6Al-4V alloy disc materials. SEM and EDS analysis were used to analyse the morphological and chemical composition of worn surfaces. The present work is expected to form a scientific basis towards developing ECSL spray technique for reducing tribological and environmental perspectives.

Surface Engineering - Applied Research and Industrial Applications

Room Pacific Salon 1 - Session G2-FrM

Component Coatings for Automotive, Aerospace, Medical, and Manufacturing Applications

Moderators: *Tetsuya Takahashi*, Kobe Steel, Ltd., Japan, *Etienne Bousser*, École Polytechnique de Montréal, Canada, *Satish Dixit*, Plasma Technology Inc., USA

8:40am **G2-FrM3 YKK's Sustainable Development: Reduction of Mold Cleaning Load by Diecast Mold Coating and Release Agent**, *M. Mizubayashi (m-mizubayashi@ykk.co.jp)*, *T. Sakuragi*, *N. Watanabe*, *M. Ishida*, YKK Corporation, Japan; *K. Matsuda*, University of Toyama, Japan; *M. Nose*, Hokuriku Polytechnic College, Japan

INVITED

In recent years, as a common philosophy in the preservation of the global environment, there is a sustainable development as a concept that is internationally widely recognized. This time, we will introduce the development of die coating and mold release agents, which are working on the continuous development of YKK and die casting technology. In the past technological development, the point of view of material strength and efficiency has been emphasized. We are working on a comprehensive development from the viewpoint of improving the total efficiency of the

equipment by reducing the mold cleaning load and reducing operator safety, health care and environmental impact. The result was very good this time. The combination of the developed an amorphous carbon film (a-C film) and the release agent, from the time of combination with the nitriding type and conventional release agent, it was confirmed that the workability is an item that was improved about 15%. The joy of the developers is that the people on the scene are satisfied with the results of the development. We want to make the most of the feature and the charm of the coating, and challenge the next generation manufacturing. I am deeply grateful to all the people who have helped me with this study.

9:20am **G2-FrM5 Effect of Plasma Electrolytic Oxidation Process on Surface Characteristics and Tribological Behavior**, *R. Cai (cai12r@uwindsor.ca)*, *C. Zhao*, *X. Nie*, University of Windsor, Canada

Alumina coatings prepared by PEO (plasma electrolytic oxidation) process have been proposed and in a validation process to replace heavy cast iron liners for internal combustion engines. The bipolar current mode in the PEO process is known as an excellent coating preparation condition. However, the industrial production would require an optimized as well as cost-efficient process. The unipolar current mode can significantly reduce the investment on coating facilities. Thus, this research was to use the unipolar mode to prepare oxide ceramic coatings on Al-Si alloy samples with different durations, i.e., 20%, 30% and 40% durations of 1000Hz. One of the samples was used with a normal bipolar mode for comparison. The influence of duty ratios on the coating's deposition rate, porosity and wear resistance was investigated. At a similar coulomb charge input ($I \times t$), the change of duty ratios from 0.8 to 0.2 had an insignificant effect on the coating deposition rates, but the coating's porosities decreased and wear resistance increased after the coated samples were polished to Ra around 25 microns and 20 microns. Dry and lubricated pin-on-disc tests indicated that the coatings produced by unipolar current mode at the lower duty ratio had comparable properties of the one prepared with the bipolar current mode. The tribological behavior of the polished surfaces was analyzed based on their surface morphology characteristics (Ra, Rpk, Vo, skewness and kurtosis). The work provides a new perspective for the optimization of PEO process for automotive application.

9:40am **G2-FrM6 Effectiveness of Electromagnetic Interference Shielding of Sputtered Nitrogen-Doped Carbon Thin Films**, *D.H. Liu (birdieliu1012@gmail.com)*, *Y.S. Lai*, National United University Miaoli, Taiwan

In this work, nitrogen-doped carbon thin films are deposited on aluminum foils by RF magnetron sputtering with different N₂ flow rates. Film properties are characterized by Raman spectroscopy, X-ray photoelectron spectroscopy, scanning electron microscopy, and transmission electron microscopy. The electrical properties are conducted by Hall measurements, and the shielding efficiency is extracted from network analyzer in the frequency range of 8.2-12.4 GHz. The Raman spectra confirms that adding small amounts of N in carbon films increases full width at half maximum of G-band and the intensity ratio (ID/IG). A red shift of the G-band is also observed. The Hall measurement reveals that the N doping acts as electron donor, leading to the increase of conductivity and carrier concentrations. Due to the improvement of electrical properties, the electromagnetic interference shielding efficiency, in terms of reflection and transmission loss, increases as well.

10:00am **G2-FrM7 Challenges for Surface Solutions for Automotive Applications**, *J. Vetter (joerg.vetter@oerlikon.com)*, *J. Becker*, Oerlikon Balzers Coating Germany GmbH, Germany; *P. Ernst*, Oerlikon Metco AG, Switzerland; *J. Crummenauer*, Oerlikon Balzers Coating Germany GmbH, Germany; *A. Müller*, Oerlikon Surface Solutions AG, BTS, Balzers, Liechtenstein

Automobile manufacturers have to consider in addition to the expectations and satisfaction of customers regarding the reliability, functionality, comfort and safety, additional aspects such as: production, consumption and environmental issues. Regional environmental legislation and shorter product life cycles require higher quality and more stringent materials requirements. Higher specific loads (thermal, mechanical etc.), weight and friction reduction (CO₂; NO_x emission reduction), longer components lifetime, improved corrosion resistance are demanding for modern automotive systems, and multifunctional surfaces like sensory functions. In addition new surface solutions are required for green car development (e.g. HEV, BEV with range extenders). Within the last decades, high performance surface solutions and new or improved surface treatments, especially in the group of plasma assisted processes, both for diffusion and deposition processes (IONITOX, PVD, PACVD, Thermal Spraying) were developed to

Friday Morning, May 24, 2019

provide economic applications for automotive parts. It will be shown that these new treatments are becoming more common in engine applications and powertrain. Generating optimized surfaces for different types of substrate materials (e.g. Al-alloys, case hardened steels, plastics etc.) and geometries (e.g. bores) also impacts the running costs. Due to the new developments within these competing surface treatments, it becomes more and more common to substitute traditional treatment-substrate-systems with advanced treatments. Both the application potential and selected examples of different surface treatments will be shown. Besides the wear and friction reduction of various components also decorative applications even for multifunctional purposes are successfully implemented in daily production. The potential of optimized functional surface generation by proper coating selection is demonstrated.

10:20am **G2-FrM8 Hard Turning with PVD Coated p-cBN**, C.J. Charlton, Kennametal Inc., USA; J. Kohlscheen (joern.kohlscheen@kennametal.com), Kennametal GmbH, Germany; D. Banerjee, Kennametal Inc., USA; C. Bareiss, Kennametal GmbH, Germany

We will give an overview of uncoated and PVD coated polycrystalline or p-cBN cutting tools that are used in finish turning on hardened steel. Examples include turning of automotive braking disks and precision shafts. Interestingly, PVD coatings can improve wear behavior in many applications. As the hardness of such thin films is comparable to the substrate values the improvement is explained by thermal and chemical protection. As many of the different p-cBN substrate materials show reduced electrical conductivity the deposition process has to be adapted. To improve adhesion and overall performance different interlayers and plasma etching cycles were applied in deposition of AlTiN arc ion plated coatings. Difference in adhesion were determined by indentation and scratch testing. Tool life was compared in turning tests of hardened steel (60 HRC) without coolant. The resulting wear patterns will be discussed.

10:40am **G2-FrM9 Arc PVD (Cr,Al,Mo)N and (Cr,Al,Cu)N Coatings for Mobility Applications**, K. Bobzin, T. Brögelmann, C. Kalscheuer (kalscheuer@iot.rwth-aachen.de), RWTH Aachen University, Germany

Efficiency during operation is besides reliability and cost effective production one of the most important demands on machines and components. Especially within the automotive sector, components need to fulfill these requirements. Since the demands for high efficiency and reliability cannot be met solely by typical base materials such as case hardened steels, physical vapor deposition (PVD) coatings for the application on highly loaded components gain increasing importance. A possible approach to reduce friction and wear in tribological systems are triboactive and tribocatalytic coatings which contain triboactive elements such as Mo and Cu which can interact with lubricants and lead to the formation of friction and wear reducing tribochemical reaction layers. Besides coating development, also the design of lubricants is in the focus of research activities to reach friction reductions. Therefore increasing interest gains towards low viscosity lubricants e.g. for e-mobility applications.

Within the current work, triboactive (Cr,Al,Mo)N and (Cr,Al,Cu)N coatings were deposited by means of cathodic arc evaporation (Arc PVD) in an industrial scale coating unit. The contents of Mo and Cu were varied. As substrate material the case hardened gear steel AISI 5115 (16MnCr5E) was used. The effects of Mo and Cu on the phase formation were investigated by means of X-ray diffraction (XRD). Analysis of the mechanical properties was conducted by nanoindentation (NI) measurements. Tribological behavior of the coatings was analyzed under continuous sliding conditions in pin on disc (PoD) tribometer under minimum quantity lubrication with lubricant amounts of $V = 0.05$ ml at a temperature $T = 80$ °C. As lubricants a low viscosity lubrication oil and a conventional mineral oil were used. Both lubricants contained Sulphur and Phosphorous (S-P) additives. Initial Hertzian contact pressure was set to $p_H \approx 1,600$ MPa. In order to investigate the influence of the counter body material on the tribological behavior, inert Si_3N_4 balls and 100Cr6 steel balls were used. Wear was analyzed by confocal laserscanning microscopy (CLSM) and scanning electron microscopy (SEM). Tribochemical interactions between the coatings and lubricants were studied by Raman spectroscopy. It was found that tribochemical interactions between Mo of the coating and S of the lubricant can lead to the in situ formation of MoS_2 in tribological contact. Triboactive (Cr,Al,Mo)N and (Cr,Al,Cu)N coatings are a promising approach to achieve reduced friction and wear in tribological systems.

11:00am **G2-FrM10 Thermal Analysis on the Application of Plasma Electrolytic Oxidation (PEO) Coatings On Automobile Engines**, X. Shen, X. Nie (xnjie@uwindsor.ca), University of Windsor, Canada; J. Tjong, Ford Motor Company, USA

The demand for the reduction of fuel consumption and emission has accelerated the replacement of traditional cast iron engine cylinders with lightweight Al-alloy-based ones due to the high strength-to-weight ratio of aluminum alloys. The thermal spray coating is commonly used to deposit on the cylinder bore to improve the cylinder wear resistance and on the piston crown to prevent the heat energy loss. Alternatively, in this paper, the plasma electrolytic oxidation (PEO) coating is adopted to deposit on the engine cylinder bore and the piston crown surface. In contrast with the thermal spray coating, the PEO coating possesses strong adhesion to the metal substrate and can have a relatively small thickness.

This paper is mainly focused on how the PEO coating affects the heat transfer in the automobile engine and investigates how the thermal behavior of the cylinder and the piston changes with the coating. Numerical simulation shows that the presence of the PEO coating can cause the occurrence of the temperature swing on the cylinder bore and the piston crown surface. The temperature swing can effectively prevent the heat loss. Moreover, the amplitude of the temperature swing increases with the coating thickness but it does not increase as the coating thickness reaches a certain value. The comparison among the different cylinder/piston materials coated with PEO coatings reveals that the effective thermal conductivity is the primary reason to cause the variation in temperature swing amplitude. In addition, most importantly, a relatively small coating thickness could be beneficial to the improvement of the engine volumetric efficiency. The main objective of the paper is to provide the design of a high-quality coating for the cylinder bore and the piston crown so as to improve the automobile engine efficiency.

Keywords: plasma electrolytic oxidation (PEO) coating, automobile engine, thermal swing, thermal analysis

11:20am **G2-FrM11 Ion Beam Stripping Process for Cutting Tools Reconditioning**, A.G. Remnev (remnev.a@shinmaywa.co.jp), ITAC Ltd., Group of ShinMaywa Industries, Japan

Presently, various kinds of hard film coatings are used in combination with cemented carbide (WC-Co) and high speed steel (HSS) cutting tools for increased longevity. For further improvement of the coated tools' life-span, their regrinding and recoating are commonly implemented. Successful recoating requires stripping off of a previous coating in order to provide sufficient adhesion. Wet electro-chemical etching (ECE) process is commonly applied for the stripping purpose. Although well established, the ECE method has some known issues such as cobalt binder leaching from the WC-Co tools, HSS corrosion, large amount of chemical waste produced. Moreover, the ECE stripping method cannot be applied to the carbon-based thin films, such as diamond and diamond like carbon (DLC), due to their chemical inertness. In this context new competitive stripping approaches are of high applicational importance.

In the present work we introduce a vacuum stripping process based on ion beam etching (IBE) of the hard films. The IBE method utilizes low energy (~1keV) high current (~0.1A) broad (~10cm) ion beams in order to create sufficient ion and radical fluxes on the tools' surface. In order to etch the metal based films, such as TiN, TiAlCrN, TiCN argon gas was introduced, while carbon based DLC and diamond films were IBE processed utilizing pure oxygen as a working gas for improved erosion rate and selectivity against the carbide material.

IBE erosion rates of commercial PVD and CVD hard coatings on various WC-Co cutting tools were experimentally measured and plasma-chemical aspects of diamond decomposition were discussed. Effect of tool geometry on the IBE uniformity was experimentally studied by measuring the local erosion rate over the tools' surface. Moreover, mathematical model of the IBE process, describing the erosion rate distribution was suggested. Surface condition of the WC-Co substrates treated by IBE were evaluated and no significant deterioration was found. Overall, it was shown that IBE provides sufficient erosion rate and uniformity without significant damage to the tool material for virtually any kind of hard coating used in today's cutting tools industry.

Bold page numbers indicate presenter

— A —

Abadian, G.: FP-ThP10, **198**; H1-2-TuA2, 121; SIT1-TuSIT1, **124**
 Abbas, A.: C3+C1-WeM2, 128
 Abboud, M.: E2-2-TuA10, 119; EP-ThP5, 193
 Abere, M.J.: C4-ThA2, **168**; C4-ThA6, 168
 Abraham, B.: B1-2-MoA1, 92
 Abro, M.A.: A1-3-WeM12, **126**
 Abstoss, K.G.: A1-1-TuM8, 102
 Adams, D.P.: C4-ThA2, 168; C4-ThA6, **168**
 Addou, F.: B2-2-FrM5, 208
 Adesina, Y.: AP-ThP5, **176**; E1-3-FrM11, **212**
 Afshar, A.: B4-4-WeA6, 138; DP-ThP26, 192
 Agüero, A.: A3-WeA4, **136**; TS2-ThM8, 161
 Aguirre Ocampo, R.: D1-2-MoA5, **96**
 Ahlgren, M.: F4-2-WeA7, 142
 Airoidi, V.T.: DP-ThP19, 191
 Akinlabi, E.T.: AP-ThP4, 176; B4-2-TuA10, 114
 Akinlabi, S.A.: AP-ThP4, 176; B4-2-TuA10, 114
 Al-Badour, A.: AP-ThP5, 176
 Albers, C.: BP-ThP37, 185
 Alem, N.: B2-1-ThA9, 165
 Aleman, A.: B6-ThM10, 152
 Alhoussein, A.A.: A1-1-TuM6, 102; E2-1-TuM5, 108
 Alling, B.: F4-2-WeA7, 142
 Allport, J.: AP-ThP2, 176
 Almer, J.: A2-1-ThM8, 150
 Almtoft, K.P.: E1-1-ThM7, 156; GP-ThP11, 201
 Alphonse, A.: F4-2-WeA11, 143
 Alrefae, M.: F3-TuA1, 119
 Altangerel, D.: B7-TuA3, 115
 Alvarez, F.: B4-3-WeM2, **126**; E1-2-ThA11, 171
 Ambriz-Vargas, F.: CP-ThP27, **189**
 Amini, S.: D1-2-MoA3, 96
 Anders, A.: FP-ThP6, 198
 Anderson, J.: G4+G5+G6-ThA1, **173**
 Andreev, N.: B1-2-MoA11, 93
 Anselme, K.: D3-TuM4, **106**
 Antunes, V.: B4-3-WeM2, 126
 Aouadi, S.M.: A2-1-ThM5, 149; A2-1-ThM9, 150
 Appleget, C.: C3+C2+C1-ThM8, **154**
 Araujo-Monsalvo, V.M.: E1-3-FrM6, 211
 Arciniega-Martínez, J.L.: B4-2-TuA3, **113**
 Ares de Parga, G.: B4-2-TuA8, 114
 Argibay, N.: E3-WeM1, 129
 Argyropoulos, C.: C3+C2+C1-ThM9, 154
 Arias, P.: B6-ThM10, 152
 Arigela, V.G.: H3-1-WeM3, **132**; H3-2-WeA9, 145
 Armstrong, B.L.: A1-1-TuM1, 101; A1-3-WeM4, 125
 Arndt, M.: B6-ThM12, 153; BP-ThP41, 185; TS1-1-WeM4, 133
 Arroyave Franco, M.: E1-4-WeA5, 141
 Arruda, D.C.: DP-ThP19, 191
 Arunachalam, N.: D1-1-MoM7, 88
 Asensio, M.C.: F3-TuA8, 120
 Ashok, A.: C4-ThA9, 169
 Ast, J.: A2-2-ThA3, 163
 Attarzadeh, R.: TS2-ThM9, 162
 Audigié, P.: A3-WeA4, 136
 Aureli, M.: C4-ThA3, 168
 Avila, J.: F3-TuA8, 120
 Awais, R.: D3-TuM6, 106
 Azzi, M.: E1-1-ThM6, 156; EP-ThP30, 197
 Azzopardi, A.: B1-2-MoA2, 92; FP-ThP9, 198

— B —

Bachu, S.: B2-1-ThA9, 165
 Bäche, O.: B2-1-ThA5, **165**
 Badhirappan, G.P.: C4-ThA9, **169**
 Bagcivan, N.: E1-2-ThA10, 171
 Bahrami, A.: B5-2-FrM4, 209; E1-3-FrM5, 211
 Bai, T.: C2-WeA9, 139
 Baik, Y.: GP-ThP23, **203**; HP-ThP12, 205
 Baker, M.: C3+C1-WeM4, 129
 Bakhit, B.: B4-1-TuM4, 104
 Bakkar, S.: A2-1-ThM9, 150
 Balaji, G.: C4-ThA9, 169
 Balasundraprabhu, R.: C4-ThA9, 169
 Balat-Pichelin, M.: B2-1-ThA7, 165
 Balazsi, K.: B1-3-TuM6, 104; B5-1-ThA4, 166
 Baloukas, B.: C3+C1-WeM4, 129
 Banakh, O.: DP-ThP22, 191
 Banerjee, D.: B2-1-ThA8, 165; BP-ThP1, 178; G2-FrM8, 213
 Banks, C.E.: F3-TuA3, 119
 Barbosa, M.: CP-ThP23, 188
 Bareiss, C.: G2-FrM8, 213
 Barman, T.B.: TSP-ThP6, 206
 Barnier, V.: F3-TuA8, 120
 Barquete, D.M.: BP-ThP28, 183
 Barr, C.M.: H3-2-WeA3, 143
 Barrallier, L.: H1-2-TuA5, 122
 Barrios, A.: H2-1-MoM4, **89**
 Bartosik, M.: B4-2-TuA1, 113; B5-1-ThA5, 167; B6-ThM2, 151; BP-ThP19, 181; BP-ThP35, 184
 Batková, Š.: F1-TuM4, 109; F4-1-WeM2, **131**
 Batory, D.: TSP-ThP2, **206**
 Beake, B.D.: H3-2-WeA2, **143**
 Beaufort, M.F.: E2-2-TuA2, 118
 Becker, J.: E3-WeM5, 130; G2-FrM7, 212
 Beganovic, N.: E3-WeM5, 130
 Bejarano, G.: D3-TuM8, 107; DP-ThP25, 192
 Bellido-Gonzalez, V.: B1-2-MoA2, **92**; B3-2-MoA5, 94; FP-ThP9, **198**
 Belviso, F.: E1-2-ThA8, **170**
 Bensalah, W.: D2-TuA1, 116
 Berastegui, P.: TS1-1-WeM5, 134
 Berger, K.: BP-ThP37, 185
 Bergeron, F.: A1-3-WeM10, **125**
 Berlia, R.: H1-2-TuA3, 121
 Berman, D.: A2-1-ThM9, 150; E3-WeM3, 129
 Bermejo Sanz, J.: A3-WeA5, 136
 Bernardes, C.: E1-3-FrM1, **210**
 Bernatova, K.: B7-TuA2, 115
 Berndorf, S.: B4-4-WeA7, 138
 Bertram, R.: B3-1-MoM2, 86; B3-2-MoA2, 94
 Berumen, J.O.: D2-TuA4, 116
 Beyerlein, I.J.: H2-2-MoA7, **98**
 Biederman, H.: F1-TuM1, 108
 Bierwisch, N.: H2-2-MoA10, **98**; HP-ThP9, **205**
 Bijalwan, P.: B5-2-FrM9, **210**
 Bijukumar, D.: D2-TuA5, 116; D3-TuM7, 106
 Bilek, M.M.: B5-1-ThA6, 167
 Biring, S.: C3+C2+C1-ThM10, 154
 Bissell, L.: F3-TuA5, 120
 Bitar-Nehme, E.B.-N.: EP-ThP30, 197
 Bittau, F.: C3+C1-WeM2, 128
 Bleu, Y.: F3-TuA8, **120**
 Bloesch, D.: B1-2-MoA5, 92; G4+G5+G6-ThA5, 173
 Bo, W.X.: EP-ThP28, 197
 Bobzin, K.: BP-ThP23, 182; BP-ThP4, 179; E3-WeM4, 130; F4-2-WeA5, 142; G2-FrM9, 213
 Bocher, P.: H3-2-WeA8, 144

Bogdanowicz, R.: D2-TuA10, 117; F3-TuA11, **120**
 Boichot, R.: B2-1-ThA6, 165; B2-2-FrM5, 208
 Bolívar, F.J.: DP-ThP4, 190; E2-2-TuA3, 118
 Bolvardi, H.: B4-2-TuA1, 113; B6-ThM9, 152; FP-ThP3, 197
 Bolz, S.: G1+G3-ThM2, 158
 Boman, M.: B2-2-FrM7, 208; B2-2-FrM8, **208**; BP-ThP20, 182
 Böör, K.: B2-2-FrM8, 208; BP-ThP20, **182**
 Borges, J.: D3-TuM2, 105
 Boris, D.R.: C2-WeA5, 139
 Borja Goyeneche, E.N.: B4-1-TuM6, 105; BP-ThP39, 185
 Bourquard, F.: F3-TuA8, 120
 Bousser, É.: A1-3-WeM10, 125; A1-3-WeM3, 125; C3+C1-WeM4, 129; E1-1-ThM6, 156; H3-2-WeA8, 144; TS2-ThM3, 161
 Bouvard, G.: D1-1-MoM3, 88
 Boveri, G.: TS2-ThM2, **160**; TS2-ThM5, 161
 Bowden, M.D.: F2-1-ThM11, 158
 Boyce, B.L.: H3-2-WeA3, 143
 Bradley, J.W.: F2-1-ThM11, **158**
 Braun, R.: B1-3-TuM2, 103
 Brenning, N.: B7-TuA9, 115; F2-1-ThM8, 158
 Brenning, R.M.: B2-2-FrM7, 208
 Briggs, S.A.: H3-2-WeA3, 143
 Brindley, J.: FP-ThP9, 198
 Brodu, A.: C3+C2+C1-ThM7, **154**; GP-ThP24, **203**
 Brögelmann, T.: BP-ThP23, 182; BP-ThP4, 179; E3-WeM4, 130; F4-2-WeA5, 142; G2-FrM9, 213
 Broitman, E.: EP-ThP18, **195**; G4+G5+G6-ThA11, **174**
 Brown, R.: B1-2-MoA2, 92; FP-ThP9, 198
 Brown, S.: TS2-ThM11, **162**; TSP-ThP2, 206
 Brown, S.G.R.: TSP-ThP4, 206
 Brugnara, R.H.: E1-2-ThA10, **171**
 Brümmer, A.: EP-ThP23, 196
 Buchinger, J.: BP-ThP19, 181; BP-ThP35, 184
 Buchwalder, A.: G4+G5+G6-ThA9, **174**
 Buechel, C.: G4+G5+G6-ThA5, **173**
 Buenrostro Arvizu, M.G.: EP-ThP11, 194
 Bull, S.J.: H2-2-MoA1, **97**
 Bumgardner, J.: D2-TuA2, 116
 Burghammer, M.: B4-4-WeA2, 137
 Bursikova, V.: B1-3-TuM6, 104; B5-1-ThA4, 166
 Burzynski, K.: TS3+4-2-MoA5, **99**
 Butler, A.: B7-TuA9, 115
 — C —
 C. Rodrigues, D.: D3-TuM3, 105
 Cabrerizo Vélchez, M.: TS2-ThM4, 161
 Cada, M.: B7-TuA11, **115**; D2-TuA10, 117; G4+G5+G6-ThA7, 174
 Cadet, C.: AP-ThP11, 178
 Cahn, G.: TS4-1-MoM4, **90**
 Cai, R.: EP-ThP27, 197; G2-FrM5, **212**
 Caíta Tapia, A.D.: B4-1-TuM6, **105**; BP-ThP39, **185**
 Callisti, M.: H3-2-WeA4, 144
 Calvo-Dahlborg, M.: TSP-ThP4, **206**
 Cammarata, A.: E1-1-ThM5, **156**; E1-2-ThA6, 170
 Campos, P.: GP-ThP7, 201
 Campos-Silva, I.E.: B4-1-TuM5, 105; B4-2-TuA3, 113; B4-3-WeM6, 127; E1-1-ThM3, 155
 Camps, E.: D2-TuA4, 116
 Cano, D.: BP-ThP36, 185

Author Index

- Čapek, J.: F1-TuM4, 109; F4-1-WeM2, 131; F4-2-WeA6, 142; FP-ThP17, 199; FP-ThP3, 197
- Capote, G.: B3-1-MoM5, 87
- Cardoso-Legorreta, E.: AP-ThP6, 177
- Carlet, M.: BP-ThP23, 182
- Carlström, C-F.: F4-2-WeA7, 142
- Carton, J.: CP-ThP22, 188
- Carvalho, S.: E1-3-FrM8, 211
- Casserly, T.: B3-2-MoA3, **94**; G1+G3-ThM8, 160
- Castelluccio, G.: H2-1-MoM4, 89
- Cavaleiro, A.: B3-2-MoA7, 95; E1-3-FrM8, 211; E1-4-WeA3, 140; FP-ThP6, 198
- Cavaleiro, D.: E1-3-FrM8, **211**
- Cavarroc, M.: A1-3-WeM10, 125; A1-3-WeM3, 125; E3-WeM10, **130**
- Cemin, F.: FP-ThP10, 198
- Černý, M.: B6-ThM2, 151
- Čerstvý, R.: F4-1-WeM2, 131
- Cha, S.C.: G1+G3-ThM12, **160**
- Chacko, A.R.: D1-2-MoA8, **96**
- Chandra, R.: F4-2-WeA3, 141; GP-ThP16, 202; GP-ThP19, 202
- Chang, C.L.: GP-ThP1, **200**
- Chang, H.Y.: GP-ThP2, 200
- Chang, K.-S.: B1-2-MoA8, **93**; BP-ThP33, 184; F4-1-WeM10, 131; TS1-2-WeA10, 147; TS1-2-WeA2, 145; TSP-ThP9, 207
- Chang, L.: B1-2-MoA7, 93
- Chang, L.C.: B4-3-WeM12, 128; BP-ThP7, 179
- Chang, S.H.: D1-1-MoM6, 88
- Chang, S.Y.: BP-ThP2, **178**; BP-ThP6, 179
- Chang, X.X.: B5-1-ThA9, 167
- Chang, Y.-C.: D1-1-MoM2, 87
- Chang, Y.-Y.: B4-4-WeA4, 138; B6-ThM3, 151
- Chao, L.C.: B4-4-WeA4, **138**
- Chapon, P.: HP-ThP6, 204
- Charlton, C.J.: BP-ThP1, 178; G2-FrM8, 213
- Charpentier, L.: B2-1-ThA7, 165
- Chason, E.: H1-2-TuA2, 121
- Chausseau, M.F.: HP-ThP6, 204
- Chen, A.J.: F2-2-ThA7, **172**
- Chen, C.H.: B5-2-FrM8, 210
- Chen, C.M.: F3-TuA4, 120
- Chen, D.Y.: B2-1-ThA6, 165; B2-1-ThA7, **165**
- Chen, H.C.: TSP-ThP6, 206
- Chen, H.-H.: F4-1-WeM1, **131**
- Chen, H.T.: DP-ThP6, 190
- Chen, M.: H3-2-WeA7, **144**
- Chen, M.J.: D1-1-MoM6, 88
- Chen, P.-C.: DP-ThP5, 190
- Chen, P.-W.: C3+C1-WeM3, **128**
- Chen, S.C.: C3+C2+C1-ThM10, 154
- Chen, W.C.: BP-ThP27, 183; BP-ThP9, 180
- Chen, X.: H3-2-WeA5, 144
- Chen, Y.: C2-WeA10, **140**
- Chen, Y.C.: A2-1-ThM4, 149
- Chen, Y.H.: C3+C2+C1-ThM10, **154**; F3-TuA4, 120
- Chen, Y.I.: B4-3-WeM12, 128; BP-ThP7, **179**
- Chen, Y.L.: D1-1-MoM6, 88
- Chen, Y.Y.: TS1-2-WeA6, **146**
- Chen, Y-F.: E2-2-TuA9, 118
- Cheng, F.-Y.: E2-2-TuA9, 118
- Cheng, K.Y.: D2-TuA5, **116**
- Cheng, L.C.: C2-WeA11, **140**
- Cheng, Y.L.: CP-ThP1, 185
- Chisholm, C.: H3-2-WeA3, 143
- Chistyakov, R.: B1-2-MoA1, **92**
- Chiu, K.A.: B1-2-MoA7, 93
- Chiu, L.Y.: B1-1-MoM5, **86**
- Chiu, Y.-C.: DP-ThP5, 190
- Chng, E.J.: D2-TuA2, 116
- Choi, K.: TS2-ThM7, 161
- Choi, Y.: HP-ThP12, 205
- Chou, C.C.: B1-2-MoA12, **93**
- Chou, C.M.: B5-1-ThA9, 167; D1-1-MoM2, 87; DP-ThP11, 191
- Chou, C.-M.: TSP-ThP9, 207
- Choudhury, T.: B2-1-ThA9, 165
- Choukourov, A.: F1-TuM1, 108
- Christensen, B.H.: E1-1-ThM7, 156
- Christien, F.C.: F3-TuA8, 120
- Chu, J.P.: D1-1-MoM6, **88**
- Chubarov, M.: B2-1-ThA9, **165**
- Chung, C.J.: B5-1-ThA9, 167; D1-1-MoM2, 87; DP-ThP11, 191; DP-ThP6, **190**
- Chung, Y.W.: EP-ThP19, 195
- Chyntara, S.: D1-1-MoM6, 88
- Cieslar, M.: F1-TuM1, 108
- Čiperová, Z.: B1-2-MoA4, **92**
- Claerbout, V.E.P.: E1-2-ThA5, **170**
- Clegg, W.J.: H2-2-MoA4, 98
- Colas, J.: B2-1-ThA7, 165
- Cole-Baker, A.: A1-1-TuM2, 101
- Contin, A.: BP-ThP28, 183
- Contla-Pacheco, A.D.: E1-1-ThM3, **155**
- Contreras, E.: B6-ThM6, **152**; EP-ThP3, **193**
- Corat, E.J.: B3-1-MoM4, 87; B3-1-MoM5, 87; BP-ThP28, 183
- Cordill, M.J.: E2-1-TuM3, **107**; EP-ThP6, 194; TS3+4-2-MoA3, 99; TS3+4-2-MoA4, 99; TS3+4-2-MoA8, 100
- Cordista, N.: B4-4-WeA6, 138; DP-ThP26, **192**
- Cormier, J.: H1-1-TuM3, 109
- Cornide, J.: TSP-ThP4, 206
- Corona-Gomez, J.: BP-ThP42, **185**; E2-2-TuA8, **118**
- Correia, R.F.B.: BP-ThP28, 183
- Cortés Suárez, V.J.: EP-ThP11, 194; HP-ThP4, 204
- Cortínez, J.: B6-ThM6, 152; EP-ThP3, 193
- Costa, D.: D3-TuM2, 105
- Costa-Barbosa, A.: D3-TuM2, 105
- Coudon, F.: AP-ThP3, 176
- Cougnon, F.G.: TS3+4-2-MoA9, **100**
- Cremer, R.: G1+G3-ThM9, **160**
- Crespo Villegas, J.: A1-3-WeM3, **125**
- Crummenauer, J.: G2-FrM7, 212
- Cruz Avilés, A.: AP-ThP6, 177
- Cselle, T.: B1-2-MoA5, 92; G4+G5+G6-ThA5, 173
- Cucatti, S.C.: B4-3-WeM2, 126
- Curry, J.: E3-WeM1, 129
- Czettel, C.: B2-1-ThA11, 166; B2-1-ThA4, 165; B4-4-WeA3, 138; B4-4-WeA7, 138; H1-1-TuM7, 110; H1-2-TuA4, 122
- Czigany, Z.: B1-3-TuM6, 104; B5-1-ThA4, 166
- D —
- da Silva Sobrinho, A.S.: DP-ThP23, 192
- Dahlborg, U.: TSP-ThP4, 206
- Dahotre, N.B.: A2-1-ThM5, 149
- Dai, M.J.: BP-ThP31, 184; EP-ThP16, 195
- Dai, X.: B5-1-ThA6, 168; FP-ThP16, 199
- Damm, D.: BP-ThP28, 183
- Dams, N.: B3-2-MoA5, 94; G1+G3-ThM4, 159
- Daniel, B.: B1-2-MoA2, 92
- Daniel, R.: B4-4-WeA2, 137
- DaSilva, V.: EP-ThP4, 193
- Daves, V.: B2-1-ThA4, 165; B4-4-WeA3, 138
- De Bosscher, W.: B7-TuA1, 114
- de Mello, S.R.S.: E1-2-ThA11, 171
- de Miguel Gamó, T.: A1-3-WeM2, 125; A3-WeA6, 137
- de Vasconcelos, G.: BP-ThP28, 183
- Dean, D.: D1-2-MoA9, 97
- Debus, J.: EP-ThP23, 196
- Dedoncker, R.: TS1-1-WeM2, **133**
- Dehm, G.: H3-1-WeM3, 132; H3-2-WeA9, 145
- Delgado, A.: B5-2-FrM4, 209
- Delgado-Brito, A.M.: B4-1-TuM5, **105**
- Depla, D.: B7-TuA3, **115**; TS1-1-WeM2, 133; TS3+4-2-MoA9, 100
- Dhananjaya, M.: CP-ThP9, **186**
- Di Gioacchino, F.: H2-2-MoA4, 98
- Diao, D.F.: EP-ThP17, **195**
- Ding, H.H.: D1-1-MoM3, 88
- Do, H.: B1-2-MoA7, 93
- Döbeli, M.: A2-2-ThA3, 163
- Dobler, C.: A3-WeA3, 136
- Dobrenizki, L.: E1-2-ThA10, 171
- Dobrovodsky, J.: B3-2-MoA8, 95
- Dobrygin, W.: B3-2-MoA1, 94
- Dolatbadi, A.: TS2-ThM3, 161; TS2-ThM9, **162**
- Dommann, A.: A2-2-ThA3, 163
- Donaldson, O.: H2-1-MoM6, **89**
- Dong, Z.: A1-1-TuM6, 102
- Donnelly, S.E.: TS1-2-WeA5, 146
- Donnet, C.D.: F3-TuA8, 120
- Doñu Ruiz, M.A.: EP-ThP11, **194**; HP-ThP4, 204
- Doris, F.: TS1-1-WeM4, 133
- Doumanidis, C.: C4-ThA3, **168**; C4-ThA7, 169
- Downey, B.P.: C2-WeA5, 139
- Drees, D.: E1-1-ThM7, 156
- Drieu La Rochelle, J.: E2-2-TuA2, 118
- Drnovšek, A.: B1-3-TuM4, **103**
- Drouet, M.: E2-2-TuA2, 118
- Dryepondt, S.N.: A1-1-TuM1, 101; A1-3-WeM4, **125**
- Dublanche-Tixier, C.: C3+C2+C1-ThM7, 154
- Duchoň, T.: F4-1-WeM2, 131
- Ducros, C.: C3+C2+C1-ThM7, 154; GP-ThP24, 203
- Duguet, T.: B2-2-FrM5, **208**; B2-2-FrM6, 208
- Duh, J.G.: B4-3-WeM11, 128; B6-ThM4, 151; BP-ThP14, 181; BP-ThP15, 181; TSP-ThP7, 206
- Durmaz, A.R.D.: H2-1-MoM3, 89
- Dutta, M.: B5-2-FrM9, 210
- E —
- Eberl, C.: AP-ThP11, 178; H2-1-MoM3, 89
- Echavarría, A.M.: D3-TuM8, **107**; DP-ThP25, **192**
- Echeverría, F.: D1-2-MoA5, 96
- Echeverrigaray, F.G.: E1-2-ThA11, 171
- Echeverry-Rendón, M.: D1-2-MoA5, 96
- Ecker, W.: B2-1-ThA4, 165; B4-4-WeA3, 138
- Eckert, J.: EP-ThP6, 194
- Eddy Jr., C.R.: C2-WeA5, 139
- Edmondson, P.D.: TS1-2-WeA5, 146
- Edwards, T.E.J.: H2-2-MoA4, **98**
- Efeoğlu, I.: B6-ThM1, **150**; BP-ThP30, **184**
- Efremov, M.: B3-2-MoA6, 94
- Egan, G.C.: C4-ThA2, 168
- Ehiasarian, A.P.: A1-1-TuM8, 102; F2-1-ThM7, **157**
- Ek, M.E.: B2-2-FrM7, 208
- Eklund, P.: F4-2-WeA7, 142
- El Mansori, M.: H1-2-TuA5, 122
- Elahinia, M.: D1-2-MoA9, 97
- El-Awady, J.A.: H2-1-MoM1, **88**
- Elbers, M.: BP-ThP37, 185
- Elias-Espinosa, M.: AP-ThP6, 177; BP-ThP24, 182; BP-ThP25, 182
- Ellis-Terrell, C.: G4+G5+G6-ThA6, **174**
- Emieux, F.: GP-ThP24, 203
- Encinas Sánchez, V.: A1-3-WeM2, 125; A3-WeA6, 137
- Engwall, A.: F2-2-ThA3, **171**
- Erdemir, A.: E1-2-ThA9, 171; EP-ThP4, 193

Author Index

- Eriguchi, K.: G4+G5+G6-ThA4, **173**
 Eriksson, A.O.: BP-ThP41, 185
 Ernst, P.: G2-FrM7, 212
 Eryilmaz, O.L.: EP-ThP4, **193**
 Escobar, D.: E1-4-WeA5, 141; EP-ThP26, 196
 Esparza, J.: BP-ThP22, 182
 Espinoza Orías, A.: D2-TuA8, **117**
 Espinoza, R.: GP-ThP6, 201
 Esteve, J.: BP-ThP36, 185
 Euchner, H.: B6-ThM12, 153; BP-ThP34, 184
 Evans, A.: A1-1-TuM2, 101
 Evaristo, M.: E1-4-WeA3, **140**
 Evertz, S.: TS1-2-WeA9, 147
 — F —
 Faber, K.T.: A2-1-ThM8, 150
 Falcão, R.: B3-1-MoM4, **87**; DP-ThP19, **191**
 Fang, Y.S.: B1-2-MoA7, **93**
 Farooq, A.: GP-ThP22, **203**
 Fatoba, O.S.: AP-ThP4, **176**; B4-2-TuA10, **114**
 Fayomi, S.: D2-TuA11, 117
 Feder, R.: C3+C2+C1-ThM9, 154
 Fehr, A.: F2-2-ThA8, **172**
 Fekete, M.: B1-3-TuM6, 104; B7-TuA2, 115
 Feldner, P.: H2-2-MoA6, **98**
 Feng, Y.Q.: B4-3-WeM10, **127**
 Fernandes, F.: E1-3-FrM8, 211
 Fernandez, I.: B3-2-MoA5, 94; F2-1-ThM9, **158**; G1+G3-ThM4, 159; TS3+4-2-MoA10, 100
 Fernández-Valdés, D.: B4-3-WeM6, **127**
 Ferreira, F.: B3-2-MoA7, 95; FP-ThP6, 198
 Ferreira, J.: CP-ThP23, 188
 Ficek, M.: F3-TuA11, 120
 Fietzke, F.: B1-3-TuM1, **103**; B4-3-WeM4, 127; G1+G3-ThM3, 159
 Figueroa, C.A.: B4-3-WeM2, 126; E1-2-ThA11, **171**
 Figueroa-Lopez, U.: E1-1-ThM3, 155
 Finazzi, G.: C3+C2+C1-ThM7, 154
 Fischer, M.: F4-2-WeA8, **142**; FP-ThP5, **197**
 Fisher, T.S.: F3-TuA1, **119**
 Flock, D.: TS1-2-WeA4, 146
 Flores, L.M.: EP-ThP12, 194
 Flores, M.: EP-ThP12, **194**; FP-ThP11, 198
 Flores-Cova, L.: FP-ThP11, **198**
 Flores-Martinez, M.: D2-TuA4, 116
 Flores-Rentería, M.: AP-ThP6, 177; BP-ThP25, 182
 Fones, A.: D1-2-MoA3, 96
 Fortunato, E.: F4-1-WeM3, **131**
 Fox, C.: A1-2-TuA9, **112**
 Fraile, A.F.: B5-1-ThA3, **166**
 Franco, D.: E2-1-TuM4, 107
 Francois, M.: E2-1-TuM5, 108
 Frank, M.: B2-2-FrM10, 209
 Franz, R.: B1-3-TuM4, 103; TS1-2-WeA3, 146
 Friák, M.F.: B6-ThM2, 151; BP-ThP19, 181
 Fridrici, V.: D1-1-MoM3, **88**; E1-1-ThM4, 156
 Frutos, E.F.: B5-1-ThA3, 166
 Fu, Q.: F2-2-ThA9, 172
 Fuger, C.: B6-ThM12, 153
 Fugita, L.T.N.: F3-TuA3, 119
 Fujii, K.: BP-ThP26, 183
 Fukumasu, N.: B3-1-MoM5, 87; E1-3-FrM1, 210
 Furgeaud, C.: H1-2-TuA2, **121**
 Furuki, T.: EP-ThP22, 196; EP-ThP24, 196
 — G —
 Gabriel, H.: B3-2-MoA5, 94; G1+G3-ThM4, **159**
 Gachot, C.: E1-2-ThA9, 171
 Gaedike, B.: G1+G3-ThM5, **159**
 Gaffar, A.: F3-TuA3, 119
 Gaiaschi, S.: HP-ThP6, 204
 Gaitán, G.B.: DP-ThP4, 190
 Galetz, M.C.: A2-2-ThA8, 164; A3-WeA3, 136
 Gamboa Mendoza, B.J.: B4-1-TuM6, 105; BP-ThP39, 185
 Gammer, C.: EP-ThP6, 194
 Ganesan, G.V.R.: B5-1-ThA6, **167**
 Gao, Z.H.: A1-1-TuM4, 101
 Garcia Fuentes, G.: BP-ThP22, 182
 Garcia Sanchez, J.A.: HP-ThP4, 204
 García, E.: D2-TuA4, **116**
 García, J.A.: BP-ThP22, **182**; GP-ThP5, 200
 García, P.: TS2-ThM8, 161
 García-Martín, G.: A1-3-WeM2, 125; A3-WeA6, **137**
 Garrelie, F.: F3-TuA8, 120
 Gasem, Z.: AP-ThP5, 176
 Gassner, M.: B2-1-ThA4, 165
 Gault, B.: H1-1-TuM3, **109**
 Gauter, S.: D1-2-MoA8, 96
 Gazal, Y.: B2-2-FrM5, 208
 Ge, F.F.: A1-2-TuA4, **112**
 Geers, C.: E1-2-ThA10, 171
 Gennaro, S.: B3-2-MoA3, 94; G1+G3-ThM8, 160
 Gentleman, M.M.: A2-1-ThM7, **150**
 George, M.: FP-ThP7, 198
 George, S.M.: F4-2-WeA9, **143**
 Gerdin, J.: BP-ThP20, 182
 Géringier, J.: D1-1-MoM3, 88; D2-TuA1, **116**
 Ghafoor, N.: B4-1-TuM4, **104**
 Ghai, P.: GP-ThP20, **203**
 Ghimire, A.: BP-ThP6, 179
 Ghimire, K.: C3+C2+C1-ThM13, 155
 Gholinia, A.: C3+C2+C1-ThM12, 155
 Ghosh, S.K.: AP-ThP1, 176
 Gibson, J.: H3-1-WeM1, **132**
 Gies, A.: E3-WeM5, **130**
 Gildersleeve, E.: A2-2-ThA4, 163
 Gimeno, S.: GP-ThP5, **200**
 Giroire, B.: E3-WeM10, 130
 Glavin, N.: F3-TuA5, 120; TS3+4-2-MoA5, 99
 Gleibe, K.: F3-TuA5, 120
 Gleich, S.G.: H3-2-WeA9, 145
 Glushko, O.: EP-ThP6, **194**; TS3+4-2-MoA3, **99**
 Godard, P.: CP-ThP13, 187; E2-2-TuA2, 118
 Goddard, D.: A1-1-TuM2, 101
 Göken, M.: H2-2-MoA5, 98; H2-2-MoA6, 98
 Gomez, J.S.: BP-ThP28, 183
 Gómez, M.A.: B6-ThM6, 152; E2-2-TuA3, 118; EP-ThP3, 193
 Gómez-Vargas, O.: AP-ThP6, **177**; B4-2-TuA8, 114; BP-ThP24, 182; BP-ThP25, 182
 Gong, C.Z.: F2-2-ThA2, 171
 Gonzalez Arrabal, R.: B3-2-MoA5, 94
 Goorsky, M.S.: B6-ThM10, 152; C2-WeA9, 139
 Gopalakrishnan, R.: D2-TuA2, **116**; D3-TuM6, 106
 Gopalan, H.G.: H3-2-WeA9, **145**
 Gostilo, V.: H3-2-WeA6, 144
 Goswami, M.: B2-1-ThA1, **164**
 Göthelid, E.: F4-2-WeA7, 142
 Goudeau, P.: CP-ThP13, 187
 Gozhyk, I.: H1-2-TuA11, 123; HP-ThP7, 204
 Grachev, S.: H1-1-TuM6, 110; H1-2-TuA11, 123; HP-ThP7, 204
 Graham, S.: TS4-1-MoM4, 90
 Grancic, B.: B5-2-FrM6, **209**; BP-ThP3, 178
 Grantham, Z.: B4-4-WeA6, 138
 Greczynski, G.: B4-1-TuM4, 104; F2-2-ThA5, **172**; SIT2-WeSIT1, 135
 Greene, J.E.: B4-1-TuM4, 104; F2-1-ThM8, 158; F2-2-ThA5, 172; HL-WeHL3, **148**; SIT2-WeSIT1, 135
 Greenhalgh, R.C.: C3+C1-WeM2, 128
 Grigoriev, S.: B1-2-MoA11, 93
 Grossias, C.: CP-ThP13, 187
 Gu, G.: BP-ThP29, 183
 Gu, J.: A2-1-ThM5, 149; A2-1-ThM9, **150**
 Gudmundsson, J.T.: B7-TuA9, 115; F1-TuM5, **109**; F2-1-ThM8, 158
 Guerin, P.: CP-ThP13, 187
 Guezmil, M.: D2-TuA1, 116
 Guida, L.: D3-TuM3, 105
 Guillon, M.G.: B4-3-WeM13, 128
 Guipont, V.: A2-1-ThM1, 149; AP-ThP3, 176
 Gunda, R.K.: E1-3-FrM12, 212; EP-ThP31, 197
 Gunduz, I.E.: C4-ThA3, 168; C4-ThA7, 169
 Günther, M.: B3-2-MoA1, **94**
 Guo, C.Q.: BP-ThP31, **184**
 Guo, J.: B5-1-ThA6, 168; FP-ThP16, 199
 Guo, Q.: A1-1-TuM1, 101
 Guo, Y.: C3+C2+C1-ThM12, 155; CP-ThP19, 187
 Gupta, G.: TS4-1-MoM5, 90
 Gupta, S.: H2-2-MoA2, 97
 Gustus, R.: B3-1-MoM3, 87
 — H —
 Haga, Y.: TS4-1-MoM3, 90
 Hahn, R.: B4-2-TuA1, **113**; B6-ThM12, 153; BP-ThP19, 181; BP-ThP34, 184
 Haiblíková, V.: H3-1-WeM2, 132
 Hajihoseini, H.: F1-TuM5, 109
 Hakala, T.J.: E1-1-ThM7, 156
 Haldan, D.: B3-1-MoM2, 86
 Halvarsson, M.: B2-1-ThA5, 165
 Hamilton, H.: D1-2-MoA3, 96
 Hamouda, A.M.S.: AP-ThP8, 177
 Hans, M.: BP-ThP41, 185; H1-1-TuM5, **110**
 Hanus, J.: F1-TuM1, 108
 Harder, B.: A2-2-ThA5, 163
 Harrison, Z.: D3-TuM6, **106**
 Harsani, M.: BP-ThP3, 178
 Hart, N.: CP-ThP12, 187
 Hasegawa, S.: G4+G5+G6-ThA4, 173
 Hashemiastaneh, S.: D3-TuM7, 106
 Hasikova, J.I.: H3-2-WeA6, **144**
 Hattar, K.: H3-2-WeA3, **143**
 Hatton, P.: C3+C1-WeM2, **128**
 Hattrick-Simpers, J.: TS1-1-WeM10, 134
 Hatzenbichler, L.: B4-3-WeM3, 127
 Hauert, R.: D1-1-MoM4, **88**
 Haviar, S.: F1-TuM4, **109**; F4-1-WeM2, 131
 Haynes, J.A.: A2-2-ThA4, 163
 He, J.: H1-1-TuM3, 109
 He, J.H.: A2-1-ThM6, **149**
 He, J.L.: A1-1-TuM9, 102; B5-1-ThA9, 167; C3+C2+C1-ThM3, 153; D1-1-MoM2, 87; DP-ThP11, 191; DP-ThP6, 190; F3-TuA4, 120
 Heaney, P.J.: B3-2-MoA6, **94**
 Heckman, E.: TS3+4-2-MoA5, 99
 Heckman, N.: H3-2-WeA3, 143
 Heller, E.: TS3+4-2-MoA5, 99
 Helmersson, U.: F2-1-ThM8, **158**
 Heraud, L.: H1-2-TuA5, 122
 Heraud, Q.: H1-2-TuA11, **123**; HP-ThP7, **204**
 Hermerschmidt, F.: TS4-1-MoM6, **91**
 Hernandez-Rodrigues, E.N.: DP-ThP16, 191; GP-ThP18, **202**
 Herren, B.: A2-1-ThM8, **150**
 Herrera Jimenez, E.J.: H3-2-WeA8, **144**
 Hess, M.: B3-1-MoM2, 86; B3-2-MoA2, **94**
 Hettlinger, J.: D1-2-MoA3, 96
 Hibino, T.: EP-ThP24, 196
 Higuchi, K.: B4-1-TuM7, 105; B4-2-TuA9, 114; BP-ThP26, 183
 Higuchi, T.: G4+G5+G6-ThA4, 173
 Hilfiker, M.: C3+C2+C1-ThM9, 154
 Hill, S.: B4-4-WeA6, 138; DP-ThP26, 192

Author Index

- Hinder, S.: C3+C1-WeM4, 129
 Hippler, R.H.: G4+G5+G6-ThA7, 174
 Hirn, S.: TS1-2-WeA3, 146
 Hirpara, J.G.: GP-ThP16, **202**
 Hishinuma, Y.: H1-2-TuA9, 122
 Hnilica, J.: B7-TuA2, 115
 Ho, W.F.: DP-ThP10, 191; DP-ThP9, **190**
 Ho, W.Y.: B5-2-FrM8, 210; BP-ThP27, 183; BP-ThP9, 180
 Hodge, A.M.: C3+C2+C1-ThM8, 154; E2-2-TuA4, **118**
 Höhn, M.: B4-3-WeM4, 127
 Holec, D.: B4-3-WeM3, 127; B5-1-ThA5, 167; B6-ThM2, 151; B6-ThM5, 151; BP-ThP19, 181; BP-ThP35, 184
 Holzapfel, D.M.: BP-ThP41, **185**; TS1-2-WeA9, 147
 Homma, H.: B2-1-ThA3, 164
 Hong, K.P.: F4-2-WeA11, 143
 Hopfeld, M.: TS1-2-WeA4, 146
 Hosemann, P.: B1-3-TuM4, 103; H3-2-WeA1, **143**
 Hou, H.J.: EP-ThP16, 195
 Hou, X.H.: TS2-ThM7, **161**; TSP-ThP1, 206; TSP-ThP6, **206**
 Houška, J.: F4-1-WeM2, 131
 Hovsepian, P.: A1-1-TuM8, **102**
 Hrebik, J.: F2-1-ThM10, **158**
 Hruby, H.: B4-4-WeA2, 137
 Hsain, Z.: E3-WeM1, 129
 Hsiao, W.Y.: DP-ThP10, 191
 Hsiao, Y.T.: BP-ThP2, 178
 Hsieh, J.H.: D1-2-MoA4, **96**; F4-1-WeM5, 131
 Hsieh, P.-Y.: B5-1-ThA9, 167; C3+C2+C1-ThM3, 153; D1-1-MoM2, 87; DP-ThP6, 190; F3-TuA4, **120**
 Hsu, C.H.: GP-ThP21, 203
 Hsu, H.C.: DP-ThP10, **191**; DP-ThP9, 190
 Hsu, L.C.: B5-2-FrM8, **210**; BP-ThP27, **183**; BP-ThP9, 180
 Hsu, S.K.: DP-ThP10, 191; DP-ThP9, 190
 Hsueh, P.: F4-1-WeM5, 131
 Hu, H.: CP-ThP2, **186**
 Huang, C.H.: GP-ThP1, 200
 Huang, C.R.: TSP-ThP7, **206**
 Huang, F.: A1-2-TuA4, 112; C2-WeA10, 140
 Huang, J.-H.: A1-1-TuM7, 102; B1-2-MoA12, 93; B4-3-WeM10, 127; B4-4-WeA1, **137**; E2-2-TuA9, 118
 Huang, J.L.: B1-1-MoM4, 86; C2-WeA11, 140; CP-ThP31, 189; F1-TuM3, 108; F4-1-WeM1, 131
 Huang, J.T.: C3+C2+C1-ThM3, **153**
 Huang, S.Y.: C3+C2+C1-ThM10, 154
 Huang, S.-Y.: D1-1-MoM2, **87**
 Huang, T.: A2-1-ThM5, 149; A2-1-ThM9, 150; FP-ThP16, 199
 Huang, T.-C.: GP-ThP17, 202
 Huang, X.: G4+G5+G6-ThA6, 174
 Huang, Y.H.: B1-1-MoM4, **86**
 Huang, Z.-W.: TSP-ThP9, **207**
 Hubicka, Z.: B7-TuA11, 115; D2-TuA10, 117; G4+G5+G6-ThA7, **174**
 Hudec, T.: E1-3-FrM2, **210**
 Hug, H.J.: D1-2-MoA8, 96; F4-2-WeA8, 142; FP-ThP5, 197
 Hulkko, J.: B2-2-FrM8, 208
 Hultman, L.: B4-1-TuM4, 104; F2-2-ThA5, 172; F4-2-WeA7, 142; SIT2-WeSIT1, 135
 Huminiuc, T.H.: B5-1-ThA3, 166; B5-2-FrM4, 209; E1-3-FrM2, 210
 Hunault, P.: HP-ThP6, **204**
 Hung, J.: B5-2-FrM8, 210; BP-ThP27, 183; BP-ThP9, 180
 Hung, S.B.: TS1-1-WeM6, **134**; TS1-2-WeA6, 146
 Hung, Y.L.: A1-1-TuM9, 102
 Hunold, O.: A2-2-ThA3, **163**
 Hurand, S.: CP-ThP13, 187
 Hurtado, A.: B6-ThM6, 152; EP-ThP3, 193
 Hurtado, C.: DP-ThP19, 191
 Hussien, A.: C4-ThA3, 168
 Hwang, S.H.: B2-2-FrM9, 209
 — I —
 Ianno, N.: CP-ThP18, 187
 Ibáñez, P.F.: TS2-ThM4, **161**
 Ibrahim, H.: D1-2-MoA9, **97**
 Ikari, Y.: G1+G3-ThM7, 159; TSP-ThP8, 206
 Ilic, E.: D1-1-MoM4, 88
 Imamiya, M.: BP-ThP13, 180
 Imamura, S.: B2-1-ThA2, 164
 Ingvarsson, S.: F1-TuM5, 109
 Iñiguez, C.: DP-ThP16, **191**
 Inspektor, A.: B1-2-MoA3, **92**
 Irving, B.J.: E1-2-ThA2, **169**
 Ishida, M.: G2-FrM3, 212
 Ishigaki, T.: B2-1-ThA3, 164
 Islam, A.: B5-2-FrM9, 210
 Islam, S.: F1-TuM6, **109**
 Isomura, Y.: G1+G3-ThM7, 159; TSP-ThP8, 206
 Itagaki, N.: B2-2-FrM9, 209
 Ito, A.: EP-ThP22, **196**
 Iwaniak, A.: AP-ThP9, **177**; H3-2-WeA10, **145**
 Izaii, V.: BP-ThP3, 178
 Izu, Y.: BP-ThP13, **180**
 Izumi, H.: TS4-1-MoM3, 90
 — J —
 Jäger, N.: B4-4-WeA2, 137
 Jain, R.K.: B1-1-MoM3, **86**
 Jaiswal, J.: F4-2-WeA3, 141; GP-ThP19, 202
 Jakutis Neto, J.J.: DP-ThP23, 192
 Janssen, W.: B2-1-ThA5, 165
 Jansson, U.: TS1-1-WeM5, 134
 Jaroš, M.: B1-2-MoA4, 92
 Jasien, C.: C4-ThA5, 168
 Jawaid, A.: F3-TuA5, 120
 Jedrzejczak, A.: TSP-ThP2, 206
 Jennings, J.A.: D3-TuM6, 106
 Jeong, E.: CP-ThP24, 188
 Jeppesen, C.S.: GP-ThP11, 201
 Jha, R.: B2-1-ThA1, 164
 Jian, S.R.: HP-ThP8, 205
 Jílek (Jr.), M.: B1-2-MoA5, 92
 Jílek (Sr.), M.: B1-2-MoA5, 92
 Jiménez, C.J.: A1-1-TuM6, 102
 Jimenez, M.J.M.: B4-3-WeM2, 126
 Jiménez, O.: EP-ThP12, 194; FP-ThP11, 198
 Johansson, K.: TS1-1-WeM3, 133
 Johansson-Jöesaar, M.P.: F4-2-WeA7, 142
 Joross, H.: TS1-1-WeM10, **134**
 Joshi, S.S.: A2-1-ThM5, 149
 Juang, J.Y.: HP-ThP8, 205
 Juárez-Navarro, C.A.: B4-2-TuA3, 113
 Juez Lorenzo, M.: A3-WeA5, 136
 Junda, M.M.: C3+C2+C1-ThM13, 155
 Jung, M.Y.: HP-ThP12, 205
 Jung, Y.G.: A2-2-ThA7, 163
 — K —
 Kabatova, M.: B3-2-MoA8, 95
 Kabel, J.: H3-2-WeA1, 143
 Kacher, J.: H2-2-MoA2, 97
 Kagerer, S.: F4-2-WeA6, **142**; FP-ThP17, **199**
 Kainz, C.: B2-1-ThA11, **166**
 Kakandar, E.: H2-1-MoM4, 89
 Kalapala, M.V.: CP-ThP21, **188**; F4-2-WeA4, **142**
 Kalscheuer, C.: BP-ThP4, 179; E3-WeM4, 130; F4-2-WeA5, 142; G2-FrM9, **213**
 Kamataki, K.: B2-2-FrM9, 209
 Kamiya, S.: TS4-1-MoM3, **90**
 Kane, K.A.: A2-1-ThM3, **149**
 Kang, B.K.: HP-ThP12, **205**
 Kang, D.: CP-ThP12, 187
 Kapsa, P.: D1-1-MoM3, 88
 Karner, J.: E3-WeM5, 130
 Kaspar, J.: TS1-2-WeA1, 145
 Kateb, M.: F1-TuM5, 109
 Katoh, Y.: H3-2-WeA1, 143
 Kaulfuss, F.: B1-2-MoA6, 92; TS1-2-WeA1, 145
 Kaur, D.: C4-ThA8, 169; CP-ThP30, 189
 Kaur, J.: B1-1-MoM3, 86
 Kbibou, M.: H1-2-TuA5, **122**
 Keckes, J.: B4-4-WeA2, 137
 Keleş, A.: B6-ThM1, 150; BP-ThP30, 184
 Kellmann, L.-B.: TS1-2-WeA4, 146
 Kelly, P.: A1-1-TuM2, **101**; A1-1-TuM4, 101; F3-TuA3, 119
 Kempe, P.: H3-1-WeM2, **132**
 Keraudy, J.: F2-1-ThM8, 158
 Keshri, A.K.: B5-2-FrM9, 210
 Kgoete, F.: E2-1-TuM6, **108**
 Khalil, K.: E2-1-TuM5, 108
 Khan, A.M.: EP-ThP19, **195**
 Khang, L.: DP-ThP26, 192
 Khanna, A.: B1-1-MoM3, 86
 Khelfaoui, F.: E1-1-ThM6, 156
 Kido, Y.: B2-1-ThA2, **164**
 Kilic, U.: C3+C2+C1-ThM9, 154; CP-ThP18, 187
 Kim, B.K.: B4-2-TuA2, **113**; GP-ThP15, 202
 Kim, H.: AP-ThP10, 177
 Kim, H.J.: GP-ThP15, 202
 Kim, H.K.: BP-ThP17, 181; CP-ThP20, **188**; HP-ThP5, 204
 Kim, I.S.: A2-2-ThA7, 163
 Kim, J.: B7-TuA11, 115; C2-WeA7, 139; EP-ThP24, 196
 Kim, J.-H.: EP-ThP20, **195**
 Kim, J.W.: CP-ThP20, 188
 Kim, R.: F3-TuA5, 120
 Kim, S.M.: CP-ThP20, 188
 Kim, W.R.: EP-ThP20, 195
 Kim, Y.: GP-ThP15, 202
 Kirchlechner, C.K.: H3-1-WeM3, 132; H3-2-WeA9, 145
 Kirnbauer, A.: BP-ThP32, **184**; TS1-1-WeM12, **134**
 Kitajima, A.: B4-1-TuM7, 105; B4-2-TuA9, 114; BP-ThP26, 183
 Kiyokawa, D.: B4-2-TuA9, **114**; BP-ThP26, 183
 Klein, P.: B5-1-ThA4, 166; B7-TuA2, 115
 Kleinbichler, A.: E2-1-TuM3, 107
 Klemberg-Sapieha, J.E.: A1-3-WeM10, 125; A1-3-WeM3, 125; E1-1-ThM6, 156; EP-ThP30, **197**; H3-2-WeA8, 144; TS2-ThM11, 162; TS2-ThM3, 161; TSP-ThP2, 206
 Klima, S.: B4-4-WeA2, 137
 Klimashin, F.F.: B6-ThM5, 151; BP-ThP18, 181
 Klostermann, H.: G1+G3-ThM3, **159**
 Klünsner, T.: B4-4-WeA3, 138
 Kment, S.: G4+G5+G6-ThA7, 174
 Knittel, S.: A1-3-WeM10, 125; A1-3-WeM3, 125
 Ko, K.Y.: G1+G3-ThM12, 160
 Kodambaka, S.: B6-ThM10, 152
 Koelker, W.: B2-2-FrM10, 209; G1+G3-ThM2, 158
 Koga, K.: B2-2-FrM9, **209**
 Koganemaru, M.: TS4-1-MoM3, 90
 Koh, I.H.J.: DP-ThP23, 192

Author Index

- Koh, J.: CP-ThP12, 187
 Kohlhauser, B.: E1-2-ThA9, **171**
 Kohlscheen, J.: BP-ThP1, **178**; G2-FrM8, **213**
 Kohulak, O.: BP-ThP3, 178
 Kokalj, D.: EP-ThP23, 196; F2-2-ThA9, **172**
 Kolarik, V.: A3-WeA5, **136**
 Koller, C.M.: BP-ThP32, 184; E1-2-ThA9, 171; TS1-1-WeM12, 134
 Koloszári, S.: B1-3-TuM4, 103; B4-2-TuA1, 113; BP-ThP32, 184; F4-2-WeA6, 142; FP-ThP17, 199; FP-ThP3, 197; TS1-2-WeA9, 147
 Komsa, H.-P.: F3-TuA9, **120**
 Kong, Y.: F2-2-ThA2, 171
 König, T.: A2-2-ThA8, **164**
 Kontis, P.: H1-1-TuM3, 109
 Korenyi-Both, A.L.: E3-WeM3, 129; TS3+4-2-MoA11, **100**
 Korlacki, R.: C3+C2+C1-ThM9, 154
 Korte-Kerzel, S.: H3-1-WeM1, 132
 Kos, Š.: B1-2-MoA4, 92
 Kostoglou, N.K.: C4-ThA7, 169
 Kotrlóvá, M.: B1-3-TuM5, **103**
 Kousaka, H.: EP-ThP22, 196; EP-ThP24, **196**
 Koutna, N.: B6-ThM2, **151**; B6-ThM5, 151; BP-ThP19, **181**; E1-2-ThA9, 171
 Koyanagi, T.: H3-2-WeA1, 143
 Kozák, T.: F2-1-ThM5, **157**; F4-2-WeA6, 142; FP-ThP17, 199; FP-ThP3, 197
 Kraetzschmar, B.G.: G1+G3-ThM3, 159
 Kranzmann, A.: A1-1-TuM8, 102
 Kratochvíl, J.: D2-TuA10, 117; F3-TuA11, 120
 Krauß, S.: H2-2-MoA5, **98**
 Krbal, M.: F4-1-WeM2, 131
 Kreiml, P.: TS3+4-2-MoA4, **99**
 Kroker, M.: B1-3-TuM6, **104**
 Krsek, V.: B1-2-MoA5, 92
 Kruis, E.: F2-2-ThA9, 172
 Krülle, T.: B1-2-MoA6, **92**
 Kruppe, N.C.: BP-ThP23, 182
 Kubart, T.: B3-2-MoA7, 95
 Kuczyk, M.: TS1-2-WeA1, **145**
 Kulczyk-Malecka, J.: A1-1-TuM4, 101; F3-TuA3, **119**
 Kumar, A.: C4-ThA8, 169; CP-ThP30, **189**
 Kumar, N.: F1-TuM4, 109
 Kümmel, J.: B2-1-ThA5, 165
 Kunche, C.K.: CP-ThP4, 186
 Kuo, W.-C.: D2-TuA12, **117**; DP-ThP2, **190**
 Kups, T.: TS1-2-WeA4, 146
 Kus, P.: BP-ThP3, 178
 Kuyel, B.: F4-2-WeA11, **143**
 Kuzminova, A.: F1-TuM1, 108
 Kvetkova, L.: B3-2-MoA8, 95
 Kylian, O.: D2-TuA10, 117; F1-TuM1, **108**
 — L —
 Lai, G.-H.: GP-ThP17, 202
 Lai, X.M.: B3-2-MoA9, 95; C3+C2+C1-ThM11, 155
 Lai, Y.S.: G2-FrM6, 212
 Lambertj, A.: TS3+4-2-MoA9, 100
 Lance, M.J.: A2-1-ThM3, 149; A2-2-ThA4, **163**
 Landälv, L.L.: F4-2-WeA7, **142**
 Lorangeira, J.: CP-ThP23, 188
 Largeau, L.: H1-1-TuM6, 110
 Lasanta Carrasco, M.I.: A1-1-TuM8, 102; A1-3-WeM2, 125; A3-WeA6, 137
 Laska, N.: B1-3-TuM2, 103
 Latarius, J.: BP-ThP37, **185**
 Lau, S.H.: H1-2-TuA8, 122
 Laugel, N.: A1-2-TuA9, 112; G4+G5+G6-ThA3, **173**
 Lavenstein, S.: H2-1-MoM1, 88
 Lavery, N.: TSP-ThP4, 206
 Lazzari, R.: H1-2-TuA11, 123; HP-ThP7, 204
 Lechner, A.: H1-1-TuM7, 110
 Lee, C.Y.: CP-ThP1, **185**
 Lee, D.B.: A1-3-WeM12, 126
 Lee, J.H.: G1+G3-ThM12, 160
 Lee, J.W.: B6-ThM4, 151
 Lee, J.-W.: B4-3-WeM11, 128; D1-2-MoA1, **95**; TS1-1-WeM6, 134; TS1-2-WeA6, 146
 Lee, J.-W.: F2-2-ThA7, 172
 Lee, J.-W.: DP-ThP7, **190**
 Lee, K.: A2-1-ThM10, **150**; A2-1-ThM8, 150; B4-2-TuA2, 113
 Lee, S.H.: BP-ThP17, **181**; HP-ThP5, 204
 Lee, S.W.: H1-2-TuA9, 122
 Lee, S.-W.: H3-1-WeM5, **132**
 Lee, S.Y.: BP-ThP17, 181; CP-ThP20, 188; HP-ThP5, 204
 Legros, M.: H1-1-TuM2, 109
 Lej, C.M.: DP-ThP5, **190**
 Leite, D.M.G.: DP-ThP23, 192
 Lemmer, O.: B2-2-FrM10, 209
 Lemmon, J.: CP-ThP12, 187
 Lengaigne, J.: TS2-ThM11, 162; TS2-ThM3, **161**; TSP-ThP2, 206
 Lenis, J.A.: DP-ThP4, **190**; E2-2-TuA3, **118**
 Lepple, M.: A2-1-ThM11, **150**
 Leson, A.: B1-2-MoA6, 92; TS1-2-WeA1, 145
 Letzig, D.: D1-2-MoA6, 96
 Levi, C.G.: A2-1-ThM11, 150
 Lewin, E.: TS1-1-WeM3, **133**
 Lewis, S.: H1-2-TuA8, 122
 Leyendecker, T.: B2-2-FrM10, 209; G1+G3-ThM2, 158
 Leyens, C.: B1-2-MoA6, 92; TS1-2-WeA1, 145
 Li, C.: D1-2-MoA4, 96; F4-1-WeM5, **131**
 Li, C.L.: D1-1-MoM6, 88
 Li, F.: HP-ThP11, 205
 Li, J.J.: BP-ThP29, **183**
 Li, K.Y.: H3-2-WeA7, 144
 Li, L.: BP-ThP31, 184
 Li, Q.: EP-ThP16, 195
 Li, S.Y.: BP-ThP33, **184**; F4-1-WeM10, **131**
 Li, X.B.: C3+C2+C1-ThM11, **155**
 Li, Y.: A1-1-TuM9, **102**; BP-ThP42, 185; E2-2-TuA8, 118
 Liang, T.: BP-ThP4, 179
 Liao, E.Y.: F3-TuA4, 120
 Liao, M.E.: B6-ThM10, 152; C2-WeA9, **139**
 Liao, M.H.: C3+C2+C1-ThM10, 154
 Liao, Y.: C4-ThA3, 168
 Liberatore, A.M.A.: DP-ThP23, 192
 Lider, A.: H3-2-WeA4, 144
 Lien, S.-Y.: GP-ThP21, 203
 Lilova, K.: A2-1-ThM11, 150
 Limbeck, A.: BP-ThP34, 184
 Lin, C.-M.: HP-ThP8, 205
 Lin, C.-P.: D1-2-MoA1, 95
 Lin, C.W.: B5-1-ThA9, **167**; DP-ThP11, **191**
 Lin, J.: CP-ThP17, **187**
 Lin, J.L.: B1-1-MoM6, **86**
 Lin, K.: G4+G5+G6-ThA6, 174
 Lin, K.C.: C3+C2+C1-ThM4, **153**; CP-ThP31, **189**
 Lin, M.: A1-1-TuM9, 102; E1-4-WeA2, **140**
 Lin, M.T.: E2-2-TuA9, **118**
 Lin, S.S.: BP-ThP31, 184; EP-ThP16, 195
 Lin, S.Y.: BP-ThP2, 178
 Lin, T.Y.: DP-ThP7, 190
 Lin, Y.C.: B4-3-WeM11, **128**; BP-ThP14, **181**
 Lin, Y.H.: F1-TuM3, **108**
 Lin, Y.L.: CP-ThP1, 185
 Lin, Z.X.: B4-3-WeM13, **128**; E1-3-FrM7, 211
 Lindahl, E.: B2-2-FrM8, 208; BP-ThP20, 182
 Liskiewicz, T.: H3-2-WeA2, 143
 List-Kratochvíl, E.: TS4-1-MoM6, 91
 Liu, B.W.: B4-3-WeM12, 128
 Liu, C.: H3-2-WeA7, 144
 Liu, C.L.: A2-1-ThP4, **149**
 Liu, C.P.: C2-WeA11, 140; F4-1-WeM1, 131
 Liu, D.H.: G2-FrM6, **212**
 Liu, H.: A1-1-TuM4, 101
 Liu, H.C.: B5-2-FrM8, 210
 Liu, J.L.: TS2-ThM7, 161; TSP-ThP6, 206
 Liu, Q.W.: D1-2-MoA4, 96
 Liu, S.-M.: GP-ThP21, 203
 Liu, Y.: H1-1-TuM2, 109
 Liu, Y.C.: B4-3-WeM13, 128; E1-3-FrM7, **211**; GP-ThP13, **201**
 Liu, Y.H.: B4-3-WeM12, **128**
 Liu, Z.: B2-1-ThA8, **165**
 Lo, W.L.: B6-ThM4, **151**; BP-ThP15, **181**
 Lobmaier, L.: B6-ThM5, 151
 Lofaj, F.: B3-2-MoA8, **95**
 Lomello, F.: A1-1-TuM3, 101
 Londoño, R.F.: EP-ThP26, 196
 Lopes Dias, N.F.: B3-1-MoM3, **87**
 Lopez Perrusquia, N.: EP-ThP11, 194; HP-ThP4, **204**
 Lopez-Suero, D.: B4-1-TuM5, 105
 Loquai, S.L.: A1-3-WeM10, 125; A1-3-WeM3, 125
 Lorin, G.: GP-ThP24, 203
 Lou, B.-S.: D1-2-MoA1, 95; DP-ThP7, 190; F2-2-ThA7, 172
 Louring, S.: E1-1-ThM7, 156
 Lousa, A.: BP-ThP36, **185**
 Lu, G.H.: B5-1-ThA9, 167
 Lu, J.: B4-1-TuM4, 104; F4-2-WeA7, 142; G1+G3-ThM4, 159
 Lu, N.: TS4-1-MoM1, **90**
 Lubaszka, P.: AP-ThP9, 177
 Lucas, S.: B7-TuA1, 114
 Luchtenberg, P.A.: GP-ThP7, **201**
 Ludwig, A.: H3-1-WeM3, 132
 Lümkeemann, A.: B1-2-MoA5, 92; B4-3-WeM3, 127; G4+G5+G6-ThA5, 173
 Lundin, D.: B7-TuA2, 115; B7-TuA9, 115; F2-1-ThM8, 158; FP-ThP10, 198
 Lusvarghib, L.: TS1-2-WeA3, 146
 — M —
 Ma, H.: HP-ThP3, 204
 Ma, Y.H.: F2-2-ThA2, 171
 Macauley, C.A.: A2-1-ThM11, 150
 Machado, I.F.: E1-3-FrM1, 210
 Maeder, X.: A2-2-ThA3, 163; H2-1-MoM4, 89; H2-2-MoA4, 98
 Mahmood, K.: FP-ThP18, **200**
 Mairaj Deen, K.: GP-ThP22, 203
 Makinen, S.K.: H1-1-TuM3, 109
 Maldonado Dominguez, K.: HP-ThP10, **205**
 Malik, G.: F4-2-WeA3, **141**; GP-ThP19, **202**
 Mallick, M.: D1-1-MoM7, **88**
 Manik, G.: DP-ThP24, 192
 Manns, T.: B2-1-ThA5, 165
 Marcel, C.: F2-2-ThA4, 171
 Marchand, B.: AP-ThP3, 176
 Marquez Herrera, A.: GP-ThP18, 202
 Marquez, A.: DP-ThP16, 191
 Marti, A.: D1-2-MoA3, 96
 Martinez-Trinidad, J.: B4-1-TuM5, 105; E1-1-ThM3, 155
 Martins, R.: F4-1-WeM3, 131
 Martinu, L.: A1-3-WeM10, 125; A1-3-WeM3, 125; EP-ThP30, 197; H3-2-WeA8, 144; TS2-ThM11, 162; TS2-ThM3, 161
 Marugi, K.: A1-3-WeM5, 125; AP-ThP13, 178
 Maruko, T.: BP-ThP11, 180; BP-ThP12, **180**; BP-ThP13, 180
 Maskrot, H.: A1-1-TuM3, 101
 Massi, M.: DP-ThP23, **192**

Author Index

- Mastail, C.: H1-2-TuA2, 121
 Mathew, M.T.: D2-TuA5, 116; D3-TuM7, **106**
 Mathiasen, C.: GP-ThP11, 201
 Matsuda, K.: G2-FrM3, 212; H1-2-TuA9, **122**
 Matthews, A.: A1-1-TuM9, 102; C3+C1-WeM4, 129; C3+C2+C1-ThM12, 155; CP-ThP19, 187; E1-4-WeA2, 140; G4+G5+G6-ThA3, 173; GP-ThP3, 200
 Matthews, D.T.A.: EP-ThP21, **195**
 Maurel, V.: A2-1-ThM1, **149**; AP-ThP11, 178; AP-ThP3, **176**
 Maury, F.: B2-2-FrM5, 208; B2-2-FrM6, **208**
 Maus, J.: B3-1-MoM2, 86
 Maus-Friedrichs, W.: B3-1-MoM3, 87
 Mayr, P.: A1-1-TuM8, 102
 Mayrhofer, P.H.: B4-2-TuA1, 113; B5-1-ThA5, 167; B6-ThM12, 153; B6-ThM2, 151; B6-ThM5, **151**; B6-ThM9, 152; BP-ThP18, **181**; BP-ThP19, 181; BP-ThP32, 184; BP-ThP34, 184; BP-ThP35, 184; E1-2-ThA9, 171; F4-2-WeA6, 142; FP-ThP17, 199; FP-ThP3, 197; TS1-1-WeM12, 134
 McKenzie, D.R.: B5-1-ThA6, 167
 McKnight, R.: G4+G5+G6-ThA6, 174
 McMaster, S.: H3-2-WeA2, 143
 McNallan, M.: D2-TuA5, 116
 Mehraban, S.: TSP-ThP4, 206
 Meindlhumer, M.: B4-4-WeA2, **137**
 Meissner, T.: A3-WeA3, 136
 Mejía, H.D.: D3-TuM8, 107; DP-ThP25, 192
 Melih, A.: EP-ThP2, **193**
 Melo-Máximo, D.V.: E1-3-FrM5, 211; E1-3-FrM6, 211
 Melo-Máximo, L.: E1-3-FrM6, 211
 Mendala, B.: A1-3-WeM5, 125; AP-ThP13, 178; AP-ThP9, 177
 Mendizabal, L.: GP-ThP5, 200
 Mendoza, G.M.: B4-2-TuA2, 113
 Meneses-Amador, A.: B4-2-TuA3, 113; B4-3-WeM6, 127
 Meng, F.: C2-WeA10, 140
 Meng, W.J.: H2-2-MoA3, **97**
 Mercier, F.: B2-1-ThA6, 165; B2-1-ThA7, 165
 Merle, B.: H2-2-MoA5, 98; H2-2-MoA6, 98; H3-1-WeM4, **132**
 Meth, J.: TS4-1-MoM4, 90
 Meyer, D.J.: C2-WeA5, 139
 Meza, R.: E1-4-WeA6, 141
 Mezlini, S.: D2-TuA1, 116
 Michau, A.: A1-1-TuM3, 101; B2-2-FrM5, 208; B2-2-FrM6, 208
 Michau, D.: E3-WeM10, 130
 Michel, A.: H1-2-TuA2, 121
 Michel, E.G.: E2-1-TuM4, 107
 Michels, A.F.: E1-2-ThA11, 171
 Michler, J.: H2-2-MoA4, 98
 Mihut, D.M.: B4-4-WeA6, 138; DP-ThP26, 192
 Mikula, M.: B5-2-FrM6, 209; BP-ThP3, 178; E1-3-FrM2, 210
 Milassin, G.: TS3+4-2-MoA8, 100
 Milhet, X.: H1-1-TuM2, **109**
 Millan-Ramos, B.: D1-2-MoA6, 96
 Minea, T.: B7-TuA9, **115**; F2-1-ThM3, 157; F2-1-ThM6, 157; FP-ThP10, 198; FP-ThP7, 198
 Mingó, B.: C3+C2+C1-ThM12, 155; CP-ThP19, 187
 Mischler, S.: D1-1-MoM4, 88
 Mishra, M.: TS4-1-MoM5, **90**
 Missaoui, J.: E1-2-ThA6, **170**
 Mitma Pillaca, E.J.D.: GP-ThP8, **201**
 Mitterer, C.: B1-2-MoA10, 93; B2-1-ThA11, 166; B2-1-ThA4, 165; B4-3-WeM3, **127**; B4-4-WeA2, 137; C4-ThA7, 169; EP-ThP6, 194; H1-1-TuM7, 110; TS3+4-2-MoA4, 99
 Miyakawa, W.T.: DP-ThP23, 192
 Mizubayashi, M.: G2-FrM3, **212**
 Mock, A.: C2-WeA1, **139**; C3+C2+C1-ThM9, 154; CP-ThP18, 187
 Mocuta, C.: E2-2-TuA2, 118
 Modes, T.: B1-3-TuM1, 103
 Mohammadtaheri, M.: BP-ThP42, 185
 Mojica-Villegas, A.: B4-1-TuM5, 105
 Moldenhauer, H.: EP-ThP23, **196**
 Molina Aldareguia, J.M.: B3-2-MoA5, 94
 Monaghan, D.: B1-2-MoA2, 92; FP-ThP9, 198
 Monclus, M.A.: B3-2-MoA5, 94
 Monsifrot, E.: B2-2-FrM5, 208; B2-2-FrM6, 208
 Monterrosa, A.M.: H3-2-WeA3, 143
 Montes Ruiz-Cabello, F.J.: TS2-ThM4, 161
 Montigaud, H.: H1-1-TuM6, 110; H1-2-TuA11, 123; HP-ThP7, 204
 Moon, G.D.: CP-ThP24, **188**
 Mora, J.: TS2-ThM8, **161**
 Moraes, V.: B4-3-WeM3, 127; B6-ThM12, 153; B6-ThM9, **152**; BP-ThP34, **184**
 Moreau, C.: CP-ThP27, 189; TS2-ThM9, 162
 Moreno Palmerin, J.: GP-ThP18, 202
 Morgado-Gonzalez, I.: AP-ThP6, 177; BP-ThP24, **182**; BP-ThP25, 182
 Morstein, M.: B4-3-WeM3, 127
 Moseler, M.: E1-3-FrM3, **210**
 Moskovkin, P.: B7-TuA1, 114
 Mosquera, M.: A1-1-TuM8, 102
 Motallebzadeh, A.: E2-2-TuA10, 119; EP-ThP5, 193
 Motylenko, M.: B4-3-WeM4, 127; B4-4-WeA7, 138
 Mouftiez, A.: B4-3-WeM6, 127
 Mourya, S.: F4-2-WeA3, 141; GP-ThP19, 202
 Mraz, S.: B1-2-MoA10, 93
 Mu, Y.: H2-2-MoA3, 97
 Muhl, S.: D2-TuA4, 116; E1-3-FrM5, 211; E1-3-FrM9, **211**
 Mühlbacher, M.: EP-ThP6, 194
 Müller, A.: G2-FrM7, 212
 Munroe, P.: TS1-1-WeM1, 133
 Muralidharan, G.M.: A1-1-TuM1, 101; A1-3-WeM4, 125
 Muratore, C.: F3-TuA5, 120; TS3+4-2-MoA5, 99
 Musil, J.: B1-2-MoA4, 92
 Myoung, S.W.: A2-2-ThA7, **163**
 — N —
 N'Gom, M.: C3+C2+C1-ThM5, **153**
 Nagaraj, R.: D2-TuA5, 116
 Nahif, F.: EX-TuEx1, **111**
 Nait-Ali, A.: H1-1-TuM2, 109
 Najarian, V.: E1-1-ThM6, 156
 Nakamura, H.: B2-1-ThA3, 164
 Nakatani, T.: B2-2-FrM9, 209
 Narala, S.K.R.: B4-2-TuA4, 113; E1-3-FrM12, 212; EP-ThP31, 197
 Naraparaju, R.: B1-3-TuM2, 103
 Narasimalu, S.: A1-1-TuM6, 102
 Nass, K.: B3-1-MoM5, 87
 Nauenburg, K.-D.: G1+G3-ThM11, 160
 Navabpour, P.: AP-ThP2, 176
 Nava-Sánchez, J.L.: B4-3-WeM6, 127
 Navrotsky, A.: A2-1-ThM11, 150
 Neels, A.: A2-2-ThA3, 163
 Nêmcova, A.: C3+C2+C1-ThM12, 155
 Nemetz, A.W.: B4-4-WeA3, **138**
 Nepal, N.: C2-WeA5, 139
 Neumeier, S.: H1-1-TuM3, 109
 Neuß, D.: TS1-2-WeA9, 147
 Neville, A.: H3-2-WeA2, 143
 Ngo, D.: C3+C1-WeM4, 129
 Nicolai, J.: E2-2-TuA2, 118
 Nicolini, P.: E1-2-ThA2, 169; E1-2-ThA5, 170; E1-2-ThA7, **170**
 Nie, X.: EP-ThP27, **197**; G2-FrM10, **213**; G2-FrM5, 212
 Nielsen, L.P.: E1-1-ThM7, **156**; GP-ThP11, **201**
 Nii, H.: B4-3-WeM5, 127
 Nikitin, D.: F1-TuM1, 108
 Nimsch, U.: TS1-2-WeA1, 145
 Nishimura, K.: H1-2-TuA9, 122
 Nishiyama, K.: TSP-ThP8, 206
 Noh, Y.: GP-ThP15, 202
 Noma, M.: G4+G5+G6-ThA4, 173
 Northam, M.: A2-2-ThA5, 163
 Norymberczyk, L.: H3-2-WeA10, 145
 Nose, M.: G2-FrM3, 212
 Nyakiti, L.O.: C2-WeA5, 139
 Nyholm, L.: TS1-1-WeM3, 133; TS1-1-WeM5, 134
 — O —
 Obasi, G.: A1-1-TuM2, 101
 Oboegbu, M.J.: AP-ThP4, 176
 Obrusnik, A.: B1-3-TuM6, 104; G1+G3-ThM1, **158**
 Oellers, T.: H3-1-WeM3, 132
 Oh, J.S.: B2-2-FrM9, 209
 Oh, S.: C2-WeA7, **139**
 Öhman, S.Ö.: B2-2-FrM7, **208**
 Okamoto, N.: B4-1-TuM7, 105; B4-2-TuA9, 114; BP-ThP26, 183
 Okimoto, T.: G1+G3-ThM7, **159**; TSP-ThP8, **206**
 Okle, P.: H1-2-TuA1, 121
 Okuno, S.: B2-1-ThA2, 164
 Olabi, A.: CP-ThP22, 188
 Oladoye, A.: CP-ThP22, **188**
 Olaya Florez, J.J.: B4-1-TuM6, 105; BP-ThP39, 185; E1-4-WeA5, 141; EP-ThP26, 196
 Olejnicek, J.: G4+G5+G6-ThA7, 174
 Oliveira, A.: DP-ThP23, 192
 Oliveira, J.C.: B3-2-MoA7, **95**; FP-ThP6, **198**
 Oliver, W.C.: H2-2-MoA9, **98**
 Onofre, C.F.: B5-2-FrM4, 209
 Ortega-Aviles, M.: E1-1-ThM3, 155
 Ortiz-Domínguez, M.: AP-ThP6, 177; B4-2-TuA8, 114; BP-ThP24, 182; BP-ThP25, 182
 Oseguera-Peña, J.: B4-1-TuM5, 105; B4-2-TuA8, 114; E1-3-FrM5, 211; E1-3-FrM6, 211; E1-4-WeA6, 141
 Oskay, C.: A3-WeA3, **136**
 Ospina, R.: E1-4-WeA5, 141; EP-ThP26, 196
 Ougier, M.: A1-1-TuM3, **101**
 Özerinç, S.: E2-2-TuA10, **119**; EP-ThP5, **193**
 — P —
 Page, N.: D1-2-MoA3, 96
 Paladines, R.: D1-2-MoA3, 96
 Palaparty, S.: E1-3-FrM12, **212**; EP-ThP31, **197**
 Paliwal, A.: C3+C2+C1-ThM10, 154
 Pan, C.-H.: TS1-2-WeA2, 145
 Pan, W.-C.: E2-2-TuA9, 118
 Pandey, K.K.: B5-2-FrM9, 210
 Pang, X.L.: E2-2-TuA11, **119**
 Pantoya, M.: F1-TuM6, 109
 Panzarino, J.: H2-1-MoM6, 89
 Papa, F.: B3-2-MoA3, 94; F2-1-ThM9, 158; G1+G3-ThM8, **160**; TS3+4-2-MoA10, 100
 Pardhasaradhi, S.P.: H2-2-MoA9, 98
 Pardo-Perez, A.: D1-1-MoM4, 88
 Park, H.J.: G1+G3-ThM12, 160
 Park, I.-W.: AP-ThP10, **177**
 Park, J.S.: CP-ThP6, **186**; CP-ThP7, 186
 Park, S.: GP-ThP15, **202**

Author Index

- Park, T.G.: CP-ThP6, 186; CP-ThP7, **186**
 Park, Y.K.: CP-ThP24, 188
 Paseuth, A.: B2-1-ThA2, 164
 Passerone, D.: F4-2-WeA8, 142; FP-ThP5, 197
 Pathak, A.: B5-2-FrM9, 210
 Patnaik, P.: B4-4-WeA5, 138
 Paturi, U.M.R.: B4-2-TuA4, **113**; EP-ThP31, 197
 Paulus, M.: BP-ThP37, 185
 Paumier, F.: CP-ThP13, 187
 Pawar, S.: C4-ThA8, **169**; CP-ThP30, 189
 Pecerskis, A.: H3-2-WeA6, 144
 Pedersen, P.M.: GP-ThP11, 201
 Peng, L.F.: B3-2-MoA9, 95; C3+C2+C1-ThM11, 155
 Peng, Z.: H1-1-TuM3, 109
 Pereira, A.: GP-ThP24, 203
 Pereira-Silva, P.: D3-TuM2, 105
 Pérez Mendoza, G.J.: EP-ThP11, 194
 Perez Pasten-Borja, R.: B4-1-TuM5, 105
 Pérez Trujillo, F.J.: A1-3-WeM2, **125**; A3-WeA6, 137
 Perez, J.: EP-ThP12, 194
 Pérez-Alvarez, J.: FP-ThP11, 198
 Periyasamy, S.: E3-WeM6, 130
 Perry, D.: FP-ThP9, 198
 Peterson, R.L.: C2-WeA3, **139**
 Petrov, I.: B4-1-TuM4, 104; F2-1-ThM8, 158; F2-2-ThA5, 172; SIT2-WeSIT1, **135**
 Pflug, A.: B7-TuA1, 114
 Pierron, O.N.: H2-1-MoM4, 89; H2-2-MoA2, **97**; TS4-1-MoM4, 90
 Pignedoli, C.A.: F4-2-WeA8, 142; FP-ThP5, 197
 Pikul, J.H.: E3-WeM1, **129**
 Pillai, R.P.: A1-1-TuM1, **101**
 Pinheiro, R.A.: BP-ThP28, 183
 Pint, B.A.: A2-1-ThM3, 149; A2-2-ThA4, 163
 Pippan, R.: C4-ThA7, 169
 Pleskunov, P.: F1-TuM1, 108
 Podraza, N.J.: C3+C2+C1-ThM13, **155**
 Poerschke, D.: A2-2-ThA1, **163**
 Pohler, M.: B4-4-WeA7, 138
 Polacek, M.: B5-1-ThA4, 166
 Polcar, T.: B5-1-ThA3, 166; H3-2-WeA4, **144**
 Polcar, T.P.: B5-2-FrM4, 209; E1-1-ThM5, 156; E1-2-ThA2, 169; E1-2-ThA7, 170; E1-3-FrM2, 210
 Polcik, P.: B4-3-WeM3, 127; B6-ThM12, 153; B6-ThM9, 152; BP-ThP34, 184; TS1-1-WeM12, 134; TS1-2-WeA9, 147
 Polop, C.: E2-1-TuM4, 107
 Polyakov, M.: A2-2-ThA3, 163
 Pone, A.: H3-2-WeA6, 144
 Pons, M.: B2-1-ThA6, 165; B2-1-ThA7, 165; B2-2-FrM5, 208
 Popoola, O.M.: CP-ThP26, 189; E1-4-WeA4, 141; E1-4-WeA7, 141; FP-ThP12, 199
 Popoola, P.A.: CP-ThP26, 189; D2-TuA11, 117; E1-4-WeA4, 141; E1-4-WeA7, 141; E2-1-TuM6, 108; FP-ThP12, 199
 Poruba, A.: B7-TuA11, 115
 Poulon-Quintin, A.: E3-WeM10, 130
 Praetzas, C.: B4-4-WeA3, 138
 Preuss, M.: A1-1-TuM2, 101
 Price, J.: B1-2-MoA2, 92
 Prieto Ríos, C.: A3-WeA1, **136**
 Primetzhofer, D.: BP-ThP41, 185
 Prysiaznyj, V.: D2-TuA10, 117
 Puetz, W.: B2-2-FrM10, 209
 Pugh, M.: TS2-ThM9, 162
 Purandare, Y.: A1-1-TuM8, 102
 Pürstl, J.T.: H2-2-MoA4, 98
 Putz, B.: TS3+4-2-MoA8, **100**
- Pyclik, L.: A1-3-WeM5, 125; AP-ThP13, **178**
 — Q —
 Qiao, R.: H1-2-TuA8, 122
 Qiu, R.: B2-2-FrM8, 208; BP-ThP20, 182
 Quintana, I.: GP-ThP5, 200
 Quintero, J.H.: EP-ThP26, 196
 — R —
 Raabe, D.: H1-1-TuM3, 109
 Raadu, M.A.: B7-TuA9, 115; F2-1-ThM8, 158
 Radny, T.: G1+G3-ThM11, 160
 Rafaja, D.: B4-3-WeM4, 127; B4-4-WeA7, 138
 Raffield, C.D.: B4-4-WeA6, 138
 Raghavan, S.: A2-2-ThA5, 163
 Rahman, M.M.: A1-2-TuA8, **112**
 Rahman, S.M.: E1-3-FrM10, **211**
 Rai, R.: F3-TuA5, **120**
 Raimondo, M.: TS2-ThM2, 160; TS2-ThM5, **161**
 Raja, T.: E3-WeM6, **130**
 Rajagopalan, J.: H1-2-TuA3, 121; HP-ThP1, 204
 Ramirez, G.: E1-2-ThA9, 171
 Ramirez, M.: B3-1-MoM5, 87; GP-ThP8, 201
 Ramm, J.: A2-2-ThA3, 163
 Rao, S.: D3-TuM7, 106
 Rasmussen, P.: H1-2-TuA3, **121**; HP-ThP1, **204**
 Ratayski, U.: B4-3-WeM4, **127**
 Ratova, M.: F3-TuA3, 119
 Rausch, M.: B1-2-MoA10, **93**; TS3+4-2-MoA4, 99
 Rebelo de Figueiredo, M.: B1-3-TuM4, 103
 Rebholz, C.G.: C3+C1-WeM4, 129; C4-ThA3, 168; C4-ThA7, **169**
 Reddy, S.P.: CP-ThP4, **186**
 Redwing, J.: B2-1-ThA9, 165
 Regalla, S.P.: E1-3-FrM12, 212
 Řehák, P.R.: B6-ThM2, 151
 Reidy, R.F.: A2-1-ThM9, 150
 Reifsnnyder Hickey, D.: B2-1-ThA9, 165
 Remnev, A.G.: G2-FrM11, **213**
 Renault, P.O.: CP-ThP13, **187**; E2-2-TuA2, **118**
 Renk, O.: C4-ThA7, 169
 Restrepo-Parra, E.: E1-4-WeA5, **141**; EP-ThP26, **196**
 Revel, A.: F2-1-ThM3, 157; F2-1-ThM6, **157**; FP-ThP7, **198**
 Rezek, B.: E1-2-ThA7, 170
 Richards, B.: A2-1-ThM7, 150
 Riedl, H.: B4-2-TuA1, 113; B6-ThM12, **153**; B6-ThM9, 152; E1-2-ThA9, 171; F4-2-WeA6, 142; FP-ThP17, 199; FP-ThP3, **197**
 Riul, A.R.: B4-3-WeM2, 126
 Rivera Chaverra, M.J.: E1-4-WeA5, 141
 Rivera-López, J.E.: B4-2-TuA3, 113
 Rivero, P.J.: BP-ThP22, 182
 Robledo, S.: D1-2-MoA5, 96
 Roch, T.: B5-2-FrM6, 209; BP-ThP3, 178; E1-3-FrM2, 210
 Rodil, S.E.: B5-2-FrM4, **209**; D1-2-MoA6, 96
 Rodrigues, M.S.: D3-TuM2, 105
 Rodríguez Arevalo, S.D.: B4-1-TuM6, 105; BP-ThP39, 185
 Rodríguez Ripoll, M.: E1-2-ThA9, 171
 Rodríguez Valverde, M.A.: TS2-ThM4, 161
 Rodríguez, R.: BP-ThP22, 182
 Rodríguez, S.: A3-WeA4, 136
 Rodríguez-Castro, G.A.: B4-2-TuA3, 113; B4-3-WeM6, 127; E1-3-FrM5, 211; E1-3-FrM6, 211
 Rogers, J.: PL-MoPL3, **85**
 Rogov, A.: GP-ThP3, 200
 Rojas, T.C.: B3-2-MoA5, 94
- Rojo-Blanco, C.: E1-3-FrM9, 211
 Rollett, A.D.: B1-2-MoA3, 92
 Romanus, H.: TS1-2-WeA4, 146
 Ronkainen, H.: E1-1-ThM7, 156
 Rosén, J.: B4-1-TuM4, 104
 Rosenthal, M.: B4-4-WeA2, 137
 Rossmann, L.: A2-2-ThA5, **163**
 Rota, A.: E1-2-ThA7, 170
 Rougier, A.: F2-2-ThA4, 171
 Rowley-Neale, S.J.: F3-TuA3, 119
 Ruan, J.-J.: TS1-2-WeA2, **145**; TSP-ThP9, 207
 Ruan, J.-W.: CP-ThP31, 189
 Rudigier, H.: TS1-1-WeM4, 133
 Rueß, H.: TS1-2-WeA9, 147
 Ruiz-Rios, A.: E1-1-ThM3, 155
 Rupapara, H.: TS1-2-WeA4, 146
 Rupert, T.: H2-1-MoM5, **89**; H2-1-MoM6, 89
 Rupp, S.: B3-1-MoM2, 86
 Ryan, P.J.: F2-1-ThM11, 158
 Ryl, J.: F3-TuA11, 120
 — S —
 Sabbadini, S.: A1-3-WeM5, 125
 Sáenz-Trevizo, A.: C3+C2+C1-ThM8, 154
 Saha, B.: C3+C1-WeM5, **129**
 Sainith, V.: E1-1-ThM4, **156**
 Saito, T.: B4-1-TuM7, **105**; B4-2-TuA9, 114; BP-ThP26, **183**
 Sakakita, H.: EP-ThP24, 196
 Sakalley, S.: C3+C2+C1-ThM10, 154
 Sakamoto, Y.: BP-ThP11, 180; BP-ThP12, 180; BP-ThP13, 180
 Sakuma, T.: BP-ThP13, 180
 Sakuragi, T.: G2-FrM3, 212
 Saldana Rovles, A.: GP-ThP18, 202
 Saleem, A.: GP-ThP22, 203
 Salem, A.: D2-TuA1, 116
 Sälker, J.A.: H3-2-WeA5, 144
 Salvador, P.A.: B1-2-MoA3, 92
 Sampaio, P.: D3-TuM2, 105
 Sampath, S.: A2-2-ThA4, 163
 Sanchette, F.: A1-1-TuM6, 102
 Sánchez Fuentes, L.: HP-ThP4, 204
 Sanchez Lara, S.: B4-4-WeA6, 138
 Sanchez Lopez, J.C.: B3-2-MoA5, 94
 Sanchez-Lara, S.: B4-4-WeA6, **138**
 Sandlöbes, S.: H3-1-WeM1, 132
 Sanginés de Castro, R.S.: BP-ThP8, 179; HP-ThP10, 205
 Sangiovanni, D.G.: B5-2-FrM6, 209; B6-ThM7, **152**
 Sanni, O.: D2-TuA11, **117**
 Santiago Varela, J.A.: B3-2-MoA5, **94**; G1+G3-ThM4, 159
 Santiago, F.: E1-4-WeA6, **141**
 Santos, M.A.: DP-ThP23, 192
 Sardar, S.: CP-ThP12, **187**
 Sari, F.N.: CP-ThP31, 189
 Saringer, C.: H1-2-TuA4, **122**
 Sarkar, R.: HP-ThP1, 204
 Sartory, B.: H1-1-TuM7, 110
 Sathishkumar, D.: C4-ThA9, 169
 Satrapinsky, L.: BP-ThP3, 178; E1-3-FrM2, 210
 Sauques, L.: F2-2-ThA4, 171
 Savadkouei, K.: HP-ThP6, 204
 Scenini, F.: A1-2-TuA9, 112
 Schaaf, P.: TS1-2-WeA4, 146
 Schäfer, J.: B4-4-WeA3, 138
 Schäfer, R.: G1+G3-ThM11, **160**
 Schalk, N.: B2-1-ThA11, 166; B2-1-ThA4, **165**; H1-1-TuM7, 110; H1-2-TuA4, 122
 Scheffel, B.: B4-3-WeM4, 127
 Scheu, C.S.: H3-2-WeA9, 145
 Schiffrers, C.: B2-2-FrM10, 209; G1+G3-ThM2, **158**

Author Index

- Schlegel, M.L.: A1-1-TuM3, 101; A1-1-TuM6, 102
- Schmid, U.: B5-1-ThA7, **167**
- Schmidt, O.: B3-2-MoA1, 94
- Schmitt, J.A.: E1-1-ThM6, 156; EP-ThP30, 197
- Schmitt, T.: E1-1-ThM6, **156**; H3-2-WeA8, 144
- Schmitt, T.S.: EP-ThP30, 197
- Schmutz, P.: D1-1-MoM4, 88
- Schneider, J.M.: B1-2-MoA10, 93; BP-ThP41, 185; H1-1-TuM5, 110; H3-2-WeA5, 144; H3-2-WeA9, 145; TS1-2-WeA9, **147**
- Schneider, M.: B5-1-ThA7, 167
- Schubert, E.: C3+C2+C1-ThM9, **154**; CP-ThP18, **187**
- Schubert, M.: C3+C2+C1-ThM9, 154; CP-ThP18, 187
- Schuler, J.D.: H2-1-MoM5, 89
- Schulz, E.: E1-2-ThA10, 171
- Schulz, U.: B1-3-TuM2, **103**
- Schulz, W.: A1-1-TuM8, 102
- Schuster, F.: A1-1-TuM3, 101; A1-1-TuM6, 102; B2-2-FrM5, 208; B2-2-FrM6, 208
- Schütze, G.: B3-2-MoA1, 94
- Schwarzer, N.: EP-ThP13, **194**; F4-1-WeM11, **132**; H2-2-MoA10, 98; HP-ThP9, 205
- Scopece, D.: F4-2-WeA8, 142; FP-ThP5, 197
- Sebastiani, M.: H2-1-MoM7, **89**
- Segu, D.Z.: EP-ThP14, **194**
- Sekine, T.: TS4-1-MoM3, 90
- Sekora, D.: C3+C2+C1-ThM9, 154; CP-ThP18, 187
- Semprimoschnig, C.: TS3+4-2-MoA8, 100
- Sen, S.: H3-2-WeA4, 144
- Seo, H.J.: CP-ThP24, 188
- Serpini, E.: E1-2-ThA7, 170
- Serra, R.: B3-2-MoA7, 95
- Sethi, S.K.: DP-ThP24, **192**
- Seydoux, C.: C3+C2+C1-ThM7, 154
- Sezemycki, P.: D2-TuA10, 117
- Sha, C.: TS1-1-WeM1, **133**
- Shaleni, V.: C4-ThA9, 169
- Shang, H.F.: A1-2-TuA3, **112**
- Shao, S.: H2-2-MoA3, 97
- Shao, T.M.: A1-2-TuA3, 112; B6-ThM11, **153**
- Sharifi, N.: TS2-ThM11, 162; TS2-ThM9, 162
- Sharma, nil.: FP-ThP15, **199**
- Sharobem, T.: A2-1-ThM6, 149
- Shelemin, A.: F1-TuM1, 108
- Shen, X.: G2-FrM10, 213
- Shen, Y.H.: BP-ThP33, 184; F4-1-WeM10, 131
- Shen, Y.-L.: E2-1-TuM1, **107**
- Shesadri, S.: H1-2-TuA8, 122
- Shi, Q.: BP-ThP31, 184
- Shi, W.: B4-2-TuA2, 113
- Shin, C.H.: G1+G3-ThM12, 160
- Shin, S.J.: F2-2-ThA3, 171
- Shirani, A.: E3-WeM3, 129
- Shiratan, M.: B2-2-FrM9, 209
- Shishido, N.: TS4-1-MoM3, 90
- Shore, D.: GP-ThP3, **200**
- Signor, L.: H1-1-TuM2, 109
- Silva, F.: D3-TuM7, 106
- Silva-Bermudez, P.: D1-2-MoA6, **96**
- SilviaAlvarez, D.F.: GP-ThP18, 202
- Simmons, M.: TS3+4-2-MoA10, 100
- Simonot, L.: H1-2-TuA2, 121
- Singh, B.R.: B2-1-ThA1, 164
- Singh, M.: DP-ThP24, 192
- Singh, P.: B2-1-ThA1, 164
- Sitnikov, N.: B1-2-MoA11, 93
- Slim, M.F.: E2-1-TuM5, 108
- Smietana, M.: D2-TuA10, 117
- Smith, G.C.: F3-TuA3, 119
- Smith, R.: C3+C1-WeM2, 128
- Snure, M.: TS3+4-2-MoA5, 99
- Snyders, R.: TS3+4-2-MoA6, **100**
- Soares, P.: GP-ThP7, 201
- Šob, M.S.: B6-ThM2, 151; BP-ThP19, 181
- Sobaszek, M.: F3-TuA11, 120
- Sokolov, A.D.: H3-2-WeA6, 144
- Solar, P.: F1-TuM1, 108
- Soler, R.S.: H3-2-WeA9, 145
- Solis-Romero, J.: AP-ThP6, 177; B4-2-TuA8, **114**; BP-ThP24, 182; BP-ThP25, **182**
- Sologubenko, A.S.: H1-2-TuA1, **121**; HP-ThP3, 204
- Song, H.: GP-ThP2, **200**
- Song, J.: E1-3-FrM10, 211
- Song, M.G.: HP-ThP5, **204**
- Sorour, A.: E1-3-FrM11, 212
- Soucek, P.: B1-3-TuM6, 104; B5-1-ThA4, **166**
- Souza, J.: D3-TuM7, 106
- Souza, R.M.: E1-3-FrM1, 210
- Sparenberg, A.: BP-ThP37, 185
- Spolenak, R.: H1-2-TuA1, 121; H3-2-WeA7, 144; HP-ThP3, 204; TS1-2-WeA7, 147
- Srinath, A.: TS1-1-WeM3, 133
- Stamate, E.: B7-TuA4, **115**
- Stangebye, S.: H2-2-MoA2, 97
- Stangier, D.: B3-1-MoM3, 87; BP-ThP37, 185; EP-ThP23, 196; F2-2-ThA8, 172; F2-2-ThA9, 172
- Stark, A.: H1-2-TuA4, 122
- Steinhoff, M.K.: TS1-2-WeA9, 147
- Steinmann, P.-A.: DP-ThP22, **191**
- Stelzer, B.: H3-2-WeA5, **144**
- Sternemann, C.: BP-ThP37, 185
- Stiens, D.: B2-1-ThA5, 165
- Stokes, J.: CP-ThP22, 188
- Stoyanov, P.: E3-WeM11, **130**
- Stranak, V.: G4+G5+G6-ThA7, 174
- Stranak, V.S.: D2-TuA10, **117**; F3-TuA11, 120
- Straub, T.S.: AP-ThP11, **178**; H2-1-MoM3, **89**
- Stripe, B.: H1-2-TuA8, 122
- Stupavskaya, M.: B5-1-ThA4, 166
- Stylianou, R.: B2-1-ThA4, 165
- Su, J.: B2-1-ThA6, **165**; B2-1-ThA7, 165
- Su, Y.-H.: TS1-2-WeA10, 147; TS1-2-WeA2, 145; TSP-ThP9, 207
- Subacius, A.: C3+C1-WeM4, **129**
- Subba Reddy, N.: B4-2-TuA4, 113
- Subedi, B.: C3+C2+C1-ThM13, 155
- Subedi, D.B.: A1-3-WeM11, **126**
- Sugiyama, H.: TS4-1-MoM3, 90
- Sun, H.: AP-ThP2, **176**; C3+C2+C1-ThM10, 154
- Sun, Y.: BP-ThP29, 183
- Suresh, V.: D2-TuA2, 116
- Surmeier, G.: BP-ThP37, 185
- Suzuki, A.: BP-ThP13, 180
- Suzuki, H.: TSP-ThP8, 206
- Švec Jr., P.: BP-ThP3, 178; E1-3-FrM2, 210
- Svensson, J.-E.: A1-2-TuA1, **112**
- Swadzba, L.: A1-3-WeM5, 125; AP-ThP13, 178; AP-ThP9, 177
- Swadzba, R.: A1-3-WeM5, **125**; AP-ThP13, 178; AP-ThP7, **177**; AP-ThP9, 177
- Sweet, M.L.: A2-1-ThM3, 149; A2-1-ThM7, 150
- Szkodo, M.: F3-TuA11, 120
- U —
- Tada, D.: DP-ThP19, 191
- Taiariol, T.: B3-1-MoM4, 87
- Takamatsu, H.: EP-ThP22, 196
- Takoudis, C.: D3-TuM7, 106
- Talke, F.E.: E1-2-ThA3, **169**
- Tamura, M.: B5-2-FrM5, **209**
- Tan, S.: B2-1-ThA8, 165
- Tanaka, C.: B4-1-TuM7, 105; B4-2-TuA9, 114
- Tanaka, K.: B6-ThM10, **152**; EP-ThP22, 196
- Tanaka, M.: H1-2-TuA9, 122
- Tandieng, D.: H1-1-TuM2, 109
- Tao, H.: B4-3-WeM11, 128
- Tauchi, Y.: TSP-ThP8, 206
- Tavakoli, A.H.: HP-ThP11, **205**
- Taylor, G.: D1-2-MoA3, **96**
- Terziyska, V.L.: B4-3-WeM3, 127; TS3+4-2-MoA4, 99
- Teulé-Gay, L.: E3-WeM10, 130
- Texier, D.: AP-ThP11, 178
- Theveneau, M.: AP-ThP3, 176
- Thiaudière, D.: CP-ThP13, 187; E2-2-TuA2, 118
- Thiex, M.: BP-ThP23, **182**; E3-WeM4, **130**
- Thorwarth, K.: D1-1-MoM4, 88; D1-2-MoA8, 96; F4-2-WeA8, 142; FP-ThP5, 197
- Tian, Q.X.: F2-2-ThA2, 171
- Tian, X.B.: F2-2-ThA2, **171**
- Tillmann, W.: B3-1-MoM3, 87; BP-ThP37, 185; EP-ThP23, 196; F2-2-ThA8, 172; F2-2-ThA9, 172
- Ting, I.S.: A1-1-TuM7, **102**
- Ting, J.J.: TS1-2-WeA10, 147
- Ting, J.-M.: B1-1-MoM5, 86; BP-ThP33, 184; CP-ThP31, 189; F4-1-WeM10, 131; TS1-2-WeA10, **147**; TS1-2-WeA2, 145; TSP-ThP9, 207
- Tint, S.: D1-2-MoA3, 96
- Tjong, J.: G2-FrM10, 213
- Tkadletz, M.: B2-1-ThA11, 166; B2-1-ThA4, 165; B4-3-WeM3, 127; C4-ThA7, 169; H1-1-TuM7, **110**; H1-2-TuA4, 122
- Todt, J.: B4-4-WeA2, 137
- Todt, M.: B5-1-ThA5, 167; BP-ThP35, 184
- Togni, A.: TS1-2-WeA3, 146
- Tolan, M.: BP-ThP37, 185
- Toledo-Romo, F.: E1-3-FrM6, **211**
- Tonneau, R.: B7-TuA1, **114**
- Torp, B.: G4+G5+G6-ThA5, 173
- Torres San Miguel, C.R.: EP-ThP11, 194; HP-ThP4, 204
- Torres, R.: GP-ThP7, 201
- Totik, Y.: B6-ThM1, 150; BP-ThP30, 184
- Toyoda, H.: TSP-ThP8, 206
- Tracz, J.: A1-3-WeM5, 125; AP-ThP13, 178
- Trant, M.: F4-2-WeA8, 142; FP-ThP5, 197
- Trava-Airoldi, V.J.: B3-1-MoM4, 87; B3-1-MoM5, **87**; BP-ThP28, **183**; GP-ThP8, 201
- Treadwell, L.: H3-2-WeA3, 143
- Tripathi, R.: AP-ThP1, **176**
- Truchlý, M.: B5-2-FrM6, 209; BP-ThP3, **178**; E1-3-FrM2, 210
- Trujillo, J.P.: A1-1-TuM8, 102
- Tsai, M.-H.: GP-ThP17, **202**
- Tsai, P.-S.: GP-ThP17, 202
- Tsai, Y.J.: GP-ThP1, 200
- Tseng, I.-H.: GP-ThP17, 202
- Tseng, Y.C.: HP-ThP8, **205**
- Tsikata, S.: F2-1-ThM3, **157**; FP-ThP7, 198
- Tsou, H.K.: DP-ThP6, 190
- Tsuchiya, T.: H1-2-TuA9, 122
- Tudhope, A.: B3-2-MoA3, 94; G1+G3-ThM8, 160
- Tunes, M.A.: TS1-2-WeA5, 146
- Tvarog, D.: B7-TuA11, 115
- U —
- Ujah, C.O.: E1-4-WeA4, **141**; FP-ThP12, **199**
- Ukrainsev, E.: E1-2-ThA7, 170
- Ulrich, S.: G1+G3-ThM11, 160
- Unocic, K.: A1-1-TuM1, 101
- Urabe, K.: G4+G5+G6-ThA4, 173
- Ushakov, S.V.: A2-1-ThM11, 150
- Uyor, U.O.: CP-ThP26, **189**; E1-4-WeA7, **141**

Author Index

— V —

Vachhani, S.: B1-3-TuM4, 103
 Valeri, S.: E1-2-ThA7, 170
 Van Campen, D.: H1-1-TuM2, 109
 van der Poel, S.H.: EP-ThP21, 195
 Van Paeppegem, W.: TS3+4-2-MoA9, 100
 Vanderesse, N.: H3-2-WeA8, 144
 Vasco, E.: E2-1-TuM4, **107**
 Vasconcelos, G.: B3-1-MoM4, 87
 Vasina, P.: B1-3-TuM6, 104; B5-1-ThA4, 166; B7-TuA2, **115**
 Vaz, F.: CP-ThP23, **188**; D3-TuM2, **105**
 Vega-Morón, R.C.: E1-3-FrM5, **211**; E1-3-FrM6, 211
 Velic, D.: B2-1-ThA4, 165
 Vereschaka, A.: B1-2-MoA11, **93**
 Vernhes, L.: E1-1-ThM6, 156
 Vernon, E.: A1-1-TuM2, 101
 Veronesi, F.: TS2-ThM2, 160; TS2-ThM5, 161
 Vetter, J.: E3-WeM5, 130; G2-FrM7, **212**
 Victor, J.L.: F2-2-ThA4, **171**
 Victoria-Hernandez, J.: D1-2-MoA6, 96
 Villabos, C.: BP-ThP36, 185
 Villanueva, J.: D3-TuM7, 106
 Villardi de Oliveira, C.: A1-1-TuM6, **102**
 Villarroel, R.: GP-ThP6, 201
 Viloan, R.P.B.: F2-1-ThM8, 158
 Vincent, B.: F2-1-ThM3, 157; FP-ThP7, 198
 Vishnyakov, V.: AP-ThP2, 176; TS1-2-WeA5, **146**
 Viswanathan, V.: A2-2-ThA5, 163
 Vitelaru, C.: B3-2-MoA7, 95
 Vo, H.: B1-3-TuM4, 103
 Voevodin, A.A.: E3-WeM3, **129**
 Volpi, M.: H1-2-TuA1, 121
 Volu, R.M.: BP-ThP28, 183
 Voronkoff, J.: H1-1-TuM6, **110**
 — W —
 Wachesk, C.: B3-1-MoM4, 87; DP-ThP19, 191
 Wagner, A.: B5-1-ThA5, **167**; BP-ThP35, **184**
 Wagner, N.J.: C4-ThA5, **168**
 Wain, R.: A1-2-TuA9, 112
 Walls, J.M.: C3+C1-WeM2, 128
 Walton, S.: C2-WeA5, 139
 Wang, A.N.: TS1-2-WeA4, **146**
 Wang, C.: B5-1-ThA6, **168**; CP-ThP2, 186; FP-ThP16, **199**
 Wang, C.J.: TS1-1-WeM6, 134; TS1-2-WeA6, 146
 Wang, D.Y.: B5-2-FrM8, 210; BP-ThP27, 183; BP-ThP9, **180**
 Wang, J.: CP-ThP17, 187
 Wang, J.: TS2-ThM7, 161
 Wang, J.-B.: DP-ThP7, 190; F2-2-ThA7, 172
 Wang, Q.J.: EP-ThP19, 195
 Wang, S.C.: F1-TuM3, 108
 Wang, S.T.: B4-3-WeM13, 128; E1-3-FrM7, 211
 Wang, W.: BP-ThP31, 184
 Wang, Y.: B6-ThM10, 152; C2-WeA9, 139
 Wang, Y.M.: F2-2-ThA3, 171
 Wardini, J.: H2-1-MoM5, 89
 Warnk, T.: B3-1-MoM2, 86
 Warrior, N.: TSP-ThP1, 206
 Watanabe, N.: G2-FrM3, 212
 Watanabe, S.: EP-ThP2, 193

Waware, U.: AP-ThP8, **177**
 Wei, C.B.: BP-ThP31, 184; EP-ThP16, **195**
 Wei, R.: G4+G5+G6-ThA6, 174
 Wei, W.: A2-1-ThM5, **149**; A2-1-ThM9, 150
 Wei, W.-C.J.: TS1-2-WeA6, 146
 Weick, S.: A3-WeA5, 136
 Weißmantel, S.: B3-1-MoM2, **86**; B3-2-MoA2, 94
 Welters, M.: BP-ThP4, **179**; F4-2-WeA5, **142**
 Weng, S.Y.: B6-ThM3, 151
 Wennberg, A.: B3-2-MoA5, 94; F2-1-ThM9, 158; G1+G3-ThM4, 159; TS3+4-2-MoA10, **100**
 Wheeler, J.M.: H3-2-WeA7, 144; HP-ThP3, **204**; TS1-2-WeA7, **147**
 Wheeler, R.: F3-TuA5, 120
 Wheeler, V.D.: C2-WeA5, **139**
 Wheelis, S.: D3-TuM3, **105**
 Widrig, B.: A2-2-ThA3, 163
 Wieclaw, G.: AP-ThP9, 177
 Winkler, J.: B1-2-MoA10, 93; TS3+4-2-MoA4, 99
 Wisnivesky, D.: B4-3-WeM2, 126
 Witala, B.: A1-3-WeM5, 125; AP-ThP13, 178; AP-ThP9, 177
 Wittel, B.: G4+G5+G6-ThA5, 173
 Wittig, A.: EP-ThP23, 196
 Woda, M.: B2-2-FrM10, **209**
 Wojcik, T.: B6-ThM12, 153; FP-ThP3, 197
 Wolfe, M.: TS4-1-MoM4, 90
 Wong, M.S.: B4-1-TuM2, **104**; BP-ThP6, **179**
 Wu, C.-F.: D2-TuA12, 117
 Wu, C.J.: A2-2-ThA6, **163**
 Wu, F.B.: B4-3-WeM13, 128; E1-3-FrM7, 211; TSP-ThP7, 206
 Wu, G.M.: CP-ThP25, **189**
 Wu, H.: EP-ThP19, 195
 Wu, P.-W.: DP-ThP5, 190
 Wu, S.: B1-1-MoM4, 86
 Wu, S.C.: DP-ThP10, 191; DP-ThP9, 190
 Wu, T.-C.: DP-ThP2, 190
 Wu, W.C.: D1-2-MoA7, 96
 Wu, W.-Y.: GP-ThP21, **203**
 Wunderlich, R.: TSP-ThP4, 206
 Wüstefeld, C.: B4-4-WeA7, **138**
 — X —
 Xia, A.: B1-3-TuM4, 103; TS1-2-WeA3, **146**
 Xiao, P.: A1-1-TuM4, **101**; A2-1-ThM4, 149
 Xiao, Y.: HP-ThP3, 204; TS1-2-WeA7, 147
 Xiaobo, W.: EP-ThP28, **197**
 Xie, Z.: TS1-1-WeM1, 133
 Xing, P.: TS2-ThM3, 161
 Xu, F.: TSP-ThP1, 206
 Xu, J.: CP-ThP12, 187
 Xu, S.: CP-ThP2, 186
 — Y —
 Yalamanchili, K.: TS1-1-WeM4, **133**
 Yamada, K.: EP-ThP2, 193
 Yamamoto, K.: B4-3-WeM5, **127**
 Yamashita, M.: G4+G5+G6-ThA4, 173
 Yan, H.: GP-ThP12, **201**
 Yan, J.W.: H1-2-TuA10, **123**
 Yan, S.: BP-ThP29, 183
 Yanagisawa, K.: B2-1-ThA3, **164**
 Yang, B.I.: A2-2-ThA7, 163
 Yang, C.H.: GP-ThP1, 200

Yang, Q.: B4-4-WeA5, **138**; BP-ThP42, 185; E2-2-TuA8, 118
 Yang, S.: AP-ThP2, 176
 Yang, X.: H1-2-TuA8, 122
 Yang, Y.-C.: D1-2-MoA1, 95; D1-2-MoA7, **96**; DP-ThP7, 190; F2-2-ThA7, 172; GP-ThP13, 201
 Yang, Y.J.: B6-ThM3, **151**
 Yavas, H.Y.: B5-1-ThA3, 166; H3-2-WeA4, 144
 Yeh-Liu, L.K.: B6-ThM4, 151
 Yeo, C.D.: E1-3-FrM10, 211
 Yerokhin, A.: A1-2-TuA9, 112; C3+C2+C1-ThM12, **155**; CP-ThP19, **187**; E1-4-WeA2, 140; E3-WeM3, 129; G4+G5+G6-ThA3, 173; GP-ThP3, 200
 Yi, P.Y.: B3-2-MoA9, 95; C3+C2+C1-ThM11, 155
 Yi, S.: D1-2-MoA6, 96
 Yoo, R.: CP-ThP6, 186; CP-ThP7, 186
 Yun, W.: H1-2-TuA8, **122**
 — Z —
 Zabinski, J.: E3-WeM3, 129
 Zabransky, L.: B1-3-TuM6, 104; B5-1-ThA4, 166
 Zagonel, L.F.: B4-3-WeM2, 126
 Zaid, H.: B6-ThM10, 152
 Zálešák, J.: B4-4-WeA2, 137; BP-ThP19, 181
 Zambrano, D.: GP-ThP6, **201**
 Zangrossi, F.: TSP-ThP1, **206**
 Zapata, M.: DP-ThP16, 191
 Zauner, L.: B6-ThM9, 152; F4-2-WeA6, 142; FP-ThP3, 197
 Zehnder, C.: H3-1-WeM1, 132
 Zeman, P.: B1-3-TuM5, 103; F4-2-WeA6, 142; FP-ThP17, 199
 Zemlicka, R.: B1-2-MoA5, **92**
 Zendejas Medina, L.: TS1-1-WeM5, **134**
 Zeng, A.: B3-2-MoA6, 94
 Zeng, Y.: BP-ThP11, **180**
 Zenker, R.: G4+G5+G6-ThA9, 174
 Zgheib, E.: E2-1-TuM5, **108**
 Zha, W.: EP-ThP27, 197
 Zhang, D.: B3-2-MoA9, **95**
 Zhang, L.: CP-ThP2, 186
 Zhang, P.L.: GP-ThP12, 201
 Zhang, W.: FP-ThP16, 199
 Zhang, X.: A1-1-TuM4, 101; H2-2-MoA3, 97
 Zhang, Z.: A1-1-TuM4, 101; B6-ThM2, 151
 Zhao, C.: EP-ThP27, 197; G2-FrM5, 212
 Zhao, L.: B4-4-WeA5, 138
 Zheng, T.-W.: B4-4-WeA1, 137
 Zheng, Y.: TS2-ThM7, 161
 Zheng, Y.Z.: BP-ThP7, 179
 Zhou, X.: G4+G5+G6-ThA11, 174
 Zhou, Z.: TS1-1-WeM1, 133
 Zhu, H.: A1-2-TuA4, 112
 Zhu, X.: CP-ThP2, 186
 Zikan, P.: B1-3-TuM6, 104; G1+G3-ThM1, 158
 Zimmer, O.: B1-2-MoA6, 92; TS1-2-WeA1, 145
 Zimmermann, M.: TS1-2-WeA1, 145
 Zitek, M.: B1-3-TuM5, 103
 Zubizarreta, C.: GP-ThP5, 200
 Zywitzki, O.: B1-3-TuM1, 103

ICMCTF 2019 EXHIBIT PROGRAM

Science drives technology and technology enables the science!

Come to the exhibit hall to meet the vendors who offer the products and services required for the analysis and characterization of metallurgical coatings, thin films and surface modification. Let them help you achieve your research goals and fulfill your laboratory needs.

Enjoy free lunch on Tuesday and Wednesday and join us for the Exhibit Hall Reception Tuesday evening from 5:30 to 7:00pm.

Exhibits are located in the Grand Exhibit Hall and are open Tuesday and Wednesday only!! (The Grand Exhibit Hall is located just past the ICMCTF registration area).

EXHIBIT HALL DAYS/HOURS

| | | |
|-----------|--------|------------|
| Tuesday | May 21 | 12pm - 7pm |
| Wednesday | May 22 | 10am - 2pm |

IN THIS SECTION:

| | |
|-----------------------------|-----|
| Exhibit Hall Overview | 221 |
| Exhibitor List & Floor Plan | 223 |
| Sponsor Listing | 224 |
| Advertisements | 225 |
| Product Locator | 234 |
| Exhibitor Profiles | 240 |



ICMCTF 2019 EXHIBIT PROGRAM



VISIT THE EXHIBITS !

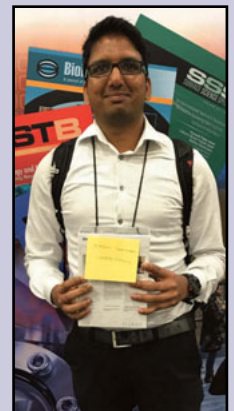
- See the Latest Technology
- Network with Colleagues & Exhibitors
- Free Light Lunch
- Exhibit Hall Reception (Tuesday 5:30)
- Raffle Drawings

EXHIBIT HALL HOURS:

| | |
|-----------|------------|
| Tuesday | 12pm - 7pm |
| Wednesday | 10am - 2pm |

Visit the sponsoring exhibitor booths to pick up your tickets to enter the daily raffle drawings...

GREAT PRIZES !!!





ICMCTF 2019 EXHIBITORS



Blue listings indicate our generous sponsors

| BOOTH | COMPANY | BOOTH | COMPANY |
|------------|--|------------|--|
| 314 | AGS Plasma Systems, Inc. | 324 | Micro Materials, Ltd. |
| 208 | AJA International, Inc. | 227 | Nano4Energy SLNE |
| 205 | Anton Paar USA | 326 | NANOVEA |
| 312 | AVS Membership & Logo Items | 219 | NETA |
| 310 | AVS Publications | 207 | Oerlikon Balzers |
| 226 | Bruker Nano Surfaces | 309 | Pfeiffer Vacuum Technology, Inc. |
| 323 | CemeCon AG | 328 | Plansee SE |
| 212 | Duniway Stockroom Corp. | 204 | Plasmaterials, Inc. |
| 308 | Ebatco | 329 | Process Materials Inc. |
| 108 | Elsevier BV | 221 | ProTech Materials |
| 327 | Eurofins EAG | 104 | PROTO |
| 223 | FemtoTools AG | 229 | PVT Plasma und Vakuum Technik GmbH |
| 306 | GE Golobal Research | 103 | R.D. Mathis Company |
| 213 | Hidden Analytical, Inc. | 107 | RAFFLE ZONE |
| 305 | Horiba Scientific | 315 | Robeko GmbH & Co. KG |
| 211 | IHI Ionbond, Inc. | 206 | Rtec Instruments, Inc. |
| 209 | Ionex Corporation | 307 | Semilab USA LLC |
| 106 | Kaufman & Robinson, Inc. | 214 | SEO (Surface Electro Optics) |
| 218 | KLA Corporation | 318 | Solecon Laboratires, Inc. |
| 319 | Kobe Steel, Ltd. | 222 | UC Components |
| 304 | Kurt J. Lesker Company | 215 | voestalpine eifeler Coatings North America |
| 316 | MeiVac, Inc. | 215 | voestalpine eifeler Vacotec GmbH |
| 321 | Melec GmbH | | |



ICMCTF 2019 SPONSORS

oerlikon
balzers

PLATITE®

Advanced Coating Systems
SWISS  QUALITY

 **eifeler**
VACOTEC

HAUZER

INDUSTRIAL PLASMA SOLUTIONS

BERNEX

SWISS CVD SOLUTIONS



ELSEVIER

PLANSEE 

 **Anton Paar**

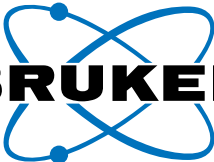
ionbond
IHI GROUP

GEMCON
The Tool Coating

 **KENNAMETAL**®

KLA 

PLASMATERIALS

 **BRUKER**

 **SEMILAB**



ICMCTF sincerely thanks the 2019 Sponsors for their support of the ICMCTF Conference and Exhibit Hall Events.

The CC800[®] HiPIMS

„Markets change, so the materials they process change too. High-performance materials place high demands on precision tools in machining. Whoever already carries the innovation gene within them today will succeed on the competitive markets of tomorrow!“

Dr. Toni Leyendecker – CEO CemeCon AG



hipims.cemecon.com

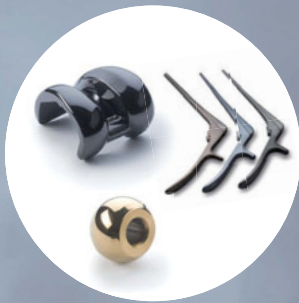
CEMECON
The Tool Coating

ionbond

IHI GROUP

HIGH QUALITY COATING SOLUTIONS ENGINEERED FOR FUNCTIONAL, MEDICAL AND DECORATIVE APPLICATIONS

Ionbond is one of the largest service providers for hard, wear-resistant, and low friction coatings. Our technology portfolio enables us to select the coating process best suited for each individual application.



Medical



Decorative



Components



Forming & Molding Tools



Cutting Tools



Automotive

info@ionbond.com | www.ionbond.com

HAUZER

INDUSTRIAL PLASMA SOLUTIONS



hauzer.nl

IHI GROUP

YOUR PARTNER IN RESEARCH



2017 Impact Factor
1.939

THIN SOLID FILMS is an international journal which serves scientists and engineers working in the fields of thin-film synthesis, characterization, and applications. The field of thin films, which can be defined as the confluence of materials science, surface science, and applied physics, has become an identifiable unified discipline of scientific endeavour.

For full aims and scope and editorial board go to:
journals.elsevier.com/thin-solid-films

Editor-in-Chief

J.E. Greene

Associate Editors

**P. Desjardins
T.A. Gessert
Z.H. Barber
D. Abou-Ras
C. S. Lee**



2017 Impact Factor
2.906

SURFACE AND COATINGS TECHNOLOGY

is an international archival journal publishing scientific papers on surface and interface engineering to modify and improve the surface properties of materials for protection in demanding contact conditions or aggressive environments, or for enhanced functional performance. Contributions range from original scientific articles concerned with applied research or direct applications of coatings, to invited reviews of current technology in specific areas.

For full aims and scope and editorial board go to:
journals.elsevier.com/surface-and-coatings-technology

Editor-in-Chief

A. Matthews

Editors

**G. Abadias
S. Aouadi
L. Lusvarghi
H.C. Man
P.J. Martin
J. Patscheider
I. Petrov
C. Rebholz
S.M.A. Shibli**



2017 Impact Factor
2.067

VACUUM is an international rapid publications journal with a focus on short communication. All papers are peer-reviewed, with the review process for short communication geared towards very fast turnaround times. The journal also published full research papers, thematic issues and selected papers from leading conferences.

A report in *Vacuum* should represent a major advance in an area that involves a controlled environment at pressures of one atmosphere or below.

The scope of the journal includes: Vacuum, Plasma science, Surface science, Materials science.

For full aims and scope and editorial board go to:
journals.elsevier.com/vacuum

Editor-in-Chief

L.G. Hultman

Editor

P. Eklund

Special Issue Editor

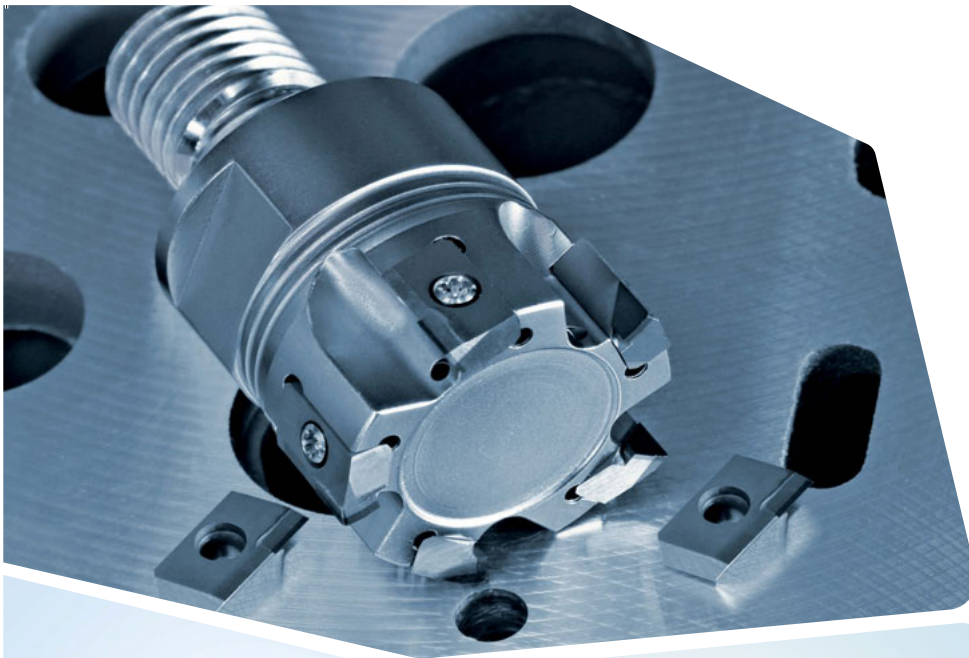
J.S. Colligon

Associate Editors

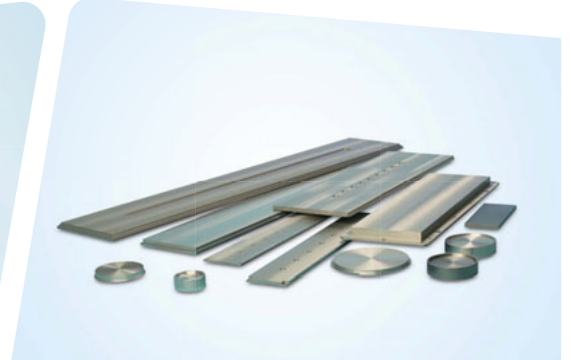
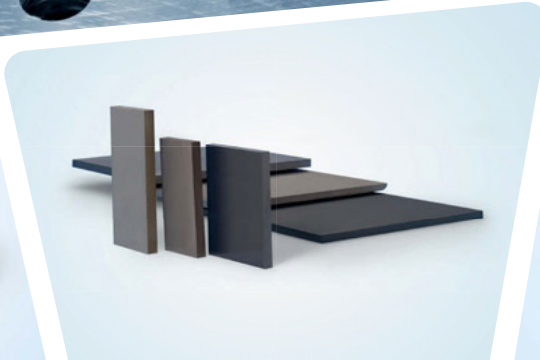
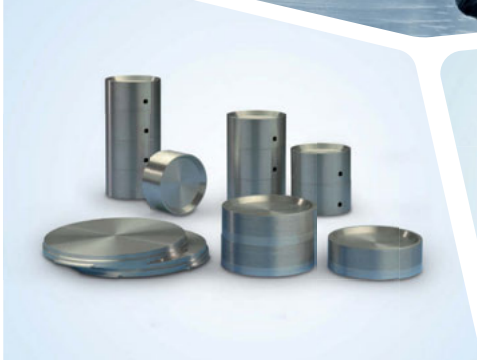
**O.B. Malyshev
P. Mayrhofer
L. Sabbatini**



Proudly Sponsoring the ICMCTF Cyber Café



PLANSEE



HIGH PERFORMANCE **TARGET MATERIALS** FOR PVD HARD COATING SOLUTIONS

Plansee is the leading supplier for high quality powder metallurgical target materials.

Our portfolio covers a wide range of standard compositions & dimensions which are available from stock. Reliable products, excellent service and a powerful innovation team, make Plansee the valuable partner of your choice.

Plansee Composite Materials GmbH
Siebenbürgerstraße 23, 86983 Lechbruck am See, Germany
Tel: +49 8862 773 0, Fax: +49 8862 773 198, plansee-cm@plansee.com

**VISIT US
BOOTH
#328!**

COME AND VISIT US
AT BOOTH 215
OR CONTACT US:
sales@eifeler-vacotec.com



BE ONE STEP AHEAD WITH OUR COATING SYSTEMS

Exigent and innovative vacuum special systems for the international market.

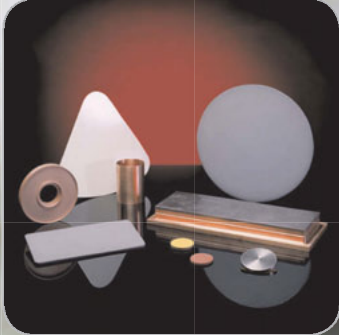
Thanks to its more than 25 years of experience in the area of vacuum technology, voestalpine eifeler Vacotec GmbH has installed more than 200 PVD coating systems in 12 countries with more than 20 locations and acquired a considerable level of know-how which is integrated into the design and the construction of the latest generation of systems.

voestalpine eifeler Vacotec GmbH
www.eifeler.com

voestalpine
ONE STEP AHEAD.

SCM **Super Conductor Materials Inc.**

Sputtering Targets



Crucible Liners



Evaporation Material



www.scm-inc.com
sales@scm-inc.com
1 845 368 0240

Made in USA
Since 1987



USE THE INDUSTRY REFERENCE IN SCRATCH TESTING: REVETEST RST³

- Scratch resistance and coating adhesion
- Scratch with automatic detection of critical loads
- Patented synchronized “Panorama” mode
- Conventional hardness measurements

Get in touch: www.anton-paar.com/surface-characterization

Visit us Booth #321



Cutting-Edge Technology by MELEC GmbH HiPIMS Superimpose with DC or Mid.- Frequency



**DC Pulse Power Controller SPIK3000A
Industrial scale
5kW -90 kW DC AVERAGE POWER**

• HiPIMS • Mid.Frequency (MF) • DC

Motivation for HiPIMS acceptance in the industry

- Highest depositionrate ➔ HiPIMS in combination with DC or Mid-Frequency, 4-5 times higher
- Reducing / preventing of arcing / poisoning ➔ HiPIMS used in pulse package mode
- Highest process stability tuning; reproduceable ➔ HiPIMS/MF used in bipolar pulse mode
- Low cost retrofit applications, single magnetron ➔ Use of your existing DC power supply combined with HiPIMS

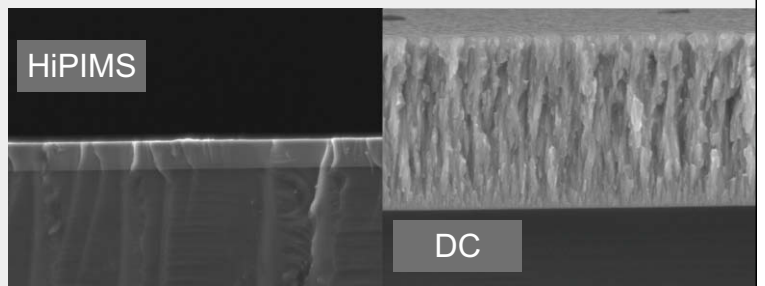
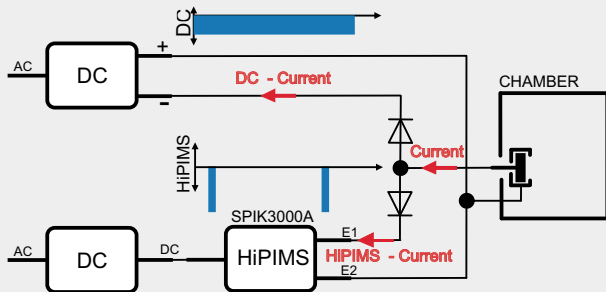
Improvements of coating using HiPIMS

- Higher ion bombardment
- Better coating adhesion
- Harder coating
- Denser films

Superimposed Processes for higher deposition rate

- HiPIMS + DC
- HiPIMS + MF

**Electric Circuit:
Superimposed HiPIMS / DC
using Single Magnetron**



MELEC GmbH
Dr.-Rudolf-Eberle-Str. 27
D-76534 Baden-Baden
Germany
Tel.: +49(0)7223 28145 -01
Fax: +49(0)7223 28145 -09
E-Mail: info@melec.de

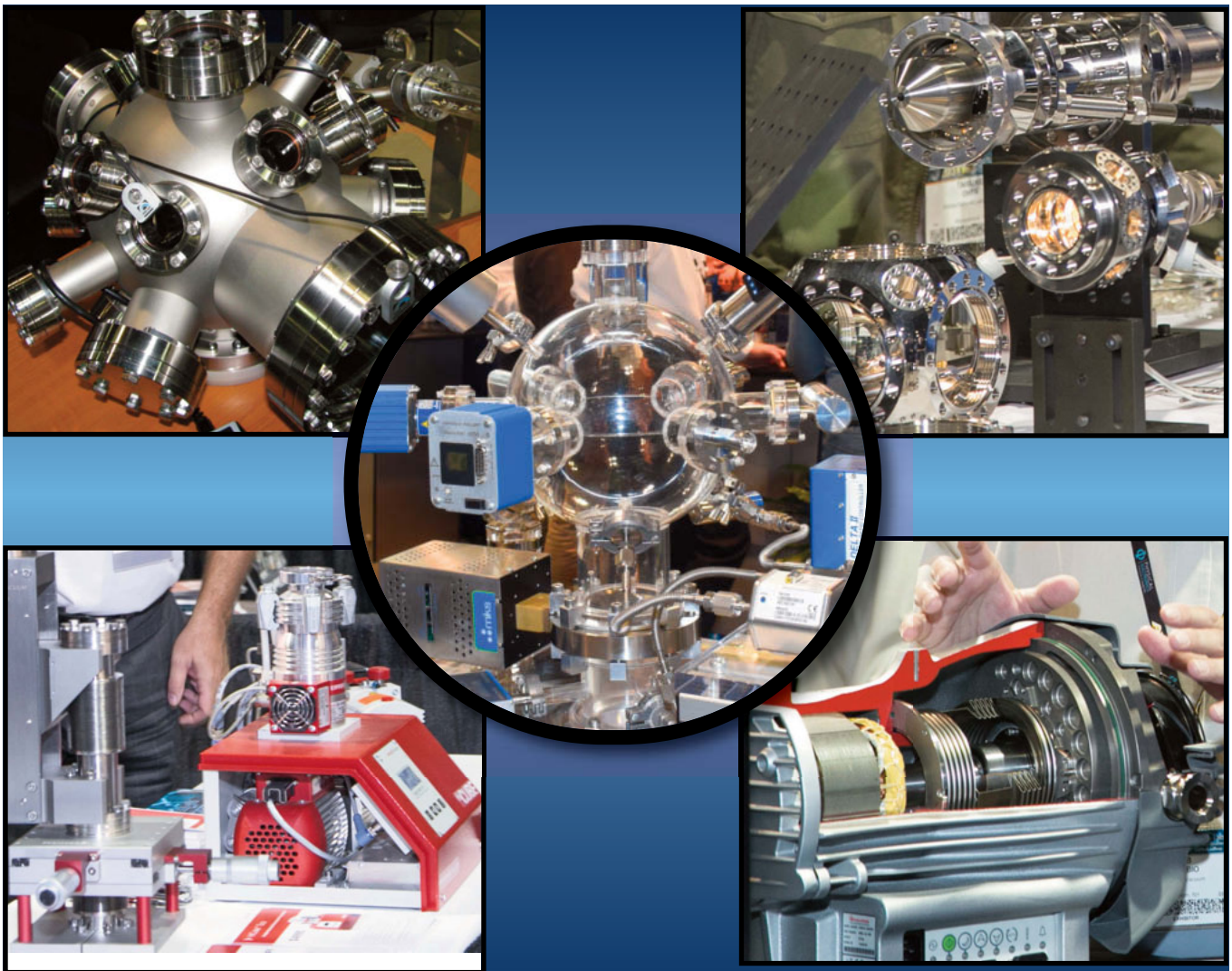
Contact:

Günter Mark, CEO
Tel. +49(0)7223 28145 -10
guenter.mark@melec.de

www.melec.de

PRODUCT LOCATOR

**Not sure what vendor supplies what you're looking for?
The Product Locator will help you find the vendors you need.
Product categories are listed alphabetically followed by the
supplier(s) and their corresponding booth location.**



PRODUCT LOCATOR

PRODUCT CATEGORIES FOLLOWED BY THE EXHIBITORS WHO OFFER THEM

Analytical & Testing Services

| | |
|--|-----|
| Bruker Nano Surfaces | 226 |
| Ebatco | 308 |
| GE Research–Material Characterization Svcs | 306 |
| KLA Corporation | 218 |
| NANOVEA | 326 |
| NETA | 219 |
| PROTO | 104 |
| Solecon Laboratories, Inc. | 318 |

Analytical Instrumentation

| | |
|----------------------------------|-----|
| Anton Paar USA | 205 |
| Bruker Nano Surfaces | 226 |
| Ebatco | 308 |
| Hiden Analytical, Inc. | 213 |
| Horiba Scientific | 305 |
| KLA Corporation | 218 |
| Micro Materials, Ltd. | 324 |
| NANOVEA | 326 |
| NETA | 219 |
| Pfeiffer Vacuum Technology, Inc. | 309 |
| PROTO | 104 |
| SEO (Surface Electro Optics) | 214 |

Backing Plates

| | |
|------------------------|-----|
| Kurt J. Lesker Company | 304 |
| Plasmaterials, Inc. | 204 |
| Process Materials Inc. | 329 |
| Robeko GmbH & Co. KG | 315 |

Bonding

| | |
|------------------------|-----|
| IHI Ionbond, Inc. | 211 |
| Kurt J. Lesker Company | 304 |
| Plasmaterials, Inc. | 204 |
| Process Materials Inc. | 329 |
| ProTech Materials | 221 |
| Robeko GmbH & Co. KG | 315 |

Bonding Techniques

| | |
|----------------------|-----|
| IHI Ionbond, Inc. | 211 |
| NETA | 219 |
| ProTech Materials | 221 |
| Robeko GmbH & Co. KG | 315 |

Consulting Services

| | |
|--|-----|
| GE Research–Material Characterization Svcs | 306 |
|--|-----|

Chemical: Surface Treating Services

| | |
|-------------------|-----|
| IHI Ionbond, Inc. | 211 |
|-------------------|-----|

Coating Machines/Instruments

| | |
|--|-----|
| AGS Plasma Systems, Inc. | 314 |
| AJA International, Inc. | 208 |
| Anton Paar USA | 205 |
| CemeCon AG | 323 |
| Kobe Steel, Ltd. | 319 |
| Kurt J. Lesker Company | 304 |
| Oerlikon Balzers | 207 |
| PVT Plasma und Vakuum Technik GmbH | 229 |
| Robeko GmbH & Co. KG | 315 |
| SEO (Surface Electro Optics) | 214 |
| voestalpine eifeler Coatings North America | 215 |
| voestalpine eifeler Vacotec GmbH | 215 |

Consulting

| | |
|----------------------------|-----|
| Ebatco | 308 |
| Kobe Steel, Ltd. | 319 |
| Solecon Laboratories, Inc. | 318 |

Crucible Liners

| | |
|------------------------|-----|
| Kurt J. Lesker Company | 304 |
| Plasmaterials, Inc. | 204 |
| Process Materials Inc. | 329 |
| R.D. Mathis Company | 103 |

Custom Vacuum Systems

| | |
|----------------------------------|-----|
| AGS Plasma Systems, Inc. | 314 |
| AJA International, Inc. | 208 |
| Kurt J. Lesker Company | 304 |
| MeiVac, Inc. | 316 |
| Pfeiffer Vacuum Technology, Inc. | 309 |
| ProTech Materials | 221 |
| voestalpine eifeler Vacotec GmbH | 215 |

CVD Diamond Coatings

| | |
|--------------------------|-----|
| CemeCon AG | 323 |
| IHI Ionbond, Inc. | 211 |
| Kaufman & Robinson, Inc. | 106 |
| MELEC GmbH | 321 |

PRODUCT LOCATOR

Detectors / Multipliers

| | |
|-------------------------|-----|
| Hidden Analytical, Inc. | 213 |
| Horiba Scientific | 305 |

E-Beam Gun Power Supplies

| | |
|--------------|-----|
| MeiVac, Inc. | 316 |
|--------------|-----|

E-Beam Gun Sweeps

| | |
|--------------|-----|
| MeiVac, Inc. | 316 |
|--------------|-----|

E-Beam Guns

| | |
|--------------------------|-----|
| AGS Plasma Systems, Inc. | 314 |
| Kurt J. Lesker Company | 304 |
| MeiVac, Inc. | 316 |

E-Beam Parts and Accessories

| | |
|---------------------|-----|
| MeiVac, Inc. | 316 |
| R.D. Mathis Company | 103 |
| UC Components | 222 |

Equipment, Used Fittings, Gaskets, Flanges, Seals

| | |
|------------------------|-----|
| Duniway Stockroom Corp | 212 |
| Kurt J. Lesker Company | 304 |
| UC Components | 222 |

Evaporation Materials

| | |
|-------------------------|-----|
| AJA International, Inc. | 208 |
| Kurt J. Lesker Company | 304 |
| Plasmaterials, Inc. | 204 |
| Process Materials Inc. | 329 |
| ProTech Materials | 221 |
| R.D. Mathis Company | 103 |
| Robeko GmbH & Co. KG | 315 |

Film Thickness Systems/Equipment

| | |
|----------------------|-----|
| Anton Paar USA | 205 |
| Bruker Nano Surfaces | 226 |
| Horiba Scientific | 305 |
| KLA Corporation | 218 |
| NETA | 219 |
| PROTO | 104 |

Gas Control Systems

| | |
|------------------------|-----|
| Kurt J. Lesker Company | 304 |
| R.D. Mathis Company | 103 |
| Robeko GmbH & Co. KG | 315 |

Gauges, Tubes

| | |
|----------------------------------|-----|
| Duniway Stockroom Corp. | 212 |
| Kurt J. Lesker Company | 304 |
| Pfeiffer Vacuum Technology, Inc. | 309 |

HIPIMS

| | |
|------------------------------------|-----|
| CemeCon AG | 323 |
| Kobe Steel, Ltd. | 319 |
| Kurt J. Lesker Company | 304 |
| MELEC GmbH | 321 |
| PVT Plasma und Vakuum Technik GmbH | 229 |
| Robeko GmbH & Co. KG | 315 |

Ion / Electron Guns

| | |
|--------------------------|-----|
| Hidden Analytical, Inc. | 213 |
| Kaufman & Robinson, Inc. | 106 |
| Kurt J. Lesker Company | 304 |

Ion Beam Deposition Systems/Guns

| | |
|--------------------------|-----|
| AGS Plasma Systems, Inc. | 314 |
| AJA International, Inc. | 208 |
| Hidden Analytical, Inc. | 213 |
| Kaufman & Robinson, Inc. | 106 |
| Kurt J. Lesker Company | 304 |

Leak Detectors

| | |
|----------------------------------|-----|
| Hidden Analytical, Inc. | 213 |
| Pfeiffer Vacuum Technology, Inc. | 309 |

Magnetron Sputtering Cathodes

| | |
|-------------------------|-----|
| AJA International, Inc. | 208 |
| Ionex Corporation | 209 |
| Kobe Steel, Ltd. | 319 |
| Kurt J. Lesker Company | 304 |
| MeiVac, Inc. | 316 |
| MELEC GmbH | 321 |
| Plansee SE | 328 |
| Process Materials Inc. | 329 |
| ProTech Materials | 221 |
| Robeko GmbH & Co. KG | 315 |

PRODUCT LOCATOR

Magnetron Sputtering Equipment

| | |
|--------------------------|-----|
| AGS Plasma Systems, Inc. | 314 |
| AJA International, Inc. | 208 |
| CemeCon AG | 323 |
| Hiden Analytical, Inc. | 213 |
| Ionex Corporation | 209 |
| Kobe Steel, Ltd. | 319 |
| Kurt J. Lesker Company | 304 |
| MeiVac, Inc. | 316 |
| MELEC GmbH | 321 |
| ProTech Materials | 221 |
| R.D. Mathis Company | 103 |
| Robeko GmbH & Co. KG | 315 |

Materials / Standards

| | |
|------------------------|-----|
| Anton Paar USA | 205 |
| Kurt J. Lesker Company | 304 |
| Micro Materials, Ltd. | 324 |
| Plansee SE | 328 |
| Plasmaterials, Inc. | 204 |
| Process Materials Inc. | 329 |
| ProTech Materials | 221 |
| PROTO | 104 |
| R.D. Mathis Company | 103 |

Materials Testing

| | |
|--|-----|
| Anton Paar USA | 205 |
| Bruker Nano Surfaces | 226 |
| Ebatco | 308 |
| Horiba Scientific | 305 |
| GE Research–Material Characterization Svcs | 306 |
| KLA Corporation | 218 |
| Micro Materials, Ltd. | 324 |
| NANOVEA | 326 |
| PROTO | 104 |
| Rtec Instruments, Inc. | 206 |

MEMS EQUIPMENT

| | |
|--------------------------|-----|
| AGS Plasma Systems, Inc. | 314 |
| FemtoTools AG | 223 |

Metrology Equipment/Systems

| | |
|----------------------|-----|
| Bruker Nano Surfaces | 226 |
| Ebatco | 308 |
| Horiba Scientific | 305 |
| KLA Corporation | 218 |
| NANOVEA | 326 |
| NETA | 219 |
| Semilab USA LLC | 307 |

Microscopy

| | |
|--|-----|
| Anton Paar USA | 205 |
| Bruker Nano Surfaces | 226 |
| Ebatco | 308 |
| GE Research–Material Characterization Svcs | 306 |
| Horiba Scientific | 305 |
| KLA Corporation | 218 |
| NETA | 219 |

NanoFabrication Systems

| | |
|--------------------------|-----|
| AGS Plasma Systems, Inc. | 314 |
|--------------------------|-----|

NanoIndenters

| | |
|-----------------------|-----|
| Anton Paar USA | 205 |
| Bruker Nano Surfaces | 226 |
| Ebatco | 308 |
| Micro Materials, Ltd. | 324 |
| NANOVEA | 326 |

NanoMechanical Testing Systems

| | |
|-----------------------|-----|
| Anton Paar USA | 205 |
| Bruker Nano Surfaces | 226 |
| Ebatco | 308 |
| Micro Materials, Ltd. | 324 |
| NANOVEA | 326 |

Ovens, Vacuum

| | |
|-------------------|-----|
| ProTech Materials | 221 |
|-------------------|-----|

Particle Monitoring

| | |
|------------------------|-----|
| Ebatco | 308 |
| Hiden Analytical, Inc. | 213 |
| Horiba Scientific | 305 |

Planar Magnetron Cathodes

| | |
|----------------------|-----|
| Kobe Steel, Ltd. | 319 |
| MeiVac, Inc. | 316 |
| Plansee SE | 328 |
| ProTech Materials | 221 |
| Robeko GmbH & Co. KG | 315 |

Precious Metal Alloys

| | |
|---------------------|-----|
| Plasmaterials, Inc. | 204 |
| R.D. Mathis Company | 103 |

Precious Metal Refining

| | |
|---------------------|-----|
| Plasmaterials, Inc. | 204 |
|---------------------|-----|

PRODUCT LOCATOR

Process Controllers/Monitors

| | |
|----------------------------------|-----|
| NETA | 219 |
| Robeko GmbH & Co. KG | 315 |
| voestalpine eifeler Vacotec GmbH | 215 |

Profilometers

| | |
|----------------------|-----|
| Bruker Nano Surfaces | 226 |
| NANOVEA | 326 |

Publishers

| | |
|------------------|-----|
| AVS Publications | 310 |
| Elsevier BV | 108 |

Pumps, Equipment, Services & Supplies

| | |
|----------------------------------|-----|
| Duniway Stockroom Corp. | 212 |
| Kobe Steel, Ltd. | 319 |
| Kurt J. Lesker Company | 304 |
| Pfeiffer Vacuum Technology, Inc. | 309 |

RAMAN Spectroscopy

| | |
|-------------------|-----|
| Anton Paar USA | 205 |
| Horiba Scientific | 305 |

RF Systems/Generators/Power Supplies

| | |
|--------------------------|-----|
| AGS Plasma Systems, Inc. | 314 |
| Ionex Corporation | 209 |
| Kurt J. Lesker Company | 304 |
| MeiVac, Inc. | 316 |
| Nano4Energy SLNE | 227 |

Scanning Probe Microscopy Systems

| | |
|----------------------|-----|
| Anton Paar USA | 205 |
| Bruker Nano Surfaces | 226 |
| Ebatco | 308 |
| Horiba Scientific | 305 |
| NETA | 219 |

Software

| | |
|-------------------|-----|
| Horiba Scientific | 305 |
| Kobe Steel, Ltd. | 319 |
| MELEC GmbH | 321 |

Spectrometer Accessories

| | |
|------------------------|-----|
| Hiden Analytical, Inc. | 213 |
| Horiba Scientific | 305 |
| UC Components | 222 |

Sputtering Deposition System

| | |
|------------------------------------|-----|
| AGS Plasma Systems, Inc. | 314 |
| AJA International, Inc. | 208 |
| CemeCon AG | 323 |
| Hiden Analytical, Inc. | 213 |
| Kaufman & Robinson, Inc. | 106 |
| Kobe Steel, Ltd. | 319 |
| Kurt J. Lesker Company | 304 |
| MELEC GmbH | 321 |
| Plansee SE | 328 |
| Process Materials Inc. | 329 |
| ProTech Materials | 221 |
| PVT Plasma und Vakuum Technik GmbH | 229 |
| voestalpine eifeler Vacotec GmbH | 215 |

Sputtering Deposition Targets

| | |
|------------------------|-----|
| Kurt J. Lesker Company | 304 |
| Plasmaterials, Inc. | 204 |
| ProTech Materials | 221 |
| R.D. Mathis Company | 103 |
| Robeko GmbH & Co. KG | 315 |

Tensiometers

| | |
|------------------------------|-----|
| SEO (Surface Electro Optics) | 214 |
|------------------------------|-----|

Thickness Monitors/Measurement

| | |
|----------------------------|-----|
| Anton Paar USA | 205 |
| Ebatco | 308 |
| Hiden Analytical, Inc. | 213 |
| Horiba Scientific | 305 |
| KLA Corporation | 218 |
| Kurt J. Lesker Company | 304 |
| MeiVac, Inc. | 316 |
| NETA | 219 |
| PROTO | 104 |
| Solecon Laboratories, Inc. | 318 |

PRODUCT LOCATOR

Thin Film Vacuum Coating

| | |
|------------------------------------|-----|
| AGS Plasma Systems, Inc. | 314 |
| AJA International, Inc. | 208 |
| Anton Paar USA | 205 |
| CemeCon AG | 323 |
| IHI Ionbond, Inc. | 211 |
| Kaufman & Robinson, Inc. | 106 |
| Kobe Steel, Ltd. | 319 |
| Kurt J. Lesker Company | 304 |
| MeiVac, Inc. | 316 |
| Micro Materials, Ltd. | 324 |
| Plansee SE | 328 |
| Process Materials Inc. | 329 |
| ProTech Materials | 221 |
| PVT Plasma und Vakuum Technik GmbH | 229 |
| Robeko GmbH & Co. KG | 315 |
| voestalpine eifeler Vacotec GmbH | 215 |

ToF SIMS Instruments

| | |
|------------------------|-----|
| Hiden Analytical, Inc. | 213 |
|------------------------|-----|

Tribology Equipment/Services

| | |
|-----------------------|-----|
| Anton Paar USA | 205 |
| Bruker Nano Surfaces | 226 |
| Ebatco | 308 |
| Micro Materials, Ltd. | 324 |

Tubing/Piping/Bellows Assemblies

| | |
|-------------------------|-----|
| Duniway Stockroom Corp. | 212 |
|-------------------------|-----|

Vacuum System Accessories

| | |
|--------------------------|-----|
| Duniway Stockroom Corp. | 212 |
| Hiden Analytical, Inc. | 213 |
| Kaufman & Robinson, Inc. | 106 |
| Kurt J. Lesker Company | 304 |
| MeiVac, Inc. | 316 |
| ProTech Materials | 221 |
| R.D. Mathis Company | 103 |
| UC Components | 222 |

Vacuum System Replacement Parts

| | |
|-------------------------|-----|
| Duniway Stockroom Corp. | 212 |
| Kurt J. Lesker Company | 304 |
| MeiVac, Inc. | 316 |
| ProTech Materials | 221 |
| UC Components | 222 |

Valves

| | |
|----------------------------------|-----|
| Duniway Stockroom Corp. | 212 |
| Hiden Analytical, Inc. | 213 |
| Kurt J. Lesker Company | 304 |
| MeiVac, Inc. | 316 |
| Pfeiffer Vacuum Technology, Inc. | 309 |

X-Ray Photoelectron Spectrometers

| | |
|-------------------|-----|
| Anton Paar USA | 205 |
| Horiba Scientific | 305 |



COMPANY PROFILES

AGS Plasma Systems, Inc.
3064 Kenneth Street
Santa Clara, CA 95054
Phone: 408-855-8686
www.agsplasma.com

PLASMA • ETCH • PVD • PECVD Celebrating our 28th Year in Plasma! Now offering the Ideal Vacuum Cube Range and introducing the Penta-PVD series of modular deposition systems Products: -MPS Series - Plasma Etching & Deposition Systems Our Modular Process System offers the ultimate machine for thin film research and development through production. MPS-150, MPS-200, MPS-300, MPS-450, and our bench-top TT-150 too! Advanced Reactor technologies, such as ICP, RIE, RIE/PE, PECVD and PVD are available as standard modules. -Penta-PVD™ - Versatile coating system -Ideal Vacuum Cube - Modular High-Vacuum Chamber System

314

AVS
125 Maiden Lane 15th Floor
New York, NY 10038
Phone: 212-248-0200
www.avs.org

As an interdisciplinary, professional Society, AVS supports networking among academic, industrial, government, and consulting professionals involved in a variety of disciplines: chemistry, physics, biology, mathematics, all engineering disciplines, business, sales through common interests related to the basic science, technology development, and commercialization of materials, interfaces, and processing area. Each year, AVS hosts local and international meetings, publishes four journals, honors member through its awards and recognition program, provides training via our short courses, and offers career services.

312



AJA International, Inc.
P.O. Box 246
North Scituate, MA 02060
Phone: 781-545-7365
www.ajaint.com

Thin Film Deposition Systems (Sputtering, E-beam, Thermal, Ion Beam, PLD and Multi-Technique). Ion Beam Etch Systems with SIMS (Ion Milling, RIBE). R&D and Pilot Scale Equipment. UHV and HV Magnetron Sputter Sources and Thermal Evaporation Sources. Wide range of Substrate Holders featuring Azimuthal Rotation, RF/DC Biasing, Heating, Water Cooling, LN2 Cooling and Tilting. Sputter Targets and Evaporation Materials. RF/DC Power Supplies.

208

AVS Publications
125 Maiden Lane 15th Floor
New York, NY 10038
Phone: 212-248-0200
www.avs.org

Broaden or share your knowledge in one of AVS' journals *JVST A*, *JVST B*, *Surface Science Spectra*, *Biointerphases* and the recently launched *AVS Quantum Science* by AVS and AIP Publishing. The scope of AVS Quantum Science is, at its core, the study of measurement. Measuring the smallest possible (quantized) value of a physical property opens the door for understanding additional characteristics and processes that occur on small, medium, and large scales. AVS and AIP Publishing also offer, eSpectra, a data product to plot, compare and validate your data, as well optionally share your data. See more about the journals including the latest Special Topic Collections, Featured Articles and Editor's Picks on the journal websites or visit us at Booth 310.

310



Anton Paar USA
10215 Timber Ridge Dr.
Ashland, VA 23005
Phone: 804-550-1051
www.anton-paar.com/us-en/

Anton Paar is the leader in the development of instruments for surface mechanical properties characterization with over 30 years' experience in both research and industrial fields. Our product line includes: •Nano and micro indentation: For hardness and modulus. Most stable on the market •Revetest, nano and micro scratch: For thin film adhesion, fracture, and deformation. For research and QC applications •Tribometers: High temperature and linear reciprocating options •Calotest: Fast coating thickness measurements

205

Bruker Nano Surfaces
3400 East Britannia Drive Suite 150
Tucson, AZ 85706
Phone: 520-741-1044
www.bruker.com/nano

Bruker is a world-leading manufacturer of metrology and testing solutions with a suite of technologies for thin film characterization including contact and non-contact surface profilers, mechanical testers and nanoindenters. Visit our booth (#226) to see our latest technologies and application stories. Check us out online at www.bruker.com/nano.

226



COMPANY PROFILES

CemeCon AG

Adenauerstrasse 20A4
52146 Wuersele, Germany
Phone: 49-2405-4470-100

www.cemecon.com

CemeCon highlights for the 2019 ICMCTF: Pure HiPIMS Coatings with a deposition rate as high as 2 $\mu\text{m}/\text{hour}$ - this makes the CC800 HIPIMS the ideal piece of equipment for industrial HiPIMS production and for cutting edge thin films research. The next generation Diamond Coatings for graphite moulds for curved displays for cell phones and CFRP/composites for the aircraft industry.



323

Duniway Stockroom Corp.

48501 Milmont Drive
Fremont, CA 94538-7335
Phone: 650-969-8811

www.duniway.com

Duniway Stockroom specializes in vacuum equipment and supplies; ion pumps and controls; flanges, gaskets, bolts and nuts; vacuum gauges and controls; mechanical pumps and rebuild kits; supplies (oils, greases, hoses, bell jars) diffusion pumps and leak detectors. Equipment rebuilding services and a variety of reconditioned equipment. Free Catalog.

212

Ebatco

7154 Shady Oak Road
Eden Prairie, MN 55344
Phone: 952-334-5486

www.ebatco.com

Ebatco is an internationally renowned nanotechnology development and service company. Ebatco specializes in providing high-quality products, consulting and contract lab services for worldwide clients in the areas of testing instruments and equipment, advanced material characterization, and nanotechnology. Ebatco provides one-stop-shop solutions for your daily challenges through nanoscale analytical lab services, expert-level consultation, and first-class scientific instruments. The product and service portfolio of Ebatco encompasses instruments, tools, equipment and lab services that are designed to boost and facilitate nanotechnology applications in industrial environments. We are ready to assist you to implement the best-possible solutions for success in the fields of surface processing, surface treatment, surface engineering, coating and thin film deposition, and material property testing and measurement.

308

Elsevier BV

Radarweg 29 Amsterdam
Radarweg 29, Amsterdam 1043 NX
Netherlands

Phone: 31-20-485-2268

www.elsevier.com

As the world's leading publisher of science and health information, Elsevier serves more than 30 million scientists, students and health and information professionals worldwide. Elsevier is the proud publisher of the best journals in this field: Thin Solid Films, Surface and Coating Technology, Vacuum, Surface Science, Applied Surface Science, Progress in Surface Science and Surface Science Reports. We help customers advance science and health by providing world-class information and innovative tools that help them make critical decisions, enhance productivity and improve outcomes.



108

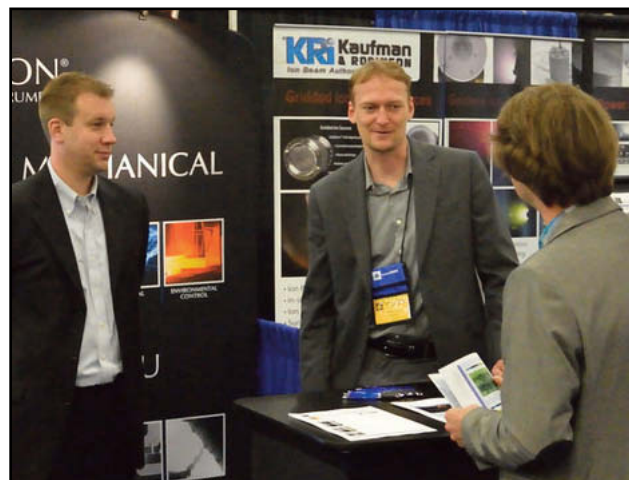
eurofin EAG

810 Kifer Road
Sunnyvale, CA 94086
Phone: 408-530-3500

www.eag.com/mc

Eurofins, EAG Laboratories is a global scientific services company serving clients across a vast array of technology-related industries. Through multidisciplinary expertise in materials and engineering sciences, EAG Laboratories helps companies innovate and improve products, ensure quality and safety, protect intellectual property. Stop by to learn more about our capabilities in surface analysis and materials characterization services.

327



COMPANY PROFILES

FemtoTools AG 223
Furtbachstrasse 4
Buchs ZH , 8107 • Switzerland
Phone: 41 448444425 • www.femtotools.com

Swiss high-tech company offering award-winning, ultra high-precision instruments for mechanical testing and robotic handling in the micro- and nanodomains. Our instruments meet the challenging requirements of semiconductor technology, microsystem development, materials science, micromedicine and biotechnology. FemtoTools' microrobotic handling and measurement instruments feature highly sensitive microforce sensing probes and force sensing microgrippers that are the result of a specially developed microelectromechanical system (MEMS)-based manufacturing process. The unmatched sensitivity and accuracy of our innovative systems redefines the standards for true quantitative investigations in the micro- and nanodomains.

GE Research—Material Characterization Services 306
1 Research Circle
Building K1-2D1
Niskayuna, New York 12309

Phone: 518-387-5882 • <https://www.ge.com/research/>
Let GE Global Research's Material Characterization team solve your most pressing material and project issues. We offer a wide range of analysis capabilities for metals, ceramics, and composites to polymers, chemical and natural materials. We can support material forensics, method origination, and supply chain solutions for your business. The team can apply over 50 characterization techniques and 1000+ unique methods to make sure materials meet customer defined criteria. Reach out to us today at: material.characterization@ge.com

Hidden Analytical, Inc. 213
37699 Schoolcraft Road
Livonia, MI 48150
Phone: 734-542-6666 • www.hiddenanalytical.com

Hidden Analytical manufactures an extensive range of high performance quadrupole mass spectrometers for plasma characterization studies, surface science applications, precision gas analysis and vacuum diagnostics. Showcasing the latest systems for residual and process gas analysis, plasma surface interactions, etch and deposition studies and Langmuir Probe measurements. For complete plasma characterization Hidden's EQP mass and energy analyzer and ESPion Langmuir Probe provide comprehensive analysis of both the plasma particle distribution and primary electrical parameters.

Horiba Scientific 305
3880 Park Avenue
Edison, NJ 08820-3012
Phone: 732-494-8660
www.horiba.com/scientific

Elemental Metal Infrared Analyzers (EMIA) measure gases extracted during combustion in a programmable High Frequency furnace directly with no conversion; The EMGA series offers analytical functions and stable control techniques providing fast, high precision analysis of materials ranging from micro-quantity to high-concentration samples; SLFA sulfur-in-oil analyzers offer cost effective methods to measure new low sulfur fuels, diesel and RG. Micro-XRF Analyzers include XGT X-ray Fluorescence micro-analyzers combining fast, non-destructive elemental analysis of energy dispersive X-ray Fluorescence with the ability to pinpoint individual particles with diameters down to 10µm in size. Automated sample scanning provides detailed images of element distribution over areas as large as 10cm x 10cm. Check out our new MESA-50 EDXRF Analyzer for applications including forensics, geology, materials, archaeology, and RoHS/ELV compliance testing.

IHI Ionbond, Inc. 211
1823 East Whitcomb Avenue
Madison Heights, MI 48071
Phone: 248-398-9100-2214
www.ionbond.com



Ionbond is a leader in state-of-the-art PVD, PACVD and CVD coating technology. Ionbond offers coating services for hard, wear resistant, low friction and decorative coatings. Ionbond's product portfolio features standard and custom engineered coatings which include pre- and post-coating treatments for cutting, forming and molding tools. Ionbond also provides coatings for components used in general industrial, automotive, aerospace, racing, medical and decorative applications. Ionbond has a worldwide presence through a network of over 39 service centers across Europe, North America and Asia. The cutting-edge technological infrastructure enables Ionbond's specialists to provide designs that meet customer's performance goals and are cost-competitive. Visit us at ICMCTF Booth # 211. More Information: www.ionbond.com.

COMPANY PROFILES

Ionex Corporation
20 Cabot Blvd Suite 300
Mansfield, MA 02048
Phone: 508-618-1266
www.ionexcorp.com

209

Ionex is the first company globally to offer a turn key HDP-magnetron source technology which are application driven, market specific and retrofittable. Ionex's HDP-magnetron deposition source technology is focused on rate, scalability and superior film properties. Our deposition technology offers the industrial market but not limited to a true alternative to Arc deposition due to its high ionization and high deposition rates producing dense, hard and smooth thin films without macro particles.

Kaufman & Robinson, Inc.
1330 Blue Spruce Drive
Fort Collins, CO 80524
Phone: 970-495-0187
www.ionsources.com

106

KRI engineers and manufactures broad beam ion and plasma products that are used world-wide. Our innovative and patented vacuum-based process tools interact with materials at the atomic level. We manufacture a wide range of ion and plasma sources, electron neutralizers, and power supplies on site. Our products and employees can assist you with your thin film depositions, etching processes, and material modifications. KRI was founded in 1978 by Dr. Harold Kaufman, and has been a leader in the research and development of broad beam sources for over four decades. Our employees have a wealth of experience and knowledge within the industry that help to make KRI the ion source authority that you can depend on.

KLA Corporation
1 Technology Drive
Milpitas, CA 95035
Phone: 408-375-3000
www.kla.com/

218



The Nano Indenter product line extends KLA-Tencor's surface metrology product suite to include a range of products well matched to customer's broader requirements for nanoscale mechanical testing. The Nano Indenter G200 is an accurate, flexible, user-friendly instrument for nanomechanical testing. Electromagnetic actuation allows unparalleled dynamic range in force and displacement, enabling measurement of deformation over six orders of magnitude, from nanometers to millimeters.

Kobe Steel, Ltd.
9-12 Kita-Shinagawa 5-Chome
Shinagana-ku, Tokyo 141-8688 Japan
Phone: 81-3-5739-6761
www.kobelco.co.jp/english/machinery/products/function/index.html

319

KOBELCO operates in a wide range of fields that provide the very foundation of society, including both the materials sector (iron and steel, welding, aluminum and copper) and the machinery sector (industrial machinery, construction machinery, engineering, and the environmental business). Among KOBELCO's industrial machinery business, our department is designing, manufacturing and selling coating systems since 1986. We are offering standard batch systems, in-line systems, and specialized coating systems for piston rings, etc. KOBELCO also developed coating technologies like UBMS systems, AIP/UBMS Hybrid system, and expanding PVD system applications. Over 400 units installed worldwide. In USA, we have a facility in Illinois, KOBAC (KOBELCO Advanced Coating (America) Inc. In Germany, company KCS Europe is representing KOBELCO. Both facilities are equipped our AIP-S40 system and are ready for demonstrations and sample testing from customers.

Kurt J. Lesker Company
1925 Route 51
Jefferson Hills, PA 15025-3681
Phone: 412-387-9200
www.lesker.com

304

KJLC® is "Enabling Technology for a Better World," while offering unparalleled customer support. R&D and batch production tools & materials for a wide variety of applications. Automated vacuum systems for PVD and ALD, chambers, components, thin film deposition sources, and pure materials. Featured products: e-beam sources; thermal evaporation sources, including low temp sources for organic films; R&D and production sputter sources; our new HIPIMS power supplies; feedthroughs; pumps and oils; valves.

COMPANY PROFILES

MeiVac, Inc. 316
5830 Hellyer Avenue
San Jose, CA 95138-1004
Phone: 408-362-1000 • www.meivac.com

MeiVac Process Systems have been widely used in Data Storage and general vacuum applications for more than 40 years. The Component group supports thin film production and R&D applications with deposition sources, substrate heaters, and process pressure control valves. VQ throttle valves, MAK sputter sources, e-Vap e-beam evaporation sources, HTR substrate heaters and their associated power supplies have long been the products of choice for a wide array of thin film deposition applications. Throttle Valves, Sputter Sources, Evaporation Sources and Substrate Heaters will be on display in the booth.

MELEC GmbH 321
Dr.-Rudolf-Eberle-Str. 15
Baden-Baden, 76534 Germany
Phone: +49-72232814510 • www.melec.de

MELEC GmbH develops and manufactures: •HiPIMS -, Mid-Frequency - and DC-Power Supplies •Dynamic voltage & current measurement systems •Software Applications using: Single & Dual Magnetron Sputtering, Synchronized Pulse BIAS, Pulse Packages, Superimposed HiPIMS with DC or MF; Pulsed cathodic arc deposition combined with DC; Plasma CVD power supplies. New HIPIMS/DC Pulse Power Controller SPIK3000A for industrial scale!

Micro Materials, Ltd. 324
Willow House - Yale Business Village Ellice Way
Wrexham, LL13 7YP • United Kingdom
Phone: 44-1978-261-615 • www.micromaterials.co.uk

Our NanoTest system offers a range of methods of materials characterisation including nanoindentation, nano-impact and nano-scratch and wear measurements. MML has pioneered nanomechanical testing in real-world conditions. The NanoTest offers unique testing modules, among them the high temperature testing module which allows testing of a sample heated up to temperatures of 850°C. The patented MML nano-impact and fatigue system affords unrivalled information on fracture and fatigue behaviour. Close collaboration with our users drives R&D programs to expand the testing capability of our NanoTest even further, ensuring MML customers are always at the cutting edge of nanomechanical testing. Our new Acoustic Emission module allows measurement of acoustic signals during indentation, impact or scratch tests.

Nano-Master, Inc. 322
3019 Alvin Devane Blvd.
Suite 300
Austin, Texas 78741
Phone: 512-385-4552
http://www.nanomaster.com

manufactures equipment for Semiconductor, MEMS, Optoelectronics, Nanotechnology and Photovoltaic applications. NANO-MASTER products include PECVD Systems for deposition of SiO₂, Si₃N₄, DLC and CNT; PA-MOCVD Systems for InGaN and AlGaIn; Reactive Sputtering, Co-Sputtering, and Combinatorial Sputtering Systems; Thermal and E-beam Evaporators, Ion Beam Milling and Reactive Etching Systems; Atomic Layer Deposition Tools; Megasonic Wafer/Mask Cleaners and Photoresist Stripping Equipment.

Nano4Energy SLNE 227
Calle Luis Camoens 9, la planta
VAT: ES B96069101
Madrid 2801
Spain
Phone: 34 622305290
http://nano4energy.eu
nano4energy.eu

Cutting edge process development for the thin film and sputtering industry. The company focus is to build bridges between the science communities and production industry by adapting state of the art laboratory processes to industrial use. We have a strong background in technology for thin film photovoltaic technology as well as monomer deposition for organic barrier layers using one step all in vacuum processes. Nano4Energy is an advanced technology R&D company in the area of thin film surface engineering.



COMPANY PROFILES

NANOVEA
6 Morgan Street Ste 156
Irvine, CA 92618
Phone: 949-461-9292
www.nanovea.com

326

Nanovea began designing and manufacturing instruments after years of experience in providing solutions for profilometry, mechanical and tribology applications. Firmly aligned with its vision, Nanovea aims to simplify advanced measurement technology to stimulate materials engineering for the common good. Ease of use, advanced automation and the dedication to superior accuracy are the driving forces behind Nanovea's full range of Profilometers, Mechanical Testers and Tribometers. Unlike other manufacturers, Nanovea also provides Laboratory & consulting services. Thus, clients are given access to years of experience in finding solutions to improve quality control and materials development. Nanovea offers many critically important tests including surface roughness, nanoindentation, scratch and wear testing among many others. Nanovea's instruments can be found internationally in distinguished educational and industrial organizations.

NETA
1, rue François Mitterrand
Talence, 33400
France
Phone: 33-564310005
www.neta-tech.com

219

Neta has designed and manufactured the JAX-M1. This patented state-of-the-art technique has enabled material to be characterized at nanometric scale without contact and causing no destruction. Our products are dedicated to industrial and scientific applications with the aim to be very user-friendly. Our turnkey ASOPS imaging solutions are well adapted to different applications: nondestructive test for thin film characterization as well as cell's nanometric ultrasound.

Oerlikon Balzers
1700 E Golf Road
Schaumburg, IL 60173
Phone: 847-619-5541
www.oerlikon.com

207

We are the world technology leader in the growing surface solutions market.



Pfeiffer Vacuum Technology, Inc.
24 Trafalgar Square
Nashua, NH 03063
Phone: 603-578-6500
www.pfeiffer-vacuum.com

309

Pfeiffer Vacuum provides vacuum solutions from a single source. We supply a full range of hybrid and magnetically levitated turbo pumps, backing pumps, measurement and analysis devices and systems. The newest member of the Pfeiffer Vacuum Group, Nor-Cal Products, manufactures high quality vacuum components, chambers and valves.

Plansee SE
115 Constitution Blvd.
Franklin, MA 02038
Phone: 508-553-3800
www.plansee.com

328

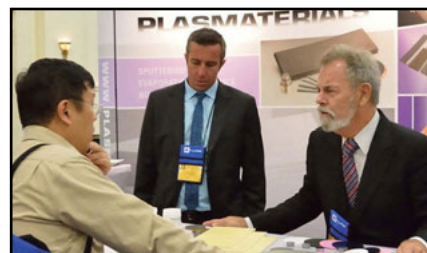
Plansee offers superior sputtering targets and arc cathodes for hard coating. Founded as a privately-owned enterprise in 1921, its expertise is in high-melting metals and compound materials. Whether in the electronics, coating, or aerospace industry, whenever conventional materials reach their limits, Plansee goes beyond the boundaries. We oversee the entire process from raw materials to the final product as the manufacturing, research, and development is done in our state-of-the-art facility.



Plasmaterials, Inc.
2268 Research Drive
Livermore, CA 94550
Phone: 925-447-4030
www.plasmaterials.com

204

PLASMATERIALS, Inc., since 1987, has been supplying the Thin Film Industry with high quality sputtering targets and evaporation materials for use in PVD equipment and related applications. These materials are well suited for industrial applications, laboratory processing, research and development applications, pilot production applications as well as full scale production. In addition, we offer backing plates, e-beam starter sources, crucible liners and bonding services. For more information, please contact us.



COMPANY PROFILES

Process Materials Inc.
5625 Brisa Street Suite B
Livermore, CA 94550
Phone: 925-245-9626
www.processmaterials.com

329

Materials: High purity; sputtering targets and evaporation materials. Bonding services, backing plates and plasma spraying. Products include metals, alloys, and ceramics. A leading source known for quality, consistency and dependability. Exact specifications, delivered on time.

ProTech Materials
20919 Cabot Blvd
Hayward, CA 94545
Phone: 650-292-5435
www.protechmaterials.com

221

Leading supplier of vacuum coating materials since 1997. Headquarters & manufacturing located in Hayward, CA. Known for delivery of high quality products. Key personnel have average of 20+ years experience in target manufacturing and thin film deposition. Strong technical capability with Engineering and Material Science with a strong emphasis on providing superior customer service.

PROTO
12350 Universal Drive
Taylor, MI 48180-4070
Phone: 734-946-0974
protoxrd.com/

104

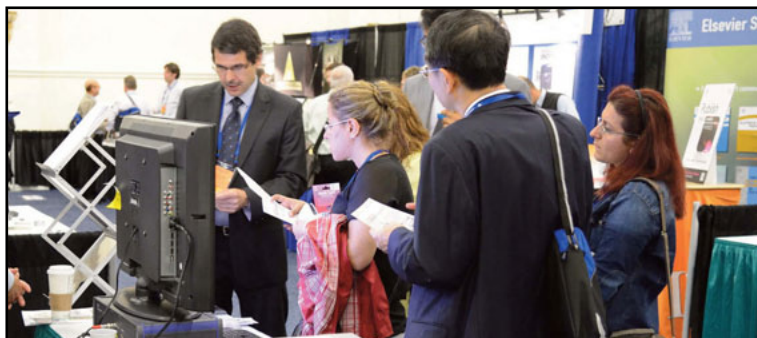
PROTO is a leading provider of innovative x-ray diffraction (XRD) systems. Our team of application scientists and engineers ensure that you get the correct system and support for all of your applications. PROTO's product line includes x-ray diffractometers for characterizing powder, single crystal, and thin-film materials.

PVT Plasma und Vakuum Technik GmbH 229
Rudolf-Diesel-Str. 7
Bensheim, 64625 Germany
Phone: 49-6251-856560
www.pvtvacuum.de

Since 1985 PVT Plasma und Vakuum Technik GmbH is a leading manufacturer of industrial and R&D PVD coating equipment for wear-, and erosion-resistant coatings, such as nano-structured single - and multilayers TiN, Ti(C,N), TiAlN, AlTiN, AlCrN and Si - and/or B - doped coatings by arc-evaporation (HiParc) for the cutting tool, automotive and aircraft industry. HiPIMS V+ and dc-pulsed magnetron-sputtering are used for tribological DLC - coatings, but also for super-smooth, ultra-dense hard coatings for any kind of wear-resistant applications. The coating systems are characterized by user friendliness, excellent reproducibility, industrial reliability, and efficiency.

R.D. Mathis Company 103
2840 Gundry Avenue
Signal Hill, CA 90755
Phone: 562-426-7049
www.rdmathis.com

Evaporation Sources and Materials. We offer the highest quality and widest selection of evaporation sources, E-Beam Liners and evaporation materials for the thin film coating industries. Our Catalog offers a comprehensive selection of Tungsten, Molybdenum and Tantalum sources as well as custom fabrication. We also offer a wide variety of E-Beam Liners and evaporation materials including gold, silver, nickel, aluminum, etc. we also offer a wide selection of Sputtering targets in various sizes. Our "LV Series" Low Voltage, High Current Power Supplies and our "GP 100" Inert Gas Purifier are available to compliment your evaporation process. www.rdmathis.com



COMPANY PROFILES

Robeko GmbH & Co. KG

315

**An der Heide 3b
Mehlingen, Rhineland-Palatinate 67678
Germany
Phone: 49-63039996700
www.robeko.de**

robeko is dedicated to components, materials and services for sputtering and microwave PECVD. robeko manufactures sputtering targets and microwave plasma sources. The sources are used for pretreatment of substrates and for PECVD deposition of DLC- and optical coatings. The circular source comes with a DN200ISO flange and is capable for powers of 3kW. A linear microwave plasma source is under development. In addition we distribute high quality products for sputtering, like rotatable and planar magnetrons, spectroscopic plasma monitors, HIPIMS power supplies.

Rtec Instruments, Inc.

206

**1810 Oakland Road, B
San Jose, CA 95131
Phone: 408-708-9226
www.rtec-instruments.com**

Rtec-instruments develops and manufactures tribology, mechanical and surface inspection and analysis testers. Our latest generation of Multi-functional Tribometer (MFT series) can achieve 3D in-line imaging function via integrated optical profilometer. This unique feature give users the ability to study, monitor and plot friction, wear, roughness, volume wear. change with time. Our latest generation of Universal Profilometer (UP series) combines Interferometry, Confocal, Dark Field Imaging, Variable focus in one unit. This allows it to measure any kind of sample – transparent, opaque, steep slopes, ultra-flat, thin/ thick films.



Semilab USA LLC

307

**10770 N. 46th Street Suite E700
Tampa, FL 33617
Phone: 813-977-2244
www.semilab.hu**

We design, produce and sell metrology equipment for the characterization of semiconductor and photovoltaic materials, for monitoring the manufacturing process of semiconductor devices, flat panel displays and solar cells, and also for R&D purposes in these areas. We offer a variety of measurement techniques; most of them are non-contact and non-destructive. Many of our technologies can be flexibly integrated into different platforms, ranging from simple handheld devices and table-top systems with high resolution mapping capability to fully automated stand-alone production control tools for mid-range and high-level fablines. We also offer in-line measurements for solar cell production lines.

SEO (Surface Electro Optics)

214

**946 Kosek
Suwon, GI 16643 South Korea
Phone: 82 312 989 561
www.s-eo.com**

SEO Co., is proud to be recognized in Contact angle, Dynamic Contact angle(DCA), surface Tension & Thermal Conductivity through innovative, excellent training and support customer .Our Phoenix-MT series & P-Smart is the world's most powerful QC,R&D grande wettability and with the DCA 200 series offer a complete line of surface chemistry Applications. www.s-eo.com

Solecon Laboratories, Inc.

318

**770 Trademark Drive
Reno, NV 89521
Phone: 775-853-5900
www.solecon.com**

Spreading resistance analysis (SRA) is especially useful for its depth accuracy (+/-3%) and sensitivity to ultra-low dopant concentrations. SRA can be performed at any stage of the wafer fab process, and is used extensively for: Epitaxial deposition - thickness, resistivity, and auto doping issues, ion implant verification, dopant contamination, diffusions in general - deep or shallow. We will be happy to discuss the possibility of running complimentary analyses to demonstrate our capabilities on your samples. Please contact Sheila Loftis at 775-853-5900 or sheila@solecon.com

COMPANY PROFILES

UC Components
18700 Adams Ct
Morgan Hill, CA 95037
Phone: 408-782-1929
www.ucomponents.com

222



Reduce out-gassing & eliminate virtual leaks from your vacuum system with RediVac® Fasteners & O-Rings from UC Components. Speed your pump-down with vented, cleaned, coated, plated, & polished screws as well as baked fluoroelastomer seals. The UC RediVac® line includes thousands of sizes and configurations to meet your application needs including center and slot-vented screws with seven different finish options including Au, Ag, and WS2. Purchase, quote or download a print at www.ucomponents.com.

voestalpine eifeler Coatings North America 215
3800 Commerce Drive
St. Charles, IL 60174
Phone: 630-587-1220
www.eifeler.com/northamerica



voestalpine eifeler Coatings North America provides customers in Canada, Mexico and the US with high performance PVD coatings. From our US locations in: California, Illinois, Michigan, Ohio and Tennessee, we offer specialty coatings for Stamping/Forming/Cutting and Medical applications. Customers benefit from our range of high quality coatings delivered by experienced teams ensuring projects are completed on time, the first time.

voestalpine eifeler Vacotec GmbH 215
Hansaallee 321
Duesseldorf, 40549
Germany
Phone: +49 211 522-2417




www.eifeler.com/en/voestalpine-eifeler-vacotec-gmbh/
For 25 years, voestalpine eifeler Vacotec builds innovative coating systems for the international market. We offer a considerable level of know-how in vacuum technology and technical expertise incorporated into our technology, design and construction of the latest generation of turnkey PVD solutions and hard wear-resistant coatings. Our innovative R&D, engineering, quality manufacturing and our international customer service guarantee for your success.

Visit as many sponsoring exhibitors as you can on Tuesday and Wednesday to obtain multiple raffle tickets to increase your chances of winning great prizes !!
Look for the sponsor signs on the carpet in front of the participating exhibitor's booth and ask for a ticket !



PLATIT®

Advanced Coating Systems
SWISS  QUALITY

Quality • Innovation • Support



Bring Coating Services & Expertise In-House

- Control quality and generate profits
- Expand your cutting tool manufacturing business
- Compete with quick turnaround and flexibility
- Our equipment assures state-of-the-art coatings now & the future
- Spare parts and consumables stocked in Chicago
- The BEST personal support in North America



Platit, Inc.

1840 Industrial Drive, Suite 220
Libertyville, IL 60048 • USA
Phone: 1-855-475-2848
Web: www.platitusa.com
Email: pvdcoating@platitusa.com



ICMCTF

47th International Conference on
Metallurgical Coatings and Thin Films

Mark Your Calendars for ICMCTF 2020!

April 26 - May 1, 2020

Town & Country Hotel and Convention Center
San Diego, California, USA

Sponsored by the AVS Advanced Surface Engineering Division:
<http://www2.avs.org/conferences/icmctf>

CONFERENCE OVERVIEW

The International Conference on Metallurgical Coatings and Thin Films (ICMCTF) is the premier international conference in the field of **thin-film deposition, characterization, and advanced surface engineering** promoting global exchange of ideas and information among **scientists, technologists, and manufacturers**. The Conference includes more than 60 high-profile invited speakers, in over 50 sessions, across twelve technical and topical symposia, several featured **lectures**, as well as focused **topic sessions, short courses, an equipment exhibition, an awards program, and daily social networking events**.

ICMCTF 2020 DEADLINES

- ▶ **Abstract Submission:**
October 1, 2019
- ▶ **Award Nominations:**
October 1, 2019
- ▶ **Manuscript Submission:**
March 20, 2020
- ▶ **Early Registration:**
March 20, 2020

ICMCTF FUTURE DATES

- 2021:** April 25-30, 2021
- 2022:** May 22-27, 2022
- 2023:** May 21-26, 2023

General Chair 2020:

Christopher Muratore
University of Dayton
cmuratore1@udayton.edu

Program Chair 2020:

Grzegorz (Greg) Greczynski
Linköping University
grzegorz.greczynski@liu.se

Conference Management:

Yvonne Towse
Della Miller
Jeannette DeGennaro
Heather Korff
icmctf@icmctf.org

